British Journal of Pharmacology

September 1991

Volume 104 Number 1 pages 1–284

Br. J. Pharmacol. (1991), **104**, 3–4

SPECIAL REPORT

CP-93,129, a potent and selective 5-HT_{1B} receptor agonist blocks neurogenic plasma extravasation within rat but not guinea-pig dura mater

Toshio Matsubara, [1]Michael A. Moskowitz & Barkjang Byun

Stroke Research Laboratory, Neurosurgical and Neurology Services, Massachusetts General Hospital, Harvard Medical School, Boston, MA 02114, U.S.A.

Pretreatment with CP-93,129 blocked plasma extravasation in rat dura mater induced by electrical trigeminal ganglion stimulation when administered at $\geqslant 140\,nmol\,kg^{-1}$, i.v. but did not affect plasma leakage in guinea-pig at 460 or $1400\,nmol\,kg^{-1}$. Sumatriptan, a 5-HT_{1D}-like receptor agonist, blocked plasma extravasation in the guinea-pig model when administered at $7\,nmol\,kg^{-1}$. In as much as CP-93,129 binds with micromolar affinities to 5-HT_{1A}, 5-HT_{1C}, 5-HT_{1D}, and 5-HT_2 recognition sites, and with nanomolar affinity to the 5-HT_{1B} receptor subtype, blockade of plasma extravasation in the rat dura mater may be mediated by 5-HT_{1B} receptors whereas the 5-HT_{1D} receptor may be more relevant to the guinea-pig.

Keywords: 5-HT_{1B} receptors; 5-HT_{1D} receptors; migraine; dura mater; neurogenic inflammation

Introduction 5-HT_{1B} and 5-HT_{1D} are pharmacologically distinct but analogous subtypes of 5-hydroxytryptamine (5-HT) receptors which mediate similar functions in different species. 5-HT_{1B} binding sites are present in rat and mouse brain but are not found in membranes prepared from guinea-pig or human brain (Hoyer & Middlemiss, 1989). CP-93,129, the tautomer of 5-hydroxy-3(4-1,2,5,6-tetrahydropyridyl)-4-azaindole, exhibits marked affinity for 5-HT_{1B} binding sites in rat brain membranes (IC_{50} 15 nM with [^{3}H]-5-HT) and selectively inhibits adenylate cyclase activity in brain areas possessing a high density of 5-HT_{1B} (rat substantia nigra) but not 5-HT_{1A} (guinea-pig hippocampus) or 5-HT_{1D} (guinea-pig substantia nigra) receptors (Macor *et al.*, 1990).

5-HT_1 receptors mediate inhibition of plasma leakage within rat dura mater following trigeminal electrical stimulation (Buzzi *et al.*, 1991b). Leakage is attenuated or blocked in the rat by pretreatment with 5-carboxamidotryptamine $\gg$ 5-benzyloxytryptamine > dihydroergotamine > sumatriptan > 8-hydroxydipropylaminotetralin in descending order of potency. This potency order is most consistent with a 5-HT_{1B} or 5-HT_{1D} response among the known 5-HT_1 family of receptors although methiothepin did not block the effect of sumatriptan nor metergoline the effects of 5-CT.

Studies were therefore undertaken in order to clarify the receptor subtype which mediates inhibition of neurogenic plasma extravasation, and to examine one possible functional correlate of the marked ligand binding selectivity.

Methods *Electrical trigeminal stimulation* Male Sprague-Dawley rats (150–200 g) and male Hartley guinea-pigs (200–250 g) (Charles River Laboratories, Wilmington, MA, U.S.A.) were anaesthetized with pentobarbitone (50 or $40\,mg\,kg^{-1}$, i.p., rats or guinea-pigs, respectively), placed in a stereotaxic frame with the incisor bar set at −1.5 mm (rats) or −4.0 mm (guinea-pigs). Symmetrical burr holes were drilled 3.0 mm laterally and 3.7 mm posteriorly from bregma (rats) or 4.0 mm and 4.0 mm, respectively in guinea-pigs. [^{125}I]-BSA $50\,\mu Ci\,kg^{-1}$ was then injected. After 5 min, electrodes were lowered 9.5 mm (rats) or 10.5 mm (guinea-pigs) from dura mater. The right ganglion was stimulated (5 min, 1.2 mA, 5 Hz, 5 ms duration). Ten minutes before stimulation and 5 min before [^{125}I]-albumin administration, rats were injected with CP-93,129 (46, 140 or $460\,nmol\,kg^{-1}$; $n = 5$, 9 or 6, respectively). Guinea-pigs were injected with CP-93,129 (460 or $1400\,nmol\,kg^{-1}$; $n = 7$, 8, respectively) or sumatriptan (2, 7 $nmol\,kg^{-1}$; $n = 5$, 6, respectively). Each dose was tested in at least two separate experiments. Animals were perfused with saline via the left cardiac ventricle for 2 (rats) or 3 min (guinea-pigs) at constant pressure (100 mmHg) to remove intravascular [^{125}I]-BSA. The dura mater was dissected as previously described (Markowitz *et al.*, 1987; Buzzi & Moskowitz, 1990) and radioactivity determined on the two sides.

Capsaicin administration The left femoral vein was exposed in pentobarbitone-anaesthetized guinea-pigs, and CP-93,129 injected. Five minutes later, [^{125}I]-BSA ($50\,\mu Ci\,kg^{-1}$) was injected as a bolus. After an additional 5 min, capsaicin ($0.5\,\mu mol\,kg^{-1}$) or vehicle was infused over 3 min. Ten minutes later, animals were perfused with saline as described above.

Data analysis [^{125}I]-BSA extravasation is expressed as the ratio: c.p.m. mg^{-1} (stimulated side)/c.p.m. mg^{-1} (unstimulated side). In capsaicin experiments, data are expressed as % c.p.m. mg^{-1} between vehicle- and drug-treated animals. Results are expressed as mean ± s.e.mean. Unpaired Student's t test was used for statistical analysis. Probability values (P) of less than 0.05 were considered significant.

Drugs [^{125}I]-bovine serum albumin (BSA; New England Nuclear, Boston, MA) and sumatriptan (Glaxo Ltd, Hertfordshire, England) were diluted in saline; capsaicin (Polyscience Inc., Wilmington, Pennsylvania) was solubilized in saline:ethanol:Tween 80 8:1:1; CP-93,129 (Pfizer, Inc, Groton, CT, U.S.A.) was dissolved in dimethylsulphoxide:saline 1:9. All drugs were injected intravenously ($1\,ml\,kg^{-1}$). The same volume of vehicle was administered.

Results There was no mortality after electrical stimulation or drug administration. CP-93,129 ($140\,nmol\,kg^{-1}$) did not change arterial blood pressure when intra-arterial monitoring (20 min) was performed in selected animals ($n = 3$ rats).

Albumin (c.p.m. mg^{-1} wet wt.) was 16.0 ± 1.6 (rats) and 17.3 ± 1.2 (guinea-pigs) on the side contralateral to stimu-

[1] Author for correspondence.

lation. Leakage ipsilateral to the stimulation was 28.8 ± 2.8 (rats) and 28.3 ± 2.1 (guinea-pigs). The ratio ranged from 1.6–2.1 (rats) or from 1.3–2.0 (guinea-pigs) in 5 (rats) or 6 (guinea-pigs) separate experiments.

The amount of protein leakage on the unstimulated side did not differ between vehicle- or CP-93,129-treated rats or guinea-pigs. The data (c.p.m. mg^{-1} wet wt.) contralateral to stimulation in rat was 20.1 ± 2.2 (vehicle, $n = 5$) versus 21.5 ± 3.4 ($n = 5$) after 46 nmol kg^{-1}, 16.2 ± 1.9 (vehicle, $n = 8$) versus 14.7 ± 1.5 ($n = 9$) after 140 nmol kg^{-1}, and 15.3 ± 1.7 (vehicle, $n = 4$) versus 17.2 ± 3.2 ($n = 6$) after 460 nmol kg^{-1}.

Pretreatment with CP-93,129 (140 or 460 nmol kg^{-1}) decreased the ratio in rats but not guinea-pigs (460, 1400 nmol kg^{-1}). Sumatriptan (7 nmol kg^{-1}) decreased the ratio in the guinea-pigs from 1.60 ± 0.12 to 1.15 ± 0.06 (Figure 1).

Capsaicin increased [^{125}I]-BSA leakage in guinea-pig dura mater but CP-93,129 (1400 nmol kg^{-1}) did not block the extravasation response [149 ± 7% in capsaicin-treated group ($n = 9$) versus 139 ± 5% in CP-93,129-treated animals ($n = 8$)].

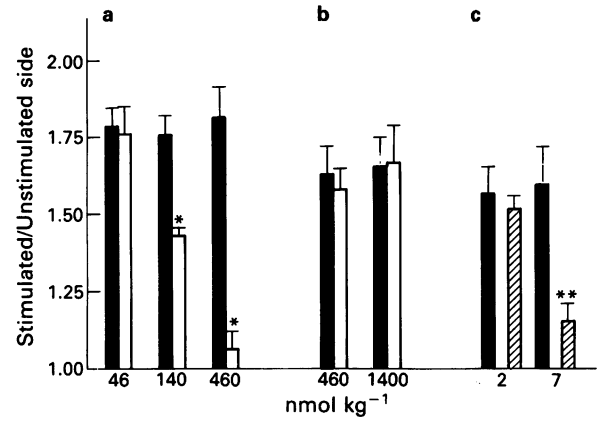

Figure 1 CP-93,129, a potent and selective 5-HT_{1B} receptor agonist, blocks neurogenic plasma extravasation within rat (a) but not guinea-pig (b) dura mater whereas sumatriptan, a potent 5-HT_{1D}-like agonist, blocks the response in the guinea-pig dura mater (c). CP-93,129 (46, 140, 460 nmol kg^{-1}, i.v. to rats; 460, 1400 nmol kg^{-1}, i.v. to guinea-pigs) or sumatriptan (2, 7 nmol kg^{-1}, i.v. to guinea-pigs) was administered to pentobarbitone-anaesthetized animals at the indicated doses 10 min prior to electrical trigeminal stimulation (1.2 mA, 5 Hz, 5 ms, 5 min) and 5 min prior to [^{125}I]-albumin (i.v., 50 μCi kg^{-1}) (see Methods). Animals were perfused with saline, and the tissues removed and counted for radioactivity. Data are expressed as the ratio of c.p.m. mg^{-1} on the stimulated and unstimulated sides. The solid columns represent the vehicle-treated animals. The open columns represent the CP-93,129-treated animals, the hatched columns the sumatriptan-treated animals; vertical bars show s.e.mean. * $P < 0.005$ or ** $P < 0.01$ as compared to vehicle-treated animals.

Discussion The importance of the 5-HT_{1B} receptor in the rat plasma extravasation model is documented in this report. The virtual selectivity of CP-93,129 for the 5-HT_{1B} recognition site provides strong evidence in support of this conclusion. Ligand binding experiments indicate that CP-93,129 exhibits 200 fold greater affinity for 5-HT_{1B} than 5-HT_{1A} (rat cortex), 150 fold greater affinity for 5-HT_{1B} than 5-HT_{1D} (bovine striatum), 400 fold greater affinity for 5-HT_{1B} than 5-HT_{1C} (pig choroid plexus), 2,400 fold greater affinity for 5-HT_{1B} than 5-HT_2 binding sites (Macor *et al.*, 1990). The compound does not bind to dopamine, noradrenaline or adenosine recognition sites.

CP-93,129 was inactive when tested in the guinea-pig model at 1,400 nmol kg^{-1} whereas sumatriptan was quite potent. The threshold dose of sumatriptan in the guinea-pig electrical stimulation model was 30 fold lower than in the rat model. This correlates with the apparent greater affinity (26 fold) of sumatriptan at the 5-HT_{1D} than 5-HT_{1B} recognition sites (Hoyer *et al.*, 1989).

Inhibition of neurogenic plasma extravasation in rat dura mater is mediated by prejunctional 5-HT_1 heteroreceptors (Buzzi *et al.*, 1991b). Receptor activation attenuates mast cell secretion and degranulation, platelet aggregation, endothelial activation which develops within postcapillary venules during electrical trigeminal ganglion stimulation (Buzzi *et al.*, 1990; Dimitriadou *et al.*, 1990). Dihydroergotamine or sumatriptan does not block the substance P- or neurokinin A-induced extravasation (Saito *et al.*, 1988; Buzzi & Moskowitz, 1990) but attenuates stimulation-induced elevations in plasma immunoreactive calcitonin gene-related peptide levels within sagittal sinus blood (Buzzi *et al.*, 1991a).

5-HT_{1B} receptor-mediated inhibition of neurotransmitter release is well known within rat brain (Macor *et al.*, 1990). Taken together with the data reported here, an important inhibitory role for the 5-HT_{1B} receptor in both the peripheral and central nervous system of rodents such as the rat seems likely.

Supported by NIH grant NS 21558.

References

BUZZI, M.G., CARTER, W.B., SHIMIZU, T., HEATH, H. & MOSKOWITZ, M.A. (1991a). Dihydroergotamine and sumatriptan attenuate the increase in plasma CGRP levels within rat superior sagittal sinus during electrical trigeminal stimulation. *Neuropharmacol.*, (in press).

BUZZI, M.G., DIMITRIADOU, V., THEOHARIDES, T.C. & MOSKOWITZ, M.A. (1990). Morphological effects of electrical trigeminal ganglion stimulation (ETG) on intra- and extracanial vessels. *Soc. Neurosci.*, **16**, 160.

BUZZI, M.G. & MOSKOWITZ, M.A. (1990). The antimigraine drug, sumatriptan (GR43175), selectively blocks neurogenic plasma extravasation from blood vessels in dura mater. *Br. J. Pharmacol.*, **90**, 202–206.

BUZZI, M.G., MOSKOWITZ, MA., PEROUTKA, S.J. & BYUN, B. (1991b). Further characterization of the putative 5-HT receptor which mediates blockade of neurogenic plasma extravasation in rat dura mater. *Br. J. Pharmacol.*, (in press).

DIMITRIADOU, V., BUZZI, M.G., LAMBRACHT-HALL, M., MOSKOWITZ, M.A. & THEOHARIDES, T.C. (1990). *In vivo* and *in vitro* ultrastructural evidence for stimulation of dura mast cells by neuropeptides. *Soc. Neurosci.*, **16**, 161.

HOYER, D. & MIDDLEMISS, D.N. (1989). Species difference in the pharmacology of terminal 5-HT autoreceptors in mammalian brain. *Trends Pharmacol. Sci.*, **10**, 130–132.

HOYER, D., SCHOEFFTER, P. & GRAY, J.A. (1989). A comparison of the interactions of dihydroergotamine, ergotamine and GR 43175 with 5-HT_1 receptor subtypes. *Cephalalgia*, **9**(Suppl 10), 340–341.

MACOR, J.E., BURKHART, J.H., HEYM, J.H., IVES, J.L., LEBEL, L.A., NEWMAN, M.E., NIELSEN, J.A., RYAN, K., SCHULZ, D.W., TORGERSEN, L.K. & KOE, B.K. (1990). 3-(1,2,5,6-Tetrahydropyrid-4-yl) pyrrolo[3,2-b]pyrid-5-one: a potent and selective serotonin (5-HT_{1B}) agonist and rotationally restricted phenolic analogue of 5-methyl-3-(1,2,5,6-tetrahydropyrid-4-yl)indole. *J. Med. Chem.*, **33**, 2087–2093.

MARKOWITZ, S., SAITO, K. & MOSKOWITZ, M.A. (1987). Neurogenically mediated leakage of plasma protein occurs from blood vessels in dura mater but not brain. *J. Neurosci.*, **7**, 4129–4136.

SAITO, K., MARKOWITZ, S. & MOSKOWITZ, M.A. (1988). Ergot alkaloids block neurogenic extravasation in dura mater: Proposed action in vascular headache. *Ann. Neurol.*, **24**, 732–737.

(Received March 11, 1991
Accepted May 9, 1991)

Br. J. Pharmacol. (1991), **104**, 5–6

SPECIAL REPORT

Coronary vasodilatation induced by endotoxin in the rabbit isolated perfused heart is nitric oxide-dependent and inhibited by dexamethasone

†Russell E.A. Smith, Richard M.J. Palmer & [1]Salvador Moncada

Wellcome Research Laboratories, Langley Court, Beckenham, Kent BR3 3BS and †King's College Hospital, London SE5 9RS

The coronary vasoconstriction induced by the thromboxane mimetic U46619 (9, 11 dideoxy methanoepoxy 9α, 11α prostaglandin $F_{2\alpha}$, 3–30 nM) was significantly attenuated in hearts obtained from rabbits treated with endotoxin (lipopolysaccharide, LPS, 200 μg kg^{-1}, i.v.) 4 h before isolation of the heart. Under these conditions the vasoconstriction induced by two inhibitors of nitric oxide (NO) synthase, N^G-monomethyl-L-arginine (L-NMMA) and N-iminoethyl-L-ornithine (L-NIO) (1–100 μM for each) was significantly enhanced when compared to that induced in hearts from control animals. Both the decreased response to U46619 and the increased response to inhibitors of NO synthase were significantly attenuated by administration of dexamethasone (4 mg kg^{-1}, i.v.) 90 min before treatment with LPS. These data are consistent with the induction, by LPS, of an NO synthase, and the inhibition of this induction by dexamethasone. The enhanced NO synthesis contributes to the haemodynamic changes known to occur in endotoxin shock.

Keywords: Nitric oxide synthase; endotoxin; coronary circulation; dexamethasone; rabbit isolated heart

Introduction Endotoxin shock is characterized by hypotension and resistance to the actions of vasoconstrictors (Parratt, 1973; Suffredini *et al.*, 1989). Recently these changes have been attributed to the induction of an NO synthase which has been shown to occur in the endothelial and smooth muscle layer of rings of aortae exposed to endotoxin (lipopolysaccharide, LPS) *in vitro* (Rees *et al.*, 1990a) and *in vivo* (Knowles *et al.*, 1990). The NO synthase responsible for this pathological release of NO is distinct from the constitutive NO synthase in the vascular endothelium responsible for the physiological regulation of vascular tone and blood pressure (Moncada *et al.*, 1991). Both the constitutive and the inducible NO synthases are inhibited by the L-arginine analogues N^G-monomethyl-L-arginine (L-NMMA) and N-iminoethyl-L-ornithine (L-NIO) (Amezcua *et al.*, 1989; Rees *et al.*, 1990a,b). Furthermore, the glucocorticoid dexamethasone inhibits the induction of the inducible enzyme without affecting the activity of the constitutive enzyme (Rees *et al.*, 1990a; Knowles *et al.*, 1990).

In the present studies we have investigated the responses of the resistance vessels of hearts obtained from rabbits treated with LPS to the vasoconstrictor U46619 and to L-NMMA and L-NIO. We have also studied the effects on these responses of prior treatment of the animals with dexamethasone.

Methods Male New Zealand White rabbits (2.0–2.5 kg) were given LPS (*S. typhosa*, DIFCO, 200 μg kg^{-1}, i.v.). After 4 h the animals were anaesthetized and the heart isolated and perfused retrogradely at constant flow (25 ml min^{-1}) with Krebs buffer at 37°C gassed with 5% CO_2 in O_2 and containing indomethacin (5 μM), according to the method of Langendorff, as described previously (Amezcua *et al.*, 1988). Coronary perfusion pressure (CPP) was recorded as an index of vascular tone. The effect on CPP of 5 min infusions of U46619 (9, 11 dideoxy methanoepoxy 9α, 11α prostaglandin $F_{2\alpha}$), 3–30 nM, was recorded.

The response to L-NMMA and L-NIO (1–100 μM) was determined after adjusting the resting CPP to 35–45 mmHg with a continuous infusion of U46619. In some experiments animals were given dexamethasone (4 mg kg^{-1}, i.v.) 90 min prior to treatment with LPS. Data are expressed as the mean ± s.e.mean for *n* experiments and were analyzed by ANOVA with differences considered significant when $P < 0.05$.

Results The vasoconstrictor response to U46619 (Figure 1) was significantly reduced in hearts from animals treated with LPS when compared with hearts from untreated control animals. At 30 nM U46619, CPP increased by

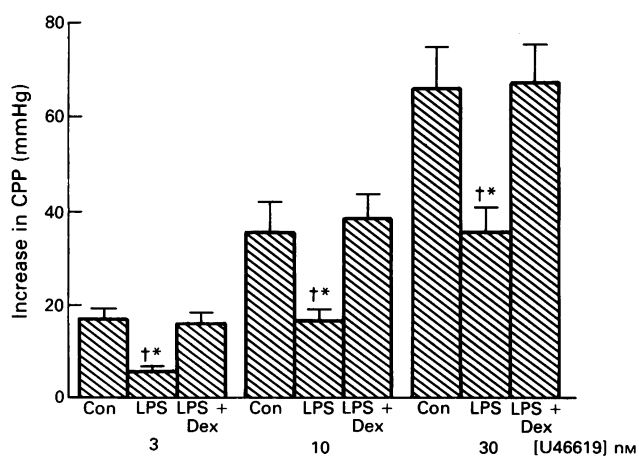

Figure 1 Effect of U46619 on coronary perfusion pressure (CPP, mmHg). U46619 (3–30 nM) caused a concentration-dependent rise in CPP in control hearts (Con) which was significantly attenuated by treatment of the animals with endotoxin lipopolysaccharide (LPS, 200 μg kg^{-1}). This effect was prevented by prior treatment with dexamethasone (4 mg kg^{-1}; LPS + Dex). Each column is the mean of 11–12 experiments; s.e.mean shown by vertical bars. †$P < 0.05$ against control and *$P < 0.05$ against LPS + Dex hearts. The basal CPP was 15.9 ± 1.9 mmHg for control hearts, 12.3 ± 0.8 mmHg for LPS-treated hearts and 13.9 ± 1.1 mmHg for dexamethasone-pretreated hearts (NS).

[1] Author for correspondence.

35.8 ± 5.2 mmHg ($n = 12$) in LPS-treated hearts and by 66.2 ± 8.9 mmHg ($n = 11$) in control hearts. This effect of LPS was prevented by administration of dexamethasone before treatment with LPS (Figure 1). L-NIO (100 μM) caused a significant increase in CPP in control hearts (Figure 2a). This effect of L-NIO was significantly potentiated in hearts from LPS-treated animals, such that greater increases in CPP were observed at 1-100 μM L-NIO. Administration of dexamethasone before LPS treatment significantly attenuated this increased response to L-NIO (Figure 2a). Similar results were obtained with L-NMMA (1–100 μM, Figure 2b).

The increases in CPP induced by these concentrations of U46619 and L-NMMA were not significantly different in hearts from untreated animals or in hearts obtained from animals treated only with dexamethasone 5.5 h prior to isolation of the heart.

Discussion Treatment of rabbits with LPS leads to a reduction in the *ex vivo* response of the coronary circulation to the vasoconstrictor U46619 and to an enhanced response to L-NMMA and L-NIO, two inhibitors of NO synthase. These findings are similar to those observed in rat aortic rings exposed to LPS *in vitro* (Rees *et al.*, 1990a) and are consistent with the induction of an NO synthase in the wall of resistance vessels of the coronary circulation leading to an increase in the synthesis of NO and therefore to vasodilatation. The excessive NO thus formed functionally antagonizes the responses to U46619 and produces a greater response to L-NMMA and L-NIO, which constrict through inhibition of NO synthesis. The altered response to these compounds is prevented by prior administration of dexamethasone, which inhibits the induction of NO synthase in the rat aorta *in vitro* (Rees *et al.*, 1990a) and *in vivo* (Knowles *et al.*, 1990). Thus, our results provide further evidence to support the conclusion that the vasodilatation and the resistance to vasoconstrictors observed during endotoxin shock are attributable to the induction of an NO synthase in the vasculature and that the prevention of these haemodynamic changes by glucocorticoids is due to inhibition of the induction of this enzyme.

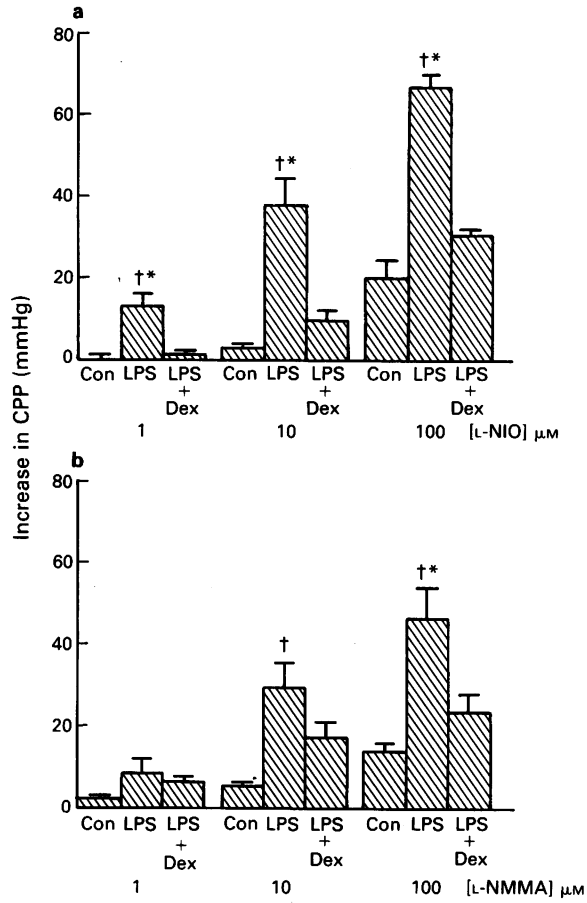

Figure 2 Effects of (a) N-iminoethyl-L-ornithine (L-NIO) and (b) N^G-monomethyl-L-arginine (L-NMMA) on coronary perfusion pressure (CPP mmHg). Both compounds (1–100 μM) caused a concentration-dependent rise in CPP (Con) which was significantly enhanced by treatment of the animals with endotoxin lipopolysaccharide (LPS, 200 μg kg^{-1}). This effect was attenuated to levels not significantly different from control values by prior treatment with dexamethasone (4 mg kg^{-1}; LPS + Dex). Each column is the mean of 4–5 experiments with L-NIO and 7–8 experiments with L-NMMA, s.e.mean shown by vertical bars. †$P < 0.05$ against control and *$P < 0.05$ against LPS + Dex hearts. Resting CPP in control hearts prior to infusion was 39.5 ± 1.3 mmHg ($n = 4$) for L-NIO and 38.3 ± 1.4 mmHg ($n = 7$) for L-NMMA and was not significantly different in the treatment groups.

References

AMEZCUA, J.L., DUSTING, G.J., PALMER, R.M.J. & MONCADA, S. (1988). Acetylcholine induces vasodilatation in the rabbit isolated heart through the release of nitric oxide, the endogenous nitrovasodilator. *Br. J. Pharmacol.*, **95**, 830–834.

AMEZCUA, J.L., PALMER, R.M.J., DE SOUZA, B.M. & MONCADA, S. (1989). Nitric oxide synthesised from L-arginine regulates vascular tone in the coronary circulation of the rabbit. *Br. J. Pharmacol.*, **97**, 1119–1124.

KNOWLES, R.G., SALTER, M., BROOKS, S.L. & MONCADA, S. (1990). Anti-inflammatory glucocorticoids inhibit the induction by endotoxin of nitric oxide synthase in the lung, liver and aorta of the rat. *Biochem. Biophys. Res. Commun.*, **172**, 1042–1048.

MONCADA, S., PALMER, R.M.J. & HIGGS, E.A. (1991). Nitric oxide: physiology, pathophysiology and pharmacology. *Pharmacol. Revs.*, **43**, 109–142.

PARRATT, J.R. (1973). Myocardial and circulatory effects of *E. coli* endotoxin; modification of responses to catecholamines. *Br. J. Pharmacol.*, **47**, 12–25.

REES, D.D., CELLEK, S., PALMER, R.M.J. & MONCADA, S. (1990a). Dexamethasone prevents the induction by endotoxin of a nitric oxide synthase and the associated effects on vascular tone. An insight into endotoxin shock. *Biochem. Biophys. Res. Commun.*, **173**, 541–547.

REES, D.D., PALMER, R.M.J., SCHULZ, R., HODSON, H.F. & MONCADA, S. (1990b). Characterization of three inhibitors of endothelial nitric oxide synthase *in vitro* and *in vivo*. *Br. J. Pharmacol.*, **101**, 746–752.

SUFFREDINI, A.F., FROMM, R.E., PARKER, M.M., BRENNER, M., KOVACS, J.A., WESLEY, R.A. & PARILLO, J.E. (1989). The cardiovascular response of normal humans to the administration of endotoxin. *New Engl. J. Med.*, **321**, 280–287.

(Received June 17, 1991
Accepted July 1, 1991)

Br. J. Pharmacol. (1991), **104**, 7–14

Cardiovascular profile of 5 novel nitrate-esters: a comparative study with nitroglycerin in pigs with and without left ventricular dysfunction

L.J. van Woerkens, W.J. van der Giessen & [1]P.D. Verdouw

Laboratory for Experimental Cardiology, Thoraxcentre, Erasmus University Rotterdam, Rotterdam, The Netherlands

1 Four cumulative 10 min intravenous infusions of 0.05, 0.2, 0.5 and 2.0 mg min^{-1} were used to compare the cardiovascular profile of 5 novel nitrate-esters dissolved in Intralipid 10% to that of nitroglycerin (GTN) in conscious pigs.

2 Infusion of Intralipid 10% alone had no effect on any of the systemic haemodynamic parameters. GTN infusions decreased mean arterial blood pressure dose-dependently from 94 ± 2 mmHg to 79 ± 3 mmHg ($P < 0.05$) and raised cardiac output from 2.74 ± 0.09 l min^{-1} to 3.40 ± 0.18 l min^{-1} ($P < 0.05$) due to an increase in heart rate (by up to 43 ± 3%), as stroke volume decreased slightly. Systemic vascular resistance decreased (by 32 ± 3%) and left ventricular end-diastolic pressure fell from 5.2 ± 0.4 mmHg to 2.2 ± 0.5 mmHg (both $P < 0.05$).

3 The novel compounds CEDO 8811, CEDO 8834 and CEDO 8901 increased cardiac output only at the highest dose (7%, 8% and 9%, respectively). There was no change in mean arterial blood pressure as the increase in cardiac output was counterbalanced by arterial vasodilatation. All three compounds reduced left ventricular end-diastolic pressure slightly.

4 CEDO 8816 was a more potent arterial and venodilator than the aforementioned CEDO compounds, as the decreases in systemic vascular resistance and left ventricular end-diastolic pressure were already significant at lower doses. The fall in stroke volume was fully compensated by the increase in heart rate and as a result cardiac output increased by 11 ± 3% ($P < 0.05$) at the highest dose.

5 CEDO 8956 was the most potent vasodilator of the novel compounds and exhibited a cardiovascular profile similar to that of GTN. Left ventricular end-diastolic pressure decreased significantly during infusion of 0.2 mg min^{-1}. Mean arterial blood pressure decreased by 11 ± 2% ($P < 0.05$) in spite of an increase in cardiac output by up to 20 ± 2% ($P < 0.05$), due to a decrease (by 27 ± 1%, $P < 0.05$) in systemic vascular resistance. The increases in heart rate (20 ± 5%, $P < 0.05$) and $LVdP/dt_{max}$ (38 ± 4%, $P < 0.05$) were, however, considerably less after CEDO 8956 than after GTN.

6 The potential of CEDO 8956 in the treatment of chronic left ventricular dysfunction was evaluated during administration to conscious pigs (21–23 kg), in which the left circumflex coronary artery was ligated 4 weeks earlier. In these animals, baseline values for cardiac output and $LVdP/dt_{max}$ were lower and those of systemic vascular resistance and left ventricular end-diastolic pressure were higher than in the first group of experiments.

7 Both GTN and CEDO 8956 in doses of 0.05 to 2.0 mg min^{-1} increased cardiac output dose-dependently (by up to 34% and 19%, respectively). The decrease in systemic vascular resistance was larger with GTN (35%) than with CEDO 8956 (17%), which resulted in a 13% decrease in mean arterial pressure during infusion of GTN, whereas there was no change in mean arterial pressure during infusion of CEDO 8956. Both compounds increased $LVdP/dt_{max}$ (by 48% and 30%, respectively) and lowered left ventricular end-diastolic pressure to normal levels.

8 At a dose of 1.0 mg min^{-1}, both GTN and CEDO 8956 increased left ventricular blood flow parallel to the increase in myocardial oxygen demand. At this dose, GTN also caused vasodilatation in the vascular beds of the brain, kidneys and adrenals. With CEDO 8956 no significant changes were achieved.

9 We conclude that the cardiovascular profile of CEDO 8956 in both normal animals and in animals with chronic left ventricular dysfunction warrants further study on its usefulness in the treatment of a number of cardiovascular disorders.

Keywords: Nitrate-esters; nitroglycerin; myocardial infarction; left ventricular dysfunction; systemic haemodynamics; coronary blood flow; regional blood flows; conscious pigs.

Introduction

Nitroglycerin (glyceryltrinitrate, GTN) has remained one of the major drugs used in the acute treatment of ischaemic heart disease, despite an attenuation of the therapeutic effects in a substantial group of patients in the long term. In search of new nitrate-like drugs a number of structurally different compounds have been synthesized. In this study we evaluated the systemic haemodynamic effects of these 5 novel nitrate-esters in conscious instrumented pigs and compared the results to those obtained with GTN. We have earlier shown that the magnitude of the responses obtained under pathophysiological conditions, might be different from those obtained under normal conditions (Van der Giessen *et al.*, 1989). We therefore selected the most potent of the novel compounds for further study in conscious pigs with mild left ventricular dysfunction secondary to a chronic coronary artery occlusion. The major characteristics of this model are a depressed cardiac output and myocardial contractility, while left ventricular filling pressure is elevated. Mean arterial blood pressure is maintained by peripheral vasoconstriction. In this model, in addition to the effects on systemic haemodynamics, we also evaluated the effects on regional blood flows using radioactive labelled microspheres.

[1] Author for correspondence.

Methods

The experimental procedures were approved by the Committee on animal experiments of the Erasmus University Rotterdam, and complied to the guidelines for the use and care of experimental animals as put forward by the council of the American Physiological Society (DHEW Publication No. (NIH) 80-23, 1980).

Surgical procedures

After an overnight fast, 25 cross-bred Landrace x Yorkshire pigs of either sex (19–21 kg at the time of surgery), pretreated with 600 mg of a mixture of procaine penicillin-G and benzathine penicillin-G intramuscularly (Duplocillin, Gist-Brocades NV, Delft, The Netherlands), were sedated with an intramuscular injection of 30 mg kg^{-1} ketamine HCl (Aeskoket, Aesculaap BV, Boxtel, The Netherlands). Subsequently the animals were intubated and mechanically ventilated with a mixture of oxygen and nitrous oxide (1:2) to which 1–4% (v/v) enflurane was added. Under sterile conditions, a jugular vein and a common carotid artery were cannulated for infusion of drugs or solvent and measurement of arterial blood pressure, respectively. The chest was opened via the third left intercostal space and an electromagnetic flow probe (Skalar, Delft, The Netherlands) was positioned around the ascending aorta for the measurement of aortic blood flow. The heart was exposed via the fifth intercostal space and a pressure transducer (Konigsberg Instruments Inc., Pasadena, CA, U.S.A.) was implanted into the left ventricle of the heart through its apex for recording of left ventricular pressure. The left atrium was cannulated for recording of left atrial pressure which, together with the arterial blood pressure, was used for calibration of the Konigsberg transducer signals.

In 16 of the 25 animals, the proximal segment of the left circumflex coronary artery (LCXCA) was permanently ligated for the induction of a myocardial infarction. In these animals the left atrial cannula was also used for the injection of radioactive microspheres to determine regional blood flows. After instrumentation was completed, a period of 30 min was allowed before closure of the chest. During this period ventricular tachycardia and ventricular fibrillation (occurring exclusively in the group with coronary artery ligation) were treated with d.c.-countershock. The chest was then closed and the wires tunnelled to the back, and the animals were allowed to recover from surgery.

Post-surgical period

The animals received daily intravenous doses of 500 mg amoxicillin (Clamoxil, Beecham Farma B.V., Amstelveen, The Netherlands) and, during the first week only, 500 mg kanamycin (Kanymex, Gist Brocades N.V., Delft, The Netherlands) to prevent infection. Catheters were flushed daily with an isotonic saline solution containing 500 iu ml^{-1} heparin. During the first month of the post-operative recovery period the animals were adapted to the laboratory facilities (8 to 10 sessions), while haemodynamic parameters were monitored. The experimental protocols were executed when systemic haemodynamics remained stable for at least 1 h, usually 4 weeks after instrumentation. All measurements were done while the animals were quietly resting in a constraining jacket.

Two animals with an intact coronary circulation were excluded from further study because of failure of the electrical signals. From the 16 pigs in which the left circumflex coronary artery was occluded, 5 animals died suddenly during the early post-operative period, most likely secondary to a ventricular arrhythmia. One animal was killed because of an infection.

Experimental protocols

In the animals with the intact coronary circulation 4 consecutive 10 min intravenous infusions with increasing doses of 0.05, 0.2, 0.5 and 2.0 mg min^{-1} (2.2 ± 0.1, 8.7 ± 0.2, 21.8 ± 0.5 and 87 ± 2 $\mu g\,kg^{-1}\,min^{-1}$, respectively) GTN, CEDO 8956, CEDO 8811, CEDO 8816, CEDO 8834 or CEDO 8901 dissolved in Intralipid 10% or equal volumes of Intralipid 10% were administered during separate runs of the protocol. Heart rate, arterial blood pressure, mean aortic blood flow, left ventricular pressure and its first derivative ($LVdP/dt$) were recorded at the end of each infusion period. Stroke volume was calculated by dividing mean aortic blood flow and heart rate, while systemic vascular resistance was determined by dividing mean arterial blood pressure and mean aortic blood flow. In all experiments infusions of different compounds or solvent in the same animals were separated by at least 24 h.

In the animals with the infarction 5 consecutive 10 min intravenous infusions with increasing doses of 0.05, 0.2, 0.5, 1.0 and 2.0 mg min^{-1} (2.3 ± 0.1, 9.2 ± 0.3, 23.0 ± 0.8, 46.1 ± 1.5 and 92 ± 3 $\mu g\,kg^{-1}\,min^{-1}$, respectively) were used to compare the cardiovascular effects of CEDO 8956 to those of GTN. As control, the Intralipid 10% solvent was infused with equal volumes. In these animals regional organ blood flows were also determined at baseline and after infusion of 1 mg min^{-1} of both compounds, by injection of a batch of 1–2 × 10^6 carbonized plastic microspheres (15 ± 1 μm (s.d.) in diameter) labelled with either ^{95}Nb, ^{103}Ru, ^{113}Sn or ^{141}Ce (NEN Chemicals GmbH, Dreieich, Germany) into the left atrium. To calculate regional blood flows a reference blood sample was withdrawn from the cannula in the carotid artery at a rate of 10 ml min^{-1}, starting 15 s before the injection of microspheres, until 90 s after completion of the injection of the microspheres. At the end of the experiments animals were killed with an overdose of sodium pentobarbitone. From the animals various organs (adrenals, liver, spleen, stomach, small intestine, brain and kidneys) and representative aliquots of several tissues (abdominal skin, skeletal muscle) were excised, weighed and put into vials. The hearts were fixed in formaldehyde (10% v/v) and 48 h later the atria and right ventricle were cut off the left ventricle. The normal myocardium of the left ventricle was divided into three layers of equal thickness: subepicardium, mid-myocardium and subendocardium. The infarcted area of the left ventricle was separated from the normal myocardium, and counted as a whole.

The radioactivity was counted and the amount of blood flow to the various tissues ($\dot{Q}_{tis}$) was calculated as:

$$\dot{Q}_{tis}\ (ml\,min^{-1}) = (I_{tis}/I_{art}) \times \dot{Q}_{art},$$

where I_{tis} and I_{art} are the radioactivity in a particular tissue and that of the arterial blood sample respectively, and $\dot{Q}_{art}$ is the rate of withdrawal of the blood sample.

Drugs

The drugs used in this study were CEDO 8811 (3,3-diphenyl-1-propanol nitrate), CEDO 8816 (1,6-hexanediol dinitrate), CEDO 8834 (3-phenyl-3-(4-pyridyl)-1-propanol nitrate. 4-methylbenzenesulphonate), CEDO 8901 (1-(4-nitrophenoxy)-2, 3-propanediol dinitrate), and CEDO 8956 (1,4-(*trans*)-di(hydroxymethyl)cyclohexane dinitrate).

All CEDO compounds were synthesized by Cedona Pharmaceuticals, Haarlem, The Netherlands, by standard methods as described elsewhere (European Patent Application EP 0 35 9335 A2) and dissolved in Intralipid 10% (Kabi Vitrum, Stockholm, Sweden) in a concentration of 1 mg ml^{-1}. The compounds were made available by courtesy of Drs. J. Bron and J.F. van der Werf. GTN (Nitro-POHL, G. Pohl-Boskamp GmbH, Hohenlockstedt, Germany) was used in an aqueous solution of 1 mg ml^{-1}.

Statistical analysis

All data are presented as the mean ± s.e.mean. The significance of the effects of the drugs have been evaluated by comparing the changes from baseline induced by the drugs to the changes from baseline during infusion of the solvent, using analysis of variance. Significance was accepted for $P < 0.05$. A

Table 1 Cardiovascular effects of solvent (Intralipid 10%) in 7 conscious pigs with a normal coronary circulation (control) and in 9 conscious pigs with left ventricular dysfunction (LVD) secondary to a chronic occlusion of the left circumflex coronary artery

			Intralipid (ml min^{-1}) *for 10 min*				
		Baseline	*0.05*	*0.2*	*0.5*	*1.0*	*2.0*
CO	Control	2.71 ± 0.11	2.69 ± 0.10	2.71 ± 0.11	2.71 ± 0.12		2.70 ± 0.14
	LVD	2.27 ± 0.15*	2.26 ± 0.15	2.27 ± 0.15	2.27 ± 0.14	2.25 ± 0.14	2.27 ± 0.15
HR	Control	128 ± 4	129 ± 5	127 ± 3	131 ± 4		129 ± 5
	LVD	115 ± 6	114 ± 7	113 ± 5	113 ± 6	113 ± 6	114 ± 6
SV	Control	21.3 ± 0.9	21.1 ± 1.2	21.2 ± 0.7	20.8 ± 1.2		21.0 ± 1.3
	LVD	20.1 ± 1.2	20.1 ± 1.3	20.2 ± 1.2	20.3 ± 1.1	20.2 ± 1.2	20.0 ± 1.1
SAP	Control	114 ± 4	114 ± 4	114 ± 4	115 ± 4		114 ± 4
	LVD	118 ± 4	117 ± 3	117 ± 4	116 ± 4	117 ± 4	119 ± 4
MAP	Control	98 ± 3	99 ± 4	98 ± 3	99 ± 3		99 ± 3
	LVD	95 ± 3	94 ± 3	96 ± 3	95 ± 4	96 ± 4	98 ± 4
DAP	Control	80 ± 4	81 ± 4	79 ± 3	82 ± 4		83 ± 3
	LVD	77 ± 3	76 ± 2	78 ± 3	77 ± 4	79 ± 3	81 ± 4
SVR	Control	36 ± 2	37 ± 2	37 ± 2	37 ± 3		37 ± 3
	LVD	43 ± 2*	42 ± 2	43 ± 2	43 ± 2	44 ± 2	44 ± 2
LV$dP/dt_{max}$	Control	3310 ± 310	3280 ± 340	3380 ± 330	3470 ± 360		3460 ± 360
	LVD	2800 ± 230*	2690 ± 230	2810 ± 220	2860 ± 260	2840 ± 250	2850 ± 230
LVEDP	Control	4.5 ± 0.3	4.2 ± 0.5	4.3 ± 0.4	4.2 ± 0.5		4.5 ± 0.4
	LVD	14.1 ± 1.4*	14.4 ± 1.5	14.0 ± 1.5	13.9 ± 1.6	13.8 ± 1.6	14.6 ± 1.6

CO = cardiac output (l min^{-1}); HR = heart rate (beats min^{-1}); SV = stroke volume (ml); SAP = systolic arterial blood pressure (mmHg); MAP = mean arterial blood pressure (mmHg); DAP = diastolic arterial blood pressure (mmHg); SVR = systemic vascular resistance (mmHg min l^{-1}); LV$dP/dt_{max}$ = maximum rate of rise of left ventricular pressure (mmHg s^{-1}); LVEDP = left ventricular end-diastolic pressure (mmHg); Data have been presented as mean ± s.e.mean; * $P < 0.05$ vs baseline data of pigs with intact coronary circulation (control).

Bonferroni correction was used because of comparison for multiple measurements. Statistical significance of the regression lines was determined by calculating the slopes of the regression lines of the individual animals and comparing the mean slope of each group of animals by unpaired Student's *t* test.

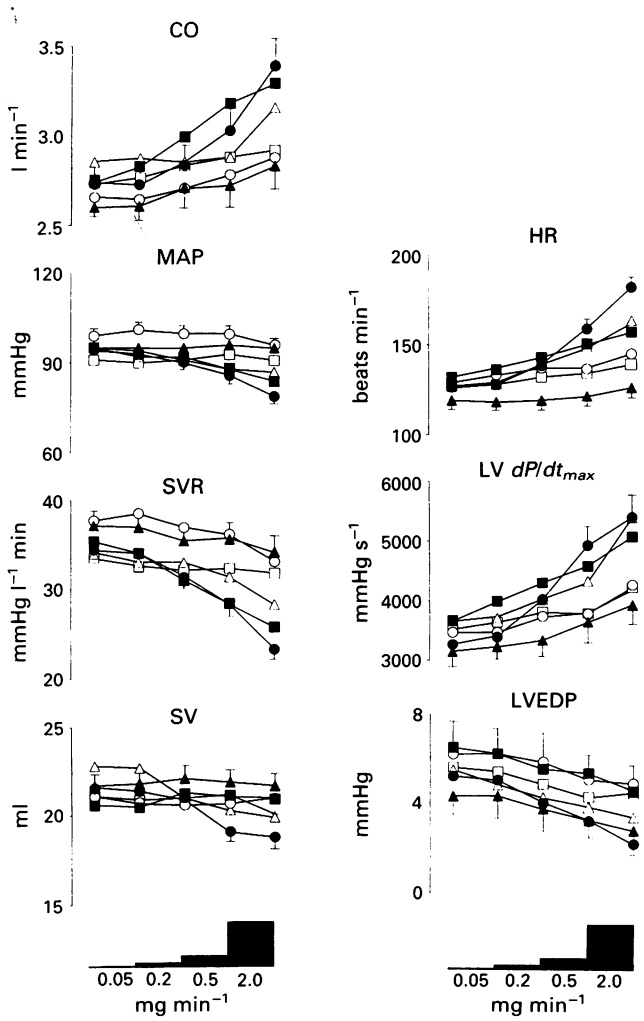

Results

Systemic haemodynamics during infusion of Intralipid (10%) in normal conscious pigs and in conscious pigs with chronic left ventricular dysfunction

Table 1 illustrates that infusion of Intralipid 10% did not lead to significant changes in any of the systemic haemodynamic parameters in the normal conscious pigs and in the animals with chronic left ventricular dysfunction. The table also shows that significant differences existed between the baseline values of both groups of animals. Similar to earlier reported findings (Van der Giessen *et al.* 1989; Van Woerkens *et al.*, 1991), we observed that occlusion of the left circumflex coronary artery had no effect on mean arterial blood pressure, because peripheral vasoconstriction counterbalanced the 20% decrease in cardiac output but that LV$dP/dt_{max}$ was 20% lower and left ventricular end-diastolic pressure had tripled in the animals with the occluded left circumflex coronary artery.

Systemic haemodynamic effects of nitroglycerin and the 5 novel nitrate-esters in normal conscious pigs

Intravenous administration of GTN caused a dose dependent increase in cardiac output (24 ± 5%, $P < 0.05$, Figure 1). Since the 43 ± 3% increase in heart rate exceeded the percentage increase in cardiac output it is obvious that stroke volume decreased ($P < 0.05$). In spite of the increase in cardiac output, mean arterial blood pressure decreased gradually. The changes in stroke volume and mean arterial pressure were only significant during the highest two infusion rates. Systemic vascular resistance had already decreased significantly after

Figure 1 Systemic haemodynamic effects of nitroglycerin (GTN) (●) and 5 novel nitrate-esters CEDO 8811 (□), CEDO 8816 (△), CEDO 8834 (○), CEDO 8901 (▲) and CEDO 8956 (■) in conscious pigs (23–25 kg) with an intact coronary circulation. CO = cardiac output; HR = heart ' rate; MAP = mean arterial blood pressure; LV$dP/dt_{max}$ = maximal rate of rise of left ventricular pressure; SVR = systemic vascular resistance; LVEDP = left ventricular end-diastolic pressure; SV = stroke volume. For reasons of clarity most of the bars for the s.e.mean and the levels of significance have been omitted in the figure (for details see the text). Data are the mean of 7 observations. The bars below the graphs depict the dose of the compounds in mg min^{-1}.

infusion of the second dose. LV$dP/dt_{max}$ increased dose-dependently. At each dose the increase in LV$dP/dt_{max}$ (5 ± 3%, 23 ± 4%, 49 ± 7% and 63 ± 4%, respectively) was larger than the increase in heart rate (1 ± 1%, 9 ± 2%, 26 ± 2% and 43 ± 3%, respectively). Left ventricular end-diastolic pressure decreased after infusion of the second dose and was further lowered during infusion of the highest dose.

No adverse reactions were observed after administration of any of the CEDO compounds. From these novel compounds, CEDO 8811, CEDO 8834 and CEDO 8901 were the least active as cardiac output increased only at the highest dose (by 7 ± 2%, 8 ± 2% and 9 ± 2%, respectively, all $P < 0.05$). Mean arterial blood pressure did not change during infusion of these compounds. Figure 1 also shows that the other haemodynamic parameters changed only moderately. With all three compounds the increases in LV$dP/dt_{max}$ (21 ± 7%, 20 ± 5% and 25 ± 3% after the highest dose, respectively, all $P < 0.05$) were larger than those in heart rate (12 ± 4%, 10 ± 2% and 6 ± 4% after the highest dose, respectively). Left ventricular end-diastolic pressure decreased slightly during the last two infusion steps.

CEDO 8816 was a slightly more potent arterial and venodilator than the three other CEDO compounds as systemic vascular resistance started to decrease (by 7 ± 3%, $P < 0.05$) during infusion of 0.5 mg min^{-1} and had decreased by 16 ± 4% ($P < 0.05$) after infusion of the highest dose. Left ventricular end-diastolic pressure had already decreased significantly during infusion of 0.2 mg min^{-1}. Stroke volume decreased (8 ± 2%, 12 ± 4% and 12 ± 2% after 0.2, 0.5 and 2.0 mg min^{-1}, respectively, $P < 0.05$), despite the reduction in afterload and the moderate positive inotropic effect of CEDO 8816 (reflected by a 46 ± 8% increase in LV$dP/dt_{max}$ against only a 27 ± 5% increase in heart rate at the highest dose). The fall in stroke volume was, however, fully compensated by the increase in heart rate (9 ± 1%, 16 ± 4% and 27 ± 5%, respectively). Consequently, cardiac output increased slightly (11 ± 3%, $P < 0.05$) at the highest dose.

CEDO 8956 caused dose-dependent increases in cardiac output of 9 ± 2%, 16 ± 2% and 20 ± 2% (all $P < 0.05$) during infusion of 0.2, 0.5 and 2.0 mg min^{-1}, respectively (Figure 1). The increases in cardiac output were secondary to the increases in heart rate, which were 9 ± 5%, 14 ± 4% and 20 ± 5%, respectively. At variance with the observations made during infusion of GTN, there were no decreases in stroke volume. Mean arterial blood pressure decreased by 7 ± 2% and 11 ± 2% during infusion of 0.5 and 2.0 mg min^{-1}, respectively. Systemic vascular resistance had already decreased by 12 ± 2% ($P < 0.05$) during infusion of 0.2 mg min^{-1}. During the highest infusion rate there was a further decrease (27 ± 1%, $P < 0.05$). Left ventricular end-diastolic pressure started to decrease during infusion of 0.2 mg min^{-1} (19 ± 5%, $P < 0.05$) and further decreased by 33 ± 5% ($P < 0.05$) during infusion of 2.0 mg min^{-1}. LV$dP/dt_{max}$ started to increase significantly during infusion 0.2 mg min^{-1} (17 ± 1%, $P < 0.05$). With the two higher infusion rates, the increments in LV$dP/dt_{max}$ were 25 ± 2% and 38 ± 4%, respectively ($P < 0.05$).

Effects of nitroglycerin and CEDO 8956 on systemic haemodynamics in conscious pigs with chronic left ventricular dysfunction

In these animals cardiac output increased dose-dependently during infusion of GTN (Table 2). Similar to the animals with normal left ventricular function, the increase in cardiac output was due to an increase in heart rate. The increase in heart rate (53 ± 8%) exceeded the increase in cardiac output (36 ± 9%) and stroke volume must therefore have decreased. Mean arterial blood pressure started to decrease during infusion of 0.5 mg min^{-1} and had fallen by 12 ± 2 mmHg ($P < 0.05$) at the end of the highest infusion rate. Because cardiac output increased, the decrease in arterial blood pressure must have been caused by arterial vasodilatation. Systemic vascular resistance was lowered by 8 ± 2% ($P < 0.05$) during infusion of 0.2 mg min^{-1}, and had fallen by 35 ± 3% after the last dose. LV$dP/dt_{max}$ increased dose-dependently by up to 48 ± 6% ($P < 0.05$), while left ventricular end-diastolic pressure was gradually lowered from 11.2 ± 1.0 mmHg to 5.6 ± 1.2 mmHg ($P < 0.05$).

The most striking difference between CEDO 8956 and GTN was that mean arterial blood pressure was unaffected during infusion of the former, whereas it decreased with GTN. Since cardiac output increased dose-dependently by up to 18% after CEDO 8956, we can calculate that the decrease in systemic vascular resistance (16%) was less than that observed during infusion of GTN (35%). As with GTN, an increase in heart rate was responsible for the increase in cardiac output.

Table 2 Cardiovascular effects of nitroglycerin (GTN) and CEDO 8956 (CED) in 10 conscious pigs with left ventricular dysfunction secondary to occlusion of the left circumflex coronary artery

			Infusions of GTN or CEDO 8956 for 10 min (mg min^{-1})				
		Baseline	*0.05*	*0.2*	*0.5*	*1.0*	*2.0*
CO	GTN	2.12 ± 0.13	2.12 ± 0.12	2.24 ± 0.12*	2.45 ± 0.12*	2.61 ± 0.12*	2.84 ± 0.19*
	CED	2.32 ± 0.15	2.32 ± 0.15	2.38 ± 0.15	2.50 ± 0.14*	2.61 ± 0.16*	2.77 ± 0.19*
HR	GTN	117 ± 8	120 ± 8	127 ± 7*	139 ± 8*	157 ± 6*	174 ± 6*
	CED	116 ± 7	118 ± 8	124 ± 8	135 ± 8*	142 ± 7*†	150 ± 8*†
SV	GTN	18.7 ± 1.3	18.2 ± 1.3	18.0 ± 1.2	18.2 ± 1.5	16.9 ± 1.1	16.7 ± 1.3
	CED	20.5 ± 1.3	20.1 ± 1.4	19.6 ± 1.3	18.8 ± 1.2	18.5 ± 1.1	19.2 ± 1.1
SAP	GTN	112 ± 4	112 ± 4	109 ± 4	104 ± 3	101 ± 2*	99 ± 3*
	CED	112 ± 4	111 ± 4	106 ± 3*	104 ± 3*	106 ± 4	107 ± 4*†
MAP	GTN	92 ± 2	92 ± 3	90 ± 3	86 ± 2*	82 ± 2*	80 ± 3*
	CED	93 ± 3	91 ± 3	89 ± 3	88 ± 3	90 ± 3†	90 ± 4†
DAP	GTN	72 ± 2	75 ± 3	74 ± 3	71 ± 2	69 ± 2*	68 ± 2
	CED	74 ± 3	75 ± 3	73 ± 3	76 ± 3	76 ± 3†	78 ± 4†
SVR	GTN	44.8 ± 2.4	44.7 ± 2.7	41.1 ± 2.3*	36.0 ± 1.8*	31.9 ± 1.3*	28.7 ± 1.2*
	CED	41.0 ± 1.9	40.4 ± 1.8	38.2 ± 1.6*	35.9 ± 1.5*	35.2 ± 1.7*†	34.0 ± 2.0*†
LV$dP/dt_{max}$	GTN	2530 ± 240	2600 ± 240	2740 ± 240	3080 ± 290*	3300 ± 320*	3700 ± 350*
	CED	2620 ± 260	2620 ± 260	2950 ± 290	2950 ± 290*	3310 ± 380*	3440 ± 410*
LVEDP	GTN	11.2 ± 1.0	10.9 ± 1.0	9.9 ± 0.8	8.6 ± 0.8*	6.3 ± 1.0*	5.6 ± 1.2*
	CED	12.4 ± 1.3	11.7 ± 1.4*	10.9 ± 1.5*	9.7 ± 1.7*	8.5 ± 1.7*	7.6 ± 1.7*

CO = cardiac output (l min^{-1}); HR = heart rate (beats min^{-1}); SV = stroke volume (ml); SAP = systolic arterial blood pressure (mmHg); MAP = mean arterial blood pressure (mmHg); DAP = diastolic arterial blood pressure (mmHg); SVR = systemic vascular resistance (mmHg min l^{-1}); LV$dP/dt_{max}$ = maximal rate of rise of left ventricular pressure (mmHg s^{-1}); LVEDP = left ventricular end-diastolic pressure (mmHg); Data have been presented as mean ± s.e.mean; * change from baseline statistically different ($P < 0.05$) from solvent-treated animals. †CEDO 8956-induced change from baseline statistically different ($P < 0.05$) from GTN-induced change.

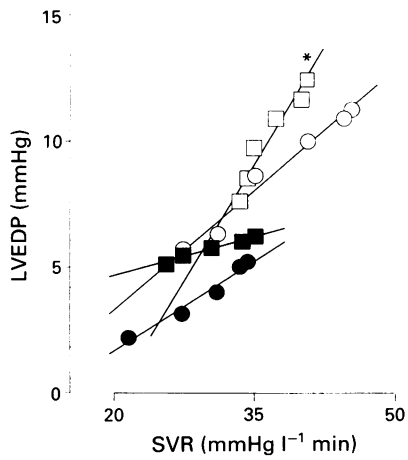

Figure 2 Relation between systemic vascular resistance (SVR) and left ventricular end-diastolic pressure (LVEDP) during incremental infusion rates of nitroglycerin (GTN) (●) and CEDO 8956 (■) in normal pigs and during incremental infusion rates of GTN (○) and CEDO 8956 (□) in conscious pigs with chronic left ventricular dysfunction. The slope of the CEDO 8956 regression line was significantly steeper in the animals with left ventricular dysfunction than in the normal animals (* $P < 0.05$).

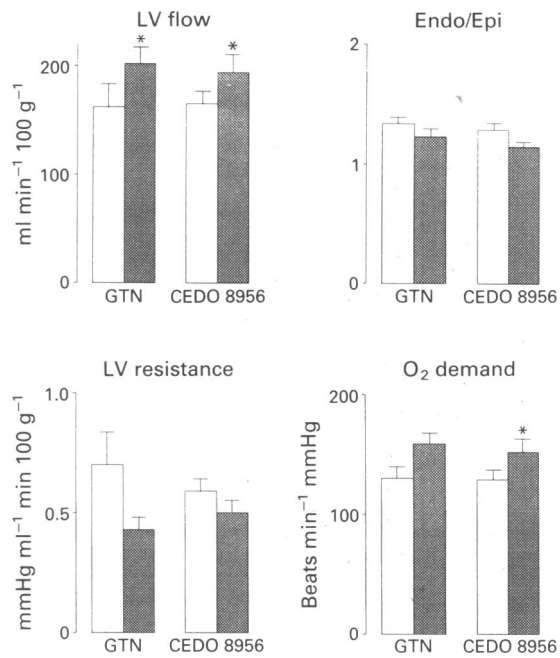

Figure 3 Transmural blood flow (LV flow) and its distribution (Endo/Epi), the coronary vascular resistance (LV resistance) remote from the site of infarction and O_2 demand in conscious pigs with a 4 week occlusion of the left circumflex coronary artery. Data were obtained at Baseline (□) and after a 10 min infusion of nitroglycerin (GTN) and CEDO 8956 at a rate of $46.1 \pm 1.5\,\mu g\,kg^{-1}\,min^{-1}$ (▨). * $P < 0.05$ vs baseline.

The increase in heart rate was significantly less with CEDO 8956 than with GTN. $LVdP/dt_{max}$ also increased (up to 30%), and like GTN, the increments were parallel to those in heart rate. Left ventricular end-diastolic pressure, however, decreased to the same degree as with GTN during the infusions of CEDO 8956.

Figure 2 illustrates the relation between the changes in systemic vascular resistance and in left ventricular end-diastolic pressure for the different experimental conditions. The figure shows that the venodilator capacity of CEDO 8956 was increased in the pigs with chronic left ventricular dysfunction as compared to the normal pigs.

Effects of nitroglycerin and CEDO 8956 on myocardial blood flow in animals with chronic left ventricular dysfunction

Because of the limited number of available isotopes, regional flow data could only be obtained at baseline and after administration of a single dose of each of the two drugs. The infusion rate of $1\,mg\,min^{-1}$ was chosen for both GTN and CEDO 8956. There were no differences in the baseline values of the two drugs (Figure 3). Myocardial O_2 demand, calculated as the product of heart rate and left ventricular systolic pressure, increased similarly during infusion of both GTN and CEDO 8956. Both GTN and CEDO 8956 increased transmural perfusion of the myocardium nourished by the non-occluded left anterior descending coronary artery. There was a modest trend towards a preferential increase of perfusion of the subepicardial layers, but the decreases in the ratio of the normalized endocardial and epicardial blood flows (endo/epi-ratio) did not reach levels of statistical significance with either drug. The decrease in the coronary vascular resistance was more pronounced with GTN than with CEDO 8956 (Figure 3). The perfusion of the central part of the myocardium in the distribution of the occluded left circumflex coronary artery increased significantly during infusion of GTN (from $25 \pm 4\,ml\,min^{-1}\ 100\,g^{-1}$ to $39 \pm 7\,ml\,min^{-1}\ 100\,g^{-1}$, $P < 0.05$), but not during that of CEDO 8956 (from $30 \pm 5\,ml\,min^{-1}\ 100\,g^{-1}$ to $36 \pm 4\,ml\,min^{-1}\ 100\,g^{-1}$).

Right ventricular blood flow increased more during administration of CEDO 8956 (from $105 \pm 9\,ml\,min^{-1}\ 100\,g^{-1}$ to $153 \pm 17\,ml\,min^{-1}\ 100\,g^{-1}$, $P < 0.05$) than during infusion of GTN (from $106 \pm 21\,ml\,min^{-1}$ to $136 \pm 13\,ml\,min^{-1}\ 100\,g^{-1}$). This difference was caused by the different effects of the drugs on arterial perfusion pressure as the decreases in coronary vascular resistance were very similar with both compounds (from $0.97 \pm 0.11\,mmHg\,min\,ml^{-1}\ 100\,g$ to $0.67 \pm 0.07\,mmHg\,min\,ml^{-1}\ 100\,g$ for GTN and from $0.96 \pm 0.10\,mmHg\,min\,ml^{-1}\ 100\,g$ to $0.67 \pm 0.09\,mmHg\ min\,ml^{-1}\ 100\,g$ for CEDO 8956).

Effects of nitroglycerin and CEDO 8956 on peripheral organ perfusion in conscious pigs with chronic left ventricular dysfunction

Infusion of $1\,mg\,min^{-1}$ of GTN resulted in significant increases in blood flow to the adrenals and the kidneys (Table 3). Calculation of the regional vascular resistances revealed that GTN induced vasodilatation in the vascular beds perfusing the brain, kidneys, adrenals and spleen but that with this dose no effect was observed in skeletal muscle, skin and liver (hepatic artery circulation only) (Table 4). CEDO 8956 was less potent at this dose in lowering systemic vascular resistance than GTN, which explains that with CEDO 8956 only a significant reduction in the resistance of the vascular bed of the adrenals was observed and that the changes in the cerebral and renal vascular resistances did not reach a level of statistical significance.

Discussion

GTN is an effective therapeutic agent in the treatment of a number of cardiovascular disorders including myocardial ischaemia, myocardial infarction and congestive heart failure (Mason *et al.*, 1971; Flaherty *et al.*, 1975; Flaherty, 1983; Packer, 1983). The principal mechanism is a direct relaxation of vascular smooth muscle and a number of investigators believed that the effect on the venous capacitance vessels was more pronounced than on the arterial resistance vessels, while others have reported less marked differences. The present study as far as performed in normal conscious pigs demonstrates a marked reduction in both left ventricular end-

Table 3 Effects of 10 min intravenous infusions of nitroglycerin (GTN) and CEDO 8956 at a rate of 1 mg min^{-1} on regional blood flows in 10 conscious pigs with left ventricular dysfunction secondary to chronic occlusion of the left circumflex coronary artery

	Baseline	*GTN*	*Baseline*	*CEDO 89*
Brain	75 ± 5	82 ± 2	71 ± 2	78 ± 4
Kidneys	421 ± 32	496 ± 40*†	424 ± 28	437 ± 28
Liver	22 ± 5	24 ± 6	22 ± 4	23 ± 5
Spleen	275 ± 22	299 ± 32	273 ± 26	228 ± 23
Adrenals	119 ± 12	219 ± 17*†	144 ± 18	166 ± 13
Stomach	47 ± 6	52 ± 7	50 ± 8	50 ± 10
Small intestine	52 ± 5	52 ± 3	50 ± 5	55 ± 7
Skin (abdomen)	6.7 ± 0.9	6.4 ± 1.1	6.9 ± 0.8	5.5 ± 0.6
Muscle (gluteus maximus)	4.9 ± 1.3	4.4 ± 0.6	3.9 ± 0.3	4.9 ± 0.7
Muscle (erector spinae)	3.8 ± 0.5	3.0 ± 0.4	3.3 ± 0.4	4.1 ± 1.1

Blood flows are expressed in ml min^{-1} 100 g^{-1} and are shown as mean ± s.e.mean. * $P < 0.05$ vs baseline; † $P < 0.05$ for GTN-induced change from baseline vs CEDO 8956-induced change from baseline.

Table 4 Effects of 10 min intravenous infusions of nitroglycerin (GTN) and CEDO 8956 at a rate of 1 mg min^{-1} on regional vascular resistances in 10 conscious pigs with left ventricular dysfunction secondary to a chronic occlusion of the left circumflex coronary artery

	Baseline	*GTN*	*Baseline*	*CEDO 895*
Brain	1.26 ± 0.09	1.01 ± 0.03*†	1.31 ± 0.05	1.17 ± 0.07
Kidneys	0.23 ± 0.02	0.18 ± 0.02*†	0.23 ± 0.02	0.21 ± 0.02
Liver	8.8 ± 3.1	6.9 ± 2.1	6.5 ± 1.7	11.1 ± 6.2
Spleen	0.35 ± 0.03	0.32 ± 0.05†	0.36 ± 0.03	0.43 ± 0.05
Adrenals	0.86 ± 0.10	0.40 ± 0.04*†	0.74 ± 0.09	0.57 ± 0.05*
Stomach	2.2 ± 0.3	1.8 ± 0.2	2.2 ± 0.3	2.1 ± 0.2
Small intestine	1.9 ± 0.2	1.6 ± 0.1	2.1 ± 0.3	1.9 ± 0.3
Skin (abdomen)	17 ± 3	17 ± 3	15 ± 2	18 ± 2
Muscle (erector spinae)	27 ± 3	31 ± 4	32 ± 4	30 ± 4

Vascular resistances are expressed in mmHg min ml^{-1} 100 g and are reported as mean ± s.e.mean. * $P < 0.05$ vs baseline; † $P < 0.05$ for GTN-induced change from baseline vs CEDO 8956-induced change from baseline.

diastolic pressure and systemic vascular resisance during infusion of GTN. When GTN was administered in animals with chronic left ventricular dysfunction the effects on left ventricular end-diastolic pressure and systemic vascular resistance were not different from those in the normal animals (Figure 2).

Of the new compounds, CEDO 8956 demonstrated a cardiovascular profile similar to that of GTN, although in the normal conscious pigs, the effect on left ventricular filling pressure was less pronounced than during GTN infusion. It could be argued that the slightly smaller increase in heart rate during infusion of CEDO 8956 was a contributing factor to this observation, but earlier studies with a number of dihydropyridine derivatives have shown that in the range of the heart rates, reported in this study, the effect of heart rate on left ventricular end-diastolic pressure is minimal (Duncker *et al.*, 1988). In the animals with left ventricular dysfunction, however, CEDO 8956 lowered left ventricular end-diastolic pressure as effectively as GTN (Table 2), while the effect on the systemic vasculature remained comparable to that induced in the normal animals (Figure 2). Both compounds increased cardiac output by an increase in heart rate rather than in stroke volume, which would be more desirable. One must keep in mind, however, that the left ventricular filling pressures in the animals with left ventricular dysfunction, although elevated were not extremely high. It is very likely that reduction of higher left ventricular filling pressure would result in a more favourable effect on stroke volume. Nevertheless, an increase in heart rate, which is a common observation with all vasodilators, increases the myocardial oxygen demand and will, in particular in hypertrophied hearts, decrease coronary flow reserve (Hoffman, 1990). Adjuvant treatment with a specific bradycardic agent may then be attractive to unload the heart without reflex-mediated tachycardia and to increase stroke volume and coronary flow reserve (Verdouw *et al.*, 1981; Canty *et al.*, 1990). The finding that CEDO 8956 did not lower mean arterial blood pressure is not necessarily a disadvantage as Cruickshank *et al.* (1987) have shown that lowering high arterial blood pressure too much may be harmful.

Contrary to earlier reported observations in dogs (Capurro *et al.*, 1977), nitroglycerin has no beneficial effect on total coronary blood flow and its distribution within the myocardium of the pig after an acute coronary artery occlusion (Most *et al.*, 1978). In the present study GTN increased blood flow to the myocardium remote from the distribution of the occluded left circumflex coronary artery. The increase appeared to be related to the increase in myocardial oxygen demand, estimated by the heart rate-left ventricular systolic pressure product. In contrast to dogs, pigs do not usually have a significant coronary collateral circulation, which may explain the differences in the observations made by Capurro *et al.* (1977) and Most *et al.* (1978). After chronic occlusion a substantial collateral flow has been observed in the fibrotic tissue of the porcine myocardium, the magnitude of which can be altered by pharmacological interventions (Van der Giessen *et al.*, 1990a). In the present study GTN also increased the flow to the fibrotic segment. It is questionable whether this increase in flow has any clinical significance as we have not been able to recruit any function by inotropic stimulation (dobutamine infusion) in this infarcted segment (unpublished observation). CEDO 8956, albeit less, also showed an increase in flow to the normal segment. A smaller increase in the heart rate-left ventricular systolic pressure product may be an index for myocardial oxygen demand, the basis for this observation. The present data cannot be used to speculate on the effects of CEDO 8956 on myocardium which is perfused by partially occluded coronary arteries. Several studies (Macho & Vatner, 1981; Hintze & Vatner, 1983) have shown that the large epicardial vessels dilate in response to nitroglycerin. Dilatation of the stenosis, which is independent of an increase in coronary artery blood flow (Adachi *et al.*, 1987) may be a major mechanism in improving an impaired oxygen balance. The design of

the present study does not provide insight into a possible dilator effect on the large epicardial vessels by CEDO 8956.

The effects of GTN on organ blood flows other than the myocardium have only been addressed in a limited number of studies. Most of these studies are in anaesthetized animals in which GTN was administered with the aim of producing severe hypotension. Colley & Sivarajan (1984) observed that during GTN infusion in halothane-anaesthetized dogs, blood flows to the brain, kidneys, liver, gastrointestinal tract and skeletal muscle were maintained, despite a reduction of mean arterial blood pressure from 82 ± 4 mmHg to 45 ± 3 mmHg, due to a 50% decrease in systemic vascular resistance. Norlén (1988) found in methomidate-anaesthetized pigs that doses of GTN which decreased systemic vascular resistance by 28% and mean arterial blood pressure by 33%, blood flows to the heart, brain, kidneys, adrenal glands, stomach and liver (hepatic artery) were not affected, but that perfusion of the spleen had decreased by 25%. The present study differs considerably from these studies, as the dose of GTN at which regional blood flows and vascular resistances were determined, lowered mean arterial blood pressure by only 12 mmHg from its baseline of 92 mmHg. Furthermore the studies were performed in conscious animals with a lowered cardiac output due to impairment of left ventricular function. In the present study cerebral blood flow was maintained and renal blood flow increased, due to local vasodilatation (Table 4). The same dose of CEDO 8956 (1 mg min^{-1}) had no effect on mean arterial blood pressure and cardiac output increased only by 12%. The effects on the regional vascular beds were therefore less pronounced than with GTN and only the vascular resistance of the adrenals was significantly decreased.

Both GTN and CEDO 8956 lacked an effect on skeletal muscle blood flow. Our present results are in agreement with an earlier report using isosorbide-dinitrate (Leier *et al.*, 1983). On the other hand we have shown an acute improvement in skeletal muscle perfusion by the calcium channel blocker nisoldipine (Van der Giessen *et al.*, 1990b). This may be important as Creager *et al.* (1985) showed in patients with heart failure that an improvement in exercise tolerance was parallelled by an increase in fore-arm blood flow. Due to the limited number of different microspheres available, regional organ blood flow data were not studied during infusion of the Intralipid 10% solvent. In an earlier paper (Van der Giessen *et al.*, 1990b), however, we showed that peripheral organ blood flows remained unchanged in conscious pigs, when systemic haemodynamic parameters remained stable, as was the case with infusion of the solvent in this report (Table 1).

In conclusion, from the novel compounds only CEDO 8956 had a cardiovascular profile similar to that of GTN and was therefore selected for further study in the conscious animals with chronic left ventricular dysfunction. In this model, CEDO 8956 normalized the depressed cardiac output by lowering left ventricular filling pressure and systemic vascular resistance. The radioactive labelled microsphere data showed that CEDO 8956, similar to GTN, caused dilatation of the coronary vascular bed remote from the infarcted area. The observations that the preload reduction by CEDO 8956 was more pronounced when left ventricular filling pressures were elevated, and that for the same decreases in left ventricular filling pressure the increase in heart rate by CEDO 8956 was less than with GTN may be attractive for cardiac patients. The cardiovascular profile of CEDO 8956, therefore warrants further studies to investigate its potential usefulness in the clinical setting. In further studies attention should be paid to the duration of action and the development of tolerance which could attenuate the therapeutic effects.

Ms Marjo van Ee is thanked for the preparation of the manuscript. The members of staff of the Laboratory for Experimental Surgery are thanked for their assistance during surgery and the post-surgical period. Ms Sylvia Schotman is thanked for her assistance during the experiments.

References

ADACHI, H., TOMOIKE, H., NISHIJIMA, H., HAYASHI, Y., YAMADA, A. & NAKAMURA, M. (1987). Effects of verapamil and nitroglycerin on coronary and systemic hemodynamics in conscious dogs. *J. Pharmacol. Exp. Ther.*, **241**, 1072–1078.

CANTY, J.M., GIGLIA, J. & KANDATH, D. (1990). Effect of tachycardia on regional function and transmural myocardial perfusion during graded coronary pressure reduction in conscious dogs. *Circulation*, **82**, 1815–1825.

CAPURRO, N.L., KENT, K.M., SMITH, H.J., AAMODT, R. & EPSTEIN, S.E. (1977). Acute coronary occlusion: prolonged increase in collateral flow following brief administration of nitroglycerin and methoxamine. *Am. J. Cardiol.*, **39**, 679–683.

COLLEY, P.S. & SIVARAJAN, M. (1984). Regional blood flow in dogs during halothane anesthesia and controlled hypotension produced by nitroprusside or nitroglycerin. *Anesth. Analg.*, **63**, 503–510.

CREAGER, M.A., MASSIE, B.M., FAXON, D.P., FRIEDMAN, S.D., KRAMER, B.L., WEINER, D.A., RYAN, T.J., TOPIC, N. & MELIDOSSIAN, C.D. (1985). Acute and long-term effects of enalapril on the cardiovascular response to exercise and exercise tolerance in patients with congestive heart failure. *J. Am. Coll. Cardiol.*, **6**, 163–170.

CRUICKSHANK, J.M., THORP, J.M. & ZACHARIAS, F. (1987). Benefits and potential harm of lowering high blood pressure. *Lancet*, **i**, 581–583.

DUNCKER, D.J., SAXENA, P.R. & VERDOUW, P.D. (1988). Systemic haemodynamics of dihydropyridine derivatives in conscious pigs with or without propranolol. *Eur. J. Pharmacol.*, **156**, 401–409.

FLAHERTY, J.T. (1983). Comparison of intravenous nitroglycerin and sodium nitroprusside in acute myocardial infarction. *Am. J. Med.*, **74**, (suppl. 6B), 53–60.

FLAHERTY, J.T., REID, P.R., KELLY, D.T., TAYLOR, D.R., WEISFELDT, M.L. & PITT, B. (1975). Intravenous nitroglycerin in acute myocardial infarction. *Circulation*, **51**, 132–139.

HINTZE, T.H. & VATNER, S.F. (1983). Comparison of effects of nifedipine and nitroglycerin on large and small coronary arteries and cardiac function in conscious dogs. *Circ. Res.*, (suppl. 1), **52**, 139–146.

HOFFMAN, J.I.E. (1990). Autoregulation and heart rate. *Circulation*, **82**, 1880–1881.

LEIER, C.V., HUSS, P., MAGORIEN, R.D. & UNVERFERTH, D.V. (1983). Improved exercise capacity and differing arterial and venous tolerance during chronic isosorbide dinitrate therapy for congestive heart failure. *Circulation*, **67**, 817–822.

MACHO, P. & VATNER, S.F. (1981). Effects of nitroglycerin and nitroprusside on large and small coronary vessels in conscious dogs. *Circulation*, **64**, 1101–1107.

MASON, D.T., ZELIS, R. & AMSTERDAM, E.A. (1971). Actions of the nitrites on the peripheral circulation and myocardial oxygen consumption: significance in the relief of angina pectoris. *Chest*, **59**, 296–305.

MOST, A.S., WILLIAMS, D.O. & MILLARD, R.W. (1978). Acute coronary occlusion in the pig: effect of nitroglycerin on regional myocardial blood flow. *Am. J. Cardiol.*, **42**, 947–953.

NORLÉN, K. (1988). Central and regional haemodynamics during controlled hypotension produced by adenosine, sodium nitroprusside and nitroglycerin. *Br. J. Anaesth.*, **61**, 186–193.

PACKER, M. (1983). New perspectives on therapeutic application of nitrates as vasodilator agents for severe chronic heart failure. *Am. J. Med.*, **74**, (suppl. 6B), 61–72.

VAN DER GIESSEN, W.J., DUNCKER, D.J., SAXENA, P.R. & VERDOUW, P.D. (1990a). Nimodipine has no effect on the cerebral circulation in conscious pigs, despite an increase in cardiac output. *Br. J. Pharmacol.*, **100**, 277–282.

VAN DER GIESSEN, W.J., VAN WOERKENS, L.J., DUNCKER, D.J., ROELANDT, J.R.T.C. & VERDOUW, P.D. (1989). The acute hemodynamic effects of nisoldipine and pimobendan in conscious pigs with chronic heart failure. *J. Cardiovasc. Pharmacol.*, **14**, 653–658.

VAN DER GIESSEN, W.J., VAN WOERKENS, L.J., SAXENA, P.R., ROELANDT, J.R.T.C. & VERDOUW, P.D. (1990b). Nisoldipine improves blood flow to skeletal muscles in conscious pigs with chronic heart failure. *Eur. Heart J.*, **11**, 552–559.

VAN WOERKENS, L.J., SCHOTMAN, S.N., VAN DER GIESSEN, W.J. & VERDOUW, P.D. (1991). Cardiovascular effects of elgodipine in conscious pigs with a normal coronary circulation and in conscious pigs with a healed myocardial infarction. *J. Cardiovasc. Pharmacol.*, (in press).

VERDOUW, P.D., HARTOG, J.M. & RUTTEMAN, A.M. (1981). Systemic and regional myocardial responses to AR-L 115 BS, a positive inotropic imidazo-pyridine, in the absence or in the presence of the bradycardiac action of alinidine. *Basic Res. Cardiol.*, **76**, 328–343.

(Received February 13, 1991
Revised April 8, 1991
Accepted April 26, 1991)

Br. J. Pharmacol. (1991), **104**, 15–20

Effect of acute and subchronic nicotine treatment on cortical efflux of [^{3}H]-D-aspartate and endogenous GABA in freely moving guinea-pigs

[1]Lorenzo Beani, Sergio Tanganelli, Tiziana Antonelli, Luca Ferraro, Michele Morari, Piero Spalluto, *Agneta Nordberg & Clementina Bianchi

Department of Pharmacology, University of Ferrara, Via Fossato di Mortara 23, 44100 Ferrara, Italy and *Department of Pharmacology, University of Uppsala, Sweden

1 The [^{3}H]-D-aspartate preloading of the parietal cortex of freely moving guinea-pigs equipped with epidural cups makes it possible to investigate drug effects on the efflux of this radiolabel, assumed as a marker of the glutamatergic structures underlying the cup. In the same model, the efflux of [^{3}H]-γ-aminobutyric acid ([^{3}H]-GABA) and endogenous GABA can be measured.

2 Nicotine, 0.9–3.6 mg kg^{-1}, s.c., or 3–5 μg, i.c.v., increased the efflux of [^{3}H]-D-aspartate but reduced that of GABA.

3 These effects were mediated through mecamylamine-sensitive receptors but the ganglionic blocking agent was devoid of any primary activity.

4 The inhibition of GABA efflux induced by nicotine 3.6 mg kg^{-1}, s.c., was abolished by methysergide 2 mg kg^{-1}, i.p. and was reduced by naloxone 3 mg kg^{-1}, i.p. pretreatment, suggesting the involvement of tryptaminergic and opioid systems. In contrast, muscarinic and catecholamine antagonists were ineffective.

5 Chronic treatment with nicotine (3.6 mg kg^{-1}, twice daily for 16 days) reduced the facilitatory effect of [^{3}H]-D-aspartate and abolished the inhibition of endogenous GABA efflux.

6 A slight increase in the number of nicotinic binding sites (by use of [^{3}H]-nicotine as ligand) was found in the neocortex of chronically treated guinea-pigs.

7 The higher degree of tolerance to chronic nicotine treatment shown by GABA as compared with [^{3}H]-D-aspartate efflux suggests that adaptative changes of the inhibitory neuronal pools prevail. This may contribute to the reinforcing and addictive properties of nicotine.

Keywords: Nicotine; guinea-pig cortex; mecamylamine; methysergide; naloxone; GABA efflux; D-aspartate efflux

Introduction

Nicotine is known to increase the firing rate of many neuronal pools and to enhance the release of a number of putative neurotransmitters, by interacting with receptors located on the cell bodies and/or nerve terminals (see Nordberg *et al.*, 1989). However, only a few investigations have been devoted to analyzing effects of nicotine on the amino acid transmitters. To date, the increased firing rate of the cerebellar glutamatergic cells (de la Garza *et al.*, 1987a), as well as enhanced glutamate release from n. accumbens slices (Gongwer *et al.*, 1987) by nicotine, have been reported. Conversely, the available data regarding γ-aminobutyric acid (GABA) are conflicting. Behavioural (Austin *et al.*, 1988) and electrophysiological studies *in vivo* (de la Garza *et al.*, 1989b) and *in vitro* (Freund *et al.*, 1988) suggest that nicotine inhibits the GABAergic structures, possibly by releasing dopamine (Austin *et al.*, 1988) or endogenous opioids (Brennan *et al.*, 1980; Dewar *et al.*, 1987). On the other hand, Limberger *et al.* (1986) and Wonnacott *et al.* (1987, 1989) reported that nicotine increased GABA efflux from caudatal slices and hippocampal synaptosomes, whereas Gongwer *et al.* (1987) did not find any effect on n. accumbens slices. These discrepancies may be due to the different brain areas studied and to the more or less integrated models employed. Since direct measurements of nicotine-induced changes of glutamate and GABA release *in vivo* are lacking, it was considered of interest to study nicotine effects on [^{3}H]-D-aspartate (assumed as a marker of endogenous glutamate) and on endogenous GABA overflow from the cerebral cortex of freely moving guinea-pigs, equipped with epidural cups.

The data here summarized demonstrate that nicotine, at doses considerably higher than those affecting acetylcholine (ACh) release (Nordberg *et al.*, 1989), increases the efflux of [^{3}H]-D-aspartate but inhibits that of GABA, through mecamylamine-sensitive receptors. These effects are reduced by chronic drug treatment, particularly as regards nicotine inhibition of GABA overflow. A preliminary account of this investigation has been published (Beani *et al.*, 1989).

Method

Guinea-pigs of either sex weighing 400–500 g were used. The animals were kept under a 12 h light/dark cycle and had free access to food and water. Implantation of the epidural cup on the left or right parietal cortex was performed under nembutal (30 mg kg^{-1}, i.p.) plus morphine (2 mg kg^{-1}, i.p.) anaesthesia, as previously described (Beani *et al.*, 1968; Beani & Bianchi, 1970). In some animals an intracerebroventricular guide cannula was also placed on the side contralateral to the cup to perform i.c.v. injections. Two days after surgery the animals were used for the release experiments.

[^{3}H]-D-aspartate efflux

Preliminary trials were carried out by placing a saline solution of [^{3}H]-D-aspartate (final concentration 0.6 μmol l^{-1}, specific activity 13.5 Ci mmol^{-1}) into the epidural cup for 5 h, in order to load the underlying cortex and to study drug effects over the washout profile curve (Beani *et al.*, 1989). Subsequently, with the aim of increasing the radiolabel uptake and efflux, the following procedure was applied: at the beginning, 0.4 ml of KCl 50 mmol l^{-1} was placed into the cup for 30 min; then, 0.4 ml of Krebs solution containing [^{3}H]-D-aspartate

[1] Author for correspondence.

0.3 μmol l^{-1} was kept in contact with the cortex for 4 h. After repeated and careful washing, 0.4 ml of normal Krebs solution was placed into the cup and renewed every 15 min. Drug treatment was performed after 4 collection periods of 15 min each, i.e., when the washout curve was levelling off to almost steady values.

The [^{3}H]-D-aspartate content of the samples (added to the scintillation liquid) was counted with a beta spectrometer (Beckman LS 1800). Some samples were run through a Dowex column CH_3COO^- form (Gaitonde, 1973), and eluted with CH_3COOH, 2 mol l^{-1}, so as to establish that their radioactivity was associated with [^{3}H]-D-aspartate standards. In addition, the amounts of [^{3}H]-D-aspartate present at the different depths of the normal and KCl-pretreated cortex were measured. After the animals were killed, the disk (3 mm diameter) of the whole cortex underlying the cup was excised immediately before starting the washout curve. Slices 400 μm thick were cut along a plane parallel to the cortical surface, dissolved in protosol and counted for their radioactivity.

GABA efflux

To study the efflux of endogenous GABA, 0.4 ml of Krebs solution containing ethanolamine-*O*-sulphate 2 mmol l^{-1} (to inhibit GABA metabolism, Beani *et al.*, 1988) was placed in the cup and renewed every 30 min for 3–4 h. The GABA content of the samples was measured with the GC-MS technique as detailed previously (Beani *et al.*, 1988).

Since the analysis of nicotine effects on glutamatergic neurones was carried out for convenience (see Discussion) by prelabelling the cortex with [^{3}H]-D-aspartate, some experiments were performed by measuring [^{3}H]-GABA outflow, so as to compare nicotine-induced changes in endogenous and ^{3}H-labelled amino acid. To this purpose, ethanolamine-*O*-sulphate pretreatment was performed as above for 3–4 h. KCl, 50 mM was then applied for 30 min, followed by [^{3}H]-GABA 0.3 μmol l^{-1} (50 Ci mmol^{-1}) preloading for 4 h. After careful washing, 0.4 ml of Krebs solution (containing ethanolamine-*O*-sulphate 2 mmol l^{-1}) was placed in the cup and renewed every 15 min. Nicotine was injected s.c. after 4 collection periods when the tritium efflux had become relatively steady. Since GABA metabolism was inhibited by ethanolamine-*O*-sulphate pretreatment, no attempt was made to ascertain to what extent the effluent tritium remained associated with GABA. In fact, under similar experimental conditions about 80%–90% of tritium proved to be represented by [^{3}H]-GABA (Young *et al.*, 1990). The samples were then measured for their tritium content as for [^{3}H]-D-aspartate (see above).

Drug treatment

In naive animals, (−)-nicotine bitartrate was injected s.c. (0.5 ml of saline solution adjusted to pH 7) 60–90 min after starting sample collection so as to determine the basal values of [^{3}H]-D-aspartate and GABA overflow as well as the drug effect on them. The time schedule of other drug treatments has been specified in Results.

Other animals were submitted to chronic nicotine treatment. The drug was injected s.c., twice daily for 16 days, at 3.6 mg kg^{-1} per day, i.e. at a dosage level 8 times higher than that previously tested for the experiments on acetylcholine release (Nordberg *et al.*, 1989). Saline-treated animals were run in parallel. On the 15th day, an epidural cup was implanted and the [^{3}H]-D-aspartate and GABA release experiments were carried out two days later. On the day of the trial, the same protocol of drug treatment as for acute nicotine experiments (injection at 9 h 00 min) was followed.

Nicotine receptor binding studies

Twelve hours after the last injection of nicotine, the animals were killed, their cerebral cortex dissected and processed for binding measurements with [^{3}H]-(−)-nicotine (7 nmol l^{-1}; specific activity 80 Ci mmol l^{-1}, Amersham, U.K.) and [^{3}H]-acetylcholine (10 nmol l^{-1}; specific activity 81 Ci mmol l^{-1}, Amersham, U.K.) in the presence of atropine 1 μmol l^{-1} (Nordberg *et al.*, 1989). The rationale for using two ligands was to label high affinity ([^{3}H]-acetylcholine) as well as additional low affinity ([^{3}H]-nicotine) binding sites (Nordberg *et al.*, 1988; Romanelli *et al.*, 1988) which have been found to be significantly increased in rats following chronic nicotine treatment at the low dose of 0.45 mg kg^{-1} but not in guinea-pigs (Nordberg *et al.*, 1989).

Drugs

Freshly prepared solutions of the following drugs were used: (−)-nicotine bitartrate, mecamylamine HCl, ethanolamine-*O*-sulphate, atropine sulphate, haloperidol and methysergide maleate (Sigma Chemical Co., St. Louis, MO, U.S.A.), naloxone (Salars, Italy). The doses are expressed as the bases. The radiochemicals and protosol were purchased from NEN.

Statistical analysis

Statistical differences were checked by ANOVA analysis followed by Dunnet's test and Newman-Keuls multiple range test, as specified in the table and figure legends.

Results

Assessment of the [^{3}H]-D-aspartate overflow method

The hypotonic KCl solution applied for 30 min gave rise to mild signs of local irritation, as shown by the appearance of occasional clones in the foreleg controlateral to the cup and by the development of spiking in the unipolar EEG, recorded from inside the cup (for technical details see Beani *et al.*, 1968). These signs rapidly disappeared soon after removal of the KCl solution. The total amount and the intracortical distribution of [^{3}H]-D-aspartate was nearly the same in KCl-treated and in control animals. However, the [^{3}H]-D-aspartate released was larger in KCl-treated than in control guinea-pigs (Table 1). In both instances, the tritium of the cup samples was exclusively represented by [^{3}H]-D-aspartate, as checked with the Dowex column separation (data not given), but its concentrations were higher and drug induced changes were more uniform in KCl-treated animals (Table 1). Interestingly, the tritium ratio between the loading solution of [^{3}H]-D-aspartate in the epidural cup (0.3 nmol ml^{-1}) and the superficial layers of the cortex 30 min after washing out the radiolabel (about 18 pmol g^{-1} see Table 1) was about 17:1, not far from the ratio between the loading solution in the microdialysis fibre and the tissue surrounding the probe as reported by Nielsen *et al.* (1989).

Table 1 Effect of KCl pretreatment on [^{3}H]-D-aspartate content per g of fresh tissue and the total efflux (150 min) from the cerebral cortex of freely moving guinea-pigs

Experimental conditions	*N° of expts.*	[^{3}H]-D-aspartate (pmol) *content*	*efflux*	*Efflux as % of content*
KCl pretreatment	5	27.8 ± 3.7[1]	1.49 ± 0.27	66 ± 2.8
No pretreatment	5	27.7 ± 4.6[1]	1.08 ± 0.32	46 ± 7.9*

* Statistically significant difference from the efflux of the non pretreated cortex, $P < 0.05$. [1] The [^{3}H]-D-aspartate content in the first (superficial), second, third and fourth (deep) slice (thickness 400 μm), calculated as percentage of the total content in the cortical disk (see methods) was 65 ± 10 (i.e., 18 pmol g^{-1}), 21 ± 3, 10 ± 3 and 3 ± 1, respectively both in normal and KCl-treated animals.

Effect of (−)-nicotine on [^{3}H-D]-aspartate

Nicotine, at doses below 0.9 mg kg^{-1}, did not change the [^{3}H]-D-aspartate overflow. Starting from 0.9 mg kg^{-1}, the drug induced a short-lasting (15–20 min) dose-related increase in the amino acid outflow, which reached the value of +70% above the basal levels at 3.6 mg kg^{-1} (Figure 1a). An evident increase in [^{3}H]-D-aspartate was also detected by injecting nicotine i.c.v. (Figure 2). The response to nicotine was prevented by local pretreatment of the cerebral cortex with tetrodotoxin 2 μmol l^{-1}, which also reduced the basal overflow by about 40% (Figure 1b). This suggests that the nerve conducted activity contributed both to the basal and to drug-induced release. The local application of the toxin did not have any discernible behavioural effect. Mecamylamine, 2 mg kg^{-1} i.p. injected 30 min before nicotine, did not itself change the profile of the washout curve but reduced the effectiveness of nicotine in a competitive fashion, shifting the dose-response curve to the right by a factor of about 2.5 (Figure 1a).

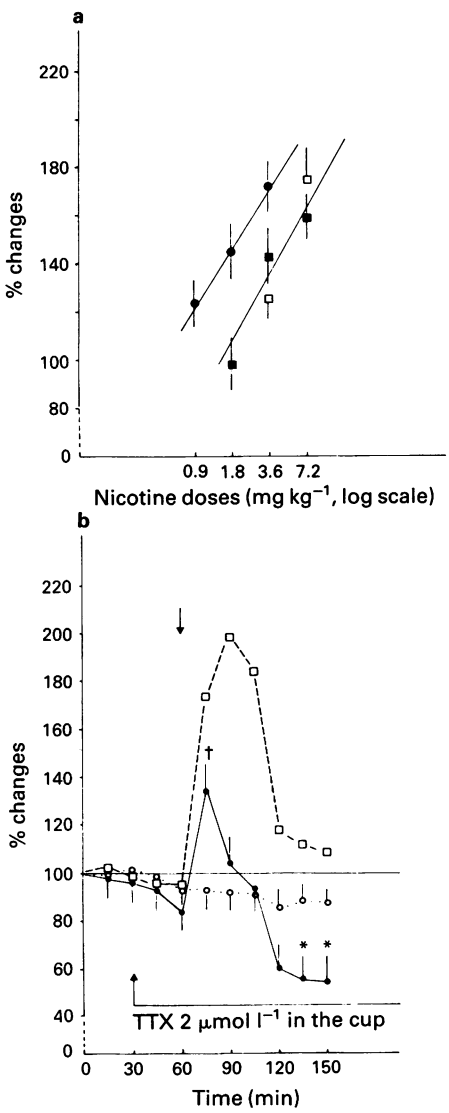

Figure 1 (a) Correlation between nicotine doses and [^{3}H]-D-aspartate efflux from the parietal cortex of normal guinea-pigs (●; $b = 82.4$, $r = 0.62$, $P < 0.01$) and mecamylamine-pretreated (8 mg kg^{-1}, i.p. 60 min before) animals (■; $b = 94.2$, $r = 0.72$, $P < 0.01$). The effect of nicotine on subchronically pretreated animals (see methods) is also shown (□). (b) Effect of topical application of tetrodotoxin (●, TTX) on the [^{3}H]-D-aspartate efflux induced by nicotine 3.6 mg kg^{-1} (at arrow). The effect of nicotine alone is shown for comparison (□). The spontaneous efflux in normal animals is also shown (○). Each point is the mean of 5–10 animals; vertical lines show s.e.mean. The values are normalized with respect to pre-injection efflux (the average efflux of [^{3}H]-D-aspartate before treatment was 0.694 ± 0.1 pmol in 15 min). The difference from control is statistically significant (* $P < 0.05$), according to ANOVA and Dunnet's test. The difference from nicotine alone is statistically significant († $P < 0.05$) according to ANOVA and Newman-Keuls multiple range test.

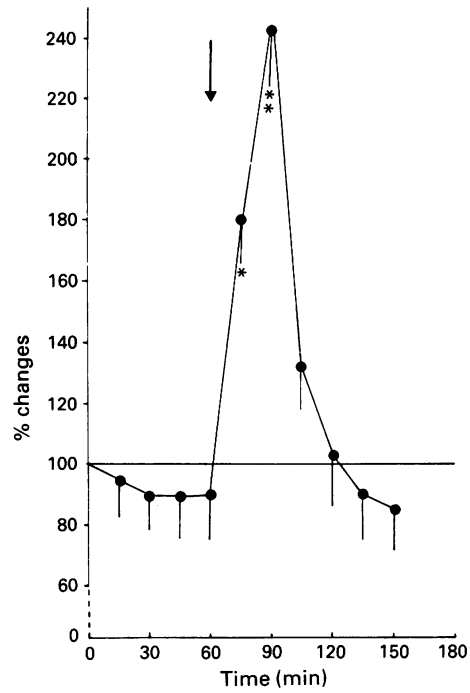

Figure 2 Effect of nicotine (5 μg at arrow) injected i.c.v. on the [^{3}H]-D-aspartate efflux from the parietal cortex of freely moving guinea-pigs. Each point is the mean of 3 animals; vertical lines show s.e.mean. The values are normalized with respect to the pre-injection release (average efflux of [^{3}H]-D-aspartate before treatment was 0.71 ± 0.06 pmol in 15 min). The difference from basal efflux is statistically significant (* $P < 0.05$, ** $P < 0.01$) according to ANOVA and Dunnet's test.

Effect of nicotine on GABA overflow

At the same doses that increased the [^{3}H]-D-aspartate efflux, nicotine reduced [^{3}H]-GABA (Figure 3a) and endogenous GABA overflow to similar extents (Figure 3b). The effect of the drug on the endogenous amino acid release was dose-related at 90 min ($r = 0.65$, $P < 0.05$). At variance with the time course of [^{3}H]-D-aspartate efflux, the inhibition of GABA overflow was long-lasting (about 2 h). Similar results were found when nicotine was injected i.c.v. (Figure 3c). Mecamylamine 2 mg kg^{-1} completely prevented the inhibition (Figure 3b). The local treatment with tetrodotoxin (0.5 μmol l^{-1} in the epidural cup for 30 min) consistently reduced the basal efflux as previously observed (Antonelli *et al.*, 1986) and prevented any further GABA reduction by nicotine 3.6 mg kg^{-1} (Figure 3d). Since nicotine is known to excite directly most of the neurones to which it is applied (Egan, 1989), the inhibition of GABA outflow suggested a drug-induced release of other transmitters which, in turn, inhibited GABA cells. Therefore, the possible involvement of some neuronal pools was tested by pretreating the animals with the proper antagonists. First of all atropine, haloperidol and prazosin were checked. None of these drugs modified the nicotine-induced GABA overflow reduction (Figure 4a). Conversely naloxone 3 mg kg^{-1} partially prevented it, while methysergide 2 mg kg^{-1} abolished any nicotine effect (Figure 4a and b).

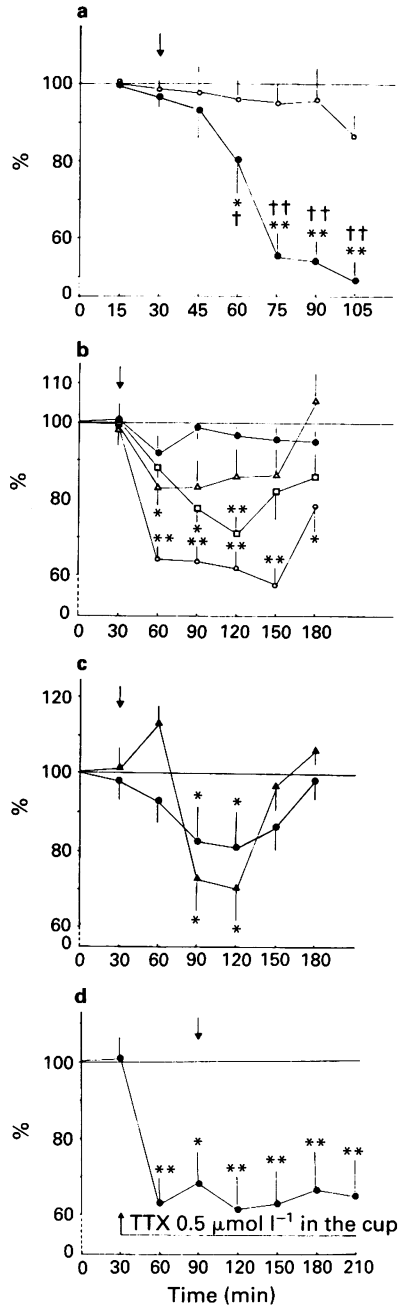

Figure 3 γ-Aminobutyric acid (GABA) efflux from the parietal cortex of freely moving guinea-pigs. (a) Effect of nicotine 3.6 mg kg^{-1} (arrow, ●) injected s.c. on [^{3}H]-GABA efflux. The spontaneous efflux in controls is also shown (○). (b) Effect of nicotine (arrow) injected s.c. (△, 0.9; □, 1.8; ○, 3.6 mg kg^{-1} and ●, 3.6 mg kg^{-1} 30 min after mecamylamine 8 mg kg^{-1}). (c) Effect of nicotine (3 μg ●, and 5 μg ▲, arrow) injected i.c.v. (d) The topical application of tetrodotoxin (TTX) prevents the inhibition of GABA efflux by nicotine 3.6 mg kg^{-1} (arrow). Each point is the mean of 5–6 animals; s.e.mean shown by vertical lines. The values are normalized with respect to the pre-injection release (average efflux before treatment was 0.036 ± 0.0039 pmol in 15 min for [^{3}H]-GABA and 26 ± 3.9 pmol cm^{-2} min^{-1} for endogenous GABA). The difference from the basal efflux is statistically significant (* $P < 0.05$; ** $P < 0.01$) according to ANOVA and Dunnet's test. The difference from spontaneous efflux in controls is statistically significant († $P < 0.05$; †† $P < 0.01$) according to ANOVA and Newman-Keuls multiple range test.

Effect of chronic (−)-nicotine treatment

In chronically treated animals a challenging dose of nicotine 3.6 mg kg^{-1}, administered 12 h after the last injection (according to the 16 day treatment schedule) caused an increase in [^{3}H]-D-aspartate efflux of only +25% (instead of +75% detected in naive animals). The recovery of the initial response was obtained with a dose of 7.2 mg kg^{-1}, indicating the development of moderate tolerance (Figure 1a). Conversely in chronically-treated guinea-pigs, nicotine 3.6 kg^{-1} no longer inhibited GABA outflow.

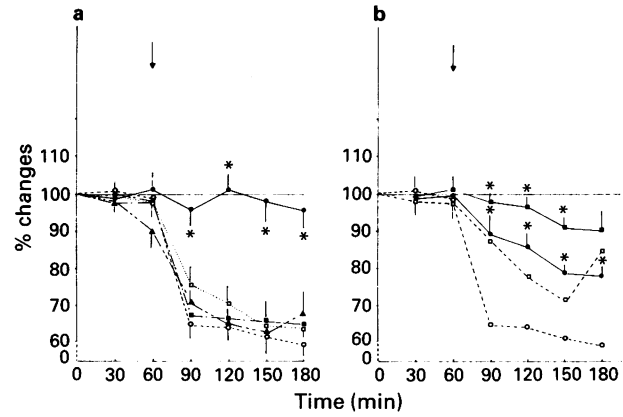

Figure 4 (a) Effect of nicotine 3.6 mg kg^{-1} (○) (arrow) on γ-aminobutyric acid (GABA) efflux from the cerebral cortex of freely moving guinea-pigs pretreated: with prazosin 15 μg kg^{-1} (▲), methysergide 2 mg kg^{-1} (●) (injected 30 min before); atropine 10 mg kg^{-1} (■) and haloperidol 2 mg kg^{-1} (□) (injected 60 min before). (b) Effect of nicotine 1.8 mg kg^{-1} (□ ··· □) and 3.6 mg kg^{-1} (○ ··· ○) (arrow) in guinea-pigs pretreated; with naloxone 3 mg kg^{-1} i.p. ((■) 15 min before nicotine 1.8 mg^{-1} and (●) before nicotine 3.6 mg kg^{-1}). Each point is the mean of 5–6 animals; s.e.mean shown by vertical lines. The values are normalized with respect to the pre-injection release. The average release before treatment was 27.5 ± 2.6 pmol cm^{-2} min^{-1}. The difference from nicotine alone is statistically significant (* $P < 0.05$) according to ANOVA and Newman-Keuls multiple range test.

Binding studies

An apparent up-regulation of nicotinic binding sites was previously found in rats but not in the guinea-pigs chronically treated with nicotine 0.45 mg kg^{-1} (Nordberg *et al.*, 1989). Such up-regulation was also evident in this latter species treated with nicotine 3.6 mg kg^{-1} (Table 2), but the extent of this change barely passed the limits of statistical significance and was restricted to the experiments with [^{3}H]-nicotine as a ligand.

Discussion

In a previous study (Nordberg *et al.*, 1989) it was shown that the time course and extent of the nicotine (0.45–0.9 mg kg^{-1}) effect on acetylcholine release from the cortex of rats and guinea-pigs was much the same, suggesting a similarity in the responsiveness of the two species to this drug. Since guinea-pigs are more suitable for the cortical cup technique, the decision was taken to make further investigations into the effect of nicotine on amino acid release in this last species alone.

The unmetabolizable analogue of glutamate, [^{3}H]-D-aspartate, has been widely used to study the activity of the glutama-

Table 2 Nicotinic receptors in the guinea-pig cerebral cortex following chronic treatment with nicotine (3.6 mg kg^{-1}), twice daily for 16 days

Experimental conditions	*Receptors* [^{3}H]-*ACh*	[^{3}H]-*nicotine*
Controls	1.8 ± 0.2 (5)	7.4 ± 0.50 (12)
Nicotine	2.4 ± 0.30 (5)	9.7 ± 1.08 (5)*

The values are pmol g^{-1} protein ± s.e.mean. The number of animals is shown in parentheses. * Significantly different from controls, $P < 0.05$.

tergic neurones *in vitro* and *in vivo* (Davies & Johnston, 1976; Huxtable *et al.*, 1985; Neilsen *et al.*, 1989). Recently, identical drug effects on the release of endogenous glutamate and [^{3}H]-D-aspartate from hippocampal slices have been reported (Marchi *et al.*, 1990). The choice of [^{3}H]-D-aspartate seems particularly convenient for studying glutamatergic neurone function *in vivo* since the glutamate coming from the blood can make a significant contribution to the overall amount of the amino acid present in the cup samples. This interference may overshadow drug effects on the neuronal release of this putative transmitter. The simple analysis of the [^{3}H]-D-aspartate washout curve was considered the best way to obtain information about the direction of nicotine-induced changes in amino acid release. In fact, the local application of selective inhibitors of glutamate uptake and/or metabolism (in order to amplify the responses) increases its extracellular concentration and, consequently, influences the activity of the entire neuronal network under the cup, thus complicating interpretation of the results. Topical pretreatment with a hypotonic KCl solution appears to be a procedure which increases the validity of the method, as shown by the higher amounts of [^{3}H]-D-aspartate released and by the more uniform responses in comparison with animals not pretreated.

The present findings clearly show that nicotine dose-dependently affected, in the opposite direction, [^{3}H]-D-aspartate and endogenous (or ^{3}H-labelled) GABA overflow from the cerebral cortex of naive, freely moving guinea-pigs. Its effect appears to be central in origin (Figures 2 and 3c) since nicotine injected i.c.v. gave rise to a response similar to that after s.c. administration.

Clearly, a peripheral component, as suggested by Hajos & Engberg (1988), cannot be ruled out. The doses required to change GABA and [^{3}H]-D-aspartate efflux were higher than those able to increase ACh release, indicating that the cholinergic structures impinging upon the neocortex are more responsive to nicotine than are the amino acid neurones. These neurones clearly respond to nicotine 3.6 mg kg^{-1} s.c., a dose which is 7–9 times lower than the LD_{50} (s.c.) in rats and guinea-pigs (Negherbon, 1959). As previously shown for the increase in cortical ACh *in vivo* (Nordberg *et al.*, 1989), these effects, are also mediated through nicotinic receptors of the neuronal type, as they are prevented by mecamylamine. On the other hand, the lack of any influence of mecamylamine on the basal [^{3}H]-D-aspartate efflux (as well as on basal GABA efflux) seems to rule out any physiological cholinergic nicotinic control over glutamate and GABA neurones in normal animals.

The excitatory properties generally attributed to nicotine, may be directly responsible for the increased [^{3}H]-D-aspartate overflow, the prevailing neuronal origin of which has been demonstrated (Figure 1). Thus, the present data are in accordance with those of de la Garza *et al.* (1987a) *in vivo* and with the report of Gongwer *et al.* (1987) *in vitro*. Conversely, the inhibition of GABA release in the conscious animal appears to be an indirect effect, due to the stimulation of nicotinic receptors located on other neuronal systems which, in turn, inhibit GABA cells. Clearly, this mechanism may no longer be operative in brain slices and is surely absent in synaptosomes.

Therefore, these simplified preparations may display excitatory responses to nicotine (Limberger *et al.*, 1986; Wonnacott *et al.*, 1989) provided some nicotinic receptors are present in the structures releasing the transmitter under study. Since atropine, haloperidol and prazosin did not prevent the reduction in GABA release, it is conceivable that the well-documented changes in acetylcholine, dopamine and noradrenaline release induced by nicotine (Balfour, 1982; Grenhoff & Svensson, 1989) are not the reason for the reduction in GABA overflow from the guinea-pig parietal cortex. Instead, the present results agree with the conclusion of Brennan *et al.* (1980) and Dewar *et al.* (1987) that the endogenous opioids released by nicotine are involved in the GABA response (Figure 4a and b). In addition, the results shown in Figure 4a demonstrate for the first time that 5-hydroxytryptamine (5-HT) plays a crucial role in the nicotine-induced inhibition of GABA release. In fact, methysergide prevented nicotine effects. In view of the existence of many 5-HT receptor subtypes, and taking into account the complexity of the *in vivo* model, further studies are needed to define the subtype and the location of these receptors.

The different duration of nicotine-induced changes in [^{3}H]-D-aspartate and GABA overflow is another point requiring some comment. In fact, the facilitation of [^{3}H]-D-aspartate is short-lived while the inhibition of GABA release is long lasting. Considering the different time courses of nicotine effects on the release of other putative transmitters (Imperato *et al.*, 1986; Nordberg *et al.*, 1989) a complex neurochemical (and behavioural) picture arises. This may explain the biphasic nicotine influence on locomoter activity of the rat (inhibition followed by facilitation, see Freeman *et al.*, 1987; Clarke & Kumar, 1983) as well as the increased alertness and decreased anxiety, the two overlapping stages of behavioural and subjective signs caused by nicotine in smokers (Pomerleau, 1986).

The results of the studies carried out in chronically treated guinea-pigs fit well with the expectations. In fact, as previously reported for the nicotine-induced increase in cortical ACh release (Nordberg *et al.*, 1989), even the increase in [^{3}H]-D-aspartate was less evident after chronic treatment. However, the inhibition of GABA efflux was no longer evident. This different degree of tolerance displayed by the glutamatergic and GABAergic cells confirms previous observations on the prevailing tolerance to the inhibitory nicotine effects on behaviour (Morrison & Stephenson, 1972). The persistent glutamatergic response may contribute to the maintenance (or enhancement) of the locomotor activation in chronically treated animals and may be another factor determining the reward in man (Pomerleau & Pomerleau, 1984; Russell, 1989), together with the well documented maintenance of the dopamine response (Clarke, 1990).

The moderate increase in the number of the nicotinic binding sites, which is limited to [^{3}H]-nicotine as ligand and can be detected only after 3.6 mg kg^{-1} per day for 16 days (but not after 0.45 mg kg^{-1} per day, see Nordberg *et al.*, 1989), confirms that, in the guinea-pig, the adaptation to chronic nicotine is not associated with consistent changes in the number or affinity of the receptors, as in other animal species, including man (Nordberg *et al.*, 1989; Wonnacott, 1990). However, in every instance, reduced responsiveness to the chronic drug administration develops.

We wish to thank Mr G. Marzola for technical assistance. This work was supported by CNR grant 'Progetto Strategico 1990: Meccanismi di release dei neurotrasmettitori e loro controllo'.

References

ANTONELLI, T., BEANI, L., BIANCHI, C., RANDO, S., SIMONATO, M. & TANGANELLI, S. (1986). Cortical acetylcholine release is increased and γ-aminobutyric acid outflow is reduced during morphine withdrawal. *Br. J. Pharmacol.*, **89**, 853–860.

AUSTIN, M.C. & KALIVAS, P.W. (1988). The effect of cholinergic stimulation in the nucleus accumbens on locomotor behaviour. *Brain Res.*, **441**, 209–214.

BALFOUR, D.J.K. (1982). The effects of nicotine on brain neurotransmitter systems. *Pharmacol. Rev.*, **16**, 269–282.

BEANI, L. & BIANCHI, C. (1970). Effects of adrenergic blocking and antiadrenergic drugs on the acetylcholine release from the exposed cerebral cortex of the conscious animal. In *Drugs and Cholinergic Mechanisms in the CNS*. ed. Heilbronn, E. & Winter, A. pp. 369–386, Stockholm: Research Institute of National Defence.

BEANI, L., BIANCHI, C., SANTINOCETO, L. & MARCHETTI, P. (1968). The cerebral acetylcholine release in conscious rabbit with semi-permanently implanted epidural cups. *Int. J. Neuropharmacol.*, **7**, 469–481.

BEANI, L., BIANCHI, C., TANGANELLI, S., ANTONELLI, T., SIMONATO, M. & RANDO, S. (1988). Inversion of the alpha-2 and alpha-1 noradrenergic control of the cortical release of acetylcholine and γ-aminobutyric acid in morphine tolerant guinea pigs. *J. Pharmacol. Exp. Ther.*, **247**, 294–300.

BEANI, L., BIANCHI, C., FERRARO, L., NILSSON, L., NORDBERG, A., ROMANELLI, L., SPALLUTO, P., SUNDWALL, A. & TANGANELLI, S. (1989). Effect of nicotine on the release of acetylcholine and aminoacids in the brain. *Prog. Brain Res.*, **79**, 149–155.

BRENNAN, M.J.W., CANTRIL, R.C. & WYLIE, B.A. (1980). Modulation of synaptosomal GABA release by enkephalin. *Life Sci.*, **27**, 1097–1101.

CLARKE, P.B.S. (1990). Dopaminergic mechanisms in the locomotor stimulant effects of nicotine. *Biochem. Pharmacol.*, **40**, 1427–1432.

CLARKE, P.B.S. & KUMAR, R. (1983). The effects of nicotine on locomotor activity in non-tolerant and tolerant rats. *Br. J. Pharmacol.*, **78**, 329–337.

DAVIES, L.P. & JOHNSTON, G.A.R. (1976). Uptake and release of D- and L-aspartate by rat brain slices. *J. Neurochem.*, **26**, 1007–1014.

DEWAR, D., JENNER, P. & MARSDEN, C.D. (1987). Effects of opioid agonist drugs on the *in vitro* release of [^{3}H]-GABA, [^{3}H]-dopamine and [^{3}H]5-HT from slices of globus pallidus. *Biochem. Pharmacol.*, **36**, 1738–1741.

EGAN, T.M. (1989). Single studies of the actions of agonists and antagonists on nicotinic receptors in the central nervous system. In *Prog. Brain Res.* (Nicotinic receptors in the CNS), **79**, 73–83.

FREEMAN, G.B., SHERMAN, K.A. & GIBSON, G.E. (1987). Locomotor activity as predictor of times and dosages for studies of nicotine's neurochemical actions. *Pharmacol. Biochem. Behav.*, **26**, 305–312.

FREUND, K.R., JUNGSCHAFFER, A.D., COLLINS, C.A. & WEHNER, M.J. (1988). Evidence for modulation of GABAergic neurotransmission by nicotine. *Brain Res.*, **453**, 215–220.

GAITONDE, M.F. (1973). Methods for the isolation and determination of glutamate, glutamine, aspartate and γ-aminobutyrate in brain. In *Research Methods in Neurochemistry*, ed. Marks, N. & Rodnight, R. vol. 2, pp. 321–359. New York: Plenum Press.

GARZA, R. DE LA, BICKFORD-WINNER, P.C., HOFFER, B.J. & FREEDMAN, R. (1987a). Heterogeneity of nicotine actions in the rat cerebellum: an *in vivo* electrophysiologic study. *J. Pharmacol. Exp. Ther.*, **240**, 689–695.

GARZA, R. DE LA, FREEDMAN, R. & HOFFER, J. (1989b). Nicotine-induced inhibition of cerebellar Purkinje neurons: specific actions of nicotine and selective blockade by mecamylamine. *Neuropharmacology*, **28**, 495–501.

GONGWER, M., ROBISON, P. & McBRIDE, W.J. (1987). Cholinergic control of aminoacid and monoamine transmitters in slices of nucleus accumbens. *Abs. Soc. Neurosci.*, **13**, 703.

GRENHOFF, J. & SVENSSON, T.H. (1989). Pharmacology of nicotine. *Br. J. Addict.*, **84**, 477–492.

HAJOS, M. & ENGBERG, J. (1988). Role of primary sensory neurones in the central effects of nicotine. *Psychopharmacology*, **94**, 468–470.

HUXTABLE, R.J., LEHMAN, A. & SANDBERG, M. (1985). *In vivo* release of D-aspartic acid and taurine in seizure susceptible rats. *Acta Neurol. Scand.*, **72**, 238–239.

IMPERATO, A., MULAS, A. & DI CHIARA, G. (1986). Nicotine preferentially stimulates dopamine release in the limbic system of freely moving rats. *Eur. J. Pharmacol.*, **132**, 337–338.

LIMBERGER, N., SPATH, C. & STARKE, K. (1986). A search for receptors modulating the release of γ-[^{3}H]-aminobutyric acid in rabbit caudate nucleus slices. *J. Neurochem.*, **46**, 1109–1117.

MARCHI, M., BESANA, E. & RAITERI, M. (1990). Oxiracetam increases in the release of endogenous glutamate from depolarized rat hippocampal slices. *Eur. J. Pharmacol.*, **185**, 247–249.

MORRISON, C.F. & STEPHENSON, J.A. (1972). The occurrence of tolerance to a central depressant effect of nicotine. *Br. J. Pharmacol.*, **46**, 141–156.

NEGHERBON, W.O. (1959). In *Insecticides, Handbook of Toxicology*, Vol. III, National Acad Sci., ed. Negherbon W.O. p. 509. Philadelphia and London: W.B. Saunders Company.

NIELSEN, E.S., AARSLEW-JENSEN, M., KROGSGAARD-LARSEN, P. & SCHOUSBUE, A. (1989). Baclofen-induced calcium-dependent stimulation of *in vivo* release of [^{3}H]-D-aspartate from rat hippocampus monitored by intracerebral microdialysis. *Neurochem. Res.*, **14**, 321–326.

NORDBERG, A., ADEM, A., NILSSON, L., ROMANELLI, L. & ZHANG, X. (1988). Heterogeneous cholinergic nicotine receptors in the CNS. In *Nicotinic Acetylcholine Receptors in the Nervous System.* ed. Clementi, F., Gotti, C. & Sher, E. pp. 331–350. Berlin, Heidelberg: Springer-Verlag.

NORDBERG, A., ROMANELLI, L., SUNDWALL, A., BIANCHI, C. & BEANI, L. (1989). Effect of acute and subchronic nicotine treatment on cortical acetylcholine release and on nicotinic receptors in rats and guinea-pigs. *Br. J. Pharmacol.*, **98**, 71–78.

POMERLEAU, O.F. (1986). Nicotine as a psychoactive drug: anxiety and pain reduction. *Psychopharmacol. Bull.*, **22**, 865–869.

POMERLEAU, O.F. & POMERLEAU, C.S. (1984). Neuroregulators and the reinforcement of smoking: towards a behavioral explanation. *Neurosci. Biobehav. Rev.*, **8**, 503–513.

ROMANELLI, L., ÖHMAN, B., ADEM, A. & NORDBERG, A. (1988). Subchronic treatment to rats with nicotine: interconversion of nicotinic receptor subtypes in brain. *Eur. J. Pharmacol.*, **148**, 289–291

RUSSELL, M.A.H. (1989). Subjective and behavioural effects of nicotine in humans: some sources of individual variations. *Prog. Brain Res.*, **79**, 289–302.

WONNACOTT, S. (1990). The paradox of nicotine acetylcholine receptor upregulation by nicotine. *Trends Pharmacol. Sci.*, **11**, 216–219.

WONNACOTT, S., FRYER, L., LUNT, G.G., FREUND, R.K., JUNGSCHAFFER, D.A. & COLLINS, A.C. (1987). Nicotinic modulation of gabaergic transmission in the hippocampus. *Soc. Neurosci.*, **14**, 1352.

WONNACOTT, S., IRONS, J., RAPIER, C., THORNE, B. & LUNT, G. (1989). Presynaptic modulation of transmitter release by nicotinic receptors. *Prog. Brain Res.*, **79**, 157–163.

YOUNG, A.M.J., FOLEY, P.M. & BRADFORD, H.F. (1990). Preloading *in vivo*: a rapid and reliable method for measuring γ-aminobutyric acid and glutamate effluxes by mycrodialysis. *J. Neurochem.*, **55**, 1060–1063.

(Received December 6, 1990
Revised April 22, 1991
Accepted April 26, 1991)

Br. J. Pharmacol. (1991), **104**, 21–24

Nitric oxide synthase in cultured endocardial cells of the pig

R. Schulz, *J.A. Smith, †M.J. Lewis & [1]S. Moncada

Wellcome Research Laboratories, Langley Court, Beckenham, Kent BR3 3BS and Departments of *Cardiology and †Pharmacology & Therapeutics, University of Wales College of Medicine, Heath Park, Cardiff CF4 4XN

1 Endocardial cells release factors which regulate myocardial contractility and guanosine 3':5'-cyclic monophosphate (cyclic GMP) levels. One of these factors is indistinguishable from endothelium-derived relaxing factor (EDRF).

2 The effluent from pig heart endocardial cells cultured on microcarrier beads caused the relaxation of a pig coronary artery ring denuded of endothelium. This relaxation was enhanced by a combination of superoxide dismutase and catalase and was attenuated by haemoglobin, which binds nitric oxide (NO), and by inhibitors of NO synthase, N^G-monomethyl-L-arginine (L-NMMA) or N^G-nitro-L-arginine.

3 A Ca^{2+}-, L-arginine- and NADPH-dependent enzyme activity which generated NO was detected by a specific spectrophotometric assay in cytosol prepared from endocardial cells. The formation of NO was inhibited in a concentration-dependent manner by L-NMMA (but not D-NMMA) and this could be partially reversed upon addition of excess L-arginine.

4 Like endothelial cells from the blood vessels, the endocardial cells possess the ability to synthesize NO, which may act to regulate myocardial contractility.

Keywords: Endocardium; endothelium-derived relaxing factor (EDRF); nitric oxide; cell culture

Introduction

Vascular endothelial cells generate nitric oxide (NO) from the terminal guanidino nitrogen atom(s) of L-arginine (Palmer *et al.*, 1987; 1988a). This NO, which causes the relaxation of vascular smooth muscle (Palmer *et al.*, 1987; Hutchinson *et al.*, 1987) and inhibits platelet aggregation (Radomski *et al.*, 1987; Furlong *et al.*, 1987), explains the biological actions of endothelium-derived relaxing factor (EDRF, Furchgott & Zawadzki, 1980). An NADPH-dependent enzyme, now known as NO synthase, was found in the cytosolic fraction of endothelial cells (Palmer & Moncada, 1989; Mülsch *et al.*, 1989; Mayer *et al.*, 1989). This enzyme catalyses the formation of NO from L-arginine, yielding L-citrulline as the co-product (Palmer & Moncada, 1989). The L-arginine to NO pathway has now been shown to exist in a variety of cells (Moncada & Higgs, 1990) where it serves as the transduction mechanism for the stimulation of the soluble guanylate cyclase (Moncada *et al.*, 1989).

The endocardial cells are ontogenetically similar to the endothelium. Analogous to the role of the endothelium in the regulation of vascular tone, it has been shown that the endocardium plays a role in modulating the contractility of cardiac muscle (Lewis *et al.*, 1990; Smith *et al.*, 1991). Cultured endocardial cells release a factor indistinguishable from EDRF as well as a factor(s), putatively termed endocardin, which exerts a positive inotropic action in isolated papillary muscle segments selectively denuded of endocardium (Smith *et al.*, 1991). In the present study we have identified and partially characterized a NO synthesizing enzyme present in the cytosol of cultured endocardial cells.

Methods

Endocardial cell culture

Endocardial cells were isolated from freshly obtained pig hearts as previously described (Smith *et al.*, 1991). Briefly, cells were harvested by exposure of the right ventricle to 0.2% collagenase in medium E199 and cultured in complete medium (medium E199 supplemented with 10% foetal bovine serum, 10% newborn bovine serum, glutamine (6 mM), benzylpenicillin (200 u ml^{-1}), streptomycin (200 $\mu g\,ml^{-1}$), and kanamycin (100 $\mu g\,ml^{-1}$)) in fibronectin-coated 75 cm^2 plastic tissue culture flasks. Flasks were coated with fibronectin by exposure to a sterile solution of fibronectin (10 $\mu g\,ml^{-1}$) in 10 mM HEPES (pH 7.3) for 1 h. Confluent cells were subcultured by brief exposure (3–5 min) to a 0.85% saline solution containing 0.05% trypsin and 0.02% EDTA. Newborn calf serum was added to inactivate the trypsin and the cell suspension was centrifuged (200 *g* for 5 min) and resuspended in complete medium. Cells used in this study were either primary cultures or those in first passage, exhibited cobblestone morphology, and incorporated fluorescent labelled acetylated low density lipoprotein (Smith *et al.*, 1991).

Determination of EDRF release by bioassay

Endocardial cells were grown on microcarrier culture beads as described (Gryglewski *et al.*, 1986a; Smith *et al.*, 1991); 0.5–0.8 ml of cell-covered beads (approximately 7.5×10^6 cells ml^{-1} beads) were washed in saline and placed in a 2 ml polypropylene syringe and superfused at a flow rate of 3.5 ml min^{-1} with oxygenated Krebs-Ringer solution at 35°C containing indomethacin (1 μM). The effluent of the cell column was used to superfuse an endothelium-denuded pig coronary artery ring preparation mounted as previously described (Christie & Lewis, 1988). The ring was preconstricted submaximally with prostaglandin $F_{2\alpha}$ (1 μM) and 5-hydroxytryptamine (5-HT, 1 μM) infused distal to the cells and changes in isometric tension were recorded.

Preparation of endocardial cytosol

Culture medium was removed and the cells were washed three times with Dulbecco's phosphate buffered saline (PBS). Cells were removed from the flasks by trypsinization, placed in an equal volume of culture medium and centrifuged (200 *g* for 10 min). The cell pellet was washed twice with PBS before resuspending the cells at a concentration of approximately 30–70 $\times 10^6$ cells ml^{-1} in ice-cold homogenization buffer containing 320 mM sucrose, 10 mM HEPES, 0.1 mM EDTA, 1 mM DL-dithiothreitol, 100 $\mu g\,ml^{-1}$ phenylmethylsulphonyl fluoride, 10 $\mu g\,ml^{-1}$ leupeptin, 10 $\mu g\,ml^{-1}$ soybean trypsin inhibitor, and 2 $\mu g\,ml^{-1}$ aprotinin (adjusted to pH 7.2 at 20°C with HCl). The cells were homogenized by sonicating twice for 3 s at 100 W with an ultrasonic probe (Soniprep, MSE). The homogenate was centrifuged at 150,000 *g* for 35 min at 4°C

[1] Author for correspondence at the Wellcome Research Laboratories.

and the supernatant was incubated with cation-exchange resin (AG 50W-X8) for 5 min at 4°C to deplete endogenous L-arginine. Upon settling of the resin, the supernatant was kept on ice and used within 2 h for determination of NO synthase activity.

Spectrophotometric determination of nitric oxide synthase activity

The formation of NO in cytosol was measured spectrophotometrically by the method of Feelisch & Noack (1987) based upon the rapid and stoichiometric reaction of NO with oxyhaemoglobin to yield methaemoglobin and nitrate. Cytosol was added in a 1:1 ratio (vol/vol) to the assay buffer (50 mM phosphate buffer, 1 mM $MgCl_2$, 10 μM oxyhaemoglobin, pH 7.2) at 37°C into a prewarmed cuvette. L-Arginine (30 μM), $CaCl_2$ (200 μM) and NADPH (100 μM) were added to initiate the reaction and the change in the difference in the absorbance at 401 and 421 nm (extinction coefficient 77,200 $M^{-1} cm^{-1}$) was monitored at 37°C with a double beam dual wavelength spectrophotometer (Shimadzu UV-3000) at a band width of 5 nm. The rate of NO synthesis was linear for 10 min. The Ca^{2+}-dependency of NO synthase was assayed in the presence of 1 mM EGTA and free Ca^{2+} was controlled by the addition of $CaCl_2$ solution to the reaction mixture (Knowles *et al.*, 1989). The protein content of the cytosol was determined with bicinchoninic acid protein assay reagent, using bovine serum albumin as a standard.

Chemicals

Cell culture materials (Flow and Sigma), N^G-monomethyl-L-arginine (L-NMMA) and D-NMMA acetate salts (Wellcome), cation exchange resin (AG 50W-X8, 200–400 mesh; Bio-Rad), bicinchoninic acid protein assay reagent (Pierce) and NADPH tetrasodium salt (Boehringer Mannheim) were obtained as indicated. Human haemoglobin was prepared as described (Paterson *et al.*, 1976). All other reagents were from BDH or Sigma.

Statistics

All values are expressed as mean ± s.e.mean of n experiments and were compared by Student's t test for paired or unpaired data, as appropriate, with $P < 0.05$ considered as statistically significant.

Results

Detection of EDRF by bioassay

Effluent from the perfused column of endocardial cells contained a diffusible factor which induced a relaxation of the bioassay detector tissue. This relaxation, measured as the percentage decrease of the initial tension, was enhanced in the presence of superoxide dismutase and catalase (73.9 ± 14.2 versus 36.9 ± 9.4%; $P < 0.01$; $n = 8$) and was completely abolished in the presence of haemoglobin (0.5 μM, $n = 6$) (Figure 1). Furthermore, the relaxation to the effluent from the cell column was completely reversed by addition of inhibitors of NO synthase, L-NMMA (50 μM, $n = 12$), or N^G-nitro-L-arginine (20 μM, $n = 4$) to the solution perfusing the cell column (data not shown).

Detection of nitric oxide by spectrophotometry

Addition of L-arginine (0.3–30 μM) to the cytosol, in the presence of NADPH (100 μM) and $CaCl_2$ (200 μM), caused a concentration-dependent increase in the rate of formation of NO to a maximum at 30 μM of 5.67 ± 0.80 pmol $min^{-1} mg^{-1}$ protein ($n = 3$; data not shown). In the absence of L-arginine or NADPH, or if D-arginine (30 μM) was substituted for L-arginine, the rate of NO synthesis was below the limit of detection (< 0.1 pmol $min^{-1} mg^{-1}$ protein; $n = 3$ for each).

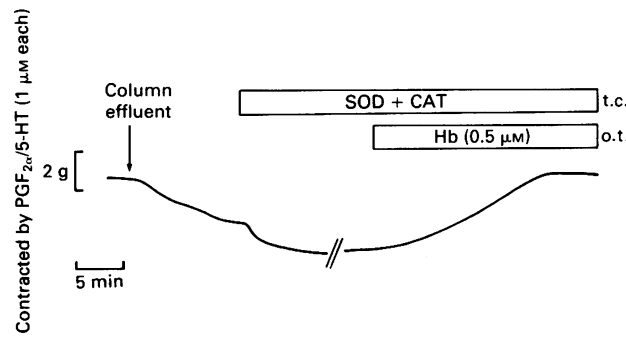

Figure 1 Bioassay of endothelium-derived relaxing factor (EDRF) release from a perfused column of cultured endocardial cells, recorded as the change in tension of the detector tissue, a preconstricted ring of coronary artery of the pig denuded of endothelium. Exposure to the effluent from the endocardial cells caused the detector tissue to relax. This effect was enhanced by superoxide dismutase (SOD, 30 u ml^{-1}) and catalase (CAT, 100 u ml^{-1}) infused through the column (t.c.) and was reversed by oxyhaemoglobin (Hb, 0.5 μM) infused over the bioassay tissue (o.t.). The tracing was redrawn and shortened by a 20 min period, represented by the double bar, and is representative of 6 experiments.

In the presence of L-arginine (30 μM), the synthesis of NO was inhibited in a concentration-dependent manner by L-NMMA ($n = 3$; Figure 2). L-NMMA (30 μM) abolished the formation of NO, an effect that was partially reversible upon addition of a ten fold molar excess of L-arginine (300 μM; $n = 3$). In the presence of D-NMMA (30 μM) there was a slight reduction in the rate of NO synthesis from 3.74 ± 0.72 to 2.92 ± 0.81 pmol $min^{-1} mg^{-1}$ protein ($n = 3$, data not shown) which was not statistically significant.

In the absence of free Ca^{2+} (1 mM EGTA), there was no measurable formation of NO by endocardial cell cytosol ($n = 3$). The addition of Ca^{2+} (resultant free Ca^{2+} concentration 0.1–71 μM) resulted in a concentration-dependent rise in the rate of NO synthesis with an EC_{50} value of 0.65 ± 0.10 μM ($n = 3$; Figure 3).

Discussion

We have demonstrated the release from endocardial cells of a factor with the characteristics of EDRF. It caused the relax-

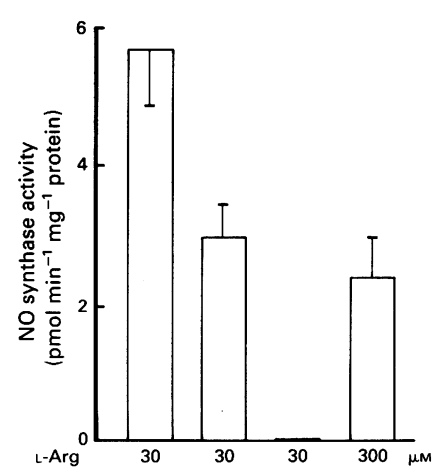

Figure 2 Effect of N^G-monomethyl-L-arginine (L-NMMA) on the formation of NO in endocardial cell cytosol. Addition of L-arginine (L-Arg, 30 μM) initiated the formation of NO which was inhibited by L-NMMA (3 and 30 μM). The formation of NO by L-Arg (30 μM) was abolished with L-NMMA (30 μM) and could be partially reversed by addition of a ten fold molar excess of L-Arg (300 μM). Each column is the mean of 3 separate experiments; vertical bars show s.e.mean.

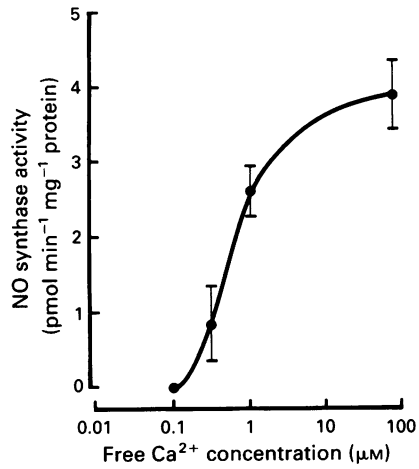

Figure 3 Ca^{2+}-dependence of NO synthesis in endocardial cell cytosol. The rate of synthesis of NO from L-arginine (30 μM) at free Ca^{2+} concentrations defined by Ca^{2+}/EGTA buffers is shown. Each point is the mean of 3 separate experiments; vertical bars show s.e.mean.

ation of vascular smooth muscle (Furchgott & Zawadzki, 1980) and its effect was potentiated by superoxide dismutase which prevents the breakdown of EDRF by superoxide anion (Gryglewski *et al.*, 1986b), and inhibited by haemoglobin (Martin *et al.*, 1985), which avidly binds NO (Gibson & Roughton, 1957). Furthermore the release of EDRF from endocardial cells was inhibited by L-NMMA and N^G-nitro-L-arginine (Palmer *et al.*, 1988b; Rees *et al.*, 1990a; Moore *et al.*, 1990), specific inhibitors of the NO synthase. It has also been demonstrated that substance P provokes an endocardium-dependent increase in guanosine 3':5'-cyclic monophosphate (cyclic GMP) levels in isolated papillary muscles of the ferret which is abolished by haemoglobin (Smith *et al.*, 1991). These results suggest that endocardial cells have the ability to synthesize NO, which accounts for the biological actions of EDRF (Palmer *et al.*, 1987).

Using a spectrophotometric assay specific for the detection of NO (Feelisch & Noack, 1987), we have now demonstrated that the cytosol of endocardial cells contains a Ca^{2+}-, L-arginine- and NADPH-dependent enzyme which synthesizes NO. The formation of NO in the cytosol was inhibited in an enantiomeric specific fashion by L-NMMA, but not D-NMMA, an effect which was reversible upon addition of excess L-arginine. These results, along with the strict Ca^{2+}-dependency of NO synthesis in the cytosol, suggest that the enzyme present in endocardial cells is similar to that found in endothelial cells (Palmer & Moncada, 1989; Mülsch *et al.*, 1989; Mayer *et al.*, 1989; Rees *et al.*, 1990a), the brain (Knowles *et al.*, 1989; Bredt & Snyder, 1990), platelets (Radomski *et al.*, 1990a) and the adrenal gland (Palacios *et al.*, 1989).

The physiological role of NO released from the endocardium is unclear. It has previously been shown that EDRF released from porcine endocardial cells shortens the contraction time of isolated papillary muscle preparations (Smith *et al.*, 1991). Furthermore, infusions of sodium nitroprusside, which spontaneously releases NO, into the coronary circulation produced an abbreviation of myocardial contraction in the Langendorff perfused heart of the ferret (Fort & Lewis, 1991), an effect which could not be observed when the drug was given into the ventricle. It has also been suggested that the endocardium may down-regulate the release of atrial natriuretic factor through an EDRF-dependent mechanism (Sanchez-Ferrer *et al.*, 1990). In addition the endocardium is responsible for the negative inotropic effect of vasopressin in isolated papillary muscles of the cat (Schoemaker *et al.*, 1990). Whether this action is mediated by the release of NO or through the suppression of the tonic release of an endocardial-derived myocardial contraction prolonging factor which has been described and given the name 'endocardin' (Smith *et al.*, 1991), remains to be determined.

It is apparent that there are similarities between the endocardium, with its potential role in the regulation of myocardial function and in providing a non-thrombogenic surface, and the endothelium, which plays a crucial role in the regulation of vascular tone and platelet activity. Endocardial damage has been shown to occur in isolated papillary muscles exposed to eosinophils taken from patients with hypereosinophilic syndrome or to 5-HT (Shah *et al.*, 1989; 1990). Whether the damage to the endocardium, seen during hypereosinophilia or in conditions like carcinoid syndrome (Olsen & Spry, 1985; Tornebrandt *et al.*, 1986; Spry, 1987), affects the local synthesis of NO and through this contributes to the cardiomyopathy associated with these disorders, requires further investigation.

It is now evident that there is another form of NO synthase which is Ca^{2+}-independent, as first described in macrophages (Hibbs *et al.*, 1988; Marletta *et al.*, 1988; Stuehr *et al.*, 1989), which releases NO as part of their cytotoxic activities against tumour cells and microorganisms (Hibbs *et al.*, 1990). Recently it has been shown that vascular endothelial (Radomski *et al.*, 1990b) and smooth muscle cells (Rees *et al.*, 1990b; Knowles *et al.*, 1990; Busse & Mülsch, 1990) can also express the Ca^{2+}-independent inducible form of the enzyme upon exposure to bacterial endotoxins and cytokines, which is likely to play a role in the pathological vasodilatation seen in endotoxin shock and cytokine therapies. It remains to be investigated whether the endocardium can also express this form of NO synthase and if this release of NO affects cardiac function during conditions of immunological activation.

We wish to thank Annie Higgs for help in the preparation of this manuscript. R.S. is a fellow of the Medical Research Council of Canada and the Alberta Heritage Foundation for Medical Research. This work was supported by a grant from the British Heart Foundation.

References

BREDT, D.S. & SNYDER, S.H. (1990). Isolation of nitric oxide synthetase, a calmodulin-requiring enzyme. *Proc. Natl. Acad. Sci., U.S.A.*, **87**, 682–685.

BUSSE, R. & MÜLSCH, A. (1990). Induction of nitric oxide synthase by cytokines in vascular smooth muscle cells. *FEBS Lett.*, **275**, 87–90.

CHRISTIE, M.I. & LEWIS, M.J. (1988). Vascular smooth muscle sensitivity to endothelium-derived relaxing factor is different in different species. *Br. J. Pharmacol.*, **95**, 630–636.

FEELISCH, M. & NOACK, E.A. (1987). Correlation between nitric oxide formation during degradation of organic nitrates and activation of guanylate cyclase. *Eur. J. Pharmacol.*, **139**, 19–30.

FORT, S. & LEWIS, M.J. (1991). Regulation of myocardial contractile performance by sodium nitroprusside in the isolated perfused heart of the ferret. *Br. J. Pharmacol.*, **102**, 351P.

FURCHGOTT, R.F. & ZAWADZKI, J.V. (1980). The obligatory role of endothelial cells in the relaxation of arterial smooth muscle by acetylcholine. *Nature*, **288**, 373–376.

FURLONG, B., HENDERSON, A.H., LEWIS, M.J. & SMITH, J.A. (1987). Endothelium-derived relaxing factor inhibits in vitro platelet aggregation. *Br. J. Pharmacol.*, **90**, 687–692.

GIBSON, Q.H. & ROUGHTON, F.J.W. (1957). The kinetics and equilibria of the reactions of nitric oxide with sheep haemoglobin. *J. Physiol. (Lond.)*, **136**, 507–526.

GRYGLEWSKI, R.J., MONCADA, S. & PALMER, R.M.J. (1986a). Bioassay of prostacyclin and endothelium-derived relaxing factor (EDRF) from porcine aortic endothelial cells. *Br. J. Pharmacol.*, **87**, 685–694.

GRYGLEWSKI, R.J., PALMER, R.M.J. & MONCADA, S. (1986b). Superoxide anion is involved in the breakdown of endothelium-derived relaxing factor. *Nature*, **320**, 454–456.

HIBBS, J.B. Jr., TAINTOR, R.R., VAVRIN, Z. & RACHLIN, E.M. (1988). Nitric oxide: a cytotoxic activated macrophage effector molecule. *Biochem. Biophys. Res. Commun.*, **157**, 87–94. (Erratum published (1989) *Biochem. Biophys. Res. Commun.*, **158**, 624).

HIBBS, J.B. Jr., TAINTOR, R.R., VAVRIN, Z., GRANGER, D.L., DRAPIER, J.-C., AMBER, I.J. & LANCASTER, J.R. Jr. (1990). Synthesis of nitric oxide from a terminal guanidino nitrogen atom of L-arginine: a molecular mechanism regulating cellular proliferation that targets intracellular iron. In *Nitric Oxide from L-Arginine: a Bioregulatory System.* ed. Moncada, S. & Higgs, E.A. pp. 189–224. Amsterdam: Elsevier.

HUTCHINSON, P.J.A., PALMER, R.M.J. & MONCADA, S. (1987). Comparative pharmacology of EDRF and nitric oxide on vascular strips. *Eur. J. Pharmacol.*, **141**, 145–151.

KNOWLES, R.G., PALACIOS, M., PALMER, R.M.J. & MONCADA, S. (1989). Formation of nitric oxide from L-arginine in the central nervous system: A transduction mechanism for stimulation of the soluble guanylate cyclase. *Proc. Natl. Acad. Sci., U.S.A.*, **86**, 5159–5162.

KNOWLES, R.G., SALTER, M., BROOKS, S.L. & MONCADA, S. (1990). Anti-inflammatory glucocorticoids inhibit the induction by endotoxin of nitric oxide synthase in the lung, liver and aorta of the rat. *Biochem. Biophys. Res. Commun.*, **172**, 1042–1048.

LEWIS, M.J., SHAH, A.M., SMITH, J.A. & HENDERSON, A.H. (1990). Does endocardium modulate myocardial contractile performance? *Cardioscience*, **1**, 83–87.

MARLETTA, M.A., YOON, P.S., IYENGAR, R., LEAF, C.D. & WISHNOK, J.S. (1988). Macrophage oxidation of L-arginine to nitrite and nitrate: nitric oxide is an intermediate. *Biochemistry*, **27**, 8706–8711.

MARTIN, W., VILLANI, G.M., JOTHIANANDAN, D. & FURCHGOTT, R.F. (1985). Selective blockade of endothelium-dependent and glyceryl trinitrate-induced relaxation by hemoglobin and by methylene blue in the rabbit aorta. *J. Pharmacol. Exp. Ther.*, **232**, 708–716.

MAYER, B., SCHMIDT, K., HUMBERT, R. & BÖHME, E. (1989). Biosynthesis of endothelium-derived relaxing factor: a cytosolic enzyme in porcine aortic endothelial cells Ca^{2+}-dependently converts L-arginine into an activator of soluble guanylyl cyclase. *Biochem. Biophys. Res. Commun.*, **164**, 678–685.

MONCADA, S. & HIGGS, E.A. (1990). *Nitric Oxide from L-Arginine: a Bioregulatory System.* Amsterdam: Elsevier.

MONCADA, S., PALMER, R.M.J. & HIGGS, E.A. (1989). Biosynthesis of nitric oxide from L-arginine: a pathway for the regulation of cell function and communication. *Biochem. Pharmacol.*, **38**, 1709–1715.

MOORE, P.K., AL-SWAYEH, O.A., CHONG, N.W.S., EVANS, R.A. & GIBSON, A. (1990). L-N^G-nitro arginine (L-NOARG) a novel, L-arginine reversible inhibitor of endothelium-dependent vasodilatation *in vitro*. *Br. J. Pharmacol.*, **99**, 408–412.

MÜLSCH, A., BASSENGE, E. & BUSSE, R. (1989). Nitric oxide synthesis in endothelial cytosol: evidence for a calcium-dependent and a calcium-independent mechanism. *Naunyn-Schmiedebergs Arch. Pharmacol.*, **340**, 767–770.

OLSEN, E.G.J. & SPRY, C.J.F. (1985). Relation between eosinophilia and endomyocardial disease. *Prog. Cardiovasc. Dis.*, **27**, 241–254.

PALACIOS, M., KNOWLES, R.G., PALMER, R.M.J. & MONCADA, S. (1989). Nitric oxide from L-arginine stimulates the soluble guanylate cyclase in adrenal glands. *Biochem. Biophys. Res. Commun.*, **165**, 802–809.

PALMER, R.M.J. & MONCADA, S. (1989). A novel citrulline-forming enzyme implicated in the formation of nitric oxide by vascular endothelial cells. *Biochem. Biophys. Res. Commun.*, **158**, 348–352.

PALMER, R.M.J., FERRIGE, A.G. & MONCADA, S. (1987). Nitric oxide release accounts for the biological activity of endothelium-derived relaxing factor. *Nature*, **327**, 524–526.

PALMER, R.M.J., ASHTON, D.S. & MONCADA, S. (1988a). Vascular endothelial cells synthesize nitric oxide from L-arginine. *Nature*, **333**, 664–666.

PALMER, R.M.J., REES, D.D., ASHTON, D.S. & MONCADA, S. (1988b). L-arginine is the physiological precursor for the formation of nitric oxide in endothelium-dependent relaxation. *Biochem. Biophys. Res. Commun.*, **153**, 1251–1256.

PATERSON, R.A., EAGLES, P.A.M., YOUNG, D.A.B. & BEDDELL, C.R. (1976). Rapid preparation of large quantities of human haemoglobin with low phosphate content by counter-flow dialysis. *Int. J. Biochem.*, **7**, 117–118.

RADOMSKI, M., PALMER, R.M.J. & MONCADA, S. (1987). The anti-aggregating properties of vascular endothelium: interactions between prostacyclin and nitric oxide. *Br. J. Pharmacol.*, **92**, 639–646.

RADOMSKI, M.W., PALMER, R.M.J. & MONCADA, S. (1990a). An L-arginine/nitric oxide pathway in human platelets regulates aggregation. *Proc. Natl. Acad. Sci., U.S.A.*, **87**, 5193–5197.

RADOMSKI, M.W., PALMER, R.M.J. & MONCADA, S. (1990b). Glucocorticoids inhibit the expression of an inducible, but not the constitutive, nitric oxide synthase in vascular endothelial cells. *Proc. Natl. Acad. Sci., U.S.A.*, **87**, 10043–10047.

REES, D.D., PALMER, R.M.J., SCHULZ, R., HODSON, H. & MONCADA, S. (1990a). Characterization of three inhibitors of endothelial nitric oxide synthase *in vitro* and *in vivo*. *Br. J. Pharmacol.*, **101**, 746–752.

REES, D.D., CELLEK, S., PALMER, R.M.J. & MONCADA, S. (1990b). Dexamethasone prevents the induction by endotoxin of a nitric oxide synthase and the associated effects on vascular tone: an insight into endotoxin shock. *Biochem. Biophys. Res. Commun.*, **173**, 541–547.

SANCHEZ-FERRER, C.F., BURNETT, J.C., Jr., LORENZ, R.R. & VANHOUTTE, P.M. (1990). Possible modulation of release of atrial natriuretic factor by endothelium-derived relaxing factor. *Am. J. Physiol.*, **259**, H982–H986.

SCHOEMAKER, I.E., MEULEMANS, A.L., ANDRIES, L.J. & BRUTSAERT, D.L. (1990). Role of endocardial endothelium in positive inotropic action of vasopressin. *Am. J. Physiol.*, **259**, H1148–H1151.

SHAH, A.M., ANDRIES, L.J., MEULEMANS, A.L. & BRUTSAERT, D.L. (1989). Endocardium modulates myocardial inotropic response to 5-hydroxytryptamine. *Am. J. Physiol.*, **257**, H1790–H1797.

SHAH, A.M., BRUTSAERT, D.L., MEULEMANS, A.L., ANDRIES, L.J. & CAPRON, M. (1990). Eosinophils from hypereosinophilic patients damage endocardium of isolated feline heart muscle preparations. *Circulation*, **81**, 1081–1088.

SMITH, J.A., SHAH, A.M. & LEWIS, M.J. (1991). Factors released from endocardium of the ferret and pig modulate myocardial contraction. *J. Physiol.* **439**, 1–14, 1991.

SPRY, C.J.F. (1987). Eosinophils and endomyocardial fibrosis: a review of clinical and experimental studies, 1980–86. In *Cardiomyopathy Update I. Pathogenesis of Myocarditis and Cardiomyopathy.* ed. Kawai, C. & Abelmann, W. pp. 293–310. Tokyo: University of Tokyo Press.

STUEHR, D., GROSS, S., SAKUMA, I., LEVI, R. & NATHAN, C. (1989). A macrophage product responsible for cytostasis and respiratory inhibition in tumor target cells. *J. Exp. Med.*, **169**, 1011–1020.

TORNEBRANDT, K., ESKILSSON, J. & NOBIN, A. (1986). Heart involvement in metastatic carcinoid disease. *Clin. Cardiol.*, **9**, 13–19.

(Received March 18, 1991
Accepted April 29, 1991)

Br. J. Pharmacol. (1991), **104**, 25–30

The effect of TYB-3823, a new antiarrhythmic drug, on sodium current in isolated cardiac cells

Jiro Miyamoto, [1]Ichiro Hisatome, Satoshi Matsuoka, Hiromoto Kosaka, Yasutaka Kurata, Yasunori Tanaka, Takahiro Nawada, Hiroshi Kotake, Hiroto Mashiba & *Ryoichi Sato

1st Department of Internal Medicine, Tottori University School of Medicine, Nishimachi 36-1, Yonago, 683, Japan and *1st Department of Internal Medicine, Kinki University, Osaka, 589, Japan

1 Sodium current (I_{Na}) blockade by TYB-3823, a newly synthesized antiarrhythmic agent, was investigated in isolated single ventricular myocytes by use of the whole cell patch-clamp technique.

2 TYB-3823 blocked I_{Na} under steady-state conditions ($K_{d,rest} = 500\,\mu M$, $K_{d,i} = 4.9\,\mu M$), findings consistent with a shift in the steady state I_{Na} availability curve to more negative potentials.

3 TYB-3823 produced use-dependent block at 2 Hz in conjunction with increase in pulse duration (5–300 ms), that was markedly enhanced at less negative holding potentials.

4 The time course of the onset of block was accelerated and the degree of use-dependent block was decreased at more negative holding potential. The time course of the onset of block was accentuated with enhancing block at more positive holding potentials.

5 The time course of recovery from use-dependent block was accelerated at more negative holding potentials but was accentuated at more positive holding potentials.

6 These results suggest that both tonic block and use-dependent block of sodium channels in cardiac tissue might result from an interaction of TYB-3832 with sodium channels mainly in the inactivated channel states and the kinetics of the interaction between drug and receptor may be modulated by the inactivation gate.

Keywords: Na current; TYB-3823; cardiac myocytes; whole cell voltage-clamp

Introduction

The newly synthesized drug TYB-3823 (1-(2,6,-dimethylphenyl)-4,4,-dimethyl-aminoguanidine hydrochloride) has a potent and long-lasting inhibitory action against supraventricular and ventricular arrhythmias induced by aconitine, ouabain, or coronary ligation-reperfusion in rats, guinea-pig and dogs (Kurthy *et al.*, 1985). The previous experiments in dog isolated ventricular myocytes (Varro *et al.*, 1987) and guinea-pig papillary muscles (Kodama *et al.*, 1988) have shown that TYB-3823 suppresses the maximum upstroke velocity (V_{max}) of action potentials and shortening of action potential duration. These studies were based on measurement of V_{max} of cardiac action potentials. However, V_{max} may not be a linear measurement of I_{Na} in cardiac tissue (Cohen *et al.*, 1984). Therefore it was considered important to elucidate the blocking mechanism of TYB-3823 on I_{Na} in guinea-pig ventricular myocytes, under voltage-clamp conditions.

In the present study, we used the whole cell patch clamp technique to assess the kinetics of I_{Na} blockade by TYB-3823 on single guinea-pig ventricular myocytes. We found that the TYB-3823 could produce resting block only at depolarized holding potentials, suggesting a high affinity of TYB-3823 for the inactivated state of the Na channel. TYB-3823 also shifted the steady state inactivation curve in the negative potential direction and produced use-dependent block markedly at low holding potentials, results consistent with the findings that TYB-3823 slows recovery from inactivation state. It is concluded from these results that TYB-3823 has a high affinity for the inactivated state of the Na channel.

Methods

Single guinea-pig ventricular myocytes were isolated by the enzymatic dissociation technique similar to that previously described by Powell *et al.* (1980) and Ehara *et al.* (1989). Sodium currents of single ventricular cells were recorded by the whole cell clamp technique (Hamil *et al.*, 1981). The chamber was continuously perfused with low sodium Tyrode solution at a temperature of 17°C and of the following composition (mM): NaCl 10, CsCl 5, $CaCl_2$ 1.8, $MgCl_2$ 0.5, D-glucose 11, HEPES 20 and tetramethylammonium chloride 125. The solution was titrated to a pH of 7.35 with 1 M tetramethylammonium hydroxide. The internal solution of the suction pipette was composed of (mM): CsF 145, NaF 10 and HEPES 5 and titrated to a pH of 7.2 with 1 M CsOH. Use of these solutions allowed effective isolation of I_{Na} from other ionic currents. Pipettes had tip resistances less than 0.5 MΩ. Compensation for series resistance was done empirically by applying series resistance compensation to speed the decay of capacitive transient. After compensation, capacitive transients were within 500 μs. The membrane current signal was recorded on video tapes (video recorder, Mitsubishi HV-F73) through a PCM converter (SHOSHIN EM, PCM-PP16) for later computer analysis (NEC PC98XL). Several criteria have been outlined to permit indirect determination of the adequacy of space-clamp control in cardiac preparations. Under our experimental conditions (Hisatome *et al.*, 1987; Miyamoto *et al.*, 1989), current recordings from isolated myocytes satisfied the criteria described by Colatsky & Tsien (1979).

To study the tonic block of TYB-3823 on I_{Na}, low pulse frequency (0.01 Hz) was used, sufficient to ensure full recovery from rate dependent block of I_{Na}. Thereby, drug-induced decrease in I_{Na} is defined as tonic block. The amount of tonic block is calculated as % decrease in I_{Na} after perfusion with drug as compared to control. To study the use-dependent block, rest periods of 180 s were interposed between the trains of stimuli. I_{Na} decreased during a pulse train and reached a new steady state. The amount of use-dependent block is calculated as % decrease of I_{Na} in the new steady state with respect to that of the first pulse (Hisatome *et al.*, 1990). TYB-3823 was kindly supplied by Toyobo & Co., Ltd., Osaka, Japan; this drug is synthesized by Biogal (Debrecen, Hungary) as G.Y.K.I. 38233 and licensed to Toyobo.

[1] Author for correspondence.

Results

Voltage-dependency and block of Na current by TYB-3823

Figure 1a shows the families of Na currents under control conditions (upper panel) and after administration of TYB-3823, 30 μM (lower panel). Na current were elicited by depolarizing pulses to selected test potentials from a holding potential (HP) of −90 mV every 90 s. After 8 min exposure to TYB-3823, the Na current was reduced to about 60% of the control value. Figure 1b shows the current-voltage relationship before and 8 min after exposure to 30 μM TYB-3823. TYB-3823 blocked the Na currents without changes in either threshold potential, peak potential or equilibrium potential. Figure 2 shows the relationship between fraction of tonic block and the concentration of TYB-3823 at HP = −90 mV. Each point represents a mean value of the blocked ratio of I_{Na} at each concentration ($n = 4$). The sigmoidal curves drawn through the data points are described according to the following equation:

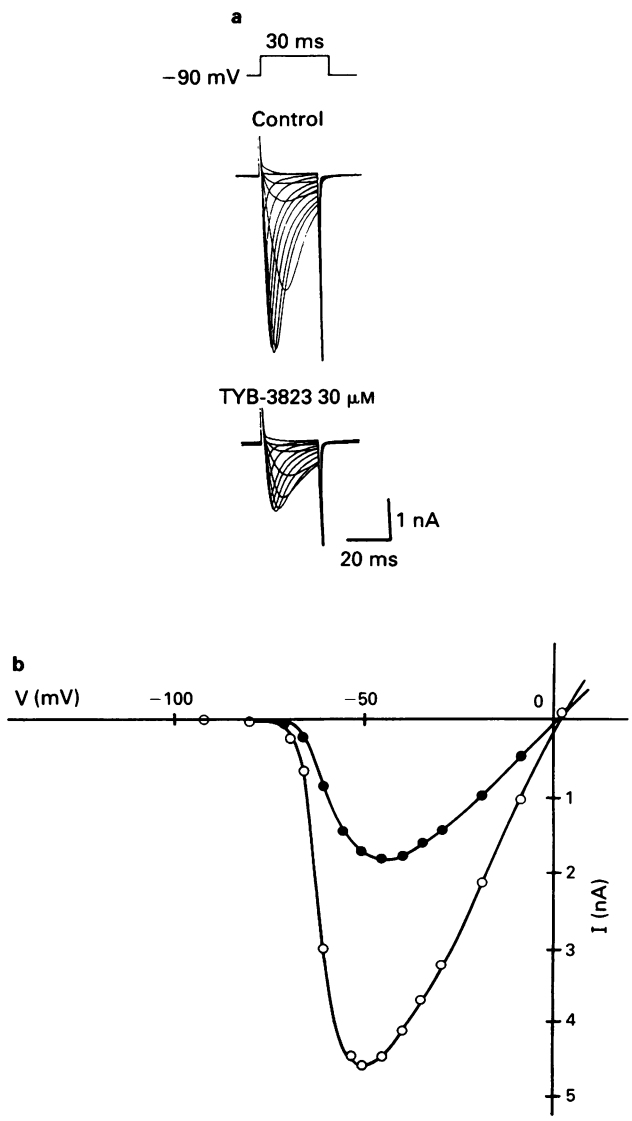

Figure 1 Voltage-dependence of TYB-3823 block of Na current. (a) Families of Na current traces under control conditions and after 30 μM TYB-3823 administration were obtained by applying 5 mV step pulses of 30 ms from a holding potential of −90 mV. Calibration shows 1 nA of current amplitude and 20 ms of time scale. (b) Current-voltage relationship for the peak current under control conditions and in the presence of 30 μM TYB-3823. Na current was blocked at all test potentials without affecting the current-voltage relationship.

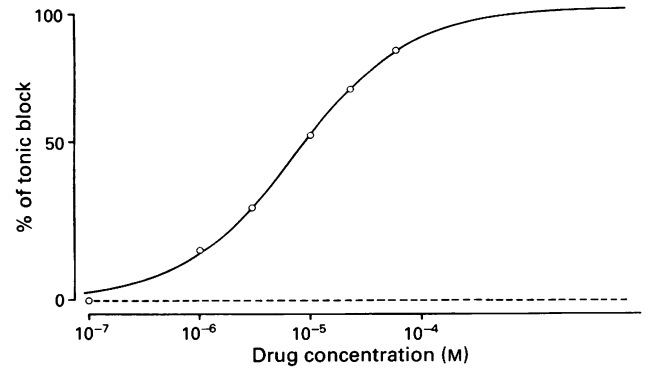

Figure 2 Concentration-dependent TYB-3823 block of Na current. Relationship between blocked reaction of Na current (ordinate scale) and the concentration of TYB-3823 (abscissa scale) are shown. I_{Na} was elicited by a test pulse to −20 mV from HP = −90 mV. The sigmoidal curve was drawn as a best fit to equation (see text). Slope factor was 0.97 and K_d was 15 μM.

$$y = (1 + K_{d,app}/[D])^{-1} \quad (1)$$

where y represents fraction of block, $K_{d,app}$ is apparent dissociation constant at HP = −90 mV and [D] is the drug concentration. $K_{d,app}$ was 15×10^{-6} M at HP = −90 mV.

Resting block by TYB-3823

Figure 3 shows the steady state availability curve for Na current under control conditions and after exposure to TYB-3823 (30 and 200 μM). I_{Na} availability was assessed at selected membrane prepulse potentials by use of a standard two-pulse protocol. A 1 s prepulse to the designated level of membrane potential was followed by a 0.5 ms interval and then by a 30 ms test pulse to −20 mV. This two pulse sequence was applied once every 90 s. The curves drawn through the data points are described by the following equation:

$$h = \{1 + \exp[(V_m - V_h)/k]\}^{-1} \quad (2)$$

where V_m is the prepulse potential, V_h is the prepulse potential at which h = 0.5 and k is a slope factor. At very negative HP (HP = −140 mV), high doses of TYB-3823 could reduce the maximum available I_{Na}. This decrease in I_{Na} at HP = −140 mV and low pulse frequency is defined as resting blockade of I_{Na} by TYB-3823. Although 30 μM TYB-3823 could not produce significant resting block, 200 μM TYB-3823

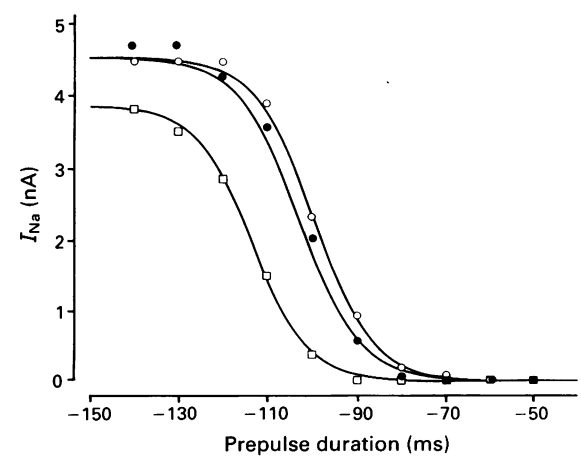

Figure 3 Dose-dependent effects of TYB-3823 on Na availability curve. Prepulse potential where I_{Na} is one-half maximum (V_h) and the slope factor (k) was calculated using Boltzmann distribution: $h = 1/1 + \exp[(V_m - V_h)/k]$ where V_m = prepulse potential. V_h was −95.3 mV and k was 6.3 (○, control), −102.8 mV and 6.3 in 30 μM TYB-3823 (●) and −113.3 mV and 6.2 in 200 μM TYB-3823 (□), respectively.

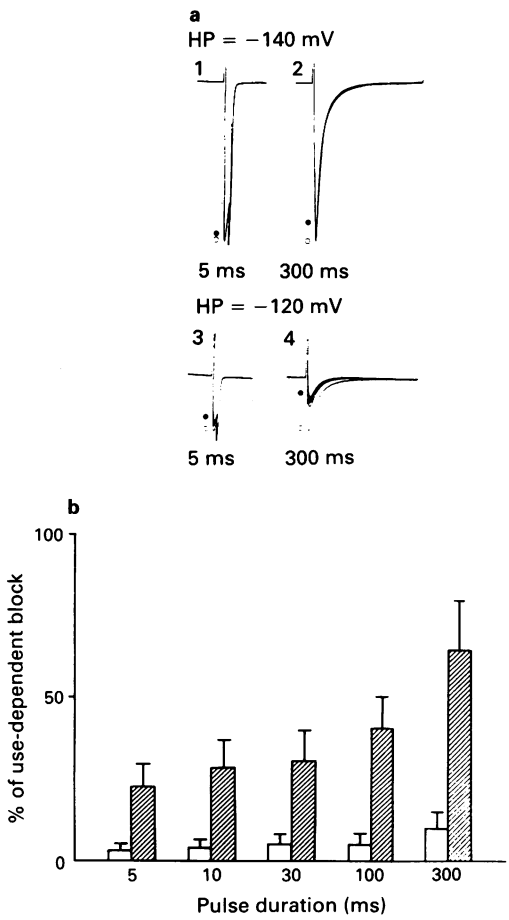

Figure 4 The relationship between pulse duration and use-dependent block at 2 Hz in the presence of 100 μM TYB-3823: effects of holding potential. (a) (1–4): I_{Na} elicited during a train of pulse to −20 mV from HP = −140 mV or −120 mV at 2 Hz. Open circle shows I_{Na} at 1st pulse and closed circle I_{Na} at 10th pulse, duration of which is 5 ms (1) and 300 ms (2) at HP = −140 mV, 5 ms (3) and 300 ms (4) at HP = −120. For calibration, see Figure 1a. (b) The relationship between pulse duration and phasic block at 2 Hz in the presence of 100 μM TYB-3823. Vertical bars show s.e. (n = 4) of use-dependent block at various pulse durations at HP = −140 (open columns) and −120 mV (hatched columns).

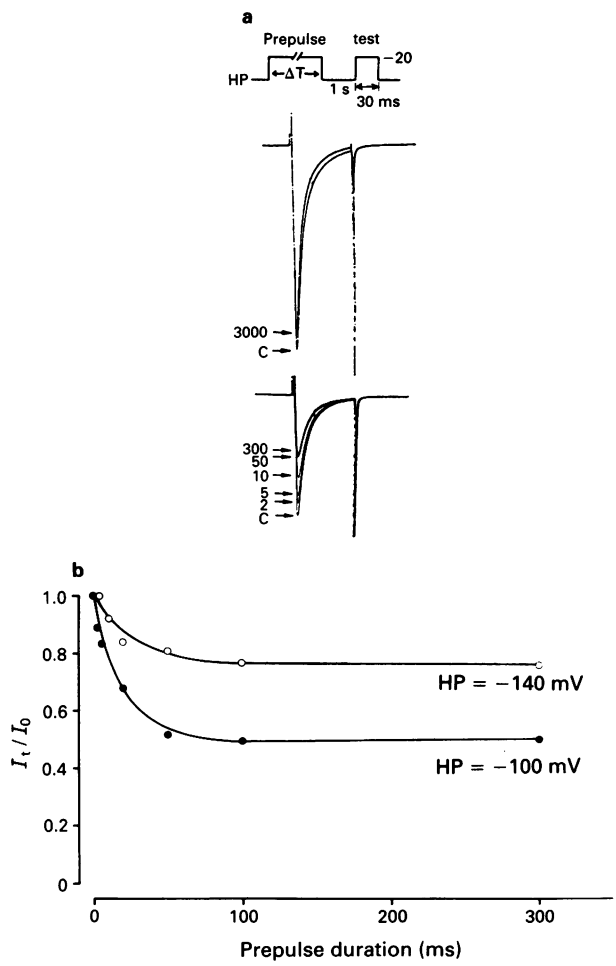

Figure 5 The time course of onset block in the presence of 100 μM TYB-3823. (a) The two-pulse protocol was used to assess the onset of use-dependent block. I_{Na} elicited by control (bottom arrow) and the test pulse following each conditioning pulse, the duration of which was 2, 5, 10, 50, 300, or 3000 ms (upper arrow) is shown in the presence of 100 μM TYB-3823. HP was −140 and −100 mV and test potential was −20 mV. For calibration, see Figure 1a. (b) The time constant of onset of block were 29 ms and 135 ms at HP = −140 (○) and −100 mV (●), respectively.

reduced maximum I_{Na} by 20% (n = 4) on average. TYB-3823 also shifted the Na availability curve toward more negative potentials in a dose-dependent manner without changes in slope factor. Therefore, resting block was observed only at a high dose of TYB-3823, and the I_{Na} blocking action of TYB-3823 was markedly dependent on membrane potential. According to equation (1), $K_{d,rest}$, i.e., dissociation constant in rested state, was 500 × 10^{-6} M.

Use-dependent block by TYB-3823

In addition to tonic block, TYB-3823 produced use-dependent block of I_{Na}. The magnitude of the use-dependent block of I_{Na} was dependent on the pulse duration and holding potential. Figure 4a(1) shows I_{Na} elicited by the first depolarizing pulse from HP = −140 to −20 mV (open circle) and 10th pulse (closed circle) in the presence of 100 μM TYB-3823 at 2 Hz, of which pulse duration was short (5 ms). Figure 4a(2) shows I_{Na} elicited by the long pulse duration (300 ms) from HP = −140 mV. Even long train pulses could produce only a small amount of use-dependent block at HP = −140 mV. Figure 4a(3) shows I_{Na} elicited by a first depolarizing pulse (open circle) from HP = −120 to −20 mV, and 10th pulse (closed circle) in the presence of 100 μM TYB-3823 at 2 Hz, with a short pulse duration (5 ms). Figure 4a(4) shows I_{Na} elicited by a long duration pulse (300 ms) from HP = −120 mV at 2 Hz. Even short duration pulses could reveal TYB-3823-induced use-dependent block of I_{Na}. Figure 4b shows the % of use-dependent block at 2 Hz by train pulses of 5, 10, 30, 100 and 300 ms in the presence of 100 μM TYB-3823 at HP = −140 and −120 mV (n = 4). The % of use-dependent block is calculated by the peak current for the 10th pulse normalized relative to that of the first pulse. The degree of use-dependent block at each HP increased with increase in the pulse duration. In addition, more cumulative block was observed at more depolarized HP. These results suggest that the magnitude of use-dependent block by TYB-3823 was dependent on both the HP and the pulse duration. It is worth noticing that even short duration pulses such as 5 or 10 ms produced use-dependent block, and the proportion of use-dependent block induced by 5 and 10 ms duration pulses relative to that by 300 ms was about 30% at either HP = −120 or −140 mV.

Onset of use-dependent block of I_{Na} by TYB-3823

The above data suggest that onset of use-dependent block by TYB-3823 might be fast. Therefore, this possibility was tested by use of a two-pulse protocol as follows. In the presence of 100 μM TYB-3823, a prepulse (2 to 300 ms) to −20 mV from

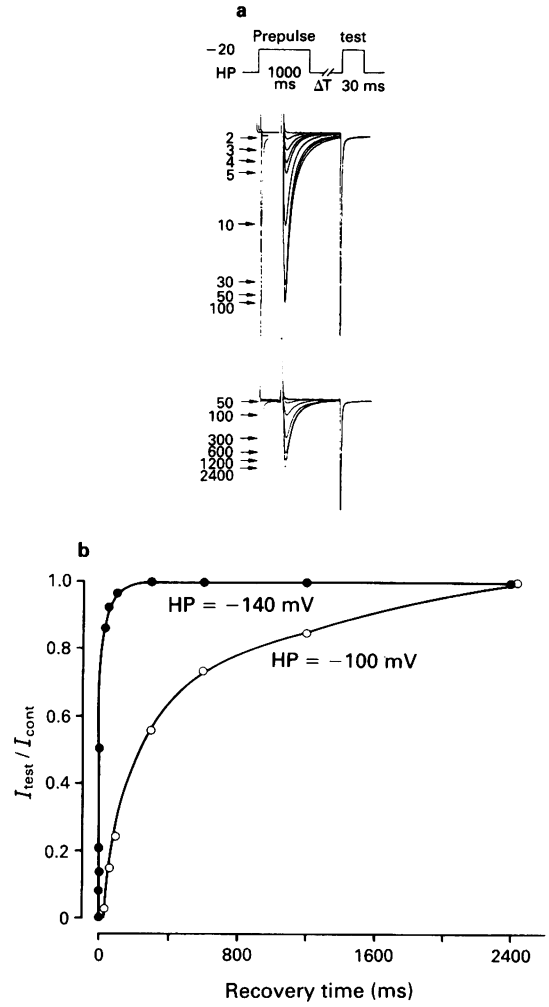

Figure 6 Effects of TYB-3823 on the recovery from inactivation of I_{Na}. Recovery of I_{Na} from inactivation was assessed by two-pulse protocol shown in the inset in upper part of (a). (a) I_{Na} elicited by the test pulse to −20 mV following 1000 ms prepulse is shown after selected recovery times (ms) as shown by arrows from HP = −140 and −100 mV in the presence of 100 μM TYB-3823. For calibration, see Figure 1a. (b) I_{Na} elicited during test pulse (I_{test}) was normalized to that elicited by the control pulse (I_{cont}). At HP = −140 mV (●), I_{Na} recovered within 300 ms, whereas at HP = −100 mV (○) full recovery of I_{Na} required more than 3 s.

HP = −140 and HP = −100 mV was followed by a 1 s recovery period and a test pulse to −20 mV from each HP to assess current recovery as shown in the pulse protocol of Figure 5a. This sequence was applied at 90 s interval to avoid build-up of use-dependent block. The upper panel of Figure 5a shows the original current traces followed by 10 μs prepulse (control) and by 3000 ms prepulse at HP = −140 mV. The lower panel of Figure 5a shows the original current traces followed by 10 μs, 2, 5, 10, 50, and 300 ms prepulse at HP = −100 mV. Figure 5b shows % of onset of use-dependent block following prepulse duration varying from 2 to 300 ms in the presence of 100 μM TYB-3823 at HP = −140 (open circles) and −100 mV (closed circles). More positive HP accelerated the degree of onset of block, which was already revealed from prepulse duration = 2 ms at HP = −100 mV. This experiment indicates that, at less negative HP, even short pulse durations such as 2 ms could induce use-dependent block of I_{Na}, and block was also enhanced at longer prepulse durations such as 100 and 300 ms. By contrast, the more negative holding potential accentuated the degree of onset block. The onset of block was fitted by a single exponential curve. The time constants of onset of block were 39 and 175 ms at HP = −140 and −100 mV, respectively, which suggested that more negative HP accelerated the time constant of onset of block.

Recovery from inactivation of I_{Na} in the presence of TYB-3823

Recovery from inactivation was assessed by the protocol shown in the inset of Figure 6a. A 1000 ms prepulse was followed by a variable recovery period and a test pulse to assess the amount of current recovered at HP = −140 and −100 mV. Each two-pulse sequence was applied at 90 s interval. The upper panel of Figure 6a shows the original current traces at HP = −140 mV and the lower panel of Figure 6a shows the original current traces at HP = −100 mV. Figure 6b shows that the peak current for each test pulse was normalized to that for the preceding control pulse and plotted as a function of recovery time. At HP = −140 mV (closed circles), the Na current recovered rapidly, being described by single exponential with a time constant of 27 ms in the presence of 100 μM TYB-3823. The time course of recovery was slowed markedly at HP = −100 mV, and was characterized by the time constant of 587 ms. Thus, the more positive HP slowed recovery from inactivation markedly, a finding consistent with its effects in inducing use-dependent block.

Discussion

The present experiments have shown that the TYB-3823 decreased I_{Na} of guinea-pig ventricular myocytes, in both a tonic and use-dependent fashion, and also shifted the Na channel availability curve in the hyperpolarizing direction. The time constant for the decay of capacitive transients did not change before and after administration of TYB-3823, so that the shift of the inactivation curve was not due to a voltage drop across the residual series resistance. We tried to reconcile the present results with the modulated receptor hypothesis (Hille, 1977; Hondeghem & Katzung, 1977). According to the modulated receptor theory, (1) drugs bind to the receptor site or very close to the sodium channel, (2) the affinity of the receptor of the drug is modulated by the channel state: rested, inactivated and activated state, (3) drug-associated channels differ from the drug-free channels in that they do not conduct and their ability to be activated is shifted to more negative potentials. It is known that the tonic block is composed of rested and inactivated state block. A simplified scheme showing the relation between TYB-3823 and inactivation and the resting state is reproduced, which was shown by Bean *et al.* (1983).

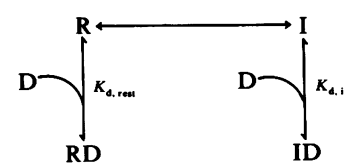

where D is the drug molecule, R is the rested state, RD is the resting state with the neutral form of drug bound; I and ID are the corresponding forms of inactivation. Therefore, the apparent affinity for TYB-3823 ($1/K_{d,app}$) will depend largely on the apportionment of channels between rested and inactivated state (comprising fraction h and 1 − h, respectively) as following equation:

$$1/K_{d,app} = h/K_{d,rest} + (1 - h)/K_{d,i} \quad (3)$$

where h is the fraction of channels in the rested state in the absence of drug and $K_{d,i}$ is the dissociation constant for

binding to the inactivated state. $K_{d,rest}$ is the dissociation constant in the rested state. $K_{d,app}$ at HP = −90 mV was 15×10^{-6} M. $K_{d,rest}$ was 500×10^{-6} M ($n = 3$) and $K_{d,i}$ was 4.9×10^{-6} M.

Mean shift of the inactivation curve induced by the drug is obtained from the following equation:

$$dV_h = k \ln\{(1 + [D]/K_{d,rest})/(1 + [D]/K_{d,i})\} \quad (4)$$

where dV_h is the shift of inactivation curve, k is the slope factor of inactivation curve and [D] is drug concentration.

In order to confirm our calculation, we applied our data to the above equation. In the presence of 200 μM TYB-3823, the hyperpolarizing shift is calculated to be 20 mV, which was very close to the experimental data (18.2 mV). These results suggest that under steady state conditions, TYB-3823 had a very low affinity for the rested state, and blocked the Na channel mainly by binding to the inactivated state, resulting in a decrease in number of the sodium channels available.

Use-dependent block is produced when the drug-channel interaction is too slow to reach equilibrium within a single cycle of Na channel activation and inactivation. Drug binding to open channels and resting channels is also attributed to the accessibility of the receptor, which is controlled by the Na channel gate (Stimers *et al.*, 1985; Tanguy & Yeh, 1985). That is, the use-dependent block is attributed to a specific interaction between the sodium channel and the charged form of the drug molecules. This use-dependent blocking action is explained by two different theories, the modulated receptor hypothesis as already mentioned in the previous section and the guarded receptor hypothesis (Starmer *et al.*, 1984). In the latter, the affinity of the binding site of the drug is constant, but access to the binding site is guarded by activation and/or inactivation gates, such that the forward binding rate is faster when the channel is open or inactivated than under resting conditions. The present experiment showed that TYB-3823 exerted pronounced use-dependent block dependent on the longer duration of the depolarizing pulse and the more depolarized level of the holding potential. Thus, a train of long pulses (300 ms) could produce a small amount of Na channel block at HP = −140 mV, because at this holding potential, Na channels are predominantly in the rested state conformation but not in the inactivated state conformation. By contrast, at HP = −120 mV, even a train of brief pulses (5 ms) produced a large degree of use-dependent block and this degree of block was enhanced by a train of longer pulses (300 ms), because at this holding potential, Na channels are partially in the inactivated state conformation. These results suggest that TYB-3823 has little effect on the Na channel in its activated state, but binds to the inactivated state, i.e., inactivated gate (state)-dependent block, resulting in block of I_{Na} due to a decrease in the number of channels available. Since TYB-3823 can be supposed to block inactivated channels with an affinity that is larger compared to that for the rested state channels, at depolarized holding potentials (where tonic block is marked and most channels are distributed between drug bound and unbound inactivated state) rapid train pulses can increase the fraction of inactivated state.

It is worthwhile to notice that the time course of both onset block and recovery from block was accelerated at more negative holding potentials while decreasing the degree of use-dependent block, and was accentuated at more positive holding potentials while increasing the degree of use-dependent block. Based on the guarded receptor hypothesis, the receptor site should lie within the channel lumen and the charged form of the drug would reach it from the pore. At more negative holding potentials, the access of drug molecules to the binding site could not be guarded by the inactivation gate. Under these conditions, the drug molecules could easily gain access to the binding site and could also easily leave the site, which might reflect on the fast kinetics of drug-receptor interaction, resulting in a decrease in the degree of use-dependent block due to a reduction in the time that the drug was present on the receptor. By contrast, at more positive holding potentials, the access of drug molecules to the binding site would be guarded by the inactivation gate. In this condition, the drug not only could hardly gain access to the binding site but also would have difficulty leaving the site, which might reflect on the slow (intermediate) kinetics of drug-receptor interaction, resulting in an enhanced degree of use-dependent block because of the longer time the drug was present on the receptor. Kodama *et al.* (1989) recently demonstrated that at a resting membrane potential of −90 mV, TYB-3823 should be regarded as an intermediate kinetic class 1 drug according to the scheme of Campbell (1988) using V_{max} of the action potential in multicellular preparations, which is in favour of our data at a more positive holding potential. However, at more negative holding potentials, this substance has been proposed as a fast kinetic Class 1 drug and assumed to have the characteristics of inactivated channel blockers rather than activated channel blockers. In summary, our results show that TYB-3823 is a potent blocker of Na current in guinea-pig ventricular myocytes. The magnitude of tonic and use-dependent block may be a major factor in the anti-arrhythmic efficiency in depolarized tissue in such conditions as ischaemia.

We appreciate the excellent secretarial assistance of Miss Keiko Iwata.

References

BEAN, B.P., COHEN, A.J. & TSIEN, R.W. (1983). Lidocaine block of sodium channels. *J. Gen. Physiol.*, **81**, 613–642.

CAMPBELL, T.J. (1988) Resting and rate-dependent depression of maximum rate of depolarization (V_{max}) in guinea pig ventricular action potentials by mexiletine, disopyramide, and encainide. *J. Cardiovasc. Pharmacol.*, **12**, 1273–1286.

COHEN, C.J., BEAN, B.P. & TSIEN, R.W. (1984). Maximal upstroke velocity as an index of available sodium conductance. Comparison of maximal upstroke velocity and voltage-clamp measurements of sodium current in rabbit Purkinje fibers. *Circ. Res.*, **54**, 636–651.

COLATSKY, T.J. & TSIEN, R.W. (1979) Sodium channels in rabbit cardiac Purkinje fibers. *Nature*, **278**, 265–268.

EHARA, T., MATSUOKA, S. & NOMA, A. (1989). Measurement of reversal potential of Na^+-Ca^{2+} exchange current in single guinea-pig ventricular cells. *J. Physiol.*, **410**, 227.

HAMIL, O.P., MARTY, A., NEHER, E., SAKMANN, B. & SIGWORTH, F.J. (1981). Improved patch-clamp techniques for high-resolution current recording from cells and cell-free membrane patches. *Pflügers Arch.*, **391**, 85–100.

HILLE, B. (1977). Local anesthesics: hydrophilic and hydrophobic pathways for the drug-receptor reaction. *J. Gen. Physiol.*, **69**, 497–515.

HISATOME, I., SATO, R., NISHIMURA, M. & SINGER, D.H. (1987). External proton blocks Na^+ current in isolated guinea-pig ventricular myocytes. *Circulation*, **76**, 110 (Abstract).

HISATOME, I., MATSUOKA, S., MIYAMOTO, J., SAWAGUCHI, M., OMODANI, K., OSAKI, S., KOTAKE, H., MASHIBA, H. & SATO, R. (1990). Blocking effect of 1389-S on the sodium current in isolated guinea-pig ventricular myocytes. *Eur. J. Pharmacol.*, **179**, 447–451.

HONDEGHEM, L.M. & KATZUNG, B.G. (1977). Time- and voltage-dependent interactions of antiarrhythmic drugs with cardiac sodium channels. *Biochem. Biophys. Acta*, **472**, 373–398.

KODAMA, I., MORIMOTO, M., TOYAMA, J. & SHIBATA, S. (1989). Electrophysiologic effects of TYB-3823, a new antiarrhythmic agent, on isolated guinea pig ventricular muscles. *J. Cardiovasc. Pharmacol.*, **13**, 616–623.

KURTHY, M., ROBLOCZY, G. & VARRO, A. (1985). New antiarrhythmic agent with positive cardiac actions (GYKI-38233). Advances in Pharmacological Research and Practice Proceedings, 4th Congress of the Hungarian Pharmacology Society, Budapest. Vol. 1, Pharmacology of the Vascular System, 2. pp. 211–215. Pergamon: Oxford.

MIYAMOTO, J., SATO, R., WASSERSTROM, J.A. & SINGER, D.H. (1989). Amiodarone shows strong resting block of cardiac I_{Na} after

removal of inactivation gate with chrolamine-T. *Biophys. J.*, **55**, 288a (Abstract).

POWELL, T., TERRAR, D.A. & TWIST, V.W. (1980). Electrical properties of individual cells isolated from adult rat ventricular myocardium. *J. Physiol.*, **302**, 131.

STARMER, C.F., GRANT, A.O. & STRAUSS, H.C. (1984). Mechanisms of use-dependent block of sodium channels in excitable membranes by local anesthetics. *Biophys. J.*, **46**, 15–27.

STIMERS, J.R., BEZANILLA, F. & TAYLOR, R.E. (1985). Sodium channel activation in the squid axon. Steady-state properties. *J. Gen. Physiol.*, **85**, 65–82.

TANGUY, J. & YEH, J.Z. (1988). Batrachotoxin uncouples gating charge immobilization from fast Na inactivation in squid giant axons. *Biophys. J.*, **54**, 719–730.

VARRO, A., REBLOCZKY, G., KUTHY, G.Y.M., JASZLISTS, L. & ERCZI, J. (1987). B-GYKI 38233—a new antifibrillatory agent with positive myocardial and coronary action. *Xth Congress of IUPHAR*, Sydney.

(Received August 30, 1990
Accepted May 1, 1991)

Br. J. Pharmacol. (1991), **104**, 31–38

Inhibition of the release of endothelium-derived relaxing factor *in vitro* and *in vivo* by dipeptides containing N^G-nitro-L-arginine

Christoph Thiemermann, Marina Mustafa, P. Achim Mester, Jane A. Mitchell, [1]Markus Hecker & John R. Vane

The William Harvey Research Institute, St. Bartholomew's Hospital Medical College, Charterhouse Square, London EC1M 6BQ

1 We have shown that dipeptides containing N^G-nitro-L-arginine (NO_2Arg) inhibit the biosynthesis of endothelium-derived relaxing factor (EDRF) *in vitro* and *in vivo*.

2 In anaesthetized rats, intravenous administration at 1–30 mg kg^{-1} of the methyl ester of NO_2Arg, NO_2-Arg-L-phenylalanine (NO_2Arg-Phe), L-alanyl-NO_2Arg (Ala-NO_2Arg) or NO_2Arg-L-arginine (NO_2Arg-Arg) produced dose-related increases in mean arterial blood pressure (MABP) which were unaffected by D-arginine (D-Arg; 20 mg kg^{-1} min^{-1} for 15 min), but prevented by co-infusions of L-arginine (L-Arg; 20 mg kg^{-1} min^{-1} for 15 min) or by their parent dipeptides.

3 NO_2Arg methyl ester, NO_2Arg-Phe methyl ester or Ala-NO_2Arg methyl ester (10 mg kg^{-1}, i.v.) also inhibited the reduction in MABP caused by the endothelium-dependent vasodilator, acetylcholine (30 μg kg^{-1} min^{-1} for 3 min), but not those induced by glyceryl trinitrate (20 μg kg^{-1} min^{-1} for 3 min) or iloprost (6 μg kg^{-1} min^{-1} for 3 min) which act directly on the vascular smooth muscle.

4 Moreover, NO_2Arg methyl ester, NO_2Arg-Phe methyl ester or NO_2Arg-Arg methyl ester (100 μM) inhibited the acetylcholine-induced relaxation of rabbit aortic strips, and NO_2Arg-Phe methyl ester (30 μM) blocked the stimulated (bradykinin, 30 pmol) release of EDRF from bovine aortic endothelial cells grown on microcarrier beads.

5 In endothelial cells grown in L-Arg-deficient medium, L-Arg-containing dipeptides such as L-Arg-L-Phe, L-Ala-L-Arg or L-Arg-L-Arg increased both the basal and stimulated release of EDRF. Moreover, the L-Arg containing dipeptides, but not their NO_2Arg analogues, were rapidly cleaved by these cells.

6 Thus, dipeptides containing NO_2Arg can directly interfere with the biosynthesis of EDRF *in vitro* and *in vivo*. Moreover, the potentiation of EDRF release from endothelial cells deprived of L-Arg by dipeptides containing L-Arg suggests that such peptides may serve as an additional or alternative substrate for the biosynthesis of EDRF.

Keywords: L-arginine; peptide(s); endothelium-derived relaxing factor; biosynthesis; haemodynamics; bioassay

Introduction

Endothelium-derived relaxing factor (EDRF), released from the vascular endothelium by a variety of stimuli, potently relaxes vascular smooth muscle (Furchgott, 1984) and inhibits platelet aggregation and adhesion (Azuma *et al.*, 1986; Radomski *et al.*, 1987) via stimulation of soluble guanylate cyclase in the target cell (Rapaport & Murad, 1983). Nitric oxide (NO; Palmer *et al.*, 1987) or possibly a closely related molecule, such as S-nitroso-L-cysteine (Myers *et al.*, 1990), accounts for the biological activity of EDRF. NO is formed via the oxidation of one of the guanidino nitrogens of the amino acid L-arginine (L-Arg). The enzymatic pathway for its biosynthesis in cytotoxic macrophages (Marletta *et al.*, 1988), endothelial (Palmer *et al.*, 1988; Mülsch *et al.*, 1989) and cerebellar cells (Bredt & Snyder, 1990) involves a NADPH- and calcium- or magnesium-dependent dioxygenase which catalyzes the conversion of L-Arg to L-citrulline (L-Cit) and NO. In addition to these cells, NO biosynthesis has also been ascribed to astrocytes (Murphy *et al.*, 1990), hepatocytes (Billiar *et al.*, 1990), mast cells (Salvemini *et al.*, 1990), platelets (Radomski *et al.*, 1990), polymorphonuclear leukocytes (Rimele *et al.*, 1988), vascular smooth muscle (Wood *et al.*, 1990), the central (Garthwaite *et al.*, 1988) and peripheral nervous system (Bult *et al.*, 1990), and the adrenal gland (Palacios *et al.*, 1989).

The L-Arg analogue, N^G-monomethyl-L-arginine (MeArg), is an inhibitor of the metabolism of L-Arg to nitrogen oxides in cytotoxic macrophages (Hibbs *et al.*, 1987; Iyenger *et al.*, 1987) and also prevents the release of EDRF from vascular endothelial cells (Rees *et al.*, 1989a; Sakuma *et al.*, 1988). Interestingly, MeArg may be a naturally occurring substance (Paik & Kim, 1975). MeArg also inhibits the formation of NO by cytosolic fractions from activated macrophages (Stuehr *et al.*, 1989), endothelial cells (Mülsch *et al.*, 1989) and rat forebrain tissues (Knowles *et al.*, 1989). The most striking biological effect of MeArg is its long lasting pressor effect in rabbits, rats or guinea-pigs (Rees *et al.*, 1989b; Whittle *et al.*, 1989; Aisaka *et al.*, 1989). This effect, together with its attenuation by L-Arg, but not D-Arg, suggests that a continuous, presumably flow-induced release of EDRF exerts a tonic vasodilator influence. The question whether this release is fundamentally different from the stimulated release induced by acetylcholine or bradykinin, is a matter of intense investigation, and has also been addressed in the present study.

Another L-Arg analogue, N^G-nitro-L-arginine (NO_2Arg) methyl ester, is also a potent inhibitor of EDRF biosynthesis *in vitro*, producing an L-Arg-reversible inhibition of the vasodilator effects of acetylcholine in rabbit aortic rings and the rat perfused mesentery (Moore *et al.*, 1989). NO_2Arg methyl ester also inhibits the release of EDRF from bovine aortic endothelial cells in culture (Ishii *et al.*, 1990). When compared to MeArg, NO_2Arg methyl ester is a more potent inhibitor of endothelium-dependent relaxations *in vitro* (Moore *et al.*, 1989; Ishii *et al.*, 1990; Hecker *et al.*, 1990a, Rees *et al.*, 1990), and produces a more pronounced and longer-lasting increase in blood pressure in the anaesthetized rat (Hecker *et al.*, 1990a; Rees *et al.*, 1990). These differences in potency may be partly due to the extensive metabolism by the endothelium of MeArg to L-Cit and subsequently to L-Arg, for NO_2Arg methyl ester is not metabolized in this way (Hecker *et al.*, 1990a).

Interestingly, L-Arg-containing peptides may be additional or alternative substrates for the biosynthesis of EDRF (Hecker *et al.*, 1990b). To explore further this possibility, we investigated the effects of three dipeptides,

[1] Author for correspondence.

NO_2Arg-L-phenylalanine (NO_2Arg-Phe) methyl ester, L-alanine-NO_2Arg (Ala-NO_2Arg) methyl ester and NO_2Arg-L-arginine (NO_2Arg-Arg) methyl ester, on (1) haemodynamic parameters in the anaesthetized rat, (2) the endothelium-dependent relaxation of rabbit isolated aortic strips, and (3) the release of EDRF from bovine aortic endothelial cells in culture. In addition, we have studied the metabolism of L-Arg-L-Phe, L-Ala-L-Arg and L-Arg-L-Arg and their NO_2Arg derivatives by cultured endothelial cells, and have investigated whether L-Arg-containing dipeptides can influence the release of EDRF from these cells or from an intact endothelium *in vitro* and *in vivo*.

Methods

Surgical procedure

Male Wistar rats (245–320 g; Glaxo Laboratories Ltd., Greenford, Middx.) were anaesthetized with thiopentone sodium (Trapanal; 120 mg kg^{-1}, i.p.). The trachea was cannulated to facilitate respiration and the rectal temperature was maintained at 37°C by means of a rectal probe connected to a homeothermic blanket (BioScience, Sheerness, Kent, U.K.). The right carotid artery was cannulated and connected to a Transamerica type 4-422-0001 pressure transducer for the measurement of phasic and mean arterial blood pressure and heart rate on a Grass model 7D polygraph recorder (Glass Instruments, Quincy, Mass., U.S.A.). The left jugular vein, the right femoral vein and the left femoral vein were cannulated for the administration of drugs.

Organ bath experiments

Male New Zealand White rabbits (2.0–2.6 kg) were anaesthetized with sodium pentobarbitone (Sagatal; 60 mg kg^{-1}, i.v.) and subsequently exsanguinated. The thoracic aorta was rapidly removed, cleared of adhering periadventitial fat and cut into rings of 5 mm width. The rings were cut open and mounted in 20 ml organ baths filled with warmed (37°C), oxygenated (95% O_2/5% CO_2) Krebs solution (pH 7.4) consisting of (mM): NaCl 118, KCl 4.7, KH_2PO_4 1.2, $MgSO_4$ 1.17, $CaCl_2$ 2.5, $NaHCO_3$ 25, glucose 5.6, EDTA 0.05 and indomethacin 0.006. Isometric force was measured with Biegestab K30 type 351 transducers (Hugo Sachs Elektonik, F.R.G.) and recorded on a Watanabe WRT 281 physiograph. A tension of 2 g was applied and the strips were equilibrated for 90 min, changing the Krebs solution every 15 min.

Endothelial cell culture

Endothelial cells were isolated from bovine aortae as previously described (de Nucci *et al.*, 1988). They were grown to confluence in plastic flasks for 5–7 days, removed by treatment with 0.05% (w/v) trypsin, seeded onto Cytodex-3 microcarrier beads (Pharmacia Ltd, Central Milton Keynes) and grown to confluence (5–7 days) in Dulbecco's modified Eagle's medium containing L-Arg (0.6 mM), 10% foetal calf serum, L-glutamine (4 mM), penicillin (500 iu ml^{-1}), streptomycin (500 μg ml^{-1}) and gentamycin (100 μg ml^{-1}). In experiments where the cells were cultured for 24 h in the absence of L-Arg, Minimum Essential Medium without L-Arg containing L-glutamine (2 mM) was used.

Superfusion bioassay cascade

Endothelial cells on beads (approximately 6×10^7 cells) were packed into a jacketed chromatography column and perfused at 5 ml min^{-1} with warmed (37°C) oxygenated (95% O_2/5% CO_2) Krebs solution containing superoxide dismutase (SOD, 10 units ml^{-1}) to stabilize EDRF and indomethacin (5.6 μM) to block the formation of cyclo-oxygenase products. The effluent from the column superfused a cascade (Vane, 1964) of four spirally cut, rabbit aortic strips with the endothelium removed (RbA) separated from the column by 1, 4, 7, and 10 s, respectively. All compounds tested were first infused over the assay tissues (o.t.) as a control and then through the column of endothelial cells (t.c.). The detector tissues were preconstricted by infusions of the stable thromboxane A_2 analogue U46619 (30 nM; 9,11-dideoxy-9$_\alpha$,11$_\alpha$-methanoepoxy-prostaglandin $F_{2\alpha}$) or phenylephrine (100 nM). Tissue lengths were detected by auxotonic levers attached to Harvard isotonic transducers and displayed on a six channel Watanabe recorder (type WR3101). The tissues were calibrated by the relaxant effects of glyceryl trinitrate (GTN), and the sensitivities adjusted electronically to give similar recordings of the relaxations.

High performance liquid chromatography (h.p.l.c.) analysis

The h.p.l.c. analysis of the endothelial cell amino acid content was performed as previously described (Hecker *et al.*, 1990a). Briefly, endothelial cells (3.5×10^6 cells/100 μl beads) were washed 5–10 times with 9 vol of Krebs solution, lysed by adding an excess of methanol (5:1, v/v), and then centrifuged for 10 min at 10,000 *g*. An aliquot (50 μl) of the supernatant was mixed with 50 μl of *o*-pthaldialdehyde reagent (Sigma, Poole, Dorset) for 1 min at room temperature, and 25 μl of this mixture were applied to a 250 × 4.6 mm (i.d.) Ultratechsphere ODS-5 h.p.l.c. column (HPLC Technology, Macclesfield) fitted with a 50 × 4.6 mm (i.d.) guard column. The column was eluted at ambient temperature by using a convex gradient (ACS model 352 ternary gradient system, setting 3) from 0% solvent A (100% methanol)/100% solvent B (10 mM KH_2PO_4/acetonitrile/methanol/tetrahydrofuran 84.0:7.5:7.5:1, v/v) to 100% solvent A/0% solvent B over 30 min followed by 100% solvent A for 5 min. The flow rate was set to 1 ml min^{-1} and the fluorescence of the eluate was continuously monitored (Waters model 420 fluorescence detector) at 425 nm (excitation wavelength 338 nm). The endogenous amino acids were identified by comparison with authentic standards, and their intracellular concentration was calculated by use of standard calibration curves and assuming an endothelial cell volume of 0.5 pl (Hecker *et al.*, 1990b).

Materials

NO_2Arg methyl ester, acetylcholine hydrochloride (ACh), noradrenaline, phenylephrine, superoxide dismutase (SOD) and the amino acids were obtained from Sigma Chemical Co. (Poole, Dorset). NO_2Arg-Phe methyl ester, Ala-NO_2Arg methyl ester, NO_2Arg-Arg methyl ester, L-Arg-L-Phe, L-Ala-L-Arg and L-Arg-L-Arg were obtained from Bachem Feinchemikalien AG (Bubendorf, Switzerland). The peptides were >98% pure, as judged by h.p.l.c. analysis, did not contain any contaminants active in the biological preparations used, and their L-Arg content was <0.1%. All other peptides were from either Bachem or Sigma. The purity of some of these peptides was also verified by h.p.l.c. analysis. Sodium pentobarbitone (Sagatal) was purchased from May & Baker (Dagenham) and sodium thiobarbitone (Trapanal) was from Byk Gulden (Konstanz, F.R.G.). GTN (Nitronal) was supplied by Lipha Pharmaceuticals Ltd. (West Drayton). Collagenase was obtained from Lorne Diagnostics (Suffolk) and trypsin, Minimum Essential Medium and Dulbecco's modified Eagle's medium were obtained from Flow Laboratories (Irvine, U.K.). Iloprost was a generous gift from Schering AG (Berlin, F.R.G.) and U46619 from Dr J. Pike (The Upjohn Company, Kalamazoo, U.S.A.). All other chemicals and solvents were obtained in the highest commercially available quality from either Sigma or BDH Ltd. (Dagenham).

Statistical comparison

All values in the figures and text are expressed as mean ± s.e.mean of *n* observations. A two-way analysis of

variance (ANOVA) or a two-tailed Student's t test were used to compare means among different groups and to analyse intragroup variation (Wallenstein *et al.*, 1980; SPSS Inc., Chicago, IL, U.S.A.). A P value of less than 0.05 was considered statistically significant.

Results

Effect of NO_2Arg-containing dipeptides in vivo

In anaesthetized rats (control data), the average values of mean arterial blood pressure (MABP) and heart rate were 123 ± 2 mmHg and 379 ± 9 beats min^{-1}, respectively (n = 68). As with NO_2Arg methyl ester itself, bolus i.v. injections of NO_2Arg-Phe methyl ester, Ala-NO_2Arg methyl ester or NO_2Arg-Arg methyl ester (1–30 mg kg^{-1}) induced dose-dependent increases in MABP (Figure 1) which reached maximum levels within 5–10 min. These pressor responses were long-lasting (see Table 1 for Ala-NO_2Arg methyl ester) and higher doses produced pressor responses of longer duration, e.g. Ala-NO_2Arg methyl ester at 10 mg kg^{-1} produced an increase in MABP lasting for 30–45 min as compared to an increase in MABP lasting for up to 2 h at a dose of 30 mg kg^{-1}. The pressor responses to all three dipeptides were not associated with a significant change in heart rate (data not shown). Ala-NO_2Arg methyl ester produced dose-related increases in MABP similar in maximum and duration to those of NO_2Arg-Phe methyl ester, whereas NO_2Arg-Arg methyl ester was slower in onset (data not shown) and at 30 mg kg^{-1} significantly less potent than Ala-NO_2Arg methyl ester or NO_2Arg-Phe methyl ester (P < 0.05; Figure 1). Moreover, in pithed rats Ala-NO_2Arg methyl ester (10 mg kg^{-1}) produced the same pressor effect (42 ± 2 mmHg; n = 3) as in the anaesthetized control group (48 ± 2 mmHg; n = 24).

Figure 2 summarizes the effects of L-Arg and D-Arg on the pressor responses obtained with NO_2Arg methyl ester, NO_2Arg-Phe methyl ester, Ala-NO_2Arg methyl ester or NO_2Arg-Arg methyl ester. Intravenous infusions of L-Arg (20 mg kg^{-1} min^{-1} for 15 min) had no effect on resting MABP (see Table 1), but significantly attenuated (70% inhibition; P < 0.001) the increases in MABP induced by NO_2Arg methyl ester (10 mg kg^{-1}), whereas D-Arg (20 mg kg^{-1} min^{-1} for 15 min) was without effect (Figure 2). Similarly, L-Arg infusions attenuated the pressor responses induced by NO_2Arg-Phe methyl ester, Ala-NO_2Arg methyl ester or NO_2Arg-Arg methyl ester (70, 63 and 81% inhibition, respectively; P < 0.001), whereas D-Arg was inactive.

Intravenous infusions of L-Arg-L-Phe, L-Ala-L-Arg or L-Arg-L-Arg (free acid form; 20 mg kg^{-1} min^{-1} for 15 min) did not cause a significant fall in MABP (see Table 1 for L-Ala-L-Arg). However, co-infusions of L-Ala-L-Arg or L-Arg-L-Arg completely prevented (4 ± 3 mmHg (n = 3) for L-Ala-L-Arg and 3 ± 2 mmHg (n = 3) for L-Arg-L-Arg) the increase in MABP induced by their NO_2Arg derivatives (48 ± 2 mmHg

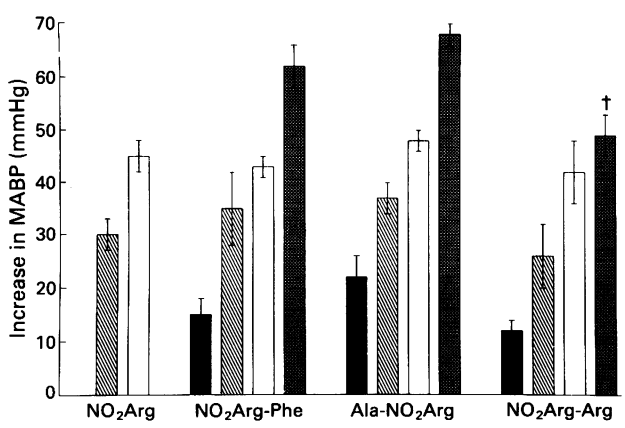

Figure 1 Effect of intravenous bolus injections of N^G-nitro-L-arginine methyl ester (NO_2Arg methyl ester), NO_2Arg-Phe methyl ester, Ala-NO_2Arg methyl ester or NO_2Arg-Arg methyl ester on mean arterial blood pressure (MABP) of anaesthetized rats. The figure depicts the increases in MABP induced by NO_2Arg methyl ester, NO_2Arg-Phe methyl ester, Ala-NO_2Arg methyl ester or NO_2Arg-Arg methyl ester at 1 mg kg^{-1} (solid columns; n = 3–4), 3 mg kg^{-1} (hatched columns; n = 4–17), 10 mg kg^{-1} (open columns; n = 7–24) and 30 mg kg^{-1} (cross-hatched columns; n = 3). † Significant difference (P < 0.05) between the effect of NO_2Arg-Arg methyl ester and NO_2Arg-Phe methyl ester or Ala-NO_2 methyl ester at 30 mg kg^{-1}.

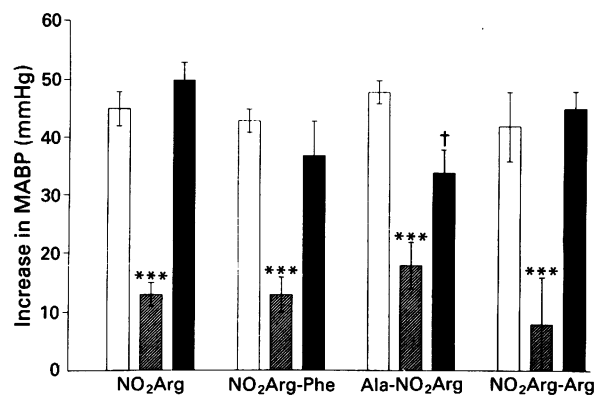

Figure 2 Attenuation by L-arginine (L-Arg), but not D-Arg, of the vasopressor effects of N^G-nitro-L-arginine methyl ester (NO_2Arg methyl ester), NO_2Arg-Phe methyl ester, Ala-NO_2Arg methyl ester or NO_2Arg-Arg methyl ester. The figure shows the increases in mean arterial blood pressure (MABP) following i.v. bolus injections of NO_2Arg methyl ester, NO_2Arg-Phe methyl ester, Ala-NO_2Arg methyl ester or NO_2Arg-Arg methyl ester at 10 mg kg^{-1} in the absence (open columns; n = 7–24) or presence of either L-Arg (20 mg kg^{-1} min^{-1} for 15 min i.v.; hatched columns; n = 3–8) or D-Arg (20 mg kg^{-1} min^{-1} for 15 min i.v.; solid columns; n = 3). ***Significant difference (P < 0.001) between infusions in the absence or presence of L-Arg; † significant difference (P < 0.05) between infusions in the presence or absence of D-Arg.

Table 1 Reversal of the pressor effect of L-alanyl-N^G-nitro-L-arginine methyl ester (Ala- NO_2Arg) by L-arginine (L-Arg) or L-alanyl-L-arginine (L-Ala-L-Arg)

		MABP (mmHg)					
Group	n	0 min	5 min	10 min	15 min	20 min	30 min
Ala-NO_2Arg	5	120 ± 4	157 ± 4	155 ± 5	156 ± 5	152 ± 4	144 ± 7
+ L-Arg	5	120 ± 3	160 ± 3	153 ± 5	137 ± 5*	126 ± 5*	125 ± 4*
+ L-Ala-L-Arg	5	124 ± 4	171 ± 7	163 ± 7	146 ± 3*	133 ± 4*	130 ± 6*
L-Arg	6	112 ± 7	110 ± 2	112 ± 3	110 ± 3	111 ± 3	117 ± 5
L-Ala-L-Arg	5	121 ± 9	124 ± 3	123 ± 3	121 ± 3	117 ± 3	117 ± 5

Changes in mean arterial blood pressure (MABP) in anaesthetized rats. Different groups of animals received: Ala-NO_2Arg (10 mg kg^{-1} i.v. at 0 min); Ala-NO_2Arg (10 mg kg^{-1} i.v. at 0 min) plus L-Arg-infusion (20 mg kg^{-1} min^{-1} i.v. for 15 min starting at 5 min); Ala-NO_2Arg (10 mg kg^{-1} i.v. at 0 min) plus L-Ala-L-Arg (20 mg kg^{-1} min^{-1} i.v. for 15 min starting at 5 min); L-Arg (20 mg kg^{-1} min^{-1} i.v. for 15 min starting at 5 min) or L-Ala-L-Arg (20 mg kg^{-1} min^{-1} i.v. for 15 min starting at 5 min).
* P < 0.05 when the MABP values of group 2 or 3 were compared to group 1 at the same time point.

($n = 24$) for Ala-NO_2Arg and 42 ± 6 mmHg ($n = 7$) for NO_2Arg-Arg at 10 mg kg^{-1}, respectively). These two dipeptides (see Table 1 for L-Ala-L-Arg) as well as L-Arg also reversed established pressor responses caused by their NO_2Arg derivatives (Table 1). Similar experiments with L-Arg-L-Phe were complicated by the fact that L-Arg-L-Phe is a potent pressor peptide in the anaesthetized rat at doses as low as 10 μg kg^{-1}, causing a simultaneous increase in MABP and heart rate (Thiemermann *et al.*, 1991). None the less L-Arg-L-Phe (20 mg kg^{-1} for 15 min) reversed the increase in MABP induced by NO_2Arg-Phe methyl ester (10 mg kg^{-1}).

Successive infusions (3 min) of the endothelium-dependent vasodilator acetylcholine (ACh; 30 μg kg^{-1} min^{-1} at -10, 5, 15, 30, 45 and 60 min) induced a fall in MABP which was reproducible during the 60 min experimental protocol ($n = 4$, data not shown). Pretreatment with NO_2Arg methyl ester, NO_2Arg-Phe methyl ester or Ala-NO_2Arg methyl ester (10 mg kg^{-1}) significantly inhibited the fall in MABP induced by ACh (Figure 3) with a maximum suppression 15 min after application of the inhibitor ($P < 0.05$ at 5, 15, 30 and 45 min; data not shown). In contrast, NO_2Arg methyl ester, NO_2Arg-Phe methyl ester or Ala-NO_2Arg methyl ester did not inhibit the decrease in MABP caused by the endothelium-independent vasodilator GTN (20 μg kg^{-1} min^{-1} for 3 min) and potentiated the hypotensive effect of iloprost (6 μg kg^{-1} min^{-1} for 3 min; $P < 0.01$; Figure 3).

Endothelium-dependent relaxations in vitro

Incubations of rabbit aortic strips with NO_2Arg methyl ester, NO_2Arg-Phe methyl ester or NO_2Arg-Arg methyl ester (all at 100 μM) had no effect on the resting tone of the tissues. When untreated tissues were preconstricted with noradrenaline, ACh produced a concentration-dependent relaxation (EC_{50} 90 ± 7 nM; $n = 35$), and a further contraction at concentrations exceeding 1 μM. Preincubations with NO_2Arg methyl ester (100 μM for 20 min) then caused a decrease in the maximum relaxation to ACh from 69 ± 6 to $18 \pm 6\%$ ($n = 4$; $P < 0.001$), representing a $72 \pm 10\%$ inhibition. Relaxations to ACh were not restored after removal of the inhibitor and 3 consecutive 15 min incubations with fresh Krebs solution. However, addition of L-Arg (1 mM), but not D-Arg ($n = 4$), to the Krebs solution (3 consecutive 15 min incubations), reversed the inhibitory effect of NO_2Arg methyl ester ($n = 4$; $P < 0.01$), so that relaxations to ACh were not significantly different from control responses. In control tissues the three consecutive dose-response curves for ACh were identical and not altered by additions of L-Arg or D-Arg (data not shown).

Similarly, NO_2Arg-Phe methyl ester (100 μM for 20 min) produced a significant inhibition of the relaxant effects of ACh. The EC_{50} for ACh was shifted by a factor of 12.5 from 80 nM to 1 μM, and the maximum relaxation to ACh was reduced from $89 \pm 3\%$ to $58 \pm 11\%$ ($n = 21$; $P < 0.001$). L-Arg (1 mM; 3 consecutive 15 min incubations) reversed the inhibitory effect of NO_2Arg-Phe methyl ester ($n = 6$; $P < 0.01$; Figure 4a), whereas D-Arg did not ($n = 4$). In contrast to the inhibition of endothelium-dependent relaxations, NO_2Arg-Phe methyl ester (100 μM for 20 min) did not affect the endothelium-independent relaxations induced by GTN (0.2–9 nM; $n = 3$; data not shown).

When compared to NO_2Arg methyl ester or NO_2Arg-Phe methyl ester, NO_2Arg-Arg methyl ester (100 μM for 20 min)

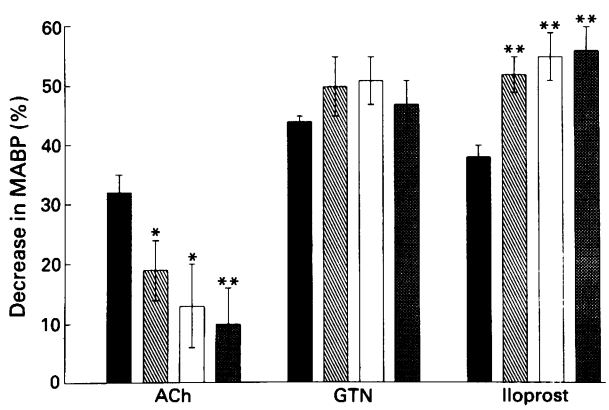

Figure 3 Effect of N^G-nitro-L-arginine methyl ester (NO_2Arg methyl ester), NO_2Arg-Phe methyl ester or Ala-NO_2Arg methyl ester on the vasodilator responses to acetylcholine (ACh; 30 μg kg^{-1} min^{-1} for 3 min), glyceryl trinitrate (GTN; 20 μg kg^{-1} min^{-1} for 3 min) or iloprost (6 μg kg^{-1} min^{-1} for 3 min). The figure depicts the decreases in MABP of $n = 5$ experiments in the absence (solid columns) or presence of NO_2Arg methyl ester (hatched columns), NO_2Arg-Phe methyl ester (open columns) or Ala-NO_2Arg methyl ester (cross-hatched columns). The inhibitors were injected as a bolus (10 mg kg^{-1}) 15 min before the vasodilator was infused intravenously. Significant differences, * $P < 0.05$ or ** $P < 0.01$, from control experiments.

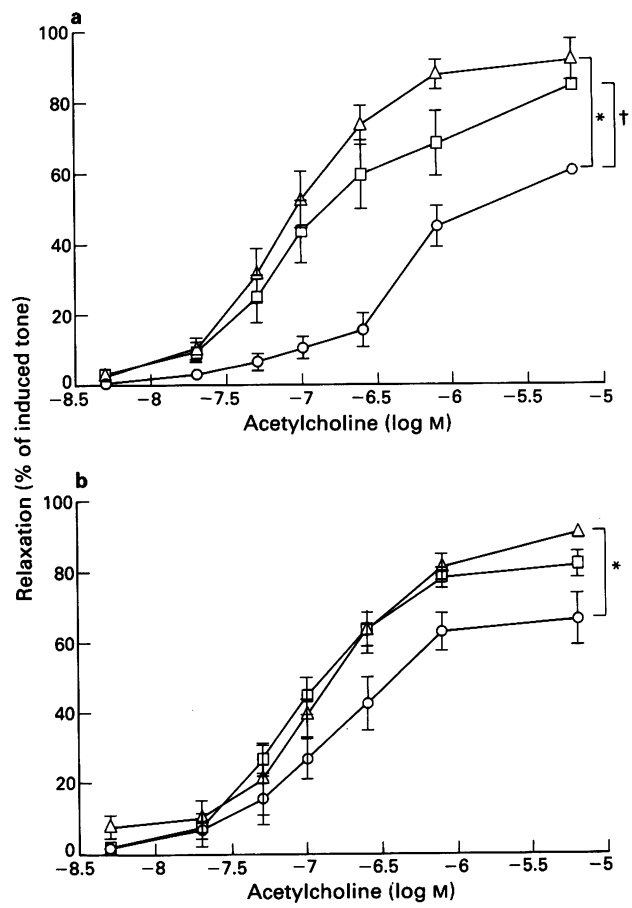

Figure 4 Inhibition by (a) N^G-nitro-L-arginine-L-phenylalanine methyl ester (NO_2Arg-Phe methyl ester) or (b) NO_2Arg-Arg methyl ester of the endothelium-dependent relaxation of rabbit aortic strips. The tissues were preconstricted with noradrenaline (10–20 nM) to approximately 1 g of tension and a cumulative dose-response curve to acetylcholine (ACh; 6 nM–6 μM; △) was constructed. The NO_2Arg-containing dipeptides (100 μM) were added 20 min before the construction of a second dose-response curve to ACh (○). After removal of the inhibitor, the tissues were incubated three times with L-Arg (1 mM) for 15 min followed by a third dose-response curve to ACh (□). The figure shows the mean changes in tension with s.e.mean (vertical bars) (expressed as % relaxation of induced tone) $n = 4$–5 experiments with aortic strips from different rabbits. * and † denote significant differences (by two-way analysis of variance) between the relaxant effects of ACh in the presence or absence of NO_2Arg-Phe methyl ester ($P < 0.001$) or NO_2Arg-Arg methyl ester ($P < 0.05$) and between the inhibitory activity of NO_2Arg-Phe methyl ester in the presence or absence of L-Arg ($P < 0.01$), respectively.

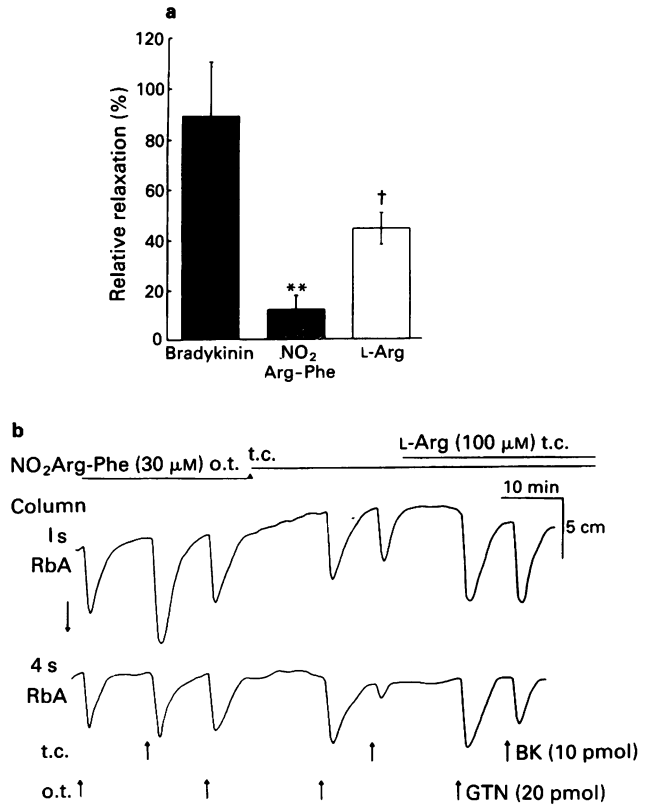

Figure 5 N^G-nitro-L-arginine-L-phenylalanine methyl ester (NO_2-Arg-Phe methyl ester) inhibits the release of EDRF from cultured endothelial cells as detected by the cascade bioassay. For experimental details refer to Methods. In (a) is shown the relaxation of the detector tissues (expressed as % relaxation relative to the response caused by glyceryl trinitrate) induced by bradykinin (BK; 10 pmol) in $n = 3$ experiments using different batches of endothelial cells. The solid column shows responses in the absence of NO_2Arg-Phe methyl ester (30 μM t.c.), the hatched column in the presence of NO_2Arg-Phe methyl ester, and the open column in the presence of both NO_2Arg-Phe methyl ester and L-Arg (100 μM) ** and † denote significant differences between NO_2Arg-Phe methyl ester and control ($P < 0.01$) and NO_2Arg-Phe methyl ester and L-Arg ($P < 0.05$). (b) An original trace of two rabbit aortic strips (RbA) separated from the column of endothelial cells by 1 and 4 s, respectively. Glyceryl trinitrate (GTN; 20 pmol) was given as a bolus injection over the detector tissues (o.t.) to calibrate their responses to EDRF released by BK (10 pmol) infused through the column of endothelial cells (t.c.). Note, that when infused o.t., NO_2Arg-Phe methyl ester (30 μM) had no effect on the tone of the detector tissues and did not interfere with the detection of EDRF, but elicited an increase in tone of the first RbA when infused t.c., indicating a reduction in the flow-induced release of EDRF. This effect was reversed by co-infusions of L-Arg (100 μM).

caused a weak but significant inhibition of the relaxation induced by ACh (23 ± 3% inhibition of the maximum relaxation to ACh; $n = 10$; Figure 4b), reducing its activity by about 2 fold (EC_{50} for ACh increased from 100 nM to 200 nM; $n = 10$; $P < 0.05$). This effect was completely reversed by L-Arg (1 mM; 3 consecutive 15 min incubations; $n = 3$), but not by D-Arg (1 mM; 3 consecutive 15 min incubations; $n = 6$). In contrast to L-Arg (0.001–10 mM), the parent dipeptides, L-Arg-L-Phe, L-Ala-L-Arg or L-Arg-L-Arg (free acid form) caused significant relaxations of the rabbit aortic strips at concentrations above 100 μM, which, however, were not strictly endothelium-dependent (data not shown).

EDRF release from cultured endothelial cells

Infusions of NO_2Arg-Phe methyl ester (30 μM) over the detector tissues in the cascade (o.t.) did not affect the relaxations induced by GTN (20 pmol; o.t.) or by EDRF released after injections of bradykinin (BK; 10 pmol) through the column of endothelial cells (t.c.) ($n = 4$; Figure 5b). When infused t.c., however, NO_2Arg-Phe methyl ester elicited an increase in tone of the aortic strips which was greatest on the first RbA (denoting a reduction in flow-induced EDRF release) and significantly inhibited the release of EDRF induced by BK (86% inhibition from 90 ± 21% relaxation to 12 ± 6%; $n = 3$; $P < 0.01$; Figure 5a). Co-infusions of L-Arg (100 μM) partially reversed the inhibitory effect of NO_2Arg-Phe methyl ester (50% inhibition from 90 ± 21% relaxation to 44 ± 6%; $n = 3$; $P < 0.05$). These effects of NO_2Arg-Phe methyl ester were similar to those produced by NO_2Arg methyl ester (Hecker *et al.*, 1990a).

In 28 of 31 experiments (i.e. 90%) with endothelial cells cultured for 24 h in the absence of L-Arg, dipeptides containing L-Arg, such as L-Arg-L-Phe ($n = 14$), L-Ala-L-Arg ($n = 6$), L-Arg-L-Arg ($n = 6$), L-Arg-L-Ile ($n = 3$) or L-Arg-L-Leu ($n = 2$) (all at 50 μM; free acid or methyl ester form) increased the flow-induced release of EDRF, and in 9 of 20 experiments (i.e. 45%) also the bradykinin-stimulated release of EDRF (data not shown). In addition L-Arg but not D-Arg (50 μM), to a similar extent as the dipeptides, potentiated the stimulated release of EDRF from L-Arg-depleted endothelial cells in 11 of 19 experiments (i.e. 58%), increased flow-induced EDRF release in 6 of 19 experiments (i.e. 32%), and had no effect in 2 experiments (data not shown).

Table 2 Metabolism of L-alanyl-N^G-nitro-L-arginine methyl ester (Ala-NO_2Arg methyl ester), NO_2Arg-Arg methyl ester or NO_2Arg-Phe methyl ester by cultured endothelial cells

	Net increase in intracellular L-Arg or NO_2Arg (μM)		
Dipeptide	10 min	30 min	60 min
L-Ala-L-Arg	1618 ± 308	2513 ± 532	3715 ± 1281
Ala-NO_2Arg[1]	334 ± 186*	1064 ± 494	1057 ± 194*
L-Arg-L-Arg	633 ± 18	1519 ± 93	2249 ± 218
NO_2Arg-Arg[1]	15 ± 9***	91 ± 25***	129 ± 17***
L-Arg-L-Phe	419 ± 88	1564 ± 188	2378 ± 180
NO_2Arg-Phe[1]	23 ± 16**	286 ± 143**	566 ± 102***

The NO_2Arg derivatives or their parent dipeptides (100 μM) were incubated with endothelial cells deprived of L-Arg (7×10^6 cells on 200 μl microcarrier beads in 1 ml Krebs solution) for 0, 10, 30 or 60 min at 37°C followed by h.p.l.c. analysis. NO_2Arg (free acid or methyl ester form) could not be detected by the fluorescence method employed. Therefore, its concentration has been inferred from the parallel increase in L-Ala, L-Arg or L-Phe, respectively. The table shows the mean (±s.e.mean) increases in L-Arg or NO_2Arg after subtraction of the corresponding time control levels. The asterisks denote NO_2Arg levels (NO_2Arg derivative) significantly different ($P < 0.05$, 0.01 or 0.001) from the corresponding L-Arg concentrations (parent dipeptide).
($n = 3$; * $P < 0.05$; ** $P < 0.01$; *** $P < 0.001$; [1]methyl ester)

Metabolism of dipeptides containing L-Arg and their NO_2Arg derivatives by bovine aortic endothelial cells

When L-Arg-L-Phe (100 μM) was incubated with Arg-depleted endothelial cells in Krebs solution, there was a rapid, time-dependent increase in both L-Arg and L-Phe. The cleavage of the dipeptide was completely prevented by co-incubations with a mixture of protease inhibitors (bestatin and phosphoramidon, 5 μg ml^{-1}; amastatin, aprotinin, captopril, leupeptin and trypsin-chymotrypsin inhibitor, 50 μg ml^{-1}; phenylmethylsulphonyl fluoride, 0.5 mM; data not shown). When compared to L-Arg-L-Phe, L-Phe was liberated from NO_2Arg-Phe methyl ester at a significantly slower rate ($P < 0.01$ at 10 and 30 min; $P < 0.001$ at 60 min; Table 2). L-Ala-L-Arg (100 μM) was more rapidly cleaved than L-Arg-L-

Phe ($P < 0.05$ at 10 and 30 min), whereas L-Arg-L-Arg (100 μM) was metabolized at virtually the same rate (Table 2). In contrast, the metabolism of NO_2Arg-Arg methyl ester was considerably slower than that of NO_2Arg-Phe methyl ester ($P < 0.01$ at 60 min) or Ala-NO_2Arg methyl ester ($P < 0.01$ at 10, 30 and 60 min). When compared to NO_2Arg-Phe methyl ester (net increase in NO_2Arg after 10 min 23 $\pm$ 16 μM; $n = 3$) or NO_2Arg-Arg methyl ester (15 $\pm$ 9 μM after 10 min; $n = 3$), the cleavage of Ala-NO_2Arg methyl ester led to a more rapid liberation of NO_2Arg (334 $\pm$ 187 μM after 10 min; $n = 3$).

Discussion

The inhibition by MeArg of the biosynthesis of EDRF/NO by vascular endothelial cells *in vitro* (Rees *et al.*, 1989a; Sakuma *et al.*, 1988) is associated with a sustained rise in systemic blood pressure in anaesthetized rabbits (Rees *et al.*, 1989b), guinea-pigs (Aisaka *et al.*, 1990) and rats (Whittle *et al.*, 1989; Tolins *et al.*, 1990; Walder *et al.*, 1990) and conscious rats *in vivo* (Gardiner *et al.*, 1990). The MeArg-induced rise in blood pressure in the rat is associated with a decrease in glomerular filtration rate and urinary guanosine 3';5'-cyclic monophosphate (cyclic GMP) excretion (Tolins *et al.*, 1990) as well as a reduced conductance in the renal, mesenteric, carotid and hindquarter vascular beds (Gardiner *et al.*, 1990). In human volunteers, infusion of MeArg into the brachial artery or dorsal vein inhibits the vasodilator responses to ACh and bradykinin, but not GTN (Vallance *et al.*, 1989). Although MeArg reduces the blood flow in the brachial artery by approximately 40%, it does not cause vasoconstriction in the dorsal vein, suggesting that a continuous release of NO regulates vascular tone in the arterial, but not in the venous part of the human circulation (Vallance *et al.*, 1989). The pressor effect of MeArg and its reversal by L-Arg, but not D-Arg, form the basis of the hypothesis that a continuous or flow-induced release of NO, derived from the metabolism of L-Arg, maintains the vasculature of several species including man in a vasodilated state (Rees *et al.*, 1989b).

NO_2Arg methyl ester is a more potent inhibitor of EDRF/NO biosynthesis than MeArg *in vitro* (Moore *et al.*, 1989; Rees *et al.*, 1990) and *in vivo* (Hecker *et al.*, 1990a; Walder *et al.*, 1990; 1991; Gardiner *et al.*, 1990). These differences in potency between MeArg and NO_2Arg methyl ester may be due to (1) a faster uptake of NO_2Arg by the endothelium (methyl ester instead of free acid form); (2) a higher affinity of the NO_2Arg derivative for EDRF/NO-synthase; and/or (3) differences in metabolism of both L-Arg analogues by the endothelium. Indeed, we have previously demonstrated (Hecker *et al.*, 1990a) that MeArg, but not NO_2Arg methyl ester, is substantially metabolised by cultured endothelial cells to L-Cit and subsequently to L-Arg, which both in turn would reduce the degree of inhibition of the NO-forming enzyme(s) afforded by MeArg.

Here we demonstrate that the methyl esters of NO_2Arg-Phe, Ala-NO_2Arg or NO_2Arg-Arg are novel and potent inhibitors of EDRF/NO biosynthesis *in vitro* and *in vivo*. For example NO_2Arg-Phe methyl ester fits the following criteria for an inhibitor of EDRF/NO biosynthesis: (1) it inhibited the basal and bradykinin-stimulated release of EDRF from cultured endothelial cells in an L-Arg-reversible manner; (2) it inhibited the endothelium-dependent, but not endothelium-independent, vasodilator responses *in vitro* and *in vivo* and these effects were again reversed by L-Arg; and (3) intravenous application of NO_2Arg-Phe methyl ester to anaesthetized rats produced a dose-related increase in blood pressure which was prevented by co-infusions of L-Arg, but not D-Arg.

Likewise, Ala-NO_2Arg methyl ester and NO_2Arg-Arg methyl ester caused dose-related pressor effects in the anaesthetized rat which were largely prevented by coinfusions of L-Arg, but not D-Arg. Moreover, infusions of the parent dipeptides L-Ala-L-Arg or L-Arg-L-Arg did not exert any haemodynamic effects in the anaesthetized rat, but completely prevented the pressor effects of the NO_2Arg derivatives. Even when given after the pressor effect was already established, L-Arg or the parent dipeptides reduced the elevated blood pressure so that baseline values were obtained within 15–20 min. This was also true for NO_2Arg-Phe methyl ester; however, attempts to prevent its pressor effect by co-infusions of L-Arg-L-Phe were hampered by the finding that L-Arg-L-Phe itself increased blood pressure and heart rate in the anaesthetized rat by enhancing plasma noradrenaline levels via a central mechanism (Thiemermann *et al.*, 1991).

These results demonstrate that NO_2Arg-containing dipeptides are novel inhibitors of EDRF/NO biosynthesis *in vitro* and *in vivo*. The fact that the methyl esters of NO_2Arg-Phe, Ala-NO_2Arg and NO_2Arg-Arg produce a substantial increase in mean arterial blood pressure in the anaesthetized rat supports the hypothesis that a continuous flow-induced release of NO, derived from the L-Arg/NO pathway in the endothelium, is of substantial importance for the physiological regulation of vascular tone and, hence, blood pressure.

Although there is some evidence that MeArg may produce its pressor effect in the anaesthetized rat by causing a central activation of the sympathetic nervous system (Sakuma *et al.*, 1990), it seems unlikely that the pressor effects of either NO_2Arg methyl ester or the NO_2Arg-containing dipeptides are brought about by a central effect, for the pressor responses to NO_2Arg methyl ester (P.K. Moore, personal communication) or Ala-NO_2Arg methyl ester (this study) were not reduced in pithed rats.

The similarities between NO_2Arg methyl ester and the NO_2Arg-containing dipeptides as inhibitors of NO-biosynthesis raises the question as to whether these dipeptides act in their own right or after cleavage to NO_2Arg. When compared to L-Arg-L-Arg, the cleavage of NO_2Arg-Arg methyl ester by Arg-depleted, cultured endothelial cells was slow and a significant intracellular concentration of NO_2Arg, i.e. 100 μM was attained only after 30–60 min. Thus, the release of NO_2Arg from NO_2Arg-Arg methyl ester does not appear to account for its inhibitory activity *in vitro*. This conclusion is reinforced by our findings that cultured endothelial cells spontaneously generate 150–750 μM intracellular L-Arg within 30–60 min which would compete with any NO_2Arg cleaved from the peptide (Hecker *et al.*, 1990a,b). Freshly isolated, rabbit aortic endothelial cells have an even higher level of L-Arg (4 mM; Swierkosz *et al.*, 1990). The potent pressor effect of NO_2Arg-Arg methyl ester *in vivo* compared to its rather weak effect on EDRF release *in vitro*, however, suggests that some cleavage to the more active NO_2Arg is occurring *in vivo*.

In contrast to NO_2Arg-Arg methyl ester, the inhibitory potency of NO_2Arg-Phe methyl ester appears to be equivalent *in vitro* and *in vivo*. NO_2Arg-Phe methyl ester is a more potent inhibitor of the release of EDRF from the rabbit aorta and a more potent vasopressor agent than MeArg *in vivo*, but both compounds are equally effective in inhibiting the release of EDRF from cultured endothelial cells. However, the uptake of exogenous MeArg (40 μM) by these cells leads to an intracellular accumulation of approximately 3 mM MeArg within 10 min (Hecker *et al.*, 1990a), whereas the cleavage of NO_2Arg-Phe methyl ester (100 μM outside the cell) results only in the formation of about 20 μM NO_2Arg inside the cell over the same period of time. This strongly suggests that NO_2Arg-Phe methyl ester directly inhibits the biosynthesis of EDRF/NO *in vitro* and probably also *in vivo*.

Unlike NO_2Arg-Phe methyl ester or NO_2Arg-Arg methyl ester, the inhibitory activity of Ala-NO_2Arg methyl ester *in vivo* and *in vitro* may be associated with its breakdown to NO_2Arg, for this was much more rapid *in vitro* (see Table 2). Moreover, our findings cannot rule out the possibility that NO_2Arg-Arg methyl ester or NO_2Arg-Phe methyl ester are cleaved by cells other than endothelial cells while circulating in the blood or when passing through metabolically active organs such as the lung of the liver. Our present data on the

metabolism of these peptides, however, could also be interpreted as indicating that a NO_2Arg-containing dipeptide with a hydrophobic residue such as NO_2Arg-Phe is a better fit for the active site of EDRF/NO synthase and, hence, may be protected from proteolytic cleavage, whereas the other two analogues (alkyl or basic residue) cannot avidly bind to the enzyme and exert their inhibitory activity via breakdown to NO_2Arg.

The di-oxygenase-like enzymes responsible for the biosynthesis of NO exist in at least two distinct forms (see Nathan & Stuehr, 1990), both of which require NADPH and a divalent cation (calcium or magnesium) as a co-factor. The so-called 'constitutive' type is present in endothelial, cerebellar and polymorphonuclear cells and can synthesize NO in a matter of seconds following stimulation by agonists such as bradykinin, N-methyl-D-aspartate or formyl-methionyl-leucyl-phenylalanine. In contrast, the 'inducible' type can be expressed in endothelial cells, hepatocytes, macrophages, monocytes or tumour cells after 4–18 h following activation of the cell with cytokines, tumour necrosis factor or bacterial lipopolysaccaride. MeArg is a more potent inhibitor of the 'inducible' enzyme (Nathan & Stuehr, 1990; Gross *et al.*, 1990), whereas NO_2Arg methyl ester is a more potent inhibitor of the 'constitutive' enzyme (Moore *et al.*, 1989; Ishii *et al.*, 1990; Hecker *et al.*, 1990a; Nathan & Stuehr, 1990). The NO_2Arg-containing dipeptides, in particular NO_2Arg-Phe methyl ester, have a similar inhibitory profile to that of NO_2Arg methyl ester and are likely to be effective inhibitors of the 'constitutive' enzyme present in endothelial cells.

The inhibition by these NO_2Arg-containing dipepetides of the release of EDRF *in vitro* in conjunction with the potentiating effect of their parent dipeptides on the release of EDRF from endothelial cells deficient in L-Arg may be interpreted as indicating that an L-Arg containing small peptide can serve as an additional or alternative substrate for the biosynthesis of EDRF/NO. On the basis of the present findings, however, it is difficult to ascertain whether the ability of the parent dipeptides to reverse the blockade of EDRF production or to enhance EDRF release does not require their hydrolysis to L-Arg. None the less, one such peptide, L-Arg-L-Asp, has been shown to be a substrate for the biosynthesis of NO by cytotoxic macrophages (Iyengar *et al.*, 1987), endothelial cell homogenates, cerebellar cells and neutrophils (see Collier & Vallance, 1989). Moreover, endothelial cells contain both the 'constitutive' and the 'inducible' form of EDRF/NO synthase (Kilbourn & Belloni, 1990; Nathan & Stuehr, 1990), and the generation of L-Arg by L-Arg-deprived endothelial cells is associated with an increase in stimulated but not flow-induced EDRF release (Mitchell *et al.*, 1990). It is, therefore, tempting to speculate that biosynthesis of EDRF under flow conditions is catalyzed by an enzyme similar to that in macrophages using an L-Arg-containing peptide as a substrate, whereas the agonist-triggered EDRF formation requires free L-Arg. Although this hypothesis needs to be explored further, our present findings and those mentioned above (see Collier & Vallance, 1989) suggest that the substrate specificity of the EDRF/NO synthase in endothelial cells is not necessarily restricted to L-Arg .

In conclusion, the novel peptidyl inhibitors of EDRF/NO biosynthesis may not only be helpful in clarifying the possibly divergent pathways of its formation *in vitro*, but should also be useful tools for elucidating the physiological and pathophysiological significance of this autacoid *in vivo*.

The authors are indebted to Hayley J. Harris for her help with the organ bath studies, Ivana Vojnovic and Desmond T. Walsh for supporting the h.p.l.c measurements, and Elisabeth G. Wood for the constant supply of cultured endothelial cells. This work was supported by a grant from Glaxo Group Research Ltd.

References

AISAKA, K., GROSS, S.S., GRIFFITH, O.W. & LEVI, R. (1989). N^G-methylarginine, an inhibitor of endothelium-derived nitric oxide synthesis, is a potent pressor agent in the guinea-pig: does nitric oxide regulate blood pressure *in vivo*? *Biochem. Biophys. Res. Commun.*, **160**, 881–885.

AZUMA, H., ISHIKAWA, M. & SEKIZAKI, S. (1986). Endothelial-dependent inhibition of platelet aggregation. *Br. J. Pharmacol.*, **97**, 411–415.

BILLIAR, T.R., CURREN, R.D., STUEHR, D.J., STADLER, J., SIMMONS, R.L. & MURRAY, S.A. (1990). Inducible cytosolic enzyme activity for the production of nitrogen oxides from L-arginine in hepatocytes. *Biochem. Biophys. Res. Commun.*, **168**, 1034–1040.

BREDT, D.A. & SNYDER, S.H. (1990). Isolation of nitric oxide synthetase, a calmodulin-requiring enzyme. *Proc. Natl. Acad. Sci. U.S.A.*, **87**, 682–685.

BULT, H., BOECKXSTAENS, G.E., PELCKMANS, P.A., JORDAENS, F.H., VAN MAERCKE, Y.M. & HERMAN, A.G. (1990). Nitric oxide as an inhibitory non-adrenergic non-cholinergic neurotransmitter. *Nature*, **345**, 346–347.

COLLIER, J. & VALLANCE, P. (1989). Second messenger role for NO widens to nervous and immune system. *Trends. Pharmacol. Sci.* **10**, 427–431.

DE NUCCI, G., GRYGLEWSKI, R.J., WARNER, T.D. & VANE, J.R. (1988). Receptor mediated release of endothelium-derived relaxing factor and prostacyclin from bovine endothelial cells is coupled. *Proc. Natl. Acad. Sci. U.S.A.*, **85**, 2334–2337.

FURCHGOTT, R.F. (1984). The role of endothelium in the responses of vascular smooth muscle to drugs. *Annu. Rev. Pharmacol. Toxicol.*, **24**, 175–197.

GARDINER, S.M., COMPTON, A.M., KEMP, P.A. & BENNETT, T. (1990). Regional and cardiac haemodynamic effects of N^G-nitro-L-arginine methyl ester in conscious Long Evans rats. *Br. J. Pharamcol.*, **101**, 625–631.

GARTHWAITE, J., CHARLES, S.L. & CHESS-WILLIAMS, R. (1988). Endothelium-derived relaxing factor release on activation of NMDA receptors suggests a role as intracellular messenger in the brain. *Nature*, **336**, 385–388.

GROSS, S.S., STUEHR, D.J., AISAKA, K., JAFFE, E.A., LEVI, R. & GRIFFITH, O.W. (1990). Macrophage and endothelial cell nitric oxide synthesis: Cell-type selective inhibition by N^G-aminoarginine, N^G-nitroarginine and N^G-methylarginine. *Biochem. Biophys. Res. Commun.*, **170**, 96–103.

HECKER, M., MITCHELL, J.A., HARRIS, H.J., KATSURA, M., THIEMERMANN, C. & VANE, J.R. (1990a). Endothelial cells metabolize N^G-monomethyl-L-arginine to L-citrulline and subsequently to L-arginine. *Biochem. Biophys. Res. Commun.*, **167**, 1037–1043.

HECKER, M., SESSA, W.C., HARRIS, H.J., ÄNGAARD, E.E. & VANE, J.R. (1990b). The metabolism of L-arginine and its significance for EDRF biosynthesis: Cultured endothelial cells recycle L-citrulline to L-arginine. *Proc. Natl. Acad. Sci. U.S.A.*, **87**, 8612–8616.

HIBBS, J.B., TAITOR, R.R. & VAVRIN, Z. (1987). Macrophage cytotoxicity: role for L-arginine deiminase and imino nitrogen oxidation to nitrite. *Science*, **235**, 473–475.

ISHII, K., CHANG, B., KERWIN, J.F., HUANG, Z. & MURAD, F. (1990). N^G-nitro-L-arginine: a potent inhibitor of endothelium-derived relaxing factor formation. *Eur. J. Pharmacol.*, **176**, 219–223.

IYENGER, R., STUEHR, D.J. & MARLETTA, M.A. (1987). Macrophage synthesis of nitric oxide, nitrate, and N-nitrosamines: precursors and role of the respiratory burst. *Proc. Natl. Acad. Sci. U.S.A.*, **84**, 6369–6373.

KILBOURN, R.G. & BELLONI, P. (1990). Endothelial cell production of nitrogen oxides in response to interferon in combination with tumor necrosis factor, interleukin-1, or endotoxin. *J. Natl. Cancer Inst.*, **82**, 772–776.

KNOWLES, R.G., PALACIOS, M., PALMER, R.M.J. & MONCADA, S. (1989). Formation of nitric oxide from L-arginine in the CNS: a transduction mechanism for the stimulation of the soluble guanylate cyclase. *Proc. Natl. Acad. Sci. U.S.A.*, **86**, 5159–5162.

MARLETTA, M.A., YOON, P.A., IYENGAR, R., LEAF, C.D. & WISHNOK, J.S. (1988). Macrophage oxidation of L-arginine to nitrite and nitrate: Nitric oxide is an intermediate. *Biochemistry*, **27**, 8706–8711.

MITCHELL, J.A., HECKER, M. & VANE, J.R. (1990). The generation of L-arginine in endothelial cells is linked to the release of

endothelium-derived relaxing factor. *Eur. J. Pharmacol.*, **176,** 253–254.

MOORE, P.K., AL-SWAYEH, O.A., CHONG, N.S.W., EVANS, R. & GIBSON, A. (1989). L-N^G-nitro-arginine, a novel L-arginine-reversible inhibitor of endothelium-dependent vasodilation *in vitro*. *Br. J. Pharmacol.*, **99,** 408–412.

MÜLSCH, A., BASSENGE, E. & BUSSE, R. (1989). Nitric oxide synthesis in endothelial cytosol: Evidence for a calcium-dependent and a calcium-independent mechanism. *Naunyn-Schmiedebergs Arch. Pharmacol.*, **340,** 767–770.

MURPHY, S., MINOR, R.L., WELK, G. & HARRISON, D.G. (1990). Evidence for an astrocyte-derived vasorelaxing factor with properties similar to nitric oxide. *J. Neurochem.*, **55,** 349–351.

MYERS, P.R., MINOR, R.L., GUERRA, R., BATES, J.N. & HARRISON, D.G. (1990). Vasorelaxant properties of the endothelium-derived relaxing factor more closely resemble S-nitrosocysteine than nitric oxide. *Nature*, **345,** 161–163.

NATHAN, C.F. & STUEHR, D.J. (1990). Does endothelium-derived nitric oxide have a role in cytokine-induced hypotension? *J. Natl. Cancer Inst.*, **82,** 726–728.

PAIK, W.K. & KIM, S. (1975). Protein methylation: Chemical, enzymological, and biological significance. *Adv. Enzymol.*, **42,** 227–238.

PALACIOS, M., KNOWLES, R.G., PALMER, R.M.J. & MONCADA, S. (1989). Nitric oxide from L-arginine stimulates the soluble guanylate cyclase in adrenal glands. *Biochem. Biophys. Res. Commun.*, **165,** 802–809.

PALMER, R.M.J., ASHTON, D.A. & MONCADA, S. (1988). Vascular endothelial cells synthesize nitric oxide from L-arginine. *Nature*, **333,** 664–666.

PALMER, R.M.J., FERRIDGE, A.G. & MONCADA, S. (1987). Nitric oxide accounts for the biological activity of endothelium-derived relaxing factor. *Nature*, **327,** 524–526.

RADOMSKI, M.W., PALMER, R.M.J. & MONCADA, S. (1987). Endogenous nitric oxide inhibits human platelet adhesion to vascular endothelium. *Lancet*, **ii,** 1057–1058.

RADOMSKI, M.W., PALMER, R.M.J. & MONCADA, S. (1990). An L-arginine/nitric oxide pathway present in human platelets regulates aggregation. *Proc. Natl. Acad. Sci. U.S.A.*, **87,** 5193–5197.

RAPOPORT, R.M. & MURAD, F. (1983). Agonist-induced endothelium-dependent relaxation of rat thoracic aorta may be mediated through cGMP-dependent protein phosphorylation. *Nature*, **306,** 174–176.

REES, D.D., PALMER, R.M.J., HODSEN, H.F. & MONCADA, S. (1989a). A specific inhibitor of nitric oxide formation from L-arginine attenuates endothelium-dependent relaxation. *Br. J. Pharmacol.*, **96,** 418–424.

REES, D.D., PALMER, R.M.J. & MONCADA, S. (1989b). Role of endothelium-derived nitric oxide in the regulation of blood pressure. *Proc. Natl. Acad. Sci. U.S.A.*, **86,** 3375–3379.

REES, D.D., PALMER, R.M.J., SCHULZ, R., HODSON, H.F. & MONCADA, S. (1990). Characterization of three inhibitors of endothelial nitric oxide synthase *in vitro* and *in vivo*. *Br. J. Pharmacol.*, **101,** 746–752.

RIMELE, T.J., STURM, R.J., ADAMS, L.M., HENRY, D.E., HAESLIP, R.J., WEICHMAN, B.M. & GRIMES, D. (1988). Interaction of neutrophils with vascular smooth muscle: identification of a neutrophil-derived relaxing factor. *J. Pharmacol. Exp. Ther.*, **245,** 102–111.

RUBANYI, G.M., ROMERO, J.C. & VANHOUTTE, P.M. (1986). Flow-induced release of endothelium-derived relaxing factor. *Am. J. Physiol.*, **250,** H1145–H1149.

SAKUMA, I., STUEHR, D.J., GROSS, S.S., NATHAN, C. & LEVI, R. (1988). Identification of arginine as a precursor of endothelium-derived relaxing factor. *Proc. Natl. Acad. Sci. U.S.A.*, **85,** 8664–8667.

SAKUMA, T.H., YOSHIOKA, M., SAITO, H., YASUDA, H., GROSS, S.S. & LEVI, R. (1990). Sympatho-excitatory effect of a selective inhibitor of endothelium-derived nitric oxide synthesis, L-N^G-methyl-L-arginine, in anaesthetized rats. *Eur. J. Pharmacol.*, **183,** 650.

SALVEMINI, D., MASINI, E., ÄNGAARD, E.E., MANNIONI, P.F. & VANE, J.R. (1990). Synthesis of a nitric oxide-like factor from L-arginine by rat serosal mast cells: stimulation of guanylate cyclase and inhibition of platelet aggregation. *Biochem. Biophys. Res. Commun.*, **169,** 596–601.

STUEHR, D.J., GROSS, S.S., SAKUMA, I., LEVI, R. & NATHAN, C.F. (1989). Activated murine macrophages secrete a metabolite of arginine with the bioactivity of endothelium-derived relaxing factor and the chemical reactivity of nitric oxide. *J. Exp. Med.*, **169,** 1011–1020.

SWIERKOSZ, T.A., MITCHELL, J.A., SESSA, W.C., HECKER, M. & VANE, J.R. (1990). L-Glutamine inhibits the release of endothelium-derived relaxing factor from the rabbit aorta. *Biochem. Biophys. Res. Commun.*, **172,** 143–148.

TOLINS, J.P., PALMER, R.M.J., MONCADA, S. & RAIJ, L. (1990). Role of endothelium-derived relaxing factor in regulation of renal haemodynamic responses. *Am. J. Physiol.*, **258,** H665–H622.

THIEMERMANN, C., AL-DAMLUJI, S., HECKER, M. & VANE, J.R. (1991). FMRFamide and L-Arg-L-Phe increase blood pressure and heart rate in the anaesthetised rat by central stimulation of the sympathetic nervous system. *Biochem. Biophys. Res. Commun.*, **175,** 318–324.

VALLANCE, P., COLLIER, J. & MONCADA, S. (1989). Effects of endothelium-derived nitric oxide on peripheral arteriolar tone in man. *Lancet*, **ii,** 997–999.

VANE, J.R. (1964). The use of isolated organs for detecting active substances in the circulating blood. *Br. J. Pharmacol. Chemother.*, **23,** 360–365.

WALDER, C.E., THIEMERMANN, C. & VANE, J.R. (1990). Endothelium-derived relaxing factor participates in the increased blood flow in response to pentagastrin in the rat stomach mucosa. *Proc. R. Soc. B.*, **241,** 195–200.

WALDER, C.E., THIEMERMANN, C. & VANE, J.R. (1991). Endothelium-derived relaxing factor plays an important role in the regulation of renal cortical blood flow in the rat. *Br. J. Pharmacol.*, **102,** 967–973.

WALLENSTEIN, S., ZUCKER, C.L. & FLEISS, J.L. (1980). Some statistical methods useful in circulation research. *Circ. Res.*, **47,** 1–9.

WHITTLE, B.J.R., LOPEZ-BELMONTE, J. & REES, D.D. (1989). Modulation of the vasodepressor actions of acetylcholine, bradykinin, substance P and endothelin in the rat by a specific inhibitor of nitric oxide formation. *Br. J. Pharmacol.*, **98,** 646–652.

WOOD, K.S., BIGG, G.M., BYRNS, R.E. & IGNARRO, L.J. (1990). Vascular smooth muscle-derived relaxing factor (MDRF) and its close similarity to nitric oxide. *Biochem. Biophys. Res. Commun.*, **170,** 86–88.

(Received November 26, 1990
Revised April 5, 1991
Accepted May 1, 1991)

Br. J. Pharmacol. (1991), **104**, 39–44

Pharmacology of the putative M_4 muscarinic receptor mediating Ca-current inhibition in neuroblastoma × glioma hybrid (NG 108-15) cells

[1]M.P. Caulfield & D.A. Brown

Department of Pharmacology, University College London, Gower Street, London WC1E 6BT

1 We have assessed the potency of a range of agonists and antagonists on the muscarinic receptor responsible for inhibiting the Ca-current (I_{Ca}) in NG 108-15 hybrid cells.

2 Acetylcholine (ACh), oxotremorine-M and carbachol were potent 'full' agonists (EC_{50} values were 0.11 μM, 0.14 μM and 2 μM, respectively). Maximum inhibition of peak high-threshold I_{Ca} by these agonists was 39.5%. (±)-Muscarine, methylfurmethide and arecaidine propargyl ester (APE) were 'partial' agonists, with EC_{50} values of 0.54 μM, 0.84 μM and 0.1 μM, respectively.

3 Atropine, pirenzepine and himbacine were potent antagonists of muscarinic inhibition of I_{Ca}, with apparent pK_B values of 9.8, 7.74 and 8.83, respectively. Methoctramine was relatively weak ($pK_B = 7.63$). Atropine and pirenzepine depressed maximum responses to agonists, probably because these antagonists have relatively slow dissociation rates.

4 The characteristic pharmacological profile found for the M_4 receptors in these functional experiments (himbacine high affinity, pirenzepine moderate to high affinity, methoctramine low affinity) corresponds well with data from earlier binding experiments (Lazareno *et al.*, 1990). Since mRNA hybridising to probes for the m4 receptor genotype can be detected in these cells, it is suggested that these pharmacological characteristics identify the equivalent expressed receptor subtype M_4.

Keywords: M_4 muscarinic receptor; Ca current; neuroblastoma cell; acetylcholine; himbacine; pirenzepine; methoctramine; muscarine; oxotremorine-M

Introduction

There are at least five muscarinic acetylcholine receptor genotypes, designated m1 to m5 (Kubo *et al.*, 1986a,b; Bonner *et al.*, 1987; Peralta *et al.*, 1987; Buckley *et al.*, 1989). Receptors expressed from genes m1, m2 and m3 may correspond to those defined pharmacologically as M_1, M_2 and M_3 (see Hulme *et al.*, 1990).

One cell type which appears to express mRNA from the m4 genotype is the NG 108-15 mouse neuroblastoma × rat glioma hybrid cell (Peralta *et al.*, 1987; Fukuda *et al.*, 1988). Recent ligand-binding experiments on muscarinic receptors expressed in these cells have shown a unique profile of antagonist binding constants, suggesting that it is now possible to define a corresponding pharmacological M_4 subtype (Lazareno *et al.*, 1990).

The functional role of this subtype is not yet clear, but one possibility is that it might mediate some of the presynaptic inhibitory effects of muscarinic agonists. The reason for suggesting this is that differentiated NG 108-15 cells express a variety of neural ion channels (see Brown & Higashida, 1988; Robbins & Sim, 1989) and that one effect of stimulating the endogenous muscarinic receptor in these cells is to inhibit a voltage-gated Ca-current (Higashida *et al.*, 1990). An effect of this type might (arguably) contribute to the inhibition of transmitter release (Miller, 1990).

Hence, in these present experiments, we have tested the effects of some different muscarinic agonists and antagonists on the Ca-current in differentiated NG 108-15 cells, in order to define further the pharmacological profile of this putative M_4 receptor as seen from a functional viewpoint.

Some of these data have been presented in preliminary form (Caulfield *et al.*, 1991).

[1] Author for correspondence.

Methods

Ca-currents

NG 108-15 cells (passage numbers 11-96) were 'differentiated' with either 10 μM prostaglandin E_1 plus 50 μM isobutylmethylxanthine for 4–10 days (Docherty, 1988) or 200 μM dibutyryl cyclic AMP for 9–28 days (Higashida *et al.*, 1990) prior to recording. Dishes of cells were perfused at 5–10 ml min^{-1} with a modified Krebs solution (pH 7.4; 22°C–24°C; pre-bubbled with 95% O_2/5% CO_2) containing (mM): NaCl 120, KCl 3, $CaCl_2$ 2.5, $MgCl_2$ 1.2, $NaHCO_3$ 23, HEPES 5, D-glucose 11. Tetrodotoxin (0.5 μM) was included in the medium to suppress Na^+ currents. The whole-cell variant of the patch-clamp technique (Hamill *et al.*, 1981) was used to record voltage-activated Ca-currents. Patch electrodes (3–9 MΩ, usually 4–5 MΩ) were filled with a solution containing (mM): CsCl 110, tetraethylammonium chloride (TEA) 25, $MgCl_2$ 3, EGTA 3, HEPES 40 (adjusted to pH 7.4 with CsOH). After formation of a gigohm seal (1 GΩ–4GΩ) between electrode and cell membrane and breaking through into 'whole-cell' recording, the cell was voltage-clamped at −80 mV (occasionally −90 mV) with an Axoclamp-2A amplifier (Axon Instruments) in switch-clamp mode at a switching frequency of 4–10 kHz. Ca-currents were recorded as the composite currents evoked by stepping for 100 ms (occasionally 500 ms) to 0 mV or +10 mV (cf. Docherty, 1988).

It has previously been shown that the use of TEA to inhibit K^+ currents activated concomitantly by the depolarizing voltage steps reduces the potency of muscarinic agonists and antagonists in this system (Caulfield, 1991). Elimination of contaminating outward K^+ currents was therefore achieved by allowing sufficient time for the Cs in the pipette solution to diffuse into the cell. This could be monitored by the progressive increase in inward current seen during a 100 ms depolarizing command pulse and experiments were not started until this current had stabilized (cf. Caulfield, 1991).

Data analysis

The effects of muscarinic agonists were measured as the percentage reduction of peak inward Ca-current. Currents were measured with respect to the zero current line. Agonists were applied until no further reduction in peak current amplitude was seen. Stepwise cumulative additions of agonist concentrations without agonist-free periods between applications were used only where responses to each dose of agonist determined in this manner did not differ significantly from corresponding responses obtained by discrete application of each agonist concentration. Dose-effect relationships were analyzed by determining the least-squares fit of data to the function $y = y_{max} x^n/(x^n + K^n)$, where y is percentage inhibition of currents, y_{max} is maximum inhibition, x is agonist concentration and n is a 'slope factor'. Where agonist dose-effect data were pooled, data obtained in each individual experiment were expressed as a percentage of the maximum response to ACh (3 μM or 10 μM) in that experiment and the least-squares fit to the pooled mean responses was weighted by the inverse of the corresponding variances. These and all subsequent curve fitting procedures were carried out by use of 'Sigma Plot 4' computer software (Jandel Scientific).

Antagonist potencies were measured in experiments in which antagonists were at apparent equilibrium, as assessed by stabilization of responses to a continually adjusted submaximal agonist dose. Effects of antagonists producing rightward parallel shifts of agonist dose-response curves were quantified by calculating the K_B value using the Gaddum-Schild equation: $K_B = B/(DR - 1)$, where K_B is the apparent antagonist dissociation constant, B is antagonist concentration and DR is the ratio of the EC_{50} value for the agonist dose-effect curve in the presence of antagonist to that for the control agonist curve.

Some antagonists reduced the maximum agonist response and shifted the dose-effect curve rightward. These data were analyzed by determining the least squares fit of the function:

$$A = \frac{(1 - p_B)}{p_B} \frac{K_A A'}{K_A/p_B + A'}$$

which is a rearrangement in hyperbolic form of the equation:

$$\frac{A}{A + K_A} = \frac{A'(1 - p_B)}{A' + K_A}$$

where A and A' are agonist concentrations producing matched responses in the absence and in the presence of antagonist, respectively, K_A is agonist dissociation constant and p_B is the proportion of receptors occupied by antagonist (see Rang, 1965; Furchgott, 1966).

The antagonist K_B was then estimated from:

$$K_B = \frac{B(1 - p_B)}{p_B}$$

which is a rearrangement of the Langmuir isotherm

$$p_B = \frac{B}{B + K_B}$$

where B is antagonist concentration.

Materials

The following compounds were obtained from Semat: methoctramine tetrachloride, (±)-muscarine chloride, oxotremorine-M methiodide. Atropine sulphate, ACh chloride, pirenzepine dichloride, carbachol chloride and isobutylmethylxanthine (IBMX) were purchased from Sigma Chemicals. BM-5 (N-methyl-N(1-methyl-4-pyrrolodino-2-butynyl)acetamide) was a generous gift of Dr A.D. Michel (Glaxo Group Research Ltd.). Dr R.B. Barlow very kindly supplied samples of APE (arecaidine propargyl ester) and McN A 343 (4-chlorophenyl-carbamoyloxy-2-butynyl trimethyl ammonium chloride). We thank Dr S.H. Lazareno (MRC Collaborative Centre, London) for a kind gift of himbacine. Prof. H. Higashida (Kanazawa University) generously sent supplies of high purity dibutyryl cyclic AMP.

Results

Agonists

Application of muscarinic agonists produced reversible (usually within 5 min) and reproducible inhibition of the Ca-current (Figure 1). Prolonged application of agonist (>2 min) resulted in some recovery from inhibition, which may have been due to desensitization of the agonist effect (data not shown). The agonists inhibited a transient high-voltage-activated component of the current, with little effect on the component of inward current remaining at the end of a 500 ms depolarizing step (Figure 1). This resembles the pattern of Ca-current inhibition by noradrenaline in these cells (Docherty & McFadzean, 1989).

The inhibitory effect of muscarinic agonists varied greatly between cells and batches of cells, even though all of the cells appeared morphologically 'differentiated'. In 61 cells exhibiting high-voltage activated currents (cf. Docherty, 1988), the mean maximum inhibition (±s.e.mean) was 40% ± 2, ranging from 15% to 76%. Muscarinic inhibition was small (<5%) or absent in recordings made over a 15 month period from 285 cells which only had a low voltage-activated Ca-current (cf. Docherty, 1988). This variability in responsiveness of batches of cells seemed not to be due to any of the following factors: passage number, culture conditions (e.g., serum concentration, culture substrate, CO_2 concentration in incubator atmosphere), differentiating agent (dibutyryl cyclic AMP, prostaglandin E_1 (PGE_1)/IBMX), duration of exposure to differentiating agent (5 days to 4 months), pipette solution contents (with or without ATP 1 mM/GTP 0.1 mM, or an ATP-regenerating system) or recording temperature (22°C–37°C). It stands in contrast to the high proportion of noradrenaline-responsive cells (193/205) reported by Docherty & McFadzean (1989), but is more in accord with the low mean inhibition (about 14%) seen in native NG 108-15 cells by Higashida *et al.* (1990).

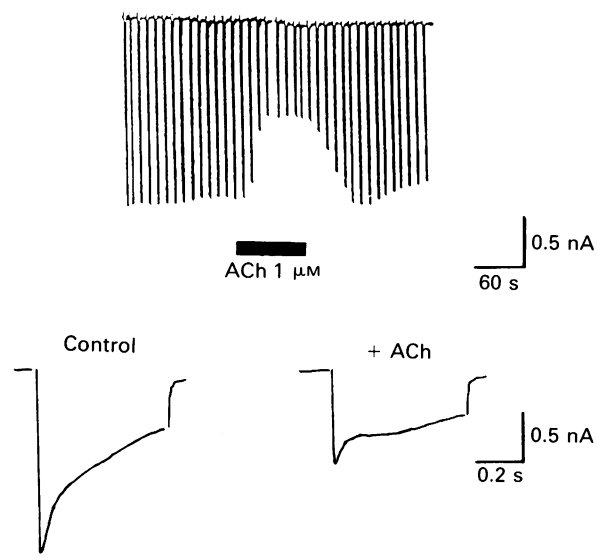

Figure 1 Inhibition of calcium current (I_{Ca}) in NG 108-15 cells by acetylcholine (ACh). The downward deflections in the upper trace represent peak inward Ca-currents evoked by stepping for 100 ms to a command potential of 0 mV from a holding potential of −80 mV. Steps were made every 10 s. The lower expanded traces show the current evoked by the same command step applied for 500 ms, before and during the peak effect of ACh. For clarity, capacity transients at the beginning and end of the current have been masked.

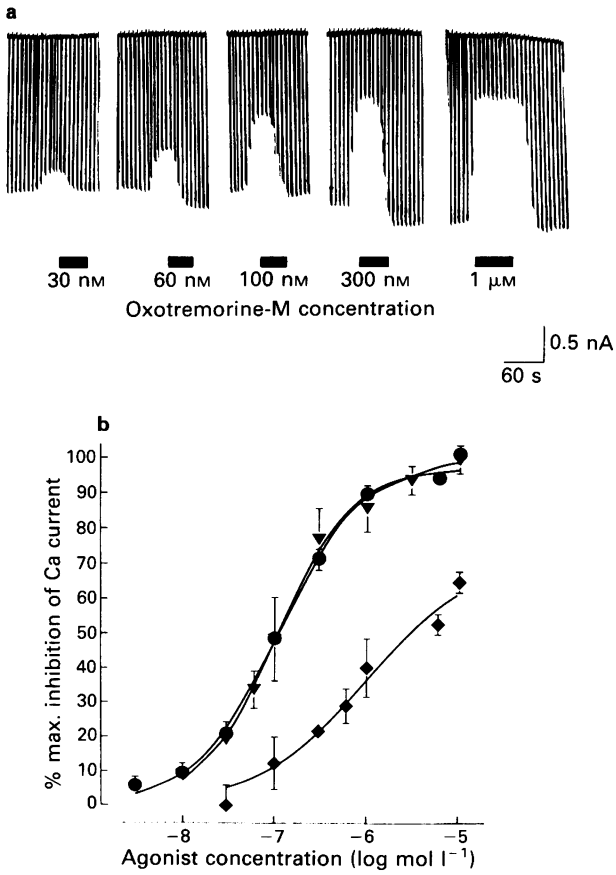

Figure 2 (a) A representative experiment showing inhibition of Ca-current by increasing concentrations of oxotremorine-M. Downward deflections show peak Ca-current amplitude (see Figure 1). (b) Dose-effect relationships for agonist inhibition of Ca-current. Points represent mean normalized responses (see Methods for calculations and curve-fitting procedures) and vertical bars show s.e.mean values for acetylcholine (ACh) (●), oxotremorine-M (▼) and muscarine (◆). K and n values (see Methods) for the curves fitted to the pooled mean agonist responses were 0.1 μM and 1.07 for oxotremorine-M, 0.11 μM and 0.9 for ACh and 0.76 μM and 0.85 for muscarine.

Figure 2 shows dose-effect curves obtained with the muscarinic agonists ACh, oxotremorine-M and muscarine. The potency of ACh was increased about 3 fold in the presence of neostigmine, suggesting the presence of functionally-active cholinesterase on the cells (McGee *et al.*, 1978). Results obtained with these and other agonists are summarized in Table 1. Muscarine was a 'partial agonist' with a lower maximal effect than oxotremorine-M, ACh or carbachol. Estimates of the maximum effect of muscarine were obtained from the curve fitted to the pooled normalised data (see Methods). Methylfurmethide and APE were potent agonists, but also produced lower maximum responses than ACh or oxotremorine-M. The putative M_1 receptor-selective agonist McN A 343 did not reduce Ca-currents at concentrations up to 100 μM, but this latter concentration of McN A343 abolished the response to a subsequent dose of ACh (1 μM; $n = 2$). Similar effects were seen with the oxotremorine analogue, BM-5, which has been reported to be a selective agonist for the adenylate-cyclase coupled receptors in heart and in NG 108-15 cells (Baumgold & Drobnick, 1989). BM-5 had no inhibitory effects at concentrations up to 10 μM, but this concentration of BM-5 shifted the ACh dose-response curve to the right (49 and 52 fold, $n = 2$) in a parallel way, suggesting an apparent antagonist K_B of about 0.2 μM.

Antagonists

In 8 out of 17 experiments, antagonist application increased the peak Ca current (Figure 3). This enhancement by antagonists was not observed in the remaining 9 experiments. The mean increase (± s.e.mean) in these 8 experiments was 18% ± 4. There was no apparent relation between this effect and either the antagonist used or the antagonist concentration. One explanation might be that the antagonist relieved a state of partial inhibition resulting from spontaneous or induced release of ACh from these cholinergic cells (McGee *et al.*, 1978). Notwithstanding, the overall effect of the antagonists on agonist dose-response curves was consistent, regardless of whether or not this enhancement occurred.

Table 1 Potencies of muscarinic agonists as inhibitors of the Ca-current in NG 108-15 cells

Agonist	$-log\ EC_{50}$ (s.e.mean)	EC_{50} (μM)	n	*Maximum response* (s.e.mean)
Acetylcholine	6.49 (0.1)	0.32	4	100
Acetylcholine + neostigmine 1 μM	6.95 (0.1)	0.11	11	100
Oxotremorine-M	6.85 (0.18)	0.14	4	100 (3)
Muscarine	6.27 (0.3)	0.54	4	73 (7)
APE	6.71 (0.28)	0.19	4	81 (6)
Methylfurmethide	6.1	0.84	2	57
Carbachol	5.7	2	2	100

APE = arecaidine propargyl ester.

The antagonists studied fell into two groups. Himbacine (Gilani & Cobbin, 1986) and methoctramine shifted agonist dose-effect curves to the right without any significant reduction in maximum agonist response (Figure 4). This enabled calculation of apparent K_B values for these compounds from the estimated dose-ratios (Table 2). At a low concentration (30 nM), pirenzepine shifted the agonist curves rightward without reducing maximum responses, but at higher concentrations, the maximum was decreased (Figure 5a). Atropine (1–10 nM) also reduced maximum agonist responses (data not shown). This effect is not due to irreversible binding of antagonist to receptor (e.g. Furchgott, 1966; Barlow *et al.*, 1991), as the inhibitory effects of pirenzepine (Figure 5b) and atropine (data not shown) reversed within 30 min on perfusing with antagonist-free medium.

It is more likely that the reduction in maximum agonist response results from a low receptor reserve and slow dissociation of antagonist from the receptor, so that the antagonist behaves as if it were irreversible, as previously described by Rang (1965). The data were therefore analyzed using the function set out by Rang (1965) and Furchgott (1966), as modified by Barlow *et al.* (1991; see Methods section), allowing estimation of apparent antagonist K_B values (Figure 6 and Table 2). Included for comparison in Table 2 are data from the radioligand binding experiments of Lazareno *et al.* (1990) on NG

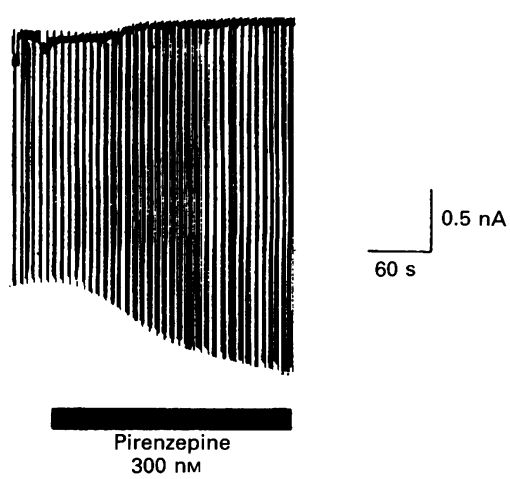

Figure 3 Pirenzepine increases Ca-current amplitude. Downward deflections represent peak Ca-current, as in Figure 1.

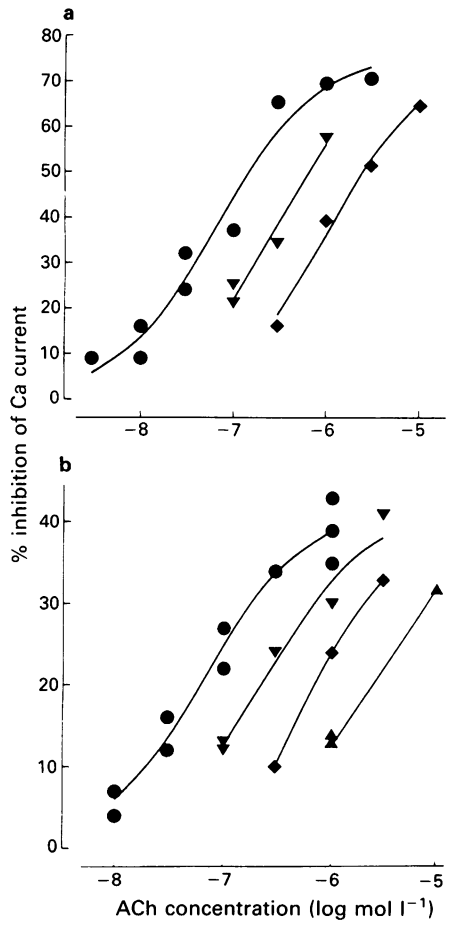

Figure 4 Sample experiments showing acetylcholine (ACh) dose-effect curves for Ca-current inhibition in the absence (●) and (a) in the presence of 10 nM (▼) and 30 nM (◆) himbacine and (b) in the presence of 100 nM (▼), 300 nM (◆) and 1 μM (▲) methoctramine. Curves were fit by least squares procedures (see Methods) where there were four or more data points; otherwise curves were drawn by eye. The control curve for the himbacine experiment was fit with a K value of 0.07 μM, n of 0.81 and y_{max} of 75.8%. Estimated himbacine dose-ratios were 4.5 (10 nM) and 17.7 (30 nM). The control curve for the methoctramine experiment was fit with a K value of 0.07 μM, n of 0.94 and y_{max} of 42.1%. Estimated methoctramine dose-ratios were 4 (100 nM), 8 (300 nM) and 21 (1 μM).

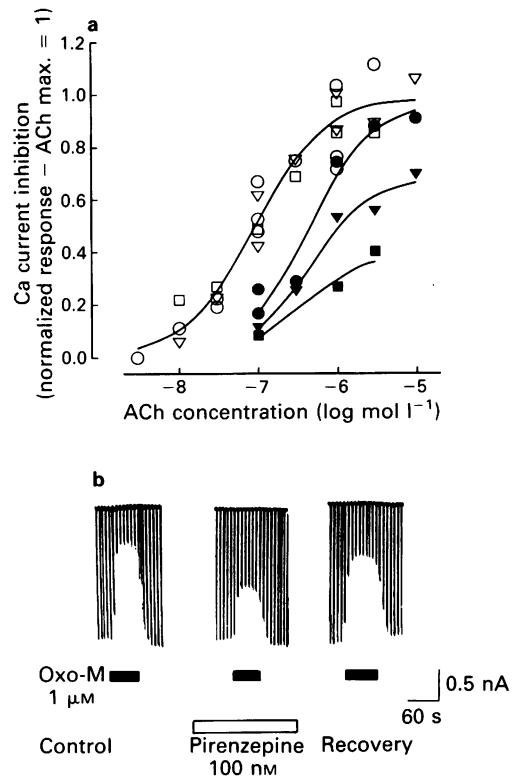

Figure 5 Representative experiments showing the effect of 30 nM (●), 100 nM (▼) and 300 nM (■) pirenzepine on respective acetylcholine (ACh) dose-effect curves (○ ▽ □) for Ca-current inhibition. Data from 3 experiments were pooled by normalizing responses to the fitted ACh maximum response in each experiment and curves were generated by least-squares procedures (see Methods). Fitted K values for the three control curves were 0.93 μM, 0.98 μM and 0.92 μM; fitted n values were 0.96, 1.1 and 0.76. Fitted parameters for the pirenzepine curves were: K = 0.43 μM, n = 1.1, y_{max} = 0.98 (pirenzepine 30 nM); K = 0.45 μM, n = 1.1, y_{max} = 0.69 (pirenzepine 100 nM). The curve for the experiment with 300 nM pirenzepine was drawn by eye. (b) Oxotremorine-M (Oxo-M) inhibition of Ca-current (represented by downward deflections, as in Figure 1) is reduced by pirenzepine. Recovery of response is shown after 30 min perfusion with antagonist-free medium.

108-15 cells and rabbit lung (which express the m4 receptor gene) and on M_1, M_2 and M_3 receptor-containing preparations. The pK_B value for pirenzepine obtained directly from the dose-ratio shifts in the two experiments with 30 nM pirenzepine was slightly higher than the value estimated by the Rang/Furchgott analysis of data from experiments with higher pirenzepine concentrations, although the difference was not significant ($P > 0.05$, t test).

The use of the Rang/Furchgott analysis, which regards the antagonists as effectively irreversible, also allows estimation of agonist dissociation constants (see Methods). The mean pK_A (± s.e.mean) estimated for ACh in this manner was 6.05 ± 0.24, corresponding to a K_A of 0.89 μM.

Discussion

The profile of antagonist affinities deduced from these experiments accords quite closely with those predicted from previous ligand-binding experiments (Michel *et al.*, 1989; Lazareno *et al.*, 1990). Thus, the absolute and relative

Table 2 Antagonist potencies against muscarinic inhibition of Ca-current in NG 108-15 cells

				pK_B *from radioligand binding**				
				M_4 *sites*				
Antagonist	pK_B (± s.e.mean)	K_B (nM)	n	*NG*	*Lung*	M_1	M_2	M_3
Atropine	9.8 (0.39)	0.15	3		9.56	9.55	9.01	9.51
Pirenzepine	7.74 (0.23)	18.2	7	7.2	7.55	8.02	6.48	7.09
(100 nM–300 nM)	7.53 (0.27)	29.5	5					
(30 nM)	8.25 (0.5)	5.6	2					
Methoctramine	7.63 (0.23)	23	4	8.09	7.83	7.6	8.34	6.88
Himbacine	8.83 (0.13)	1.5	3	8.53	8.47	7.16	8.34	7.09

* Data from antagonist displacement experiments of Lazareno *et al.* (1990). NG = NG 108-15 cells; Lung = rabbit lung, M_1 = [^{3}H]-pirenzepine binding to rat cerebral cortex; M_2 and M_3 = [^{3}H]-N-methylscopolamine binding to rat heart and rat submandibular gland, respectively.

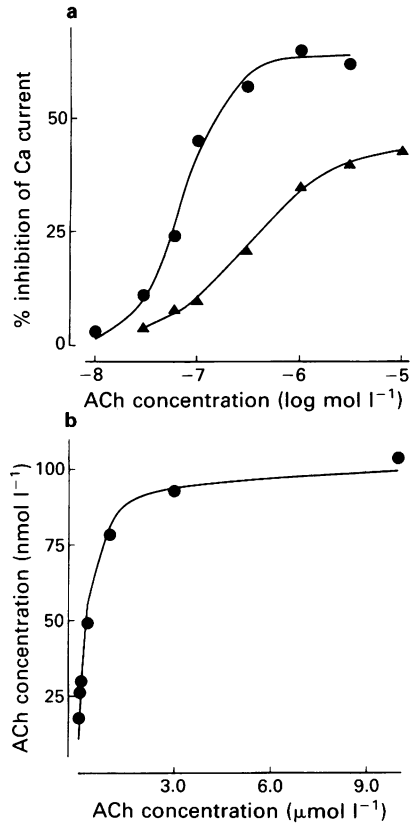

Figure 6 (a) A representative experiment showing the reduction of maximum inhibition of Ca-current by acetylcholine (ACh) by 100 nM pirenzepine. Curves were fit by least-squares procedures (see Methods) and the best-fit parameters were: control $K = 0.07\,\mu M$, n = 1.9, $y_{max} = 63\%$; pirenzepine, $K = 0.31\,\mu M$, n = 1, $y_{max} = 44\%$. (b) The same data fit to the hyperbolic function

$$A = \frac{(1 - p_B)}{p_B} \frac{K_A A'}{K_A/p_B + A'}$$

(see Barlow *et al.*, 1991)

where A is plotted on the ordinate and A' on the abscissa scale. A and A' are ACh concentrations in the absence and presence of antagonist, respectively; K_A is agonist dissociation constant and p_B is the proportion of receptors occupied by antagonist. The curve was drawn with K_A and p_B values of 0.2 μM and 0.6, respectively.

potencies of himbacine, pirenzepine and methoctramine measured against muscarinic inhibition of I_{Ca} are very similar to the ligand displacement potencies on putative M_4 receptors in both NG 108-15 cells and rabbit lung (Lazareno *et al.*, 1990), and clearly differ from their potencies at M_1, M_2 or M_3 binding sites (Lazareno *et al.*, 1990) or at the corresponding receptor subtypes in functional assays (e.g. Brown *et al.*, 1980; Lazareno & Roberts, 1989). Although the potency of pirenzepine against I_{Ca} inhibition (pK_B 7.74) was slightly higher than its binding potency in NG 108-15 cells (pK_B 7.2; Lazareno *et al.*, 1990), the accuracy of functional pK_B calculations is probably limited by the non-parallel shift of the dose-response curve (see below). Also, equivalent differences between binding and functional potencies for pirenzepine have been noted at M_1 receptors (Brown *et al.*, 1980) and it is possible that other factors such as uptake into cells may affect measurements. Therefore, M_4 receptors seem to preserve their unique antagonist profile when measured by a functional assay. Our experiments further suggest that they might best be distinguished operationally from M_1 receptors by their high sensitivity to himbacine rather than by their slightly lower sensitivity to pirenzepine.

In contrast to the unique profile for antagonist potencies, the potencies of the agonists we tested were roughly comparable with those observed in a functional assay for M_1 receptor activation (e.g. Brown *et al.*, 1980). However, several points are noteworthy.

Firstly, there seems to be a rather low receptor reserve for Ca-current inhibition, even for 'full' agonists such as acetylcholine, carbachol and oxotremorine-M, such that high concentrations of pirenzepine and atropine reduced the maximum agonist effect. This is to be expected from the interaction of an agonist with a slowly dissociating antagonist when there are few 'spare receptors' (Rang, 1965). At first sight this seems an inadequate explanation for the depression, since methoctramine and himbacine had similar or lower apparent K_B values than pirenzepine, so might be expected to dissociate slowly, yet produced a parallel shift of the agonist dose-response curve. However, pirenzepine appears to have a much slower dissociation rate than that predicted from its equilibrium constant. Thus, the rate constant for dissociation of [^{3}H]-pirenzepine from M_4 receptors in rabbit lung is only 1.5 times greater than that for dissociation of [^{3}H]-N-methylscopolamine, whereas the ratio of the equilibrium constants is 480 (Lazareno *et al.*, 1990). Analysis of the data for pirenzepine block yielded an apparent dissociation equilibrium constant for acetylcholine of 0.89 μM, so that a just-maximal concentration of 3 μM would have to occupy about 77% of the available receptors. Although this occupancy is somewhat greater than that predicted from the dose-ratio shift produced by concentrations of pirenzepine below those which depressed the maximum response, the concept of a low receptor reserve is substantiated by the fact that muscarine, methylfurmethide and APE appeared to behave as 'partial' agonists, with a lower maximum effect than that produced by acetylcholine or oxotremorine-M.

Secondly, and perhaps related to the apparent low receptor reserve, McN A 343 and BM-5 did not exhibit clear agonist activity but instead behaved as antagonists. BM-5 has previously been reported to exert partial agonist activity in respect of inhibition of prostaglandin-stimulated adenylate cyclase in NG 108-15 cells, with an EC_{50} value of 0.4 μM (Baumgold & Drobnick, 1989). This accords reasonably well with the apparent antagonist K_B (0.2 μM) obtained in the present experiments. This suggests that the same receptor may be responsible both for inhibition of adenylate cyclase and inhibition of the Ca-current, but that it couples less efficiently to the latter. It should be noted that inhibition of I_{Ca} is not due to inhibition of adenylate cyclase, since it is not affected by high intracellular concentrations of cyclic AMP (Higashida *et al.*, 1990) and further that the two responses are likely to be mediated by different GTP-binding proteins (see McFadzean *et al.*, 1989).

The present results have some bearing on the pharmacological identification of muscarinic receptors responsible for Ca-current inhibition (and possibly for inhibiting transmitter release) in other cells. Thus, whereas in most cells inhibition of I_{Ca} is resistant to high concentrations of pirenzepine (e.g. Mochida & Kobayashi, 1986; Gahwiler & Brown, 1987; Song *et al.*, 1989; Tse *et al.*, 1990), in rat sympathetic neurones inhibition is potently antagonized by pirenzepine, leading to the suggestion that it is mediated by an M_1 receptor (Wanke *et al.*, 1987). However, experiments on DNA-transfected NG 108-15 cells suggest that only m2 or m4 genotypic receptors are capable of inhibiting I_{Ca} and that neither m1 nor m3 genotypic receptors can couple efficiently to this current (Higashida *et al.*, 1990). The present data offer a way of resolving this difficulty, since they suggest that M_4 receptors could be responsible for the high pirenzepine sensitivity of I_{Ca}-block in sympathetic neurones. Likewise, if Ca-current inhibition does indeed contribute to presynaptic inhibition, then the high potency of pirenzepine against muscarinic presynaptic inhibition in the hippocampus (Dutar & Nicol, 1988; Sheridan & Sutor, 1990), olfactory cortex (Williams & Constanti, 1988) and septum (Hasuo *et al.*, 1988) might also reflect involvement of the putative M_4 receptor. Other instances of high presynaptic potency of pirenzepine include muscarinic inhibition of sympathetic transmission in rabbit ear artery (Choo *et al.*,

1986), acetylcholine release in chick heart (Jeck *et al.*, 1988) and sympathetic transmission at rabbit vas deferens (Eltze, 1988). In the latter case, the argument in favour of an M_4 receptor is strengthened by the equivalent high potency of himbacine.

Thus, the present observations provide a functional counterpart to previous ligand-binding studies which may indicate a role for M_4 receptors in a variety of nerve cells.

This work was supported by a grant from the Medical Research Council. We are grateful to Dr R.B. Barlow for invaluable help with computations and to Dr J. Robbins, Dr R.J. Docherty and Dr S.H. Lazareno for encouragement and helpful discussion. We thank Prof. H. Higashida for his advice on tissue culture.

References

BARLOW, R.B., McMILLEN, L.S. & VEALE, M.A. (1991). The use of 4-diphenylacetoxy-N-(2-chloroethyl)-piperidine (4-DAMP mustard) for estimating the apparent affinities of some agonists acting at muscarinic receptors in guinea-pig ileum. *Br. J. Pharmacol.*, **102**, 657–662.

BAUMGOLD, J. & DROBNICK, A. (1989). An agonist that is selective for adenylate cyclase-coupled muscarinic receptors. *Mol. Pharmacol.*, **36**, 465–470.

BONNER, T.I., BUCKLEY, N.J., YOUNG, A.C. & BRANN, M.R. (1987). Identification of a family of muscarinic receptor genes. *Science*, **237**, 527–532.

BROWN, D.A., FORWARD, A. & MARSH, S. (1980). Antagonist discrimination between ganglionic and ileal muscarinic receptors. *Br. J. Pharmacol.*, **71**, 362–364.

BROWN, D.A. & HIGASHIDA, H. (1988). Voltage- and calcium-activated potassium currents in mouse neuroblastoma × glioma hybrid cells. *J. Physiol.*, **397**, 149–165.

BUCKLEY, N.J., BONNER, T.I., BUCKLEY, C.M. & BRANN, M.R. (1989). Antagonist binding properties of five cloned muscarinic receptors expressed in CHO-K1 cells. *Mol. Pharmacol.*, **35**, 469–476.

CAULFIELD, M.P. (1991). Muscarinic receptor-mediated inhibition of voltage-activated Ca current in neuroblastoma × glioma hybrid (NG 108-15) cells-reduction of muscarinic agonist and antagonist potency by tetraethylammonium (TEA). *Neurosci. Lett.* (in press).

CAULFIELD, M.P., BROWN, D.A. & BARLOW, R.B. (1991). A pharmacological study of the M_4 muscarinic receptor mediating inhibition of the voltage-gated Ca-current in neuroblastoma × glioma hybrid (NG 108-15) cells. *Br. J. Pharmacol.*, **102**, 149P.

CHOO, L.K., MITCHELSON, F. & VONG, Y.M. (1986). Interaction of some muscarinic agonists and antagonists at the prejunctional muscarinic receptor in the rabbit ear artery preparation. *Br. J. Pharmacol.*, **87**, 733–740.

DOCHERTY, R.J. (1988). Gadolinium selectively blocks a component of calcium-current in rodent neuroblastoma × glioma hybrid (NG108-15) cells. *J. Physiol.*, **398**, 33–47.

DOCHERTY, R.J. & McFADZEAN, I. (1989). Noradrenaline-induced inhibition of voltage-sensitive calcium currents in NG108-15 hybrid cells. *Eur. J. Neurosci.*, **1**, 132–140.

DUTAR, P. & NICOL, R.A. (1988). Classification of muscarinic responses in hippocampus in terms of receptor subtypes and second-messenger systems: electrophysiological studies *in vitro*. *J. Neurosci.*, **8**, 4214–4224.

ELTZE, M. (1988). Muscarinic M_1- and M_2-receptors mediating opposite effects on neuromuscular transmission in rabbit vas deferens. *Eur. J. Pharmacol.*, **151**, 205–221.

FUKUDA, K., HIGASHIDA, H., KUBO, T.I., MAEDA, A., AKIBA, I., BUJO, H., MISHINA, M. & NUMA, S. (1988). Selective coupling with K^+ currents of muscarinic acetylcholine receptor subtypes in NG 108-15 cells. *Nature*, **335**, 355–358.

FURCHGOTT, R.F. (1966). The use of β-haloalkylamines in the differentiation of receptors and in the determination of dissociation constants of receptor-agonist complexes. *Adv. Drug Res.*, **3**, 21–55.

GAHWILER, B.H. & BROWN, D.A. (1987). Muscarine affects calcium-currents in rat hippocampal pyramidal cells *in vitro*. *Neurosci. Lett.*. **76**, 301–306.

GILANI, S.A.H. & COBBIN, L.B. (1986). The cardio-selectivity of himbacine: a muscarine receptor antagonist. *Naunyn Schmiedebergs Arch. Pharmacol.*, **332**, 10–20.

HAMILL, O.P., MARTY, A., NEHER, E., SAKMANN, B. & SIGWORTH, F.J. (1981). Improved patch-clamp techniques for high-resolution current recording from cells and cell-free membrane patches. *Pflüger's Arch.*, **391**, 85–100.

HASUO, H., GALLAGHER, J.P. & SHINNICK-GALLAGHER, P. (1988). Disinhibition in the rat septum mediated by M_1 muscarinic receptors. *Brain Res.*, **438**, 323–327.

HIGASHIDA, H., HASHII, M., FUKUDA, K., CAULFIELD, M.P., NUMA, S. & BROWN, D.A. (1990). Selective coupling of different muscarinic acetylcholine receptors to neuronal calcium currents in DNA-transfected cells. *Proc. R. Soc.* B., **242**, 68–74.

HULME, E.C., BIRDSALL, N.J.M. & BUCKLEY, N.J. (1990). Muscarinic receptor subtypes. *Annu. Rev. Pharmacol. Toxicol.*, **30**, 633–673.

JECK, D., LINDMAR, R., LOFFELHOLZ, K. & WANKE, M. (1988). Subtypes of muscarinic receptor on cholinergic nerves and atrial cells of chicken and guinea-pig hearts. *Br. J. Pharmacol.*, **93**, 357–366.

KUBO, T., MAEDA, A., SUGIMOTO, K., AKIBA, I., MIKAMI, A., TAKAHASHI, H., HAGA, T., HAGA, K., ICHIYAMA, A., KANGAWA, K., MATSUO, H., HIROSE, T. & NUMA, S. (1986a). Primary structure of porcine cardiac muscarinic acetylcholine receptor deduced from the cDNA sequence. *FEBS Lett.*, **209**, 367–372.

KUBO, T., FUKUDA, K., MIKAMI, A., MAEDA, A., TAKAHASHI, H., MISHINA, M., HAGA, T., HAGA, K., ICHIYAMA, A., KANGAWA, K., KOJIMA, M., MATSUO, H., HIROSE, T. & NUMA, S. (1986b). Cloning, sequencing and expression of complementary DNA encoding the muscarinic acetylcholine receptor. *Nature*, **323**, 411–416.

LAZARENO, S., BUCKLEY, N.J. & ROBERTS, F.F. (1990). Characterisation of muscarinic M_4 binding sites in rabbit lung, chicken heart and NG 108-15 cells. *Mol. Pharmacol.*, **38**, 805–815.

LAZARENO, S. & ROBERTS, F.F. (1989). Functional and binding studies with muscarinic M_2-subtype selective antagonists. *Br. J. Pharmacol.*, **98**, 309–317.

McFADZEAN, I., MULLANEY, I., BROWN, D.A. & MILLIGAN, G. (1989). Antibodies to the GTP binding protein, G_0, antagonize noradrenaline-induced calcium current inhibition in NG108-15 hybrid cells. *Neuron*, **3**, 177–182.

McGEE, R., SIMPSON, P., CHRISTIAN, C., MATA, M., NELSON, P. & NIRENBERG, M. (1978). Regulation of acetylcholine release from neuroblastoma × glioma hybrid cells. *Proc. Nat. Acad. Sci. U.S.A.*, **75**, 1314–1318.

MICHEL, A.D., DELMENDO, R., STEFANICH, E. & WHITING, R.L. (1989). Binding characteristics of the muscarinic receptor subtype of the NG108-15 cell line. *Naunyn Schmiedebergs Arch. Pharmacol.*, **340**, 62–67.

MILLER, R.J. (1990). Receptor-mediated regulation of calcium channels and neurotransmitter release. *FASEB J.*, **4**, 3291–3299.

MOCHIDA, S. & KOBAYASHI, H. (1986). Activation of M_2 muscarinic receptors causes an alteration of action potentials by modulation of Ca entry in isolated sympathetic neurons of rabbits. *Neurosci. Lett.*, **72**, 199–204.

PERALTA, E.G., ASHKENAZI, A., WINSLOW, J.W., SMITH, D.H., RAMACHANDRAN, J. & CAPON, D.J. (1987). Distinct primary structures, ligand-binding properties and tissue-specific expression of four human muscarinic acetylcholine receptors. *EMBO J.*, **6**, 3923–3929.

RANG, H.P. (1965). The kinetics of action of acetylcholine antagonists in smooth muscle. *Proc. R. Soc.* B, **161**, 488–510.

ROBBINS, J. & SIM, J. (1990). A transient outward current in NG 108-15 neuroblastoma × glioma hybrid cells. *Pflüger's Arch.*, **416**, 130–137.

SHERIDAN, R.D. & SUTOR, B. (1990). Presynaptic M_1 muscarinic cholinoceptors mediate inhibition of excitatory synaptic transmission in the hippocampus *in vitro*. *Neurosci. Lett.*, **108**, 273–278.

SONG, S.Y., SAITO, S., NOGUCHI, K. & KONISHI, S. (1989). Different GTP-binding proteins mediate regulation of calcium channels by acetylcholine and noradrenaline in rat sympathetic neurons. *Brain Res.*, **494**, 383–386.

TSE, A., CLARK, R.B. & GILES, W.R. (1990). Muscarinic modulation of calcium current in neurones from the interatrial septum of bullfrog heart. *J. Physiol.*, **427**, 127–149.

WANKE, E., FERRONI, A., MALGAROLI, A., AMBROSINI, A., POZZAN, T. & MELDOLESI, J. (1987). Activation of muscarinic receptor selectively inhibits a rapidly inactivated Ca^{2+} current in rat sympathetic neurons. *Proc. Natl. Acad. Sci.*, U.S.A., **84**, 4313–4317.

WILLIAMS, S.H. & CONSTANTI, A. (1988). A quantitative study of the effects of some muscarinic antagonists on the guinea-pig olfactory cortex slice. *Br. J. Pharmacol.*, **93**, 855–862.

(Received March 20, 1991
Revised May 8, 1991
Accepted May 9, 1991)

Br. J. Pharmacol. (1991), **104**, 45–48

The antimigraine drugs ergotamine and dihydroergotamine are potent 5-HT_{1C} receptor agonists in piglet choroid plexus

Anthony M. Brown, Tracey L. Patch & Alberto J. Kaumann

SmithKline Beecham Pharmaceuticals, The Frythe, Welwyn, Herts, AL6 9AR

1 Fozard & Gray (1989) proposed that migraine is mediated by stimulation of 5-HT_{1C} receptors. We have examined the interaction of two effective anti-migraine agents, ergotamine and dihydroergotamine (DHE), with these receptors. Binding (inhibition of labelling by [^{3}H]-mesulergine) and agonist activity (phosphoinositide hydrolysis) were measured in piglet choroid plexus, a tissue rich in 5-HT_{1C} receptors.

2 The pK_D for [^{3}H]-mesulergine binding was 8.4. Ergotamine and DHE both inhibited [^{3}H]-mesulergine binding with a pK_D of 7.1. This was similar to the potency of *m*-chlorophenylpiperazine (*m*-CPP) (pK_D 7.4) and rather less than that of 5-hydroxytryptamine (5-HT) (pK_D 8.1).

3 Both ergotamine and DHE were full agonists (pEC_{50}s 7.5 and 7.6 respectively) with potencies similar to that of 5-HT (pEC_{50} 7.7) and greater than that of *m*-CPP (pEC_{50} 7.1). Mesulergine 10^{-7} M produced near-parallel rightward shifts of the concentration-response curves for all these agents of 1.8–2.2 log units, consistent with an action of the agonists at the same receptor.

4 There was no effect of prazosin, spiperone, mepyramine or atropine on the phosphoinositide hydrolysis induced by ergotamine, ruling out an action via α_1-adrenoceptors, 5-HT_2, histamine H_1, or muscarinic receptors.

5 It is concluded that, together with 5-HT, ergotamine and DHE are the most potent 5-HT_{1C} agonists reported so far. These findings do not support the theory that 5-HT_{1C} receptor activation causes migraine.

Keywords: 5-HT_{1C} receptor stimulation; choroid plexus; phospholipase C; ergotamine; dihydroergotamine

Introduction

Fozard & Gray (1989) proposed that a variety of drugs that prevent migraine may do so by blocking cerebral 5-HT_{1C} receptors. Their proposal was based on the observation by Brewerton *et al.* (1988) of a high incidence of migraine-like headache induced by a single oral dose of *m*-chlorophenylpiperazine (*m*-CPP). The incidence of headache was significantly greater in subjects with a personal or family history of migraine. Fozard & Gray (1989) based their argument on the relative high affinity of *m*-CPP for 5-HT_{1C} receptors (Hoyer, 1989), its relative high potency as an enhancer of inositol phosphate levels in pig choroid plexus (Schoeffter & Hoyer, 1989) and its selectivity for 5-HT_{1C} receptors over other 5-HT_1 receptor subtypes and 5-HT_2 receptors (Hoyer, 1989).

The classical antimigraine drugs, ergotamine and dihydroergotamine (Bowman & Rand, 1980), have been reported to possess affinity for the 5-HT_{1C} receptor which is similar to the affinity of *m*-CPP (Hoyer, 1989). In view of this affinity, we investigated whether these ergot analogues possessed agonist properties in the 5-HT_{1C} receptor system of piglet choroid plexus. We found that the ergots are powerful agonists. To establish the relationship between agonist potency and affinity, we labelled the 5-HT_{1C} receptors with [^{3}H]-mesulergine and used the ergots as binding inhibitors. The effects and affinities of the ergots were compared to those of 5-hydroxytryptamine (5-HT) and *m*-CPP.

Methods

Measurement of inositol phosphate accumulation

The method for measuring accumulation of inositol phosphates was a modification of that described by Schoeffter & Hoyer (1989) for choroid plexus from pig. Piglets (Camborough Hi-Bred, 5–9 days old) from a local farm were anaesthetized with halothane and killed by removal of the heart (Kaumann, 1990). The skull was opened, the brain removed and the choroid plexus rapidly dissected and transferred to Na-Krebs medium at 37°C, gassed with 95% O_2:5% CO_2. The Na-Krebs medium contained (mM): Na^+ 149, K^+ 6.4, Mg^{2+} 1.3, Ca^{2+} 0.8, Cl^- 128, HCO_3^- 26, phosphate 1.4, SO_4^{2-} 1.3 and glucose 10. For each experiment, plexi were collected and pooled from 9 piglets. After the last choroid plexus had been removed (total time less than 2 h), the choroid plexi were cross chopped on a McIlwain tissue chopper set at 300 μm. The slices were washed twice by allowing them to settle under gravity, removing the supernatant and then resuspending them in fresh, gassed Na-Krebs at 37°C. After each resuspension, the slices were incubated for about 10 min before further processing, with gassing over the surface of the suspension. The slices were finally suspended in 6 ml of fresh Na-Krebs and 50 μCi of [^{3}H]-*myo*-inositol (10–20 Ci mmol^{-1}; stock solution dried under nitrogen and redissolved in Na-Krebs), was added. The slices were then incubated for 1.5 to 2 h at 37°C with constant gassing directed as a jet on to the surface of the suspension to provide good mixing.

After this incubation, 40 ml of Li-Krebs (as Na-Krebs but with 10 mM NaCl replaced by 10 mM LiCl) was added. The slices were mixed with a plastic Pasteur pipette and allowed to settle. The supernatant was discarded and replaced with fresh Li-Krebs and the slices incubated for 5 min at 37°C. This process was repeated twice more and the slices were finally resuspended in an appropriate volume of Li-Krebs containing (final concentrations in incubation vials) 100 μM pargyline (to inhibit monoamine oxidase), 6 μM cocaine (to inhibit possible tissue 5-HT uptake) and 0.2 mM ascorbic acid (to inhibit oxidation of 5-HT) and stirred gently with magnetic stirring ready for distribution to the incubation vials.

Incubations were carried out in Beckman Biovials in Li-Krebs for 1 h at 37°C in a shaking water bath. The total incubation volume was 300 μl. Li was included in the incubation medium to prevent breakdown of inositol monophosphate and hence cause the inositol phosphates to accumulate over the incubation period. Drugs were added in a total volume of 20 μl. Agonists (5-HT, ergots and *m*-CPP) were dissolved in 2 mM ascorbic acid and were added in 10 μl. Mesulergine was dissolved in Li-Krebs containing 0.2 mM ascorbic acid and added in 10 μl. Incubations were started by addition to each vial of 280 μl of the slice suspension. The vial contents were

gassed/mixed with a jet of 95% O_2:5% CO_2 and sealed. Incubations were terminated by addition to each vial of 300 μl of 7% perchloric acid after which the vials were placed on ice for 15 min. The contents of the vials were then centrifuged and 0.55 ml of the supernatant mixed well with 0.625 ml of (trioctylamine:1,1-2-trichlorotrifluoroethane, 1:1) to extract the perchloric acid. After centrifugation, 0.4 ml of the top (aqueous) phase was pipetted on to columns containing ion exchange resin (Biorad AG 1-X8, 200–400 mesh, formate form) in 5 ml Milli-Q purified water. The columns were washed with a further 20 ml water to remove inositol. The inositol phosphates were then eluted into scintillation vials with 10 ml of a solution containing 1.05 M ammonium formate and 0.1 M formic acid. ^3H content of each vial was then determined by scintillation counting.

Binding studies

Preparation of membranes from piglet choroid plexus and measurement of binding to 5-HT_{1C} receptors with [^3H]-mesulergine were essentially as described by Pazos *et al.* (1984) for pig choroid plexus. Incubations were at 37°C for 30 min in a medium containing 50 mM Tris-Cl (pH 7.7 at room temperature), 4 mM $CaCl_2$, 10 μM pargyline, 0.1% ascorbic acid, and in a total volume of 1 ml. For binding inhibition studies, drugs were added in 250 μl, [^3H]-mesulergine (final concentration about 1 nM) in 250 μl and membranes in 500 μl (30–75 μg protein/assay tube), with all incubation tubes on ice. The incubations were started by transfer of the tubes to a waterbath at 37°C and terminated after 30 min by rapid filtration through Whatman GF/C filters (presoaked in polyethyleneimine, 0.5%, for 2 h to reduce non-specific binding) on a Brandel Harvester followed by three rapid washes with 3 ml of ice-cold 50 mM Tris-Cl (pH 7.4 at room temperature), 4 mM $CaCl_2$. The filters were then transferred to scintillation vials and counted for ^3H in Ready Protein scintillation fluid (Beckman). Protein was determined by the method of Bradford (1976).

The saturation binding isotherm for [^3H]-mesulergine was determined by use of a range of [^3H]-mesulergine concentrations between 0.05 and 80 nM. Mesulergine 1 μM was used to define non-specific binding. At 1 nM [^3H]-mesulergine, as used in the binding inhibition experiments, approximately 60% of the total ^3H binding was specific. For all binding experiments, data were analysed by non-linear regression with GraFit (Erithacus Software Ltd., Staines, U.K.) on a Tandon PCA20 computer. Both saturation binding and binding inhibition data were well fitted by equations assuming interactions at a single site and yielding a value for the binding equilibrium constant, K_D.

Drugs

Ergotamine, dihydroergotamine, 5-HT hydrochloride, atropine sulphate and prazosin were from Sigma, Mepyramine maleate was from May and Baker, *m*-CPP and spiperone were obtained from Research Biochemicals Incorporated. Mesulergine was a gift from the Sandoz Company, Basle. [^3H]-mesulergine was obtained from Amersham International and [^3H]-*myo*-inositol from New England Nuclear.

Results

Both ergotamine and dihydroergotamine were full agonists. Their potency was almost as high as that of 5-HT and 3 times higher than that of *m*-CPP (Figure 1, Table 1). Mesulergine, 10^{-7} M, caused surmountable blockade of the effects of all the agonists, shifting the concentration-effect curves in nearly parallel manner and to similar extent (Figure 1). The similarity of the concentration ratios for these agonists (Table 1) suggests the involvement of the same receptor. Spiperone 10^{-7} M had no effect on the response to 5-HT 10^{-6} M or ergotamine 10^{-6} M (Table 2), ruling out the involvement of 5-HT_2 receptors. The effects of micromolar concentrations of ergotamine were also not altered by the histamine H_1 antagonist, mepyramine (10^{-6} M), the muscarinic antagonist atropine (10^{-6} M) or the α_1-adrenoceptor antagonist, prazosin (10^{-6} M) (Table 2).

[^3H]-mesulergine bound in a saturable manner to sites with a pK_D of 8.4 and density of $-\log_{10}(K_D)$, M

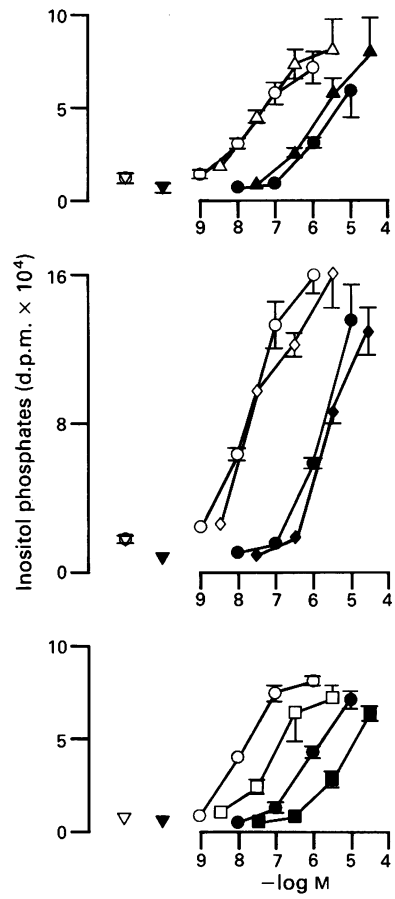

Figure 1 Effects of agonists on the accumulation of inositol phosphates in slices of piglet choroid plexus in the absence (open symbols) and presence (closed symbols) of mesulergine 10^{-7} M. (○, ●), 5-hydroxytryptamine; (△, ▲), ergotamine; (◇, ◆), dihydroergotamine; (□, ■), *m*-chlorophenylpiperazine; (▽, ▼), basal accumulation. Each panel shows a separate experiment carried out on pooled choroid plexi from 9 piglets. Each point is the mean of triplicate determinations; vertical bars show s.e.mean. Where not shown, the error bar is smaller than the symbol.

Table 1 Effects of agonists on inositol phosphate accumulation and inhibition of binding of [^3H]-mesulergine in piglet choroid plexus

	Inositol phosphate accumulation			*Binding*
Drug	*n* (piglets)	pEC_{50}[a]	log(CR)[b]	pK_D[c]
5-HT	27	7.7	1.8	8.1
Ergotamine	9	7.5	2.0	7.1
Dihydroergotamine	9	7.6	2.2	7.1
m-CPP	9	7.1	1.9	7.4

m-CPP = *m*-chlorophenylpiperazine.
[a] $pEC_{50} = -\log_{10}(EC_{50})$, M.
[b] CR = concentration ratio of agonist with 10^{-7} M mesulergine.
[c] $pK_D = -\log_{10}(K_D)$, M.

Table 2 Effects of receptor antagonists on 5-hydroxytryptamine (5-HT)- and ergotamine-induced inositol phosphate accumulation in piglet choroid plexus

Condition	*Inositol phosphate accumulation* (d.p.m.)
Experiment 1	
Basal	12,044 ± 99
5-HT (1 μM)	223,483 ± 26,235
5-HT (1 μM) + spiperone (0.1 μM)	250,843 ± 29,976
Ergotamine (1 μM)	205,994 ± 4,980
Ergotamine (1 μM) + spiperone (0.1 μM)	195,221 ± 7,853
Ergotamine (1 μM) + atropine (1 μM)	227,011 ± 4,697
Ergotamine (1 μM) + mepyramine (1 μM)	227,683 ± 17,225
Experiment 2	
Basal	8,584 ± 315
Ergotamine (3.3 μM)	68,815 ± 8,324
Ergotamine (3.3 μM) + prazosin (1 μM)	78,835 ± 12,233

0.52 ± 0.05 pmol mg^{-1} protein (mean ± s.e.mean, $n = 10$; experiments not shown). 5-HT, ergotamine, dihydroergotamine and *m*-CPP inhibited binding in a fashion consistent with interaction of a single site with pK_D values shown in Table 1.

Discussion

Our data are consistent with 5-HT$_{1C}$ receptor-mediated phospholipase C stimulation by both ergotamine and dihydroergotamine. Our binding affinity estimates for 5-HT, ergotamine, dihydroergotamine, *m*-CPP and [^{3}H]-mesulergine in piglet choroid plexus membranes agree with the corresponding affinities of the compounds for 5-HT$_{1C}$ receptors of choroid plexus of adult pigs reported by Hoyer (1989). Mesulergine antagonized with similar affinity the effects of the four agonists. This evidence, taken together, is consistent with an interaction of the four agonists with 5-HT$_{1C}$ receptors labelled and blocked by mesulergine.

The EC_{50} values of 5-HT, ergotamine and dihydroergotamine roughly agree with the corresponding K_D values (Table 1), suggesting that there is negligible receptor reserve under our conditions. Some 5-HT$_{1C}$ receptor reserve has been reported for the effects of 5-HT in rat choroid plexus (Sanders-Bush & Breeding, 1990).

Ergotamine and dihydroergotamine are known to interact with other receptors which stimulate phospholipase C, including 5-HT$_2$ (Hoyer, 1989) and α_1-adrenoceptors (Megens *et al.*, 1986). Since these receptors might be present in piglet choroid plexus, we examined the effects of antagonists on the ergotamine-induced inositol phosphate accumulation in choroid plexus slices. Neither 10^{-7} M of the 5-HT$_2$ antagonist spiperone (pK_D at 5-HT$_2$ receptors, 8.8; pK_D at 5-HT$_{1C}$ receptors, 5.9; Hoyer, 1989) nor 10^{-6} M of the α_1-adrenoceptor antagonist prazosin (pK_D 10.0; Watson & Abbott, 1991) inhibited the effect of micromolar concentrations of ergotamine, ruling out roles for either of these receptors. The absence of α_1-adrenoceptors on choroid plexus is consistent with the findings of Conn & Sanders-Bush (1986) in rat choroid plexus. We also tested whether two further phospholipase C-linked receptors, muscarinic and histamine H$_1$ receptors, might be involved in the effect of ergotamine in this tissue. However, neither atropine 10^{-6} M, (pK_D at muscarinic receptors, 9.3; Fisher, 1985) nor mepyramine 10^{-6} M (pK_D at histamine H$_1$ receptors 9.1; Hill, 1990) altered ergotamine-induced inositol phosphate accumulation.

The high agonistic potency of the antimigraine drugs ergotamine and dihydroergotamine at 5-HT$_{1C}$ receptors would appear to be inconsistent with the hypothesis of Fozard & Gray (1989) that activation of these receptors induces migraine. Indeed, it might be expected from the data presented here that these agents would be more potent inducers of migraine than *m*-CPP. However, the two ergots only occasionally cause headache (Bowman & Rand, 1980), possibly related to abuse (Andersson, 1975).

One possible explanation for this apparent inconsistency might be that the ergots are poorly brain penetrant. The chemical nature of ergotamine and dihydroergotamine makes it unlikely that they would readily cross the blood-brain barrier (Ziegler, 1990). However, there is some evidence for brain penetration of both substances although the amounts detected are small. For example, 20–50 ng g^{-1} of [^{3}H]-ergotamine and 10 ng g^{-1} of [^{3}H]-dihydroergotamine have been reported in rat brain following 0.5–1 mg kg^{-1} oral or i.v. administration (Eckert *et al.*, 1978). These amounts of the two drugs, if evenly distributed, would suffice to yield concentrations greater than 10 nM at cerebral 5-HT$_{1C}$ receptors and could well cause phospholipase C stimulation as seen in the piglet choroid plexus. Interestingly, 1 mg kg^{-1} i.p. dihydroergotamine increases wakefulness and modifies sleep patterns in rats, consistent with a central site of action (Loew *et al.*, 1978). Ergotamine has also been measured in human cerebrospinal fluid after oral administration of a therapeutic dose (Ala-Hurula *et al.*, 1979) although some concern has been expressed about the specificity of the analytical method used in this study (Sanders *et al.*, 1986).

These data suggest that some headache might be expected with ergots if the hypothesis of Fozard & Gray (1989) is correct for, given the high agonistic potency of the compounds, even a small amount of brain penetration should result in some activation of cerebral 5-HT$_{1C}$ receptors. It is conceivable that the therapeutic effects of the two ergots, presumably exerted through cerebral vascular constriction (Bowman & Rand, 1980), overshadow some possible 5-HT$_{1C}$ receptor stimulation. The present data therefore suggest a need to regard the hypothesis of Fozard & Gray (1989) with some caution though they are not sufficient to reject it. In addition, *m*-CPP also causes a considerable release of hypothalamic 5-HT (Pettibone & Williams, 1984) which could play an additional role in the production of headache.

We conclude that ergotamine and dihydroergotamine, together with 5-HT, are the most potent agonists of 5-HT$_{1C}$ receptors described so far (Schoeffter & Hoyer, 1989; Hoyer, 1989).

References

ALA-HURULA, V., MYLLYLÄ, V.V., ARVELA, P., KÄRKI, N.T. & HOKKANEN, E. (1979). Systemic availability of ergotamine tartrate after three successive doses and during continuous medication. *Eur. J. Clin. Pharmacol.*, **16**, 355–360.

ANDERSSON, P.G. (1975). Ergotamine headache. *Headache*, **15**, 118–121.

BOWMAN, W.C. & RAND, M.J. (1980). *Textbook of Pharmacology*. Oxford: Blackwell Scientific Publications.

BRADFORD, M. (1976). A rapid and sensitive method for the quantitation of microgram quantities of protein utilizing the principle of protein-dye binding. *Anal. Biochem.*, **72**, 248–254.

BREWERTON, T.D., DENNIS, L.M., MUELLER, E.A. & JIMERSON, D.C. (1988). Induction of migraine-like headaches by the serotonin agonist *m*-chlorophenyl-piperazine. *Clin. Pharmacol. Ther.*, **43**, 605–609.

CONN, P.J. & SANDERS-BUSH, E. (1986). Agonist-induced phosphoinositide hydrolysis in choroid plexus. *J. Neurochem.*, **47**, 1754–1760.

ECKERT, H., KIECHEL, J.R., ROSENTHALER, J., SCHMIDT, R. & SCHREIER, E. (1978). Biopharmaceutical aspects. Analytical methods, pharmacokinetics, metabolism and bioavailability. In *Ergot Alkaloids and Related Compounds* ed. Berde, B. & Schild, H.O. pp. 719–803. Berlin: Springer-Verlag.

FISHER, S.K. (1985). Inositol lipids and signal transduction at CNS muscarinic receptors. In *Subtypes of Muscarinic Receptors II.* ed. Levine, R.R., Birdsall, N.J.M., Giachetti, A., Hammer, R., Iversen,

L.L., Jenden, D.J. & North, R.A. Supplement to *Trends Pharmacol. Sci.*, pp. 61–65. Amsterdam: Elsevier.

FOZARD, J.R. & GRAY, J.A. (1989). 5-HT_{1C} receptor activation: a key step in the initiation of migraine? *Trends Pharmacol. Sci.*, **10**, 307–309.

HILL, S.J. (1990). Distribution, properties, and functional characteristics of three classes of histamine receptor. *Pharmacol. Rev.*, **42**, 45–83.

HOYER, D. (1989). Biochemical mechanisms of 5-HT receptor-effector coupling in peripheral tissues. In *The Peripheral Actions of 5-Hydroxytryptamine* ed. Fozard, J.R. pp. 72–99. Oxford: University Press.

KAUMANN, A.J. (1990). Piglet sinoatrial 5-HT receptors resemble human atrial 5-HT_4-like receptors. *Naunyn-Schmiedebergs Arch. Pharmacol.*, **342**, 619–622.

LOEW, D.M., VAN DEUSEN, E.B. & MEIER-RUGE, W. (1978). Effects on the central nervous system. In *Ergot Alkaloids and Related Compounds* ed. Berde, B. & Schild, H.O., pp. 421–531. Berlin: Springer-Verlag.

MEGENS, A.A.H.P., LEYSEN, J.E., AWOUTERS, F.H.L. & NIEMEGEERS, C.J.E. (1986). Further validation of *in vivo* and *in vitro* pharmacological procedures for assessing the α_1/α_2-selectivity of test compounds: (1) α-adrenoceptor antagonists. *Eur. J. Pharmacol.*, **129**, 49–55.

PAZOS, A., HOYER, D. & PALACIOS, J.M. (1984). The binding of serotonergic ligands to the porcine choroid plexus: characterization of a new type of serotonin recognition site. *Eur. J. Pharmacol.*, **106**, 539–546.

PETTIBONE, D.J. & WILLIAMS, M. (1984). Serotonin-releasing effects of substituted piperazines *in vitro*. *Biochem. Pharmacol.*, **33**, 1531–1535.

SANDERS, S.W., HAERING, N., MOSBERG, H. & JAEGER, H. (1986). Pharmacokinetics of ergotamine in healthy volunteers following oral and rectal dosing. *Eur. J. Clin. Pharmacol.*, **30**, 331–334.

SANDERS-BUSH, E. & BREEDING, M. (1990). Serotonin 5-HT_{1C} receptor reserve in choroid plexus masks receptor subsensitivity. *J. Pharmacol. Exp. Ther.*, **252**, 984–988.

SCHOEFFTER, P. & HOYER, D. (1989). Interaction of arylpiperazines with 5-HT_{1A}, 5-HT_{1B}, 5-HT_{1C} and 5-HT_{1D} receptors: do discriminatory 5-HT_{1B} receptor ligands exist? *Naunyn-Schmiedebergs Arch. Pharmacol.*, **339**, 675–683.

WATSON, S.P. & ABBOTT, A. (1991). *Trends Pharmacol. Sci. Receptor Nomenclature Supplement*, 1991, p. 4. Cambridge: Elsevier Science Publishers.

ZIEGLER, A. (1990). Treatment: where are we going? In *Migraine: a Spectrum of Ideas*. ed. Sandler, M. & Collins, G.M. pp. 294–300. Oxford: University Press.

(Received April 15, 1991
Accepted May 10, 1991)

Br. J. Pharmacol. (1991), **104**, 49–52

Prostacyclin activates tachykinin release from capsaicin-sensitive afferents in guinea-pig bronchi through a ruthenium red-sensitive pathway

[1]Cristina Elisabetta Mapp, *Leonardo Michele Fabbri, *Anna Boniotti & †Carlo Alberto Maggi

Institute of Occupational Medicine, University of Padua, Padua, Italy; *Institute of Pulmonary Diseases, Section on Experimental Pathophysiology, University of Ferrara, Ferrara, Italy and †Pharmacology Department, Research Laboratories, A. Menarini Pharmaceuticals, Florence, Italy

1 We have investigated the ability of prostacyclin (PGI_2) to contract guinea-pig isolated bronchi and the possible involvement of capsaicin-sensitive primary afferents in the response to PGI_2.

2 PGI_2 (0.1–100 μM) produced concentration-dependent contractions of the guinea-pig isolated bronchi. *In vitro* capsaicin desensitization (10 μM for 30 min followed by washing) significantly reduced the PGI_2-induced contraction at all concentrations tested. A capsaicin-resistant component of contraction (40–60% of the overall response) was also evident.

3 Ruthenium red (3 μM), an inorganic dye which acts as a selective functional antagonist of capsaicin, significantly decreased PGI_2-induced contractions, without affecting the response to substance P, neurokinin A or acetylcholine.

4 MEN 10, 207, (Tyr^5, D-Trp^{6,8,9}, Arg^{10})-neurokinin A (4–10) (3 μM), a selective antagonist of NK_2-tachykinin receptors, significantly decreased PGI_2-induced contractions and neurokinin A-induced contractions, without affecting the response to acetylcholine.

5 The effect of ruthenium red and MEN 10,207 on the one hand, and that of ruthenium red and capsaicin on the other was non additive.

6 These results indicate that PGI_2-induced contraction of the guinea-pig isolated bronchi involves two distinct mechanisms, one of which involves transmitter (tachykinins) release from peripheral endings of capsaicin-sensitive primary afferents. In as much as PGI_2-activation of primary afferents is sensitive to ruthenium red, we suggest that PGI_2 shares a common mechanism of tachykinin release with that activated by capsaicin.

Keywords: Prostaglandins; capsaicin-sensitive primary afferents; tachykinins; guinea-pig bronchi; ruthenium red

Introduction

Prostaglandins are synthesized and released by almost every tissue in the body and participate in several different biological functions (Moncada & Vane, 1983). Prostacyclin (PGI_2), an unstable endoperoxide derivative which belongs to the family of prostaglandins, is a potent vasodilator and it is the principal metabolite of arachidonic acid formed by vascular endothelial cells (Bunting *et al.*, 1976).

The lung is one of the major sites of prostaglandin synthesis and inactivation, and PGI_2 and PGE_2 may affect lung functions in separate and sometimes opposite directions. In fact, prostaglandins of the E series relax airway smooth muscle and prostacyclin reverses the bronchospasm induced by acetylcholine, histamine and prostaglandin $F_{2\alpha}$ (Wasserman *et al.*, 1980). However, these bronchodilator prostaglandins cause bronchoconstriction in both normal and asthmatic subjects when administered either by aerosol (Mathe *et al.*, 1975) or by intravenous infusion (Smith & Cuthbert, 1976). Since subjects complained of cough and irritation of the upper respiratory tract, it is possible that stimulation of sensory nerves was involved in these 'paradoxical' effects induced by inhaled PGI_2 and by PGE_2, which usually are classified as bronchodilator prostaglandins. This hypothesis is supported by the findings of Roberts *et al.* (1985) who showed that PGI_2 stimulated both pulmonary and bronchial C-fibres in dogs. They recorded reflex changes in smooth muscle tension in an innervated segment of the upper trachea which was not itself exposed to the direct action of PGI_2 and PGE_2, and found a tracheal contraction which was reflex in origin, initiated by nonmyelinated fibres. Roberts *et al.* (1985) postulated that, in susceptible human subjects, the threshold concentration of bronchodilator prostaglandins that stimulates the afferent vagal C-fibres is lower than the threshold concentration required for a direct bronchodilator effect. PGI_2 also stimulates pulmonary C-fibres in species other than dogs, such as rabbits (Armstrong *et al.*, 1981). Moreover, PGI_2 is released during pulmonary oedema (Van Grondelle *et al.*, 1984), and vagal reflexes evoked by this condition in the absence of congestion result largely from stimulation of lung C-fibres (Roberts *et al.*, 1986). PGI_2 is also the major arachidonate metabolite via the cyclo-oxygenase pathway produced during vasoconstriction by the rat isolated lung (Voelkel *et al.*, 1981). Recently, it has been shown that infusion of 5-hydroxytryptamine (5-HT) in the canine isolated lung lobe perfused with blood at constant flow, increased plasma levels of 6-keto-$PGF_{1\alpha}$, the principal hydrolysis product of PGI_2 (El-Kashef *et al.*, 1990).

We carried out this study to determine whether PGI_2 contracts bronchial smooth muscle in guinea-pigs and whether the mechanism of contraction might involve the activation of capsaicin-sensitive primary afferents.

Methods

Male Hartley-outbred guinea-pigs (Rodentia Laboratories, Torre Pallavicina, Bergamo) weighing 300–400 g were anaesthetized with pentobarbitone sodium (50 mg kg^{-1}, i.p.). The lungs were removed rapidly and immersed in oxygenated Krebs-Henseleit solution containing the following (mM): NaCl 118.3, KCl 4.7, $MgSO_4$ 1.2, KH_2PO_4 1.2, $NaHCO_3$ 25.0, $CaCl_2$ 2.5 and D-(+)-glucose 11.1. The main bronchi were dissected free of loose connective tissue and were prepared in two

[1] Author for correspondence at Istituto di Medicina del Lavoro, Universitá degli Studi di Padova, Via J Facciolati 71, 35100 Padova, Italy.

rings. The rings were mounted in glass chambers filled with 15 ml of Krebs-Henseleit solution that was maintained at 37°C and aerated continuously by bubbling it with a mixture of 95% O_2 and 5% CO_2, which produced a pH of 7.4. We measured isometric tension of rings of bronchial smooth muscle continuously by connecting the tissue to a force-displacement transducer (Grass FTO3), and recorded the responses on a Battaglia Rangoni model KV380 polygraph recorder. The tissues were allowed to equilibrate for 90 min with the resting tension maintained at 5 mN. During equilibration the medium was changed every 20 min. Contractions were normalized by expressing each muscle tension measured as a percentage of the active tension obtained in response to acetylcholine (ACh, 1 mM). The response to ACh was supramaximal and highly reproducible.

To study the effect of PGI_2 in main bronchi from guinea-pigs, we assessed the effects of increasing concentrations of PGI_2 (0.1–100 μM). After the equilibration period, 1 mM acetylcholine was added, and the response was monitored. Then the bronchial rings were rinsed until tension returned to resting values. After washing, increasing concentrations of PGI_2 were added cumulatively. Each successive concentration was added only after the previous response had reached a constant value. Six experiments were performed for each concentration of PGI_2.

To study the effect of putative inhibitors on PGI_2-induced contractions, we measured the responses induced by 1 mM acetylcholine. The rings were rinsed until the tension returned to resting values. After washing, we performed parallel experiments on paired bronchial rings from the same animal. The possible involvement of capsaicin-sensitive primary afferents in the response to PGI_2 was assessed by using three different pharmacological treatments: *in vitro* capsaicin desensitization, MEN 10,207 and ruthenium red.

For *in vitro* capsaicin desensitization, one bronchial ring of each pair was exposed to 10 μM capsaicin for 30 min and then repeatedly washed. The effect of PGI_2 was studied when tension returned to resting values.

In as much as tachykinin release has been implicated in the bronchial contraction produced by capsaicin-sensitive afferents (Lundberg *et al.*, 1983; Maggi *et al.*, 1990a; 1991), the effect of PGI_2 was also investigated in the presence of MEN 10,207 (3 μM, contact time 30 min) a competitive antagonist of NK_2-tachykinin receptors (indicated as Peptide I in Maggi *et al.*, 1990b). MEN 10,207 has been shown to abolish the non-cholinergic contraction produced by sensory nerves activation in the guinea-pig isolated bronchus (Maggi *et al.*, 1991).

The effect of ruthenium red (3 μM, contact time 30 min) on PGI_2-induced bronchial contraction was also investigated because this dye has been shown to act as a selective functional antagonist of capsaicin-activated transmitter release from sensory nerves in the bronchi (Maggi *et al.*, 1989).

We also examined (1) the effect of ruthenium red on substance P (1 μM), on neurokinin A (1 nM) and on acetylcholine (0.1 μM)-induced responses; (2) the effect of MEN 10,207 on acetylcholine (0.1 μM) and on neurokinin A (1 nM)-induced responses.

Materials and reagents

Prostacyclin, acetylcholine, capsaicin, and ruthenium red were obtained from Sigma Chemical Co. (St. Louis, MO, U.S.A.). Substance P and neurokinin A were obtained from Peninsula (St. Helens, England). MEN 10,207 (Tyr^5, D-Trp^{6,8,9}, Arg^{10})-neurokinin A was synthesized by Dr P. Rovero, Department of Chemistry, A. Menarini Pharmaceuticals, Florence, Italy, by conventional solid phase methods.

Statistical analysis

Each value is mean ± standard error of the mean (s.e.mean). The effect of putative inhibitors on PGI_2-induced contractions was compared by a two-tailed Student's test for paired data. To test for a possible additive effect of MEN 10,207 and ruthenium red and of capsaicin and ruthenium red, we analyzed the data by using two-way analysis of variance. $P < 0.05$ was considered significant.

Results

PGI_2 (0.1–100 μM) caused a concentration-dependent, rapidly developing and sustained contraction of the guinea-pig isolated main bronchus (Figure 1). At 100 μM the PGI_2-induced contraction averaged 73.4 ± 8.2% of the maximal response to acetylcholine.

In vitro capsaicin desensitization (10 μM for 30 min) reduced PGI_2-induced contractions at all concentrations tested. A residual, capsaicin-resistant response to PGI_2 was however still evident, which ranged between 10–25% of maximal response to acetylcholine. This protocol of *in vitro* capsaicin desensitization completely abolished (Maggi *et al.*, unpublished data) the contractile response to capsaicin or the atropine-resistant contraction to electrical field stimulation (cf. Maggi *et al.*, 1990a,c) for at least 3 h.

The effect of ruthenium red, capsaicin pretreatment and MEN 10,207 on PGI_2-induced contractions is shown in Figure 2. Capsaicin pretreatment (10 μM for 30 min) produced a significant inhibition of PGI_2-induced contractions. In control rings, the response to PGI_2 averaged 27.5 ± 4.7% and 40.8 ± 7.3% at 1 and 10 μM, respectively. The corresponding values in rings pretreated with capsaicin were 8.1 ± 2.5% and 22.5 ± 4.5%, respectively ($P < 0.001$, $P < 0.05$, $n = 10$; Figure 2).

Ruthenium red (3 μM) reduced PGI_2-induced contractions. In control rings, the response to PGI_2 averaged 17.9 ± 2.6% and 25.6 ± 3.5% at 1 and 10 μM, respectively. The corresponding values in the presence of ruthenium red were 9.0 ± 1.3% and 13.6 ± 4.5% ($P < 0.01$, $P < 0.005$, $n = 7$; Figure 2). Ruthenium red did not affect substance P-induced contractions (45.9 ± 10.0% in control rings and 50.7 ± 12.6% in the presence of ruthenium red, $n = 5$, $P > 0.05$). Likewise, ruthenium red failed to affect the response to neurokinin A which averaged 27.3 ± 4.4% in control rings and 21.8 ± 3.0% in the presence of the dye ($n = 5$, $P > 0.05$), nor did it affect the acetylcholine-induced contraction (36.7 ± 4.5% in control rings and 38.5 ± 3.9% in the presence of the dye, $n = 5$, $P > 0.05$).

Addition of MEN 10,207 (3 μM) had a significant inhibitory effect on PGI_2-induced contractions. In control rings, the

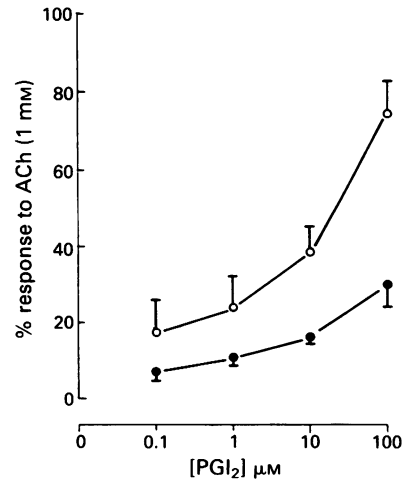

Figure 1 Effect of prostacyclin (PGI_2) on guinea-pig main bronchi before (○) and after capsaicin (10 μM) (●). Each point is the mean of six experiments; vertical bars show s.e.mean.

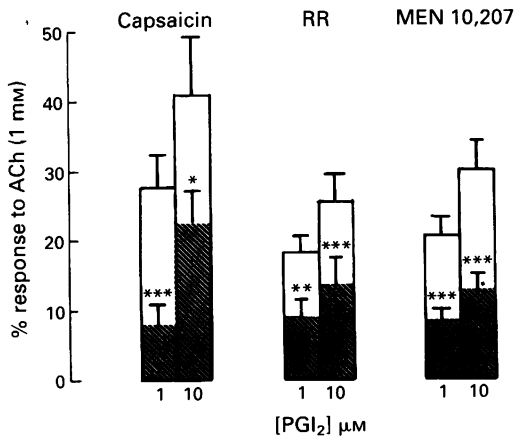

Figure 2 Effect of pretreatment with capsaicin (10 μM), ruthenium red (RR, 3 μM), and MEN 10,207 (3 μM) on the contractile response to prostacyclin (PGI_2, 1 μM, 10 μM). Capsaicin, ruthenium red and MEN 10,207 significantly inhibited PGI_2-induced contractions. Control rings: open columns; pretreated rings: shaded columns. $^{**}P < 0.01$; $^{***}P < 0.005$ and $^{*}P < 0.05$.

response to PGI_2 averaged 20.2 ± 2.7% and 30.0 ± 4.0%, at 1 and 10 μM, respectively. The corresponding values in the presence of MEN 10,207 were 7.8 ± 2.0% and 12.7 ± 5.9%, respectively ($P < 0.001$, $P < 0.001$, $n = 7$, Figure 2). MEN 10,207 did not affect acetylcholine-induced contractions. In control rings, the response to acetylcholine averaged 25.9 ± 5.3%, whereas in the presence of MEN 10,207 it was 23.4 ± 3.0% ($n = 8$, $P > 0.05$). MEN 10,207 reduced the responses to neurokinin A. In control rings, it was 28.1 ± 7.7% of acetylcholine maximum, whereas in rings pretreated with MEN 10,207 it was 13.6 ± 4.1% ($n = 9$, $P < 0.01$). The effect of ruthenium red and of MEN 10,207 on PGI_2-induced contractions was non-additive (Figure 3). For PGI_2 (1 μM), the response induced was 20.7 ± 7.6% in control rings and 9.9 ± 2.1% in rings pretreated with both the agents. For PGI_2 (10 μM), the response was 38.2 ± 9.5% in control rings and 17.7 ± 5.7% in rings pretreated with ruthenium red and MEN 10,207. Also the inhibitory effect of ruthenium red and of capsaicin pretreatment on PGI_2-induced contractions was non-additive (Figure 3). In control rings, the response to PGI_2 averaged 28.0 ± 9.5% and 51.6 ± 9.2% of the maximum

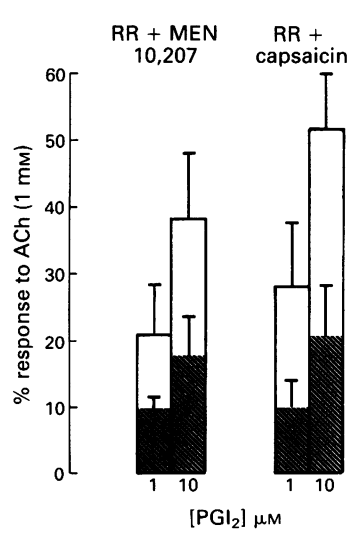

Figure 3 Effect of pretreatment with MEN 10,207 (3 μM) plus ruthenium red (RR, 3 μM) and of capsaicin (10 μM) + ruthenium red (3 μM) on the contractile response to prostacyclin (PGI_2, 1 μM, 10 μM). Control rings: open columns; pretreated rings: shaded columns. Two-way analysis of variance did not show any additive effect between agents ($F = 0.396$, $P > 0.05$ and $F = 1.087$, $P > 0.05$ respectively for MEN 10,207 + RR, and for capsaicin + RR).

at 1 and 10 μM, respectively. The corresponding values in the presence of ruthenium red and after capsaicin pretreatment were 10.0 ± 4.0% and 20.8 ± 7.1% of the maximum, respectively. In both cases, the statistical analysis by two-way analysis of variance did not show any additive effect between the agents ($F = 0.396$, $P > 0.05$ and $F = 1.087$, $P > 0.05$ respectively for MEN 10,207 + ruthenium red, and capsaicin + ruthenium red).

Discussion

The present study shows that PGI_2 produces contraction of the guinea-pig isolated bronchi which is partly (40–60%) dependent on tachykinin release from peripheral endings of capsaicin-sensitive primary afferents.

We used *in vitro* capsaicin desensitization to inactivate selectively sensory nerves of the guinea-pig bronchus. Our results indicate that the response to PGI_2 is partly dependent upon transmitter release from primary afferents and that a fraction of the overall response does not involve sensory nerve activation. The contraction of the isolated bronchi produced by activation of capsaicin-sensitive primary afferents is thought to be almost entirely, if not exclusively, mediated by peptides of the tachykinin family (Lundberg *et al.*, 1983; Maggi *et al.*, 1990a; 1991). It was therefore expected that the response to PGI_2 would be partly sensitive to tachykinin antagonists: such an assumption has been validated by experiments with MEN 10,207, a selective antagonist of NK_2-tachykinin receptors (Rovero *et al.*, 1990; Maggi *et al.*, 1990b). This has also been previously shown (Maggi *et al.*, 1991) to be effective in blocking the noncholinergic bronchial response to sensory nerves activation. MEN 10,207 inhibited the PGI_2-induced response to about the same extent as that produced by *in vitro* capsaicin desensitization and the effect of the two treatments was non-additive. The latter indicates that the inhibitory action of MEN 10,207 is restricted to that fraction of PGI_2 action which involves activation of sensory nerves.

In recent years, evidence has been obtained indicating the existence of multiple modes of transmitter release from peripheral endings of capsaicin-sensitive primary afferents (see Maggi 1991, for review). In particular, the inorganic dye, ruthenium red, has emerged as a useful tool to address this issue. Although ruthenium red is endowed with several types of pharmacological actions at both cell membrane levels and intracellularly, it behaves as a selective functional antagonist of capsaicin in a number of preparations (Maggi, 1991). Ruthenium red prevents the opening of the cation channel coupled with the capsaicin receptor on the membrane of primary afferents (Dray *et al.*, 1990) while it does not bind to the capsaicin receptor (Szallasi & Blumberg, 1990). At the concentration employed in this study, ruthenium red has been shown to prevent selectively sensory nerve activation by capsaicin in the guinea-pig isolated bronchi (Maggi *et al.*, 1989).

In the present experiments, ruthenium red reduced the effect of PGI_2 to the same extent as that produced by either capsaicin pretreatment or by MEN 10,207, and its inhibitory action was non-additive with that of the latter two treatments. This indicates that the inhibitory action of ruthenium red is restricted to that fraction of PGI_2 response which involves tachykinin release from primary afferents. As ruthenium red did not affect the response to exogenously administered substance P or neurokinin A, we conclude that its action toward PGI_2 occurs at a prejunctional level, by inhibiting transmitter release from capsaicin-sensitive afferents, i.e. the same mechanism whereby ruthenium red acts as a functional antagonist of capsaicin (cf. Maggi *et al.*, 1989). The latter conclusion also suggests that PGI_2 and capsaicin share a common mechanism of tachykinin release in the guinea-pig bronchi, which is ruthenium red-sensitive.

The possibility that PGI_2 might interact with the capsaicin receptor on primary afferents seems unlikely, because PGI_2

does not compete with radiolabelled resiniferatoxin for the resiniferatoxin/capsaicin receptor on membranes from dorsal root ganglion neurones (Szallasi & Blumberg, 1990; A. Szallasi, personal communication). We therefore interpret our findings as an indication that PGI_2 activates tachykinin release from primary afferents in guinea-pig bronchi through a mechanism independent of the capsaicin receptor which however shares a common, ruthenium red-sensitive site of action, putatively represented by the cationic channel coupled with the capsaicin receptor.

The potent bronchoconstrictor effect of many prostaglandins has suggested their participation in the pathogenesis of bronchial asthma (Mathe *et al.*, 1973). PGE_2 and PGI_2 have been usually considered to counteract the effects of bronchoconstrictor prostaglandins. The results of the present study and of previous studies (Choudry *et al.*, 1989) suggest a different role for these bronchodilator prostaglandins. Choudry *et al.* (1989) showed that inhaled PGE_2 increased the cough response to a high dose of the provocative agent, capsaicin, without affecting the sensitivity. The authors suggested that this prostaglandin can increase the response of unmyelinated sensory neurones. On the other hand, the implication of our study is that PGI_2 can contract bronchial smooth muscle, and that tachykinins are partly involved.

In conclusion our findings indicate that PGI_2, a major prostanoid produced in the lungs of several species, exerts a contractile action on the guinea-pig isolated bronchi which involves, in part, tachykinin release from capsaicin-sensitive afferents and suggest that PGI_2 and capsaicin activate a common secretory mechanism (ruthenium red-sensitive).

This work was supported in part by grants from the National Research Council (89.02961.04, 89.02664.04, 90.01508.CT04), the Italian Ministry of Education, and by Regione Veneto.

References

ARMSTRONG, D.J. & MILLER, S.A. (1981). Intrapulmonary C-fibres contribute to the afferent arm of the vagally mediated responses to right atrial injections of prostacyclin into rabbits. *J. Physiol.*, **301**, 65P–66P.

BUNTING, S., GRYGLEWSKI, R., MONCADA, S. & VANE, J.R. (1976). Arterial walls generate from prostaglandin endoperoxides a substance (prostaglandin X) which relaxes strips of mesenteric and coeliac arteries and inhibits platelet aggregation. *Prostaglandins*, **12**, 897–913.

CHOUDRY, N.B., FULLER, R.W. & PRIDE, N.B. (1989). Sensitivity of the human cough reflex: effect of inflammatory mediators prostaglandin E, bradykinin, and histamine. *Am. Rev. Respir. Dis.*, **140**, 137–141.

DRAY, A., FORBES, C.A. & BURGESS, G.M. (1990). Ruthenium red blocks the capsaicin-induced increase in intracellular calcium and activation of membrane currents in sensory neurones, as well as the activation of peripheral nociceptors in vitro. *Neurosci. Lett.*, **110**, 52–59.

EL-KASHEF, H.A., WENDELL, F.H. & INA, C.E. (1990). Prostacyclin production with serotonin, increased flow, or elevated venous pressure in dog lung. *J. Appl. Physiol.*, **69**, 1283–1289.

LUNDBERG, J.M., SARIA, A., BRODIN, E., ROSELL, S. & FOLKERS, K. (1983). A substance P antagonist inhibits vagally-induced increase vascular permeability and bronchial smooth muscle contraction in the guinea-pig. *Proc. Natl. Acad. Sci. U.S.A.*, **80**, 1120–1124.

MAGGI, C.A. (1991). Capsaicin and primary afferent neurones: from basic science to human therapy? *J. Auton. Nervous System.* **33**, 1–14.

MAGGI, C.A., PATACCHINI, R., BAROLDI, P., THEODORSSON, E. & MELI, A. (1990a). Immunoblockade by a specific tachykinin antiserum of the non-cholinergic contractile responses in the guinea-pig isolated bronchus. *J. Auton. Pharmacol.*, **10**, 173–179.

MAGGI, C.A., PATACCHINI, R., GIULIANI, S., ROVERO, P., DION, S., REGOLI, D., GIACHETTI, A. & MELI, A. (1990b). Competitive antagonists discriminate between NK_2 tachykinin receptor subtypes. *Br. J. Pharmacol.*, **100**, 588–592.

MAGGI, C.A., PATACCHINI, R., PERRETTI, F., MEINI, S., MANZINI, S., SANTICIOLI, P., DEL BIANCO, E. & MELI, A. (1990c). The effect of thiorphan and epithelium removal on contractions and tachykinin release produced by activation of capsaicin-sensitive afferents in the guinea-pig isolated bronchus. *Naunyn Schmiedebergs Arch. Pharmacol.*, **341**, 74–79.

MAGGI, C.A., PATACCHINI, R., ROVERO, P. & SANTICIOLI, P. (1991). Tachykinin receptors and noncholinergic bronchoconstriction in the guinea-pig isolated bronchi. *Am. Rev. Respir. Dis.*, (in press).

MAGGI, C.A., PATACCHINI, R., SANTICIOLI, P., GIULIANI, S., DEL BIANCO, E., GEPPETTI, P. & MELI, A. (1989). The "efferent" function of capsaicin-sensitive nerves, ruthenium red discriminates between different mechanisms of action. *Eur. J. Pharmacol.*, **170**, 167–177.

MATHE, A.A. & HEDQVIST, P. (1975). Effect of prostaglandin $F_{2\alpha}$ and E_2 on airway conductance in healthy subjects and asthmatic patients. *Am. Rev. Respir. Dis.*, **111**, 313–320.

MATHE, A.A., HEDQVIST, P., HOLMGREN, A. & SVANBORG, N. (1973). Bronchial hyperreactivity to prostaglandin $F_{2\alpha}$ and histamine in patients with asthma. *Br. Med. J.*, **1**, 193–196.

MONCADA, S. & VANE, J.R. (1983). Prostacyclin, thromboxane and leukotrienes. Introduction to Symposium. *Br. Med. Bull.*, **39**, p. 209.

ROBERTS, A.M., SCHULTZ, H.D., GREEN, J.F., ARMSTRONG, D.J., KAUFMAN, M.P., COLERIDGE, H.M. & COLERIDGE, J.C.G. (1985). Reflex tracheal contraction evoked in dogs by bronchodilator prostaglandins E_2 and I_2. *J. Appl. Physiol.*, **58**, 1823–1831.

ROBERTS, A.M., BHATTACHARYA, J., SCHULTZ, H.D., COLERIDGE, H.M. & COLERIDGE, J.C.G. (1986). Stimulation of pulmonary vagal afferent C-fibers by lung edema in dogs. *Circ. Res.*, **58**, 512–522.

ROVERO, P., PESTELLINI, V., MAGGI, C.A., PATACCHINI, R., REGOLI, D. & GIACHETTI, A. (1990). A highly selective NK-2 tachykinin receptor antagonist containing D-tryptophan. *Eur. J. Pharmacol.*, **175**, 113–115.

SMITH, A.P. & CUTHBERT, M.F. (1976). The response of normal and asthmatic subjects to prostaglandins E and F by different routes, and their significate in asthma. In *Advances in Prostaglandin and Thromboxane Research.* ed. Samuelsson, B. & Paoletti, R. Vol. I, pp. 449–459. New York: Raven.

SZALLASI, A. & BLUMBERG, P.M. (1990). Specific binding of resiniferatoxin, an ultrapotent capsaicin analog by dorsal root ganglion membranes. *Brain Res.*, **524**, 106–111.

VAN GRONDELLE, A., WORTHEN, G.S., ELLIS, D., MATHIAS, M.M., MURPHY, C., STRIFE, R.J., REEVES, J.T. & VOELKEL, N.F. (1984). Altering hydrodynamic variables influences PGI_2 production by isolated lungs and endothelial cells. *J. Appl. Physiol.*, **57**, 388–395.

VOELKEL, N.F., GERBER, J.G., McMURTRY, I.F., NIES, A.S. & REEVES, J.T. (1981). Release of vasodilator prostaglandin, PGI_2, and isolated rat lung during vasoconstriction. *Circ. Res.*, **48**, 207–213.

WASSERMAN, M.A., DUCHARME, D.W., WENDLING, M.G., GRIFFIN, R.L. & DEGRAAF, G.L. (1980). Bronchodilator effects of prostacyclin (PGI_2) in dogs and guinea pigs. *Eur. J. Pharmacol.*, **66**, 53–63.

(Received December 13, 1990
Revised April 15, 1991
Accepted May 10, 1991)

Br. J. Pharmacol. (1991), **104**, 53–58

Effects of N^G-substituted analogues of L-arginine on NANC relaxation of the rat anococcygeus and bovine retractor penis muscles and the bovine penile artery

Xiaorong Liu, John S. Gillespie, Ian F. Gibson & [1]William Martin

Department of Pharmacology, University of Glasgow, Glasgow, G12 8QQ

1 The effects of two inhibitors of nitric oxide synthase, N^G-monomethyl L-arginine (L-NMMA) and N^G-nitro L-arginine (L-NOARG), were examined on non-adrenergic non-cholinergic (NANC) inhibitory transmission in the rat anococcygeus, bovine retractor penis (BRP) and bovine penile artery.

2 In the rat anococcygeus, L-NMMA (10–1000 μM) produced a concentration-dependent augmentation of guanethidine (30 μM)-induced tone and inhibited NANC relaxation at all frequencies tested (0.1–20 Hz): the maximum inhibition obtained was 56 ± 6% (n = 6). L-NOARG (0.3–30 μM) also augmented tone and inhibited NANC relaxation in a concentration-dependent manner, but unlike L-NMMA the maximum inhibition was 100%.

3 In the BRP, L-NMMA (10–100 μM) had no effect on tone or NANC-induced relaxation, but at 1000 μM tone was increased and NANC relaxation inhibited by 25 ± 7% (n = 6). L-NOARG (0.3–30 μM) produced a concentration-dependent increase in tone and inhibition of NANC relaxation. As in the rat anococcygeus, inhibition of NANC relaxation was complete.

4 The effects of L-NMMA and L-NOARG were stereospecific since D-NMMA (10–1000 μM) and D-NOARG (1–1000 μM) had no effect on tone or NANC relaxation of the rat anococcygeus or BRP.

5 L-Arginine (10–300 μM) had no effect by itself on NANC-induced relaxation of the rat anococcygeus or BRP. It did, however, reverse the ability of L-NMMA (10–1000 μM) to augment tone and inhibit NANC relaxation in the rat anococcygeus and BRP. The actions of low concentrations L-NOARG (0.3–10 μM) were also reversed by L-arginine (300 μM), but those of higher concentrations were not. D-Arginine (1000 μM) had no effect on the ability of L-NMMA or L-NOARG to augment tone and inhibit NANC relaxation in the anococcygeus and BRP.

6 On the bovine penile artery, both L-NMMA (100 μM) and L-NOARG (30 μM) augmented the tone induced by guanethidine (30 μM) and 5-hydroxytryptamine (0.2 μM) in an endothelium-dependent manner. L-NMMA had no effect on NANC-induced relaxation, but inhibited acetylcholine-induced endothelium-dependent relaxation. L-NOARG abolished NANC relaxation at all frequencies tested and inhibited acetylcholine-induced relaxation. D-NOARG (30 μM) had no effect on NANC or acetylcholine-induced relaxation.

7 The ability of L-NOARG to abolish NANC-induced relaxation in the rat anococcygeus, BRP and bovine penile artery suggests that the L-arginine-nitric oxide pathway mediates neurotransmission in all three tissues. The effectiveness of L-NMMA in blocking NANC relaxation in the rat anococcygeus but not the BRP and bovine penile artery suggests a species difference in the neuronal nitric oxide synthase. The neuronal and endothelial nitric oxide synthases in the penile artery also appear to differ.

Keywords: Anococcygeus; retractor penis; penile artery; NANC nerves; L-arginine; nitric oxide; N^G-monomethyl L-arginine; N^G-nitro L-arginine

Introduction

Endothelium-derived relaxing factor (EDRF, Furchgott & Zawadzki, 1980) has recently been identified as nitric oxide derived from the terminal guanidino nitrogen(s) of L-arginine (Palmer *et al.*, 1987; 1988). This synthesis of nitric oxide can be blocked competitively with N^G-monomethyl L-arginine (L-NMMA), but its D-isomer is inactive (Rees *et al.*, 1989). The L-arginine-nitric oxide system is not, however, restricted to the endothelium: it has been described in macrophages (Marletta *et al.*, 1988), neutrophils (McCall *et al.*, 1989), the brain (Garthwaite *et al.*, 1988; 1989) and adrenal gland (Palacios *et al.*, 1989). Although the functions of the L-arginine-nitric oxide system in the brain are unknown, we and others have proposed that it mediates non-adrenergic, non-cholinergic (NANC) inhibitory neurotransmission in the anococcygeus of the rat and mouse (Gillespie *et al.*, 1989; Li & Rand, 1989; Martin & Gillespie, 1990; Gibson *et al.*, 1990). This proposal was based on the ability of L-NMMA but not D-NMMA to inhibit NANC-induced relaxation in these tissues in an L-arginine-reversible manner. One obstacle to the acceptance of nitric oxide as the NANC neurotransmitter is the finding that L-NMMA is a poor inhibitor of NANC relaxation in the analogous muscle in the bull, the retractor penis muscle (Gillespie & Xiaorong, 1989). The majority of evidence obtained previously, demonstrating the involvement of soluble guanylate cyclase and the blocking action of haemoglobin (Bowman *et al.*, 1982; Bowman & Drummond, 1984), had suggested that the neurotransmitters in the rat anococcygeus and bovine retractor penis (BRP) were similar. We had found, however, that NANC relaxation was blocked by the superoxide anion generators, pyrogallol and hydroquinone, in the rat anococcygeus but not in the BRP (Gillespie & Sheng, 1990). Superoxide anion is known to inactivate nitric oxide (Gryglewski *et al.*, 1986; Rubanyi & Vanhoutte, 1986), and these observations might be consistent with nitric oxide being the NANC neurotransmitter in the anococcygeus but not in the BRP. Following the recent observation that N^G-nitro L-arginine was a more potent and effective inhibitor of NANC relaxation in the anococcygeus of the mouse and rat than L-NMMA (Gibson *et al.*, 1990; Hobbs & Gibson, 1990), we wished to re-evaluate the involvement of the L-arginine-nitric oxide system in the NANC innervation of the BRP. In this study we compared the effects of L-NMMA and L-NOARG on NANC-induced

[1] Author for correspondence.

relaxation in rat anococcygeus and BRP. Furthermore, we examined the actions of these inhibitors on NANC-induced vasodilatation of the bovine penile artery, a tissue which receives the same inhibitory innervation as the BRP (Klinge & Sjöstrand, 1974).

Methods

Preparation of tissues

Bovine penises were obtained from a local abattoir and transported to the laboratory where the retractor penis muscles and proximal segments of the dorsal penile artery were dissected out and freed of connective tissues. Some tissues were used that day, others were stored at 4°C in Krebs solution for use the following day. BRP muscle strips 2–3 mm wide and 1–1.5 cm long were cut for tension recording and penile artery segments 3 cm long were cut for pressure recording. Rat anococcygeus muscles were isolated as previously described (Gillespie, 1972). BRP and anococcygeus muscle strips were mounted under 1–2 g resting tension within Ag-AgCl ring electrodes in 10 ml organ chambers and bathed in Krebs solution containing (mM): NaCl 118, KCl 4.8, $CaCl_2$ 2.5, $MgSO_4$ 1.2, KH_2PO_4 1.2, $NaHCO_3$ 24, glucose 11, and gassed with 5% CO_2 in air. Tension was measured with Grass FTO3C isometric tension transducers and displayed on a Grass Polygraph. Penile artery segments were cannulated, inserted into Ag-AgCl ring electrodes, placed in 10 ml organ chambers and perfused with Krebs solution at 37°C at a constant flow of 3 ml min^{-1} by means of a Watson Marlow pump. Pressure was recorded with Statham pressure transducers and displayed on a Grass Polygraph. In some experiments ring segments of penile artery were used to examine acetylcholine-induced endothelium-dependent relaxation. In the BRP, the anococcygeus and the penile artery, adrenergic motor responses were blocked and tone induced by treatment with guanethidine (30 μM). In most experiments with the penile artery, guanethidine-induced tone was low and was increased further with 5-hydroxytryptamine (0.1–3 μM). Electrical field stimulation was delivered at supramaximal voltage with a Grass S44 or a Harvard stimulator. A pulse width of 0.5 ms was used for the BRP and anococcygeus but on the penile artery this was reduced to 0.1 ms to avoid direct stimulation of muscle fibres.

Drugs

L-Arginine hydrochloride, D-arginine (free base), N^G-nitro L-arginine (L-NOARG) and 5-hydroxytryptamine creatinine sulphate were obtained from Sigma, guanethidine sulphate from CIBA, N^G-nitro D-arginine from Bachem, and N^G-monomethyl L-arginine (L-NMMA) and N^G-monomethyl D-arginine (D-NMMA) were generous gifts from Dr R.M.J. Palmer, Wellcome Laboratories. Glyceryl trinitrate (10% w/w in lactose) was obtained from Napp Laboratories. All drugs were dissolved in saline (0.9%).

Results

Effects of L-NMMA and L-NOARG on the rat anococcygeus and bovine retractor penis

On the rat anococcygeus in the presence of guanethidine (30 μM) L-NMMA (10–1000 μM) and L-NOARG (0.3–30 μM) each produced a concentration-dependent inhibition of NANC relaxation at all frequencies tested (0.1–20 Hz, Figures 1, 2 and 3). At a frequency of 10 Hz, the maximum blockade produced by L-NMMA (1000 μM) was 56 ± 6% ($n = 6$), and that produced by L-NOARG (30 μM) was 98 ± 1% (IC_{50} 1.5 ± 0.4 μM, $n = 10$). On the BRP, L-NMMA (10–1000 μM) was less effective in blocking NANC relaxation than on the rat anococcygeus (Figures 1 and 3): at a frequency of 10 Hz, the maximum blockade produced by L-NMMA (1000 μM) was 25 ± 7% ($n = 6$). In contrast, L-NOARG (0.3–30 μM) was as effective in blocking NANC relaxation on the BRP as on the rat anococcygeus: the maximum blockade produced by L-NOARG (30 μM) was 100 ± 1% (IC_{50} 2.3 ± 0.3 μM, $n = 6$, Figures 2 and 3).

An additional action of L-NMMA and L-NOARG was the ability to augment guanethidine-induced tone: on the rat anococcygeus L-NMMA (10–1000 μM) and L-NOARG (0.3–30 μM) each augmented tone in a concentration-dependent manner to a maximum of around 20% (Figures 1 and 2). On the BRP, L-NOARG (0.3–30 μM) augmented tone but L-NMMA did not produce this effect below 1000 μM.

The ability of both L-NMMA and L-NOARG to block NANC relaxation and increase tone was completely reversed by washing. The stereoisomers D-NMMA (10–1000 μM) and D-NOARG (1–100 μM) had no effect on NANC relaxation or guanethidine-induced tone in the anococcygeus or BRP (Figures 2 and 3).

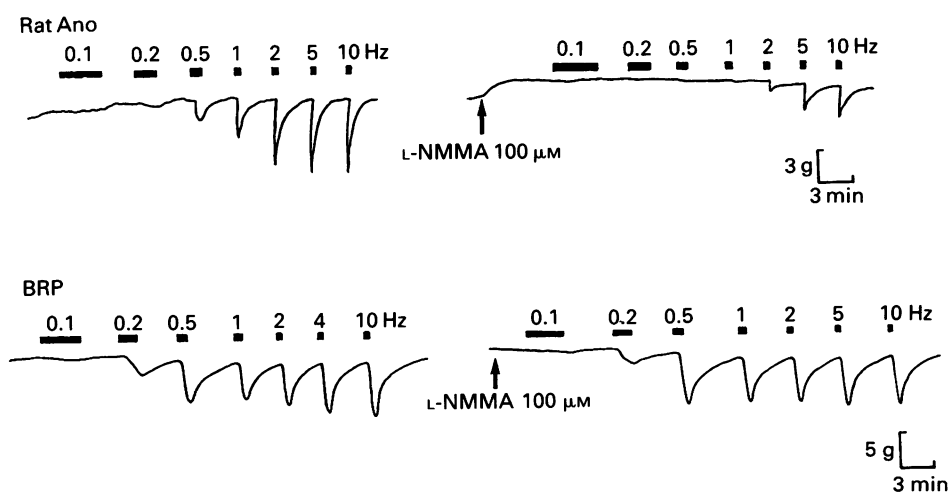

Figure 1 In the presence of guanethidine (30 μM)-induced tone, electrical field stimulation of rat anococcygeus (Rat Ano) and bovine retractor penis (BRP) muscles with a fixed number of 20 pulses (0.5 ms, supramaximal voltage) elicited frequency-dependent relaxation. The application of N^G-monomethyl L-arginine (L-NMMA, 100 μM) raised guanethidine-induced tone and inhibited NANC-induced relaxation of the rat anococcygeus at all frequencies tested but had no effects on the BRP. The frequency and duration of stimulation is shown above each response.

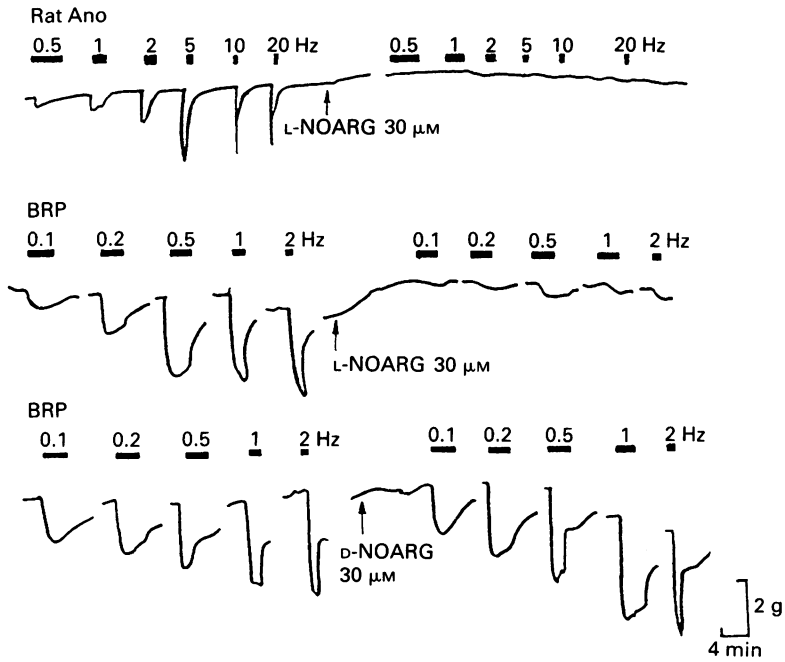

Figure 2 N^G-nitro L-arginine (L-NOARG, 30 μM) raised guanethidine (30 μM)-induced tone and inhibited NANC relaxation of rat anococcygeus (Rat Ano) and bovine retractor penis (BRP) muscles at all frequencies tested. N^G-nitro D-arginine (D-NOARG, 30 μM) had no effect on tone or NANC-induced relaxation of the BRP. The frequency and duration of stimulation is shown above each response. The rat anococcygeus was stimulated at a fixed number of 100 pulses (0.5 ms, supramaximal voltage), and on the BRP, 100 pulses were delivered at 2 Hz, 1 Hz and 0.5 Hz and 50 and 20 pulses at 0.2 Hz and 0.1 Hz, respectively.

Effects of L-arginine

L-Arginine at concentrations up to 300 μM had no significant effect on the magnitude of NANC relaxation of the rat anococcygeus or BRP at any frequency tested (0.1–20 Hz). L-Arginine (10–300 μM), but not D-arginine (1000 μM) did, however, reverse the ability of L-NMMA and L-NOARG to increase tone and block NANC relaxation of the anococcygeus and BRP: the effects of L-NMMA at all concentrations were reversed but only those of L-NOARG at submaximal concentrations were reversed. Figure 4 shows blockade of NANC relaxation of the BRP by L-NOARG (10 μM) and its

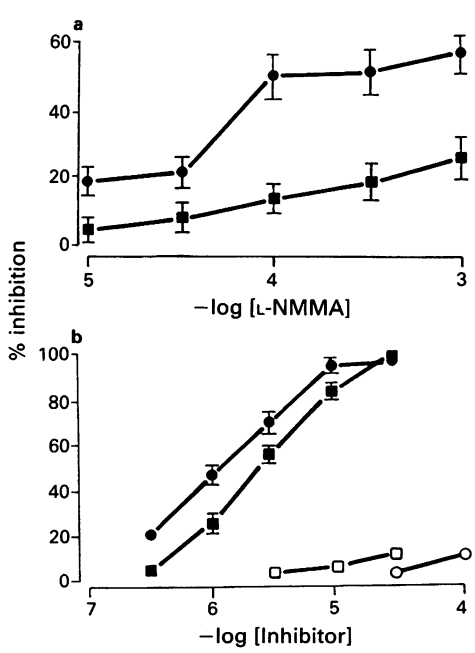

Figure 3 Concentration-effect curves showing the ability of N^G-monomethyl L-arginine (L-NMMA, a) and N^G-nitro L-arginine (L-NOARG) and N^G-nitro D-arginine (D-NOARG, b) to inhibit NANC-induced relaxation of the rat anococcygeus (circles) and bovine retractor penis (squares) muscles stimulated at a frequency of 10 Hz (0.5 ms, supramaximal voltage). Results obtained with the L- and D-isomers and indicated by filled and open symbols, respectively. Points are the mean and vertical bars indicate the s.e.mean of 6–10 observations.

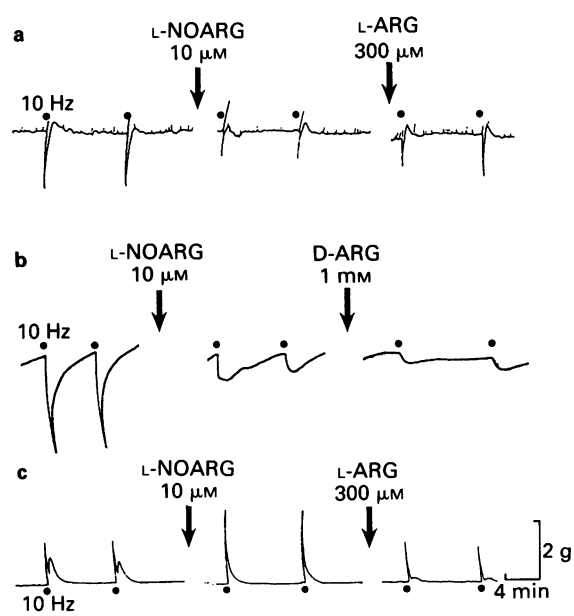

Figure 4 In the presence of guanethidine (30 μM)-induced tone, NANC-induced relaxation of the bovine retractor penis muscle (10 Hz, 0.5 ms, 100 pulses, supramaximal voltage) was inhibited in the presence of N^G-nitro L-arginine (L-NOARG, 10 μM) (a and b). In the continued presence of L-NOARG, blockade was reversed by the addition of L-arginine (300 μM) but not D-arginine (1000 μM). In the absence of tone, adrenergic motor responses were augmented by L-NOARG (10 μM) and this was reversed by the addition of L-arginine (300 μM) (c). All NANC responses shown following drug treatment indicate the responses obtained upon equilibration of the drugs. Dots indicate the moment of electrical stimulation.

reversal by L-arginine (300 μM) but not D-arginine (1000 μM). This figure also shows that at low tone and in the absence of guanethidine, adrenergic motor responses are augmented by L-NOARG (10 μM) and this is reversed by L-arginine (300 μM).

Selectivity of L-NMMA and L-NOARG

L-NMMA and L-NOARG have previously been shown to block NANC relaxation of rat and mouse anococcygeus without affecting relaxation induced by nitric oxide or nitrovasodilators (Gillespie *et al.*, 1989; Gibson *et al.*, 1990). Figure 5 shows that on the BRP also, L-NOARG (30 μM) has no effect on the relaxation induced by glyceryl trinitrate (0.01–1 μM).

Bovine penile artery

In isolated segments of bovine penile artery, adrenergic motor responses were blocked and active tone induced by a combination of 5-hydroxytryptamine (0.1–1 μM) and guanethidine (30 μM) to produce a perfusion pressure of 200–300 mmHg. Both L-NMMA (100 μM) and L-NOARG (30 μM) augmented perfusion pressure by 10–20%, and this was abolished following endothelial removal (data not shown). L-NMMA had no effect on NANC vasodilatation, but L-NOARG abolished NANC vasodilatation at all frequencies (1–20 Hz, Figure 6). In isolated ring segments of penile artery, however, the endothelium-dependent relaxation induced by acetylcholine (0.01–3 μM) was inhibited following pretreatment with either L-NMMA (100 μM) or L-NOARG (30 μM) (Figure 7). D-NOARG (30 μM) had no effect on tone, or on NANC- or acetylcholine-induced vasodilatation (data not shown).

Discussion

Evidence presented previously suggesting the involvement of the L-arginine-nitric oxide system in NANC neurotransmission in the anococcygeus of the rat and mouse is strong (Gillespie *et al.*, 1989; Li & Rand, 1989; Gibson *et al.*, 1990). Thus L-NMMA, an inhibitor of nitric oxide synthesis from L-arginine in neurones and other cells (Knowles *et al.*, 1989; Moncada *et al.*, 1989) inhibits NANC relaxation in these tissues by 50–60%, but the inactive D-isomer does not. The effects of L-NMMA can be reversed by the addition of L-arginine indicating that the inhibition is competitive in nature. It is likely that blockade by L-NMMA results from an action in the NANC nerve terminals since the relaxant actions of nitric oxide or nitrovasodilators, which like those of the inhibitory nerves arise through stimulation of soluble guanylate cyclase (Katsuki *et al.*, 1977; Bowman & Drummond, 1984), are completely unaffected. We cannot at this point, however, rule out an alternative possibility that the NANC transmitter acts post-junctionally to trigger nitric oxide formation from L-arginine. It was surprising therefore to find in the analogous muscle to the anococcygeus in the bull, the retractor penis muscle, that L-NMMA is a poor inhibitor of NANC relaxation (Gillespie & Xiaorong, 1989). One potential explanation of this difference is that the L-arginine-nitric oxide system mediates NANC transmission in the anococcygeus but not the bovine retractor penis (BRP). Further evidence in

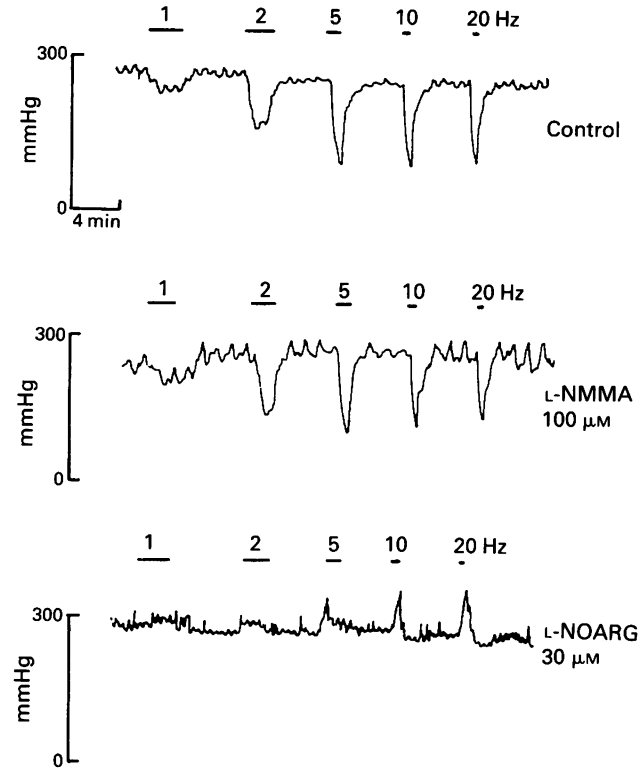

Figure 6 In the isolated, perfused bovine penile artery in the presence of pressure developed in response to guanethidine (30 μM) and 5-hydroxytryptamine (8×10^{-7} M), electrical field stimulation (0.1 ms, supramaximal voltage, 200 pulses) induced frequency-dependent NANC vasodilatation. NANC vasodilatation was unaffected by N^G-monomethyl L-arginine (L-NMMA, 100 μM), but was abolished at all frequencies by N^G-nitro L-arginine (L-NOARG, 30 μM). When L-NMMA and L-NOARG were used, the concentration of 5-hydroxytryptamine was reduced to 2×10^{-7} M to offset the endothelium-dependent augmentation of pressure induced by these agents. The frequency and duration of stimulation is shown above each response.

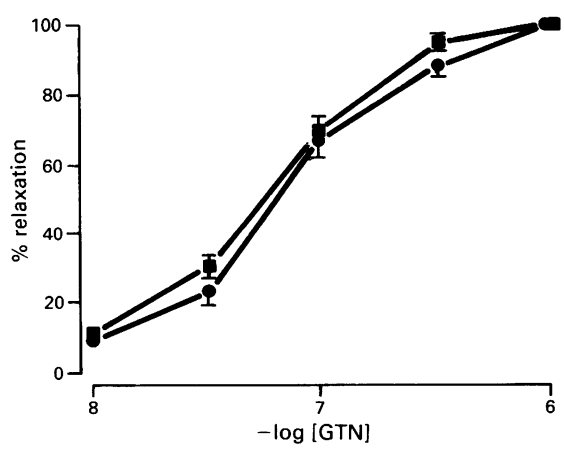

Figure 5 In the presence of guanethidine (30 μM)-induced tone, glyceryl trinitrate (GTN, 0.01–1 μM) induced concentration-dependent relaxation of the bovine retractor penis muscle (●). N^G-nitro L-arginine (L-NOARG, 30 μM, ■) had no effect on glyceryl trinitrate-induced relaxation. Points are the mean and vertical bars indicate the s.e.mean of 10 observations.

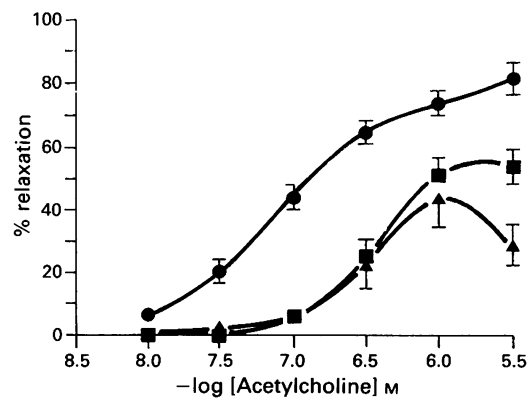

Figure 7 Concentration-effect curves showing acetylcholine-induced endothelium-dependent relaxation of untreated rings of bovine penile artery (●) and the blockade of this relaxation following treatment with N^G-monomethyl L-arginine (100 μM, ▲) or N^G-nitro L-arginine (30 μM, ■). Points are the mean and vertical bars indicate the s.e.mean of at least 6 observations.

support of this is the ability of the superoxide radical generators, pyrogallol and hydroquinone, to inhibit NANC relaxation in the anococcygeus but not the BRP (Gillespie & Sheng, 1990), although, alternatively, this could reflect different levels of superoxide dismutase in the two tissues. It became clear, however, when we examined the effects of L-NOARG, a more potent and selective inhibitor of NANC relaxation in the anococcygeus of the mouse and rat (Gibson *et al.*, 1990; Hobbs & Gibson, 1990) that NANC relaxation of the BRP could be completely abolished. Furthermore, as previously shown for rat anococcygeus (Hobbs & Gibson, 1990), blockade was stereoelective since D-NOARG was completely inactive. When L-NOARG-induced blockade was complete, reversal by L-arginine was unconvincing, but submaximal blockade could be partially reversed suggesting it was competitive in nature. D-Arginine was unable to reverse this blockade as was shown previously for mouse and rat anococcygeus (Gibson *et al.*, 1990; Hobbs & Gibson, 1990). Our finding that L-NOARG had no effect on glyceryl trinitrate-induced relaxation of the BRP, confirms previous reports of a lack of effect of this substance on nitrovasodilator-induced relaxation in the anococcygeus of the mouse and rat (Gibson *et al.*, 1990; Hobbs & Gibson, 1990), and suggests that as with L-NMMA, blockade of NANC relaxation occurs by a pre-junctional action.

The bovine penile artery receives the same parasympathetic innervation as the BRP (Klinge & Sjöstrand, 1974), and consistent with this, we found that NANC vasodilatation in this tissue was similarly resistant to blockade by L-NMMA, but abolished by L-NOARG. It is likely therefore that the ability of L-NMMA to inhibit NANC relaxation in the anococcygeus of the rat and mouse but to have little effect in the BRP or bovine penile artery results from a species difference, probably in the nitric oxide synthase enzyme. Acetylcholine-induced endothelium-dependent relaxation of the bovine penile artery was, however, inhibited by both L-NMMA and L-NOARG suggesting that the nitric oxide synthases in the endothelium and NANC nerves of this tissue also differ. Previous studies in which the rank order of potency of a range of analogues of L-arginine have been examined on endothelial cells, macrophages, neutrophils, brain and adrenal gland have already suggested the existence of different forms of the enzyme nitric oxide synthase (Iyengar *et al.*, 1987; Hibbs *et al.*, 1987; Rees *et al.*, 1990). In addition to blocking NANC relaxation, we found that L-NOARG potentiated adrenergic motor responses in the BRP. This observation is in keeping with earlier observations that inhibition of the NANC nerves with haemoglobin or by hypoxia potentiates motor responses (Bowman & McGrath, 1985) and highlights the mutually antagonistic actions of the motor and inhibitory nerves.

Recent evidence obtained with L-NMMA and L-NOARG suggests a wide occurrence of nerves utilizing the L-arginine-nitric oxide system in the peripheral autonomic nervous system. For example, such nerves appear to relax the rabbit corpus cavernosum (Ignarro *et al.*, 1990), which like the anococcygeus, retractor penis and penile artery is innervated by the sacral parasympathetic outflow. These findings taken together indicate an important role for nitric oxide in penile erection. Such NANC responses are not, however, limited to tissues receiving a sacral parasympathetic innervation; it has also been proposed that neurogenic relaxation of dog cerebral and superior mesenteric artery (Toda & Okamura, 1990) and ileocolonic junction (Bult *et al.*, 1990), guinea-pig trachea (Tucker *et al.*, 1990), and rat oesophagus (Will *et al.*, 1990) involve the L-arginine-nitric oxide system. Furthermore, an immunohistochemical study has revealed the presence of the enzyme nitric oxide synthase in nerves in the periphery as well in the CNS (Bredt *et al.*, 1990).

The use of the L-arginine-nitric oxide system by a nerve presents a novel concept in neurotransmission, difficult to reconcile with the classical view of neurotransmitters stored in vesicles and released in a quantal manner. It is not easy to conceive of a small membrane permeant, highly reactive substance such as nitric oxide being stored in vesicles. Furthermore, the rapid onset of blockade by the nitric oxide synthase inhibitors, L-NMMA and L-NOARG, suggests that nitric oxide is synthesized on demand by the nerves and not stored. The strict calcium-dependence of neurally-derived nitric oxide synthase (Knowles *et al.*, 1989) suggests, however, that in common with other nerves, neurotransmission is triggered by an influx of calcium. Further studies are required to determine precisely the mechanisms governing excitation-secretion coupling in NANC nerves utilizing the L-arginine-nitric oxide system.

In addition to blocking NANC relaxation, L-NMMA and L-NOARG, but not their D-isomers, augmented tone in the rat anococcygeus, BRP and bovine penile artery. In the latter tissue this was strictly endothelium-dependent and is probably related to inhibition of basal synthesis of EDRF (nitric oxide). In the rat anococcygeus and BRP, however, it is likely to be related to inhibition of spontaneous synthesis of nitric oxide by the inhibitory nerves. This is suggested by the effectiveness of L-NOARG in blocking NANC relaxation and raising tone in both tissues whereas L-NMMA was relatively ineffective on both the NANC response and tone in the BRP.

In conclusion, the effectiveness of L-NOARG in inhibiting NANC relaxation of the rat anococcygeus, BRP and bovine penile artery in an L-arginine-reversible manner suggests that the L-arginine-nitric oxide system mediates neurotransmission in all three tissues. The effectiveness of L-NMMA in blocking NANC relaxation in the rat anococcygeus but not in the BRP or bovine penile artery suggests a species difference in the neuronal nitric oxide synthase enzyme. The nitric oxide synthase enzyme in the endothelium and NANC nerves of the bovine penile artery also appear to differ.

This work was supported by the British Heart Foundation and the Medical Research Funds of the University of Glasgow. X.L. is supported by a Glasgow University Post-graduate Scholarship and an O.R.S. award.

References

BOWMAN, A. & DRUMMOND, A.H. (1984). Cyclic GMP mediates neurogenic relaxation in the bovine retractor penis muscle. *Br. J. Pharmacol.*, **81**, 665–674.

BOWMAN, A., GILLESPIE, J.S. & POLLOCK, D. (1982). Oxyhaemoglobin blocks non-adrenergic inhibition in the bovine retractor penis muscle. *Eur. J. Pharmacol.*, **85**, 221–224.

BOWMAN, A. & McGRATH, J.C. (1985). The effect of hypoxia on neuroeffector transmission in the bovine retractor penis and rat anococcygeus muscles. *Br. J. Pharmacol.*, **85**, 869–875.

BREDT, D.S., HWANG, P.M. & SNYDER, S.H. (1990). Localisation of nitric oxide synthase indicating a neural role for nitric oxide. *Nature*, **347**, 768–770.

BULT, H., BOECKXSTAENS, G.E., PELCKMANS, P.A., JORDAENS, F.H., VAN MAERCKE, Y.M. & HERMAN, A.G. (1990). Nitric oxide as an inhibitory non-adrenergic non-cholinergic neurotransmitter. *Nature*, **345**, 346–347.

FURCHGOTT, R.F. & ZAWADZKI, J.V. (1980). The obligatory role of endothelial cells in the relaxation of arterial smooth muscle by acetylcholine. *Nature*, **288**, 373–376.

GARTHWAITE, J., CHARLES, S.L. & CHESS-WILLIAMS, R. (1988). Endothelium-derived relaxing factor release on activation of NMDA receptors suggests role as intercellular messenger in the brain. *Nature*, **336**, 385–388.

GARTHWAITE, J., GARTHWAITE, G., PALMER, R.M.J. & MONCADA, S. (1989). NMDA receptor activation induces nitric oxide synthesis from arginine in rat brain slices. *Eur. J. Pharmacol.*, **172**, 413–416.

GIBSON, A., MIRZAZADEH, S., HOBBS, A.J. & MOORE, P.K. (1990). L-N^G-monomethyl arginine and L-N^G-nitro arginine inhibit non-

adrenergic, non-cholinergic relaxation of the mouse anococcygeus muscle. *Br. J. Pharmacol.*, **99**, 602–606.

GILLESPIE, J.S. (1972). The rat anococcygeus muscle and its response to nerve stimulation and to some drugs. *Br. J. Pharmacol.*, **45**, 404–416.

GILLESPIE, J.S., LIU, X. & MARTIN, W. (1989). The effects of L-arginine and N^G-monomethyl L-arginine on the response of the rat anococcygeus to NANC nerve stimulation. *Br. J. Pharmacol.*, **98**, 1080–1082.

GILLESPIE, J.S. & SHENG, H. (1990). The effects of pyrogallol and hydroquinone on the response to NANC nerve stimulation in the rat anococcygeus and the bovine retractor penis muscles. *Br. J. Pharmacol.*, **99**, 194–196.

GILLESPIE, J.S. & XIAORONG, L. (1989). The effect of arginine and L–N monomethyl arginine on the response of the bovine retractor penis to stimulation of its NANC nerve. *Br. J. Pharmacol.*, **97**, 453P.

GRYGLEWSKI, R.J., MONCADA, S. & PALMER, R.M.J. (1986). Bioassay of prostacyclin and endothelium-derived relaxing factor (EDRF) from porcine aortic endothelial cells. *Br. J. Pharmacol.*, **87**, 685–694.

HIBBS, J.B. JR., VAVRIN, Z. & TAINTOR, R.R. (1987). L-arginine is required for expression of the activated macrophage effector mechanism causing selective metabolic inhibition in target cells. *J. Immunol.*, **138**, 550–565.

HOBBS, A.J. & GIBSON, A. (1990). L-N^G-nitro-arginine and its methyl ester are potent inhibitors of non-adrenergic, non-cholinergic transmission in the rat anococcygeus. *Br. J. Pharmacol.*, **100**, 749–752.

IGNARRO, L.J., BUSH, P.A., BUGA, G.M., WOOD, K.S., FUKOTO, J.M. & RAJFER, J. (1990). Nitric oxide and cyclic GMP formation upon electrical field stimulation cause relaxation of corpus cavernosum smooth muscle. *Biochem. Biophys. Res. Commun.*, **170**, 843–850.

IYENGAR, R., STUEHR, D.J. & MARLETTA, M.A. (1987). Macrophage synthesis of nitrite, nitrate and N-nitrosamines: precursors and role of the respiratory burst. *Proc. Natl. Acad. Sci. U.S.A.*, **84**, 6369–6373.

KATSUKI, S., ARNOLD, W., MITTAL, C.K. & MURAD, F. (1977). Stimulation of guanylate cyclase by sodium nitroprusside, nitroglycerine and nitric oxide in various tissue preparations and comparisons to the effects of sodium azide and hydroxylamine. *J. Cyclic Nucleotide Res.*, **3**, 23–25.

KLINGE, E. & SJÖSTRAND, N.O. (1974). Contraction and relaxation of the retractor penis muscle and the penile artery of the bull. *Acta Physiol. Scand.*, Suppl. **420**, 1–88.

KNOWLES, R.G., PALACIOS, M., PALMER, R.M.J. & MONCADA, S. (1989). Formation of nitric oxide from L-arginine in the central nervous system: A transduction mechanism of the stimulation of soluble guanylate cyclase. *Proc. Natl. Acad. Sci. U.S.A.*, **86**, 5159–5162.

LI, C.G. & RAND, M.J. (1989). Evidence for a role of nitric oxide in the neurotransmitter system mediating relaxation of the rat anococcygeus muscle. *Clin. Exp. Pharmacol. Physiol.*, **16**, 933–938.

McCALL, T.B., BOUGHTON-SMITH, N.K., PALMER, R.M.J., WHITTLE, B.J.R. & MONCADA, S. (1989). Synthesis of nitric oxide from L-arginine by neutrophils. Release and interaction with superoxide anion. *Biochem. J.*, **261**, 293–296.

MARLETTA, M.A., YOON, P.S., IYENGAR, R., LEAF, C.D. & WISHNOK, J.S. (1988). Macrophage oxidation of L-arginine to nitrite and nitrate: nitric oxide is an intermediate. *Biochemistry*, **27**, 8706–8711.

MARTIN, W. & GILLESPIE, J.S. (1990). L-arginine-derived nitric oxide: the basis of inhibitory transmission in the anococcygeus and retractor penis muscles. In *Novel Peripheral Neurotransmitters*. ed. Bell, C. pp. 65–79. New York: Pergamon Press.

MONCADA, S., PALMER, R.M.J. & HIGGS, E.A. (1989). Biosynthesis of nitric oxide from L-arginine. A pathway for the regulation of cell function and communication. *Biochem. Pharmacol.*, **38**, 1709–1715.

PALACIOS, M., KNOWLES, R.G., PALMER, R.M.J. & MONCADA, S. (1989). Nitric oxide from L-arginine stimulates soluble guanylate cyclase in adrenal glands. *Biochem. Biophys. Res. Commun.*, **165**, 802–809.

PALMER, R.M.J., ASHTON, D.S. & MONCADA, S. (1988). Vascular endothelial cells synthesize nitric oxide from L-arginine. *Nature*, **333**, 664–666.

PALMER, R.M.J., FERRIGE, A.G. & MONCADA, S. (1987). Nitric oxide release accounts for the biological activity of endothelium-derived relaxing factor. *Nature*, **327**, 524–526.

REES, D.D., PALMER, R.M.J., HODSON, H.F. & MONCADA, S. (1989). A specific inhibitor of nitric oxide formation from L-arginine attenuates endothelium-dependent relaxation. *Br. J. Pharmacol.*, **96**, 418–424.

REES, D.D., PALMER, R.M.J., SCHULZ, R., HODSON, H.F. & MONCADA, S. (1990). Characterisation of three inhibitors of endothelial nitric oxide synthase *in vitro* and *in vivo*. *Br. J. Pharmacol.*, **101**, 746–752.

RUBANYI, G.M. & VANHOUTTE, P.M. (1986). Superoxide anions and hyperoxia inactivate endothelium-derived relaxing factor. *Am. J. Physiol.*, **250**, H822–H827.

TODA, N. & OKAMURA, T. (1990). Modification by L-N^G-monomethyl arginine (L-NMMA) of the response to nerve stimulation in isolated dog mesenteric and cerebral arteries. *Jpn. J. Pharmacol.*, **52**, 170–173.

TUCKER, J.F., BRAVE, S.R., CHARALAMBOUS, L., HOBBS, A.J. & GIBSON, A. (1990). L-N^G-nitro arginine inhibits non-adrenergic, non-cholinergic relaxation of guinea-pig isolated tracheal smooth muscle. *Br. J. Pharmacol.*, **100**, 663–664.

WILL, S., BIEGER, D. & TRIGGLE, C.R. (1990). NO: possible role in TTX-sensitive field-stimulated relaxations of the rat oesophageal tunica muscularis mucosae. *Eur. J. Pharmacol.*, **183**, 2419–2420.

(Received December 14, 1990
Revised April 24, 1991
Accepted May 13, 1991)

Br. J. Pharmacol. (1991), **104**, 59–64

Regional coronary haemodynamic effects of two inhibitors of nitric oxide synthesis in anaesthetized, open-chest dogs

Vincent Richard, Alain Berdeaux, Christophe Drieu la Rochelle & [1]Jean-François Giudicelli

Laboratoire de Pharmacologie, Faculté de Médecine Paris Sud, 63 rue Gabriel Péri, 94276 Le Kremlin-Bicêtre Cédex, France

1 The role of endothelial nitric oxide synthesis from L-arginine in the regulation of coronary vascular tone and myocardial tissue perfusion was evaluated in anaesthetized, open-chest dogs. Coronary blood flow was measured with an electromagnetic flow probe placed around the left circumflex coronary artery. Coronary vascular resistance was calculated from mean arterial blood pressure and mean coronary blood flow, whereas regional myocardial tissue flow was determined by use of the radioactive microspheres technique.

2 N^G-monomethyl L-arginine (L-NMMA) and N^G-nitro-L-arginine methyl ester (L-NAME), administered directly into the left circumflex artery, induced a small increase in arterial blood pressure and an increase in coronary vascular resistance. However, myocardial tissue perfusion, assessed by the microspheres technique (whether subendocardial, subepicardial, or transmural), was unaffected by L-NMMA or L-NAME.

3 Acetylcholine, administered intracoronarily, induced an increase in left circumflex coronary blood flow and a decrease in coronary vascular resistance, without affecting systemic haemodynamics. This coronary vasodilator effect of acetylcholine was markedly inhibited by L-NMMA and L-NAME, the latter being a more potent antagonist than the former.

4 These results indicate that the endothelial L-arginine pathway is largely responsible for the coronary vasodilator effect of acetylcholine. However, although basal release of nitric oxide from L-arginine apparently contributes to the regulation of resting coronary vascular tone, blockade of this pathway does not affect myocardial tissue perfusion, possibly because of compensatory mechanisms occurring at the level of small arterioles and/or capillaries.

Keywords: Endothelium; endothelium-derived relaxing factor; coronary circulation; regional myocardial blood flow; microspheres; acetylcholine; L-arginine; nitric oxide

Introduction

Vascular endothelial cells synthesize nitric oxide (NO) from L-arginine (Palmer *et al.*, 1988a), and this pathway accounts for the biological action of the endothelium-derived relaxing factor initially described by Furchgott & Zawadzki (1980). The biosynthesis of NO by vascular endothelial cells is antagonized by N^G-substituted analogues of L-arginine, especially N^G-monomethyl-L-arginine (L-NMMA; Palmer *et al.*, 1988b) and N^G-nitro-L-arginine methyl ester (L-NAME; Moore *et al.*, 1990; Rees *et al.*, 1990; Mülsch & Busse, 1990). *In vitro*, both inhibitors induce an endothelium-dependent increase in tone of isolated vascular rings (e.g. Palmer *et al.*, 1988b) and a rise in coronary perfusion pressure in isolated hearts (Amezcua *et al.*, 1989). In addition, administration of these L-arginine analogues *in vitro* results in a marked inhibition of endothelium-dependent relaxations to various agonists, including acetylcholine (e.g. Palmer *et al.*, 1988b).

In vivo, systemic administration of either L-NMMA or L-NAME causes dose-dependent hypertension and regional vasoconstriction (Aisaka *et al.*, 1989; Whittle *et al.*, 1989; Gardiner *et al.*, 1990a,b,c; Rees *et al.*, 1990), and these *in vivo* effects of L-NMMA and L-NAME are consistent with inhibition of basal release of nitric oxide from vascular endothelial cells. In anaesthetized rabbits, systemic administration of L-NAME induces a reduction in regional tissue perfusion (microspheres technique) in various vascular territories, including the coronary bed (Humphries *et al.*, 1991). In conscious dogs, i.v. administration of L-NMMA induces hypertension and vasoconstriction of both large epicardial coronary arteries and coronary resistance vessels (Chu *et al.*, 1990). However, in this last study, the constriction of the coronary resistance bed remains modest, suggesting a preferential action of nitric oxide on large conductance as compared to small resistance coronary arteries. Whether this vasoconstriction of the coronary resistance bed is sufficient to induce in dogs a reduction in regional myocardial tissue perfusion, is not known.

In addition, in contrast to *in vitro* data, the hypotensive and vasodilator responses to acetylcholine *in vivo* in both anaesthetized and conscious animals are only very moderately affected by L-NMMA or L-NAME (Aisaka *et al.*, 1989; Rees *et al.*, 1990; Gardiner *et al.*, 1990c). Furthermore, in conscious rats, the regional vasodilator effects of acetylcholine in different vascular beds are virtually unaffected by L-NAME (Gardiner *et al.*, 1990c). In situations in which acetylcholine induces marked hypotension, the regional responses obtained are likely to be the consequence of both a direct vasodilator effect and indirect influences such as neurohumoral and (at least in the conscious animals) baroreflex mechanisms that occur in response to acetylcholine-induced hypotension (Gardiner *et al.*, 1990c), and these indirect influences are probably unaffected by L-arginine analogues. To avoid such confounding factors, it is essential to evaluate the effects of the inhibitors on the response to acetylcholine administered locally at doses that do not markedly affect blood pressure.

Thus, we designed the present study to assess, in anaesthetized open-chest dogs, the effects of two inhibitors of endothelium-derived nitric oxide, L-NMMA and L-NAME, administered directly into the left circumflex coronary artery, on regional myocardial blood flow (assessed by the microspheres technique) and its transmural distribution (endocardial/epicardial flow ratios), and on the responses to acetylcholine infused into the coronary artery at doses that do not affect systemic haemodynamics.

Methods

Experimental preparation

Experiments were performed on 11 mongrel dogs of either sex, weighing 15–25 kg. Animals were anaesthetized with

[1] Author for correspondence.

35 mg kg^{-1} i.v. sodium pentobarbitone and ventilated by a Harvard respirator with room air supplemented with low-flow oxygen. Arterial blood gases were checked periodically and maintained within a physiological range by adjusting ventilator variables as needed. A saline-filled catheter was inserted into the right femoral artery and advanced in the ascending thoracic aorta for the measurement of arterial blood pressure and for withdrawal of reference arterial blood samples required for determining tissue flow (see below). A left thoracotomy was performed in the fourth intercostal space and the heart was suspended in a pericardial cradle. A saline-filled catheter was placed in the left atrial appendage for later injection of radioactive microspheres. The left circumflex (LCX) coronary artery was isolated distal to its atrial appendage but proximal to its first marginal branch. Phasic and mean left circumflex coronary blood flow were continuously recorded with a Gould electromagnetic flow probe (2–3 mm internal diameter) placed around the isolated segment of the artery. Coronary vascular resistance was calculated as mean arterial pressure/mean coronary blood flow. A small heparin-filled 3F teflon catheter (Plastimed, France) was inserted into the circumflex artery proximal to the blood flow probe with a metal guide. Care was taken so that the tip of the catheter did not interfere with the electromagnetic blood flow signal. Left circumflex coronary blood flow was monitored continuously during the intracoronary cannulation, in order to verify that the cannulation was not associated with significant impairment of coronary perfusion. The intracoronary catheter was secured to the chest and was left in place throughout the experiment; patency of the catheter was verified periodically by flushing 1 ml of heparinized saline.

Experimental protocol

After a stabilization period of at least 15 min, heart rate, blood pressure and LCX blood flow were measured. Increasing doses of acetylcholine (ACh; 0.03, 0.1 and 0.3 μg kg^{-1}) were then injected into the circumflex coronary artery as 2 min infusions (0.5 ml min^{-1}). Such infusions of ACh typically induced an initial peak increase in LCX blood flow (within the first 20–30 s of infusion), followed by a plateau which remained stable until the end of the infusion. Thus, the effects of inhibitors of the blood flow response to acetylcholine were monitored both at the peak dilator effect of acetylcholine and during the plateau phase. In all experiments, coronary blood flow was allowed to return to baseline before subsequent administration of ACh. In addition, the vehicle (saline) was periodically infused over 2 min (0.5 ml min^{-1}) to verify the absence of effect on coronary blood flow.

After establishment of the control dose-response curve to acetylcholine, the animals were allowed to stabilize for at least 15 min, then the first (control) radioactive microspheres were administered (see below). The animals were assigned to either L-NMMA ($n = 5$) or L-NAME ($n = 6$). Subsequently, increasing doses of the selected inhibitor (0.1, 0.3 and 1 mg kg^{-1}, cumulative doses) were infused into the coronary artery over 2 min (0.5 ml min^{-1}). The response to one dose of ACh (0.1 μg kg^{-1}) was again assessed after each dose of the inhibitor. In order to measure the effects of L-NMMA or L-NAME on regional myocardial blood flow, the second and third radioactive microspheres were injected after the administration of the two highest doses of the inhibitors (i.e. 0.3 and 1 mg kg^{-1}), but before administration of acetylcholine. Fifteen min after the last microspheres injection, increasing doses of D-arginine and L-arginine were administered. Initially, we attempted to deliver L-arginine through the intracoronary catheter, but this procedure was associated with the development of severe ventricular arrhythmias, including episodes of ventricular tachycardia associated with marked transient decreases in blood pressure, and the arrhythmias became even more severe when acetylcholine was infused after L-arginine. Because of this, the haemodynamic effects of L-arginine administered intracoronarily could not be analyzed, but, in 7 dogs (4 from the L-NMMA and 3 from the L-NAME group), D- and L-arginine were also administered intravenously at the dose of 60 mg kg^{-1}. Administration of L-arginine through the intravenous route was associated with less severe arrhythmias. Thus the effect of L-arginine on the baseline haemodynamic effects of L-NMMA and L-NAME are described only in this subset of 7 animals. However, even in these conditions, administration of acetylcholine was associated with the development of severe arrhythmias. Hence, it was not possible to assess the reversal by L-arginine of the inhibitory effects of L-NMMA and L-NAME on acetylcholine-induced dilatation.

Measurement of regional myocardial blood flows

The distribution of regional myocardial tissue flows was assessed by the radioactive microspheres technique. At the times indicated in the experimental design, approximately 2×10^6 microspheres (diameter 15 ± 3 μM), labelled with ^{46}Sc, ^{103}Ru or ^{141}Ce (New England Nuclear, Boston, Massachusetts), were injected through the catheter in the left arterial appendage, followed by a 10 ml saline flush. Beginning just before and continuing for 90 s after injection, a reference sample of arterial blood was withdrawn from the femoral artery at a rate of 20 ml min^{-1}. Reference blood samples were collected in 6 separate aliquots in order to ensure that all radioactivity had been cleared from the circulation at the end of the sampling. At the end of the experiment, the animals received approximately 2000 units of heparin i.v., then the heart was excised. The anatomic boundaries of the circumflex perfusion bed were delineated by dual perfusion of dyes at physiological perfusion pressure in the left main coronary artery and the circumflex coronary artery. The perfusate to the circumflex bed contained triphenyl tetrazolium chloride (TTC), while that to the left main coronary artery contained Monastral blue dye (0.5%). The heart was then incubated at 37°C for 20 min, then fixed for at least 3 days in 4% formalin. With this technique, the left circumflex appears stained red, while the rest of the left ventricle is stained blue. After fixation, the right ventricle was removed and discarded, and the left ventricle was cut in 5 transverse sections, from base to apex. The most basal and apical sections were discarded. On each of the remaining three slices, a transmural sample representing 50–60% of the left circumflex perfusion bed was cut using the two stains as a guide, and a corresponding section was cut inside the perfusion bed of the left anterior descending coronary artery. Each region was then subdivided into subendocardial, midmyocardial and subepicardial thirds. Only the results obtained in the left circumflex perfusion bed (which received L-NMMA or L-NAME) are described here.

All samples were weighed, and the radioactivity of the samples, as well as that of the reference blood samples, was measured in a gamma counter (Compugamma, LKB Co.) with correction made for background activity and for overlap of isotope spectra. Myocardial blood flow was calculated from the formula: Tissue flow = (Tissue counts)(Reference flow)/Reference counts, and was expressed relative to sample weight (ml min^{-1} g^{-1}). Transmural mean regional blood flow was calculated as the weighted mean of the three transmural samples, and the endocardium/epicardium blood flow ratio was calculated. Finally, regional vascular resistance was calculated as diastolic blood pressure/transmural mean regional blood flow.

Drugs

Acetylcholine hydrochloride, D-arginine, L-arginine, L-NAME hydrochloride, triphenyl tetrazolium chloride and monastral blue were all obtained from Sigma Chimie (la Verpillère, France). L-NMMA acetate was a gift from Dr S. Moncada (Wellcome Research Laboratories, Beckenham, Kent, UK). All drugs were freshly prepared at the time of the experiment and dissolved in sterile saline.

Statistics

All values are expressed as mean ± s.e.mean. Intragroup comparisons were made by analysis of variance for repeated measures, followed by modified *t* test when ANOVA was significant. A P value <0.05 was considered statistically significant.

Results

Effects of acetylcholine

The peak haemodynamic and coronary effects of increasing doses of acetylcholine, administered into the coronary artery, are summarized in Table 1. Infusion of acetylcholine induced a marked, dose-dependent increase in left circumflex coronary blood flow (maximal increase: 98.2 ± 13.2%), and a dose-dependent decrease in coronary resistance (maximal decrease 46.1 ± 4.0%). These coronary effects of acetylcholine were not associated with significant modifications of systemic haemodynamics: the maximal decrease in mean blood pressure observed at the highest dose of acetylcholine was 3.0 ± 1.6%, which represents an average decrease of 3 mmHg (not statistically significant, NS). Heart rate remained constant throughout the infusion of acetylcholine. Thus, local administration of acetylcholine specifically dilated coronary arterioles without affecting systemic haemodynamics.

Haemodynamic effects of L-NMMA and L-NAME

The systemic and coronary haemodynamic effects of increasing doses of L-NMMA and L-NAME (0.1, 0.3 and 1 mg kg^{-1}), measured 15 min after the end of infusion, are shown in Figure 1. Both L-NMMA and L-NAME increased blood pressure only at the highest dose (1 mg kg^{-1}). This hypertension remained modest: 13 ± 4 mmHg with L-NMMA, and 16 ± 5 mmHg with L-NAME. Both inhibitors induced at the highest dose a small, but significant bradycardia (average decrease 19 ± 5 beats min^{-1} with L-NMMA, and 18 ± 6 beats min^{-1} with L-NAME). This bradycardia was already present with L-NAME at the dose of 0.3 mg kg^{-1}. L-NAME induced a significant reduction of coronary blood flow only at the highest dose (1 mg kg^{-1}). At the same dose, L-NMMA also slightly reduced coronary blood flow, although this reduction was not significant. However, both L-NMMA and L-NAME induced at the same dose a significant increase in coronary vascular resistance. This effect was more marked with L-NAME than with L-NMMA (maximal increase in resistance: L-NAME 43.4 ± 8.6% vs L-NMMA 28.0 ± 7.2%).

Effects of L- and D-arginine

D-Arginine and L-arginine (both at 60 mg kg^{-1}) were administered i.v. to a subset of 7 animals (see Methods). D-Arginine had no effects on the haemodynamic responses to L-NMMA or L-NAME. L-Arginine partially reversed the responses to L-NMMA and to L-NAME, but more markedly so the effects of L-NMMA. Thus, the increase in mean arterial pressure induced by L-NMMA was reduced from 12.1 ± 4.9% to 5.9 ± 2.9% (NS), and the increase in coronary resistance from 29.9 ± 8.5% to 14.2 ± 10.5% (NS), whereas the increase in blood pressure induced by L-NAME was reduced from 14.5 ± 4.9% to 10.9 ± 5.1% (NS), and the increase in coronary resistance was reduced from 45.2 ± 13.5% to 38.3 ± 10.6% (NS).

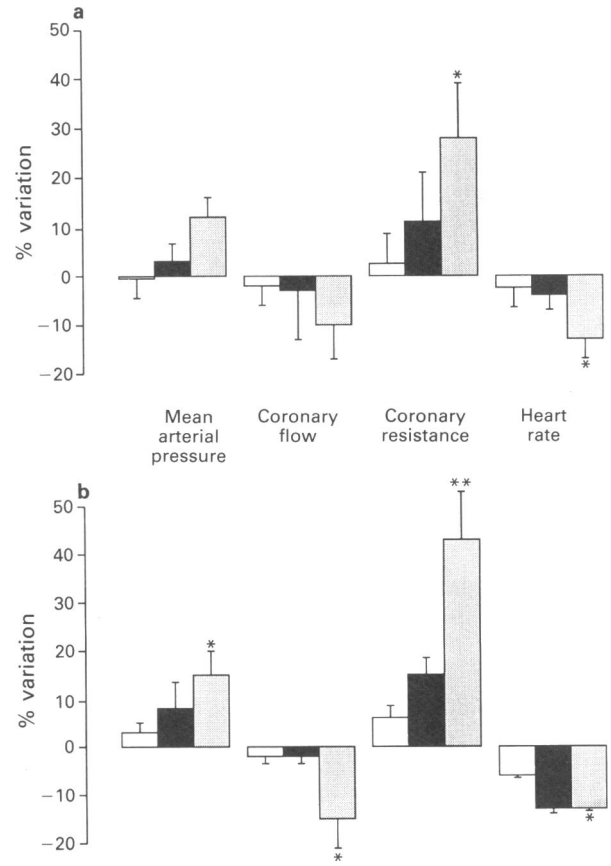

Figure 1 Effect of NG-monomethyl-L-arginine (L-NMMA, a) and N^G-nitro-L-arginine methyl ester (L-NAME, b) on mean arterial blood pressure, mean coronary blood flow, mean coronary resistance, and heart rate. Open columns, 0.1 mg kg^{-1}; solid columns, 0.3 mg kg^{-1} and stippled columns, 1 mg kg^{-1} L-NMMA or L-NAME.
* $P < 0.05$, and ** $P < 0.01$ vs baseline.

Effects of L-NMMA and L-NAME on regional blood flow and regional resistance

The effects of the two highest doses of L-NMMA and L-NAME (0.3 and 1 mg kg^{-1}) on endocardial, epicardial and transmural blood flows, as well as on endocardial/epicardial ratios, are shown in Figures 2 and 3. L-NMMA and L-NAME at the doses used had no effect on endocardial, epicardial or transmural blood flows, or on the endocardial/epicardial ratios.

The calculated regional resistance is shown in Figure 4. Both L-NMMA (1 mg kg^{-1}) and L-NAME (0.3 and 1 mg kg^{-1}) induced small, and non significant increases in regional resistance.

Table 1 Peak systemic and coronary haemodynamic effects of acetylcholine (0.03–0.3 μg kg^{-1}) administered into the coronary artery in anaesthetized, open-chest dogs

	Heart rate		*Mean blood pressure*			*Mean coronary flow*	*Mean coronary resistance*	
Acetylcholine (μg kg^{-1})	Baseline (beats min^{-1})	Δ%	Baseline (mmHg)	Δ%	Baseline (ml min^{-1})	Δ%	Baseline (mmHg ml^{-1} min)	Δ%
0.03	160.0 ± 5.8	−0.4 ± 0.4	108.3 ± 4.5	−0.1 ± 0.8	53.2 ± 6.5	39.7 ± 8.7*	2.27 ± 0.27	−26.6 ± 4.0*
0.1	154.3 ± 5.3	0.0 ± 0.0	107.4 ± 4.6	−1.3 ± 0.6	50.4 ± 6.3	76.5 ± 11.7*	2.41 ± 0.31	−42.1 ± 3.8*
0.3	152.9 ± 5.6	−0.4 ± 0.4	108.2 ± 4.9	−3.0 ± 1.6	53.2 ± 6.7	98.2 ± 13.2*	2.36 ± 0.35	−46.1 ± 4.0*

* P at least <0.05 vs baseline.

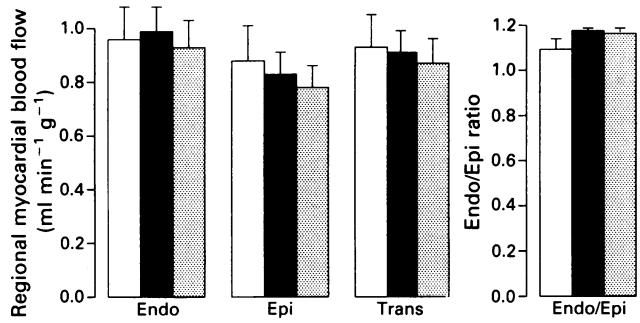

Figure 2 Effect of N^G-monomethyl-L-arginine (L-NMMA) on regional myocardial blood flow. Open columns, control; solid columns L-NMMA 0.3 mg kg^{-1}; stippled columns, L-NMMA 1 mg kg^{-1}. Endo: subendocardial area; Epi: subepicardial area; Trans: transmural mean; Endo/Epi = subendocardial/subepicardial flow ratios.

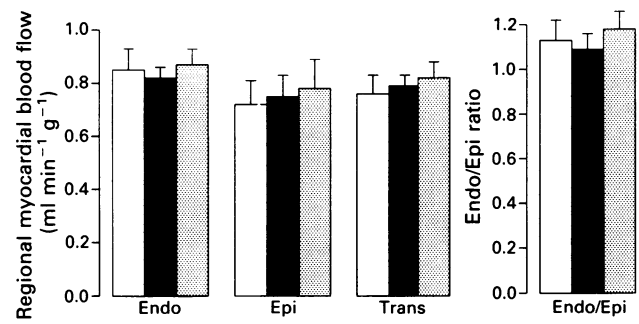

Figure 3 Effect of N^G-nitro-L-arginine methyl ester (L-NAME) on regional myocardial blood flow. Open columns, control; solid columns, L-NAME 0.3 mg kg^{-1}; stippled columns, L-NAME 1 mg kg^{-1}. Endo: subendocardial area; Epi: subepicardial area; Trans: transmural mean; Endo/Epi = subendocardial/subepicardial flow ratios.

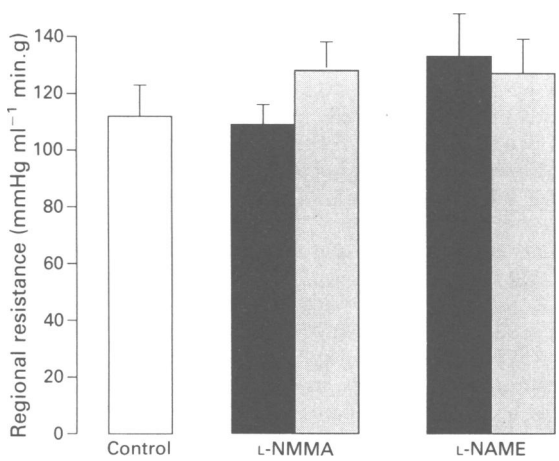

Figure 4 Effect of N^G-monomethyl-L-arginine (L-NMMA) and N^G-nitro-L-arginine methyl ester (L-NAME) on regional myocardial tissue resistance. Regional resistance was calculated as diastolic arterial pressure/transmural mean regional myocardial blood flow. Open columns, control; solid columns, 0.3 mg kg^{-1}; stippled columns, 1 mg kg^{-1} L-NMMA or L-NAME.

Effect of L-NMMA and L-NAME on the response to acetylcholine

The effects of L-NMMA and L-NAME on the coronary vasodilator response to acetylcholine are shown in Figures 5 and 6. Since acetylcholine by itself did not induce any systemic haemodynamic changes and in particular did not change arterial blood pressure, changes in coronary resistance were the opposite of changes in coronary blood flow; only the effects of acetylcholine on coronary blood flow are represented here. Both L-NMMA (1 mg kg^{-1}) and L-NAME (0.3 and 1 mg kg^{-1}) significantly inhibited the peak dilator effect of

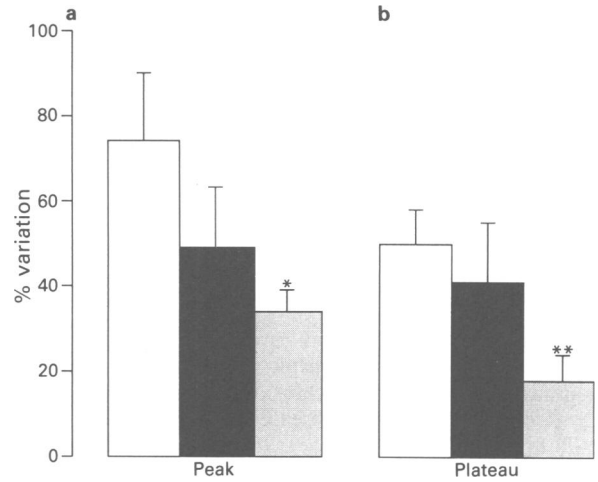

Figure 5 Effect of N^G-monomethyl-L-arginine (L-NMMA) on the coronary flow response to acetylcholine (0.1 μg kg^{-1}). The coronary flow response was assessed both at peak (a) and during the plateau phase (b) (see Methods). Open columns, control; solid columns, L-NMMA 0.3 mg kg^{-1}; stippled columns, L-NMMA 1 mg kg^{-1}.
* $P < 0.05$, and ** $P < 0.01$ vs control.

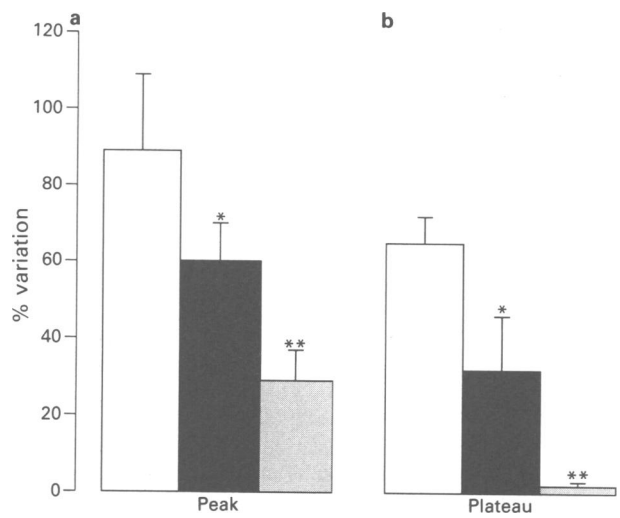

Figure 6 Effect of N^G-nitro-L-arginine methyl ester (L-NAME) on the coronary flow response to acetylcholine (0.1 μg kg^{-1}). The coronary flow response was assessed both at peak (a) and during the plateau phase (b) (see Methods). Open columns, control; solid columns, L-NAME 0.3 mg kg^{-1}; stippled columns, L-NAME 1 mg kg^{-1}.
* $P < 0.05$, and ** $P < 0.01$ vs control.

acetylcholine. This inhibitory effect was more marked when the dilator effect of acetylcholine was assessed during the stable phase. In this situation, the inhibitory effect of L-NMMA was significant only at the dose of 1 mg kg^{-1}, whereas that of L-NAME was already significant at the dose of 0.3 mg kg^{-1}. At the highest dose used (1 mg kg^{-1}), L-NMMA and L-NAME reduced the peak dilator effect of acetylcholine by an average 55% and 63%, respectively, and the dilator effect at the plateau phase by 67% and 93%, respectively.

Discussion

There is now convincing evidence from *in vitro* data that L-arginine is the precursor of endothelium-derived nitric oxide. L-Arginine induces the release of nitric oxide from L-arginine-depleted endothelial cells (Palmer *et al.*, 1988a) and evokes potent relaxations in L-arginine-depleted isolated blood vessels (Gold *et al.*, 1990; Schini *et al.*, 1991). Furthermore, several L-arginine analogues, including L-NMMA and L-NAME, inhibit NO synthase (Palmer & Moncada, 1989;

Mülsch & Busse, 1990; Rees *et al.*, 1990) and nitric oxide formation in cultured endothelial cells (Palmer *et al.*, 1988b; Ishii *et al.*, 1990; Mitchell *et al.*, 1990). In addition, these L-arginine analogues markedly inhibit the endothelium-dependent relaxation to acetylcholine in isolated blood vessels (Palmer *et al.*, 1988b; Moore *et al.*, 1990; Rees *et al.*, 1990). Thus, L-NMMA and L-NAME are valuable tools for studying the importance of the endothelial L-arginine pathway *in vitro*, but also *in vivo*.

The primary objective of the present study was to delineate in anaesthetized, open-chest dogs the contribution of endothelium-derived nitric oxide to the maintenance of coronary arteriolar tone (electromagnetic probe) and regional myocardial tissue perfusion (radioactive microspheres), and to the coronary vasodilator effect of locally administered acetylcholine. Our data indicate that L-NMMA and L-NAME induce an increase in left circumflex coronary resistance and markedly inhibit the coronary vasodilator effects of acetylcholine, but do not significantly affect regional myocardial tissue perfusion.

The marked inhibition of acetylcholine-induced vasodilatation by L-NMMA and L-NAME observed in the present study is at variance with previous studies performed in rats, rabbits and guinea-pigs, in which the vasodilator effect of acetylcholine was not markedly affected by these L-arginine analogues. For example, in anaesthetized guinea-pigs (Aisaka *et al.*, 1989) and rats (Rees *et al.*, 1990), as well as in conscious rats (Gardiner *et al.*, 1990a,b,c), administration of L-NMMA or L-NAME consistently induced hypertension, but did not markedly affect the maximal hypotensive response to intravenously administered acetylcholine, although the L-arginine analogues tended to reduce the duration of this hypotensive phase. Furthermore, in conscious rats, the regional (renal, mesenteric and hindquarter) vasodilator effects of acetylcholine were not markedly affected by L-NAME (Gardiner *et al.*, 1990c). Several hypotheses were advanced to explain this lack of inhibition *in vivo*; one possibility is that, *in vivo*, the vasodilator response to acetylcholine, as well as that to other endothelium-dependent vasodilators (e.g. bradykinin), is partly nitric oxide-independent (Gardiner *et al.*, 1990c), or is mediated through the release of nitric oxide from intracellular stores that do not rely on mobilization of L-arginine (Aisaka *et al.*, 1989). In this regard, the fact that, in the presence of L-NMMA or L-NAME, the peak hypotensive response to acetylcholine was not affected, but the duration of acetylcholine-induced hypotension was reduced (Aisaka *et al.*, 1989; Rees *et al.*, 1990), would suggest that acetylcholine-induced vasodilatation is the result of two events: (1) an initial vasodilatation which depends on the release of NO or an NO-like molecule (e.g. S-nitrosothiol; Myers *et al.*, 1990) from a preformed endothelial pool, and (2) a sustained vasodilator phase which depends on the biosynthesis of nitric oxide from L-arginine. In our experiments, acetylcholine administered as a slow infusion induced an early peak coronary vasodilator phase, which was followed by a plateau phase lasting until the end of the infusion, and the inhibitory effects of L-NMMA and L-NAME were more marked during the plateau phase than at the peak vasodilator phase. This differential inhibition supports the hypothesis that at least part of the initial vasodilatation induced by acetylcholine might not require a *de novo* synthesis of NO (Aisaka *et al.*, 1989). If this were true, then it would be expected that the vasodilatation induced by acetylcholine administered as a bolus injection would not be markedly affected by L-arginine analogues, since the vasodilatation induced in these conditions is very short lasting and thus probably does not rely on *de novo* synthesis of nitric oxide form L-arginine. Interestingly, in conscious rats, the inhibitory effect of L-NAME on acetylcholine-induced dilatation is more marked when acetylcholine is administered as a slow infusion (Gardiner *et al.*, 1991), than when administered as a bolus injection (Gardiner *et al.*, 1990c).

One major difference between our study and those previous *in vivo* experiments is that we administered acetylcholine directly into the coronary arterial bed. In these conditions, the acetylcholine-induced coronary vasodilatation was observed in the absence of any systemic haemodynamic modification. This is in contrast with previous experiments, in which systemically administered acetylcholine consistently induced marked hypotension and reflex tachycardia. In these conditions, it is likely that the vasodilator response to acetylcholine is the result of various influences, including baroreflex, neurohumoral and autoregulatory mechanisms (Gardiner *et al.*, 1990c), all of which are probably unaffected by L-NMMA or L-NAME. Our experiments show that, when acetylcholine is administered locally in the absence of systemic modifications, the regional vasodilator response obtained is indeed largely mediated through the L-arginine-nitric oxide pathway.

One intriguing result of our experiments is that local administration of L-NMMA and L-NAME induced a rise in left circumflex coronary resistance and a decrease in left circumflex blood flow (measured with an electromagnetic flow probe), but did not affect regional myocardial tissue flow or tissue resistance (measured by the microspheres technique). This apparent discrepancy could be explained on the basis that the coronary flow measured with the electromagnetic probe is the reflection of the tone of the totality of the coronary resistance bed, including small arteries (100–300 μm diameter) and arterioles ($< 100\,\mu$m), whereas the 15 μm diameter microspheres reflect flow at the level of the smallest arterioles. One could conceive that only the larger resistance arteries are affected by L-NMMA and L-NAME, a situation evidenced by the increase in global coronary resistance, whereas the smaller nutritive arterioles do not constrict upon administration of these L-arginine analogues, thus explaining that tissue flow was not affected.

The fact that small coronary arterioles do not constrict after administration of L-NMMA or L-NAME would suggest either that basal release of nitric oxide from L-arginine does not occur at the level of these small arterioles, or that these arterioles are not sensitive to nitric oxide produced from L-arginine in endothelial cells. Such an heterogeneous release of EDRF has already been reported in isolated dog coronary arteries (Hoeffner *et al.*, 1989). In isolated small coronary arteries of the pig (Tschudi *et al.*, 1991), and in pressurized mesenteric resistance arteries of the rat (Dohi *et al.*, 1990), administration of L-NMMA induced vasoconstriction, suggesting that these vessels do release nitric oxide from L-arginine under basal conditions, at least *in vitro*. However, in these experiments, only the larger ($> 100\,\mu$m diameter) resistance arteries were studied, and those contribute to less than 50% of total resistance in various vascular beds, including the coronary circulation (Chillian *et al.*, 1986). To date, it is not clear whether the endothelium of the smallest arterioles does or does not release nitric oxide in the basal state. However, the hypothesis that small arterioles do not release nitric oxide is supported by preliminary experiments in anaesthetized, open-chest dogs showing that topically administered ACh induces vasodilatation of large ($> 100\,\mu$m) arterioles, but fails to dilate the smaller ($< 100\,\mu$m) arterioles (Komaru *et al.*, 1990).

The hypothesis that small arterioles are insensitive to endothelium-derived nitric oxide is also supported by the recent observation that coronary arterioles ($< 100\,\mu$m) do not respond to the organic nitrate nitroglycerin, but are responsive to S-nitrosothiols (Kurtz *et al.*, 1991). Since this lack of response to nitroglycerin could be reversed by L-cysteine, this suggests that the active metabolite of nitroglycerin is a nitrosothiol compound, and that small coronary arterioles lack the specific sulphydryl pool necessary for the production of the active S-nitrosothiol. If one assumes, as has been suggested recently, that EDRF is a nitrosothiol rather than authentic nitric oxide (Myers *et al.*, 1990), then it is likely that small coronary arterioles will not be capable of producing this active nitrosothiol, because of the absence of sulphydryl groups.

One alternative explanation for the lack of effect of L-NMMA and L-NAME on regional myocardial tissue flow is that the constriction of small coronary arteries and arterioles

is not associated with a net reduction of tissue flows, because of compensatory dilator mechanisms that occur in response to the constriction of 'upstream' vessels. This phenomeon has already been observed with other vasoconstrictors, e.g. α-adrenoceptor agonists; indeed, in anaesthetized cats, α-adrenoceptor stimulation results in constriction of coronary arteries larger than 100 μm, whereas dilatation predominates in vessels less than 100 μm in diameter, and regional myocardial tissue flow (microspheres) does not change (Chillian *et al.*, 1989). This implies that there may be independent regulatory mechanisms for the control of vasomotor tone in different microvascular segments of the coronary circulation; whereas neurohumoral control mechanisms predominate at the level of small arteries and large arterioles, metabolic and myogenic influences may regulate smaller arterioles. Thus, one can hypothesize that 'downstream' dilatation due to a metabolic and/or myogenic mechanism (i.e. intrinsic autoregulatory adjustments) would maintain normal tissue perfusion despite the 'upstream' constriction induced by L-NMMA or L-NAME. Finally, constriction of small arteries and arterioles could induce a recruitment of myocardial tissue capillaries, thus compensating for the decreased tissue perfusion. Both compensatory dilatation of smaller arterioles and recruitment of new capillaries could thus contribute to the maintenance of tissue flow (and its transmural distribution) despite coronary vasoconstriction observed in our experiments with L-NMMA and L-NAME.

Conclusions

The present results obtained in anaesthetized dogs after intracoronary administration of L-NMMA and L-NAME suggest that the endothelial L-arginine pathway is responsible for the coronary vasodilator effect of locally administered acetylcholine. In addition, although basal release of nitric oxide from L-arginine apparently contributes to the regulation of coronary vascular tone, blockade of this pathway does not affect myocardial tissue perfusion, possibly because of compensatory mechanisms occurring at the level of the smallest arterioles and/or capillaries.

We are grateful to Dr S. Moncada for his generous gift of L-NMMA. We also wish to thank Dr A.A. Abena for his help during surgical preparation of the animals and A. Bizé for his expert technical assistance.

References

AISAKA, K., GROSS, S.S., GRIFFITH, O.W. & LEVI, R. (1989). L-arginine availability determines the duration of acetylcholine-induced systemic vasodilation *in vivo*. *Biochem. Biophys. Res. Commun.*, **163**, 710–717.

AMEZCUA, J.L., PALMER, R.M.J., DE SOUZA, B.M. & MONCADA, S. (1989). Nitric oxide synthesized from L-arginine regulates vascular tone in the coronary circulation of the rabbit. *Br. J. Pharmacol.*, **97**, 1119–1124.

CHILIAN, W.M., LAYNE, S.M., EASTHAM, C.L. & MARCUS, M.L. (1989). Heterogenous microvascular coronary α-adrenergic vasoconstriction. *Circ. Res.*, **64**, 376–388.

CHU, A., CHAMBERS, D.E., LIN, C.C., KUEHL, W.D. & COBB, F.R. (1990). Nitric oxide modulates epicardial coronary basal vasomotor tone in awake dogs. *Am. J. Physiol.*, **258**, H1250–H1254.

DOHI, Y., THIEL, M.A., BÜHLER, F.R. & LÜSCHER, T.F. (1990). Activation of endothelial L-arginine pathway in resistance arteries. Effect of age and hypertension. *Hypertension*, **15**, 170–179.

FURCHGOTT, R.F. & ZAWADZKI, J.V. (1980). The obligatory role of endothelial cells in the relaxation of arterial smooth muscle by acetylcholine. *Nature*, **288**, 373–376.

GARDINER, S.M., COMPTON, A.M., BENNETT, T., PALMER, R.M.J. & MONCADA, S. (1990a). Control of regional blood flow by endothelium-derived nitric oxide. *Hypertension*, **15**, 486–492.

GARDINER, S.M., COMPTON, A.M., KEMP, P.A. & BENNETT, T. (1990b). Regional and cardiac haemodynamic effects of N^G-nitro-L-arginine methyl ester in conscious, Long Evans rats. *Br. J. Pharmacol.*, **101**, 625–631.

GARDINER, S.M., COMPTON, A.M., KEMP, P.A. & BENNETT, T. (1990c). Regional and cardiac haemodynamic responses to glyceryl trinitrate, acetylcholine, bradykinin and endothelin-1 in conscious rats: effects of N^G-nitro-L-arginine methyl ester. *Br. J. Pharmacol.*, **101**, 632–639.

GARDINER, S.M., KEMP, P.A. & BENNETT, T. (1991). Effects of N^G-nitro-L-arginine methyl ester on vasodilator responses to acetylcholine, 5'-N-ethylcarboxamidoadenosine or salbutamol in conscious rats. *Br. J. Pharmacol.*, (in press).

GOLD, M.E., WOOD, K.S., BYRNS, R.E., BUGA, G.M. & IGNARRO, L.J. (1990). L-arginine-dependent vascular smooth muscle relaxation and cGMP formation. *Am. J. Physiol.*, **259**, H1813–H1821.

HOEFFNER, U., BOULANGER, C. & VANHOUTTE, P.M. (1989). Proximal and distal dog coronary arteries respond differently to basal EDRF but not to NO. *Am. J. Physiol.*, **256**, H828–H831.

HUMPHRIES, R.G., CARR, R.D., NICOL, A.K., TOMLINSON, W. & O'CONNOR, S.E. (1991). Coronary vasoconstriction in the conscious rabbit following intravenous infusion of L-N^G-nitro-arginine. *Br. J. Pharmacol.*, **102**, 565–566.

ISHII, K., CHANG, B., KERWIN, J.F. JR., HUANG, Z.J. & MURAD, F. (1990). N-nitro-L-arginine: a potent inhibitor of endothelium-derived relaxing factor formation. *Eur. J. Pharmacol.*, **176**, 219–223.

KOMARU, T., LAMPING, K.G., EASTHAM, C.L., HARRISON, D.G., MARCUS, M.L. & DELLSPERGER, K.C. (1990). Effect of an arginine analog on acetylcholine-induced coronary microvascular dilation. *Circulation*, **82**, (Suppl. III), III-702 (Abstract).

KURTZ, M.A., LAMPING, K.G., BATES, J.N., EASTHAM, C.L., MARCUS, M.L. & HARRISON, D.G. (1991). Mechanisms responsible for the heterogenous coronary microvascular response to nitroglycerin. *Circ. Res.*, **68**, 847–855.

MITCHELL, J.A., HECKER, M. & VANE, J.R. (1990). The generation of L-arginine in endothelial cells is linked to the release of endothelium-derived relaxing factor. *Eur. J. Pharmacol.*, **176**, 253–254.

MOORE, P.K., AL-SWAYEH, O.A., CHONG, N.W.S., EVANS, R.A. & GIBSON, A. (1990). L-N^G-nitro arginine (L-NOARG), a novel, L-arginine reversible inhibitor of endothelium-dependent vasodilatation *in vitro*. *Br. J. Pharmacol.*, **99**, 408–412.

MÜLSCH, A. & BUSSE, R. (1990). N^G-nitro-L-arginine (N^5-[imino(nitro amino)methyl]-L- ornithine) impairs endothelium-dependent dilation by inhibiting cytosolic nitric oxide synthesis from L-arginine. *Naunyn-Schmiedebergs Arch. Pharmacol.*, **341**, 143–147.

MYERS, P.R., MINOR JR., R.L., GUERRA JR., R., BATES, J.N. & HARRISON, D.G. (1990). Vasorelaxant properties of the endothelium-derived relaxing factor more closely resemble S-nitrosocysteine than nitric oxide. *Nature*, **345**, 161–163.

PALMER, R.M.J., ASHTON, D.S. & MONCADA, S. (1988a). Vascular endothelial cells synthesize nitric oxide from L-arginine. *Nature*, **333**, 664–666.

PALMER, R.M.J., REES, D.D., ASHTON, D.S. & MONCADA, S. (1988b). L-arginine is the physiological precursor for the formation of nitric oxide in endothelium-dependent relaxation. *Biochem. Biophys. Res. Commun.*, **153**, 1251–1256.

PALMER, R.M.J. & MONCADA, S. (1989). A novel citrulline-forming enzyme implicated in the formation of nitric oxide by vascular endothelial cells. *Biochem. Biophys. Res. Commun.*, **158**, 348–352.

REES, D.D., PALMER, R.M.J., SCHULZ, R., HODSON, H.F. & MONCADA, S. (1990). Characterization of three inhibitors of endothelial nitric oxide synthase *in vitro* and *in vivo*. *Br. J. Pharmacol.*, **101**, 746–752.

SCHINI, V.B. & VANHOUTTE, P.M. (1991). L-arginine evokes both endothelium-dependent and -independent relaxations in L-arginine-depleted aortas of the rat. *Circ. Res.*, **68**, 209–216.

TSCHUDI, M., RICHARD, V., BÜHLER, F.R. & LÜSCHER, T.F. (1991). Importance of endothelium-derived nitric oxide in porcine coronary resistance arteries. *Am. J. Physiol.*, **260**, H13–H20.

WHITTLE, B.J.R., LOPEZ-BELMONTE, J. & REES, D.D. (1989). Modulation of the vasodepressor actions of acetylcholine, bradykinin, substance P and endothelin in the rat by a specific inhibitor of nitric oxide formation. *Br. J. Pharmacol.*, **98**, 646–652.

(Received April 24, 1991
Revised May 9, 1991
Accepted May 13, 1991)

Br. J. Pharmacol. (1991), **104**, 65–70

Fenoverine inhibition of calcium channel currents in single smooth muscle cells from rat portal vein and myometrium

[1]J. Mironneau, S. Arnaudeau & C. Mironneau

Laboratoire de Physiologie Cellulaire et Pharmacologie Moléculaire, INSERM CJF 88-13, Université de Bordeaux II, 3 place de la Victoire, 33076 Bordeaux Cédex, France

1 The effects of fenoverine, an antispasmodic drug, have been studied on the Ca^{2+} channel currents of isolated cells from rat portal vein and pregnant myometrium by the patch-clamp technique (whole-cell configuration).

2 Fenoverine inhibited both fast and slow Ca^{2+} channel currents in a concentration-dependent manner. Half-inhibition of fast Ca^{2+} channel current (holding potential of -70 mV) and slow Ca^{2+} channel current (holding potential of -40 mV) in portal vein smooth muscle were obtained at concentrations of 7.5 and 1.9 μM, respectively. In myometrium, the fenoverine concentration which blocked 50% of the slow Ca^{2+} channel current (holding potential of -70 mV) was 2.3 μM.

3 Administration of fenoverine at rest reduced both Ca^{2+} channel currents. Currents activated repetitively, at a rate between 0.05 and 0.1 Hz, were inhibited equally which indicates an absence of use-dependent inhibition.

4 When cells held at depolarized membrane potentials at which fast or slow Ca^{2+} channel currents were strongly inactivated, the inhibitory effects of fenoverine were enhanced on both Ca^{2+} channel currents which indicates that the fenoverine-induced inhibition was voltage-dependent. The fenoverine concentrations which blocked the inactivated Ca^{2+} channels were 5–7 times lower than those which blocked the resting Ca^{2+} channels.

5 Our results show that fenoverine depresses inward currents through fast and slow Ca^{2+} channels. This effect may be explained by the preferential binding of fenoverine to resting Ca^{2+} channels. In addition, fenoverine has a higher afinity for inactivated Ca^{2+} channels than for resting channels.

Keywords: Ca^{2+} channels; Ca^{2+}-channel antagonists; fenoverine; antispasmodic drug; smooth muscle

Introduction

Fenoverine, (piperonyl-4-piperazinyl)-2-(phenothiazinyl-10)-1-ethanone, is an antispasmodic drug which is known to inhibit contraction of smooth muscles elicited either by electrical stimulation or by potassium depolarization (Gonella *et al.*, 1987).

Since the activation of voltage-dependent Ca^{2+} channels is associated with electrical and mechanical activity in smooth muscle (Mironneau, 1973), the inhibition of these channels by drugs which abolish excessive myoelectric activity might be useful to reduce gastro-intestinal disorders. The purpose of the present study was to test whether fenoverine has calcium channel blocking properties in visceral (myometrium) and vascular (portal vein) smooth muscle by studying its effects on Ca^{2+} channel currents in single smooth muscle cells by the patch-clamp technique. We have found that fenoverine depressed inward current through fast and slow Ca^{2+} channels and bound not only to the resting state of the Ca^{2+} channels but also that it had a higher affinity for the inactivated state.

Methods

Electrical activity

The cells were isolated from rat portal vein and pregnant myometrium (18–19 days gestation) as previously described (Loirand *et al.*, 1986; Amédée *et al.*, 1986). They were maintained in primary culture and used during the first 36 h. The electrode, electronics and data recording have been described in detail previously (Loirand *et al.*, 1989; Honoré *et al.*, 1989). The cells were investigated with patch pipettes in the whole-cell clamp mode (Hamill *et al.*, 1981). The patch pipettes were filled with a solution containing (mM): CsCl 130, $ATPNa_2$ 5, $MgCl_2$ 4, HEPES 10 (pH 7.3 with CsOH), EGTA 10. Outward K^+ currents were blocked with a CsCl pipette which suggests that internal dialysis was complete. Ca^{2+} channel currents were corrected digitally for leakage and capacitative currents by subtraction of scaled currents traces obtained with hyperpolarizing or small depolarizing pulses from the holding potential.

Solutions and drugs

The extracellular medium (reference solution) contained (mM): NaCl 130, CsCl 5.6, $BaCl_2$ 5, $MgCl_2$ 1.24, glucose 11, Tris 8.3 (pH 7.4 with HCl). The temperature of the bathing solution was kept at 30 ± 1°C and the solution was exchanged within 1 min. The stimulation frequency was 0.05 Hz except where indicated otherwise in the text. For studies of inhibition mechanisms fenoverine was applied with a pressure ejector from a glass pipette placed close to the cell membrane (100 μm).

Fenoverine was a gift from Delalande (Paris) and isradipine was a gift from Sandoz (Paris). They were diluted from a stock solution in 10^{-1} M dimethyl sulphoxide (DMSO). Thus, at the maximal fenoverine concentration used (10^{-4} M), the DMSO concentration was 10^{-5} M and had no effect on the Ca^{2+} channel current.

Statistical analysis

Concentration-effect relationships were computer-fitted with a nonlinear least-squares programme for the analysis of sigmoidal curves (De Lean *et al.*, 1978). The results are expressed as mean ± s.e.mean for n experiments and significance was tested by means of Student's t test. P values less than 0.05 were considered to be significant.

[1] Author for correspondence.

Results

Effects of fenoverine on the fast Ba^{2+} current of single cells isolated from rat portal vein smooth muscle

Previous experiments in portal vein smooth muscle cells have revealed two distinct classes of voltage-dependent Ca^{2+} channels that can be separated kinetically and pharmacologically (Loirand *et al.*, 1986, 1989). A rapidly inactivating Ba^{2+} current (fast current) was present when cells were held at a negative potential (−70 mV) in the presence of 10 mM isradipine which blocked the slow Ba^{2+} current. Under these conditions, application of 10 μM fenoverine resulted in a strong inhibition of the fast Ba^{2+} current at any given voltage step without any change in the voltage threshold, the potential for the maximal current and the apparent reversal potential (Figure 1). In all experiments measurements were made only when the cells reached steady-state, i.e. within 1.5–2 min at a stimulation frequency of 0.05 Hz. The effects of fenoverine were totally reversed within 2–3 min after returning to the reference solution. The steady-state inhibitory effect of increasing concentrations of fenoverine was measured at a stimulation frequency of 0.05 Hz on the maximal Ba^{2+} current obtained at a test potential of 0 mV (Figure 2). The concentration of fenoverine required to reduce the amplitude of the fast Ba^{2+} current by 50% (IC_{50}) was 7.5 ± 1.7 μM (n = 6).

Mechanisms of fenoverine inhibition of the fast Ba^{2+} current

A standardized protocol was used to assess the relative contribution of initial, conditioned and tonic blockade of the Ba^{2+} current by fenoverine (Figure 3a). We recorded a train of Ba^{2+} current elicited by depolarizing voltage-clamp pulses applied at 0.05 Hz under control conditions, followed by a rest period lasting 1.7 min during which fenoverine (10 μM) was perfused (○). A second identical voltage-clamp depolarization train was then applied. Blockade was estimated by measuring the difference in peak Ba^{2+} current between control and test drug conditions when steady-state blockade was obtained. The initial blockade was assessed as the difference in peak

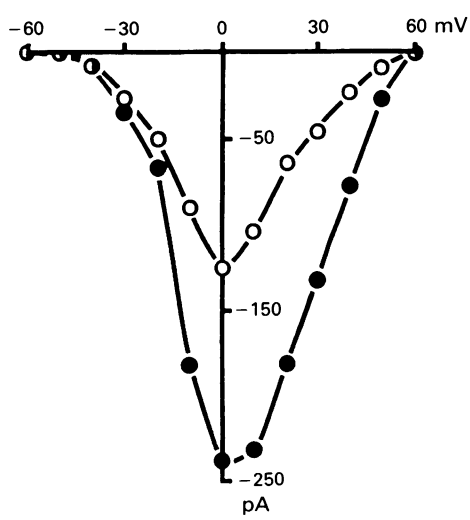

Figure 1 Inhibitory effect of 10 μM fenoverine on the fast Ba^{2+} current of rat isolated portal vein smooth muscle cells in primary culture. The holding potential was −70 mV and the cells were superfused in the presence of 10 nM isradipine to block the slow Ba^{2+} current. Current-voltage relationships were obtained by plotting the peak current against the membrane potential in control (●) and after addition of 10 μM fenoverine for 3 min (○). Stimulation frequency was 0.05 Hz.

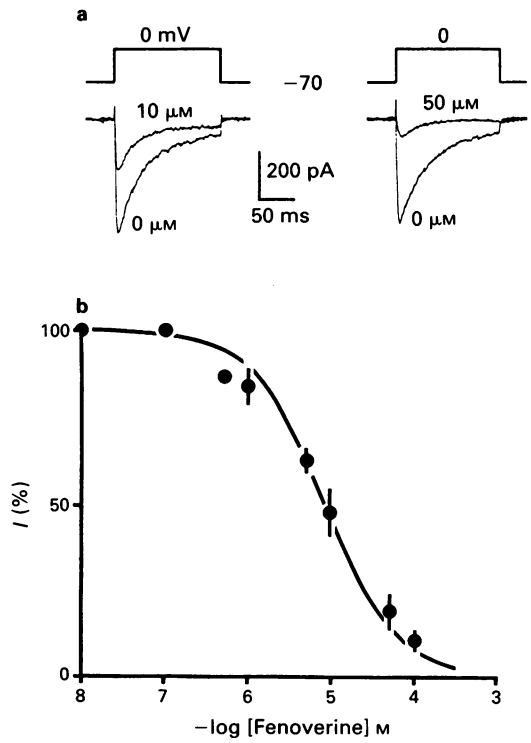

Figure 2 Concentration-effect relationship of the inhibitory action of fenoverine on the fast Ba^{2+} current of portal vein smooth muscle cells. (a) The Ba^{2+} current elicited from a holding potential of −70 to 0 mV was inhibited by addition of 10 μM and 50 μM fenoverine. (b) Concentration-response curve for the effects of fenoverine on the fast Ba^{2+} current elicited from a holding potential of −70 mV. Ordinate scale: % of maximal Ba^{2+} current. Abscissa scale: log of drug concentration (M). The continuous curve represents the nonlinear least-square regression curve to the data assuming a Hill coefficient of 1. Each point represents the mean response of 6 cells with the s.e. shown by vertical lines. The stimulation frequency was 0.05 Hz.

Ba^{2+} current between the control and the first pulse after drug exposure which was 62.6 ± 3.0% (n = 3). Conditioned blockade was the difference between the peak Ba^{2+} current for the first and the last pulses after drug exposure without rest period (●). The Ba^{2+} current inhibition was 62.0 ± 6.0% (n = 3) and was not different from that observed after a 1.3 min rest period ($P > 0.05$). Increasing the stimulation frequency to 0.1 Hz had no effect on the time course and the steady-state inhibition of fast Ba^{2+} current in the presence of fenoverine. Tonic blockade was defined as the blockade of Ba^{2+} current that could not be removed during a rest period of 2 min when the membrane potential was held at −90 mV. As hyperpolarizing the membrane did not restore the Ba^{2+} current we can assume that the blockade was largely tonic.

The next possibility we tested was that membrane depolarization could alter the effectiveness of fast Ba^{2+} current blockade by fenoverine. The influence of fenoverine on the voltage-dependent inactivation of the fast Ba^{2+} current was examined with a two-pulse protocol (Figure 3b, inset). A test pulse to 0 mV (V_2) from a holding potential of −70 mV was preceded by a prepulse (V_1) of 30 s duration and of variable amplitude. The decrease of the test current was taken as an index of availability of the fast Ba^{2+} current. Relative availability was expressed by plotting the test current against the prepulse potential value. The amplitude of the test current was normalized to its value at the most negative prepulse (I/I_{max}). As shown in Figure 3b, in the presence of 10 μM fenoverine, the curve was shifted to more negative membrane potential by 9.2 ± 3 mV (n = 6) without a change of the mean slope factor (k = 6). Using an approach described by Bean *et al.* (1986), we could estimate the dissociation constants for fenoverine

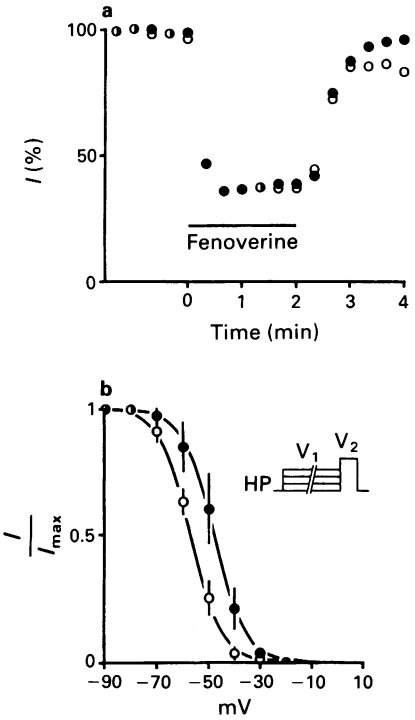

Figure 3 Effects of frequency of command pulses and membrane potential on the fast Ba^{2+} current of portal vein smooth muscle cells. (a) Command pulses applied repetitively at 0.05 Hz before, during the application of 10 μM fenoverine and after removal of fenoverine (●). The current was normalized to its maximal value in control conditions. Steady-state effect of fenoverine was obtained within 1 min. After complete recovery, the same protocol was applied except that the effect of fenoverine was tested after a rest period of 1.3 min (○). Fenoverine was applied with a pressure ejector from a glass pipette placed close to the cell membrane. The command pulses were 150 ms in duration and 70 mV in amplitude. The holding potential was −70 mV and the cells were superfused in the presence of 10 nM isradipine. (b) Steady-state availability curves of the fast Ba^{2+} current in isolation before (●) and after addition of 10 μM fenoverine (○) against membrane potential. For these experiments inhibition of Ba^{2+} currents ranged between 45 and 55%. The test potential (V_2) was 0 mV and duration of the conditioning pulse (V_1) was 30 s (inset). The data were fitted by curves of form $1/[1 + \exp(V - V_h)/k]$ where V_h was the potential at which half of the current was inactivated. For the control curve (●), $V_h = -47$ mV and $k = 6.1$. For the curve in the presence of fenoverine (○), $V_h = -57$ mV and $k = 5.9$. In the presence of fenoverine, the measurements of Ba^{2+} current were made when the cells reached steady state i.e. within 2–3 min at a stimulation frequency of 0.03 Hz. The current was normalized to its value at the most negative membrane potential.

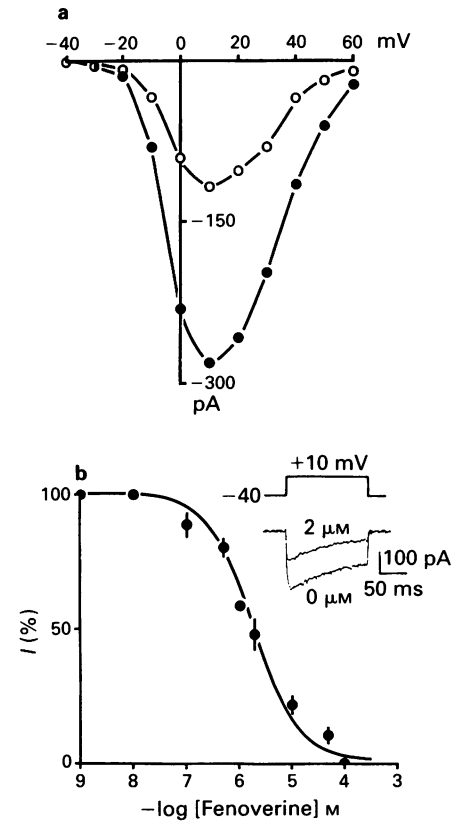

Figure 4 Effects of fenoverine on the slow Ba^{2+} current of portal vein smooth muscle cells. (a) Current-voltage relationships in control (●) and after addition of 2 μM fenoverine. The slow Ba^{2+} current was elicited from a holding potential of −40 mV. (b) Concentration-response curve for the effects of fenoverine on the slow Ba^{2+} current elicited from a holding potential of −40 mV. Percentage maximal current was plotted against the logarithmic value of fenoverine concentration. The continuous curve represents nonlinear regression to the data points assuming a Hill coefficient of 1. Each point represents the mean response of 6 cells with the s.e. shown by vertical lines. The stimulation frequency was 0.05 Hz. Inset: Ba^{2+} current traces in absence and presence of 2 μM fenoverine.

binding to the resting and inactivated states, assuming one-to-one binding of drug to resting and inactivated Ca^{2+} channels. The dissociation constant for binding to the inactivated state (k_i) can be calculated from the equation:

$$\Delta V_h = k \ln[(1 + [\text{drug}]/K_i)/(1 + [\text{drug}]/K_r)]$$

where ΔV_h is the shift of the mid-point of the steady-state availability curve, k is the slope factor of the availability curve, [drug] is the concentration of fenoverine used (10 μM), and K_r is 7.5 μM. Using the shift of 9.2 mV caused by 10 μM fenoverine gave a value K_i of 1 μM. The ratio K_r/K_i was 7.5 which indicates a higher affinity of fenoverine for the inactivated fast Ca^{2+} channels than for resting channels.

Effect of fenoverine on the slow Ba^{2+} current of portal vein smooth muscle

In order to study the effects of fenoverine on the slow Ca^{2+} channels, experiments were carried out with a holding potential of −40 mV where most (if not all) fast Ca^{2+} channels were inactivated. Figure 4a shows a typical inhibitory effect of 2 μM fenoverine on the current-voltage relationship of the slow Ba^{2+} current. The maximal Ba^{2+} current was inhibited by 53 ± 6% ($n = 6$) without any change in the voltage threshold, the potential for the maximal current and the apparent reversal potential. The measurements were made only when the cells reached steady-state, i.e. within 1.5–2 min at a stimulation frequency of 0.05 Hz. The effects of fenoverine were partially reversed after 3–4 min return to reference solution. The concentration-response curve (Figure 4 b) shows that the concentration of fenoverine required to reduce the slow Ba^{2+} current by 50% (IC_{50}) was 1.9 ± 0.9 μM ($n = 6$).

As shown in Figure 5a, the blockade of the slow Ba^{2+} current by 2 μM fenoverine was similar at the end of a rest period of 1.3 min (44.3 ± 14.7%, $n = 3$) or when currents were activated at a frequency of 0.05 Hz (47.3 ± 14.7, $n = 3$). The difference was not significant ($P > 0.05$). In the presence of 2 μM fenoverine, the voltage-dependent availability curve of the slow Ba^{2+} current was slightly shifted to more negative membrane potential by 4.6 ± 0.3 mV ($n = 6$) without a change in the mean slope factor ($k = 4$). As the shift of the mid-point of the availability curve was suppressed after removal of fenoverine, we estimated that the dissociation constant (K_i) for fenoverine binding to inactivated slow Ca^{2+} channels was 0.39 μM. The ration K_r/K_i was 6.4. A better confidence for this mechanism of action is provided below by use of myometrial cells where only slow Ca^{2+} channels have been identified (Honoré *et al.*, 1989).

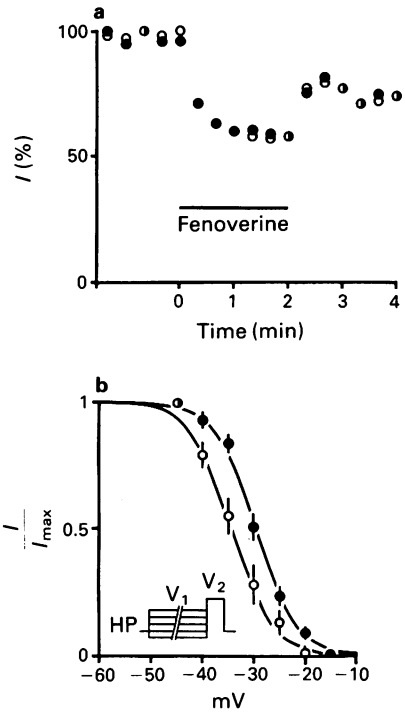

Figure 5 Effects of frequency of command pulses and membrane potential on the slow Ba^{2+} current of portal vein smooth muscle cells. (a) Command pulses applied repetitively at 0.05 Hz in the absence and presence of 2 μM fenoverine (●). The current was normalized to its maximal value in control. After recovery, the same protocol was applied except that the effect of fenoverine was tested after a rest period of 1.3 min (○). The command pulses were 150 ms in duration and 50 mV in amplitude. The holding potential was −40 mV. (b) Steady-state availability curve in isolation before (●) and after addition of 2 μM fenoverine (○). At this concentration, fenoverine inhibition ranged between 50 and 55%. The test potential (V_2) was +10 mV and the duration of the conditioning pulse (V_1) was 30 s (inset). For the control curve (●), $V_h = -30$ mV and $k = 4$. For the curve in the presence of fenoverine (○), $V_h = -35$ mV and $k = 4.2$. The current was normalized to its value at the most negative membrane potential. Stimulation frequency was 0.03 Hz.

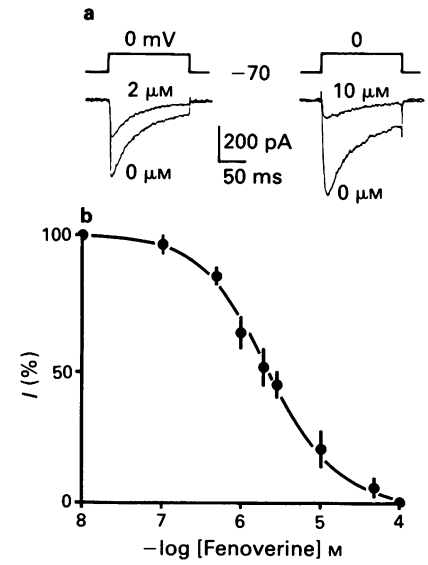

Figure 6 Concentration-effect relationship of the inhibitory action of fenoverine on the slow Ba^{2+} current of isolated myometrial cells from pregnant rat. (a) The Ba^{2+} current elicited from a holding potential of −70 mV to 0 mV was inhibited by addition of 2 μM and 10 μM fenoverine (in two different cells). (b) Concentration-response curve for the effects of fenoverine on the slow Ba^{2+} current elicited from a holding potential of −70 mV. Percentage maximal current was plotted against the logarithmic value of fenoverine concentration. The continuous curve represents the nonlinear regression to the data assuming a Hill coefficient of 1. Each point represents the mean response of 6 cells with s.e. shown by vertical lines. The stimulation frequency was 0.05 Hz.

Effects of fenoverine on the slow Ba^{2+} current in myometrium

In myometrial cells isolated from pregnant rats, the voltage-dependent Ca^{2+} channel is mainly of the slow-type (Honoré *et al.*, 1989; Ohya & Sperelakis, 1989). However, the sensitivity of myometrial cells to dihydropyridines is reported to be about 3–5 times lower than that of vascular smooth muscle cells (Honoré *et al.*, 1989).

Fenoverine inhibited in a concentration-dependent manner the slow Ba^{2+} current of myometrial cells held at a membrane potential of −70 mV (Figure 6). The IC_{50} was estimated to be 2.3 ± 0.9 μM ($n = 6$), a value similar to that obtained for vascular smooth muscle cells. The experimental points were closely distributed along a sigmoid curve with a slope of 1. The blockade of the slow Ba^{2+} current by 2 μM fenoverine was similar at the end of a rest period of 1.3 min or when currents were activated at a frequency of 0.05 Hz (Figure 7a). The difference was not significant ($P > 0.05$, $n = 5$). As hyperpolarizing the membrane for 2 min at −90 mV did not restore the slow Ba^{2+} current, this result suggests that the blockade of the slow Ca^{2+} channels was largely tonic. Calculation of the dissociation constant for fenoverine binding to inactivated slow Ca^{2+} channels was obtained by comparing the availability curves constructed from a holding potential of −70 mV in the absence and presence of 2 μM fenoverine. As the shift of the mid-point of the steady-state availability curve was 6.5 ± 0.7 mV ($n = 6$) and the mean slope factor, $k = 5$, this gave a value for K_i of 0.34 μM. These results indicate that fenoverine has a similar affinity for the slow Ca^{2+} channels in both vascular and myometrial smooth muscle whatever the value of the holding potential (−70 or −40 mV).

Discussion

The electrophysiological data presented in this paper show that fenoverine, at micromolar concentrations, caused an inhibition of both fast and slow Ca^{2+} channels in smooth muscle cells of rat portal vein. This is of particular interest as most Ca^{2+} inhibitors have been shown to inhibit selectively slow Ca^{2+} channels in neurones (Fox *et al.*, 1987), cardiac muscle cells (Bean, 1985) and smooth muscle cells (Benham *et al.*, 1987; Hering *et al.*, 1988). Isradipine, a dihydropyridine derivative, blocks the fast Ca^{2+} current at concentrations 300 times higher than those used to block the slow Ca^{2+} current (Loirand *et al.*, 1989). Similarly, fenoverine is more effective in blocking the slow Ba^{2+} current in vascular and myometrial smooth muscle cells (IC_{50} = 1.9–2.3 μM). Fenoverine inhibition of both fast and slow Ba^{2+} currents is obtained without any significant modification of the apparent reversal potential, which suggests that the drug decreases the voltage-dependent Ba^{2+} conductance of the smooth muscle cell membrane.

Recent studies have provided new informations regarding the mechanism of Ca^{2+} channel blockade by organic Ca^{2+} channel inhibitors (Uehara & Hume, 1985; Klöckner & Isenberg, 1986; Dacquet *et al.*, 1987). The results of all these experiments support the idea that the inhibition of Ca^{2+} channels can be modulated by stimulation frequency and the membrane potential. The inhibitory effect of fenoverine was not enhanced when the cell was stimulated by repetitive depolarizing clamp pulses (0.05–0.1 Hz), which indicates that the rate at which Ca^{2+} channels are activated does not play a key role in the inhibitory effect of fenoverine (absence of use-dependence). Moreover, the inhibitory effect of fenoverine on Ca^{2+} channels is enhanced at more depolarized long-lasting holding potentials. The relative potency of fenoverine calculated from the dissociation constants for binding to resting

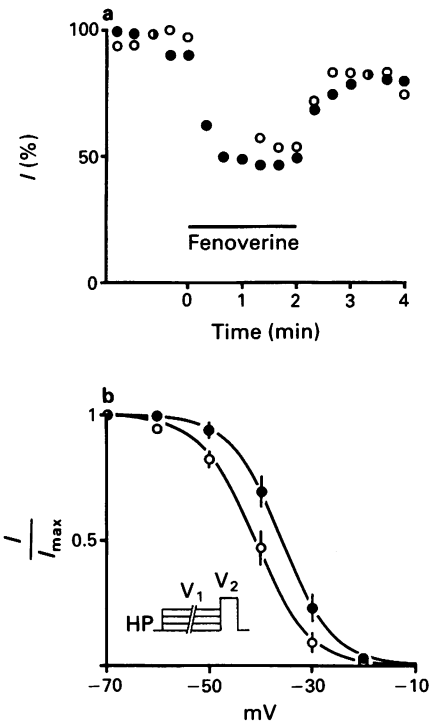

Figure 7 Effects of frequency of command pulses and membrane potential on the slow Ba^{2+} current of myometrial cells. (a) Command pulses applied repetitively at 0.05 Hz in the absence and presence of 2 μM fenoverine (●). The current was normalized to its maximal value in control conditions. After recovery, the same protocol was applied except that the effect of fenoverine was tested after a rest period of 1.3 min (○). The command pulse was 150 ms in duration and 70 mV in amplitude. The holding potential was −70 mV. (b) Steady-state availability curve in isolation before (●) and after addition of 2 μM fenoverine (○). At this concentration fenoverine inhibition ranged between 49 and 55%. The test potential (V_2) was 0 mV and the duration of the conditioning pulse (V_1) was 30 s (inset). For the control curve (●), $V_h = -35$ mV and $k = 5$. For the curve in the presence of fenoverine (○), $V_h = -41$ mV and $k = 5.2$. The current was normalized to its value at the most negative membrane potential. Stimulation frequency was 0.03 Hz.

channels (K_r) and to inactivated channels (K_i) was estimated to be 5–7, a value similar to that calculated for isradipine in vascular smooth muscle cells (Loirand *et al.*, 1989). Therefore, our results can be interpreted according to the 'modulated receptor hypothesis' (Hondeghem & Katzung, 1984) which postulates that the binding of the antagonistic drug is dependent on the channel state (resting, open or inactivated state). Our experimental results are consistent with the binding of fenoverine to resting Ca^{2+} channels (fast and slow-type). Increasing the number of inactivated Ca^{2+} channels at depolarized holding potentials increased the fenoverine-induced blockade as assessed by a preferential binding of the drug to the inactivated Ca^{2+} channel state. However, binding of fenoverine to the inactivated state of the Ca^{2+} channels would be expected to induce a use-dependent blockade on repetitive depolarizations (150 ms) by holding the channels in a drug-bound inactivated state. Because virtually all drug-free slow channels of myometrial cells are in the resting state at holding potentials of −70 mV, this result suggests that fenoverine only binds to the inactivated state when long-lasting holding potentials (30 s) were applied. This discrepancy has been previously observed for nifedipine in rabbit artery (Hering *et al.*, 1988) and suggests that repetitive depolarizing pulses are too brief to allow high affinity binding to the inactivated state of the Ca^{2+} channels. Quantitative determination of the contribution of use-dependent blockade of slow Ca^{2+} channels to the actions of Ca^{2+} channel antagonists during short repetitive depolarizations may require additional experimental procedures such as single channel recordings or rapid photoconversion procedures.

In conclusion, our results demonstrate that fenoverine, at pharmacological concentrations, inhibits both fast and slow Ba^{2+} currents in smooth muscle. The results suggest that fenoverine may reduce smooth muscle contractility by inhibiting the slow Ca^{2+} channels which constitute the major Ca^{2+} entry pathway during action potential generation and excitation-contraction coupling, and modulate spike firing by inhibiting the fast Ca^{2+} channels which are believed to contribute to modulation of vascular activity.

This work was supported by grants from Ministère de la Recherche et de la Technologie, Ministère de l'Education Nationale, Fondation pour la Recherche Médicale, Région Aquitaine, Centre National des Etudes Spatiales, and Laboratoires Delalande, France. We thank Mrs N. Biendon for excellent assistance.

References

AMEDEE, T., MIRONNEAU, C. & MIRONNEAU, J. (1986). Isolation and contractile responses of single pregnant rat myometrial cells in short-term primary culture and the effects of pharmacological and electrical stimuli. *Br. J. Pharmacol.*, **88**, 873–880.

BEAN, B. (1985). Two kinds of calcium channels in canine atrial cells. Differences in kinetics, selectivity and pharmacology. *J. Gen. Physiol.*, **86**, 1–30.

BEAN, B., STUREK, M., PUGA, A. & HERMSMEYER, K. (1986). Calcium channels in muscle cells isolated from rat mesenteric arteries: modulation by dihydropyridine drugs. *Circ. Res.*, **59**, 229–235.

BENHAM, C., HESS, T. & TSIEN, R. (1987). Two types of calcium channels in single smooth muscle cells from rabbit ear artery studied with whole-cell and single-channel recordings. *Circ. Res.*, **61**, I10–I16.

DACQUET, C., LOIRAND, G., MIRONNEAU, C., MIRONNEAU, J. & PACAUD, P. (1987). Spironolactone inhibition of contraction and calcium channels in rat portal vein. *Br. J. Pharmacol.*, **92**, 535–544.

DE LEAN, A.P., MUNSON, P.J. & RODBARD, D. (1978). Simultaneous analysis of families of sigmoidal curves: Applications to bioassay, radioligand assay and physiological dose-response curves. *Am. J. Physiol.*, **235**, E97–E102.

FOX, A., NOWYCKY, M. & TSIEN, R. (1987). Kinetic and pharmacological properties distinguish three types of calcium currents in chick sensory neurones. *J. Physiol.*, **394**, 149–172.

GONELLA, J., LALANNE, C. & MIRONNEAU, J. (1987). Fenoverine: a novel synchronizer of smooth muscle motility by interference with cellular calcium flow. *Curr. Med. Res. Op.*, **10**, 427–435.

HAMILL, O.P., MARTY, A., NEHER, E., SAKMANN, E. & SIGWORTH, F.J. (1981). Improved patch-clamp techniques for high-resolution current recording from cells and cell-free membranes patches. *Pflügers Arch.*, **391**, 85–100.

HERING, S., BEECH, D.J., BOLTON, T.B. & LIM, S.P. (1988). Action of nifedipine or Bay k 8644 is dependent on calcium channel state in single smooth muscle cells from rabbit ear artery. *Pflügers Arch.*, **411**, 590–592.

HONDEGHEM, L.M. & KATZUNG, B.G. (1984). Antiarrhythmic agents: the modulated receptor mechanism of action of sodium and calcium channel-blocking drugs. *Annu. Rev. Pharmacol. Toxicol.*, **24**, 387–423.

HONORE, E., AMEDEE, T., MARTIN, C., DACQUET, C., MIRONNEAU, C. & MIRONNEAU, J. (1989). Calcium channel current and its sensitivity to (+)-isradipine in cultured pregnant rat myometrial cells. An electrophysiological and a binding study. *Pflügers Arch.*, **414**, 477–483.

KLOCKNER, U. & ISENBERG, G. (1986). Tiapamil reduces the calcium inward current of isolated smooth muscle cells. Dependence on holding potential and pulse frequency. *Eur. J. Pharmacol.*, **127**, 165–171.

LOIRAND, G., PACAUD, P., MIRONNEAU, C. & MIRONNEAU, J. (1986). Evidence for two distinct calcium channels in rat vascular

smooth muscle cells in short-term primary culture. *Pflügers Arch.*, **407**, 566–568.

LOIRAND, G., MIRONNEAU, C., MIRONNEAU, J. & PACAUD, P. (1989). Two types of calcium currents in single smooth muscle cells from rat portal vein. *J. Physiol.*, **412**, 333–349.

MIRONNEAU, J. (1973). Excitation-contraction coupling in voltage-clamped uterine smooth muscle. *J. Physiol.*, **233**, 127–141.

OHYA, Y. & SPERELAKIS, N. (1989). Fast Na^+ and slow Ca^{2+} channels in single uterine muscle cells from pregnant rat. *Am. J. Physiol.*, **257**, C408–412.

UEHARA, A. & HUME, J.R. (1985). Interactions of organic calcium channel antagonists with calcium channels in single frog atrial cells. *J. Gen. Physiol.*, **85**, 621–647.

(Received April 2, 1991
Revised May 10, 1991
Accepted May 13, 1991)

Br. J. Pharmacol. (1991), **104**, 71–76

Antagonism of relaxin by glibenclamide in the uterus of the rat *in vivo*

[1]Sandra J. Downing & M. Hollingsworth

Smooth Muscle Research Group, Department of Physiological Sciences, University of Manchester, Oxford Road, Manchester M13 9PT

1 The effects of glibenclamide (a blocker of adenosine triphosphate [ATP]-dependent K^+-channels) on the inhibition of uterine contractions by relaxin, salbutamol and cromakalim were compared *in vivo*.

2 Glibenclamide (20 mg kg^{-1}) did not antagonize salbutamol. Glibenclamide produced a parallel rightward shift in the dose-response curve to cromakalim with a 5.5 fold decrease in uterine sensitivity (post-vehicle log ID_{50}, −0.87 mg kg^{-1}; post-glibenclamide log ID_{50}, −0.07 mg kg^{-1}). Glibenclamide produced a non-parallel rightward shift in the dose-response curve to relaxin (post-vehicle log ID_{50}, 0.99 μg kg^{-1}; post-glibenclamide log ID_{50}, 2.28 μg kg^{-1}).

3 Glibenclamide reversed established inhibition of uterine contractions by cromakalim or relaxin but not that by salbutamol.

4 Insulin produced no antagonism of relaxin on isolated uterus of the rat, demonstrating that glibenclamide antagonism of relaxin *in vivo* is not by released insulin. Apamin did not antagonize relaxin *in vivo*, suggesting that small calcium-activated K^+-channels are not involved in the action of relaxin.

5 Comparison of the lack of antagonism of salbutamol with the non-competitive-like antagonism of relaxin by glibenclamide suggests that relaxin does not relax uterine smooth muscle predominantly by increasing intracellular adenosine 3′, 5′-cyclic monophosphate concentrations. Comparison of the non-competitive-like antagonism of relaxin and the competitive-like antagonism of cromakalim by glibenclamide suggests that the two relaxants may share, in part, a common mechanism of action and that additional mechanism(s) may also be involved in the inhibitory action of relaxin.

Keywords: Relaxin; uterus; glibenclamide; salbutamol; cromakalim; potassium channels

Introduction

Relaxin, a polypeptide hormone of molecular weight 6500 daltons, is a potent, selective and reversible inhibitor of uterine contractions *in vivo* and *in vitro* (Porter *et al.*, 1979; Sanborn *et al.*, 1980; Cheah & Sherwood, 1981; Bradshaw *et al.*, 1981). Relaxin has been shown to be important for the maintenance of myometrial quiescence during late pregnancy in the rat (Downing & Sherwood, 1985a,b) and for delivery of live young in the rat and pig (Nara *et al.*, 1982; Downing & Sherwood, 1985a). The mechanism by which relaxin inhibits uterine contractions is not fully understood. Relaxin has been shown to increase myometrial adenosine 3′,5′-cyclic monophosphate (cyclic AMP) concentrations *in vitro* in a concentration-dependent manner (Cheah & Sherwood, 1980; Judson *et al.*, 1980; Sanborn *et al.*, 1980). However, the time course of changes in cycle AMP concentrations and activity of cyclic AMP-dependent protein kinase are not well correlated with the time course of inhibition of uterine contractions (Judson *et al.*, 1980; Sanborn *et al.*, 1980; Kemp & Niall, 1981). Relaxin also induces inactivation of myosin light chain kinase by phosphorylation (Nishikori *et al.*, 1983), which may be a cyclic AMP-dependent event, and promotes calcium ion efflux from myometrial cells in culture (Rao & Sanborn, 1986).

Potassium channel opening may also be a mechanism by which relaxin inhibits uterine contractions. Relaxin inhibits uterine spasm induced by a low concentration (20 mM) of potassium chloride *in vitro*, but does not inhibit uterine spasm induced by a higher concentration (30 mM) (St-Louis, 1981). It has recently been suggested that such observations are indicative of a relaxant action of agents involving K^+-channels (Edwards & Weston, 1990). Relaxin is also antagonized *in vitro* by the non-selective K^+-channel blocker, tetraethylammonium (unpublished results). Glibenclamide, an oral hypoglycaemic agent which is a relatively selective blocker of ATP-dependent K^+ channels (Sturgess *et al.*, 1988; Escande *et al.*, 1989; Standen *et al.*, 1989) has been used *in vivo* to demonstrate antagonism of the hypotensive and uterine-relaxant actions of the K^+-channel opener cromakalim (Buckingham *et al.*, 1989; Cavero *et al.*, 1989; Quast & Cook, 1989; Piper *et al.*, 1990). Apamin is another highly selective blocker of K^+-channels, in this case the small calcium-activated K^+-channel (Weir & Weston, 1986; Cook & Hof, 1988).

The aims of this study were to determine whether relaxin inhibition of uterine contractions *in vivo* involved K^+-channel opening by using the antagonists glibenclamide and apamin. The antagonism of relaxin by glibenclamide was compared with that of cromakalim and the β-adrenoceptor agonist salbutamol, which inhibits uterine contractions by cyclic AMP-mediated mechanisms. Some preliminary results have been published (Downing & Hollingsworth, 1990a).

Methods

Female rats, 200–250 g, purchased from Charles River Ltd., UK, were anaesthetized with tribromoethanol, 240 mg kg^{-1} i.p., bilaterally ovariectomized, a small latex balloon placed in one uterine horn and the right jugular vein cannulated (Downing & Sherwood, 1985b). The balloon and cannula tubing were passed s.c. to the back of the neck, exteriorized and passed through a 40 cm protective metal spring, which allowed the animals almost unrestricted movement within the cage throughout the recording period. All rats were given 5 mg kg^{-1} morphine sulphate s.c. for post-operative analgesia. The animals were allowed 24 h for recovery from surgery before continuous recording of uterine contractions in conscious animals started. Contractions, recorded as intra-uterine pressure cycles with Elcomatic EM750 or Statham P23Db pressure transducers and Grass Polygraphs, were quantified as integral of the area under the pressure curve. The rats were allocated to one of the following three experimental procedures:

[1] Author for correspondence.

(1) *Effect of glibenclamide on inhibition of uterine contractions by salbutamol, cromakalim and relaxin*

The uterine responses to bolus i.v. doses of salbutamol (10, 50, 200 $\mu g\,kg^{-1}$, 60 rats), cromakalim (0.05, 0.1, 0.25 $mg\,kg^{-1}$, 80 rats) or porcine relaxin (2, 5, 20 $\mu g\,kg^{-1}$, 80 rats) were recorded for 60 min and expressed as percentage inhibition of integral of uterine contractions recorded for the 60 min before each bolus dose. Three hours were allowed to elapse between each relaxant bolus to allow the relaxant to clear. Four hours after the last bolus dose of relaxant, the rats were given an intravenous infusion of either glibenclamide (20 $mg\,kg^{-1}$) or vehicle (0.02N sodium hydroxide in 4% glucose w/v, 5 $ml\,kg^{-1}$) over 5 min. A single i.v. bolus dose of relaxant (salbutamol, 10, 50 or 200 $\mu g\,kg^{-1}$; cromakalim, 0.05, 0.1, 0.25, 0.5, 1.0, 1.6 or 2.5 $mg\,kg^{-1}$; relaxin, 2, 5, 50 or 200 $\mu g\,kg^{-1}$, 10 rats per bolus dose) was given at 15 min after the end of infusion. Due to the short duration of action of glibenclamide *in vivo* in the rat, only a single bolus dose of relaxant could be used after infusion. The percentage inhibition of integral of uterine contractions was determined over 60 min as before. Pre-infusion log ID_{50} values for each animal and post-infusion log ID_{50} values from mean data were calculated by probit analysis and were compared statistically by analysis of variance followed by Student's *t* test. Slopes of the pre- and post-infusion dose-response curves were calculated by linear regression.

(2) *Glibenclamide reversal of inhibition of uterine contractions by salbutamol, cromakalim and relaxin*

After 120 min control recording of uterine contractions, rats were given a single i.v. bolus dose of salbutamol (200 $\mu g\,kg^{-1}$, 21 rats), cromakalim (0.25 $mg\,kg^{-1}$, 25 rats) or relaxin (20 $\mu g\,kg^{-1}$, 24 rats). Three hours later, the relaxant dose was repeated followed after 5 min by an i.v. infusion of glibenclamide (20 $mg\,kg^{-1}$) or vehicle (5 $ml\,kg^{-1}$) over 5 min. Uterine contractions were recorded for 120 min after the relaxant bolus dose. A separate group of animals received i.v. infusion of glibenclamide (20 $mg\,kg^{-1}$, 5 rats) or vehicle (5 $ml\,kg^{-1}$, 6 rats) without prior treatment with relaxant and uterine contractions were recorded for 120 min after infusion. Recordings were analysed in successive 10 min periods after bolus injection of relaxant and expressed as percent control integral. Statistical comparisons between groups were made by analysis of variance.

(3) *Effect of apamin on relaxin inhibition of uterine contractions*

The uterine responses to bolus i.v. doses of relaxin (2, 5, 20 $\mu g\,kg^{-1}$) were recorded as described in treatment (1). The animals then received an i.v. infusion of apamin (0.15 $mg\,kg^{-1}$, 18 rats) or saline (1 $ml\,kg^{-1}$, 18 rats) over 20 min. Thirty minutes after the end of infusion, the animals received a single bolus i.v. dose of relaxin (2, 5 or 20 $\mu g\,kg^{-1}$). Pre- and post-infusion log ID_{50} values and slopes of the dose-response curves were calculated as in treatment (1).

The effect of insulin on relaxin inhibition of uterine contractions in vitro

A further group of 10 rats were subjected to bilateral ovariectomy only. Twenty-four hours after surgery the animals were killed, uteri removed and cleaned of fat. Each uterine horn was opened longitudinally and cut into longitudinal strips of approximately 1 cm length. The strips were mounted for isometric recording under 1 g tension in a physiological salt solution maintained at 37°C, gassed with 95% O_2/5% CO_2 and equilibrated for 1 h. The spontaneous mechanical responses were measured as integrated tension by the method of Granger *et al.* (1985). Porcine insulin was then added to the tissue bath to produce concentrations of 50, 500 or 5000 $ng\,ml^{-1}$ (10 strips per group), and vehicle (25 μM hydrochloric acid) added to a further 10 strips. After a further 15 min equilibration, concentration-response curves to cumulative additions of porcine relaxin (2.5–160 $ng\,ml^{-1}$) were constructed. Log IC_{50} values were calculated by probit analysis and compared statistically by analysis of variance followed by Student's *t* test.

Drugs and solutions

Porcine relaxin was isolated and purified from pregnant sow ovaries by the method of Sherwood & O'Byrne (1974). Relaxin was bioassayed *in vitro* by inhibition of the electrically-stimulated uterus from oestrogen-treated rats (100 $\mu g\,kg^{-1}$ 17-β oestradiol benzoate s.c.), with porcine relaxin, kindly donated by Dr O.D. Sherwood, as standard. The relaxin preparation was found to be equipotent with highly purified relaxin. Cromakalim was supplied by Smith-Kline Beecham (Surrey), salbutamol by Glaxo Ltd (Ware) and glibenclamide by Hoechst Ltd (Hounslow). Porcine insulin and apamin were purchased from Sigma Chemical Co (Poole, Dorset), tribromoethanol from Fluka Chemicals (Glossop), and morphine sulphate from Evans Ltd (Dunstable). Latex for manufacture of intra-uterine balloons was kindly donated by Revertex Ltd, Harlow, Essex.

Results

(1) *Effect of glibenclamide on inhibition of uterine contractions by salbutamol, cromakalim and relaxin*

Dose-response curves for inhibition of uterine contractions by salbutamol, cromakalim and relaxin before and after infusion of glibenclamide or vehicle are shown in Figures 1, 2 and 4. Log ID_{50} values and slopes of the dose-response curves for the three relaxants before and after infusion of glibenclamide or vehicle are given in Table 1. Inhibition by salbutamol of uterine contractions was unaffected by infusion of either glibenclamide or vehicle (Figure 1). No significant differences were observed between log ID_{50} values or slopes of the dose-response curves for pre- and post-infusion responses to salbutamol (Table 1) in vehicle- or glibenclamide-infused rats.

Inhibition by cromakalim of uterine contractions was unaffected by vehicle infusion (Figure 2a). In contrast, the dose-response curve for cromakalim was shifted to the right after glibenclamide infusion compared with the pre-infusion uterine responses (Figure 2b). A 5.5 fold reduction in uterine sensitivity to cromakalim was produced by glibenclamide infusion ($P < 0.05$). The slope of the post-infusion dose-response curve, however, was unchanged by glibenclamide treatment (Table 1).

Relaxin reversibly inhibited uterine contractions with immediate onset of action (Figure 3a). The relaxin inhibition of uterine contractions was unaffected by vehicle infusion (Figure 4a). Glibenclamide infusion, however, produced a marked reduction in uterine response to relaxin compared with pre-infusion responses (Figures 3b and 4b, Table 1). A 19 fold reduction in uterine sensitivity to relaxin, at 50% inhibition, was observed in glibenclamide-infused rats ($P < 0.05$). In contrast to its antagonism of cromakalim, glibenclamide treatment also produced a marked reduction in the slope of the dose-response curve to relaxin ($P < 0.05$; Table 1).

(2) *Glibenclamide reversal of inhibition of uterine contractions by salbutamol, cromakalim and relaxin*

Salbutamol (200 $\mu g\,kg^{-1}$) produced a sustained reduction in uterine contractions for a period of 90 min (Figure 5). The inhibition of uterine contractions was maintained during and after infusion of either vehicle or glibenclamide (20 $mg\,kg^{-1}$, Figure 5a, Table 2). Cromakalim (0.25 $mg\,kg^{-1}$) also produced

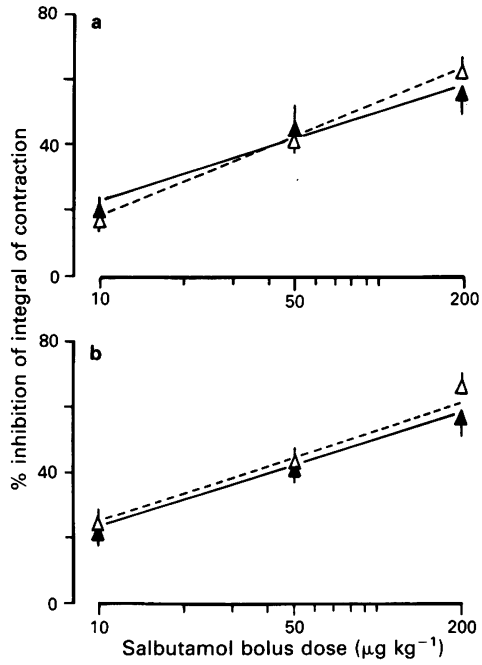

Figure 1 Effect of salbutamol i.v. (a) on uterine contractions before (△) and after (▲) infusion of vehicle (0.02N sodium hydroxide in 4% glucose, 5 ml kg^{-1} i.v.), $n = 30$ rats preinfusion, 10 rats per point postinfusion. Effect of salbutamol i.v. (b) on uterine contractions before (△) and after (▲) infusion of glibenclamide (20 mg kg^{-1} i.v.), $n = 30$ rats preinfusion, 10 rats per point postinfusion. Ordinate scales: inhibition of integral of uterine contraction over 60 min as % of integral for 60 min preceding i.v. bolus dose. Abscissa scales: dose of salbutamol on a log scale.

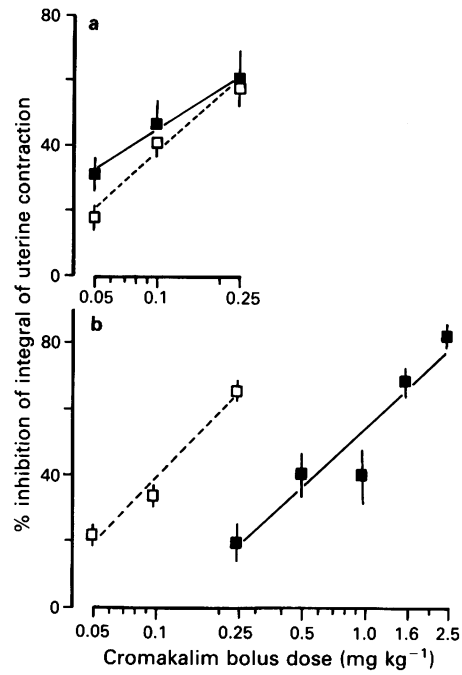

Figure 2 Effect of cromakalim i.v. (a) on uterine contractions before (□) and after (■) infusion of vehicle (0.02N sodium hydroxide in 4% glucose, 5 ml kg^{-1} i.v.), $n = 30$ rats preinfusion, 10 rats per point postinfusion. Effect of cromakalim i.v. (b) on uterine contractions before (□) and after (■) infusion of glibenclamide (20 mg kg^{-1} i.v.), $n = 50$ rats preinfusion, 10 rats per point postinfusion. Ordinate scales: inhibition of integral of uterine contraction over 60 min as % of integral for 60 min preceding i.v. relaxant bolus. Abscissa scales: dose of cromakalim on a log scale.

prolonged reduction in uterine contractions which was not modified by infusion of vehicle (Table 2). Infusion of glibenclamide after cromakalim bolus dose significantly ($P < 0.05$–< 0.001) increased the integral of uterine contractions for 80 min after infusion. Additionally, glibenclamide infusion appeared to have increased uterine contractions above control levels of uterine activity recorded prior to cromakalim bolus, for a period of 60 min after infusion (Figure 5b). Relaxin

Table 1 Log ID_{50} values and slopes of dose-response curves for inhibition of uterine contractions

Relaxant		*Vehicle infusion*		*Glibenclamide infusion*	
		Preinfusion	*Postinfusion*	*Preinfusion*	*Postinfusion*
Salbutamol	log ID_{50} (μg kg^{-1})	1.88 ± 0.07	1.99	1.83 ± 0.07	1.93
	95% CL	1.72 – 2.05	1.72 – 2.46	1.67 – 1.90	1.75 – 2.35
	Slope (% (log μg kg^{-1})$^{-1}$)	34.6 ± 3.9	28.9 ± 6.9	32.8 ± 3.4	28.2 ± 5.9
Cromakalim	log ID_{50} (mg kg^{-1})	−0.76 ± 0.06	−0.87	−0.81 ± 0.05[a]	−0.07[a]
	95% CL	−0.87 – −0.62	−1.03 – −0.62	−0.88 – −0.75	−0.17 – 0.04
	Slope (%(log mg kg^{-1})$^{-1}$)	56.7 ± 9.1	41.0 ± 11.1	64.0 ± 6.6	58.8 ± 8.1
Relaxin	log ID_{50} (μg kg^{-1})	1.03 ± 0.03	0.99	1.00 ± 0.04[b]	2.28[b]
	95% CL	0.96 – 1.09	0.87 – 1.07	0.96 – 1.10	2.04 – 3.03
	Slope (% (log μg kg^{-1})$^{-1}$)	55.2 ± 3.8	45.7 ± 4.0	56.6 ± 4.3[c]	20.4 ± 4.1[c]

Log ID_{50} values are means ± s.e. mean. Values with same superscripts are significantly different: [a, b, c] $P < 0.05$.

Table 2 Uterine responses to bolus dose of relaxant (% inhibition over 60 min) in vehicle and glibenclamide-infused rats

	Vehicle infusion		*Glibenclamide infusion*	
Relaxant	*Control response*	*Test response*	*Control response*	*Test response*
Salbutamol (200 μg kg^{-1})	59.8 ± 8.7%	62.6 ± 4.2%	52.6 ± 7.7%	52.1 ± 5.2%
Cromakalim (0.25 mg kg^{-1})	58.5 ± 3.6%	51.4 ± 6.9%	62.2 ± 6.6%[a]	7.2 ± 3.3%[a]
Relaxin (20 μg kg^{-1})	52.3 ± 7.0%	65.2 ± 4.2%	65.4 ± 7.7%[b]	35.3 ± 6.2%[b]

Values are means ± s.e. mean. Means with the same superscripts are significantly different: [a] $P < 0.001$, [b] $P < 0.01$.

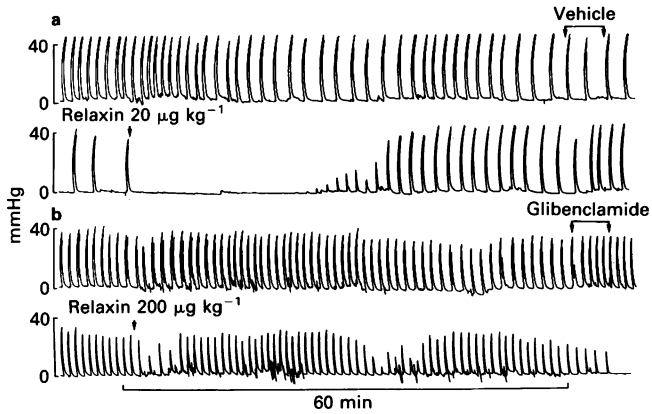

Figure 3 Recording of uterine contractions from two rats given an infusion of vehicle i.v. followed 15 min later with relaxin 20 $\mu g\,kg^{-1}$ i.v. (a) or given an infusion of glibenclamide, 20 $mg\,kg^{-1}$ i.v., followed 15 min later with relaxin, 200 $\mu g\,kg^{-1}$ i.v. (b).

(20 $\mu g\,kg^{-1}$) produced prolonged inhibition of uterine contractions for 120 min which was not modified by infusion of vehicle (Figure 5c, Table 2). Glibenclamide infusion in these animals produced a significant increase in uterine contractions for a period of 50 min ($P < 0.05$), although reversal of relaxin inhibition was only partial, since integral of uterine contractions did not reach pre-relaxin control levels (Figure 5c).

No significant change in integral of uterine contractions was observed after vehicle or glibenclamide infusion in the absence of prior relaxant treatment (Figure 5d).

(3) *Effect of apamin on relaxin inhibition of uterine contractions*

Uterine responses to bolus i.v. doses of relaxin were unaffected by infusion of either saline or apamin (0.15 $mg\,kg^{-1}$). Pre- and post-infusion log ID_{50} values for inhibition by relaxin of uterine contractions were similar in both saline (pre-infusion, 1.03 $\mu g\,kg^{-1}$, 95% CL, 0.91–1.17; post-infusion, 0.98 $\mu g\,kg^{-1}$, 95% CL, 0.76–1.38) and apamin-infused rats (pre-infusion, 1.07 $\mu g\,kg^{-1}$, 95% CL, 0.96–1.24; post-infusion, 1.03 $\mu g\,kg^{-1}$, 95% CL, 0.81–1.47). Similarly, the slopes of the dose-response curves to relaxin were unchanged in either saline (pre-infusion, 54.7 ± 7.1% $(\mu g\,kg^{-1})^{-1}$; post-infusion, 53.4 ± 13.6% $(\mu g\,kg^{-1})^{-1}$) or apamin-infused rats (pre-infusion, 50.2 ± 6.4% $(\mu g\,kg^{-1})^{-1}$; post-infusion, 53·8 ± 13.7% $(\mu g\,kg^{-1})^{-1}$). No antagonism of relaxin by apamin was therefore observed *in vivo*.

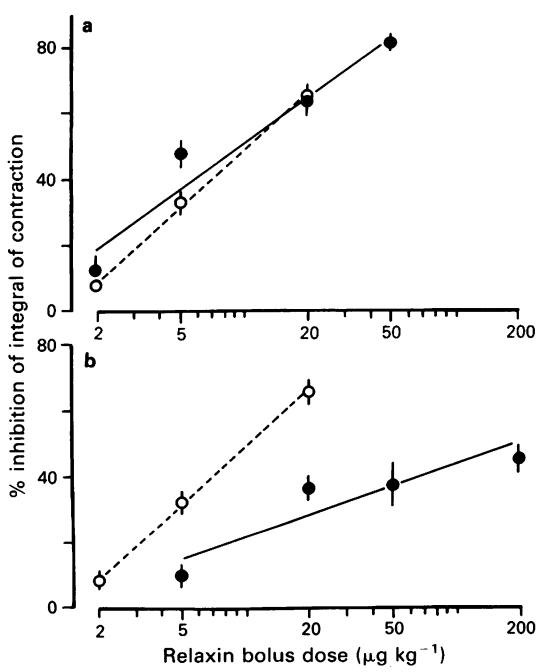

Figure 4 Effect of relaxin i.v. (a) on uterine contractions before (○) and after (●) infusion of vehicle (0.02N sodium hydroxide in 4% glucose, 5 $ml\,kg^{-1}$ i.v.), $n = 40$ rats preinfusion, 10 rats per point postinfusion. Effect of relaxin i.v. (b) on uterine contractions before (○) and after (●) infusion of glibenclamide (20 $mg\,kg^{-1}$, i.v.), $n = 40$ rats preinfusion, 10 rats per point postinfusion. Ordinate scales: inhibition of integral of uterine contraction over 60 min as % of integral for 60 min preceding i.v. relaxant dose. Abscissa scales: dose of relaxin on a log scale.

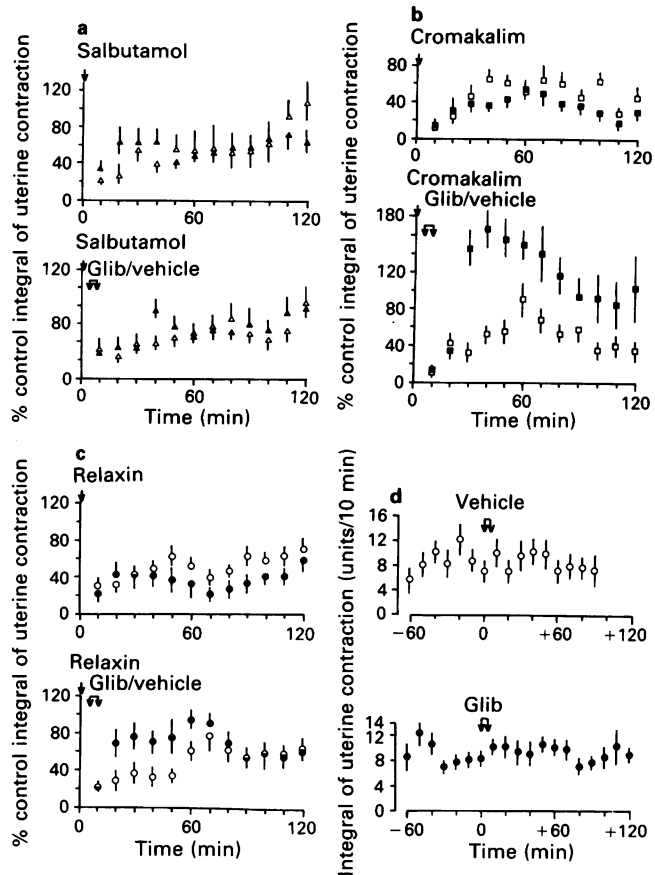

Figure 5 (a) Upper panel: preinfusion uterine response to salbutamol 200 $\mu g\,kg^{-1}$, i.v. (△) pre-vehicle, 10 rats; (▲) pre-glibenclamide, 11 rats. Lower panel: effect of vehicle (△) or glibenclamide (Glib) 20 $mg\,kg^{-1}$, i.v. (▲) (indicated by arrows) on uterine response to salbutamol, 200 $\mu g\,kg^{-1}$, i.v. (b) Upper panel: uterine response to cromakalim, 0.25 $mg\,kg^{-1}$, i.v. (□) pre-vehicle, 12 rats; (■) pre-glibenclamide, 13 rats. Lower panel: effect of vehicle (□) or glibenclamide 20 $mg\,kg^{-1}$, i.v. (■) (indicated by arrows) on uterine response to cromakalim, 0.25 $mg\,kg^{-1}$, i.v. (c) Upper panel: uterine response to relaxin, 20 $\mu g\,kg^{-1}$, i.v. (○) pre-vehicle, 12 rats; (●) pre-glibenclamide, 12 rats. Lower panel: effect of vehicle (○) or glibenclamide 20 $mg\,kg^{-1}$, i.v. (●) (indicated by arrows) on uterine response to relaxin 20 $\mu g\,kg^{-1}$, i.v. (d) Upper panel: effect of vehicle, 0.02N NaOH in 4% glucose 5 $ml\,kg^{-1}$ i.v. (indicated by arrows) on uterine contractions, (○), 5 rats. Lower panel: effect of glibenclamide, 20 $mg\,kg^{-1}$ i.v. (indicated by arrows) on uterine contractions. (●), 6 rats. Ordinate scales: integral of uterine contractions per 10 min period as % of mean integral of 12 × 10 min control periods (a–c); integral of uterine contractions as units per 10 min (d), Abscissa scales: time.

Effect of insulin on relaxin inhibition of uterine contractions in vitro

Relaxin produced a concentration-related inhibition of spontaneous uterine contractions (Figure 6). The sensitivity of uteri to relaxin was not modified by prior incubation of strips with high concentrations of porcine insulin or its vehicle (Figure 6).

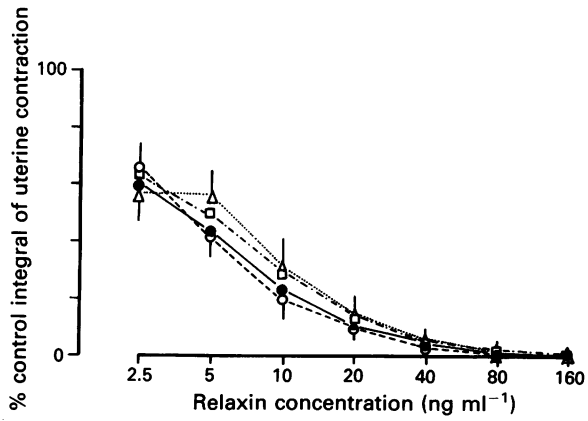

Figure 6 Effect of relaxin on uterine contractions *in vitro* in the absence of (○) and presence of porcine insulin (△, 50 ng ml^{-1}; □, 500 ng kg^{-1}; ●, 5000 ng ml^{-1}; $n = 10$ tissues per group). Ordinate scales: integral of uterine contraction remaining as % of integral prior to relaxin addition. Abscissa scales: concentration of relaxin on a log scale. Symbols represent means and vertical lines show s.e.mean.

Log IC_{50} values for inhibition of uterine contractions by relaxin were similar among the four treatment groups: vehicle 0.69 ± 0.07 ng ml^{-1}; 50 ng ml^{-1} insulin, 0.8 ± 0.1 ng ml^{-1}; 500 ng ml^{-1} insulin, 0.78 ± 0.08 ng ml^{-1}; 5000 ng ml^{-1} insulin, 0.71 ± 0.04 ng ml^{-1}. No antagonism was observed, therefore, of porcine relaxin by porcine insulin *in vitro*.

Discussion

Glibenclamide interaction with salbutamol and cromakalim

The interaction between the ATP-dependent K^+-channel blocker glibenclamide with three uterine relaxants has been investigated. Salbutamol, a β-adrenoceptor agonist, acts via activation of adenylate cyclase and subsequent generation of cyclic AMP, which mediates intracellular events leading to smooth muscle relaxation (Johansson & Andersson, 1980). Uterine responses to salbutamol were unaffected by either prior glibenclamide treatment or by glibenclamide infusion after salbutamol inhibition of uterine contractions had been established, demonstrating that cyclic AMP-mediated inhibition is not prevented by glibenclamide. In contrast, glibenclamide produced significant reduction (5.5 fold) in uterine sensitivity to cromakalim. The parallel rightward shift in the dose-response curve to cromakalim by glibenclamide is consistent with the competitive-like antagonism of cromakalim observed in uterine tissue *in vitro* (Piper *et al.*, 1990). Glibenclamide was also effective in reversing established uterine inhibition by cromakalim and appears to have stimulated uterine contractions above control values in these animals. Cromakalim has a prolonged duration of inhibition of uterine contractions (Downing *et al.*, 1989). At 5 h after the control high dose of cromakalim (0.25 mg kg^{-1}), there may have been some residual effect of the drug. Glibenclamide treatment alone had no stimulatory effect on uterine contractions, which also supports the view that its antagonism of cromakalim is not by an indirect mechanism, or functional antagonism. The lack of effect of glibenclamide alone on uterine contractions is also in accord with *in vitro* observations (Piper *et al.*,1990).

Glibenclamide antagonism of relaxin

Glibenclamide treatment significantly reduced uterine sensitivity to relaxin. In contrast to the parallel shift in the dose-response curve to cromakalim by glibenclamide, the slope of the post-glibenclamide dose-response curve to relaxin was markedly reduced compared with the pretreatment dose-response curve. An explanation of the change in slope of the dose-response curve is that the antagonism of relaxin by glibenclamide could be by an indirect mechanism. Glibenclamide is known to induce release of insulin by blocking ATP-dependent K^+-channels in pancreatic β-cells (Geisen, 1988; Sturgess *et al.*, 1988) and the dose of glibenclamide used in the present study is in excess of those required for its hypoglycaemic action (Geisen, 1988; Quast & Cook, 1989). Insulin is purported to have a similar tertiary structure to relaxin (Dodson *et al.*, 1982), although there is less than 20% amino acid sequence homology between the two polypeptide hormones. Insulin, released by glibenclamide, could act as an indirect antagonist of relaxin. However, no antagonism of porcine relaxin by porcine insulin was observed in uterine tissue *in vitro* (Figure 6) suggesting that insulin is not involved in glibenclamide antagonism. Other indirect mechanism(s) may operate to produce glibenclamide antagonism of relaxin which could result from an action of glibenclamide unrelated to its ATP-dependent K^+-channel blocking properties.

If glibenclamide is acting as a blocker of ATP-dependent K^+-channels in the uterus *in vivo*, the interaction between glibenclamide and relaxin may be of a non-competitive, allosteric nature similar to that observed with minoxidil sulphate in rat aorta (Newgreen *et al.*, 1990). An additional explanation of the results is that the reduction in slope of the post-glibenclamide dose-response curve (Figure 4) reflects multi-component mechanisms of the action of relaxin. Increase in myometrial cyclic AMP concentrations resulting from relaxin action *in vitro* have been reported (Sanborn *et al.*, 1980), although the increases are short lived. It is possible that cyclic AMP-mediated events predominate during early stages of relaxin inhibition, but K^+-channel opening may be important for maintenance of uterine quiescence. In this way, low doses of relaxin, with a short duration of effect, would be relatively little affected by glibenclamide due to prominence of cyclic AMP-mediated inhibition. Higher doses of relaxin, with more prolonged duration of action and greater involvement of K^+-channel opening, would be more affected by glibenclamide. Despite the antagonism of both cromakalim and relaxin by glibenclamide, cross tolerance between them was not observed (Downing & Hollingsworth, 1990b). The latter observation suggests that the site of tolerance development is situated prior to a possible common mechanism in the sequence of events leading to smooth muscle relaxation.

Apamin and relaxin

Apamin, a selective blocker of low conductance calcium activated K^+-channels (Weir & Weston, 1986; Cook & Hof, 1988), had no effect on relaxin-induced inhibition of uterine contractions. Similarly, apamin was found to be ineffective against cardiovascular effects of cromakalim *in vivo* but potentiated angiotensin (Cook & Hof, 1988). It is unlikely, therefore, that low conductance calcium-activated K^+-channels are involved in the action of relaxin in the uterus.

Relaxin and signal transduction

In addition to an increase in myometrial cyclic AMP concentrations and activation of cyclic AMP-dependent protein kinase, relaxin has also been shown to promote calcium efflux (Rao & Sanborn, 1986; Ginsberg *et al.*, 1988; Anwer *et al.*, 1989) and produce inactivation of myosin light chain kinase (Nishikori *et al.*, 1983). The relative importance of cyclic AMP or K^+-channel opening in mediating these later events in smooth muscle relaxation is not known. K^+-channel opening is thought to induce smooth muscle relaxation by hyperpolarization of the cell membranes to a degree which prevents opening of calcium channels and influx of calcium ions necessary for contractile activity as well as modifying intracellular calcium ion homeostasis more directly (Edwards & Weston, 1990).

In conclusion, the lack of antagonism of salbutamol compared with the non-competitive-like antagonism of relaxin by glibenclamide suggests that increase in intracellular cyclic AMP concentrations is not the predominant mechanism by which relaxin inhibits uterine contractions. The competitive-like antagonism of cromakalim compared with the non-competitive like antagonism of relaxin may suggest that the two relaxants share, in part, a common mechanism of action and that additional mechanism(s) may be involved in the inhibitory action of relaxin.

We thank Action Research for financial support, Dr T.C. Hamilton (SmithKline Beecham) for cromakalim, Hoechst for glibenclamide and J. Dawkins, Congerstone, for the supply of pregnant sow ovaries.

References

ANWER, K., HOVINGTON, J.A. & SANBORN, B.M. (1989). Antagonism of contractants and relaxants at the level of intracellular calcium and phosphoinositide turnover in the rat uterus. *Endocrinology*, **124**, 2995–3002.

BRADSHAW, J.M.C., DOWNING, S.J., MOFFAT, A., HINTON, J.C. & PORTER, D.G. (1981). Demonstration of some of the physiological properties of rat relaxin. *J. Reprod. Fert.*, **63**, 145–153.

BUCKINGHAM, R.E., HAMILTON, T.C., HOWLETT, D.R., MOOTOO, S. & WILSON, C. (1989). Inhibition by glibenclamide of the vasorelaxant action of cromakalim in the rat. *Br. J. Pharmacol.*, **97**, 57–64.

CAVERO, I., MONDOT, S. & MESTRE, M. (1989). Vasorelaxant effects of cromakalim in rats are mediated by glibenclamide-sensitive potassium channels. *J. Pharmacol. Exp. Ther.*, **248**, 1261–1268.

CHEAH, S.H. & SHERWOOD, O.D. (1980). Target tissues for relaxin in the rat – tissue distribution of injected ^{125}I-labeled relaxin and tissue changes in adenosine 3′, 5′-monophosphate levels after *in vitro* relaxin incubation. *Endocrinology*, **106**, 1203–1209.

CHEAH, S.H. & SHERWOOD, O.D. (1981). Effects of relaxin on *in vivo* uterine contractions in conscious and unrestrained estrogen-treated and steroid-untreated ovariectomised rats. *Endocrinology*, **109**, 2076–2083.

COOK, N.S. & HOF, R.B. (1988). Cardiovascular effects of apamin and BRL34915 in rats and rabbits. *Br. J. Pharmacol.*, **93**, 121–131.

DODSON, G.G., ELIOPOULOS, E.E., ISAACS, N.W., McCALL, M.J., NIALL, H.D. & NORTH, A.C.T. (1982). Rat relaxin: Insulin-like fold predicts a likely receptor binding region. *Int. Biol. Macromol.*, **4**, 399–405.

DOWNING, S.J. & HOLLINGSWORTH, M. (1990a). Antagonism of relaxin by glibenclamide in the uterus of the rat *in vivo*. *Br. J. Pharmacol.*, **99**, 10P.

DOWNING, S.J. & HOLLINGSWORTH, M. (1990b). Uterine tolerance to relaxants *in vivo*: lack of cross tolerance between relaxin, salbutamol and cromakalim. *Br. J. Pharmacol.*, **100**, 488P.

DOWNING, S.J., MILLER, M. & HOLLINGSWORTH, M. (1989). Tolerance to cromakalim in the rat uterus *in vivo*. *Br. J. Pharmacol.*, **96**, 732–738.

DOWNING, S.J., & SHERWOOD, O.D. (1985a). The physiological role of relaxin in the pregnant rat. I. The influence of relaxin on parturition. *Endocrinology*, **116**, 1200–1205.

DOWNING, S.J. & SHERWOOD, O.D. (1985b). The physiological role of relaxin in the pregnant rat: II. The influence of relaxin on uterine contractile activity. *Endocrinology*, **116**, 1206–1214.

EDWARDS, G. & WESTON, A.H. (1990). Potassium channel openers and vascular smooth muscle relaxation. *Pharmacol. Ther.*, **48**, 237–258.

ESCANDE, D., THURINGER, D., LE GUERN, S., COURTEIX, J., LAVILLE, M. & CAVERO, I. (1989). Potassium channel openers act through an activation of ATP-sensitive K^+-channels in guinea-pig cardiac myocytes. *Pflügers Arch.*, **414**, 669–675.

GEISEN, K. (1988). Special pharmacology of the new sulfonylurea glimepiride. *Arzneim. Forsch.*, **38**, 1120–1130.

GINSBERG, F.W., ROSENBERG, C.R., SCHWARTZ, M., COLON, J.M. & GOLDSMITH, L.T. (1988). The effect of relaxin on calcium fluxes in the rat uterus. *Am. J. Obstet. Gynecol.*, **159**, 1395–1401.

GRANGER, S.E., HOLLINGSWORTH, M. & WESTON, A.H. (1985). A comparison of several calcium antagonists on uterine, vascular and cardiac muscles from the rat. *Br. J. Pharmacol.*, **85**, 255–262.

JOHANSSON, S.R.M. & ANDERSSON, R.G.G. (1980). Effects of β-adrenergic agonists on rat uterine motility and cAMP levels in vivo. *Acta Pharmacol. Toxicol.*, **47**, 5–10.

JUDSON, D.G., PAY, S. & BHOOLA, K.D. (1980). Modulation of cyclic AMP in isolated rat uterine tissue slices by porcine relaxin. *J. Endocrinol.*, **87**, 153–159.

KEMP, B.E. & NIALL, H.D. (1981). Effect of relaxin on the activation of cAMP-dependent protein kinase in rat uterus. In *Relaxin.* ed. Bryant-Greenwood, G.D., Niall, H.D. & Greenwood, F.G. pp. 273–275. New York: Elsevier/North Holland.

NARA, B.S., WELK, F.A., RUTHERFORD, J.E., SHERWOOD, O.D. & FIRST, N.L. (1982). Effect of relaxin on parturition and frequency of live births in pigs. *J. Reprod. Fert.*, **66**, 359–365.

NEWGREEN, D.T., BRAY, K.M., McHARG, A.D., WESTON, A.H., DUTY, S., BROWN, B.S., KAY, P.B., EDWARDS, G., LONGMORE, J. & SOUTHERTON, J.S. (1990). The action of diazoxide and minoxidil sulphate on rat blood vessels: a comparison with cromakalim. *Br. J. Pharmacol.*, **100**, 605–613.

NISHIKORI, K., WEISBRODT, N.W., SHERWOOD, O.D. & SANBORN, B.M. (1983). Effects of relaxin on rat uterine myosin light chain kinase activity and myosin chain light phosphorylation. *J. Biol. Chem.*, **258**, 2468–2474.

PIPER, I., MINSHALL, E., DOWNING, S.J., HOLLINGSWORTH, M. & SADRAELI, H. (1990). Effects of several potassium channel openers and glibenclamide on the uterus of the rat. *Br. J. Pharmacol.*, **101**, 901–907.

PORTER, D.G., DOWNING, S.J. & BRADSHAW, J.M.C. (1979). Relaxin inhibits spontaneous and prostaglandin-driven myometrial activity in anaesthetised rats. *J. Endocrinol.*, **83**, 183–192.

QUAST, U. & COOK, N.S. (1989). *In vitro* and *in vivo* comparison of two K^+channel openers, diazoxide and cromakalim, and their inhibition by glibenclamide. *J. Pharmacol. Exp. Ther.*, **250**, 261–271.

RAO, M.R. & SANBORN, B.M. (1986). Relaxin increases calcium efflux from rat myometrial cells in culture. *Endocrinology*, **119**, 435–437.

SANBORN, B.M., KUO, H.S., WEISBRODT, N.W. & SHERWOOD, O.D. (1980). The interaction of relaxin with the rat uterus. I. Effect on cyclic nucleotide levels and spontaneous contractile activity. *Endocrinology*, **106**, 1210–1215.

SHERWOOD, O.D. & O'BYRNE, E.M. (1974). Purification and characterization of porcine relaxin. *Arch. Biochem. Biophys.*, **160**, 185–196.

ST-LOUIS, J. (1981). Relaxin inhibition of KCl-induced uterine contractions *in vitro*: an alternative bioassay. *Can. J. Physiol. Pharmacol.*, **59**, 507–512.

STANDEN, N.B., QUAYLE, J.M., DAVIES, N.W., BRAYDEN, J.E., HUANG, Y. & NELSON, M.T. (1989). Hyperpolarizing vasodilators activate ATP-sensitive K^+ channels in arterial smooth muscle. *Science*, **245**, 177–180.

STURGESS, N.C., KOZLOWSKI, R.Z., CARRINGTON, C.A., HALES, C.N. & ASHFORD, M.L.J. (1988). Effects of sulphonylureas and diazoxide on insulin secretion and nucleotide-sensitive channels in an insulin-secreting cell line. *Br. J. Pharmacol.*, **95**, 83–94.

WEIR, S.W. & WESTON, A.H. (1986). Effect of apamin on responses to BRL34915, nicorandil and other relaxants in the guinea-pig taenia coli. *Br. J. Pharmacol.*, **88**, 113–120.

(Received April 12, 1991
Revised May 4, 1991
Accepted May 14, 1991)

Br. J. Pharmacol. (1991), **104**, 77–84

Cross tachyphylaxis to endothelin isopeptide-induced hypotension: a phenomenon not seen with proendothelin

Anne-Charlotte Le Monnier de Gouville & [1]Icilio Cavero

Rhône-Poulenc Rorer, Centre de Recherche de Vitry-Alfortville, 13 quai Jules Guesde, BP 14, 94403 Vitry sur Seine Cedex, France

1 In anaesthetized rats, an i.v. injection of endothelin-1 (0.25 nmol kg^{-1}) evoked a rapidly appearing (maximal effect within 15 s) and short lasting (3 min) fall in blood pressure with tachyphylaxis occurring so that it was reduced by 50% by the last of 4 injections given 10 min apart. This property was also shared by endothelin-2, endothelin-3 and vasoactive intestinal contractor (VIC).

2 Cross tachyphylaxis between the isopeptides occurred. However, under the same experimental conditions the hypotensive effects of acetylcholine, adenosine, atrial natriuretic peptide (ANP) and substance P were reproducible and not modified in animals in which endothelin-1 no longer lowered blood pressure. Thus, the mechanism of the hypotensive action of endothelin peptides is different from that of acetylcholine, adenosine, ANP, and substance P.

3 In pithed rats, endothelin-1 (0.25 nmol kg^{-1}) and its precursor human proendothelin (h-proendothelin) (0.5 nmol kg^{-1}) induced pressor responses of a similar magnitude, which for h-proendothelin (up to 5.0 nmol kg^{-1}) were not preceded by a hypotensive phase. The pressor effects of endothelin-1, like those of vasopressin, were reproducible upon repeated i.v. injections.

4 Rats given a 10 min infusion (0.1 nmol kg^{-1} min^{-1}) of endothelin-1 showed no hypotensive response to an i.v. bolus injection of endothelin-1, whereas animals pretreated with an equipressor infusion of h-proendothelin did not develop tachyphylaxis to endothelin-1.

5 In pithed rats, endothelin-1, at a dose inducing the same maximal increase in blood pressure as h-proendothelin, was approximately 3 fold more potent as a mesenteric vasoconstrictor than h-proendothelin. These results suggest that if h-proendothelin is processed to endothelin-1, this transformation is not uniform throughout the vascular system.

6 The pressor response of h-proendothelin in pithed rats was dose-dependently inhibited by phosphoramidon (2.5–5.0 mg kg^{-1}). However, this compound did not antagonize the effects of endothelin-1 (0.25 nmol kg^{-1}) or those of h-proendothelin (0.5 nmol kg^{-1}) once developed.

7 Although some of these results may suggest that h-proendothelin does not undergo *in vivo* conversion to endothelin-1, the results obtained with phosphoramidon suggest that h-proendothelin is converted into endothelin-1. Therefore, the amount of endothelin-1 so produced can elicit pressor responses or regional vasoconstriction, but is insufficient to lower blood pressure and to inhibit endothelin-1-induced hypotension.

8 The mechanism of the tachyphylaxis does not appear to be depletion of endothelium-derived relaxing factor, since agents coupled to the latter endogenous vasorelaxant substance do not exhibit cross-tachyphylaxis with endothelin-1. It is suggested that upon repeated or sustained exposure to endothelin-1, the endothelin-1 receptors mediating hypotension decrease in number and/or undergo conformational changes making them refractory to activation. Alternatively, the depletion of a blood-borne agent responsible for the hypotension could be involved.

Keywords: Hypotension; endothelin; tachyphylaxis; proendothelin; systemic pressor responses; phosphoramidon; regional blood flow.

Introduction

Endothelin-1 initially isolated by Yanagisawa *et al.* (1988) from the supernatant of cultured porcine aortic endothelial cells is a 21-amino acid peptide with two intrachain disulphide bonds. Endothelin-1 is synthesized as a 203-amino acid prepropeptide which is then cleaved by an endopeptidase to proendothelin, generally called big-endothelin. The latter peptide consists of 38 and 39 amino acids for human (h-proendothelin) and porcine (p-proendothelin) proendothelin-1 respectively and is then processed into endothelin-1 by an 'endothelin converting enzyme' which is present in endothelial cells (Ikegawa *et al.*, 1990; Matsumura *et al.*, 1990a, b; Ohnaka *et al.*, 1990) and in vascular smooth muscle cells (Hioki *et al.*, 1991).

Since the discovery of endothelin-1, other isopeptides called endothelin-2, endothelin-3 and vasoactive intestinal contractor (VIC) of similar structure have been identified in mammalian species (Inoue *et al.*, 1989; Saida *et al.*, 1989). They differ from endothelin-1 by 2, 6 and 3 amino acids respectively.

The i.v. administration of endothelin-1 or its isopeptides, to rats, evokes a rapidly appearing and short lasting fall in blood pressure, followed by a moderate pressor effect. In contrast, p-proendothelin produces only a monophasic pressor response (Kashiwabara *et al.*, 1989). Additionally, when a series of i.v. injections of endothelin-1 was given to the same animal, the initial hypotensive effect progressively faded and only a pressor response remained (Le Monnier de Gouville *et al.*, 1990).

The first objective of this study was to assess whether tachyphylaxis to endothelin-1 extends to endothelin isopeptides. Furthermore, attempts were made to determine the mechanism of the tachyphylaxis. Finally, the cardiovascular profile of endothelin-1 and h-proendothelin were compared in order to investigate whether or not the pharmacological properties of h-proendothelin could be entirely accounted for by its transformation to endothelin-1.

[1] Author for correspondence.

Methods

Anaesthetized rats

Male normotensive rats (Crl:SD CD, Charles River Laboratory, 76410 St Aubin-les-Elbeuf) weighing 240–270 g were anaesthetized with sodium pentobarbitone (60 mg kg^{-1}, i.p.) and artificially ventilated with room air (1 ml 100 g^{-1} of body weight, 60 strokes min^{-1}) with a rodent ventilator, (Biological Research Apparatus, Comerio, VA, Italy). The left carotid artery and femoral veins were cannulated for blood pressure measurement and i.v. injections respectively. After an equilibration time of 15 min, treatments were begun. Heart rate was measured with a cardiotachometer (triggered by pressure pulses) and blood pressure recorded on a polygraph (Linearcorder Mk VII, Graphtec Corp., Tokyo, Japan).

Series 1 Four consecutive i.v. bolus injections of either endothelin-1 (0.25 nmol kg^{-1}), endothelin-2 (0.5 nmol kg^{-1}), endothelin-3 (0.5 nmol kg^{-1}) or VIC (0.5 nmol kg^{-1}) were administered to 4 separate groups of 5 to 10 animals. A 10 min interval was left between two consecutive injections of peptide and the last one was followed by an i.v. dose of either acetylcholine (0.5 μg kg^{-1}) or adenosine (200 μg kg^{-1}).

Series 2 In 6 separate groups of 4 to 7 rats, 4 i.v. boluses of either ANP (30 μg kg^{-1}), adenosine (200 μg kg^{-1}), or substance P (1 μg kg^{-1}) were administered, followed by an i.v. bolus injection of endothelin-1 (0.25 nmol kg^{-1}). In 2 other groups of 4–6 rats, an i.v. bolus of ANP or substance P was preceded by 4 successive boluses of endothelin-1 (0.25 nmol kg^{-1}, i.v.), as described in Series 1.

Series 3 The hypotensive effects of 4 consecutive i.v. bolus injections of endothelin-1 (0.25 nmol kg^{-1}) were studied in a group of 5 animals which were subjected to nephrectomy the day before the experimental procedure. During a brief period (10 min) of ether anaesthesia, laparotomy was performed, the renal arteries and veins were ligated and then the kidneys were removed.

Series 4 In 12 groups of 4–6 animals, a 10 min i.v. infusion (0.1 nmol kg^{-1} min^{-1}) of either endothelin-1, endothelin-2, endothelin-3, VIC or h-proendothelin was given and 8, 30 or 120 min later an i.v. bolus injection of endothelin-1 (0.25 nmol kg^{-1}) was administered. In other sets of experiments, an i.v. bolus injection of each peptide (0.25 nmol kg^{-1}) was given 8 min after the start of an i.v. infusion of endothelin-1, endothelin-2, endothelin-3 or VIC (0.1 nmol kg^{-1} min^{-1}). In each group of 4–6 animals only an infusion followed by a bolus of endothelin peptides was studied.

Pithed rats

Male normotensive rats (Crl:SD CD, Charles River Laboratory) were briefly anaesthetized with ether. After rapid cannulation of the trachea for artificial ventilation they were pithed by inserting a stainless steel rod into the spinal canal via the right orbit. The right carotid artery was ligated and the vagi cut. The left carotid artery and the femoral vein(s) were catheterized for blood pressure measurements and drug administrations respectively.

Series 1 Three consecutive i.v. bolus injections of either endothelin-1 (0.25 nmol kg^{-1}) or vasopressin (20 mi u kg^{-1}) were given to groups of 5 to 6 rats. Blood pressure was allowed to recover to initial values before each subsequent injection.

Series 2 A 0.5 nmol kg^{-1} i.v. bolus dose of h-proendothelin and a 0.25 nmol kg^{-1}, i.v. bolus dose of endothelin-1 (which give similar maximal increases in systemic blood pressure) were chosen to study the effects of these peptides on regional blood flows (n = 6–7). In laparotomized rats, Doppler blood flow velocity probes were placed on the aorta at its exit from the diaphragm and on the renal artery. In order to minimize the surgical trauma mesenteric and hindquarter (measured from the terminal aorta) blood flows were recorded in a separate group of rats. Each flow probe was connected to a pulsed Doppler preamplifier (Crystal Biotech Inc., Holliston, MA). Changes in blood flow velocity were taken as an estimate of changes in cardiac output since they have been shown to be similar to values measured with an electromagnetic flow probe (Richer *et al.*, 1987) and thus they are unlikely to undergo the 'aliasing phenomenon' recently described as a source of error with Doppler flow probes placed on the ascending aorta of conscious rats (Gardiner *et al.*, 1990b). These parameters were used to calculate regional vascular resistances (mmHg kHz^{-1}) by dividing mean systemic blood pressure (mmHg) by Doppler shifts (kHz). In 12 separate groups of animals, the blood pressure effects of endothelin-1 and h-proendothelin given as i.v. bolus injections (0.25 to 1.0 nmol kg^{-1}) or as 10 min infusions (0.01 to 0.1 nmol kg^{-1} min^{-1}) were compared (n = 4–7 per group).

Series 3 A 0.5 nmol kg^{-1} i.v. bolus of h-proendothelin or 0.25 nmol kg^{-1} of endothelin-1 was administered in rats (n = 5–7) pretreated 5 min earlier with phosphoramidon (2.5 or 5.0 mg kg^{-1} given over 5 min) or saline (0.25 ml kg^{-1}). In a separate group of 5 rats, phosphoramidon was injected (5 mg kg^{-1}, i.v. over 5 min) once the pressor response to proendothelin (0.5 nmol kg^{-1}, i.v.) had reached a steady state.

Series 4 Four consecutive i.v. bolus injections of either endothelin-1 (0.25 nmol kg^{-1}), endothelin-2 (0.5 nmol kg^{-1}), endothelin-3 (0.5 nmol kg^{-1}) or VIC (0.5 nmol kg^{-1}) were administered to 4 independent groups of 5–6 animals in which the low blood pressure (due to the pithing procedure) was elevated by an i.v. infusion of vasopressin (6 mi u kg^{-1} min^{-1}) to levels similar to those present in intact rats. A 10 min interval was observed between two consecutive injections to allow the changed blood pressure to recover to control values.

Series 5 The low blood pressure value of pithed rats was elevated by 20, 30 and 40 mmHg by adjusting the infusion rates of i.v. vasopressin, h-proendothelin or endothelin-1. When a steady-state response was attained, an i.v. bolus injection of either endothelin-1 (0.25 nmol kg^{-1}), adenosine (200 μg kg^{-1}) or acetylcholine (0.5 μg kg^{-1}) was studied in separate groups of 5–7 animals.

Analysis of the results

Results are given as means ± s.e. mean. The significance ($P < 0.05$) of the results was assessed by paired or unpaired Student's t test. The s.e. mean of some of the points in the figures were too small to be represented graphically.

Drugs

The following drugs were used: acetylcholine bromide (Sigma Chemical Co, St Louis, MO, USA), adenosine (Rhone-Poulenc Rorer, Vitry-sur-Seine, France), rat ANP (Peninsula, St Helens, U.K.), phosphoramidon (Sigma Chemical Co), substance P (Sigma Chemical Co), vasopressin acetate (Sigma Chemical Co), sodium pentobarbitone (Sanofi Santé Animale, St Jean de la Rulelle, France), endothelin-1, endothelin-2, endothelin-3, VIC and h-proendothelin (Novabiochem, Laufelfingen, Switzerland). Peptides were dissolved in standard saline containing 0.5% bovine serum albumin (Sigma Chemical Co) which in the case of VIC was mixed with acetic acid 0.1% v/v. The solution obtained was dispensed into small vials of 100 μl (2 to 6 μg per vial) and stored at −20°C. At the end of the experiment any remaining solution was discarded.

Results

Anaesthetized rats

Effects of repeated i.v. bolus injections of endothelin and other depressor agents. In anaesthetized rats, endothelin-1 given as an i.v. bolus injection (0.25 nmol kg^{-1}) evoked a rapidly appearing decrease in blood pressure which attained a maximum within the initial 15 s and lasted approximately 3 min. However, the hypotensive effect waned progressively upon repeated administration of endothelin-1 and was reduced by 50% at the fourth injection (Figure 1). A similar pattern was found for the hypotension induced by endothelin-2, endothelin-3 and VIC. In contrast, tachyphylaxis did not occur with i.v. adenosine (200 μg kg^{-1}), acetylcholine (0.5 μg kg^{-1}), or substance P (1.0 μg kg^{-1}) (Table 1).

The maximal hypotensive response to endothelin-1, determined under control conditions (-49 ± 3 mmHg, $n = 10$), was not altered in animals which had received 4 successive i.v. bolus doses of acetylcholine, adenosine, ANP, or substance P. Indeed, the values of these responses were -50 ± 2 ($n = 5$), -51 ± 3 ($n = 5$), -45 ± 4 ($n = 8$) and -56 ± 4 mmHg ($n = 4$), respectively. Furthermore, after 4 successive i.v. bolus doses of endothelin-1 (0.25 nmol kg^{-1}), the hypotensive effects of adenosine, acetylcholine, ANP, and substance P were not changed significantly.

In nephrectomized rats, the hypotensive effects of repeated doses of endothelin-1 showed tachyphylaxis as in intact animals. In the latter preparation, the blood pressure falls for the first and fourth dose of endothelin-1 were -65 ± 4, and -30 ± 4 mmHg ($n = 4$), whereas the corresponding values for nephrectomized rats were -57 ± 3 and -33 ± 2 mmHg ($n = 5$).

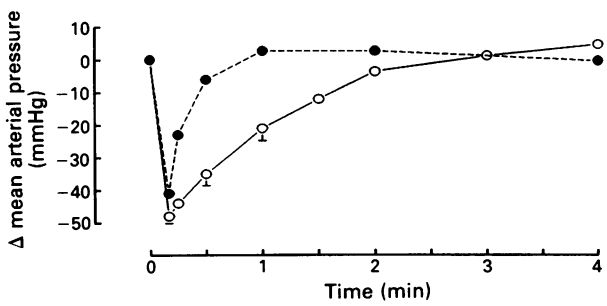

Figure 1 Time-course of the mean carotid artery blood pressure decreases (Δ MAPa) produced by i.v. endothelin-1 (0.25 nmol kg^{-1}; ○) and acetylcholine (0.5 μg kg^{-1}, i.v.; ●) in anaesthetized rats. Initial values for mean carotid artery blood pressures were 123 ± 4 mmHg ($n = 5$) and 133 ± 4 mmHg ($n = 5$) respectively.

Hypotensive responses to endothelin-1 after an infusion of endothelin isopeptides or h-proendothelin Ten min i.v. infusions of endothelin-1, endothelin-2, endothelin-3 or VIC (0.1 nmol kg^{-1} min^{-1}) produced initial falls in blood pressure which attained their maxima (-13 ± 3, $n = 5$; -1 ± 2, $n = 17$; -20 ± 3, $n = 19$ and -8 ± 3 mmHg, $n = 18$, respectively) within the first 3 min of the onset of the infusion. Thereafter, this effect disappeared and was followed by a moderate pressor response which reached a maximum towards the end of the infusion of endothelin-1, endothelin-2, endothelin-3 or VIC (13 ± 2, 12 ± 3, 7 ± 2 and 9 ± 2 mmHg, respectively).

An i.v. bolus dose of endothelin-1 (0.25 nmol kg^{-1}) injected 8 min after starting an infusion of saline evoked a short lasting hypotension (maximum -50 ± 1 mmHg, $n = 17$). In animals ($n = 5$) infused with endothelin-1 (0.1 n mol kg^{-1} min^{-1}, i.v. over 8 min) this effect was entirely absent, whereas in rats infused with the same molar dose of endothelin-2, endothelin-3 or VIC, it was reduced by 57 ± 6 ($n = 5$), 70 ± 6 ($n = 5$) and $67 \pm 5\%$ ($n = 4$) respectively. When studied 120 min after the end of the infusion of endothelin-1 ($n = 5$), endothelin-2 ($n = 5$) or VIC ($n = 6$), the maximal hypotensive responses to endothelin-1 recovered to values similar to those measured in matched control animals ($n = 21$). In contrast, in the group pretreated with endothelin-3 ($n = 10$), the response to endothelin-1 was still inhibited by 40% (Figure 2).

In rats given an 8 min i.v. infusion (0.1 nmol kg^{-1} min^{-1}) of either endothelin-2, endothelin-3 or VIC, the hypotensive effects of 0.25 nmol kg^{-1} i.v. of endothelin-1, endothelin-2, endothelin-3 or VIC were inhibited. By contrast, the responses to acetylcholine (0.5 μg kg^{-1}, i.v.) remained unchanged (Table 2).

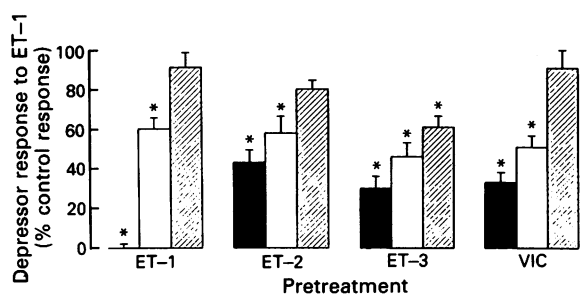

Figure 2 Hypotensive responses to an i.v. bolus injection of endothelin-1 (0.25 nmol kg^{-1}) injected 8 (solid columns), 30 (open columns) or 120 (hatched columns) min after starting a 10 min i.v. infusion (pretreatment) of endothelin-1, endothelin-2, endothelin-3 or VIC (0.1 nmol kg^{-1} min^{-1}, i.v.) in anaesthetized rats ($n = 5$–6 per group). The results are expressed as % of control response obtained in matched groups of animals pretreated with saline. Each group of rats received a single i.v. bolus dose of endothelin-1. *Significant difference ($P < 0.05$, paired t test) from control values (-50 ± 1 mmHg, $n = 17$; -47 ± 2 mmHg, $n = 13$; -44 ± 2 mmHg, $n = 22$ at 8, 30 and 120 min respectively).

Table 1 Maximal falls in mean carotid artery blood pressure induced by 4 repeated (10 min apart) i.v. bolus injections of endothelin-1 (0.25 nmol kg^{-1}), endothelin-2 (0.5 nmol kg^{-1}), endothelin-3 (0.5 nmol kg^{-1}), vasoactive intestinal contractor (VIC, 0.5 nmol kg^{-1}), acetylcholine (ACh 0.5 μg kg^{-1}), adenosine (200 μg kg^{-1}), atrial natriuretic peptide ANP (30 μg kg^{-1}) and substance P (1 μg kg^{-1}) in anaesthetized rats

		Maximum decrease in mean arterial pressure (mmHg)			
		Injection number			
Compound	n	1	2	3	4
Endothelin-1	10	-49 ± 3	-45 ± 2	-30 ± 2*	-23 ± 1*
Endothelin-2	5	-44 ± 1	-32 ± 2*	-17 ± 3*	-10 ± 4*
Endothelin-3	5	-45 ± 3	-25 ± 1*	-7 ± 1*	$+12 \pm 1$*
VIC	6	-57 ± 3	-37 ± 3*	-27 ± 3*	-22 ± 4*
ACh	5	-41 ± 1	-44 ± 2	-46 ± 2	-44 ± 1
Adenosine	5	-44 ± 4	-39 ± 1	-42 ± 2	-41 ± 3
ANP	8	-34 ± 3	-30 ± 4	-30 ± 5	-28 ± 5
Substance P	4	-39 ± 2	-40 ± 4	-44 ± 5	-44 ± 3

* Response is significantly decreased ($P < 0.05$: paired t test) when compared to that produced by the first injection.

Table 2 Maximal falls in mean carotid artery artery blood pressure induced by i.v. bolus injections of 0.25 nmol kg^{-1} of endothelin-1 (ET-1), endothelin-2 (ET-2), endothelin-3 (ET-3), vasoactive intestinal contractor (VIC) and acetylcholine (0.5 μg kg^{-1}), given 8 min after starting a 10 min i.v. infusion (pretreatment) of either saline, endothelin-1, endothelin-2, endothelin-3, VIC or h-proendothelin (0.1 nmol kg^{-1} min^{-1})

	Maximal change in mean arterial pressure (mmHg) *induced by an i.v. bolus of*				
Pretreatment	*ET-1*	*ET-2*	*ET-3*	*VIC*	*ACh*
Saline	−50 ± 1	−61 ± 1	−58 ± 3	−61 ± 1	−53 ± 3
Endothelin-1	1 ± 3*	−9 ± 3*	−10 ± 2*	−11 ± 3*	−50 ± 4
Endothelin-2	−21 ± 3*	−17 ± 3*	−10 ± 4*	−5 ± 2*	−47 ± 2
Endothelin-3	−15 ± 6*	−14 ± 2*	−21 ± 4*	−14 ± 3*	−52 ± 2
VIC	−16 ± 3*	−16 ± 3*	−17 ± 3*	−15 ± 1*	−52 ± 3
h-proendothelin	−57 ± 3	−48 ± 2	−62 ± 3	−54 ± 4	−53 ± 2

* Significant difference ($P < 0.05$: paired t test) from the response obtained after an infusion of saline.

The infusion of h-proendothelin (0.1 nmol kg^{-1} min^{-1} over 10 min) evoked a small monophasic blood pressure increase (16 ± 4 mmHg, $n = 6$) which reached a plateau within 7 min. In this preparation, the hypotensive response produced by an i.v. bolus injection of one of the endothelin peptide was not changed when studied 8 min after starting the infusion of h-proendothelin (Figure 3).

Pithed rats

Pressor effects of repeated i.v. bolus injections of endothelin-1 and vasopressin In pithed rats ($n = 6$), endothelin-1 (0.25 nmol kg^{-1}) evoked a pressor response the magnitude of which increased significantly ($P < 0.01$: paired t test) with repeated injections. Under the same experimental conditions, the pressor responses to repeated i.v. bolus doses of vasopressin (20 mi u kg^{-1}) ($n = 5$) also showed a slight enhancement (Figure 4).

Haemodynamic effects of h-proendothelin In pithed rats, i.v. bolus injections of *h*-proendothelin (0.25, 0.5 and 1.0 nmol kg^{-1}) evoked slowly appearing, dose-dependent monophasic pressor responses which attained their maxima (13 ± 3, $n = 4$; 32 ± 5, $n = 6$ and 63 ± 5 mmHg, $n = 6$, respectively) 7 to 15 min after administration. In contrast, with endothelin-1 (0.25 nmol kg^{-1}) the pressor effect (39 ± 3 mmHg, $n = 6$) was preceded by an initial, brief, fall (−10 ± 1 mmHg) in blood pressure. H-proendothelin was slightly less potent (on a molar basis) than endothelin-1. A 0.25 nmol kg^{-1}, i.v. bolus dose of endothelin-1 evoked a rapid increase in mean carotid artery blood pressure which reached a maximum within 2 to 3 min and waned during the subsequent 20 to 50 min. A 0.5 nmol kg^{-1} i.v. bolus dose of h-proendothelin induced an increase in blood pressure which was of slow onset. A plateau lasting for 5 min was reached 10 min after the administration of h-proendothelin, then the response declined slowly (Figure 5).

The pressor effect to endothelin-1 (0.25 nmol kg^{-1}, $n = 7$) was accompanied by an increase in renal blood flow, a decrease in mesenteric blood flow but no significant change in cardiac output or hindquarters blood flow. The corresponding vascular resistances were all increased, with the mesenteric bed being the most affected. An i.v. bolus administration of h-proendothelin (0.5 nmol kg^{-1}, $n = 6$) evoked a slow increase in renal blood flow which reached a maximum (33 ± 6%, $n = 6$) within 15 min and then declined slowly (Figure 5). Cardiac output, hindquarters and mesenteric blood flows were not significantly affected. With the exception of renal vascular resistance, which remained unchanged, there were similar increases for all other calculated vascular resistances. These effects attained a maximum within 15 min and then they decreased slowly.

When given as a 10 min i.v. infusion, h-proendothelin (0.01, 0.03 and 0.1 nmol kg^{-1} min^{-1}) evoked slowly-developing, dose-dependent pressor responses, the maxima of which for the two lowest doses studied were approximately 50% smaller (10 ± 2 mmHg, $n = 5$ and 21 ± 3 mmHg, $n = 5$, $P < 0.05$, t test) than those evoked by the same molar dose of endothelin-1 (18 ± 2 mmHg, $n = 5$; 47 ± 6 mmHg, $n = 4$). However, for the highest dose studied, h-proendothelin and endothelin-1 produced virtually the same maximal response (61 ± 4 mmHg, $n = 6$; 64 ± 3 mmHg $n = 5$, respectively) although the rate of onset appeared to be faster for endothelin-1 than h-proendothelin effects.

Effects of phosphoramidon on the pressor effects of h-proendothelin and endothelin-1 In pithed rats ($n = 12$), phos-

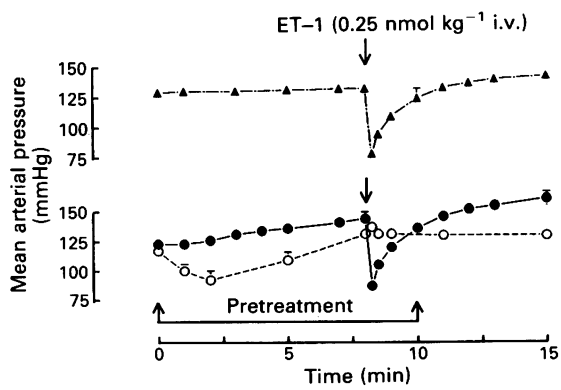

Figure 3 Mean carotid artery blood pressure effects of a 10 min i.v. infusion (pretreatment) of saline (▲) and 0.1 nmol kg^{-1} min^{-1} of either endothelin-1 (ET-1, ○) and h-proendothelin (●) in anaesthetized rats ($n = 6$ per group). The response to an i.v. bolus injection of endothelin-1 (0.25 nmol kg^{-1}) was studied 8 min after starting the infusion of either saline, endothelin-1 or h-proendothelin.

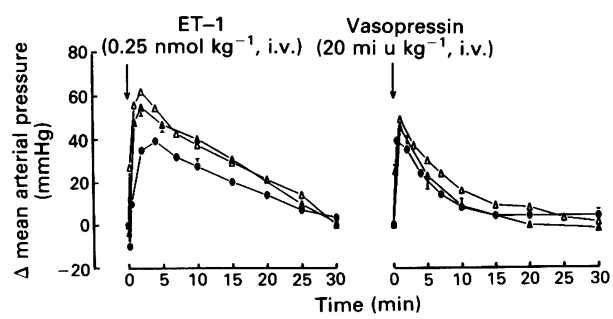

Figure 4 Time course of the changes in mean arterial blood pressure induced by 3 consecutive i.v. bolus injections (●: first, ▲: second and △: third) of endothelin-1 (ET-1, 0.25 nmol kg^{-1}) or vasopressin (20 mi u kg^{-1}) in pithed rats. The initial blood pressure values before each injection of endothelin-1 and vasopressin were 64 ± 3, 68 ± 2, 66 ± 2 mmHg ($n = 6$) and 61 ± 3, 65 ± 3, 66 ± 3 mmHg ($n = 5$) respectively. Note that for the two first injections of endothelin-1 the pressor effects were preceded by a small transient fall in blood pressure.

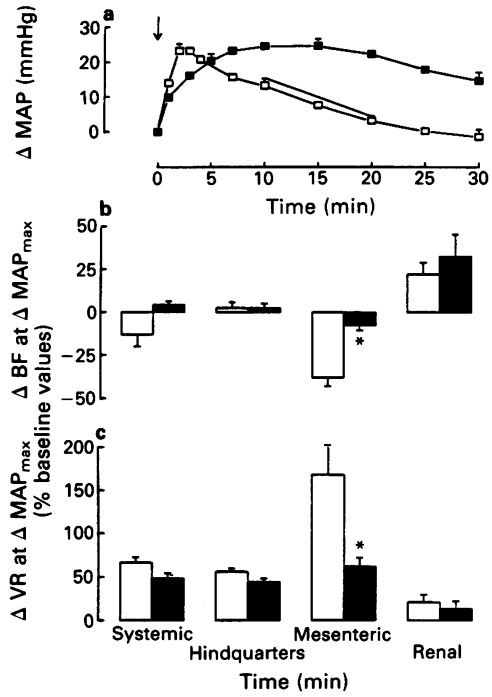

Figure 5 (a) Time courses of the changes in mean carotid artery blood pressure (Δ MAP) induced by an i.v. bolus injection of endothelin-1 (□: 0.25 nmol kg^{-1}) and h-proendothelin (■: 0.5 nmol kg^{-1}) in pithed rats (n = 6–8 per group). (b and c) Changes in cardiac output systemic, hindquarters, mesenteric and renal blood flows (Δ BF) and vascular resistances (Δ VR) at the maximal pressor response (Δ MAP_{max}) to endothelin-1 (3 min) and proendothelin (15 min).
*Significant difference ($P < 0.05$, t test) between endothelin-1 and proendothelin.

phoramidon (2.5 or 5.0 mg kg^{-1} given over 5 min) did not change baseline blood pressure, but inhibited in a dose-dependent manner, the pressor response to h-proendothelin (0.5 nmol kg^{-1}). In contrast, phosphoramidon (5.0 mg kg^{-1}, i.v.) failed to exert this effect when it was administered at the maximum of the pressor effect of h-proendothelin (Figure 6). Similarly, phosphoramidon (5.0 mg kg^{-1}, i.v.). did not affect the pressor effects of endothelin-1 (0.25 nmol kg^{-1}, i.v. bolus).

Hypotensive effects of repeated i.v. bolus injections of endothelin peptides in pitched rats with vasopressin-supported blood pressure In pithed rats, an i.v. infusion of vasopressin produced a sustained increase in blood pressure (121 ± 2 mmHg from 57 ± 1 mm Hg, n = 21). In this vasopressin-supported preparation, i.v. administration of endothelin-1 (0.25 nmol kg^{-1}), endothelin-2 (0.5 nmol kg^{-1}), endothelin-3 (0.5 nmol kg^{-1}) or VIC (0.5 nmol kg^{-1}) produced similar falls in blood pressure (Figure 7). When the same peptides were injected repeatedly, their hypotensive effects waned such that, at the fourth injection endothelin-1, endothelin-3 and VIC produced only pressor responses whereas endothelin-2 still evoked a small decrease in blood pressure (Figure 7).

Effects of endothelin-1 injected after an infusion of endothelin-1 or h-proendothelin In pithed rats given a 10 min i.v. infusion of h-proendothelin (0.1 nmol kg^{-1} min^{-1} i.v.), the response to an i.v. bolus of endothelin-1 (0.25 nmol kg^{-1}) was a decrease in blood pressure of a similar magnitude to that measured in matched control preparations. In contrast, endothelin-1 evoked only a pressor response in rats which were infused with an i.v. dose of endothelin-1 giving the same pressor response as h-proendothelin (Figure 8).

Relationship between pressor responses to endothelin-1 and initial blood pressure levels In pithed rats with blood pressure elevated by an i.v. infusion of either vasopressin or h-proendothelin, the magnitude of the hypotensive responses to endothelin-1 (0.25 nmol kg^{-1}, i.v) was a direct function of the initial blood pressure value. In contrast, this relationship could not be demonstrated for endothelin-1 (0.25 nmol kg^{-1}) when it was studied in pithed rats with blood pressure elevated by an i.v. infusion of endothelin-1 (Figure 9). Interestingly, acetylcholine (0.5 μg kg^{-1}) and adenosine (200 μg kg^{-1}) produced

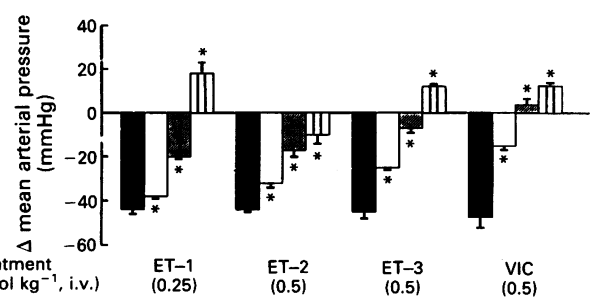

Figure 7 Maximal changes in mean carotid artery blood pressure (Δ MAP_{max}) produced by 4 successive (10 min apart) i.v. bolus doses of endothelin-1 (0.25 nmol kg^{-1}), endothelin-2 (0.5 nmol kg^{-1}), endothelin-3 (0.5 nmol kg^{-1}) and vasoactive intestinal contractor (VIC) (0.5 nmol kg^{-1}) in pithed rats (n = 5–6 per group) with blood pressure supported by an i.v. infusion of vasopressin. Solid column: first; open column: second; hatched column: third and striped column: fourth injection.
*Significant difference ($P < 0.05$, paired t test) from the first injection.

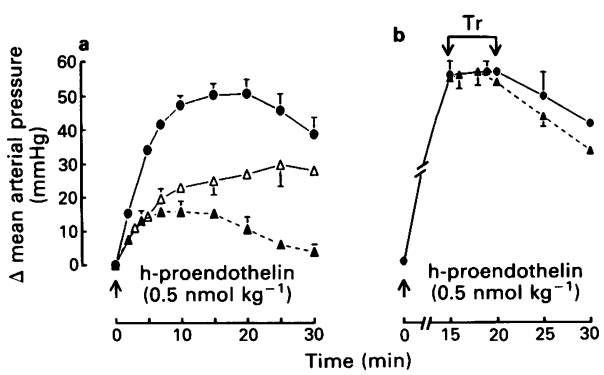

Figure 6 (a) Time course of the change in mean carotid artery blood pressure induced by an i.v. bolus injection of proendothelin (0.5 nmol kg^{-1}) in pithed rats (n = 5–7 per group) pretreated with either saline (●) or phosphoramidon (2.5 (Δ) and 5.0 (▲) mg kg^{-1} i.v. given over 5 min). (b) Effects of a 5 min i.v. infusion (Tr) of phosphoramidon (▲) (5 mg kg^{-1}) or saline (●) on the blood pressure effects of h-proendothelin (0.5 nmol kg^{-1}, i.v) in pithed rats.

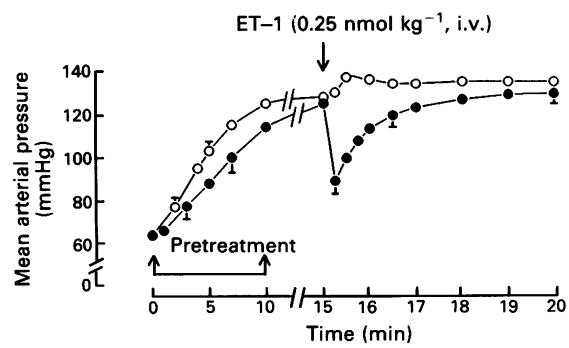

Figure 8 Effects on mean carotid artery blood pressure of an i.v. bolus injection of endothelin-1 (ET-1, 0.25 nmol kg^{-1}) in pithed rats (n = 5–6 per group) which were pretreated 15 min earlier with a 10 min i.v. infusion (0.1 nmol kg^{-1} min^{-1}) of either h-proendothelin (●) or endothelin-1 (○).

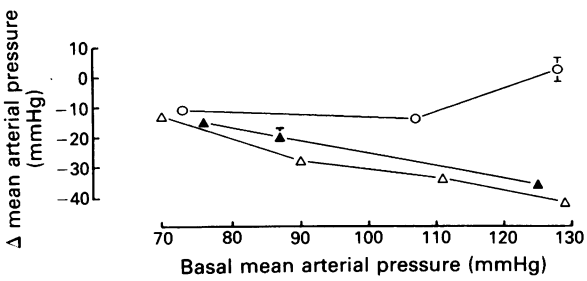

Figure 9 Relationship between the changes in mean carotid artery blood pressure (Δ MAP) produced by an i.v. bolus injection of endothelin-1 (0.25 nmol kg^{-1}) and pre-injection blood pressure values obtained by i.v. infusions of appropriate amounts of either vasopressin (△), h-proendothelin (▲), or endothelin-1 (○), in pithed rats ($n = 6$ for each group). A significant ($P < 0.05$) straight line correlation ($r = 0.96$) exists between the responses to endothelin-1 (0.25 nmol kg^{-1}, i.v. bolus) and basal blood pressure for the rats infused with vasopressin and h-proendothelin but not those receiving endothelin-1. The slopes of the latter regression lines were significantly different ($P < 0.05$) from zero.

maximal decreases in blood pressure which were directly related to the level of basal blood pressure regardless of whether the latter was increased with vasopressin or endothelin-1.

Discussion

In intact anaesthetized rats and in pithed rats with vasopressin-supported blood pressure, i.v. bolus injections of endothelin-1, adenosine, acetylcholine, ANP and substance P produced rapidly appearing, albeit transient, falls in blood pressure. However, for endothelin-1, these effects were not reproducible and decreased progressively in magnitude when the peptide was administered repeatedly at 10 min intervals. The hypotensive activity of endothelin-1 was also markedly reduced in animals which received an 8 min infusion of endothelin-1. This homologous tachyphylaxis, once developed, was reversible since it was no longer demonstrable 2 h after the end of endothelin-1 infusion.

Endothelin-2, endothelin-3, and VIC behaved like endothelin-1, in as much as their hypotensive effects showed tachyphylaxis. More importantly, once an animal became resistant to the depressor effects of one peptide then, it no longer responded to the others. These findings indicate that there is a cross-tachyphylaxis between these isopeptides and that a mechanism common to all of them might be responsible for their hypotensive activity.

If the receptor activated by endothelin isopeptides undergoes transient membrane internalization or acquires a conformational state making it unresponsive to any additional stimulation for a certain time, then repeated and short spaced administrations of endothelin isopeptides will decrease the number of functional receptors to a value below that necessary to obtain a response. This suggestion is directly supported by results obtained in radioligand experiments (Hirata *et al.*, 1988) which demonstrate that the maximal binding capacity for endothelin-1 declines during a prolonged exposure of a membrane preparation to endothelin-1. Furthermore, bound endothelin-1 is very poorly dissociable from its binding sites (Robaut *et al.*, 1990). If endothelin-1 behaves in the same manner under *in vivo* conditions, the persistence of endothelin-1 at its receptor sites makes them unavailable for activation. If this suggestion is correct, it would require that the occupied receptor becomes rapidly uncoupled since on the one hand, the hypotensive effects of endothelin-1 are short lasting and, on the other hand, the tachyphylaxis requires approximately 2 h to wane. Furthermore, since the vasoconstrictor response to endothelin-1 does not undergo tachyphylaxis, endothelin-1 is unlikely to bind persistently to receptors mediating increases in blood pressure unless the number of these receptors is overwhelming and the total amount of repeatedly administered endothelin-1 is not sufficient to decrease them below a critical value.

Alternatively or additionally, if endothelin-1 liberates an endogenous vasodilator substance which is rapidly depletable, multiple injections of this peptide would lead to a tachyphylactic response. We have no argument in favour or against this contention. What can be stated with confidence is that nitric oxide mobilised by acetylcholine or substance P to produce their hypotensive effects is an unlikely endogenous candidate since these vasodilators do not exhibit cross-tachyphylaxis with endothelin-1. These conclusions are consistent with the experiments of Gardiner *et al.* (1989) who found that N^G-monomethyl-L-arginine does not impair the hindquarters vasodilators effects of endothelin-1. Similarly, cyclic AMP and cyclic GMP would appear not to be responsible for the endothelin-induced hypotension since the decrease in blood pressure produced by adenosine and ANP (which use these coupling mechanisms) is not affected in animals with a tachyphylaxis developed to endothelin-1. Furthermore, the time-course of the hypotensive response to ANP is entirely different from that to endothelin-1 (Le Monnier de Gouville *et al.*, 1990; Fozard & Part, 1990; Gardiner *et al.*, 1990a). Finally, the fact that endothelin-1 tachyphylaxis also occurred in nephrectomized or vasopressin-supported pithed rats excludes the kidney or the central nervous system as possible anatomical structures from which endothelin-1 would directly or indirectly liberate a vasodilator substance. However, this vasodilator substance could be of blood origin as suggested by Ohlstein *et al.* (1990).

A goal of this investigation was also to assess whether h-proendothelin possessed the same pharmacological profile as endothelin-1 of which it is the immediate precursor. In pithed rats, h-proendothelin (1 nmol kg^{-1}, i.v.) produced a monophasic pressor response which was of a similar magnitude to that obtained with an equimolar dose of endothelin-1. This finding is in agreement with the results of Kashiwabara *et al.* (1989) but not with those of MacMahon *et al.* (1989) who obtained a pressor effect with a 40 amino acid p-proendothelin only when the peptide was injected after pre-incubation with chymotrypsin. Recent publications (Fukuroda *et al.*, 1990; Matsumura *et al.*, 1990c; McMahon *et al.*, 1991) and this investigation demonstrate that the pressor effects of h-proendothelin in pithed rats can be inhibited dose-dependently by phosphoramidon which is a metallopeptidase inhibitor. This finding allows the conclusion that the functional effects of h-proendothelin are mediated by endothelin-1 unless phosphoramidon is a blocker of a specific receptor for h-proendothelin. The latter possibility can be discarded since this investigation demonstrates that phosphoramidon does not antagonize the already developed pressor effects of h-proendothelin. Thus, if h-proendothelin is processed by an endothelin converting enzyme, the lack of pressor effects of the p-proendothelin used by McMahon *et al.* (1989) can be explained by assuming that this peptide is not a substrate of the rat endothelin converting enzyme. In contrast, in pithed rats the 39 amino acid p-proendothelin produces pressor effects which are more susceptible to phosphoramidon inhibition than those of h-proendothelin (unpublished results).

In contrast to the results of Douglas & Hiley (1991), in our hands a major difference between endothelin-1 and its precursor is the lack of initial depressor response in intact anaesthetized rats after an i.v. bolus injection of even a large dose of h-proendothelin. On the basis of the demonstration that h-proendothelin is processed to endothelin-1 (D'Orleans-Juste *et al.*, 1990), two possible mechanisms may be advanced to explain this observation. First, h-proendothelin is converted to endothelin but the rate of transformation is too slow (as the onset of action of the pressor effect suggests) to yield receptor biophase concentrations attainable with an i.v. bolus of endothelin-1. Alternatively and complementarily, i.v. injected h-proendothelin may be converted at the level of vascular

regions where the receptors mediating the hypotensive effects of endothelin-1 are poorly represented.

Another difference between endothelin-1 and h-proendothelin is their haemodynamic profile. At a dose producing the same systemic pressor effect, the increase in mesenteric vascular resistance was 2.7 times greater for endothelin-1 than for h-proendothelin. This finding can be accounted for if h-proendothelin is poorly converted to endothelin-1 in the mesenteric vascular bed. Thus, the rate of h-proendothelin conversion appears to be a feature of individual vascular beds which may be accounted for by an uneven distribution of the endothelin-converting enzyme.

In anaesthetized rats, an i.v. bolus injection of endothelin-1 (0.25 nmol kg^{-1}) given 5 min after the end of a 10 min infusion of h-proendothelin (0.1 nmol kg^{-1} min^{-1}, i.v) induced a hypotensive response similar to that obtained in control animals. In contrast, in a matched group of animals pretreated with endothelin-1, an i.v. bolus injection of the latter peptide failed to lower blood pressure. Furthermore, in pithed rats, doses of h-proendothelin carefully selected to produce the same persistent pressor response as endothelin-1 did not inhibit the blood pressure lowering effects of an i.v. bolus injection of endothelin-1. Although these results and those of Hoffman *et al.* (1990), who showed that proendothelin but not endothelin-1 evokes renal vasodilatation, could be interpreted as functional evidence against the transformation of h-proendothelin into endothelin-1, this possibility can no longer be held on the basis of the findings with phosphoramidon discussed above. We suggest that endothelin-1 derived from the bioconversion of h-proendothelin has a limited accessibility to endothelin-1 receptors mediating hypotension and this prevents the development of tachyphylaxis which appears to require the exposure of these endothelin receptors to large quantities of endothelin-1. An indirect argument in favour of this suggestion is that the putative endothelin-converting enzyme has not been detected in the blood stream but has been found in endothelial cells (Ikegawa *et al.*, 1990; Matsumura *et al.*, 1990a,b; Ohnaka *et al.*, 1990) and smooth muscle cells (Hioki *et al.* 1991). Thus, endothelin-1 processed locally from h-proendothelin is likely to have a distribution which will be considerably different from that of i.v. injected endothelin-1. This contention is favoured by the different haemodynamic profile of endothelin-1 and h-proendothelin injected i.v. Thus, h-proendothelin studies could provide a better experimental approach for assessing the cardiovascular effects of endogenously released endothelin-1 since the injection of h-proendothelin would produce endothelin-1 firstly at sites where the endothelin-converting enzyme is located.

In conclusion, these experiments show that the hypotensive response to endothelin isopeptides undergoes rapid and cross-tachyphylaxis. Since this phenomenon is not extended to the pressor effect, the receptors mediating hypertension and hypotension should be distinct membrane structures. Furthermore, the tachyphylaxis found with endothelin isopeptides does not exist for vasodilators such as ANP, substance P, acetylcholine, and adenosine implying that it results from a mechanism not shared by the latter agonists. Finally, the *in vivo* cardiovascular effects of h-proendothelin are accountable (at least partly) for by its conversion to endothelin-1, but the latter peptide has a biophase destiny different from that of i.v. injected endothelin-1 since h-proendothelin does not exert hypotensive activity, its haemodynamic profile differs from that of endothelin-1 and its administration is not accompanied by the development of tachyphylaxis to the hypotensive effects of endothelin-1.

The authors wish to thank warmly Chantal Thiry, for her help in the realisation of part of the experiments described herein, and Karen Birmingham, for improving the English style of the manuscript. Our thanks are also extended to Dr J. Fozard for his critical review of the manuscript.

References

D'ORLEANS-JUSTE, P., LIDBURY, P., WARNER, T. & VANE, J. (1990). Intravascular big-endothelin increases circulating levels of endothelin-1 and prostanoids in the rabbit. *Biochem. Pharmacol.*, **39**, R21–R22.

DOUGLAS, S. & HILEY, R. (1991). Responses to endothelin-1, human proendothelin (1–38) and porcine proendothelin (1–39) in the rat on intravenous administration and in the blood perfused mesentery. *Neurochem. Int.*, **18**, 445–454.

FOZARD, J. & PART, M. (1990). No major role for atrial natriuretic peptide in the vasodilator responses to endothelin-1 in the spontaneously hypertensive rat. *Eur. J. Pharmacol.*, **180**, 153–159.

FUKURODA, T., NOGUCHI, K., TSUCHIDA, S., NISHIKIBE, M., IKEMOTO, F., OKADA, K. & YANO, M. (1990). Inhibition of biological actions of big-endothelin-1 by phosphoramidon. *Biochem. Biophys. Res. Commun.*, **172**, 390–395.

GARDINER, S., COMPTON, A., BENNETT, T., PALMER, R. & MONCADA, S. (1989). N^G-monomethyl-L-arginine does not inhibit the hindquarters vasodilator action of endothelin-1 in conscious rats. *Eur. J. Pharmacol.*, **171**, 237–240.

GARDINER, S., COMPTON, A. & BENNETT, T. (1990a). Regional haemodynamic effects of endothelin-1 and endothelin-3 in conscious Long Evans and Brattleboro rats. *Br. J. Pharmacol.*, **99**, 107–112.

GARDINER, S., COMPTON, A., BENNETT, T. & HARTLEY, C. (1990b) Can pulsed doppler technique measure changes in aortic blood flow in conscious rats? *Am. J. Physiol.*, **259**, H448–H456

HIOKI, Y., OKADA, K., ITO, H. MATSUYAMA, K. & YANO, M. (1991) Endothelin converting enzyme of bovine carotid artery smooth muscles. *Biochem. Biophys. Res. Commun.*, **174**, 446–451.

HIRATA, Y., YOSHIMI, H., TAKAICHI, S., YANAGISAWA, M. & MASAKI, T. (1988). Binding and receptor down-regulation of a novel vasoconstrictor endothelin in cultured rat vascular smooth muscle cells. *FEBS Lett.*, **239**, 13–17.

HOFFMAN, A., GROSSMAN, E. & KEISER, H. (1990). Opposite effects of endothelin-1 and big-ET (1–39) on renal function in rats. *Eur. J. Pharmacol.*, **182**, 603–606.

IKEGAWA, R., MATSUMURA, Y., TAKAOKA, M. & MOROMOTO, S. (1990). Evidence for pepstatin-sensitive conversion of porcine big-endothelin to endothelin-1 by the endothelial cell extract. *Biochem. Biophys. Res. Commun.*, **167**, 860–866.

INOUE, A., YANAGISAWA, M., KIMURA, S., KASUYA, Y., MIYAUCHI, T., GOTO, K. & MASAKI, T. (1989). The human endothelin family: three structurally and pharmacologically distinct isopeptides predicted by three separate genes. *Proc. Natl. Acad. Sci. U.S.A.*, **86**, 2863–2867.

KASHIWABARA, T., INAGAKI, Y., OHTA, H., IWAMATSU, A., NOMIZU, M., MORITA, A. & NISHIKORI, K. (1989). Putative precursors of endothelin have less vasoconstrictor activity in vitro but potent pressor effect in vivo. *FEBS Lett.*, **247**, 73–76.

LE MONNIER DE GOUVILLE, A-C., MONDOT, S., LIPPTON, H., HYMAN, A. & CAVERO, I. (1990). Hemodynamic and pharmacological evaluation of the vasodilator and vasoconstrictor effects of endothelin-1 in rats. *J. Pharmacol. Exp. Ther.*, **252**, 300–311.

MACMAHON, E., FOK, K., MOORE, W., SMITH, C., SIEGEL, N. & TRAPANI, A. (1989). In vitro and in vivo activity of chymotrypsin-activated big endothelin (porcine 1–40). *Biochem. Biophys. Res. Commun.*, **163**, 424–429.

MCMAHON, E., PALOMO, M., MOORE, W., MCDONALD, J., & STERN, M. (1991). Phosphoramidon bocks the pressor activity of porcine big endothelin-1-(1-39) in vivo, and conversion of big endothelin-1-(1-39) to endothelin-1(1-21) in vitro. *Proc. Natl. Acad. Sci., USA*, **88**, 703–707.

MATSUMURA, Y., IKEGAWA, R., TAKAOKA, M. & MOROMOTO, S. (1990a). Conversion of porcine big endothelin by an extract from the porcine aortic endothelial cells. *Biochem. Biophys. Res. Commun.*, **167**, 203–210.

MATSUMURA, Y., IKEGAWA, R., TSUKAHARA, Y., TAKAOKA, M. & MORIMOTO, S. (1990b). Conversion of big endothelin-1 to endothelin-1 by two types of metallopeptidases derived from porcine aortic endothelial cells. *FEBS Lett.*, **272**, 166–170.

MATSUMURA, Y., HISAKI, K., TAKAOKA, M. & MORIMOTO, S. (1990c). Phosphoramidon, a metallopeptidase inhibitor, supresses the hypertensive effect of big endothelin-1. *Eur. J. Pharmacol.*, **185**, 103–106.

OHNAKA, K., TAKAYANAGI, R., YAMAUCHI, T., OKAZAKI, H.,

OHASHI, M., UMEDA, F. & NAWATA, H. (1990). Identification and characterization of endothelin converting activity in cultured bovine endothelial cells. *Biochem. Biophys. Res Commun.*, **168**, 1128–1136.

OHLSTEIN, E., VICKERY, L., SAUERMELCH, C. & WILLETTE, N. (1990) Vasodilation induced by endothelin: role of EDRF and prostanoids in rat hindquarter. *Am. J. Physiol.*, **259**, H1835–H1841.

RICHER, C., LEFEVRE-BORG, F., LECHAIRE, J., GOMENI, C., GOMENI, R., GIUDICELLI, J.-F. & CAVERO, I. (1987). Systemic and regional hemodynamic characterization of alpha-1 and alpha-2 adrenoceptor agonists in pithed rats. *J. Pharmacol. Exp. Ther.*, **240**, 944–953.

ROBAUT, C., MONDON, F., BANDET, J., FERRÉ, F. & CAVERO, I. (1991). Regional distribution and pharmacological characterization of [^{125}I]ET-1 biding sites in human foetal placental vessels. *Placenta*, **12**, 55–67.

SAIDA, K., MITSUI, Y. & ISHIDA, N. (1989). A novel peptide, vasoactive intestinal contractor, of a new (endothelin) peptide family. *J. Biol. Chem.*, **264**, 14613–14616.

YANAGISAWA, M., KURIHARA, H., KIMURA, S., TOMOBE, Y., KOBAYASHI, M., MITSUI, Y., YAZAKI, Y., GOTO, K. & MASAKI, T. (1988). A novel potent vasoconstrictor peptide produced by vascular endothelial cells. *Nature*, **332**, 411–415.

(Received November 2, 1990
Revised March 10, 1991
Accepted May 15, 1991)

Br. J. Pharmacol. (1991), **104**, 85–90

Electrophysiological studies of the $GABA_A$ receptor ligand, 4-PIOL, on cultured hippocampal neurones

U. Kristiansen, [1]†J.D.C. Lambert, *E. Falch & *P. Krogsgaard-Larsen

PharmaBiotec Research Centre, Department of Biology and *Department of Organic Chemistry, The Royal Danish School of Pharmacy, 2, Universitetsparken, DK-2100 Copenhagen Ø and †Institute of Physiology, University of Aarhus, DK-8000 Århus C, Denmark

1 Whole-cell, patch-clamp recordings from cultured hippocampal neurones have been used to characterize the action of the $GABA_A$ ligand, 5-(4-piperidyl)isoxazol-3-ol (4-PIOL). The action of 4-PIOL was compared with that of the established $GABA_A$ agonist, isoguvacine.

2 With a symmetrical Cl^- gradient across the membrane and a holding potential of −60 mV, both isoguvacine and 4-PIOL evoked an inward current. The reversal potentials of the responses to both agents were identical (+8.8 mV, $n = 4$) and the current/voltage relationships showed outward-going rectification.

3 The response to 300 μM 4-PIOL was completely blocked by the $GABA_A$ antagonist, bicuculline methobromide (BMB, 10 μM). The pA_2 of BMB was >6.46. With 2 mM 4-PIOL about 15% of the response remained in the presence of 100 μM BMB. This may represent a non-specific component of the response to large concentrations of 4-PIOL.

4 4-PIOL was about 200 times less potent as an agonist than isoguvacine. Because of the rapid fade (desensitization) of isoguvacine-induced currents, the maximum response to this agonist was not determined. However, the response to 2 mM 4-PIOL was only a small fraction of that evoked by submaximal concentrations of isoguvacine.

5 Setting the response to 1 mM 4-PIOL as maximum, the EC_{50} for 4-PIOL was 91 μM (95% confidence limits: 73–114 μM).

6 4-PIOL antagonized the response to isoguvacine with a parallel shift to the right of the dose-response curve. The antagonist action of 4-PIOL was about 30 times weaker than that of BMB. When allowance was made for the intrinsic agonist action of 4-PIOL, the K_i was 116 μM (95% confidence limits: 102–130 μM). This was not significantly different from EC_{50} ($P = 0.86$; non-parametric Mann-Whitney test).

7 It is concluded that 4-PIOL is a partial agonist at the $GABA_A$ receptor on cultured hippocampal neurones.

Keywords: 4-PIOL (5-(4-piperidyl)isoxazol-3-ol); THIP analogue; $GABA_A$ partial agonist/antagonist; whole-cell patch-clamp; cultured hippocampal neurones; isoguvacine; bicuculline methobromide

Introduction

Dysfunctions of the central γ-aminobutyric acid (GABA) neurotransmitter system have been associated with hyperkinetic neurological disorders such as Huntington's chorea (DiChiara & Gessa, 1981), epilepsy (Meldrum, 1982; Nistico *et al.*, 1986) and tardive dyskinesia (Thaker *et al.*, 1989). While GABA replacement therapy is a rational approach to these disorders, administration of the specific $GABA_A$ agonist 4,5,6,7-tetrahydroisoxazolo[4,5-*c*]pyridin-3-ol (THIP) (Krogsgaard-Larsen *et al.*, 1977) does not significantly ameliorate the symptoms of chorea (Foster *et al.*, 1983), epilepsy (Petersen *et al.*, 1983) or tardive dyskinesia (Korsgaard *et al.*, 1982). This may reflect rapid desensitization of the target $GABA_A$ receptors (Mathers, 1987) as a result of constant activation by THIP. If this is the case, low-efficacy $GABA_A$ agonists would, in principle, be of therapeutic interest. We have therefore attempted to develop agents with this pharmacological profile. Here we describe experiments with the THIP analogue, 5-(4-piperidyl) isoxazol-3-ol (4-PIOL) (Figure 1), which has been shown to act as a relatively weak $GABA_A$ agonist on cat spinal neurones (Byberg *et al.*, 1987) but also antagonizes muscimol-stimulated benzodiazepine binding to rat cortical membranes (Falch *et al.*, 1990). We have used the whole-cell, patch-clamp technique to characterize the agonist/antagonist profile of 4-PIOL on cultured hippocampal neurones. Part of this work has been published as an abstract (Kristiansen *et al.*, 1990).

[1]Author for correspondence.

Methods

Electrophysiological recordings using the whole-cell patch-clamp technique were made on cultured hippocampal neurones.

Tissue culture

Neurones were cultured from the hippocampi of 17–18 day old rat embryos essentially according to Brewer & Cotman (1989): 5×10^{-5} cells were placed in 35 mm petri dishes which

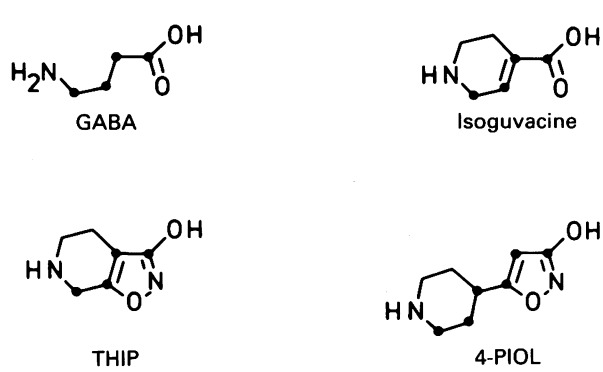

Figure 1 Structures of the GABA analogues which are relevant to this study.

sometimes contained coverslips treated with poly-L-lysine. Plating medium was based on Minimum Essential Medium with Earle's salts (without glutamine, Gibco 041-01090) to which the following were added: 10% horse serum (heat inactivated), 10% foetal calf serum, 50 i.u. ml^{-1} penicillin, 50 $\mu g\,ml^{-1}$ streptomycin, 0.5 mM glutamine. After one day, the plating medium was completely exchanged with feeding medium (2 ml). This had the same composition as the plating medium, except that the foetal calf serum was removed, horse serum reduced to 5% and supplemented with the additives specified by Romijn *et al.* (1982). The medium was replenished twice a week by exchanging 1 ml with fresh feeding medium. Mitosis was inhibited with 5'-fluoro-2'-deoxyuridine (15 $\mu g\,ml^{-1}$) plus uridine (35 $\mu g\,ml^{-1}$) at the time when visual inspection showed a confluent background layer of cells. Some of the cultures were made from neurones which had been cryo-preserved in 8% dimethyl sulphoxide (Mattson & Kater, 1988).

Electrophysiological recording

A 35 mm petri dish was used as the recording chamber, which was either the dish in which the culture was grown or a fresh dish into which a coverslip containing the culture was transferred. The dish was placed on the stage of an Olympus inverted phase contrast microscope, where the individual neurones were viewed at × 200. The culture medium was replaced with about 4 ml artificial balanced salt solution (ABSS), which was continuously renewed by constant perfusion at 0.5 ml min^{-1} at room temperature (20–22°C). The composition of ABSS was (in mM): NaCl 140, KCl 3.5, Na_2HPO_4 1.25, $MgSO_4$ 2, $CaCl_2$ 2, glucose 10 and HEPES 10. pH was 7.35 at 22°C. Tetrodotoxin (0.25–0.5 × 10^{-6} M) was added to the ABSS to block spontaneous synaptic activity.

Standard patch-clamp techniques (Hamill *et al.*, 1981) were used to record from neurones in the whole-cell configuration using a List EPC-7 amplifier. The patch electrodes were pulled and polished on the morning of the experiment and filled just before use. They were manufactured from 1.2 mm o.d. glass (Clark Electromedical) by use of a Sutter P-87 electrode puller. The tips were polished with a Narishige MF-83 microforge to an opening of about 1 μm, which gave resistances of 2–5 MΩ. The standard medium for filling the patch electrodes had the following composition (in mM): KCl 140, $MgCl_2$ 1, $CaCl_2$ 1, EGTA 10, K_2ATP 2 and HEPES 10; pH 7.3 at 22°C (Edwards *et al.*, 1989).

A holding potential (V_h) of −60 mV was usually used. Superimposed on this were command potentials of −10 mV (duration 60 ms, 1.5 Hz) to monitor membrane conductance (G_M). Low frequency, whole-cell currents were plotted on a low fidelity chart recorder during the experiment. The signals were also recorded on a video recorder with a modified pulse code modulator (Lamb, 1985) for subsequent analysis and measurement of the conductance pulses using a Nicolet model 4094C digital oscilloscope.

The drugs used and their sources were: 4-PIOL (5-(4-piperidyl)isoxazol-3-ol), synthesized according to Byberg *et al.* (1987); isoguvacine, synthesized according to Krogsgaard-Larsen & Christiansen (1979); bicuculline methobromide (BMB) (Sigma). These were premixed at the required concentration by diluting stock solutions in ABSS. The solutions were applied in the vicinity (about 100 μm) of the recorded neurone from a multi-barrelled perfusion pipette constructed from 7 hypodermic syringe needles (Carbone & Lux, 1987). The ends of the needles were housed in a glass cap with an opening of about 100 μm. Six of the barrels contained drug solutions, which were applied in random order, while the seventh was used as an exhaust. Shortly before application of a solution was required, the tap separating the reservoir from the hypodermic needle was turned on. The drug solution was then released by gravity feed into the cap of the pipette, where it was siphoned off by the exhaust. On interrupting the exhaust barrel by manual operation of a 3-way tap, the drug-containing solution emerged rapidly from the cap and completely surrounded the neurone. Drugs were applied for 10 s every 1 min, with the exception of experiments including isoguvacine at concentrations in excess of 20 μM, where applications were made every second minute so as to ensure full recovery to a constant baseline for at least 30 s between applications. Applications to the neurone of the perfusion medium alone caused no alteration in the holding current.

Where appropriate, K_i was calculated from the relationship $K_i = [I]/(\text{concentration ratio} - 1)$.

Results

Following the establishment of a whole-cell recording, when the current required to clamp E_M at −60 mV had stabilized and was < 100 pA, agonist application began. The experimental protocol was not started until responses to evenly spaced applications of the same concentration of agonist were constant.

Quantification of the agonist-induced responses

At the usual holding potential of −60 mV, 10 s applications of isoguvacine or 4-PIOL evoked net inward currents. These were accompanied by an increase in G_M as witnessed by the larger currents required to step the voltage by −10 mV (Figure 3). Responses were quantified by measuring the peak whole-cell current. With responses to isoguvacine at a concentration of 10 μM or less, the current reached a plateau which was maintained throughout the application. With larger concentrations, however, the agonist-evoked current rose quickly to a peak from which it slowly declined with a concomitant decline of G_M (Figures 3 and 4). This fading, which is probably due to receptor desensitization, means that responses to larger concentrations of isoguvacine would probably be underestimated. In consideration of this, and the limited number of barrels in the perfusion pipette, concentrations of isoguvacine were limited to those which evoked responses of comparable size to those of 4-PIOL.

The $GABA_A$ agonist action of 4-PIOL

Dose-response curve to 4-PIOL The maximum agonist-induced whole-cell currents varied according to the size of the cell. The responses were therefore normalized so that they could be pooled for statistical analysis. The response to 2 mM 4-PIOL (the highest concentration used) was set to 100% and responses to lower concentrations expressed as fractions of this. Dose-response curves to 4-PIOL were determined in 12 neurones (Figure 2). The concentration of 4-PIOL required to produce a just-detectable response was about 10 μM.

The EC_{50} for the agonist effect of 4-PIOL was determined by linear regression analysis for responses to 30, 100 and 300 μM, which lie on the linear portion of the dose-response curve (Figure 2a). When the response to 2 mM is set to 100%, the EC_{50} for 4-PIOL is 118 μM (95% confidence limits: 99–141 μM). However, it is likely that about 15% of the response to 2 mM 4-PIOL represents an unspecific action (Figure 2a and see below). When the response to 1 mM 4-PIOL is normalized to 100%, the EC_{50} for 4-PIOL is 91 μM (95% confidence limits: 73–114 μM).

Since maximal responses to isoguvacine were not obtained, it is not possible to calculate EC_{50} for this agonist. However, the response to 2 mM 4-PIOL was about the same as that to 10 μM isoguvacine and 14% of the response to 40 μM isoguvacine.

The effect of bicuculline methobromide on responses to 4-PIOL Figure 2b shows that the response to 300 μM 4-PIOL was completely and reversibly blocked by 10 μM BMB. This was the case for all of the six neurones tested and the result is included in Figure 2a. On the other hand, the response to

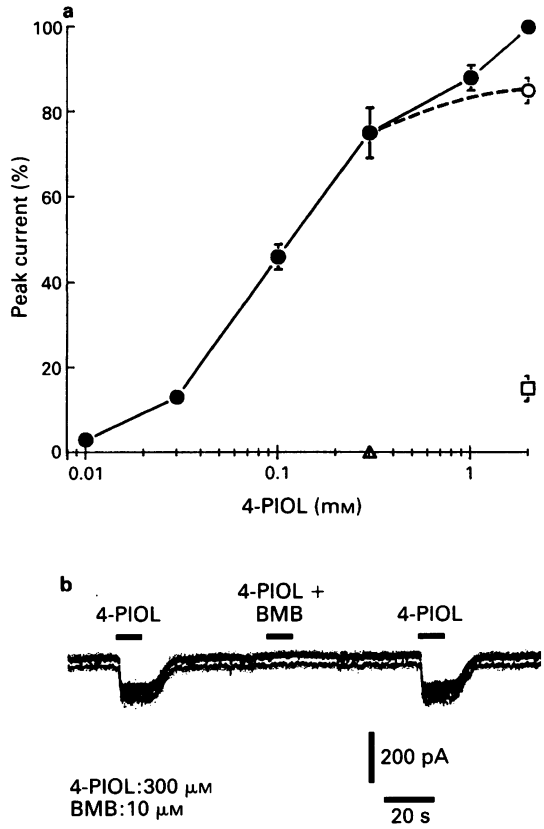

Figure 2 (a) Dose-response curve for 4-PIOL. 4-PIOL was applied at the six concentrations shown to cultured hippocampal neurones ($n = 12$ for all concentrations except 0.01 mM where $n = 4$). The responses were measured as the peak of the whole-cell current (●). For each neurone, the response to 2 mM 4-PIOL was normalized to 100%. Bicuculline methobromide (BMB) 10 μM, abolished the response to 0.3 mM 4-PIOL ($n = 4$, △: see also (b)), while 100 μM BMB did not completely antagonize the response to 2 mM 4-PIOL ($n = 11$, □); (○) indicates the response to 2 mM 4-PIOL following subtraction of the BMB-resistant component and has been joined (stippled line) to the response to 0.3 mM 4-PIOL (which contained no BMB-insensitive component). (b) Whole-cell patch-clamp recordings from a cultured hippocampal neurone showing antagonism of the response to 4-PIOL (300 μM) by concurrent application of BMB (10 μM).

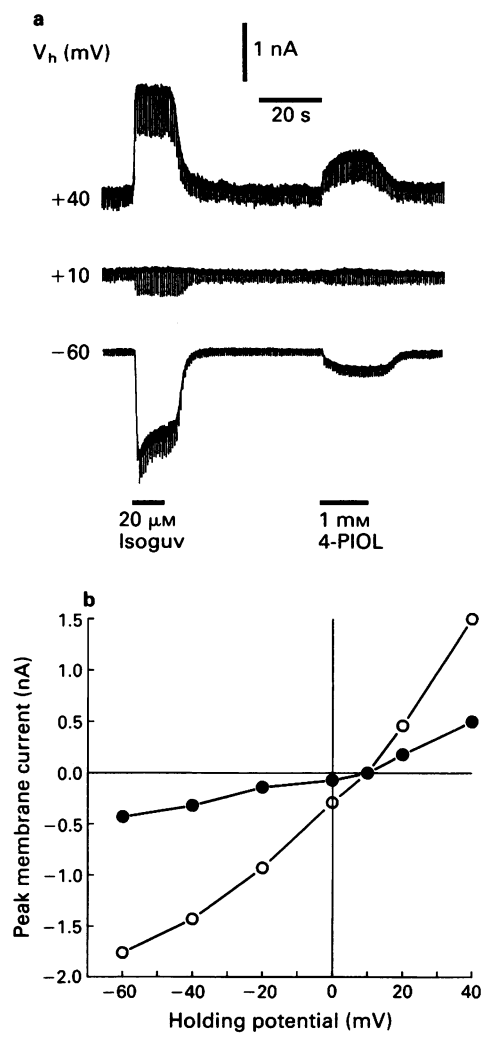

Figure 3 Current-voltage relationship for isoguvacine (Isoguv) and 4-PIOL. (a) Traces showing the currents required to clamp E_M at the three holding potentials (V_h) shown. The traces are modulated by negative-going transients which reflect the current required to shift E_M by −10 mV relative to V_h. These increase in size with depolarization (outward rectification). The response to both agents reversed at +10 mV, where there was no net change in I_M, but an increase in G_M. Note that, while the agonist-evoked increases in I_M are approximately symmetrical, the displacements from the reversal potential are +30 mV and −70 mV respectively, which is indicative of outward rectification. (b) Plots from the same cell of the peak agonist-evoked current against V_h for 4-PIOL (1 mM: ●) and isoguvacine (20 μM: ○). Both relationships show outward rectification and the reversal potentials for the two agonists are identical (+10 mV).

2 mM 4-PIOL was only blocked by 85 ± 3% (s.e.mean; $n = 11$) in the presence of a ten times larger concentration of BMB (100 μM). After subtraction of the BMB-resistant component of the response to 2 mM 4-PIOL, there was no significant difference between responses to 0.3, 1 and 2 mM ($P > 0.05$) which suggests that the dose-response relationship of the BMB-sensitive part of the response to 4-PIOL had reached a plateau.

Current-voltage relationship for 4-PIOL The current-voltage (I/V) relationship for 4-PIOL was compared with that of isoguvacine. I/V curves of the type shown in Figure 3 were constructed for 4 cells. The reversal potential for the response to 4-PIOL was 8.8 ± 2.0 mV, which was the same as that for the response to isoguvacine (8.8 ± 2.3 mV). The I/V curves for both agents showed outward rectification.

The $GABA_A$ antagonist action of 4-PIOL

The effect of 4-PIOL on responses to isoguvacine When isoguvacine and 4-PIOL were applied simultaneously to a neurone, the resulting response was not the algebraic sum of the response to the two agonists when applied alone. The net response was always smaller than that to isoguvacine and approached the size of the response to 4-PIOL alone (Figure 4a). The recorded current in the presence of both agonists will partly reflect the agonist action of 4-PIOL. Figure 4b shows that the antagonism of the response to 20 μM isoguvacine is progressively increased with increasing concentrations of 4-PIOL. The net response to isoguvacine has been estimated by subtracting the response evoked by 4-PIOL when applied alone.

The effect of 4-PIOL on the dose-response curve for isoguvacine is shown in Figure 5. The antagonism of responses to isoguvacine by 4-PIOL was investigated on the basis of a symmetrical (2 + 2) dose assay (Colquhoun, 1971). Both the upper and the lower parts of the log dose-response curve showed a parallel shift to the right in the presence of 4-PIOL ($P > 0.05$). This is compatible with competitive antagonism. K_i was calculated to be 142 μM (95% confidence limits: 126–159 μM). When account is taken of the intrinsic activity of 4-PIOL by subtracting its agonist effect, K_i was 116 μM (95% confidence limits: 102–130 μM).

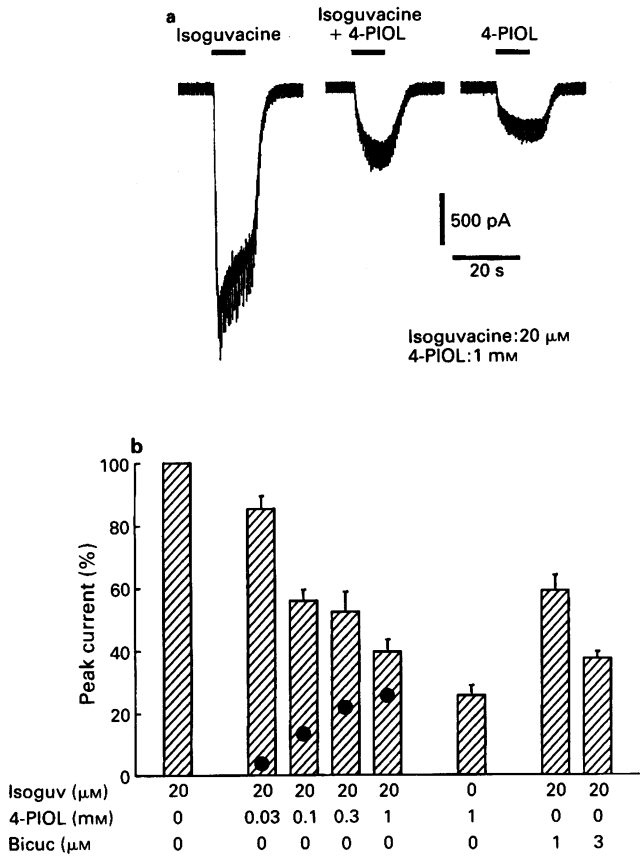

Figure 4 (a) Interactions of 4-PIOL and isoguvacine. The response to isoguvacine (20 μM) was reduced by 72% when 4-PIOL (1 mM) was applied simultaneously. 4-PIOL alone evoked a response which was 60% of that to the combined application. The fast deflections are the currents required to evoke -10 mV changes in V_h. (b) The effect of 4-PIOL and bicuculline on the response to 20 μM isoguvacine (Isoguv) ($n = 10$). The concentrations of the ligands applied from the perfusion pipette are given below the histogram. The response to 20 μM isoguvacine alone has been set as 100% (first column on the left) and other responses are expressed as a fraction of this. The response to isoguvacine is progressively reduced with increasing concentrations of 4-PIOL; (●) show the intrinsic agonist effect of 4-PIOL alone (see Figure 2 and the response to 1 mM 4-PIOL alone). The columns to the right show the antagonistic effect of two concentrations of bicuculline (Bicuc) on the response to isoguvacine ($n = 10$).

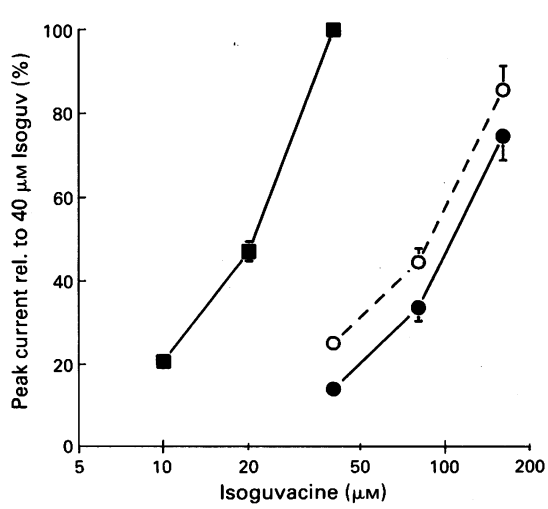

Figure 5 $GABA_A$ antagonist action of 4-PIOL. A dose-response curve to isoguvacine has been constructed where the response to 40 μM has been set as 100% ($n = 9$, ■). 4-PIOL (500 μM) caused a shift to the right of the relationship (○); (●) show the relationship after allowance has been made for the intrinsic activity of 4-PIOL.

Since the 95% confidence intervals for EC_{50} and K_i are not symmetrically distributed about the mean, these values cannot be compared by a normal t test. Instead, K_i ($n = 9$) and EC_{50} ($n = 12$) were calculated for each cell and compared by the non-parametric Mann-Whitney test. This showed that there was no significant difference between EC_{50} and K_i either when the response to 1 mM ($P = 0.86$) or 2 mM ($P = 0.70$) 4-PIOL was set to 100% for calculation of the EC_{50}.

Comparison of 4-PIOL with bicuculline methobromide Figure 4b shows that the IC_{50} of BMB on responses to isoguvacine is about 2 μM. When allowance is made for the intrinsic agonist effect of 4-PIOL, 100 μM 4-PIOL and 3 μM BMB are roughly equipotent, i.e. 4-PIOL is about 30 times weaker as a $GABA_A$ antagonist than BMB.

The action of 4-PIOL on cultured spinal cord neurones

The only previous electrophysiological experiments with 4-PIOL have been performed with extracellular recordings in the cat spinal cord, where 4-PIOL was shown to be a weak GABA agonist (Byberg *et al.*, 1987). We have also tested the action of 4-PIOL on two spinal neurones (which were cultured from mouse embryos according to the methods given in Jensen & Lambert (1986)). Exactly the same profile of action was found as that reported above for the hippocampal neurones.

Discussion

The response to 1 mM 4-PIOL is blocked by the specific $GABA_A$ antagonist, BMB (Figure 2). This is a strong indication that 4-PIOL is acting at the $GABA_A$ receptor. In the presence of 10 μM BMB the dose-response relationship for 4-PIOL is shifted to the right with a concentration ratio >30 (Figure 2a), from which $K_i < 0.34$ and $pA_2 > 6.46$. This compares with pA_2 values of 5.88 for the action of bicuculline methochloride (BMC) on responses to muscimol in the rat cuneate nucleus (Simmonds, 1982) and of 6.24 for BMC on responses to isoguvacine in the rat hippocampus (Kemp *et al.*, 1986).

About 15% of the response to 2 mM 4-PIOL is not blocked by 100 μM BMB (Figure 2a), which probably reflects a 'non-specific' effect of the agonist at this high concentration. The presence of such a non-specific component would explain why the dose-response relationship does not reach a plateau (Figure 2a). In light of this, it is probably more correct to calculate EC_{50} either from the response to 2 mM after subtraction of the BMB-resistant component, or from the response to 1 mM 4-PIOL (where the BMB-resistant component probably represents less than 5% of the overall response (Figure 2a)).

Other evidence that 4-PIOL is a $GABA_A$ agonist is obtained by comparing its action with the established $GABA_A$ agonist, isoguvacine. Firstly, the reversal potential to isoguvacine and 4-PIOL were identical (Figure 3), which indicates that the same ionic mechanism is involved. Secondly, the I/V relationship for responses to isoguvacine and 4-PIOL both showed outward rectification, which has been shown to be a characteristic of responses to GABA (Segal & Barker, 1984a; Weiss *et al.*, 1988). This has previously been thought to be due to rectification of the $GABA_A$ channel (Gray & Johnston, 1985) or modulation of its kinetics by the transmembrane potential (Segal & Barker, 1984a). Recent analysis at the single-channel level, however, has shown that depolarization increases the probability that $GABA_A$ ionophores will open (Weiss, 1988).

There is a general consensus that the decline of the whole-cell currents during maintained application of agonist results from desensitization of the $GABA_A$ receptor (Wong & Watkins, 1982; Numann & Wong, 1984; Thalmann & Hershkowitz, 1985; Weiss *et al.*, 1988; Tehrani *et al.*, 1989), although a change in E_{Cl^-} may also be involved (Segal & Barker, 1984b; Huguenard & Alger, 1986). While we also report

fading of responses to isoguvacine, it is noteworthy that the response did not show the same degree of fade when mediated by an outward current (Figure 3). This was observed in all neurones where the response to isoguvacine was evoked at appreciably positive levels of potential. Responses to 4-PIOL showed no tendency to desensitize. This might be considered to be an important difference between the two agents. However, the response to the maximum concentration of 4-PIOL (2 mM) was of similar amplitude to that of 10 μM isoguvacine, which also did not desensitize.

4-PIOL, with an EC_{50} of 91 μM, is about 200 times weaker than isoguvacine. Because of complications with desensitization, we have not determined the maximum response to isoguvacine. However, the largest response evoked by 4-PIOL was only a small fraction of that to submaximal concentrations of isoguvacine. Thus, since 4-PIOL is unable to evoke the full $GABA_A$ response of which the tissue is capable, it has the character of a partial agonist.

A weak partial agonist will occupy the receptor, but will not be very effective in transforming the ionophore to the conducting state. At the same time, however, it will prevent a full agonist from gaining access to the receptor and will therefore exhibit the characteristics of an antagonist. This was indeed the case for 4-PIOL. It antagonized responses to isoguvacine (Figure 4) with a parallel shift to the right of the dose-response curve (Figure 5). While this is compatible with competitive antagonism, it is not definitive proof (Simmonds, 1982). The limitations of our perfusion system precluded a full Schild analysis. Assuming that the responses to isoguvacine lie on curves which have undergone a parallel shift to the right in the presence of 4-PIOL, dose-ratios to isoguvacine in the presence of 30 and 100 μM 4-PIOL can be calculated. The slope of the resulting Schild plot is 1.14 (95% confidence limits: 0.81–1.47). When allowance is made for the intrinsic agonist action of 4-PIOL, K_i was 116 μM. There was no significant difference between EC_{50} and K_i for 4-PIOL, as would be expected for a partial agonist.

In view of the fact that 4-PIOL has been proposed as a $GABA_A$ ligand which has no effect on benzodiazepine binding, the actions of both benzodiazepine agonists and inverse agonists (Jensen & Lambert, 1986) will be investigated in electrophysiological experiments. However, it is possible that the presently demonstrated low intrinsic activity of 4-PIOL might explain the lack of effect on benzodiazepine binding, while the antagonism of muscimol-induced stimulation of benzodiazepine binding by 4-PIOL (Falch *et al.*, 1990) could be explained by the dominant antagonist profile of 4-PIOL.

Possible therapeutic applications of 4-PIOL

To the best of our knowledge, 4-PIOL represents the first substance which has been characterized as a low efficacy partial agonist at $GABA_A$ receptors. A slight reduction in $GABA_A$ ergic transmission, as is achieved with partial inverse agonists at the benzodiazepine receptor (Lambert *et al.*, 1988; Izquierdo, 1989), can enhance awareness, learning and memory. 4-PIOL has a dominant antagonist profile and may therefore exhibit the anxiogenic and pro-convulsant (or frank convulsant) effects associated with the more effective inverse agonists at the benzodiazepine receptor. It is possible, however, that these undesirable effects could be offset by the modest agonist activity of 4-PIOL. At physiological pH 4-PIOL itself is predominantly ionized and will not, therefore, penetrate the blood-brain barrier to any significant extent. In accordance with this, systemic administration of 4-PIOL evokes no pharmacological effects (Suzdak & Krogsgaard-Larsen, unpublished observations). This pharmacokinetic obstacle may be overcome by synthesizing new 4-PIOL analogues which are predominantly uncharged at the physiological pH.

We thank the Danish Medical Research Council and Aarhus University's Research Fund for financial support. Kirsten Kandborg is thanked for preparation of the cultures and Morten Skovgaard Jensen for help with some of the initial experiments.

References

BREWER, G.J. & COTMAN, C.W. (1989). Survival and growth of hippocampal neurons in defined medium at low density: Advantages of a sandwich culture technique or low oxygen. *Brain Res.*, **494**, 65–74.

BYBERG, J.R., LABOUTA, I.M., FALCH, E., HJEDS, H., KROGSGAARD-LARSEN, P., CURTIS, D.R. & GYNTHER, B.D. (1987). Synthesis and biological activity of a GABA-A agonist which has no effect on benzodiazepine binding and structurally related glycine antagonists. *Drug Des. Del.*, **1**, 261–274.

CARBONE, E. & LUX, H.D. (1987). Kinetics and selectivity of a low-voltage-activated calcium current in chick and rat sensory neurones. *J. Physiol.*, **386**, 547–570.

COLQUHOUN, D. (1971). *Lectures on Biostatistics.* Oxford: Clarendon Press.

DICHIARA, G. & GESSA, G.L. (1981). *GABA and the Basal Ganglia.* New York: Raven Press.

EDWARDS, F.A., KONNERTH, A., SAKMANN, B. & TAKAHASHI, T. (1989). A thin slice preparation for patch clamp recordings from neurones of the mammalian central nervous system. *Pflügers Arch.*, **414**, 600–612.

FALCH, E., LARSSON, O.M., SCHOUSBOE, A. & KROGSGAARD-LARSEN, P. (1990). GABA-A agonists and GABA uptake inhibitors. *Drug Dev. Res.*, **21**, 169–188.

FOSTER, N.L., CHASE, T.N., DENARO, A., HARE, T.A. & TAMMINGA, C.A. (1983). THIP treatment and Huntington's chorea. *Neurology*, **33**, 637–639.

GRAY, R. & JOHNSTON, D. (1985). Rectification of single GABA-gated chloride channels in adult hippocampal neurons. *J. Neurophysiol.*, **54**, 134–142.

HAMILL, O.P., MARTY, A., NEHER, E., SAKMANN, B. & SIGWORTH, F.J. (1981). Improved patch-clamp techniques for high-resolution current recording from cells and cell-free membrane patches. *Pflügers Arch.*, **391**, 85–100.

HUGUENARD, J.R. & ALGER, B.E. (1986). Whole-cell voltage-clamp study of the fading of GABA-activated currents in acutely dissociated hippocampal neurons. *J. Neurophysiol.*, **56**, 1–18.

IZQUIERDO, I. (1989). A game with shifting mirrors. *Trends Pharmacol. Sci.*, **10**, 473–476.

JENSEN, M.S. & LAMBERT, J.D.C. (1986). Electrophysiological studies in cultured mouse CNS neurones of the action of an agonist and an inverse agonist at the benzodiazepine receptor. *Br. J. Pharmacol.*, **88**, 717–731.

KEMP, J.A., MARSHALL, G.R. & WOODRUFF, G.N. (1986). Quantitative evaluation of the potencies of GABA-receptor agonists and antagonists using the rat hippocampal slice preparation. *Br. J. Pharmacol.*, **87**, 677–684.

KORSGAARD, S., CASEY, D.E., GERLACH, J., HETMAR, O., KALDAN, B. & MIKKELSEN, L.B. (1982). The effect of tetrahydroisoxazolopyridinol (THIP) in tardive dyskinesia. *Arch. Gen. Psychiatry*, **39**, 1017–1021.

KRISTIANSEN, U., LAMBERT, J.D.C., FALCH, E. & KROGSGAARD-LARSEN, P. (1990). Electrophysiological studies of the $GABA_A$ ligand, 4-PIOL. *Eur. J. Neurosci.*, **Suppl. 3**, 25.

KROGSGAARD-LARSEN, P. & CHRISTIANSEN, T.R. (1979). GABA agonists. Synthesis and structure-activity studies on analogues of isoguvacine and THIP. *Eur. J. Med. Chem.*, **14**, 157–164.

KROGSGAARD-LARSEN, P., JOHNSTON, G.A.R., LODGE, D. & CURTIS, D.R. (1977). A new class of GABA agonist. *Nature*, **268**, 53–55.

LAMB, T.D. (1985). An inexpensive digital tape recorder suitable for neurophysiological signals. *J. Neurosci. Methods*, **15**, 1–13.

LAMBERT, J.D.C., PETERSEN, E.N., JENSEN, M.S. & JENSEN, L.H. (1988). Modulatory sites associated with the GABA receptor-ionophore complex and the development of new, potentially specific therapeutic agents. In *Neurotransmitters and Cortical Function.* ed. Avoli, M., Reader, T.A., Dykes, R.W. & Gloor, P. pp.

207–226. New York: Plenum Press.

MATHERS, D.A. (1987). The $GABA_A$ receptor: new insights from single-channel recording. *Synapse*, **1**, 96–101.

MATTSON, M.P. & KATER, S.B. (1988). Isolated hippocampal neurons in cryopreserved long-term cultures: development of neuroarchitecture and sensitivity to NMDA. *Int. J. Dev. Neurosci.*, **6**, 439–452.

MELDRUM, B.S. (1982). Pharmacology of GABA. *Clin. Neuropharmacol.*, **5**, 293–316.

NISTICO, G., ENGEL, J., FARIELLO, R.G., LLOYD, K.G. & MORSELLI, P.L. (1986). *Neurotransmitters, Seizures and Epilepsy*, Vol. III. New York: Raven Press.

NUMANN, R.E. & WONG, R.K.S. (1984). Voltage-clamp study on GABA response desensitization in single pyramidal cells dissociated from the hippocampus of adult guinea pigs. *Neurosci. Lett.*, **47**, 289–294.

PETERSEN, H.R., JENSEN, I. & DAM, M. (1983). THIP: a single-blind controlled trial in patients with epilepsy. *Acta Neurol. Scand.*, **67**, 114–117.

ROMIJN, H.J., HABETS, A.M.M.C., MUD, M.T. & WOLTERS, P.S. (1982). Nerve outgrowth, synaptogenesis and bioelectric activity in fetal rat cerebral cortex tissue cultured in serum-free, chemically defined medium. *Dev. Brain Res.*, **2**, 583–589.

SEGAL, M. & BARKER, J.L. (1984a). Rat hippocampal neurons in culture: properties of GABA-activated Cl^- ion conductance. *J. Neurophysiol.*, **51**, 500–515.

SEGAL, M. & BARKER, J.L. (1984b). Rat hippocampal neurons in culture: voltage-clamp analysis of inhibitory synaptic connections. *J. Neurophysiol.*, **52**, 469–487.

SIMMONDS, M.A. (1982). Classification of some GABA antagonists with regard to site of action and potency in slices of rat cuneate nucleus. *Eur. J. Pharmacol.*, **80**, 347–358.

TEHRANI, M.H.J., HABLITZ, J.J. & BARNES, JR, E.M. (1989). cAMP increases the rate of $GABA_A$ receptor desensitization in chick cortical neurons. *Synapse*, **4**, 126–131.

THAKER, G.K., NGUYEN, J.A. & TAMMINGA, C.A. (1989). Increased saccadic distractability in tardive dyskinesia: functional evidence for subcortical GABA dysfunction. *Biol. Psychiatry*, **25**, 49–59.

THALMANN, R.H. & HERSHKOWITZ, N. (1985). Some factors that influence the decrement in the response to GABA during its continuous iontophoretic application to hippocampal neurons. *Brain Res.*, **342**, 219–233.

WEISS, D.S. (1988). Membrane potential modulates the activation of GABA-gated channels. *J. Neurophysiol.*, **59**, 514–527.

WEISS, D.S., BARNES, JR, E.M. & HABLITZ, J.J. (1988). Whole-cell and single-channel recordings of GABA-gated currents in cultured chick cerebral neurons. *J. Neurophysiol.*, **59**, 495–513.

WONG, R.K.S. & WATKINS, D.J. (1982). Cellular factors influencing GABA response in hippocampal pyramidal cells. *J. Neurophysiol.*, **48**, 938–951.

(Received November 6, 1990
Revised May 8, 1991
Accepted May 16, 1991)

Br. J. Pharmacol. (1991), **104**, 91–96

Further evidence for the existence of NK_2 tachykinin receptor subtypes

[1]Riccardo Patacchini, *Mara Astolfi, **Laura Quartara, **Paolo Rovero, Antonio Giachetti & Carlo Alberto Maggi

Pharmacology Department, A. Menarini Pharmaceuticals, Via Sette Santi 3 50131, Florence; *Pharmacology Department, Menariñi Sud, Pomezia, Rome and **Chemistry Department, A. Menarini Pharmaceuticals, Florence, Italy

1 We have evaluated the biological activity of a number of neurokinin A (4–10), (NKA (4–10)) analogues in the endothelium-deprived rabbit isolated pulmonary artery (RPA) and hamster isolated trachea (HT), two tissues rich in different NK_2 receptor subtypes.

2 MDL 28,564, a pseudopeptide selective for NK_2 receptor sites, behaved as a full agonist in the RPA, while in the HT it competitively antagonized NKA or [βAla^8]-NKA (4–10) contractile effects.

3 The peculiar behaviour of MDL 28,564 in the RPA and HT may be explained neither by a difference in receptor reserve between the two organs (the reserve being three times greater in RPA than in the HT) nor by a different affinity for the two receptor subtypes (identical dissociation constants, pK_A or pK_B, calculated in the RPA and in the HT). On the other hand, MDL 28,564 displayed a very different intrinsic efficacy for the two receptor subtypes.

4 The novel peptides MEN 10,295 ([Trp^7, βAla^8]-NKA-(4–10)) and MEN 10,296 ([Tyr^5, Trp^7, βAla^8]-NKA-(4–10)) behaved as weaker agonists than MDL 28,564 in the RPA, but retained appreciable agonist activity also in the HT.

5 The novel peptides: MEN 10,282 ([Tyr^5, D-Trp^{6,8}, Trp^9, Arg^{10}]-NKA-(4–10)), MEN 10,449 ([diI-Try^5, D-Trp^{6,8,9}, Arg^{10}]-NKA-(4–10)) and the cyclic hexapeptide L 659,877 (cyclo [Leu-Met-Gln-Trp-Phe-Gly]) behaved as competitive antagonists against NKA contractile effects both in the RPA and HT. MEN 10,282 and MEN 10,449 were unable to distinguish between the NK_2 receptor subtypes, having almost the same affinity in the two organs. On the other hand L 659,877 was about 15 times more potent in the HT than in the RPA.

6 These results provide further evidence for NK_2 receptors heterogeneity and are useful in outlining pharmacological features of the two subtypes present in the RPA and HT.

Keywords: Tachykinins; tachykinin receptors; NK_2 receptor subtypes; tachykinin antagonists; pseudopeptides

Introduction

The tachykinin (TK) receptors (NK_1, NK_2, NK_3) have been defined on the basis of their sensitivity to the natural peptides, substance P (SP), neurokinin A (NKA) and neurokinin B (NKB) and to a number of synthetic TK agonists selective for one of the three TK receptors (Buck *et al.*, 1984; 1988; Lee *et al.*, 1986; Drapeau *et al.*, 1987; Dion *et al.*, 1987; Regoli *et al.*, 1987; 1988; 1989; Maggi *et al.*, 1987; Rovero *et al.*, 1989). The identification, through cloning studies of three receptor proteins belonging to the G-protein superfamily, which possess the pharmacological character of the above receptors, supports this classification (Masu *et al.*, 1987; Yokota *et al.*, 1989; Hershey & Krause, 1990).

However, a number of experimental observations obtained with novel TK antagonists are not explained by the present classification of TK receptors. For example, McKnight *et al.* (1988) found that L 659,877 and other cyclic TK antagonists possess a very different affinity (pA_2 values) when tested in two isolated organs endowed with NK_2 receptors, the rat vas deferens and guinea-pig trachea, suggesting the existence of a distinct receptor in the latter organ (termed NK_4). Further, Van Giersbergen *et al.* (1991) have reported that L 659,877 is about 20 times more potent in inhibiting [^{125}I]-NKA specific binding on NK_2 receptor sites present on hamster urinary bladder membranes than on NK_2 sites expressed in a murine fibroblast cell line (SKLKB82#3) transfected with the bovine stomach cDNA.

Recently we found (Maggi *et al.*, 1990) marked differences in the affinity estimates for selective NK_2 antagonists in two preparations which have been shown to contain an apparently homogeneous class of NK_2 receptors: the endothelium-deprived rabbit isolated pulmonary artery (RPA) and hamster isolated trachea (HT). Thus, MEN 10,207 (referred to as peptide I in Maggi *et al.*, 1990), a selective NK_2 antagonist (Rovero *et al.*, 1990), was about 100 times more potent in the RPA than in the HT while a converse picture was obtained with a linear peptide antagonist termed R396 (referred to as peptide III in Maggi *et al.*, 1990). MEN 10,207 exhibits also a marked difference in inhibiting [^{125}I]-NKA binding to NK_2 sites, being about 120 times more potent at the NK_2 receptors expressed by a murine fibroblast cell line (SKLKB82#3), than at the receptors present on hamster urinary bladder membranes (Van Giersbergen *et al.*, 1991).

Collectively, these data suggest that the NK_2 receptor is heterogeneous in respect to antagonists which detect differences in the NK_2 receptor present in different tissues. Here we present further evidence supporting this conclusion. As probes of the NK_2 receptor we have used a number of NK_2 ligands, including L 659,877 and MDL 28,564. This latter compound, a pseudopeptide analogue of NKA-(4–10), maintains selective affinity for NK_2 receptor sites (Harbeson *et al.*, 1990), but exhibits diverging actions in tissues endowed with NK_2 receptors: in the guinea-pig trachea it is a full agonist, while in the hamster urinary bladder or the rat vas deferens it is virtually inactive as an agonist and also possesses antagonist activity (Buck *et al.*, 1990). Because of the peculiar behaviour of MDL 28,564, the 'receptor reserve' for NKA in the RPA and HT has been evaluated, in order to evaluate the role of tissue factors in producing the biological response to TK agonists in the two organs. The affinity constant (K_A) and relative intrinsic efficacy of NKA and MDL 28,564 have also been estimated for TK receptors of RPA and HT.

Part of this work has been presented at the meeting: 'SP and related peptides: cellular and molecular physiology', held in Worcester (U.S.A.) on July 18–21, 1990.

[1] Author for correspondence.

Methods

General

Male albino rabbits (3.0–3.5 kg) and Syrian golden hamsters (100–120 g) were stunned and bled. Endothelium-denuded strips of rabbit pulmonary artery (RPA) or rings of the hamster trachea (HT) were excised and prepared for isometric tension recording in oxygenated (96% O_2 and 4% CO_2) Krebs solution in 5 ml organ baths, as described previously (Maggi *et al.*, 1990). Cumulative concentration-response curves to the agonists were obtained, each concentration being added when the effect of the preceding one had reached a steady state. Preliminary experiments indicated lack of desensitization of both RPA or HT to the cumulative administration of peptides. pD_2 values were calculated as $-\log$ molar concentration of agonist producing 50% of maximal effect (EC_{50}). The effect of the TK-antagonists (contact time 15 min) was studied as described previously (Maggi *et al.*, 1990). Antagonist activity was evaluated by the Schild plot method (Arunlakshana & Schild, 1959). Since all TK-antagonists studied yielded a slope not different from unity, the pA_2 values reported were calculated by the constrained plot method (slope constrained to -1) as described by Tallarida *et al.* (1979). Neither antagonists of muscarinic receptors, adrenoceptors and histamine receptors, nor inhibitors of cyclo-oxygenase, lipo-oxygenase or peptidases were used in this study since previous investigations have demonstrated that the tachykinin contractile effect in the RPA and HT is a direct phenomenon, not influenced by the above agents (D'Orleans-Juste *et al.*, 1985; Maggi *et al.*, 1989; 1990). The potency of agonists relative to that of NKA was evaluated by the ratio of the respective EC_{50}s.

The amino acid sequence of peptides used in this study is shown in Table 1.

Determination of dissociation constant (K_A) and receptor reserve values

To determine the agonist affinity (dissociation constant, K_A) and the receptor reserve for NKA in the two bioassays we used the 'partial irreversible blockade' method described by Furchgott (Furchgott, 1966; Furchgott & Bursztyn, 1967). Cumulative concentration-response curves to NKA were constructed both in the RPA and HT, before and after incubation of the tissues with the alkylating agent phenoxybenzamine (Pbz). Previously Pbz, in concentration up to 100 μM, has been shown to reduce NK_2 receptor number without affecting the affinity of iodinated NKA in binding experiments conducted on hamster and rat urinary bladder membranes (Buck & Burcher, 1987). Therefore, to avoid changes in ligand affinity, Pbz concentrations employed in the present study were in the 10–50 μM range, with an exposure time (30 min) which was half of that used by Buck & Burcher (1987). Notably, other investigators working on peptide receptors (Lin & Musacchio, 1983; Vaught *et al.*, 1986) have used alkylating conditions similar to ours.

Pbz was left in contact for 30 min with the tissues. At the end of the incubation period Pbz was washed out repeatedly for 30 min, before repetition of the curve to NKA (40 min after Pbz washout). Concentration-response curves to NKA (or to other TK-agonists), performed in matched preparations before and after incubation for 30 min with the vehicle employed to dissolve Pbz according to the above schedule, proved to be very reproducible, confirming the reliability of the rightward shifts observed in the Pbz-treated tissues. Reciprocal equieffective doses of NKA before and after Pbz treatment were plotted. From the slope and intercept of the straight line fitting the points, the value for K_A and the fraction of receptors remaining unblocked (q) were calculated (Furchgott, 1966; Furchgott & Bursztyn, 1967). Since the extent of alkylation by a given concentation of Pbz was variable, we selected the experiments in which receptors alkylated were at least 50% of total, to minimize the experimental errors produced by low doses of agonist in constructing the reciprocal plot, as suggested by Kenakin (1987). For the same reason, equiactive concentrations of NKA were selected from the upper region of the depressed dose-response curve. The K_A value for MDL 28,564 in the RPA was evaluated in the same manner. Receptor reserve, regarded as the fraction of the total receptor pool not required for a maximal tissue response, is difficult to quantify experimentally. We choose to express the 'reserve' as the ratio between the concentration of NKA required for half maximal receptor occupancy (K_A) and half maximal response (EC_{50}) (Kenakin, 1987). The fractional occupancy of receptors (ρ) required to elicit half maximal response was calculated on the basis of Clark's equation:

$$\rho = \frac{[AR]}{[Rt]} = \frac{[A]}{[A] + K_A} \quad (1)$$

by substituting [A] with EC_{50} and using K_A obtained in each experiment.

Measurement of relative efficacy of neurokinin A and MDL 28, 564

The relative efficacy of MDL 28,564 and NKA ($\varepsilon_{NKA}/\varepsilon_{MDL}$) for the NK_2 receptor in the RPA was calculated by the method of Furchgott & Bursztyn (1967). By this method the relative efficacy of agonists can be obtained from the ratio of their fractional receptor occupancy (ρ) according to:

$$\varepsilon_1/\varepsilon_2 = \rho_2/\rho_1 \quad (2)$$

We calculated 'ρ' by the law of mass action (1), where [A] is the molar concentration of agonist, and K_A is the dissociation constant determined for NKA and MDL 28,564 on paired strips from the same animal by the method of irreversible alkylation with Pbz (see the above section). Control pre-Pbz response data for each agonist were then replotted to obtain response vs log ρ. The antilog of the distance between the two curves along the abscissae, was taken as the relative efficacy (Furchgott & Bursztyn, 1967).

Statistical analysis

Each value in the text, tables or figures is mean ± s.e.mean. Statistical analysis was performed by means of Student's t test for paired or unpaired data. Regression analysis of log concentration-effect curves was performed by the least squares

Table 1 Amino acid sequences of peptides used in this study

NKA-(4–10)	H-Asp-Ser-Phe-Val-Gly-Leu-Met-NH_2
[βAla^8]-NKA-(4–10)	H-Asp-Ser-Phe-Val-βAla-Leu-Met-NH_2
MEN 10,295	H-Asp-Ser-Phe-Trp-βAla-Leu-Met-NH_2
MEN 10,296	H-Asp-Tyr-Phe-Trp-βAla-Leu-Met-NH_2
MEN 10,207	H-Asp-Tyr-D-Trp-Val-D-Trp-D-Trp-Arg-NH_2
MEN 10,282	H-Asp-Tyr-D-Trp-Val-D-Trp-Trp-Arg-NH_2
MEN 10,449	H-Asp-(diI)Tyr-D-Trp-Val-D-Trp-D-Trp-Arg-NH_2
MDL 28,564	H-Asp-Ser-Phe-Val-Gly-LeuΨ(CH_2NH)Leu-NH_2
L 659,877	cyclo(Leu-Met-Gln-Trp-Phe-Gly)
R 396	AcLeu-Asp-Gln-Trp-Phe-Gly-NH_2

method, considering linear such curves between 20 and 80% of the maximal response. EC_{50} and 95% confidence limits were calculated accordingly.

Peptides

NKA, NKA (4–10), [βAla^8]-NKA (4–10), MEN 10,295, MEN 10,296, MEN 10,207, MEN 10,282 and MEN 10,449 were synthesized in our laboratory by conventional solid-phase methods. L 659,877 was obtained from Cambridge R.B. (Cambridge, U.K.). MDL 28,564 and R 396 were kind gifts of Dr S.H. Buck, Marion Merrell Dow Research Institute, and Prof. D. Regoli, Department of Physiology and Pharmacology, University of Sherbrooke, Canada, respectively. Phenoxybenzamine (Pbz) was from Smith Kline & French s.p.a. (Milano, Italy). Final concentration of MEN 10,449 higher than 10 μM could not be tested because of precipitation in the organ bath. Stock solutions of Pbz (100 mM) were made by dissolving the drug in 0.05 N HCl. Water dilutions were made from frozen stock solutions just before use.

Results

Effect of MDL 28, 564

In the RPA, MDL 28,564 acted as a full agonist, being about 17 and 30 times less potent than NKA or NKA (4–10), respectively (Table 2; Figure 1a); its maximal response averaged 91% (95% C.L. = 82–100) of that to NKA. As shown in Figure 1b, the response to MDL 28,564 was competitively antagonized by MEN 10,207 and R 396 with a pA_2 of 7.87 ± 0.03 (n = 6) and 5.49 ± 0.05 (n = 6) respectively. These pA_2 values were similar to those obtained in comparable experimental conditions against NKA, or the selective NK_2 receptor agonist [βAla^8]-NKA (4–10) (Maggi *et al.*, 1990).

The dissociation constant (K_A) as well as the receptor reserve for MDL 28,564 in the RPA was calculated following partial irreversible alkylation with Pbz (Figure 2; Table 3). Both the K_A value (646.5 nM) and receptor reserve found for MDL 28,564 were lower than those for NKA in this organ (Table 3).

In the HT, MDL 28,564 (3–30 μM) beside producing a slight, not concentration-dependent contraction (not exceeding 10% of the response to NKA, or NKA (4–10), Figure 1c, n = 14) competitively antagonized the response to NKA (Figure 1d) or [βAla^8]-NKA (4–10) with pA_2 values of 6.21 ± 0.09 and 6.25 ± 0.12 (n = 12 and 4, respectively). Therefore, in spite of the different mode of action of MDL 28,564, no difference was

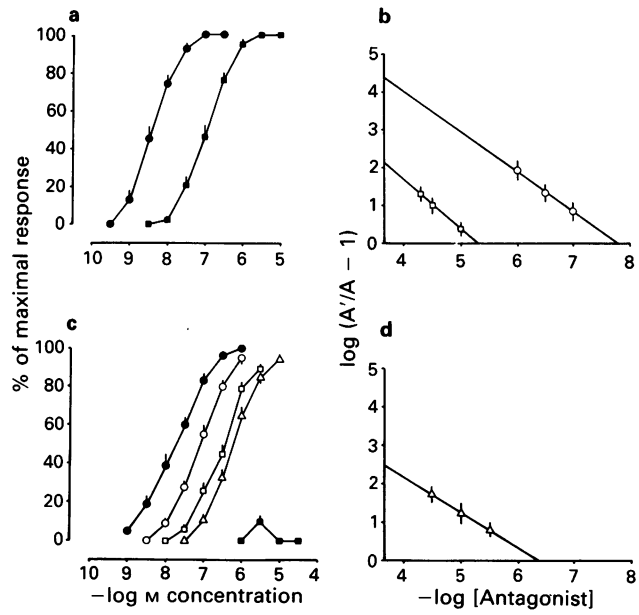

Figure 1 (a) Concentration-response curve to neurokinin A (NKA) (●) or MDL 28,564 (■) in the endothelium-deprived rabbit pulmonary artery (RPA). Each value is mean of 8–12 experiments with s.e. shown by vertical lines. (b) Schild plots showing the antagonism of MDL 28,564-induced contractions of the RPA by MEN 10,207 (○) and R 396 (□). Each value is mean of 4 experiments; s.e. shown by vertical lines. (c) Concentration-response curve to neurokinin A in the hamster isolated trachea (HT) in control (●, n = 12) or in the presence of various concentrations of MDL 28,564 (○, 3 μM; □, 10 μM; △, 30 μM; contact time 15 min for each concentration, n = 4 each); (■) effect of MDL 28,564 alone. Each value is mean of 4–6 experiments; s.e. shown by vertical lines. (d) Schild plot showing the antagonism of the contractile response to NKA in the HT by MDL 28,564. Each value is mean of 4 experiments; vertical lines show s.e.

Table 2 Comparison of the activity of various NK_2 receptor ligands in the endothelium-denuded rabbit pulmonary artery (RPA) and in the hamster trachea (HT)

	RPA			*HT*		
Peptide	pD_2	α	pA_2	pD_2	α	pA_2
NKA	8.10** (8.0–8.20)	1	...	7.30 (7.21–7.39)	1	...
NKA (4–10)	8.34** (8.14–8.54)	1 (0.9–1.1)	...	7.45 (7.30–7.60)	1 (0.9–1.1)	...
MDL 28,564	6.86 (6.74–6.98)	0.91 (0.82–1.0)	...	...	...	6.21 (5.99–6.42)
MEN 10,295	6.31 (6.0–6.61)	0.98 (0.9–1.1)	...	5.71 (5.4–6.01)	0.57 (0.47–0.67)	...
MEN 10,296	6.0 (5.77–6.23)	0.85 (0.77–0.93)	...	5.76 (5.38–6.14)	0.75 (0.65–0.85)	...
MEN 10,207§	...	...	7.89** (7.71–8.06)	...	...	5.94 (5.72–6.18)
MEN 10,282	...	...	6.47 (6.13–6.81)	...	...	6.12 (5.77–6.47)
MEN 10,449	...	...	5.60 (5.33–5.88)	...	...	5.58 (5.25–5.90)
L 659,877	...	...	6.72 (6.50–7.0)	...	...	7.92 (7.84–8.0)

Each value is mean of at least 6 determinations. In parentheses are 95% C.L.
$pD_2 = -\log EC_{50}$.
pA_2 values were obtained by means of the constrained plot method as described by Tallarida *et al.* (1979).
α = intrinsic activity, expressed as a fraction of the maximal response to neurokinin A.
** Significantly different from the corresponding value in HT: $P < 0.01$.
§ Data for MEN 10,207 are from Maggi *et al.*, 1990.

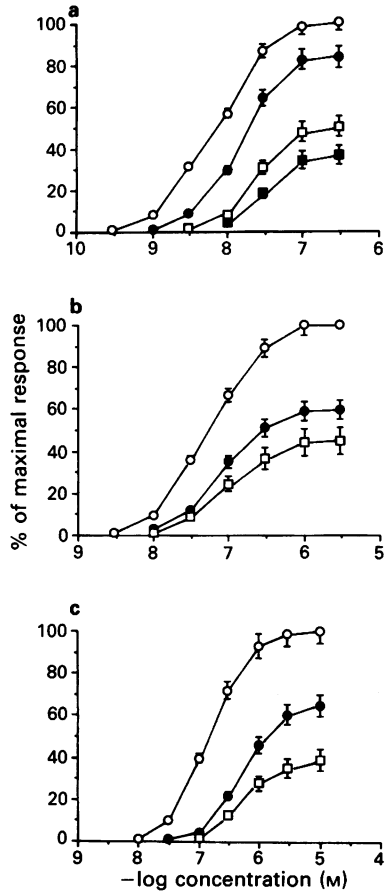

Figure 2 (a) Concentration-response curves to neurokinin A in the endothelium-deprived rabbit pulmonary artery (RPA) before (○) or after 30 min incubation with phenoxybenzamine 10 μM (●), 30 μM (□) and 50 μM (■). (b) Concentration-response curves to neurokinin A in the hamster isolated trachea (HT) before (○) or after 30 min incubation with phenoxybenzamine 10 μM (●) and 20 μM (□). (c) Concentration-response curves to MDL 28,564 in the RPA before (○) or after 30 min incubation with phenoxybenzamine 10 μM (●) and 15 μM (□).

Table 3 Irreversible antagonism by phenoxybenzamine of neurokinin A (NKA) and MDL 28,564 contractile effects in the endothelium-denuded rabbit pulmonary artery (RPA) and of NKA contractile effect in the hamster trachea (HT)

Values	*RPA*		*HT*
Agonists	*MDL 28,564*	*NKA*	*NKA*
EC_{50} (nM)	162.4	8.0**	50.9
	(121.6–203.2)	(6.4–9.6)	(40.9–60.9)
K_A (nM)	645.5	79.8**	169.7
	(344.2–948.8)	(53.0 – 106.5)	(132.1–207.3)
Reserve	3.1	11.1**	3.62
	(2.04–4.16)	(7.4–14.8)	(2.7–4.5)
q (%)	30.3	21.9	33.7
	(22.3–38.2)	(16.1–27.7)	(27.8–39.6)
ρ (%)	26.9	11.6**	24.1
	(20.2–33.5)	(7.9–15.3)	(18.7–29.5)

Each value is mean of at least 12 determinations plus 95% C.L. Phenoxybenzamine (10–50 μM) was left in contact with tissues for 30 min.
EC_{50} = agonist concentration producing 50% of maximal response.
K_A = agonist concentration producing 50% of maximal receptor occupancy.
Reserve = K_A/EC_{50}.
q = fraction of receptors remained unblocked after incubation with phenoxybenzamine.
ρ = fractional occupancy of receptors by NKA or MDL 28,564 required to elicit half maximal response.
** Significantly different from the corresponding value in HT: $P < 0.01$.

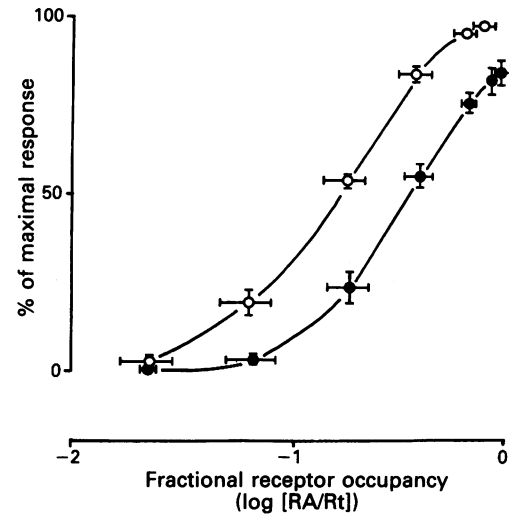

Figure 3 Comparison of the efficacy of neurokinin A (NKA, ○) (ε_{NKA}) relative to that of MDL 28,564 (●) (ε_{MDL}) on the NK_2 receptor of the rabbit pulmonary artery ($\varepsilon_{NKA}/\varepsilon_{MDL}$ = 2.2). Ordinates: percentage of the maximal response to NKA in each experiment. Abscissae: logarithms of the receptor occupancy of various concentration of agonists. Each value represents mean of 6 determinations; s.e. shown by bars.

found between the affinity of this peptide for the NK_2 receptor in the RPA (K_A = 646.5 nM; pK_A = 6.19) or in the HT ($pA_2 = pK_B$ = 6.21 or 6.25).

Effect of other NKA-(4–10) analogues and L 659,877

MEN 10,295 and MEN 10,296, two analogues of [βAla^8]-NKA (4–10) (see Table 1), behaved as full or virtually full agonists in the RPA (Table 2), being 60 and 125 times less potent than NKA, respectively. In the HT they still behaved as agonists, even if with lower potency and intrinsic activity, as compared to the RPA (Table 2).

MEN 10,282 and MEN 10,449, two close analogues of MEN 10,207 (Table 1), acted as competitive antagonists, producing a concentration-dependent rightward shift of the curve to NKA in the RPA. Their affinity values were between 1.5 and 2.5 log units lower than those found for MEN 10,207, in the same organ (Table 2). In the HT, both MEN 10,282 and MEN 10,449 competitively antagonized the contractile effect to NKA, with potencies similar to those observed in the RPA (Table 2). Therefore both compounds were equipotent in the two preparations examined.

L 659,877, a cyclic TK antagonist (McKnight *et al.*, 1988), acted as a potent competitive antagonist of NKA contractile effects, both in RPA and HT (Table 2). In the latter organ L 659,877 was about 15 times more potent than in the RPA.

Receptor reserve for neurokinin A in rabbit pulmonary artery and hamster trachea

The dissociation constants (K_A) calculated for NKA in the RPA and HT by the method of partial irreversible alkylation of NK_2 receptors with Pbz (Figure 2), were found to be close but significantly different from each other (Table 3). The receptor reserve for NKA in the RPA was sizeable, being about 3 times higher than in the HT (Table 3). The receptor occupancy required to obtain half maximal response to NKA averaged 11.6% in the RPA and 24.1% in the HT.

Relative efficacy of neurokinin A and MDL 28,564 in the rabbit pulmonary artery

The relative efficacy of NKA and MDL 28,564 for the NK_2 receptor in the RPA was evaluated by the procedure of Furchgott & Bursztyn (1967) (see Methods for details). By using the K_A values for both NKA and MDL 28,564 in the

RPA, an occupancy-response curve was constructed (Figure 3) from which the relative efficacy between NKA and MDL 28,564 ($\varepsilon_{NKA}/\varepsilon_{MDL}$) was calculated. NKA intrinsic efficacy was 2.2 times higher than that of MDL 28,564 for the NK_2 receptor in the RPA. Such a comparison was impossible in the HT, because of the lack of intrinsic efficacy for MDL 28,564 which is unable to act as agonist up to 30 μM, a concentration sufficient to occupy 98% of total NK_2 receptors.

Discussion

We have previously provided evidence for the existence of NK_2 receptor subtypes in the RPA and HT, which are recognized with very different affinity by certain antagonists, such as R 396 (100 times more potent in the HT than in the RPA) or MEN 10,207 (100 times more potent in the RPA than in the HT) (Maggi *et al.*, 1990). The results of the present investigation point to differences in the character of NK_2 receptors mediating contractility in the RPA and HT, hence they support the concept of NK_2 receptor heterogeneity.

One of the tools employed in this study, the selective NK_2 ligand MDL 28,564 (Buck *et al.*, 1990), showed full agonist activity in the RPA, while it acted as a competitive antagonist in the HT. The contractile responses elicited by MDL 28,564 in the RPA appear to involve the same receptor activated by NKA, as indicated by the similar pA_2 values obtained with MEN 10,207 and R 396 against MDL 28,564 (present findings) or NKA and [βAla^8]-NKA (4–10) (Maggi *et al.*, 1990) as agonists. The behaviour of MDL 28,564 could be explained either in terms of differences in receptor coupling and/or density (tissue factors) between the RPA and HT or by differences existing between the two NK_2 receptors present in the above tissues. The aim of the present work was to verify these possibilities. In order to obtain a measure of the extent of tissue factors in the HT and RPA, we compared the receptor reserve for NKA in these latter organs. Indeed the size of the receptor reserve for NKA observed in the RPA and HT was slightly greater (about 3 times) in the former than that in the latter tissue. Such a difference could explain the lower potency (from 3 to 7 times) observed for NKA and other NK_2 receptor agonists in the HT as compared to the RPA (cf. Maggi *et al.*, 1990 and present findings). However, it appears doubtful that the smaller receptor reserve, measured in the HT, could explain the total loss of agonist activity for MDL 28,564 in this tissue. On the other hand the present results do indicate that the main cause of the behaviour of MDL 28,564 is the different intrinsic efficacy displayed by the compound for the two NK_2 receptors. In fact the intrinsic efficacy of MDL 28,564 in the RPA was only 2.2 times lower than that of NKA, while it was virtually undetectable in the HT. Indirect evidence supporting this hypothesis comes from the results obtained with MEN 10,295 and MEN 10,296, two [βAla^8]-NKA (4–10) analogues showing weaker agonist properties than MDL 28,564 in the RPA. If 'tissue factors', i.e. receptor coupling and density, which are regarded as completely drug-independent parameters, were the determinants for the loss of MDL 28,564 agonist activity in the HT, then these factors would have similarly affected the agonist activity of MEN 10,295 and MEN 10,296 in the former organ. On the contrary MEN 10,295 and 10,296 maintain agonist properties in the HT, demonstrating that tissue factors are of little relevance for the expression of agonist activity in the RPA and HT within this class of peptides. Measurements of affinity constants (true affinity, K_A) for MDL 28,564 and NKA did not provide a means of distinguishing between subtypes. In fact MDL 28,564 binds to both subtypes with comparable affinity (in terms of pK_A or pK_B), and the difference in the K_A value noted for the natural ligand NKA, though significant, is too small to indicate receptor heterogeneity. A similar behaviour of MDL 28,564 has been reported by Buck *et al.* (1990) for other tissues containing NK_2 receptors: the guinea-pig trachea on one hand and the hamster urinary bladder and rat vas deferens on the other (see also Introduction). These findings suggest that the pseudopeptide MDL 28,564, derived from the NKA (4–10) sequence by reduction of the bond between positions 9 and 10, recognizes putative NK_2 receptor subtypes with similar affinity but possesses sufficient intrinsic efficacy for only one of the subtypes. On the basis of these data one may speculate that the terminal region of the sequence (e.g. the residues 9 and 10) is crucially involved in receptor activation, while the remaining sequence contributes to receptor recognition and binding.

An interesting finding emerges from the comparison of various antagonists containing D-Trp in their sequence. For example MEN 10,282 and MEN 10,449, two close analogues of MEN 10,207, are as potent as the parent compound in the HT but are weaker antagonists than MEN 10,207 in the RPA. This observed reduction of antagonist potency occurring in the latter tissue, suggests that MEN 10,207 possesses rather exacting structural requirements which determine its ability to bind with high affinity to the RPA NK_2 subtype. On the other hand the cyclic antagonist L 659,877 exhibits greater potency (15 times) in inhibiting NK_2 receptor-mediated responses in the HT relative to the RPA, suggesting that, among antagonists, the ability to selectively recognize subtypes is not confined to the NKA sequence. From the limited examples presented here it appears that the NK_2 receptor of the HT may accommodate a wider range of chemical moieties.

In conclusion this investigation provides further evidence for NK_2 receptor heterogeneity. On the basis of the present and previous findings (Maggi *et al.*, 1990) we conclude that the NK_2 receptor subtype present in the RPA is recognized with the highest affinity by MEN 10,207 and with high intrinsic efficacy (full agonist activity) by MDL 28,564. On the contrary the NK_2 receptor subtype present in the HT is recognized with the highest affinity by L 659,877, and with low (or absent) intrinsic efficacy (antagonist activity) by MDL 28,564.

References

ARUNLAKSHANA, O. & SCHILD, H.O. (1959). Some quantitative uses of drug antagonists. *Br. J. Pharmacol. Chemother.*, **14**, 48–58.

BUCK, S.H. & BURCHER, E. (1987). Differential sensitivity to phenoxybenzamine alkylation among types of neurokinin binding sites. *Neuropeptides*, **9**, 33–39.

BUCK, S.H., BURCHER, E., SCHULTZ, C.W., LOVENBERG, W. & O'DONAHUE, T.L. (1984). Novel pharmacology of substance K binding sites: a third type of tachykinin receptor. *Science*, **226**, 987–989.

BUCK, S.H., HARBESON, S.L., HASSMANN III, C.F., SHATZER, S.A., ROUISSI, N., NANTEL, F. & VAN GIERSBERGEN, P.L.M. (1990). [Leu$^9\psi$(CH$_2$NH)Leu^{10}]-Neurokinin A (4–10) (MDL 28,564) distinguishes tissue tachykinin peptide NK_2 receptors. *Life Sci.*, **47**, PL-37-PL41.

BUCK, S.H., PRUSS, R.M., KRSTENANSKY, J.L., ROBINSON, P.J. & STAUDERMAN, K.A. (1988). A tachykinin peptide receptor joins an elite club. *Trends Pharmacol. Sci.*, **9**, 3–5.

DION, S., D'ORLEANS-JUSTE, P., DRAPEAU, G., RHALEB, N.E., ROUISSI, N.E., TOUSIGNANT, C. & REGOLI, D. (1987). Characterization of neurokinin receptors in various isolated organs by the use of selective agonists. *Life Sci.*, **41**, 2269–2276.

D'ORLEANS-JUSTE, P., DION, S., DRAPEAU, G. & REGOLI, D. (1985). Different receptors are involved in the endothelium-mediated relaxation and the smooth muscle contraction of the rabbit pulmonary artery in response to substance P and related neurokinins. *Eur. J. Pharmacol.*, **125**, 37–44.

DRAPEAU, G., D'ORLEANS-JUSTE, P., DION, S., RHALEB, N.E., ROUISSI, N.E. & REGOLI, D. (1987). Selective agonists for substance P and neurokinin receptors. *Neuropeptides*, **10**, 43–48.

FURCHGOTT, R.F. (1966). The use of β-haloalkylamines in the differentiation of receptors and in the determination of dissociation constants of receptor-agonist complexes. In *Advances in Drug Research*. ed. Harper, N.J. & Simmonds, A.B. Vol. 3, pp. 21–55. New York, N.Y.: Academic Press, Inc.

FURCHGOTT, R.F. & BURSZTYN, P. (1967). Comparison of dissociation constants and of relative efficacies of selected agonists acting on parasympathetic receptors. *Ann. N.Y. Acad. Sci.*, **144**, 882–899.

HARBESON, S.L., BUCK, S.H., HASSMANN III, C.F. & SHATZER, S.A. (1990). Synthesis and biological activity of [$\psi(CH_2NH)$] analogs of neurokinin A (4–10). In *Peptides: Chemistry, Structure and Biology*. ed. Rivier, J.E. & Marshall, G.R. pp. 180–181. Leiden: Escom.

HERSHEY, A.D. & KRAUSE, J.E. (1990). Molecular characterization of a functional cDNA encoding the rat substance P receptor. *Science*, **247**, 958–962.

KENAKIN, T.P. (1987). *Pharmacologic Analysis of Drug-Receptor Interaction*. New York, N.Y.: Raven Press.

LEE, C.M., CAMPBELL, N.J., WILLIAMS, B.J. & IVERSEN, L.L. (1986). Multiple tachykinin binding sites in peripheral tissue and brain. *Eur. J. Pharmacol.*, **130**, 209–216.

LIN, C.W. & MUSACCHIO, J.M. (1983) The determination of dissociation constants for substance P and substance P analogues in the guinea-pig ileum by pharmacological procedures. *Mol. Pharmacol.*, **23**, 558–562.

MAGGI, C.A., GIULIANI, S., SANTICIOLI, P., REGOLI, D. & MELI, A. (1987). Peripheral effects of neurokinins: functional evidence for the existence of multiple receptors. *J. Autonom. Pharmacol.*, **7**, 11–21.

MAGGI, C.A., PATACCHINI, R., GIULIANI, S., ROVERO, P., DION, S., REGOLI, D., GIACHETTI, A. & MELI, A. (1990). Competitive antagonists discriminate between NK_2 tachykinin receptor subtypes. *Br. J. Pharmacol.*, **100**, 588–592.

MAGGI, C.A., PATACCHINI, R., ROVERO, P. & MELI, A. (1989). The hamster isolated trachea: a new preparation for studying NK-2 receptors. *Eur. J. Pharmacol.*, **166**, 435–440.

MASU, Y., NAKAYAMA, K., TAMAKI, H., HARADA, Y., KUNO, M. & NAKANISHI, S. (1987). cDNA cloning of bovine substance-K receptor through oocyte expression system. *Nature*, **329**, 836–838.

McKNIGHT, A.T., MAGUIRE, J.J., WILLIAMS, B.J., FOSTER, A.C., TRIDGETT, R. & IVERSEN, L.L. (1988). Pharmacological specificity of synthetic peptides as antagonists at tachykinin receptors. *Reg. Pept.*, **22**, 127.

REGOLI, D., DRAPEAU, G., DION, S. & COUTURE, R. (1988). New selective agonists for neurokinin receptors: pharmacological tools for receptor characterization. *Trends Pharmacol. Sci.*, **9**, 290–295.

REGOLI, D., DRAPEAU, G., DION, S. & D'ORLEANS-JUSTE, P. (1987). Pharmacological receptors for substance P and neurokinins. *Life Sci.*, **40**, 109–116.

REGOLI, D., DRAPEAU, G., DION, S. & D'ORLEANS-JUSTE, P. (1989). Receptors for substance P and related neurokinins. *Pharmacology*, **38**, 1–15.

ROVERO, P., PESTELLINI, V., PATACCHINI, R., GIULIANI, S., SANTICIOLI, P., MAGGI, C.A., MELI, A. & GIACHETTI, A. (1989). A potent and selective agonist for NK_2 tachykinin receptor. *Peptides*, **10**, 593–595.

ROVERO, P., PESTELLINI, V., MAGGI, C.A., PATACCHINI, R., REGOLI, D. & GIACHETTI, A. (1990). A highly selective NK_2 tachykinin receptor antagonist containing D-tryptophan. *Eur. J. Pharmacol.*, **175**, 113–115.

TALLARIDA, R.J., COWAN, A. & ADLER, M.W. (1979). pA_2 and receptor differentiation: a statistical analysis of competitive antagonism. *Life Sci.*, **25**, 637–654.

VAN GIERSBERGEN, P.L.M., SHATZER, S.A., HENDERSON, A.K., LAI, J., NAKANISHI, S., YAMAMURA, H.I. & BUCK, S.H. (1991). Characterization of a tachykinin peptide NK_2 receptor transfected into murine fibroblast B82 cells. *Proc. Natl. Acad. Sci. U.S.A.*, **88**, 1661–1666.

VAUGHT, J.L., SCOTT, R.W. & JACOBY, H.I. (1986). A differentiation between peripheral and central neurokinin receptors using phenoxybenzamine. *Eur. J. Pharmacol.*, **125**, 325–331.

YOKOTA, Y., SASAI, Y., TANAKA, K., FUJIWARA, T., TSUCHIDA, K., SHIGEMOTO, R., KAKIZUKA, A., OHKUBO, H. & NAKANISHI, S. (1989). Molecular characterization of a functional cDNA for rat substance P receptor. *J. Biol. Chem.*, **264**, 17649–17652.

(Received December 3, 1990
Revised April 23, 1991
Accepted May 16, 1991)

Br. J. Pharmacol. (1991), **104**, 97–104

ICI D7114 a novel selective β-adrenoceptor agonist selectively stimulates brown fat and increases whole-body oxygen consumption

[1]Brian R. Holloway, Ralph Howe, Balbir S. Rao, Donald Stribling, Rachel M. Mayers, Martyn G. Briscoe & Jacqueline M. Jackson

ICI Pharmaceuticals, Alderley Park, Macclesfield, Cheshire, SK10 4TG

1 ICI D7114 is a novel, β-adrenoceptor agonist which stimulates whole body oxygen consumption in conscious rats, cats and dogs and brown adipose tissue (BAT) activity in conscious rats. Treatment of rats with ICI D7114 stimulated oxygen consumption (ED_{50}, 0.04 mg kg^{-1}, p.o.) and BAT mitochondrial guanosine diphosphate (GDP)-binding (ED_{50}, 0.15 mg kg^{-1}, p.o.) with no chronotropic effects on the heart at these doses.

2 Reference β-adrenoceptor agonists, isoprenaline and clenbuterol, also stimulated oxygen consumption and BAT activity but were less selective because they also produced effects on heart rate at these doses.

3 Treatment of conscious rats with ICI D7114 did not attenuate the chronotropic effects on the heart of a subsequent isoprenaline challenge.

4 Administration of ICI D7114 or of its acid metabolite had no effect in a cat soleus muscle model of tremor or on blood potassium levels in the conscious dog, indicating lack of effects at β_2-adrenoceptors.

5 The results indicate that ICI D7114 may have activity at atypical β-adrenoceptors in brown adipose tissue leading to increased whole body oxygen consumption.

Keywords: Brown adipose tissue; non-shivering thermogenesis; ICI D7114; β_3-agonist; uncoupling protein

Introduction

Obesity is associated with increased risk of hypertension, hyperlipidaemia, ischaemic heart disease, non-insulin dependent diabetes and excessive mortality (National Institute of Health Consensus Development Panel, 1985). There is clear evidence that weight reduction may have a beneficial impact on some of the risks associated with obesity (Build Study, 1979). Despite the undoubted benefits of weight reduction, the results of dieting are often disappointing, one main reason being that reduction in energy intake leads to compensatory decreases in energy expenditure (Bray, 1969; Ravussin *et al.*, 1985); thus there is less weight loss than would be expected. Increasing energy expenditure *per se* or preventing the compensatory decrease in energy expenditure during dieting, offer alternative approaches to the treatment of obesity.

Extensive research has shown that there is an adaptive component of energy expenditure which takes place in the absence of muscle movement and it has been called non-shivering thermogenesis (NST). Experiments have shown that animals can increase NST when exposed to a cold environment (Smith & Roberts, 1964). Animals induced to overeat increase NST thereby reducing the impact of increased energy intake on body weight and fat stored (Rothwell & Stock, 1979). Conversely, dieting induces a compensatory decrease in NST (Rothwell & Stock, 1983a). Animals with a genetically determined predisposition to obesity may also have a decreased capacity for NST (Rothwell *et al.*, 1983b).

Experiments in animals have demonstrated that the major proportion of capacity for NST resides in brown adipose tissue (BAT) (Foster & Frydman, 1979). In cold-exposed rats or overfed rats, increased activity of BAT accounts for the enhanced capacity for NST. Conversely, in dieting (Rothwell & Stock, 1982) or genetically obese animals (Ashwell *et al.*, 1985) decreased activity of BAT leads to reduced capability for NST. BAT is richly innervated by the sympathetic nervous system (SNS) and the physiological effector of BAT is noradrenaline acting through β-adrenoceptors (Girardier & Seydoux, 1986).

Non-specific sympathomimetics can stimulate energy expenditure but also have widespread, undesirable side effects on the cardiovascular system and other tissues associated with agonist activity at β_1 and β_2-adrenoceptors. Arch and colleagues (1984) reported data on a series of compounds which were more potent in stimulating brown fat cell lipolysis than in stimulating either atria or trachea. One of these compounds BRL 26830A was demonstrated to increase energy expenditure in man and to cause weight loss (Connacher *et al.*, 1988). However, these therapeutic effects were accompanied by tremor, indicating the possibility of β_2-adrenoceptor-mediated side effects. We have recently demonstrated that a novel β-adrenoceptor agonist, ICI D7114, and its acid metabolite (Figure 1) are potent stimulants of oxygen consumption by isolated brown fat cells and have only low potency effects on atria and trachea (Holloway *et al.*, 1990). In the present paper the properties of ICI D7114 and its major metabolite are discussed. The results indicate that ICI D7114 is a potent and selective stimulant of whole body oxygen consumption with little effect on heart rate in the rat. In addition, administration of ICI D7114 did not produce β_2-adrenoceptor-mediated effects such as tremor or hypokalaemia. Other β-agonists failed to exhibit such selectivity in the same tests. The results suggest that ICI D7114 may be useful in the treatment of obesity and related diseases such as diabetes.

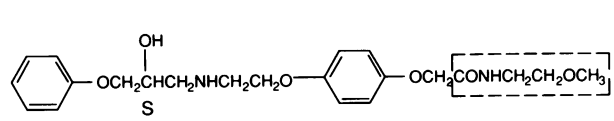

Figure 1 Structure of ICI D7114; (---) metabolized to -COOH *in vivo*.

[1] Author for correspondence at: ICI Pharmaceuticals, Bioscience II Department, Mereside, Alderley Park, Macclesfield, Cheshire SK10 4TG.

Methods

Measurement of oxygen consumption

Male, Wistar rats (Alderley Park strain, 145–175 g) were housed at a temperature of 25°C for at least two days before fasting overnight. After being fasted, individual rats were placed in airtight water jacketed chambers held at a temperature of 25°C. Resting oxygen consumption was then measured for a total of 60 min with a closed circuit system (Arundel *et al.*, 1984). At the end of this period rats treated with ICI D7114 or clenbuterol were dosed by gavage with the compounds dissolved in aqueous 0.025% polysorbate. The volume of solution given orally was 5.0 ml kg^{-1} body weight. In the case of rats treated with isoprenaline, the compound was dissolved in saline and administered by the subcutaneous route in a volume of 1.0 ml kg^{-1}. Control rats were given excipient alone. After dosing, the rats were returned to the chambers and oxygen consumption measured for at least a further 60 min. Oxygen consumption readings from the first 15 min after the rats were put into the chambers were discarded because of the high locomotor activity of the control and treated rats. Oxygen consumption was measured continually but expressed as 5 min means. Resting oxygen consumption, before dosing was taken as the mean of the lowest, three consecutive 5 min values. Peak oxygen consumption after dosing was defined as the mean of the highest, three consecutive readings. Increases in oxygen consumption were determined as the difference between the mean post and predose levels and were expressed as ml O_2 min^{-1} (kg body $weight^{0.75})^{-1}$.

Oxygen consumption in dogs and cats was estimated with an open-circuit system as described by Holloway *et al.* (1985). This method does not correct for possible changes in the respiratory exchange ratio. However even maximum changes in respiratory quotient would introduce an error in the measurement of only 6.3%. Animals were trained to sit for periods of several hours in a large ventilated box. The effects of ICI D7114 on oxygen consumption in dogs were assessed in two series of experiments. In the first series, four dogs received gelatin capsules containing 0.1, 1.0 or 10.0 mg kg^{-1} of ICI D7114 or a placebo capsule containing lactose. Each dog received each treatment with a washout period of at least one week between treatments. In the second series the effects of 0.01, 0.03 and 0.1 mg kg^{-1} ICI D7114 were compared with placebo. The effects of treatment with placebo capsules or capsules containing 0.1 or 10.0 mg kg^{-1} of ICI D7114 were also assessed in five cats in the same way as described for dogs. When the effects of treatment on oxygen consumption were assessed, animals were placed in the box and oxygen consumption measured for a baseline period of 1 h. After this period the animals were given a placebo or drug containing capsule and oxygen consumption was measured continuously for a further 4 h.

All values for oxygen consumption were corrected to Standard Temperature and Pressure (STP).

Measurement of brown adipose tissue guanosine diphosphate binding

Male, Wistar rats (Alderley Park strain, 150–175 g) were housed at 4°C for 5 days and then transferred to housing at a temperature of 25°C for 2 days. Housing at 4°C increased the amount of BAT so that there was sufficient material to carry out the assay, and capacity for guanosine diphosphate (GDP)-binding was increased. Transfer to a warm room at the end of cold exposure resulted in low basal GDP-binding. After 48 h at 25°C the rats were dosed in the same way as described for metabolic rate experiments. One hour after dosing the rats were killed by cervical dislocation. The interscapular BAT was dissected and placed in a small beaker containing 1 ml ice cold 0.25 M sucrose, 5 mM N-tris (hydroxymethyl)-2-amino-ethane sulphonate (TES), 0.2 mM EDTA, pH 7.2. The samples of BAT were finely minced with scissors and homogenized in a total volume of 10 ml of buffer with a Braun teflon and glass homogenizer at 1400 r.p.m. with four complete strokes. The homogenate was filtered through four layers of gauze and the gauze was washed with a further 5 ml of buffer. The filtered homogenate and washings were poured into a 15 ml centrifuge tube and made up to volume with buffer. A crude mitochondrial fraction was prepared by centrifugation in a Sorvall RC-5B refrigerated centrifuge at 4°C. The homogenate was centrifuged at 8000 *g* for 15 min. The resulting pellet was resuspended in 2 ml of 0.25 M sucrose. Mitochondrial protein was determined by the method of Lowry *et al.* (1951) with a bovine serum albumin standard. Mitochondrial [^{3}H]-GDP-binding was determined by the method of Nicholls (1976). Briefly, 0.25 ml aliquots of each mitochondrial sample were incubated in triplicate for 1 min in a medium containing 100 mM sucrose, 20 mM TES, 10 mM choline chloride, 5 μM rotenone, 100 μM sodium atractyloside and 0.5 μCi ml^{-1} [^{14}C]-sucrose. At this time [^{3}H]-GDP was added to give a final concentration of 10 μM and a specific activity of 1.0 μCi ml^{-1}. Following a further period of 1 min incubation the mitochondria were collected on filters (Whatman GF/F) which had been washed with 1 ml of distilled water. The mitochondria and filters were washed twice with 1.0 ml aliquots of distilled water. Filtration and washing operations were carried out with a Brandel cell harvester (Semat, St. Albans, England). Radioactivity remaining in the filters was determined by liquid scintillation counting using PCS scintillant (Amersham, England). GDP-binding was calculated after allowing for the extra-matrix volume trapped on the filter as estimated from the sucrose space and expressed in terms of mg mitochondrial protein. In preliminary experiments non-specific binding was determined in the presence of 200 μM GDP as at this concentration [^{3}H]-GDP is maximally displaced from the GDP-binding sites and non-specific binding is a constant proportion of the free nucleotide. By use of the method described, non-specific binding was negligible (<1%) and was not affected by drug treatment. Therefore in the results reported no correction was made for non-specific binding.

Heart rate in conscious rats

Newly weaned (21–25 days) male rats were caged in groups of three in a room at a temperature of 29°C and allowed free access to laboratory chow and water. In preliminary experiments, housing rats at 29°C (thermoneutral temperature for the rat) was found to lead to decreased activity of BAT and capacity for NST. Therefore this procedure reduced propensity for reflex tachycardia secondary to stimulation of metabolic rate and allowed an assessment of the effect of compounds on heart rate which were due to direct effects on the cardiovascular system. After 10–14 days the rats were trained to rest in specially constructed chambers. Foot-pad electrodes in the base of the chambers allowed collection of ECG signals and determination of heart rate. On day 15 the rats were dosed with a solution of ICI D7114, other drugs or vehicle prepared as described above. After dosing, rats were placed in the chambers and 15 min later heart rate was measured at 5 min intervals for the next 15 min. Heart rate was expressed as the mean of the three readings for each rat. Each experiment was carried out according to a 6 × 6 latin square design.

The cat model of tremor

The effects of ICI D7114 and salbutamol were assessed in a cat model of tremor based on that of Bowman & Zaimis (1958). The effects of the acid metabolite of ICI D7114 were also assessed in this model since metabolism studies had demonstrated that after oral administration of ICI D7114 the acid was the major metabolite (unpublished observations). Cats of either sex (2–4 kg) were fasted overnight before being anaesthetized with chloralose (80 mg kg^{-1}, i.p.), and pheno-

barbitone (12 mg kg^{-1}, i.p.). The left femoral vein was cannulated for the administration of drugs. A catheter was also placed in the carotid artery for monitoring blood pressure and heart rate. The animals were ventilated naturally through a tracheotomy. Throughout the experiment blood gases were maintained within normal limits. The left hind leg was then securely fixed, the soleus muscle isolated and the calcaneal tendon sectioned before being attached to a calibrated force transducer. The sciatic nerve was exposed through an incision in the hind leg 2–3 cm from the abdomen and a bipolar electrode placed on the nerve. The nerve was then stimulated with a train of stimuli (frequency 5–10 Hz) with a Grass stimulator once every 10 s, with a pulse width of 0.15 ms and an initial voltage of 1 V. Once a muscle twitch had been obtained the voltage was gradually increased until a maximum twitch tension was obtained.

The preparation was then stimulated for 20 min before the administration of drugs. After this time a priming dose of isoprenaline (0.5 μg kg^{-1}, i.v.) was given. When twitch tension had returned to basal levels a dose-response relating intravenous injections of isoprenaline in the range 0.01–1.0 μg kg^{-1}, i.v. to peak changes in soleus muscle twitch tension was constructed. When soleus muscle twitch tension had returned to control values cumulative dose-response curves relating intravenous injections of ICI D7114 its acid metabolite or salbutamol to twitch tension were obtained.

The potency of the test compound in reducing soleus muscle twitch tension was expressed as the dose (ED_{50}) causing 50% of the maximal effect of the compound. The intrinsic sympathomimetic activity (ISA) was expressed as a percentage of the maximal change brought about by isoprenaline.

Blood potassium in conscious dogs

Dogs with indwelling venous and arterial catheters were dosed with capsules containing ICI D7114 or a placebo preparation of lactose. Blood samples were taken via the catheters at intervals after dosing for the determination of blood potassium with a Nova Stat Profile blood gas analyser. For comparison the effects of adrenaline infusion were determined in the same dogs in separate experiments.

Drugs

ICI D7114 and its acid metabolite were synthesized at ICI Pharmaceuticals. Isoprenaline, adrenaline and salbutamol were obtained from Sigma, Chemical Company Ltd., Poole, Dorset. Clenbuterol was a gift from Boehringer Ingelheim.

Statistics

Student's *t* test was used to test the significance of the difference between two independent samples. Except where stated otherwise, the system of notation illustrated below is used to indicate the level of significance (*P*) of the difference between the means of two sets of observations, i.e. control and treated groups: NS, not significantly different = $P > 0.05$; $*P < 0.05$; $**P < 0.01$; $***P < 0.001$.

Results

Oxygen consumption

Acute, oral administration of ICI D7114 to Wistar rats caused a rapid and sustained increase in oxygen consumption (Figure 2). In a dose-response study the mean resting oxygen consumption of all of the rats before dosing was 14.4 ml min^{-1} (kg$^{.75}$)$^{-1}$ ($n = 55$). Administration of the dosing vehicle alone was associated with a transient, peak increase in oxygen consumption of 3.2 ± 0.6 ml min^{-1} (kg$^{.75}$)$^{-1}$ ($n = 9$). When ICI D7114 was given at 0.03 mg kg^{-1} or greater, there were peak increases in oxygen consumption which were significantly greater than that after dosing the vehicle alone (Figure 3). The greatest increase in oxygen consumption was 10.1 ± 0.4 ml min^{-1} (kg$^{.75}$)$^{-1}$ ($n = 6$) and occurred after a dose of 10 mg kg^{-1} ICI D7114. In this experiment the dose of ICI D7114 causing 50% (ED_{50}) of the maximal increase in oxygen consumption was estimated to be 0.03 mg kg^{-1} using a curve-fitting programme. In a total of three experiments the mean ED_{50} for the effects of ICI D7114 on oxygen consumption was 0.04 ± 0.01 mg kg^{-1}. Subcutaneous administration of isoprenaline also stimulated oxygen consumption (Figure 2). In three experiments the ED_{50} for the effects of isoprenaline on peak oxygen consumption was 0.05 ± 0.03 mg kg^{-1} (Table 3).

Acute administration of ICI D7114 to male Beagle dogs (Table 1) and to cats (Table 2) of either sex also stimulated oxygen consumption without any apparent increase in motor

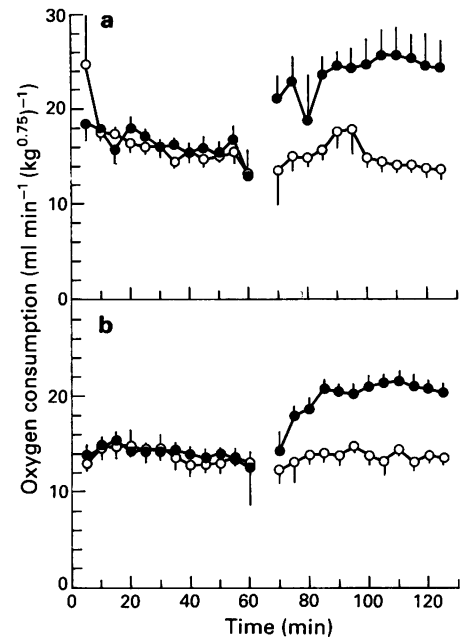

Figure 2 Time course for whole body oxygen consumption in rats treated with ICI D7114, isoprenaline or excipient. Resting oxygen consumption was measured in all rats from 0 to 60 min. Rats were then dosed by gavage with 1 mg kg^{-1} ICI D7114 (●, $n = 5$) or excipient (○, $n = 6$) (a), or given subcutaneous injections of 1 mg kg^{-1} isoprenaline (●, $n = 7$) (b).

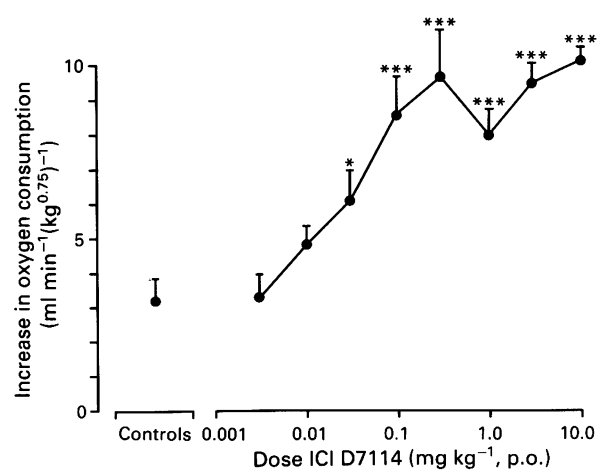

Figure 3 Effect of ICI D7114 on oxygen consumption in conscious, Wistar rats. Results are means of observations in at least four animals for each dose of drug; s.e.mean are depicted by vertical lines.

Table 1 Effects of acute administration of ICI D7114 on oxygen consumption in dogs

	Change in oxygen consumption after dosing (ml min^{-1} (kg$^{.75}$)$^{-1}$)					
	Dose of ICI D7114 (mg kg^{-1}, p.o.)					
Time after dosing (min)	0 (8)	0.01 (4)	0.03 (4)	0.1 (7)	1.0 (4)	10.0 (4)
30	0.04 ± 0.53	0.73 ± 0.55	−0.20 ± 0.45	1.33 ± 0.48	1.70 ± 1.45	0.43 ± 1.15
60	−0.23 ± 0.38	0.35 ± 0.25	0.23 ± 0.46	2.76 ± 0.95*	2.03 ± 0.93*	3.77 ± 3.10
90	−0.71 ± 0.42	0.48 ± 1.08	0.80 ± 0.44	4.45 ± 1.15**	2.97 ± 0.61***	4.00 ± 3.00
120	−0.09 ± 0.40	−0.32 ± 1.08	0.70 ± 0.37	3.26 ± 0.66***	5.20 ± 1.56*	3.38 ± 1.86
150	−0.71 ± 0.23	0.15 ± 1.20	2.18 ± 0.87*	3.16 ± 0.77**	6.75 ± 2.34*	2.77 ± 0.93*
180	−0.26 ± 0.82	−0.42 ± 1.63	0.97 ± 0.50*	3.73 ± 1.12*	4.63 ± 1.14**	4.35 ± 1.65*
210	−1.33 ± 0.92	−0.26 ± 0.96	0.53 ± 0.99	3.31 ± 0.39**	4.30 ± 1.10**	4.55 ± 1.36**
240	0.31 ± 0.34	1.65 ± 1.32	2.42 ± 1.09	2.50 ± 0.30***	3.60 ± 1.30	3.75 ± 0.72***

Results are mean ± s.e.mean of the number of observations indicated in parentheses. Each figure is the mean 30 min oxygen consumption after dosing minus the mean oxygen consumption measured for 30 min before dosing.

activity. Resting oxygen consumption in the dogs was 15.5 ± 0.4 ml min^{-1} (kg$^{.75}$)$^{-1}$ (n = 8). Doses as low as 0.03 mg kg^{-1} ICI D7114 caused an apparent increase in oxygen consumption in the dogs although this effect only achieved statistical significance at two time points. At a dose of 0.1 mg kg^{-1} ICI D7114 significantly increased oxygen consumption between 0.5 and 4.0 h after dosing. The peak increase in oxygen consumption at this dose was 28.7% above resting values. The maximum increase (43% above resting values) in oxygen consumption was achieved at a dose of 1.0 mg kg^{-1}. In cats, resting oxygen consumption was 10.3 ± 0.5 ml min^{-1} (kg$^{.75}$)$^{-1}$ (n = 5) and acute administration of 0.1 mg kg^{-1} ICI D7114 increased oxygen consumption in the cats by 2–3 ml min^{-1} (kg$^{.75}$)$^{-1}$ (19–29%) over basal values. Oxygen consumption was increased relative to basal values in cats treated with 0.1 mg kg^{-1} ICI D7114 for up to 4 h after administration, though this effect was not significant at all time points. In cats treated with 10 mg kg^{-1} ICI D7114, oxygen consumption was increased by up to 4.8 ml min^{-1} (kg$^{.75}$)$^{-1}$ (47%) compared to resting values.

Brown adipose tissue

The effect of ICI D7114 on oxygen consumption in the rat is associated with activation of brown adipose tissue as assessed by measurement of BAT mitochondrial GDP-binding. The results of three typical experiments are shown in Figure 4. Doses of ICI D7114 as low as 0.03 mg kg^{-1} tended to increase GDP-binding though this effect achieved significance in only one experiment. In two out of the three experiments summarised, a dose of 0.1 mg kg^{-1} significantly increased BAT mitochondrial GDP-binding. At a dose of 0.3 mg kg^{-1} ICI D7114 there were significant ($P < 0.001$) increases in GDP-binding in all three experiments. Maximum effects on GDP-binding were achieved at doses of 1.0 mg kg^{-1} or greater of ICI D7114. Based on figures derived from a total of nine separate experiments, the dose (ED_{50}) of ICI D7114 which increased BAT GDP-binding by 50% of the maximum was calculated to be 0.15 mg kg^{-1} with 95% confidence limits of 0.09–0.26 mg kg^{-1}.

Heart rate

Administration of ICI D7114 to conscious rats at a dose of 0.1 mg kg^{-1} had no effect on heart rate 15–30 min after dosing (Figures 5 and 6). Even at higher doses of ICI D7114 effects

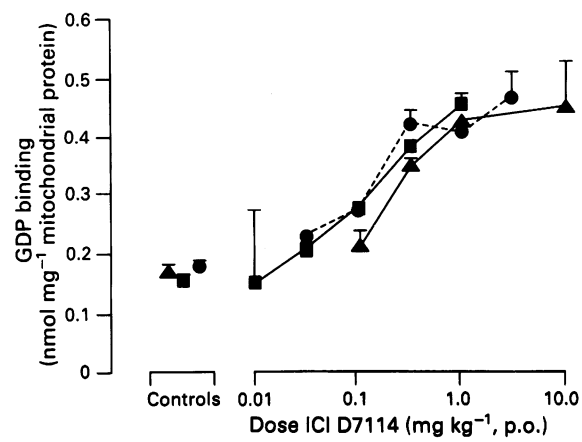

Figure 4 Effect of ICI D7114 on brown adipose tissue GDP binding in Wistar rats. The results of three separate experiments are summarised (different symbols denote the three experiments). In each experiment control values are the mean and s.e.mean (vertical bars) of observations in six rats, whilst results in treated animals are the mean and s.e.mean of observations in three rats.

Table 2 Effects of acute administration of ICI D7114 on oxygen consumption in cats

	Change in oxygen consumption after dosing (ml min^{-1} (kg$^{.75}$)$^{-1}$)		
	Dose of ICI D7114 (mg kg^{-1}, p.o.)		
Time after dosing (min)	0	0.1	10.0
30	−0.48 ± 0.45	2.82 ± 0.57**	2.72 ± 1.15*
60	−0.36 ± 0.35	2.78 ± 1.37	4.18 ± 0.65**
90	−0.34 ± 0.21	2.08 ± 0.97	4.80 ± 0.60***
120	−0.48 ± 0.36	2.26 ± 0.92	4.14 ± 0.51
150	0.94 ± 0.50	2.66 ± 1.24	2.80 ± 0.56
180	1.02 ± 0.72	2.20 ± 0.89	2.90 ± 0.62
210	1.10 ± 0.45	3.06 ± 0.97	3.02 ± 0.56*
240	0.86 ± 0.57	2.80 ± 0.94	2.84 ± 0.54*

Results are mean ± s.e.mean for 5 observations. Each figure is the mean 30 min oxygen consumption after dosing minus the mean oxygen consumption measured for 30 min before dosing.

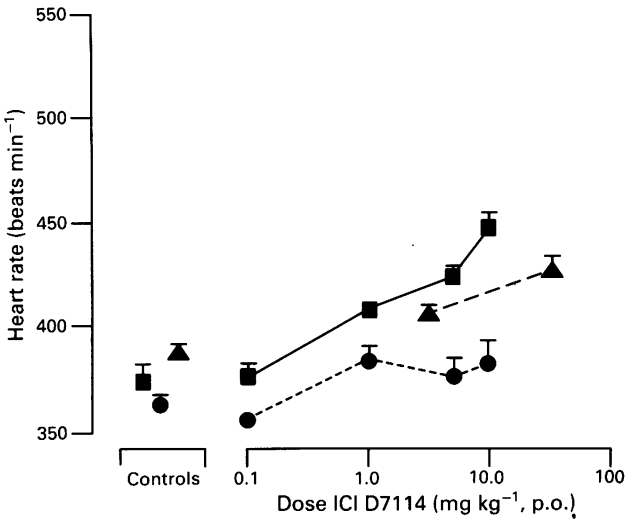

Figure 5 Effect of ICI D7114 on heart rate in conscious Wistar rats. The results of three separate experiments are summarised (different symbols denote the three experiments). In each experiment each value is the mean of three readings taken from 15–30 min in animals.

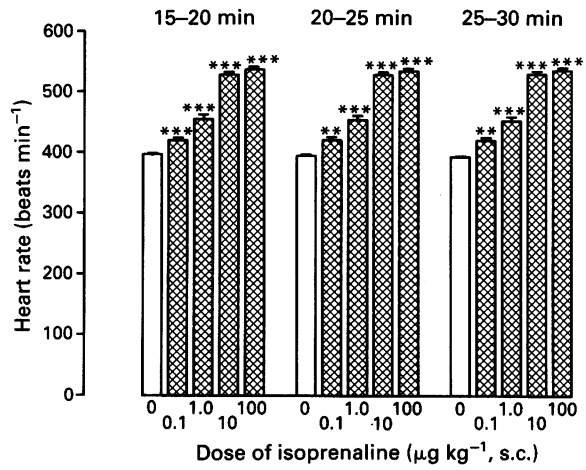

Figure 7 Time course for the effects of isoprenaline on heart rate in conscious Wistar rats. Rats were given subcutaneous injections of isoprenaline (cross hatched columns) or excipient (open columns). Heart rate was measured at 5 min intervals from 15–30 min after dosing. Results are the mean of observations in six animals in each group; s.e.mean shown by vertical bars.

on heart rate were small. The maximal effects of ICI D7114 on oxygen consumption and on BAT GDP-binding were attained at a dose of 1.0 mg kg^{-1}. At the same dose, heart rate was increased by 21 beats min^{-1} (not significantly different from controls) in one experiment and by 35 beats min^{-1} ($P < 0.01$) in a second. The greatest increase in heart rate (75 beats min^{-1}; $P < 0.001$) recorded was in one experiment where rats were given 10.0 mg kg^{-1} ICI D7114. In a second experiment where rats received this dose, heart rate was increased only by 22 beats min^{-1} (not significantly different from controls) and in one experiment where rats received a dose of 34.3 mg kg^{-1} ICI D7114 the maximum heart rate measured was 430 ± 2 beats min^{-1} an increase of 42 beats ($P < 0.001$). Although heart rate was measured over a shorter time course than metabolic rate or BAT activity, the results illustrated in Figure 6 indicate that tachycardia was maximal 15 min after administration of ICI D7114 and did not increase further at later time points.

In contrast to ICI D7114, isoprenaline had very potent effects on heart rate (Figure 7). Doses of isoprenaline as low as 0.1 μg kg^{-1} significantly increased heart rate 15–30 min after dosing. Furthermore, whereas the dose of ICI D7114 which increased oxygen consumption by 50% had little effect on heart rate, doses of isoprenaline that were below the ED_{50} on metabolic rate increased heart rate by up to 150 beats.

The sub-maximal effects of the compound on heart rate in the rat do not appear to be due to partial agonist activity at a receptor which can be stimulated by isoprenaline as pretreatment with ICI D7114 did not attenuate the effects of an isoprenaline challenge on heart rate in conscious rats (Figure 8). An acute dose (3 mg kg^{-1}, p.o.) of ICI D7114 produced a small increase in heart rate in its own right but did not attenuate the effects of a subsequent isoprenaline challenge.

Table 3 shows the effects of other β-adrenoceptor agonists in the conscious rat models. After parenteral administration, isoprenaline increased heart rate to 500 beats min^{-1} at a dose of 0.01 mg kg^{-1} with ED_{50} of 0.17 and 0.05 mg kg^{-1} on GDP-binding and oxygen consumption, respectively. Similarly the selective β_2-adrenoceptor agonist, clenbuterol, increased heart rate at doses that had little effect on thermogenesis.

Effects of ICI D7114 and its acid metabolite in animal models of β_2-adrenoceptor-mediated activity

Neither ICI D7114 nor its acid metabolite demonstrated any agonist activity in the cat model of tremor. No decrease in

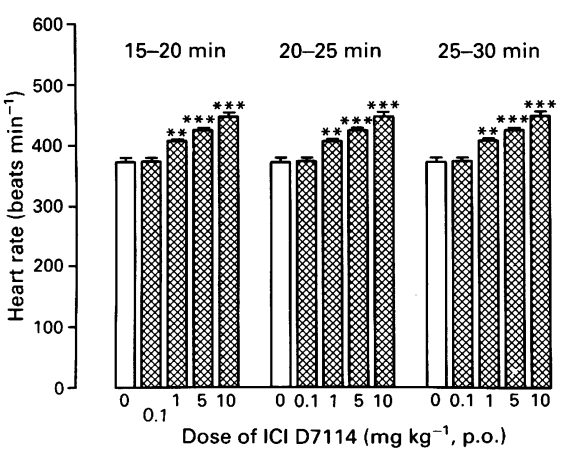

Figure 6 Time course for the effects of ICI D7114 on heart rate in conscious Wistar rats. Rats were dosed by gavage with ICI D7114 (cross-hatched columns) or excipient (open columns). Heart rate was measured at 5 min intervals from 15–30 min after dosing. Results are the mean of observations in six animals in each group; s.e.mean shown by vertical bars.

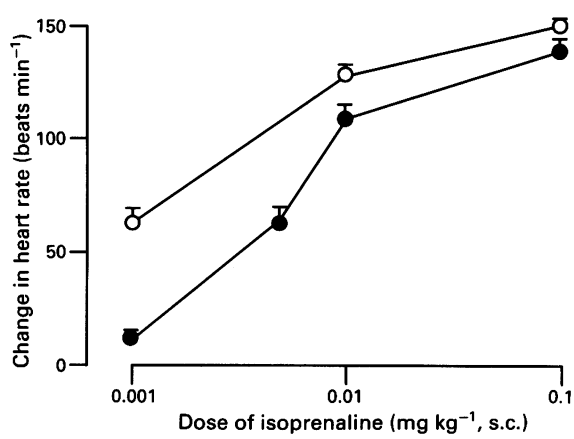

Figure 8 Effects of ICI D7114 on isoprenaline-induced tachycardia. Rats were treated with 3.0 mg kg^{-1}, p.o. ICI D7114 (○) or excipient (●). Thirty minutes later the animals were given subcutaneous injections of isoprenaline or saline. Heart rate was measured 15–30 min after the last injection. Results are the mean of observations in six animals in each group; s.e.mean shown by vertical bars.

Table 3 Effects of β-adrenoceptor agonists on brown adipose tissue (BAT), oxygen consumption and heart rate in conscious rats

Compound	Route of administration	BAT mitochondrial GDP-binding (ED_{50}, mg kg^{-1})	Oxygen consumption (ED_{50}, mg kg^{-1})	Heart rate D_{500} (mg kg^{-1})
Isoprenaline	s.c.	0.17 ± 0.04 (3)	0.05 ± 0.03 (3)	0.010 (1)
Clenbuterol	p.o.	0.39 ± 0.03 (3)	0.15 (1)	<0.1 (1)
ICI D7114	p.o.	0.15 ± 0.05 (9)	0.04 ± 0.01 (3)	>34.4 (4)

D500 = The dose of compound which increases heart rate to 500 beats min^{-1}.
Results are the mean ± s.e.mean of the number of experiments indicated in parentheses.

tension or increase in rate of relaxation was observed on administration of the compound (Table 4). In contrast to the effects of D7114 and its acid metabolite, both salbutamol and isoprenaline were potent agonists in this model.

In the conscious dog, infusion of adrenaline elicits an immediate hypokalaemic effect (Figure 9). Treatment of dogs with 0.1–10.0 mg kg^{-1}, p.o., ICI D7114 had no significant effect on blood potassium levels for up to 4 h after giving the compound (Figure 10) even though all of these doses had marked effects on oxygen consumption (Table 1).

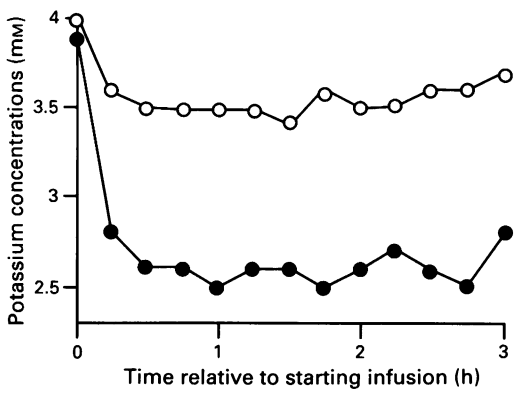

Figure 9 Effects of adrenaline infusion (2 μg min^{-1}, i.v.) (●) on blood potassium levels in conscious dogs. Control dogs (○) received infusions of an equivalent amount of saline. Results are the mean of observations in four dogs at each time point.

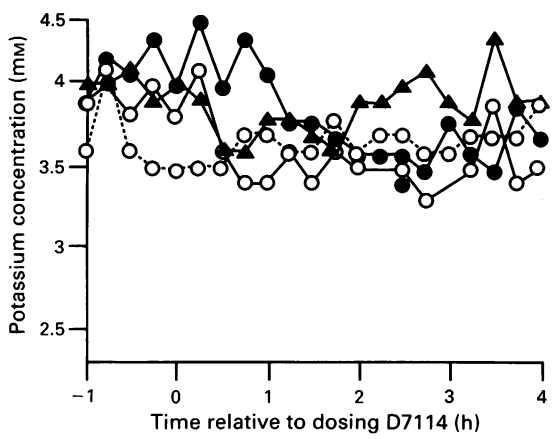

Figure 10 Effects of ICI D7114 on blood potassium levels in conscious dogs. Treated dogs received a capsule containing 0.1 (▲), 1.0 (●) or 10.0, (○——○) mg kg^{-1} ICI D7114. Control dogs (○ - - - ○) were dosed with a capsule containing a placebo preparation. The results are the mean of observations in four dogs at each time point.

Discussion

ICI D7114 potently stimulated oxygen consumption in the rat, dog and cat. The effects of the compound on increased oxygen consumption were not associated with any observed changes in locomotor activity. In the rat, the effects of the compound on oxygen consumption were associated with an increase in the activity of BAT as determined by mitochondrial purine nucleotide (GDP) binding. Levels of GDP-binding reflect the activity of the 'proton conductance pathway' associated with the inner mitochondrial membrane 'uncoupling protein', which is unique to BAT and which allows extremely high rates of respiration uncoupled to ATP-synthesis (Nicholls & Locke, 1984; Trayhurn *et al.*, 1987). These results indicate that in the rat at least, increased activity of BAT may contribute to the increase in whole body oxygen consumption in animals treated with ICI D7114, although other tissues may also be involved. Changes in the activity of BAT may also have a role in the increased oxygen consumption in other species treated with ICI D7114. Although there is an age-related decline in the activity of BAT in the dog (Ashwell *et al.*, 1987) adipose tissue in this species retains a thermogenic response to acute adrenergic stimulation even in adult dogs (Holloway *et al.*, 1985). Furthermore, when dogs were treated for two weeks with a β-adrenoceptor agonist (LY 79730) there was clear immunological evidence of increased uncoupling protein in adipose tissue depots (Ashwell *et al.*, 1987) and an increased thermogenic response to the compound (Holloway *et al.*, 1985). Similar results have been obtained in dogs treated with ICI D7114 for periods of two weeks or longer (Champigny, personal communication). Although the effects of β-adrenoceptor agonists on cat adipose tissue have not been studied, Loncar *et al.* (1986) demonstrated that short term cold exposure led to an increase in the apparent activity of BAT as judged by histological criteria.

The administration of ICI D7114 to rats selectively increased oxygen consumption and brown fat activity with attenuated effects on heart rate. Maximal effects on thermogenesis were achieved at doses that had only minimal effects on heart rate. In rats receiving 1 mg kg^{-1} ICI D7114, oxygen consumption was increased from 15 min until at least 65 min after dosing. During this period there was a small (21–35 beats min^{-1}) increase in heart rate measured between 15 and 30 min after dosing. Although heart rate was not measured after this

Table 4 Effects of ICI D7114 and its acid metabolite on the twitch tension of soleus muscle in the anaesthetized cat

Compound	Number of observations	Relaxation of twitch tension (ED_{50} μg kg^{-1}, i.v.)	% isoprenaline maximum
Isoprenaline	8	0.15 ± 0.02	100
Salbutamol	3	0.23 ± 0.06	100
ICI D7114	3	>4444	—
Acid metabolite of ICI D7114	3	>4444	—

Results are the mean ± s.e.mean of observations in the number of animals indicated.

period, it appeared to be maximal after 15–20 min as there was no significant further increase up to 30 min after dosing. In rats given 0.1 mg kg^{-1} ICI D7114, oxygen consumption and activity of BAT were increased although there was no change in heart rate during the time it was measured. At the highest dose of ICI D7114 tested (34.3 mg kg^{-1}) the maximum heart rate measured was 430 beats min^{-1} which was an increase of 42 beats min^{-1} over control values.

It is likely that some of the increase in heart rate in rats treated with ICI D7114 is secondary to the effects of the compound on oxygen consumption. An increase in whole body oxygen consumption of over 50% must be accompanied by increased cardiac output which may be achieved at least in part by increased heart rate. The data demonstrated that in the conscious rat, ICI D7114 selectively stimulated BAT and oxygen consumption with little effect on heart rate. This selectivity is not a consequence of poor absorption of ICI D7114 after oral administration at high doses. There was no difference in the effects of ICI D7114 on heart rate whether administered by parenteral or oral routes (data not shown).

In contrast isoprenaline, a non-selective β-adrenoceptor agonist, exhibited no such selectivity and caused marked tachycardia at doses below those causing a 50% increase in oxygen consumption and brown fat activity. The conscious rat models demonstrated the novelty of ICI D7114 which had more potent effects on brown fat and metabolic rate compared to direct β_1-mediated effects on the heart. The rat models also discriminated against potent β_2-agonists such as clenbuterol which can increase heart rate by both direct and reflex-mediated effects.

The direct effects of ICI D7114 and its acid metabolite at β_2-adrenoceptors have also been assessed in two further tests; an animal model of tremor in the anaesthetized cat and by estimation of blood potassium in conscious dogs. The quantitative measurement of sympathomimetic-induced tremor in experimental animals is difficult because the animals must be conscious and unrestrained. However, it has been demonstrated by Bowman & Zaimis (1958) that the action of sympathomimetics on the stimulated contractions of slow contracting muscles of anaesthetized animals is mediated by a β_2-adrenoceptor. β_2-Adrenoceptor agonists (e.g. salbutamol) produce a decrease in the tension and an increase in the rate of relaxation of maximal twitches of cat soleus muscle, so that the overall tension of the twitch is reduced. In dogs, activity of β_2-receptors has been shown to provoke a hypokalaemic response (Todd & Vick, 1971; Brown, 1985). ICI D7114 had no effect in either of these models even when tested at doses in excess of those known to stimulate oxygen consumption.

Other β-adrenoceptor agonists have been developed which exhibit selectivity for brown fat and thermogenesis (Arch *et al.*, 1984; 1987; Holloway *et al.*, 1989; Meir *et al.*, 1989). This selectivity may reside in activity at an atypical β-receptor. The classification of brown fat β-adrenoceptors has only been addressed in recent years. Previous work using agonists and antagonists suggested that the properties of the receptor mediating lipolysis in isolated white fat cells were not compatible with the involvement of either β_1- or β_2-adrenoceptors (reviewed by Zaagsma & Nahorski, 1990). The results of Arch *et al.* (1984) provided the first evidence that the β-adrenoceptor which mediated brown fat cell lipolysis was similar to the white fat cell receptor and different from β_1- and β_2-adrenoceptors. This group reported results with a new series of agonists that selectively stimulated brown fat (Arch *et al.*, 1984) and white fat (Wilson *et al.*, 1984) lipolysis. One compound in this series (BRL 37344A) was 400 and 20 fold more potent in stimulating lipolysis than atrial rate (β_1) or tracheal relaxation (β_2) respectively.

Evidence of a potential candidate for the atypical receptor has come from the isolation of a human gene encoding for a third (β_3) β-adrenoceptor and the preliminary identification of messenger RNA for this receptor in adipose tissue (Emorine *et al.*, 1989). Agonists which have been demonstrated to have potent and selective effects on BAT and whole body oxygen consumption are also potent agonists of adenosine 3',5'-cyclic monophosphate (cyclic AMP) accumulation in Chinese hamster ovary cells transfected with the β_3-receptor. Therefore the selectivity of ICI D7114 for BAT and thermogenesis may be due to selective stimulation of the β_3-receptor, although Zaagsma & Nahorski (1990) have highlighted some differences between the atypical receptor controlling lipolysis and the receptor isolated by Emorine *et al.* (1989).

One compound (BRL 26830A) reported to be a selective agonist of brown fat (Arch *et al.*, 1984) has been demonstrated to increase thermogenesis and to enhance greatly weight loss in obese patients on a low calorie diet (Connacher *et al.*, 1988). However, the beneficial effects of the compound were associated with a feeling of tremulousness. This side effect may be related to activity at β_2-receptors as BRL 26830A and a related analogue BRL 35135A were shown to have activity in the cat model of tremor and to cause hypokalaemia in conscious dogs (Holloway *et al.*, 1989). In contrast ICI D7114 exhibited no such activity, appearing to be free from activity at the β_2-receptor. Therefore, ICI D7114 may be useful in the treatment of obesity and maturity-onset diabetes, free from unwanted side effects at the β_2-receptor.

References

ARCH, J.R.S., AINSWORTH, A.T., CAWTHORNE, M.A., PIERCY, V., SENNITT, M.A., THODY, V., WILSON, C. & WILSON, S. (1984). Atypical beta-adrenoreceptor on brown adipocytes as a target for antiobesity drugs. *Nature*, **309**, 163–165.

ARCH, J.R.S., PIERCY, V., THURLBY, P.L., WILSON, C. & WILSON, S. (1987). Thermogenic and lipolytic drugs for the treatment of obesity: old ideas and new possibilities. In *Recent Advances in Obesity Research*, Vol. V, pp. 300–318, ed. Berry, E.M., Blondheim, S.H., Eliahau, H.E. & Shafrir, E. London: John Libbey.

ARUNDEL, P.A., HOLLOWAY, B.R. & MELLOR, P.M. (1984). A low-cost modular oxygen-consumption device for small animals. *J. Appl. Physiol: Respir. Environ. Exercise Physiol.*, **57**, 1591–1593.

ASHWELL, M., HOLT, S.J., JENNINGS, G., STIRLING, D.M., TRAYHURN, P. & YORK, D.A. (1985). Measurement by radioimmunoassay of the mitochondrial uncoupling protein from brown adipose tissue of obese (ob/ob) mice and Zucker (fa/fa) rats at different ages. *FEBS Lett.*, **179**, 233–237.

ASHWELL, M., STIRLING, D.M., FREEMAN, S. & HOLLOWAY, B.R. (1987). Immunological, histological and biochemical assessment of brown adipose tissue activity in neonatal, control and beta-stimulant-treated adult dogs. *Int. J. Obesity*, **11**, 357–365.

BOWMAN, W.S. & ZAIMIS, E. (1958). The effects of adrenaline, noradrenaline and isoprenaline on skeletal muscle contractions in the cat. *J. Physiol.*, **144**, 92–107.

BRAY, G. (1969). Effect of caloric restriction on energy expenditure in obese patients. *Lancet*, **ii**, 397–398.

BROWN, M.J. (1985). Hypokalaemia from β_2-receptor stimulation by circulating epinephrine. *Am. J. Cardiol.*, **56**, 3D–9D.

BUILD STUDY 1979 (1980). *Society of Actuaries and Association of Life Insurance Medical Directors of America, Chicago.*

CONNACHER, A.A., JUNG, R.T. & MITCHELL, P.E.G. (1988). Weight loss in obese subjects on a restricted diet given BRL 26830A, a new atypical beta-adrenoceptor agonist. *Br. Med. J.*, **296**, 1217–1220.

EMORINE, L.J., MARULLO, S., BRIEND-SUTREN, M.-M., PATEY, G., TATE, K., DELAVIER-KLUTCHKO, C. & STROSBERG, D. (1989). Molecular characterisation of the human Beta-3 adrenergic receptor. *Science*, **245**, 1118–1121.

FOSTER, D.O. & FRYDMAN, M.L. (1978). Nonshivering thermogenesis in the rat. II Measurements of blood flow with microspheres point to brown adipose tissue as the dominant site of the calorigenesis induced by noradrenaline. *Can. J. Physiol. Pharmacol.*, **56**, 110–122.

GIRARDIER, L. & SEYDOUX, J. (1986). Neural control of brown adipose tissue. In *Brown Adipose Tissue*. pp. 122–151 ed. Trayhurn, P. & Nicholls, D.G. London: Edward Arnold.

HOLLOWAY, B.R., BRISCOE, M., GROWCOTT, J., WILSON, C., STOCK, M.J. & SUDERA, D. (1990). In vitro and in vivo selectivity of the

beta-3 adrenoceptor agonist ICI D7114 for brown fat and thermogenesis. In *Adrenoceptors: Structure, Mechanisms, Function. Advances in Pharmacological Sciences.* Pp. 313–314. ed. Szabadi, E. Basel: Birkhauser Verlag.

HOLLOWAY, B.R., STRIBLING, D., FREEMAN, S. & JAMIESON, L. (1985). The thermogenic role of adipose tissue in the dog. *Int. J. Obesity* **9,** 423–432.

HOLLOWAY, B.R., HOWE, R., RAO, B.S. & STRIBLING, D. (1989). ICI 198157: a novel selective agonist of brown fat and thermogenesis. In *Obesity in Europe 88,* pp. 323–328. ed. Bjorntorp, P. & Rossner, S. London: John Libbey.

LONCAR, D., BEDRICA, L., MAYER, J., CANNON, B., NEDERGAARD, J., AFZELIUS, B.A. & SVAJGER, A. (1986). The effect of intermittent cold treatment on the adipose tissue of the cat. Apparent transformation from white to brown adipose tissue. *J. Ultrastructure Mol. Struct. Res.,* **97,** 119–129.

LOWRY, O.H., ROSENBROUGH, N.J. & FARR, A.L. (1951). Protein measurement with the folin-phenol reagent. *J. Biol. Chem.,* **193,** 265–275.

MEIR, M.K., BLUM-KAELIN, D., GEROLD, M., ISLER, D. & MUELLER, M. (1989). Ro40–2148: A novel thermogenic β-agonist with anti-obesity activity. In *Obesity in Europe, 88.* pp. 329–338. ed. Bjorntorp, P. & Rossner, S. London: John Libbey.

NATIONAL INSTITUTES OF HEALTH CONCENSUS DEVELOPMENT PANEL (1985). Health Implications of Obesity. *Ann. Intern. Med.,* **103,** 1073–1077.

NICHOLLS, D.G. (1976). Hamster brown adipose tissue mitochondria. Purine nucleotide control of the ion conductance of the inner membrane, the nature of the nucleotide binding site. *Eur. J. Biochem.,* **62,** 223–228.

NICHOLLS, D.G. & LOCKE, R.M. (1984). Thermogenic mechanisms in brown fat. *Physiol. Rev.,* **64,** 1–65.

RAVUSSIN, E., BURNAND, B., SCHUTZ, Y. & JEQUIER, E. (1985). Energy expenditure before and during energy restriction in obese patients. *Am. J. Clin. Nut.,* **41,** 753–759.

ROTHWELL, N.J. & STOCK, M.J. (1979). A role for brown adipose tissue in diet-induced thermogenesis. *Nature,* **281,** 31–35.

ROTHWELL, N.J. & STOCK, M.J. (1982). Effect of chronic food restriction on energy balance, thermogenic capacity, and brown adipose tissue activity in the rat. *Biosci. Rep.,* **2,** 543–549.

ROTHWELL, N.J. & STOCK, M.J. (1983a). Diet induced thermogenesis. In *Mammalian Thermogenesis*: ed. Giradier, L. & Stock, M.J. pp. 208–233. London: Chapman & Hall.

ROTHWELL, N.J., & STOCK, M.J. (1983b). Acute effects of fat and carbohydrate on metabolic rate in normal, cold-acclimated and lean and obese (fa/fa) Zucker rats. *Metabolism,* **32,** 371–376.

SMITH, R.E. & ROBERTS, J.C. (1964). Thermogenic activity of BAT in cold acclimated rats. *Am. J. Physiol.,* **206,** 143–148.

TODD, E.P. & VICK, R.L. (1971). Kalaemotropic effect of epinephrine: analysis with adrenergic agonists and antagonists. *Am. J. Physiol.,* **220,** 1964–1969.

TRAYHURN, P., ASHWELL, M., JENNINGS, G., RICHARD, D. & STIRLING, D.M. (1987). Effect of warm or cold exposure on GDP-binding and uncoupling protein in rat brown fat. *Am. J. Physiol.,* **252,** E237–E243.

WILSON, C., WILSON, S., PIERCY, V., SENNITT, M.V. & ARCH, J.R.S. (1984). The rat lipolytic β-adrenoceptor: studies using novel β-adrenoceptor agonists. *Eur. J. Pharmacol.,* **100,** 309–319.

ZAAGSMA, J. & NAHORSKI, S.R. (1990). Is the adipocyte β-adrenoceptor a prototype for the recently cloned atypical "β_3-adrenoceptor"? *Trends Pharmacol. Sci.,* **11,** 3–7.

(Received January 16, 1991
Revised April 18, 1991
Accepted May 17, 1991)

Br. J. Pharmacol. (1991), **104**, 105–112

Effects of 5-HT uptake inhibitors, agonists and antagonists on the burying of harmless objects by mice; a putative test for anxiolytic agents

[1]K. Njung'e & [2]S.L. Handley

Pharmaceutical Sciences Institute, Aston University, Aston Triangle, Birmingham B4 7ET

1 The effects of 5-hydroxytryptamine (5-HT) uptake inhibitors, agonists and antagonists have been evaluated on mouse marble-burying behaviour, a putative test for anxiolytic agents. The high levels of locomotor activity occurring on first exposure to a circular runway (runway activity) were used as a separate test of non-specific drug effects.

2 Fluvoxamine, zimeldine, indalpine and citalopram dose-dependently inhibited burying without affecting runway activity. 5-Hydroxytryptophan (5-HTP, with carbidopa), 5-methoxy-N,N-dimethyltryptamine, 8-hydroxy-2-(di-n-propylamino) tetralin (8-OHDPAT), buspirone, gepirone and ipsapirone reduced burying only at doses reducing runway activity. RU 24969 increased runway activity at all effective doses. 1-(2,5-Dimethoxy-4-iodophenyl)-2 aminopropane (DOI), 1,-(3-trifluoromethylphenyl) piperazine (TFMPP) and 1-(3-chlorophenyl)-piperazine (mCPP) potently and differentially reduced burying at doses below those affecting runway activity.

3 5-HT antagonists only reduced burying at high doses which also reduced runway activity. Burying inhibition by DOI was antagonized by ritanserin, ICI 169 369 and cyproheptadine but not by pindolol or a low (0.25 mg kg^{-1}) dose of metergoline. Burying inhibition by mCPP was not altered by any of these agents except that it was potentiated by pindolol 5 mg kg^{-1}.

4 Zimeldine burying inhibition was potentiated by ritanserin, ICI 169 369, ICS 205–930, cyproheptadine and pindolol. Runway activity was not affected by these drug combinations.

5 Zimeldine was administered in drinking water at a dose of 10 mg kg^{-1} daily for 21 days. Burying inhibition had disappeared by day 14 and did not recur 24 or 48 h after withdrawal at which times responses to DOI were at control levels.

6 Selective inhibition of marble burying was not found to be a property of 5-HT-related putative and actual anxiolytics such as buspirone, gepirone, ipsapirone, ritanserin and ondansetron. Nevertheless it was a general property of both 5-HT uptake inhibitors and 5-HT releasing agents; this generality suggests that elevated synaptic 5-HT could be responsible for the effects of these latter agents. The action of DOI may be attributable to effects at the 5-HT$_2$ receptor but those of the 5-HT agonist and releasing agent mCPP, and the uptake inhibitor zimeldine, could not be attributed to effects at any one 5-HT receptor subtype. This, together with the potentiating effect of several 5-HT antagonists on the response to zimeldine, raises the possibility of multiple interactions between 5-HT receptor subtypes.

Keywords: Antidepressive agents; anxiety disorders; animal behaviour; fenfluramine; 5-hydroxytryptamine; 5-HT antagonists; zimeldine

Introduction

Rodents bury harmless as well as noxious objects in their bedding (e.g. Terlecki *et al.*, 1979; Poling *et al.*, 1981; Broekkamp *et al.*, 1986). It has been suggested that the burying of glass marbles by mice could constitute a useful test for anxiolytic activity, since it was differentially inhibited by a variety of anxiolytics at doses which did not alter swim-induced grooming when the latter was used to control for non-specific effects (Broekkamp *et al.*, 1986; Broekkamp & Jenck, 1989). The properties of this model have recently been further investigated (Njung'e & Handley, 1991) and no evidence was found that mice treat marbles as an aversive stimulus, as would be expected of an anxiety model (Gray, 1982). Inhibition of marble burying may therefore be a correlational test of anxiolytic activity, according to the classification proposed by Treit (1985); that is, a test which models something other than anxiety but is affected by anxiolytic agents. However, although this test is responsive to benzodiazepines, ethanol and meprobamate (Broekkamp *et al.*, 1986), it appears that 5-hydroxytryptamine (5-HT)-related putative and actual anxiolytics may not selectively inhibit this burying (Broekkamp & Jenck, 1989; Broekkamp *et al.*, 1989).

The profile of the effects of monoamine uptake inhibitors is however of considerable interest. 5-HT uptake inhibitors selectively reduced marble burying at doses that did not affect grooming while mixed and noradrenaline-selective agents were found to be inactive (Broekkamp & Jenck, 1989; Broekkamp *et al.*, 1989). Antidepressants have recently been found to be effective against anxiety disorders (reviewed by Nutt & Glue, 1989). In the case of obsessive-compulsive disorder, this effectiveness appears to be confined to 5-HT uptake inhibitors (reviewed by Winslow & Insel, 1990). Since burying behaviour did not habituate, the possibility exists that it is compulsive (Njung'e & Handley, 1991).

The inhibition of burying caused by 5-HT uptake inhibitors may be due to their ability to increase the availability of 5-HT at one or more subtypes of the 5-HT receptor. The present work was therefore undertaken in an attempt to elucidate the role of 5-HT receptors in the inhibition of marble burying behaviour.

In order to control for the specificity of burying inhibition, it is necessary to test separately for general behavioural impairment (Broekkamp & Jenck, 1989) to avoid any confounding by behavioural competition between this control measure and marble burying (Njung'e & Handley, 1991). Previous work with marble burying used inhibition of swim-induced grooming to detect non-specific effects (Broekkamp *et al.*, 1986; 1989; Broekkamp & Jenck, 1989). However grooming is not amenable to instrumental measurement and is time

[1] Present address: Kenya Medical Research Institute, P.O. Box 54840 Nairobi, Kenya.
[2]Author for correspondence.

consuming to quantify. In addition, it may not be an independent measure since some 5-HT agonists induce grooming behaviour (e.g. Heaton *et al.*, 1988) and 5-HT uptake inhibitors may themselves increase certain aspects of grooming (S.M. Dursun, personal communication). We have shown that zimeldine and diazepam preferentially inhibit burying compared to locomotion in a circular runway (Njung'e & Handley, 1991). The high levels of activity which occur on initial introduction to a circular runway (runway activity) may therefore offer a more suitable control with which to detect non-specific drug effects. The differential effects on marble burying and runway activity of four 5-HT uptake inhibitors, fluvoxamine, zimeldine, indalpine and citalopram, and the 5-HT releasing agent fenfluramine, were therefore determined.

The clinical effects of 5-HT reuptake inhibitors take some time to develop. In contrast, these agents selectively inhibit burying on first dose (Broekkamp *et al.*, 1986; Broekkamp & Jenck, 1989; Njung'e & Handley, 1991). If differential inhibition of marble burying has relevance to their clinical effects, it should at least be demonstrable on chronic, as well as acute dosing. The effects of 21 days administration of zimeldine have therefore been investigated.

A preliminary account of part of this work has been communicated to the British Pharmacological Society (Njung'e & Handley, 1989).

Methods

Female mice (23–35 g, Aston-bred MF1) were held in groups of 20 under a 12 h light/12 h dark cycle (lights on 08 h 00 min), with free access to food (Pilsbury Ltd diet 41B) and tap water for at least 3 days before experiments which took place between 10 h 00 min and 18 h 00 min.

Marble-burying behaviour

As we have described (Njung'e & Handley, 1991), each mouse was placed individually in a polypropylene cage (42 × 24 × 12 cm) containing 20 clean glass marbles evenly spaced on 5 cm deep sawdust. The cage-lid was a metal grid. No food or water was present. The number of marbles at least 2/3 buried was counted 30 min later. Vehicle control mice were tested concurrently. Drug or vehicle was administered i.p. 30 min before testing except for 8-hydroxy-2-(di-n-propylamino)tetralin (8-OHDPAT) (10 min) and 5-methoxy-N,N-dimethyltryptamine (5-MeODMT) (20 min). In drug interaction experiments, antagonists were administered i.p. 10 min before the agonist or 5-HT uptake inhibitor. In the experiment with subchronic zimeldine, zimeldine or saline was injected i.p. on day 1. The mice were then offered tap water (control group) or zimeldine in tap water (test group) as their only drinking fluid for 21 days, the concentration of zimeldine being adjusted each day for the mean weight of the test group and the amount of fluid consumed on the previous day. Naive mice were withdrawn at random from the treatment and control groups for measurement of burying behaviour, 30 min after the first i.p. injection and at the corresponding time of day (10 h 00 min to 12 h 00 min) on each test day thereafter.

Runway activity

Where agents significantly affected burying, locomotor activity was measured separately in groups of 6 mice at representative doses. Individual mice were placed for 5 min in a circular runway (width 6 cm, outer radius of curvature 38 cm) mounted on an Animex activity meter (LKB-Farad, tuned to 40 μA; sensitivity 25 μA). The output of the Animex Activity Meter is in arbitrary counts. Two Animex/runways were used. For each meter, it was established that the above settings were correct to give maximal counts for translocational movements without recording static activities. However, one meter consistently gave a greater number of arbitrary counts than the other. For this reason, each test dose was investigated on one apparatus only, these runs being interspersed with those for the corresponding vehicle control mice on the same apparatus. Pretreatment times and time of day corresponded to those for the corresponding tests of drug effects on marble burying.

Statistical analysis

Non-parametric tests were used, Wilcoxon/Mann-Whitney for the 2-sample and Kruskal-Wallis analysis of variance for the n-sample case (Siegal & Castellan, 1988). The mean and its standard error have however been used in the figures to illustrate central tendency. The significance of drug interactions was assessed by Tukey's test after 2-way analysis of variance.

Drugs used

Buspirone (Bristol Myers), carbidopa (Merck, Sharp & Dohme), citalopram (Duphar), cyproheptadine (Merck Sharp & Dohme), DOI (1-2,5-dimethoxy-4-iodophenyl)-2-aminopropane) (Research Biochemicals), fenfluramine (Sigma), fluvoxamine (Duphar), gepirone (Bristol Myers), ondansetron (1,2,3,9-tetrahydro-9-methyl-3[(C2-methyl-1H-imidazol-1-yl)-methyl]-4H-carbazol-4-one) (Glaxo), 8-OHDPAT (8-hydroxy-2-(di-n-propyl-amino)tetralin) (Research Biochemicals), RU 24969 (5-methoxy-3(tetrahydro-pyridin-4-yl)1H-indole) (Roussel Uclaf), 5-MeODMT (5-methoxy-N,N-dimethyltryptamine) (Sigma), ICI 169,369 (2-(2-dimethylaminoethylthio)-3-phenylquinone) (ICI), ICS 205–930 ((3-α-tropanyl)-1H-indole-3-carboxylic acid ester) (Sandoz), indalpine (Roussel Uclaf), ipsapirone (Troponwerke), ketanserin (Janssen), metergoline (Farmitalia), methysergide (Sandoz), mCPP (1-(3-chlorophenyl)-piperazine) (Research Biochemicals), pindolol (Sigma), 5-HTP (5-hydroxytryptophan) (Sigma), ritanserin (Janssen), TFMPP (1-(3-trifluoromethylphenyl) piperazine) (Research Biochemicals), zimeldine (Astra) were all dissolved in 0.9% sodium chloride (saline) which was also used as the vehicle control.

Results

5-HT uptake inhibitors

Figure 1 shows that fluvoxamine, indalpine, citalopram (each 1–20 mg kg^{-1}) and zimeldine (1–30 mg kg^{-1}) dose-dependently reduced marble burying. Runway activity was not significantly affected, even at the highest dose of each agent used (Table 1).

5-HTP and fenfluramine

The 5-HT releasing agent fenfluramine (1–10 mg kg^{-1}) also dose-dependently reduced marble burying (Figure 2) without affecting runway activity (Table 1). Carbidopa (9 mg kg^{-1}), when given alone, reduced marble burying (Figure 2) but not runway activity (Table 1). When co-administered with 9 mg kg^{-1} carbidopa, 5-hydroxytryptophan (5-HTP, 5 mg kg^{-1}) significantly reduced both marble burying and runway activity compared with the carbidopa control, higher doses of 5-HTP further reduced marble burying (Figure 2 and Table 1).

5-HT agonists

Data on marble burying are given in Figure 2 while that for runway activity is given in Table 1. mCPP (1–20 mg kg^{-1}), TFMPP (1–20 mg kg^{-1}) and DOI (0.01–5.0 mg kg^{-1}) dose-dependently reduced marble burying while only the highest dose of mCPP or TFMPP, 20 mg kg^{-1} reduced runway activity. DOI (0.1 and 5.0 mg kg^{-1}) did not reduce runway activity at any dose. In contrast, 8-OHDPAT (10 mg kg^{-1}), buspirone

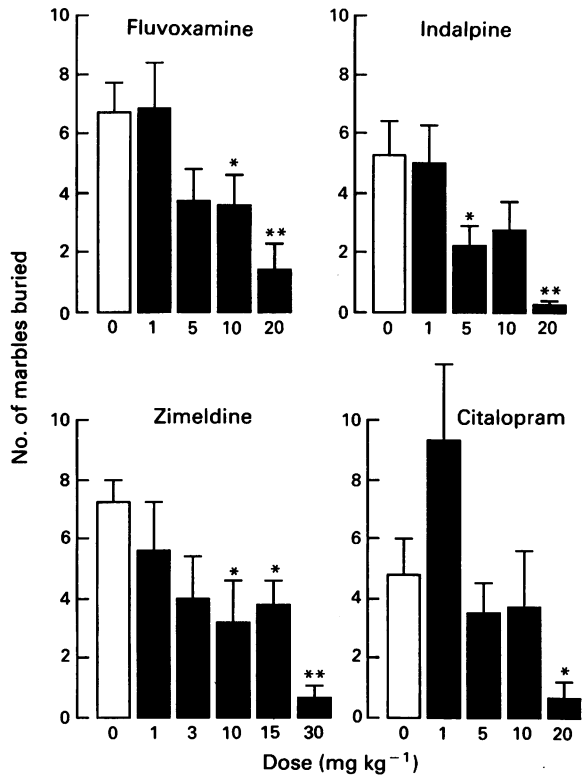

Figure 1 Effects of four 5-hydroxytryptamine uptake inhibitors on marble burying. Data are the mean number of marbles buried by female MF1 mice in a 30 min period starting 30 min after i.p. injection of vehicle (open columns) or uptake inhibitor (solid columns). Vertical bars represent s.e.mean. There were at least 6 mice per group. $*P < 0.05$; $**P < 0.01$.

(20 mg kg^{-1}) and gepirone (10 and 20 mg kg^{-1}) only reduced marble burying at high doses which also inhibited runway activity. Ipsapirone failed to affect either marble burying (5–20 mg kg^{-1}) or runway activity (20 mg kg^{-1}). RU 24969 (0.1–10 mg kg^{-1}) dose-dependently reduced marble burying, however, at the threshold dose for a significant reduction, 2.5 mg kg^{-1}, RU 24969 already produced a marked increase in runway activity.

5-HT antagonists

Table 2 shows that pindolol (5 and 10 mg kg^{-1}), ICI 169369 (1–10 mg kg^{-1}), ICS 205930 (0.1–10 mg kg^{-1}) and ondansetron (0.01–1.0 mg kg^{-1}) failed to affect marble burying. The remaining antagonists reduced marble burying only at doses at or above those reducing runway activity (Table 2): ritanserin at 20 mg kg^{-1}, ketanserin at 1 and 10 mg kg^{-1}, methysergide at 5 and 10 mg kg^{-1}, metergoline at 1.0 mg kg^{-1} and cyproheptadine at 5 mg kg^{-1}.

Effect of antagonists on DOI and mCPP responses

Figure 3 shows that the response to DOI (0.1 mg kg^{-1}) was dose-dependently reduced by ritanserin (0.2–1.0 mg kg^{-1}) and also by ICI 169369 (at 10.0 although not at 5.0 mg kg^{-1}) and cyproheptadine 2.0 mg kg^{-1}. Metergoline (0.25 mg kg^{-1}) and pindolol (5.0 mg kg^{-1}) were without effect. In no case was runway activity significantly altered by these treatments alone or in combination (Table 3). Inhibition of burying by mCPP 2.5 mg kg^{-1} (Figure 4) was not antagonized by ritanserin (5 mg kg^{-1}), cyproheptadine (1.0 and 2.0 mg kg^{-1}) or metergoline, 0.25 mg kg^{-1} and again there were no effects on runway activity (Table 3). Pindolol (5.0 mg kg^{-1}) significantly potentiated the effect of this dose of mCPP on marble burying without changing runway activity.

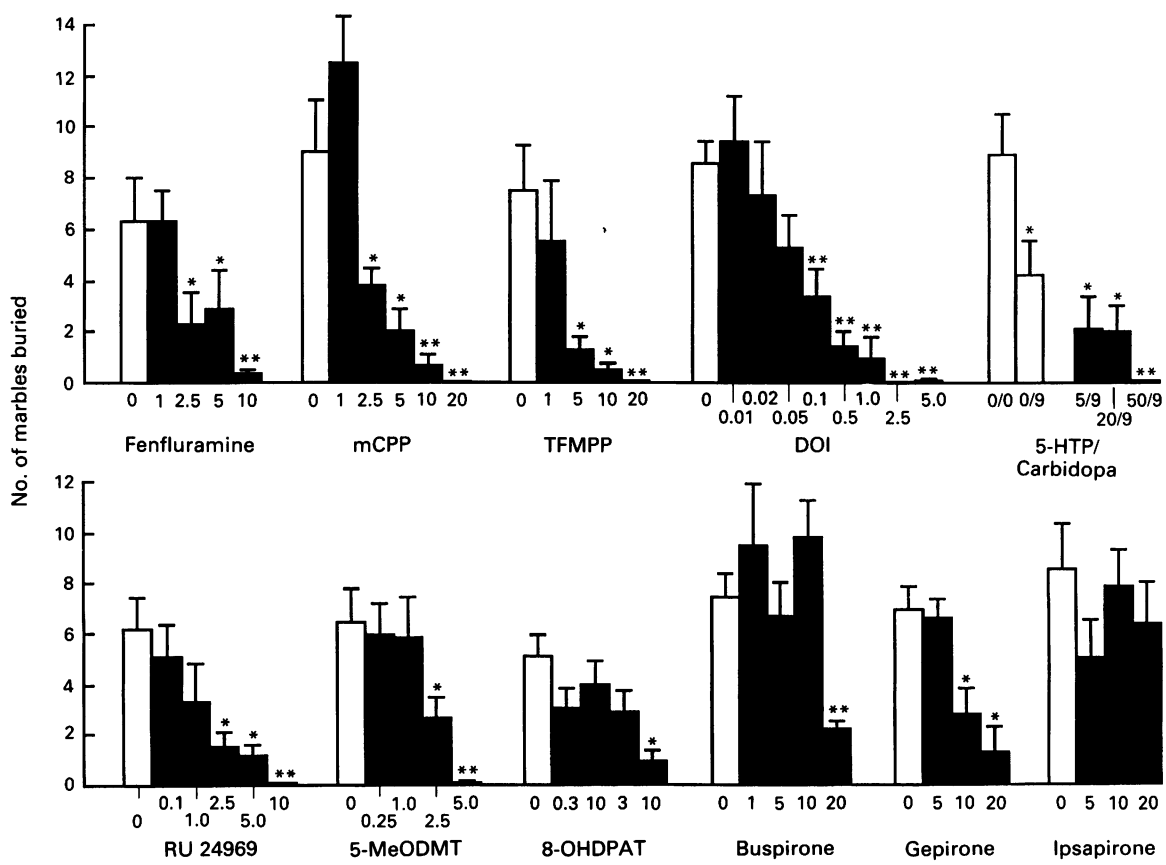

Figure 2 Effects of 5-hydroxytryptamine agonists on marble burying. Data are the mean number of marbles buried by female MF1 mice in a 30 min period starting 10 min (8-OHDPAT), 20 min (5-MeODMT) or 30 (other agents) min after i.p. injection of vehicle (open columns) or agonist (solid columns). Vertical bars represent s.e.mean. There were at least 6 mice per group. $*P < 0.05$; $**P < 0.01$. For abbreviations see Methods.

Table 1 Effects of 5-hydroxytryptamine (5-HT)-related agents on runway activity

Agent	Dose (mg kg^{-1})	Animex counts in 5 min (±s.e.mean) Agent	Vehicle-control	P
Fluvoxamine	20	284 ± 22	240 ± 24	NS
Indalpine	20	510 ± 26	500 ± 14	NS
Citalopram	20	513 ± 25	481 ± 20	NS
Zimeldine	3	197 ± 15	209 ± 8	NS
	10	445 ± 23	483 ± 25	NS
	30	198 ± 33	240 ± 24	NS
Fenfluramine	10	226 ± 22	209 ± 8	NS
Carbidopa + saline	9	418 ± 40	481 ± 35	NS
Carbidopa + 5-HTP	9	314 ± 19	418 ± 40	0.01*
MCPP	2.5	556 ± 24	483 ± 25	NS
	10	539 ± 21	481 ± 20	NS
	20	118 ± 19	217 ± 16	0·05
TFMPP	20	259 ± 18	391 ± 14	0·01
DOI	0.1	224 ± 27	209 ± 8	NS
	5	274 ± 27	240 ± 24	NS
RU 24969	2.5	843 ± 39	481 ± 35	0·01
5-MeODMT	2.5	421 ± 16	500 ± 14	0.01
8-OHDPAT	2.5	333 ± 64	526 ± 23	0.05
	10	62 ± 20	209 ± 8	0.01
Buspirone	20	223 ± 22	391 ± 14	0.01
Gepirone	10	368 ± 16	481 ± 35	0.05
	20	28 ± 6	209 ± 8	0.01
Ipsapirone	20	159 ± 28	164 ± 10	NS

Abbreviations for agents used are given in Methods. Data are in arbitrary counts (mean ± s.e.mean) from Animex activity meter when mice were placed in a circular runway over a 5 min period starting 10 (DOI), 20 (5-MeODMT) or 30 (other agents) min after i.p. injection of agent or vehicle control and is for at least 6 animals/group.

* In this experiment, the data in the vehicle control column are for carbidopa 9 mg kg^{-1} and significance is for 5-HTP/carbidopa compared with this carbidopa control.

Effect of antagonists on responses to zimeldine, fluvoxamine and fenfluramine

Figure 5 demonstrates that ritanserin (5.0 mg kg^{-1}), ICI 169,369 (10 mg kg^{-1}), ICS 205–930 (10 mg kg^{-1}), pindolol (5 mg kg^{-1}) and cyproheptadine (2 mg kg^{-1}) significantly potentiated the response to zimeldine 10 mg kg^{-1}. These agents did not affect runway activity either alone or in combination with zimeldine (Table 3). Similarly, ritanserin 1 mg kg^{-1} potentiated the effect of zimeldine 3 mg kg^{-1} (mean number of marbles buried in 30 min: vehicle 5.3 ± 1.2, ritanserin 12.0 ± 0.4, zimeldine 4.0 ± 1.4, combination 1.9 ± 1.1). Metergoline, 0.25 mg kg^{-1} was inactive. Ritanserin 5 mg kg^{-1} also potentiated the responses to fluvoxamine (5 mg kg^{-1}) and fenfluramine (1 mg kg^{-1}) (Figure 6). In neither case was runway activity affected (Table 3).

Subchronic administration of zimeldine

Zimeldine 10 mg kg^{-1} daily was given on day 1 by i.p. injection and significantly inhibited marble burying (Figure 7); this dose was then administered in drinking water for a further 20 days (Methods). Initially, this regimen resulted in a significant inhibition of marble burying but this had disappeared by day 14. No significant difference was found between animals maintained on tap water and those maintained on zimeldine for the remainder of the treatment period or 24 to 48 h after withdrawal of zimeldine. In addition, the response of these mice to DOI, 0.1 mg kg^{-1}, was no different from that of the control mice that had been maintained on tap water.

Discussion

As previously found (Njung'e & Handley, 1991), this Aston-bred MF1 mouse strain buried on average less than half the 20 marbles presented, thus potentially allowing both increases

Table 2 Effects of 5-hydroxytryptamine (5-HT) antagonists on marble burying and runway activity

Antagonist/Dose		Marbles buried Vehicle	Antagonist	Runway activity Vehicle	Antagonist
Ritanserin	1	8.1 ± 1.5	6.3 ± 1.5		
	5	8.5 ± 1.8	4.8 ± 2.0	483 ± 25	455 ± 36
	10	8.5 ± 1·8	6·8 ± 2.4	161 ± 16	137 ± 28
	20	8.5 ± 1.8	2.1 ± 1.2*	558 ± 24	371 ± 35*
ICI 169 369	1	8.3 ± 1.7	6.1 ± 2.0		
	5	10.2 ± 1.9	12.7 ± 2.1		
	10	6.1 ± 0.8	6.8 ± 1.7	209 ± 8.3	214 ± 19
Ketanserin	1	10 ± 2.5	1.3 ± 0.8**	556 ± 24	470 ± 25*
Cyproheptadine	1	10.1 ± 2.1	10.7 ± 2.6		
	2	10.1 ± 2.1	5.2 ± 2.6		
	5	10.1 ± 2.1	3.2 ± 2.2*	507 ± 26	376 ± 62*
Methysergide	1	8.0 ± 2.3	6.0 ± 2.4		
	5	8.8 ± 1.4	2.3 ± 1.1**	550 ± 13	471 ± 45*
Metergoline	0.10	4.3 ± 0.93	3.0 ± 1.3		
	0.25	4.3 ± 0.93	3.5 ± 1.3		
	1	6.2 ± 1.5	0.0**	484 ± 16.2	394 ± 17**
Pindolol	5	8.9 ± 1.6	8.3 ± 2.2		
	10	10.0 ± 2.5	9.2 ± 2.2		
ICS 205–930	0.1	7.5 ± 1.3	5.7 ± 1.6		
	1.0	7.5 ± 1.3	9.0 ± 2.1		
	10	7.5 ± 1.3	6.5 ± 2.1		
Ondansetron	0.01	8.8 ± 1.4	10.3 ± 0.8		
	0.1	8.8 ± 1.4	8.3 ± 1.5		
	1.0	8.9 ± 1.4	7.7 ± 1.1		

Doses are in mg kg^{-1}. Data are in arbitrary counts (mean ± s.e.mean) from Animex activity meter when mice were placed in a circular runway over a 5 min period starting 30 min after i.p. injection of agent or vehicle control and is for at least 6 animals/group. *$P < 0.05$; **$P < 0.01$ compared with vehicle controls.

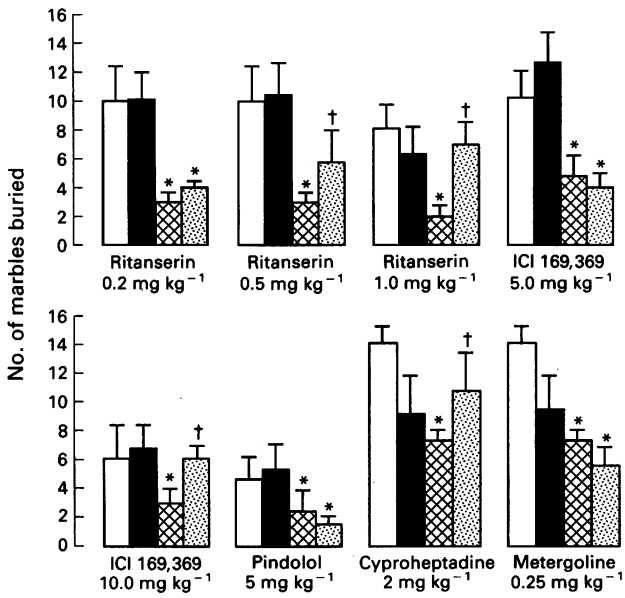

Figure 3 Effects of some 5-hydroxytryptamine antagonists on the inhibition of marble burying induced by DOI 0.1 mg kg^{-1}, i.p. Antagonist or vehicle was administered i.p. 10 min before DOI and data are the mean number of marbles buried by female MF1 mice in a 30 min period starting 30 min after vehicle/vehicle (open columns), antagonist/vehicle (solid columns), vehicle/DOI (cross-hatched columns) or antagonist/DOI (stippled columns). Vertical bars represent s.e.mean. There were at least 6 mice per group. $*P < 0.05$; $**P < 0.01$ with respect to vehicle/vehicle. $\dagger P < 0.05$; $\dagger\dagger P < 0.01$ with respect to vehicle/DOI. For abbreviations, see Methods.

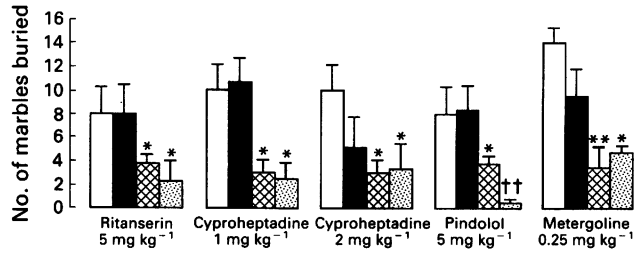

Figure 4 Effects of some 5-hydroxytryptamine antagonists on the inhibition of marble burying induced by mCPP 2.5 mg kg^{-1} i.p. Antagonist or vehicle was administered i.p. 10 min before mCPP and data are the mean number of marbles buried by female MF1 mice in a 30 min period starting 30 min after vehicle/vehicle (open columns), antagonist/vehicle (solid columns), vehicle/mCPP (cross-hatched columns) or antagonist/mCPP (stippled columns). Vertical bars represent s.e.mean. There were at least 6 mice per group. $*P < 0.05$; $**P < 0.01$ with respect to vehicle/vehicle. $\dagger P < 0.05$; $\dagger\dagger P < 0.01$ with respect to vehicle/mCPP. For abbreviations, see Methods.

and decreases in burying to be seen. There was some day to day variation in the number of marbles buried. This was also the case with runway activity and emphasizes the importance of concurrent controls in both paradigms. We have previously shown that female mice bury marbles as readily as males and that most marbles are buried when these are evenly distributed (Njung'e & Handley, 1991). These conditions were therefore adopted for the present experiments.

Fluvoxamine, zimeldine, indalpine and citalopram dose-dependently reduced burying, but had no effect on runway activity, confirming the pattern of effects previously observed using swim-induced grooming (Broekkamp *et al.*, 1986; 1989; Broekkamp & Jenck, 1989). The 5-HT releasing agent, fenfluramine, also differentially inhibited burying, reinforcing the possibility that such an effect could be due to increased synaptic availability of 5-HT.

Among the agonists tested, those with appreciable affinity for 5-HT$_{1A}$ receptors (8-OHDPAT, buspirone, gepirone, ipsapirone, 5-MeODMT, also 5-HTP) (Hamon *et al.*, 1986) failed to reduce burying except at high doses which also reduced runway activity. This suggests that 5-HT$_{1A}$ receptors are not involved in selective inhibition of burying. RU 24969 binds to both 5-HT$_{1A}$ and 5-HT$_{1B}$ receptors, its effects were however difficult to evaluate because it caused hyperlocomotion in the runway activity test at all effective doses. The remaining agonists, TFMPP, mCPP and DOI, selectively reduced burying at doses not affecting runway activity. DOI inhibited burying at doses well below those causing head-twitch (Heaton *et al.*, 1988), so that competition of marble burying with this behaviour is not a likely explanation of its effects. These agents have in common a high affinity for 5-HT$_{1C}$ receptors (Hoyer, 1988; Kennett *et al.*, 1989; Hoyer & Schoeffter, 1989; Hoyer *et al.*, 1989). However, DOI also binds strongly to 5-HT$_2$ receptors and mCPP and TFMPP to 5-HT$_{1B}$ receptors (Garratini *et al.*, 1989; Hoyer & Schoeffter, 1989). In addition, RU 24969, mCPP and TFMPP have been demonstrated to cause a major release of 5-HT from hypothalamic or hippocampal slices (Pettibone & Williams, 1984; Auerbach *et al.*, 1990).

Although a wide range of 5-HT antagonists was investigated, none increased burying. This suggests that resting levels of 5-HT neuronal activity may be too low to modulate

Table 3 Effects of drug combinations on runway activity

Antagonist		*Agent*		*Vehicle/ Vehicle*	*Antagonist/ Vehicle*	*Vehicle/ Agent*	*Antagonist/ Agent*
Ritanserin	5	Zimeldine	3	240 ± 24	235 ± 29	197 ± 15	211 ± 33
ICI 169369	10	Zimeldine	10	483 ± 25	490 ± 26	445 ± 23	398 ± 22
ICS 205930	10	Zimeldine	10	483 ± 25	467 ± 22	445 ± 23	550 ± 33
Pindolol	5	Zimeldine	10	483 ± 25	489 ± 18	445 ± 23	418 ± 26
Cyproheptadine	1	Zimeldihe	10	470 ± 28	466 ± 23	459 ± 19	422 ± 27
Metergoline	0.25	Zimeldine	10	429 ± 28	401 ± 27	432 ± 22	437 ± 26
Ritanserin	5	Fenfluramine	1	483 ± 25	455 ± 36	486 ± 28	398 ± 47
Ritanserin	5	Fluvoxamine	5	483 ± 25	455 ± 36	513 ± 13	472 ± 13
Ritanserin	5	mCPP	2.5	483 ± 25	455 ± 36	556 ± 24	520 ± 33
Pindolol	5	mCPP	2.5	483 ± 25	489 ± 18	556 ± 24	485 ± 21
Cyproheptadine	2	mCPP	2.5	470 ± 28	466 ± 23	534 ± 26	521 ± 30
Metergoline	0.25	mCPP	2.5	429 ± 28	410 ± 27	534 ± 26	508 ± 27
Ritanserin	1	DOI	0.1	267 ± 17	256 ± 21	302 ± 22	261 ± 29
ICI 169369	10	DOI	0.1	267 ± 17	234 ± 19	302 ± 22	254 ± 31
Cyproheptadine	2	DOI	0.1	389 ± 23	341 ± 32	426 ± 31	402 ± 28
Pindolol	5	DOI	0.1	324 ± 21	301 ± 17	342 ± 15	327 ± 25
Metergoline	0.25	DOI	0.1	324 ± 21	352 ± 20	342 ± 15	322 ± 19

Doses are in mg kg^{-1}. Data are in arbitrary counts (mean ± s.e.mean) from Animex activity meter when mice were placed in a circular runway over a 5 min period and are for at least 6 animals/group. Antagonists were injected i.p. 10 min before agent i.p. and observation started 30 min later. There were no statistically significant effects.

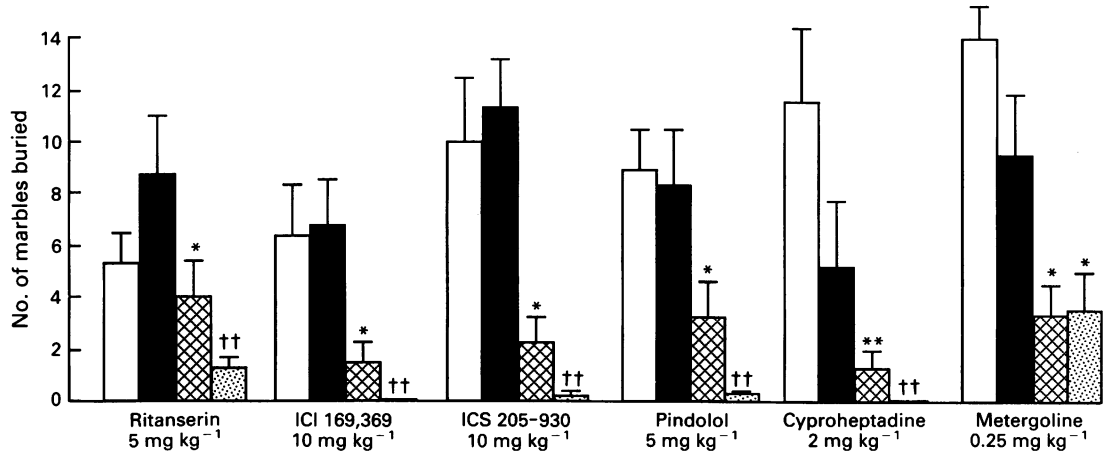

Figure 5 Effects of some 5-hydroxytryptamine antagonists on the inhibition of marble burying induced by zimeldine 10 mg kg^{-1}, i.p. Antagonist or vehicle was administered i.p. 10 min before zimeldine and data are the mean number of marbles buried by female MF1 mice in a 30 min period starting 30 min after vehicle/vehicle (open columns), antagonist/vehicle (solid columns), vehicle/zimeldine (cross-hatched columns) or antagonist/zimeldine (stippled columns). Vertical bars represent s.e.mean. There were at least 6 mice per group. $*P < 0.05$, $**P < 0.01$ with respect to vehicle/vehicle. $\dagger P < 0.05$; $\dagger\dagger P < 0.01$ with respect to vehicle/zimeldine.

burying. The lack of effect of 5-HT$_2$ antagonists, despite the potent activity of DOI, would also be consistent with recent suggestions that 5-HT$_2$ receptors receive little impetus from endogenous 5-HT under normal circumstances (Darmani *et al.*, 1990; Leysen *et al.*, 1990). No antagonist reduced burying at doses which did not also reduce runway activity.

The effects of antagonists on DOI- and mCPP-induced inhibition of burying were investigated in an attempt to elucidate the receptor subtypes(s) involved. Since pindolol, even at the high dose of 5 mg kg^{-1}, did not antagonize these responses, it appears that 5-HT$_{1B}$ receptors are unlikely to be important. Indeed, pindolol potentiated the effect of mCPP, suggesting that activation of 5-HT$_{1B}$ receptors by this agent may have been minimizing its effect at other receptors (Darmani *et al.*, 1990). The common action of DOI and mCPP at 5-HT$_{1C}$ receptors appears to be ruled out as a mechanism of burying inhibition because the 5-HT$_2$/5-HT$_{1C}$ antagonists ritanserin and cyproheptadine (Hoyer, 1988) prevented the effect of DOI but had no effect on mCPP responses even at higher doses. Metergoline was ineffective against both agonists but the dose was limited by the strong effects of this agent on runway activity. It therefore appears likely that the burying inhibition caused by DOI was due to an action at 5-HT$_2$ receptors but that the similar effect of mCPP was not due to its direct actions at either 5-HT$_{1B}$ or 5-HT$_{1C}$ receptors.

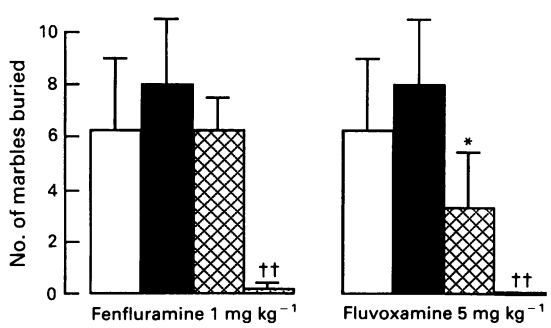

Figure 6 Effects of ritanserin 5 mg kg^{-1} on the inhibition of marble burying induced by fenfluramine or fluvoxamine. Ritanserin or vehicle was administered i.p. 10 min before fenfluramine 1 mg kg^{-1} i.p. or fluvoxamine 5 mg kg^{-1} i.p. (agents) and data are the mean number of marbles buried by female MF1 mice in a 30 min period starting 30 min after vehicle/vehicle (open columns), ritanserin/vehicle (solid columns), vehicle/agent (cross-hatched columns) or ritanserin/agent (stippled columns). Vertical bars represent s.e.mean. There were at least 6 mice per group. $*P < 0.05$; $**P < 0.01$ with respect to vehicle/vehicle. $\dagger\dagger P < 0.01$ with respect to vehicle/agent.

Four 5-HT uptake inhibitors, as well as the 5-HT releaser fenfluramine and the three direct agonists which can also cause 5-HT release, mCPP, TFMPP and RU 24969, selectively inhibited burying. Increased synaptic 5-HT is therefore likely to be an important factor in causing selective burying inhibition. Nevertheless, none of the antagonists tested reduced the effect of zimeldine or mCPP, indicating that increased activation of any one subtype of the 5-HT receptor is unlikely to be the cause. Despite the ability of ritanserin to reduce the effect of DOI, this antagonist also had no effect on burying inhibition caused by fluvoxamine or the 5-HT releaser fenfluramine, as well as zimeldine and mCPP.

These same antagonists, with the exception of metergoline which was dose-limited by reduced runway activity at higher doses, actually potentiated the effect of zimeldine on burying, leaving runway activity unaffected. This unexpected effect was investigated by examining the action of ritanserin on a further uptake inhibitor, fluvoxamine, and a 5-HT releaser, fenfluramine, with the same result. Since potentiation was not seen when ritanserin was given with mCPP, it could be speculated that the direct agonist actions of this latter agent prevented its occurrence. The mechanism of the potentiation is unclear. It may be a consequence of interactions between several different 5-HT receptor subtypes activated by elevated synaptic 5-HT. Such interactions are known to occur between pairs of 5-HT receptor subtypes (Backus *et al.*, 1990) but neither their extent nor their significance are yet fully understood. For instance, 5-HT$_{1A}$ and 5-HT$_2$ receptors interact in such a way that both 5-HT$_2$ agonists (Arnt & Hyttel, 1989) and antagonists (Backus *et al.*, 1990) potentiate the '5-HT syndrome' induced by stimulation of 5-HT$_{1A}$ receptors. Moreover, ritanserin enhanced the behavioural activation induced by the 5-HT$_{1B}$ agonist RU 24969 (Goodwin & Green, 1985). There is also evidence that 5-HT$_{1B}$ receptors activation inhibits 5-HT$_2$ receptor-mediated scratching (Darmani *et al.*, 1990). These latter workers have suggested that there is a 5-HT$_1$-receptor-mediated damping mechanism with the function of reducing excessive 5-HT$_2$ receptor stimulation. However, there is also evidence of behavioural specificity among these effects since the 5-HT$_{1A}$ agonist, 8-OHDPAT, reduced the head-twitch response to DOI but increased the ability of this latter agent to induce scratching (Heaton & Handley, 1989). These investigations have so far examined only interactions between pairs of receptors but they predict that multiple interactions would also occur.

The onset of the clinical effects of 5-HT uptake inhibitors is delayed; however, their ability to inhibit burying was seen on first dose. The subchronic effect of zimeldine was therefore studied during daily administration for 21 days. The inhibi-

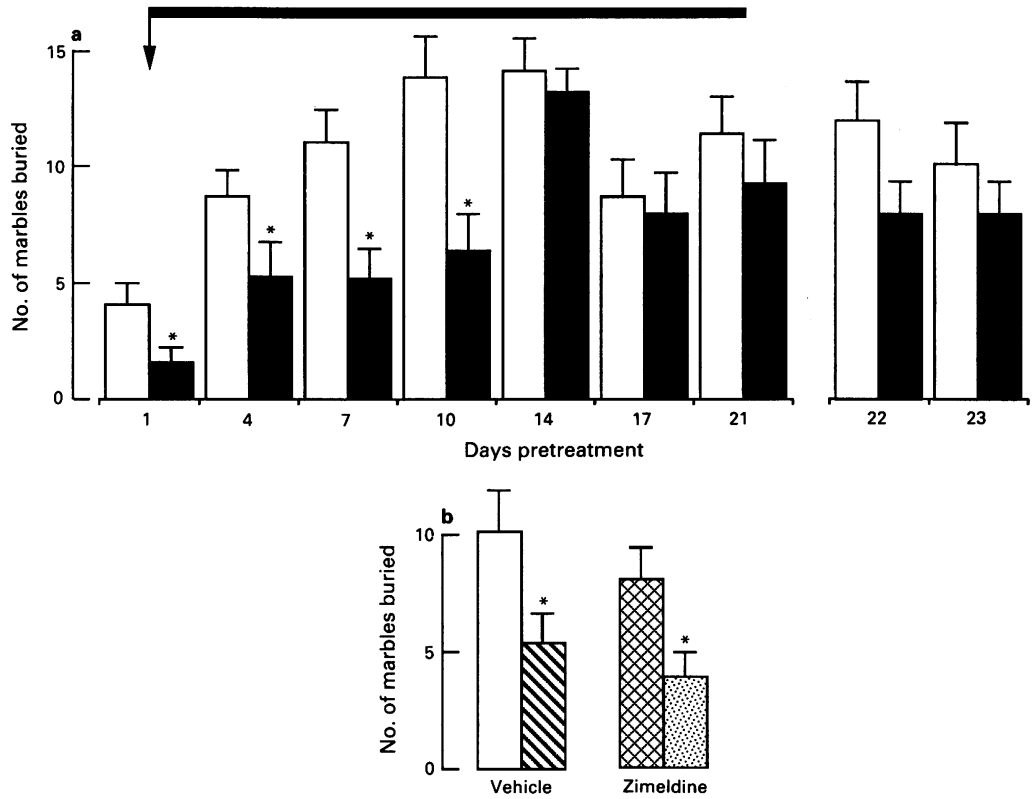

Figure 7 Effect on marble burying of 21 days treatment with zimeldine. Zimeldine 10 mg kg^{-1}, daily was given i.p. on day 1 (arrow) and, dissolved in tap water, as the only drinking fluid thereafter (horizontal bar). Control mice received saline vehicle i.p. on day 1 only. Naive mice were randomly selected from each treatment group for testing on each occasion. Data are the mean number of marbles buried by female MF1 mice in a 30 min period starting 30 min after the first injection of zimeldine and at the same time of day on each measurement day thereafter. (a) Shows the effect of this subchronic treatment on marble burying; *$P < 0.05$ with respect to control on the same day. (b) Represents the response to DOI 0.1 mg kg^{-1}, i.p., 48 h after cessation of treatment (open column, vehicle i.p. in control mice; hatched column, DOI 0.1 mg kg^{-1} in control mice; cross-hatched column, vehicle i.p. in zimeldine-treated mice, stippled column, DOI 0.1 mg kg^{-1} i.p. in zimeldine-treated mice). *$P < 0.05$ with respect to vehicle/vehicle or zimeldine/vehicle controls.

tion of burying had disappeared by day 14 and had not returned 48 h after withdrawal. This finding was complicated by an apparent increase in burying by controls. This was not an effect of repeated exposure to marbles since naive mice were taken from treated and vehicle groups on each occasion; successive removal of mice may have induced a stress response in those remaining. Whatever the explanation, it did not account for the diminution of the zimeldine response because this response disappeared abruptly between days 10 and 14 while vehicle control responses were identical on both days. The disappearance of the burying response on and after day 14 did not appear to be due to desensitization of 5-HT$_2$ receptor mechanisms since the burying response to DOI was unaffected 48 h after zimeldine withdrawal.

The significance of harmless object burying behaviour is as yet unclear. There is no evidence that it actually models anxiety (Njung'e & Handley, 1991) so it remains at best a correlational model for the detection of anxiolytics according to the criteria of Treit (1985). However the present findings confirm and extend those of Broekkamp *et al.* (1989) to demonstrate that it does not detect the activity of actual and putative 5-HT-related anxiolytics such as buspirone, gepirone, ipsapirone, ritanserin and ondansetron. Its possible use as a model for obsessive-compulsive disorder (Broekkamp & Jenck, 1989, see also Njung'e & Handley, 1991) falls down in that the actions of at least one 5-HT uptake inhibitor were not maintained. However, irrespective of the relationship, if any, between burying behaviour and anxiety, this behaviour has demonstrated unexpected interactions between 5-HT uptake inhibitors and 5-HT antagonists which are worth consideration in the context of any future clinical use of such combinations. These findings also raise the possibility that multiple interactions may occur between 5-HT receptor subtypes.

We thank Janssen Pharmaceutical for financial support and K. Manani, Mita Parmar and V. Brown for their enthusiastic assistance. Kung'u Njung'e was a Commonwealth Scholar during the time this work was performed.

References

ARNT, J., & HYTTEL, J. (1989). Facilitation of 8-OHDPAT-induced forepaw treading of rats by the 5-HT$_2$ agonist DOI. *Eur. J. Pharmacol.*, **161**, 45–51.

AUERBACH, S.B., KAMALAKANNAN, N. & RUTTER, J.J. (1990). TFMPP and RU24969 enhance serotonin release from rat hippocampus. *Eur. J. Pharmacol.*, **190**, 51–57.

BACKUS, L.I., SHARP, T. & GRAHAME-SMITH, D.G. (1990). Behavioural evidence for a functional interaction between central 5-HT$_2$ and 5-HT$_{1A}$ receptors. *Br. J. Pharmacol.*, **100**, 793–799.

BROEKKAMP, C.L., BERENDSEN, H.H.G., JENCK, F. & VAN DELFT, A.M.L. (1989). Animal models for anxiety and response to serotonergic drugs. *Psychopathology*, **22**, 2–12.

BROEKKAMP, C.L. & JENCK, F. (1989). The relationship between various animal models of anxiety, fear-related psychiatric symptoms and response to serotonergic drugs. In *Behavioural Pharmacology of 5-HT*. ed. Bevan, P., Cools, A.R., & Archer, T. pp. 321–335. London: Lawrence Erlbaum Associates.

BROEKKAMP, C.L., RIJK, H.W., JOLY-GELOUIN, D. & LLOYD, K.L.

(1986). Major tranquillizers can be distinguished from minor tranquillizers on the basis of effects on marble burying and swim-induced grooming in mice. *Eur. J. Pharmacol.*, **126**, 223–229.

DARMANI, N.A., MARTIN, B.R., PANDEY, U. & GLENNON, R.A. (1990). Pharmacological characterisation of ear-scratch response in mice as a behavioural model for selective 5-HT_2-receptor agonists and evidence for 5-HT_{1B}- and 5-HT_2- receptor interactions. *Pharmacol. Biochem. Behav.*, **37**, 95–99.

GARRATINI, S., MENNINI, T. & SAMANIN, R. (1989). Reduction of food intake by manipulation of central serotonin. *Br. J. Psychiatr.*, **155**, 41–51.

GOODWIN, G.M. & GREEN, A.R. (1985). A behavioural and biochemical study in mice and rats of putative selective agonists and antagonists for 5-HT_1 and 5-HT_2 receptors. *Br. J. Pharmacol.*, **84**, 743–753.

GRAY, J.A. (1982). *The Neuropsychology of Anxiety.* Oxford: Clarendon Press.

HAMON, M., COSSERY, J.-M., SPAMPINATO, U. & GOZLAN, H. (1986). Are there selective ligands for 5-HT_{1A} and 5-HT_{1B} receptor binding sites in brain? *Trends Pharmacol. Sci.*, **7**, 336–338.

HEATON, J.C.P. & HANDLEY, S.L. (1989). Comparison of DOI-induced scratching and head-twitch behaviours: differential action of 8-OHDPAT. *Br. J. Pharmacol.*, **98**, 687P.

HEATON, J.C.P., NJUNG'E, K. & HANDLEY, S.L. (1988). Behavioural profile of 1-(2,5-dimethoxy-4-iodophenyl)-2-aminopropane (DOI) a selective 5-HT_2 agonist. *Br. J. Pharmacol.*, **94**, 388P.

HOYER, D. (1988). Molecular pharmacology and biology of 5-HT_{1C} receptors. *Trends Pharmacol. Sci.*, **9**, 89–94.

HOYER, D. & SCHOEFFTER, P. (1989). Are TFMPP, mCPP and CGS 12066 selective for 5-hydroxytryptamine 5-HT_{1B} receptors? *Br. J. Pharmacol.*, **96**, 9P.

HOYER, D. WAEBER, C., SCHOEFFTER, P., PALACIOS, J.M. & DRAVID, A. (1989). 5-HT_{1C} receptor-mediated stimulation of inositol phosphate production in pig choroid plexus. A pharmacological characterisation. *Naunyn-Schmiedebergs Arch. Pharmacol.*, **339**, 252–258.

KENNETT, G.A., WHITTON, P., SHAH, K. & CURZON, G. (1989). Anxiogenic-like effects of mCPP and TFMPP in animal models are opposed by 5-HT_{1C} receptor antagonists. *Eur. J. Pharmacol.*, **164**, 445–454.

LEYSEN, J.E. & PAUWELS, P.J. (1990). Central and peripheral 5-HT_2 receptors: role in physiological versus pathological conditions. In *Serotonin. From Cell Biology To Pharmacology and Therapeutics*, ed. Paoletti, R., Vanhoutte, P.P., Brunello, M. & Maggi, F.M. pp. 323–329. Boston: Kluwer Academic Publishers.

NJUNG'E, K. & HANDLEY, S.L. (1989). Which 5-HT receptors are involved in the inhibition of object burying behaviour by 5-HT uptake inhibitors? *Br. J. Pharmacol.*, **98**, 684P.

NJUNG'E, K. & HANDLEY, S.L. (1991). Evaluation of marble burying as a model of anxiety. *Pharmacol. Biochem. Behav.*, **38**, 63–67.

NUTT, D.J. & GLUE, P. (1989). Clinical pharmacology of anxiolytics: a psychopharmacological perspective. *Pharmacol. Ther.*, **44**, 309–334.

PETTIBONE, D.J. & WILLIAMS, M. (1984). Serotonin-relating effects of substituted piperazines in vitro. *Biochem. Pharmacol.*, **33**, 1531–1535.

POLING, A., CLEARY, J. & MONAGHAN, M. (1981). Burying by rats in response to aversive and nonaversive stimuli. *J. Exp. Anal. Behav.*, **35**, 31–44.

SIEGAL, S. & CASTELLAN, N.J.Jr. (1988). *Nonparametric Statistics for the Behavioural Sciences.* New York: McGraw-Hill.

TERLECKI, L.J., PINEL, J.P.J. & TREIT, D. (1979). Conditioned and unconditioned defensive burying in the rat. *Learn. Motivat.*, **10**, 337–350.

TREIT, D. (1985). Animal models for the study of anti-anxiety agents: a review. *Neurosci. Behav. Rev.*, **9**, 203–222.

WINSLOW, J. T. & INSEL, T.R. (1990). Neurobiology of obsessive compulsive disorder: a possible role for serotonin. *J. Clin. Psychiatr.*, **51** (Suppl.), 27–31.

(Received February 27, 1991
Accepted May 17, 1991)

Br. J. Pharmacol. (1991), **104**, 113–116

The role of the L-arginine-nitric oxide pathway in relaxation of the opossum lower oesophageal sphincter

[1]*†A. Tøttrup, *M.A. Knudsen & *H. Gregersen

Department of *Surgical Gastroenterology L and of †Obstetrics and Gynaecology, Aarhus kommunehospital, DK-8000 Aarhus, Denmark

1 The role of the L-arginine-nitric oxide pathway in lower oesophageal sphincter (LOS) relaxation and oesophageal peristalsis was investigated.

2 Twenty four adult opossums were anaesthetized and the right vagus nerve was isolated in the neck and sectioned. Electrical stimulation, applied to the peripheral end of the nerve, resulted in a frequency-dependent relaxation of the LOS, and peristaltic and non-peristaltic contractions in the oesophageal body.

3 N^{ω}-nitro-L-arginine (L-NNA, 10^{-8}–10^{-5} mol kg^{-1}), an inhibitor of the L-arginine-nitric oxide pathway, inhibited LOS relaxation in a dose-dependent manner, but did not affect resting LOS pressure. At the highest dose of L-NNA no relaxation of the LOS was elicited in response to vagal stimulation. The effect of L-NNA, (10^{-5} mol kg^{-1}) was fully reversed by infusion of 10^{-4} mol kg^{-1} L-arginine. Peristaltic velocity and amplitude of contractions in the oesophageal body were unaffected by L-NNA.

4 Infusion of sodium nitroprusside reduced LOS pressure to zero, and the drug was equally potent in control animals ($-\log ED_{50}$: 8.1 ± 0.2 mol kg^{-1}) and in animals pretreated with L-NNA ($-\log ED_{50}$: 8.2 ± 0.3 mol kg^{-1}). This suggests that the effect of L-NNA was not directly on guanylate cyclase.

5 A significant elevation of blood pressure was recorded after administration of L-NNA (10^{-5} mol kg^{-1}).

6 It is suggested that the L-arginine-nitric oxide pathway plays an important functional role for relaxation of the LOS, but not for oesophageal peristalsis. Whether the active substance is nitric oxide or a related nitroso-compound remains to be settled.

Keywords: Non-adrenergic non-cholinergic; nitric oxide; NANC nerves; L-arginine metabolism; oesophageal peristalsis; nitroprusside, N^{ω}-nitro-L-arginine

Introduction

Resting tone in the lower oesophageal sphincter (LOS) is independent of neuronal activity and thus 'myogenic' in nature (Goyal & Rattan, 1976). The sphincter relaxes during swallowing, and this relaxation is caused by an activation of non-adrenergic, non-cholinergic (NANC) nerves (Goyal & Rattan, 1975). The transmitter substance of these NANC nerves has not yet been identified but recent *in vitro* studies have suggested that nitric oxide (NO), or a related product of the L-arginine-NO pathway, is involved in the mediation of NANC inhibition in a number of tissues, including the LOS (Gillespie *et al.*, 1989; Li & Rand, 1989; Bult *et al.*, 1990; Gibson *et al.*, 1990; Tucker *et al.*, 1990; Tøttrup *et al.*, 1991). NO is synthesized from L-arginine (Palmer *et al.*, 1988), and this process is inhibited by a number of L-arginine analogues with a substituted guanidino group (Rees *et al.*, 1989a; Moore *et al.*, 1990). Most of the reports so far published concern the effects of L-arginine analogues on the responses to transmural field stimulation in isolated muscle preparations from different NANC innervated organs. To what extent the findings in isolated tissues are valid for *in vivo* organ function remains to be settled. The aim of the present study was to investigate the role of the L-arginine-NO pathway in motor function of the distal oesophageal body and the LOS, *in vivo*.

Methods

Twenty four North American opossums (*Didelphis virginiana*, 1100–2650 g) were anaesthetized with intraperitoneal pentobarbitone (35 mg kg^{-1}). Twelve animals had been given atropine (30 μg kg^{-1}, i.v.) as premedication to reduce shortening of the oesophagus during peristalsis and to avoid bradycardia in relation to manipulation and stimulation of the vagus nerve. Since atropine previously has been shown to affect the contractile pattern of the oesophageal body to vagal stimulation (Dodds *et al.*, 1978) data from these animals were not included in the calculations of peristaltic velocity and amplitude of contractions. On the other hand, atropine inhibits the shortening of the longitudinal muscle of the oesophagus during vagal stimulation (Dodds *et al.*, 1978) thereby preventing movement of the oesophagus in relation to the catheter, but leaves LOS relaxation unaffected, at least in the dose used for the present experiments (Goyal & Rattan, 1975). To avoid aspiration of saliva and saline, a rubber tube was inserted in the trachea, but the animals were kept on spontaneous respiration. The right vagus nerve was isolated in the neck, and sectioned. Electrical stimulation, applied to the peripheral end of the nerve, was delivered in trains of impulses, separated by 1 min (1 s train duration, 0.4 ms impulse duration, 20–50 V, varying frequency). Oesophageal pressures were monitored by a 4 channel, perfused catheter assembly. Each channel had a side hole for pressure recording, and the distal hole was covered with a 2 cm long 'cuff' for continuous measurement of LOS pressure (Gustavsson & Tucker, 1988). The three proximal side holes were located 1, 3 and 5 cm above the cuff, respectively. The catheter was constantly perfused (0.2 ml min^{-1}) with bubble-free saline by a low compliance, pneumohydraulic system and pressures were registered on an Elema Siemens Mingograph by external transducers (Elema Siemens 746, Sweden). The LOS was located by a slow pull-through technique, and the cuff was placed to yield the highest possible resting sphincter pressure. In addition, the following criteria were used to ensure optimal placement of the catheter: (1) a distinct relaxation of the LOS should be recorded in response to vagal stimulation, (2) within 20 s after cessation of vagal stimulation, LOS pressure should have returned to pre-stimulus level. All pressures mentioned are end-expiratory and given with the fundic pressure as reference. Peristaltic velocity was calculated by measuring the time interval between the major upstroke of the peristaltic contraction at the different measuring sites in the oesophageal body. Arterial blood pressure was continuously monitored in 6 animals by a catheter inserted in the femoral artery. All drugs were dissolved in

[1]Author for correspondence at: Department of Surgical Gastroenterology L, Aarhus kommunehospital, 8000 Aarhus C, Denmark.

0.9% saline, and given as intravenous bolus injections (1 ml kg^{-1}) over 20 s in cumulatively increasing doses through a cannula inserted in the external jugular vein or in the cephalic vein. Responses were compared by a paired or an unpaired Student's t test, where appropriate.

Determination of ED_{50}-values

The dose producing half-maximal effect (ED_{50}) was assessed by linear interpolation on the semilogarithmic dose-response curve and was expressed as $-\log ED_{50}$.

Drugs

Atropine (Danish Pharmacy Labs); sodium pentobarbitone (Danish Pharmacy Labs); N^{ω}-nitro-D-arginine (D-NNA, Serva), L-arginine, N^{ω}-nitro-L-arginine (L-NNA) and sodium nitroprusside were obtained from Sigma Chemical Co.

Results

Basal performance

Resting LOS pressure was 31 ± 3 mmHg above fundic pressure (Table 1). No spontaneous contractile activity was observed in the oesophageal body except when the animals swallowed spontaneously or when electrical stimulation was applied to the vagus nerve. Vagal stimulation resulted in peristaltic or simultaneous contractions in the oesophageal body and relaxation of the LOS. The latter was frequency-dependent and reached 80% at 10 Hz (Figure 1). The onset of the LOS relaxation began 1–3 s after cessation of vagal stimulation, while contraction at the recording site 3 cm above the LOS began 2–4 s after cessation of the stimulus. The response of the oesophageal body to vagal stimulation varied. In 6 out of 12 animals not given atropine, peristaltic contractions with a propagation velocity <6 cm s^{-1} were constantly elicited. In the remaining 6 animals the velocity of propagation was much faster, and occasionally simultaneous contractions were evoked. All measurements of peristaltic velocity and amplitude were made in animals exhibiting the first-named type of contractions, since these most closely resemble swallowing-induced peristalsis (Dodds *et al.*, 1978).

Effects of L-NNA, D-NNA and L-arginine

Administration of L-NNA resulted in a dose-dependent inhibition of LOS relaxation (Figures 1 and 2). The maximal effect at each dose of L-NNA was seen after approximately 10 min. At 10^{-5} mol kg^{-1}, the LOS failed to relax in response to vagal stimulation at any frequency studied (Figure 1). Resting LOS pressure did not change after infusion of L-NNA (Table 1). The effect of L-NNA (10^{-5} mol kg^{-1}) was fully reversed by infusion of L-arginine, 10^{-4} mol kg^{-1} (Figures 1 and 2). This reversal by L-arginine was maximal after 10–15 min. In animals not given L-arginine, the effect of L-NNA persisted to the end of the study period (at least 30 min after last injection of L-NNA). D-NNA had no influence on LOS relaxation induced by vagal stimulation (Figure 1). Peristaltic velocity was 3.6 ± 0.6 cm s^{-1} in the oesophageal body when a frequency of 10 Hz was used for vagal stimulation. This parameter and the amplitude of contractions were unchanged after infusion of L-NNA (Table 1).

Table 1 Effects of N^{ω}-nitro-L-arginine (L-NNA 10^{-5} mol kg^{-1}) on blood pressure, lower oesophageal sphincter (LOS) pressure and oesophageal peristalsis

	Control	*After L-NNA*	P
Systolic pressure ($n = 6$)	107 ± 12	127 ± 11	<0.05
Diastolic pressure ($n = 6$)	70 ± 5	85 ± 6	<0.05
LOS pressure ($n = 12$ and 7)	31 ± 3	30 ± 3	0.83
Oesophageal peristalsis			
Velocity (cm s^{-1}) ($n = 6$)	3.7 ± 0.6	4.0 ± 0.6	0.81
Pressure amplitude ($n = 6$)	76 ± 7	77 ± 6	0.87

Pressures are given in mmHg. Values are means with s.e.mean indicated. A paired Student's t test was used for statistical comparisons. P represents probability.

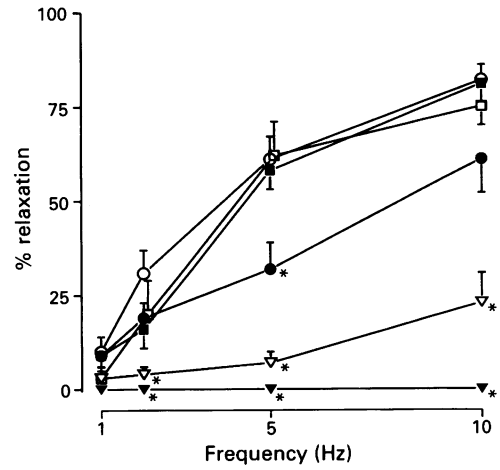

Figure 1 The influence of N^{ω}-nitro-L-arginine (L-NNA) on vagally-induced relaxation of the lower oesophageal sphincter (LOS). Vagal stimulation (1 s trains of impulses, 0.4 ms impulse duration) produced a frequency-dependent relaxation of the LOS (control: ○). L-NNA dose-dependently (*$P < 0.01$) inhibited LOS relaxation (●: 10^{-7} mol kg^{-1}; ▽: 10^{-6} mol kg^{-1}; ▼: 10^{-5} mol kg^{-1}). The effect of L-NNA, 10^{-5} mol kg^{-1} was reversed by infusion of L-arginine, 10^{-4} mol kg^{-1} (□). D-NNA, 10^{-5} mol kg^{-1} (■), had no influence on the relaxations induced by vagal stimulation. All drugs were given intravenously as bolus injections over 20 s. Each point is mean of 7–10 observations with s.e.mean shown by vertical bars.

Effect of sodium nitroprusside

Infusion of sodium nitroprusside, which was given either in untreated animals or when 10^{-5} mol kg^{-1} of L-NNA had abolished LOS responses to vagal stimulation, resulted in a dose-dependent and complete relaxation of LOS pressure ($-\log ED_{50}$: 8.1 ± 0.2 mol kg^{-1} and 8.2 ± 0.3 mol kg^{-1} in control- and L-NNA pretreated animals, respectively; $n = 4$ and 8). Arterial blood pressure was reduced to 15–35 mmHg (systolic) and 5–15 mmHg (diastolic) with the highest dose of sodium nitroprusside (10^{-5} mol kg^{-1}). A comparable

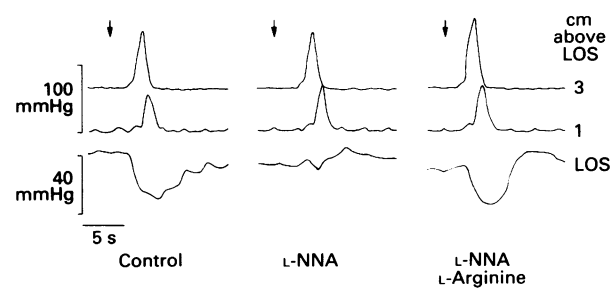

Figure 2 The effect of vagal stimulation on pressures in the oesophageal body and the lower oesophageal sphincter (LOS). The lower tracings represent the LOS and the two upper tracings represent recordings 1 and 3 cm above the LOS, respectively. All three responses were induced by stimulation of the right vagus (1 s train, 40 V, 0.4 ms impulse duration and 10 Hz). Arrows at the top indicate cessation of the stimulus train. The control response is shown on the left. The response in the middle, labelled L-NNA, represents the response recorded 10 min after infusion of N^{ω}-nitro-L-arginine (L-NNA, 10^{-5} mol kg^{-1}). The right response shows the reversing effect of L-arginine (10^{-4} mol kg^{-1}) on LOS relaxation in the same animal. Notice that the peristaltic contractions are unchanged.

reduction in blood pressure by bleeding has been shown to cause only a minor decrease in LOS pressure (Goyal & Rattan, 1980).

Discussion

The external muscle layers of the gastrointestinal tract receive a potent inhibitory innervation, which is thought to play a role in peristalsis and relaxation of sphincters. It is evident that the transmitter(s) mediating the inhibitory responses is neither acetylcholine nor noradrenaline, and it is therefore designated as NANC in character. Different substances, including vasoactive intestinal polypeptide (VIP) and adenosine triphosphate (ATP) have been proposed as participating in the NANC responses of several gut muscles, but significant data fail to support these candidates as principal mediators of NANC inhibition in the oesophagus (Daniel *et al.*, 1983; Torphy *et al.*, 1986). Recently, *in vitro* studies have shown that NO, or a related nitroso compound, might be involved in NANC inhibition of both gastrointestinal and non-gastrointestinal smooth muscle (Gillespie *et al.*, 1989; Li & Rand, 1989; Gibson *et al.*, 1990; Bult *et al.*, 1990; Tucker *et al.*, 1990; Tøttrup *et al.*, 1991). The evidence presented in these studies is based on the assumption that NO, or a related nitroso compound, is synthesized from L-arginine, and that the process is inhibited by L-arginine analogues with a substituted N-guanidino group. Of these analogues, L-NNA seems to be one of the most potent (Moore *et al.*, 1990).

The present finding that vagally-induced relaxation of the LOS was abolished by intravenous administration of L-NNA implies a physiological role of the L-arginine-NO pathway in LOS relaxation. The reversal by L-arginine and the lack of effect of the D-isomer (D-NNA) support this view. The hypothesis is further strengthened by earlier reports that guanosine 3':5'-cyclic monophosphate (cyclic GMP) levels increase during NANC stimulation of the LOS (Torphy *et al.*, 1986), since NO and other nitrogen-containing compounds are potent stimulators of guanylate cyclase (Arnold *et al.*, 1977; Rapoport & Murad, 1983; Boulanger *et al.*, 1990). Sodium nitroprusside, another activator of guanylate cyclase, relaxed the LOS completely when vagally-induced relaxation was absent due to the influence of L-NNA. Moreover, the sensitivity to sodium nitroprusside was identical whether or not the animals had been given L-NNA indicating that the inhibitory influence of L-NNA was not directly on the guanylate cyclase. During 'resting' conditions, NO does not seem to be released in an amount to affect the LOS, since L-NNA had no effects on resting LOS pressure. By contrast, a significant rise in arterial blood pressure was recorded after infusion of L-NNA (Table 1) supporting results of an earlier investigation (Rees *et al.*, 1989b).

NANC inhibition of the circular muscle layer of the oesophageal body has been shown to precede the peristaltic wave of contraction (Rattan *et al.*, 1983; Sugarbaker *et al.*, 1984; Paterson, 1989), and gradients in the latency from cessation of the inhibition to the onset of the contraction have been suggested to play a role in the mechanism of peristalsis (Weisbrodt & Christensen, 1972; Christensen *et al.*, 1979; Paterson, 1989). The inhibitory NANC transmitter of the oesophageal body is probably a product of the L-arginine-NO pathway, since the inhibitory junction potential evoked by stimulation of these nerves is abolished by L-NNA (E.E. Daniel, personal communication), and the prominent 'off' contraction elicited in circular oesophageal muscle strips by transmural field stimulation disappears after L-NNA (Knudsen & Tøttrup, unpublished observations). The short trains used for vagal stimulation in the present study are optimal for relaxation of the lower oesophageal sphincter, but less well suited for studies of oesophageal peristalsis since both contractions with a normal propagation velocity as well as contractions propagating much faster may be elicited (Dodds *et al.*, 1978). In animals showing only the first-named type of contractions, L-NNA did not affect either velocity of propagation or amplitude of contractions. This suggests that, at least under experimental conditions, the inhibitory innervation is not essential for the basic pattern of oesophageal peristalsis. A 'myogenic' mechanism may therefore exist for determination of propagation (Bartlet, 1973; Sarna *et al.*, 1977; Helm *et al.*, 1989), although this mechanism may allow contractions to propagate in both directions when the nerves are blocked.

Two crucial questions that cannot be addressed from the present findings are: (1) is NO the active agent, and (2) is NO, or the closely related compound, a transmitter in the classical sense? Vascular endothelial cells liberate a relaxing factor (endothelium-derived relaxing factor, EDRF) in response to certain stimuli, and several lines of evidence have suggested that EDRF is identical to NO (Palmer *et al.*, 1987; Ignarro *et al.*, 1987). Certain pharmacological differences between EDRF and NO (Shikano *et al.*, 1987) have been demonstrated, and recent experiments have shown a closer similarity between EDRF and a nitrosothiol (Myers *et al.*, 1990; Wei & Kontos, 1990). A linkage to another molecule would clearly be an advantage in the nervous system, since storage of NO is unlikely, due to its instability after contact with oxygen and the superoxide anion (Gryglewski *et al.*, 1986). This leads directly to the question of the compound as a neurotransmitter. The enzyme required for conversion of L-arginine to NO (and citrulline) has recently been demonstrated by immunohistochemical staining in the brain, in autonomic nerves and in the myenteric plexus (Bredt *et al.*, 1990) favouring a transmitter role of NO or the closely related compound. If this is true, we anticipate that the substance released upon activation is either not stored as other neurotransmitters, or is different from NO. The cellular location of the process, however, might also be extraneuronal.

In conclusion, the present findings show that L-NNA is an efficient inhibitor of the NANC-mediated LOS relaxation in intact opossums. This indicates an important role of the L-arginine-NO pathway in LOS motor function. Propagated contractions in the oesophageal body may be generated when the L-arginine-NO pathway is blocked. Further characterization of this mediator system in the LOS, and elsewhere, may be of major clinical importance.

Supported by grants from the Aarhus University Research Foundation and The NOVO Foundation, Denmark.

References

ARNOLD, W.P., MITTAL, C.K., KATSUKI, S. & MURAD, F. (1977). Nitric oxide activates guanylate cyclase and increases guanosine 3' : 5'-cyclic monophosphate levels in various tissue preparations. *Proc. Natl. Acad. Sci. U.S.A.*, **74**, 3203–3207.

BARTLET A.L. (1973). Myogenic peristalsis in isolated preparations of chicken oesophagus. *Br. J. Pharmacol.*, **48**, 36–47.

BREDT, D.S., HWANG, P.M. & SNYDER, S.H. (1990). Localization of nitric oxide synthase indicating a neural role for nitric oxide. *Nature*, **347**, 768–770.

BOULANGER, C., SCHINI, V.B., MONCADA, S. & VANHOUTTE, P.M. (1990). Stimulation of cyclic GMP production in cultured endothelial cells of the pig by bradykinin, adenosine diphosphate, calcium ionophore A23187 and nitric oxide. *Br. J. Pharmacol.*, **101**, 152–156.

BULT, H., BOECKXSTAENS, G.E., PELCKMANS, P.A., JORDAENS, F.H., MAERCKE, Y.M., VAN & HERMAN, A.G. (1990). Nitric oxide as an inhibitory non-adrenergic non-cholinergic neurotransmitter. *Nature*, **345**, 346–347.

CHRISTENSEN, J., ARTHUR, C. & CONKLIN, J.L. (1979). Some determinants of latency of off-response to electrical field stimulation in circular layer of smooth muscle of opossum esophagus. *Gastroenterology*, **77**, 677–681.

DANIEL, E.E., HELMY-ELKHOLY, A., JAGER, L.P. & KANNAN, M.S. (1983). Neither a purine nor VIP is the mediator of inhibitory nerves of opossum oesophageal smooth muscle. *J. Physiol.*, **336**, 243–260.

DODDS, W.J., CHRISTENSEN, J., DENT, J., WOOD, J.D. & ARNDORFER, R.C. (1978). Esophageal contractions induced by vagal stimulation in the opossum. *Am. J. Physiol.*, **235**, E392–E401.

GIBSON, A., MIRZAZADEH, S., HOBBS, A.J. & MOORE, P.K. (1990). L-N^G-monomethyl arginine and L-N^G-nitro arginine inhibit non-adrenergic, non-cholinergic relaxation of the mouse anococcygeus muscle. *Br. J. Pharmacol.*, **99**, 602–606.

GILLESPIE, J.S., LIU, X. & MARTIN, W. (1989). The effects of L-arginine and N^G-monomethyl L-arginine on the response of the rat anococcygeus muscle to NANC nerve stimulation. *Br. J. Pharmacol.*, **98**, 1080–1082.

GOYAL, R.K. & RATTAN, S. (1975). Nature of the vagal inhibitory innervation to the lower oesophageal sphincter. *J. Clin. Invest.*, **55**, 1119–1126.

GOYAL, R.K. & RATTAN, S. (1976). Genesis of basal sphincter pressure: effect of tetrodotoxin on lower esophageal sphincter pressure in opossum *in vivo*. *Gastroenterology*, **71**, 62–67.

GOYAL, R.K. & RATTAN, S. (1980). Effects of sodium nitroprusside and verapamil on lower esophageal pressure. *Am. J. Physiol.*, **238**, G40–G44.

GRYGLEWSKI, R.J., PALMER, R.M.J. & MONCADA, S. (1986). Superoxide anion is involved in the breakdown of endothelium-derived vascular relaxing factor. *Nature*, **320**, 454–456.

GUSTAVSSON, S. & TUCKER, R. (1988). Manometry. In *An Illustrated Guide to Gastrointestinal Motility*. ed. Kumar, D. & Gustavsson, S. pp. 67–80. Chichester: John Wiley & Sons.

HELM, J., BRO, S.L., DODDS, W.J. & SARNA, S.K. (1989). A myogenic mechanism accounts for peristalsis in the opossum smooth-muscle esophagus. *J. Gastrointestinal. Motil.*, **1**, 57.

IGNARRO, L.J., BUGA, G.M., WOOD, K.S., BYRNS, R.E. & CHAUDHURY, G. (1987). Endothelium-derived relaxing factor produced and released from artery and vein is nitric oxide. *Proc. Natl. Acad. Sci. U.S.A.*, **84**, 9265–9269.

LI, C.G. & RAND, M.J. (1989). Evidence for a role of nitric oxide in the neurotransmitter system mediating relaxation of the rat anococcygeus muscle. *Clin. Exp. Pharmacol. Physiol.*, **16**, 933–938.

MOORE, P.K., AL-SWAYEH, O.A., CHONG, N.W.S., EVANS, R.A. & GIBSON, A. (1990). L-N^G-nitro arginine (L-NOARG), a novel, L-arginine reversible inhibitor of endothelium-dependent vasodilatation *in vitro*. *Br. J. Pharmacol.*, **99**, 408–412.

MYERS, P.R., MINOR, R.L. JR, GUERRA, R. JR, BATES, J.N. & HARRISON, D.G. (1990). Vasorelaxant properties of the endothelium-derived relaxing factor more closely resemble S-nitrosocysteine than nitric oxide. *Nature*, **345**, 161–163.

PALMER, R.M.J., FERRIGE, A.G. & MONCADA, S. (1987). Nitric oxide release accounts for the biological activity of endothelium-derived relaxing factor. *Nature*, **327**, 524–526.

PALMER, R.M.J., REES, D.D., ASHTON, D.S. & MONCADA, S. (1988). L-arginine is the physical precursor for the formation of nitric oxide in endothelium-dependent relaxation. *Biochem. Biophys. Res. Commun.*, **53**, 1251–1256.

PATERSON, W.G. (1989). Electric correlates of peristaltic and nonperistaltic contractions in the opossum smooth muscle esophagus. *Gastroenterology*, **97**, 665–675.

RAPOPORT, R.M. & MURAD, F. (1983). Endothelium-dependent and nitrovasodilator-induced relaxation of vascular smooth muscle: role of cyclic GMP. *J. Cyclic. Nucleotide Res.*, **9**, 281–296.

RATTAN, S., GIDDA, J.S. & GOYAL, R.K. (1983). Membrane potential and mechanical responses of the opossum esophagus to vagal stimulation and swallowing. *Gastroenterology*, **85**, 922–928.

REES, D.D., PALMER, R.M.J., HODSON, H.F. & MONCADA, S. (1989a). A specific inhibitor of nitric oxide formation from L-arginine attenuates endothelium-dependent relaxation. *Br. J. Pharmacol.*, **96**, 418–424.

REES, D.D., PALMER, R.M.J. & MONCADA, S. (1989b). Role of endothelium-derived nitric oxide in the regulation of blood pressure. *Proc. Natl. Acad. Sci. U.S.A.*, **86**, 3375–3378.

SARNA, S.K., DANIEL, E.E. & WATERFALL, W.E. (1977). Myogenic and neural control systems for oesophageal motility. *Gastroenterology*, **73**, 1345–1352.

SHIKANO, K., OHLSTEIN, E.H. & BERKOWITZ, B.A. (1987). Differential selectivity of endothelium-derived relaxing factor and nitric oxide in smooth muscle. *Br. J. Pharmacol.*, **92**, 483–485.

SUGARBAKER, D.J., RATTAN, S. & GOYAL, R.K. (1984). Mechanical and electrical activity of oesophageal smooth muscle during peristalsis. *Am. J. Physiol.*, **246**, G145–G150.

TORPHY, T.J., FINE, C.F., BURMAN, M., BARNETTE, M.S. & ORMSBEE, H.S. III. (1986). Lower oesophageal sphincter relaxation is associated with increased cyclic nucleotide content. *Am. J. Physiol.*, **251**, G786–G793.

TUCKER, J.F., BRAVE, S.R., CHARALAMBOUS, L., HOBBS, A.J. & GIBSON, A. (1990). L-N^G-nitro arginine inhibits non-adrenergic, non-cholinergic relaxations of guinea-pig isolated tracheal smooth muscle. *Br. J. Pharmacol.*, **100**, 663–664.

TØTTRUP, A., SVANE, D. & FORMAN, A. (1991). Nitric oxide mediating NANC inhibition in opossum lower oesophageal sphincter. *Am. J. Physiol.*, **260**, G385–G389.

WEI, E.P. & KONTOS, H.A. (1990). H_2O_2 and endothelium-dependent cerebral arteriolar dilation. Implications for the identity of endothelium-derived relaxing factor generated by acetylcholine. *Hypertension*, **16**, 162–169.

WEISBRODT, N.W. & CHRISTENSEN, J. (1972). Gradients of contraction in the opossum esophagus. *Gastroenterology*, **62**, 1159–1166.

(Received April 16, 1991
Revised May 17, 1991
Accepted May 20, 1991)

Br. J. Pharmacol. (1991), **109**, 117–122

Effects of adenosine 3′:5′-cyclic monophosphate and guanine nucleotides on calcium-evoked ACTH release from electrically permeabilized AtT-20 cells

Simon Guild

Department of Pharmacology, University of Glasgow, Glasgow G12 8QQ

1 The mouse AtT-20/D16-16 anterior pituitary tumour cell line was used as a model system for the investigation of adenosine 3′:5′-cyclic monophosphate (cyclic AMP)-mediated enhancement of calcium-evoked adrenocorticotrophin (ACTH) secretion.

2 AtT-20 cells were permeabilized by subjecting the cells to intense electric fields. Exposure of permeabilized cells to calcium (1 mM) in the external medium significantly stimulated ACTH secretion over the first 20 min of exposure. This calcium-stimulated ACTH secretion was dependent upon the presence of MgATP (5 mM).

3 The amount of ACTH secreted, in a 20 min incubation at 37°C, from permeabilized cells depended upon the free calcium concentration in the permeabilization medium. Calcium stimulated ACTH secretion from permeabilized cells in the concentration range of 10^{-7}–10^{-5} M (half maximal = 7×10^{-7} M). Cyclic AMP(10^{-4} M) increased the amount of ACTH secreted at each effective concentration of calcium. However, cyclic AMP did not alter the potency of calcium as a stimulant of ACTH secretion.

4 Guanosine 5′-O-(3-thiotriphosphate) (GTP-γ-S, 10^{-4} M) stimulated ACTH secretion from permeabilized cells in the absence of calcium and was additive with calcium-evoked ACTH secretion up to a maximum which could be stimulated by calcium acting singly. Guanosine 5′-O-(2-thiodiphosphate) (GDP-β-S, 10^{-4} M) inhibited calcium-evoked ACTH secretion from permeabilized cells.

5 GTP-γ-S stimulated ACTH secretion from permeabilized cells in a concentration-dependent manner. The nucleotide significantly stimulated ACTH secretion at concentrations of 10^{-5} M and above. Cyclic AMP (10^{-4} M) increased the amount of ACTH secretion evoked by effective concentrations of GTP-γ-S.

6 The results of the present study support the hypothesis that, in AtT-20 cells, cyclic AMP is acting at some site, distal to calcium entry, which modulates the ability of an increase in cytosolic calcium concentration to stimulate ACTH secretion. One such site may be a GTP-binding protein which the present study suggests may mediate the effects of calcium upon the secretory apparatus. These GTP-binding proteins may be a target for regulation by cyclic AMP.

Keywords: Cyclic AMP; calcium; G-proteins; anterior pituitary tumour cell line; ACTH

Introduction

Corticotrophin-releasing factor (CRF), the most potent and effective natural stimulant of adrenocorticotrophin (ACTH) release, activates both adenylate cyclase and adenosine 3′:5′-cyclic monophosphate (cyclic AMP)-dependent protein kinase (PKA) in homogenates of rat anterior pituitary (Aguilera *et al.*, 1983) and a tumour cell line of the mouse anterior pituitary (AtT-20/D16-16) (Miyazaki *et al.*, 1984; Litvin *et al.*, 1984). Other agents that increase the cellular content of cyclic AMP, such as forskolin, and 8-bromo-cyclic AMP, also stimulate ACTH secretion from corticotrophs and AtT-20 cells (Aguilera *et al.*, 1983; Axelrod & Reisine, 1984; Heisler & Reisine, 1984; Litvin *et al.*, 1984; Miyazaki *et al.*, 1984). These findings suggest that elevation of cellular cyclic AMP content and activation of PKA may be an important step in the stimulation of ACTH secretion by CRF.

Extracellular calcium is necessary for the stimulation of ACTH secretion but not the stimulation of cyclic AMP production (Axelrod & Reisine, 1984; Miyazaki *et al.*, 1984). Furthermore, CRF, forskolin and 8 bromo-cyclic AMP also elevate cytosolic calcium concentrations in AtT-20 cells (Luini *et al.*, 1985; Reisine & Guild, 1985; Guild *et al.*, 1986; Guild & Reisine, 1987). Since an increase in the cellular levels of calcium has been proposed as a necessary and sufficient stimulus to trigger hormone secretion (Douglas, 1968), it is conceivable that cyclic AMP influences hormone secretion via an interaction with the calcium messenger system in AtT-20 cells.

The interaction between cyclic AMP and calcium in AtT-20 cells in on at least at two levels. Firstly, cyclic AMP potentiates voltage-dependent calcium entry into AtT-20 cells and raises cytosolic free calcium concentrations (Luini *et al.*, 1985; Guild & Reisine, 1987). Secondly, cyclic AMP potentiates the ability of a particular increase in cytosolic calcium concentration to stimulate ACTH secretion (Guild *et al.*, 1986). These data suggest that an additional important action of this cyclic nucleotide is distal to the entry of calcium into the cytosol to modulate the action of changes in cytosolic calcium, including those evoked by cyclic AMP itself, upon the secretory apparatus. In the present study, the electrical permeabilization technique (Knight & Baker, 1982) was used to test this hypothesis further. This technique has been used previously in this laboratory to investigate the interaction between cyclic AMP and calcium upon hormone secretion from dispersed cells of the intermediate lobe of the rat pituitary (Yammamoto *et al.*, 1987) and the 7315c rat anterior pituitary tumour cell line (Guild *et al.*, 1988). These previous findings strongly suggested a post-calcium site of action in the stimulus-secretion coupling pathway for cyclic AMP-mediated stimulation of hormone secretion.

The mechanisms linking changes in cytosolic calcium concentration to changes in hormone secretion remain largely unknown and therefore possible targets for cyclic AMP-dependent phosphorylation are not immediately obvious. There is increasing evidence that GTP-binding proteins are also involved in mediating the effects of second messengers upon cellular function. GTP analogues have been reported to stimulate exocytosis from secretory cells by a mechanism independent of their actions upon the signal-transduction processes (Burgoyne, 1987). It has been suggested that a late stage in the stimulus-secretion coupling may involve a direct regulation of exocytosis by GTP-binding proteins, dubbed G_E by Gomperts and his co-workers (Barrowman *et al.*, 1986). Pre-

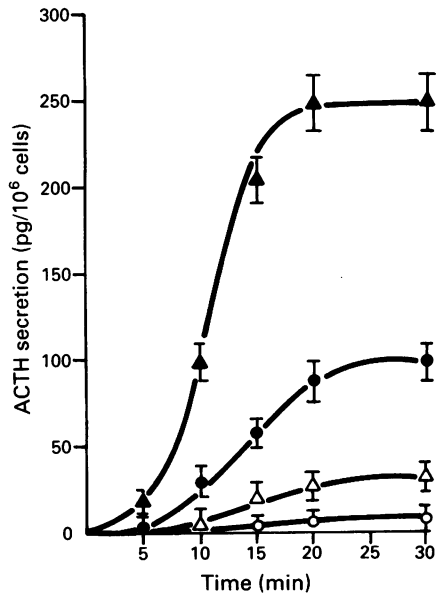

Figure 1 Time course of adrenocorticotrophin (ACTH) secretion from permeabilized AtT-20 cells. Cells, permeabilized as described in the methods (5 discharges of 2.5 kV cm^{-1}), were incubated for the indicated time periods in standard permeabilization medium modified to contain (1) no calcium and no MgATP (○), (2) no calcium but MgATP (5 mM) (●), (3) calcium (1 mM) but no MgATP (△), or (4) calcium (1 mM) and MgATP (5 mM) (▲). The amount of ACTH secreted into the medium during each time period was determined by radioimmunoassay, as described in the methods. The results are expressed as the means from 3 separate experiments; s.e.mean shown by the vertical bars.

vious findings have suggested that a GTP-binding protein may mediate the effects of changes in cytosolic free calcium concentration on hormone secretion (Luini & De Matteis, 1988; 1990).

The principal aim of this study was to investigate the post-calcium site of action of cyclic AMP in AtT-20 cells (Guild *et al.*, 1986) and to test whether this is at the level of a GTP-binding protein. The results of the present study support the hypothesis that, in AtT-20 cells, cyclic AMP is acting at some site distal to changes in the free cytosolic calcium concentration to potentiate calcium-evoked ACTH secretion. Furthermore, GTP-binding proteins mediate the effect of calcium upon the secretory apparatus. A site of regulation by cyclic AMP may lie at or beyond the level of these GTP-binding proteins controlling secretion.

Methods

Culture of AtT-20 cells

Cells of the mouse AtT-20/D16-16 pituitary tumour were grown and subcultured in Dulbecco's Modified Eagle's Medium (DMEM) containing glucose 4.5 g l^{-1} and supplemented with 10% (w/v) foetal calf serum, as previously described (Reisine, 1984). Cells were plated in 75 cm^2 flasks (Nunc, Gibco, UK) at an initial density of 2 × 10^6 cells/flask and were used 7–9 days after subculturing (80–90% confluency). Routinely between 10–20 × 10^6 cells were harvested from each culture flask.

Preparation of AtT-20 cells for experiments

The culture medium was removed, cells adhering to the substrate were washed 3 times with 10 ml of DMEM supplemented with 0.1% (w/v) bovine serum albumin (DMEM/BSA) and then incubated for 1 h in 10 ml of fresh DMEM/BSA at 37°C in a humidified atmosphere of 5% CO_2 in air. The DMEM/BSA was then decanted and the cells liberated from the substrate by Trypsin/EDTA. The cells were washed twice by centrifugation (200 *g*, 5 min) and resuspension in a balanced salt solution of the following composition (mM): NaCl 145, KCl 5.6, $CaCl_2$ 2, $MgCl_2$ 0.5, glucose 5.6, HEPES 5, sodium ascorbate 0.5 and BSA 0.1% (w/v); pH 7.4. After washing, the cells were suspended at a density of 10^6 cells ml^{-1} in this buffer and incubated for a further 30 min at 37°C. The cell suspension was then centrifuged (200 *g*, 5 min) and the cell pellet washed twice by resuspension/centrifugation (200 *g*, 5 min) in the standard permeabilization buffer of the following composition (mM): potassium glutamate 129, PIPES (potassium salt) 20, glucose 5, ATP 5, EGTA 5, BSA 0.1% (w/v); pH 6.6. The cells were finally resuspended in this buffer at a density of 10^7 ml^{-1} and electrically permeabilized by subjection to intense electric fields of brief duration (Knight & Baker, 1982). The nuclear stain, ethidium bromide, is normally impermeant and fluorescent only when in contact with nucleic acid. It can, therefore, be used as an indicator of cell permeabilization. To determine the parameters that lead to 100% permeabilization, the cells were subjected to varying numbers of discharges of varying voltages and subsequently stained with ethidium bromide (50 μM) as previously described (Guild *et al.*, 1988). Optimum permeabilization parameters were also determined for the ability of calcium, added to the external medium, to stimulate ACTH secretion from permeabilized cells as previously described (Guild *et al.*, 1988). For both indicators of permeabilization, optimum parameters were determined to be 5 discharges of 2500 V cm^{-1} (data not shown) and were subsequently adopted in these experiments. The time period for which the cells remained permeabilized was also determined by methods previously described (Guild *et al.*, 1988) and it was found that AtT-20 cells remained permeabilized for 60 min (data not shown).

Measurement of calcium-stimulated ACTH from permeabilized AtT-20 cells

The standard protocol for the determination of ACTH secretion from permeabilized AtT-20 cells was as follows: permeabilized cells were suspended at a cell density of 10^6 cells ml^{-1} in a series of calcium-EGTA buffers chosen to give a free calcium concentration in the range 10^{-9}–10^{-3} M. At this point, the zero time samples were centrifuged (10,000 *g*, 30 s) and an aliquot of the supernatant was stored for subsequent measurement of ACTH content. The cell suspensions were incubated at 37°C for 20 min at which point incubations were terminated by centrifugation (10,000 *g*, 30 s) and removal of the supernatant. The ACTH content of the supernatant was measured by radioimmunoassay. In each experiment, sextuplicate samples were run for each condition. The modifications to this standard protocol which were made to permit the measurement of the effect of cyclic AMP and guanine nucleotides, upon calcium-stimulated ACTH secretion from permeabilized AtT-20 cells, are described in the legends to the figures.

Preparation of calcium-EGTA buffers

In experiments involving the exposure of permeabilized cells to a range of free calcium concentrations in the external medium, calcium-EGTA buffers were employed to obtain the desired free calcium concentration (Portzehl *et al.*, 1964). Various quantities of volumetric 1 M $CaCl_2$ and $MgCl_2$ were added to the standard permeabilization buffer to give the required free calcium concentration and a free magnesium concentration of 1 mM when in equilibrium with 5 mM EGTA and 5 mM MgATP (present in the standard buffer) at pH 6.6. The exact quantity of $CaCl_2$ and $MgCl_2$ to be added was calculated by use of a computer programme written on the basis of previously published programmes for hand held calculators (Perrin & Sayce, 1967; Fabiato & Fabiato, 1979). The free calcium concentration of these Ca-EGTA buffers was checked

by a calcium-sensitive electrode (Affolter & Siegel, 1979) and calibrated by use of calcium standards (Tsien & Rink, 1980).

Radioimmunoassays

The radioimmunossay for ACTH was performed as previously described (Reisine, 1984). The amount of ACTH released by 10^6 cells was expressed as the amount present at the end of the specified incubation period less the amount present at zero time.

Statistics

Each experiment was repeated three times, on different days. A two-sided, 0.05 level, paired *t* test was used to determine if the effect of a treatment was significant.

Materials

The following substances (with their sources) were used: cyclic AMP, ATP, BSA (fraction V) from Sigma, UK; guanosine 5'-O-(3-thiotriphosphate) (GTP-γ-S) and guanosine 5'-O-(2-thiodiphosphate) (GDP-β-S) from Boehringer Mannheim, UK; DMEM, foetal calf serum and trypsin/EDTA were purchased from GIBCO, UK; human ACTH antiserum and human ACTH for standards was the gift of the National Hormone and Pituitary programme, Baltimore, MD, U.S.A.; [^{125}I]-ACTH tracer was the gift of Dr F. Antoni, University of Edinburgh. All other chemicals used were of Analar grade and readily commercially available.

Results

Characterization of calcium-stimulated ACTH secretion

Permeabilized AtT-20 cells secreted ACTH in response to 1 mM external calcium (Figure 1). The ability of calcium to stimulate ACTH secretion was dependent upon the presence of MgATP (5 mM) in the incubation medium. Calcium (1 mM) stimulated an ACTH secretion of 251 ± 10 pg/10^6 cells in a 20 min period in the presence of MgATP but only 24 ± 3 pg/10^6 cells in the absence of MgATP. Interestingly, MgATP alone was able to stimulate significantly ACTH secretion from permeabilized AtT-20 cells in an apparently calcium-independent manner but to a much lesser extent than in the presence of calcium. The time course studies revealed that significant calcium-stimulated ACTH secretion was detectable after 5 min of exposure and that it reached a plateau after 20 min. Consequently, 20 min was chosen as the incubation period for subsequent experiments.

Calcium-evoked ACTH secretion from permeabilized AtT-20 cells was dependent upon the concentration of free calcium in the permeabilization medium (Figure 2). Calcium stimulated ACTH secretion in a concentration-dependent manner between 10^{-7} and 10^{-5} M ($EC_{50} = 7 \times 10^{-7}$ M). Cyclic AMP (10^{-4} M) enhanced calcium-dependent ACTH secretion from permeabilized AtT-20 cells. The amount of ACTH secreted at each effective concentration of calcium was increased (the maximum effect was a 2 fold increase). Cyclic AMP did not significantly change either the EC_{50} of the calcium concentration-effect curve ($EC_{50} = 7 \pm 1 \times 10^{-7}$ M in the absence and $5 \pm 1 \times 10^{-7}$ M in the presence of cyclic AMP) or the concentration of calcium which caused a maximal effect.

The effect of guanine nucleotides upon ACTH secretion from permeabilized AtT-20 cells

The non-hydrolysable GTP analogue, GTP-γ-S (10^{-4} M), which persistently activates GTP-binding proteins, signifi-

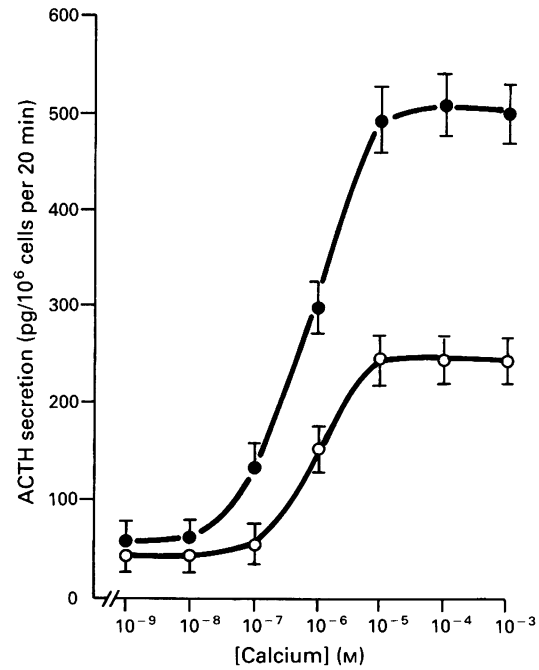

Figure 2 Effect of adenosine 3':5'-cyclic monophosphate (cyclic AMP) on calcium-dependent adrenocorticotrophin (ACTH) secretion from permeabilized AtT-20 cells. Permeabilized cells were incubated in standard permeabilization medium containing various proportions of calcium and EGTA, such that the indicated concentrations of free calcium resulted, either in the presence (●) or absence (○) of cyclic AMP (10^{-4} M). The amount of ACTH secreted was determined. The results are expressed as the means from 3 separate experiments; s.e.mean shown by vertical bars.

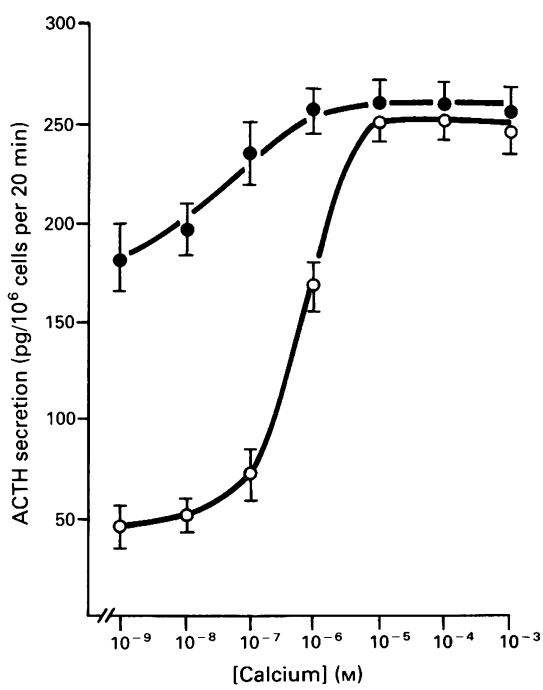

Figure 3 Effect of guanosine 5'-0-(3-thiotriphosphate (GTP-γ-S) on calcium-dependent adrenocorticotrophin (ACTH) secretion from permeabilized AtT-20 cells. Permeabilized cells were incubated in standard permeabilization medium containing various proportions of calcium and EGTA, such that the indicated concentrations of free calcium resulted, either in the presence (●)or absence (○)of GTP-γ-S (10^{-4} M). The amount of ACTH secreted was determined. The results are expressed as the means from 3 separate experiments; s.e. mean shown by vertical bars.

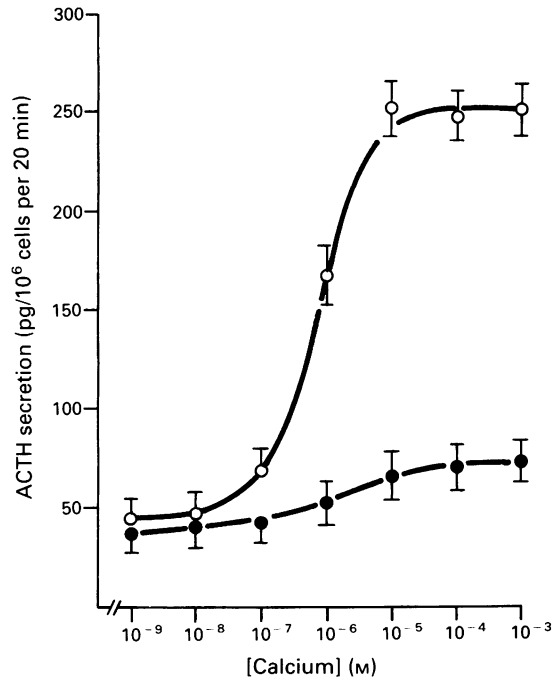

Figure 4 Effect of guanosine 5'-0-(2-thiodiphosphate) (GDP-β-S) on calcium-dependent adrenocorticotrophin (ACTH) secretion from permeabilized AtT-20 cells. Permeabilized cells were incubated in standard permeabilization medium containing various proportions of calcium and EGTA, such that the indicated concentrations of free calcium resulted, either in the presence (●) or absence (○) of GDP-β-S (10^{-4} M). The amount of ACTH secreted was determined. The results are expressed as the means from 3 separate experiments; s.e.mean shown by vertical bars.

cantly stimulated ACTH secretion in the absence of calcium (free calcium concentration of 10^{-9} M, Figure 3). This effect of GTP-γ-S (10^{-4} M) was additive with the stimulation of ACTH secretion evoked by increasing concentrations of free calcium

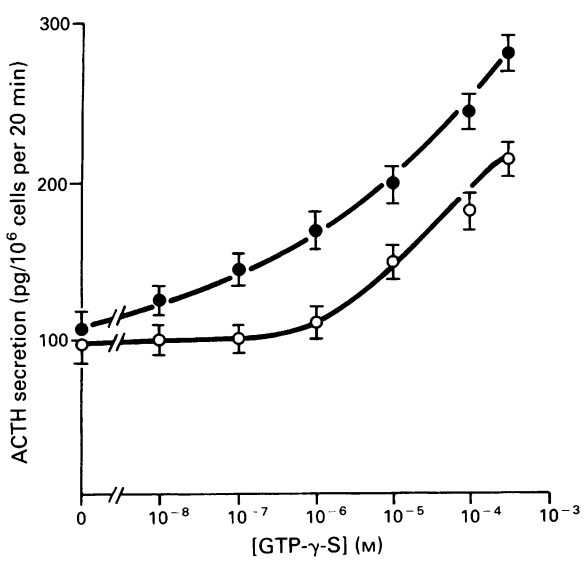

Figure 5 Effect of adenosine 3':5'-cyclic monophosphate (cyclic AMP) on guanosine 5'-0-(3-thiotriphosphate) (GTP-γ-S)-stimulated adrenocorticotrophin (ACTH) secretion from permeabilised AtT-20 cells. Permeabilised cells were incubated in the standard permeabilization medium supplemented with the indicated concentrations of GTP-γ-S either in the presence (●) or absence (○) of cyclic AMP (10^{-4} M). The amount of ACTH secreted was determined. The results are expressed as the means for 3 separate experiments; s.e.mean shown by the vertical bars.

but only up to a maximal value which could be achieved by calcium acting alone. The stable GDP analogue, GDP-β-S (10^{-4} M), used as a method of competing with GTP and thus inhibiting the activation of GTP-binding proteins, inhibited calcium-evoked ACTH secretion (Figure 4). The stimulation of ACTH secretion evoked by 10^{-5} M free calcium was inhibited by 80% in the presence of GDP-β-S (10^{-4} M). The stimulation of ACTH secretion by GTP-γ-S in the absence of calcium was concentration-dependent (Figure 5). The threshold concentration for GTP-γ-S stimulation of ACTH secretion was 10^{-6} M and would appear to be approaching a maximal effect at 3×10^{-4} M. Cyclic AMP (10^{-4} M) enhanced the stimulation of ACTH secretion stimulated by GTP-β-S at all concentrations of the nucleotide investigated. Thus cyclic AMP potentiated both calcium- and guanine nucleotide-stimulated ACTH secretion.

Discussion

Permeabilizing AtT-20 cells by use of the high voltage technique did not impair their ability to undergo exocytosis. Permeabilized tumour cells maintained a secretory response which was dependent upon the free cytosolic calcium concentration and the presence of MgATP. This latter finding is in agreement with previous reports from both this (Yamamoto *et al.*, 1987; Guild *et al.*, 1988) and other laboratories (Knight & Baker, 1982; Bittner *et al.*, 1986; Vallar *et al.*, 1987) in which MgATP has been found to be necessary for secretion in several cell types including digitonin-permeabilized AtT-20 cells (Luini & De Matteis, 1988). Tumour cells permeabilized in the absence of calcium and MgATP did not release ACTH to any significant extent, suggesting that release due to cellular damage was not significant.

Permeabilized AtT-20 cells exhibited increased ACTH secretion when the intracellular calcium concentration was increased between 10^{-7} and 10^{-5} M ($EC_{50} = 7 \times 10^{-7}$ M). These data are entirely consistent with those obtained from several cell types by various permeabilization techniques (for review see Knight & Scrutton, 1986). In addition, the calcium concentration range of 10^{-7}–10^{-5} M is similar to that found in digitonin-permeabilized AtT-20 cells (Luini & De Matteis, 1988) and our own results in dispersed intermediate lobe pituitary cells (Yamamoto *et al.*, 1987) and electrically-permeabilized 7315c cells (Guild *et al.*, 1988). These comparisons indicate that electrically-permeabilized AtT-20 cells may be a useful system for the further investigation of the effects of cyclic AMP upon calcium-evoked ACTH secretion.

Cyclic AMP enhanced calcium-dependent secretion from permeabilized AtT-20 cells. This implies that, in permeabilized AtT-20 cells, cyclic AMP does not enhance hormone secretion by increasing the cytosolic calcium concentration, since any such increases would be buffered by the calcium-EGTA buffers (which are designed to maintain the desired free calcium concentrations). By implication, increased calcium entry into the cytosol from either intra- or extracellular sources (Luini *et al.*, 1985; Guild *et al.*, 1986; Guild & Reisine, 1987; Reisine & Guild, 1987) may not be the only mechanism by which cyclic AMP enhances secretion and an ability to enhance ACTH secretion evoked by a particular increment in cytosolic calcium may be an important additional mechanism. This is consistent with our previous work with intact AtT-20 cells (Guild *et al.*, 1986). If cyclic AMP were to increase the cytosolic calcium concentration in a compartment critical for secretion, then calcium would be more potent in stimulating secretion in its presence. Since this was not observed, the principal site of action of cyclic AMP in enhancing ACTH secretion from permeabilized AtT-20 cells must be distal to the entry of calcium into the cytosol. The fact that cyclic AMP increases the capacity of the AtT-20 cell to release ACTH in

response to a particular increment in cytosolic calcium leads to the speculation that cyclic AMP alters a rate-limiting step in the calcium-dependent release pathway or alters the fusion of secretory vesicles with the cell membrane. It was this speculation which led to the studies of the effects of guanine nucleotides in permeabilized AtT-20 cells.

A new role for GTP-binding proteins has emerged from the use of GTP analogues in permeabilized secretory cells (Burgoyne, 1987) in which they have been reported to stimulate exocytosis by a mechanism independent of their actions upon signal-transduction processes (Bittner *et al.*, 1986; Howell *et al.*, 1987; Vallar *et al.*, 1987). Both membrane fusion and microtubule assembly are sensitive to guanine nucleotides and it is therefore possible that one of these could be the site at which the control of exocytosis is exerted (Barrowman *et al.*, 1986). A postulated GTP-binding protein involved in the control of exocytotic secretion has been dubbed G_E by Gomperts and his co-workers (Barrowman *et al.*, 1986) implying that it is directly involved in membrane fusion in exocytosis. Recent studies in digitonin-permeabilized AtT-20 cells have indicated a role for GTP-binding proteins, perhaps G_E, in the stimulation of ACTH secretion in this cell line (Luini & De Matteis, 1988; 1990). We have shown here that GTP-γ-S is able to stimulate ACTH secretion, in a concentration-dependent manner, in the absence of calcium. In addition, GDP-β-S inhibited calcium-evoked ACTH secretion. These findings strongly support the contention that a GTP-binding protein(s) mediates the stimulation of ACTH secretion evoked by increases in cytosolic calcium concentration.

The nature of the GTP-binding protein directly regulating exocytosis remains unknown. The *ras* (*Ha-*, *Ki*, and *N-ras*) and *ras*-like genes (*rho*, *ral*, *R-ras*, Yptl, *rab2* and *Sec4*) encode an evolutionarily conserved family of proteins, with molecular weights of 20–25,000, which exhibit both GTP/GDP binding and GTPase activities (Barbacid, 1987). It has been suggested that the product of a *ras* gene is a GTP-binding protein involved in the regulation of exocytosis based on the evidence that microinjection of the protein product of a human *ras* gene resulted in degranulation of mast cells (Bar-Sagi & Feramisco, 1986). Interestingly small molecular weight GTP-binding proteins have been implicated as molecular switches in the processing, packaging and exocytosis in constitutive exocytosis in yeast (Salminen & Novick, 1987; Segev *et al.*, 1988; Bourne *et al.*, 1990). Furthermore, the Sec4 gene product Sec4p, rapidly associates with the cytoplasmic surface of secretory vesicles as well as the inner surface of the plasma membrane of the yeast cells (Goud *et al.*, 1988) and has been proposed as important in the promotion of fusion of the secretory vesicle and plasma membranes (Bourne *et al.*, 1990). However, any comparison with the secretory system investigated here is severely limited by the lack of a stimulated exocytotic pathway in yeast and the fact that constitutive membrane traffic in yeast is inhibited by GTP-γ-S (Bourne, 1988).

The ability of cyclic AMP to potentiate GTP-γ-S-evoked ACTH secretion suggests that the site of interaction between calcium and cyclic AMP is either at or at some point distal to the GTP-binding protein(s) mediating the effects of calcium upon the secretory apparatus. Interestingly, small molecular weight GTP-binding proteins have been identified as PKA phosphorylation targets (Lazarowski *et al.*, 1989; Nagata *et al.*, 1989). Furthermore, PKA phosphorylates proteins in intact AtT-20 cells of molecular weight in the range 20–25,000 Da (Bishop *et al.*, 1987; Rougon *et al.*, 1989). It is therefore an attractive idea that cyclic AMP could be acting at the level of a small molecular weight GTP-binding protein or the proteins associated with the regulation of their activity (for review see Bourne *et al.*, 1990) to produce the observed ability of this cyclic nucleotide to potentiate calcium-evoked hormone secretion.

The author would like to acknowledge the financial support of the Wellcome Trust.

References

AFFOLTER, H. & SIEGEL, E. (1979). A simple system for the measurement of ion activities with solvent polymeric membrane electrodes. *Anal. Biochem.*, **97**, 315–319.

AGUILERA, G., HARWOOD, J., WILSON, J., BROWN, J. & CATT, K. (1983). Mechanism of action of corticotropin-releasing factor and other regulators of corticotropin release in rat pituitary cells. *J. Biol. Chem.*, **258**, 8039–8045.

AXELROD, J. & REISINE, T. (1984). Stress hormones: Their interaction and regulation. *Science*, **224**, 452–459.

BARBACID, M. (1987). *Ras* genes. *Annu. Rev. Biochem.*, **56**, 779–827.

BARROWMAN, M.M., COCKCROFT, S. & GOMPERTS, B.D. (1986). Two roles for guanine nucleotides in the stimulus-secretion sequence of neutrophils. *Nature*, **319**, 504–507.

BAR-SAGI, D. & FERAMISCO, J. (1986). Induction of membrane ruffling and fluid-phase pinocytosis in quiescent fibroblasts by *ras* proteins. *Science*, **233**, 1061–1068.

BISHOP, J.F., FARAH, J.M., PATEL, J. & O'DONOHUE, T.L. (1987). Activation of distinct second messenger systems in anterior pituitary corticotropin tumour cells alters the phosphorylation states of both shared and distinct cytosolic proteins. *Mol. Cell. Endocrinol.*, **52**, 17–26.

BITTNER, M.A., HOLZ, R.W. & NEUBIG, R.R. (1986). Guanine nucleotide effects on catecholamine secretion from digitonin-permeabilised adrenal chromaffin cells. *J. Biol. Chem.*, **261**, 10182–10188.

BOURNE, H.R. (1988). Do GTPases direct membrane traffic in secretion. *Cell*, **53**, 669–671.

BOURNE, H.R., SANDERS, D.A. & McCORMICK, F. (1990). The GTP-ase superfamily: a conserved switch for diverse cell functions. *Nature*, **348**, 125–132.

BURGOYNE, R.D. (1987). Control of exocytosis. *Nature*, **328**, 112–113.

DOUGLAS, W. (1968). Stimulus-secretion coupling: The concept and clues from chromaffin and other cells. *Br. J. Pharmacol.*, **34**, 451–474.

FABIATO, A. & FABIATO, F. (1979). Calculator programmes for computing the composition of the solutions containing multiple metals and ligands used for experiments in skinned muscle cells. *J. Physiol. Paris*, **75**, 463–505.

GOUD, B., SALMINEN, A., WALWORTH, N.C. & NOVICK, P.J. (1988). A GTP-binding protein required for secretion rapidly associates with secretory vesicles and the plasma membrane in yeast. *Cell*, **53**, 753–768.

GUILD, S., FREY, E.A., POCOTTE, S.L. & KEBABIAN, J.W. (1988). Adenosine 3':5'-cyclic monophosphate-mediated enhancement of calcium-evoked prolactin release from electrically permeabilized 7315c tumour cells. *Br. J. Pharmacol.*, **94**, 737–744.

GUILD, S., ITOH, Y., KEBABIAN, J.W., LUINI, A. & REISINE, T. (1986). Forskolin enhances basal and potassium evoked hormone release from normal and malignant pituitary tissue. The role of calcium. *Endocrinology*, **118**, 268–279.

GUILD, S. & REISINE, T. (1987). Molecular mechanisms of corticotropin-releasing factor stimulation of calcium mobilization and adrenocorticotropin release from anterior pituitary tumour cells. *J. Pharmacol. Exp. Ther.*, **241**, 125–130.

HEISLER, S. & REISINE, T. (1984). Forskolin stimulates adenylate cyclase activity, cAMP accumulation and ACTH secretion from mouse pituitary tumours. *J. Neurochem.*, **42**, 1659–1665.

HOWELL, T.W., COCKCROFT, S. & GOMPERTS, B.D. (1987). Essential synergy between Ca^{2+} and guanine nucleotides in exocytotic secretion from permeabilized rat mast cells. *J. Cell Biol.*, **105**, 191–197.

KNIGHT, D.E. & BAKER, P.F. (1982). Calcium-dependence of catecholamine release from adrenal medulary cells after exposure to intense electric fields. *J. Memb. Biol.*, **68**, 107–140.

KNIGHT, D.E. & SCRUTTON, M.C. (1986). Gaining access to the cytosol: the technique and some applications of electropermeabilization. *Biochem. J.*, **234**, 497–50.

LAZAROWSKI, E.R., LACAL, J.C. & LAPETINA, E.G. (1989). Agonist-induced phosphorylation of an immunologically *ras*-related protein in human erythroleukaemia cells. *Biochem. Biophys. Res. Commun.*, **161**, 972–978.

LITVIN, Y., PASMANTIER, R., FLEISCHER, N. & EHRLICHMAN, J.

(1984). Hormonal activation of the cAMP-dependent protein kinases in AtT-20 cells. Preferential activation of the protein kinase 1 by corticotropin-releasing factor, isoproterenol and forskolin. *J. Biol. Chem.*, **259**, 10296–10303.

LUINI, A. & DE MATTEIS, M.A. (1988). Dual regulation of ACTH secretion by guanine nucleotides in permeabilized AtT-20 cells. *Cell. Mol. Biol.*, **8**, 129–138.

LUINI, A. & DE MATTEIS, M.A. (1990). Evidence that receptor-linked G protein inhibits exocytosis by a post-second messenger mechanism at AtT-20 cells. *J. Neurochem.*, **54**, 30–38.

LUINI, A., LEWIS, D.,GUILD, S., CORDA, D. & AXELROD, J. (1985). Hormone secretagogues elevate cytosolic calcium by increasing cAMP in corticotropin-secreting cells. *Proc. Natl. Acad. Sci. U.S.A.*, **82**, 8034–8038.

MIYAZAKI, K., REISINE, T. & KEBABIAN, J.W. (1984). Cyclic AMP-dependent protein kinase activity in rodent pituitary tissue; possible role in cAMP-dependent hormone secretion. *Endocrinology*, **115**, 1933–1945.

NAGATA, K. NAGAO, S. & NOZAWA, Y. (1989). Low Mr GTP-binding proteins in human platelets: cyclic AMP-dependent kinase phosphorylates m22KG(I) in membrane but not c21KG in cytosol. *Biochem. Biophys. Res. Commun.*, **160**, 235–242.

PERRIN, D.D. & SAYCE, I.G. (1967). Computer calculation of equilibrium concentrations in mixtures of metal ions and complexing species. *Talanta*, **14**, 833–842.

PORTZEHL, H., CALDWELL, P.C. & REUGG, J.C. (1964). The dependence of contraction and relaxation of muscle fibres from the crab *Maia squinado* on the internal concentration of free calcium *Biochem. Biophys. Res. Commun.*, **79**, 581–591.

REISINE, T. (1984). Somatostatin desensitization; Loss of the ability of somatostatin to inhibit cAMP accumulation and ACTH release. *J. Pharmacol. Exp. Ther.*, **229**, 14–20.

REISINE, T. & GUILD, S. (1985). Pertussis toxin blocks somatostatin inhibition of calcium mobilization and densentizes somatostatin receptors. *J. Pharmacol. Exp. Ther.*, **235**, 551–557.

ROUGON, G., BARBET, J. & REISINE, T. (1989). Protein phosphorylation induced by phorbol esters and cyclic AMP in anterior pituitary cells: possible role in adrenocorticotrophin release and synthesis. *J. Neurochem.*, **52**, 1270–1278.

SALMINEN, A. & NOVICK, P.J. (1987). A *ras*-like protein is required for a post-golgi event in yeast secretion. *Cell*, **49**, 527-538.

SEGEV, N., MULHOLLAND, J. & BOTSTEIN, D. (1988). The yeast GTP-binding YPT1 protein and a mammalian counterpart are associated with the secretion machinery. *Cell*, **52**, 915–924.

TSIEN, R.Y. & RINK, T.J. (1980). Neutral carrier ion-selective microelectrodes for measurement of intracellular free calcium. *Biochim. Biophys. Acta*, **599**, 623–638.

VALLAR, L., BIDEN, T.J. & WOLLHEIM, C.B. (1987). Guanine nucleotides induce a Ca^{2+}-independent insulin secretion from permeabilized R1Nm5F cells. *J. Biol. Chem.*, **262**, 5049–5056.

YAMAMOTO, T., FURUKI, Y., GUILD, S. & KEBABIAN, J.W. (1987). Adenosine 3′,5′-cyclic monophosphate stimulates secretion of α-melanocyte-stimulating hormone from permeabilized cells of the intermediate lobe of the rat pituitary. *Biochem. Biophys. Res. Commun.*, **145**, 1076–1084.

(Recieved April 9, 1991
Revised May 9, 1991
Accepted May 23, 1991)

Br. J. Pharmacol. (1991), **104**, 123–127

Ca^{2+} ion sequestration by guinea-pig tracheal cartilage: its influence on trachealis reactivity to KCl

[1]Paul Gupta, [2]Anthony Markham & Rae M. Morgan

School of Pharmacology, Sunderland Polytechnic, Sunderland, SR1 3SD

1 The contractile response of guinea-pig isolated trachealis to KCl has been studied in the presence and absence of cartilage.

2 Dissection of cartilage from the trachealis resulted in both a rightward displacement of the concentration-response curve to KCl (EC_{50} value: intact strip, 26.9 ± 3.7 mM $n = 5$; dissected strip, 38.7 ± 2.6 mM $n = 5$; $P < 0.05$), and a reduction in the contractile response to KCl (30 mM) observed in a nominally Ca^{2+}-free medium.

3 Removal of cartilage from the trachealis did not alter the responsiveness of the tissue to $CaCl_2$ (2.5 mM) when added to K^+ depolarized tissues.

4 Muscle-denuded cartilage rings were prepared by surgical removal of the trachealis muscle. Autoradiographic studies, and a direct comparison of Ca^{2+} (2.5 mM) uptake with that of sorbitol (2.5 mM) showed that cartilage *per se* had a high capacity to accumulate Ca^{2+} ions by a process which was resistant to iodoacetate (100 μM), diflunisal (100 μM) and boiling.

5 The uptake of ^{45}Ca into isolated cartilage was unaltered by the addition of orthovanadate (500 μM), verapamil (10 μM), diltiazem (10 μM) or Bay K 8644 (10 μM), but was significantly reduced ($P < 0.05$) in the presence of $LaCl_3$ (1–10 mM).

6 We conclude, like previous studies, that cartilage may supply a pool of Ca^{2+} ions to airway smooth muscle during the generation of tension in a noninally Ca^{2+}-free medium, and that $LaCl_3$ may provide an experimental tool to elucidate further the role of non-muscle Ca^{2+}-depots in smooth muscle contraction.

Keywords: Calcium; tracheal cartilage; guinea-pig; KCl

Introduction

Calcium ion entry blockers are less potent on airway smooth muscle (Advenier *et al.*, 1984; Yousif & Triggle, 1986) than on vascular and intestinal smooth muscles (Shimizu *et al.*, 1980; Karaki *et al.*, 1982; Andersson *et al.*, 1983). Although the mechanisms responsible for this tissue selectivity are unclear (Naylor & Dillon, 1986; Triggle, 1987), Ca^{2+} ion entry blockers have been shown to be least effective against agents that evoke a contractile response by the mobilization of intracellular Ca^{2+} ion stores (Cauvin *et al.*, 1988).

However, there is evidence that differences in Ca^{2+} ion entry blocker potency occur against K^+ ions (as KCl) in different types of smooth muscle (Yousif & Triggle, 1986). This presents the possibility that there are inherent differences in the functional binding properties of Ca^{2+} ion entry blockers, although binding data in smooth muscle membrane fractions from different tissues are similar (Bristow *et al.*, 1984; Yousif *et al.*, 1985).

In 1983, Foster and co-workers demonstrated a pronounced uptake of Ca^{2+} ions by cartilage-rich segments of guinea-pig trachea which was inhibited by K^+ ion enrichment of the bathing medium (Foster *et al.*, 1983). Subsequent studies by Raeburn *et al.* (1986; 1987a) suggested that cartilage may supply Ca^{2+} ions during K^+- and histamine-evoked contractures of guinea-pig trachealis. Since high concentrations (mM) of extracellular Ca^{2+} ions have been demonstrated directly to reduce both the Ca^{2+} ion channel blockade induced by Ca^{2+} ion entry blockers (Lee & Tsien, 1983), and reduce binding to specific recognition sites (Garcia *et al.*, 1986), the release of Ca^{2+} ions from cartilage may reduce the functional binding of Ca^{2+} ion entry blockers. Indeed, in the study by Raeburn *et al.* (1987a), cartilage removal was shown to increase the effectiveness of verapamil against K^+ ions and histamine. It appears, therefore, that if cartilage does supply Ca^{2+} ions to the trachealis muscle, then the elevated local Ca^{2+} ion concentration at the site of the Ca^{2+} ion channel may be sufficient to reduce the efficacy of calcium entry blockers, and therefore account for their relatively low potency on airway smooth muscle.

The aim of the work described here was to determine the role of cartilage in modulating the reactivity of airway smooth muscle. Since the presence of cartilage may be of importance in the contraction of guinea-pig trachealis, the mechanisms controlling Ca^{2+} ion sequestration in isolated muscle-free tracheal cartilage were also investigated.

Methods

Dunkin-Hartley guinea-pigs of either sex (700–1000g) were killed by stunning and bleeding. Tracheae were excised from the animals, dissected free of adhering fat and connective tissue and then prepared as described below:

Isometric recording of tension changes evoked by KCl

Tracheae were opened by cutting longitudinally through the cartilage rings diametrically opposite the trachealis muscle. Segments of trachea, two cartilage rings in width, were mounted in isolated organ baths (10 ml) containing Krebs solution gassed with 95% O_2 and 5% CO_2 at 37°C. In test experiments, cartilage was surgically removed from the tracheal segment. Histological examination of these tissues demonstrated that a small amount of cartilage (approximately 5%) remained after dissection. These preparations will be referred to as cartilage-reduced tissues. Attachments were made to both preparations with hooks attached to nylon threads (Mustad, hooks to nylon, size 18).

The initial resting load imposed on intact or cartilage-reduced tissues was 1.0 g. The tissues were equilibrated for 60 min, during which time the bathing fluid was changed at

[1] Present address: Department of Biomedical Research, Wyeth Laboratories, Huntercombe Lane South, Taplow, Maidenhead, Berkshire, SL6 0PH.

[2] Author for correspondence.

15 min intervals. Both intact and cartilage-reduced tissues partially relaxed from the initial 1 g loading tension during the 60 min equilibration. The tension in the preparations was measured with a Grass FT03C force-displacement transducer and displayed on a Grass 79D polygraph. The effects of KCl (10–100 mM) were studied by constructing cumulative concentration-response curves with a 12 min contact time. Two single applications of KCl (30 mM) were then made at 20 min intervals, after which tissues were washed in Krebs solution and allowed to relax for a further 20 min. They were then equilibrated in nominally Ca^{2+}-free Krebs solution (prepared by omission of $CaCl_2$) for 40 min, the media being changed at 5 min intervals, before the effect of KCl (30 mM) was retested. Tissue responsiveness at the end of each experiment was tested by the addition of $CaCl_2$ (2.5 mM), whilst the previous KCl dose remained in the tissue bath. Peak tension (resting tension under 1 g load plus generated tension) was then measured and compared with the peak tension observed following the second addition of KCl (30 mM) to tissues suspended in Ca^{2+}-containing Krebs solution.

^{45}Ca-binding to cartilage

Under a light microscope, tracheae were placed on the dorsal surface and the trachealis muscle was dissected away from the open-ended cartilaginous support. Individual cartilage segments were then dissected free.

Groups of three individual cartilage segments were incubated in Krebs solution (2 ml) gassed with 95% O_2 and 5% CO_2, at 37°C for 15 min, in either the absence or presence of test compounds. Cartilage was then blotted and transferred to Krebs solution, containing ^{45}Ca (0.5 μCi ml^{-1}, 2 ml total volume) and test drug if appropriate, gassed with 95% O_2 and 5% CO_2 at 37°C. ^{45}Ca-binding was measured, after blotting, by solubilization of cartilage in 0.5 ml Soluene at 60°C for 60 min, 0.25 ml of solubilized tissue was added to 10 ml scintillant (PCS, Amersham), dark-adapted overnight and ^{45}Ca activity measured in a Beckman LS 7500 liquid scintillation counter. In experiments investigating the effect of high temperature on ^{45}Ca-binding to cartilage, cartilage was boiled in Krebs solution for 15 min before addition to the ^{45}Ca-containing medium. In experiments involving sorbitol ([^{14}C]-sorbitol, 0.27 μCi ml^{-1}) or lanthanum chloride ($LaCl_3$), a modified sorbitol-Krebs solution or a modified Tris-HCl buffered Krebs solution (pH 7.4) were used respectively. Experiments involving Bay K 8644 were carried out under sodium lamp illumination to reduce photolytic degradation.

Autoradiographical procedures

Cartilage was pre-loaded with ^{45}Ca (10 nCi ml^{-1}) in Krebs solution for 2 h, removed from the medium and frozen in the vapour of liquid nitrogen. Serial transverse sections (20 μm) were cut in a cryostat (Bright Instruments) from the ventral apex of the cartilage at −10°C and were then mounted on gelatin-coated glass microscope slides which were dried in air, and exposed to autoradiography film (Amersham Hyperfilm-βmax) at room temperature for 21 days. The autoradiographs were developed in Kodak D19 developer for 5 min and the distribution of ^{45}Ca was then assessed by visual inspection.

Histological procedures

Serial 20 μm transverse sections of wax-embedded cartilage specimens were prepared with a microtome knife and stained with Ehrlich's haematoxylin and Van Gieson's counterstain as described by Gupta (1990).

Drugs and solutions

The following solutions were used; Krebs solution (mM): NaCl 118, KCl 4.7, $MgSO_4$ 1.0, KH_2PO_4 0.9, $CaCl_2$ 2.5, $NaHCO_3$ 25.0, glucose 11.1; Tris-HCl buffered Krebs solution (mM): NaCl 143, $MgSO_4$ 1.0, Tris-HCl 2.5, KCl 4.7, $CaCl_2$ 2.5, glucose 11.1 (gassed with 100% O_2, pH 7.4). Nominally Ca^{2+}-free Krebs solution and sorbitol-containing Krebs solution were prepared by omission of $CaCl_2$ and addition of sorbitol (2.5 mM) respectively.

Sodium iodoacetate, sodium orthovanadate, diltiazem hydrochloride and verapamil hydrochloride were purchased from Sigma Chemical Company, St. Louis, MO, U.S.A.; lanthanum chloride was purchased from British Drug Houses Ltd., Poole, Dorset; diflunisal was a gift from Merck, Sharpe & Dohme, Hoddsdon, U.K.; and Bay K 8644 was a gift from Bayer A.G., Pharmaceutical Research, F.R.G. ^{45}Ca (specific activity 2.12 mCi 165 μg^{-1} Ca^{2+}) and D-[^{14}C]-sorbitol (specific activity 274 mCi mmol^{-1} D-sorbitol) were purchased from Amersham International.

Bay K 8644 was dissolved in 100% v/v dimethyl sulphoxide (DMSO) and diflunisal in 4% v/v N-methyl-D-glucamine. All other drugs were dissolved in distilled and deionised water.

Statistical analysis of data

Results are expressed as the geometric mean ± s.e.mean for n separate experiments using tissues from different animals. EC_{50} values (concentration of KCl required to produce 50% of the maximum response attainable to KCl in the initial curve) and IC_{50} values (concentration of compound required to inhibit maximum ^{45}Ca-binding to cartilage by 50%) were calculated. Differences between means were determined by a paired Student's t test, after checking the homogeneity of the variances. P values less than 0.05 were considered to be significantly different.

Results

Histological examination of tissues

Following surgical removal of the cartilage support, or the trachealis muscle, from tracheal strips, tissues were examined histologically. No lesions in smooth muscle or cartilage morphology were detected following either surgical procedure when dissected tissues were compared with intact tissues. These observations are in agreement with results from a previous study which also indicated that cartilage removal does not cause obvious muscle damage (Raeburn *et al.*, 1987b).

Effect of cartilage removal on trachealis contracture responses to KCl

KCl (10–100 mM) evoked concentration-dependent contractions of both intact and cartilage-reduced trachealis preparations (Figure 1a), although the latter were less sensitive to KCl and the maximal tension developed was reduced (sensitivity, intact strip EC_{50} 26.9 ± 3.7 mM, $n = 5$; cartilage-reduced strip EC_{50} 38.7 ± 2.6 mM, $n = 5$, $P < 0.05$: maximal tension developed, intact strip 1860 ± 443 mg tension, $n = 5$; cartilage-reduced strip 417 ± 96 mg tension, $n = 5$, Figure 1b).

Two challenges with KCl (30 mM) separated by a 20 min interval gave reproducible responses (maximal tension developed, intact strip 673 ± 112 and 665 ± 113 mg tension, both $n = 5$, $P > 0.05$; cartilage-reduced strip, 128 ± 17 and 115 ± 16 mg tension, both $n = 5$, $P > 0.05$). The response to a third KCl challenge (30 mM) made in a nominally Ca^{2+}-free medium, was reduced compared with that seen in Ca^{2+}-containing Krebs solution. This reduction was greater in cartilage-reduced strips than in controls (peak tension developed, intact strip in Ca^{2+}-containing medium 665 ± 103 mg, $n = 5$; after Ca^{2+} removal, 400 ± 59 mg, $n = 5$, $P < 0.05$: cartilage-reduced strips in Ca^{2+}-containing medium 115 ± 16 mg, $n = 5$; after Ca^{2+} removal, 19 ± 7 mg, $n = 5$, $P < 0.001$). These observations suggested that in the intact tissues, KCl-evoked contractures may be enhanced by the presence of cartilage, or that removal of cartilage caused muscle damage. When $CaCl_2$ (2.5 mM) was added in the presence of KCl (30 mM), a second contracture was superimposed on that

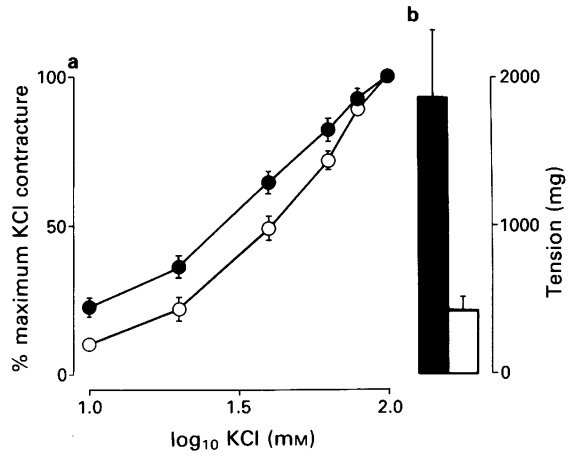

Figure 1 Log concentration-response curve to KCl on intact and cartilage-reduced guinea-pig trachealis preparations. (a) The cumulative administration of KCl (10–100 mM) produced concentration-dependent contractures of both intact (●) and cartilage-reduced (○) preparations. Results are expressed as a percentage of the maximum response to KCl. (b) Representation of data from (a) as maximum tension generated (absolute values) by intact (solid column) and cartilage-reduced (open column) trachealis preparations following the cumulative administration of KCl up to a concentration of 100 mM. All data represent the means of five different experiments with s.e.mean shown by vertical bars.

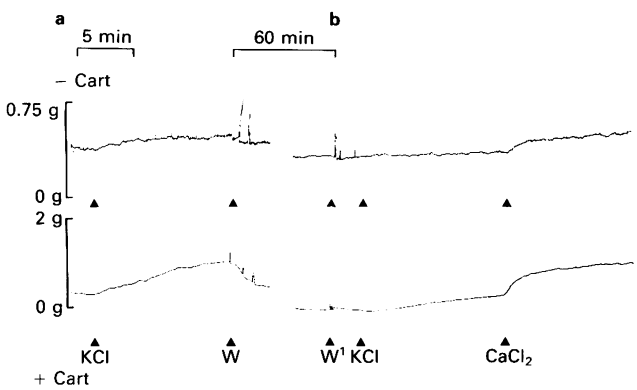

Figure 2 Typical contracture of intact and cartilage-reduced trachealis preparations to KCl in normal and Ca^{2+}-free Krebs solution. Typical contracture responses of cartilage-reduced (−Cart; upper panel) and intact (+Cart; lower panel) guinea-pig trachealis preparations to KCl (30 mM). (a) Two additions of KCl (30 mM; 12 min exposure) were administered at 20 min intervals to preparations in Krebs solution; responses were found to be exactly reproducible, and only the second response is shown. Tissues were then washed in Krebs solution (W), allowed to relax for a further 20 min and then washed in Ca^{2+}-free Krebs for 40 min. (b) The final washing procedure in Ca^{2+}-free Krebs is denoted by W^1, after which KCl (30 mM) was administered for 12 min and contracture responses recorded. After the 12 min exposure of KCl, $CaCl_2$ (2.5 mM) was added for a further 12 min.

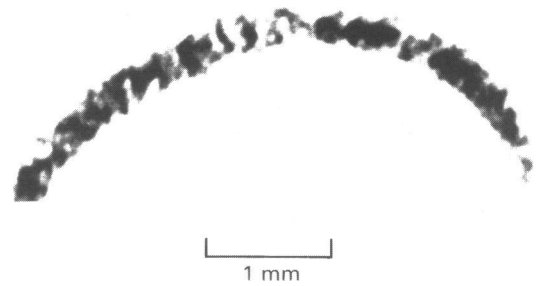

Figure 3 Autoradiograph showing the binding or sequestration of ^{45}Ca in the cartilage of guinea-pig trachea. Following 2 h incubation with ^{45}Ca (10 nCi ml^{-1}), a transverse section (20 μm thickness) of tracheal cartilage was cut in which the knife passed through the ventral portion of one of the cartilage rings. Note, in the autoradiogram prepared from such a section, that the radiolabel became uniformly distributed within the cartilage. The autoradiogram does not provide sufficient resolution to reveal the intraperichondrial distribution of ^{45}Ca in any detail.

due to KCl (peak tension developed, intact strips 1120 ± 127 mg, $n = 5$; cartilage-reduced strips 246 ± 67 mg, $n = 5$). In both tissues, the peak tension following $CaCl_2$ (2.5 mM) equalled the peak tension developed previously in response to KCl (30 mM) in Ca^{2+}-containing Krebs solution (Figure 2). This suggested that the difference in response of the intact and cartilage-reduced strips to KCl in Ca^{2+}-free Krebs solution resulted from cartilage removal.

Binding of ^{45}Ca to cartilage

Incubation of cartilage with ^{45}Ca (0.5 μCi ml^{-1}) in Krebs solution (Ca^{2+} 2.5 mM) from 10 to 120 min resulted in a time-dependent binding (at 10 min 1.33 ± 0.12 and at 120 min 3.64 ± 0.25 pmol ^{45}Ca mg^{-1} cartilage, both $n = 5$, $P < 0.001$). All subsequent data (except autoradiographic experiments) refer to values obtained following a 30 min incubation.

After incubation in ^{45}Ca (0.5 μCi ml^{-1} for 2 h), cartilage sections (thickness 20 μm) were exposed to autoradiography film. Inspection of the film revealed a relatively even distribution of ^{45}Ca throughout each section of the cartilage (Figure 3). Experiments were then performed with sorbitol (a marker of passive tissue equilibration processes; Foster, 1968) in a modified sorbitol-containing Krebs solution (see methods). With incubation of the tissues in this medium, Ca^{2+} uptake, but not that of sorbitol, exhibited time-dependent characteristics (Ca^{2+} uptake, 10 min 3.38 ± 0.35 and 30 min 6.52 ± 0.76 nmol Ca^{2+} mg^{-1} cartilage, both $n = 4$, $P < 0.001$; sorbitol uptake, 10 min 1.24 ± 0.08 and 30 min 1.35 ± 0.03 nmol sorbitol mg^{-1} cartilage, $n = 4$, $P > 0.05$). The mean Ca^{2+} ion: sorbitol ratios, defined as the mol ratio of Ca^{2+} ion/sorbitol accumulated following cartilage incubation in the modified Krebs medium for a fixed time period (Ca^{2+} ion: sorbitol ratio 10 min 2.73, $n = 4$; 30 min 4.81, $n = 4$), suggested that part of

Table 1 Effect of various compounds on ^{45}Ca binding to tracheal cartilage

Treatment	*Concentration* (μM)	^{45}Ca (pmol mg^{-1} cartilage) *Control*	*Test*
Boil	—	2.83 ± 0.18 (5)	2.87 ± 0.27 (5)
Iodoacetate	100	2.68 ± 0.19 (4)	2.59 ± 0.17 (4)
Diflunisal	100	2.62 ± 0.24 (7)	2.54 ± 0.23 (7)
Orthovanadate	500	2.61 ± 0.28 (6)	2.58 ± 0.23 (6)
Diltiazem	10	2.68 ± 0.19 (4)	2.48 ± 0.15 (4)
Verapamil	10	2.61 ± 0.23 (6)	2.56 ± 0.14 (6)
Bay K 8644	10	2.52 ± 0.11 (4)	2.61 ± 0.23 (4)
$LaCl_3$	100	2.48 ± 0.09 (6)	2.35 ± 0.16 (6)
	1000	2.48 ± 0.09 (6)	2.00 ± 0.17 (6)*
	10000	2.48 ± 0.09 (6)	0.66 ± 0.06 (6)**

* $P < 0.05$ when compared with control and ** $P < 0.001$ when compared with control. Number of observations are given in parentheses.

the Ca^{2+} ion accumulation occurred by a process additional to those factors determining passive sorbitol equilibration with the tissue.

Inhibition of ^{45}Ca uptake into cartilage

Boiling cartilage in Krebs solution for 15 min did not alter ^{45}Ca uptake (Table 1). ^{45}Ca uptake was unaffected by iodoacetate (100 μM), diflunisal (100 μM), orthovanadate (500 μM), diltiazem (10 μM), verapamil (10 μM) and Bay K 8644 (10 μM) (Table 1).

The effect of $LaCl_3$ was investigated in a modified Tris-buffered Krebs solution (pH 7.4, see methods). This modified medium did not alter the control amounts of ^{45}Ca accumulated by cartilage. However, $LaCl_3$ (IC_{50} 4.07 $\pm$ 0.70 mM, $n = 6$) did reduce ^{45}Ca uptake (Table 1).

Discussion

Calcium ion entry blockers are less potent relaxants of airway smooth muscle than is the case with other types of smooth muscle. Although the mechanism of such tissue selectivity is not understood, the presence of cartilage in the guinea-pig trachealis has been implicated previously (Raeburn *et al.*, 1986; 1987a). This paper examines the properties of tracheal cartilage and considers its influence on airway smooth muscle reactivity to calcium.

Both the Ca^{2+} ion: sorbitol binding ratios, and autoradiographic evidence showed that cartilage acts as a large depot for Ca^{2+} ions. The accumulation of Ca^{2+} ions by cartilage is a non-biological, adenosine 5'-triphosphate (ATP)-independent event, since boiling and inhibition of ATP synthesis by iodoacetate or diflunisal did not change the rate of uptake. Furthermore, high concentrations of calcium ion entry blockers, Bay K 8644 or orthovanadate did not alter Ca^{2+} uptake into tracheal cartilage. Previous studies with osteosarcoma cells have indicated that Ca^{2+} ion movements may occur via Ca^{2+} ion channels (Guggino *et al.*, 1988) and depend upon Ca^{2+}-ATPase in growth-plate cartilage (Akisaka & Gay, 1985). Therefore, the Ca^{2+} ion regulatory mechanisms reported for osteosarcoma cells and growth-plate cartilage appear to be distinct from those occurring in tracheal cartilage. The only means of inhibiting Ca^{2+} ion uptake into tracheal cartilage revealed in this study was the administration of La^{3+}, suggesting that the uptake process is governed by a physical rather than a biological mechanism. Preliminary experiments indicate that the transition elements such as Cd^{3+} and Mn^{2+}, share with La^{3+}, this ability to inhibit Ca^{2+} ion uptake (Gupta unpublished observations). Thus, the movement of Ca^{2+} ions into cartilage and smooth muscle of the trachea occur by quite different processes.

Does cartilage contribute Ca^{2+} ions that are used in smooth muscle contraction? In agreement with an earlier study by Raeburn *et al.* (1987a), when cartilage was removed from tracheal strips, a rightward displacement of the concentration-response curve to KCl was observed, indicating that KCl is more able to supply Ca^{2+} ions for muscle contraction when cartilage is present than when it is absent. In the cartilage-reduced tissues, the total maximal tension generated to KCl (100 mM) was only 22% of that found in intact tissues. It could thus be argued that the pharmacological changes observed following cartilage removal were the result of muscle damage occurring during dissection. If this were the case, then damage was not apparent upon histological examination of intact and dissected tissues, where no obvious lesions in muscle morphology were observed following dissection. One factor that may have led to the lower level of maximal tension generated could have been that a lower proportion of muscle fibres were aligned with the hook attachments in cartilage-reduced preparations.

KCl (30 mM)-induced contractures of cartilage-reduced tissues were reduced more by Ca^{2+} ion removal than the corresponding responses of intact tissues. This may suggest that KCl-promoted Ca^{2+} release from cartilage provides a means whereby contractile responses of the trachealis muscle to KCl can be preserved despite removal of Ca^{2+} from the bathing medium. However, that Ca^{2+} release from the cartilage plays an important role in supporting KCl-induced contraction of trachealis in a medium containing physiological amounts of Ca^{2+} seems unlikely. In this situation the interstitial fluid provides a large, readily-available pool of extracellular Ca^{2+} which is in intimate contact with all the trachealis cells. In contrast, the majority of trachealis cells do not lie in close proximity to the cartilaginous Ca^{2+} pool.

Ca^{2+} ions derived from cartilage, in addition to those available in the extracellular fluid, could reduce the binding of calcium entry blockers, and therefore explain their low functional potency in this tissue. Evidence in support of this hypothesis has been provided previously in binding (Garcia *et al.*, 1986; Guggino *et al.*, 1988) and functional studies (Lee & Tsien, 1983). However since cartilage is absent from the lower respiratory tract, it is improbable that cartilage could exert a general influence on the efficacy of calcium ion entry blockers in pulmonary tissue. It is conceivable though that simple connective tissue could influence the functional potency of calcium ion entry blockers because of the following; (a) it is found in abundance between both the trachealis muscle bundles (Dixon & Small, 1983) and throughout the respiratory tract; (b) it can also bind high levels of Ca^{2+} ions (Villamil *et al.*, 1973) and (c) it may be integrally involved in the translocation of Ca^{2+} ions from the extracellular compartment into the intracellular compartment during smooth muscle contraction (Loutzenhiser & Van Breeman, 1983). Connective tissue is found to a variable extent in all smooth muscle preparations and could thus be responsible for apparent tissue selectivity. How the transition elements may affect the proposed antagonism by reducing the Ca^{2+} ion supply remains to be determined.

The authors would like to express their gratitude to Dr J.M. Sneddon and Professor D.F. Weetman for their assistance in the preparation of this manuscript.

Diflunisal was a gift from Merck Sharp and Dohme Ltd. (U.K. and U.S.A.). Bay K 8644 was a gift from Bayer AG., Pharmaceutical Research, FRG.

The authors gratefully acknowledge the financial support of the Science and Engineering Research Council (PG).

References

ADVENIER, C., CERRINA, J., DUROUX, P., FLOCH, A. & RENIER, A. (1984). Effects of five different organic calcium antagonists on guinea-pig isolated trachea. *Br. J. Pharmacol.*, **82**, 727–733.

AKISAKA, T. & GAY, C.V. (1985). Ultrastructural localisation of calcium-activated adenosine triphosphatase (Ca^{2+}-ATPase) in growth-plate cartilage. *J. Histochem. Cytochem.*, **33**, 925–932.

ANDERSSON, K.E., EDVINSON, L., MACKENZIE, E.T., SKARBY, T. & YOUNG, A.R. (1983). Influence of extracellular calcium and calcium antagonists on contractions induced by potassium and prostaglandin $F_{2\alpha}$ in isolated cerebral and mesenteric arteries of the cat. *Br. J. Pharmacol.*, **79**, 135–140.

BRISTOW, M.R., GINSBURG, R., LASER, J.A., McAULEY, B.J. & MINOBE, W. (1984). Tissue response selectivity of calcium antagonists is not due to heterogeneity of [^{3}H]-nitrendipine binding sites. *Br. J. Pharmacol.*, **82**, 309–320.

CAUVIN, C., TEJERINA, M., HWANG, O., KAI-YAMAMOTO, M. & VAN BREEMAN, C. (1988). The effect of Ca^{2+} antagonists on isolated rat and rabbit mesenteric resistance vessels. *Ann. N.Y. Acad. Sci.*, **522**, 338–350.

DIXON, J.S. & SMALL, R.C. (1983). Evidence of poor conduction of muscle excitation in the longitudinal axis of guinea-pig isolated trachea. *Br. J. Pharmacol.*, **79**, 75–83.

FOSTER, R.W. (1968). A correlation between inhibition of the uptake of ^3H from (±)-^3H-noradrenaline and potentiation of the responses to (−)-noradrenaline in the guinea-pig isolated trachea. *Br. J. Pharmacol. Chemother.*, **33**, 357–367.

FOSTER, R.W., SMALL, R.C. & WESTON, A.H. (1983). The spasmogenic action of potasium chloride in guinea-pig trachealis. *Br. J. Pharmacol.*, **80**, 553–559.

GARCIA, M.L., KING, F., SIEGL, P.K.S., REUBEN, J.P. & KACZOROWSKI, G.J. (1986). Binding of Ca^{2+} entry blockers to cardiac sarcolemmal membrane vesicles. *J. Biol. Chem.*, **261**, 8146–8157.

GUGGINO, S.E., WAGNER, J.A., SNOWMAN, A.M., HESTER, L.D., SACKTOR, B. & SNYDER, S.H. (1988). Phenylalkylamine-sensitive calcium channels in osteoblast-like osteosarcoma cells. *J. Biol. Chem.*, **263**, 10155–10161.

GUPTA, P. (1990). The control of intracellular calcium homeostasis by aspirin-like drugs and its relationship to mediator function. *Ph. D. Thesis, Sunderland Polytechnic.*

KARAKI, H., MURAKAMI, K., NAGAGAWA, H., OXAKI, H. & URAKAWA, N. (1982). Effect of calmodulin antagonists on tension and cellular calcium content in depolarized vascular and intestinal smooth muscles. *Br. J. Pharmacol.*, **77**, 661–666.

LEE, K.S. & TSIEN, R.W. (1983). Mechanism of action of calcium channel blockade by verapamil, D600, diltiazem and nitrendipine in single dialysed heart cells. *Nature*, **302**, 790–794.

LOUTZENHISER, R. & VAN BREEMAN, C. (1983). Involvement of extracellularly bound calcium in the activation of arterial smooth muscle. *Blood Vessels*, **20**, 295–305.

NAYLOR, W.G. & DILLON, J.S. (1986). Calcium antagonists and their mode of action: an historical overview. *Br. J. Clin. Pharmacol.*, **21**, 97S–107S.

RAEBURN, D., HAY, D.W.P., FARMER, S.G. & FEDAN, J.S. (1987a). Influence of cartilage on reactivity and on the effectiveness of verapamil in guinea-pig isolated airway smooth muscle. *J. Pharmacol. Exp. Ther.*, **242**, 450–454.

RAEBURN, D., HAY, D.W.P., MUCCITELLI, R.M., DEY, R.D. & FEDAN, J.S. (1987b). The development of tone in the smooth muscle of the guinea-pig isolated tracheal preparation may be influenced by prostanoids released from adjacent airway cartilage. *Prostaglandins*, **33**, 651–661.

RAEBURN, D., RODGER, I.W., HAY, D.W.P. & FEDAN, J.S. (1986). The dependence of airway smooth muscle on extracellular Ca^{2+} for contraction is influenced by the presence of cartilage. *Life Sci.*, **38**, 1499–1505.

SHIMIZU, K., OHTA, T. & TODA, N. (1980). Evidence for greater susceptibility of isolated dog cerebral arteries to Ca antagonists than peripheral arteries. *Stroke*, **11**, 261–265.

TRIGGLE, D.J. (1987). Calcium channel ligands. *Annu. Rev. Pharmacol. Toxicol.*, **27**, 347–369.

VILLAMIL, M.F., RETTORI, V. & YEYATI, N. (1973). Calcium exchange and distribution in the arterial wall. *Am. J. Physiol.*, **224**, 1314–1319.

YOUSIF, F.B., BOLGER, G.T., RUZUCKY, A. & TRIGGLE, D.J. (1985). Ca^{2+} channel antagonist actions in bladder smooth muscle: comparative pharmacologic and [^3H]nitrendipine binding studies. *Can. J. Physiol. Pharmacol.*, **63**, 453–462.

YOUSIF, F.B. & TRIGGLE, D.J. (1986). Inhibitory actions of a series of Ca^{2+} channel antagonists against agonist and K^+ depolarization induced responses in smooth muscle: an assessment of selectivity of action. *Can. J. Physiol. Pharmacol.*, **64**, 273–283.

(Received October 19, 1990
Revised April 18, 1991
Accepted May 16, 1991)

Br. J. Pharmacol. (1991), **104**, 128–132

Quantitative assessment of increased airway microvascular permeability to ^{125}I-labelled plasma fibrinogen induced by platelet activating factor and bradykinin

K.E. Pedersen, P.J. Rigby & [1]R.G. Goldie

Department of Pharmacology, University of Western Australia, Perth, Nedlands, 6009, Australia

1 We have used ^{125}I-labelled fibrinogen (I-FN) in experiments monitoring plasma extravasation from vessels within guinea-pig trachea and peripheral lung tissue in response to platelet activating factor (PAF) and bradykinin (BK). Retained tissue radioactivity derived from I-FN was detected by direct measurement and by autoradiography.

2 Both PAF and BK caused concentration-dependent increases in radioactivity in trachea and peripheral lung, with PAF being approximately 1000 times more potent than BK at both sites. On a wet weight basis, mean tracheal leakage responses to PAF and BK were approximately 6 times and 2 times greater respectively than those in peripheral lung. Furthermore, in trachea, the maximal response to PAF was nearly twice that to BK, although they were approximately equiactive in peripheral lung. The dipeptidyl carboxypeptidase inhibitor, enalapril (1 mg kg^{-1}, i.v.), increased the potency of BK by approximately 40 fold.

3 In trachea, PAF (50 ng kg^{-1}, i.v.)-induced leakage was selectively inhibited by the PAF receptor antagonist, WEB 2086 (5–50 μg kg^{-1}), while responses to BK (50 μg kg^{-1}, i.v.) were selectively inhibited by the BK_2 receptor antagonist NPC 349 (0.5–1 mg kg^{-1}). Neither PAF nor BK-induced leakage were significantly altered by pretreatment with the histamine H_1-receptor antagonists mepyramine (10 μg kg^{-1}) or ketotifen (50 μg kg^{-1}) or the leukotriene receptor antagonist SKF 104353. These data indicate that both agonists caused direct, specific receptor operated increases in tracheal vascular permeability to plasma macromolecules. The α/β-adrenoceptor agonist adrenaline (100 μg kg^{-1}) caused modest inhibition of leakage induced by BK, but not of the leakage response to PAF.

4 Peripheral airway leakage responses to both PAF and BK were also detected by light microscopic autoradiography in paraffin-embedded tissue sections. This was possible since a significant amount of extravasated I-FN was apparently precipitated and fixed in the extravascular space as ^{125}I-labelled fibrin. Autoradiograms showed that both agonists caused increases in peripheral bronchial circulation microvascular permeability to I-FN. No evidence for leakage in alveolar wall capillaries or in pulmonary blood vessels was observed. Quantitation of such autoradiographic data will allow a comprehensive evaluation of the effects of putative asthma mediators on microvascular permeability throughout the respiratory tree.

Keywords: Platelet activating factor; bradykinin; vascular leakage; autoradiography; guinea-pig lung and trachea

Introduction

Inflammation, which is often a major feature in bronchial asthma (Barnes, 1988), is closely linked to increased microvascular permeability and oedema (Ryan & Majno, 1977; Persson, 1987). Not surprisingly, airway wall oedema is also a well recognized feature of severe asthma (Huber & Koessler, 1922; Dunnill, 1960). Importantly, many of the putative inflammatory mediators of asthma, including platelet activating factor (PAF) (Page *et al.*, 1984; Cuss *et al.*, 1986) and bradykinin (BK) (Barnes, 1987, Fuller *et al.*, 1987), have been shown to induce the extravasation of plasma macromolecules from the airway microvasculature into the extracellular submucosa and airway lumen (Saria *et al.*, 1983; Persson, 1986; Evans *et al.*, 1987; 1988; Erjefalt & Persson, 1989).

Studies to the present time have largely concentrated on measurement of mediator-induced plasma leakage from tracheal microvessels and have used readily diffusable plasma markers such as FITC-dextran, albumin (radiolabelled or associated with Evans blue dye) (Persson, 1987; Boschetto *et al.*, 1989), or colloidal carbon particles (O'Donnell & Barnett, 1987). In the present study, we were interested in establishing the microvascular sites throughout the respiratory tree at which increased permeability was induced in response to PAF and BK. ^{125}I-labelled fibrinogen (I-FN) is a relatively large plasma protein (340 kDa) which can be used as a marker of plasma extravasation. Importantly, this protein can be rapidly cleaved during activation of the coagulation system in the extravascular space, precipitating as non-diffusible ^{125}I-labelled fibrin (Saldeen, 1969). This property allowed us to obtain a quantitative assessment of the extent of tracheal and peripheral lung plasma leakage, in addition to an autoradiographic evaluation of leakage sites throughout the lung.

Methods

Male guinea-pigs (SR/C Tricolour) weighing 280–350 g were premedicated with diazepam (10 mg kg^{-1}, i.p.) and anaesthetized with 1 ml kg^{-1} Hypnorm (0.315 mg kg^{-1} fentanyl citrate and 10 mg kg^{-1} fluranisone, i.m.). The right jugular vein was cannulated for the intravenous administration of drugs. Animals received I-FN (100 μCi kg^{-1}) and 2 min later a blood sample (0.3 ml) was taken from the contralateral jugular vein for the estimation of blood radioactivity and packed cell volume (PCV). After a further 1 min, PAF (1–250 ng kg^{-1}) or BK (1–250 μg kg^{-1}) was intravenously administered. In some experiments, the effects of antagonists selective for various drug receptor types were tested against PAF or BK-induced plasma leakage. Unless otherwise stated, these antagonists were administered intravenously 10 min before PAF or BK.

The abdominal and thoracic cavities were opened 15 min after agonist administration and a clamp placed on the thoracic vena cava. Assessment of the time course of tissue accumulation of I-FN showed that the response was maximal at this time point. The abdominal vena cava was then severed

[1] Author for correspondence.

and a blood sample collected for estimates of radioactivity and PCV. An infusion of 20 ml of isotonic saline (5 ml min^{-1}). Residual circulating I-FN following this flushing procedure was <3% of the initial blood level.

The lungs were removed and the trachea and lower left lung lobe dissected free, gently blotted dry on filter paper (Whatman No. 1), weighed and the radioactivity estimated in a gamma counter (Packard, model 5650). These tissue specimens were then fixed in buffered formal saline (BFS) for a further 24 h, and processed for embedding in paraffin wax and sectioned at 5 μm. Sections were de-waxed in xylene, air dried and dipped into liquified NTB-2 nuclear track emulsion at 43°C. These assemblies were air dried and placed in light-tight boxes containing dessicant for 21 days at 4°C. Autoradiograms were developed in Dektol (Kodak) diluted 1:1 with distilled water for 3 min, rinsed in 1% acetic acid containing 2.5% Hypam hardener (Ilford), fixed in Hypam Rapid fix (Ilford) containing 2.5% Hypam hardener, for 3 min and washed in distilled water. Sections were then stained with Gill's haematoxylin for 1 min, dehydrated in graded solutions of ethanol, cleared in xylene and mounted under glass coverslips in DePeX mounting medium. Autoradiograms were viewed with an Olympus (BH-2) photo-microscope under light and dark-field illumination.

Data analysis

Tissue radioactivity derived from retained I-FN was used to assess specific leakage of plasma (μl g^{-1} wet weight of tissue). This was calculated by dividing the tissue radioactivity by the product of the plasma radioactivity of I-FN in 1 μl of plasma and the weight of each tissue sample to obtain the volume of extravasated plasma in 1 g of tissue. Non-specific leakage was taken as that occurring after administration of 0.9% w/v sodium chloride (1 ml kg^{-1}) in place of BK, or 0.9% w/v sodium chloride (1 ml kg^{-1}) containing 0.25% bovine serum albumin in place of PAF. Specific leakage was calculated by subtracting non-specific from the total plasma leakage occurring after the administration of PAF or BK.

Data were examined by analysis of variance and Fisher's least significant difference test and treatment effects considered significant if the probability of differences (P) was <0.05.

Drugs

Platelet activating factor (L-α-phosphotidylcholine, β-acetyl-O-alkyl), lyso-PAF (L-α-lysophosphotidylcholine, β-acetyl-O-alkyl), adrenaline bitartrate, histamine dihydrochloride, mepyramine hydrochloride, bradykinin (Sigma); enalapril maleate (Merck Sharp & Dohme); NPC 349 (D-Arg-[Hyp^3, Thi^{5,8}, D-Phe^7]-BK, Nova); WEB-2086 (3-(4-(2-chlorophenyl)-9-methyl-6H-thieno-(3,2-f)(1,2,4)-triazolo-(3,3-α)(1,4)-diazepine-2-yl)-1-(4-morpholinyl)-1-propanone, Boehringer Ingelheim); SKF 104353 (2(s)-hydroxy-3(R)-[(2-carboxyethyl)thio]-3-[2-(8-phenyloctyl)phenyl]-propanoic acid, SmithKline Beecham); Hypnorm (Janssen-Cilag); diazepam (David Bull); ketotifen (Sandoz); ^{125}I-labelled human fibrinogen (approximately 100 μCi mg^{-1}; Amersham).

Results

Trachea

Intravenous PAF (1–250 ng kg^{-1}; Figure 1a) or BK (1–250 μg kg^{-1}; Figure 1b) caused concentration-dependent increases in tracheal radioactivity derived from circulating plasma I-FN. The highest doses of these agonists cause marked changes in breathing pattern including gasping and short periods of apnoea. The maximum response to PAF was approximately 2 fold greater than that observed after the administration of BK. Conversely, lyso-PAF (250 ng kg^{-1}, i.v.) was apparently inactive (Figure 2a). Concentrations causing

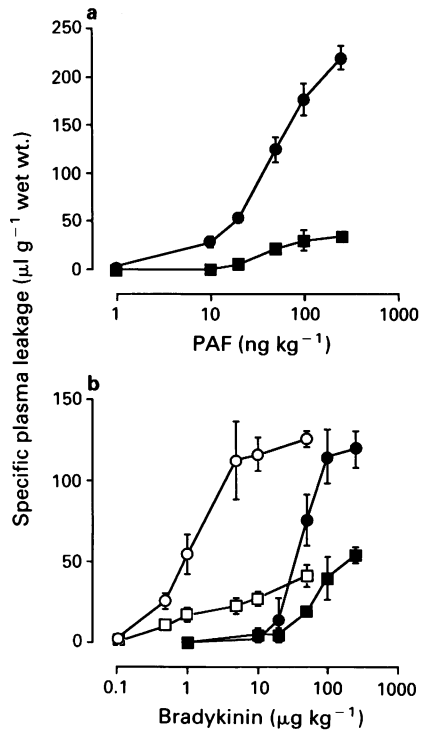

Figure 1 Dose-response relationships for (a) intravenous platelet activating factor (PAF) or (b) intravenous bradykinin (BK)-induced specific plasma leakage (μl g^{-1} wet weight tissue) in guinea-pig trachea (●, ○) and lung parenchyma (■, □), determined from measurements of tissue radioactivity derived from [^{125}I]-labelled fibrinogen (100 μCi kg^{-1}). Data for BK shown with open symbols was obtained following pretreatment with enalapril (1 mg kg^{-1}, i.v.). Vertical bars represent s.e.mean of 5–10 observations.

50% of the maximum plasma leakage (EC_{50}) for PAF and BK were approximately 42 ng kg^{-1} and 40 μg kg^{-1} respectively. Radioactivity derived from I-FN remaining in tracheal tissue from guinea-pigs given only saline or saline containing 0.25% BSA, represented background leakage equivalent to 16.9 ± 1.5 μl g^{-1} wet wt (saline; n = 5) and 18.3 ± 1.7 μl g^{-1} wet wt (BSA saline; n = 6). These were only 10% and 18% of the mean levels of total leakage occurring after administration of PAF (50 ng kg^{-1}) and BK (50 μg kg^{-1}) respectively. The potency of BK was increased by approximately 40 fold by pretreatment with enalapril (1 mg kg^{-1}, i.v.) (EC_{50} = 1.0 μg kg^{-1}), an inhibitor of dipeptidyl carboxypeptidase (Figure 1b). In contrast, enalapril failed to alter the potency of PAF (P > 0.05).

The PAF receptor antagonist WEB-2086 (5–50 μg kg^{-1} i.v.) caused concentration-dependent inhibition of PAF (50 ng kg^{-1})-induced I-FN leakage in trachea. At 50 μg kg^{-1}, WEB-2086 reduced PAF-induced leakage by 96% (Figure 2a, P < 0.001). PAF-induced leakage was not significantly inhibited by the administration of the selective histamine H_1-receptor antagonists mepyramine (10 μg kg^{-1}) or ketotifen (50 μg kg^{-1}), the selective BK_2-receptor antagonist NPC 349 (1 mg kg^{-1}, administered 1 min prior to PAF), or the selective leukotriene receptor antagonist SKF 104353 (0.5 mg kg^{-1}). Pretreatment with adrenaline (50–100 μg kg^{-1}) 5 or 10 min before challenge with PAF also failed to alter significantly plasma leakage in the trachea (Figure 2a; P > 0.05).

BK-induced microvascular leakage in the trachea was not significantly reduced by WEB 2086 (50–100 μg kg^{-1}), mepyramine (10 μg kg^{-1}) or SKF 104353 (0.5 mg kg^{-1}). However, NPC 349 (0.4–1 mg kg^{-1}, i.v.) administered 1 min before BK caused a dose-dependent inhibition of I-FN leakage caused by this peptide. At 1 mg kg^{-1}, NPC 349 reduced BK-induced leakage by 70% (Figure 2b). Pretreatment with adrenaline (100 μg kg^{-1}) administered 5 min prior to BK, reduced the

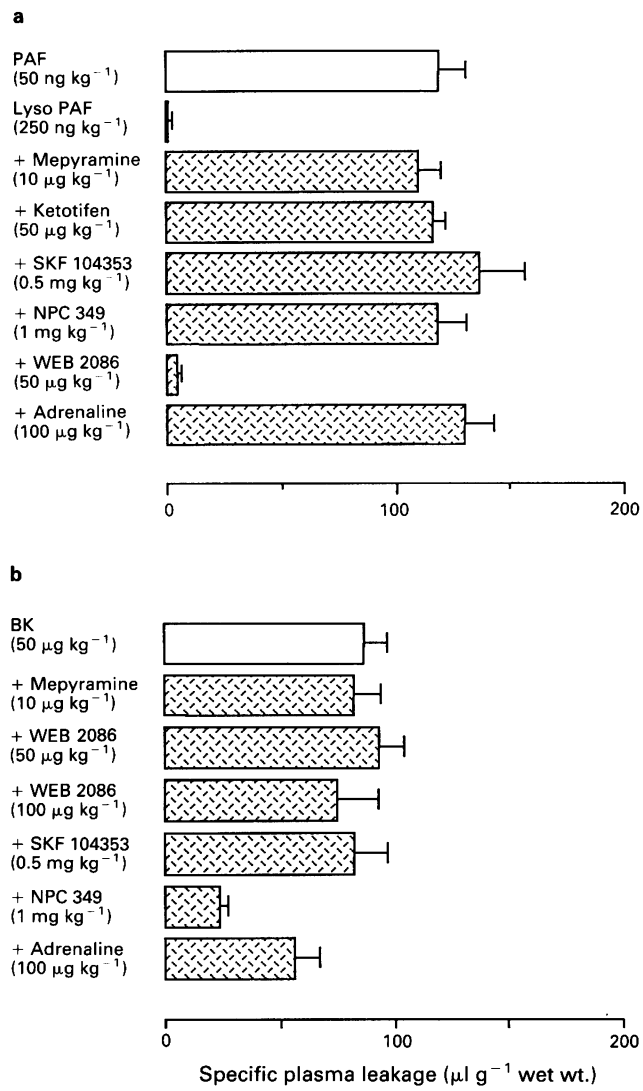

Figure 2 Effects of (a) platelet activating factor (PAF), 50 ng kg^{-1}, i.v.) and lyso-PAF (250 ng kg^{-1}, i.v.) or (b) bradykinin (BK, 50 μg kg^{-1}, i.v.) on the specific vascular leakage of plasma in guinea-pig trachea. The influence of drugs on PAF or BK-induced plasma leakage are indicated by the hatched columns. Horizontal bars represent s.e.mean of 4–10 observations.

leakage response to this agonist by approximately 35% (Figure 2b, $P > 0.05$). No such effect was observed when the pretreatment time was extended to 10 min or when the dose of adrenaline was reduced to 50 μg kg^{-1}.

Parenchyma

In guinea-pig lung parenchyma, the mean background level of I-FN leakage produced following saline challenge was 8.0 ± 1.5 μl g^{-1} wet wt. ($n = 5$) and was 7.4 ± 1.4 μl g^{-1} wet wt. ($n = 6$) after BSA saline challenge. Following exposure to lyso-PAF (250 ng kg^{-1}, i.v.), the mean leakage level was 2.6 ± 1.2 μl g^{-1} wet wt. ($n = 4$). Background leakage was 23% and 24% of the total leakage induced by PAF (50 ng kg^{-1}) and BK (50 μg kg^{-1}) respectively. These agonists were approximately equi-effective in that they caused similar mean maximum levels of plasma leakage (Figure 1). However, for both agonists these levels were only 17% and 45% respectively of those seen in trachea. These weaker responses made accurate quantitation of the effects of appropriate receptor-selective antagonists impracticable.

Autoradiographic detection of PAF or BK-induced leakage sites

Trachea Autoradiographs revealed that both PAF (50 ng kg^{-1}) and BK (50 μg kg^{-1}) caused plasma leakage from vessels of the microcirculation within the tracheal submucosa between the airway epithelium and smooth muscle and in deeper tissue beneath the tracheal smooth muscle (Figure 3). Autoradiographic grain numbers over vessel lumen space were low and similar to numbers determined over non-tissue space. There was no evidence of I-FN leakage across the airway basement membrane into the epithelium, although some extracellular space between smooth muscle layers was infiltrated. Autoradiographic grains derived from I-FN were concentrated in the adventitial space surrounding each vessel. As observed in experiments quantitating tissue radioactivity, WEB-2086 (50 μg kg^{-1}) selectively inhibited PAF-induced I-FN leakage.

Parenchyma In peripheral lung tissue, autoradiographic grains identifying sites of PAF or BK-induced leakage were observed only in association with vessels of the bronchial circulation i.e. with small vessels within the walls of bronchi (Figure 4). As observed in trachea, the luminal space of these blood vessels and of vessels of the pulmonary circulation were associated with very low numbers of autoradiographic grains. Furthermore, the epithelium of these peripheral airways was not penetrated by I-FN sequestered from the vasculature. Numbers of autoradiographic grains similar to background levels determined over non-tissue were evident over alveolar septae, indicating the absence of significant I-FN leakage from alveolar capillaries. Similarly, there was no evidence of plasma leakage from large pulmonary vessels.

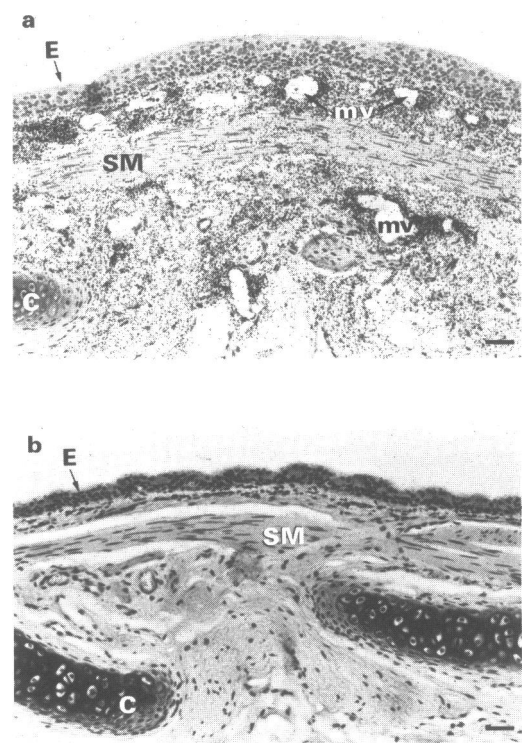

Figure 3 Light-field photomicrographs of transverse paraffin sections (5 μm) of guinea-pig trachea stained with haemotoxylin, from animals given (a) platelet activating factor (PAF, 50 ng kg^{-1}, i.v.), or (b) 0.9% w/v NaCl solution containing 0.25% bovine serum albumin. In (a), autoradiographic grains (black dots) derived from the vascular exudation of ^{125}I-labelled fibrinogen (I-FN, 100 μCi kg^{-1}) are seen concentrated in the perimeter adventitia of submucosal microvessels (mv) of the bronchial circulation. Sequestered I-FN did not penetrate the tracheal epithelium (E). Smooth muscle = SM. Cartilage = C. Bar = 100 μm.

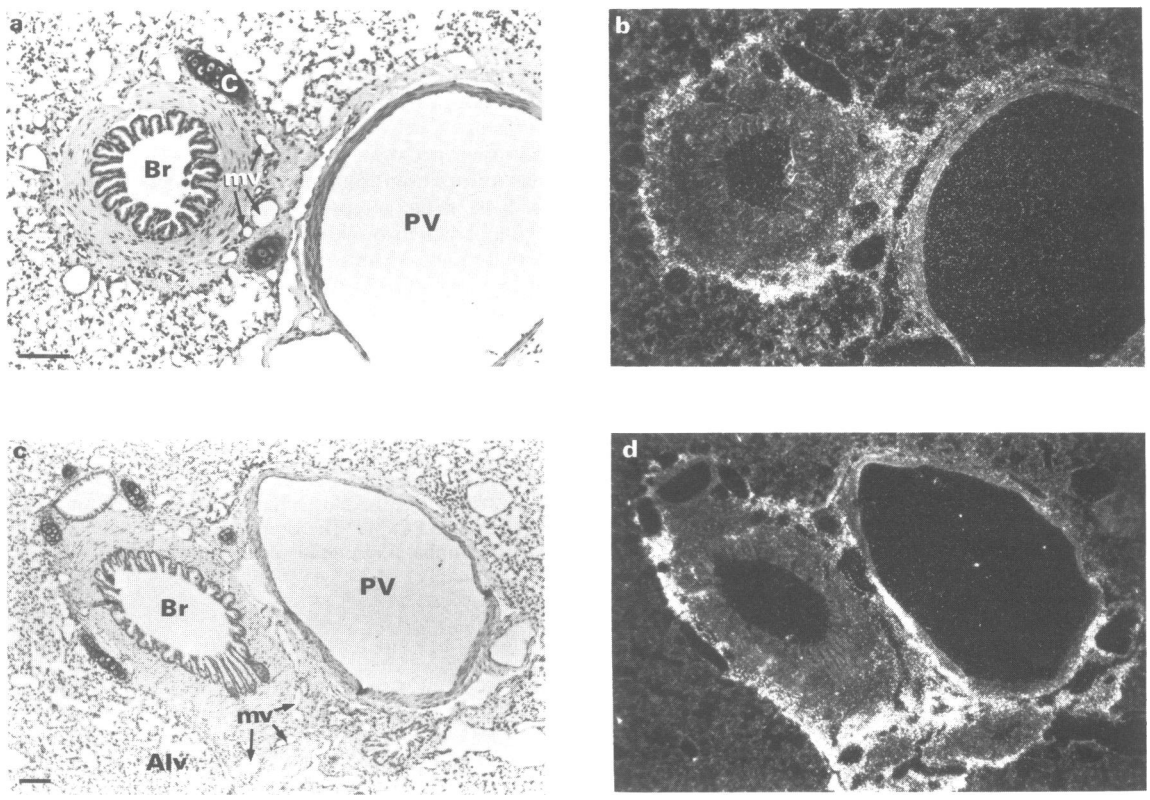

Figure 4 Photomicrographs of paraffin sections (5 μm) of guinea-pig peripheral lung stained with haemotoxylin from an animal given (a, b) platelet activating factor (PAF, 50 ng kg^{-1}, i.v.), or (c, d) bradykinin (BK, 50 μg kg^{-1}, i.v.). Dark-field photomicrographs (b, d) show autoradiographic grains (white dots) derived from ^{125}I-labelled fibrinogen (I-FN; 100 μCi kg^{-1}) extravasated from microvessels (mv) within bronchi (Br). The bronchial epithelium was not penetrated by I-FN. No signs of I-FN leakage from capillaries in alveoli (Alv) or from vessels of the pulmonary circulation (PV) were present. Cartilage = C. Bar = 100 μm.

Discussion

This study describes a new method for evaluating mediator-induced increases in airway microvascular permeability. The use of radiolabelled fibrinogen as a plasma marker, which following extravasation is deposited as radiolabelled fibrin, allows for the sensitive detection of the sites of leakage throughout the respiratory tree, as well as for the quantification of leakage at these sites.

In the present study both PAF and BK caused selective, concentration-dependent leakage of plasma I-FN from the bronchial microcirculation of the trachea and more distal airways. In the trachea, the maximum response to PAF was approximately twice that to BK. This may in part be due to the use of Hypnorm as an anaesthetic, since opiates can inhibit the neurogenic component of the response to BK (Belvisi *et al.*, 1989; Rogers *et al.*, 1990). Furthermore, PAF was approximately 1000 times more potent than BK both in the trachea and in peripheral airways. In the present system, leakage responses to both agonists were apparently directly mediated via specific receptor-operated mechanisms. For example, PAF-induced tracheal leakage was virtually abolished in the presence of the PAF receptor antagonist WEB 2086, but was not significantly altered in the presence of histamine H_1-receptor antagonists, the leukotriene receptor antagonist SKF 104353, or the BK_2-receptor antagonist, NPC 349. Similarly, the BK-induced response was significantly reduced by the receptor subtype-selective antagonist, NPC 349 and was therefore apparently mediated via BK_2 receptors (Jin *et al.*, 1989; Ichinose & Barnes., 1990). In contrast, Rogers *et al.* (1990) have recently reported a component of BK-induced plasma leakage in guinea-pig airways which was sensitive to WEB 2086 (1–1000 μg kg^{-1}) and which was thus mediated by PAF. This component was not evident in the present model.

Adrenaline has been reported to inhibit PAF-induced leakage in guinea-pig trachea via an α-adrenoceptor-mediated reduction in bronchial blood flow (Boschetto *et al.*, 1989) and to blunt the microvascular leakage response to other inflammatory mediators including histamine (Persson & Erjefalt, 1979). In the present study, the leakage response to BK was significantly reduced by adrenaline, but only when the pretreatment time was reduced to 5 min and the concentration raised to 100 μg kg^{-1}. In contrast, PAF-induced leakage was unaffected by all adrenaline pretreatments used. Our results are consistent with the failure of noradrenaline to attenuate significantly the airway leakage response to PAF in the rat (Sirois *et al.*, 1990). The reason for the disparity between these studies and the data of Boschetto *et al.* (1989) is unclear. Differences in the methods used to assess plasma leakage, including the use of different plasma markers, may be relevant.

In guinea-pig peripheral lung, mean maximal leakage responses to PAF and BK were only 17% and 45% respectively of those observed in the trachea. Attempts to quantify the effects of various potential inhibitors of peripheral lung leakage responses induced by EC_{50} doses of PAF and BK were unsuccessful in view of the relatively low control signals obtained. However, autoradiography revealed that at these doses, both mediators caused marked leakage of I-FN which was concentrated at sites around the perimeter of microvessels within peripheral bronchi. No leakage of I-FN was detected in response to either mediator in peripheral alveoli or in vessels of the pulmonary circulation. It has previously been estimated that the volume density of peripheral airways in human lung is only approximately 5% of the total tissue volume (Bertram *et al.*, 1983). Peripheral airways might be expected to account for a similar proportion of the total tissue volume in guinea-pig lung. Since it was only the microvessels within these peripheral airway structures that became leaky in response to PAF and BK, the small volume of responding tissue would account for the apparently weak signal detected on a wet wt. basis. However, if peripheral airway volume density was taken into account, it may be that the bronchial circulation within

peripheral airways was more sensitive to these leakage promoting mediators than were similar tracheal microvessels. A quantitative autoradiographic approach is required to evaluate this possibility.

Specific binding sites for PAF receptor and BK receptor ligands have been detected in areas containing bronchial microvessels in guinea-pig trachea and peripheral airways (Mak & Barnes, 1989; Goldie *et al.*, 1990). These may be specific receptors responsible for mediating endothelial cell contraction, thereby promoting intercellular gap formation and vascular leakage (Persson, 1986; 1987).

As in peripheral airways, autoradiography showed that in trachea, extravasated I-FN was concentrated in and around the extraluminal periphery of submucosal microvessels of the bronchial circulation. I-FN was not detected in significant amounts beyond the submucosa/epithelium interface. This is in contrast to results obtained when albumin was used as a marker of plasma extravasation, which demonstrated PAF-induced leakage across the epithelium into the tracheal lumen (Erjefalt & Persson, 1989). This may reflect the greater size of I-FN and/or the precipitation of this marker as fibrin.

This study has shown that PAF and bradykinin cause marked, selective increases in the permeability of the bronchial circulations of both the trachea and peripheral airways. The autoradiographic method currently employed enables assessments of vascular leakage in peripheral lung elements as well as in proximal conducting airways. The use of quantitative autoradiographic techniques such as we have recently used in drug receptor studies in the lung (Henry *et al.*, 1990a,b), will also allow accurate measurement of the effects of mediators of asthma on vascular permeability in peripheral airways, as well as of the influence of anti-asthma drugs on this process.

This research was supported by grants from the National Health and Medical Research Council (Australia) and from the Clive and Vera Ramaciotti Foundations (Australia). The authors also wish to thank Boehringer Ingelheim for their gift of WEB-2086, Sandoz Australia for their gift of ketotifen, SmithKline Beecham (U.S.A.) for their gift of SKF 104353 and the Nova Pharmaceutical Corporation (U.S.A.) for their gift of NPC 349. The generous supply of Hypnorm by Janssen-Cilag (Australia) is also gratefully acknowledged.

References

BARNES, P.J. (1987). Inflammatory mediator receptors and asthma. *Am. Rev. Respir. Dis.*, **135**, S26–S31.

BARNES, P.J. (1988). Inflammatory mediators and asthma. *Pharmacol. Rev.*, **40**, 49–84.

BELVISI, M.G., ROGERS, D.F. & BARNES, P.J. (1989). Neurogenic plasma extravasation: inhibition by morphine in guinea-pig airways in vivo. *J. Appl. Physiol.*, **66**, 268–272.

BERTRAM, J.F., GOLDIE, R.G., PAPADIMITRIOU, J.M. & PATERSON, J.W. (1983). Correlations between pharmacological responses and structure of human lung parenchyma strips, *Br. J. Pharmacol.*, **80**, 107–114.

BOSCHETTO, P., ROBERTS, N.M., ROGERS, D.F. & BARNES, P.J. (1989). Effect of antiasthma drugs on microvascular leakage in guinea-pig airways. *Am. Rev. Respir. Dis.*, **139**, 416–421.

CUSS, F.M., DIXON, C.M.S. & BARNES, P.J. (1986). Effects of inhaled platelet activating factor on pulmonary function and bronchial responsiveness in man. *Lancet* **ii**, 189–192.

DUNNILL, M.S. (1960). The pathology of asthma with special reference to changes in the bronchial mucosa. *J. Clin. Pathol.*, **13**, 27–33.

ERJEFALT, I. & PERSSON, C.G.A. (1989). Inflammatory passage of plasma macromolecules into airway wall and lumen. *Pulm. Pharmacol.*, **2**, 93–102.

EVANS, T.W., CHUNG, K.F., ROGERS, D.F. & BARNES, P.J. (1987). Effect of platelet activating factor on airway vascular permeability: possible mechanisms. *J. Appl. Physiol.*, **63**, 479–484.

EVANS, T.W., DENT, G., ROGERS, D.F., AURSUDKIJ, B., CHUNG, K.F. & BARNES, P.J. (1988). Effect of a Paf antagonist, WEB 2086, on airway microvascular leakage in the guinea-pig and platelet aggregation in man. *Br. J. Pharmacol.*, **94**, 164–168.

FULLER, R.W., DIXON, C.M.S., CUSS, F.M.C. & BARNES, P.J. (1987). Bradykinin,-induced bronchoconstriction in man: mode of action. *Am. Rev. Respir. Dis.*, **135**, 176–180.

GOLDIE, R.G., PEDERSEN, K.E., RIGBY, P.J. & PATERSON, J.W. (1990). PAF receptors in guinea-pig and human lung. *Agents Actions*, **31**, 243–246.

HENRY, P.J., RIGBY, P.J. & GOLDIE, R.G. (1990a). Distribution of β_1- and β_2-adrenoceptors in mouse trachea and lung: a quantitative autoradiographic study. *Br. J. Pharmacol.*, **99**, 136–144.

HENRY, P.J., RIGBY, P.J., SELF, G.J., PREUSS, J.M.H. & GOLDIE, R.G. (1990b). Relationship between endothelin-1 binding site densities and constrictor activities in human and animal airway smooth muscle. *Br. J. Pharmacol.*, **100**, 786–792.

HUBER, H.L. & KOESSLER, K.K. (1922). The pathology of bronchial asthma. *Arch. Int. Med.*, **30**, 689–701.

ICHINOSE, M. & BARNES, P.J. (1990). Bradykinin-induced airway microvascular leakage and bronchoconstriction are mediated via a bradykinin B_2 receptor. *Am. Rev. Respir. Dis.*, **142**, 1104–1107.

JIN, L.S., SEEDS, E., PAGE, C.P. & SCHACHTER, M. (1989). Inhibition of bradykinin-induced bronchoconstriction in the guinea-pig by a synthetic B_2 receptor antagonist, *Br. J. Pharmacol.*, **97**, 598–602.

MAK, J.C.W. & BARNES, P.J. (1990). Bradykinin receptors in lung: Characterization and autoradiographic mapping. *Am. Rev. Respir. Dis.*, **141** (Part 2), A726.

O'DONNELL, S.R. & BARNETT, C.J.K. (1987). Microvascular leakage to platelet activating factor in guinea-pig trachea and bronchi. *Eur. J. Pharmacol.*, **138**, 385–396.

PAGE, C.P., ARCHER, C.B., PAUL, W. & MORLEY, J. (1984). Paf-acether: a mediator of inflammation and asthma. *Trends Pharmacol. Sci.*, **5**, 239–241.

PERSSON, C.G.A. (1986). Role of plasma exudation in asthmatic airways. *Lancet*, **ii**, 1126–1129.

PERSSON, C.G.A. (1987). Leakage of macromolecules from the tracheobronchial microcirculation. *Am. Rev. Respir. Dis.*, **135**, S71–S75.

PERSSON, C.G.A. & ERJEFALT, I. (1979). Terbutaline and adrenaline inhibit leakage of fluid and protein in guinea-pig lung. *Eur. J. Pharmacol.*, **55**, 199–201.

ROGERS, D.F., DIJK, S. & BARNES, P.J. (1990). Bradykinin-induced plasma exudation in guinea-pig airways: involvement of platelet activating factor. *Br. J. Pharmacol.*, **101**, 739–745.

RYAN, G.B. & MAJNO, G.B. (1977). Acute inflammation: a review. *Am. J. Pathol.*, **86**, 185–276.

SALDEEN, T. (1969). Quantitative determination of intravascular coagulation in the lungs of experimental animals. *Scand. J. Haematol.*, **6**, 205–215.

SARIA, A., LUNDBERG, J.M., SKOFITSCH, G. & LEMBECK, F. (1983). Vascular protein leakage in various tissues induced by substance P, capsaicin, bradykinin, serotonin, histamine and by antigen challenge. *Naunyn-Schmiedebergs Arch. Pharmacol.*, **324**, 212–218.

SIROIS, M.G., PLANTE, G.E., BRAQUET, P. & SIROIS, P. (1990). Role of eicosanoids in PAF-induced increases of vascular permeability in rat airways. *Br. J. Pharmacol.*, **101**, 896–900.

(Received November 19, 1990
Revised May 7, 1991
Accepted May 20, 1991)

Br. J. Pharmacol. (1991), **104**, 133–138

Changes of quantal transmitter release caused by gadolinium ions at the frog neuromuscular junction

[1]Jordi Molgó, [2]Esperanza del Pozo, [3]Josep E. Baños & Denise Angaut-Petit

Laboratoire de Neurobiologie Cellulaire et Moléculaire, C.N.R.S., 91198 Gif sur Yvette Cédex, France

1 The actions of the trivalent cation, gadolinium (Gd^{3+}), were studied on frog isolated neuromuscular preparations by conventional electrophysiological techniques.

2 Gd^{3+} (450 μM) applied to normal or formamide-treated cutaneous pectoris nerve-muscle preparations induced, after a short delay, a complete block of neuromuscular transmission. The reversibility of the effect was dependent on the time of exposure.

3 Gd^{3+} (5–450 μM) had no consistent effect on the resting membrane potential of the muscle fibres.

4 Gd^{3+} (5–40 μM) applied to preparations equilibrated in solutions containing high Mg^{2+} and low Ca^{2+} reduced the mean quantal content of endplate potentials (e.p.ps) in a dose-dependent manner. Under those conditions, 3,4-diaminopyridine (10 μM) consistently reversed the depression of evoked quantal release.

5 The calcium current entering motor nerve terminals, revealed after blocking presynaptic potassium currents with tetraethylammonium (10 mM) in the presence of elevated extracellular Ca^{2+} (8 mM), was markedly reduced by Gd^{3+} (0.2–0.5 mM).

6 Gd^{3+} (40–200 μM) increased the frequency of spontaneous miniature endplate potentials (m.e.p.ps) in junctions bathed either in normal Ringer solution or in a nominally Ca^{2+}-free medium supplemented with 0.7 μM tetrodotoxin. This effect may be due to Gd^{3+} entry into the nerve endings since it is not reversed upon removal of extracellular Gd^{3+} with chelators (1 mM EGTA or EDTA). Gd^{3+} also enhanced the frequency of me.p.ps appearing after each nerve stimulus in junctions bathed in a medium containing high Mg^{2+} and low Ca^{2+}.

7 Gd^{3+}, in concentrations higher than 100 μM, decreased reversibly the amplitude of m.e.p.ps suggesting a postsynaptic action.

8 It is concluded that the block of nerve-impulse evoked quantal release caused by Gd^{3+} is related to its ability to block the calcium current entering the nerve endings, supporting the view that Gd^{3+} blocks N-type Ca^{2+} channels; while the enhancement of spontaneous quantal release is probably the result of Gd^{3+} entry into motor nerve endings. Besides its dual prejunctional effects on quantal release it is suggested that Gd^{3+} exerts a postsynaptic action on the endplate acetylcholine receptor-channel complex.

Keywords: Gadolinium; neuromuscular junction; acetylcholine release; motor nerve terminals; calcium channels

Introduction

It is generally accepted that nerve-impulse evoked transmitter release from nerve terminals is triggered by the phasic entry of calcium through voltage-sensitive membrane channels (for a recent review see Augustine *et al.*, 1987). Various types of calcium channels have been identified in neurones based on their single channel conductances, activation and inactivation properties and sensitivity to pharmacological agents (for a review see Miller, 1987). These channels have been tentatively termed T-, N-, and L-type calcium channels. Organic calcium channel antagonists, such as verapamil and dihydropyridines which block only L-channels, do not influence evoked acetylcholine release at frog neuromuscular junctions (Gotgilf & Magazanik, 1977; Nachshen & Blaustein, 1979; Arnon *et al.*, 1988). ω-Conotoxin which is a potent irreversible blocker of both L- and N-channels, consistently blocks nerve-impulse evoked transmitter release at frog neuromuscular junctions (Kerr & Yoshikami, 1984; Enomoto *et al.*, 1986; Sano *et al.*, 1987). Gadolinium (Gd^{3+}) has recently been shown in rodent neuroblastoma × glioma hybrid cells to block only one component of whole-cell current, possibly that through the N-type Ca^{2+} channel (Docherty, 1988; Brown *et al.*, 1989). As the type of Ca^{2+} channel involved in nerve-impulse-evoked transmitter release from motor nerve terminals is not yet well defined, it was of interest to study the effects of Gd^{3+} on both quantal transmitter release and the presynaptic calcium current from frog motor nerve terminals.

Methods

Experiments were performed at 20–22°C on the cutaneous pectoris nerve-muscle preparation isolated from 20–25 g male frogs (*Rana esculenta*). The standard Ringer solution had the following composition in mM: NaCl 110.0, KCl 2.1, $CaCl_2$ 1.8, and N-2-hydroxyethylpiperazine-N'-2-ethanesulphonic acid (HEPES) 5.0, buffered at pH 7.2. In some experiments the Ca^{2+} and Mg^{2+} concentrations were varied as specified in the results. All preparations were kept for 1 h in solutions with altered Ca^{2+} and Mg^{2+} concentrations to allow for equilibration. When changes were made in the ionic composition of the bathing solution, osmolarity was maintained by changing NaCl concentration.

When necessary, the mechanical activity of cutaneous pectoris muscles was uncoupled from the membrane surface depolarization by use of 2 M formamide (see del Castillo & Escalona de Motta, 1978). Preparations were not used until complete recovery of the resting membrane potential of the muscle fibres.

Membrane potentials, miniature endplate potentials (m.e.p.ps), endplate potentials (e.p.ps) and indirectly elicited action potentials were recorded with intracellular glass capillary microelectrodes filled with 3 M KCl (8–12 MΩ resistance)

[1] Author for correspondence.

[2] Permanent address: Universidad de Granada, Facultad de Medicina, Departamento de Farmacologia y Terapéutica, 18012 Granada, Spain.

[3] Permanent address: Universitat Autónoma de Barcelona, Facultat de Medicina, Departament de Farmacologia i Psiquiatria, 08193 Bellaterra (Barcelona), Spain.

by conventional intracellular recording techniques. The nerve was stimulated, unless otherwise stated, at a rate of 0.5 Hz with supramaximal current pulses of 50 μs duration through a glass suction electrode.

The quantal content (m) of e.p.ps was estimated either by the direct method (m = mean amplitude of e.p.ps/mean amplitude of me.p.ps) or by the method of failures ($m = \ln(N/N_0)$; where N = number of trials and N_0 number of failures of release).

Presynaptic currents were recorded either from nerve terminals by use of heat-polished microelectrodes (2–5 MΩ resistance) filled with standard Ringer solution or from the perineural space of fine superficial motor nerve bundles with 2 M NaCl-filled microelectrodes (10–15 MΩ resistance) as previously described (Gundersen *et al.*, 1982; Mallart, 1984). At the perineural space the signals generated at the endings upon invasion of nerve impulses are recorded with inverse polarity (Mallart, 1984). In all cases positivity at the recordings electrode is signalled by upward deflections. In all perineural recordings (+)-tubocurarine (30 μM) and procaine (50–100 μM) were added to the physiological solution to abolish completely postsynaptic activity and to prevent spontaneous repetitive nerve firing in the presence of tetraethylammonium (TEA). Superficial nerves and endplates were observed at a magnification × 400 with a microscope fitted with a water immersion × 40 Zeiss objective (working distance 1.6 mm) and interference contrast (Nomarski) optics.

Electrical signals were, after conventional amplification, digitized, displayed on a digital oscilloscope and simultaneously recorded on video tape with the aid of a modified digital audio processor (Sony PCM 701 ES) and a video cassette recorder (Sony SLC 9F). Data were collected and analysed with the aid of an IBM-AT microcomputer equipped with a TM-100 Labmaster analogue and digital interface board (Scientific solutions, U.S.A.) and modified pClamp software (Axon Instruments, U.S.A.). An event detector (AI 2020, Axon Instruments) was used to detect synaptic events.

Drugs used were: formamide, (+)-tubocurarine, tetrodotoxin, 3,4-diaminopyridine, ethyleneglycol-*bis*-(β-aminoethylether) N,N',-tetraacetic acid (EGTA), ethylenediaminetetraacetic acid (EDTA), (Sigma, St. Louis, MO, U.S.A.); procaine hydrochloride (Merck, Darmstadt, Germany); tetraethylammonium bromide (Koch-Light, Haverhill, U.K.) and gadolinium chloride (Ventron, Karlsruche, Germany). Since the supplier of gadolinium did not specify the moles of water content present in the $GdCl_3$ sample, the chloride concentration was determined in every stock solution made. All salts were of analytical grade.

Statistical analysis of data was performed with Student's *t* test (two tailed). Values are expressed as mean ± s.e.mean. Data were considered significant at $P < 0.05$.

Results

Effect of Gd^{3+} on neuromuscular transmission

Nerve stimulation of cutaneous pectoris muscles, previously treated with formamide (see Methods), elicited at junctional areas action potentials without contraction triggered by e.p.ps (Figure 1a). Under these conditions, addition of 450 μM Gd^{3+} to the normal Ringer solution reduced, in a few minutes, the amplitude of e.p.ps which could no longer reach the threshold for action potential generation in the muscle fibre. Finally Gd^{3+} completely blocked neuromuscular transmission

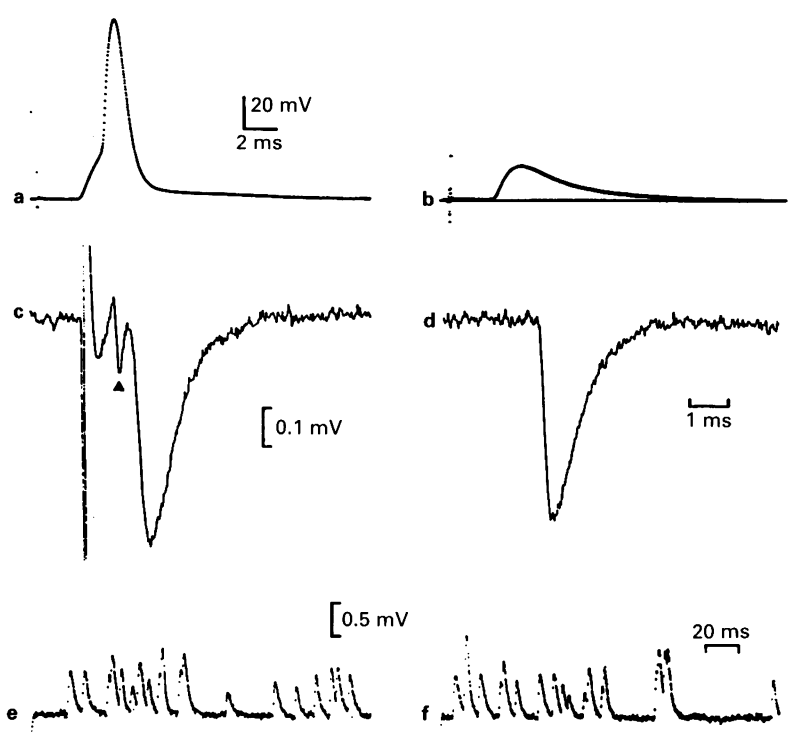

Figure 1 Effects of Gd^{3+} on neuromuscular transmission in three different neuromuscular preparations. (a) Action potential elicited by nerve stimulation (0.5 Hz) in a junction perfused with standard Ringer solution in which excitation-contraction was uncoupled by formamide. (b) Superimposed recordings obtained on the same junction 1 and 3 min after the addition of Gd^{3+} (0.45 mM) to the standard Ringer solution. Note that at this concentration, Gd^{3+} completely suppressed the evoked e.p.p. Resting membrane potential during measurements in (a) and (b) −81 mV. Same calibration for (a) and (b). (c) Extracellular focal recordings obtained from a junction perfused with low Ca^{2+} (0.6 mM) high Mg^{2+} (6 mM) Ringer solution showing that upon nerve stimulation, presynaptic currents (▲) can be recorded in the presence of Gd^{3+} (40 μM) even when transmitter release is greatly inhibited. (d) Spontaneous miniature endplate current recorded on the same synaptic site as (c). Note that the evoked and spontaneous postsynaptic currents have similar amplitudes and time courses. (e) and (f) Intracellular m.e.p.ps recorded in a junction perfused with the same Ringer as in (c) showing that in the presence of Gd^{3+} (100 μM) the blockade of evoked transmitter release is followed by an increase in m.e.p.p. frequency.

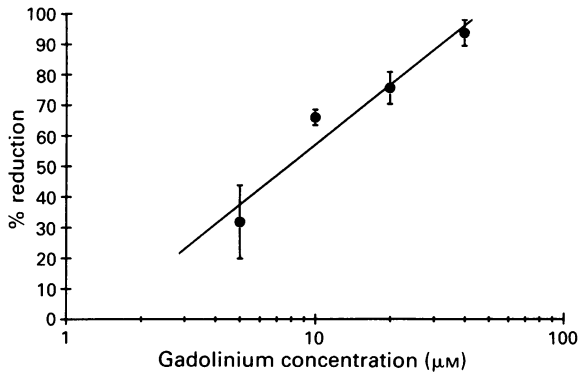

Figure 2 Dose-dependent reduction of the mean quantal content of e.p.ps by Gd^{3+}. The extracellular medium contained low Ca^{2+} (0.5 mM) and high Mg^{2+} (6 mM). Each point represents the percent reduction ± s.e. as compared to respective control obtained in a single junction. Data were obtained from 4–8 different preparations.

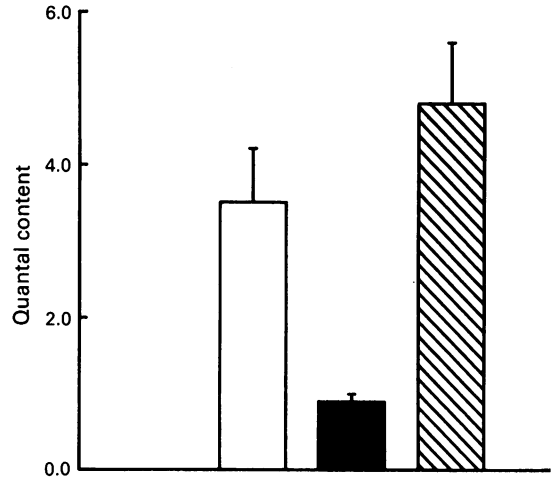

Figure 3 Reduction in quantal content of e.p.ps produced by 10 μM Gd^{3+} (solid column) over controls (open column) and its reversal by 10 μM 3,4-diaminopyridine (hatched column). Preparation bathed in low Ca^{2+} (0.5 mM)-high Mg^{2+} (6 mM) Ringer solution. Each column represents the mean of 3 values obtained in different preparations; s.e. shown by vertical bars. The quantal content was estimated by the direct method. Gd^{3+} was applied for 20 min, while 3,4-diaminopyridine was applied for 15 min in the continuous presence of Gd^{3+}.

(Figure 1b). The effect of Gd^{3+} was reversible, provided preparations were exposed for 10–15 min and washed with Gd^{3+}-free solution. Gd^{3+} in the range of concentrations used (5–450 μM) had no consistent effect on the resting membrane potential of the muscle fibres. A similar blockade of neuromuscular transmission by Gd^{3+} was observed at junctions in which excitation-contraction coupling was unaffected. The inhibitory effect of Gd^{3+} on neuromuscular transmission raised the possibility that the cation may have pre- and/or postsynaptic actions at the neuromuscular junction.

Gd^{3+} on evoked quantal release

In preparations in which the normal release of transmitter was reduced by a medium containing low Ca^{2+} (0.5 mM) and high Mg^{2+} (6 mM), the addition of Gd^{3+} (5–40 μM) produced a dose-dependent increase in the number of failures of release, during trains of nerve stimulation at 0.5 Hz, and a decrease in the mean quantal content of e.p.ps (Figure 2). Extracellular focal recordings from endplate regions revealed that blockade of quantal release caused by Gd^{3+} was neither due to an impairment of the presynaptic action potential to reach the nerve terminal (Figure 1c), nor the result of a postsynaptic blockade, since miniature endplate currents could be recorded from the same synaptic sites (Figure 1d) and had a similar amplitude and time course to unitary evoked responses. These results indicate that Gd^{3+}, in the range of concentrations studied, reduces the number of transmitter quanta released by each nerve impulse.

A notable feature in Gd^{3+}-blocked junctions was the observation that nerve stimulation at low rates (0.2–0.5 Hz) evoked a period of high frequency me.p.ps after each stimulus, even when failures of evoked transmitter release occurred as shown in representative recordings (Figure 1e, f).

3,4-Diaminopyridine (3,4-DAP) (5–10 μM), which by blocking voltage-sensitive K^+ channels in motor endings prolongs the duration of the presynaptic depolarization, enhancing Ca^{2+} influx and consequently evoked transmitter release (Molgó, 1982), consistently reversed the depression of nerve-impulse evoked transmitter release caused by Gd^{3+} in the low Ca^{2+}-high Mg^{2+} medium as shown in Figure 3.

Effects of Gd^{3+} on presynaptic Ca^{2+} currents

The possibility that blockade of evoked transmitter release in Gd^{3+}-treated junctions reflects inhibition of Ca^{2+} entry in presynaptic terminals was directly investigated by use of perineural current recordings. The calcium current entering the nerve terminals is not readily detectable in recordings performed in standard Ringer solution but can be revealed after blocking outward K^+ currents (Gundersen *et al.*, 1982; Mallart, 1984).

To study the effects of Gd^{3+} on presynaptic Ca^{2+} currents experiments were performed in the presence of TEA, which blocks voltage- and calcium-dependent K^+ currents in motor terminals (Mallart, 1984; Hevron *et al.*, 1986), together with elevated extracellular Ca^{2+} levels. Figure 4a, shows typical perineural recordings obtained in preparations perfused with

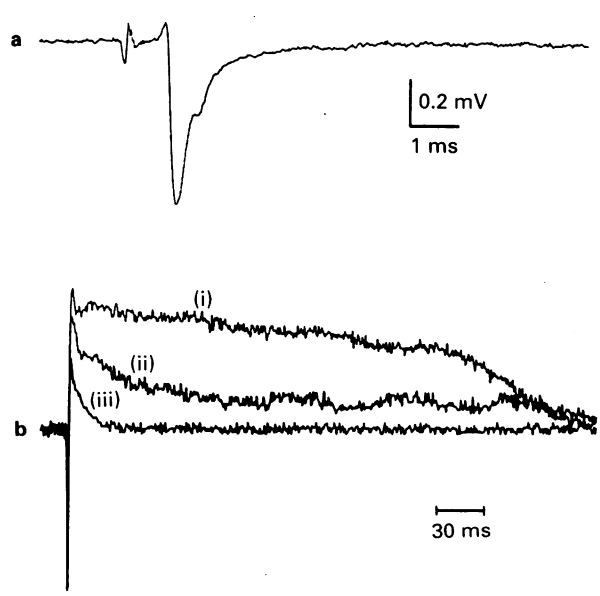

Figure 4 Presynaptic currents recorded from the perineural space of a small preterminal nerve bundle. (a) Control (average of 5 tracings). (b) (i) Single trace obtained on the same recording site 20 min after the addition of 10 mM tetraethylammonium. The upward deflection signals the prolonged calcium current. (ii) and (iii) show the progressive blockade of the calcium current after the addition of 0.5 mM Gd^{2+}. Note in (iii) the presence of an inward current (presumably carried by Na^+) entering the terminals that was unaffected by Gd^{3+}. Recordings obtained in Ringer solution containing 8 mM Ca^{2+} and 30 μM (+)-tubocurarine. In (b), procaine (100 μM) was added to avoid repetitive nerve firing. Stimulation rate was 0.5 Hz in (a) and 0.008 Hz in (b).

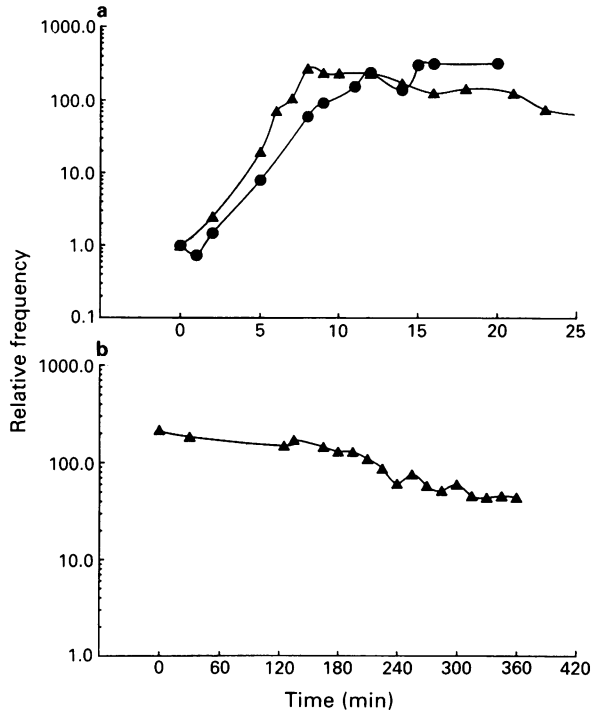

Figure 5 (a) Time course of the increase in m.e.p.p. frequency caused by 40 μM Gd^{3+} at two different neuromuscular junctions equilibrated for respectively 1 h in a nominally calcium-free solution containing 2 mM Mg^{2+} and 0.7 μM tetrodotoxin (▲) and in standard Ringer solution containing 2 mM Mg^{2+} (●). (b) Time course of me.p.p. frequency at a single junction previously exposed for 30 min to 40 μM Gd^{3+} and then washed with a nominally calcium-free solution containing 1 mM EGTA. In (a) and (b) each point represents the relative increase in m.e.p.p. frequency as compared to respective controls.

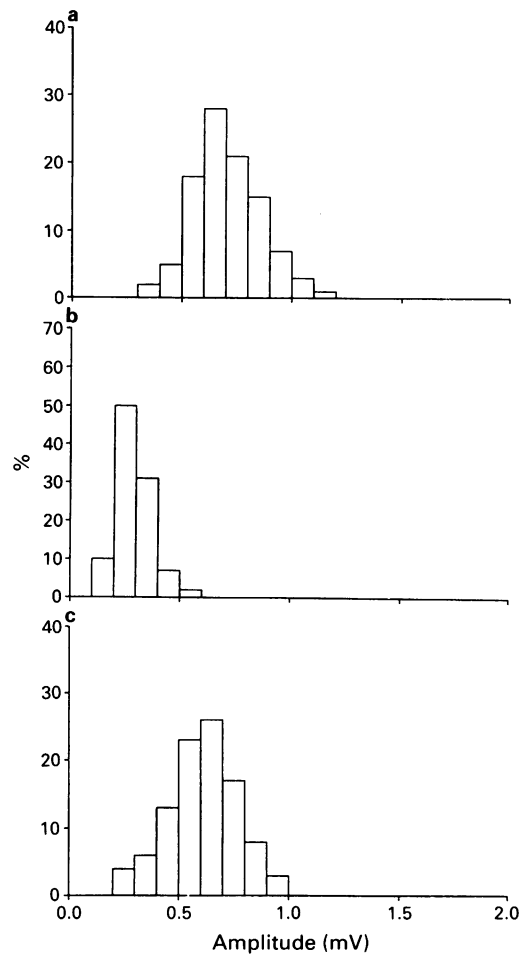

Figure 6 Amplitude distribution of spontaneous m.e.p.ps recorded at the same endplate in standard Ringer solution (a), after 20 min exposure to 200 μM Gd^{3+} added to the Ringer solution (b) and after washing out Gd^{3+} for 15 min from the external medium. Mean resting membrane potential during measurements was −82.6 mV.

Ringer solution containing 8 mM Ca^{2+}. Two current components can be distinguished. The early component has been ascribed to the sodium current which flows into the motor axons at the nodes of Ranvier and promotes depolarization of their terminals. The second component corresponds to the potassium current which underlies spike repolarization in the terminals (Mallart, 1984; Hevron *et al.*, 1986). Under these conditions addition of 10 mM TEA to the solution allowed the development of a long-lasting plateau current (Figure 4b(i)).

Several lines of evidence identified the plateau current as an inward Ca^{2+} current in the terminals (I_{Ca}): (1) I_{Ca} was not present or could be suppressed in a calcium-free medium; (2) divalent cations like Co^{2+} (10 mM) and Cd^{2+} (0.2 mM), well known calcium channel blockers, abolished I_{Ca}. Calcium plateaus of long duration (several hundred ms) could be evoked only when low frequency stimulation (<0.03 Hz) was used. At higher rates, shortening of the plateau duration occurred probably because of calcium-channel inactivation by intraterminal Ca^{2+} accumulation. Using low rates of nerve stimulation we found that 0.2–0.5 mM Gd^{3+} suppressed I_{Ca}, as shown in Figure 4(b(ii), (iii)). Although the positive current component which remains after Gd^{3+} action was not fully investigated, it is likely that it may be due to Na^{+} ions entering the terminals, since it was also observed after Co^{2+}- and Cd^{2+}-blockade of calcium currents (results not shown).

Gd^{3+} on spontaneous quantal release

Addition of Gd^{3+} to the standard Ringer solution in concentrations of 40–200 μM caused, within a few min, a significant rise in spontaneous quantal release recorded as m.e.p.p. frequency. Simple withdrawal of Gd^{3+} from the medium did not interrupt the marked increase in m.e.p.p. frequency. With continued application of Gd^{3+}, the frequency reached a maximum usually in the range of 100–150 Hz, and subsequently subsided slowly. A similar effect was observed in junctions bathed in a nominally Ca^{2+}-free medium containing 2 mM Mg^{2+} supplemented with 0.7 μM tetrodotoxin (Figure 5a). As shown in Figure 5b, removal of extracellular Gd^{3+} by continuous perfusion with a Gd^{3+}-free and Ca^{2+}-free solution containing 1 mM EGTA (Figure 5b) or 1 mM EDTA (not shown) to chelate extracellular traces of Gd^{3+} did not completely reverse the increase in me.p.p. frequency caused by Gd^{3+}. These experiments indicate that Gd^{3+} can itself act to increase quantal release in the nominal absence of external Ca^{2+}. This effect presumably depends upon entry of Gd^{3+} into the nerve endings, since it is slowly, if at all, reversed upon removal of extracellular Gd^{3+}.

Gd^{3+}, in addition to increasing the frequency of me.p.ps, also caused at concentrations equal or higher than 100 μM a reduction in m.e.p.p amplitude. Thus, a 20 min exposure to 100 μM or 200 μM Gd^{3+} depressed the amplitude of m.e.p.ps to 0.70 ± 0.12 ($n = 3$) and 0.36 ± 0.05 ($n = 3$) respectively of control values (mean ± s.e.). These effects of Gd^{3+}, in contrast to those on the frequency of m.e.p.ps were reversible upon 15–20 min washing with a Gd^{3+}-free medium. Figure 6 shows an example of the amplitude distribution of m.e.p.ps and the shift of the modal value to lower amplitude levels during the action of Gd^{3+} and, to control levels during the washing out of Gd^{3+} from the medium. With 450 μM Gd^{3+}, me.p.ps were no longer detectable by intracellular recordings at junctional areas of the muscle fibres.

Discussion

The present results show that Gd^{3+} has a dual action on quantal transmitter release from frog motor nerve terminals since it blocks nerve-impulse evoked transmitter release and enhances spontaneous quantal release recorded as m.e.p.p. frequency. In that respect the action of Gd^{3+} is similar to that previously observed with other trivalent lanthanide cations like lanthanum (Blioch *et al.*, 1968; Heuser & Miledi, 1971), praseodynium (Alnaes & Rahamimoff, 1974) and erbium (Metral *et al.*, 1978).

Gd^{3+} was previously found to inhibit twitch tension evoked by nerve stimulation on the frog isolated sartorius nerve-muscle preparation (Bowen, 1972) and to block skeletal muscle contraction (Hambly & Dos Remedios, 1977). The present results indicate that the block of evoked quantal transmitter release caused by Gd^{3+} can be ascribed to its ability to block the calcium current entering motor endings, as shown by perineural recordings. The results support the view that Gd^{3+} blocks N-type Ca^{2+} channels (Docherty, 1988) and suggest that such channels are the major type involved in nerve-impulse evoked transmitter release from frog motor nerve terminals. These findings agree with previous studies showing that Gd^{3+} inhibits [^{3}H]-noradrenaline and vasopressin release (Bourne & Trifaró, 1982; Muscholl *et al.*, 1985) and effectively reduced depolarization-induced $^{45}Ca^{2+}$ uptake into cultured chromaffin cells and rat brain synaptosomes (Nachshen, 1984).

The calcium current entering frog motor nerve terminals differed from the one recorded at mouse preparations by the fact that long-lasting plateau currents could not be obtained in the latter preparations in the presence of TEA alone, but only after the combined action of TEA and 3,4-DAP (Dreyer & Penner, 1987; Anderson & Harvey, 1987; Tabti *et al.*, 1989). This was taken as evidence for the presence of a TEA-resistant potassium current in mouse motor nerve terminals which develops with a relatively slow time course and which is sensitive to 3,4-DAP (Dreyer & Penner, 1987; Tabti *et al.*, 1989). Since calcium plateau magnitude and duration depend on the balance between Ca^{2+} and K^+ permeabilities (Katz & Miledi, 1971), we suggest that frog motor nerve terminals lack the slowly activating, TEA-insensitive potassium current, reported in mammalian terminals allowing therefore the development of calcium plateaus after blocking both the voltage-dependent and the calcium-activated potassium currents.

In addition to its blocking action on nerve-impulse-evoked transmitter release, Gd^{3+} was found to enhance asynchronous quantal release from motor terminals. On isolated adrenal medullary cells and in the rat neurohypophysis no effect of Gd^{3+} was detected on the basal release of [^{3}H]-noradrenaline and vasopressin (Bourne & Trifaró, 1982; Muscholl *et al.*, 1985) while in striatal synaptosomal preparations Gd^{3+} slightly increased basal [^{3}H]-dopamine release (Sheer, 1989). The increase in spontaneous quantal release caused by Gd^{3+} is most probably the result of its entry into motor nerve terminals and its intracellular action is reminiscent of the action of La^{3+} (Curtis *et al.*, 1986). The action of Gd^{3+} in enhancing m.e.p.p. frequency may be either secondary to an increase in intraterminal Ca^{2+} concentration, caused by the interference of energy-dependent Ca^{2+} sequestering systems within the motor terminals or may be due to a direct intracellular action at a site that governs quantal transmitter release.

In addition to the presynaptic effects discussed here, Gd^{3+} was found to reduce reversibly me.p.p. amplitude by what seemed to be a reduction in the sensitivity of the postsynaptic membrane to the transmitter. Further experiments will be necessary to understand the action(s) of Gd^{3+} on the endplate acetylcholine receptor-channel complex. Thus, both pre- and postjunctional actions seem to be implicated in the effects of Gd^{3+} at the neuromuscular junction.

We thank Prof. E. Muscholl for his valuable comments regarding the purity and source of Gd^{3+} used in the present study and Mrs M. Teixido-Aymerich for determining the chloride concentration in our stock solutions of Gd^{3+}.

This study was supported in part by grants from Direction des Recherches Etudes et Techniques and by Association Française contre les Myopathies. E.D.P. and J.B. were supported by the programme Ayudas para estancias en el extranjero de la Universidad de Granada, Spain and by Ajuts per l'ampliació d'estudis i estàncies a l'estranger of CIRIT (Generalitat de Catalunya, Spain).

References

ALNAES, E. & RAHAMIMOFF, R. (1974). Dual action of Praseodymium (Pr^{3+}) on transmitter release at the frog neuromuscular synapse. *Nature*, **274**, 478–479.

ANDERSON, A.J. & HARVEY, A.L. (1987). ω-Conotoxin does not block the verapamil-sensitive calcium channels at mouse motor nerve terminals. *Neurosci. Lett.*, **82**, 177–180.

AUGUSTINE, G.J., CHARLTON, M.P. & SMITH, S.J. (1987). Calcium action in synaptic transmitter release. *Annu. Rev. Neurosci.*, **10**, 633–693.

ARNON, A., DAVID, G., HEVRON, E. & YAARI, Y. (1988). Calcium currents in frog motor nerve terminals. *Soc. Neurosci. Abstr.*, **14**, 68.

BLIOCH, Z.L., GLAGOLEVA, I.M., LIBERMAN, E.A., & NENASHEV, V.A. (1968). A study of the mechanism of quantal transmitter release at a chemical synapse. *J. Physiol.*, **199**, 11–35.

BOURNE, G.W. & TRIFARO, J.M. (1982). The gadolinium ion: a potent blocker of calcium channels and catecholamine release from cultured chromaffin cells. *Neuroscience*, **7**, 1615–1622.

BOWEN, J.M. (1972). Effects of rare earths and yttrium on striated muscle and the neuromuscular junction. *Can J. Physiol. Pharmacol.*, **50**, 603–611.

BROWN, D.A., DOCHERTY, R.J. & McFADZEAN, I. (1989). Calcium channels in vertebrate neurons. *Ann. New York Acad. Sci.*, **560**, 358–372.

CURTIS, M.J., QUASTEL, D.M.J. & SAINT, D.A. (1986). Lanthanum as a surrogate for calcium in transmitter release at mouse motor nerve terminals. *J. Physiol.*, **373**, 243–260.

DEL CASTILLO, J. & ESCALONA DE MOTTA, G. (1978). A new method for excitation-contraction uncoupling in frog skeletal muscle. *J. Cell Biol.*, **78**, 782–784.

DOCHERTY, R.J. (1988). Gadolinium selectively blocks a component of calcium current in rodent neuroblastoma × glioma hybrid (NG108-15) cells. *J. Physiol.*, **398**, 33–47.

DREYER, F. & PENNER, R. (1987). The action of presynaptic snake toxins on membrane currents of the mouse motor nerve terminals. *J. Physiol.*, **386**, 455–463.

ENOMOTO, K., SANO, K., SHIBUYA, Y. & MAENO, T. (1986). Blockade of transmitter release by a synthetic venom peptide, ω-conotoxin. *Proc. Jpn. Acad., Ser. B*, **62**, 267–270.

GOTGILF, I.M. & MAGAZANIK, L.G. (1977). Action of calcium channels blocking agents (verapamil, D-600 and manganese ions) on transmitter release from motor nerve endings of frog muscle. *Neurofiziologia*, **9**, 415–422. (in Russian)

GUNDERSEN, C.B.S., KATZ, B. & MILEDI, R. (1982). The antagonism between botulinum toxin and calcium in motor nerve terminals. *Proc. R. Soc. B*, **216**, 369–376.

HAMBLY, B.D. & DOS REMEDIOS, C.G. (1977). Responses of skeletal muscle fibres to lanthanide ions. Dependence of the twitch response on ionic radii. *Experientia*, **33**, 1042–1044.

HEUSER, J. & MILEDI, R. (1971). Effect of lanthanum ions on function and structure of frog neuromuscular junctions. *Proc. R. Soc. B*, **179**, 247–260.

HEVRON, E., DAVID, G., ARNON, A. & YAARI, Y. (1986). Acetylcholine modulates two types of presynaptic potassium channels in vertebrate motor nerve terminals. *Neurosci. Lett.*, **72**, 87–92.

KATZ, B. & MILEDI, R. (1971). The effect of prolonged depolarization on synaptic transfer in the stellate ganglion of the squid. *J. Physiol.*, **216**, 503–512.

KERR, L.M. & YOSHIKAMI, D.C. (1984). A venom peptide with a novel presynaptic blocking action. *Nature*, **308**, 282–284.

MALLART, A. (1984). Presynaptic currents in frog motor endings. *Pflugërs Arch.*, **400**, 8–13

METRAL, S., BONNETON, C., HORT-LEGRAND, C. & REYNES, J. (1978). Dual action of erbium on transmitter release at the frog neuromuscular synapse. *Nature*, **271**, 773–775.

MILLER, R.J. (1987). Multiple calcium channels and neuronal function. *Science*, **235**, 46–52.

MOLGO, J. (1982). Effects of aminopyridines on neuromuscular transmission. In *Aminopyridines and Similarly Acting Drugs: Effects on Nerves, Muscles and Synapses.* ed. Lechat, P., Thesleff, S. & Bowman, W.C. *Advances in the Biosciences*, Vol. 35, pp. 95–116. Oxford: Pergamon Press.

MUSCHOLL, E., RACKE, K. & TRAUT, A. (1985). Gadolinium ions inhibit exocytotic vasopressin release from the rat neurohypophysis. *J. Physiol.*, **365**, 419–434.

NACHSHEN, D.A. (1984). Selectivity of the Ca binding site in synaptosome Ca channels. *J. Gen. Physiol.*, **83**, 941–967.

NACHSHEN, D.A. & BLAUSTEIN, M.P. (1979). The effect of some organic 'calcium antagonists' on Ca influx in presynaptic nerve terminals. *Mol. Pharmacol.*, **16**, 579–586.

SANO, K., ENOMOTO, K. & MAENO, T. (1987). Effects of synthetic ω-conotoxin, a new type Ca^{2+} antagonist, on frog and mouse neuromuscular transmission. *Eur. J. Pharmacol.*, **141**, 235–241.

SCHEER, H.W. (1989). Interactions between α-latrotoxin and trivalent cations in rat striatal synaptosomal preparations. *J. Neurochem.*, **52**, 1590–1597.

TABTI, N., BOURRET, C. & MALLART, A. (1989). Three potassium currents in mouse motor nerve terminals. *Pflügers Arch.*, **413**, 395–400.

(Received April 19, 1991
Accepted May 28, 1991)

Br. J. Pharmacol. (1991), **104**, 139–144

Endothelium-derived relaxing factor inhibits the endothelin-1-induced increase in protein kinase C activity in rat aorta

D. Lang & [1]M.J. Lewis

Departments of Pharmacology & Therapeutics and Cardiology, University of Wales College of Medicine, Heath Park, Cardiff CF4 4XN

1 Particulate and cytosolic protein kinase C (PKC) activity was measured in rat aortae with and without endothelium, following exposure to endothelin-1 (10^{-8} M) for various time intervals.

2 Endothelin-1 induced two peaks of particulate PKC activity, occurring at 30 s and 10 min exposure times in both endothelium-intact and endothelium-denuded preparations. Cytosolic PKC activity fell below baseline at all incubation times studied.

3 In endothelium-denuded preparations, elevation of guanosine 3':5'-cyclic monophosphate (cyclic GMP) levels with sodium nitroprusside (10^{-6} M) or atrial natriuretic peptide (10^{-6} M) and, in endothelium-intact preparations with the calcium ionophore A23187 (10^{-6} M), inhibited the activation of particulate PKC activity seen after incubation with endothelin-1 for 30 s. The inhibitory effect of A23187 was prevented by prior incubation of the endothelium-intact vessels with the nitric oxide synthetase inhibitor, L-N^G-nitro arginine (5×10^{-5} M).

4 These results indicate that EDRF acting via cyclic GMP can inhibit the activation of PKC induced by endothelin-1 in rat aorta.

Keywords: Rat aorta; EDRF; protein kinase C; endothelin; L-N^G-nitro arginine

Introduction

In vascular smooth muscle, protein kinase C (PKC) is present in relatively high concentrations (Nishizuka, 1984) and is presumed to play an important role in the regulation of tone, particularly during the tonic phase of contraction (Rasmussen *et al.*, 1987; Haller *et al.*, 1990). Several constrictor agonists including endothelin have now been shown to cause activation and translocation of PKC from the cytosolic to the particulate fraction of vascular smooth muscle cells (Haller *et al.*, 1990) and it has been shown that these events are responsible for the maintenance of tone during the tonic phase of contraction.

Nitric oxide is now known to be the active principle of endothelium-derived relaxing factor (EDRF; Palmer *et al.*, 1987). It induces vascular smooth muscle relaxation by the activation of soluble guanylate cyclase and elevation of intracellular levels of guanosine 3':5'-cyclic monophosphate (cyclic GMP) (for review see Griffith *et al.*, 1988). However, the precise mechanism whereby cyclic GMP induces smooth muscle relaxation is not fully understood. It is known that cyclic GMP inhibits phosphatidylinositol (PI) hydrolysis in vascular smooth muscle (Rapoport, 1986) and platelets (Takai *et al.*, 1981). More recently it has been shown that in both vascular smooth muscle and endothelium this effect of cyclic GMP leads to inhibition of agonist-induced inositol 1,4,5-trisphosphate (IP_3) production (Lang & Lewis, 1989; 1991). However, this effect of cyclic GMP on IP_3 production does not adequately explain the mechanism of inhibition of vascular smooth muscle tone during the tonic phase of contraction, which involves PKC activation.

In the present study therefore we have investigated the effects of EDRF and other cyclic GMP elevating agents, on endothelin-1-induced activation of PKC in rat aorta.

Methods

Tissue preparation

Male Wistar rats (250–300 g) were killed by cervical dislocation and their thoracic aortae removed and placed into Krebs-Ringer bicarbonate (KRB) solution of the following composition (mM): NaCl 95.5, KCl 4.8, $MgSO_4$ 1.2, $CaCl_2$ 2.5, KH_2PO_4 1.2, $NaHCO_3$ 25, glucose 11 and indomethacin 0.001. The vessels were cleaned of all fat and connective tissue and each divided into 4 equal lengths. Paired lengths were used in each experiment. The endothelium was removed from some of the vessels by gentle rubbing of the intimal surface with a wooden stick. The sections were placed in KRB gassed with 95% O_2:5% CO_2 and left to equilibrate for at least 60 min at 37°C.

Protein kinase C assay

The PKC activity was measured with a commercially available kit (Amersham International, U.K.). The assay is dependent on PKC catalysing the transfer of a radiolabelled [^{32}P]-phosphate of ATP to the threonine group of a substrate peptide which is specific for PKC. The assay is a modification of a previously described technique (Hannun *et al.*, 1985).

At the end of each experiment each vessel was homogenized in an ice-cold hypotonic lysis buffer and the cytosolic and particulate PKC fractions separated by ultracentrifugation. These fractions were stored on ice and their PKC activity measured within 4 h of the initial homogenization. The protein content of each sample was measured immediately following the assay of PKC activity, as described previously (Collins *et al.*, 1988). The cytosolic fraction was also assayed for its cyclic GMP content with a commercially available radioimmunoassay kit (New England Nuclear Research Products, Germany), after being stored at −20°C for up to 1 month. PKC activity is expressed as fmol phosphate transferred $min^{-1}\,\mu g^{-1}$ protein and the cyclic GMP content as fmol μg^{-1} protein.

Experimental protocol

Endothelin-1 was chosen as the constrictor agonist and all experiments were carried out in KRB gassed with 95% O_2:5% CO_2, pH 7.4 at 37°C. Vessels with and without endothelium were exposed to endothelin-1 (10^{-8} M) for 30 s, 1, 2, 5, 10, 20 and 30 min. The time showing peak PKC activity was chosen for all subsequent experiments. In all experiments, untreated vessels were included for measurement of basal PKC activity.

[1] Author for correspondence at Department of Pharmacology & Therapeutics.

For investigation of the effects of cyclic GMP on PKC activity, two series of experiments were performed. In the first series, endothelium-denuded vessels were exposed for 30 s, 1, 2, 5 and 10 min to sodium nitroprusside (10^{-5} M) or atrial natriuretic peptide (ANP, 10^{-6} M) alone. In the second series vessels denuded of endothelium were incubated with either agent for the stated times followed by a 30 s exposure to endothelin-1 (10^{-8} M), the time at which PKC activity is maximally induced by endothelin-1.

To study the effect of EDRF on endothelin-1-induced PKC activity, endothelium-intact preparations were exposed to the calcium ionophore A23187 (10^{-6} M) alone for 30 s, 1, 2, 5 and 10 min. In other experiments endothelium-intact vessels were incubated with A23187 for the stated times, followed by a 30 s exposure to endothelin-1 (10^{-8} M). This second series of experiments were repeated to include a 30 min pre-incubation with the nitric oxide synthetase inhibitor L-N^G-nitro arginine (L-NNA, 5×10^{-5} M; Moore *et al.*, 1990), before each addition of A23187. Also, endothelium-intact vessels were exposed to endothelin-1 (10^{-8} M) alone for 30 s 1, 2, 5 and 10 min following a 30 min pre-incubation with L-NNA (5×10^{-5} M).

Calculation and statistics

PKC activity and cyclic GMP levels were determined as described in the respective kits.

Each data point represents the mean ± standard error of the mean (s.e.mean) of at least 4 separate experiments. Control measurements were made repeatedly throughout the course of the study.

For analysis of within-group data a one-way analysis of variance was used followed by Dunnett's multiple range test to identify significant differences where $P < 0.05$. For between-group data, a one-way analysis of variance was followed by Tukey's multiple range test to identify significant differences where $P < 0.05$.

Drugs

All drugs were purchased from Sigma Chemical Co., Dorset, England. Endothelin-1 and human sequence atrial natriuretic peptide were used. All other chemicals used were analytical reagent standard.

Results

Endothelin-1

Figure 1a and 1b show the changes in cytosolic and particulate PKC activity respectively following incubation of endothelium-intact and -denuded vessels with endothelin-1 for the times indicated. As can be seen, in the intact preparations cytosolic PKC activity was significantly different from baseline levels only after 20 and 30 min exposure to endothelin-1. The particulate enzyme showed two distinct peaks of activity which were significantly different from basal. These occurred after 30 s and 10 min of agonist exposure.

In the denuded preparations cytosolic activity was significantly reduced below baseline values after 5 and 10 min exposure to endothelin-1, returning to baseline levels thereafter. Like the endothelium-intact preparations, the particulate activity in the denuded preparations showed significant increases above basal at 30 s and 10 min.

Figure 1c shows that endothelin-1 caused no significant changes in intracellular cyclic GMP levels at any of the times studied. The data do show, however, that basal levels of cyclic GMP in endothelium-intact preparations (Figure 1c) are approximately 9 times greater than in endothelium-denuded preparations.

For all subsequent experiments a 30 s exposure to endothelin-1 was chosen to investigate the effects of the cyclic GMP-elevating interventions on PKC activity.

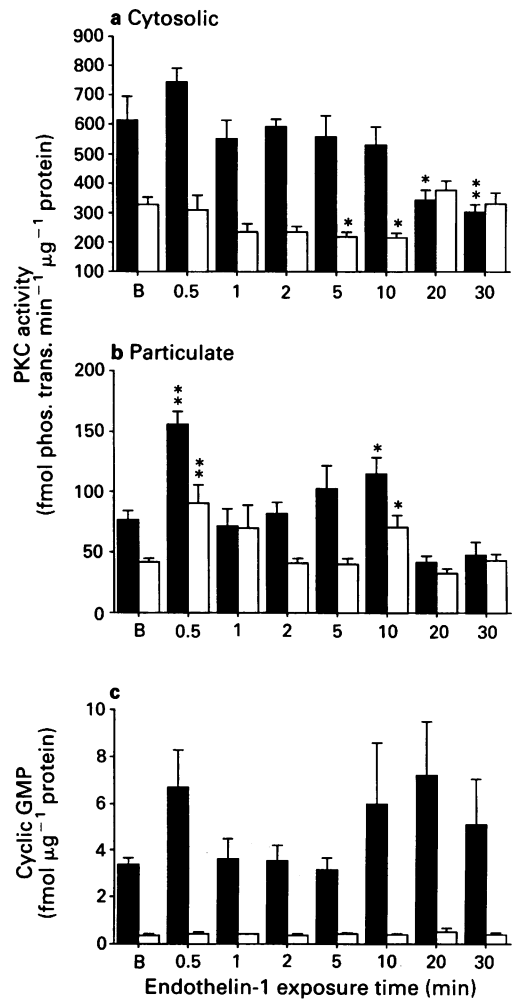

Figure 1 Changes in cytosolic (a) and particulate (b) protein kinase C (PKC) activity in endothelium-intact (closed columns) and -denuded (open columns) rat aortae following incubation with endothelin-1 for 0.5, 1, 2, 5, 10, 20 and 30 min. Changes in cyclic GMP levels in the same experiment are also shown (c). Values are the mean of 4–6 determinations from 8 separate experiments; vertical bars show s.e.mean. *$P < 0.05$; **$P < 0.01$ compared with basal values (B).

Sodium nitroprusside

Endothelium-denuded preparations only were used for these studies. As shown in Figures 2a and 2b, neither cytosolic nor particulate PKC activities were altered from basal values following exposure of the tissues to sodium nitroprusside alone.

The changes in cytosolic and particulate PKC activities induced by endothelin-1 in the presence of sodium nitroprusside are also shown in Figures 2a and 2b. As can be seen, cytosolic activity was also unchanged by endothelin-1 in the presence of sodium nitroprusside at any of the incubation times studied. Likewise, the increase in particulate PKC activity following exposure to endothelin-1 was inhibited by prior incubation with sodium nitroprusside for 30 s 1, 2, 5 and 10 min, though at 10 min values were significantly greater than basal.

Pre-incubation of the vessels with sodium nitroprusside alone for 30 s and also when followed by endothelin-1, resulted in an approximate 180 fold increase in the levels of cyclic GMP above basal values (Figure 2c); exposure to sodium nitroprusside for longer periods also significantly increased cyclic GMP levels but the extent of the increase was less than that seen at 30 s, being about 25 times the basal values at 10 min in both experiments.

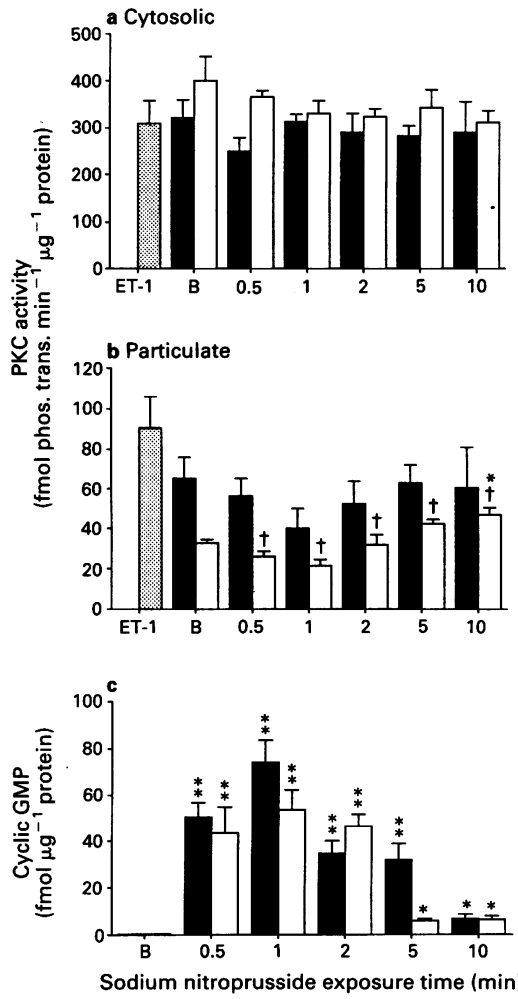

Figure 2 Changes in cytosolic (a) and particulate (b) protein kinase C (PKC) activity in endothelium-denuded rat aortae following incubation with sodium nitroprusside alone for 0.5, 1, 2, 5 and 10 min (closed columns) and following similar incubations with sodium nitroprusside before exposure to endothelin-1 for 30 s (open columns). Changes in cyclic GMP levels in the same experiments are also shown (c). Values are mean of 4–6 determinations from 5 separate experiments; vertical bars show s.e.mean. $*P < 0.05$; $**P < 0.01$ compared with basal values (B); $\dagger P < 0.05$ compared to exposure to endothelin-1 (ET-1) alone for 30 s in endothelium-denuded preparations (stippled column).

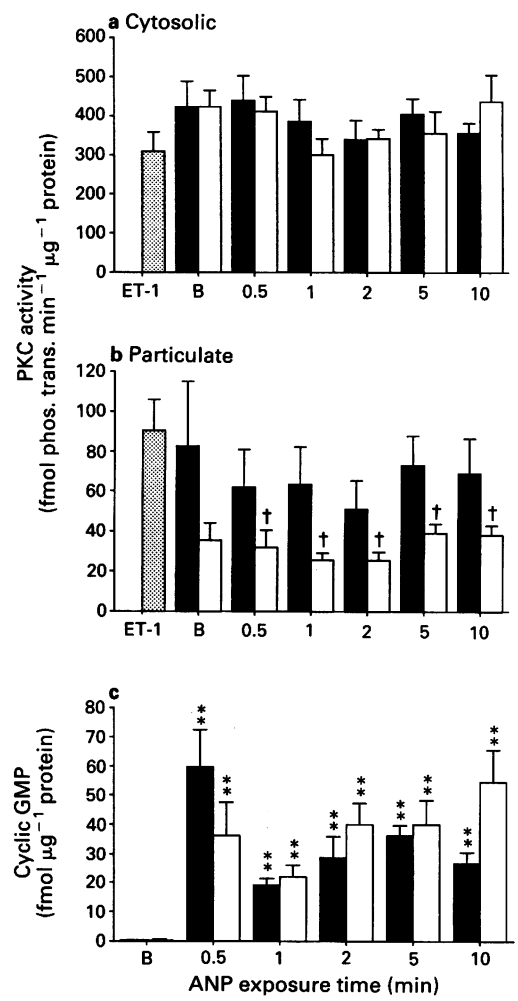

Figure 3 Changes in cytosolic (a) and particulate (b) protein kinase C (PKC) activity in endothelium-denuded rat aortae following incubation with atrial natriuretic peptide (ANP) alone for 0.5, 1, 2, 5 and 10 min (closed columns) and following similar incubations with ANP before exposure to endothelin-1 for 30 s (open columns). Changes in cyclic GMP levels in the same experiments are also shown. Values are mean of 4–6 determinations from 5 separate experiments; vertical bars show s.e.mean. $**P < 0.01$ compared with basal values (B); $\dagger P < 0.05$ compared to exposure to endothelin-1 (ET-1) alone for 30 s in endothelium-denuded preparations (stippled column).

Atrial natriuretic peptide

In the presence of ANP alone neither the cytosolic nor particulate PKC activities were altered significantly at any of the incubation periods studied (Figure 3a and 3b). The particulate activity in the presence of ANP alone was approximately double the values found in the presence of endothelin-1, though none of the points reached was significantly different. Pre-incubation with ANP for up to 10 min significantly inhibited the changes in particulate PKC activity induced by a 30 s exposure to endothelin-1, levels remaining unchanged from basal (Figure 3b).

A significant increase in cyclic GMP levels above basal values was observed following incubation with ANP alone or in the presence of endothelin-1 (Figure 3c).

Endothelium-derived relaxing factor

Calcium ionophore-induced EDRF release in endothelium-intact preparations resulted in a significant reduction in basal cytosolic PKC activity following the 5 and 10 min incubation periods (Figure 4a). A significant reduction in basal particulate activity was also observed following 1 min incubation with A23187 (Figure 4b).

Changes in cytosolic and particulate PKC activity in endothelium-intact vessels pre-incubated for various times with A23187 followed by endothelin-1 exposure, are also shown in Figures 4a and 4b respectively. Cytosolic activity fell gradually throughout the whole time course of the experiment, reaching significance compared with basal activity at the 10 min incubation period. Particulate activity also tended to fall compared with basal values though significance was not achieved at any incubation time studied.

When compared to the data obtained in the presence of endothelin-1 alone (Figure 1a), cytosolic activity in the presence of both A23187 and endothelin-1 was significantly reduced at all A23187 incubation times studied. A similar significant reduction was observed in particulate activity when compared to that seen with endothelin-1 alone (Figure 1b).

A23187, alone and in the presence of endothelin-1, significantly increased cyclic GMP levels above basal values, at each incubation time studied (Figure 4c). Peak cyclic GMP levels were achieved after 5 min incubation with A23187 both in the absence and presence of endothelin-1.

The effect of L-NNA on the changes induced by A23187 in endothelium-intact vessels in the presence of endothelin-1 is

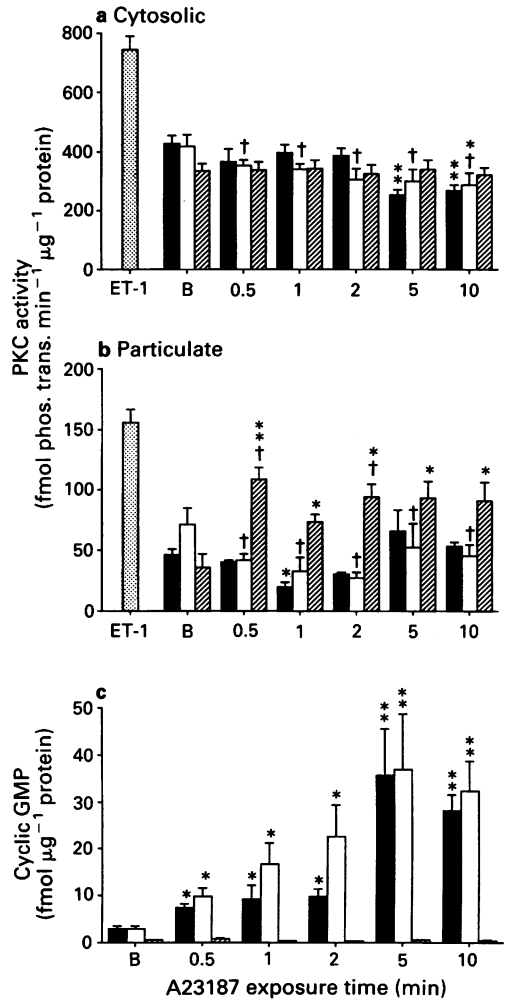

Figure 4 Changes in cytosolic (a) and particulate (b) protein kinase C (PKC) activity in endothelium-intact rat aortae following incubation with A23187 alone for 0.5, 1, 2, 5 and 10 min (closed columns) and following similar incubations with A23187 before exposure to endothelin-1 for 30 s (open columns). Changes following preincubation with L-N^G-nitro arginine before A32187 and endothelin-1 are also included (hatched columns). Changes in cyclic GMP levels in the same experiments are also shown. Values are mean of 4–6 determinations from 8 separate experiments; vertical bars show s.e.mean. $^*P < 0.05$; $^{**}P < 0.01$ compared to basal values (B); $\dagger P < 0.05$ compared to exposure to endothelin-1 (ET-1) alone for 30 s in endothelium-intact preparations (stippled column).

again shown in Figure 4. Cytosolic PKC activity, compared to basal values, was unaffected by the presence of this nitric oxide synthetase inhibitor. Particulate activity however was significantly enhanced at all time points when compared to basal values following incubation with A23187 and endothelin-1 in the presence of L-NNA.

Compared to the data obtained in the absence of L-NNA, cytosolic PKC activity was not significantly altered by L-NNA. Particulate activity was however significantly different from that obtained in the absence of L-NNA at the 30 s and 2 min incubation periods with A23187.

Figure 4c shows that in the presence of L-NNA, A23187 did not increase cyclic GMP levels above basal values at all incubation times studied.

To test the effect of L-NNA itself on endothelin-1-induced changes in PKC activity, endothelium-intact preparations were incubated for 30 min prior to exposure to endothelin-1 for various times. The PKC response to endothelin-1 was similar to that observed in the absence of L-NNA (Figure 1a and 1b) but with no significant increase in particulate PKC occurring after 10 min exposure to endothelin-1 (data not shown).

Discussion

Endothelin-1 is a potent vasoconstrictor peptide producing a contractile response in vascular smooth muscle which is slow in onset and unusually long-lasting (Yanagisawa *et al.*, 1988). It has been suggested that PKC plays an important part in mediating this contractile response (Danthuluri & Brock, 1990). The data presented here show that exposure of rat vascular smooth muscle to endothelin-1 results in the production of two temporally separated, transient increases in particulate, or membrane bound, PKC activity. The first and largest, increase occurs after only 30 s exposure to endothelin-1 with the second increase developing later at 10 min. This transient, biphasic response occurs both in the presence and absence of endothelium.

It is interesting to note that endothelin-1 did not significantly increase cyclic GMP levels in the aortic preparations. A recent report by Topouzis and colleagues (1991) showed a small, transient, early increase (1 min) in cyclic GMP in rat aortic rings in response to endothelin-1 (10^{-8} M) which was dependent on the presence of endothelium. The reasons for the discrepancy between their data and those of the present study are difficult to explain. One possibility is the different experimental conditions used in the two studies.

It has been suggested (Nishizuka, 1984) that under basal conditions PKC is found located mainly in the cytosol (cytosolic fraction). Then, after cell activation, it is rapidly translocated to the membrane (particulate fraction), where it becomes associated with membrane phospholipids. If this is the case then an increase in particulate PKC activity should be associated with a corresponding decrease in cytosolic PKC activity. However, to date, opinion on this matter is conflicting. For example, prolactin stimulation of rat aortic smooth muscle has been shown to lead to simultaneous increases in both particulate and cytosolic PKC activity (Sauro *et al.*, 1989). In contrast, agonist-induced decreases in cytosolic PKC activity with corresponding increases in particulate PKC activity have been shown by a number of workers (Wheeler-Jones *et al.*, 1989; Chambers *et al.*, 1990; Haller *et al.*, 1990). An unusual situation occurs in platelets in that either dual activation of both cytosolic and particulate enzymes can occur or, alternatively, the cytosolic activity decreases while the particulate activity increases depending on which aggregating agent is used (Salari *et al.*, 1990).

The biphasic activation of particulate PKC shown here is not accompanied by a simultaneous decrease in cytosolic PKC activity. In the presence of endothelium and in response to endothelin-1, cytosolic activity is decreased significantly only after 20 and 30 min of agonist exposure. In the absence of endothelium however cytosolic activity is decreased after 5 and 10 min of endothelin-1 exposure, thereafter returning to levels comparable with basal activity. It appears therefore, that in the absence of endothelium this return to basal levels may well represent a re-translocation of PKC from the membrane to the cytosol. Why this difference between endothelium-intact and denuded preparations should occur is not at all evident. It is possible that endothelial cells release a substance, perhaps EDRF, that prevents the retranslocation of the PKC. Further work is needed to explain this phenomenon.

The lack of any real association between increases in particulate PKC activity and decreases in cytosolic PKC activity in the presence of endothelin-1 leads us to suggest that in this model, the two pools of the PKC isoenzymes may be acting independently of one another. There is no reason to believe that the response to other agonists would be similar however. Other workers have examined the effects of endothelin-1 exposure on PKC activity in vascular smooth muscle. One such study (Haller *et al.*, 1990) in intact strips of bovine carotid artery showed endothelin-1 to cause a sustained elevation in particulate PKC activity over 50 min. This was accompanied by a corresponding decrease in cytosolic PKC activity. These results would therefore seem to disagree with

those of the present study. Why this discrepancy should exist is not clear. One explanation is that a species difference may exist. A possible difference between aortic and carotid artery tissue could also be responsible.

If PKC is responsible for the sustained phase of agonist-induced vascular smooth muscle contraction, changes in the intracellular levels of diacylglycerol (DAG), the specific activator of PKC (Nishizuka, 1984) are also of importance. The DAG response of vascular smooth muscle to endothelin-1 has been studied by a number of groups. For example, cultured cells from bovine and rat aortae were shown to develop maximum levels of DAG at 1–2 min after exposure, decaying to basal levels thereafter (Resink *et al.*, 1988). In contrast, in cultured aortic smooth muscle cells of rat (Griendling *et al.*, 1989) and rabbit (Sunako *et al.*, 1989; 1990) endothelin-1 has been shown to produce a biphasic increase in DAG levels with an early transient increase being followed by a more sustained increase. This biphasic production would correlate well with the biphasic activation of particulate PKC shown in the present study.

Another vasoconstrictor, angiotensin II, also produces a biphasic DAG response in vascular smooth muscle cells (Griendling *et al.*, 1986; Sunako *et al.*, 1989; 1990). As inositol 1,4,5-trisphosphate (IP_3) is produced from phosphatidylinositol 4,5 bisphosphate (PIP_2) at the same time as DAG (Berridge & Irvine, 1984) some of these workers (Griendling *et al.*, 1986; Sunako *et al.*, 1989) also measured the IP_3 response of these cells to angiotensin II. Both groups found the IP_3 response to be rapid and transient compared to the biphasic DAG response. This suggests that the early transient DAG phase is derived from PIP_2 hydrolysis while a large part of the late sustained DAG phase could come from other major membrane-associated phospholipids such as PI (Griendling *et al.*, 1986) or phosphatidylcholine (PC) (Griendling *et al.*, 1989).

The present study also clearly shows that an elevation of intracellular cyclic GMP levels by either EDRF, sodium nitroprusside or ANP causes an inhibition of the particulate PKC response to endothelin-1. No discernible changes in cytosolic PKC activity were noted under the same conditions. We have previously shown that cyclic GMP causes inhibition of IP_3 production in both vascular smooth muscle (Lang & Lewis, 1989) and cultured endothelial cells of the pig (Lang & Lewis, 1991). An inhibition of DAG production from PIP_2 could account for the effect of cyclic GMP on the early rise in endothelin-1-induced particulate PKC, since cyclic GMP is thought to exert its effect at the site of the G protein coupling receptor to phospholipase C (Hirata *et al.*, 1990).

Our observations on the effects of cyclic GMP on PKC activity confirm those of other groups using bovine vascular smooth muscle (Ahlner *et al.*, 1988), and rat aortic smooth muscle (Sauro & Fitzpatrick, 1990a,b).

Although inhibition of PIP_2 hydrolysis by cyclic GMP can account for inhibition of the early activation of PKC by endothelin-1, cyclic GMP elevating agents have been shown to cause a reversal of the sustained or tonic phase of endothelin-1-induced contraction in vascular smooth muscle (Yanagisawa *et al.*, 1988; Bonhomme *et al.*, 1989; Miller *et al.*, 1989). This suggests that cyclic GMP may also inhibit the sustained production of DAG and the late phase of PKC activation.

In conclusion, endothelin-1 causes a biphasic activation of particulate PKC activity in rat aortic smooth muscle. The study also shows that EDRF, acting via cyclic GMP, inhibits the first phase of particulate PKC activation, thus providing further evidence for the mechanism of EDRF-induced relaxation in vascular smooth muscle.

This work was supported by a grant from the British Heart Foundation.

References

AHLNER, J., AXELSSON, K.L., KARLSSON, J-O.G. & ANDERSSON, R.G.G. (1988). Glyceryl trinitrate inhibits phosphatidylinositol hydrolysis and protein kinase C activity in bovine mesenteric artery. *Life Sci.*, **43**, 1241–1248.

BERRIDGE, M.J. & IRVINE, R.F. (1984). Inositol trisphosphate, a novel second messenger in cellular signal transduction. *Nature*, **312**, 315–321.

BONHOMME, M.C., CANTIN, M. & GARCIA, R. (1989). Relaxing effect of artrial natriuretic factor on endothelin–precontracted vascular strips. *Proc. Soc. Exp. Biol. Med.*, **191**, 309–315.

CHAMBERS, T.C., CHALIKONDA, I. & EILON, G. (1990). Correlation of protein kinase C translocation, P-glycoprotein phosphorylation and reduced drug accumulation in multi drug resistant human KB cells. *Biochem. Biophys. Res. Commun.*, **169**, 253–259.

COLLINS, P., HENDERSON, A.H., LANG, D. & LEWIS, M.J. (1988). Endothelium-derived relaxing factor and nitroprusside compared in noradrenaline–and K^+–contracted rabbit and rat aortae. *J. Physiol.*, **400**, 395–404.

DANTHULURI, N.R. & BROCK, T.A. (1990). Endothelin receptor-coupling mechanisms in vascular smooth muscle: a role for protein kinase C. *J. Pharmacol. Exp. Ther.*, **254**, 393–398.

GRIENDLING, K.K., RITTENHOUSE, S.E., BROCK, T.A., EKSTEIN, L.S., GIMBRONE, M.A. & ALEXANDER, R.W. (1986). Sustained diacylglycerol formation from inositol phospholipids in angiotensin II-stimulated vascular smooth muscle cells. *J. Biol. Chem.*, **261**, 5901–5906.

GRIENDLING, K.K., TSUDA, T. & ALEXANDER, R.W. (1989). Endothelin stimulates diacylglycerol accumulation and activates protein kinase C in cultured vascular smooth muscle cells. *J. Biol. Chem.*, **26**, 8237–8240.

GRIFFITH, T.M., LEWIS, M.J., NEWBY, A.C. & HENDERSON, A.H. (1988). Endothelium-derived relaxing factor. *J. Am. Coll. Cardiol.*, **12**, 797–806.

HALLER, H., SMALLWOOD, J.I. & RASMUSSEN, H. (1990). Protein kinase C translocation in intact vascular smooth muscle strips. *Biochem J.*, **270**, 375–381.

HANNUN, Y.A., LOOMIS, C.R. & BELL, R.M. (1985). Activation of protein kinase C by Triton X-100 mixed micelles containing diacylglycerol and phosphatidylserine. *J. Biol. Chem.*, **260**, 10039–10040.

HIRATA, M., KOHSE, K.P., CHANG, C.H., IKEBE, T. & MURAD, F. (1990). Mechanism of cylic GMP inhibition of inositol phosphate formation in rat aorta segments and cultured bovine aortic smooth muscle cells. *J. Biol. Chem.*, **265**, 1268–1273.

LANG, D. & LEWIS, M.J. (1989). Endothelium-derived relaxing factor inhibits the formation of inositol trisphosphate by rabbit aorta. *J. Physiol.*, **411**, 45–52.

LANG, D. & LEWIS, M.J. (1991). Inhibition of inositol 1,4,5-trisphosphate formation by cyclic GMP in cultured aortic endothelial cells in the pig. *Br. J. Pharmacol.*, **102**, 277–281.

MILLER, V.M., KOMORI, K., BURNETT, J.C. & VANHOUTTE, P.M. (1989). Differential sensitivity to endothelin in canine arteries and veins. *Am. J. Physiol.*, **257**, H1127–H1131.

MOORE, P.K., AL-SWAYEH, O.A., CHONG, N.W.S., EVANS, R.A. & GIBSON, A. (1990). L-N^G-nitro arginine (L-NOARG), a novel, L-arginine-reversible inhibitor of endothelium-dependent vasodilatation *in vitro*. *Br. J. Pharmacol.*, **99**, 408–412.

NISHIZUKA, Y. (1984). The role of protein kinase C in cell surface signal transduction and tumour promotion. *Nature*, **308**, 693–698.

PALMER, R.M.J., FERRIDGE, A.G. & MONCADA, S. (1987). Nitric oxide release accounts for the biological activity of endothelium-derived relaxing factor. *Nature*, **327**, 524–526.

RAPOPORT, R.M. (1986). Cyclic guanosine monophosphate inhibition of contraction may be mediated through inhibition of phosphatidyl inositol hydrolysis in rat aorta. *Circ. Res.*, **58**, 407–410.

RASMUSSEN, H., TAKUWA, Y. & PARK, S. (1987). Protein kinase C in the regulation of smooth muscle contraction. *FASEB. J.*, **1**, 177–185.

RESINK, T.J., SCOTT-BURDEN, T. & BÜHLER, F.R. (1988). Endothelin stimulates phospholipase C in cultured vascular smooth muscle cells. *Biochem. Biophys. Res. Commun.*, **157**, 1360–1368.

SALARI, H., DURONICO, V., HOWARD, S., DEMOS, M. & PELECH, S. L. (1990). Translocation-independent activation of protein kinase C by platelet factor, thrombin and prostacyclin. *Biochem J.*, **267**,

689–696.

SAURO, M.D., BUCKLEY, A.R., RUSSELL, D.H. & FITZPATRICK, D. F. (1989). Prolactin stimulation of protein kinase C activity in rat aortic smooth muscle. *Life Sci.*, **44**, 1787–1792.

SAURO, M.D. & FITZPATRICK, D.F. (1990a). Atrial natriuretic factor inhibits protein kinase C activation in rat aortic smooth muscle. *FASEB J.*, **4**, A334.

SAURO, M.D. & FITZPATRICK, D.F. (1990b). Atrial peptides inhibit protein kinase C-mediated contraction in rat aorta. *Eur. J. Pharmacol.*, **180**, 373–376.

SUNAKO, M., KAWAHARA, Y., HIRATA, K., TSUDA, T., YOKOYAMA, M., FUKUZAKI, H. & TAKAI, Y. (1990). Mass analysis of 1,2-diacylglyerol in cultured rabbit vascular smooth muscle cells. Comparison of stimulation by angiotensin II and endothelin. *Hypertension.*, **15**, 84–88.

SUNAKO, M., KAWAHARA, Y., KARIYA, K., ARAKI, S., FUKUZAKI, H. & TAKAI, Y. (1989). Endothelin-induced biphasic formation of 1,2-diacylglycerol in cultured rabbit vascular smooth muscle cells – mass analysis with a radioenzymatic assay. *Biochem. Biophys. Res. Commun.*, **160**, 744–750.

TAKAI, Y., KAIBUCHI, K., MATSUBARA, T. & NISHIZUKA, Y. (1981). Inhibitory action of guanosine 3',5'-monophosphate on thrombin-induced phosphatidylinositol turnover and protein phosphorylation in human platelets. *Biochem. Biophys. Res. Commun.*, **101**, 61–67.

TOPOUZIS, S., HUGGINS, J.P., PELTON, J.T. & MILLER, R.C. (1991). Modulation by endothelium of the responses induced by endothelin-1 and by some analogues in rat isolated aorta. *Br. J. Pharmacol.*, **102**, 545–549.

WHEELER-JONES, C.P.D., PATEL, Y., KAKKAR, V.V. & KRISHNAMURTH, S. (1989). Receptor- and phorbol-ester-mediated redistribution of protein kinase C in human platelets. *Biochem. J.*, **263**, 969–972.

YANAGISAWA, H., KURIHARA, H., KIMURA, S., TOMOBE, Y., KOBAYASHI, M., MITSUI, Y., YAZAKI, Y., GOTO, K. & MASAKI, T. (1988). A novel potent vasoconstrictor peptide produced by vascular endothelial cells. *Nature*, **332**, 411–415.

(Received February 11, 1991
Revised May 14, 1991
Accepted May 29, 1991)

Br. J. Pharmacol. (1991), **104**, 145–150

Pharmacological analysis of agonist-antagonist interactions at acetylcholine muscarinic receptors in a new urinary bladder assay

*P.A.C. Durant, [1]†N.P. Shankley, *N.J. Welsh & *J.W. Black

†James Black Foundation, 68 Half Moon Lane, London SE24 9JE and *Department of Analytical Pharmacology, King's College School of Medicine & Dentistry, The Rayne Institute, 123 Coldharbour Lane, London SE5 9NU

1 Agonist-antagonist interactions at acetylcholine (ACh) muscarinic receptors have been analysed by use of an improved urinary bladder assay, isolated and intact, from the mouse. With 5-methylfurmethide as agonist, validated cumulative concentration-effect curves were obtained in less than 7 min by re-dosing before the response plateaux began to fade.

2 The pK_B value estimated for pirenzepine was 6.76. The pK_B values estimated for atropine and N-methylatropine from data obtained at concentrations which produced dose-ratios greater than 20 and 60 were 8.90 and 9.58, respectively.

3 The deviation from simple competitive behaviour at low dose-ratios with atropine and N-methylatropine was consistent with the operation of saturable antagonist removal processes. The deviation observed with atropine was corrected by pre-incubation with methylbutyrate, an alternative substrate for 'atropine esterase'.

4 The simple competitive behaviour of N-methylatropine was restored following pre-incubation with the neuronal choline uptake blocker hemicholinium-3 (HC-3). However, the pK_B estimated for N-methylatropine under these conditions was low. This latter result could be accounted for by the observed behaviour of HC-3 as a competitive antagonist of ACh muscarinic receptors ($pK_B = 4.01$).

5 We conclude that the modified mouse urinary bladder assay is suitable for the quantitative analysis of muscarinic receptor interactions. In addition, we postulate the existence of a previously undescribed uptake mechanism for quaternary muscarinic receptor antagonists.

Keywords: Receptor, muscarinic; parasympatholytics; parasympathomimetics; muscle, smooth, bladder; ammonium compounds; urinary tract, bladder; hemicholinium-3; esterase.

Introduction

The need for the development of new selective drugs to control the function of the urinary bladder is widely recognized (see McGuire, 1986). One approach is to use understood pharmacological principles and methods to define receptor targets (Black, 1989). Tactically, pharmacological models of agonist and antagonist action are applied in an attempt to relate experimental data to the model-defined chemical parameters which are imagined to govern ligand-receptor interactions. The challenge is to develop bioassays which can provide data of the necessary quality both to test the applicability of a model and to determine the confidence held in particular parameter estimates.

In vitro assays currently used for the pharmacological investigation of the urinary bladder are hindered by the intrinsic properties of the smooth muscle. The characteristic basal spontaneous activity which often increases during agonist-induced contraction and the transient nature of agonism, both make response level determination difficult (Edvardsen & Setekleiv, 1968; Sibley, 1984). As a result, experimental designs have evolved in which the preparations are superfused or washed between repeated applications of either single agonist doses or pulses of electrical stimulation (Holt *et al.*, 1985; 1986; Santicioli *et al.*, 1986). These experimental designs are, in our hands at least, inherently uneconomical and the data obtained highly variable. In addition, those assays using strips of bladder muscle are potentially further complicated because of the known regional variation in the hormone receptor (Levin *et al.*, 1980) and innervation density (Taira, 1972).

We describe the development of an *in vitro*, intact, mouse urinary bladder preparation for pharmacological assay. The assay has been validated by performing standard competitive analyses on the interaction between 5-methylfurmethide, an acetylcholine (ACh) muscarinic receptor agonist and three competitive antagonists, atropine, N-methylatropine and pirenzepine, previously well-characterized on other biosystems (see Black & Shankley, 1985). These validation procedures disclosed a new antagonist removal process and some of its properties.

[1] Author for correspondence.

Methods

Urinary bladder assay

Bladders removed from adult male mice (18–28 g of Charles River CD-1 albino strain) were placed in Krebs-Henseleit solution of the following composition (in mM): Na^+ 143, K^+ 5.9, Ca^{2+} 2.5, Mg^{2+} 1.2, Cl^- 128, HPO_4^{2-} 1.0, SO_4^{2-} 1.2, D-glucose 10 and HCO_3^- 25. The whole bladder was drained, trimmed of extraneous tissue, ligated between two stainless steel wires and placed in an organ bath containing 20 ml of the above solution at 37°C, gassed with 95% O_2 and 5% CO_2. Tension was continuously recorded with an isometric transducer following the application of a 2 g load.

Guinea-pig trachea assay

Tissues were prepared as tracheal strips essentially as described by Emmerson & Mackay (1979). Briefly, the whole trachea from male guinea-pigs (Dunkin Hartley 400–600 g) was removed and cleared of extraneous tissue. The trachea was examined to locate the smooth muscle layer (posterior aspect). The anterior cartilage was cut longitudinally. The trachea was then pinned open on a board and kept moist with Krebs solution. The connective tissue between two rings was

cut on one side; then, the muscle layer was cut, leaving two adjacent rings separated from the rest of the trachea. Threads were tied to the open ends of the rings. Each preparation was suspended in an organ bath under identical recording conditions to those used for the bladder assay with the exception of the application of a 1 g load.

Experimental protocols

After the cumulative agonist dosing regime was established (see Results), the following protocol was used for the analysis of competitive antagonism. Twelve preparations were used simultaneously and after an initial 60 min stabilization period (solution replaced every 20 min), tissues were incubated for a further 60 min in the absence or presence of antagonist before a single cumulative concentration-effect curve was obtained using 5-methylfurmethide (5-MeF). Indomethacin (3 μM) was also included during this period in the tracheal assay to minimize interference from cyclo-oxygenase products. In additional experiments, tissues were also preincubated with hexamethonium (100 μM), methylbutyrate (100 μM), taurocholate (100 μM), choline (100 μM) or hemicholinium-3 (HC-3, 500 μM) for 60 min. Antagonist and other drug treatments were allocated on a block design so that each organ bath received a different treatment during the course of an experiment. Between 4 and 8 replicates were obtained for each treatment group.

Data analysis

Responses were expressed as changes in tension measured from the baseline immediately prior to starting the cumulative agonist concentration-effect curve or electrical stimulation. The concentration-effect curve data from individual preparations were fitted to a logistic function which provided estimates of the midpoint location ($\log[A_{50}]$), maximal asymptote (α) and midpoint slope (p) parameters, as described previously (Black & Shankley, 1985). These parameters were expressed as mean $\pm$ s.e.mean and used for both the analysis of the data and for display purposes by using them to simulate logistic curves which are shown superimposed upon the mean experimental data.

Competitive antagonism experiments were analysed according to methods described previously (Black *et al.*, 1985). In brief, if no significant differences were found in slopes and asymptotes of the curves in the absence and presence of the antagonist as tested by one-way ANOVA, then the $\log[A_{50}]$ values in the absence ($[A_{50}]$) and presence ($[A_{50}]^B$) of antagonist (B) were directly fitted to the following derivative of the Schild equation:

$$\log[A_{50}]^B = \log[A_{50}] + \log\left(1 + \frac{[B]^b}{10^{\log K_B}}\right)$$

If b, which is equivalent to the Schild slope parameter, was found to be not significantly different from unity, a second fit was performed with b constrained to unity, allowing the antagonist equilibrium dissociation constant (K_B) to be estimated as $\log K_B \pm$ s.e. For display purposes, mean $\log[A_{50}]$ data were expressed as dose-ratios (r) and plotted in Schild plot space.

A combined dose-ratio analysis was performed as described previously (Shankley *et al.*, 1988). In brief, data from the interaction between HC-3 (300 μM) and atropine (10 nM) in the presence of methylbutyrate (100 μM) were analysed to test compliance with the additive and multiplicative models.

A model describing the saturable uptake of a competitive antagonist (see Shankley, 1985; Kenakin & Beek, 1987) was used to simulate the data from the interaction between both N-methylatropine and atropine with 5-MeF. The following relation was used, $\log(r - 1) = \log[B_a] + pK_B$, where $[B_a]$, [B] in the receptor compartment, is given by the following equations,

$$[B_a] = \frac{-b + \sqrt{b^2 + 4ac}}{2a}$$

where $a = 1$, $b = (K_{BU} + U_M/k - [B])$ and $c = K_{BU}[B]$.

U_M is the maximum rate of uptake, k the diffusion rate constant for entry into the receptor compartment and K_{BU} the Michaelis-Menten constant.

Similarly, the combined competitive antagonism of muscarinic receptors by HC-3 (C) and N-methylatropine (B) was simulated using the relationship (Black *et al.*, 1986), $\log(r - 1) = \log([B]/K_B(1 + [C]/K_C))$ where K_B and K_C are the equilibrium dissociation constants for the two antagonists. The simultaneous expression of combined antagonism and antagonist uptake was simulated as follows,

$$\log(r - 1) = \log\left(\frac{[B_a]}{K_B(1 + [C]/K_C)}\right)$$

where $[B_a]$ is obtained from the equation describing the uptake system which is given above.

Drugs

Where possible, all drugs were freshly prepared in distilled water; methylbutyrate and indomethacin had to be prepared initially in absolute ethanol. The total volume of solvent added to the 20 ml organ bath did not exceed 350 μl. Drugs and their sources were as follows: atropine sulphate, N-methylatropine nitrate, hemicholinium-3 bromide, choline chloride, hexamethonium bromide, indomethacin, taurocholic acid (Sigma Chemical Co. Ltd.), methylbutyrate (Aldrich Chemical Co. Ltd.), 5-methylfurmethide iodide (Wellcome Research Laboratories Ltd.), pirenzepine dihydrochloride (A.B. Hassle Ltd.).

Results

Characterization of 5-methylfurmethide concentration-effect relations

Mouse urinary bladders, exposed to 5-MeF at concentrations between 0.1 μM and 10 μM, responded by a rapid increase in tone. After reaching a brief plateau, the tone faded with a half-life of a few minutes. Soon after the fade began, the muscle developed irregular, high frequency, twitch contractions (Figure 1a). This combination of fade and irregular twitchings made the identification and measurement of a 'steady-state' level nearly impossible. Apparently, 5-MeF concentration-effect relations would have to be measured from randomised sequences of individual doses, a difficult experimental design for studying agonist-antagonist interactions comprehensively.

Attempts to suppress the spontaneous activity of the bladder by pharmacological means were unsuccessful. Experiments were performed in the absence of calcium and in the presence of 1%, 3% and 10% of normal calcium concentration (2.5 mM) at organ bath temperatures of either 24°C and 37°C. Similarly, increasing the magnesium concentration (1.2 mM) up to 10 fold, in either a normal or low calcium solution (1%) did not affect spontaneous activity although the magnitude of the responses to 5-MeF was reduced.

However, one of us (P.A.C.D.) discovered that when a higher concentration of 5-MeF was added at the initial, twitch-free plateau of a previous dose-response, the superimposed contraction suppressed the onset of spontaneous twitching which was expected to develop after the antecedent dose. Thus it was possible, in a mere 7 min to obtain a complete agonist concentration-effect curve by cumulative dosing before the onset of fade at each level (Figure 1b). No significant differences were found between peak responses during

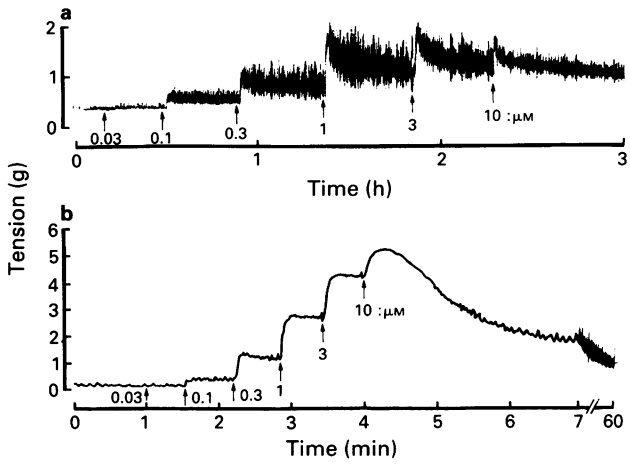

Figure 1 Experimental traces showing cumulative 5-methylfurmethide concentration-effect curves obtained on the intact mouse urinary bladder assay. Traces show (a) the development of fade and spontaneous activity following several minutes of exposure to the agonist and (b) the well-defined curve following adoption of the fast-dosing regime.

sequential cumulation of doses and those obtained from single doses given on a randomized schedule (Table 1). This table also shows that the experimental price to be paid for the ease and speed of cumulative dosing is serial correlation which shows up as progressively increasing variances.

Interaction between pirenzepine and 5-methylfurmethide

Pirenzepine, a polar derivative of benzodiazepine, is classified as a selective muscarinic receptor antagonist (Hulme *et al.*, 1990). It is useful for distinguishing M_1-receptors ($pK_B \sim 8.0$) from M_2- and M_3-receptors ($pK_B \sim 6.8$).

Pirenzepine, equilibrated with bladder muscle at concentrations between 0.3 μM–30 μM regularly moved the location of 5-MeF concentration-effect curves according to the Gaddum-Schild equation (Figure 2). The other parameters of the curves, slope and maximum, were not significantly changed. The simple competitive behaviour of pirenzepine was characterized by a pK_B estimate of 6.76 ± 0.09 (d.f. = 33). This value corresponds to the affinity of pirenzepine for M_2- and M_3-receptors.

Interaction between atropine and 5-methylfurmethide

Atropine, a basic organic ester, is classified as a non-selective antagonist of muscarinic receptors with a $pK_B \sim 9.0$.

On urinary bladder muscle, atropine produced concentration-dependent (3 nM–300 nM), parallel displacement of 5-MeF concentration-effect curves. Their slope parameters and maximal asymptotes were not altered. However, unlike pirenzepine, the displacements produced by atropine did not conform to the rectilinear simplicity of the Gaddum-Schild equation for competitive antagonism (Figure 2). The Schild plot, concave to the log[antagonist] axis, approached an asymptote of unit slope which gave an apparent pK_B intercept

Table 1 Comparison of the initial responses (tension, g ± s.e.mean, $n = 6$) to 5-methylfurmethide (5-MeF) obtained following single and cumulative dosing on the mouse urinary bladder assay

[5-MeF]: μM	Single dosing	Cumulative dosing
0.1	0.98 ± 0.19	1.20 ± 0.20
1	3.38 ± 0.20	3.60 ± 0.45
10	5.50 ± 0.29	5.33 ± 0.82

No significant differences were found (unpaired t test, $P > 0.05$).

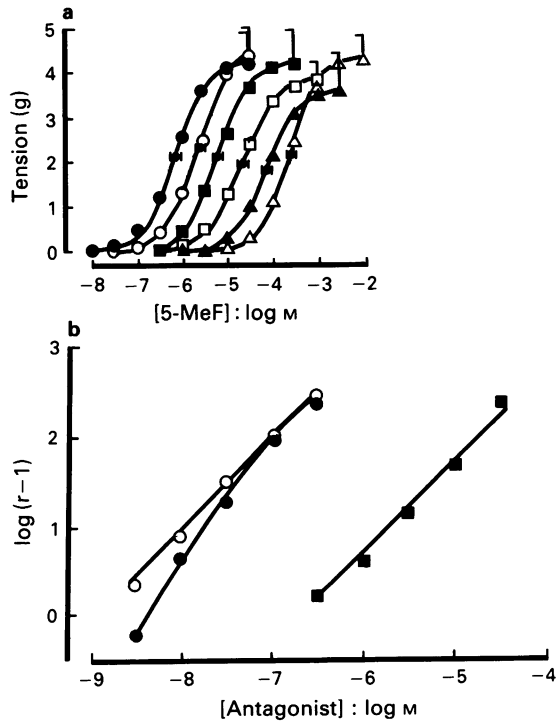

Figure 2 Atropine and pirenzepine pK_B determination on the mouse urinary bladder assay. (a) Methylfurmethide (5-MeF) concentration-effect curves obtained in the absence (●) and presence of atropine (nM), 3 (○), 10 (■), 30 (□), 100 (▲) and 300 (△) and in the presence of methylbutyrate (100 μM). (b) Schild plots for the 5-MeF/atropine (●), 5-MeF/atropine in the presence of methylbutyrate (100 μM) (○) and 5-MeF/pirenzepine (■) interactions on the mouse urinary bladder assay. The curve drawn through the data obtained from the 5-MeF/atropine interaction in the absence of methylbutyrate was simulated using a model describing the saturable removal of atropine (see legend to Figure 4 for details). pK_B estimates were as follows: atropine (+methylbutyrate) $pK_B = 8.99 \pm 0.07$, $b = 1.07 \pm 0.05$, pirenzepine $pK_B = 6.76 \pm 0.09$, $b = 1.11 \pm 0.07$.

of 8.90 ± 0.06 (d.f. = 25). Underreading of the effectiveness of atropine at low dose-ratios could occur if the tissue had a saturable removal process for atropine which operated in the vicinity of the cell surface receptors (Black & Shankley, 1985). In fact, Kenakin & Beek (1987), using rabbit ileum, found a similar saturable process which they attributed to the operation of an 'atropine esterase'. They showed that the enzyme could be inhibited by incubation with an excess (100 μM) of methylbutyrate, a substrate for the enzyme. Urinary bladders similarly incubated with methylbutyrate had the simple competitive behaviour of atropine fully restored, characterized by $pK_B = 8.99 \pm 0.07$ (d.f. = 28).

Interaction between N-methylatropine and 5-methylfurmethide

N-methylatropine, the highly polar quaternary ammonium derivative of atropine, is classified, like atropine itself, as a non-selective muscarinic receptor antagonist but with a $pK_B \sim 9.6$.

N-methylatropine produced concentration-dependent (3 nM–300 nM) parallel displacement of 5-MeF concentration-effect curves without alteration of slope parameters or upper asymptotes. Like atropine, the Schild plot was concave to the log[antagonist] axis but, at the higher dose-ratios, approached an asymptote of unit slope (Figure 3). Data from this region gave $pK_B = 9.58 \pm 0.07$ (d.f. = 20). Once again, it was possible to simulate these data with the model which describes the saturable uptake of a competitive antagonist (Figures 3 and 4). However, in this case, preincubation with methylbutyrate (100 μM) failed to disclose simple competitive

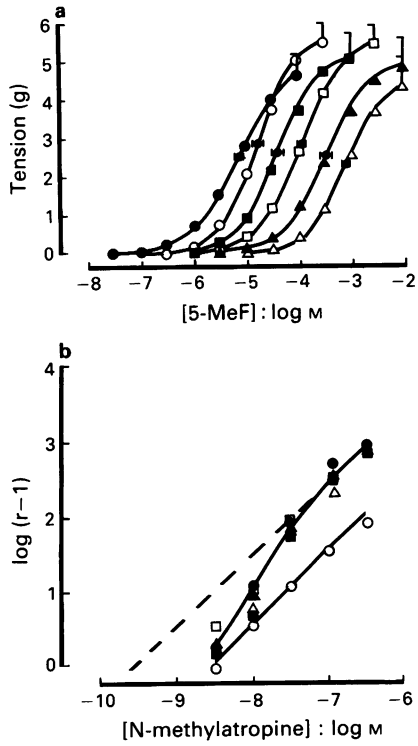

Figure 3 N-methylatropine pK_B determination on the mouse urinary bladder assay. (a) 5-Methylfurmethide (5-MeF) concentration-effect curves obtained in the presence of hemicholinium-3 (HC-3, 500 μM) and in the absence (●) and presence of N-methylatropine (nM), 3 (○), 10 (■), 30 (□), 100 (▲) and 300 (△). (b) Schild plots for the 5-MeF + N-methylatropine interaction in the absence (●) and presence of (○) HC-3 (500 μM), (■) methylbutyrate (100 μM), (□) choline (100 μM), (▲) hexamethonium (100 μM) and (△) taurocholate (100 μM). The curve drawn through the Schild plot data was simulated using a model describing the saturable removal of N-methylatropine. The pK_B value, in the absence of HC-3, (9.58 ± 0.07, b = 0.97 ± 0.09) was estimated using concentrations of N-methylatropine above 10 nM. A pK_B value of 8.61 ± 0.07, b = 0.95 ± 0.05 was estimated in the presence of HC-3.

behaviour suggesting that the N-methylatropine is not a substrate for the 'atropine esterase'.

Other antagonist removal processes were investigated. Taurocholate (100 μM), a recognized inhibitor of quaternary ammonium ion uptake in biochemical systems (Ruifrok, 1982) and hexamethonium (100 μM), a potential alternative substrate, had no effect on the Schild plot (Figure 3b). Similarly, choline (100 μM), a quaternary base with its own specific uptake process, did not affect the profile of antagonism (Figure 3b). However, preincubation with HC-3 (500 μM but not 30 μM), a specific inhibitor of the transport system which takes choline into cholinergic nerve-endings (see Ivy & Townsel, 1987), corrected the deviation from simple competitive behaviour in the Schild plot. However, the corresponding pK_B estimate of 8.61 ± 0.07 (d.f. = 21) was significantly lower than that obtained from the asymptote at high dose-ratios in the absence of HC-3 (Figure 3b).

The model simulations (Figure 4) indicate that the data obtained in the presence of HC-3 are consistent with the model describing the concomitant blockade of the N-methylatropine saturable uptake and muscarinic receptor competitive antagonism. This hypothesis was tested by application of the pharmacological resultant analysis (Figure 5). HC-3 produced concentration-dependent, parallel displacement of 5-MeF concentration-effect curves on both mouse bladder and guinea-pig trachea assays. This behaviour was compatible with HC-3 being a simple competitive antagonist of M-receptors in tracheal muscle with a $pK_B = 4.12 \pm 0.07$ (d.f. = 22). On the other hand, the Schild plot from the bladder assay was flat (b = 0.71 ± 0.04) and possibly nonlinear as well, data incompatable with simple competitive behav-

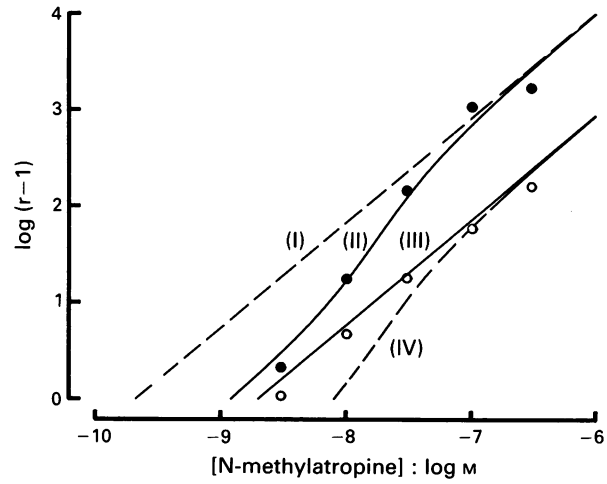

Figure 4 The effect of hemicholinium-3 (HC-3) on the N-methylatropine/5-methylfurmethide (5-MeF) interaction. Schild plots for the 5-MeF/N-methylatropine interaction in the absence (●) and presence (○) of 500 μM HC-3 on the mouse urinary bladder assay. The model-derived lines drawn superimposed on the data were obtained as described in the Methods section. Parameters as follows: (I) Simple competitive antagonism: simulated assuming a K_B value of 0.21 nM for N-methylatropine in the absence of HC-3 using the relationship $\log(r - 1) = \log[B] + pK_B$. (II) Saturable antagonist uptake in the absence of HC-3. $K_B = 0.21$ nM, $U_M = 15$ nmol s^{-1}, $k = 1$ s^{-1} and $K_{BU} = 3$ nM. (III) Antagonist uptake blocked and combined competitive antagonism of muscarinic receptors by HC-3 (C) and N-methylatropine (B). $K_B = 0.21$ nM, $K_C = 200$ μM and [C] = 500 μM. (IV) Combined competitive antagonism of muscarinic receptors by HC-3 (C) and N-methylatropine (B) with the uptake process still active. $K_B = 0.21$ nM, $K_C = 200$ μM, [C] = 500 μM and $[B_a]$ is given by the uptake model as above (II).

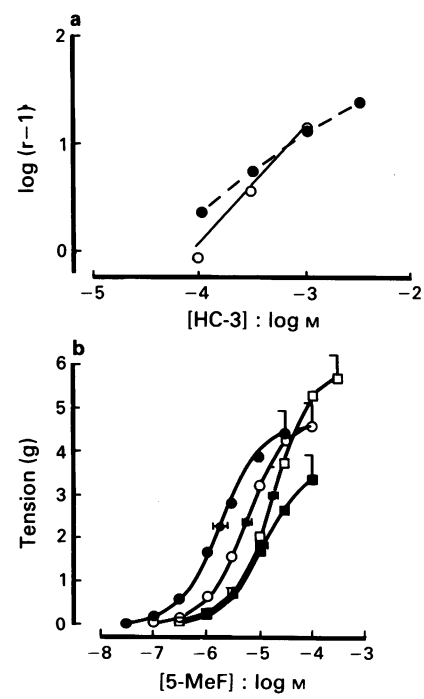

Figure 5 The effect of hemicholinium-3 (HC-3) on the N-methylatropine/5-methylfurmethide (5-MeF) interaction. (a) Schild plots for the 5-MeF/HC-3 interaction on the mouse urinary bladder (●, b = 0.71 ± 0.04) and guinea-pig trachea (○, $pK_B = 4.12 \pm 0.07$, b = 1.14 ± 0.12) assays. (b) Combined dose-ratio analysis. 5-MeF concentration-effect curves in the absence (●) and presence of (○) HC-3 (300 μM), (■) atropine (10 nM) plus methylbutyrate (100 μM) and (□) a combination of both antagonist treatments. The test statistic for the multiplicative model ($S_M = -0.32 \pm 0.18$, d.f. = 24), but not the additive model ($S_A = 0.12 \pm 0.26$, d.f. = 24), was significantly different from zero. Therefore the results are consistent with the additive model (for details of the analysis see Shankley et al., 1988).

iour. However, a combined dose-ratio analysis with atropine used as the reference antagonist showed, by the additivity of antagonism, that HC-3 was apparently acting syntopically with atropine (Figure 5). Importantly, it was not possible to simulate the effect of HC-3 on the N-methylatropine Schild plot by assuming that its action was solely due to muscarinic receptor blockade (Figure 4).

Discussion

Confidence in the application of models of drug action to bioassay data increases with the number of model-defined experimental criteria that are met. Models of agonism and antagonism, based on the applicability of the Law of Mass Action to the interactions among agonist, antagonist and receptor, require for simplicity that measurements of effect are made under equilibrium conditions. Ideally, measurements of effect are made when the agonist response achieves a clearly-defined, sustained plateau. This steady-state condition is usually assumed to indicate an underlying equilibrium condition at the receptors. The increase in tone of the urinary bladder muscle produced by 5-MeF, a muscarinic receptor agonist which is not a substrate for cholinesterases, faded rapidly after a brief plateau. We have presumed that this is due to the bladder wall plasticity which allows this organ to accommodate increases in volume without change in intravesical pressure. In spite of this, the adoption of the fast, cumulative dosing regime and increasing the chart speed did allow the reliable definition of the concentration-effect curve for 5-MeF. This was possible because each pre-fade contraction apparently suppressed not only fade but also the development of spontaneous, irregular twitch contractions.

However, the problem remained as to whether the brief period following application of the agonist to the organ bath was sufficient for equilibrium to be achieved. In reality, this problem is no different from that faced with all assays in which the receptor events are deduced rather than measured directly (perhaps as in ligand binding studies), whether or not sustained responses are achieved. Ideally, during preincubation, the antagonist diffuses into the tissue and ultimately it comes into concentration equilibrium with the receptor. According to the Law of Mass Action, the antagonist, B, will occupy a specified fraction of the available receptors. When the agonist, A, is applied, it diffuses in and competes with B to occupy receptors. This means that the occupancy of B previously established during the pre-incubation period must decrease as occupancy by A increases. For the fast dosing regime to be considered useful, this new equilibrium must be attained rapidly. A necessary but not sufficient test for rapid equilibrium was performed by analysing the interaction between 5-MeF and the three previously well-characterized muscarinic receptor antagonists. If the system was at equilibrium then the pK_B estimates would agree with those previously found (Black & Shankley, 1985). The results with pirenzepine show not only that this method of characterizing agonist concentration-effect curves exposes its expected simple competitive behaviour but, also gives a satisfactory estimate of its pK_B at M_2- or M_3-receptors (6.76 ± 0.09).

The competitive analysis with 5-MeF and atropine was initially confounded by significant deviation from competitive behaviour at low atropine concentrations. However, following pretreatment with methylbutyrate, the alternative substrate for 'atropine esterase', atropine behaved as a simple competitive antagonist and the pK_B value estimated (8.99 ± 0.07) was similar to values previously obtained on other muscarinic receptor assays (Hulme *et al.*, 1990). Interestingly, in contrast to the results of the study by Kenakin & Beek (1987), in which 'atropine esterase' activity was observed in only 25% of rabbit ileum preparations, the deviation from simple competitive behaviour was seen in all preparations in the present study. However, wide variation in the distribution and activity of the enzyme has been previously recognized (see Kenakin & Beek, 1987).

The deviation from simple competitive behaviour with N-methylatropine, in contrast to atropine, was not corrected by incubation with an excess concentration of methylbutyrate suggesting that N-methylatropine is not a substrate for 'atropine esterase'. We have previously suggested that N-methylatropine might be a substrate for a quaternary ammonium uptake system (Black & Shankley, 1985). However, as in our previous study, using the lumen-perfused mouse stomach assay, the biochemically-defined uptake inhibitor (Ruifrok, 1982), taurocholate, and the potential alternative substrates, hexamethonium and choline, were ineffective. However, the ability to estimate $\log[A_{50}]$ values in the presence of high concentrations of N-methylatropine, seemingly when the uptake process was saturated, did allow a pK_B value (9.58 ± 0.07) to be estimated which agreed with values previously found (Black & Shankley, 1985).

Considered together, the results obtained from the three competitive analyses indicate that equilibrium conditions are achieved rapidly, that is, within the period between agonist dosing and the corresponding effect level measurement.

The finding that the deviation from competitive behaviour of N-methylatropine was corrected by pre-incubation with HC-3 was initially confused by the significantly lower pK_B indicated for N-methylatropine (Figure 3). However, this result could be accounted for by assuming that the effects of HC-3 were due to concomitant uptake blockade and competitive antagonism at muscarinic receptors. The data could be simulated by assuming a pK_B value of 4.20 for HC-3 (Figure 4). The independent experiments on both the guinea-pig trachea and mouse urinary bladder assays provided estimates, 4.12 ± 0.07 and $4.01 \pm \pm 0.07$, respectively, which were very close to this model prediction. The choline uptake blocking property of HC-3 has been claimed to be unique to neuronal sites (see Ivy & Townsel; 1987) suggesting the possibility that N-methylatropine, but not atropine, is taken up by cholinergic neurones. The pharmacological significance of this finding merits further investigation. Is the N-methylatropine captured by the nerve-endings also taken up by the terminal vesicles? Is N-methylatropine released along with ACh during nerve stimulation?

In conclusion, the mouse urinary bladder assay described is suitable for the quantitative analysis of muscarinic receptor interactions. In addition we postulate the existence of a previously undescribed uptake mechanism for quaternary muscarinic receptor antagonists.

We are grateful to Dr Pauline Martin (Whitby Research Inc.) for scientific discussion and Dr Robert Hull (James Black Foundation Ltd) for his criticism of this manuscript. This study was partially funded by the Mayo Foundation, Rochester, Minnesota, U.S.A. (to P.A.C.D.) and the James Black Foundation, Dulwich, London.

References

BLACK, J.W. (1989). Drugs from emasculated hormones: The principle of syntopic antagonism. *Science*, **245**, 486–493.

BLACK, J.W., LEFF, P. & SHANKLEY, N.P. (1985). Further analysis of anomalous pK_B values for histamine H2-receptor antagonists on the isolated mouse stomach assay. *Br. J. Pharmacol.*, **86**, 581–587.

BLACK, J.W. & SHANKLEY, N.P. (1985). Pharmacological analysis of muscarinic receptors coupled to oxyntic cell secretion in the mouse stomach. *Br. J. Pharmacol.*, **86**, 601–607.

BLACK, J.W., GERSKOWITCH, V.P., LEFF, P. & SHANKLEY, N.P. (1986). Analysis of competitive antagonism when this property occurs as part of a pharmacological resultant. *Br. J. Pharmacol.*, **89**, 547–555.

EDVARDSEN, P. & SETEKLEIV, J. (1968). Distribution of adrenergic receptors in the urinary bladder of cats, rabbits and guinea-pigs. *Acta Pharmacol. Toxicol.*, **26**, 437–445.

EMMERSON, J. & MACKAY, D. (1979). The zig-zag tracheal strip. *J.*

Pharm. Pharmacol., **31**, 798.

HOLT, S.E., COOPER, M. & WYLLIE, J.H. (1985). Evidence for purinergic transmission in mouse urinary bladder and for modulation of responses to electrical stimulation by 5-hydroxytryptamine. *Eur. J. Pharmacol.*, **116**, 105–111.

HOLT, S.E., COOPER, M. & WYLLIE, J.H. (1986). On the nature of the receptor mediating the action of 5-hydroxytryptamine in potentiating responses of the mouse urinary bladder strip to electrical stimulation. *Naunyn Schmiedebergs Arch. Pharmacol.*, **334**, 333–340.

HULME, E.C., BIRDSALL, N.J.M. & BUCKLEY, N.J. (1990). Muscarinic receptor subtypes. *Annu. Rev. Pharmacol. Toxicol.*, **30**, 633–673.

IVY, M.T. & TOWNSEL, J.G. (1987). A comparative study of high affinity choline uptake and choline utilization in cholinergic and non-cholinergic tissues. *Comp. Biochem. Physiol.*, **86**, 111–120.

KENAKIN, T.P. & BEEK, D. (1987). The effects on Schild regressions of antagonist removal from the receptor compartment by a saturable process. *Naunyn Schmiedebergs Arch. Pharmacol.*, **335**, 103–108.

LEVIN, R.M., SHOFER, F.S. & WEIN A.J. (1980). Cholinergic, adrenergic and purinergic responses of sequential strips of rabbit urinary bladder. *J. Pharmacol. Exp. Ther.*, **212**, 536–540.

McGUIRE, E.J. (1986). Neuromuscular dysfunction of the lower urinary tract. Chapter 11 (pp. 616–638). In *Campbell's Urology*, Fifth edition. London: W.B. Saunders & Co.

RUIFROK, P.G. (1982). Uptake of quaternary ammonium compounds into rat liver plasma membrane vesicles. *Biochem. Pharmacol.*, **31**, 1431–1435.

SANTICIOLI, P., MAGGI, C.A. & MELI, A. (1986). The postganglionic excitatory innervation of the mouse urinary bladder and its modulation by prejunctional $GABA_B$-receptors. *J. Auton. Pharmacol.*, **6**, 53–66.

SHANKLEY, N.P., BLACK, J.W., GANELLIN, C.R. & MITCHELL, R.C. (1988). Correlation between log P_{OCT/H_2O} and pK_B estimates for a series of muscarinic and histamine H_2-receptor antagonists. *Br. J. Pharmacol.*, **94**, 264–274.

SHANKLEY, N.P. (1985). Pharmacological analysis of the regulators of gastric acid secretion. *Ph.D. thesis. University of London.*

SIBLEY, G.N.A. (1984). A comparison of spontaneous and nerve-mediated activity in bladder muscle from man, pig and rabbit. *J. Physiol.*, **354**, 431–443.

TAIRA, N. (1972). The autonomic pharmacology of the bladder. *Annu. Rev. Pharmacol.*, **12**, 197–208.

(Received April 26, 1991
Revised May 24, 1991
Accepted May 31, 1991)

Br. J. Pharmacol. (1991), **104**, 151–158

Factors affecting the regional haemodynamic responses to glyceryl trinitrate and molsidomine in conscious rats

K. Phillips, [1]S.M. Gardiner, P.A. Kemp & T. Bennett

Department of Physiology and Pharmacology, University of Nottingham Medical School, Queen's Medical Centre, Nottingham NG7 2UH

1 A series of experiments was performed in conscious, unrestrained, male, Long Evans rats, chronically instrumented for the measurement of regional haemodynamics.

2 Infusion of glyceryl trinitrate (GTN, 0.1 mg kg^{-1} min^{-1}, i.v.) for 10 min elicited tachycardia, but no sustained change in mean arterial blood pressure. Renal haemodynamics were unaffected, but there were reductions in hindquarters flow and vascular conductance together with substantial increases in flow and conductance in the mesenteric vascular bed.

3 In the presence of captopril (2 mg kg^{-1} bolus, and 1 mg kg^{-1} h^{-1} infusion, i.v.) GTN elicited significant hypotension and increases in renal blood flow and vascular conductance, indicating that activation of the renin-angiotension system opposed the dilator effects of GTN in this vascular bed. However, the mesenteric and hindquarters haemodynamic effects of GTN were not affected by captopril. In contrast, in the presence of enalaprilat (2 mg kg^{-1} bolus, and 1 mg kg^{-1} h^{-1} infusion, i.v.) there was significant enhancement of the mesenteric, as well as renal, haemodynamic effects of GTN. Hence, these results provide no evidence for the sulphydryl groups in captopril exerting a specific effect to enhance the haemodynamic actions of GTN in our experimental protocols.

4 Administration of molsidomine alone (1 mg kg^{-1}, i.v. bolus) elicited tachycardia and hypotension; there were no changes in mesenteric or hindquarters haemodynamics, but renal flow and vascular conductance fell. Thus, the hypotensive effect of molsidomine was probably due to a reduction in cardiac output, consequent upon venodilatation.

5 In the presence of captopril or enalaprilat, molsidomine evoked renal and mesenteric vasodilatations in association with hypotension, indicating that activation of the renin-angiotensin system contributed to the lack of vasodilator responses to administration of molsidomine alone. However, since the effects of enalaprilat were more marked than those of captopril (in spite of the dose of both drugs being supramaximal for inhibition of angiotensin-converting enzyme), other factors must have been involved.

6 In a separate experiment, pretreatment with the nitric oxide synthesis inhibitor, N^G-nitro-L-arginine methyl ester (1 mg kg^{-1} h^{-1}, i.v.), enhanced the mesenteric vasodilator effect of molsidomine. Collectively, these results are consistent with *in vitro* data showing that endogenous nitric oxide can inhibit the vasodilator effects of nitric oxide derived from molsidomine, and that the sulphydryl groups of captopril can protect endogenous nitric oxide from inactivation by oxygen-derived free radicals, thereby enhancing the inhibitory effect of endogenous nitric oxide on the vasodilator responses to exogenous nitric oxide derived from molsidomine (or GTN).

Keywords: Glyceryl trinitrate; molsidomine; haemodynamics; conscious rats; N^G-nitro-L-arginine methyl ester

Introduction

The demonstration that the major endothelium-derived relaxing factor is nitric oxide, synthesized from L-arginine (Palmer *et al.*, 1987; 1988), has not only opened up new areas of research (Moncada & Higgs, 1990), but has also put into context what was known already about the pharmacology of nitrovasodilators (Ignarro, 1989). Thus, the latter compounds exert their effects by virtue of releasing nitric oxide and, as with nitric oxide derived from L-arginine, the final common pathway for vasorelaxation is, probably, interaction between nitric oxide and the haem moiety of soluble guanylate cyclase, causing activation of the enzyme and hence increased production of guanosine 3′ : 5′-cyclic monophosphate (cyclic GMP) (Moncada *et al.*, 1988; Ignarro, 1989). The latter, by some means, causes reduction of free cytosolic levels of Ca^{2+} and, thereby, inhibition of the contractile process (see Kukovetz & Holzmann, 1990).

Although endogenous nitric oxide and organic nitrates have a common mode of action, some of the latter group of compounds are distinguished by the fact that tolerance to their effects develops, both *in vivo* and *in vitro* (see Katz, 1990, for review). While it is likely that the development of tolerance *in vivo* may partly be due to activation of counter-regulatory mechanisms, such as the renin-angiotensin system (RAS) (Katz, 1990), there is evidence that changes in the biochemical factors involved in the production of nitric oxide from some organic nitrates may also contribute to the development of tolerance (Ignarro, 1989; Katz, 1990). Thus, depletion of tissue sulphydryl groups retards the production of the unstable intermediate compounds through which nitric oxide is generated from some organic nitrates (Ignarro, 1989). Consistent with this proposal, supplementation with sources of sulphydryl groups has been shown to suppress tolerance to glyceryl trinitrate (GTN), for example (see Katz, 1990; Newman *et al.*, 1990). However, it should be noted that other studies have not confirmed these results (Gruetter & Lemke, 1983; Stewart *et al.*, 1988; Hogan *et al.*, 1989). Nonetheless, sulphydryl depletion as an explanation for organic nitrate tolerance has led to the proposal that sulphydryl-containing angiotensin-converting enzyme (ACE) inhibitors might be particularly useful in conjunction with organic nitrates, since they could combat both the biochemical and physiological bases of tolerance (Katz, 1990). Although *in vitro* studies (van Gilst *et al.*, 1987) have indicated that a sulphydryl-containing ACE inhibitor, but not a non-sulphydryl ACE inhibitor, prevents organic nitrate tolerance in the perfused coronary vascular bed of the rat, there have been no *in vivo* haemodynamic studies of this

[1] Author for correspondence.

phenomenon. Therefore, the first objective of the present work was to assess the regional haemodynamic effects of GTN in the absence and in the presence of captopril (a sulphydryl-containing ACE inhibitor) or enalaprilat (a non-sulphydryl ACE inhibitor).

The phenomenon of tolerance is not so apparent with compounds that produce nitric oxide spontaneously (Ignarro, 1989; Kukovetz & Holzman, 1990). Molsidomine is a drug which, following metabolic activation in the liver (Wilson *et al.*, 1986), produces nitric oxide by spontaneous decomposition (Noack & Feelish, 1989; Bohn & Schönafinger, 1989; Feelish *et al.*, 1989). Hence, comparison of the *in vivo* haemodynamic effects of molsidomine in the absence and presence of captopril or enalaprilat should allow delineation of the contribution of the RAS to the responses seen, and also the identification of any putative differences between the two ACE inhibitors under these circumstances. Therefore, this was the second objective of the present work.

There is evidence that the effects of exogenous nitric oxide derived from GTN (Moncada *et al.*, 1991) or from molsidomine (Lüscher *et al.*, 1989; Busse *et al.*, 1989; Flavahan & Vanhoutte, 1989) might be inhibited by endogenous nitric oxide, although the details of this phenomenon are not clear. Therefore, the third objective of the present work was to quantify the *in vivo* haemodynamic effects of GTN and of molsidomine in the absence and in the presence of N^G-nitro-L-arginine methyl ester (L-NAME; Moore *et al.*, 1990; Rees *et al.*, 1990), a potent inhibitor of the endogenous production of nitric oxide.

Methods

Male, Long Evans rats (350–450 g) were anaesthetized (sodium methohexitone, 60 mg kg^{-1}, i.p.) and had miniaturized, pulsed Doppler probes (Haywood *et al.*, 1981) implanted to monitor renal, mesenteric and hindquarters blood flows (Gardiner *et al.*, 1990a). Animals were given ampicillin (7 mg kg^{-1}, i.m.; Penbritin, Beechams) and left in their home cages for at least 7 days, by which time they were eating, drinking and behaving normally. Then, under brief anaesthesia (sodium methohexitone, 40 mg kg^{-1}, i.p.) an intra-arterial catheter (distal abdominal aorta via ventral caudal artery) and 3 intravenous catheters (right jugular vein) were implanted; the latter arrangement allowed separate catheters to be used for administration of GTN and molsidomine. The catheters were led subcutaneously to emerge at the back of the neck with the probe wires. The latter were soldered into a microconnector that was clamped into a harness fitted to the rat. A flexible spring was connected to the harness and the catheters ran through the spring which was supported by a counterbalanced lever. This arrangement allowed the animal free movement and permitted experiments to be carried out without disturbance (Gardiner *et al.*, 1990a). Animals were left in their home cages overnight before measurements were begun; the following experiments were then performed.

Experiment 1: Effects of glyceryl trinitrate in the absence and presence of captopril

Animals ($n = 8$) were given GTN by i.v. infusion (0.1 mg kg^{-1} min^{-1}, in a volume of 33 μl min^{-1}) over 10 min, since pilot experiments had shown this procedure produced clear-cut increases in mesenteric blood flow (see also Gardiner *et al.*, 1990b). At least 1 h after administration of GTN, a primed infusion of captopril (2 mg kg^{-1} bolus in 0.1 ml, 1 mg kg^{-1} h^{-1} at 0.3 ml h^{-1}; Muller *et al.*, 1990) was begun and, starting 1 h later, the GTN infusion was repeated.

Experiment 2: Effects of glyceryl trinitrate in the absence and presence of enalaprilat

In a separate group ($n = 8$) of rats, the above protocol was repeated except that enalaprilat was given instead of captopril, using the same dose regime.

Experiment 3: Effects of glyceryl trinitrate in the absence and presence of N^G-nitro-L-arginine methyl ester

A group of rats ($n = 8$), randomly selected from the 2 groups above, were re-challenged with GTN (dose as in experiment 1) at least 48 h after their previous exposure. After a delay of 1 h, an infusion of L-NAME (1 mg kg^{-1} h^{-1}, at 0.3 ml h^{-1}; Gardiner *et al.*, 1991) was begun, and 1 h later the animals were re-challenged with GTN.

Experiment 4: Effects of molsidomine in the absence and presence of captopril

The animals in this experiment were the same as those used in experiment 1 with each animal being randomized to receive molsidomine or GTN first, but in the same order in the absence and presence of captopril. Molsidomine was given as a bolus dose of 1 mg kg^{-1} (in 0.1 ml), and since pilot experiments had shown its effects were persistent, at least 2 h were allowed before any subsequent intervention was carried out. The protocol described in experiment 1 was followed.

Experiment 5: Effects of molsidomine in the absence and presence of enalaprilat

The animals in this experiment were those used in experiment 2, with random allocation to receive molsidomine or GTN first in the absence and presence of enalaprilat, at the dose used in experiment 2.

Experiment 6: Effects of molsidomine in the absence and presence of N^G-nitro-L-arginine methyl ester

The animals in this experiment were those studied in experiment 3, with random allocation to receive molsidomine or GTN first in the absence and presence of L-NAME (dose as in experiment 3).

Data analysis

Continuous recordings were made of phasic and mean systemic arterial blood pressure (MAP), instantaneous heart rate and mean renal, mesenteric and hindquarters Doppler shift signals; regional vascular conductances were calculated as (mean Doppler shift/MAP). Since all animals acted as their own controls, analysis was carried out on the raw data rather than percentage changes (Gardiner *et al.*, 1990a,b; 1991). Changes relative to baseline were assessed by Friedman's test (Theodorsson-Norheim, 1987). Comparisons between responses in the presence and absence of ACE inhibitors or L-NAME were carried out by use of Wilcoxon's ranks sums test applied to areas under or over curves. Wilcoxon's test was used also to compare baseline values in the same group of animals under different conditions; a P value <0.05 was taken as significant.

Drugs

Molsidomine (Sigma), captopril (Squibb, U.S.A.), enalaprilat (MSD, U.S.A.), and L-NAME hydrochloride (Sigma) were dissolved in isotonic NaCl (157 mmol l^{-1}). The pH of the captopril and enalaprilat solutions was adjusted to 7.0–7.4 with NaOH. GTN (Tridil, DuPont, U.S.A. provided as a 5 mg ml^{-1} stock solution) was diluted in isotonic NaCl.

Results

Vehicle administration had no consistent haemodynamic effects.

Experiment 1: Effects of glyceryl trinitrate in the absence and presence of captopril

Infusion of GTN alone produced tachycardia throughout the infusion period, and during the 5 min following infusion (Figure 1). However, there was no sustained reduction in MAP (Figure 1), although pulse pressure fell, and there was a very transient initial hypotension in most animals (data not shown). Renal blood flow and vascular conductance were unaffected by GTN, whereas hindquarters blood flow and vascular conductance showed significant reductions (Figure 1). In contrast, there were significant increases in mesenteric blood flow and vascular conductance (Figure 1).

Administration of captopril caused initial tachycardia, hypotension and increases in flow and conductance in the renal, mesenteric and hindquarters vascular beds. However, at the time of administration of GTN, only the renal blood flow and vascular conductance were increased relative to the resting values in the absence of captopril (Figure 1).

In the presence of captopril, GTN caused a slight, but significant, fall in MAP (AOC, 92 ± 24 units) and this effect was significantly different from the response to GTN in the absence of captopril (AOC, 31 ± 7 units) (Figure 1). In spite of this difference, the tachycardic response to GTN in the presence of captopril was not significantly different from the response to GTN alone (Figure 1). There was an increase in renal flow and vascular conductance in response to GTN in the presence of captopril (AUC, 17 ± 5 and 28 ± 7 units, respectively), and these effects were significantly different from the response to GTN alone (AUC, 7 ± 3 and 6 ± 3 units for renal flow and conductance, respectively) (Figure 1). However, the mesenteric and hindquarters haemodynamic responses to GTN were not different in the presence and absence of captopril (Figure 1).

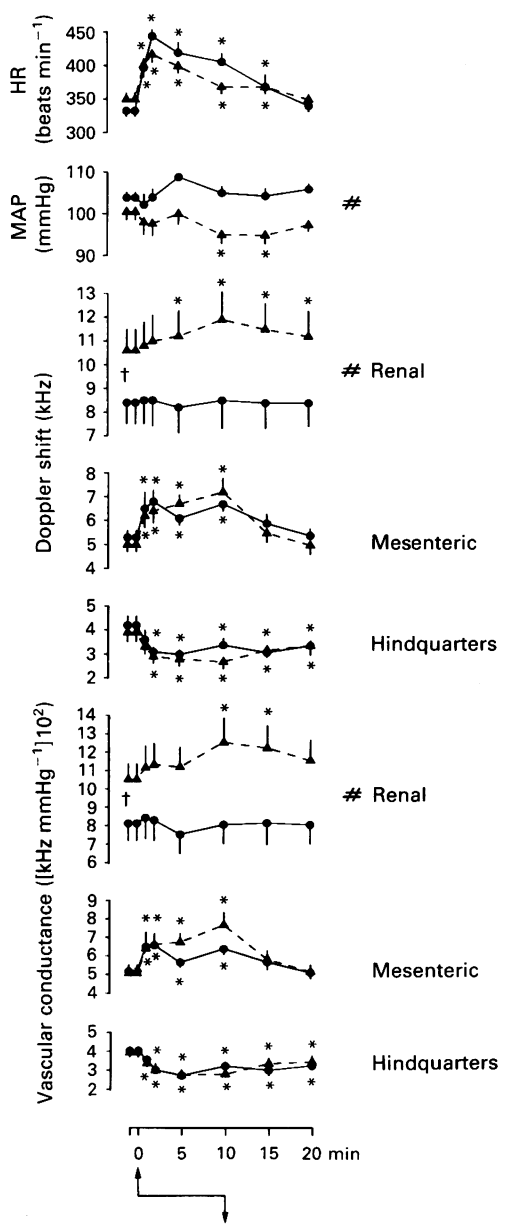

Figure 1 Cardiovascular responses to a 10 min infusion of glyceryl trinitrate at 0.1 mg kg^{-1} min^{-1} (between the arrows) in the same group (n = 8) of conscious, Long Evans rats in the absence (●) or in the presence (▲) of captopril (2 mg kg^{-1} bolus, and 1 mg kg^{-1} min^{-1}, infusion). Values are mean and bars show s.e.mean; where bars are missing they lie within the symbols. *P < 0.05 versus baseline; †P < 0.05 between resting values in the absence and presence of captopril; #P < 0.05 between responses in the absence and presence of captopril, based on areas under or over curves. MAP = mean systemic arterial blood pressure; HR = heart rate.

Experiment 2: Effects of glyceryl trinitrate in the absence and presence of enalaprilat

The responses to GTN alone were qualitatively similar to those in the group of animals in experiment 1 (Figure 2).

Administration of enalaprilat caused initial tachycardia, hypotension and increases in flow and vascular conductance in renal, mesenteric and hindquarters vascular beds. However, at the time GTN was administered, only the renal vascular bed showed increases in flow and conductance, but there was an increased mesenteric vascular conductance, in association with tachycardia and a reduction in MAP (Figure 2).

In the presence of enalaprilat, GTN caused tachycardia and a modest fall in MAP (AOC, 102 ± 26 units), but only the latter effect was different from the response to GTN alone (AOC, 43 ± 13 units) (Figure 2). There were increases in flow and vascular conductance in response to GTN in the renal and mesenteric vascular beds in the presence of enalaprilat (AUC, renal flow 21 ± 5 units; renal conductance 31 ± 8 units; mesenteric flow 50 ± 8 units; mesenteric conductance 65 ± 11 units), and all were greater than those to GTN alone (AUC, renal flow 10 ± 4 units; renal conductance 8 ± 3 units; mesenteric flow 40 ± 6 units; mesenteric conductance 37 ± 6 units) (Figure 2). Furthermore, the enhancement of the mesenteric responses to GTN was greater in the presence of enalaprilat than of captopril (AUC, mesenteric flow 26 ± 6 units; mesenteric conductance 31 ± 7 units) (Figures 1 and 2). Hindquarters haemodynamic changes following GTN were not significantly affected by enalaprilat (Figure 2).

Experiment 3: Effects of glyceryl trinitrate in the absence and presence of N^G-nitro-L-arginine methyl ester

The responses to GTN alone were as described above, although the changes in hindquarters haemodynamics were not significant in this experiment (Figure 3).

L-NAME caused bradycardia and an increase in MAP, accompanied by mesenteric and hindquarters vasoconstriction (Figure 3). Although the changes in heart rate and MAP in response to GTN in the presence of L-NAME were not significantly different from those in response to GTN alone, there was a significant hypotensive response to GTN in the presence of L-NAME (Figure 3). The renal, the mesenteric and the hindquarters responses to GTN in the absence and presence of L-NAME were not significantly different (Figure 3).

Experiment 4: Effects of molsidomine in the absence and presence of captopril

Injection of molsidomine alone caused tachycardia associated with a fall in MAP (Figure 4). Renal blood flow and vascular conductance were decreased but mesenteric and hindquarters haemodynamics were unchanged (Figure 4).

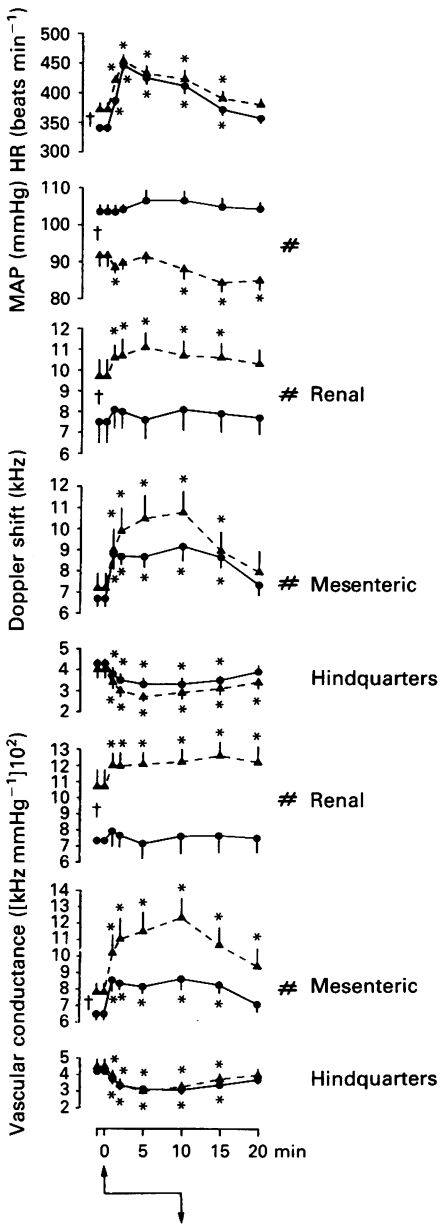

Figure 2 Cardiovascular responses to a 10 min infusion of glyceryl trinitrate at 0.1 mg kg^{-1} min^{-1} (between the arrows) in the same group (n = 8) of conscious, Long Evans rats in the absence (●) or in the presence (▲) of enalaprilat (2 mg kg^{-1} bolus, and 1 mg kg^{-1} min^{-1}, infusion). Values are mean and bars show s.e.mean; where bars are missing they lie within the symbols. *P < 0.05 versus baseline; †P < 0.05 between resting values in the absence and presence of enalaprilat; #P < 0.05 between responses in the absence and presence of enalaprilat, based on areas under or over curves. MAP = mean systemic arterial blood pressure; HR = heart rate.

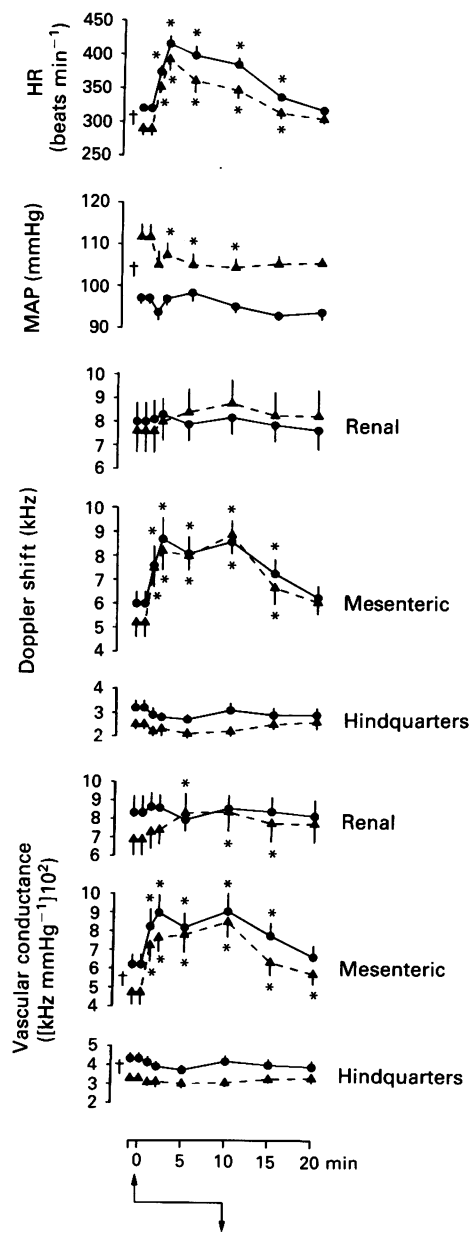

Figure 3 Cardiovascular responses to a 10 min infusion of glyceryl trinitrate at 0.1 mg kg^{-1} min^{-1} (between the arrows) in the same group (n = 8) of conscious, Long Evans rats in the absence (●) or in the presence (▲) of N^{G}-nitro-L-arginine methyl ester (L-NAME) (1 mg kg^{-1} min^{-1}, infusion). Values are mean and bars show s.e.mean; where bars are missing they lie within the symbols. *P < 0.05 versus baseline; †P < 0.05 between resting values in the absence and presence of L-NAME. MAP = mean systemic arterial blood pressure; HR = heart rate.

The animals in this experiment were those in experiment 1, hence, the effects of captopril were qualitatively similar to those described under experiment 1.

In the presence of captopril, the changes in heart rate and MAP in response to molsidomine were not different from those seen in response to molsidomine alone. However, there were increases in flow and vascular conductance in the mesenteric vascular bed (AUC, 33 ± 6 and 66 ± 8 units, respectively) and an increase in renal vascular conductance (AUC, 50 ± 17 units) that were significantly different from the changes evoked by molsidomine alone (AUC, mesenteric flow 3 ± 1 units; mesenteric conductance 17 ± 6 units; renal conductance 2 ± 1 units) (Figure 4). In contrast, even in the presence of captopril, molsidomine had no effect on hindquarters haemodynamics (Figure 4).

Experiment 5: Effects of molsidomine in the absence and presence of enalaprilat

The responses to molsidomine alone in this group of rats were qualitatively similar to those studied in experiment 4 (Figure 5).

The animals in this experiment were those in experiment 2, hence, the effects of enalaprilat were qualitatively similar to those described under experiment 2.

In the presence of enalaprilat, the hypotensive effect of molsidomine was clearly enhanced (molsidomine alone AOC, 426 ± 65 units; molsidomine in the presence of enalaprilat AOC, 1046 ± 154 units), although its tachycardic effect was unchanged (Figure 5). While renal blood flow fell (AOC, 49 ± 18 units), this change was less than that in response to molsidomine alone (AOC, 124 ± 24 units) (Figure 5), and in

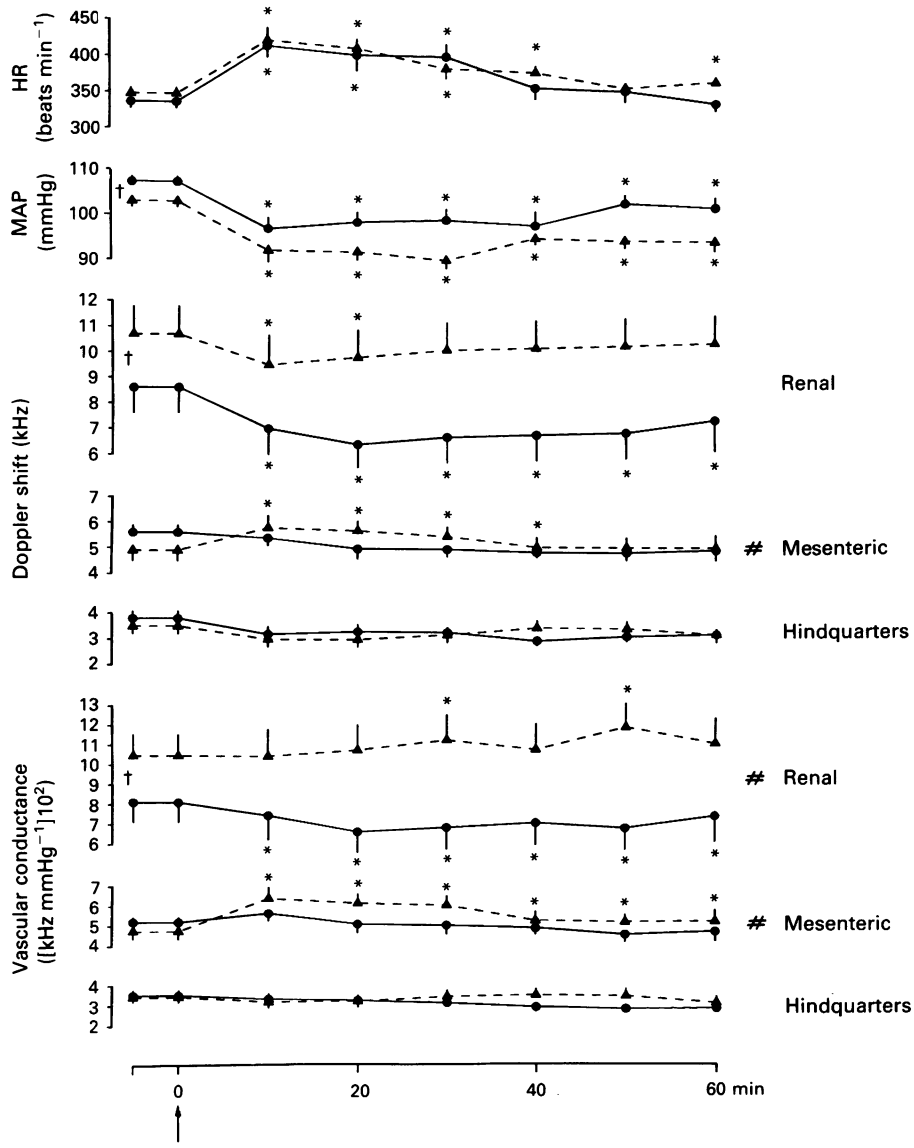

Figure 4 Cardiovascular responses to molsidomine (0.1 mg kg^{-1} bolus at arrow) in the same group (n = 8) of conscious, Long Evans rats in the absence (●) or in the presence (▲) of captopril (2 mg kg^{-1} bolus, and 1 mg kg^{-1} min^{-1}, infusion). Values are mean and bars show s.e.mean; where bars are missing they lie within the symbols. *P < 0.05 versus baseline; †P < 0.05 between resting values in the absence and presence of captopril; #P < 0.05 between responses in the absence and presence of captopril, based on areas under or over curves. MAP = mean systemic arterial blood pressure; HR = heart rate.

the presence of enalaprilat there was a renal vasodilatation in response to molsidomine (AUC, 100 ± 15 units), rather than a vasconstriction as seen with molsidomine alone (AOC, 96 ± 19 units) (Figure 5). Likewise, enalaprilat unmasked substantial increases in flow and vascular conductance in response to molsidomine in the mesenteric vascular bed (AUC, flow 62 ± 17 units; conductance 177 ± 35 units), and this effect was greater (P < 0.05) than that in the presence of captopril. As in captopril-treated rats, molsidomine had no effects on hindquarters haemodynamics in the presence of enalaprilat (Figure 5).

Experiment 6: Effects of molsidomine in the absence and presence of N^G-nitro-L-arginine methyl ester

The qualitative effects of molsidomine alone were as described above (Figure 6). The animals in this experiment were those in experiment 3, hence, the effects of L-NAME were as described under experiment 3.

In the presence of L-NAME the hypotensive effect of molsidomine was unchanged, although there was a slight enhancement of its tachycardic action (AUC, molsidomine alone 2988 ± 357 units; molsidomine + L-NAME 4481 ± 537 units) and renal vasconstrictor effects (AOC, molsidomine alone 66 ± 21 units; molsidomine + L-NAME 114 ± 27 units) (Figure 6). In contrast, there were increases in mesenteric blood flow and vascular conductance in response to molsidomine in the presence of L-NAME (AUC, flow 51 ± 15 units; conductance 69 ± 15 units), and these were significantly different from the changes in the absence of L-NAME (AUC, flow 19 ± 9 units; conductance 45 ± 8 units) (Figure 6). Molsidomine had no effects on hindquarters haemodynamics in the presence of L-NAME (Figure 6).

Discussion

The present work had three main objectives that can be restated in the form of the following questions:

Are the regional haemodynamic effects of GTN enhanced more by captopril (a sulphydryl-containing ACE-inhibitor) than by enalaprilat (an ACE-inhibitor lacking a sulphydryl group)? The answer to this question is no, at least under the

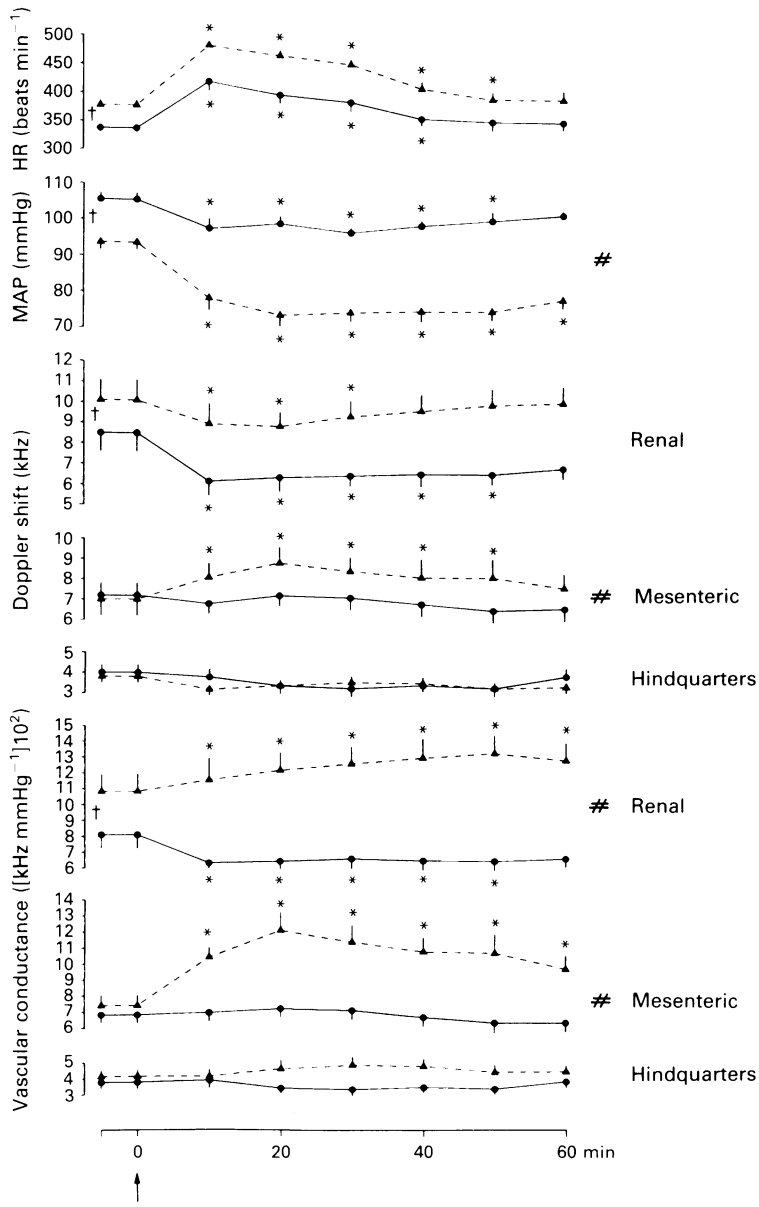

Figure 5 Cardiovascular responses to molsidomine (0.1 mg kg^{-1} bolus at arrow) in the same group (n = 8) of conscious, Long Evans rats in the absence (●) or in the presence (▲) of enalaprilat (2 mg kg^{-1} bolus and 1 mg kg^{-1} min^{-1}, infusion). Values are mean and bars show s.e.mean; where bars are missing they lie within the symbols. *$P < 0.05$ versus baseline; †$P < 0.05$ between resting values in the absence and presence of enalaprilat; #$P < 0.05$ between responses in the absence and presence of enalaprilat, based on areas under or over curves. MAP = mean systemic arterial blood pressure; HR = heart rate.

conditions of our experiment. While it could be argued that the exposure to GTN was too short to elicit tolerance, it is clear from the results of Stewart *et al.* (1988) that within 1 min of the onset of GTN infusion functional tolerance can develop. Moreover, it was apparent from the present results that both captopril and enalaprilat unmasked a renal vasodilator response to GTN, indicating that a component of 'tolerance' attributable to GTN-induced activation of the RAS was present. However, it was notable that, although there was a tendency for GTN to cause an enhanced mesenteric vasodilatation in the presence of captopril, this effect was not significant, whereas enalaprilat caused a clear augmentation of the mesenteric haemodynamic effects of GTN. Since both ACE inhibitors were given in doses that were supra-maximal for their effects on the RAS (Muller *et al.*, 1990) then a factor other than ACE inhibition must have been responsible for the difference between their effects on the mesenteric responses to GTN. There is some *in vitro* evidence for endogenous nitric oxide inhibiting responses to nitric oxide derived from GTN (Moncada *et al.*, 1991). If the sulphydryl groups of captopril act as selective scavengers of oxygen-derived free radicals (McMurray & Chopra, 1991) that inactivate nitric oxide (see Ignarro, 1989), then in the presence of captopril there could have been a greater inhibition by endogenous nitric oxide of the vasodilator response to nitric oxide derived from GTN. However, enalaprilat, lacking sulphydryl groups, and thus not acting to preserve endogenous nitric oxide, would not augment the inhibitory effects on the responses to nitric oxide derived from GTN. Inhibition of ACE with enalaprilat could thus remove the counter-regulatory vasconstrictor effects of the RAS and reveal a greater component of GTN-induced vasodilatation than seen in the presence of captopril. However, it is not clear why such an effect should not be apparent in the renal vascular bed.

As suggested elsewhere (Kiff *et al.*, 1991), the marked mesenteric vasodilator response to GTN in the absence of a hindquarters vasodilatation could have been due to differential biotransformation (Kawamoto *et al.*, 1990) of GTN to nitric oxide in the two vascular beds. However, the finding that neither captopril nor enalaprilat revealed a hindquarters vaso-

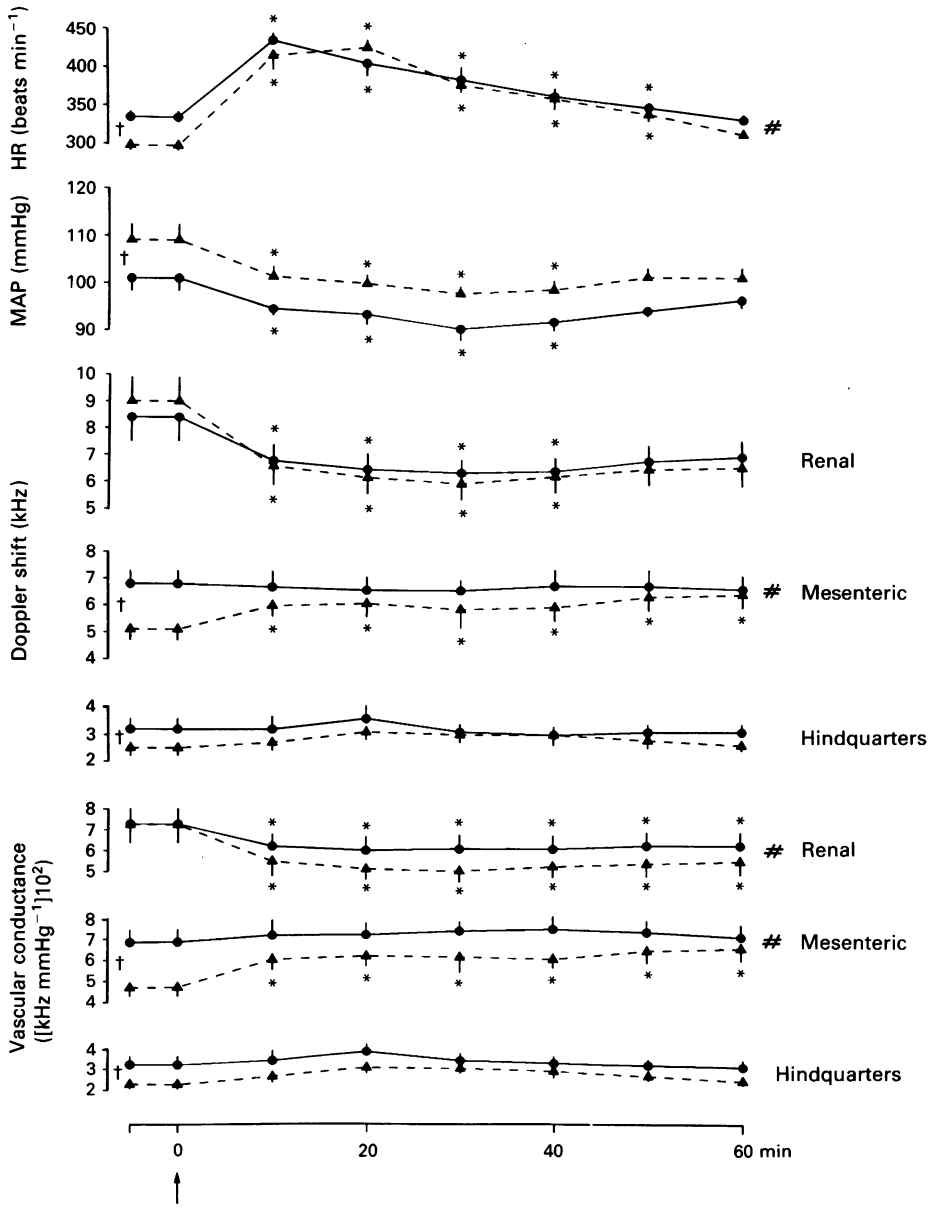

Figure 6 Cardiovascular responses to molsidomine (0.1 mg kg^{-1} bolus at arrow) in the same group (n = 8) of conscious, Long Evans rats in the absence (●) or in the presence (▲) of N^{G}-nitro-L-arginine methyl ester (L-NAME) (1 mg kg^{-1} min^{-1}, infusion). Values are mean and bars show s.e.mean; where bars are missing they lie within the symbols. *P < 0.05 versus baseline; †P < 0.05 between resting values in the absence and presence of L-NAME; #P < 0.05 between responses in the absence and presence of L-NAME, based on areas under or over curves. MAP = mean systemic arterial blood pressure; HR = heart rate.

dilator response to GTN indicates that the sulphydryl groups of captopril were not sufficient to promote a vasodilator effect of GTN in that vascular bed, and hence deficiency of sulphydryl groups may not have been the reason for the lack of a vasodilator response. Since the mesenteric vascular bed showed a substantial and maintained mesenteric vasodilator response to GTN it would be worthwhile in future experiments to determine if prolonged infusions of, or repeated dosing with, GTN produce tolerance in that vascular bed and, if so, whether or not captopril is more effective than enalaprilat in suppressing such tolerance.

What are the regional haemodynamic effects of molsidomine, and are they differentially affected by captopril or enalaprilat? Molsidomine caused hypotension and a tachycardia, presumably of reflex origin. It is notable that in the presence of molsidomine alone there were no changes in mesenteric or hindquarters haemodynamics, and there were reductions in renal blood flow and vascular conductance. Hence the hypotension was probably due to a fall in cardiac output, possibly resulting from venodilatation (Grund *et al.*, 1978). It is feasible that systemic generation of nitric oxide from molsidomine was responsible for this effect and consequent activation of counter-regulatory mechanisms over-rode any molsidomine-induced reductions in vascular conductances. The difference between GTN and molsidomine in this respect could have been due to local production of nitric oxide from GTN, especially in the mesenteric vascular bed, exerting a particularly potent effect at that site, compared to the less localized effects of nitric oxide generated spontaneously from molsidomine. However, it appears that molsidomine may be a more potent venodilator than GTN, as reported by Grund *et al.* (1978), since there was no indication that GTN caused a fall in cardiac output.

Captopril revealed renal and mesenteric vasodilator responses to molsidomine, consistent with activation of the RAS opposing its vasodilator effects, but enalaprilat had more marked effects than captopril on the mesenteric responses to molsidomine, possibly for the reasons discussed above in connection with GTN.

Are the regional haemodynamic effects of GTN or molsidomine affected by N^G-nitro-L-arginine methyl ester? Although L-NAME had haemodynamic effects consistent with suppression of endothelial nitric oxide production (Gardiner *et al.*, 1990a), it did not have a significant influence on the responses to GTN. However, there was a mesenteric vasodilator response to molsidomine in the presence of L-NAME that was not seen in its absence. Thus, these results are consistent with removal of a negative interaction between endogenous nitric oxide and that derived from molsidomine; the apparent lack of interaction between endogenous nitric oxide and that derived from GTN could have been due to the relative doses of L-NAME and GTN used (Moncada *et al.*, 1991).

In conclusion, it is clear that the nitrovasodilators, GTN and molsidomine, have different regional haemodynamic effects in conscious rats, although both elicit functional activation of the RAS. However, pretreatment with enalaprilat causes greater augmentation of the responses to GTN and molsidomine than does captopril. Hence, these results do not show a selective ability of the sulphydryl groups of captopril to enhance responses to GTN or molsidomine. Rather, they are consistent with an augmented inhibition of the responses to exogenous nitric oxide (derived from GTN or molsidomine) in the presence of captopril, possibly due to the sulphydryl groups of the latter protecting endogenous nitric oxide from inactivation by oxygen-derived free radicals.

References

BOHN, H. & SCHÖNAFINGER, K. (1989). Oxygen and oxidation promote the release of nitric oxide from sydnonimines. *J. Cardiovasc. Pharmacol.*, **14**, Suppl. 11, S6–S12.

BUSSE, R., POHL, U., MÜLSCH, A. & BASSENGE, E. (1989). Modulation of the vasodilator action of SIN-1 by the endothelium. *J. Cardiovasc. Pharmacol.*, **14**, Suppl. 11, S81–S85.

FEELISCH, M., OSTROWSKI, J. & NOACK, E. (1989). On the mechanism of NO release from sydnonimines. *J. Cardiovasc. Pharmacol.*, **14**, Suppl. 11, S13–S22.

FLAVAHAN, N.A. & VANHOUTTE, P.M. (1989). Mechanisms underlying the inhibitory interaction between the nitrovasodilator SIN-1 and the endothelium. *J. Cardiovasc. Pharmacol.*, **14**, Suppl. 11, S86–S90.

GARDINER, S.M., COMPTON, A.M., KEMP, P.A. & BENNETT, T. (1990a). Regional and cardiac haemodynamic effects of N^G-nitro-L-arginine methyl ester in conscious, Long Evans rats. *Br. J. Pharmacol.*, **101**, 625–631.

GARDINER, S.M., COMPTON, A.M., KEMP, P.A. & BENNETT, T. (1990b). Regional and cardiac haemodynamic responses to glyceryl trinitrate, acetylcholine, bradykinin and endothelin-1 in conscious rats: effects of N^G-nitro-L-arginine methyl ester. *Br. J. Pharmacol.*, **101**, 632–639.

GARDINER, S.M., KEMP, P.A. & BENNETT, T. (1991). Effects of N^G-nitro-L-arginine methyl ester on vasodilator responses to infusions of acetylcholine, 5'-N-ethylcarboxamidoadenosine or salbutamol in conscious rats. *Br. J. Pharmacol.*, **103**, 1725–1732.

GRUETTER, C.A. & LEMKE, S.M. (1985). Dissociation of cysteine and glutathione levels from nitroglycerin-induced relaxation. *Eur. J. Pharmacol.*, **111**, 85–95.

GRUND, E., MÜLLER-RUCHHOLTZ, E.R., LAPP, E.R., LÖSCH, H.-M. & LOCHNER, W. (1978). Comparative study of nitroglycerin and molsidomine: effects on the integrated systemic venous bed and the arterial pressure in dogs. *Arzneim.-Forsch.*, **28**, 1624–1628.

HAYWOOD, J.R., SHAFFER, R., FASTENOW, C., FINK, G.D. & BRODY, M.J. (1981). Regional blood flow measurement with pulsed Doppler flowmeter in conscious rat. *Am. J. Physiol.*, **241**, H273–H278.

HOGAN, J.C., LEWIS, M.J. & HENDERSON, A.H. (1989). N-acetylcysteine fails to attenuate haemodynamic tolerance to glyceryl trinitrate in healthy volunteers. *Br. J. Clin. Pharmacol.*, **28**, 421–426.

IGNARRO, L.J. (1989). Biological actions and properties of endothelium-derived nitric oxide formed and released from artery and vein. *Circ. Res.*, **65**, 1–21.

KATZ, R.J. (1990). Mechanisms of nitrate tolerance: a review. *Cardiovasc. Drugs Ther.*, **4**, 247–252.

KAWAMOTO, J.H., MCLAUGHLIN, B.E., BRIEN, J.F., MARKS, G.S. & NAKATSU, K. (1990). Biotransformation of glyceryl trinitrate and elevation of cyclic GMP precede glyceryl trinitrate-induced vasodilation. *J. Cardiovasc. Pharmacol.*, **15**, 714–719.

KIFF, R.J., GARDINER, S.M., COMPTON, A.M. & BENNETT, T. (1991). Selective impairment of hindquarters vasodilator responses to bradykinin in conscious Wistar rats with streptozotocin-induced diabetes mellitus. *Br. J. Pharmacol.*, **103**, 1357–1362.

KUKOVETZ, W.R. & HOLZMANN, S. (1990). Mechanisms of nitrate-induced vasodilatation and tolerance. *Eur. J. Clin. Pharmacol.*, **38**, Suppl. 1, S9–S14.

LÜSCHER, T.F., RICHARD, V. & YANG, Z. (1989). Interaction between endothelium-derived nitric oxide and SIN-1 in human and porcine blood vessels. *J. Cardiovasc. Pharmacol.*, **14**, Suppl. 11, S76–S80.

McMURRAY, J. & CHOPRA, M. (1991). Influence of ACE inhibitors on free radicals and reperfusion injury: pharmacological curiosity or therapeutic hope? *Br. J. Clin. Pharmacol.*, **31**, 373–379.

MONCADA, S. & HIGGS, E.A. (1990). *Nitric Oxide from L-Arginine: A Bioregulatory System.* Amsterdam, Excerpta Medica.

MONCADA, S., PALMER, R.M.J. & HIGGS, A.E. (1988). The discovery of nitric oxide as the endogenous nitrovasodilator. *Hypertension*, **12**, 365–372.

MONCADA, S., REES, D.D., SCHULZ, R. & PALMER, R.M.J. (1991). Development and mechanism of a specific supersensitivity to nitrovasodilators after inhibition of vascular nitric oxide synthesis *in vivo*. *Proc. Natl. Acad. Sci. U.S.A.*, **88**, 2166–2170.

MOORE, P.K., AL-SWAYEH, O.A., CHONG, N.W.S., EVANS, R.A. & GIBSON, A. (1990). L-N^G-nitro arginine (L-NOARG), a novel, L-arginine-reversible inhibitor of endothelium-dependent vasodilatation *in vitro*. *Br. J. Pharmacol.*, **99**, 408–412.

MULLER, A.F., GARDINER, S.M., COMPTON, A.M. & BENNETT, T. (1990). Regional haemodynamic effects of captopril, enalaprilat and lisinopril in conscious water-replete and water-deprived Brattleboro rats. *Clin. Sci.*, **79**, 393–401.

NEWMAN, C.M., WARREN, J.B., TAYLOR, G.W., BOOBIS, A.R. & DAVIES, D.S. (1990). Rapid tolerance to the hypotensive effects of glyceryl trinitrate in the rat: prevention by N-acetyl-L-but not N-acetyl-D-cysteine. *Br. J. Pharmacol.*, **99**, 825–829.

NOACK, E. & FEELISCH, M. (1989). Molecular aspects underlying the vasodilator action of molsidomine. *J. Cardiovasc. Pharmacol.*, **14**, Suppl. 11, S1–S5.

PALMER, R.M.J., FERRIGE, A.G. & MONCADA, S. (1987). Nitric oxide release accounts for the biological activity of endothelium-derived relaxing factor. *Nature*, **327**, 524–526.

PALMER, R.M.J., ASHTON, D.S. & MONCADA, S. (1988). Vascular endothelial cells synthesize nitric oxide from L-arginine. *Nature*, **333**, 664–666.

REES, D.D., PALMER, R.M.J., SCHULZ, R., HODSON, H.F. & MONCADA, S. (1990). Characterization of three inhibitors of endothelial nitric oxide synthase *in vitro* and *in vivo*. *Br. J. Pharmacol.*, **101**, 746–752.

STEWART, D.J., MÜNZEL, T., HOLTZ, J. & BASSENGE, E. (1988). Discrepancy between initial and steady-state resistance vessel responsiveness to short-term nitroglycerin exposure in the hindlimb of conscious dogs. *J. Cardiovasc. Pharmacol.*, **12**, 144–151.

THEODORSSON-NORHEIM, E. (1987). Friedman and Quade tests: BASIC computer program to perform non-parametric two-way analysis of variance and multiple comparisons on ranks of several related samples. *Comput. Biol. Med.*, **17**, 85–99.

VAN GILST, W.H., DE GRAEFF, P.A., SCHOLTENS, E., DE LANGEN, C.D.J. & WESSELING, H. (1987). Potentiation of isosorbide dinitrate-induced coronary dilatation by captopril. *J. Cardiovasc. Pharmacol.*, **9**, 254–255.

WILSON, I. D., WATSON, K.V., TROKE, J., ILLING, H.P.A. & FROMSON, J.M. (1986). The metabolism of [^{14}C]N-ethoxycarbonyl-3-morpholinosydnonimine (molsidomine) in laboratory animals. *Xenobiotica*, **16**, 1117–1128.

(Received April 9, 1991
Revised May 23, 1991
Accepted June 17, 1991)

Br. J. Pharmacol. (1991), **104**, 159–165

Substance P modulates the time course of nicotinic but not muscarinic catecholamine secretion from perfused adrenal glands of rat

Xin-Fu Zhou, Philip D. Marley & [1]Bruce G. Livett

Department of Biochemistry, University of Melbourne, Parkville 3052, Vic. Australia

1 Substance P (SP) and acetylcholine (ACh) are contained within the splanchnic nerve terminals in the adrenal gland and can be released in response to stress. In the rat, the release of ACh brings about secretion of catecholamines (CA) by acting on nicotinic and muscarinic receptors on the adrenal chromaffin cells.

2 In the present study, we have used a rat isolated adrenal gland preparation to investigate the effects of SP, perfused at different concentrations, on CA secretion evoked by 10^{-5} M nicotine and 10^{-4} M muscarine.

3 In the first 10 min stimulation period (S1), in the absence of SP, nicotine (10^{-5} M) evoked substantial and equal secretion of noradrenaline (NA) and adrenaline (Ad). In a second 10 min stimulation period (S2), carried out 18 min after S1, the nicotinic response was desensitized. In contrast, the muscarinic response, which preferentially evoked Ad secretion in S1 (Ad/NA: 8.7/1), was well maintained in S2.

4 SP present in S1 had no effect on desensitization of the subsequent nicotinic response in S2.

5 At low concentrations (10^{-7}–10^{-10} M), SP changed the time course of nicotine-induced CA secretion during S1 by enhancing CA secretion in the first 4 min and inhibiting CA secretion thereafter. The maximal effect occurred at 10^{-9} M SP.

6 At a higher concentration (10^{-5} M), SP inhibited total nicotinic CA secretion throughout S1 and produced a biphasic secretion of CA (depressed in the presence of SP and enhanced after wash out of SP). Pre-exposure of adrenal glands to SP (10^{-9} to 10^{-5} M) for 10 min produced marked inhibition of the nicotine-induced CA secretion.

7 In contrast to the effect of SP on the nicotinic response, SP from 10^{-9} to 10^{-5} M had no effect on muscarinic CA secretion.

8 This difference in sensitivity of the nicotinic and muscarinic responses to SP points to a diversity of mechanisms available for control of adrenal catecholamine secretion. In addition to the ability of SP to increase or decrease the total amount of adrenal CA secretion, dependent on the concentration of SP, the present study shows that SP can change the time-course of nicotinic CA secretion. These results with the rat adrenal gland perfused *in vitro* suggests both a quantitative and temporal role for SP as a novel modulator of adrenal CA secretion.

Keywords: Substance P; adrenal medulla; noradrenaline; adrenaline; nicotine; catecholamine; muscarine; neuromodulation

Introduction

Catecholamine (CA) secretion from the adrenal gland is mediated by acetylcholine (ACh) released from splanchnic nerve terminals innervating the adrenal medulla (Feldberg *et al.*, 1934). In most mammals, ACh activates both nicotinic and muscarinic receptors to evoke secretion (Feldberg *et al.*, 1934; Douglas & Poisner, 1965; Critchley *et al.*, 1986; for review see Livett, 1987). In recent years, substantial evidence has accumulated indicating that, in addition to the classical neurotransmitter ACh, a large number of endogeneous neuropeptides are involved in the regulation of CA secretion either as neurotransmitters or as neuromodulators (for review, see Marley & Livett, 1985; Livett, 1987).

Substance P (SP)-like immunoreactivity has been identified in nerve terminals innervating the adrenal medulla of man (Linnoila *et al.*, 1980), pig (Kong *et al.*, 1989), and rat (Kuramoto *et al.*, 1987). In the rat, SP nerves in the adrenal medulla originate from the sensory neurones in the ipsilateral dorsal root ganglia rather than cholinergic motor neurones in the spinal cord (Zhou *et al.*, 1990). In addition, SP can be released *in vivo* from the adrenal medulla in response to physiological stress (Vaupel *et al.*, 1988). Bovine adrenal medullary membranes have specific high affinity binding sites for SP (Geraghty *et al.*, 1990) that are distinct from the classical NK_1, NK_2 and NK_3 receptors in other systems. However, the possible functional role of SP in adrenal medullary secretion remains unclear.

Functional studies indicate that SP has no effect on the basal secretion or veratridine- or potassium-induced secretion from bovine isolated chromaffin cells (Livett *et al.*, 1979; Boksa & Livett, 1984a). However, SP does inhibit nicotine- or ACh-evoked CA secretion (Livett *et al.*, 1979; Role *et al.*, 1981), and preincubation with SP can protect against desensitization of the nicotinic response (Boksa & Livett, 1984b; Khalil *et al.*, 1988a). In contrast to these studies in chromaffin cells in which SP protected against desensitization of the nicotinic response, in PC12 cells, a rat phaeochromocytoma cell line, SP enhanced desensitization of the nicotinic response as measured by sodium influx in response to nicotinic agonists (Stallcup & Patrick, 1980; Simasko *et al.*, 1985; 1987). More recently, Boyd & Leeman (1987) reported that SP treatment of PC12 cells in the absence of agonist caused the nicotinic acetylcholine receptor to become subsequently non-responsive to agonists.

The rat adrenal medulla possesses both functional nicotinic and muscarinic receptors (Wakade, 1981). Previous studies in perfused rat adrenal glands have shown that SP modulates adrenal CA secretion evoked by electrical field stimulation (Zhou & Livett, 1990b). However, the involvement of nicotinic vs muscarinic responses in this process has not been determined. SP is the most potent mammalian tachykinin for modulating nicotinic receptor function (Khalil *et al.*, 1988b; Boyd & Leeman, 1987). Therefore, in the present study, we

[1] Author for correspondence.

have used rat isolated perfused adrenal glands and studied: (1) the effect of SP on CA secretion evoked by nicotine and muscarine; (2) the effect of SP on the desensitization of the nicotinic response; and (3) the effect of pre-exposure to SP on the subsequent nicotinic CA secretion. We found that SP had multiple effects on nicotinic CA secretion but had no effect on muscarinic-induced CA secretion.

Methods

Preparation of the perfused adrenal gland

Adult male and female Buffalo rats, 250 to 350 g, were used throughout. The rats were anaesthetized with Equithesin (a mixture of pentobarbitone and chloral hydrate, i.p., 2.6 ml kg^{-1}, for detail, see Tagerud & Cuello, 1979) and an L-shaped incision was made on the left side of the abdomen. The left adrenal gland was isolated and perfused essentially as described by Wakade (1981). In this preparation the adrenal vein was cannulated rather than the renal vein to reduce leakage from collaterals (Zhou & Livett, 1990b). After cannulation, the gland was isolated from the rat, put in a heated chamber (circulated with 37°C water) and perfused at 125 μl min^{-1} with Krebs bicarbonate solution, consisting of (mM): NaCl 118.4, $NaHCO_3$ 25, KCl 4.7, $CaCl_2$ 2.5, $MgCl_2$ 1.18, KH_2PO_4 1.2 and glucose 11.7. The perfusion solution was gassed with 95% O_2 and 5% CO_2 to a final pH of 7.4.

Effect of substance P on nicotine-evoked catecholamine secretion

For testing the effect of SP on the nicotinic CA secretion, two protocols were used. In one protocol (Figures 1, 2 and 3), CA release was evoked by perfusing with 10^{-5} M nicotine for two 10 min periods, separated by an 18 min rest period. In the first stimulation period (S1), SP at different concentrations (0–10^{-5} M) was perfused into the adrenal gland for 2 min before and 10 min during the nicotine perfusion. In the second stimulation period (S2), SP was omitted to test the effect of SP present in the first stimulation on desensitization of nicotine-induced CA secretion in the second stimulation. The perfusate was collected every 2 min for CA assay.

In the second protocol (Figure 4), the adrenal gland was stimulated once by perfusion with 10^{-5} M nicotine. SP (10^{-9} to 10^{-5} M) was perfused for 10 min before and for 10 min during perfusion with 10^{-5} M nicotine.

Effect of substance P on muscarine-evoked catecholamine secretion

For testing the effect of SP on muscarinic CA secretion (Figures 5 and 6), adrenal glands were stimulated twice by perfusion with 100 μM muscarine for 10 min. In S1, only 100 μM muscarine was perfused; in S2, SP at different concentrations was perfused for 2 min before and 10 min during perfusion with 100 μM muscarine. There was an 18 min interval between the two stimulations. The perfusate was collected every 2 min for CA assay.

Measurement of endogeneous catecholamines

The perfusates were acidified with perchloric acid (PCA, 0.4 M final concentration) and stored at −20°C until assay. For determination of noradrenaline (NA) and adrenaline (Ad), the perfusate was centrifuged at 4000 *g* for 10 min at 2°C. The supernatant was mixed with 3,4-dihydroxybenzylamine (DHBA, 2 nmol ml^{-1}) in 0.1 M PCA. The samples were injected into a high performance liquid chromatography (h.p.l.c.) system and NA and Ad were detected electrochemically as described previously (Livett *et al.*, 1987).

Statistics

The data were plotted as means ± s.e.mean. The amount of CA secreted in each fraction during S1 and S2 was added to obtain the total CA secretion during each stimulation. In the experiments with muscarine, the ratios of S2/S1 were calculated in order to assess the effect of SP during S2. The differences among the control and test groups were assessed by ANOVA.

Results

Effect of substance P on the time course of nicotine-evoked catecholamine secretion

The basal release of NA and Ad was in the order of 25 and 35 pmol 2 min^{-1} respectively. SP at concentrations from 10^{-10} to 10^{-5} M had no effect on basal CA release. In the absence of SP, NA and Ad secretion increased significantly during the first 6 min perfusion with 10^{-5} M nicotine and declined thereafter (Figures 1 and 2, control). NA and Ad output reached 605 ± 125 and 720 ± 100 pmol 2 min^{-1}, respectively, at maximal response. CA secretion in response to the same concentration of nicotine during S2 was reduced by approximately 50%.

SP had biphasic effects on the time course of CA secretion evoked by 10^{-5} M nicotine depending on the concentration of SP (Figures 1 and 2). In control glands perfused with nicotine (10^{-5} M), CA secretion reached its peak at 6 to 8 min and then had declined by 10 min after the start of the perfusion with

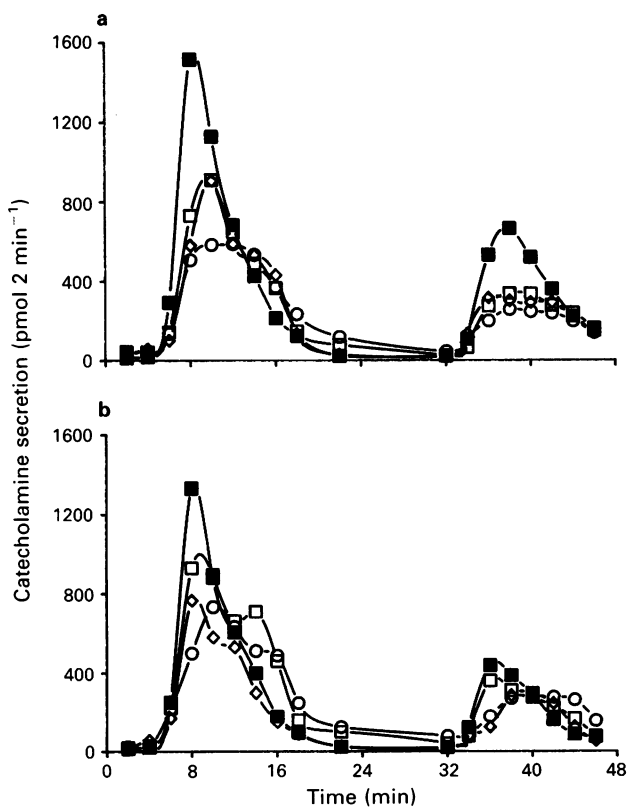

Figure 1 Effect of substance P (SP, 0, 10^{-10}, 10^{-9} or 10^{-8} M) on the time course of catecholamine (CA) secretion evoked by 10^{-5} M nicotine from rat perfused adrenal glands. After two basal samples were collected, the glands were stimulated with 10^{-5} M nicotine for 10 min twice with an 18 min interval between the two stimulations. Different concentrations of SP were added to the perfusion 2 min before and 10 during the first stimulation. Fractions were collected for CA assay every 2 min. Data are plotted as the means of 5 experiments (the error bars were 5 to 15% of the means and were omitted for clarity): (a) noradrenaline; (b) adrenaline; (○) control; (◇) SP 10^{-10} M; (■) SP 10^{-9} M; (□) SP 10^{-8} M.

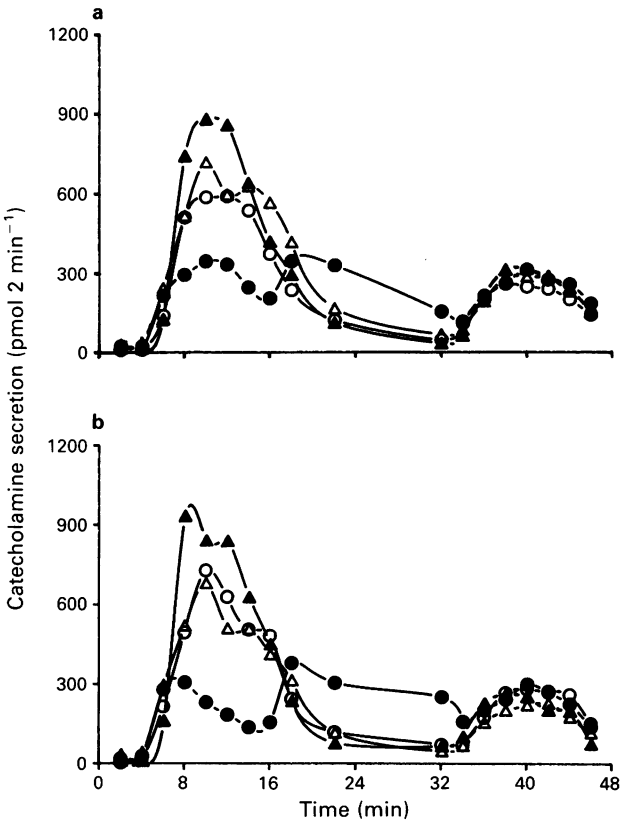

Figure 2 Effect of substance P (SP, 0, 10^{-7}, 10^{-6}, or 10^{-5} M) on the time course of catecholamine secretion evoked by 10^{-5} M nicotine from rat perfused adrenal glands. The experimental procedure was the same as in Figure 1. (a) Noradrenaline; (b) adrenaline; (○) control; (▲) SP 10^{-7} M; (△) SP 10^{-6} M; (●) SP 10^{-5} M.

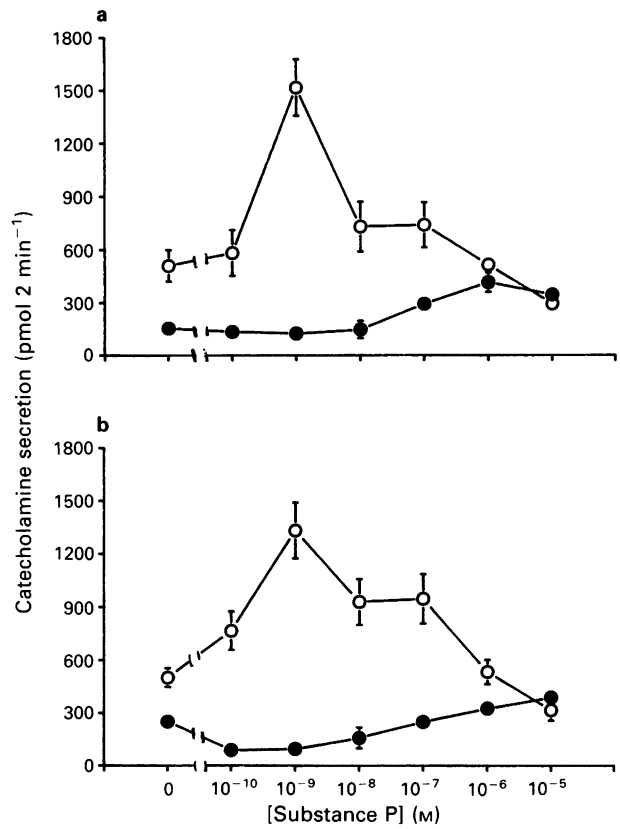

Figure 3 Effect of substance P (SP, 10^{-10}–10^{-5} M) on catecholamine (CA) secretion at 4 min and 14 min after perfusion of rat adrenal glands with nicotine (10^{-5} M). Data on CA secretion at 4 min and 14 min after nicotine in Figures 1 and 2 were replotted (means ± s.e.mean, $n = 5$) as a function of SP concentration (ANOVA test: at 4 min after nicotine, noradrenaline (NA): $F = 5.6$, $P < 0.01$; adrenaline (Ad): $F = 5.2$, $P < 0.01$; at 14 min after nicotine: NA: $F = 4.9$, $P < 0.01$; Ad: $F = 4.5$, $P < 0.01$). (a) NA; (b) Ad; (○) 4 min after nicotine; (●) 14 min after nicotine.

nicotine. In the presence of SP (10^{-9} M), CA secretion reached the maximum more rapidly, at 4 min after nicotine, when NA levels were 2.8 times and Ad levels 2.5 times higher than those in control (analysis of variance in all groups: NA: $F = 5.6$, $P < 0.01$; Ad: 4.8, $P < 0.01$) (Figure 3) and then declined rapidly by 6 and 8 min. In the presence of SP at 10^{-7}, 10^{-8} and 10^{-10} M, the changes were similar to those at 10^{-9} M but less pronounced (Figures 1, 2 and 3).

SP at 10^{-5} M also markedly changed the time course of CA secretion (Figure 2) but in a different manner from that seen with the low concentrations of SP. CA secretion in the presence of 10^{-5} M SP was almost the same as in the control during the first 2 min of nicotine stimulation; however, it decreased during the second and the third 2 min fractions. When the perfusion of SP and nicotine was stopped, NA secretion rebounded from 220 to 390 pmol 2 min^{-1} ($n = 5$) and Ad from 180 to 420 pmol 2 min^{-1} ($n = 5$). As shown in Figure 2, SP at 10^{-6} M also increased CA secretion after perfusion of SP was stopped (Figure 3).

Effect of substance P on the desensitization of the nicotinic response

In the control group (no SP in S1), the total NA and Ad output during S2 were 1440 ± 280 and 1880 ± 400 pmol (Figures 1 and 2). SP (10^{-10}–10^{-5} M) in the first 10 min stimulation had no significant effect on CA secretion during the second 10 min stimulation (in the absence of SP), 18 min later.

Effect of pre-exposure to substance P on catecholamine secretion

Pre-exposure of the adrenal glands to SP had a marked effect on the subsequent CA secretory response to nicotine. As shown in Figure 4, when SP (10^{-9} to 10^{-5} M) was present in the perfusion solution for 10 min before and 10 min during 10^{-5} M nicotine stimulation, both NA and Ad secretion were markedly inhibited in a concentration-dependent manner. As shown in Figure 4, CA secretion was almost completely inhibited by SP at 10^{-5} M. These results contrast with those where SP was exposed to the adrenal glands for only 2 min before nicotine (see Figures 1 and 2).

Effect of substance P on the time course of catecholamine secretion evoked by muscarine

As shown in Figure 5 and Figure 6, the basal secretion of NA and Ad was similar in the presence or absence of SP. In the absence of SP during S1, muscarine (10^{-4} M) preferentially increased Ad secretion (Ad/NA = 8.7 ± 0.4). In the first 2 min of stimulation during S1, NA secretion increased 2–3 fold over the basal (45 ± 5 pmol 2 min^{-1}), whereas Ad increased 12 fold over the basal to 270 ± 30 pmol 2 min^{-1}. Ad secretion continued to increase in the subsequent fractions reaching a maximum of 480 ± 80 pmol 2 min^{-1} and was maintained at this level until perfusion of muscarine was stopped. The time course and extent of Ad and NA secretion during S2 in the control was similar to that during S1. SP (10^{-9} to 10^{-5} M) for 2 min before and 10 min during S2 had no significant effect on the time course of NA or Ad secretion in S2 induced by 10^{-4} M muscarine (Figures 5 and 6).

Effect of substance P on total catecholamine secretion evoked by muscarine

In the control group, the total amount of Ad secretion evoked by 10^{-4} M muscarine over the 10 min S1 and S2 stimulation

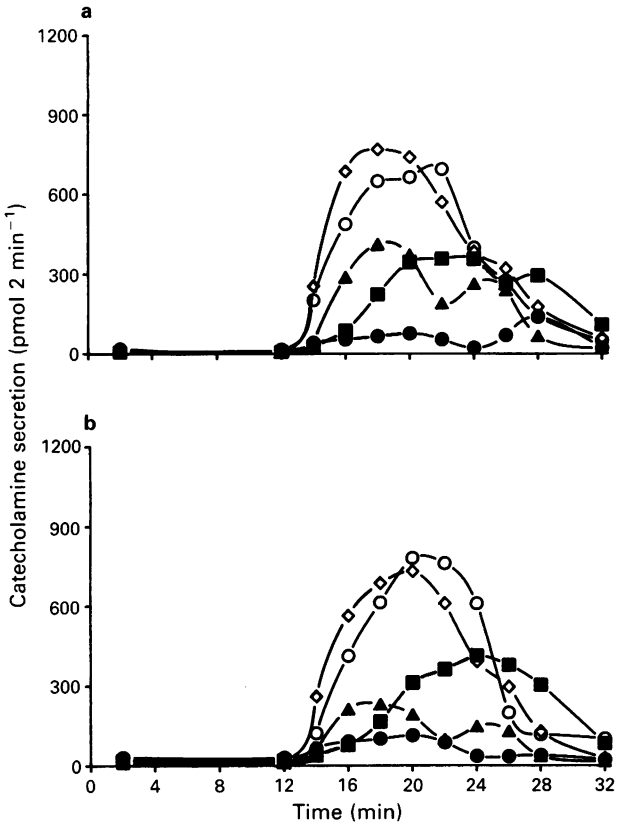

Figure 4 Effect of pre-incubation with substance P (SP) for 10 min on nicotine-induced catecholamine (CA) secretion from rat perfused adrenal glands. After a basal sample was collected, adrenal glands were perfused with SP (10^{-10} to 10^{-5} M) for 10 min before and 10 min during stimulation with 10^{-5} M nicotine. The fractions were assayed for CA and the data plotted as means of 4 experiments (error bars were 5 to 15% of means and omitted for clarity). (a) Noradrenaline; (b) adrenaline; (○) control; (◇) SP 10^{-10} M; (■) SP 10^{-9} M; (▲) SP 10^{-7} M; (●) SP 10^{-5} M.

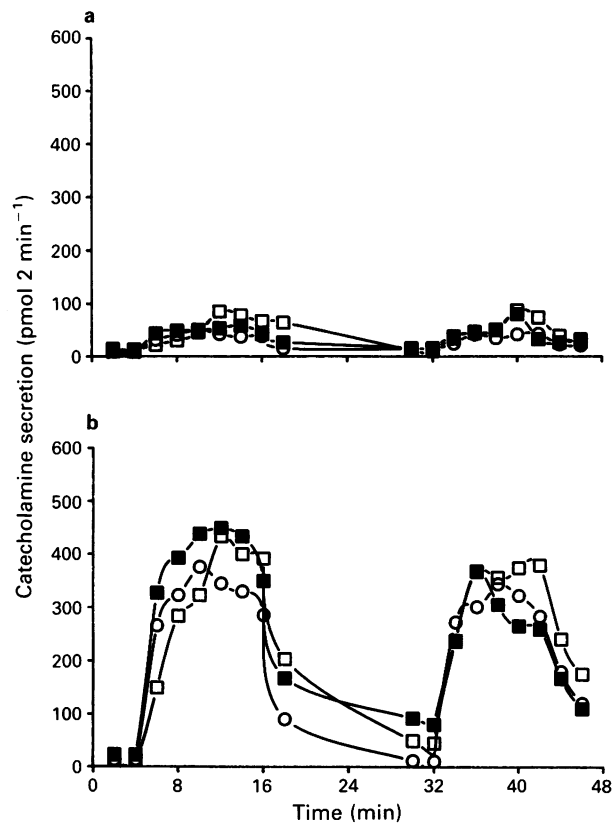

Figure 5 Effect of substance P (SP, 10^{-9}–10^{-7} M) on the time course of catecholamine (CA) secretion evoked by muscarine from rat perfused adrenal glands. After two samples were collected, the adrenal glands were perfused with 10^{-4} M muscarine for 10 min twice, with an 18 min period between. SP at concentrations from 10^{-9} to 10^{-7} M was present in the perfusion solution for 2 min before and 10 min during the second stimulation. The fractions were collected as shown in the figure for CA assay. Data are plotted as means of 5 experiments (error bars were 10%–15% of means and are omitted for the clarity). (a) Noradrenaline; (b) adrenaline; (○) control; (■) SP 10^{-9} M; (□) SP 10^{-8} M.

periods was 2012 ± 331 and 1767 ± 234 pmol, respectively and NA was 281 ± 63 and 254 ± 52 pmol respectively. In the control group (no SP), the ratios of S2/S1 were 0.95 ± 0.13 for NA and 0.84 ± 0.11 for Ad. Although the ratios of S2/S1 for NA and Ad increased slightly in the presence of SP 10^{-8} and 10^{-7} M, there were no statistically significant differences among control and test groups (ANOVA, $F = 1.17$ for Ad and $F = 0.98$ for NA, $P > 0.05$, $n = 5$).

Discussion

Facilitatory effect of substance P on the initial nicotinic response

In the present study, we compared the effects of SP on CA secretion evoked by nicotine and muscarine from perfused rat adrenal glands. We found that SP modulates nicotinic but not muscarinic CA secretion. A novel finding in the present study was that SP at the lower concentrations (10^{-10}–10^{-7} M) increased initial nicotinic CA secretion in the first two 2 min collection periods but decreased nicotinic CA secretion thereafter (Figures 1 and 2). This effect of SP was concentration-dependent, and more pronounced on NA secretion than on Ad secretion. The maximal effect occurred at 10^{-9} M SP. SP by itself had no effect on basal CA secretion from the rat adrenal glands, indicating that SP produced its effect by modulating the nicotinic secretion of adrenal catecholamines.

These results in the rat appear to differ from those in isolated bovine chromaffin cells where SP at these lower concentrations (10^{-9}–10^{-7} M) had no apparent effect on CA secretion evoked by nicotine over a 5 min collection period (Khalil *et al.*, 1988a; Boksa & Livett, 1984b). However, in the studies on adrenal chromaffin cells, an initial facilitatory effect of SP may have occurred at 2 min or 4 min but have been obscured by the fact that the release sample was collected over a 5 min-incubation period. This is reasonable, given that there are no diffusion barriers in the isolated chromaffin cells and the response to nicotine and SP could be faster than in the perfused rat preparation. Note that at 8 min after nicotine stimulation in the perfused rat preparation there was likewise no significant effect of SP (10^{-9}–10^{-7} M) on nicotine-evoked CA secretion whereas at 14 min the effects were inhibitory (Figure 3).

The mechanism by which SP facilitates CA secretion by SP in the first 4 min is not clear. SP may increase CA secretion by changing the conductance of ion channels. It has been reported that SP at 10^{-7} M depolarizes sympathetic neurones in the guinea-pig by increasing sodium permeability and decreasing potassium permeability (Dun & Minota, 1981). In autonomic ganglia, SP ($10^{-7} - 4 \times 10^{-6}$ M) mimics the non-cholinergic slow exitatory postsynaptic potential (e.p.s.p.) (Jiang *et al.*, 1982; Konishi *et al.*, 1989) and facilitates the nicotinic response (Jiang & Dun, 1986). Moreover, it has also been shown that SP at 10^{-7} M depolarizes rat chromaffin cells from the adrenal medulla by approximately 20 mV (Richter & Grunwald, 1987). Although this degree of depolarization is not sufficient to evoke CA secretion itself, the calcium influx resulting from the depolarization is thought to facilitate CA secretion evoked by nicotinic agonists.

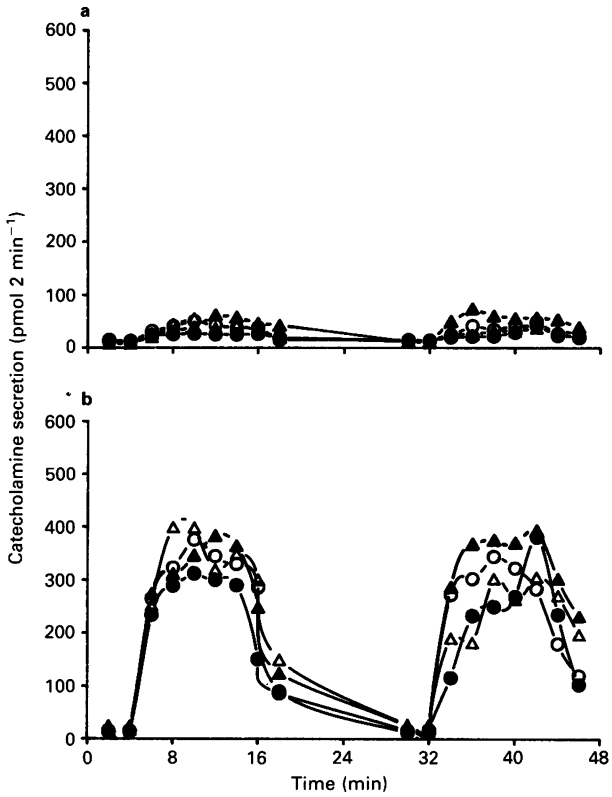

Figure 6 Effect of substance P (SP, 10^{-6}–10^{-5} M) on the time course of catecholamine secretion evoked by muscarine from rat perfused adrenal glands. The protocol was the same as in Figure 5. (a) Noradrenaline; (b) adrenaline; (○) control; (▲) SP 10^{-7} M; (△); SP 10^{-6} M; (●) SP 10^{-5} M.

It is possible that SP plays a facilitatory role in the early secretory phase via second messenger systems. It is well known that SP can stimulate hydrolysis of phospholipids and produce accumulation of inositol trisphosphate and diacylglycerol in many tissues including guinea-pig ileum, rat hypothalamus (Watson & Downes, 1983), hamster urinary bladder (Bristow *et al.*, 1987), rat parotid gland (Rollandy *et al.*, 1989) and rat skin (Thomas *et al.*, 1989). Although SP has no effect on metabolism of phosphatidylinositol phosphates (PIP) in bovine chromaffin cells (Bunn *et al.*, 1990) it does have a stimulating effect on PIP metabolism in rat adrenal medulla (Minenko & Oehme, 1987; Minenko *et al.*, 1988). An increase in cytosolic mobilization of calcium by inositol 1,4,5-trisphosphate and activation of protein kinase C by diacylglycerol may prime the calcium-sensitive secretory process so as to facilitate secretion by nicotine (Cheek *et al.*, 1989a,b). In addition, SP may facilitate nicotinic CA secretion by protecting against nicotinic receptor desensitization (Boksa & Livett, 1984b) since even low concentrations of nicotinic agonists (10^{-6} M) can cause desensitization (Boyd, 1987).

Inhibitory effect of substance P on the later nicotinic response

In the present study, we found that SP inhibited adrenal CA secretion in the later phase of nicotinic stimulation (Figures 1 and 2). This inhibitory action of SP was markedly enhanced by pre-exposure to SP for 10 min before nicotine (Figure 4). Inhibitory effects of SP on the nicotinic responses have been described for a number of different preparations including cat spinal Renshaw cells (Belcher & Ryall, 1977; Krnjevic & Lekic, 1977), bovine isolated chromaffin cells (Livett *et al.*, 1979; Role *et al.*, 1981; Boksa & Livett, 1984b), frog sympathetic ganglia and skeletal muscle endplates (Akasu *et al.*, 1983), PC-12 cells (Stallcup & Patrick, 1980; Simasko *et al.*, 1985; Boyd & Leeman, 1987), BC_3H_1 cells (Simasko *et al.*, 1985) and rat adrenal gland slices (Nieber & Oehme, 1987). This action which is Ca^{2+}-dependent and specific to nicotinic receptor function (Boksa & Livett, 1984b; Role *et al.*, 1981) has an IC_{50} for SP of about 10^{-6} M (Boksa & Livett, 1984b; Simasko *et al.*, 1987).

The mechanism by which SP inhibits nicotinic function is not clear. SP does not appear to inhibit nicotinic function by binding to the nicotine binding sites (Stallcup & Patrick, 1980; Boyd & Leeman, 1987), but rather by blocking the receptor-linked open ion channels (SP may be physically trapped within these ion channels; Stallcup & Patrick, 1980; Clapham & Neher, 1984; Simasko *et al.*, 1987). In isolated chromaffin cells and PC12 cells this action is reversible after washing out the SP (Boksa & Livett, 1984b; Boyd & Leeman, 1987). Consistent with the hypothesis that SP blocks nicotinic receptor-linked open ion channels, in the present study with the rat perfused adrenal gland preparation, CA secretion rebounded immediately after switching off both SP and nicotine. In addition, SP may act as an inhibitor of adrenal CA secretion by enhancing desensitization, as evidenced by measurement of sodium influx in rat PC-12 cells or ion currents in bovine cultured chromaffin cells (Clapham & Neher, 1984; Boyd & Leeman, 1987; Higgins & Berg, 1989).

Effect of substance P on the desensitization of the nicotinic response

In the present study, CA secretion in S2 amounted to less than 50% of S1. This reduction in CA secretion was not due to agonist-induced depletion of CA from the adrenal glands since normal adrenal glands contained 65 nmol of NA and Ad, some 20 times that secreted during S1 (Zhou & Livett, 1990a). The decline in CA secretion in S2 is more likely to be due to desensitization of the nicotinic response. SP present in S1 did not protect against the desensitization of the nicotinic response during S2. These results contrast with those in bovine cultured chromaffin cells in which SP (10^{-6} M) present together with a high concentration of nicotine (10^{-3} M) in the first incubation period protected the nicotinic response against desensitization in a second nicotinic stimulation period (Boksa & Livett, 1984b). The reason for this difference in response to SP is most likely related to the temporal differences in the experimental protocols and the previous history of the preparation (Oehme & Krivoy, 1983). The time interval between the two stimulations in the present study was longer than that in the studies in cell culture (18 min vs 20 s). Boksa & Livett (1984b) showed that the protection by SP was reversible by washout of SP. In the present study, any protective actions of SP would be lost during the prolonged perfusion time between the two stimulations.

Reports on the effect of SP on desensitization of the nicotinic response are controversial, some studies reporting SP protects against desensitization (Boksa & Livett, 1984b; Khalil *et al.*, 1988a) while others find it enhances the rate of nicotinic desensitization (Stallcup & Patrick, 1980; Clapham & Neher, 1984; Simasko *et al.*, 1985; 1987; Higgins & Berg, 1988). This apparent discrepancy of SP action may be explained by multiple actions of SP on nicotinic ACh receptors, dependent upon the time frame of these experiments and time of exposure to SP. Desensitization of the nicotinic response is known to have two phases: an initial fast phase lasting less than a second or a few seconds and a later slow phase lasting minutes or longer (Boyd, 1987). Boyd & Leeman (1987) showed that SP increased agonist-induced desensitization of nicotinic receptors in the fast phase but inhibited agonist-mediated desensitization in the later slow phase. In addition, SP also protected the receptors from agonist-mediated irreversible deactivation (Boyd & Leeman, 1987), a mechanism which may explain our finding that SP protects against nicotinic desensitization (Boksa & Livett, 1984b).

Effect of pre-exposure to substance P on the nicotinic response

The pre-exposure time with SP is important for its inhibitory action on catecholamine (CA) secretion. Boyd & Leeman (1987) reported that exposure of PC-12 cells to SP alone for 10 min caused acetylcholine receptors to become non-responsive to agonists. In the absence of nicotinic agonists SP converted the nicotinic receptor from its resting closed state to a non-functional state (Boyd & Leeman, 1987). This receptor transition did not involve the open channel state of the receptor since SP did not cause an increase in ^{22}Na influx. Our present study shows that pre-exposure of adrenal glands to SP (10^{-9} to 10^{-5} M) for 10 min caused more marked inhibition in CA secretion than did pre-exposure to SP for 2 min. In accord with the results of Boyd & Leeman (1987), this action of SP is reversible because CA secretion rebounded after termination of perfusion with SP and nicotine. This effect appears to be related to the closed state of ion channels to which SP may bind. Recently, it has been shown that bovine adrenal medullary membranes possess a novel class of binding sites for SP which unlike the NK_1 class, require both the C- and N-terminal amino acid sequence of SP (Geraghty *et al.*, 1990). The possibility that these sites represent binding of SP to the nicotinic receptor ion channel remains to be determined.

Effect of substance P on muscarinic catecholamine secretion

Muscarine at concentrations from 10^{-6} to 10^{-3} M evoked a dose-dependent secretion of Ad and NA from the perfused rat adrenal glands (data not shown). As shown in Figure 5 and Figure 6, muscarine at 10^{-4} M (close to the EC_{50}) evoked predominantly Ad secretion and had little effect on NA secretion. The Ad/NA ratio evoked by muscarine was 8.7. This contrasts with the secretion evoked by nicotine in which Ad and NA secretion were almost equal. The results in the present study in the perfused rat adrenal gland are consistent with those in the perfused cat adrenal gland described by Douglas & Poisner (1965) and Critchley *et al.* (1986). This selective secretion of Ad evoked by muscarinic agonists seems to be species-specific and was more significant in rat (Ad/NA, 8.7, present study) than in cat (Ad/NA, 3.6) and dog (Ad/NA, 2.6, Critchley *et al.*, 1986).

As shown in Figures 5 and 6, CA secretion evoked by muscarine was well maintained during the second 10 min stimulation. In contrast to nicotinic CA secretion (Figures 1 and 2), there was little desensitization of the CA secretion evoked by muscarine. SP at concentrations from 10^{-9} to 10^{-5} M had no significant effect on either the time course of the total amount of CA secretion evoked by muscarine. This result is consistent with that obtained with guinea-pig isolated chromaffin cells (Role *et al.*, 1981) and in other systems (Krnjevic & Lekic, 1977; Belcher & Ryall, 1977). The reason for the differential effects of SP on nicotinic and muscarinic CA secretion may reflect the different pathways for secretion activated by nicotine and muscarine (Harish *et al.*, 1987; Cheek *et al.*, 1989a,b).

In conclusion, SP has multiple actions on nicotinic CA secretion from the perfused rat adrenal gland *in vitro*. SP at low concentrations (10^{-7}–10^{-9} M) changed the time course of CA secretion resulting in enhancement of CA secretion in response to nicotine in the first 4 min and inhibition of secretion thereafter. At higher concentrations (10^{-5} M), SP inhibited total CA secretion followed by a rebound in CA secretion after wash out of the SP. Pre-exposure of adrenal glands to SP (10^{-9} to 10^{-5} M) for 10 min produced a more profound inhibition in CA secretion than pre-exposure to SP for 2 min. SP had no effect on muscarinic CA secretion. These results with the rat adrenal gland perfused *in vitro* suggest both a quantitative and temporal role for SP as a novel modulator of adrenal CA secretion.

We thank Mr Ian Young, Mr Tim Anning and Mr Phillip McGlashan for technical assistance. X.-F.Z. was supported by a University of Melbourne Postgraduate Award. P.D.M. is an NH&MR Research Fellow. This work was supported by a project grant to B.G.L. from the National Health and Medical Research Council (NH&MRC) of Australia.

References

AKASU, T., KOJIMA, M. & KOKETSU, K. (1983). Substance P modulates the sensitivity of the nicotinic receptor in amphibian cholinergic transmission. *Br. J. Pharmacol.*, **80**, 123–131.

BELCHER, G. & RYALL, R.W. (1977). Substance P and Renshaw cells: a new concept of inhibitory synaptic interactions. *J. Physiol.*, **272**, 105–119.

BOKSA, P. & LIVETT, B.G. (1984a). Desensitization to nicotinic cholinergic agonists and K^+, agents that stimulate catecholamine secretion in isolated adrenal chromaffin cells. *J. Neurochem.*, **42**, 607–617.

BOKSA, P. & LIVETT, B.G. (1984b). Substance P protects against desensitization of nicotinic response in isolated adrenal chromaffin cells. *J. Neurochem.*, **42**, 618–627.

BOYD, N.D. (1987). Two distinct kinetic phases of desensitization of acetylcholine receptors of clonal rat PC12 cells. *J. Physiol.*, **389**, 45–67.

BOYD, N.D. & LEEMAN, S.E. (1987). Multiple actions of substance P that regulate the functional properties of acetylcholine receptors of clonal rat PC12 cells. *J. Physiol*, **389**, 69–97.

BRISTOW, D.R., CURTIS, N.R., SUMAN-CHAUHAN, N., WATLING, K.J. & WILLIAM, B.J. (1987). Effects of tachykinins on inositol phospholipid hydrolysis in slices of hamster urinary bladder. *Br. J. Pharmacol.*, **90**, 211–217.

BUNN, S.J., MARLEY, P.D. & LIVETT, B.G. (1990). Receptor stimulated formation of inositol phosphates in cultures of bovine adrenal medullary cells: The effects of bradykinin, bombesin and neurotensin. *Neuropeptides*, **15**, 187–194.

CHEEK, T.R. & THASTRUP, O. (1989a). Internal Ca^{2+} mobilization and secretion in bovine adrenal chromaffin cells. *Cell Calcium*, **10**, 213–221.

CHEEK, T.R., O'SULLIVAN, A.J., MORETON, R.B., BERRIDGE, M.J. & BURGOYNE, R.D. (1989b). Spatial localization of the stimulus-induced rise in cytosolic Ca^{2+} in bovine adrenal chromaffin cells: Distinct nicotinic and muscarinic patterns. *FEBS Lett.*, **247**, 429–434.

CLAPHAM, D.E. & NEHER, E. (1984). Substance P reduces acetylcholine-induced currents in isolated bovine chromaffin cells. *J. Physiol.*, **347**, 255–277.

CRITCHLEY, J.A.J.H., ELLIS, P., HENDERSON, C.G., UNGAR, A. & WEST, C.P. (1986). Muscarinic and nicotinic mechanisms in the responses of the adrenal medulla of the dog and cat to reflex stimuli and to cholinomimetic drugs. *Br. J. Pharmacol.*, **89**, 831–835.

DOUGLAS, W.W. & POISNER, A.M. (1965). Preferential release of adrenaline from the adrenal medulla by muscarine and pilocarpine. *Nature*, **208**, 1102–1103.

DUN, N.J. & MINOTA, S. (1981). Effect of substance P on neurones of the inferior mesenteric ganglia of the guinea-pig. *J. Physiol.*, **321**, 259–271.

FELDBERG, W., MINZ, B. & TSUDZIMURA, H. (1934). The mechanism of nervous discharge of adrenaline. *J. Physiol.*, **81**, 286–304.

GERAGHTY, D.P., LIVETT, B.G., ROGERSON, F.M. & BURCHER, E. (1990). A novel substance P binding site in bovine adrenal medulla. *Neurosci. Lett.*, (in press).

HARISH, O.E., KAO, L.-S., RAFFANIELIO, R., WAKADE, A.R. & SCHNEIDER, A.S. (1987). Calcium dependence of muscarinic receptor-mediated catecholamine secretion from the perfused rat adrenal medulla. *J. Neurochem.*, **48**, 1730–1735.

HIGGINS, L.S. & BERG, D.K. (1988). A desensitized form of neuronal acetylcholine receptor detected by ^3H-nicotine binding on bovine adrenal chromaffin cells. *J. Neurosci.*, **8**, 1436–1446.

JIANG, Z.G. & DUN, N.J. (1986). Facilitation of nicotinic response in the guinea pig prevertebral neurons by substance P. *Brain Res.*, **363**, 196–198.

JIANG, Z.G., DUN, N.J. & KARCZMAR, A.G. (1982). A putative sensory transmitter in mammalian autonomic ganglia. *Science*, **217**, 739–741.

KHALIL, Z., MARLEY, P.D. & LIVETT, B.G. (1988a). Effect of substance P on nicotine-induced desensitization of cultured bovine adrenal chromaffin cells: possible receptor subtypes. *Brain Res.*, **459**, 282–288.

KHALIL, Z., MARLEY, P.D. & LIVETT, B.G. (1988b). Mammalian tachykinins modulate the nicotinic secretory response of cultured bovine adrenal chromaffin cells. *Brain Res.*, **459**, 289–297.

KONG, J.Y., THURESON-KLEIN, A. & KLEIN, R.J. (1989). Differential distribution of neuropeptides and serotonin in pig adrenal glands. *Neuroscience*, **28**, 765–775.

KONISHI, S., SONG, S.-Y., OGAWA, T. & KANAZAWA, I. (1989). Tachykinins produce fast and slow depolarizations in sympathetic neurons of rat coeliac-superior mesenteric ganglia. *Brain Res.*, **490**, 162–165.

KRNJEVIC, K. & LEKIC, D. (1977). Substance P selectively blocks excitation of Renshaw cells by acetylcholine. *Can. J. Physiol. Pharmacol.*, **55**, 958–961.

KURAMOTO, H., KONDO, H. & FUJITA, T. (1987). Calcitonin gene-related peptide (CGRP)-like immunoreactivity on scattered chromaffin cells and nerve fibers in the adrenal gland of rats. *Cell Tissue Res.*, **247**, 309–315.

LINNOILA, R.I., DIAUGUSTINE, R.R., HERVONEN, A. & MILLER, R.J. (1980). Distribution of (Met5)- and (Leu5)-enkephalin, vasoactive intestinal polypeptide and substance P-like immunoreactivities in human adrenal glands. *Neuroscience*, **5**, 247–2259.

LIVETT, B.G. (1987). Peptide modulation of adrenal chromaffin cell secretion. In *Stimulus-secretion Coupling in Chromaffin Cells*. ed. Rosenheck, K. & Lelkes, P.I. pp. 177–204. Boca Raton, Florida: CRC Press.

LIVETT, B.G., KOZOUSEK, V., MIZOBE, F. & DEAN, D.M. (1979). Substance P inhibits nicotinic activation of chromaffin cells. *Nature*, **278**, 256–257.

LIVETT, B.G., MARLEY, P.D., MITCHELHILL, K.I., WAN, D.C.C. & WHITE, T.D. (1987). Assessment of adrenal chromaffin cell secretion: presentation of four techniques. In *In Vitro Methods for Studying Secretion*.. ed. Poisner, A.M. & Trifaro, J.M. pp. 176–204.

MARLEY, P.D. & LIVETT, B.G. (1985). Neuropeptides in the autonomic nervous system. *CRC Critical Reviews in Clinical Neurobiology*, **1**, 201–283.

MINENKO, A., GABRYSIAK, B. & OEHME, P. (1988). Decreased SP-stimulated diesteratic hydrolysis of inositol phospholipids in adrenal medulla slices from spontaneously hypertensive rats. *Biomed. Biochim. Acta*, **47**, 31–37.

MINENKO, A. & OEHME, P. (1987). Substance P action in inositol phospholipids in rat adrenal medulla slices. *Biomed. Biochim. Acta*, **46**, 461–467.

NIEBER, K. & OEHME, P. (1987). Effect of substance P (SP) and the N-terminal SP-analogue SP (1–4) on the pre- and postsynaptic transmitter release in rat adrenal gland slices. *Biomed. Biochim. Acta*, **46**, 103–109.

OEHME, P. & KRIVOY, W.A. (1983). Substance P: a peptide with unusual features. *Trends Pharmacol. Sci.*, **4**, 531–523.

RICHTER, R. & GRUNWALD, C.H. (1987). Effect of substance P on the membrane potential of rat adrenal chromaffin cells. *Biomed. Biochim. Acta*, **46**, 837–840.

ROLE, L.W., LEEMAN, S.E. & PERLMAN, R.L. (1981). Somatostatin and substance P inhibits catecholamine secretion from isolated cells of guinea-pig adrenal medulla. *Neuroscience*, **6**, 1813–1821.

ROLLANDY, I., DREUX, C., IMHOFF, V. & ROSSIGNOL, B. (1989). Importance of the presence of the N-terminal tripeptide of substance P for the stimulation of phosphatidylinositol metabolism in rat parotid gland: a possible activation of phospholipases C and D. *Neuropeptides*, **13**, 175–185.

SIMASKO, S.M., DURKIN, J.A. & WEILAND, G.A. (1987). Effects of substance P on nicotinic acetylcholine receptor function in PC12 cells. *J. Neurochem.*, **49**, 253–260.

SIMASKO, S.M., SOARES, J.R. & WEILAND, G.A. (1985). Structure-activity relationship for substance P inhibition of carbamylcholine-stimulated $^{22}Na^{+}$ flux in neuronal (PC12) and non-neuronal (BC3H1) cell lines. *J. Pharmacol. Exp. Ther.*, **235**, 601–605.

STALLCUP, W.B. & PATRICK, J. (1980). Substance P enhances cholinergic receptor desensitization in a clonal nerve cell line. *Proc. Natl. Acad. Sci. U.S.A.*, **77**, 634–638.

TAGERUD, S.E.O. & CUELLO, A.C. (1979). Dopamine release from the rat substantia nigra *in vitro*. Effect of raphe lesions and veratridine stimulation. *Neuroscience*, **4**, 2021–2029.

THOMAS, K.L., ANDREWS, P.V., KHALIL, Z. & HELME, R.D. (1989). Substance P induced hydrolysis of inositol phospholipids in rat skin in an *in vivo* model of inflammation. *Neuropeptides*, **13**, 191–196.

VAUPEL, R., JARRY, H., SCHLOMER, H.-T. & WUTTKE, W. (1988). Differential response of substance P-containing subtypes of adrenomedullary cells to different stressors. *Endocrinology*, **123**, 2140–2145.

WAKADE, A.R. (1981). Studies on secretion of catecholamines evoked by acetylcholine or transmural stimulation of the rat adrenal gland. *J. Physiol.*, **313**, 453–480.

WATSON, S.P. & DOWNES, C.P. (1983). Substance P induced hydrolysis of inositol phospholipids in guinea-pig ileum and rat hypothalamus. *Eur. J. Pharmacol.*, **93**, 245–253.

ZHOU, X.-F. & LIVETT, B.G. (1990a). Effect of capsaicin-sensitive sensory nerves on plasma glucose and catecholamine levels during 2-deoxyglucose-induced stress in conscious rats. *Br. J. Pharmacol.*, **100**, 523–529.

ZHOU, X.-F. & LIVETT, B.G. (1990b). Substance P increases catecholamine secretion from perfused rat adrenal glands evoked by prolonged field stimulation. *J. Physiol.*, **425**, 321–334.

ZHOU, X.-F., OLDFIELD, B. & LIVETT, B.G. (1990). Substance P containing sensory neurons in the rat dorsal root ganglia innervate the adrenal medulla. *Proc. Australian Neurosci. Soc.*, **1**, 145 (Abstract).

(Received June 6, 1990
Revised October 22, 1990
Accepted November 22, 1990)

Br. J. Pharmacol. (1991), **104**, 166–170

The effects of sham and full spinalization on the systemic potency of μ- and κ-opioids on spinal nociceptive reflexes in rats

Juan F. Herrero & [1]P. Max Headley

Department of Physiology, The School of Medical Sciences, University of Bristol, University Walk, Bristol BS8 1TD

1 Flexor withdrawal reflexes to noxious mechanical pinch stimuli were recorded as single motor unit activity in α-chloralose anaesthetized rats, by means of tungsten bipolar electrodes inserted percutaneously into hindlimb flexor muscles. The relative spinal and supraspinal contributions to μ- and κ-opioid agonists in inhibiting these spinal reflexes, together with possible potency changes elicited by surgical trauma, were examined by comparing their relative potencies in spinally unoperated, sham spinalized and spinalized rats.

2 The noxious stimuli, which were of comparable intensity in the three groups, elicited similar mean firing rates of the motor units in all groups. This indicates that the excitability levels in the reflex pathway were not greatly affected by either sham or actual spinalization.

3 The μ-agonists morphine and fentanyl, and the κ-agonist U-50,488H, inhibited the reflexes in a dose-dependent manner, when administered intravenously in a $\log_2$ cumulative dose regime.

4 The surgery of sham spinalization had little effect on the potency of morphine and fentanyl, whereas it doubled the potency of U-50,488.

5 Spinalization did not affect the potency of morphine. In contrast it decreased the potency of fentanyl 2-4 fold and that of U-50,488 approximately 6 fold.

6 The effects of all agonists were antagonized by naloxone. Dose-dependence studies indicating that antagonism of U-50,488H required about 5 times the dose of naloxone that antagonized morphine.

7 The data suggest that surgical trauma to the spinal column and/or dura mater triggers supraspinal mechanisms that significantly enhance the potency of κ- but not μ-agonists.

8 It is concluded that most of the effects of systemic morphine on spinal reflexes are mediated, under all three conditions tested, by direct effects in the spinal cord. In contrast, the inhibition of reflexes by U-50,488H is mediated at both spinal and supraspinal levels, the latter being enhanced in the presence of surgical trauma. The differences between morphine and fentanyl remain unexplained.

Keywords: μ opioid; κ opioid; nociception; spinal reflexes; U-50,488H; fentanyl; morphine

Introduction

Morphine and other μ-opioids are effective analgesics and act at all levels of the neuraxis to reduce nociceptive responses, as indicated by numerous studies performed with a variety of local administration techniques, or with systemic administration with lesions of various nuclei or pathways (Yaksh, 1984; Yaksh & Noueihed, 1985; Millan *et al.*, 1989).

The relative degree to which the effects of systemic opioid agonists are produced directly at spinal rather than at supraspinal sites still remains unclear. Many reports have concluded that morphine increases the threshold in nociceptive tests primarily through supraspinal mechanisms. For example, systemic morphine was less effective in increasing the threshold in the tail flick test (which is generally accepted as a spinal reflex) in spinally transected as compared with intact rats (Advokat & Burton, 1987; Sinclair *et al.*, 1988). Lesions of the dorsolateral funiculus or of brainstem nuclei reduced the effectiveness of systemic morphine in this test (Murfin *et al.*, 1976; Basbaum *et al.*, 1977; Yaksh & Rudy, 1977; Hayes *et al.*, 1978; Barton *et al.*, 1980).

Other studies indicate that the spinal cord is relatively more important in mediating the effects of systemic μ-opioids (Yaksh & Noueihed, 1985; Millan *et al.*, 1989). Some experiments have even failed to find any supraspinal influence of systemic morphine on nociceptive responses of dorsal horn cells (Le Bars *et al.*, 1979; 1980; Chitour *et al.*, 1986). Many reports indicate that morphine has antinociceptive effects following local spinal administration (Yaksh & Noueihed, 1985; Sinclair *et al.*, 1988).

Contradictory results have also been obtained with κ-receptor agonists concerning their relative spinal and supraspinal actions (Millan, 1990). In paw-pressure, tail flick or hot-plate tests, intrathecal administration of selective κ-opioids produced markedly less antinociception than when injected either intravenously (i.v.) or intracerebroventricularly (Stevens & Yaksh, 1986; Leighton *et al.*, 1988; but see Wilcox & Hwang, 1984) except in some tests of visceral chemical nociception (Schmauss & Yaksh, 1984). On the other hand Millan (1989) clearly demonstrated that intrathecal κ-agonists reduced reflexes to noxious pinch and moderate heat stimuli, and intrathecal naloxone reduced the effects of systemic κ- (and μ-) agonists (Millan *et al.*, 1989). In electrophysiological tests local administration had variable effects between cells (Knox & Dickenson, 1987; Hope *et al.*, 1990). With systemic administration to spinalized rats, however, the selective κ-opioid U-50,488H caused consistent and naloxone-reversible reductions of the nociceptive responses of both motoneurones (Parsons & Headley, 1989; Parsons *et al.*, 1989) and dorsal horn neurones (Headley *et al.*, 1989; Dong *et al.*, 1991; see also Calthrop & Hill, 1983).

It was appropriate to clarify this situation. We have now made direct comparisons of the potencies of the μ-opioids, morphine and fentanyl, and the κ-opioid, U-50,488H, on with drawal reflexes evoked in rats by noxious mechanical pinch stimuli. Drugs were administered intravenously so as to ensure the adequate access of the test opioids to all relevant receptors (see Parsons *et al.*, 1989). The potencies of the opioid agonists were compared between intact and spinalized rats so as to assess the contribution of direct spinal effects to the overall inhibition of these nociceptive reflexes. Because it has been shown that surgery to the spinal column can enhance the direct spinal potency of opioids and anaesthetics on nociceptive reflexes (Hartell *et al.*, 1990; Hartell & Headley, 1991) it was important to include a sham-operated group when comparing intact versus spinalized animals.

[1] Author for correspondence.

A preliminary account of some of these data has appeared elsewhere (Herrero & Headley, 1990).

Methods

Animal preparation

Details of most of the methods have been described previously (Hartell & Headley, 1990). Male Wistar rats (300–380 g) were anaesthetized with halothane in O_2 and cannulae were implanted in the trachea, one carotid artery and one jugular vein. In one group (spinally unoperated) no further surgery was performed. In the other two experimental groups, a small laminectomy was performed, with infiltration of lignocaine with adrenaline, from thoracic 10 to 8 vertebrae, and the dura mater was opened. In one group (sham spinalization) no further surgery was performed and the incision was closed. In the other (spinalized group) the spinal cord was transected at thoracic segment 8 or 9 using cautery to minimise bleeding. When a larger vein was present at this level it was left intact, together with a wedge of dorsal column tissue for support, so as not to compromise the venous drainage from the cord.

Halothane was discontinued and α-chloralose was used as the maintenance anaesthetic (50 mg kg^{-1}, i.v. initially and 20 mg kg^{-1}, i.v. approximately every hour). Blood pressure was monitored continuously and experiments were terminated if systolic pressure fell below 100 mmHg. Core temperature was maintained at 37°C $\pm$ 0.5°C. All animals were left for at least 1 h after surgery before recording was started.

Stimulus presentation and recording systems

Nociceptive reflexes were elicited by use of one of two pneumatically-driven pincher devices. Most experiments were performed with a device to which a constant pneumatic pressure was applied, but from which no precise measure of applied force was obtained. In later experiments a different unit permitted a constant force to be pre-calibrated (2.5 N applied between 4 mm diameter, smooth surfaced jaws). Stimuli were applied to one of the two most lateral toes for 15 s every 3 min. Receptive fields were restricted to the foot area. The stimulus force used was always well above that required with these devices for eliciting withdrawal in conscious rats (N.A. Hartell, unpublished observations) but below that causing swelling of the foot with repeated application.

Bipolar recording electrodes were inserted percutaneously into hindlimb flexor muscles (Hartell & Headley, 1990). Extracellular recordings of single motoneurone reflex activity were made from single motor units (s.m.u.). Unit firing rate (see Figure 2), counts of spikes in stimulus related epochs and blood pressure were recorded on a chart recorder. The quantitative analysis presented below is based on counts of spikes evoked during the last 10 s of each pinch stimulus (see Parsons & Headley, 1989).

Drug administration and analysis of drug effects

Morphine hydrochloride (Richard Daniel), fentanyl citrate (Sublimaze, Janssen) and U-50,488H (*trans*-3,4-dichloro-N-methyl-N[2-(1pyrrolidinyl)-cyclohexyl] benzeneacetamide, Upjohn) were dissolved or diluted in isotonic saline and administered i.v. in a constant volume of 0.3 ml. All agonists were injected in a logarithmic base$_2$ cumulative dose regime, starting with a dose of 1 μg kg^{-1} for fentanyl and 1 mg kg^{-1} for morphine and U-50,488H. Doses were increased at 6 min intervals until the evoked response was reduced to below 20% of control. Fentanyl and U-50,488 reach their peak effect within 3 min of i.v. injection, and morphine usually within 6 min, as was observed following the last dose in each cumulative regime (not illustrated; but see Parsons & Headley, 1989; Parsons *et al.*, 1989). Most cells were tested with more than one opioid agonist. A subsequent drug was only administered after an interval of at least 30 min following recovery from the previous compound. The different agonists were therefore tested under closely comparable conditions.

Antagonism of morphine and U-50,488H was tested with cumulative i.v. doses of naloxone (Sigma) injected in a regime of 1, 10, 20, 50 and 100 μg kg^{-1} given at intervals of 6 min; administration was stopped when complete recovery of the response was obtained. Because U-50,488H is relatively short-lasting (see Figure 2) the degree of reversal by naloxone was assessed by comparing the recovery phase between two tests with U-50,488H, one without and one followed by naloxone (see Parsons *et al.*, 1989). Fentanyl was sensitive to naloxone but the dose-dependence of the antagonism was not studied. In some experiments fentanyl was used to assess whether naloxone had been adequately metabolized: it was injected at hourly intervals until its efficacy returned to pre-naloxone values.

Data are expressed as a percentage of control, where the control was taken as the mean of the three responses preceding the administration of the drug. Data were only accepted for analysis if the response recovered by at least 80% of the maximum effect of the drug, either spontaneously or following naloxone. Statistical significance was determined on pooled data by the non-parametric two-tailed Mann-Whitney U-test (Siegel & Castellan, 1988).

Results

General

Data were obtained from 84 s.m.u. in 63 rats. Spontaneous activity was low or absent in all experiments. The pre-drug neuronal firing rate during each response evoked by a noxious pinch stimulus (see Figure 2) was similar for the three groups: mean 20.6 $\pm$ 0.9 s.e.mean (n = 48) action potentials per second in spinally unoperated, 21.9 $\pm$ 1.7 (n = 15) in sham spinalized and 20 $\pm$ 2.2 (n = 21) in spinalized animals. All three opioid agonists reduced mechanical nociceptive reflexes in a dose-dependent and naloxone reversible manner.

Actions of the μ-agonists, fentanyl and morphine

Figure 1 shows pooled data of the effects of morphine in the three groups of animals. The mean ED_{50} was between 2 and 4 mg kg^{-1} and the dose necessary to depress the response below 20% of control was 4–8 mg kg^{-1} in all three groups (intact: n = 12, sham: n = 8, spinalized: n = 7); there were no significant differences between groups. The effects of morphine were fully reversed by doses of 10–20 μg kg^{-1} of naloxone (Figure 1).

Figure 1b shows that fentanyl was similarly potent in spinally unoperated and sham spinalized rats (ED_{50} 2–4 μg kg^{-1}) but that (unlike morphine) its potency was significantly reduced by spinalization (ED_{50} approximately 8 μg kg^{-1}).

Actions of the κ-agonist, U-50,488H

Typical effects of U-50,488H are illustrated in Figure 2 which shows s.m.u. recordings from three different animals, one in each experimental group, recorded under otherwise identical conditions. Pooled data are shown in Figure 3. In spinally unoperated animals the potency of this κ-opioid was similar to that of morphine (mean ED_{50} for both was 2–4 mg kg^{-1}). In sham spinalized animals U-50,488H was significantly more potent (mean ED_{50} approximately 1 mg kg^{-1}) whereas spinalization caused a 6 fold decrease in its potency (mean ED_{50} increased to approximately 8 mg kg^{-1}).

The ability of naloxone to antagonize the actions of U-50,488H was tested on a subset of these units (Figure 3b). Doses of 50–100 μg kg^{-1} of naloxone i.v. were effective in all

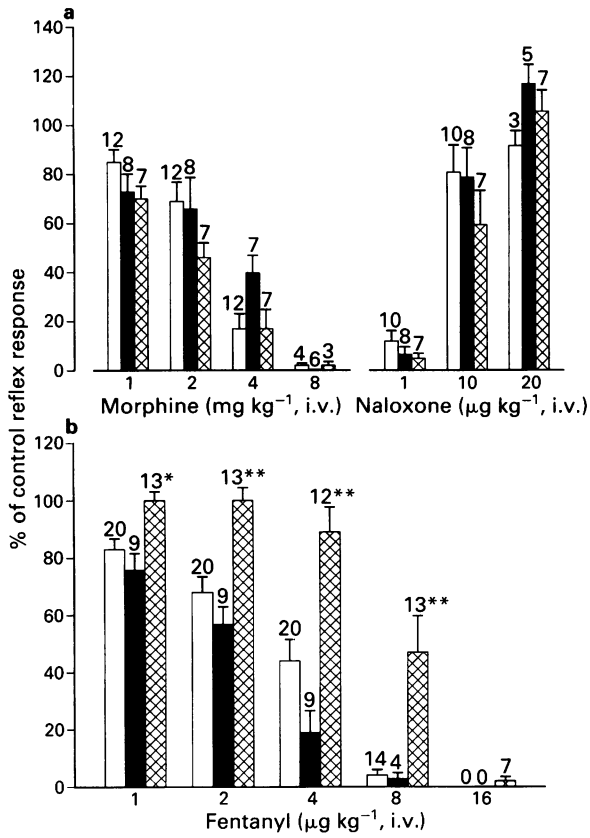

Figure 1 The effects of sham surgery and of spinalization on the potency of intravenous morphine (1–8 mg kg^{-1}, a) and fentanyl (1–16 μg kg^{-1}, b) in reducing reflex responses of single motoneurones to pinch stimuli: the spinally unoperated group is shown by open columns, the sham spinalized group by solid columns and the spinalized group by cross hatched columns. Naloxone (10–20 μg kg^{-1}, i.v.) was administered to most units immediately after the morphine tests and dose-dependently reversed the inhibition produced by morphine in all 3 groups. Error bars represent standard errors of the mean and the numbers above bars indicate the number of units recorded. Data from spinally unoperated and spinalized groups were compared statistically with those obtained from sham-spinalized rats. Significance was calculated by the Mann-Whitney U-test (* $P < 0.05$; ** $P < 0.01$).

three groups. These doses were about 5 times higher than those needed to reverse the effects of morphine (see Figure 1).

Discussion

The similarity of the firing rate during pinch stimuli for the three experimental groups suggests that tonic descending inhibition affects these nociceptive reflexes rather little under our control conditions. On the other hand the time spent looking for a stable unit was considerably shorter in spinalized rats, so that it appeared that the number of motoneurones that could be excited by the pinch stimuli was greater in this group, as might be expected from the lack of descending inhibition. The possibility that the intensity of the pinch stimuli was consistently different between the experimental groups is unlikely given the care that was taken to ensure constancy, between experiments, of the force applied.

The effects elicited by both morphine and U-50,488H were mediated by opioid receptors, for they were antagonized by low doses of naloxone. The five fold higher doses required to antagonize U-50,488H are consistent with the different sensitivity to naloxone of μ- and κ-opioid agonists as well as with binding site data (see Parsons *et al.*, 1989). Moreover the κ-agonist generally increased, whereas the μ-opioids reduced, arterial blood pressure. All these factors indicate that the agents were acting at different opioid receptors.

Our results suggest that under these experimental conditions, supraspinal actions do not contribute to the net suppression of spinal reflexes by morphine: this follows from the similar potency seen in spinally unoperated, sham spinalized and spinalized groups. This conclusion is similar to that obtained with systemic administration of morphine in other electrophysiological experiments (Le Bars *et al.*, 1979; 1980; Soja & Sinclair, 1983; Chitour *et al.*, 1986). Other authors, using behavioural tests of nociception, have however reported significant reductions of the effects of systemic morphine after producing lesions aimed at descending pathways (see Introduction).

These findings imply that some combination of the anaesthesia and the preparatory surgery may explain the greater effectiveness of morphine seen in electrophysiological recordings. In the present study the potency of morphine was not affected by the sham spinalization, suggesting that surgery *per se* was not the significant factor in the above studies. Various authors have suggested that the presence of general anaesthetics can influence the potency of opioids (see Advokat & Burton, 1987; Sinclair *et al.*, 1988). Whilst this is likely for the supraspinal actions of morphine, it is not the case for the direct spinal effects of μ-opioids: using the same technique as in the current study, Hartell & Headley (1989) found that the presence of α-chloralose (as used here) did not affect the direct spinal potency with which μ-opioids depressed nociceptive reflexes.

The potency of the other μ-agonist tested, fentanyl, was surprisingly affected differently from morphine by spinalization: following spinal section, 2–4 times the dose was necessary to have the same effect as in sham-operated animals. This difference between morphine and fentanyl remains unexplained. It is hard to perceive how the much greater lipophilicity of fentanyl could differentially affect the responses between the three experimental groups following systemic administration. Whether the difference could relate to μ-receptor subtypes, the distribution of which is reported to be different in cord and supraspinal regions (see Paul *et al.*, 1989) remains to be assessed.

U-50,488H showed clear inter-group differences. Thus the surgery of sham-spinalization doubled the potency of this κ-opioid, whilst additional spinalization decreased the potency about 6 fold. As a result U-50,488H was only half as potent in spinalized as in unoperated spinally intact animals.

The simplest interpretation of the latter findings is that the surgery sensitizes some unidentified supraspinal centres to the actions of κ- (but not μ-) opioid agonists. It is possible that this is related to the selective increase of κ-receptors seen in the periaqueductal grey during arthritis induced by Freund's Complete Adjuvant (Millan *et al.*, 1987).

When the cord is transected this supraspinal effect is removed, leaving only the direct spinal actions of U-50,488H. This κ-agonist (unlike morphine) is evidently somewhat weaker at spinal compared with the supraspinal sites that control descending inhibitions (see also Takemori *et al.*, 1988; Millan *et al.*, 1989). The potency of U-50,488H in the present sample of spinalized rats (ED_{50} 4–8 mg kg^{-1}) was similar to that in the larger sample analyzed previously (ED_{50} 4.9 mg kg^{-1}, $n = 31$, Parsons *et al.*, 1989). These doses of U-50,488 are within the range observed to be effective in behavioural tests of nociception (see Parsons *et al.*, 1989; Millan, 1989). All these data indicate that κ-opioids are effective at the level of the spinal cord.

In summary, this study appears to be the first in which selective μ- and κ-opioids have been compared electrophysiologically for spinal vs. supraspinal actions; moreover it is one of very few studies in which sham spinalization was included. Neither surgical trauma nor spinalization affected the potency of morphine on the reflex tested, indicating that under these conditions morphine reduces spinal nociceptive reflexes by a direct action within the cord. The different effects of fentanyl, which was weaker in spinalized rats, suggests that morphine and fentanyl may activate different groups of μ-receptors with

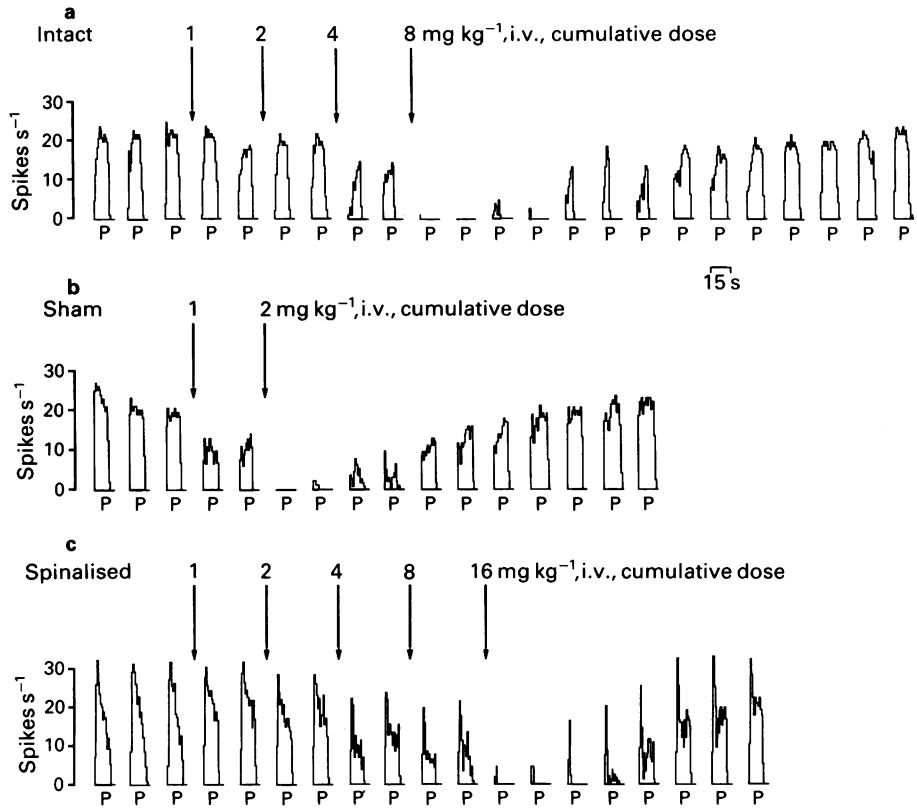

Figure 2 Effects of the κ-opioid U-50,488H on reflex responses to noxious pinch stimuli. The figure shows traces of original records of the firing rate of single motor units in hindlimb flexor muscles in response to 15 s pinch stimuli (P) repeated every 3 min (the pen recorder was halted between stimuli). One example is shown for each of the experimental groups, spinally intact (a), sham spinalization (b) and spinalized (c). The traces illustrate the typical differences in the potency of this opioid between groups.

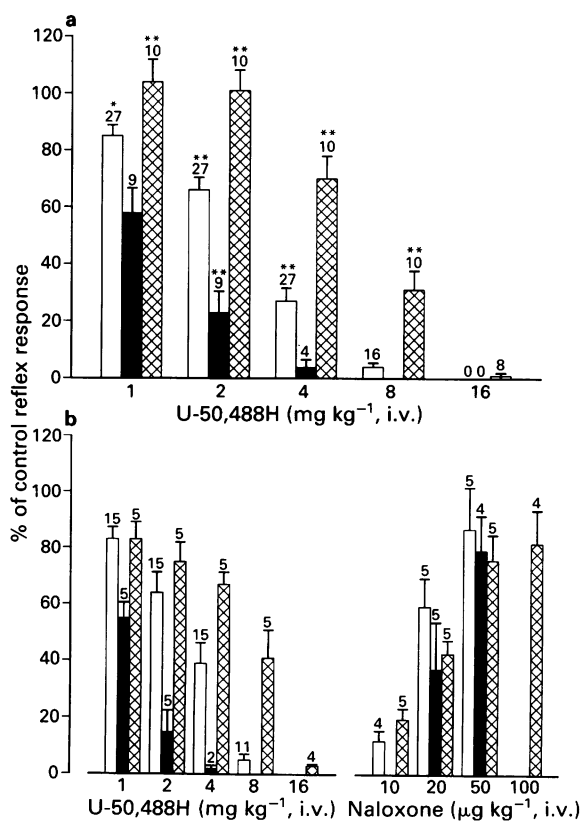

different spinal vs. supraspinal distributions. Supraspinally mediated inhibitions of spinal reflexes are activated by lower doses of the κ-agonist U-50,488 than those having direct spinal effects, but the latter still occur at behaviourally relevant doses. Trauma increased the potency of U-50,488, an effect which must be borne in mind in other studies involving surgical preparation.

We wish to thank Dr N.A. Hartell for useful discussions, Ms Mel Watson for technical assistance, Upjohn for a gift of U-50,488, and the Wellcome Trust and the Spanish Ministry of Education for financial support.

Figure 3 Effects of sham and actual spinalization on the potency of the κ-opioid agonist U-50,488 on spinal nociceptive reflexes. Pooled data presented as in Figure 1 for spinally unoperated (open columns), sham spinalized (solid columns) and spinalized groups of rats (hatched columns). Note that it was not necessary to test the higher doses in all groups. Pooled data from all tests are shown in (a); (b) shows the subset of units on which naloxone reversal of U-50,488 was assessed. The left panel indicates the effectiveness of U-50,488 on these units, and the right panel the reversal of these reductions by naloxone (10–100 μg kg^{-1}). Naloxone was similarly effective in the three groups despite the different doses of agonist administered. Data from spinalized and spinally unoperated animals were compared statistically with the data from sham-operated rats (Mann-Whitney U-test, * $P < 0.05$; ** $P < 0.01$).

References

ADVOKAT, C. & BURTON, P. (1987). Antinociceptive effect of systemic and intrathecal morphine in spinally transected rats. *Eur. J. Pharmacol.*, **139**, 335–343.

BARTON, C., BASBAUM, A.I. & FIELDS, H.L. (1980). Dissociation of supraspinal and spinal actions of morphine: a quantitative evaluation. *Brain Res.*, **188**, 487–498.

BASBAUM, A.I., MARLEY, N.J.E., O'KEEFE, J. & CLANTON, C.H. (1977). Reversal of morphine and stimulus produced analgesia by subtotal spinal cord lesions. *Pain*, **3**, 43–56.

CALTHROP, J. & HILL, R.G. (1983). The action of k-agonists on the nociceptive responses of neurones in the medullary dorsal horn of the anaesthetized rat. *Life Sci.*, **33**, Suppl. 1, 541–544.

CHITOUR, D., VILLANUEVA, L. & LE BARS, D. (1986). Lesions of dorsolateral funiculi (DLF) do not affect the depressive effects of systemic morphine upon dorsal horn convergent neuronal activities related to pain in the rat. *Brain Res.*, **377**, 397–402.

DONG, X-W., PARSONS, C.G. & HEADLEY, P.M. (1991). Effects of intravenous μ and κ receptor agonists on sensory responses of convergent neurones in the dorsal horn of spinalized rats. *Br. J. Pharmacol.*, **103**, 1230–1236.

HARTELL, N.A. & HEADLEY, P.M. (1989). The potencies of several injectable anaesthetics on a spinal, nociceptive reflex in both decerebrate and anaesthetised rats. *Br. J. Pharmacol.*, **97**, 496P.

HARTELL, N.A. & HEADLEY, P.M. (1990). Spinal effects of four injectable anaesthetics on nociceptive reflexes in rats: a comparison of electrophysiological and behavioural measurements. *Br. J. Pharmacol.*, **101**, 563–568.

HARTELL, N.A. & HEADLEY, P.M. (1991). Preparative surgery enhances the direct spinal actions of three injectable anaesthetics in the anaesthetized rat. *Pain.* (in press).

HARTELL, N.A., HEADLEY, P.M. & PARSONS, C.G. (1990). The degree of surgical intervention influences the potency with which injectable anaesthetics depress spinal nociceptive reflexes in the adult rat. *J. Physiol.*, **420**, 28P.

HAYES, R.L., PRICE, D.D., BENNETT, G.J., WILCOX, G.L. & MAYER, D.J. (1978). Differential effects of spinal cord lesions on narcotic and non-narcotic suppression of nociceptive reflexes: further evidence for the physiologic multiplicity of pain modulation. *Brain Res.*, **155**, 91–101.

HEADLEY, P.M., PARSONS, C.G., WEST, D.C. & DONG, X-W. (1989). On the influence of anaesthesia, stimulus intensity and drug access in pharmacological tests of sensory processing in the superficial dorsal horn. In *Processing of Sensory Information in the Superficial Dorsal Horn of the Spinal Cord.* ed. Cervero, F., Bennett, G.J. & Headley, P.M. *NATO ASI Series A. Life Sciences*, Vol. 176, pp. 499–511. New York: Plenum Press.

HERRERO, J.F. & HEADLEY, P.M. (1990). Relative spinal and supraspinal potencies of mu and kappa opioids in reducing spinal nociceptive reflexes. In *New Leads in Opioid Research.* ed.: Van Ree, J.M., Mulder, A.H., Wiegant, V.M. & Greidanus, T.B.W. *Int. Cong. Ser.*, Vol. 914, pp. 59–60. Amsterdam: Excerpta Medica.

HOPE, P.J., FLEETWOOD-WALKER, S.M. & MITCHELL, R. (1990). Distinct antinociceptive actions mediated by different opioid receptors in the region of lamina I and laminae III–V of the dorsal horn of the rat. *Br. J. Pharmacol.*, **101**, 477–483.

KNOX, R.J. & DICKENSON, A.H. (1987). Effects of selective and non-selective κ-opioid receptor agonists on cutaneous C-fibre-evoked responses of rat dorsal horn neurones. *Brain Res.*, **415**, 21–29.

LE BARS, D., RIVOT, J.P., GUILBAUD, G., MENETREY, D. & BESSON J.M. (1979). The depressive effect of morphine on the C fibre response of dorsal horn neurones in the spinal rat pretreated or not by pCPA. *Brain Res.*, **176**, 337–353.

LE BARS, D., GUILBAUD, G., CHITOUR, D. & BESSON, J.M. (1980). Does systemic morphine increase descending inhibitory controls of dorsal horn neurones involved in nociception? *Brain Res.*, **202**, 223–228.

LEIGHTON, G.E., RODRIGUEZ, R.E., HILL, R.G. & HUGHES, J. (1988). κ-Opioid agonists produce antinociception after i.v. and i.c.v. but not intrathecal administration in the rat. *Br. J. Pharmacol.*, **93**, 553–560.

MILLAN, M.J. (1989). Kappa-opioid receptor-mediated antinociception in the rat. I. Comparative actions of mu- and kappa-opioids against noxious thermal, pressure and electrical stimuli. *J. Pharmacol. Exp. Ther.*, **251**, 334–341.

MILLAN, M.J. (1990). κ-Opioid receptors and analgesia. *Trends Pharmacol. Sci.*, **11**, 70–76.

MILLAN, M.J., CZŁONKOWSKI, A., LIPKOWSKI, A. & HERZ, A. (1989). Kappa-opioid receptor-mediated antinociception in the rat. II. Supraspinal in addition to spinal sites of action. *J. Pharmacol. Exp. Ther.*, **251**, 342–350.

MILLAN, M.J., MORRIS, B.V., COLPAERT, F.C. & HERZ, A. (1987). A model of chronic pain in the rat: high-resolution neuroanatomical approach identifies alterations in multiple opioid system in the periaqueductal grey. *Brain Res.*, **416**, 349–353.

MURFIN, R., BENNETT, G.J. & MAYER, D.J. (1976). The effect of dorsolateral spinal cord (DLF) lesions on analgesia from morphine microinjected into the periaqueductal gray matter (PAG) of the rat. *Neuroci. Abstr.*, **2**, 946.

PARSONS, C.G. & HEADLEY, P.M. (1989). Spinal antinociceptive actions of μ- and κ-opioids: the importance of stimulus intensity in determining 'selectivity' between reflexes to different modalities of noxious stimulus. *Br. J. Pharmacol.*, **98**, 523–532.

PARSONS, C.G., WEST, D.C. & HEADLEY, P.M. (1989). Spinal antinociceptive actions and naloxone reversibility of intravenous μ- and κ-opioids in spinalized rats: potency mismatch with values reported for spinal administration. *Br. J. Pharmacol.*, **98**, 533–543.

PAUL, D., BODNAR, R.J., GISTRAK, M.A. & PASTERNAK, G.W. (1989). Different μ receptor subtypes mediate spinal and supraspinal analgesia in mice. *Eur. J. Pharmacol.*, **168**, 307–314.

SCHMAUSS, C. & YAKSH, T. (1984). *In vivo* studies on spinal opiate receptor systems mediating antinociception. II. Pharmacological profiles suggesting a differential association of mu, delta and kappa receptors with visceral chemical and cutaneous thermal stimuli in the rat. *J. Pharmacol. Exp. Ther.*, **228**, 1–12.

SIEGEL, S. & CASTELLAN, N.J. (1988). *Non-parametric Statistics for the Behavioural Sciences.* 2nd edition. New York: McGraw-Hill.

SINCLAIR, J.G., MAIN, C.D. & LO, F.G. (1988). Spinal vs. supraspinal actions of morphine on the rat tail-flick reflex. *Pain*, **33**, 357–362.

SOJA, P.J. & SINCLAIR, J.G. (1983). Spinal vs. supraspinal actions of morphine on cat spinal cord multireceptive neurons. *Brain Res.*, **273**, 1–7.

STEVENS, C.W. & YAKSH, T.L. (1986). Dynorphin A and related peptides administered intrathecally in the rat: A search for putative kappa opiate receptor activity. *J. Pharmacol. Exp. Ther.*, **238**, 833–838.

TAKEMORI, A.E., GEGONIA, Y.H., NAESETH, J.S. & PORTOGHESE, P.S. (1988). Norbinaltorphimine, a highly selective kappa-opioid antagonist in analgesic and receptor binding assays. *J. Pharmacol. Exp. Ther.*, **246**, 255–258.

WILCOX, G.L. & HWANG, S. (1984). Selective analgesia in mice after intrathecal kappa opioid agonists. *Proc. 9th Int. Cong. Pharmacol.*, p. 267. London: Macmillan.

YAKSH, T.L. (1984). Multiple opioid receptor systems in brain and spinal cord. *Eur. J. Anaesthesiol.*, **1**, 171–243.

YAKSH, T.L. & NOUEIHED, R. (1985). The physiology and pharmacology of spinal opiates. *Annu. Rev. Pharmacol. Toxicol.*, **25**, 433–462.

YAKSH, D.C. & RUDY, T.A. (1977). Studies on the direct spinal action of narcotics in the production of analgesia in the rat. *J. Pharmacol. Exp. Ther.*, **202**, 411–428.

(Received January 25, 1991
Revised April 16, 1991
Accepted April 26, 1991)

Br. J. Pharmacol. (1991), **104**, 171–177

1-*O*-hexadecyl-2-acetyl-*sn*-glycero-3-phospho (N,N,N trimethyl) hexanolamine: an analogue of platelet-activating factor with partial agonist activity

George Grigoriadis & [1]Alastair G. Stewart

Department of Physiology, University of Melbourne, Parkville, Victoria 3052, Australia

1 During studies of the role of platelet-activating factor (PAF) in macrophage superoxide anion generation (O_2^{-1}), we identified an agonist action of the putative PAF receptor antagonist 1-*O*-hexadecyl-2-acetyl-*sn*-glycero-3-phospho (N,N,N-trimethyl) hexanolamine (hexanolamine PAF) in guinea-pig macrophages. The 1-O-octadecyl form of this compound has specific antagonist actions at PAF receptors.

2 The agonist properties of hexanolamine PAF were examined in rabbit washed platelets (aggregation) and in guinea-pig peritoneal macrophages (O_2^- generation).

3 Hexanolamine PAF induced significant platelet aggregation (50% of the PAF maximum). However, the omission of bovine serum albumin (BSA) from the Tyrode buffer resulted in a diminution of the response of washed platelets during storage for 24 h at 4°C (7% of PAF maximum), whereas the maximum response to PAF was unaffected by storage for this period, irrespective of the presence of BSA.

4 Platelet aggregation induced by hexanolamine PAF was not accompanied by a detectable increase in intracellular calcium $[Ca^{2+}]_i$, whereas the aggregation response to PAF was preceded by a large rise in $[Ca^{2+}]_i$.

5 Hexanolamine PAF induced O_2^- generation in adherent macrophages, with a maximum response 45% of that to PAF. Hexanolamine PAF (100 nM), at a concentration equi-effective with PAF (1 nM) for stimulation of O_2^- generation in macrophages, induced an increase in $[Ca^{2+}]_i$ which was significantly less than that induced by PAF.

6 PAF concentration-response curves were constructed in platelets or macrophages following pretreatment with hexanolamine PAF (0.1 and 1 μM). The interaction between PAF and the putative partial agonist (hexanolamine PAF) had the characteristics expected of a partial agonist interacting with a full agonist.

7 Platelet aggregation induced by hexanolamine PAF was antagonized non-competitively by the PAF receptor antagonist, WEB 2086, whereas antagonism of PAF-induced aggregation by WEB 2086 was competitive. Macrophage O_2^- generation induced by hexanolamine PAF or PAF was antagonized by WEB 2086.

8 These data indicate that hexanolamine PAF is a partial agonist at PAF receptors in macrophages and platelets. The inability of hexanolamine PAF to increase $[Ca^{2+}]_i$ in platelets suggests that PAF receptors may be coupled to platelet aggregation by both Ca^{2+}-dependent and -independent pathways.

Keywords: Intracellular calcium; macrophages; platelet-activating factor; platelet aggregation; receptors; signal transduction

Introduction

Platelet-activating factor (PAF) is a biologically active phospholipid with pathophysiological effects extending beyond platelet activation to include mediator roles in inflammation (Braquet *et al.*, 1987; Prescott *et al.*, 1990), allergy and asthma (Barnes *et al.*, 1988).

The existence of specific receptors for PAF is supported by its potency, the precise structural requirements for biological activity, stereospecificity, the wide range of potent and specific PAF antagonists and PAF-specific desensitization in a number of cell types (see Hwang, 1990 for a review). Notwithstanding the evidence in favour of receptor-mediated actions, it has been suggested that PAF may exert physicochemical actions promoting membrane fusion (Bratton & Henson, 1989).

PAF was originally described as a soluble factor released by rabbit basophils (Beneviste *et al.*, 1972). However, a range of cell types including endothelial cells (Prescott *et al.*, 1990), are now known to retain most, if not all, the PAF that is synthesized. This distribution prompted the examination of the potential role of cell-associated PAF. Several studies have provided evidence of a second messenger role for PAF on the basis of the inhibitory effects of PAF receptor antagonists (Stewart *et al.*, 1990), inhibitors of PAF biosynthesis (Remy *et al.*, 1990) and the existence of intracellular PAF receptors (Marcheselli *et al.*, 1990).

During studies of the role of cell-associated PAF in macrophages, we examined the effects of the putative PAF receptor antagonist, hexanolamine PAF (1-*O*-hexadecyl-2-acetyl-*sn*-glycero-3-phospho (N,N,N-trimethyl)hexanolamine). This compound differs from that reported by Tokumura *et al.* (1985) to inhibit platelet aggregation, in having a hexadecyl, rather than an octadecyl alkyl ether chain on C_2 of the glycerol backbone. Our interest in hexanolamine PAF arose from the likelihood that this close structural analogue of PAF would be distributed within membranes in a manner similar to that of PAF and may therefore gain access to sites of action not available to other PAF receptor antagonists. It was considered that such a compound could facilitate the elucidation and the involvement of endogenous PAF in signal transduction mechanisms.

Methods

Platelets

Adult rabbits (2–4 kg) were anaesthetized by intravenous administration of Saffan (alphaxalone and alphadalone).

[1] Author for correspondence.

Blood was collected via a cannula placed in a carotid artery and was immediately mixed with trisodium citrate (0.38% $w v^{-1}$, final concentration) and centrifuged at 150*g* for 20 min at ambient temperature (20–24°C) (Stewart & Dusting, 1988). The resulting platelet rich plasma (PRP) was transferred to polypropylene tubes and prostacyclin (PGI_2, 300 ng ml^{-1}) was added to act as an anti-aggregatory agent during the washing procedure (Vargas *et al.*, 1982). Platelets were isolated by centrifugation (10 min at 1000*g*) and resuspended in HEPES-buffered Tyrode solution. This centrifugation/resuspension step was repeated once and the platelet count of the final solution wsa determined with a haemocytometer. The platelets were resuspended at a concentration of 2×10^8 ml^{-1} in Tyrode buffer containing 1.8 mM Ca^{2+} with or without 0.25% BSA. The washed platelets were kept at ambient temperature for at least 4 h, during which time the effects of PGI_2 subsided. In studies on the effect of storage on responsiveness, platelets were maintained at 4°C overnight and were brought to ambient temperature for 2 h before use on the following day.

Platelet aggregation

Aggregation studies were carried out at 37°C in a dual chamber aggregometer (Chrono-Log, Aggro-meter Model 540) by the spectrophotometric technique. The reference cell contained a 1 in 10 dilution of platelets and defined 100% light transmission. The aggregation data are presented either as percentage light transmission or as a percentage of the maximum response to PAF. The PAF receptor antagonist WEB 2086, was added 1 min before the addition of PAF or hexanolamine PAF, longer pre-incubation with WEB 2086 did not increase antagonism of PAF or hexanolamine PAF responses. In experiments examining the interaction of hexanolamine PAF with PAF, the response to hexanolamine PAF was allowed to plateau (approximately 2 min) before addition of PAF.

Macrophage isolation

Male Dunkin-Hartley guinea-pigs (0.3–0.7 kg) were killed by a sharp blow to the head and rapidly exsanguinated. Resident macrophages were obtained by peritoneal lavage: a 50 ml volume of sterile, heparinized (50 u ml^{-1}), phosphate-buffered saline was injected into the peritoneum and the cavity was gently massaged for ~1 min. The lavage fluid was aspirated and the cells were isolated by centrifugation (1000*g*, 4°C, 10 min) (Stewart & Dusting, 1988). The supernatant was decanted and the cells were counted and resuspended at 10^6 ml^{-1} in either 5 ml of RPMI 1640 (20% foetal calf serum (FCS), penicillin 100 u ml^{-1}, streptomycin 100 μg ml^{-1}) for cells adhered to cell culture plates or Tyrode buffer containing 0.25% bovine serum albumin (TBSA) (composition (mM): HEPES 5, NaCl 137, D-(+)-glucose 11, $NaHCO_3$ 11.9, KCl 2.7, $MgCl_2$ 0.26, NaH_2PO_4 0.4, $CaCl_2$ 1.8) for cells in suspension.

In some experiments, peritoneal lavage cells were resuspended in 0.25% TBSA at a concentration of 10^6 ml^{-1}. These cells were 70–85% macrophages as assessed by non-specific esterase or Giemsa staining which differentiates macrophages from other cell types likely to be in the peritoneal lavage fluid (including erythrocytes, lymphocytes and occasionally low numbers of neutrophils). During the assay period (40–60 min), the cells were kept in polypropylene tubes that were rocked through a 45° angle at 22 min^{-1} to prevent adherence of the cells to the sides of the tubes. The use of peritoneal lavage cell suspensions facilitated on-line measurement of cytochrome C reduction providing a detailed record of the time-course of O_2^- generation. However, the sequential nature of these experiments limited the amount of data that could be obtained. Thus, in a number of experiments, adherent peritoneal cells were used, which allowed parallel processing of a large number of aliquots of cells. Following isolation by centrifugation, cells were resuspended in RPMI 1640 at a concentration of 10^6 ml^{-1}, dispensed (0.5 ml) into 24 well plastic culture plates and allowed to adhere for at least 2 h at 37°C. At the end of this period non-adherent cells were removed and the remaining cells (80–95%) were washed twice. This method consistently provided cells which were greater than 98% viable as assessed by the trypan blue exclusion and greater than 90% were macrophages as defined by non-specific esterase and Giemsa staining.

Superoxide anion generation

Superoxide anion (O_2^-) generation was determined by a colorimetric assay based on the reduction of cytochrome C (Johnston *et al.*, 1978). The generation was followed by measuring the absorbance change at 550 nm relative to an aliquot of cells treated with superoxide dismutase (SOD, 30 u ml^{-1}) in a U-2000 double-beam spectrophotometer (Htachi Ltd., Japan). Levels of O_2^- were quantified using the extinction coefficient of 21.1 mM^{-1} and expressed as nmol per 10^6 cells. Superoxide anion was measured in macrophages in suspension or in those adhered to plastic culture plates depending on the objectives of the experiment (time-course or concentration-response). There were no differences between adherent or non-adherent macrophages in the maximum responses or the potency of PAF or of hexanolamine PAF in stimulating O_2^{-1} generation. Superoxide anion generation was measured over a period of 5 min which was adequate for maximum responses to be achieved.

Non-adherent macrophages

Briefly, 1 ml of peritoneal lavage cell suspension (10^6 cells) was added to 1 ml of freshly prepared cytochrome C (2 mg ml^{-1}) in a cuvette and preincubated for 2 min with stirring (>98% viable after the 2 min period) at 37°C in the spectrophotometer cuvette.

Adherent macrophages

The medium overlaying adherent macrophages was removed and replaced with Tyrode buffer containing 0.25% BSA and cytochrome C (1 mg ml^{-1}) and preincubated for 15 min (Stewart & Dusting, 1988). Following incubation with various agonists, the supernatants were aspirated, transferred to plastic centrifuge tubes, and spun at 1000*g* to remove any debris or detached cells. Superoxide anion generation was measured as the increase in cytochrome C reduction compared with that in a well treated with SOD (30 u ml^{-1}).

Intracellular calcium measurements in platelets

Platelets were resuspended in Tyrode buffer in the presence or absence of BSA as indicated at a concentration of 2×10^8 ml^{-1}, left for a period of at least 4 h then incubated for 30 min at 37°C with 2 μM Fura-2 acetoxy methyl ester. The platelets were then isolated by centrifugation, the supernatant was decanted and a 15 min period at 37°C allowing cytosolic esterases to cleave the acetoxy methyl ester resulting in the trapping of the Fura-2 anion. The measurement of $[Ca^{2+}]_i$ was carried out with a F-2000 fluorescence spectrophotometer (Hitachi) using excitation wavelengths alternating at 0.5 s intervals between 340 and 380 nm and the emission intensity was continuously monitored at 510 nm.

Intracellular calcium measurements in macrophages

The use of non-adherent macrophages for the measurement of $[Ca^{2+}]_i$ was required to replicate the conditions used for studies in platelets.

Leakage of Fura-2 was reported to be greatly decreased at temperatures below 37°C in a variety of cell types (Malgaroli *et al.*, 1987), so macrophages were loaded at room tem-

perature for a period of 40 min. The cells were washed with TBSA and incubated for 15 min at 37°C for cleavage of the acetoxy methyl ester, and washed once with TBSA to remove any extracellular Fura-2. The apparent increase in $[Ca^{2+}]_i$ over the time course due to the efflux of the dye has been accounted for by subtracting apparent $[Ca^{2+}]_i$ in unstimulated cells from that obtained in stimulated cells. The data resulting from this transformation represent agonist-induced increases in $[Ca^{2+}]_i$.

Stimulants were added in a volume of less than 10 μl after 2 min equilibration with stirring at 37°C. At the end of the measurement period, cells were lysed with Triton X-100 to obtain the fluorescence ratio of Fura-2 at saturating concentrations of Ca^{2+}, then the chelating agent, EGTA (10 mM) was added to obtain the fluorescence ratio of Fura-2 at zero Ca^{2+} levels. These ratios were used to calculate the $[Ca^{2+}]_i$ according to Grynkiewicz *et al.* (1985).

Data analysis

Concentration-response data for agonists were analysed by linear regression to determine the negative logarithm of the concentration that induced 50% of the maximum response ($-\log EC_{50}$), the individual differences were subsequently identified by unpaired *t* test using Bonferoni's correction for multiple comparisons. An analysis of variance (ANOVA) with repeated measures was performed when paired sets of concentration-response curves were being compared. Comparisons of single groups were made by a two-tailed paired *t* test or unpaired *t* test. A *P* value of less than 0.05 was considered to be significant. Data are presented as the means ± standard errors (s.e.) of the means of *n* observations. Concentration-response curves were fitted to a sigmoidal curve using the graphics software *Fig P* (Biosoft).

Materials

All reagents and solvents used in this study were of analytical or higher grade. RPMI 1640 and FCS were obtained from CSL (Australia) and Flow Laboratories respectively. Chemicals were obtained from the following sources: BSA, grade 5, essentially fatty acid-free; cytochrome C (horse heart type III); EGTA (ethylenebis(oxyethylenenitrilo) tetraacetic acid; formyl-methionyl-leucyl-phenylalanine (fMLP); Giemsa stain; fura-2 acetoxy methyl ester; α-naphtyl acetate esterase kit; probenecid; superoxide dismutase; Tyrode salts (Sigma Chemical Co.); hexadecyl platelet activating-factor (PAF); hexanolamine PAF (1-*O*-hexadecyl-2-acetyl-*sn*-glycero-3-phospho (N,N,N-trimethyl) hexanolamine · H_2O) (Novabiochem); HEPES (N-2-hydroxy ethylpiperazine-N-2-ethane sulphonic acid, BDH Chemicals); heparin (Fisons Pty. Ltd.); CV-6209 (2-[N-acetyl-N-(2-methoxy-3-octadecyl carbamoyloxypropoxy carbonyl) aminomethyl]-1-ethylpyridinium chloride) (Takeda Chemical Industries Ltd.); WEB 2086 (3-(4-(2-chlorophenyl)-9-methyl-6H-thieno(3,2-f), (1,2,4)-triazolo,(4,3-a), (1,4)-diazepine-2-yl)-1-(4-morpholinyl)-1-propanone), (Boehringer Ingelheim, West Germany); BN-52021 (9H-1,7a-(epoxymethano)-1H,6aH-cyclopenta(c)furo (2,3-b)furo-(3',2':3,4) cyclopenta(1,2-d)furan-5,9,12-(4H)-trione,3-tert-butylhexahydro-8-methyl) (Institut Henri Beaufour, France).

Results

The effect of hexanolamine PAF on platelet aggregation

PAF (0.01–1 nM) induced aggregation of platelets with a $-\log EC_{50}$ value of 10.13 ± 0.06 (Figure 1a). Hexanolamine PAF (0.03–3 μM) induced aggregation of platelets with a potency (6.75 ± 0.09) and maximum response (46 ± 7%) significantly less than those of PAF ($P < 0.05$, unpaired *t* test) (Figure 1a). Our initial studies indicated some variability in the height of the maximum response to hexanolamine PAF. The reasons for this variability were examined by systematic studies of the effects of platelet storage and the presence of BSA in the storage medium on the hexanolamine PAF response. The aggregation response to hexanolamine PAF was either absent or markedly decreased in platelets maintained in Tyrode solution in the absence of BSA (Table 1). In contrast, there were no differences in the maximum responses to PAF in platelets tested at 4 h and at 24 h after isolation, irrespective of the presence of BSA in the Tyrode solution (Table 1). In platelet

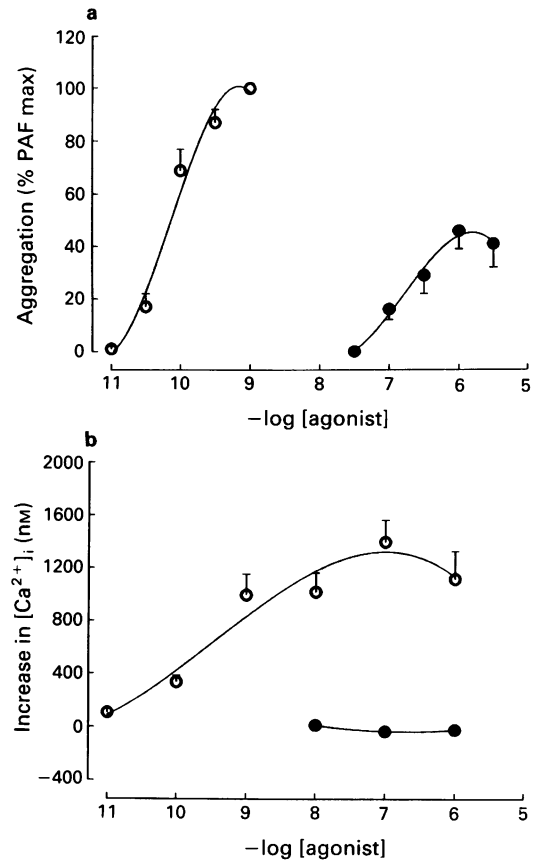

Figure 1 PAF (○) and hexanolamine PAF (●) induced aggregation (a) and increases in $[Ca^{2+}]_i$ (b) in rabbit platelets. Ordinate scales: (a) aggregation response, normalized to the maximum aggregation induced by PAF (1 nM); (b) peak increase in $[Ca^{2+}]_i$ 10–15 s after addition of stimulus (nM increase above the basal level). Abscissa scales: −logarithm of the molar concentration of the agonist. Data are presented as the means of (a) 9–14 and (b) 7–9 observations and vertical lines indicate one s.e.mean.

Table 1 The effect of storage and of bovine serum albumin (BSA) on PAF or hexanolamine PAF-induced platelet aggregation

Agonist	*Time*[2]	*Aggregation*[1] *+ BSA*	*− BSA*
PAF	4 h	74 ± 11 (8)	90 ± 1 (4)
(0.1 nM)	18–24 h	65 ± 13 (7)	90 ± 4 (7)
Hexanolamine PAF	4 h	52 ± 10 (8)	34 ± 12 (4)
(1 μM)	18–24 h	40 ± 9 (7)	6 ± 4* (7)

* $P < 0.05$, unpaired *t* test, compared with response obtained in the presence of BSA.
Data are presented as the mean ± s.e. of the mean of *n* observations.
[1] Responses for aggregation are expressed as percentage increase in light transmission.
[2] Period following platelet isolation.

preparations in which hexanolamine PAF was inactive in stimulating platelet aggregation (24 h, no BSA), the aggregation induced by PAF could still be antagonized by hexanolamine PAF (data not shown).

Intracellular calcium in platelets

PAF induced a concentration-dependent increase in $[Ca^{2+}]_i$ which paralleled the PAF-induced aggregation (Figure 1a). However, at a low concentration, PAF (0.01 nM) induced an increase in $[Ca^{2+}]_i$ (108 ± 29 nM) without inducing aggregation (1 ± 1%). Hexanolamine PAF (1 μM) induced a maximal aggregation response (46 ± 7%) with no significant effect on $[Ca^{2+}]_i$ (−21 ± 33 nM) (Figure 1b). Pretreatment of platelets for 1 min with hexanolamine PAF (0.1 and 1.0 μM) significantly inhibited the rise in $[Ca^{2+}]_i$ induced by PAF (1 nM) ($P < 0.05$, two-way ANOVA with repeated measures) (Figure 2).

Antagonism of platelet aggregation by the PAF receptor antagonist WEB 2086

To determine whether hexanolamine PAF was activating PAF receptors, we examined the inhibitory effect of the PAF receptor antagonist WEB 2086 on PAF and hexanolamine PAF-induced aggregation in platelets (Figure 3). As expected, WEB 2086 produced parallel rightward shifts of the concentration-response curve for PAF-induced aggregation without affecting the maximum responses ($P < 0.05$, paired t test) (Figure 3a). In contrast, WEB 2086 produced non-parallel rightward shifts of the concentration-response curve to hexanolamine PAF and significantly depressed ($P < 0.05$, paired t test) the maximum responses at higher concentrations (10–100 nM) (Figure 3b).

Interaction between hexanolamine PAF and PAF in platelets

The initial studies with hexanolamine PAF were suggestive of partial agonism, since the maximum responses were significantly less than those induced by PAF in platelets ($P < 0.05$, paired t test). Concentration-response curves to the full agonist were constructed in the presence of fixed concentrations of the putative partial agonist, hexanolamine PAF (Figure 4). Responses to PAF which were larger than those to hexanolamine PAF pretreatment were inhibited in a concentration-dependent manner (Figure 4a).

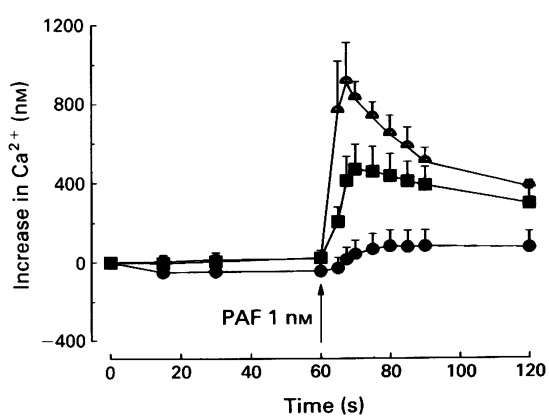

Figure 2 Effect of pretreatment with hexanolamine PAF (0.1 μM, ■ and 1 μM, ●) on PAF (1 nM)-induced rises in $[Ca^{2+}]_i$ in platelets. PAF was added 60 s after the addition of hexanolamine PAF as indicated by the arrow. Ordinate scale: increase in $[Ca^{2+}]_i$ over the basal (nM). Abscissa scale: the time (s) after the addition of hexanolamine PAF or the vehicle, Tyrode buffer (0.25% BSA, TBSA, ⌓). Data are presented as the means of 8 observations and vertical lines represent one s.e.mean.

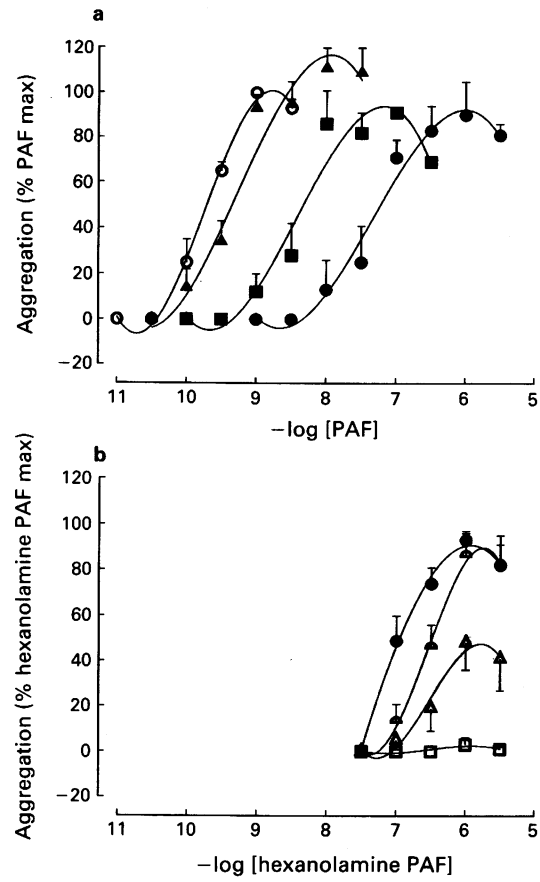

Figure 3 Effect of WEB 2086 (1–100 nM) pretreatment of PAF (a) or hexanolamine PAF (b) -induced aggregation of platelets. Ordinate scales: aggregation (a) normalized to a percentage of the maximum response to PAF; (b) normalized to a percentage of the maximum response to hexanolamine PAF. Platelets were pretreated with (a): the vehicle, TBSA (○); WEB 2086 10 nM, (▲); 100 nM, ■; 1 μM, (●); in (b): the vehicle TBSA (●); WEB 2086 1 nM (⌓); 10 nM (△); 100 nM (□). Abscissa scales: −logarithm of the molar concentration of the agonist. Data are presented as the means of (a) 5 and (b) 6–8 observations and vertical lines indicate one s.e.mean.

Activation of adherent macrophages by hexanolamine PAF

Previous studies suggest that PAF receptors in macrophages differ from those on platelets (Lambrecht & Parnham, 1986; Stewart & Dusting, 1988). It was therefore of interest to determine whether the differences between the agonist actions of PAF and hexanolamine PAF observed in platelets were also seen in macrophages.

In adherent macrophages, hexanolamine PAF induced a concentration-dependent increase in O_2^- generation that was significantly less than that induced by PAF ($P < 0.05$, unpaired t test) (Figure 5a). PAF induced a concentration-dependent increase in $[Ca^{2+}]_i$ with a $-\log EC_{50}$ not different from that for PAF-induced O_2^- generation (Figure 5a; Table 2). Hexanolamine PAF induced an increase in $[Ca^{2+}]_i$ in macrophages (in suspension) in contrast to its lack of effect in platelets (Figure 5b cf. Figure 1b). Concentrations of hexanolamine PAF (1 μM) and PAF (1 nM), which were equi-effective for stimulation of O_2^- production, induced significantly different rises in $[Ca^{2+}]_i$, (PAF 1 nM, 340 ± 36 nM, $n = 8$; hexanolamine PAF 1 μM, 181 ± 36 nM, $n = 10$) ($P < 0.05$, paired t test).

Although most studies of macrophages were carried out with adherent cells, to examine whether hexanolamine PAF

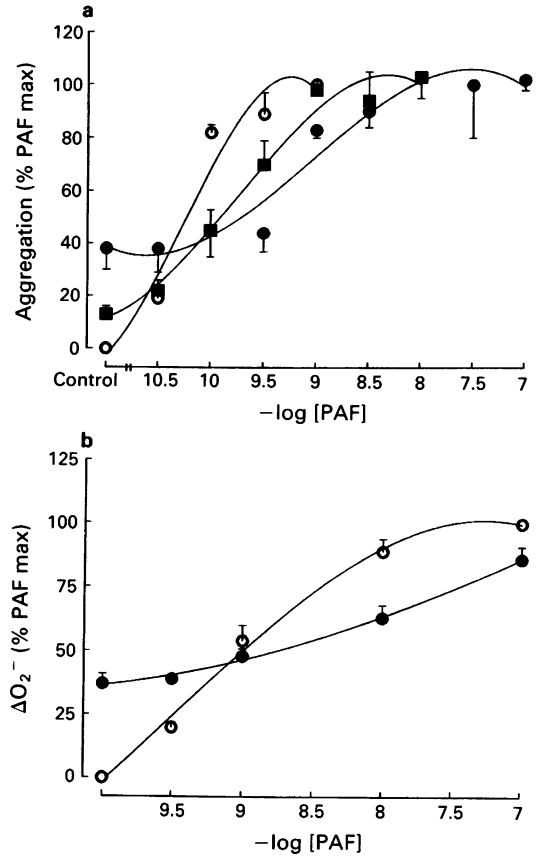

Figure 4 Effects of hexanolamine PAF pretreatment on PAF-induced aggregation of platelets (a) or generation of superoxide anion (O_2^-) in peritoneal lavage cell suspensions (b). (a) The hexanolamine PAF-induced aggregation was allowed to develop until a maximum change in light transmission occurred (usually within 2 min), then PAF was added; vehicle (TBSA) (○); hexanolamine PAF 100 nM (■), 1 μM (●). Ordinate scale: aggregation responses normalized to the maximum response to PAF (1 nM). (b) Non-adherent macrophages were pretreated for 2 min with hexanolamine PAF (●) or the vehicle (TBSA, ○) before treatment with PAF for a further 5 min period. Ordinate scale: increase in O_2^- generation over the basal, normalized to the maximum response to PAF (100 nM). Abscissa scales: −logarithm of the molar concentration of PAF. Data are presented as the means of (a) 7–12 and (b) 4 observations and vertical lines indicate one s.e.mean.

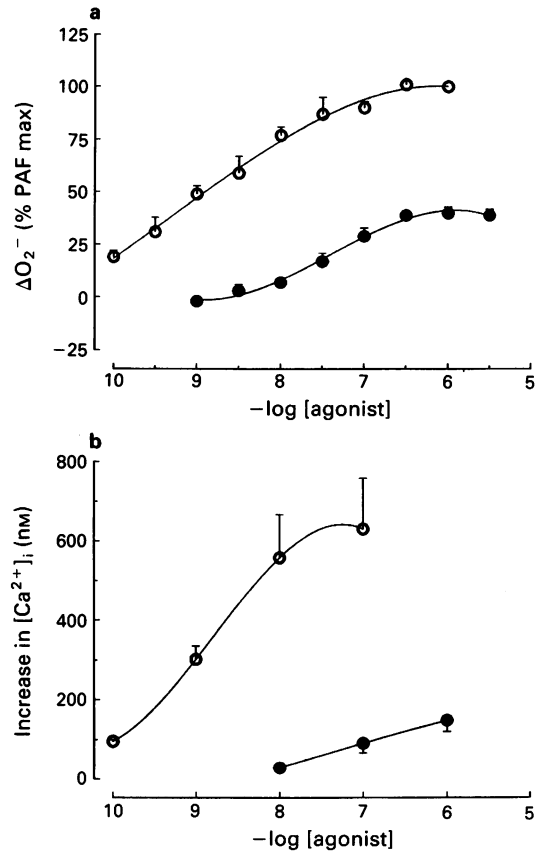

Figure 5 Stimulation of superoxide anion (O_2^-) generation and increases in intracellular calcium $[Ca^{2+}]_i$ by PAF (○) or hexanolamine PAF (●) in peritoneal lavage cells. Superoxide anion generation was measured in adherent macrophages stimulated with PAF or hexanolamine PAF for 15 min. Intracellular Ca^{2+} was measured in non-adherent peritoneal lavage cells. Ordinate scales: (a) increase in O_2^- generation over the basal, normalized to the maximum O_2^- generation induced by PAF (100 nM); (b) peak increase in $[Ca^{2+}]_i$ (nM). Abscissa scales: −logarithm of the molar concentration of the agonist. Data are presented as the means of (a) 12–18 and (b) 5–10 observations and vertical lines indicate one s.e.mean.

was a partial agonist at PAF receptors on macrophages, cells in suspension were used since this allowed experiments to be carried out under the same conditions as those for platelets. Hexanolamine PAF (1 μM) increased the response to lower concentrations of PAF and inhibited those to higher concentrations ($P < 0.05$, two-way ANOVA with repeated measures) (Figure 4b).

Table 2 The potency of PAF and hexanolamine PAF on guinea-pig macrophage superoxide anion (O_2^-) generation and increases in intracellular calcium $[Ca^{2+}]_i$

Response	*Agonist*	n	$-log\ EC_{50}$	*Max*
	PAF			
O_2^-		17	8.87 ± 0.08	14.6[1] ± 1.4
$[Ca^{2+}]_i$		8	8.67 ± 0.19	847[2] ± 201
	Hexanolamine PAF			
O_2^-		18	7.39 ± 0.11*	6.6 ± 1.0*
$[Ca^{2+}]_i$		10	7.26 ± 0.66*	181 ± 36*

* $P < 0.05$, unpaired t test, compared with corresponding responses to PAF. Data are presented as the mean ± the s.e. of the mean.
[1] Maximum increases in O_2^- generation are presented as nmol/10^6 cells.
[2] Maximum increases in $[Ca^{2+}]_i$ are presented in nM.

Antagonism of superoxide anion generation by PAF receptor antagonists

WEB 2086 (1 nM), CV 6209 (1 nM) or BN 52021 (1 μM) each inhibited O_2^- generation induced by PAF or hexanolamine PAF (Table 3). Pretreatment of adherent macrophages with either the vehicle (TBSA), WEB 2086, CV 6209 or BN 52021

Table 3 Effect of PAF-receptor antagonists on O_2^- generation in guinea-pig macrophages

	Inhibition of superoxide anion generation (%)	
Treatment	*Hexanolamine PAF* (100 nM)[1]	*PAF* (100 nM)[1]
WEB 2086 (1 nM)	43 ± 6* (4)	36 ± 12* (4)
CV 6209 (1 nM)	99 ± 9* (4)	23 ± 7* (7)
BN 52021 (1 μM)	48 ± 12* (4)	ND[2]

* $P < 0.05$, paired t test compared to control[1].
Data are presented as the mean ± s.e.mean.
[1] Control O_2^- generation, nmol/10^6 cells: hexanolamine PAF, 2.2 ± 0.6; PAF, 12.4 ± 3.7.
[2] ND, not done.

did not significantly alter the basal amount of O_2^- generated (data not shown). Furthermore, hexanolamine PAF had no effect on O_2^- generation in response to 10 nM of the chemotactic tripeptide, formyl-Met Leu Phe (nmol $O_2^-/10^6$ cells, $n = 3$: control, 6.7 ± 3.3; hexanolamine PAF 10 nM, 5.6 ± 1.9; 100 nM, 6.9 ± 2.8).

Discussion

The major finding of this study was the identification of partial agonist activity of hexanolamine PAF at PAF receptors on platelets and macrophages. Hexanolamine PAF, a close structural analogue of PAF, is the first compound identified as having partial agonist activity at PAF receptors. Interestingly, hexanolamine PAF activated a signal transduction cascade in platelets that appeared to be Ca^{2+}-independent.

The maximum response to hexanolamine PAF was approximately 50% of that to PAF in either platelets or macrophages. The PAF receptor antagonist, WEB 2086 inhibited the PAF and hexanolamine PAF responses in both platelets and macrophages indicating an action at PAF receptors. However, the antagonism by WEB 2086 of PAF-induced platelet aggregation was clearly competitive, whereas hexanolamine PAF responses were non-competitively antagonized by WEB 2086. Thus, WEB 2086 and hexanolamine PAF may interact with different parts of the PAF receptor. In macrophages, O_2^- generation induced by either hexanolamine PAF or PAF was antagonized by the PAF receptor antagonists, WEB 2086, BN 52021 or CV 6209. The characteristics of the interaction between PAF and hexanolamine PAF on both platelet and non-adherent macrophage responses resembled closely those expected of a partial agonist (Stephenson, 1956). Hexanolamine PAF appeared to act specifically at PAF receptors in platelets and macrophages, since hexanolamine PAF did not inhibit thrombin-induced aggregation at concentrations up to 1 μM (data not shown). In macrophages, hexanolamine PAF had no inhibitory effects on fMLP-induced O_2^- generation. Finally, under conditions in which hexanolamine PAF had no agonist activity (platelets stored in the absence of BSA), it acted as an antagonist of PAF, consistent with a specific action at PAF receptors. These observations strongly support the conclusion that hexanolamine PAF is a partial agonist at PAF receptors.

It was expected that a partial agonist would activate the same signal transduction pathway as a full agonist only to a lesser extent and would have antagonist activity. Hexanolamine PAF induced aggregation without producing a detectable increase in $[Ca^{2+}]_i$. Furthermore, a low concentration of PAF induced a rise in $[Ca^{2+}]_i$ (130 nM), but no platelet aggregation. It is therefore unlikely that hexanolamine PAF-induced aggregation was dependent on increases in $[Ca^{2+}]_i$ not detectable with the Fura-2 fluorescent probe. Similar observations of selective activation of a signal transduction mechanism with clonidine, a partial agonist at α_2-adrenoceptors have been observed in thoracic aortic strips (Takayanagi & Onozuka, 1989).

Tokumura *et al.* (1985) reported that the 1-*O*-octadecyl form of hexanolamine PAF was an antagonist of PAF that was essentially devoid of agonist activity. The difference between our findings and those of Tokumura *et al.* (1985) may be explained by our use of the 1-*O*-hexadecyl form of hexanolamine PAF. The potency of C_{18}-PAF is half a log less than that of C_{16}-PAF (Hanahan *et al.*, 1981); a similar effect of the altered alkyl chain length on the potency of hexanolamine PAF could explain the lack of agonist activity (Tokumura *et al.*, 1985). The mechanism by which BSA preserves aggregation responses was not identified, but does not appear to involve a maintenance of hexanolamine PAF binding, since the antagonist activity of hexanolamine PAF was unaffected by the absence of BSA in the Tyrode solution.

PAF-induced platelet aggregation occurs at least in part, through a phospholipase C/$[Ca^{2+}]_i$ dependent pathway (Morrison & Shukla, 1989). In contrast, the aggregation induced by hexanolamine PAF occurs independently of a detectable rise in $[Ca^{2+}]_i$. Adrenaline activates platelet α_2-adrenoceptors (Grant & Scrutton, 1979) without increasing inositol phospholipid hydrolysis (Siess *et al.*, 1984) or increasing Ca^{2+} uptake (Thompson & Scrutton, 1985; Siess & Lapetina, 1988). In a recent study, the PAF-receptor antagonists Ro-193704 and CV-3988, which are structurally related to PAF, were found to act as antagonists of α_2-adrenoceptors (Schattner *et al.*, 1989). Adrenaline and hexanolamine PAF may activate a common, calcium-independent signal transduction cascade, but the possibility that hexanolamine PAF binds to the α_2-adrenoceptor is excluded by our finding that the α_2-adrenoceptor antagonist, idazoxan did not inhibit aggregation induced by hexanolamine PAF (Grigoriadis & Stewart, unpublished observations).

In the presence of the non-specific inhibitor of PKC, staurosporine (Tamaoki *et al.*, 1986), sub-maximal concentrations of PAF induce platelet activation which appears to be independent of phosphatidyl inositol (PI) hydrolysis or activation of PKC (Murphy *et al.*, 1990). The residual signal transduction mechanism may be the same as that associated with activation of PAF receptors by hexanolamine PAF.

In platelets pre-incubated with the octadecyl form of hexanolamine PAF, the resting levels of PI-4-P and PI-4,5-P_2 increased despite the lack of agonist activity (Tokumura *et al.*, 1985). Formation of the newly-discovered second messenger PIP_3, which is difficult to resolve from PIP_2 on thin layer chromatography (t.l.c.), is dependent on G-proteins, but not $[Ca^{2+}]_i$ or PKC (Traynor-Kaplan *et al.*, 1989). Thus, PI-3 kinase is a candidate for the Ca^{2+}-independent signal transduction mechanism for aggregation induced by hexanolamine PAF.

Hexanolamine PAF is unique in having partial agonist activity at PAF receptors in macrophages and platelets. This partial agonism of hexanolamine PAF may be explained by the existence of two receptor populations or two affinity states of a single receptor population. Hexanolamine PAF may act as an antagonist at one subset of receptors, and as an agonist on the other. It is likely that both receptors/affinity states are PAF receptors since both are WEB 2086-sensitive.

The inability of hexanolamine PAF to increase $[Ca^{2+}]_i$ to the same extent as PAF may account for its partial agonism. Such selective activation of a part of the signal transduction mechanism may explain why some compounds act as partial agonists.

We thank Anna Christov for excellent technical assistance. This study was supported by a grant from the National Health & Medical Research Council (Australia). We also thank Dr N. Latt, Boehringer (Australia Ltd), Dr P. Braquet, IHB Laboratories, France and Dr Oka, Takeda Chemical Industries, Osaka, Japan, for generous gifts of WEB 2086, BN 52021 and CV 6209, respectively.

References

BARNES, P.J., CHUNG, K.F. & PAGE, C.P. (1988). Inflammatory mediators in asthma. *Pharmacol. Rev.*, **40**, 49–84.

BENVENISTE, J., HENSON, P.M. & COCHRANE, C.G. (1972). Leukocyte-dependent histamine release from rabbit platelets. The role of IgE, basophils and platelet-activating factor. *J. Exp. Med.*, **136**, 1356–1377.

BRAQUET, P., TOUQUI, L., SHEN, T.Y. & VARGAFTIG, B.B. (1987). Perspectives in platelet-activating factor research. *Pharmacol. Rev.*, **39**, 97–145.

BRATTON, D. & HENSON, P.M. (1989). Cellular origins of Paf. *Platelet Activating Factor and Human Disease*. ed. Barnes, P.J., Page, C.P. & Henson, P.M. pp 23–57. London: Blackwell.

GRANT, J.A. & SCRUTTON, M.C. (1979). Novel α_2-adrenoceptors primarily responsible for inducing platelet aggregation. *Nature*, **277**, 659–661.

GRYNKIEWICZ, G., POENIE, M. & TSIEN, R.Y. (1984). A new generation of Ca^{2+} indicators with greatly improved fluorescence properties. *J. Biol. Chem.*, **267**, 3440–3448.

HANAHAN, D.J., MUNDER, P.G., SATOUCHI, K., McMANUS, L.M. & PINCKARD, R.N. (1981). Potent platelet stimulating activity of enantiomers of acetyl glyceryl ether phosphorylcholine and its methoxy analogues. *Biochem. Biophys. Res. Commun.*, **99**, 183–188.

HWANG, S.B. (1990). Specific receptors of platelet-activating factor, receptor heterogeneity, and signal transduction mechanisms. *J. Lip. Med.*, **2**, 123–158.

JOHNSTON, R.B. JR., GODZICK, C.A. & COHN, Z.A. (1978). Increased superoxide anion production by immunologically activated and chemically elicited macrophages. *J. Exp. Med.*, **148**, 115–127.

LAMBRECHT, G. & PARNHAM, M. (1986). Kadseurenone distinguishes between different platelet-activating factor receptor subtypes on macrophages and polymorphonuclear leukocytes. *Br. J. Pharmacol.*, **87**, 287–289.

MALGAROLI, A., MILANI, D., MELDOLESI, J. & POZZAN, T. (1987). Fura-2 measurement of cytosolic free Ca^{2+} in monolayers and suspensions of various types of animal cells. *J. Cell. Biol.*, **105**, 2145–2155.

MARCHESELLI, V.L., ROSSOWSKA, M.J., DOMINGO, M., BRAQUET, P. & BAZAN, N.G. (1990). Distinct platelet-activating factor binding sites in synaptic endings and in intracellular membranes of rat cerebral cortex. *J. Biol. Chem.*, **265**, 9140–9145.

MORRISON, W.J. & SHUKLA, S.D. (1989). Antagonism of platelet activating factor receptor binding and stimulated phosphoinositide-specific phospholipase C in rabbit platelets. *J. Pharmacol. Exp. Ther.*, **250**, 831–835.

MURPHY, C.T., KELLIE, M.A. & WESTWICK, J. (1990). Characterization of platelet activating factor induced inositol (1,4,5)-trisphosphate production in platelets: modulation by protein kinase C. *Eur. J. Pharmacol.*, **183**, 636–637.

PRESCOTT, S.M., ZIMMERMAN, G.A. & McINTYRE, T.M. (1990). Platelet-activating factor. *J. Biol. Chem.*, **265**, 17381–17384.

REMY, E., VANDESTEENE, C. & REMACLE, J. (1990). Central role of intracellular Paf in the activation of bovine neutrophils. *Proceedings of the 7th International Conference on Prostaglandins and Related Compounds.* p. 248. Florence: Fondazione Giovanni Lorenzini.

SCHATTNER, M., PARINI, A., FOUQUE, F., VARGAFTIG, B.B. & TOUQUI, L. (1989). Selective inhibition of adrenaline-induced human platelet aggregation by the structurally related Paf antagonist Ro19-3704. *Br. J. Pharmacol.*, **96**, 759–766.

SIESS, W. & LAPETINA, E.G. (1988). Ca^{2+} mobilization primes protein kinase C in human platelets. *Biochem. J.*, **255**, 309–318.

SIESS, W., WEBER, P. & LAPETINA, E.G. (1984). Activation of phospholipase C is dissociated from arachidonate metabolism during platelet shape change induced by thrombin or platelet-activating factor. *J. Biol. Chem.*, **259**, 8286–8292.

STEPHENSON, R.P. (1956). A modification of receptor theory. *Br. J. Pharmacol.*, **11**, 379–393.

STEWART, A.G., DUBBIN, P.N., HARRIS, T. & DUSTING, G. (1990). Platelet-activating factor may act as a second messenger in the release of icosanoids and superoxide anions from leukocytes and endothelial cells. *Proc. Natl. Acad. Sci., U.S.A.*, **87**, 3215–3219.

STEWART, A.G. & DUSTING, G.J. (1988). Characterization of receptors for platelet-activating factor on platelets, polymorphonuclear leukocytes and macrophages. *Br. J. Pharmacol.*, **94**, 1225–1233.

TAKAYANAGI, I. & ONOZUKA, S. (1989). Greater tension is developed at the same level of cytosolic Ca^{2+} concentration in the presence of clonidine, an adrenergic partial agonist, than in the presence of norepinephrine. *J. Pharmacobiodyn.*, **12**, 781–786.

TAMAOKI, T., NOMOTO, H., TAKAHASHI, I., KATO, Y., MORIMOTO, M. & TOMITA, F. (1986). Staurosporine, a potent inhibitor of phospholipid/Ca^{2+} dependent protein kinase. *Biochem. Biophys. Res. Commun.*, **135**, 397–402.

THOMPSON, T. & SCRUTTON, M.C. (1985). Intracellular calcium fluxes in human platelets. *Biochem. J.*, **147**, 421–427.

TOKUMURA, A., HOMMA, H. & HANAHAN, D.K. (1985). Structural analogs of alkylacetylglycerophosphocholine inhibitory behaviour on platelet activation. *J. Biol. Chem.*, **260**, 12710–12714.

TRAYNOR-KAPLAN, A.E., THOMSON, B.L., HARRIS, A.L., TAYLOR, P., OMANN, A.M. & SKLAR, L.A. (1989). Transient increase in phosphatidylinositol 3,4-bisphosphate and phosphatidylinositol trisphosphate during activation of human neutrophils. *J. Biol. Chem.*, **264**, 15668–15673.

VARGAS, J.R., RADOMSKI, M. & MONCADA, S. (1982). The use of prostacyclin in the separation from plasma and washing of human platelets. *Prostaglandins*, **23**, 929–945.

(Received December 28, 1990
Revised April 8, 1991
Accepted April 16, 1991)

Br. J. Pharmacol. (1991), **104**, 178–182

Effects of paracetamol and aspirin on neural activity of joint mechanonociceptors in adjuvant arthritis

[1]D.S. McQueen, *A. Iggo, G.J. Birrell & *B.D. Grubb

Department of Pharmacology, University of Edinburgh Medical School, 1 George Square, Edinburgh, EH8 9JZ and *Department of Preclinical Veterinary Sciences, R(D)SVS, Summerhall, Edinburgh, EH9 1QH

1 The effects of paracetamol and lysine acetylsalicylate (L-AS) on high-threshold mechanonociceptors have been investigated by recording neural activity from the inflamed ankle joint in anaesthetized rats with mild adjuvant-induced monoarthritis.

2 Paracetamol (50 mg kg^{-1}, i.v.) and L-AS (100 mg kg^{-1}, i.v., equivalent to 50 mg kg^{-1} aspirin) both caused a maximal reduction of about 40% in mechanically-evoked discharge and of 30% in ongoing (spontaneous) activity by about 15 min after the injection: a second dose of either drug did not have any significant additional effect on discharge.

3 The prostanoid IP receptor agonist, cicaprost (0.1–0.5 μg), increased both mechanically-evoked and ongoing discharge to pre-paracetamol levels when injected close-arterially 30–50 min after paracetamol, whereas prostaglandin E_2 (PGE_2) was relatively ineffective at restoring activity.

4 The results suggest that prostacyclin (PGI_2) contributes to the sensitization of high-threshold joint mechanonociceptors in adjuvant-induced monoarthritis, and that paracetamol and L-AS both act to reduce discharge by inhibiting the synthesis of prostacyclin in the joint capsule.

5 Paracetamol has a direct peripheral action affecting joint capsule mechanonociceptors in rat adjuvant-induced arthritis which is very similar to that of the soluble aspirin preparation, L-AS. These findings, together with the existing literature concerning the anti-arthritic effects of paracetamol, are relevant to the treatment of chronic inflammatory disorders such as rheumatoid arthritis.

Keywords: Adjuvant arthritis; paracetamol; aspirin; high threshold joint mechanonociceptors

Introduction

The rat ankle joint contains high-threshold mechanoreceptors that are located in the joint capsule (Guilbaud *et al.*, 1985) and are classified as type IV articular receptors having a nociceptive function (Wyke, 1981). In the normal joint these sensory receptors only respond to intense mechanical stimuli and the afferent fibres rarely show spontaneous activity. In adjuvant-induced poly- or mono-arthritis the sensors become hypersensitive to mechanical stimuli and spontaneous activity can readily be recorded from the afferent nerve fibres (Guilbaud *et al.*, 1985; Grubb *et al.*, 1991). Prostanoids appear to be involved in this sensitization because the soluble aspirin preparation lysine acetylsalicylate (L-AS) substantially reduced both 'spontaneous' and mechanically-evoked discharge from high-threshold mechanonociceptors, possibly as a result of cyclo-oxygenase inhibition reducing prostacyclin levels within the inflamed joint (Guilbaud & Iggo, 1985).

We have developed a model of arthritis in which the lesion induced by local administration of Freund's complete adjuvant in a low dose is mild and confined to one ankle joint i.e. monoarthritis (Grubb *et al.*, 1988; Birrell *et al.*, 1990). This preparation has now been used to compare the effects of paracetamol and aspirin on afferent activity recorded from high threshold mechanonociceptors in the arthritic ankle joints of anaesthetized rats. The aim was to determine whether or not paracetamol has peripheral actions comparable with those of aspirin; a common view is that aspirin, by virtue of its anti-inflammatory action, reduces sensitization of nociceptors in chronic inflammatory states such as arthritis, whereas paracetamol has no or only weak anti-inflammatory actions at peripheral sites and is, therefore, ineffective (e.g. Rang & Dale, 1988; Bradley, 1989).

Preliminary accounts of some of this work have been published (Birrell *et al.*, 1990; McQueen *et al.*, 1990).

[1] Author for correspondence.

Methods

Experiments were performed on male Wistar rats weighing between 252 and 397 g, mean (± s.e.mean) 310 ± 12 g. Arthritis was induced between 12 and 32 days (mean 20 ± 2) before the acute experiment. Freund's complete adjuvant (1 mg ml^{-1} heat killed and dried *Mycobacterium tuberculosis*, suspended in paraffin oil; Sigma) was injected subdermally in a total volume of 0.15 ml (0.15 mg bacteria) at three separate sites around the left ankle (tibio-tarsal) joint in rats which were anaesthetized with halothane (2% in oxygen). The left ankle joint showed signs of mild inflammation within a day and the peak increase (~50%) in circumference of the joint occurred after approximately 10 days. Thereafter the inflammation remained stable for a further 25 days. The animals continued to move, behave and gain weight normally and did not differ significantly from uninjected controls or from vehicle-injected rats which had no inflammation and only a slight swelling (lasting 2–7 days) of the left ankle. The contralateral (un-injected) limb was, in terms of circumference and appearance, no different from that of uninjected controls at any time during the post-injection period ($P > 0.05$, Wilcoxon test).

Neuropharmacological experiments

The arthritic rats were anaesthetized with urethane (0.6 ml 100 g^{-1} body weight of 25% w/v aqueous ethylcarbamate solution injected i.p.) and body temperature was maintained at 37°C by an automated heating blanket connected to a thermistor probe inserted in the rectum. The trachea, a carotid artery (for B.P. monitoring), and the right femoral vein were cannulated, and a catheter was introduced into the abdominal aorta via the right femoral artery and used for intra-arterial administration of substances.

Neural recordings were obtained from fine filaments dissected from the left primary articular cutaneous ramus, a

branch of the tibial nerve which innervates the ankle joint capsule, see Guilbaud *et al.* (1985) for details. Bipolar platinum-iridium wire electrodes were used to provide an extracellular signal that was amplified (Neurolog), digitized (Sony PCM 701-ES) and recorded on video tape (Sony Betamax, SLF 25 UB), and subsequently analysed by playing back through a voltage discriminator (WPI, 120) which enabled individual action potentials to be selected for quantification, in conjunction with a CED 1401 (Cambridge Electronics) interface, by a PC compatible microcomputer (DCS.XT).

High threshold mechanoreceptors were identified by probing the left ankle joint manually with a fine-tipped rod and, once a receptive field had been found, calibrated Von Frey hairs were used to determine the threshold force needed to activate the receptor. A mechanical stimulator (Somedic) was then positioned over the site with the 1 mm diameter tip of its probe resting on the tissues above the joint. A timer was used to trigger a ramp and plateau indentation of constant amplitude (100–500 μm, usually 400 μm) and duration (2 s) repeated once every 2 min. The displacement of the probe was digitised and recorded on video tape together with the associated neural discharge.

The conduction velocity of the units recorded was measured by passing current from an electrical stimulator (Neurolog) through a pair of electrodes in the tip of the probe attached to the mechanical stimulator. This allowed small localised currents to be passed within the receptive field with the probe pressing firmly into the tissue and the conduction velocity was calculated from the time taken to reach the recording electrodes (17–35 mm away).

Estimation of salicylate and paracetamol in plasma samples

Samples of arterial blood were taken, heparin added (50 units), and the plasma separated following centrifugation. Total salicylate was estimated by colorimetry (see McQueen *et al.*, 1989) and paracetamol was measured by high performance liquid chromatography (h.p.l.c.) (Adriaennssens & Prescott, 1978).

Data analysis

Ongoing (spontaneous) neural activity was measured by averaging discharge in successive 60 s periods. Mechanically-evoked activity was determined by counting the total number of action potentials generated by each 2 s indent. Data were normalized with respect to pre-drug values (= 100%) in individual experiments.

Mean values are shown ± s.e.mean. The Wilcoxon two sample test (Colquhoun, 1971) was used to test for statistically significant differences between groups, and the null hypothesis rejected at $P \leqslant 0.05$. The paired t test was used for small samples.

Drugs

The following drugs were used, dissolved in 0.9% w/v aqueous NaCl: lysine acetylsalicylate (L-AS), (Aspegic, Synthelabo, France; the dose used was 100 mg, equivalent to 50 mg acetylsalicylic acid-aspirin), paracetamol (Aldrich), prostaglandin E_2 (Sigma), cicaprost (Searle), and ethyl carbamate (B.D.H.).

The L-AS preparation and the paracetamol were injected i.v. in a volume of 1 ml delivered over 10 s. Cicaprost was injected over 2 s into the abdominal aorta in volumes of 0.1 ml washed in with 0.2 ml saline.

Results

The high threshold mechanoreceptors recorded from arthritic ankle joints during this study were more sensitive to mechanical stimulation (mean threshold 53 ± 3 mN) than those from control joints (mean 81 ± 7 mN; $P < 0.01$). The conduction velocities of the fibres ranged from 0.3 to 2.0 ms^{-1} (mean 0.9 ± 0.1 ms^{-1}; $n = 21$ units) which means they were fine unmyelinated C fibre afferents (conduction velocity < 2.5 ms^{-1}, Schaible & Schmidt, 1983).

Responses to mechanical stimulation – effects of paracetamol and lysine acetylsalicylate

Pooled data from experiments in which the activity of high threshold mechanoreceptors recorded from the left (arthritic) ankle was evoked by mechanical stimulation of the joint are shown as absolute values in Figure 1. Paracetamol (50 mg kg^{-1}, i.v.) and L-AS (100 mg kg^{-1}, i.v.) both caused a reduction in the discharge which varied somewhat between experiments as reflected in the high s.e.mean. The variability is a consequence of pooling data that have a wide range of basal values (i.e. impulses per standard indent), coupled with the finding that individual mechanoreceptors differed in their responsiveness to paracetamol or L-AS; all showed depression of the response, but the size of the reduction and the time course was variable. There was no correlation between the circumference of the joint or the conduction velocity of the afferent fibre with the magnitude of the response to the drugs.

Normalizing the data as a % of the pre-injection control values eliminates inter-experiment variability attributable to differing basal values, and plotting the result in this way shows that paracetamol and L-AS caused similar reductions in mechanically-evoked discharge (Figure 2). The only significant difference between the effects of paracetamol and L-AS lay in the rapid transient reduction observed 6 min after paracetamol ($P < 0.05$ in comparison with L-AS). Otherwise there were no significant differences between the drugs: both reduced discharge to about half of control levels, reaching the nadir 36–46 min after the single injection. Mechanoreceptor responsiveness returned to pre-injection levels 60–80 min post-injection, but this was not investigated systematically as the preparations were generally used for further studies 46 min after the original dose, which explains the decrease to $n = 3$ in n after this time; this small sample size precluded meaningful statistical analysis for measurements at 60 min.

Effects of paracetamol and lysine acetylsalicylate on spontaneous mechanoreceptor discharge

In most, but not all, recordings of neural activity from single high threshold mechanoreceptors the units displayed spontaneous ongoing discharge, in addition to mechanically-evoked activity. Paracetamol and L-AS both reduced the spontaneous

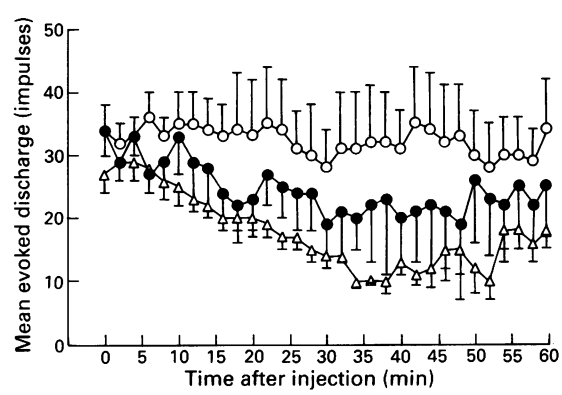

Figure 1 Effects of injecting paracetamol (50 mg kg^{-1} i.v., ●, $n = 7$), lysine acetylsalicylate (100 mg kg^{-1} i.v., △, $n = 8$), or saline (1 ml i.v., ○, $n = 9$) on the discharge evoked by mechanical stimulation of high-threshold joint mechanoreceptors in arthritic ankle joints. The mean responses are shown; s.e.mean indicated by vertical bars. From 25 min onwards n decreased, but was never less than 3.

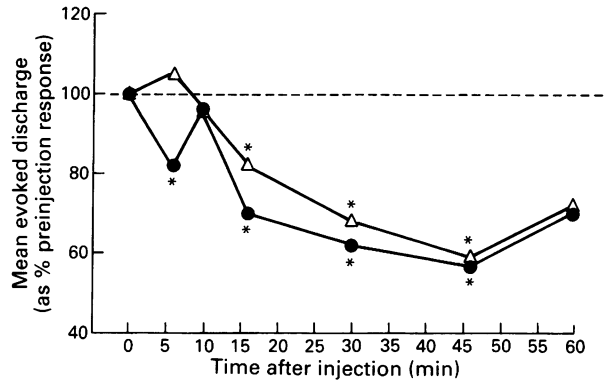

Figure 2 Normalized data showing the decrease in discharge evoked from mechanonociceptors following i.v. injection of 100 mg kg^{-1} lysine acetylsalicylate (L-AS, △, n = 3–8) or 50 mg kg^{-1} paracetamol (●, n = 3–7). The dashed line represents the pre-injection response (100%), which, in absolute terms, was 34 ± 4 impulses for paracetamol and 27 ± 3 impulses for L-AS in response to the standard indent. * $P < 0.05$, paired t test, versus pre-injection control discharge.

discharge, in comparison with the saline controls, and the overall pattern was similar (see Figure 3). L-AS transiently reduced discharge at 5 min post-injection, whereas paracetamol did not, but apart from this the effects of the drugs were similar in that both reduced spontaneous mechanoreceptor discharge to 60–70% of preinjection levels by 15 min post-injection, with some inter-experiment variability.

Additional doses of paracetamol or lysine acetylsalicylate

A second i.v. injection (same dose) was made 45 min after the first in order to determine whether any additional effect could be observed on either spontaneous or mechanically-evoked activity of the joint sensors. In three experiments a second dose of paracetamol (50 mg kg^{-1} i.v.) had no additional effect, and nor did a second dose of L-AS (100 mg kg^{-1}, i.v.) in three experiments when it was given 45 min after the original dose of salicylate. In a further three experiments L-AS (100 mg kg^{-1}, i.v.) was injected 45 min after paracetamol had been administered. The salicylate caused a further slight reduction in mechanically-evoked activity as well as in spontaneous discharge, but this reduction was not statistically significant ($P > 0.05$; time zero versus 30 min post-L-AS, paired t test).

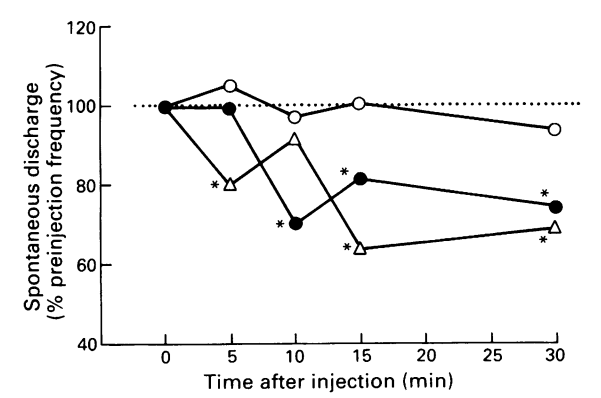

Figure 3 Effects of injecting paracetamol (50 mg kg^{-1}, i.v., ●, n = 3–8), lysine acetylsalicylate (L-AS, 100 mg kg^{-1} i.v., △, n = 3–5) or 1 ml saline (○, n = 3–9) on background (spontaneous) discharge of high-threshold joint mechanoreceptors in arthritic ankle joints. Mean discharge was averaged over 60 s before (0) and 5, 10, 15 and 30 min after the i.v. injection and expressed as a percentage of the preinjection value (dashed line = 100%). Preinjection discharge averaged 1.2 counts per second (ct s^{-1}) pre-paracetamol, 2.5 ct s^{-1} pre-L-AS, and 1.9 ct s^{-1} pre-saline. * $P < 0.05$, Wilcoxon test versus saline.

Effects of cicaprost injected after paracetamol

The prostanoid IP receptor agonist (see Coleman *et al.*, 1984, for a review on prostanoid receptor classification) cicaprost was injected 30–50 min after discharge had been reduced by paracetamol. Both spontaneous and mechanically-evoked discharge were enhanced after cicaprost (0.1–0.5 μg, i.a.), with discharge being restored to pre-paracetamol levels; similar results were obtained in the three experiments performed, and representative examples from two of them are shown in Figure 4. In a separate experiment prostaglandin E_2 (PGE_2, 3 μg, i.a.) was injected 45 min after paracetamol had reduced spontaneous and mechanically evoked mechanoreceptor discharge. There was no additional effect on evoked activity, and although spontaneous discharge increased slightly after PGE_2, the effect was transient and lasted for only 3–4 min.

Plasma concentrations of aspirin and paracetamol

Samples of blood were taken 5, 15, 30 and 45 min after a single i.v. injection of lysine acetylsalicylate (100 mg kg^{-1}, equivalent to 50 mg kg^{-1} aspirin). A second injection of the same drug was made 50–60 min after the original dose, and samples taken 5, 15 and 30 min thereafter. In a separate series

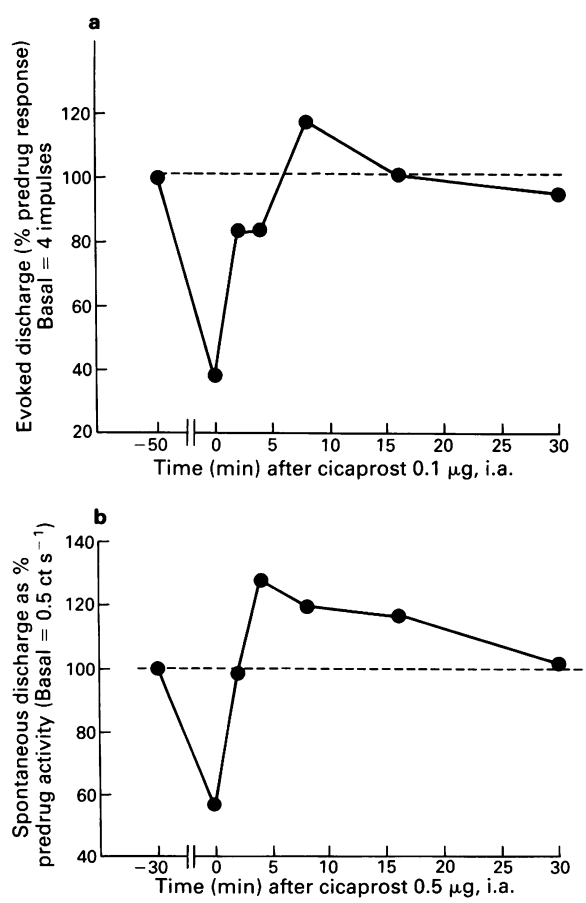

Figure 4 Data from separate experiments illustrating the ability of cicaprost (0.1–0.5 μg, i.a.) to restore (a) mechanically-evoked and (b) spontaneous discharge of high-threshold mechanoreceptors in arthritic-joints to levels comparable with those obtained before the injection of paracetamol (50 mg kg^{-1}, i.v.) given approximately 45 min earlier. Basal (100%) values were 42 impulses in (a), 0.5 ct s^{-1} in (b); cicaprost was injected at time 0.

of experiments estimations of paracetamol in plasma were made 45 min after injecting paracetamol at a dose of 50 mg kg^{-1}, i.v. The highest salicylate level was 75.9 ± 1.0 mg l^{-1} 10 min after the first dose of L-AS, declining to 50.1 ± 12.9 mg l^{-1} at 30 min. Following the second dose, corresponding levels at 5 and 30 min were 127.5 ± 23.2 and 108.2 ± 17.1 mg l^{-1} respectively of salicylate (n = 3). Paracetamol values were 16.3 ± 1.4 mg l^{-1} 45 min after the first dose, 43.9 ± 5.7 mg l^{-1} 30 min after the second (n = 3).

Discussion

Our results show that neural discharge from high threshold mechanoreceptors (presumed nociceptors) in the ankle joint of anaesthetized rats with adjuvant-induced monoarthritis is reduced by paracetamol as well as by the soluble aspirin preparation L-AS; both ongoing and mechanically-evoked discharge were affected. The effect of L-AS on these ankle joint sensors confirms previous findings in rats with either adjuvant-induced polyarthritis (Guilbaud & Iggo, 1985) or monoarthritis (Grubb *et al.*, 1991). L-AS has no effect on the activity of these sensory receptors in normal joints (Guilbaud & Iggo, 1985), so the reduction in activity seen in arthritis suggests sensitization of the receptors by a mediator which is susceptible to the action(s) of salicylate and paracetamol.

We found that PGE_2, given 30 min after paracetamol had reduced mechanoreceptor discharge, was ineffective in restoring discharge to pre-paracetamol levels. This result is similar to that obtained during earlier studies with L-AS on this preparation (Birrel *et al.*, 1990; Grubb *et al.*, 1991) and suggests that inhibition of PGE_2 production by paracetamol is not responsible for the decreased responsiveness of the sensors following administration of the drug in arthritis. In contrast, the stable and highly selective IP receptor agonist cicaprost (Skuballa *et al.*, 1986) did restore discharge rapidly, and this action was sustained. We have already shown that PGI_2, in contrast to the feeble action of PGE_2, can activate these sensory receptors in normal rat ankle joints, although the effect evoked is shorter-lasting than that of cicaprost (Birrell *et al.*, 1991). It seems likely, therefore, that PGI_2 acting at IP receptors is involved in the sensitization of high threshold mechanonociceptors observed in this model of arthritis; this is supported by the relatively rapid effect of paracetamol and of L-AS in reducing discharge, which points to involvement of a prostanoid having a short half-life in the tissues. PGI_2 meets this requirement, whereas PGE_2 does not, as discussed in detail by Guilbaud & Iggo (1985). Additional studies involving measurement of eicosanoid levels in the joint capsule would provide more direct evidence regarding the relative role of PGI_2 and PGE_2 in the sensitization of joint mechanonociceptors in this model of arthritis.

The doses of L-AS (equivalent to 50 mg kg^{-1} aspirin) and paracetamol (50 mg kg^{-1}) evidently caused maximal reductions in discharge since a second dose given 45 min after the first produced no additional effect. Paracetamol given after L-AS also failed to cause any further decrease in activity, whereas L-AS given after paracetamol did cause a further slight reduction, although this was not statistically significant. The two non-steroidal anti-inflammatory drugs appear to act via a common mechanism but the possibility that part of their action may involve separate mechanisms cannot be excluded. Further studies will be needed to investigate this aspect and also to establish whether PGE_2, or another eicosanoid with a long half-life in the tissues, contributes to the 'residual' nociceptor discharge remaining after doses of L-AS or paracetamol. Our results demonstrating that paracetamol is effective in reducing discharge from presumed nociceptors in this model of arthritis is very strong evidence for a peripheral action of the drug in or near the joint. L-AS was established as having a local rather than systemic action in desensitizing joint capsule mechanonociceptors by application to the joint (Guilbaud & Iggo, 1985), and Ferreira *et al.* (1978) proposed that the peripheral analgesic effect of paracetamol involves action of the drug at nociceptors.

There is a consensus that non-steroidal anti-inflammatory drugs act mainly in the periphery to reduce sensitization of nociceptors (e.g. Ferreira, 1972; Moncada *et al.*, 1975; Handwerker, 1976; Ferreira *et al.*, 1978; Tyers & Haywood, 1979; Martin *et al.*, 1987), and that they achieve this by inhibiting the cyclo-oxygenase enzyme involved in synthesizing prostanoids. However, a commonly held view is that paracetamol lacks anti-inflammatory properties because it is a very weak cyclo-oxygenase inhibitor, at least as far as the periphery is concerned (e.g. Rang & Dale, 1988). In fact paracetamol is quite capable of inhibiting prostaglandin biosynthesis in the periphery, although its potency varies depending on the tissue studied (see Higgs *et al.*, 1974; Flower & Vane, 1974), and it is also anti-arthritic and anti-inflammatory in a variety of acute and chronic inflammatory tests in rats, including adjuvant-induced arthritis (Vinegar *et al.*, 1976; Wong & Gardocki, 1983). Phenacetin was used as an effective treatment for rheumatoid arthritis in man, and it is generally considered that its metabolite, paracetamol, was the active agent (Smith, 1958). Paracetamol is an anti-inflammatory drug in man (McQueen, 1973; Skjelbred *et al.*, 1977) and it has been shown to reduce prostanoid levels in inflammatory exudates and in synovial fluid aspirated from the knee joints of patients with rheumatoid arthritis (Higgs *et al.*, 1974; 1976).

In conclusion, our results provide neuropharmacological evidence that paracetamol, like aspirin, has a direct action in the periphery to reduce the sensitization of presumed nociceptors in a rat model of arthritis and, given that paracetamol has fewer 'side effects' than aspirin, may be relevant to the treatment of pain and inflammation in rheumatoid arthritis.

This work was supported by a project grant from the Arthritis and Rheumatism Council, and the Oliver Bird Fund, Nuffield Foundation. G.J.B. was an SERC-CASE scholar. Laboratory facilities were provided by the Wellcome Animal Research Unit.

References

ADRIAENSSENS, P.I. & PRESCOTT, L.F. (1978). High performance liquid chromatographic estimation of paracetamol metabolites in plasma. *Br. J. Clin. Pharmacol.*, **6**, 87–88.

BIRRELL, G.J., GRUBB, B.D., IGGO, A. & McQUEEN, D.S. (1990). Actions of PGE_2 and cicaprost on the sensitivity of high-threshold mechanoreceptors in normal and inflamed ankle joints of the anaesthetized rat. *J. Physiol.*, **420**, 33P.

BIRRELL, G.J., McQUEEN, D.S., IGGO, A., COLEMAN, R.A. & GRUBB, B.D. (1991). PGI_2-induced activation and sensitization of articular mechanonociceptors. *Neurosci. Letters*, **124**, 5–8.

BRADLEY, P. (1989). *Introduction to Neuropharmacology*, Chapter 15. London: Wright.

COLEMAN, R.A., HUMPHREY, P.P.A., KENNEDY, I. & LUMLEY, P. (1984). Prostanoid receptors—the development of a working classification. *Trends Pharmacol. Sci.*, **5**, 303–306.

COLQUHOUN, D. (1971). *Lectures on Biostatistics* p. 425. Oxford: Clarendon Press.

FERREIRA, S.H. (1972). Prostaglandins, aspirin-like drugs and analgesia. *Nature*, **240**, 200–203.

FERREIRA, S.H., LORENZETTI, B.B. & CORREA, A. (1978). Central and peripheral antialgesic action of aspirin-like drugs. *Eur. J. Pharmacol.*, **53**, 39–48.

FLOWER, R.J. & VANE, J.R. (1974). 'Some pharmacologic and biochemical aspects of prostaglandin biosynthesis and its inhibition'. In *Prostaglandin Synthetase Inhibitors*. ed. Robinson, H.J. & Vane, J.R., pp. 9–18. New York: Raven Press.

GRUBB, B.D., McQUEEN, D.S., IGGO, A., BIRRELL, G.J. & DUTIA, M.B. (1988). A study of 5-HT-receptors associated with afferent nerves located in normal and inflamed rat ankle joints. *Agents Actions*, **25**, 216–218.

GRUBB, B.D., BIRRELL, G.J., McQUEEN, D.S. & IGGO, A. (1991). The role of PGE_2 in the sensitization of mechanoreceptors in normal and inflamed ankle joints of the rat. *Exp. Brain Res.*, **84**, 383–392.

GUILBAUD, G. & IGGO, A. (1985). The effect of lysine acetylsalicylate on joint capsule mechanoreceptors in rats with polyarthritis. *Exp. Brain Res.*, **61**, 164–168.

GUILBAUD, G., IGGO, A. & TEGNER, R. (1985). Sensory receptors in the ankle joint of normal and arthritic rats. *Exp. Brain Res.*, **58**, 29–40.

HANDWERKER, H. (1976). Influences of algogenic substances and prostaglandins on the discharges of unmyelinated cutaneous nerve fibres identified as nociceptors. In *Advances in Pain Research and Therapy*. ed. Bonica, J.J. & Albe-Fessard, D. Vol. 1, pp. 41–45. New York: Raven Press.

HIGGS, G.A., VANE, J.R., HART, F.D. & WOJTULEWSKI, J.A. (1974). Effects of anti-inflammatory drugs on prostaglandins in rheumatoid arthritis. In *Prostaglandin Synthetase Inhibitors*. ed. Robinson, H.J. & Vane, J.R. pp. 165–173. New York: Raven Press.

HIGGS, G.A., HARVEY, E.A., FERREIRA, S.H. & VANE, J.R. (1976). The effects of anti-inflammatory drugs on the production of prostaglandins *in vivo*. In *Advances in Prostaglandin and Thromboxane Research*. ed. Samuelson, B. & Paoletti, R. Vol. 1, p. 105. New York: Raven Press.

MARTIN, H.A., BASBAUM, A.I., KWIAT, G.C., GOETZL, E.J. & LEVINE, J.D. (1987). Leukotriene and prostaglandin sensitization of cutaneous high-threshold C- and A-delta mechanonociceptors in the hairy skin of rat hindlimbs. *Neurosci.*, **22**, 651–659.

McQUEEN, E.G. (1973). Anti-inflammatory drug mechanisms. *Drugs*, **6**, 107–117.

McQUEEN, D.S., RITCHIE, I.M. & BIRRELL, G.J. (1989). Arterial chemoreceptor involvement in salicylate-induced hyperventilation in rats. *Br. J. Pharmacol.*, **98**, 413–424.

McQUEEN, D.S., IGGO, A., BIRRELL, G.J. & GRUBB, B.D. (1990). Effects of aspirin and paracetamol on high-threshold tarsal joint mechanoreceptors in anaesthetized rats with adjuvant-induced arthritis. *J. Physiol.*, **425**, 35P.

MONCADA, S., FERREIRA, S.H. & VANE, J.R. (1975). Inhibition of prostaglandin biosynthesis as the mechanism of analgesia of aspirin-like drugs in the dog knee joint. *Eur. J. Pharmacol.*, **31**, 250–260.

RANG, H.P. & DALE, M.M. (1987). *Pharmacology*. p. 212. Edinburgh: Churchill Livingstone.

SCHAIBLE, H.-G. & SCHMIDT, R.F. (1983). Activation of group III and IV sensory units in medial articular nerve by local mechanical stimulation of knee joint. *J. Neurophysiol.*, **49**, 35–44.

SKJELBRED, P., ALBUM, B. & LOKKEN, P. (1977). Acetylsalicylic acid versus paracetamol: effects on post-operative course. *Eur. J. Clin. Pharmacol.*, **12**, 257–264.

SKUBULLA, W., SCHILLINGER, E., STURZEBECHER, S. & VORBRUGGEN, H. (1986). Synthesis of a new chemically and metabolically stable prostacyclin derivative with high and long-lasting activity. *J. Med. Chem.*, **29**, 313–314.

SMITH, P.K. (1958). *Acetophenetidin – a Critical Bibliographic Review*. New York: Interscience.

TYERS, M.B. & HAYWOOD, H. (1979). Effects of prostaglandins on peripheral nociception in acute inflammation. In *Prostaglandins and Inflammation*, ed. Rainsford, K.D. & Ford-Hutchinson, A.W. p.65. Basel: Birkhauser Verlag.

VINEGAR, R., TRUAX, J.F. & SELPH, J.L. (1976). Quantitative comparison of the analgesic and anti-inflammatory activities of aspirin, phenacetin and acetaminophen in rodents. *Eur. J. Pharmacol.*, **37**, 23–30.

WONG, S. & GARDOCKI, J.F. (1983). Anti-inflammatory and anti-arthritic evaluation of acetaminophen and its potentiation of tolmetin. *J. Pharmacol. Exp. Ther.*, **226**, 625–632.

WYKE, B. (1981). The neurology of joints: a review of general principles. *Clin. Rheum. Dis.*, **7**, 223–239.

(Received February 25, 1991
Revised April 15, 1991
Accepted May 1, 1991)

Br. J. Pharmacol. (1991), **104**, 183–189

Carotid vascular effects of ergotamine and dihydroergotamine in the pig: no exclusive mediation via 5-HT_1-like receptors

Marinus O. den Boer, Jan P.C. Heiligers & [1]Pramod R. Saxena

Department of Pharmacology, Faculty of Medicine and Health Sciences, Erasmus University Rotterdam, P.O. Box 1738, 3000 DR Rotterdam, The Netherlands

1 Though it is well known that the antimigraine drugs ergotamine and dihydroergotamine reduce carotid arteriovenous anastomotic shunting, it is uncertain whether a 5-HT_1-like receptor is responsible for this effect. Using a high dose of methiothepin (3 mg kg^{-1}), which completely blocks the carotid vascular effects of sumatriptan, we have attempted to study the role of 5-HT_1-like receptors in the carotid vascular effects of ergotamine as well as dihydroergotamine in anaesthetized pigs.

2 Both ergotamine and dihydroergotamine increased arterial blood pressure and decreased heart rate.

3 The ergot alkaloids reduced dose-dependently total carotid blood flow and conductance as a result of a selective decrease in the arteriovenous anastomotic fraction. The nutrient fraction increased, particularly to bones, tongue and salivary glands with ergotamine and to ears, head skin, bones and salivary glands with dihydroergotamine. In contrast, dural vascular conductance tended to decresae.

4 Methiothepin (3 mg kg^{-1}) partially antagonized the decrease in total carotid and arteriovenous anastomotic blood flow and conductance by the ergot alkaloids; the ED_{30} for ergotamine and dihydroergotamine (agonist dose eliciting a 30% decrease in arteriovenous anastomotic conductance) was raised by 3.1 and 5.2 fold respectively.

5 These results indicate that the effects of ergotamine and dihydroergotamine are partly mediated by methiothepin-sensitive receptors, which may probably belong to either 5-HT_1-like or α_2-adrenoceptor category. However, an important part of the effect of ergot alkaloids is left after methiothepin and this could be mediated by other, perhaps novel, receptors.

Keywords: α-adrenoceptors; arteriovenous anastomoses; carotid blood flow; cranial arteriovenous shunting in the pig; dihydroergotamine; ergotamine; ergot alkaloids; 5-hydroxytryptamine receptors; migraine; sumatriptan

Introduction

The pharmacology of the antimigraine drugs ergotamine and dihydroergotamine is complex. Apart from being capable of inhibiting the sympathetic nervous system and blunting cardiovascular reflexes (Saxena & De Vlaam-Schluter, 1974; Clark *et al.*, 1978; Saxena & Cairo-Rawlins, 1979), the ergot alkaloids possess a direct vasoconstrictor property on veins and larger arteries. Depending on the species, the blood vessel and the experimental procedure used, stimulation of both adrenoceptors (α_1 and α_2) and 5-hydroxytryptamine (5-HT_1-like and 5-HT_2) receptors have been implicated (Berde & Stürmer, 1978; Müller-Schweinitzer & Weidmann, 1978; Müller-Schweinitzer & Rosenthaler, 1987; Glusa & Markwardt, 1988; Müller *et al.*, 1988). A reduction of carotid arteriovenous anastomotic blood flow by ergotamine is a property shared by other antimigraine drugs such as dihydroergotamine, isometheptene, methysergide and sumatriptan (Johnston & Saxena, 1978; Spierings & Saxena, 1980; Saxena & Verdouw, 1984; Perren *et al.*, 1989; Saxena *et al.*, 1989; Den Boer *et al.*, 1991; Saxena & Den Boer, 1991). In different species this effect of ergotamine was only partially affected by pretreatment with phentolamine (0.5 mg kg^{-1}) and methiothepin (1 mg kg^{-1}) and not at all by pizotifen (0.5 mg kg^{-1}) or ketanserin (0.5 mg kg^{-1}) (Saxena *et al.*, 1983; Bom *et al.*, 1989a). These findings apparently excluded a major role of 5-HT_1-like, 5-HT_2 and D_2 receptors as well as α_1- and α_2-adrenoceptors.

Recent investigations have revealed that: (1) ergotamine and dihydroergotamine, besides their well known ability to bind to α_1- and α_2-adrenoceptors and D_2 receptors, show high affinities for 5-HT_1 and 5-HT_2 binding sites (Table 1), (ii) the reduction of arteriovenous anastomotic blood flow by sumatriptan, a selective 5-HT_1-like receptor agonist (Humphrey *et al.*, 1988) with antimigraine action is only partially inhibited by 1 mg kg^{-1} of methiothepin (Den Boer *et al.*, 1991), and (iii) for a full inhibition of the effect of sumatriptan, a dose of 3 mg kg^{-1} is required (Den Boer *et al.*, 1991). Thus, the adequacy of the dose of methiothepin (1 mg kg^{-1}) used in the ergotamine experiments (Bom *et al.*, 1989a) to antagonize 5-HT_1-like receptors is questionable. Therefore, the present experiments were devoted to studying the effect of 3 mg kg^{-1} methiothepin on the reduction in cranial arteriovenous anastomotic shunting by ergotamine in the pig. In addition, dihydroergotamine was included in this study, since no data are available on the receptors involved in the carotid vascular action of this ergot derivative.

Methods

General

After an overnight fast, 24 domestic pigs (Yorkshire × Landrace; 16–22 kg) were anaesthetized with azaperone (120 mg,

Table 1 Affinities (pK_i) of ergotamine, dihydroergotamine and methiothepin for different binding sites

	Ergotamine	*Dihydroergotamine*	*Methiothepin*
5-HT_{1A}	8.3[a]; 8.4[b]	8.6[a]; 8.9[bc]	7.1[b]
5-HT_{1B}	8.7[ab]	8.4[a]; 9.1[b]	7.3[b]
5-HT_{1C}	7.3[ab]	7.3[a]; 7.4[c]; 7.5[b]	7.6[b]
5-HT_{1D}	7.6[b]; 7.8[a]	7.7[bc]; 7.9[a]	7.3[b]
5-HT_2	7.7[b]; 7.9[d]	7.1[c]; 8.6[b]	8.2[e]; 8.8[b]
α_1	8.0[d]	8.2[c]	8.9[e]; 9.3[f]
α_2	8.2[d]	8.5[c]	6.9[e]; 7.3[f]
D_2	8.5[d]	7.0[e]	8.4[f]

Data from: [a] Hoyer *et al.*, 1989; [b] Hoyer, 1989; [c] McCarthy & Peroutka, 1989; [d] Leysen & Gommeren, 1984; [e] Leysen *et al.*, 1981; [f] Leysen, 1985.

[1] Author for correspondence.

i.m.) and metomidate (150 mg, i.v.), intubated and connected to a respirator (Bear 2E, BeMeds AG, Baar, Switzerland) for intermittent positive pressure ventilation with a mixture of room air and oxygen. Respiratory rate, tidal volume and oxygen supply were adjusted to keep arterial blood gas values within physiological limits (pH; 7.35–7.48; P_{CO_2}: 35–48 mmHg; P_{O_2}: 100–120 mmHg). Anaesthesia was maintained with a continuous i.v. infusion of pentobarbitone sodium (Sanofi, Paris, France) at 20 mg kg^{-1} h^{-1} for the first hour and thereafter 12 mg kg^{-1} h^{-1}.

Catheters were placed in the inferior vena cava via a femoral vein for the administration of drugs and the aortic arch via a femoral artery, connected to a Statham pressure transducer (P23 Dc, Hato Rey, Puerto Rico) for the measurement of arterial blood pressure and the withdrawal of arterial blood for determination of blood gases (ABL-2, Radiometer, Copenhagen, Denmark). Mean arterial blood pressure (MAP) was calculated from the systolic (SAP) and diastolic (DAP) arterial pressures; MAP = (SAP + 2 × DAP)/3. The common carotid arteries were dissected free and the cervical vagosympathetic trunks were cut. Blood flow was measured in one of the common carotid arteries with a flow probe (internal diameter: 2.5 or 3 mm) connected to a sine-wave electromagnetic flow meter (Transflow 600-system, Skalar, Delft, The Netherlands). Heart rate was measured with a tachograph triggered from the blood pressure or the flow signal, depending on their shape. A 0.5 mm (external diameter) needle, connected to a polyethylene tubing was inserted into the common carotid artery against the direction of the blood flow for the administration of radioactive microspheres. On the same side the jugular vein was cannulated in order to obtain venous blood samples for determining blood gases.

During the experiment body temperature was kept at about 37°C and the animal was continuously infused with 100 ml h^{-1} saline to compensate for fluid losses.

Distribution of common carotid blood flow

The distribution of common carotid blood flow was determined with 15 ± 1 (s.d.) μm diameter microspheres labelled with either ^{141}Ce, ^{113}Sn, ^{103}Ru, ^{95}Nb or ^{46}Sc (NEN Company, Dreieich, West Germany). For each measurement a suspension of about 200,000 microspheres, labelled with one of the isotopes, was mixed and injected into the carotid artery against the direction of the blood flow to ensure uniform mixing. At the end of the experiment the animals were killed and the heart, kidneys, lungs and the different cranial tissues were dissected out, weighed and put in vials. The radioactivity in these vials was counted for 5–10 min in a gamma-scintillation counter (Packard, Minaxi Autogamma 5000) using suitable windows for discriminating the different isotopes.

The ratio between the radioactivity in a particular tissue and the total radioactivity was calculated with a set of specially developed computer programmes (Saxena *et al.*, 1980). By multiplying this ratio with the total carotid blood flow value at the time of the injection, blood flow to the tissues (nutrient blood flow) was determined. No radioactivity could be detected in the heart or the kidneys, so all microspheres reaching the venous side by arteriovenous anastomoses were trapped in the lungs. Therefore, the amount of radioactivity in the lungs was used as an index for the arteriovenous anastomotic part of the common carotid blood flow (see Johnston & Saxena, 1978; Saxena & Verdouw, 1984). The respective conductances were determined by dividing blood flow by mean arterial blood pressure.

Experimental protocol

After a stabilization period of about 1 h, the animals were divided into four groups. The first group received cumulative bolus injections of ergotamine (2.5, 5, 10 and 20 μg kg^{-1}), every 25–30 min after saline pretreatment. The second group received the same doses of ergotamine, but after pretreatment with methiothepin (3 mg kg^{-1}). The third and fourth groups received cumulatively dihydroergotamine (3, 10, 30 and 100 μg kg^{-1}), every 25–30 min after pretreatment with, respectively, saline and methiothepin (3 mg kg^{-1}). All pretreatments were given i.v. over a 30 min period. Just before and after about 15–20 min after each dose of the ergot alkaloids, measurements of heart rate, mean blood pressure, carotid blood flow and its distribution and arterial and jugular venous blood gases were made.

Data presentation and statistical analysis

All data have been expressed as means ± s.e.mean. The significance of the differences between the variables within one group was evaluated with Duncan's new multiple range test, once an analysis of variance (randomized block design) had revealed that the samples represented different populations (Steel & Torrie, 1980). Between groups the respective changes at the same dose of ergotamine or dihydroergotamine were evaluated with a Student's t test. Statistical significance was accepted at $P < 0.05$ (two-tailed).

Drugs

Apart from the anaesthetics, azaperone and metomidate (both from Janssen Pharmaceutica, Beerse, Belgium), the drugs used in this study were: ergotamine tartrate (Wander-Pharma, Uden, The Netherlands), dihydroergotamine mesylate (Wander-Pharma, Uden, The Netherlands), methiothepin maleate (gift: Hoffman La Roche B.V., Mijdrecht, The Netherlands) and heparin sodium (Thromboliquine, Organon Teknika B.V., Boxtel, The Netherlands) to prevent clotting of the catheters. Methiothepin maleate was dissolved in 5 ml propylene glycol 20% in distilled water and subsequently diluted with 45 ml physiological saline. All doses refer to the respective salts.

Results

Changes in the systemic haemodynamics by the ergot alkaloids

The systemic haemodynamic effects of the ergot alkaloids are shown in Table 2. Ergotamine caused a dose-dependent decrease in heart rate up to −12 ± 3% at the maximum dose. Dihydroergotamine also reduced heart rate until the 30 μg kg^{-1} dose (−6 ± 3%) but after the highest dose heart rate had returned to baseline. Though the responses were rather small, methiothepin seemed to attenuate those caused by ergotamine.

Mean arterial blood pressure was dose-dependently increased by 29 ± 2% and 40 ± 7% at the highest dose of ergotamine and dihydroergotamine, respectively. Methiothepin attenuated the increases in blood pressure by the two compounds; it should, however, be noted that in both methiothepin pretreated groups, initial arterial blood pressure was higher (Table 2).

Changes in the arteriovenous oxygen saturation difference

Dihydroergotamine caused an increase in the difference in oxygen saturation between arterial and jugular venous blood (Table 2). Ergotamine tended to increase equally arteriovenous oxygen saturation difference, although this did not reach statistical significance. The responses to dihydroergotamine remained unaffected and those to ergotamine were even slightly accentuated in animals pretreated with methiothepin.

Changes in the carotid haemodynamics

In the four groups, between 71 and 80% of the carotid blood flow passed through arteriovenous anastomoses. In the saline-

Table 2 Effects of intravenous bolus injections of ergotamine and dihydroergotamine on systemic haemodynamic variables and arteriovenous difference in oxygen saturation after pretreatment with saline or methiothepin (3 mg kg^{-1})

	Ergotamine (μg kg^{-1})					*Dihydroergotamine* (μg kg^{-1})				
	0	2.5	5	10	20	0	3	10	30	100
Heart rate (beats min^{-1})										
Saline	88 ± 3	84 ± 3	81 ± 4*	79 ± 4*	77 ± 4*	90 ± 2	87 ± 1	85 ± 1*	84 ± 2*	89 ± 2
Methiothepin	87 ± 4	86 ± 4	85 ± 4	84 ± 3	81 ± 3*	86 ± 3	84 ± 3	83 ± 3	84 ± 3	87 ± 3
Mean arterial blood pressure (mmHg)										
Saline	85 ± 6	97 ± 7	99 ± 6*	103 ± 7*	109 ± 7*	90 ± 2	104 ± 3*	110 ± 4*	118 ± 5*	126 ± 5*
Methiothepin	95 ± 4	97 ± 6†	99 ± 7	102 ± 8†	104 ± 8†	96 ± 6	98 ± 7†	101 ± 6†	108 ± 7*†	112 ± 7*†
Arteriovenous difference in oxygen saturation (%)										
Saline	5 ± 1	7 ± 1	8 ± 1	9 ± 2	10 ± 2	6 ± 1	8 ± 1	9 ± 2	10 ± 2*	11 ± 2*
Methiothepin	7 ± 2	8 ± 2	10 ± 2	12 ± 3*	13 ± 3*	4 ± 1	5 ± 1	5 ± 1	7 ± 1*	8 ± 1*

All values have been presented as means ± s.e.mean. * $P < 0.05$ vs. baseline.
† $P < 0.05$ vs. the corresponding dose in saline pretreated animals.

pretreated animals, both ergotamine and dihydroergotamine caused dose-dependent decreases in arteriovenous anastomotic blood flow (Figures 1 and 2). At the highest dose of ergotamine (20 μg kg^{-1}, cumulatively 37.5 μg kg^{-1}), arteriovenous anastomotic blood flow had decreased by 66 ± 6%, but total carotid blood flow only by 37 ± 5% because nutrient (tissue) blood flow had increased by 76 ± 13%. The highest dose of dihydroergotamine (100 μg kg^{-1}, 143 μg kg^{-1} cumulatively) decreased arteriovenous anastomotic blood flow by 78 ± 7% and total carotid flow by 36 ± 5%, while nutrient flow increased by 72 ± 14%. Because both ergotamine and dihydroergotamine increased arterial blood pressure (Table 2), they caused even larger decreases in total carotid and arteriovenous anastomotic vascular conductances; the increases at the highest doses were: 51 ± 3% and 74 ± 4%, respectively, for ergotamine and 53 ± 5% and 84 ± 6%, respectively, for dihydroergotamine (Figures 3 and 4). Pretreatment with methiothepin (3 mg kg^{-1}) attenuated the effects of both ergotamine and dihydroergotamine on arteriovenous anastomotic blood flow and conductance; there was a 3.1 and 5.2 fold shift in the ED_{30} (dose eliciting a 30% decrease in arteriovenous anastomotic conductance) of ergotamine and dihydroergotamine, respectively.

The effects of ergotamine and dihydroergotamine on the nutrient conductance to the different tissues are shown in Figure 5. Ergotamine increased the arteriolar conductance in

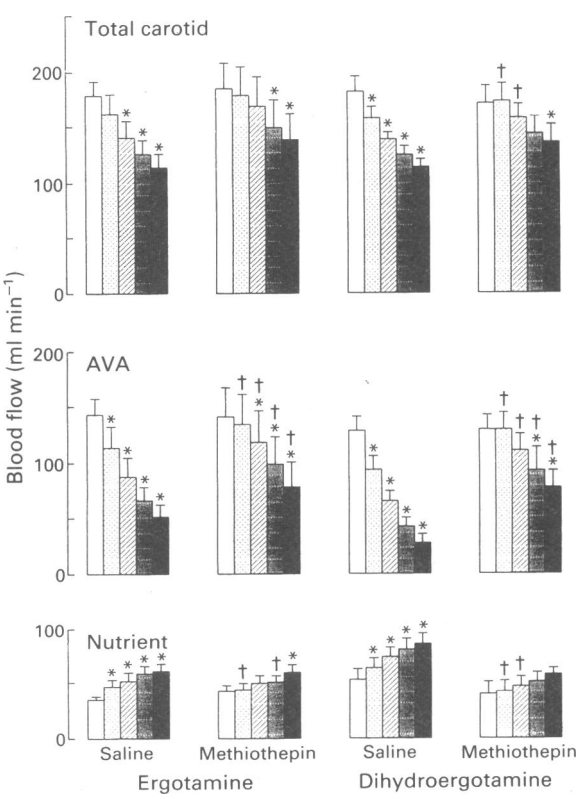

Figure 1 Effects of ergotamine and dihydroergotamine on total carotid blood flow and its arteriovenous anastomotic (AVA) and nutrient fractions in anaesthetized pigs pretreated with saline ($n = 6$ each) or methiothepin (3 mg kg^{-1}; $n = 6$ each). The five columns in each panel represent, from left to right, the following doses: ergotamine: 0 (baseline), 2.5, 5, 10 and 20 μg kg^{-1}; dihydroergotamine: 0 (baseline), 3, 10, 30 and 100 μg kg^{-1}. * $P < 0.05$ vs baseline; † $P < 0.05$ vs the corresponding dose in the saline pretreated animals.

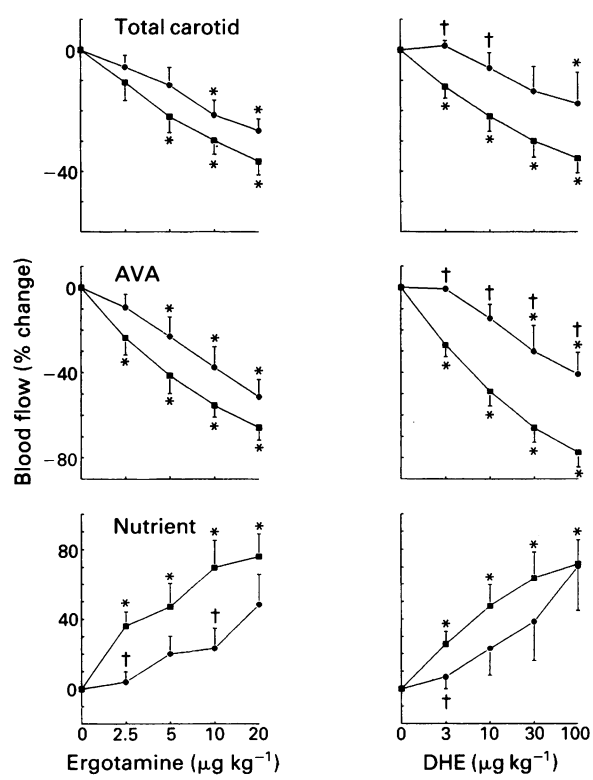

Figure 2 Percentage changes in total carotid blood flow and its arteriovenous anastomotic (AVA) and nutrient fractions induced by ergotamine and dihydroergotamine (DHE) in anaesthetized pigs pretreated with saline (■; $n = 6$ and 6, respectively) or methiothepin (3 mg kg^{-1}, ●; $n = 6$ and 6, respectively). * $P < 0.05$ vs baseline; † $P < 0.05$ vs the corresponding dose in the saline pretreated animals.

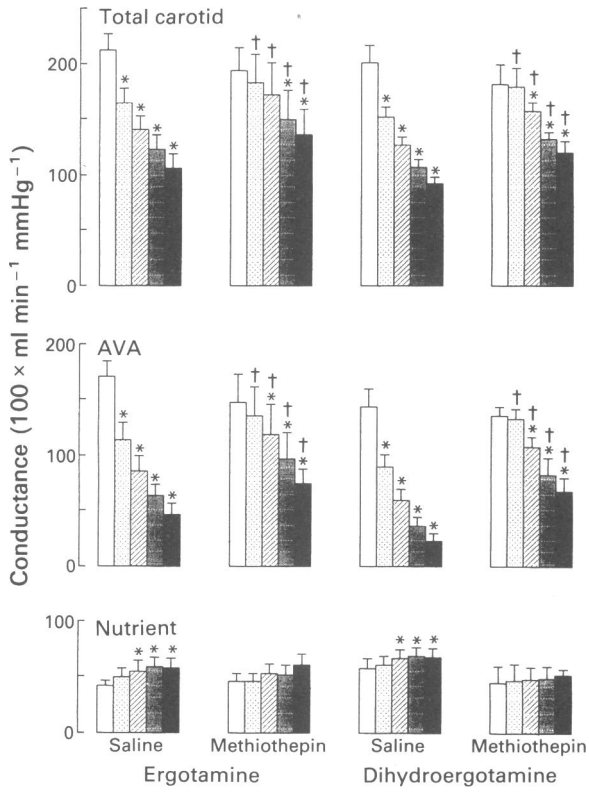

Figure 3 Effects of ergotamine and dihydroergotamine on total carotid vascular conductance and its arteriovenous anastomotic (AVA) and nutrient fractions in anaesthetized pigs pretreated with saline ($n = 6$ each) or methiothepin ($3\,mg\,kg^{-1}$; $n = 6$ each). The five columns in each panel represent, from left to right, the following doses: ergotamine: 0 (baseline), 2.5, 5, 10 and $20\,\mu g\,kg^{-1}$; dihydroergotamine: 0 (baseline), 3, 10, 30 and $100\,\mu g\,kg^{-1}$. * $P < 0.05$ vs baseline; † $P < 0.05$ vs the corresponding dose in the saline pretreated animals.

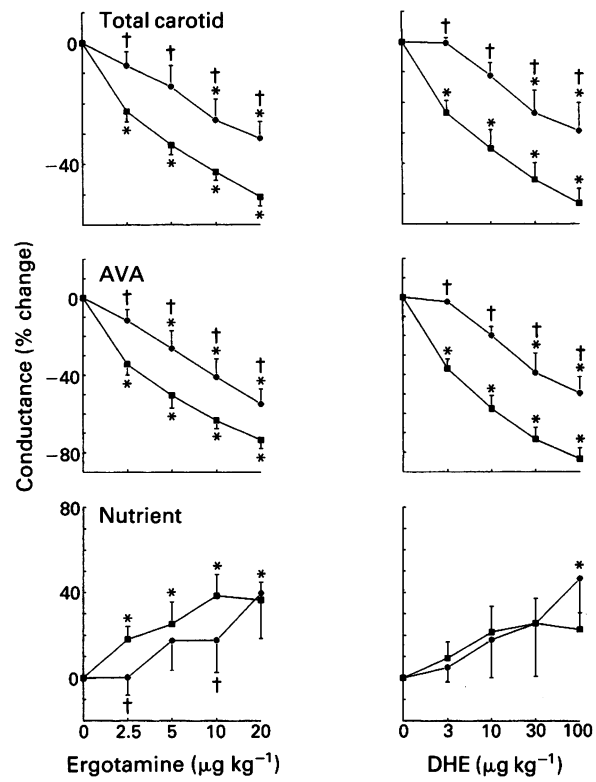

Figure 4 Percentage changes in total carotid vascular conductance and its arteriovenous anastomotic (AVA) and nutrient fractions induced by ergotamine and dihydroergotamine (DHE) in anaesthetized pigs pretreated with saline (■; $n = 6$ and 6, respectively) or methiothepin ($3\,mg\,kg^{-1}$, ●; $n = 6$ and 6, respectively). * $P < 0.05$ vs baseline; † $P < 0.05$ vs the corresponding dose in the saline pretreated animals.

the bones, tongue and salivary glands, whereas the arteriolar conductance in the other tissues remained unchanged. Methiothepin ($3\,mg\,kg^{-1}$) had no significant effect on these changes in nutrient conductance. Dihydroergotamine slightly increased the arteriolar conductance in the ears, head skin, bones and salivary glands. Methiothepin ($3\,mg\,kg^{-1}$) attenuated most of these effects.

Figure 5 also shows that, despite an increase in total nutrient conductance as well as conductance in several tissues, the conductance in the dura mater tended to decrease with both ergot alkaloids. However, this vascular effect reached statistical significance only in the case of dihydroergotamine. Methiothepin did not have a clear effect on the responses of the dural vessels.

Discussion

Systemic haemodynamics

Ergotamine reduced dose-dependently heart rate. Such a bradycardia has already been shown in different species, like dogs and man (Clark *et al.*, 1978), cats (Saxena & Cairo-Rawlins, 1979) and pigs (Schamhardt *et al.*, 1979; Bom *et al.*, 1989a). In cats, an agonist action at presynaptic dopamine receptors on sympathetic cardioaccelerator neurones has been implicated (Saxena & Cairo-Rawlins, 1979), but in rats stimulation of presynaptic α_2-adrenoceptors may be involved (Roquebert & Grenié, 1986). The mechanism involved in pigs is, however, unknown at present. Dihydroergotamine ($3–30\,\mu g\,kg^{-1}$) also reduced heart rate in a dose-dependent way, probably by the same mechanism as ergotamine; in man a moderate decrease in heart rate has been observed after $10–15\,\mu g\,kg^{-1}$ of dihydroergotamine (Harris *et al.*, 1963; Nordenfeldt & Mellander, 1972). Since the highest dose of dihydroergotamine ($100\,\mu g\,kg^{-1}$) produced less bradycardia than the lower doses in the present experiments, the drug may have a partial agonist activity on the receptor involved.

The pressor response to the ergot alkaloids is generally believed to be a peripheral action, depending much on the pre-existing sympathetic tone (Clark *et al.*, 1978). In the case of a high sympathetic tone, the sympatholytic action of the ergots predominates and no or less marked pressor responses are found, as has been the case in some earlier studies (Saxena & De Vlaam-Schluter, 1974; Bom *et al.*, 1989a). In the present investigation, arterial blood pressure was increased by both ergotamine and dihydroergotamine. In the rat, the ergot alkaloids-induced pressor response seems to be mediated partly by α_2-adrenoceptors and partly by 5-HT receptors, but probably not by α_1-adrenoceptors (Roquebert & Grenié, 1986; Müller *et al.*, 1988). Although the receptor mechanism in the pig is unknown, both the α-adrenoceptor and the 5-HT receptor antagonist potency of methiothepin may be responsible for the attenuation of the pressor responses to the two ergot alkaloids (see Table 1).

Carotid haemodynamics

Both ergotamine and dihydroergotamine caused dose-dependent decreases in carotid blood flow and vascular conductance, exclusively by affecting the arteriovenous anastomotic fraction. The effects of the drugs on the arteriovenous oxygen saturation difference is in keeping with an effect on the arteriovenous anastomoses. Heyck (1969) observed a decreased arterio-jugular venous oxygen saturation difference during migraine attacks and administration of dihydroergotamine raised this difference, as in our experiments. It is interesting to note that, despite an increase in

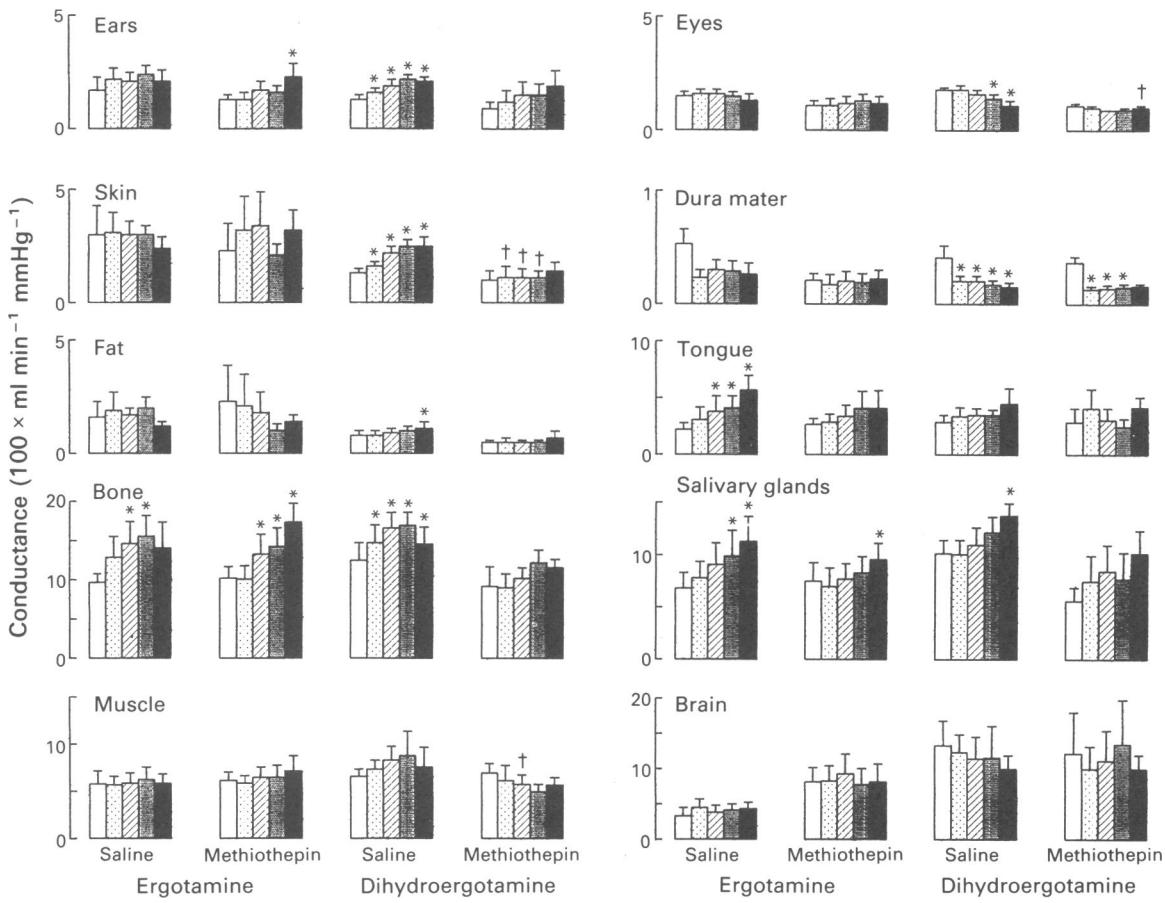

Figure 5 Effects of ergotamine and dihydroergotamine on vascular conductance in different cranial tissues in anaesthetized pigs pretreated with saline ($n = 6$ each) or methiothepin ($3\,mg\,kg^{-1}$; $n = 6$ each). The five columns in each panel represent, from left to right, the following doses: ergotamine: 0 (baseline), 2.5, 5, 10 and $20\,\mu g\,kg^{-1}$; dihydroergotamine: 0 (baseline), 3, 10, 30 and $100\,\mu g\,kg^{-1}$. * $P < 0.05$ vs baseline; † $P < 0.05$ vs the corresponding dose in the saline pretreated animals.

vascular conductance in several cranial extracerebral tissues and the nutrient conductance as a whole, dural vascular conductance decreased with the ergots. There was no effect on the cerebral component of the carotid blood flow in our experiments, which is in keeping with the observations in both animals and man that total cerebral blood flow is little affected by ergotamine and dihydroergotamine (Hatchinski *et al.*, 1978; Johnston & Saxena, 1978; Andersen *et al.*, 1987).

Pretreatment with $3\,mg\,kg^{-1}$ methiothepin partly antagonized the effects of the two ergot alkaloids. This antagonism was slightly more marked in the case of dihydroergotamine than ergotamine; the increase in ED_{30} was, respectively, 5.2 and 3.1 fold. Since methiothepin $1\,mg\,kg^{-1}$ had caused a 3.2 fold increase in ED_{30} of ergotamine in the experiments of Bom *et al.* (1989a), the higher dose of methiothepin did not seem to have any further effect. This is in contrast with sumatriptan where methiothepin dose-dependently antagonized the carotid vascular effects and with the higher dose ($3\,mg\,kg^{-1}$) a complete blockade was observed (Den Boer *et al.*, 1991). At high concentrations, methiothepin is an antagonist at 5-HT_1-like and 5-HT_2 receptors (Table 1; Bradley *et al.*, 1986) as well as at α_1- and α_2-adrenoceptors and D_2 receptors (Table 1). Since ergotamine and dihydroergotamine also have reasonable affinities for these receptors (Table 1), theoretically any of these could mediate the methiothepin-sensitive component of the effect of the ergot alkaloids. Involvement of α_1, 5-HT_2 or D_2 receptors seems less likely, since blockade of 5-HT_2 receptors by pizotifen in dogs and of 5-HT_2 and α_1 receptors by ketanserin in cats left the responses to ergotamine unchanged (Saxena *et al.*, 1983; Bom *et al.*, 1989a) and the presence of functional D_2 receptors on blood vessels is at present uncertain (De Keyser *et al.*, 1988). Since phentolamine slightly inhibited the carotid vasoconstrictor responses to ergotamine in dogs (Saxena & De Vlaam-Schluter, 1974; Saxena *et al.*, 1983), the attenuation observed with methiothepin in the present experiments could be due to blockade of postsynaptic α_2-adrenoceptors. Nevertheless, we cannot rule out the involvement of 5-HT_1-like receptors, especially since phentolamine also has a slight antagonist action at 5-HT receptors (Parsons *et al.*, 1989; Hoffman & Lefkowitz, 1990). Ergotamine and dihydroergotamine as well as sumatriptan share a high affinity for the 5-HT_{1D} subtype of the 5-HT_1-like receptors (Table 1) and all three inhibit forskolin-stimulated adenylate cyclase activity in calf substantia nigra (Hoyer & Schoeffter, 1991), a putative 5-HT_{1D} receptor mediated effect. However, a possible role of this receptor in the carotid vasoconstrictor responses to these drugs has still to be elucidated.

The present experiments show that, despite the use of a high dose ($3\,mg\,kg^{-1}$) of methiothepin, a substantial part of the arteriovenous anastomotic flow reduction by the ergot alkaloids was not amenable to blockade by methiothepin. This is in marked contrast to the antimigraine drug sumatriptan (Den Boer *et al.*, 1991) and other drugs, such as 5-HT (Saxena *et al.*, 1986), 8-OH DPAT (Bom *et al.*, 1989b), RU 24969 (Bom *et al.*, 1989c) and indorenate (Villalón *et al.*, 1990), all of which reduce arteriovenous anastomotic blood flow by acting on a 5-HT_1-like receptor which is quite susceptible to blockade by methiothepin (Saxena & Ferrari, 1989; Den Boer *et al.*, 1991). Therefore, the carotid vasoconstrictor effects of the ergot alkaloids must be mediated in part by a novel mechanism involving 'ergot receptors' that remain to be characterized. Such receptors have also been postulated in the contraction of rabbit isolated saphenous vein to the non-peptide ergot alkaloids methysergide, ergometrine and methylergometrine

(MacLennan & Martin, 1990). These contractions were clearly biphasic and only the first part was susceptible to blockade by methiothepin.

Possible mechanisms in the antimigraine effect

The exact mechanism of the antimigraine activity of the ergot alkaloids and, indeed of other drugs is under debate (see Saxena & Ferrari, 1989; Buzzi & Moskowitz, 1990; Humphrey *et al.*, 1990; Saxena, 1990). The limited understanding of the migraine syndrome itself is in large part the reason for this. Due to the unilaterality of the symptoms, migraine is likely to be caused by a neural disturbance in the central nervous system, possibly originating in the brain stem nuclei. This could lead to a dilatation of extracerebral cranial blood vessels, which has been observed, at least in some patients, during a migraine attack (Drummond & Lance, 1988; Saxena & Ferrari, 1989; Iversen *et al.*, 1990).

Notwithstanding the mechanism, a common feature of the antimigraine drugs effective against acute migraine attacks (ergotamine, dihydroergotamine and sumatriptan) is their ability to constrict, relatively selectively, arteries and arteriovenous anastomoses in the cranial circulation, without affecting tissue blood flow (Müller-Schweinitzer & Weidmann, 1978; Saxena & Ferrari, 1989; Saxena & Den Boer, 1991). Since sumatriptan does not seem to penetrate the blood brain barrier (Dallas *et al.*, 1989) and the evidence regarding penetration by ergotamine and dihydroergotamine is at best equivocal (in favour: Ala-Hurula *et al.*, 1979; Goadsby & Gundlach, 1991; against: Eckert *et al.*, 1978; Kanto *et al.*, 1981; Hovdal *et al.*, 1982), it would appear that the antimigraine effect of these drugs is related to a vascular effect, possibly involving a powerful vasoconstrictor activity on dilated and painful blood vessels. In addition, these drugs have been reported to inhibit extravasation of plasma in the dura mater following stimulation of the trigeminal ganglion in the rat (Markowitz *et al.*, 1988; Saito *et al.*, 1988; Buzzi & Moskowitz, 1990); such an effect may also contribute to the antimigraine effect of these drugs. However, the exact mechanism responsible for the inhibition of plasma extravasation is not well understood. Although an effect on receptors on sensory afferent fibres in the muscular layer of the blood vessel wall is possible, this effect could equally be secondary to vasoconstriction. Indeed, sumatriptan has been shown to have a vasoconstrictor action in human dural blood vessels (Feniuk *et al.*, 1991). Furthermore, apart from arteries and veins, the presence of arteriovenous anastomoses in the dura mater has been anatomically demonstrated (Rowbotham & Little, 1965; Kerber & Newton, 1973).

Part of this work was financially supported by Glaxo Group Research, Ware, UK. The authors wish to thank Dr W. Feniuk (Glaxo Group Research, Ware, U.K.) for his critical remarks and help in preparing the manuscript.

References

ALA-HURULA, V., MYLLYLÄ, V.V., ARVELA, P., KÄRKI, N. & HOKKANEN, E. (1979). Systemic availability of ergotamine tartrate after three successive doses and during continuous medication. *Eur. J. Clin. Pharmacol.*, **16**, 355–360.

ANDERSEN, A.R., TFELT-HANSEN, P. & LASSEN, N.A. (1987). The effect of ergotamine and dihydroergotamine on cerebral blood flow in man. *Stroke*, **18**, 120–123.

BERDE, B. & STUERMER, E. (1978). Introduction to the pharmacology of ergot alkaloids and related compounds as a basis of their therapeutic application. In *Ergot Alkaloids and Related Compounds, Handbook of Experimental Pharmacology*, Vol. 49. ed. Berde, B. & Schild, H.O. pp. 1–28. Berlin, Heidelberg, New York: Springer-Verlag.

BOM, A.H., HEILIGERS, J.P.C., SAXENA, P.R. & VERDOUW, P.D. (1989a) Reduction of cephalic arteriovenous shunting by ergotamine is not mediated by 5-HT_1-like or 5-HT_2 receptors. *Br. J. Pharmacol.*, **97**, 383–390.

BOM, A.H., VERDOUW, P.D. & SAXENA, P.R. (1989b). Carotid haemodynamics in pigs during infusions of 8-OH-DPAT: Reduction in arteriovenous shunting is mediated by 5-HT_1-like receptors. *Br. J. Pharmacol.*, **96**, 125–132.

BOM, A.H., VILLALÓN, C.M., VERDOUW, P.D. & SAXENA, P.R. (1989c). The 5-HT_1-like receptor mediating reduction of porcine carotid arteriovenous shunting by RU 24969 is not related to either the 5-HT_{1A} or the 5-HT_{1B} subtype. *Eur. J. Pharmacol.*, **171**, 87–96.

BRADLEY, P.B., ENGEL, G., FENIUK, W., FOZARD, J.R., HUMPHREY, P.P.A., MIDDLEMISS, D.N., MYLECHARANE, E.J., RICHARDSON, B.P. & SAXENA, P.R. (1986). Proposals for the classification and nomenclature of functional receptors for 5-hydroxytryptamine. *Neuropharmacology*, **25**, 563–576.

BUZZI, M.G. & MOSKOWITZ, M.A. (1990). The antimigraine drug, sumatriptan (GR43175), selectively blocks neurogenic plasma extravasation from blood vessels in dura mater. *Br. J. Pharmacol.*, **99**, 202–206.

CLARK, B.J., CHU, D. & AELLIG, W.H. (1978). Actions on the heart and circulation. In *Ergot Alkaloids and Related Compounds, Handbook of Experimental Pharmacology*, Vol. 49. ed. Berde, B. & Schild, H.O. pp. 321–420. Berlin, Heidelberg, New York: Springer-Verlag.

DALLAS, F.A.A., DIXON, C.M., McCULLOCH, R.J. & SAYNOR, D.A. (1989). The kinetics of ^{14}C-GR43175 in rat and dog. *Cephalalgia*, **9** (Suppl. 9), 53–56.

DE KEYSER, J., EBINGER, G., DE BACKER, J.P., CONVENTS, A., VANDERHEYDEN, P. & VAUQUELIN, G. (1988). Subtypes of adrenergic and dopaminergic receptors in bovine cerebral blood vessels. *Neurosci. Lett.*, **85**, 272.

DEN BOER, M.O., VILLALÓN, C.M., HEILIGERS, J.P.C., HUMPHREY, P.P.A. & SAXENA, P.R. (1991). Role of 5-HT_1-like receptors in the reduction of porcine cranial arteriovenous anastomotic shunting by sumatriptan. *Br. J. Pharmacol.*, **102**, 323–330.

DRUMMOND, P.D. & LANCE, J.W. (1988). Contribution of the extracranial circulation to the pathophysiology of headache. In *Basic Mechanisms of Headache*. ed. Olesen, J. & Edvinsson, L. pp. 321–330. Amsterdam, New York, Oxford: Elsevier Science Publishers.

ECKERT, H., KIECHEL, J.R., ROSENTHALER, J., SCHMIDT, R. & SCHREIER, E. (1978). Biopharmaceutical aspects: analytical methods, pharmacokinetics, metabolism and bioavailability. In *Ergot Alkaloids and Related Compounds, Handbook of Experimental Pharmacology*, Vol. 49, ed. Berde, B. & Schild, H.O. pp. 719–803. Berlin, Heidelberg, New York: Springer-Verlag.

FENIUK, W., HUMPHREY, P.P.A., PERREN, M.J., CONNOR, H.E. & WHALLEY, E.T. (1991). Rationale for the use of 5-HT_1-like agonists in the treatment of migraine. *J. Neurol.*, **238** (Suppl. 1), S57–S61.

GLUSA, E. & MARKWARDT, F. (1988). Influence of endothelium on the vasoconstrictor effect of dihydroergotamine in the isolated rat aorta. *Arch. Int. Pharmacodyn.*, **296**, 66–75.

GOADSBY, P.J. & GUNDLACH, A.L. (1991). Localization of ^{3}H-dihydroergotamine-binding sites in the cat central nervous system: relevance to migraine. *Ann. Neurol.*, **29**, 91–94.

HARRIS, P., BISHOP, J.M. & SEGEL, N. (1963). The effects of dihydroergotamine tartrate on the pulmonary and systemic circulations in man. *Clin. Sci. Mol. Med.*, **25**, 443–447.

HATCHINSKI, V.C., NORRIS, J.W., COOPER, P.W. & EDMEADS, J.G. (1978). Migraine and the cerebral circulation. In *Current Concepts in Migraine Research*. ed. Greene, R. pp. 11–15. New York: Raven Press.

HEYCK, H. (1969). Pathogenesis of migraine. *Res. Clin. Stud. Headache*, **2**, 1–28.

HOFFMAN, B.B. & LEFKOWITZ, R.J. (1990). Adrenergic receptor antagonists. In *The Pharmacological Basis of Therapeutics*. ed. Goodman Gilman, A., Rall, T.W., Nies, A.S. & Taylor, P. pp. 221–243. New York: Pergamon Press.

HOVDAL, H., SYVERSEN, G.B. & ROSENTHALER, J. (1982). Ergotamine in plasma and CSF after i.m. and rectal administration in humans. *Cephalalgia*, **2**, 145–150.

HOYER, D. (1989). 5-Hydroxytryptamine receptors and effector coupling mechanisms in peripheral tissues. In *The Peripheral Actions of 5-Hydroxytryptamine*. ed. Fozard, J.R. pp. 73–99. Oxford: Oxford University Press.

HOYER, D. & SCHOEFFTER, P. (1991). Interaction of dihydroergotamine (DHE), ergotamine and GR43175 (sumatriptan) with 5-HT_{1D} receptors. *Naunyn Schmiedebergs Arch. Pharmacol.*, **43**, (in press).

HOYER, D., SCHOEFFTER, P. & GRAY, J.A. (1989). A comparison of

the interactions of dihydroergotamine, ergotamine and GR43175 with 5-HT_1 receptor subtypes. *Cephalalgia*, **9**, 340–341.

HUMPHREY, P.P.A., APPERLEY, E., FENIUK, W. & PERREN, M.J. (1990). A rational approach to identifying a fundamentally new drug for the treatment of migraine. In *The Cardiovascular Pharmacology of 5-Hydroxytryptamine: Prospective Therapeutic Applications*. ed. Saxena, P.R., Wallis, D.I., Wouters, W. & Bevan, P. pp. 417–431. Dordrecht: Kluwer Academic Publishers.

HUMPHREY, P.P.A., FENIUK, W., PERREN, M.J., CONNOR, H.E., OXFORD, A.W., COATES, I.H. & BUTINA, D. (1988). GR43175, a selective agonist for the 5-HT_1-like receptor in dog isolated saphenous vein. *Br. J. Pharmacol.*, **94**, 1123–1132.

IVERSEN, H.K., NIELSEN, T.H., OLESEN, J. & TFELT-HANSEN, P. (1990). Arterial responses during migraine headache. *Lancet*, **336**, 837–839.

JOHNSTON, B.M. & SAXENA, P.R. (1978). The effect of ergotamine on tissue blood flow and the arteriovenous shunting of radioactive microspheres in the head. *Br. J. Pharmacol.*, **63**, 541–549.

KANTO, J., ALLONEN, H., KOSKI, K., KOULU, M., LAMMINTAUSTA, R., MÄNTYLÄ, R., KLEIMOLA, T. & SIIRTOLA, T. (1981). Pharmacokinetics of dihydroergotamine in healthy volunteers and in neurological patients after a single intravenous injection. *Int. J. Clin. Pharmacol. Ther. Toxicol.*, **19**, 127–130.

KERBER, C.W. & NEWTON, T.H. (1973). The macro and microvasculature of the dura mater. *Neuroradiology*, **6**, 175–179.

LEYSEN, J.E. (1985). Serotonergic binding sites. In *Serotonin and the Cardiovascular System*. ed. Vanhoutte, P.M. pp. 43–62. New York: Raven Press.

LEYSEN, J.E., AWOUTERS, F., KENNIS, L., LADURON, P.M., VANDENBERK, J. & JANSSEN, P.A.J. (1981). Receptor binding profile of R 41 468, a novel antagonist at 5-HT_2 receptors. *Life Sci.*, **28**, 1015–1022.

LEYSEN, J.E. & GOMMEREN, W. (1984). *In vitro* receptor binding profile of drugs used in migraine. In *The Pharmacological Basis of Migraine Therapy*. ed. Amery, W.K., Van Nueten, J.M. & Wauquier, A. pp. 255–266. London: Pitman Publishing Ltd.

MACLENNAN, S.J. & MARTIN, G.R. (1990). Actions of non-peptide ergot alkaloids at 5-HT_1-like and 5-HT_2 receptors mediating vascular smooth muscle contraction. *Naunyn Schmiedebergs Arch. Pharmacol.*, **342**, 120–129.

MARKOWITZ, S., SAITO, K. & MOSKOWITZ, M.A. (1988). Neurogenically mediated plasma extravasation in dura mater: effect of ergot alkaloids. A possible mechanism of action in vascular headache. *Cephalalgia*, **8**, 83–91.

McCARTHY, B.G. & PEROUTKA, S.J. (1989). Comparative neuropharmacology of dihydroergotamine and sumatriptan (GR43175). *Headache*, **29**, 420–422.

MÜLLER, H., GLUSA, E. & MARKWARDT, F. (1988). Dual effect of dihydroergotamine at vascular 5-hydroxytryptamine receptors in pithed rats. *Pharmacology*, **37**, 248–253.

MÜLLER-SCHWEINITZER, E. & ROSENTHALER, J. (1987). Dihydroergotamine: Pharmacokinetics, pharmacodynamics and mechanism of venoconstrictor action in Beagle dogs. *J. Cardiovasc. Pharmacol.*, **9**, 686–693.

MÜLLER-SCHWEINITZER, E. & WEIDMANN, H. (1978). Basic pharmacological properties. In *Ergot Alkaloids and Related Compounds, Handbook of Experimental Pharmacology*, Vol. 49. ed. Berde, B. & Schild, H.O. pp. 87–232. Berlin, Heidelberg, New York: Springer-Verlag.

NORDENFELDT, I. & MELLANDER, S. (1972). Central haemodynamic effects of dihydroergotamine in patients with orthostatic hypotension. *Acta Med. Scand.*, **191**, 115–120.

PARSONS, A.A., WHALLEY, E.T., FENIUK, W., CONNOR, H.E. & HUMPHREY, P.P.A. (1989). 5-HT_1-like receptors mediate 5-hydroxytryptamine-induced contraction of human isolated basilar artery. *Br. J. Pharmacol.*, **96**, 434–449.

PERREN, M.J., FENIUK, W. & HUMPHREY, P.P.A. (1989). The selective closure of feline carotid arteriovenous anastomoses (AVAs) by GR43175. *Cephalalgia*, **9** (Suppl. 9), 41–46.

ROQUEBERT, J. & GRENIE, B. (1986). α_2-Adrenergic agonist and α_1-adrenergic antagonist activity of ergotamine and dihydroergotamine in rats. *Arch. Int. Pharmacodyn.*, **284**, 30–37.

ROWBOTHAM, G.F. & LITTLE, E. (1965). New concepts on the aetiology and vascularization of meningiomata; the mechanisms of migraine; the chemical process of the cerebrospinal fluid; and the formations of the collections of blood or fluid in the subdural space. *Br. J. Surg.*, **52**, 21–24.

SAITO, K., MARKOWITZ, S. & MOSKOWITZ, M.A. (1988). Ergot alkaloids block neurogenic extravasation in dura mater: Proposed action in vascular headaches. *Ann. Neurol.*, **24**, 732–737.

SAXENA, P.R. (1990). Is there still a case for the shunt hypothesis in migraine. In *Migraine, a Spectrum of Ideas*. ed. Sandler, M. & Collins, G., pp. 191–197. Oxford: Oxford Medical Publications.

SAXENA, P.R., BOM, A.H. & VERDOUW, P.D. (1989). Characterization of 5-hydroxytryptamine receptors in the cranial vasculature. *Cephalagia*, **9** (Suppl. 9), 15–22.

SAXENA, P.R. & CAIRO-RAWLINS, W.I. (1979). Presynaptic inhibition by ergotamine of the responses to cardioaccelerator nerve stimulation in the cat. *Eur. J. Pharmacol.*, **58**, 305–312.

SAXENA, P.R. & DEN BOER, M.O. (1991). Pharmacology of antimigraine drugs. *J. Neurol.*, **238** (Suppl. 1), S28–S35.

SAXENA, P.R. & DE VLAAM-SCHLUTER, G.M. (1974). Role of some biogenic substances in migraine and relevant mechanism in antimigraine action of ergotamine. Studies in an experimental model for migraine. *Headache*, **13**, 142–163.

SAXENA, P.R., DUNCKER, D.J., BOM, A.H., HEILIGERS, J. & VERDOUW, P.D. (1986). Effects of MDL 72222 and methiothepin on carotid vascular responses to 5-hydroxytryptamine in the pig: Evidence for the presence of 'hydroxytryptamine$_1$-like' receptors. *Naunyn-Schmiedebergs Arch. Pharmacol.*, **333**, 198–204.

SAXENA, P.R. & FERRARI, M.D. (1989). 5-HT_1-like receptor agonists and the pathophysiology of migraine. *Trends Pharmacol. Sci.*, **10**, 200–204.

SAXENA, P.R., KOEDAM, N.A., HEILIGERS, J. & HOF, R.P. (1983). Ergotamine-induced constriction of cranial arteriovenous anastomoses in dogs pretreated with phentolamine and pizotifen. *Cephalalgia*, **3**, 71–81.

SAXENA, P.R., SCHAMHARDT, H.C., FORSYTH, R.P. & LOEVE, J. (1980). Computer programs for the radioactive microsphere technique. Determination of regional blood flows and other haemodynamic variables in different experimental circumstances. *Comp. Program. Biomed.*, **12**, 63–84.

SAXENA, P.R. & VERDOUW, P.D. (1984). Effects of methysergide and 5-hydroxytryptamine on carotid blood flow distribution in pigs: Further evidence for the presence of atypical 5-HT receptors. *Br. J. Pharmacol.*, **82**, 817–826.

SCHAMHARDT, H.C., VERDOUW, P.D., VAN DER HOEK, T.M. & SAXENA, P.R. (1979). Regional myocardial perfusion and wall thickness and arteriovenous shunting after ergotamine administration to pigs with a fixed coronary stenosis. *J. Cardiovasc. Pharmacol.*, **1**, 673–686.

SPIERINGS, E.L.H. & SAXENA, P.R. (1980). Antimigraine drugs and cranial arteriovenous shunting in the cat. *Neurology*, **30**, 696–701.

STEEL, R.G.D. & TORRIE, J.H. (1980). *Principles and Procedures of Statistics. A Biomedical Approach*, 2nd edn., Tokyo: McGraw Hill Kogakusha Ltd.

VILLALÓN, C.M., BOM, A.H., HEILIGERS, J.P.C., DEN BOER, M.O. & SAXENA, P.R. (1990). The 5-HT_1-like receptor involved in the indorenate-induced reduction of porcine cephalic arteriovenous shunting seems unrelated to either 5-HT_{1A}, 5-HT_{1B}, 5-HT_{1C} or 5-HT_{1D} receptor subtype. *Eur. J. Pharmacol.*, **190**, 167–176.

(Received February 18, 1991
Revised April 25, 1991
Accepted May 1, 1991)

Br. J. Pharmacol. (1991), **104**, 190–194

Effect of a 7-day treatment with idazoxan and its 2-methoxy derivative RX 821001 on α_2-adrenoceptors and non-adrenoceptor idazoxan binding sites in rabbits

[1]M. Portillo, M. Reverte, D. Langin, J.M. Senard, M.A. Tran, M. Berlan & [2]J.L. Montastruc

Laboratoire de Pharmacologie Médicale et Clinique, INSERM U317, Faculté de Médecine, 37 allées Jules-Guesde, 31073 Toulouse Cedex, France

1 The present study investigates the influence of a 7-day treatment with 2 mg kg^{-1}, s.c., twice daily of RX 821002 (an α_2-adrenoceptor antagonist which binds only to α_2-adrenoceptors) or idazoxan (α_2-antagonist which binds to α_2-adrenoceptors and also to non-adrenoceptor idazoxan binding sites: NAIBS) on α_2-adrenoceptor (labelled with [^{3}H]-RX 821002) and NAIBS (labelled with [^{3}H]-idazoxan) number in three tissues (adipocytes, colocytes and platelets) in the rabbit.

2 Acute administration of RX 821002 or idazoxan increased plasma non-esterified fatty acids (NEFA) and catecholamine levels with no change in plasma glucose levels.

3 The 7-day treatment with RX 821002 or idazoxan failed to influence food intake, total body weight or perirenal adipose tissue weight.

4 RX 821002 and idazoxan increased the number of [^{3}H]-RX 821002 binding sites in adipose tissue with no change in colocytes or platelets.

5 RX 821002 and idazoxan failed to modify [^{3}H]-idazoxan binding sites on adipocytes and colocytes. No significant [^{3}H]-idazoxan binding was detected on rabbit platelets.

6 The results show that a 7-day treatment with α_2-antagonists induces an up-regulation in adipocyte α_2-adrenoceptors. In contrast, this phenomenon does not involve all the tissues since colocytes and platelets escape the effects of α_2-antagonists. The data suggest a differential regulation of α_2-adrenoceptors according to their location.

7 The fact that NAIBS did not vary suggests that α_2-adrenoceptors and NAIBS are two different entities. Finally, since RX 821002 and idazoxan exert similar effects after either acute or chronic treatment, it is suggested that NAIBS are not involved in the control of catecholamine release or in NEFA or glucose metabolism.

Keywords: Idazoxan; RX 821002; α_2-adrenoceptors; non-adrenoceptor idazoxan binding sites; adipocytes; colocytes; platelets

Introduction

α_2-Adrenoceptors are the initial recognition sites on a great variety of catecholamine responsive target cells and have been widely studied in three different tissues, platelet, adipose tissue and colon, where their function is the reduction of aggregation velocity (Galitzky *et al.*, 1990b), antilipolysis (Taouis *et al.*, 1988) and probably the increase in fluid and electrolyte (Cl^- and Na^+) absorption (Nakaki *et al.*, 1982; Senard *et al.*, 1990) respectively.

Membrane receptors are dynamic entities the properties of which (number and/or affinity) can be modified by agonists, antagonists and heterologous hormones. In general, interaction with agonists promotes a 'down-regulation' phenomenon while inhibition of receptors by antagonists produces an 'up-regulation' phenomenon (Insel, 1989).

Regulation of α_2-adrenoceptor number in target cells appears to be somewhat different from that observed in other classes of adrenoceptors. Species and tissue differences have been published (Latifpour & McNeill, 1984). Reserpine treatment was reported to be associated with either no change (Nasseri *et al.*, 1985) or up-regulation (Fortin & Sundaresan, 1989) of α_2-adrenoceptors in rat vas deferens. Estan *et al.* (1990) showed up-regulation of platelet α_2-adrenoceptors with no change in adipocyte α_2-adrenoceptors in dogs treated with reserpine. Similar discrepancies can be found after treatment with α_2-adrenoceptor agonists or exposure to high levels of catecholamines: some studies showed α_2-adrenoceptor down-regulation in human (Brodde, 1982) and rabbit (Deighton *et al.*, 1988b) platelets and desensitization after exposure to high levels of noradrenaline (Deighton *et al.*, 1988a), whereas others observed no change (Hollister *et al.*, 1983; Valet *et al.*, 1989).

Various radioligands have been used for the identification of α_2-adrenoceptors such as [^{3}H]-idazoxan and its 2-methoxy derivative [^{3}H]-RX 821002. It has been shown that [^{3}H]-idazoxan, which possesses an imidazoline ring, labels more sites than do classical radiolabelled α_2-adrenoceptor antagonists like [^{3}H]-yohimbine. These additional binding sites are not competed by catecholamines and have been termed 'non-adrenergic (non-adrenoceptor) idazoxan binding sites' (NAIBS) (Langin & Lafontan, 1989; Langin *et al.*, 1990a) or imidazoline binding sites (MacKinnon *et al.*, 1989). Interestingly, other imidazoline compounds such as [^{3}H]-RX 821002 were shown to be selective for α_2-adrenoceptors and more appropriate than yohimbine in rabbits (Langin *et al.*, 1989; Senard *et al.*, 1990). It was first suggested that NAIBS might be closely related to α_2-adrenoceptors (Michel *et al.*, 1989). However, more recently it has been shown that they are independent entities and, to date, the role of NAIBS remains speculative (Parini *et al.*, 1989; Langin *et al.*, 1990b; Senard *et al.*, 1990).

The aim of the present work was to determine whether a chronic treatment with α_2-antagonists, i.e. idazoxan (an α_2-antagonist which also binds NAIBS) or its 2-methoxy derivative RX 821002 (which, although possessing an imidazoline ring, binds only to α_2-adrenoceptors and does not recognize NAIBS) is able to modify the number and affinity of α_2-adrenoceptors as well as NAIBS in various cells (adipocytes, colocytes and platelets) in the rabbit.

[1] Present address: Departamento de Nutricion y Bromatologia, Facultad de Farmacia, Universidad del Pais Vasco, Vitoria, Spain.
[2] Author for correspondence.

Methods

Animals and general procedure

The experiments were performed on white New Zealand rabbits (2.5–3.0 kg). The animals were housed individually and allowed access to food and water *ad libitum*. A 7-day treatment was carried out in several groups of eight rabbits each of which received either 0.9% saline vehicle, RX 821002 or idazoxan subcutaneously (2 mg kg^{-1} twice a day at 08 h 00 min and 18 h 00 min) for seven days. At day 8, 14 h after the last injection (i.e. at 09 h 00 min), the rabbits were anaesthetized with pentobarbitone (60 mg kg^{-1}, i.p.). Blood samples were removed from the carotid artery in heparinized tubes and immediately centrifuged. Plasma was collected and frozen at −20°C until use. Blood for platelets was also removed from the carotid artery in tubes containing 3.8% sodium citrate. Perirenal adipose tissue was removed immediately, weighed and isolated fat cells were prepared as previously described (Berlan & Lafontan, 1985). Epithelial cells were collected from the proximal colon by incubation in phosphate buffer containing 5 mM disodium edetate (EDTA), as previously described (Senard *et al.*, 1990). Cell membranes were prepared from adipocytes, colocytes and platelets according to the methods used by Berlan & Lafontan (1985), Senard *et al.* (1990) and Estan *et al.* (1990) respectively.

Radioligand binding studies

Thawed frozen membranes were re-homogenized and washed once with 50 mM Tris-HCl, 5 mM EDTA buffer, pH 7.4. Another washing was carried out with the buffer used in the binding studies. Binding experiments were performed at 25°C with shaking. A 100 µl aliquot of the membrane suspension (1 to 2 mg protein ml^{-1}) was incubated for 30 min with the radioligand in a 400 µl final volume of binding buffer (50 mM Tris-HCl, 0.5 mM $MgCl_2$, pH 7.4). The incubations were stopped by the addition of 4 ml of ice-cold washing buffer (10 mM Tris-HCl, 0.5 mM $MgCl_2$). Bound and free radioligands were separated by filtration through GF/C Whatman filters under vacuum. The filters were than washed twice with 10 ml of washing buffer and placed in scintillation vials. The radioactivity retained on the filters was determined in the presence of 4 ml of scintillation mixture (Emulsifier Safe Packard) by use of a scintillation counter (Packard) with an efficiency of 45–50%. Specific binding was defined as the difference between total and non-specific binding. For the α_2-adrenoceptor binding studies, 0.5 to 20 nM concentrations of [^{3}H]-RX 821002 were used. Non-specific binding was obtained with 10^{-6} M yohimbine. NAIBS binding was determined with [^{3}H]-idazoxan (0.5 to 20 nM) in the presence of 10^{-6} M yohimbine (in order to avoid [^{3}H]-idazoxan binding to α_2-adrenoceptors). Naphazoline 10^{-4} M was used to measure non-specific binding. K_d (equilibrium dissociation constant) and B_{max} (maximum number of binding sites) values were calculated from computer-assisted analysis of the data using the EBDA-LIGAND programme (McPherson, 1985). Protein concentration was measured according to Bradford (1974) with bovine serum albumin as standard.

Biochemical determinations

Blood glucose was determined with a glucose-oxidase technique (Biotrol Kit, Paris, France) and non-esterified fatty acids (NEFA) by the Wako enzymatic method (commercial radioimmuno-assay Kit, Biolyon, Lyon). For catecholamine determinations, blood was collected on lithium heparin with 10 mM sodium metabisulphite and centrifuged at 5000 *g* at 0°C. The plasma was stored at −80°C. Catecholamines were selectively isolated from the plasma by adsorption on activated alumina, then eluted with 0.1 M perchloric acid. Dihydroxybenzylamine was used as internal standard to monitor recovery from the extraction step. Catecholamines were assayed by high performance liquid chromatography using electrochemical (amperometric) detection (Waters h.p.l.c. system). The working electrode potential was set at 0.65 V against a Ag/AgCl reference electrode. Catecholamines were separated on a C 18 column (3.9 × 150 mm) at a constant flow rate of 1 ml min^{-1}. The electrochemical detector response was linear for concentrations ranging from 10 pg ml^{-1} to 100 pg ml^{-1}. In these conditions, the detection limit is 10 pg ml^{-1} (Valet *et al.*, 1989).

Statistical analysis

Values are the mean ± s.e. mean. Biochemical plasma values before and after treatment were analysed by Student's paired *t* test. An ANOVA *t* test was used to carry out the analysis of all other determinations. Differences were considered significant when P was less than 0.05.

Drugs and chemicals

[^{3}H]-RX 821002 (2-methoxy-1,4-[6,7-[^{3}H]-benzodioxan-2-yl-2-imidazolin HCl, 43.8 Ci mmol^{-1}) was a gift from Reckitt and Colman (Kingston upon Hull, U.K.). [^{3}H]-idazoxan (specific radioactivity 41 Ci mmol^{-1}) was from Amersham (Les Ulis, France). RX 821002 and idazoxan were provided by Reckitt and Colman (Kingston upon Hull, U.K.). Yohimbine hydrochloride, naphazoline, EDTA and bovine serum albumin were purchased from Sigma Co. (St Louis, M.O, U.S.A.). Collagenase came from Boehringer Mannheim (F.R.G.). All other chemicals and organic solvents were of reagent grade.

Results

Metabolic effects of acute injection of subcutaneous RX 821002 or idazoxan

In a preliminary study, the effects of a single dose (2 mg kg^{-1}, s.c.) of the two α_2-antagonists on glucose, NEFA and catecholamine plasma concentrations were analysed in 18-h fasting rabbits. As shown in Figure 1, RX 821002 increased NEFA plasma concentrations, the maximal effect being observed 30 min after the injection. Levels of plasma catecholamines were also increased by RX 821002 (Table 1). The response to idazoxan was quite similar the higher effect on NEFA being observed 30 min after injection (Figure 1, Table 1). Glucose plasma concentration was unaffected by acute administration of RX 821002 or idazoxan (Table 1).

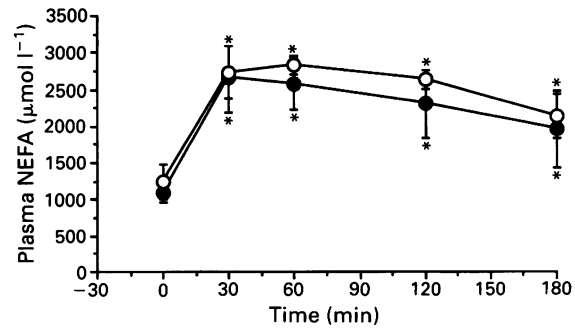

Figure 1 Effect of acute RX 821002 (2 mg kg^{-1}) (●) or idazoxan (2 mg kg^{-1}) (○) injection on plasma non-esterified fatty acid (NEFA) levels in conscious rabbits. Blood samples were removed before, 30, 60, 120 and 180 min after subcutaneous injection of the drugs. Each value represents the mean from 4 animals; vertical bars show s.e.mean. *Significantly different ($P < 0.05$) compared to the values measured at time 0.

Table 1 Effect of acute injection of RX 821002 or idazoxan (2 mg kg^{-1}, s.c.) on plasma noradrenaline (NA in pg ml^{-1}), adrenaline (Ad in pg ml^{-1}) and glucose (mmol l^{-1}) levels in 18 h-fasted conscious rabbits

Time (min)	0	60	180
		RX 821002	
NA (pg ml^{-1})	494 ± 222	1504 ± 343*	1332 ± 283**
Ad (pg ml^{-1})	278 ± 78	1404 ± 290**	1334 ± 286*
Glucose (mmol l^{-1})	7.2 ± 0.5	7.8 ± 0.5	8.1 ± 0.5
		Idazoxan	
NA (pg ml^{-1})	554 ± 232	1094 ± 242	2554 ± 1269*
Ad (pg ml^{-1})	145 ± 18	345 ± 61*	1375 ± 585*
Glucose (mmol l^{-1})	8.5 ± 0.6	9.7 ± 0.8	8.2 ± 0.5

Values are the mean ± s.e.mean from 4 animals. * $P = <0.05$; ** $P < 0.02$ when compared to time 0.

Effects of a 7-day treatment with RX 821002 or idazoxan on body weight, food intake and perirenal adipose tissue weight and endocrino-metabolical parameters

The treatment did not modify food intake of final body weight (Table 2). Adipose tissue weight was similar, in the three groups of animals (control, RX 821002 and idazoxan). Plasma glucose, NEFA, noradrenaline and adrenaline levels measured 14 h after the last subcutaneous injection of RX 821002 or idazoxan were unmodified (Table 3).

[^3H]-*RX 821002 and* [^3H]-*idazoxan binding* (Table 4).

Adipocytes Binding assays performed with [^{3}H]-RX 821002 revealed an increase in α_2-adrenoceptor number after either RX 821002 or idazoxan. No change in affinity (K_d values) was found. Hill coefficients were near to unity, suggesting that a single class of sites was labelled. [^{3}H]-idazoxan binding, used to determine NAIBS, showed no significant difference in number (B_{max}) or affinity (K_d) between the three groups of animals whatever the treatment (saline, RX 821002 or idazoxan). The Hill coefficient indicates that the radioligand ([^{3}H]-idazoxan) labelled a single class of sites.

Colocytes There was no difference in the number or affinity of α_2-adrenoceptors and NAIBS in the three groups of animals. Hill coefficients were around unity.

Platelets Only [^{3}H]-RX 821002 binding was carried out because we were unable to detect any [^{3}H]-idazoxan binding. The number of α_2-adrenoceptors and their affinity were unmodified by the 7-day treatment with RX 821002 or idazoxan.

Discussion

The aim of the present study was to investigate whether α_2-adrenoceptors or NAIBS from different tissues should be regulated by a 7-day treatment with α_2-antagonists in the rabbit. We found that α_2-antagonists (RX 821002 or idazoxan) were able to produce a tissue-specific increase in α_2-adrenoceptor number without any change in NAIBS.

The selected dose (2 mg kg^{-1}) of the two α_2-antagonists was effective, i.e. able to induce an increase in sympathetic tone in the rabbit since noradrenaline and adrenaline plasma levels strongly increased. These results agree with studies carried out with yohimbine, another α_2-adrenoceptor antagonist (Szabo *et al.*, 1989). α_2-Antagonists are known to enhance transmitter release by blockade of α_2-adrenoceptors on peripheral sympathetic nerve endings (Majewski *et al.*, 1983; Starke *et al.*, 1989). Plasma NEFA levels increased after treatment with α_2-antagonists. This effect is explained by the stimulation of lipolysis in adipose tissue due to the release of noradrenaline acting on fat cells via β-adrenoceptors (Taouis *et al.*, 1988).

Table 2 Effect of a 7-day treatment with α_2-adrenoceptor antagonists (RX 821002 or idazoxan) on body weight [measured before (initial body weight) and after (final body weight) treatment], food intake and perirenal adipose tissue weight

	Controls	*RX 821002*	*Idazoxan*
Initial body weight (kg)	2.44 ± 0.09	2.43 ± 0.09	2.60 ± 0.06
Final body weight (kg)	2.60 ± 0.11	2.56 ± 0.09	2.56 ± 0.06
Food intake (g/7 days)	985 ± 78	884 ± 67	827 ± 82
Perirenal adipose tissue weight (g)	26.06 ± 3.74	24.38 ± 2.63	25.98 ± 3.03

Animals received 0.9% saline vehicle, RX 821002 (4 mg kg^{-1} daily) or idazoxan (4 mg kg^{-1} daily) subcutaneously for seven days. Food intake represents the cumulative daily value over the experimental period (7 days). Values are the mean ± s.e.mean from 8 animals. There were no significant differences between the three groups of animals.

Table 3 Glucose, non-esterified fatty acids (NEFA) and catecholamine concentrations in plasma before and after chronic treatment with α_2-adrenoceptor antagonists

7-day treatment		*Glucose* (mmol l^{-1})	*NEFA* (μmol l^{-1})	*Noradrenaline* (pg ml^{-1})	*Adrenaline* (pg ml^{-1})
Controls	before	6.25 ± 0.2	282 ± 26	1096 ± 100	151 ± 72
	after	5.9 ± 0.3	167 ± 28	994 ± 136	179 ± 60
RX 821002	before	6.2 ± 0.1	295 ± 50	736 ± 65	85 ± 42
	after	6.3 ± 0.3	263 ± 44	663 ± 46	140 ± 60
Idazoxan	before	6.2 ± 0.2	200 ± 20	826 ± 189	178 ± 51
	after	6.6 ± 0.2	182 ± 22	789 ± 78	187 ± 27

Two subcutaneous injections of 0.9% saline vehicle (controls) or RX 821002 or idazoxan were administered as described in Methods. Blood samples were removed before starting treatment and 14 h after the last injection of the day. Values are the mean ± s.e.mean from 8 animals. There was no significant difference between the three groups of animals.

Table 4 [^{3}H]-RX 821002 and [^{3}H]-idazoxan bindings in adipocyte, colocytes and platelet membranes of the three groups of animals

7-day treatment	K_d (nM)	B_{max} (fmol mg^{-1} prot)	n(Hill)	K_d (nM)	B_{max} (fmol mg^{-1} prot)	n(Hill)
Adipocytes		*α_2-Adrenoceptors*			*NAIBS*	
Controls	8.6 ± 0.9	58 ± 8	0.98 ± 0.02	8.8 ± 0.9	274 ± 47	0.96 ± 0.01
RX 821002	9.6 ± 1.1	116 ± 13***	0.91 ± 0.01	10.5 ± 1.3	386 ± 68	0.95 ± 0.02
Idazoxan	10.4 ± 1.8	94 ± 9**	0.97 ± 0.07	7.5 ± 0.9	375 ± 67	0.99 ± 0.01
Colocytes		*α_2-Adrenoceptors*			*NAIBS*	
Controls	8.1 ± 0.6	251 ± 28	0.96 ± 0.01	8.8 ± 0.6	127 ± 28	0.97 ± 0.01
RX 821002	8.1 ± 0.7	245 ± 36	0.96 ± 0.03	6.9 ± 0.4	107 ± 23	0.95 ± 0.01
Idazoxan	8.4 ± 0.3	268 ± 39	0.98 ± 0.01	8.0 ± 0.4	149 ± 25	0.96 ± 0.01
Platelets		*α_2-Adrenoceptors*				
Controls	6.85 ± 0.77	158 ± 12	0.973 ± 0.021			
RX 821002	8.22 ± 0.42	175 ± 48	0.987 ± 0.009			
Idazoxan	7.69 ± 0.87	183 ± 37	0.975 ± 0.006			

Membranes were incubated for 30 min at 25°C with increasing concentrations of radioligands (0.5–20 nM). [^{3}H]-RX 821002 binding was performed using 10^{-6} M yohimbine for the non-specific binding and identified α_2-adrenoceptors. [^{3}H]-idazoxan binding, carried out by adding 10^{-6} M yohimbine as α_2-adrenoceptor antagonist to prevent [^{3}H]-idazoxan fixation on α_2-sites and 10^{-4} M naphazoline for the non-specific binding, was used to identify non-adrenoceptor idazoxan-binding sites (NAIBS). The protocol was described in Methods. The number of binding sites was calculated from Scatchard plots. Values are the mean ± s.e.mean from 8 animals. ** Significantly different ($P < 0.01$) when compared to the control values. *** Significantly different ($P < 0.001$) when compared to the control values. No significant NAIBS binding was found in rabbit platelets.

The main purpose of the present work was to investigate a putative regulation of α_2-adrenoceptors or NAIBS. The phenomenon of regulation has been well studied with β-adrenoceptors which are coupled to the adenylate-cyclase system in a stimulatory manner (Sibley & Lefkowitz, 1985). Regulation of systems coupled in an inhibitory manner to the adenylate-cyclase system, such as the α_2-adrenoceptor, is less understood. Moreover, most of the studies have investigated this regulation by use of adrenoceptor agonists, but, as far as we know, few studies concerned α_2-antagonists.

The first result of the present study concerns α_2-adrenoceptors located on adipocytes: their number increased after treatment with RX 821002 or idazoxan. During the development of the adipose tissue, a specific increase in α_2-adrenoceptor antilipolyic responsiveness is observed. It is related to an increment in α_2-adrenoceptor density (Carpéné *et al.*, 1983; Taouis *et al.*, 1987). In contrast, a decrease in sympathetic tone provided either by reserpine (Estan *et al.*, 1990) or 6-hydroxydopamine (Saulnier-Blache *et al.*, 1990a) administration failed to change fat cell α_2-adrenoceptors. Crampes *et al.* (1989) found no modification in adipocyte α_2-adrenoceptor response after a hypocaloric diet in humans. However, these authors observed an up-regulation of platelet α_2-adrenoceptors during this hypocaloric diet in these subjects. More recently, Saulnier-Blache *et al.* (1990b) described a specific testosterone-dependent regulation of adipocyte α_2-adrenoceptors in hamsters. The increase in adipocyte α_2-adrenoceptor number found in our study cannot be attributed to an enhanced size of the fat stock in the treated animals since no difference in perirenal adipose tissue weight between the three groups of animals was found.

In contrast, platelet α_2-adrenoceptors seem to be differently regulated since after reserpine-induced sympathectomy (Estan *et al.*, 1990) or a hypocaloric diet (Crampes *et al.*, 1989), their number increased. In healthy volunteers, chronic administration of yohimbine did not affect platelet α_2-adrenoceptors (Galitzky *et al.*, 1990a). In rabbit colon, crypt cells have a higher number of α_2-adrenoceptors than surface cells (Senard *et al.*, 1990). The present study investigated only crypt and surface α_2-adrenoceptors whatever their location along the colon. A differential regulation of lymphocytes, lung and heart α_2-adrenoceptors was previously described by Deighton *et al.* (1988a) using an agonist noradrenaline. Yakubu *et al.* (1990) found an enhanced number of α_2-adrenoceptors in forebrain without modifications in hindbrain and kidney after idazoxan in the rabbit. The present study showing no change in colocytes or platelets after two α_2-antagonists RX 821002 and idazoxan, extends this conclusion of a differential regulation of α_2-adrenoceptors according to their location.

The reasons for the differences in the regulation of α_2-adrenoceptors according to the tissue need to be discussed. First, one could suggest that the α_2-adrenoceptor subtype in the studied tissue can explain these tissue differences. However, this explanation does not hold since in the rabbit, only the α_{2A}-subtype was described in the tissues concerned (Deighton *et al.*, 1988a; Langin *et al.*, 1989; Senard *et al.*, 1990). Differences in α_2-adrenoceptor metabolism ($t_{1/2}$) depending on the tissues can also be considered. For example in the rabbit the half-life is 38 h for α_2-adrenoceptors in spleen, 6 days in the cerebral cortex (Mahan *et al.*, 1987) and around 36 h in hamster adipose tissue (Taouis *et al.*, 1987). The lack of change in platelet α_2-adrenoceptors could be explained by the fact that platelets are unnucleated cells with a half-life of near ten days. Finally, one can speculate that in the present study, the two α_2-antagonists could be stored in adipose tissue leading to a permanent blockade of adipocyte α_2-adrenoceptors when compared to the other cells (platelets and colocytes) submitted to intermittent blockade according to plasma fluctuations of RX 821002 or idazoxan.

NAIBS binding studies have been carried out in adipocytes and colocytes. Their function and regulation have not yet been established. It has been proposed that NAIBS might be involved in blood pressure regulation by the central nervous system (Bousquet *et al.*, 1984; Michel & Insel, 1989). Our results indicated that NAIBS were unaffected by treatment with RX 821002 and idazoxan in the fat cells and colocytes. Few studies have investigated NAIBS regulation: Yakubu *et al.* (1990) described a decrease in [^{3}H]-idazoxan binding on kidney but no change in forebrain or hindbrain membranes after a 5-day treatment with idazoxan in rabbits. We have no hypothesis to explain these discrepancies between their results and the present study. Since it is not established whether idazoxan acts as an agonist or an antagonist at its binding sites, it is difficult to propose a hypothesis as to the regulation of these sites. However, the fact that RX 821002 (which binds only to α_2-adrenoceptors) and idazoxan (which binds to both α_2-adrenoceptors and NAIBS) exert similar effects after either acute or chronic treatment suggests that NAIBS are not involved in the control of catecholamine release or NEFA or glucose metabolism. Finally, the present study showing a differential regulation of the two sites (α_2-adrenoceptors and NAIBS) during the treatment with the α_2-adrenoceptor antagonists indicates that they are two separate entities as suggested by biochemical approaches (Parini *et al.*, 1989).

The authors are grateful to Dr Lafontan for fruitful discussions during the preparation of the manuscript. M.P. is a recipient of a fellowship from the Ministerio de Education y Ciencia, Direccion General de Investigacion Cientifica y Technica (Spain). The authors acknowledge the technical help of Mrs Portolan, Mr Bernou and Mr Duplantier. Mrs Bontemps carefully prepared the manuscript.

References

BERLAN, M. & LAFONTAN, M. (1985). Evidence that epinephrine acts preferentially as an antilipolytic agent in human subcutaneous fat cells: assessment by analysis of beta- and alpha-adrenoceptors properties. *Eur. J. Clin. Invest.*, **15**, 341–348.

BOUSQUET, P., FELDMAN, J. & SCHWARTZ, J. (1984). Central cardiovascular effects of alpha-adrenergic drugs. Differences between catecholamines and imidazolines. *J. Pharmacol. Exp. Ther.*, **230**, 232–236.

BRADFORD, M.M. (1974). A rapid sensitive method for the quantitation of protein utilizing the principle of protein dye binding. *Anal. Biochem.*, **72**, 248–254.

BRODDE, O.E. (1982). Homogeneous class of beta 1-adrenergic receptors in rat kidney. Identification by (±) [^{125}I] iodocyanopindolol binding. *Biochem. Pharmacol.*, **31**, 1743–1747.

CARPENE, C., BERLAN, M. & LAFONTAN, M. (1983). Influence of development and reduction of fat stores on the lipolytic alpha$_2$-adrenoceptor in hamster adipocytes: comparison with adenosine and beta-adrenergic lipolytic responses. *J. Lipid Res.*, **24**, 766–774.

CRAMPES, F., MARCERON, M., BEAUVILLE, M., RIVIERE, D., GARRIGUES, M., BERLAN, M. & LAFONTAN, M. (1988). Platelet alpha$_2$-adrenoceptors and adrenergic adipose tissue responsiveness after moderate hypocaloric diet in obese subjects. *Int. J. Obesity*, **13**, 99–110.

DEIGHTON, M.M., BROWN, A.D., HAMILTON, C.A. & REID, J.L. (1988a). Regulation of adrenergic receptor number following chronic noradrenaline infusion in the rabbit. *Naunyn-Schmiedebergs Arch. Pharmacol.*, **338**, 517–522.

DEIGHTON, M.M., HAMILTON, C.D., JONES, C.R. & REID, J.L. (1988b). The effects of chronic administration of adrenaline on the function and number of adrenoceptors in the rabbit. *J. Cardiovasc. Pharmacol.*, **12**, 332–337.

ESTAN, L., SENARD, J.M., TRAN, M.A., MONTASTRUC, J.L. & BERLAN M. (1990). Reserpine induces vascular α_2-adrenergic supersensitivity and platelet α_2-adrenoceptor up-regulation in dog. *Br. J. Pharmacol.*, **101**, 329–336.

FORTIN, T.L. & SUNDARESAN, P.R. (1989). Reserpine but not surgical denervation regulates rat renal beta-adrenergic receptors. *Am. J. Physiol.*, **256**, F532-F539.

GALITZKY, J., RIVIERE, D., TRAN, M.A., MONTASTRUC, J.L. & BERLAN, M. (1990a). Pharmacodynamic effects of chronic yohimbine treatment in healthy volunteers. *Eur. J. Clin. Pharmacol.*, **39**, 447–451.

GALITZKY, J., SENARD, J.M., LAFONTAN, M., STILLINGS, M., MONTASTRUC, J.L. & BERLAN, M. (1990b). Identification of human platelet α_2-adrenoceptors with a new antagonist [^{3}H]-RX 821002, a methoxy derivative of idazoxan. *Br. J. Pharmacol.*, **100**, 862–866.

HOLLISTER, A.S., FITZGERALD, G.A., NADEAU, J.H.J. & ROBERTSON, D. (1983). Acute reduction in human platelet alpha$_2$-adrenoceptor affinity for agonist by endogenous and exogenous catecholamines. *J. Clin. Invest.*, **72**, 1498–1505.

INSEL, P.A. (1989). Structure and function of alpha-adrenergic receptors. *Am. J. Med.*, **87**, 13S-16S.

LANGIN, D. & LAFONTAN, M. (1989). [^{3}H]-idazoxan binding at non-alpha$_2$-adrenoceptors in rabbit adipocyte membranes. *Eur. J. Pharmacol.*, **159**, 199–203.

LANGIN, D. LAFONTAN, M. STILLINGS, M.K. & PARIS, H. (1989). [^{3}H] RX 821002: a new tool for the identification of alpha$_2$-adrenoceptors. *Eur. J. Pharmacol.*, **167**, 95–104.

LANGIN, D., PARIS, H. DAUZATS, M. & LAFONTAN, M. (1990a). Discrimination between alpha$_2$-adrenoceptors and [3H]-idazoxan labelled non adrenergic sites in rabbit white fat cells. *Eur. J. Pharmacol.*, **188**, 261–272.

LANGIN, D., PARIS, H. & LAFONTAN, M. (1990b). Binding of [^{3}H]-idazoxan and its methoxy derivative [^{3}H] RX 821002 in human fat cells. [^{3}H] idazoxan but no [^{3}H] RX 821002 labels additional non alpha$_2$-adrenergic binding sites. *Mol. Pharmacol.*, **37**, 876–885.

LATIFPOUR, J. & MCNEILL, J.H. (1984). Reserpine induces changes in cardiac adrenergic receptors. *Can. J. Physiol. Pharmacol.*, **62**, 23–26.

MAHAN, L.C., MCKERNAN, R. & INSEL, P.A. (1987). Metabolism of alpha- and beta-adrenergic receptors in vitro and in vivo. *Annu. Rev. Pharmacol. Toxicol.*, **27**, 215–235.

MAJEWSKI, H., HEDLER, L. & STARKE, K. (1983). Evidence for a physiological role of presynaptic alpha-adrenoceptors: modification of noradrenaline released in the pithed rabbit. *Naunyn-Schmiedebergs Arch. Pharmacol.*, **324**, 256–263.

MACKINNON, A.C., BROWN, C.M., SPEDDING, M. & KILPATRICK, A.T. (1989). [^{3}H]-idazoxan binds with high affinity to two sites on hamster adipocytes: a α_2-adrenoceptor and a non-adrenoceptor site. *Br. J. Pharmacol.*, **98**, 1143–1150.

MACPHERSON, G.A. (1985). Analysis of radioligand binding experiments: A collection of computer programs for the IBM PC. *J. Pharmacol. Meth.*, **14**, 213–228.

MICHEL, A.C., BRODDE, O.E., SCHNEPEL, B., BEHRENDT, J., TSCHADA, R., MOTULSKY, M.J. & INSEL, P.A. (1989). [^{3}H]-idazoxan and some other alpha$_2$-adrenergic drugs also bind with high affinity to a non adrenergic site. *Mol. Pharmacol.*, **35**, 324–330.

MICHEL, M.C. & INSEL, P.A. (1989). Are there multiple imidazoline binding sites? *Trends Pharmacol. Sci.*, **10**, 342–344.

NAKAKI, T., NAKADATE, T., YAMAMOTO, S. & KATO, R. (1982). Alpha$_2$-adrenergic inhibition of intestinal secretion induced by prostaglandin E1, vasoactive intestinal peptide and dibutyryl cyclic AMP in rat jejunum flux. *J. Pharmacol. Exp. Ther.*, **220**, 637–641.

NASSERI, A., BARAKEH, J.F., ABEL, P.W. & MINNEMAN, K.P. (1985). Reserpine-induced post-junctional supersensitivity in rat vas deferens and caudal artery without changes in alpha-adrenergic receptors. *J. Pharmacol. Exp. Ther.*, **234**, 350–357.

PARINI, A., COUPRY, I., GRAHAM, R.M., UZIELLI, J., ATLAS, D., LANIER, S.M. (1989). Characterization of an imidazoline guanidinium receptive site distinct from the alpha$_2$-adrenergic receptor. *J. Biol. Chem.*, **264**, 11874-11878.

SAULNIER-BLACHE, J.S., ATGIE, C., CARPENE, C., QUIDEAU, N. & LAFONTAN, M. (1990a). Hamster adipocyte alpha$_2$-adrenoceptor changes during fat mass modifications are not directly dependent on adipose tissue norepinephrine content. *Endocrinology*, **126**, 2425–2434.

SAULNIER-BLACE, J.S., LARROUY, D., CARPENE, C., QUIDEAU, N., DAUZATS, M. & LAFONTAN, M. (1990b). Photoperiodic control of adipocyte alpha$_2$-adrenoceptors in Syrian hamsters: role of testosterone. *Endocrinology*, **127**, 1245–1253.

SENARD, J.M., LANGIN, D., ESTAN, L. & PARIS, H. (1990). Identification of alpha$_2$-adrenoceptors and non adrenergic idazoxan: binding sites in rabbit colon epithelial cells. *Eur. J. Pharmacol.*, **191**, 59–68.

SIBLEY, D.R. & LEFKOWITZ, R.J. (1985). Molecular mechanism of receptor desensibilization using beta-adrenergic receptor coupled adenylate-cyclase system as a model. *Nature*, **317**, 124–129.

STARKE, K., GOTHERT, M. & KILBINGER, H. (1989). Modulation of transmitter release by presynaptic autoreceptors. *Physiol. Rev.*, **69**, 864–889.

SZABO, B., HEDLER, L. & STARKE, K. (1989). Peripheral presynaptic and central effects of clonidine, yohimbine and rauwolscine on the sympathetic nervous system in rabbits. *Naunyn-Schmiedebergs Arch. Pharmacol.*, **340**, 648–657.

TAOUIS, M., BERLAN, M., MONTASTRUC, P. & LAFONTAN, M. (1987). Characterization of dog fat cell adrenoceptors: variations in alpha$_2$- and beta-adrenergic receptors distribution according to the extent of the fat deposits and the anatomical location. *J. Pharmacol. Exp. Ther.*, **242**, 1041–1049.

TAOUIS, M., BERLAN, M., MONTASTRUC, P. & LAFONTAN, M. (1988). Mechanism of the lipid mobilizing effect of alpha$_2$-adrenergic antagonists in the dog. *J. Pharmacol. Exp. Ther.*, **247**, 1172–1180.

VALET, P., DAMASE-MICHEL, C., MONTASTRUC, J.L. & MONTASTRUC, P. (1989). Plasma catecholamines and adrenoceptors after chronic sinaortic denervation in dogs. *Fundam. Clin. Pharmacol.*, **3**, 307–320.

YAKUBU, M.A., DEIGHTON, N.M., HAMILTON, C.A. & REID, J.L. (1990). Differences in the regulation of [^{3}H]-idazoxan and [^{3}H]-yohimbine binding sites in the rabbit. *Eur. J. Pharmacol.*, **176**, 305–311.

(Received February 1, 1991
Revised April 9, 1991
Accepted May 8, 1991)

Br. J. Pharmacol. (1991), **104**, 195–201

The effects of neuropeptide Y on myocardial contractility and coronary blood flow

Sonia J. Awad, [1]Rosemarie Einstein, *Erica K. Potter & Desmond P. Richardson

Department of Pharmacology, University of Sydney, N.S.W. 2006 and *School of Physiology and Pharmacology, University of New South Wales, N.S.W. 2033, Australia

1 This study was designed to assess the effects of exogenous neuropeptide Y (NPY) on cardiac contractility and coronary blood flow (CBF) in anaesthetized dogs and to evaluate the effect of NPY on the responses to sympathetic and parasympathetic stimulation and to inotropic agents.

2 Bolus doses of NPY (500 μg), administered via the femoral vein, increased mean arterial pressure. The pressor effect was associated with reductions in heart rate, CBF and cardiac contractility.

3 The effects of NPY (500 μg) on contractility and CBF were compared with that of vasopressin (VP) (1 unit). For similar reductions in CBF, NPY and VP had similar negative inotropic effects. Thus, it is likely that the negative inotropic response to NPY is not due to a direct effect of NPY on the heart muscle but is largely due to coronary vasoconstriction.

4 In the presence of NPY (500 μg, i.v.), there was an inhibition of the positive inotropic response to stimulation of the left cardiac sympathetic nerve (2 or 5 Hz, 0.05 ms). NPY also inhibited the negative inotropic response and chronotropic response to vagal stimulation (2, 3 or 5 Hz, 0.05 ms).

5 Dose-response curves were obtained for the inotropic, chronotropic and pressor responses to cumulative infusions of noradrenaline ($n = 6$) and dobutamine ($n = 6$). NPY had no effect on these dose-response curves.

6 The effect of NPY on the responses to salbutamol and impromidine was assessed. NPY did not alter the positive inotropic, chronotropic or depressor responses to these agonists.

7 Our results indicate that NPY has direct, postsynaptic vasoconstrictor activity and the reduction in myocardial contractility and heart rate are due to a combination of coronary vasoconstriction, baroreceptor reflex activation and presynaptic inhibition of transmitter release from sympathetic nerves. The well-documented inhibitory effect of NPY on the chronotropic response to parasympathetic stimulation was confirmed and similar inhibition of the inotropic response to both sympathetic and parasympathetic stimulation was demonstrated. Since there was no modulation of the inotropic effects of exogenous α- and β- adrenoceptor or H_2-receptor agonists, it is concluded that the effects of NPY on myocardial contractility are exerted presynaptically.

Keywords: Neuropeptide Y; cardiac contractility; coronary blood flow

Introduction

Neuropeptide Y (NPY) was originally isolated from pig brain by Tatemoto and colleagues in 1982 (Tatemoto *et al.*, 1982) and its presence has since been identified throughout the peripheral nervous system. High levels of NPY have been found in the peripheral nerves of the heart and in the stellate ganglia of a number of species including cat, rat, mouse, guinea-pig, pig, dog and man (Lundberg *et al.*, 1982; Gu *et al.*, 1983; Allen *et al.*, 1986). In these structures, NPY is co-localized with noradrenaline (NA); consequently, there is a simultaneous release of NPY and NA when the nerves are stimulated (Rudehill *et al.*, 1986). This, and the presence of high concentrations of the peptide in the heart suggest that NPY may be involved in the control of cardiac function.

NPY exerts three different effects in the periphery. First there is a presynaptic inhibitory effect on transmitter release from both noradrenergic and cholinergic nerves (Lundberg *et al.*, 1982; Potter, 1987). Second there is a postsynaptic potentiation of the actions of direct vasoconstrictor agents (Edvinsson *et al.*, 1984). The third effect is a direct postsynaptic vasoconstrictor action on some blood vessels (Edvinsson *et al.*, 1984; Wahlestedt *et al.*, 1987). This effect of NPY is prolonged and is resistant to α- and β-adrenoceptor blockade (Lundberg & Tatemoto, 1982; Mabe *et al.*, 1985; and see Potter, 1988).

[1]Author for correspondence.

Although the vascular actions of NPY are well documented, the results from studies on the cardiac, in particular the inotropic, effects of NPY are conflicting. This probably arises from the wide variety of techniques and species used to examine this question. Negative inotropic, but not chronotropic, effects of NPY in the perfused rabbit heart have been reported (Allen *et al.*, 1983). Both negative inotropic and chronotropic effects in spontaneously beating guinea-pig atria have been described (Lundberg *et al.*, 1984a) but these are not found in all studies (Potter, 1987; Wahlestedt *et al.*, 1987). In other studies, direct effects of NPY have been observed on coronary arteries (Rioux *et al.*, 1986; Han & Abel, 1987) or on rat isolated myocytes (Piper *et al.*, 1989). These latter direct effects appear to depend on high local concentrations of NPY and are most easily observed in the rat (see also Zukowska-Grojec *et al.*, 1987). More recently, experiments performed on anaesthetized dogs have shown that local injection of NPY into coronary arteries will cause a local vasoconstriction (Aizawa *et al.*, 1987; Martin & Patterson, 1989) or a reduction in coronary blood flow (Allen *et al.*, 1986; Maturi *et al.*, 1989) but effects on contractility are variable (Allen *et al.*, 1986; Martin & Patterson, 1989). A decrease in contractility has been observed following intravenous injection of NPY in the anaesthetized rabbit (Minson *et al.*, 1987).

Thus, the aim of these experiments was to investigate the cardiac actions of NPY in intact animals, with particular emphasis on the effects of the peptide on cardiac contractility while measuring coronary blood flow simultaneously. The

effect of NPY on the cardiac responses to vagal and sympathetic stimulation were examined. The possibility of postsynaptic interaction between NPY and inotropic agonists was also investigated. A brief account of part of this work has been published (Awad et al., 1989).

Methods

Dogs weighing 6–20 kg were anaesthetized with pentobarbitone sodium (30 mg kg^{-1} i.v., followed by maintenance doses as required), intubated and artificially ventilated with room air. Systemic arterial blood pressure (BP) was continuously monitored via a femoral artery cannula and Statham P23AC pressure transducer. A cannula was also inserted into the femoral vein for the administration of anaesthetic, NPY and test drugs. Heart rate (HR) was recorded from the Lead II ECG connected to a tachograph (Grass 7P4G), triggered by the R-wave of the Lead II ECG. Bilateral vagotomy was performed in all dogs.

A left thoracotomy was performed at the third or fourth intercostal space. A Konigsberg catheter tip micromanometer was implanted into the left ventricle via a stab wound in the apex of the heart to measure left ventricular pressure (LVP). The first derivative of the rising phase of LVP, *dP/dt*, was obtained by an active differentiating circuit. The index of contractility used in this study, (*dP/dt*)/IIT (Goodman et al., 1972), was obtained by the division of maximum *dP/dt* by the time integral of isovolumic ventricular pressure (integrated isometric tension) during the period from the R-wave of the ECG to the peak *dP/dt*. The index was computed, beat-by-beat, by an on-line digital computer (PDP 11/34, Digital Equipment, Australia). The process is initiated by the R-wave of the Lead II ECG. Integration of LVP was continued at one millisecond intervals until maximum *dP/dt* was detected. The ratio was then computed and an analogue voltage representing the index returned to the polygraph. Units of the index were s^{-2}. All parameters were recorded on a Grass polygraph (Model 7).

Experimental protocol

Arterial blood pressure, beat by beat heart rate and contractility were measured continuously in all experiments.

Series I: the effects of exogenous neuropeptide Y on coronary blood flow and on the responses to vagal nerve stimulation Blood flow in the left anterior descending coronary artery (CBF) was measured in 8 animals with a 2 mm electromagnetic flow probe (EMI flowmeter). Both vagus nerves were cut and the distal end of the right vagus nerve was stimulated supramaximally at either 2, 3 or 5 Hz, 50 or 60 V, 0.01 to 0.05 ms (depending on the responsiveness of the dog) for 5 s every min. Once the stimulation parameters were selected for each dog, they remained constant throughout the experiment. Stimulations were repeated at least 3 times to ensure reproducibility of the response. A bolus dose of NPY (500 μg) was then administered. After 5 min, vagal stimulation was repeated every 5 min as before, for approximately 30 min. In 3 of the dogs, the effects of NPY on contractility and CBF were compared with that of vasopressin (VP, Pitressin, Parke Davis) (1 unit).

Series II: the effects of exogenous neuropeptide Y on the responses to sympathetic stimulation and noradrenaline or dobutamine infusion In 12 dogs, the left sympathetic cardiac nerve was stimulated at either 2 or 5 Hz, 20 or 50 V, 0.05 ms, (depending on the responsiveness of the dog) for 5 s in each min for 3 min. The left nerve was used because it affects mainly contractility and not heart rate (Levy et al., 1966). The right sympathetic nerve and both vagus nerves remained intact. For each dog, once the stimulation parameters were selected, they remained constant throughout the experiment. In 6 dogs NA was then infused (McGaw Volumetric Infusion Pump) at rates from 0.1 $\mu g\,kg^{-1}\,min^{-1}$ to 1.0 $\mu g\,kg^{-1}\,min^{-1}$. Each dose level was maintained until steady levels were reached before increasing the infusion rate. The remaining 6 animals received dobutamine infusions in doses from 0.5 $\mu g\,kg^{-1}\,min^{-1}$ to 20 $\mu g\,kg^{-1}\,min^{-1}$. The cardiovascular parameters were allowed to return to control before injection of NPY (500 μg). After 5 min, sympathetic nerve stimulation and drug infusion were repeated.

Series III: the effects of exogenous neuropeptide Y on the responses to salbutamol injection Salbutamol (0.5 $\mu g\,kg^{-1}$) was injected once every 10 min, 3 times in each of 6 dogs. NPY (500 μg) was then injected and after 5 min, salbutamol was injected 4 times at 10 min intervals.

Series IV: the effects of exogenous neuropeptide Y on the responses to impromidine injection Impromidine (0.7 $\mu g\,kg^{-1}$) was injected once every 15 min, 3 times in each of 6 dogs. NPY (500 μg) was then injected, and after 5 min, impromidine was injected once every 15 min for 45 min.

Analysis of results

The changes in BP, HR, CBF and contractility following the administration of NPY were tested for significance by use of *t* tests. One factor ANOVA (repeated measures) was conducted on each set of data to test the significance of the changes between control and post-NPY responses to stimulation or drug administration. The Scheffe F-test was used to test the significance of the changes. In both these tests, the significance level was set at $P < 0.05$.

Drugs used

The following drugs were used: neuropeptide Y (human 1-36) (a gift from Pacific Biotechnology, Sydney); vasopressin (Pitressin, Parke-Davis); noradrenaline (norepinephrine) bitartrate (Sigma Chemical Co.); dobutamine hydrochloride (Lilly (Aust.) & Co.); salbutamol sulphate (Glaxo (Aust.) & Co.); impromidine trihydrochloride (Smith Kline and French Laboratories); and sodium pentobarbitone (Abbott Laboratories).

Results

A bolus dose of NPY (500 μg) was administered to all 32 animals. NPY increased mean arterial pressure from 102 ± 4 mmHg to 130 ± 4 mmHg ($n = 32$; $t = -16.134$; $P < 0.001$). The pressor effect was associated with a reduction in resting heart rate from 168 ± 4 b min^{-1} to 151 ± 4 b min^{-1} ($n = 32$; $t = 14.672$; $P < 0.001$) and a significant reduction in coronary blood flow (measured only in series I) from 1.71 ± 0.24 ml min^{-1} kg^{-1} to 1.55 ± 0.26 ml $min^{-1}\,kg^{-1}$ ($n = 8$; $t = 3.65$; $P < 0.01$). Cardiac contractility fell from $2090 \pm 100\,s^{-2}$ to $1490 \pm 85\,s^{-2}$ ($n = 32$; $t = 8.186$; $P < 0.001$). The results of a typical experiment are shown in Figure 1.

The pressor effect of NPY was prompt and transient, with the peak response occurring within 1.5 min. Similarly, the maximal changes in HR, CBF and contractility occurred 1–2 min after injection of NPY (Figure 1). The duration of the effect of NPY is discussed separately below.

Series I

Right vagal stimulation was associated with marked reductions in MAP, HR, CBF and cardiac contractility. There was a long-lasting attenuation of these responses following the bolus injection of NPY. An experimental recording from one dog is shown in Figure 2 and the results from 8 dogs are summarised in Table 1. From the table, it can be seen that within 5 min of injection of NPY, the negative chronotropic response

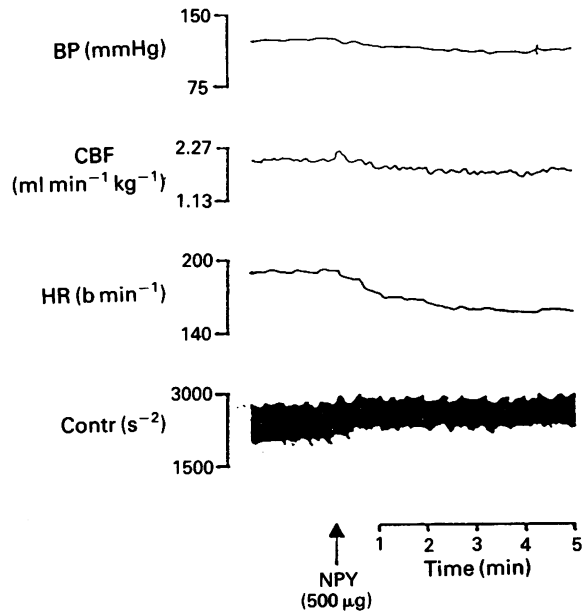

Figure 1 The effect of neuropeptide Y (NPY) on heart rate (HR), coronary blood flow (CBF), contractility (Contr) and arterial blood pressure (BP) in an anaesthetized dog.

to vagal stimulation was reduced by almost 50%. This effect was maintained over the next 5 min. Similarly, the reduction in CBF associated with vagal stimulation was reduced by approximately 40% and was further attenuated in the next 5 min.

The negative inotropic response to vagal stimulation was reduced by approximately 45%, 5 min after NPY injection. In the next 5 min, the inotropic response to vagal stimulation was reduced by approximately 50%. The depressor response to vagal stimulation was reduced by approximately 30% in the first 5 min and was further depressed in the next 5 min by approximately 40% of the control response (Table 1).

Responses to vagal stimulation were recorded for 25 min after NPY administration. In 6 of the 8 animals, resting levels of all of the cardiovascular parameters reached at least 80% of control by this time. 25 min after NPY administration, the responses to vagal stimulation were still reduced; the negative chronotropic response was 66%, the reduction in CBF was 70%, the negative inotropic response was 76% and depressor response was 71% of their respective control responses. Analysis of the data by one-factor ANOVA showed that at 25 min changes in HR, CBF and cardiac contractility in response to vagal stimulation were still significantly reduced. However, the attenuation of the depressor response to vagal stimulation was significant only for 10–20 min after NPY injection.

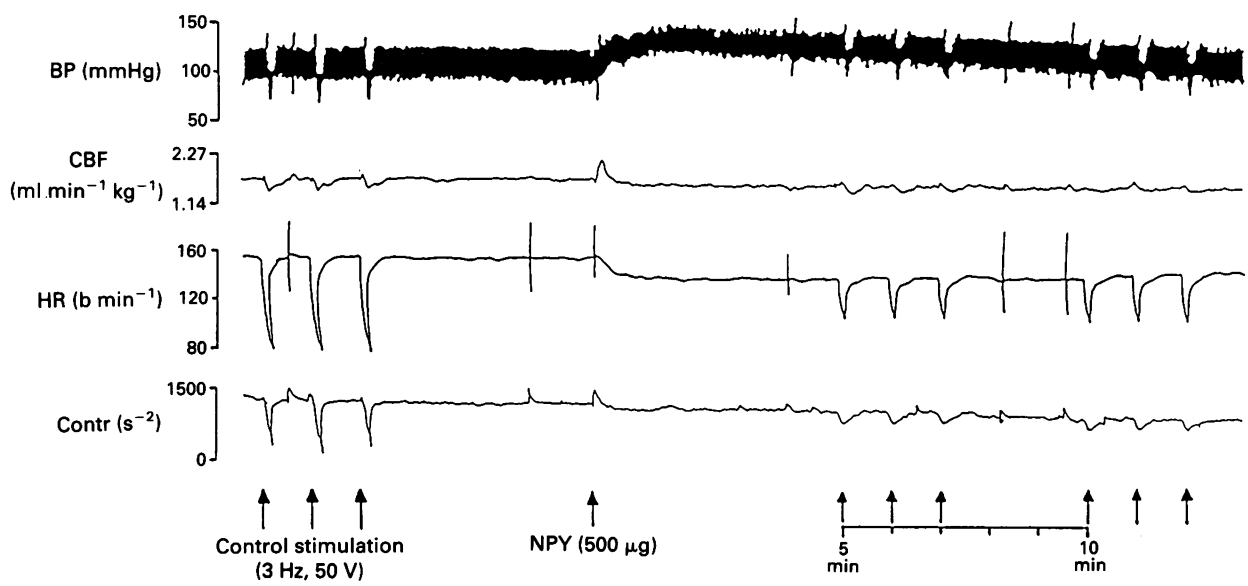

Figure 2 The effect of neuropeptide Y (NPY) on the depressor (BP), coronary blood flow (CBF), chronotropic (HR) and inotropic (Contr) responses to right vagal stimulation in an anaesthetized dog.

Table 1 The effect of neuropeptide Y (NPY) on the cardiovascular responses to right vagal stimulation

	BP (mmHg)	*HR* (min^{-1})	*CBF* ($ml\,min^{-1}\,kg^{-1}$)	*Contractility* (s^{-2})
Prestimulation	115 ± 8	175 ± 8	1.77 ± 0.23	1890 ± 270
Stimulation	91 ± 7	106 ± 6	1.38 ± 0.17	1340 ± 210
Stimulation-induced change	24 ± 3	68 ± 6	0.40 ± 0.07	550 ± 100
NPY	135 ± 8	161 ± 7	1.55 ± 0.25	1530 ± 190
5 min after NPY				
Prestimulation	131 ± 8	162 ± 7	1.60 ± 0.20	1630 ± 230
Stimulation	114 ± 7	127 ± 7	1.36 ± 0.18	1320 ± 190
Stimulation-induced change	17 ± 2	35 ± 4	0.23 ± 0.05	310 ± 60
10 min after NPY				
Prestimulation	124 ± 8	160 ± 7	1.56 ± 0.27	1700 ± 310
Stimulation	110 ± 7	124 ± 8	1.40 ± 0.24	1420 ± 240
Stimulation-induced change	14 ± 1	35 ± 5	0.16 ± 0.03	280 ± 90
25 min after NPY				
Prestimulation	120 ± 8	174 ± 8	1.63 ± 0.24	1860 ± 240
Stimulation	103 ± 8	129 ± 7	1.35 ± 0.20	1440 ± 170
Stimulation-induced change	16 ± 2	24 ± 3	0.28 ± 0.05	420 ± 90

The effects of NPY (500 μg) on contractility and CBF were compared with those of vasopressin (1 unit). VP caused a marked increase in MAP, which reached peak effect in 3 min ($n = 3$). The pressor effect was maintained for approximately 20 min, and was associated with a reduction in CBF, contractility and HR. The percentage reduction in cardiac contractility was plotted against the percentage reduction in CBF for VP and NPY in each dog (Figure 3). The relationship between reduction in CBF and reduction in contractility was similar for NPY and VP.

Series II

A record showing the effect of NPY on the response to stimulation of the left cardiac sympathetic nerve is shown in Figure 4. The results from all of the animals were combined and it was shown that during stimulation cardiac contractility increased from a mean of $1920 \pm 110\,s^{-2}$ to $2780 \pm 170\,s^{-2}$ i.e. an increase of $860 \pm 120\,s^{-2}$ ($n = 11$). Contractility decreased to $1500 \pm 170\,s^{-2}$ following NPY injection and the inotropic response to stimulation of the sympathetic nerve was reduced by 30% i.e. from a change of $860 \pm 120\,s^{-2}$ to a change of $610 \pm 100\,s^{-2}$. One factor ANOVA (repeated measures) showed that this inhibition was statistically significant.

The trace in Figure 4 shows an increase in blood pressure in response to stimulation of the cardiac sympathetic nerves which was not altered after NPY administration. Although in this particular experiment the pressor response appears substantial, when the results from all of the dogs in this group were combined, MAP increased from 114 ± 7 mmHg to 120 ± 7 mmHg. This was an increase of 6 ± 7 mmHg ($n = 11$) and after NPY the increase was from 108 ± 6 mmHg to $114 + 8$ mmHg i.e. a change of 6 ± 3 mmHg, which was not significantly different. The chronotropic response to sympathetic stimulation was variable; in some dogs, HR was reduced and in others it was increased. In either case, changes in HR were small. In the control period, HR was $161 \pm 8\,b\,min^{-1}$ and during stimulation was $160 \pm 8\,b\,min^{-1}$. This change ($-1 \pm 2\,b\,min^{-1}$, $n = 11$) was similar after NPY injection, when HR changed from $154 \pm 8\,b\,min^{-1}$ to $153 \pm 8\,b\,min^{-1}$ ($-1 \pm 1\,b\,min^{-1}$, $n = 11$).

Infusion of NA (0.1–1.0 $\mu g\,kg^{-1}\,min^{-1}$) produced dose-dependent increases in cardiac contractility and MAP. The chronotropic response associated with NA infusion was variable and displayed no consistent pattern. Figure 5 shows the combined results for each of the parameters from 6 dogs.

Dobutamine infusion produced dose-dependent increases in HR and contractility. The minor pressor response to dobutamine infusion was variable (Figure 6).

One factor ANOVA (repeated measures) showed that NPY had no significant effect on the dose-response curves obtained

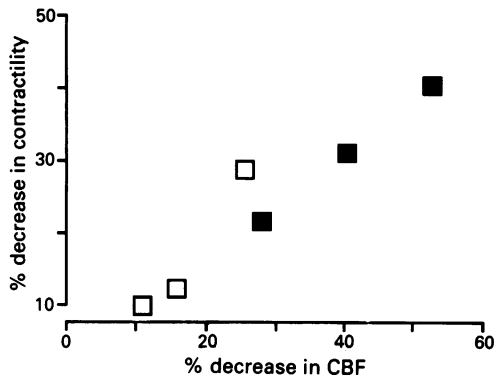

Figure 3 The effects of neuropeptide Y (500 μg) (□) and vasopressin (VP) (1 unit) (■) on cardiac contractility and coronary blood flow (CBF).

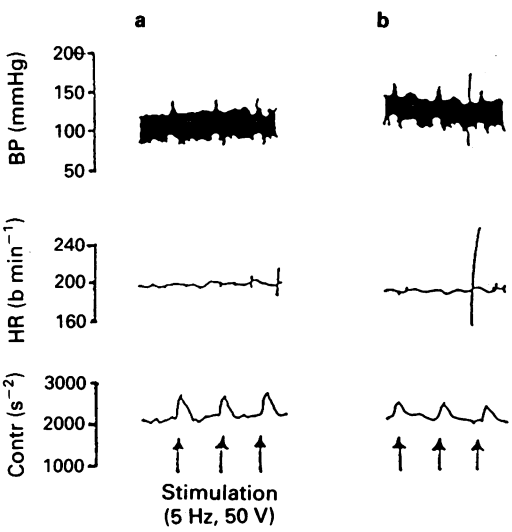

Figure 4 Effect of sympathetic stimulation on blood pressure (BP), heart rate (HR) and contractility (Contr.); (a) prior to and (b) 5 min after the injection of NPY in an anesthetized dog.

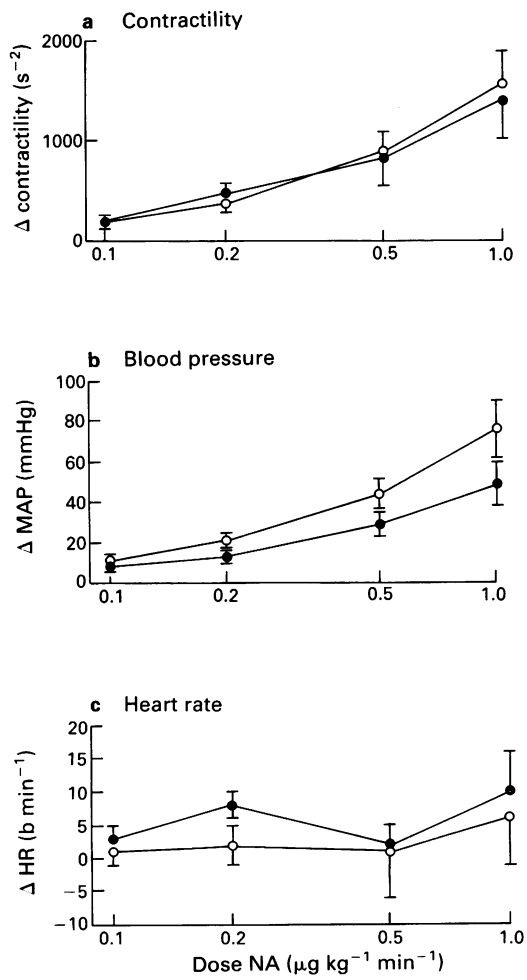

Figure 5 Dose-response curve for the effect of noradrenaline (NA) on contractility, blood pressure (MAP) and heart rate (HR) in the absence (○) and presence (●) of neuropeptide Y.

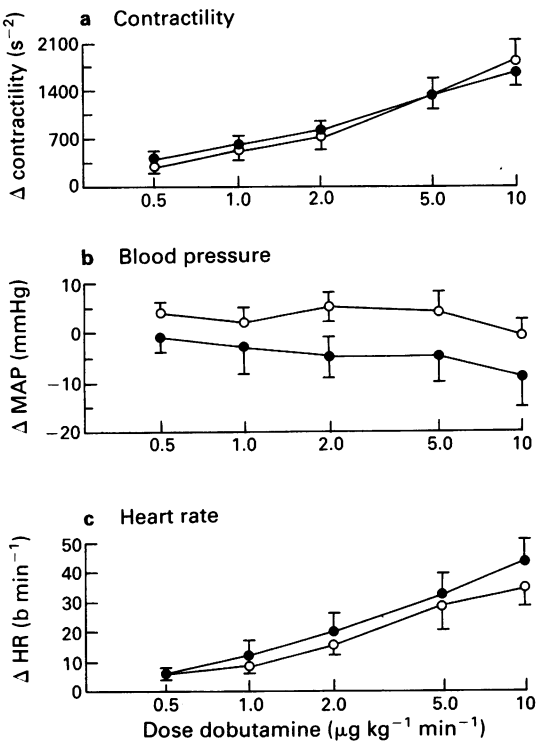

Figure 6 Dose-response curves for the effect of dobutamine on contractility, blood pressure (MAP) and heart rate (HR) in the absence (○) and presence (●) of neuropeptide Y.

for cumulative infusions of NA (Figure 5) and dobutamine (Figure 6) for contractility, HR or MAP.

Series III

The injection of salbutamol ($0.5\,\mu g\,kg^{-1}$) produced a prompt fall in MAP, from 112 ± 6 mmHg to 84 ± 6 mmHg. This depressor effect was associated with a small increase in HR, from $159 \pm 9\,b\,min^{-1}$ to $171 \pm 9\,b\,min^{-1}$ and a positive inotropic effect, increasing contractility from $2160 \pm 230\,s^{-2}$ to $3060 \pm 280\,s^{-2}$. Analysis of the data by one factor ANOVA (repeated measures) showed that there was no significant change in the inotropic, chronotropic or depressor effect of salbutamol in the presence of NPY.

Series IV

The injection of impromidine ($0.7\,\mu g\,kg^{-1}$) produced a reduction in MAP from 116 ± 9 mmHg to 96 ± 9 mmHg. This depressor action was associated with a positive chronotropic effect, increasing HR from $162 \pm 7\,b\,min^{-1}$ to $174 \pm 8\,b\,min^{-1}$, and a positive inotropic effect, increasing contractility from $2140 \pm 170\,s^{-2}$ to $2940 \pm 265\,s^{-2}$. One factor ANOVA (repeated measures) showed that at 5 min, there was no significant difference in the inotropic response to impromidine injection. NPY also had no significant effect on the chronotropic or pressor responses to impromidine injection.

Discussion

Since NPY is found in sympathetic nerves supplying the heart and has been shown to be present in coronary vessels, it has been postulated that it may be engaged in the regulation of coronary perfusion and may be responsible for coronary spasm (Aizawa *et al.*, 1985; Clarke *et al.*, 1987). NPY may also be involved in myocardial ischaemia and heart failure which are associated with hyperreactivity of the sympathetic nervous system but are resistant to adrenoceptor blockers (Zukowska-Grojec *et al.*, 1987). Thus, it was considered of interest to investigate the actions of NPY on the coronary circulation, and the way in which these effects may influence cardiac function.

The experiments described here show that intravenous injection of NPY evoked significant reductions in CBF with a parallel fall in contractility. The results of this study are in agreement with those of Maturi *et al.* (1989), who administered NPY directly into the coronary circulation of dogs. Substantial falls in coronary blood flow were seen in their animals, presumably due to the very high local concentrations which would have been present in the coronary vasculature. In the present experiments where NPY was administered intravenously, the changes in coronary blood flow were smaller. In order to determine the importance of the coronary vasoconstrictor response in these animals, the effects of NPY were compared to those of vasopressin. Vasopressin is a potent pressor agent, which is known to have no direct actions on the heart in the dog (Courtice *et al.*, 1983). Doses of 30 to 300 times greater than that required to induce vasoconstriction were necessary to elicit negative inotropic responses in canine isolated atrial preparations (Chiba, 1977). Doses of NPY and vasopressin which caused similar decreases in coronary blood flow had similar negative inotropic effects and since it has been shown that NPY acts primarily on small coronary arteries to produce vasoconstriction (Maturi *et al.*, 1989), we suggest that the fall in contractility after NPY is largely due to the accompanying decrease in coronary blood flow.

In a recent paper by Martin & Patterson (1989), intracoronary infusions of a high dose of NPY had no effect on contractility, measured as LV *dP/dt*, although there was a fall in CBF. As these authors suggested, LV *dP/dt* can be increased by increases in blood pressure. Thus the pressor effect of NPY may have increased LV *dP/dt* and thereby masked a negative inotropic response. Their results may also have been influenced by anaesthesia since, in unanaesthetized rabbits, a fall in LV *dP/dt* was seen after NPY administration (Minson *et al.*, 1987). The index of contractility used in the present experiments is less influenced by alterations in afterload (Goodman *et al.*, 1972) and thus more accurately reflects changes in the inotropic state of the heart.

The pressor effect in response to administration of NPY is associated with a fall in HR, which is probably reflex in this preparation. It is likely that withdrawal of sympathetic tone was responsible for the major part of the bradycardia. There was no difference in the chronotropic responses of intact animals and those which had been vagotomized, which is in accord with the known vagolytic actions of pentobarbitone. It is also possible that withdrawal of sympathetic tone to the ventricular myocardium contributed to the reduction in contractility. Under normal circumstances, the inotropic component of baroreceptor reflex activity in an animal at rest is small. However, this becomes of greater significance in situations where there is a high level of sympathetic tone, as was the case in the present experiments.

It has been demonstrated that NPY induces a long-lasting attenuation of the action of the vagus nerve in anaesthetized dogs (Potter, 1985). This effect is brought about by a presynaptic inhibition of cholinergic transmission (Potter, 1987). The attenuating effect of NPY has been shown for the chronotropic and depressor responses to vagal stimulation. The results of the experiments in Series I show that attenuation of the inotropic and coronary vascular responses to vagal stimulation by NPY also occurs. This is probably because the reduction in contractility and CBF are secondary to the negative chronotropic effect.

The results of the experiments in Series II confirm the data of Lundberg *et al.* (1984a) from spontaneously beating guinea-pig atria, where NPY inhibited the positive inotropic and chronotropic effects of electrical field stimulation. In the present experiments, only the left cardiac sympathetic nerve was stimulated and thus there was no significant chronotropic response. The inhibitory effect of NPY on the inotropic response to sympathetic stimulation has been shown to be exerted presynaptically, by inhibition of the release of NA from sympathetic nerve terminals (Lundberg & Stjarne, 1984; Lundberg *et al.*, 1984a). Since the dose of NPY used in these experiments was shown to reduce effectively the response to sympathetic nerve stimulation, the possibility that similar presynaptic activity could contribute to the negative inotropic response to NPY must also be considered.

A number of reports of the effects of NPY on postsynaptic receptors have been published, but no consistent findings emerge. Some authors found that NPY potentiated the vasoconstrictor response to NA (Edvinsson *et al.*, 1984; Wahlestedt *et al.*, 1985; Tseng *et al.*, 1988). These results were obtained *in vitro*, in the absence of reflex activity which may result from the pressor, chronotropic or inotropic responses to drug infusion. Others have shown that the major part of the action of NPY *in vivo* is direct vasoconstriction and not the potentiation of other vasoconstrictors, such as NA (Lundberg *et al.*, 1984b; Petty *et al.*, 1984). In the rabbit isolated perfused heart, it has been shown that NPY had no effect on NA-evoked changes in HR or dP/dt, indicating that NPY does not interact with noradrenergic transmission at its postsynaptic receptors (Allen *et al.*, 1983). Iravani & Zar (1989) also showed that NPY did not significantly modify the chronotropic and inotropic effects of NA. The results of the present study show that NPY had no effect on either the pressor or cardiac responses to NA or dobutamine infusion, indicating that NPY has no modulatory effect on postsynaptic α- or β_1-adrenoceptors. These results are in agreement with those obtained by Allen *et al.* (1983) and Iravani & Zar (1989). There was no significant change in the responses to salbutamol injection, indicating furthermore that NPY has no modulatory effect on postsynaptic β_2-adrenoceptors.

It has been demonstrated in rabbit isolated blood vessels that NPY potentiates the constriction produced by histamine (Edvinsson *et al.*, 1984; Han & Abel, 1987). Since histamine H_2-receptors mediate a positive inotropic response in the canine heart (Einstein *et al.*, 1987), the effect of NPY on these receptors was studied. NPY had no significant effect on the responses to impromidine injection, showing that NPY has no modulatory role on H_2-receptors.

In conclusion, the attenuation of the depressor and chronotropic actions of the vagus nerve by NPY was confirmed in this study. It was also shown that NPY attenuates the CBF and inotropic responses to vagal stimulation. There was no evidence from these experiments to indicate that NPY has any modulatory effects on postsynaptic adrenoceptors or histamine receptors.

The results of the present study also demonstrate that NPY produces a prompt rise in MAP, with falls in HR, CBF and myocardial contractility in anaesthetized dogs. The fall in coronary blood flow occurs as a result of coronary vasoconstriction due to direct stimulation of postsynaptic receptors. The negative inotropic response to the administration of NPY probably occurs indirectly, as a result of the reduction in blood flow through the coronary vasculature and reduced sympathetic activity.

References

AIZAWA, Y., MURATA, M., HAYASHI, M., FUNAZAKI, T., ITO, S. & SHIBATA, A. (1985). Vasoconstrictor effect of neuropeptide Y (NPY) on canine coronary artery. *Jpn. Circ. J.*, **49**, 584–588.

AIZAWA, Y., SATOH, M., AIZAWA, M., FUNAZAKI, T., NIWANO, S., MIYAJIMA, S. & SHIBATA, A. (1987). Potency and receptors involved in coronary vasoconstriction caused by neuropeptide Y(NPY). *Jpn. Heart J.*, **28**, 891–898.

ALLEN, J.M., BIRCHAM, P.M.M., EDWARDS, A.V., TATEMOTO, K. & BLOOM, S.R. (1983). Neuropeptide Y (NPY) reduces myocardial perfusion and inhibits the force of contraction of the isolated perfused rabbit heart. *Regul. Pept.*, **6**, 247–253.

ALLEN, J.M., GJORSTRUP, P., BJORKMAN, J.-AEK, L., ABRAHAMSSON, T. & BLOOM, S.R. (1986). Studies on cardiac distribution and function of neuropeptide Y. *Acta Physiol. Scand.*, **126**, 405–411.

AWAD, S. J., EINSTEIN, R. & POTTER, E.K. (1989). The effects of neuropeptide Y (NPY) on myocardial contractility. *Proceedings of Australian Society of Clinical and Experimental Pharmacologists*, p. 59.

CHIBA, S. (1977). Positive chronotropic and negative inotropic actions of vasopressin in isolated blood-perfused canine atrium. *Jpn. Heart J.*, **18**, 221–224.

CLARKE, J.G., KERWIN, R., LARKIN, S., LEE, Y., YACOUB, M., DAVIES, G.J., HACKETT, D., DAWBARN, D., BLOOM, S.R. & MASERI, A. (1987). Coronary artery infusion of neuropeptide Y in patients with angina pectoris. *Lancet*, **i**, 1057–1059.

COURTICE, G.P., KWONG, T.E., LUMBERS, E.R. & POTTER, E.K. (1984). Excitation of the cardiac vagus by vasopressin. *J. Physiol.*, **354**, 547–556.

EDVINSSON, L., EKBLAD, E., HAKANSON, R. & WAHLESTEDT, C. (1984). Neuropeptide Y potentiates the effect of various constrictor agents on rabbit blood vessels. *Br. J. Pharmacol.*, **83**, 519–524.

EINSTEIN, R., MIHAILIDOU, A.S. & RICHARDSON, D.P. (1987). Positive inotropic effects of histamine in anaesthetised dogs. *Br. J. Pharmacol.*, **92**, 445–450.

GOODMAN, A.H., ANGUS, J.A., EINSTEIN, R. & COBBIN, L.B. (1972). A device for measuring myocardial contractility. *Med. Electron. Biol. Eng.*, **10**, 483–495.

GU, J., ADRIAN, T.E., TATEMOTO, K., POLAK, J.M., ALLEN, J.M. & BLOOM, S.R. (1983). Neuropeptide tyrosine (NPY) – A major cardiac neuropeptide. *Lancet*, **i**, 1008–1010.

HAN, C. & ABEL, P.W. (1987). Neuropeptide Y potentiates contraction. *Pharmacol.*, **9**, 675–681.

IRAVANI, M.M. & ZAR, M.A. (1989). The effects of neuropeptide Y (NPY) on isolated preparation of rat right atrium. *Br. J. Pharmacol.*, **96**, 218P.

LEVY, M.N., NG, M.L. & ZIESKE, H. (1966). Functional distribution of the peripheral cardiac sympathetic pathways. *Circ. Res.*, **19**, 650–661.

LUNDBERG, J.M., HUA, X.-Y. & FRANCO-CERECEDA, A. (1984a). Effects of neuropeptide Y (NPY) on mechanical activity and neurotransmission in the heart, vas deferens and urinary bladder of the guinea-pig. *Acta Physiol. Scand.*, **121**, 325–332.

LUNDBERG, J.M., SARIA, A., ANGGARD, A., HOKFELT, T. & TERENIUS, L. (1984b). Neuropeptide Y and noradrenaline interaction in peripheral cardiovascular control. *Clin. Exp. Hypertens.* Part A., **6**, 1961–1972.

LUNDBERG, J.M. & STJARNE, L. (1984). Neuropeptide Y (NPY) depresses the secretion of ^{3}H-noradrenaline and the contractile response evoked by field stimulation, in rat vas deferens. *Acta Physiol. Scand.*, **120**, 477–479.

LUNDBERG, J.M. & TATEMOTO, K. (1982). Pancreatic polypeptide family (APP, BPP, NPY and PPY) in relation to sympathetic vasoconstriction resistant to α-adrenoceptor blockade. *Acta Physiol. Scand.*, **116**, 393–402.

LUNDBERG, J.M., TERENIUS, L., HOKFELT, T., MARTLING, C.R., TATEMOTO, K., MUTT, V., POLAK, J. & GOLDSTEIN, M. (1982). Neuropeptide Y (NPY)–like immunoreactivity in peripheral noradrenergic neurons and effects of NPY on sympathetic function. *Acta Physiol. Scand.*, **116**, 477–480.

MABE, Y., TATEMOTO, K. & HUIDOBORO-TORO, P. (1985). Neuropeptide Y-induced pressor responses: activation of a non-adrenergic mechanism, potentiation by reserpine and blockade by nifedipine. *Eur. J. Pharmacol.*, **116**, 33–39.

MARTIN, S.E. & PATTERSON, R.E. (1989). Coronary constriction due to neuropeptide Y: alleviation with cyclooxygenase blockers. *Am. J. Physiol.* **257**, H927–H934.

MATURI, M.F., GREENE, R., SPEIR, E., BURRUS, C., DORSEY, L.M.A., MARKLE, D.R., MAXWELL, M., SCHMIDT, W., GOLDSTEIN, S.R. & PATTERSON, E. (1989). Neuropeptide Y – A peptide found in human coronary arteries constricts primarily small coronary

arteries to produce myocardial ischaemia in dogs. *J. Clin. Invest.*, **83**, 1217–1224.

MINSON, R.B., McRITCHIE, R.J. & CHALMERS, J.P. (1987). Effects of neuropeptide Y on left ventricular function in the conscious rabbit. *Clin. Exp. Pharmacol. Physiol.*, **14**, 263–266.

PETTY, M.A., DIETRICH, R. & LANG, R.E. (1984) The cardiovascular effects of neuropeptide Y (NPY). *Clin. Exp. Hypertens.* Part A., **6**, 1889–1892.

PIPER, H.M., MILLAR, B.C. & McDERMOTT, B.J. (1989). The negative inotropic effect of neuropeptide Y on the ventricular cardiomyocyte. *Naunyn-Schmiedebergs Arch. Pharmacol.*, **340**, 333–337.

POTTER, E.K. (1985). Prolonged non-adrenergic inhibition of cardiac vagal action following sympathetic stimulation: Neuromodulation by neuropeptide Y? *Neurosci. Lett.*, **54**, 117–121.

POTTER, E. K. (1987). Site of action of neuropeptide Y in the heart. *Neurosci. Lett.*, **27** (Suppl.), 5112.

POTTER, E. K. (1988). Neuropeptide Y as an autonomic neurotransmitter. *Pharmacol. Ther.*, **37**, 251–273.

RIOUX, F., BACHELARD, H., MARTEL, J.C. & ST. PIERRE, S. (1986). Guinea-pig isolated heart. *Peptides*, **7**, 27–31.

RUDEHILL, A., SOLLEVI, A., FRANCO-CERECEDA, A. & LUNDBERG, J.M. (1986). Neuropeptide Y (NPY) and the pig heart: release and coronary vasoconstrictor effects. *Peptides*, **7**, 821–826.

TATEMOTO, K., CARLQUIST, M. & MUTT, V. (1982). Neuropeptide Y – A novel brain peptide with structural similarities to peptide YY and pancreatic polypeptide. *Nature*, **296**, 659–660.

TSENG, C.-J., ROBERTSON, D., LIGHT, R.T., ATKINSON, J.R. & ROBERTSON, R.M. (1988). Neuropeptide Y is a vasoconstrictor of human coronary arteries. *Am. J. Med. Sci.*, **296**, 11–16.

WAHLESTEDT, C., EDVINSSON, L., EKBLAD, E. & HAKANSON, R. (1985). Neuropeptide Y potentiates noradrenaline evoked vasoconstriction: Mode of action. *J. Pharmacol. Exp. Ther.*, **234**, 735–741.

WAHLESTEDT, C., WOHLFART, B. & HAKANSON, R. (1987). Effects of neuropeptide Y (NPY) on isolated guinea-pig heart. *Acta Physiol. Scand.*, **129**, 459–463.

ZUKOWSKA-GROJEC, Z., MARKS, E.S. & HAASS, M. (1987). Neuropeptide Y is a potent vasoconstrictor and a cardiodepressant in rat. *Am. J. Physiol.*, **253**, H1234-H1239.

(Received December 6, 1990
Revised March 8, 1991
Accepted May 8, 1991)

Br. J. Pharmacol. (1991), **104**, 202–206

Inositol 1,4,5-trisphosphate-stimulated calcium release from permeabilized cerebellar granule cells

[1]Emma M. Whitham, R.A. John Challiss & Stefan R. Nahorski

Department of Pharmacology and Therapeutics, University of Leicester, University Road, Leicester LE1 9HN

1 Muscarinic cholinoceptor stimulation of phosphoinositide hydrolysis in rat cultured cerebellar granule cells results in a rapid, transient accumulation of inositol 1,4,5-trisphosphate ($Ins(1,4,5)P_3$), which has been implicated in the release of non-mitochondrial intracellular Ca^{2+} stores. In the present study, the release of Ca^{2+} from intracellular stores and the $Ins(1,4,5)P_3$ receptor responsible for this process have been investigated.

2 Monolayers of saponin-permeabilized granule cells accumulate $^{45}Ca^{2+}$ in an ATP-dependent manner and the sequestered $^{45}Ca^{2+}$ can be concentration-dependently released by $Ins(1,4,5)P_3$ by a stereospecific and heparin-sensitive mechanism. The EC_{50} for $Ins(1,4,5)P_3$-stimulated $^{45}Ca^{2+}$ release was 80 ± 3 nM.

3 Radioligand binding studies performed on a crude granule cell membrane fraction indicated the presence of an apparently homogeneous population of stereo-specific $Ins(1,4,5)P_3$ receptors (K_D 54.7 ± 2.0 nM; B_{max} 1.37 ± 0.29 pmol mg^{-1} protein).

4 This study provides evidence for $Ins(1,4,5)P_3$-sensitive intracellular Ca^{2+} stores in primary cultures of cerebellar granule cells and suggest that these cells provide an excellent model neuronal system in which to study the relative functional roles of Ca^{2+} release from intracellular stores and Ca^{2+}-entry in neuronal Ca^{2+} homeostasis.

Keywords: Inositol 1,4,5-trisphosphate; Ca^{2+} homeostasis; cerebellar granule cell; $Ins(1,4,5)P_3$ receptors

Introduction

The cerebellar granule cell in culture provides an excellent cellular neuronal model for the investigation of transmembrane signalling phenomena and stimulus-secretion coupling mechanisms (Gallo *et al.*, 1982; Nicoletti *et al.*, 1986). The granule cell expresses a variety of neurotransmitter receptors which, upon activation by agonists, can stimulate phosphoinositidase C (PIC) activity to increase inositol phospholipid hydrolysis (Nicoletti *et al.*, 1986; Xu & Chuang, 1987; Lin *et al.*, 1990a; Whitham *et al.*, 1991). Although the majority of studies on this cell have involved the assessment of PIC activity by measuring total inositol phosphate accumulation in the presence of the uncompetitive inhibition of inositol monophosphatase by lithium, more recent studies have demonstrated increased mass accumulation of inositol 1,4,5-trisphosphate ($Ins(1,4,5)P_3$) concentration in response to muscarinic cholinoceptor stimulation (Whitham *et al.*, 1991) and increased [^{3}H]-$Ins(1,4,5)P_3$ and [^{3}H]-$Ins(1,3,4,5)P_4$ accumulations in cerebellar granule cells, labelled to equilibrium with [^{3}H]inositol, in response to glutamate (Bouchelouche *et al.*, 1989).

Since there is also some evidence that certain agonists can release Ca^{2+} from intracellular stores of granule cells (Courtney *et al.*, 1990; Irving *et al.*, 1990), it is likely that this can occur via increases in polyphosphoinositide hydrolysis (Berridge & Irvine, 1989) and activation of the stereospecific inositol polyphosphate receptors responsible for Ca^{2+} release from intracellular stores (Nahorski & Potter, 1989). However, although cerebellum contains particularly high concentrations of the $Ins(1,4,5)P_3$ receptor and has provided a suitable tissue source for the purification (Supattapone *et al.*, 1988) and cloning (Furiuchi *et al.*, 1989) of this intracellular receptor, the density of $Ins(1,4,5)P_3$ receptors within this brain area is highly heterogeneous (Worley *et al.*, 1989), with very high densities of sites in Purkinje cells, and very low levels evident in the granular layer of cerebellum (Ross *et al.*, 1989). Thus, although $Ins(1,4,5)P_3$-induced release of Ca^{2+} from crude cerebellar microsomes has been reported (Stauderman *et al.*, 1988; Joseph *et al.*, 1989) it has been assumed that the microsomal fraction exhibiting release is derived from Purkinje cells. The present study has investigated the characteristics of $Ins(1,4,5)P_3$-induced Ca^{2+} release from saponin-permeabilized monolayers of rat cerebellar granule cells and provides the first demonstration of the presence and properties of the $Ins(1,4,5)P_3$ receptor in a discrete population of primary neuronal cells.

[1] Author for correspondence.

Methods

Culture of cerebellar granule cells

This was performed as described previously (Whitham *et al.*, 1991): in brief, cells were prepared from cerebella obtained from 6–8 day old rats by mild trypsin digestion and tituration and cultured at an approximate density of 3–4 $\times$ 10^6 cells/well in multiwells precoated with poly-D-lysine (5 μg ml^{-1}). The culture medium was basal modified Eagle's medium, supplemented with 10% (v/v) foetal calf serum, 5 mM glutamine, 40 μg ml^{-1} gentamycin and containing 25 mM K^+ (Gallo *et al.*, 1987). Cultures were maintained at 37°C in a humidified atmosphere of 5% CO_2, and 20–24 h after initial plating 10 μM cytosine arabinoside was added to inhibit proliferation of non-neuronal cells. In agreement with the reports of others (Kingsbury *et al.*, 1985), these conditions produced cultures of 90–95% granule cells. All experiments were carried out after 7–9 days *in vitro*.

Cell permeabilization, Ca^{2+} loading and release

Experiments were carried out according to the methods described by Ambler & Taylor (1989). Monolayers of cells were washed three times with 'wash' buffer (in mM: KCl 140, NaCl 10, $MgCl_2$ 1.0, $CaCl_2$ 0.24, K_2HPO_4 1.0, EGTA 1.0 and HEPES 25) and then exposed to saponin, 100 μg ml^{-1} for 60 s. After saponin exposure, monolayers were carefully washed with the buffer: this treatment resulted in >90% permeabilization, as assessed with trypan blue. Monolayers were then incubated in a 'cytosol-like' buffer (in mM: KCl 120, KH_2PO_4 2, $CH_3COO.Na$ 5, HEPES 20, $MgCl_2$ 6, ATP 5, pH 6.9 containing oligomycin 2 μg ml^{-1}, $^{45}CaCl_2$ (2 μCi ml^{-1}) and the final Ca^{2+} concentration buffered at 50–100 nM for

the periods indicated in the Results section. After the loading period, fresh 'cytosol-like' buffer was added and cells challenged with the concentrations of Ins(1,4,5)P_3, for the times indicated in the Results section. At the end of this period buffer was exchanged with ice-cold 'wash' buffer to terminate the incubation and cells were solubilized with 0.1 M NaOH and radioactivity determined by scintillation counting.

Inositol 1,4,5-trisphosphate-receptor characterization

For these experiments, cerebellar granule cells were cultured in 175 cm^2 tissue-culture flasks for 7–8 days *in vitro*. Cells were scraped from the flasks and washed in ice-cold 20 mM $NaHCO_3$, 1 mM dithiothreitol, pH 8.0 and homogenized (polytron setting 5–6, 2 × 15 s). The homogenate was centrifuged at 40,000 *g* for 20 min at 4°C and the membrane pellet resuspended by homogenization in the same buffer. Membranes were washed three times by centrigugation/homogenization and the final pellet resuspended at 7–8 mg of protein ml^{-1}. Binding assays (Challiss *et al.*, 1990) were performed in a final volume of 0.12 ml at 4°C: 200–300 μg of membrane protein were added to an assay buffer (25 mM Tris/HCl, 1 mM EDTA, pH 8.0) containing approx. 15,000 d.p.m. [^{32}P]Ins(1,4,5)P_3 and various concentrations of D- or L-Ins(1,4,5)- P_3 (see Results section). Non-specific binding was determined in the presence of 10 μM D- or DL-Ins(1,4,5)P_3. Incubations were for 30 min and were terminated by centrifugation (12,000 *g*, 4 min). The supernatant was carefully removed, the pellet solubilized in 0.1 ml Lumasolve and radioactivity determined by scintillation counting.

Materials

[^{32}P]-Ins(1,4,5)P_3 (110–170 Ci $mmol^{-1}$) was generously provided as a gift by NEN(DuPont). Ins(1,4,5)P_3 was from RBI/SEMAT, and L-Ins(1,4,5)P_3 was a gift from Prof. B.V.L. Potter (Pharmacy & Pharmacology, University of Bath). Ionomycin, saponin and heparin (low mol wt) were from Sigma. All other chemicals and tissue culture reagents were obtained from the suppliers given in Whitham *et al.* (1991).

Data analysis

EC_{50} (the concentration of agent causing 50% of the maximal effect) values were estimated by computer-assisted curve-fitting using ALLFIT (DeLean *et al.*, 1978). K_D and B_{max} values were calculated following Scatchard transformation of isotope-dilution data by linear regression analysis. Results are expressed as means ± s.e.mean for *n* independent experiments throughout.

Results

Saponin-treated monolayers of cerebellar granule cells displayed a rapid and ATP-dependent uptake of $^{45}Ca^{2+}$ when incubated in the presence of 50–100 nM Ca^{2+} and oligomycin to block uptake into mitochondria (Strupish *et al.*, 1988). Under these conditions $^{45}Ca^{2+}$-uptake was half-maximal at about 5 min, and reached a steady-state level by 15 min which was maintained essentially unchanged over the subsequent 15–30 min loading period (Figure 1). The Ca^{2+} ionophore ionomycin (10 μM) released 80–90% of the $^{45}Ca^{2+}$ accumulated, suggesting that it is predominantly intravesicular. The small uptake observed in the absence of added ATP may suggest that endogenous ATP persists in these permeabilized cells or occurs by an ATP-independent uptake mechanism.

Addition of Ins(1,4,5)P_3 (1 μM) to monolayers, following a $^{45}Ca^{2+}$-loading period of 15 min, resulted in a rapid release of $^{45}Ca^{2+}$ from sequestered stores. Maximal release was observed within 30 s of Ins(1,4,5)P_3 addition and was maintained for about 5 min before slowly declining towards pre-stimulation values (Figure 2). The re-uptake of $^{45}Ca^{2+}$ was consistent with the time-course of Ins(1,4,5)P_3 metabolism by

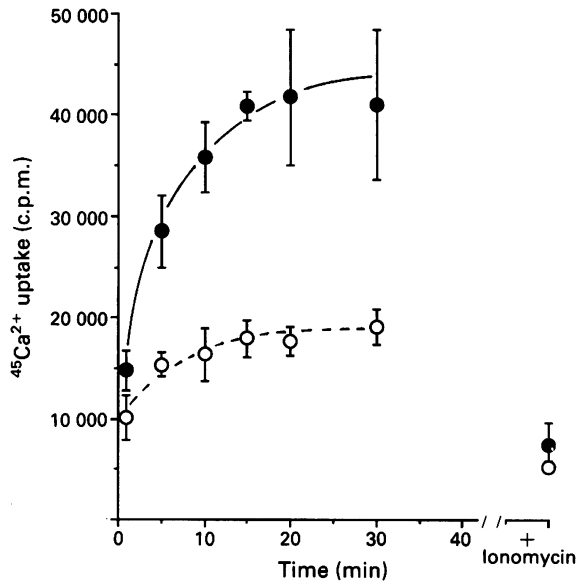

Figure 1 Time course of $^{45}Ca^{2+}$ uptake into permeabilized rat cerebellar granule cells. Saponin-permeabilized granule cell monolayers were incubated in the absence (○) or presence (●) of 5 mM ATP as described in the Methods section. Ionomycin (10 μM) released >90% of the $^{45}Ca^{2+}$ accumulated when added after 15 min. Values are shown as means of four separate experiments (s.e.mean shown by vertical bars), each performed in duplicate.

both cellular 5-phosphatase and 3-kinase routes (data not shown). Ins(1,4,5)P_3 concentration-dependently released $^{45}Ca^{2+}$ when determined 2 min after agonist challenge (Figure 3). A maximal release of 60% of the sequestered stores was observed in the presence of >1 μM Ins(1,4,5)P_3 and the EC_{50} value for the release response was 80 ± 3 nM. L-Ins(1,4,5)P_3 did not cause $^{45}Ca^{2+}$ release up to the maximal concentration tested (10 μM), demonstrating the strict stereo-selectivity of the receptor-mediated release process (Figure 3, Table 1). Furthermore, Ins(1,4,5)P_3-induced Ca^{2+} release was antagonized by addition of low mol wt. heparin (100 μg ml^{-1}) to permeabilized monolayers 15 min before agonist challenge (Table 1).

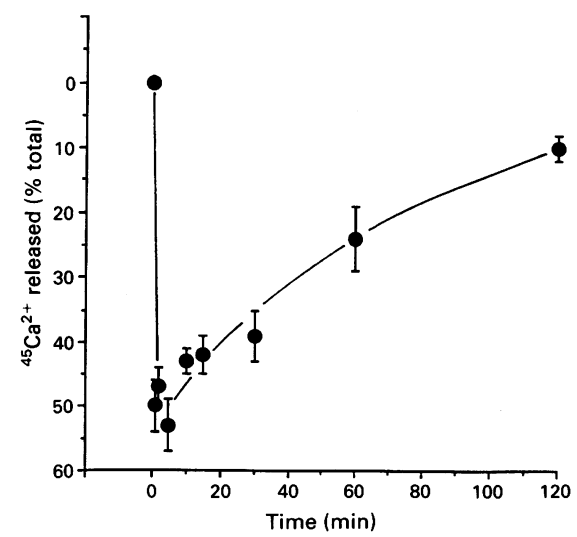

Figure 2 Kinetics of inositol 1,4,5-trisphosphate (Ins(1,4,5)-P_3)-evoked $^{45}Ca^{2+}$ release from permeabilized cerebellar granule cells. Saponin-permeabilized granule cell monolayers were $^{45}Ca^{2+}$-loaded as described in the Methods section and challenged with Ins(1,4,5)P_3 3 μM at time-zero. Values are shown as means of four separate experiments (s.e.mean shown by vertical bars), each performed in duplicate

Table 1 Effects of D and L-inositol 1,4,5-trisphosphate (D- and L-Ins(1,4,5)P_3) on $^{45}Ca^{2+}$ release, and antagonism by low mol wt heparin, in permeablilized cerebellar granule cells

Agonist/antagonist addition	*Residual* $^{45}Ca^{2+}$ (% total)	*Release* (%)
D-Ins(1,4,5)P_3 3 μM	38.5 ± 4.0	61.5
L-Ins(1,4,5)P_3 3 μM	114 ± 8	0
D-Ins(1,4,5)P_3 3 μM + low mol wt heparin 100 $\mu g\,ml^{-1}$	91 ± 4	9

Granule cell monolayers were saponin-permeabilized as described in the methods section. Where indicated low mol wt heparin was added 10 min before agonist addition. Values for vesicular $^{45}Ca^{2+}$ remaining 2 min after agonist addition are shown as means ± s.e.mean for three separate experiments, each performed in duplicate.

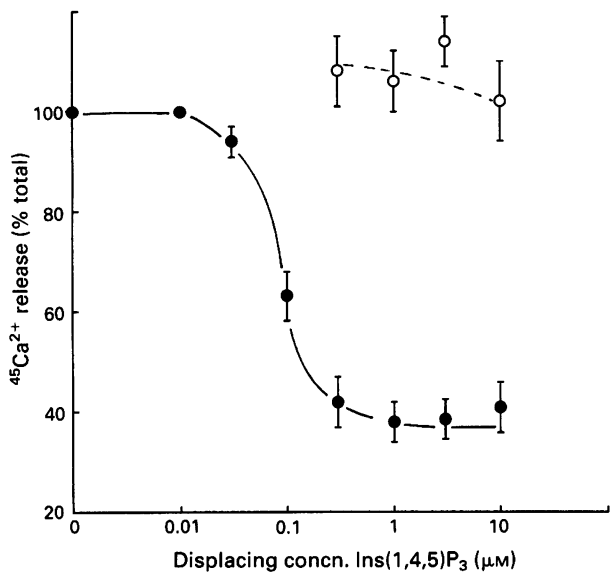

Figure 3 Concentration-dependent effects of D and L-inositol 1,4,5-trisphosphate (D- and L-Ins(1,4,5)P_3) on $^{45}Ca^{2+}$ release from permeabilized cerebellar granule cells. Saponin-permeabilized granule cell monolayers were $^{45}Ca^{2+}$-loaded as described in the Methods section and challenged with various concentrations of D-Ins(1,4,5)P_3 (●) or L-Ins(1,4,5)P_3 (○) for 2 min. Values are shown as means of four separate experiments (s.e.mean shown by vertical bars), each performed in duplicate.

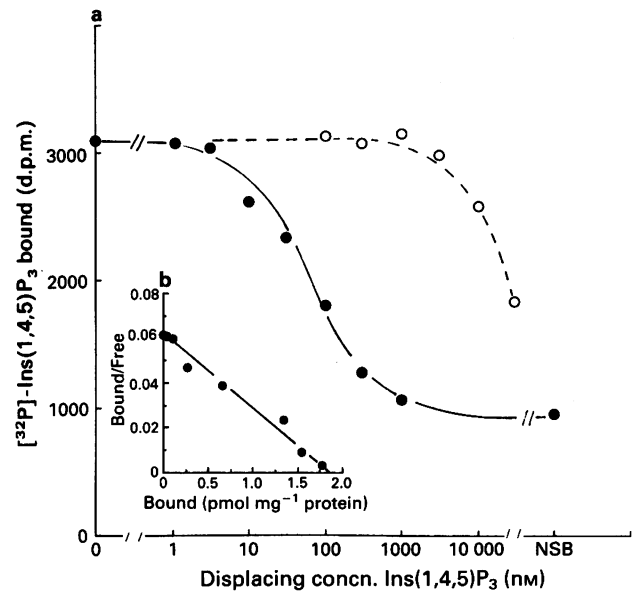

Figure 4 Concentration-dependent displacement of [^{32}P]-inositol 1,4,5-trisphosphate ([^{32}P]Ins(1,4,5)P_3) by D- and L-Ins(1,4,5)P_3 from rat cerebellar granule membranes. A crude membrane pellet was prepared as described in the Methods section. (a) Displacement of [^{32}P]Ins(1,4,5)P_3 binding by D-Ins(1,4,5)P_3 (●) or L-Ins(1,4,5)P_3 (○) is shown with the non-specific binding (NSB) component being defined in the presence of 10 μM DL-Ins(1,4,5)P_3 or 100 $\mu g\,ml^{-1}$ low mol wt heparin. The inset (b) shows the Scatchard transformation of the D-Ins(1,4,5)P_3 isotope dilution data. Data from a representative experiment are shown, with similar results being obtained on two other occasions.

The displacement of [^{32}P]-Ins(1,4,5)P_3 binding to a crude preparation of cerebellar granule cell membranes by Ins(1,4,5)-P_3 and L-Ins(1,4,5)P_3 is shown in Figure 4. Definition of the non-specific binding component by use of 10 μM Ins(1,4,5)P_3, 10 μM DL-Ins(1,4,5)P_3 or 100 $\mu g\,ml^{-1}$ low mol wt heparin gave essentially identical values, varying over a range of 30–45% of the total binding for the different membrane preparations used in the study. The receptor displayed a marked stereoselectivity, with the L-isomer being at least 300 fold less effective in its displacing activity (Figure 4). Scatchard transformation of the isotope-dilution data for Ins(1,4,5)P_3 demonstrated an apparently homogeneous population of binding sites (Figure 4 inset) with a K_D of 54.7 ± 2.0 nM and a B_{max} of 1.37 ± 0.29 pmol mg^{-1} protein.

Discussion

The cerebellar granule cell in culture provides an excellent model system which exhibits many of the phenotypic characteristics of neurones *in vivo* (Burgoyne & Cambray-Dekin, 1988; Chuang, 1989). Receptor-mediated changes in cytosolic Ca^{2+} concentration can be effected by activation of receptor-operated and voltage-operated Ca^{2+} channels (Kingsbury & Balazs, 1987; Carboni & Wojcik, 1988; Holopainen *et al.*, 1989). Thus, excitatory amino acid receptors can cause Ca^{2+} entry via direct and indirect mechanisms (Wroblewski *et al.*, 1985; Nicoletti *et al.*, 1986; Burgoyne *et al.*, 1988; Courtney *et al.*, 1990; Gallo *et al.*, 1990). In addition, 'metabotropic' excitatory amino acid receptor activation results in release of Ca^{2+} from intracellular stores (Courtney *et al.*, 1990; Irving *et al.*, 1990) making this cell a valuable preparation in which to investigate the relationship and significance of these sources of Ca^{2+} in neuronal cells. Cerebellar granule cells express several receptors linked to phosphoinositide metabolism (Xu & Chuang, 1987; Whitham *et al.*, 1991) and it is tempting to suggest that inositol polyphosphates play a role in release of Ca^{2+} stores and perhaps Ca^{2+} entry via non-voltage operated channels (Nahorski, 1988; Berridge & Irvine, 1989). Although the generation of the Ca^{2+}-mobilizing second messenger Ins(1,4,5)P_3 has not been detected in all studies (Hynie *et al.*, 1989), our own work (Whitham *et al.*, 1991) and that from other laboratories (Bouchelouche *et al.*, 1989) suggest that a large, transient increase in Ins(1,4,5)P_3 concentration occurs in granule cells in response to muscarinic agonists and glutamate, with metabolism occurring via both 5-phosphatase and 3-kinase routes (Bouchelouche *et al.*, 1989; Whitham, Challiss, & Nahorski, unpublished results).

In the present study we have established that Ins(1,4,5)P_3 can induce Ca^{2+} release from intracellular stores in per-

meabilized monolayers of granule cells. Uptake of $^{45}Ca^{2+}$ into non-mitochondrial intracellular stores occurred by an ATP-dependent, high affinity process exhibiting similar characteristics to those reported previously in many permeabilized cells or microsomal preparations (Stauderman *et al.*, 1988; Strupish *et al.*, 1988; Joseph *et al.*, 1989). The Ins(1,4,5)P_3-induced release was stereo-specific and was inhibited by low mol wt heparin, an antagonist at the Ins(1,4,5)P_3 receptor (Worley *et al.*, 1987a; Guillemette *et al.*, 1989) suggesting interaction with a receptor exhibiting properties closely resembling those identified in several other cell types. Maximally effective concentrations of Ins(1,4,5)P_3 released about 60% of sequestered $^{45}Ca^{2+}$, compared to 80–90% release by ionomycin addition. An identical proportion of $^{45}Ca^{2+}$ was released by the metabolically-stable inositol 1,4,5-trisphosphorothioate (Nahorski & Potter, 1989) (data not shown). This strategy suggests that Ins(1,4,5)P_3-sensitive and insensitive stores are present in granule cells. The nature of the Ins(1,4,5)P_3- insensitive store in certain cells suggests that Ca^{2+} release can be facilitated by caffeine, blocked by ryanodine and may serve as a Ca^{2+}-induced Ca^{2+} release site (Thayer *et al.*, 1988); however, under the present experimental conditions, we were unable to evoke release by concentrations of caffeine as high as 10 mM (Whitham, Challiss and Nahorski, unpublished results).

Although cerebellum contains the highest density of Ins(1,4,5)P_3 receptors (Worley *et al.*, 1987b, 1989) and Ins(1,4,5)P_3-receptor-encoding mRNA (Furiuchi *et al.*, 1990) of all tissues so far investigated, expression appears to be cell-type specific, with Purkinje cells possessing very high levels of receptors (Ross *et al.*, 1989; Mignery *et al.*, 1989; Maeda *et al.*, 1990) and the immunocytochemical methods employed being unable to detect Ins(1,4,5)P_3 receptors in the granule cell layer. However, in agreement with the Ca^{2+} release data, we observed stereo-specific [^{32}P]-Ins(1,4,5)P_3 binding to crude cerebellar granule cell membrane preparations. The cerebellar granule cell Ins(1,4,5)P_3 receptor exhibited a similar affinity to that reported for whole cerebellum; however, the receptor density was low (1.37 ± 0.29 pmol mg^{-1} protein), relative to the values (10–30 pmol mg^{-1} protein) reported for whole cerebellum (Willcocks *et al.*, 1987; Worley *et al.*, 1987a; Joseph & Rice, 1989), suggesting that the Ins(1,4,5)P_3 receptor density of cerebellar granule cells may be masked by that present in Purkinje cells. Furthermore, the possibility should be considered that as a neonatal culture, the presence of these sites may not reflect the mature granule cells, and the distribution of Ins(1,4,5)P_3 binding-sites in neonatal cerebellum would be worthy of further investigation.

Cerebellar granule cells possess a variety of receptors coupled to Ins(1,4,5)P_3 generation, Ins(1,4,5)P_3 receptors and the potential for second messenger-induced Ca^{2+} release from intracellular stores. It would seem probable therefore that the ability of 'metabotropic' excitatory amino acid, and perhaps muscarinic, agonists to release Ca^{2+} from intracellular stores of granule cells (Courtney *et al.*, 1990; Irving *et al.*, 1990; Ciardo & Meldolesi, 1991) involves this signalling sequence. The precise role(s) of Ins(1,4,5)P_3-stimulated changes in intracellular Ca^{2+} concentration in excitable tissues is unknown. Although there are examples of Ins(1,4,5)P_3-induced Ca^{2+}-mobilization and entry across the plasma membrane accompanying functional changes in 'neurone-like' cells (e.g. increased catecholmine release from adrenal chromaffin cells; Cheek *et al.*, 1989; O'Sullivan *et al.*, 1989), the high densities of voltage-operated Ca^{2+} channels in neuronal cells strongly suggest that extracellular Ca^{2+} is the primary source for changes in cytoplasmic Ca^{2+} (Nahorski, 1988). Observations of receptor-stimulated glutamate release from cerebellar granule cells tend to support this general view; thus Gallo *et al.* (1990) and Levi *et al.* (1991) have demonstrated that quisqualate and α-amino-3-hydroxy-5-methyl-4-isoxazolepropionate (AMPA) can increase neurotransmitter release, with the quisqualate effect being completely blocked by the 'ionotropic' quisqualate receptor antagonist 6-cyano-2,3-hydroxy-7-nitroquinoxaline. Furthermore, although endothelin-1 causes a marked stimulation of phosphoinositide turnover in granule cells (Lin *et al.*, 1990a) and stimulates transmitter release (Lin *et al.*, 1990b), this action is dependent on extracellular Ca^{2+}.

This study provides firm evidence for both Ins(1,4,5)P_3- sensitive and insensitive intracellular stores of Ca^{2+} in granule cells. It seems likely that this neuronal culture will be valuable in assessing the significance of such a source of Ca^{2+} and its possible association with voltage-independent Ca^{2+} entry.

We thank the Wellcome Trust for financial support and NEN(DuPont) for generously providing the [^{32}P]-Ins(1,4,5)P_3. E.M.W. holds a Wellcome Prize Studentship.

References

AMBLER, S.K. & TAYLOR, P. (1989). Release of nonmitochondrial sequestered Ca^{2+} from permeabilized muscle cells in culture. *Mol. Pharmacol.*, **35**, 369–374.

BERRIDGE, M.J. & IRVINE, R.F. (1989). Inositol phosphates and cell signalling. *Nature*, **341**, 197–205.

BOUCHELOUCHE, P., BELHAGE, B., FRANDSEN, A., DREJER, J. & SCHOUSBOE, A. (1989). Glutamate receptor activation in cultured cerebellar granule cells increases cytosolic free Ca^{2+} by mobilization of cellular Ca^{2+} and activation of Ca^{2+} influx. *Exp. Brain Res.*, **76**, 281–291.

BURGOYNE, R.D. & CAMBRAY-DEAKIN, M. (1988). The cellular neurobiology of neuronal development: the cerebellar granule cell. *Brain Res. Rev.*, **13**, 77–101.

BURGOYNE, R.D., PEARCE, I.A. & CAMBRAY-DEAKIN, M. (1988). N-methyl-D-aspartate raises cytosolic calcium concentration in rat cerebellar granule cells in culture. *Neurosci. Lett.*, **91**, 47–52.

CARBONI, E. & WOJCIK, W.J. (1988). Dihydropyridine binding sites regulate calcium influx through specific voltage-sensitive calcium channels in cerebellar granule cells. *J. Neurochem.*, **50**, 1279–1286.

CHALLISS, R.A.J., CHILVERS, E.R., WILLCOCKS, A.L. & NAHORSKI, S.R. (1990). Heterogeneity of [^{3}H]inositol 1,4,5-trisphosphate binding sites in adrenal cortical membranes. *Biochem. J.*, **265**, 421–427.

CHEEK, T.R., O'SULLIVAN, A.J., MORETON, R.B., BERRIDGE, M.J. & BURGOYNE, R.D. (1989). Spatial localisation of the stimulus-induced rise in cytosolic Ca^{2+} in bovine adrenal chromaffin cells: distinct nicotinic and muscarinic patterns. *FEBS Lett.*, **247**, 429–434.

CHUANG, D.-M. (1989). Neurotransmitter receptors and phosphoinositide turnover. *Annu. Rev. Pharmacol. Toxicol.*, **29**, 71–110.

CIARDO, A. & MELDOLESI, J. (1991). Regulation of intracellular calcium in cerebellar granule neurons: Effects of depolarization and of glutamatergic and cholinergic stimulation. *J. Neurochem.*, **56**, 184–191.

COURTNEY, M.J., LAMBERT, J.J. & NICHOLLS, D.G. (1990). The interactions between plasma membrane depolarization and glutamate receptor activation in the regulation of cytoplasmic free calcium in cultured cerebellar granule cells. *J. Neurosci.*, **10**, 3873–3879.

DELEAN, A., MUNSON, P.J. & RODBARD, D. (1978). Simultaneous analysis of families of sigmoidal curves, application to bioassay, radiological assay and physiological dose-response curves. *Am. J. Physiol.*, **235**, E97–E108.

FURIUCHI, T., YOSHIKAWA, S., MIYAWAKI, A., WADA, K., MAEDA, N. & MIKOSHIBA, K. (1989). Primary structure and functional expression of the inositol 1,4,5-trisphosphate binding protein P_{400}. *Nature*, **342**, 32–38.

FURIUCHI, T., SHIOTA, C. & MIKOSHIBA, K. (1990). Distribution of inositol 1,4,5-trisphosphate receptor mRNA in mouse tissues. *FEBS Lett.*, **267**, 85–88.

GALLO, V., CIOTTI, M.T., COLETTI, A., ALOISI, F. & LEVI, G. (1982). Selective release of glutamate from cerebellar granule cells differentiated in culture. *Proc. Natl. Acad. Sci. U.S.A.*, **79**, 7919–7923.

GALLO, V., KINGSBURY, A.E., BALAZS, R. & JORGENSEN, O.S. (1987). The role of depolarization in the survival and differentiation of the cerebellar granule cell in culture. *J. Neurosci.*, **7**, 203–213.

GALLO, V., GIOVANNINI, C. & LEVI, G. (1990). Modulation of non-N-

methyl-D-aspartate receptors in cultured cerebellar granule cells. *J. Neurochem.*, **54**, 1619–1625.

GUILLEMETTE, G., LAMONTAGE, S., BOULAY, G. & MOUILLAC, B. (1989). Differential effects of heparin on inositol 1,4,5-trisphosphate binding, metabolism and calcium release activity in the bovine adrenal cortex. *Mol. Pharmacol.*, **35**, 339–344.

HOLOPAINEN, I., ENKVIST, M.O.K. & AKERMAN, K.E.O. (1989). Glutamate receptor agonists increase intracellular Ca^{2+} independently of voltage-gated Ca^{2+} channels in rat cerebellar granule cells. *Neurosci. Lett.*, **98**, 57–62.

HYNIE, S., WROBLEWSKI, J.T. & COSTA, E. (1989). Profile of phosphatidyl-inositol metabolism stimulated by carbachol and glutamate in primary cultures of rat cerebellar neurons. *Neuropharmacology*, **28**, 1309–1315.

IRVING, A.J., SCHOFIELD, J.G., WATKINS, J.C., SUNTER, D.C. & COLLINGRIDGE, G.L. (1990). 1S, 3R-ACPD stimulates and L-AP3 blocks Ca^{2+} mobilization in rat cerebellar neurons. *Eur. J. Pharmacol.*, **186**, 363–365.

JOSEPH, S.K. & RICE, H.L. (1989). The relationship between inositol trisphosphate receptor density and calcium release in brain microsomes. *Mol. Pharmacol.*, **35**, 355–359.

JOSEPH, S.K., RICE, H.L. & WILLIAMSON, J.R. (1989). The effect of external calcium and pH in inositol trisphosphate-mediated calcium release from cerebellum microsomal fractions. *Biochem. J.*, **258**, 261–265.

KINGSBURY, A.E. & BALAZS, R. (1987). Effect of calcium agonists and antagonists on cerebellar granule cells. *Eur. J. Pharmacol.*, **140**, 275–283.

KINGSBURY, A.E., GALLO, V., WOODHAMS, P.L. & BALAZS, R. (1985). Survival, morphology and adhesion properties of cerebellar interneurones cultured in chemically defined and serum supplemented medium. *Dev. Brain Res.*, **17**, 17–25.

LEVI, G., PATRIZIO, M. & GALLO, V. (1991). Release of endogenous and newly synthesized glutamate and other amino acids induced by non-N-methyl-D-aspartate receptor activation in cerebellar granule cell cultures. *J. Neurochem.*, **56**, 199–206.

LIN, W.-W., LEE, C.Y. & CHUANG, D.-M. (1990a). Comparative studies of phosphoinositide hydrolysis induced by endothelin-related peptides in cultured cerebellar astrocytes, C_6-glioma and cerebellar granule cells. *Biochem. Biophys. Res. Commun.*, **168**, 512–519.

LIN, W.-W., LEE, C.Y. & CHUANG, D.-M. (1990b). Endothelin-1 stimulates the release of preloaded [^{3}H]D-aspartate from cultured cerebellar granule cells. *Biochem. Biophys. Res. Commun.*, **167**, 593–599.

MAEDA, N., NIINOBE, M. & MIKOSHIBA, K. (1990). A cerebellar Purkinje cell marker P_{400} protein is an inositol 1,4,5-trisphosphate receptor protein. Purification and characterization of $InsP_3$ receptor complex. *EMBO J.*, **9**, 61–67.

MIGNERY, G.A., SUDHOF, T.C., TAKEI, K. & DE CAMILLI, P. (1989). Putative receptor for inositol 1,4,5-trisphosphate similar to ryanodine receptor. *Nature*, **342**, 192–195.

NAHORSKI, S.R. (1988). Inositol polyphosphates and neuronal calcium homeostasis. *Trends Neurosci.*, **11**, 444–448.

NAHORSKI, S.R. & POTTER, B.V.L. (1989). Molecular recognition of inositol polyphosphates by intracellular receptors and metabolic enzymes. *Trends Pharmacol. Sci.*, **10**, 139–144.

NICOLETTI, F., WROBLEWSKI, J.T., NOVELLI, A., ALHO, H., GUIDOTTI, A. & COSTA, E. (1986). The activation of inositol phospholipid metabolism as a signal transduction system for excitatory amino acids in primary cultures of cerebellar granule cells. *J. Neurosci.*, **6**, 1905–1911.

O'SULLIVAN, A.J., CHEEK, T.R., MORETON, R.B., BERRIDGE, M.J. & BURGOYNE, R.D. (1989). Localisation and heterogeneity of agonist-induced changes in cytosolic Ca^{2+} concentration in single bovine adrenal chromaffin cells from video imaging of fura-2. *EMBO J.*, **8**, 401–411.

ROSS, C.A., MELDOLESI, J., MILNER, J.A., SATOH, T., SUPATTAPONE, S. & SNYDER, S.H. (1989). Inositol 1,4,5-trisphosphate receptor localized to endoplasmic reticulum in cerebellar Purkinje neurons. *Nature*, **339**, 468–470.

STAUDERMAN, K.A., HARRIS, G.D. & LOVENBERG, W. (1988). Characterization of inositol 1,4,5-trisphosphate-stimulated calcium release from rat cerebellar microsomal fractions. *Biochem. J.*, **255**, 677–683.

STRUPISH, J., COOKE, A.M., POTTER, B.V.L., GIGG, R. & NAHORSKI, S.R. (1988). Stereospecific mobilization of intracellular Ca^{2+} by inositol 1,4,5-trisphosphate. *Biochem. J.*, **253**, 901–905.

SUPATTAPONE, S., WORLEY, P.F., BARABAN, J.M. & SNYDER, S.H. (1988). Solubilization, purification and characterization of an inositol trisphosphate receptor. *J. Biol. Chem.*, **263**, 1530–1534.

THAYER, S.A., PERNEY, T.M. & MILLER, R.J. (1988). Regulation of calcium homeostasis in sensory neurons by bradykinin. *J. Neurosci.*, **8**, 4089–4097.

WHITHAM, E.M., CHALLISS, R.A.J. & NAHORSKI, S.R. (1991). M_3 muscarinic cholinoceptors are linked to phosphoinositide metabolism in rat cerebellar granule cells. *Eur. J. Pharmacol.*, **206**, 181–189.

WILLCOCKS, A.L., COOKE, A.M., POTTER, B.V.L. & NAHORSKI, S.R. (1987). Stereospecific recognition sites for [^{3}H]inositol 1,4,5-trisphosphate in particulate preparations of rat cerebellum. *Biochem. Biophys. Res. Commun.*, **146**, 1071–1078.

WORLEY, P.F., BARABAN, J.M., SUPATTAPONE, S., WILSON, V.S. & SNYDER, S.H. (1987a). Characterization of inositol trisphosphate receptor binding in brain. *J. Biol. Chem.*, **262**, 12132–12136.

WORLEY, P.F., BARABAN, J.M., COLVIN, J.S. & SNYDER, S.H. (1987b). Inositol trisphosphate receptor localization in brain: variable stoichiometry with protein kinase C. *Nature*, **325**, 159–161.

WORLEY, P.F., BARABAN, J.M. & SNYDER, S.H. (1989). Inositol 1,4,5-trisphosphate receptor binding: autoradiographic localization in rat brain. *J. Neurosci.*, **9**, 339–346.

WROBLEWSKI, J.T., NICOLETTI, F. & COSTA, E. (1985). Different coupling of excitatory amino acid receptors with Ca^{2+} channels in primary cultures of cerebellar granule cells. *Neuropharmacology*, **24**, 919–921.

XU, Y. & CHUANG, D.-M. (1987). Serotonergic, adrenergic and histaminergic receptors coupled to phospholipase C in cultured cerebellar granule cells of rats. *Biochem. Pharmacol.*, **36**, 2353–2358.

(Received March 7, 1991
Revised May 7, 1991
Accepted May 13, 1991)

Br. J. Pharmacol. (1991), **104**, 207–221

Structure-activity analysis of binding kinetics for NMDA receptor competitive antagonists: the influence of conformational restriction

Morris Benveniste & [1]Mark L. Mayer

Section of Neurophysiology and Biophysics, Laboratory of Developmental Neurobiology, NICHD, Building 36, Room 2A21, National Institutes of Health, Bethesda, Maryland 20892, U.S.A.

1 The kinetics of action of 17 structurally related NMDA receptor competitive antagonists were measured under voltage clamp in mouse hippocampal neurones. Analysis of the response to rapid changes in antagonist concentration during constant application of agonist was used to estimate microscopic association (k_{on}) and dissociation (k_{off}) rate constants for antagonist binding, assuming a two-equivalent site model for competitive antagonism. Dose-inhibition curves were analysed to estimate antagonist equilibrium dissociation constants.

2 For a series of 11 ω-phosphono, α-amino acids k_{on} and k_{off} varied 26 and 107 fold respectively. Rapid association and dissociation rate constants were obtained for flexible antagonist molecules such as D-2-amino-7-phosphonoheptanoic acid (D-AP7): k_{on} $1.4 \times 10^7\,M^{-1}s^{-1}$; k_{off} $20.3\,s^{-1}$. For conformationally restrained molecules such as **3S,4aR,6S,8aR**-6-phosphonomethyl-decahydroisoquinoline-3-carboxylic acid (LY 235959), association and dissociation rate constants were much slower: k_{on} $1.1 \times 10^6\,M^{-1}s^{-1}$; k_{off} $0.2\,s^{-1}$. For the D- and L-isomers of 3-(2-carboxypiperazin-4-yl)-propyl-1-phosphonic acid (CPP) estimates for k_{on} were similar, but for the L-isomer k_{off} was 10 fold faster than for the D-isomer.

3 For 2-amino-5-phosphonopentanoic acid (AP5) and its piperidine derivative *cis*-4-(phosphonomethyl) piperidine-2-carboxylic acid (CGS 19755), an increase in chain length of two methylene groups between the ω-phosphono and α-carboxylate moieties caused a 1.6 to 1.8 fold decrease in k_{on} with little change in k_{off}. In contrast, for AP5, CPP and its ω-carboxylate analogue, addition of a double bond close to the phosphonate moiety caused a 1.3 to 1.6 fold increase in k_{on}.

4 For antagonists with an ω-tetrazole moiety, k_{on} and k_{off} were 2.8–4.6 times faster than for the parent ω-phosphono compounds. A similar, but smaller increase in k_{on} and k_{off} was observed for antagonists with an ω-carboxylate moiety.

5 The slow kinetics of action of potent NMDA receptor antagonists were not an artefact of buffered diffusion. In neurones equilibrated with 200 μM D-AP7, 2 μM LY 235959 and 10 μM NMDA, a transient agonist response was recorded following a rapid switch to D-AP7-free solution. This can only be explained by differences in the binding kinetics of AP7 and LY 235959, since at equilibrium, with these concentrations, either antagonist essentially eliminates the agonist response to 10 μM NMDA.

6 For all antagonists studied, the ratio k_{off}/k_{on} was consistent with equilibrium K_i values obtained under similar experimental conditions, over a 40 fold range of potency. Comparison of these values with K_i estimates determined from both agonist ([^{3}H]-glutamate), and antagonist ([^{3}H]-CGS 19755 and [^{3}H]-CPP) radioligand competition studies revealed good correlation between data from voltage clamp and binding experiments. However, K_i values obtained in antagonist binding assays showed on average 6.5 fold higher affinity than those obtained in voltage clamp experiments; in contrast K_i values obtained in agonist binding assays showed only 1.4 fold higher affinity.

7 The insights gained from our experiments may be of use for predicting the structural features required to generate more potent NMDA receptor antagonists, and suggest that novel acyclic compounds will have greater potential for high potency than derivatives of conformationally rigid compounds with piperazine, piperidine or bicyclic ring structures.

Keywords: NMDA receptor; glutamate; kinetics, antagonist, dose-response analysis; structure-activity relationship; AP5, CPP

Introduction

Activation of N-methyl-D-aspartic acid (NMDA) receptors has been implicated in the mechanism for cell death due to hypoxia (Simon *et al.*, 1984; Choi, 1990) and in the generation of epileptic seizures (Meldrum *et al.*, 1989). The therapeutic potential of antagonists which block activation of NMDA receptors by glutamate, and by related excitatory neurotransmitters, has stimulated an extensive effort to identify novel drugs acting at this subtype of CNS glutamate receptor. This has resulted in the availability of a large number of compounds, of diverse but related structure, all of which competitively displace glutamate from the excitatory amino acid recognition site on the NMDA receptor channel complex (Collingridge & Lester, 1989). The majority of new NMDA receptor antagonists are derivatives of 2-amino-5-phosphonopentanoic acid (AP5) or 2-amino-7-phosphonoheptanoic acid (AP7) of increased potency in which the addition of ring structures, or double bonds, introduces conformational restriction of the α-amino and α- and ω-acidic groups required for NMDA receptor antagonist action. If antagonist binding is diffusion limited, the increase in equilibrium potency of conformationally restricted ligands should reflect stabilization of the receptor-antagonist complex, and a reduction in the antagonist dissociation rate constant. However, analysis with radioligand competition studies reveals that compounds with strikingly different structures, such as **3S,4aR,6S,8aR**-6-phosphonomethyl-decahydroisoquinoline-3-carboxylic acid (LY 235959, the active enantiomer of LY 274614, Ornstein *et al.*, 1991) and (E)-2-amino-4-methyl-5-phosphono-3-pentenoic acid (CGP 37849, Fagg *et al.*, 1990), can have similar equilibrium affinities for NMDA

[1] Author for correspondence.

receptors, while other compounds with similar structures, such as *cis*-4-(phosphonomethyl)piperidine-2-carboxylic acid (CGS 19755, Murphy *et al.*, 1988; Hutchison *et al.*, 1989) and 3-(2-carboxypiperazin-4-yl)-methyl-1-phosphonic acid (CMP), can have substantially different equilibrium affinities (Hays *et al.*, 1990). In view of this, we have performed a structure-activity analysis for a large series of NMDA receptor antagonists with the aim of determining how conformational restriction influences the kinetics of binding of antagonists.

The approach chosen, concentration jump analysis of antagonist binding kinetics assayed by voltage clamp recording from hippocampal neurones, has not been used previously for this type of investigation. In contrast to conventional equilibrium measurments of antagonist action, a kinetic analysis provides insight into the molecular features which determine both the rate constants of association (k_{on}) and dissociation (k_{off}) of antagonists from NMDA receptors. Using this approach, we have been able to characterize the effects of different functional groups, conformational restriction, and chain length on the kinetics of antagonist binding and dissociation.

Methods

Culture conditions and electrophysiology

Neurones were isolated from a dissection of E16-E18 C57B1/6 mouse hippocampi and plated on a confluent glial cell feeder layer grown from a dissection of P1 mouse hippocampus as previously described (Mayer *et al.*, 1989b). Experiments were generally performed 10–14 days after neurones were plated. The conditions for electrophysiological experiments involving rapid application and removal of NMDA receptor ligands have been described in detail previously (Benveniste *et al.*, 1990; Vyklicky *et al.*, 1990; Benveniste & Mayer, 1991). Briefly, neurones were voltage clamped by use of the whole cell patch clamp technique and an Axoclamp 2 amplifier (Axon Instruments) operating in switch clamp mode at a frequency of approximately 10 kHz. The holding potential was −60 mV unless specified differently. Experiments were performed at 24–27°C.

The extracellular solution consisted of (in mM): NaCl 160, KCl 2.5, $CaCl_2$ 2, $MgCl_2$ 1, glucose 10, HEPES 10, phenol red 10 $\mu g\,ml^{-1}$; adjusted to pH 7.3 and 325 mOsm. Tetrodotoxin 400 nM and bicuculline methochloride 5 μM were added to block sodium currents and inhibitory postsynaptic currents. The intracellular solution consisted of (in mM): $CsMeSO_3$ 125, CsCl 15, $CaCl_2$ 0.5, $MgCl_2$ 3, Cs_4BAPTA 5; either MgATP or Na_2ATP 2; adjusted to pH 7.2 and 305 mOsm. Agonist and antagonist solutions were similar to control extracellular solution but contained only 0.2 mM Ca and lacked Mg. Glycine was present at 3 μM for all experiments, and except where noted, NMDA was applied at 10 μM. These conditions essentially block desensitization of NMDA receptor responses (Mayer *et al.*, 1989a). Agonists and antagonists were applied to the neuronal soma and surrounding dendrites by a concentration jump technique, using a series of nine 'flowpipe' tubes, each 356 μm internal diameter, positioned approximately 100 μm from the soma. Rapid solution changes were achieved with solenoid valves, by redirecting the flow between two adjacent flowpipe barrels containing different solutions after a stepper motor had moved the desired barrel into position above the cell; only one solution flowed at any time. Previously, we have shown that with this technique the time constant for solution exchange during whole cell recording was approximately 10 ms or less (Vyklicky *et al.*, 1990).

Analysis

Antagonist association and dissociation rate constants (k_{on} and k_{off}, respectively) were determined from an iterative non-linear least squares fit of a two equivalent site model for competitive antagonism to the time-dependent response recorded following rapid application and removal of antagonists, as described previously (Benveniste & Mayer, 1991). The apparent association and dissociation rate constants for NMDA, which were required for the analysis of antagonist kinetics were previously determined to be 2.1 $\mu M^{-1} s^{-1}$ and 22.9 s^{-1}, respectively (Benveniste & Mayer, 1991). Analysis of antagonist rate constants were generally performed for two antagonist concentrations which evoked approximately 80 and 95% inhibition of the response to 10 μM NMDA, and the results pooled. The state diagram for competitive antagonism at NMDA receptors according to this scheme assumes that each of the agonist recognition sites which must be occupied by NMDA to activate ion channel gating (Patneau & Mayer, 1990) can alternatively bind an antagonist molecule, and is summarized below, where R represents the NMDA receptor, A the agonist and B the competitive antagonist, and k_{Aon} and k_{Aoff} the microscopic association and dissociation rate constants for agonist binding:

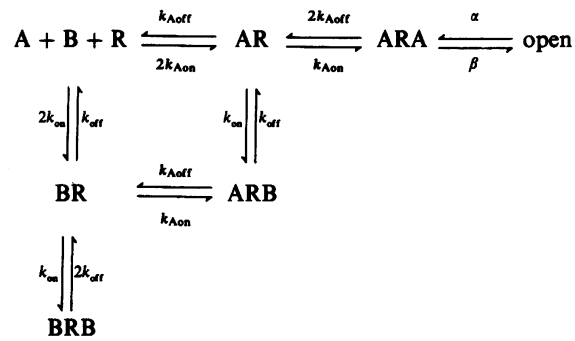

For each antagonist studied, the equilibrium microscopic dissociation constant (K_i) was determined in two ways: (1) from the ratio k_{off}/k_{on} as determined from kinetic measurements; and (2) from analysis of equilibrium dose-inhibition curves recorded with 5 concentrations of antagonist in the presence of 10 μM NMDA, and fit by non-linear regression to a 2 binding site inhibition isotherm:

$$\% \text{ of control} = \frac{100}{\left(1 + \frac{[B]}{K_0}\right)^2} \quad (1)$$

where K_0 is defined as the concentration of antagonist which displaces half of the agonist molecules occupying agonist binding sites. K_i values were then determined from the Cheng–Prusoff equation (Cheng & Prusoff, 1973):

$$K_i = \frac{K_0}{1 + \frac{[A]}{K_d}} \quad (2)$$

where K_d is the apparent microscopic equilibrium dissociation constant for binding of agonist (A), determined to be 11.0 μM from the ratio of k_{off}/k_{on} for NMDA given above.

Only 9/17 of the antagonists studied were optically resolved; however, from binding studies with the optical isomers of AP5, 4-(3-phosphonoprop-2-E-en-1-yl)piperazine-2-carboxylic acid (CPP-ene), CPP and CGP 37849 (Aebischer *et al.*, 1988; Olverman *et al.*, 1988; Fagg *et al.*, 1990), and from physiological studies with AP5, CPP-ene, and CPP (Davies & Watkins, 1982; Aebischer *et al.*, 1988), it is known that potent NMDA receptor antagonist activity occurs selectively for the D-isomers. Thus, for the analysis of k_{on} and K_i values for racemic compounds (indicated by an asterisk in Tables 1–5), a 2 fold correction was made assuming the L-isomers to be inactive. For one compound, 2-amino-4,5-(1,2-cyclohexyl)-7-phosphonoheptanoic acid (NPC 12626, Ferkany *et al.*, 1989), this correction was not justifiable, since the antagonist used was a mixture of 8 isomers, of unknown relative potency; in this case only a preliminary estimate was obtained for k_{off}, and no attempt was made to calculate k_{on} or K_i.

Voltage-dependence of the kinetics of antagonist block was analysed according to the equation:

$$k = k'e^{(V_m/H)} \quad (3)$$

where k represents the value of k_{on} or k_{off} at a given membrane potential V_m, k' is the rate constant at a membrane potential of 0 mV and H is the shift in membrane potential required to cause an e-fold change in the value of k.

All LY antagonists were a gift from Dr P. Ornstein; D- and L-CPP were provided by Professor J.C. Watkins; Dr P. Herrling provided D-CMP, D-CPP-ene and D-CPC-ene; Drs C. Angst and G. Fagg provided *trans*-APPA and CGP 37849; CGS 19755 was provided by Dr D. Bennett; CPC was supplied by Dr G. Johnson; Drs S. Borosky and Dr J. Ferkany supplied NPC 12626; all other antagonists were purchased from Tocris Neuramin (Essex). $CsMeSO_3$ was purchased from Aldrich.

Results

Agonist responses show complex kinetics in the presence of competitive antagonists

In the presence of 3 μM glycine, with a low extracellular concentration of calcium, the response to concentration jump application of NMDA shows rapid on-off kinetics, with little evidence of desensitization (Mayer *et al.*, 1989a). However, in the presence of competitive NMDA receptor antagonists, at concentrations chosen to give similar amounts of inhibition at equilibrium, the response to NMDA shows complex kinetics, which vary with the relative timing of the application of agonist and antagonist, and are different for individual antagonists.

Figure 1 illustrates the action of 17 μM D-AP7 and 1.5 μM of its piperidine analogue, *cis*-4-(3-phosphonoprop-1-yl) piperidine-2-carboxylic acid (LY 257883, Ornstein *et al.*, 1989), which at equilibrium reduced the current activated by 100 μM NMDA to 30% and 45% of control, respectively. Simultaneous application of D-AP7 and NMDA yielded an initial transient response to 43% of control, followed by a rapid decrease in inward current such that equilibrium block was achieved within 200 ms (Figure 1a, left). In contrast, the analogous experiment with LY 257883 (Figure 1a, right) yielded an initial transient response to 97% of control, and equilibrium block was achieved only 3.3 s after the start of the application of agonist and antagonist.

When the same antagonists were applied prior to the application of agonist, the response to NMDA showed strikingly different kinetics. In the presence of D-AP7 the response to NMDA reached equilibrium within 200 ms, but without any initial transient response (Figure 1b, left). In contrast, in the presence of LY 257883 the initial rapid response to NMDA (which reached only 17% of the control response recorded in the absence of antagonist) was followed by a slow increase in inward current and equilibrium block (at 45% of the control response) was not reached until 3.2 s after the start of the application of NMDA (Figure 1b, right). Similar complex responses were recorded for all of the antagonists studied, but the kinetics varied widely with individual drugs.

The time-dependent responses to NMDA recorded in the presence of D-AP7 and LY 257883 could in principle arise from a variety of mechanisms. In particular, decay of the initial transient response which was recorded during simultaneous application of agonist and antagonist could have arisen from ion channel block or enhanced desensitization. Kinetic evidence for competition between NMDA and LY 257883, illustrated in Figure 1c, eliminates the latter possibility. The simultaneous application of 30 μM LY 257883 and 100 μM NMDA yielded an initial transient response similar to that observed with lower concentrations of antagonist, but with faster kinetics. After equilibrium block was achieved the concentration of NMDA was increased from 100 μM to 1 mM (Figure 1c); this evoked a slow increase in inward current with similar kinetics to responses recorded when NMDA was applied following preincubation with LY 257883 alone (Figure 1b). The 25 fold increase in response recorded on increasing the concentration of NMDA from 100 μM to 1 mM can only arise from competition between LY 257883 and NMDA, since it is unlikely that increasing the concentration of agonist would decrease desensitization. In the absence of antagonist the increase in agonist response expected for these concentrations of NMDA, calculated using the logistic equation, with an EC_{50} for NMDA of 35 μM, n = 1.4 (Patneau & Mayer, 1990), is only 1.2 fold.

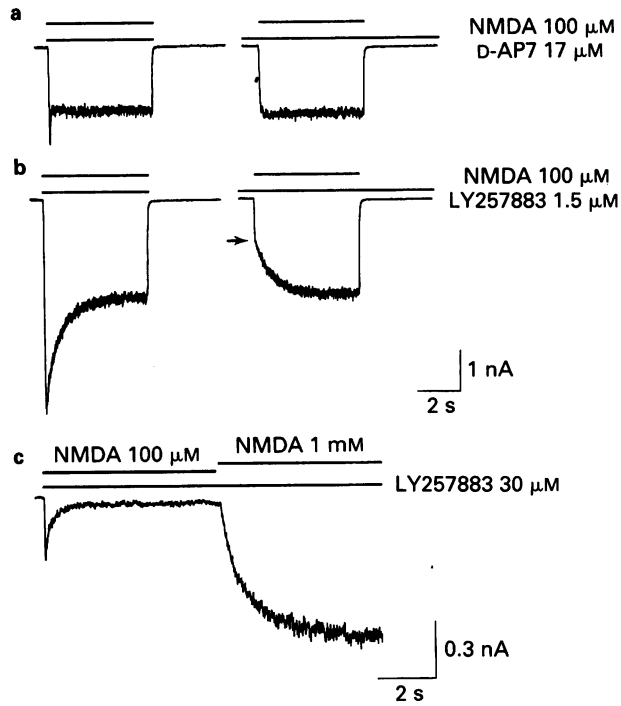

Figure 1 Responses to NMDA show complex kinetics in the presence of competitive antagonists. (a) and (b) show inward current responses to 100 μM NMDA (upper bar) recorded in the presence of (a) 17 μM D-AP7 and (b) 1.5 μM LY 257883 (lower bar); traces are from the same neurone at a holding potential of −60 mV. Antagonist doses were chosen to be approximately equipotent at equilibrium. Responses on the left were recorded when agonist and antagonist were applied simultaneously; responses on the right were recorded following a 15 s preincubation with antagonist applied alone, and in the case of LY 257883 show an initial fast component (arrow), followed by a slow inward relaxation. (c) shows that following activation and block of NMDA receptors in response to 100 μM NMDA and 30 μM LY 257883 applied simultaneously, an increase in the concentration of NMDA from 0.1 to 1 mM also produces a slow inward relaxation, without any initial fast component, but of similar time course to the inward and outward relaxations shown in (b).

The results illustrated in Figure 1a–c are entirely consistent with the competitive nature of the NMDA receptor antagonist action of ω-phosphono α-amino acids (Evans *et al.*, 1982; Harrison & Simmonds, 1985; Verdoorn *et al.*, 1989), but suggest that the kinetics of binding and dissociation for individual antagonists can vary widely. Because these antagonists have the same α-carboxylate, α-amino and ω-phosphono functional groups, it seemed possible that the kinetic differences observed in our experiments might be related to the molecular arrangement of these substituents in individual antagonists. In subsequent experiments, we measured directly the association and dissociation rate constants for a series of structurally related competitive NMDA receptor antagonists, by recording the response to application and removal of antagonists in the continuous presence of 10 μM NMDA and 3 μM glycine (e.g. Figure 2a).

Effects of conformational restriction on the kinetics of AP5-derived phosphonate antagonists

Two series of competitive NMDA receptor antagonists have been developed, by use of AP5 and AP7 as starting templates (e.g. Olverman *et al.*, 1988). In AP5 analogues, the α-carboxylate and the ω-phosphonate groups are separated by 4 carbon atoms; thus, AP5 and its derivatives will be denoted 4-atom separation analogues. For this series of antagonists, structures progress from a flexible acyclic molecule, AP5, through the conformationally restrained, but acyclic, antagonist (E)-2-amino-5-phosphono-3-pentenoic acid (*trans*-APPA, Fagg *et al.*, 1990) and its 4-methyl derivative, CGP 37849, to a cyclic derivative based on a piperidine nucleus (CGS 19755). Figure 2b shows an example of the kinetics of responses for AP5 and the above derivatives, plotted on the same time scale, and fit with a two-equivalent site model for competitive antagonism (Benveniste & Mayer, 1991). Although the concentrations of antagonist used produced similar degrees of inhibition of the NMDA evoked response (88 to 95%), the rate of onset of and recovery from block was much faster for AP5 and *trans*-APPA than for CGP 37849 and CGS 19755.

Equilibrium dose-inhibition relationships were also obtained for the above series of 4-atom separation phosphonate antagonists (Figure 3). CGP 37849 was the most potent 4-atom separation analogue, with a K_i value of 160 nM; *trans*-APPA, with a K_i of 440 nM is only slightly less potent than CGP 37849 (in agreement with radioligand competition studies, Fagg *et al.*, 1990) but exhibits strikingly different kinetics. Although CGS 19755 is more structurally constrained than CGP 37849, it is less potent, reflecting both a slower forward rate constant for binding of CGS 19755 to NMDA receptors, and once bound, faster dissociation of CGS 19755 than measured for CGP 37849 (Table 1). Comparison of equilibrium K_i values determined as shown in Figure 3 with those determined from the ratio of k_{off}/k_{on} yielded a maximum discrepancy of 2.8 fold.

The summary of these experiments (Table 1) suggests that increasing restriction of conformational flexibility reduces both k_{on} and k_{off}. Compared to D-AP5, the piperidine analogue CGS 19755 has a 3.2 fold slower association rate constant, and exhibits an 11.4 fold decrease in k_{off}. It is of interest that addition of a double bond at the 3 position of D-AP5, as in the case of *trans*-APPA, also reduces k_{off} by 4.9 fold, but actually increases k_{on}. Addition of a methyl group to the 4 position of *trans*-APPA, to form CGP 37849, causes a 1.7 fold lowering of k_{on} and a dramatic, 17.6 fold decrease in k_{off}; the latter effect accounts for the high potency of CGP 37849 relative to AP5.

Effects of conformational restriction on the kinetics of AP7-derived phosphonate antagonists

An analogous series of acyclic antagonist structures based on AP7, similar to *trans*-APPA and CGP 37849, has not been developed. However, a large number of AP7 derivatives, denoted 6-atom separation analogues, and which form a distinct structural series (Table 2), was available for analysis. Figure 4 shows examples of the kinetics of action of AP7 and two cyclic derivatives, plotted on the same time scale, and fit with a two-equivalent site model for competitive antagonism. Similar experiments were performed for D-CPP and D-CPP-ene. Although the concentrations of antagonists used for these experiments produced similar degrees of inhibition of the NMDA-evoked response, differences in the rates of onset and recovery from block were even more dramatic than observed for AP5 derivatives. From Figure 4, it is evident that the dissociation rate decreases 18.5 and 102 fold when the flexible acyclic antagonist, D-AP7, is compared to an analogue con-

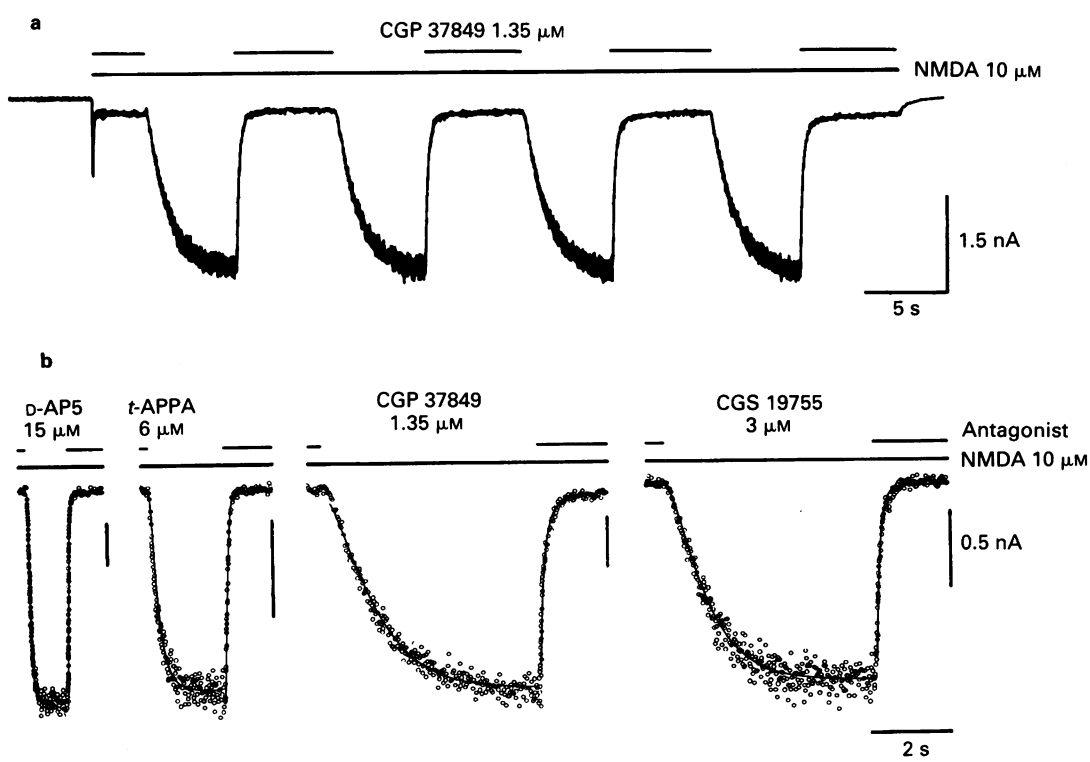

Figure 2 Kinetic analysis of NMDA receptor block by AP5 and some derivatives. The chart record in (a) shows an example of the protocol used for application of agonist and antagonist. NMDA, 10 μM, was present continuously (lower bar); 1.35 μM CGP 37849 was applied 5 times (upper bars). An increase in inward current occurred on removal of antagonist; the kinetics of onset of antagonism were recorded on return to a solution containing both NMDA and CGP 37849. Segments of records like this were digitized for further analysis. (b) Membrane current responses to 15 μM D-AP5, 6 μM *trans*-APPA, 1.35 μM CGP 37849 and 3 μM CGS 19755, recorded as described in (a). Solid lines represent a non-linear least squares fit of the response to concentration jump application of antagonists to a two equivalent site model for competitive antagonism.

Table 1 Effect of increasing conformational restriction for ω-phosphonates with 4 atom separation

	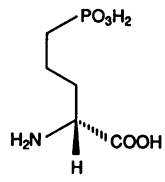 D-AP5	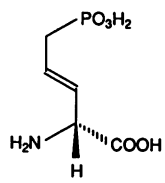 trans-APPA*	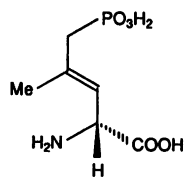 CGP 37849*	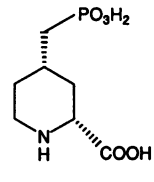 CGS 19755*
k_{on} $\mu M^{-1} s^{-1}$	22.2 ± 6.5	29.7 ± 14.3	13.0 ± 3.6	7.0 ± 2.3
k_{off} s^{-1}	19.4 ± 4.1	4.0 ± 1.3	1.1 ± 0.2	1.7 ± 0.2
k_{off}/k_{on} μM	0.92 ± 0.23	0.16 ± 0.08	0.10 ± 0.03	0.28 ± 0.13
K_i μM	1.93 ± 0.57	0.44 ± 0.14	0.16 ± 0.02	0.34 ± 0.08

Values are given as mean ± s.d. Association and dissociation rate constants were determined by kinetic analysis; K_i values were determined from equilibrium measurements with 10 μM NMDA as described in Methods.
* Indicates correction was made for a racemic mixture of 2 isomers, one of which was assumed to have negligible activity.

strained by one (LY 257883) or two rings (LY 235959). Another AP7 analogue, 2-amino-4,5-(1,2-cyclohexyl)-7-phosphonoheptanoic acid (NPC 12626), in which a cyclohexyl ring constrains rotational mobility of methylene groups at positions 4–5 in the backbone of AP7 but which leaves the α- and ω-binding groups attached to the ring via flexible methylene bridges, yielded a dissociation rate constant of 1.7 s^{-1}, similar to that obtained for LY 257883. This provides further evidence that severe conformational restriction in LY 235959 underlies the unusually slow binding kinetics observed for this compound.

Equilibrium dose-inhibition relationships were also obtained for the series of 6-atom separation phosphonate antagonists, and analysed using a two-site model (Figure 5). The potency sequence for the 6-atom analogues is LY 235959 > D-CPP-ene > LY 257883 ≈ D-CPP > D-AP7 (Table 2). Although there is a greater than 100 fold difference in the dissociation rate constants for D-AP7 and LY 235959, equilibrium measurements reveal only a 24 fold increase in potency. Indeed, equilibrium measurements highlight the modest increase in potency achieved by further conformational restriction of antagonists which already contain a ring, such as LY 257883 and D-CPP. For example, introduction of a cyclohexyl ring into LY 257883, to produce the bicyclic compound LY 235959, increases equilibrium potency only 2.1 times, whereas introduction of a piperazine or piperidine ring into AP7 produces a greater than 11 fold increase in potency (Table 2). Comparison of equilibrium K_i values for the series of 6-atom separation compounds shown in Table 2, with those determined from the ratio of k_{off}/k_{on} yielded a maximum discrepancy of 2.7 fold.

The above experiments with 4- and 6-atom separation analogues suggests that restriction of molecular flexibility, via the introduction of cyclic structures which constrain mobility of the α-carboxylate, α-amino and ω-phosphono groups required for potent NMDA receptor antagonist activity decreases both the association rate constant (lowering antagonist potency) and the dissociation rate constant (increasing antagonist potency). The relative balance of these effects determines the degree to which more potent antagonists evolve as a result of structural modification of parent compounds like AP5 and AP7.

A different strategy for conformational restriction is the introduction of unsaturated bonds, as in *trans*-APPA, CGP 37849 and D-CPP-ene. In the 4-atom separation examples

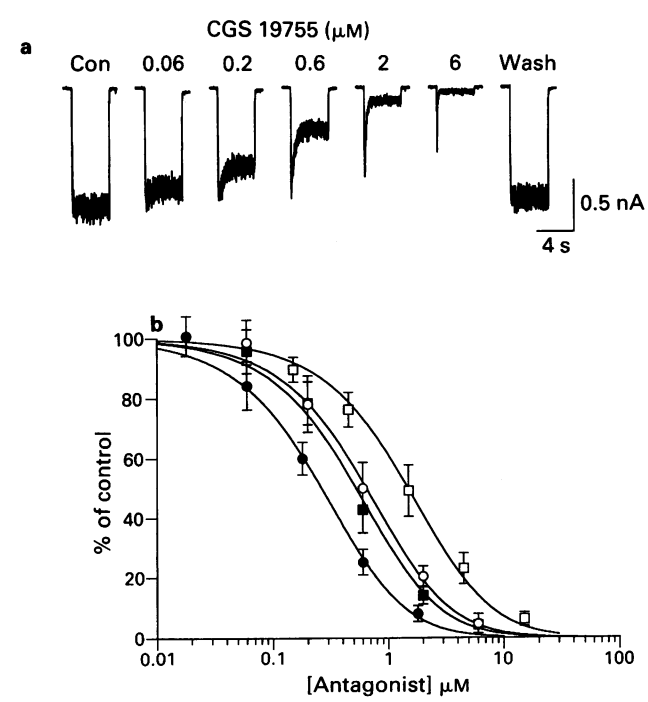

Figure 3 Equilibrium dose response analysis for NMDA receptor block by AP5 and some derivatives. (a) Responses to concentration jump application of 10 μM NMDA, applied together with the indicated concentrations of CGS 19755; 3 μM glycine was present continuously. Initially the response to NMDA overshoots its final value, because the onset of antagonism by CGS 19755 is slow to reach equilibrium. (b) Dose-response analysis for 4 antagonists. Smooth curves were obtained by non-linear regression using the equation for a two-binding site isotherm. K_0 values (in μM) are: 0.60 ± 0.06 for CGP 37849 (●), 1.29 ± 0.30 for CGS 19755 (■), 1.68 ± 0.54 for *trans*-APPA (○), and 3.68 ± 1.08 for D-AP5 (□). Data points are mean of 46–73 observations recorded from 4–6 cells for each antagonist. Error bars depict standard deviation.

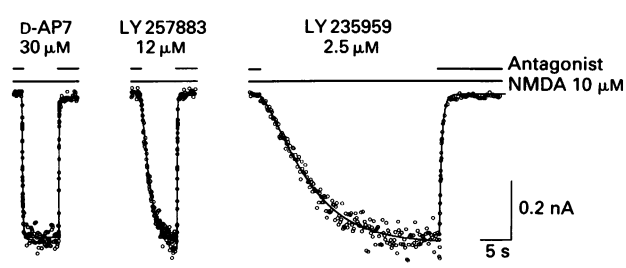

Figure 4 Conformational restriction slows binding kinetics for cyclic AP7 derivatives: 10 μM NMDA and 3 μM glycine were applied continuously (lower bar). Antagonists were applied during periods indicated by the upper bar; at the start of each record responses are at equilibrium, and increase in amplitude on removal of antagonist. Lines drawn through the data points are least squares fits of a two binding site model for competitive antagonism. D-AP7 has fast kinetics, the piperidine derivative LY 257883 intermediate kinetics similar to those illustrated in Figure 2 for CGS 19755, and the bicyclic derivative LY 235959 extremely slow kinetics.

Table 2 Effect of increasing conformational restriction for ω-phosphonates with 6 atom separation

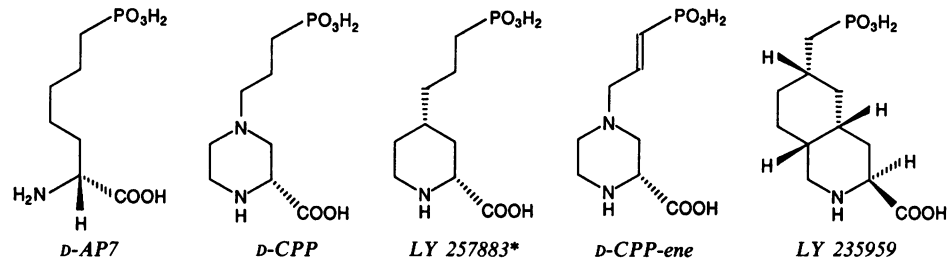

	D-AP7	D-CPP	LY 257883*	D-CPP-ene	LY 235959
k_{on} $\mu M^{-1} s^{-1}$	14.1 ± 5.4	3.6 ± 1.4	4.0 ± 1.5	4.9 ± 2.1	1.1 ± 0.6
k_{off} s^{-1}	20.3 ± 5.6	1.1 ± 0.1	1.3 ± 0.2	0.7 ± 0.2	0.2 ± 0.05
k_{off}/k_{on} μM	1.69 ± 0.87	0.37 ± 0.16	0.36 ± 0.16	0.16 ± 0.10	0.24 ± 0.15
K_i μM	4.55 ± 0.62	0.40 ± 0.04	0.37 ± 0.08	9.23 ± 0.04	0.19 ± 0.04

Values are given as mean ± s.d. Association and dissociation rate constants were determined by kinetic analysis; K_i values were determined from equilibrium measurements with 10 μM NMDA as described in Methods.
* Indicates correction was made for a racemic mixture of 2 isomers, one of which was assumed to have negligible activity.

investigated this substantially lowered the dissociation rate constant, with less effect on k_{on}, producing potent antagonists (cf. results for AP5 and *trans*-APPA given in Table 1). However, in the case of the 6-atom separation analogue D-CPP-ene, introduction of a double bond in the 6–7 position produced only a 1.6 fold decrease in dissociation rate constant (Table 2). This small effect was not unexpected, since in these compounds introduction of a double bond would be expected to produce different results: AP5 is a flexible acyclic molecule, which becomes highly constrained upon introduction of a double bond to form *trans*-APPA, while in contrast, for D-CPP rotational mobility in positions 2–4 of the backbone of AP7 is already highly constrained prior to introduction of a double bond at positions 6–7 to form D-CPP-ene.

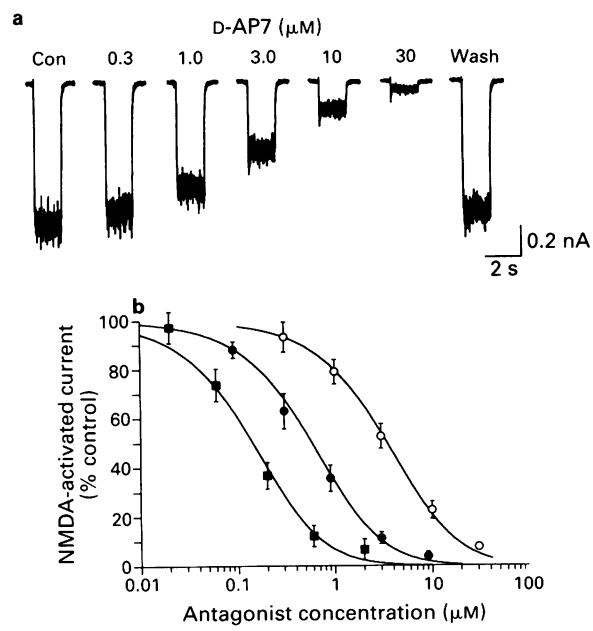

Figure 5 Analysis of equilibrium antagonist potency for AP7 and some cyclic derivatives: (a) shows inward current responses to 10 μM NMDA applied together with the indicated concentrations of D-AP7. The initial transient response to NMDA with 3, 10 and 30 μM D-AP7 is similar to that shown on a faster time scale in Figure 1a; the transient is much smaller than for the response to equipotent doses of CGS 19755 (cf. Figure 3a). Dose-inhibition curves measured at equilibrium are plotted in (b). Smooth lines were obtained by non-linear regression using the equation for a two-binding site isotherm. K_0 values (in μM) are: 0.36 ± 0.07 for LY 235959 (■), 1.40 ± 0.17 for LY 257883 (●) and 8.69 ± 1.18 for D-AP7 (○). Data points are mean of 42–60 observations recorded from 5 cells for each antagonist. Error bars depict standard deviation.

Inhibition by phosphonate antagonists is not glycine- or voltage-dependent

Although AP5 has been shown by Schild plot analysis to act as a competitive antagonist at the glutamate binding site on NMDA receptors (Evans *et al.*, 1982; Harrison & Simmonds, 1985; Verdoorn *et al.*, 1989), we were concerned that the unusually slow kinetics of action of the cyclic compounds described in Tables 1 and 2 could reflect some additional action at a site other than that at which glutamate binds to the NMDA receptor channel complex. Ascher and his colleagues have shown that the equilibrium potency of CPP does not vary with glycine concentration (Henderson *et al.*, 1990), suggesting that CPP does not bind to the glycine recognition site on NMDA receptors, and that there is no strong allosteric interaction between binding of glycine and binding of CPP. In support of this we have found that when 100 μM L-alanine, a rapidly dissociating agonist (Benveniste *et al.*, 1990), is used to activate the glycine recognition site, the kinetics of action of CPP are similar to those measured with 3 μM glycine.

The slow recovery from antagonism of NMDA receptor responses evoked by cyclic antagonists could alternatively have a component due to channel block, since drugs such as MK-801, ketamine and desipramine (MacDonald *et al.*, 1987; Huettner & Bean, 1988; Sernagor *et al.*, 1989), which block the ion channel of NMDA receptors, exhibit similar slow kinetics. For this class of drugs both the rate of recovery from block, and potency at equilibrium, show strong voltage dependence. In contrast, as illustrated in Figure 6a, the kinetics of action of D-CPP and potency of block at equilibrium are similar at holding potentials of +60 and −60 mV. Average k_{on} and k_{off} values were 3.35 ± 0.85 and 3.14 ± 1.35 $\mu M^{-1} s^{-1}$, and 1.15 ± 0.04 and 0.91 ± 0.05 s^{-1} at +60 and −60 mV respectively. Further analysis shows that k_{on} and k_{off} are essentially independent of voltage, since they increase *e*-fold for every 1060 mV and 539 mV change in membrane potential, respectively (Figure 6b). This weak voltage-sensitivity implies that the glutamate and competitive antagonist recognition sites on the NMDA receptor channel complex are likely to be at some distance from the lipid bilayer, and not modulated in an indirect manner by the membrane electric field. Since the piperazine ring of CPP contains an additional nitrogen atom which is expected to be protonated at physiological pH, it is unlikely that acyclic and piperidine derivatives of AP5 and AP7 which lack this nitrogen atom will act as channel blockers and we did not examine any voltage-dependence of the action of other antagonists.

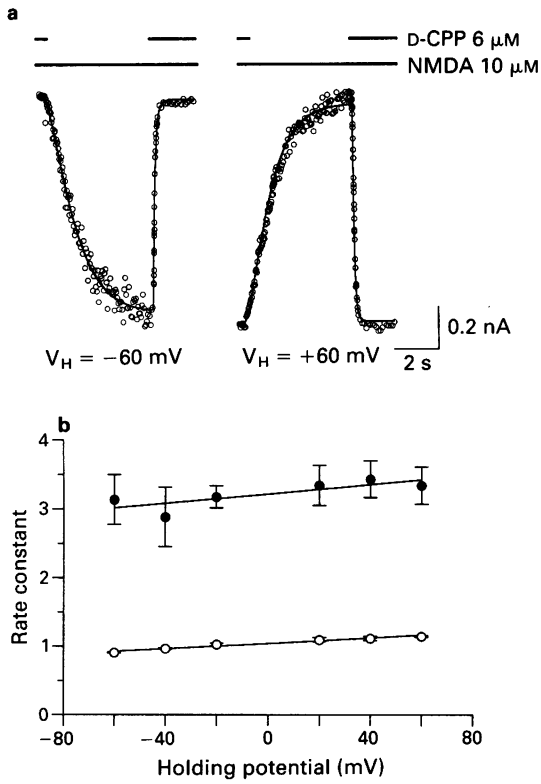

Figure 6 The kinetics of action of D-CPP show only weak voltage sensitivity: (a) shows responses recorded at holding potentials of −60 and +60 mV during concentration jump applications of D-CPP, and fit with a two site model for competitive antagonism. Initially 10 μM NMDA, 3 μM glycine and 6 μM D-CPP were applied together, and the activation of NMDA receptors allowed to reach equilibrium. During the period shown by breaks in the upper bar, the solution was changed to 10 μM NMDA and 3 μM glycine applied alone to allow study of the kinetics of recovery from and onset of block by D-CPP. (b) Analysis of 77 responses recorded from 3 neurones; data points show mean for the antagonist association rate constant k_{on}, in units of $\mu M^{-1} s^{-1}$ (●), and for the antagonist dissociation rate constant k_{off}, in units of s^{-1} (○); error bars show s.e.mean. Lines were fit by non-linear regression to equation 3, and indicate minimal voltage sensitivity in D-CPP binding kinetics.

Effects of lengthening atomic chain length between α-carboxylate and ω-phosphonate moieties

In view of evidence presented above suggesting that differences in conformational flexibility contribute to the kinetics of binding of NMDA receptor antagonists, we extended our analysis to examine the effects of varying the chain length between α and ω functional groups in phosphonate antagonists, and the effects of substitution of different ω functional groups in antagonists of similar structure. Binding studies have shown that the 6-atom separation antagonist, D-AP7 is 2.6 fold less potent than the 4-atom separation antagonist D-AP5 (Olverman *et al.*, 1988; Hays *et al.*, 1990), consistent with the 2.4 fold difference in equilibrium potency measured in the present experiments. In contrast, the 6-atom separation piperidine analogue LY 257883 is equipotent with the 4-atom separation piperidine analogue CGS 19755 in both binding (Ornstein *et al.*, 1989) and voltage clamp (Table 3) assays. In an attempt to discern possible trends due to increasing chain length on binding kinetics and equilibrium dissociation constants data from three sets of antagonists were compared (Table 3).

There is a 1.6 fold decrease in k_{on} on going from D-AP5 to D-AP7, with only a small change in k_{off}. There is a similar 1.8 fold decrease in k_{on} on addition of two methylene groups for the piperidines CGS 19755 and LY 257883, but also a 1.3 fold decrease in k_{off}; as a result there is almost no change in the potency of this pair of compounds at equilibrium. However, piperazines behave differently. The 4- and 6-atom separation piperazine analogues, D-CMP and D-CPP show a 3 fold decrease in k_{on} on addition of two methylene groups, and a much larger, 6.8 fold, decrease in k_{off}. As a result there is a 3.5 fold increase in equilibrium potency for the 6-atom separation piperazine D-CPP, in contrast to the absence of any such change for the piperidines LY 257883 and CGS 19755.

Kinetic effects of α-carbon stereochemistry

From binding and equilibrium physiological studies (Aebischer *et al.*, 1988; Olverman *et al.*, 1988), it has been shown that the L-isomers of the antagonists AP5, AP7, CPP and CPP-ene are considerably less active than the corresponding D-isomers. One difficulty with studies of this type occurs when there is a large isomeric potency ratio, since contamination of the less active isomer with only a small quantity of the more potent isomer will give an artifically high estimate of the activity of the less active ligand. One advantage of kinetic experiments is the ability to distinguish such a case, since the dissociation rate constants for active and inactive isomers would be identical if contamination with the active isomer was the cause of activity for the inactive isomer; in contrast, if both isomers bind to the receptor, with different affinity, their kinetics of action should differ. Figure 7a highlights the striking difference in the kinetics of action of the D- and L-isomers of CPP applied at approximately equipotent doses (93% and 88% inhibition, respectively). Figure 7b shows that at equilibrium L-CPP is 14.8 fold less potent than D-CPP, and Figure 8c shows that this difference in potency largely

Table 3 Comparison of ω-phosphonates with 4 and 6 atom separation

	D-AP5	D-AP7	CGS 19755*	LY 257883*	D-CMP	D-CPP
k_{on} $\mu M^{-1} s^{-1}$	22.2 ± 6.5	14.1 ± 5.45	7.0 ± 2.3	4.0 ± 1.5	10.8 ± 5.7	3.6 ± 1.4
k_{off} s^{-1}	19.4 ± 4.1	20.3 ± 5.6	1.7 ± 0.2	1.3 ± 0.2	7.5 ± 0.7	1.1 ± 0.1
k_{off}/k_{on} μM	0.92 ± 0.23	1.69 ± 0.87	0.28 ± 0.13	0.36 ± 0.16	0.97 ± 0.59	0.37 ± 0.16
K_i μM	1.93 ± 0.57	4.55 ± 0.62	0.34 ± 0.08	0.37 ± 0.04	1.41 ± 0.13	0.40 ± 0.04

Values are given as mean ± s.d. Association and dissociation rate constants were determined by kinetic analysis; K_i values were determined from equilibrium measurements with 10 μM NMDA as described in Methods.

* Indicates correction was made for a racemic mixture of 2 isomers, one of which was assumed to have negligible activity.

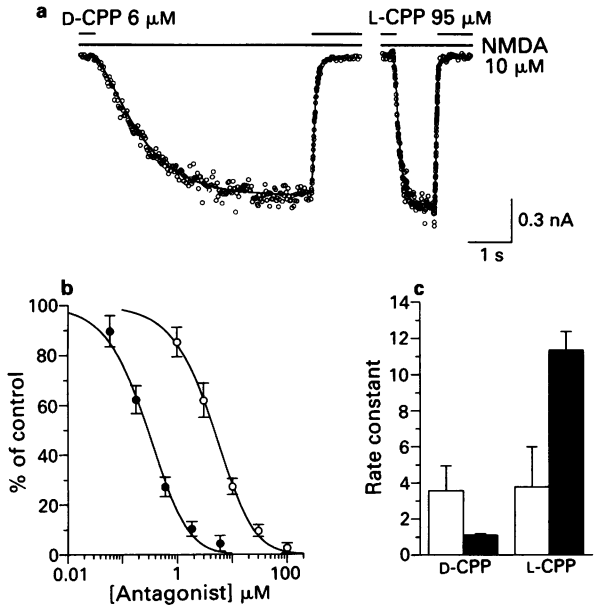

Figure 7 Comparison of D-CPP and L-CPP as NMDA receptor antagonists: (a) shows kinetic analysis of the response to D- and L-CPP. Initially 10 μM NMDA, 3 μM glycine and one of the isomers of CPP were applied together, and the activation of NMDA receptors allowed to reach equilibrium; during the period shown by breaks in the upper bar, the solution was changed to 10 μM NMDA and 3 μM glycine applied alone to allow study of the kinetics of recovery from block, and the kinetics of onset of block on reapplication of CPP. Lines drawn through the data points are least squares fits of a two binding site model for competitive antagonism. (b) Analysis of equilibrium potency for block of responses to 10 μM NMDA by D-CPP (●) and L-CPP (○); lines drawn through the data points are least squares fits of a two-site model for competitive antagonism. (c) Comparison of the association (open column, $\mu M^{-1} s^{-1}$) and dissociation (filled columns, s^{-1}) rate constants for binding of the isomers of CPP, as estimated in (a); error bars show s.d. for 36–45 observations recorded from 4–7 cells for each enantiomer at a holding potential of −60 mV.

results from the 10 fold increase in k_{off} for L-CPP. This difference in the dissociation rate constants for D- and L-CPP indicates that the NMDA receptor antagonist activity of L-CPP does not result from contamination with D-CPP.

The D- and L-isomers of CPP do not differ in any of their chemical properties or in their degree of conformational constraint. Thus, the striking change in k_{off} and the absence of large changes in k_{on} indicates that while both k_{on} and k_{off} are influenced by the degree of conformational constraint (Tables 1 and 2). However, k_{off} is influenced by an additional parameter, possibly reflecting the ability of one of the three functional groups present in phosphonic amino acid antagonists to achieve optimal orientation with its binding site on the NMDA receptor once the other two functional groups are bound.

Kinetic effects of different ω-substituted groups

Thus far, we have described only the effects of conformational restriction and stereochemistry on the kinetics of action of phosphonic amino acid antagonists. However, the chemical structure of the functional groups involved in antagonist binding to the NMDA receptor would also be expected to strongly influence kinetics. Binding studies with acyclic antagonists show that ω-phosphonate compounds exhibit at least 10 fold greater potency than observed with ω-carboxylate compounds, although potent NMDA receptor antagonist activity does occur with other ω-substituted derivatives in cyclic AP5 and AP7 derivatives (Olverman *et al.*, 1988; Olverman & Watkins, 1989; Ornstein *et al.*, 1989; Hays *et al.*, 1990). Table 4 shows the effect on k_{on} and k_{off} of replacement of the ω-phosphonate group with an ω-carboxylate group. The dicarboxylic acids studied, *cis*-3-carboxy-1-piperazinebutanoic acid (D-CPC); *cis*-4-(3-carboxyprop-1-yl)-piperidine-2-carboxylic acid (LY 221501, Ornstein *et al.*, unpublished results); and 4-(3-carboxyprop-2-E-en-1-yl) piperazine-2-carboxylic acid (D-CPC-ene), have slightly faster association rate constants than their phosphonate analogues. LY 221501 and D-CPC also show 1.9 and 1.7 fold increases in dissociation rate constant compared to their phosphonate analogues LY 257883 and D-CPP; this contributes to a decrease in equilibrium potency of 1.7 to 3 fold (Table 4). The unsaturated dicarboxylate derivative D-CPC-ene had 6 fold faster dissociation kinetics than its phosphonate analogue D-CPP-ene, and this largely accounts for the 8 fold decrease in equilibrium potency. The similar values for k_{off} and k_{on} observed when comparing the piperidine (LY 221501) and piperazine (D-CPC) dicarboxylic acid antagonists can be related to the similar results obtained when comparing the piperidine and piperazine α-carboxylate, ω-phosphonate compounds (Table 4).

Table 5 shows that substitution of the ω-phosphonate group with the tetrazole isostere also causes k_{on} and k_{off} to increase. The association rate constant for *cis*-4-((1(2)H-tetrazol-5-yl)methylpiperidine-2-carboxylic acid (LY 233053, Ornstein *et al.*, 1991) is similar to that of D-AP5 and nearly 3 times faster than that for the ω-phosphonate analogue, CGS 19755. Additionally, 3S,4aR,6S,8aR-6-((1(2)H-tetrazol-5-yl) methyl-decahydroisoquinoline-3-carboxylic acid (LY 202157, the active enantiomer of LY 233536, Ornstein *et al.*, 1991) has a 3.1 fold higher association rate constant than its ω-phosphonate analogue, LY 235959 (Table 5). Dissociation rate constants for the tetrazole antagonists are also increased over

Table 4 Effect of ω-phosphonate vs. ω-carboxylatate substitution

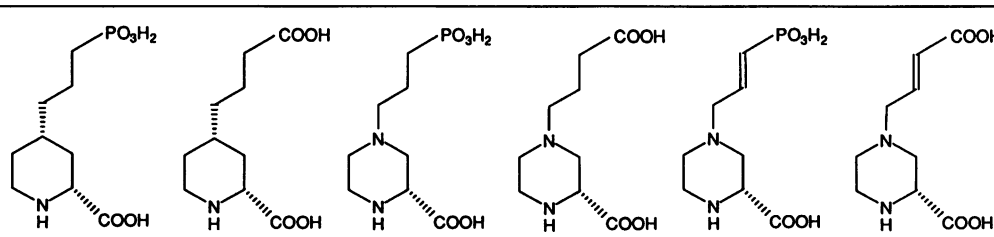

	*LY 257883**	*LY 221501**	*D-CPP*	*D-CPC*	*D-CPP-ene*	*D-CPC-ene*
k_{on} $\mu M^{-1} s^{-1}$	4.0 ± 1.5	5.6 ± 1.9	3.6 ± 1.4	5.3 ± 1.8	4.9 ± 2.1	8.2 ± 3.2
k_{off} s^{-1}	1.3 ± 0.2	2.5 ± 0.2	1.1 ± 0.1	1.9 ± 0.1	0.7 ± 0.2	4.2 ± 0.5
k_{off}/k_{on} μM	0.36 ± 0.16	0.51 ± 0.20	0.37 ± 0.16	0.41 ± 0.14	0.16 ± 0.09	0.58 ± 0.23
K_i μM	0.37 ± 0.04	1.10 ± 0.12	0.40 ± 0.04	0.69 ± 0.05	0.23 ± 0.04	0.98 ± 0.21

Values are given as mean ± s.d. Association and dissociation rate constants were determined by kinetic analysis; K_i values were determined from equilibrium measurements with 10 μM NMDA as described in Methods.

* Indicates correction was made for a racemic mixture of 2 isomers, one of which was assumed to have negligible activity.

Table 5 Effect of ω-phosphonate vs. ω-tetrazole substitution

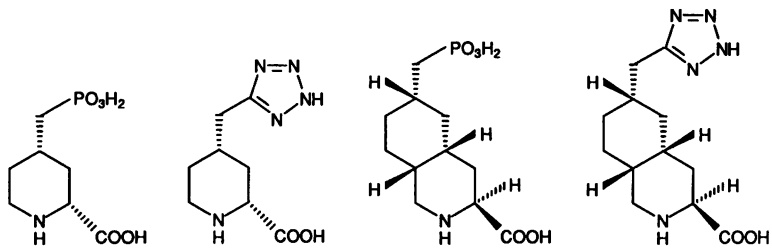

	*CGS 19755**	*LY 233053**	*LY 235959*	*LY 202157*
k_{on} $\mu M^{-1} s^{-1}$	7.0 ± 2.3	19.6 ± 11.4	1.1 ± 0.6	3.4 ± 1.0
k_{off} s^{-1}	1.7 ± 0.2	5.2 ± 0.4	0.19 ± 0.03	0.87 ± 0.10
k_{off}/k_{on} μM	0.28 ± 0.13	0.36 ± 0.18	0.24 ± 0.15	0.27 ± 0.07
K_i μM	0.34 ± 0.08	0.85 ± 0.06	0.19 ± 0.04	0.41 ± 0.05

Values are given as mean ± s.d. Association and dissociation rate constants were determined by kinetic analysis; K_i values were determined from equilibrium measurements with 10 μM NMDA as described in Methods.
* Indicates correction was made for a racemic mixture of 2 isomers, one of which was assumed to have negligible activity.

their phosphonate counterparts, with LY 233053 dissociating 3.1 fold faster than CGS 19755 and LY 202157 dissociating 4.6 fold faster than LY 235959 (Table 5). The larger increase in k_{off} relative to the increase in k_{on} when comparing phosphono amino acids to their tetrazole analogues contributes to the greater than 2 fold decrease in equilibrium potency observed for ω-tetrazole antagonists. Also note that the addition of a fused cyclohexyl ring structure to the piperidine based tetrazole LY 233053, to yield the bicyclic antagonist LY 202157, produces an 8 fold decrease in k_{on} and a 6 fold decrease in k_{off}, most likely as a result of additional conformational constraint. These changes in k_{on} and k_{off} are comparable to those observed for the corresponding phosphonate analogues (e.g. Tables 1 and 2): Comparison of the piperidine CGS 19755 to the bicyclic antagonist LY 235959 reveals a similar 6.4 fold decrease in k_{on} and an 8.5 fold decrease in k_{off}.

The slow kinetics of action of NMDA receptor antagonists are not an artefact of buffered diffusion

The rate of solution exchange in our experiments is not instantaneous; also, as is the case for nicotinic receptors at the vertebrate neuromuscular junction (Armstrong & Lester, 1979), it is possible that buffered diffusion in the restricted extracellular space between hippocampal neurones and the underlying glial cell layer could slow the rate of equilibration of ligands which bind with high affinity to NMDA receptors. These phenomena would artifically lower the rate of recovery from block, and hence give erroneously slow antagonist dissociation rate constants if antagonist molecules rebound to NMDA receptors before being washed away. In addition, an erroneously slow association rate constant would result if buffered diffusion limited the rate of rise of antagonist concentration, such that the kinetics of solution exchange, and binding kinetics determined the rate of occupancy of receptors by antagonist. Buffered diffusion should be dependent on antagonist affinity, such that high affinity antagonists would suffer larger decreases in k_{off} and k_{on}; in general, although this was the effect observed, and potent antagonists such as LY 235959 exhibit slower binding kinetics than weaker antagonists such as AP7, considerable differences exist in the kinetics of action of compounds of similar equilibrium potency (cf. CGP 37849 and LY 235959).

The occurrence of diffusion limited artefacts can be tested by use of an experimental protocol based on that outlined by Rang (1966) for the dynamics of muscarinic acetylcholine receptor responses in the presence of fast and slow acting antagonists; a similar kinetic test has been used to verify differences in the kinetics of binding of tetrodotoxin and saxitoxin to axonal membranes (Ulbricht, 1981). If two antagonists with association and dissociation rates which are genuinely different are applied in the constant presence of agonist and the response allowed to reach equilibrium, removal of the faster acting antagonist will yield a transient agonist response. This is due to the rapid dissociation and removal, by fast perfusion, of the fast acting antagonist, leaving receptor sites vacant, and out of equilibrium for binding of agonist and the slow acting antagonist. An agonist response then occurs if receptors have a higher probability of binding the agonist than of binding the slow acting antagonist; the agonist response fades as binding of agonist and the slow acting antagonist reaches equilibrium.

Figure 8a shows such an experiment for the response to 200 μM D-AP7, recorded following a 17 s equilibration with D-AP7 in the presence of 2 μM LY 235959 and 10 μM NMDA; following removal of AP7 there is transient activation of NMDA receptors before block by LY 235959 reaches its new equilibrium value in the absence of AP7. Figure 8b shows a numerical simulation of the current transient expected upon removal of D-AP7, with agonist and antagonist concentrations identical to those used for the experiment illustrated in Figure 8a. Experimentally determined values for the association and dissociation rate constants for D-AP7, LY 235959 (Table 2) and NMDA (see Methods) were used for this simulation, the result of which closely approximated the experimental data. When k_{on} and k_{off} for LY 235959 were increased only two fold, the time course of the simulated response was nearly identical to the experimental result. As a result, if buffered diffusion does slow the kinetics of binding of LY 235959, the magnitude of the distortion can be at most two fold, and would be less for antagonists of lower affinity. Another explanation for the failure of this simulation to predict exactly the time course of the experimental response could result from oversimplification of the NMDA receptor binding scheme in the two equivalent site model used for our analysis.

Comparison of antagonist binding kinetics with equilibrium potency

The above experiment suggests that our concentration jump analysis accurately estimates binding kinetics for competitive antagonists acting at NMDA receptors. Although in general, potent antagonists such as LY 235959 exhibited slower binding kinetics than weaker antagonists such as AP7, analysis of data from all 16 antagonists studied shows this trend is not absolute. Figure 9a shows the lack of strong correlation between antagonist association and dissociation rates, with equilibrium K_i values determined separately from analysis of dose-inhibition curves. The wide scatter reveals no significant correlation between k_{on} and K_i determined at equilibrium (correlation coefficient = 0.034), such that potent compounds can either have high or low association rate constants

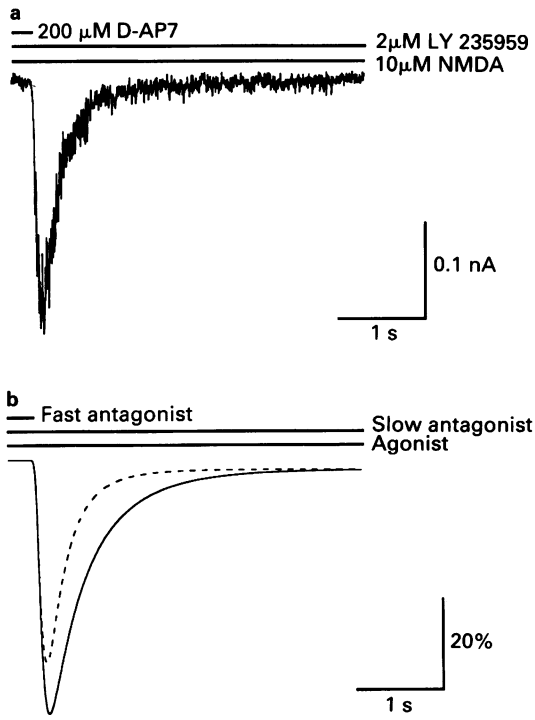

Figure 8 A kinetic test for buffered diffusion: (a) shows the response of a hippocampal neurone pre-equilibrated with 200 μM D-AP7, 2 μM LY 235959, 10 μM NMDA, and 3 μM glycine, to rapid removal of D-AP7 (upper bar). There is an initial agonist response to NMDA, which fades as block by LY 235959 returns to equilibrium. (b) Shows numerical simulations for a similar experiment; the agonist and antagonist concentrations were identical to those given in (a). The solid line shows the response obtained when the association and dissociation rate constants for the fast and slow acting antagonists are taken from values given in Table 2 for D-AP7 and LY 235959 respectively; the dashed line shows the response obtained when the association and dissociation rate constants for LY 235959 were increased two fold.

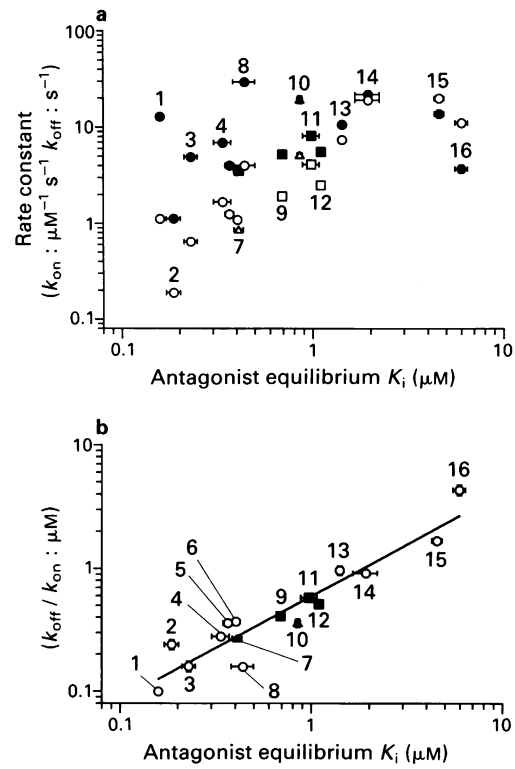

Figure 9 Antagonist binding kinetics vary widely but are good predictors of potency at equilibrium: (a) shows a plot of antagonist association rate constant k_{on} (filled symbols, $\mu M^{-1} s^{-1}$) and antagonist dissociation rate constant k_{off} (open symbols, s^{-1}) for a series of 16 ω-phosphono- (circles), ω-carboxylate (squares) and ω-tetrazolyl- (triangles) NMDA receptor competitive antagonists, plotted vs. equilibrium dissociation constants (K_i) determined from dose-inhibition analysis (Figures 3 and 5). (b) Plot of the ratio k_{off}/k_{on} for the same series of antagonists vs. equilibrium K_i. Estimates for these parameters were obtained using two site models for competitive antagonism and data points represent mean with s.e.mean shown by error bars. In (a) and (b) the antagonists studied are identified by the following key: (1) CGP 37849; (2) LY 235959; (3) D-CPP-ene; (4) CGS 19755; (5) LY 257883; (6) D-CPP; (7) LY 202157; (8) *trans*-APPA; (9) D-CPC; (10) LY 233053; (11) D-CPC-ene; (12) LY 221501; (13) D-CMP; (14) D-AP5; (15) D-AP7; (16) L-CPP.

(e.g. CGP 37849 or LY 235959, respectively). However, there is a moderate correlation between antagonist dissociation rate constant and potency (correlation coefficient = 0.753); as the antagonist dissociation rate constant decreases, the potency of the compounds increases. The latter correlation is not unexpected, since the dissociation rate constant reflects the stability of the ligand-receptor complex, with slower dissociation indicating more stable complexes, typical of the action of potent antagonists. In contrast, the association rate constant reflects the ability of the antagonist to access and interact with the binding site, but a molecule which can quickly bind to the receptor may or may not form a stable complex.

In contrast to the lack of strong correlation between k_{on}, k_{off} and K_i the ratio k_{off}/k_{on} was an excellent predictor of the microscopic dissociation constant measured at equilibrium. Figure 9b shows a plot of the ratio k_{off}/k_{on} vs. K_i determined from separate equilibrium measurements (correlation coefficient = 0.942), indicating that the ideal antagonist will access the site quickly and form a stable ligand-receptor complex. The acyclic, but conformationally restrained AP5 derivative CGP 37849 comes closest to meeting this requirement.

Comparison of NMDA and AMPA-kainate receptor antagonists

The kinetics of action of many ω-phosphonate based NMDA receptor antagonists are unusually slow, and in some cases association rate constants are perhaps 100 times less than expected from diffusion limited binding. In view of this, we briefly examined the kinetics of action of another class of glutamate receptor antagonist, represented by 6-cyano-7-nitroquinoxaline-2,3-dione (CNQX), which competitively antagonizes responses to kainate (Honoré *et al.*, 1988; Verdoorn *et al.*, 1989). For analysis of equilibrium responses to CNQX, 50 μM kainate was utilized for the dose-inhibition curve, corresponding to approximately the same level of occupancy of non-NMDA receptors by the agonist kainate as achieved with 10 μM NMDA for activation of NMDA receptors (Patneau & Mayer, 1990). Since analysis of dose-response curves gave Hill coefficients > 1 for the action of kainate in oocytes injected with brain mRNA and in cultured mouse hippocampal neurones (Verdoorn & Dingledine, 1988; Patneau & Mayer, 1990), a two site analysis was used for the action of CNQX. The K_i for CNQX under these conditions was 0.61 μM, similar to that of 0.40 μM for D-CPP (Figure 10b), and in reasonable agreement with the K_i of 300 nM estimated by electrophysiological techniques in *Xenopus* oocytes injected wih mRNA (Verdoorn *et al.*, 1989), especially when it is considered that the latter analysis used a 1 site model for competitive antagonism, which we have found increases the estimate of antagonist potency approximately 2 fold for a receptor which is instead activated by two molecules of agonist.

Despite the similar potency of D-CCP and CNQX at equilibrium, these experiments revealed marked differences in the rate of recovery from the antagonist action of D-CPP at NMDA receptors and CNQX at non-NMDA receptors

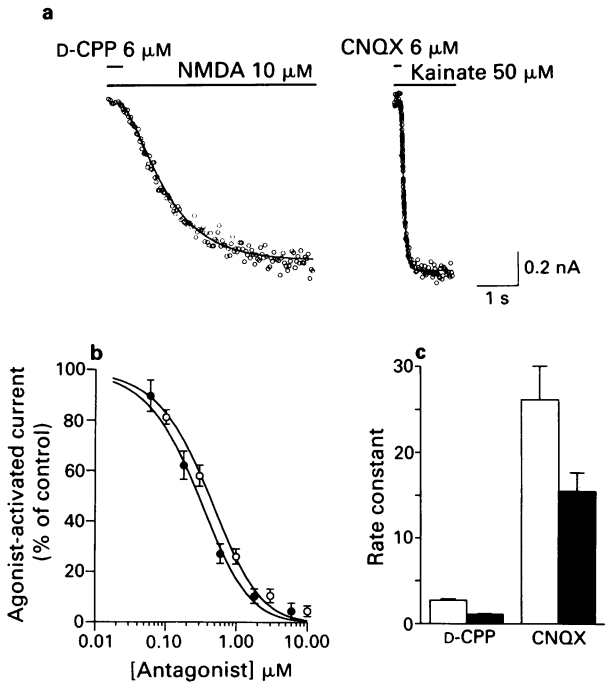

Figure 10 Comparison of the kinetics of block by D-CPP with those of CNQX, a non-NMDA receptor antagonist: (a) shows kinetic analysis of the response to removal of 6 μM D-CPP or 6 μM CNQX. Initially 10 μM NMDA, 3 μM glycine and 6 μM D-CPP were applied together, and the activation of NMDA receptors allowed to reach equilibrium, after which the solution was changed to 10 μM NMDA and 3 μM glycine applied alone to allow study of the kinetics of recovery from block (left). The same protocol was used for the response to 6 μM CNQX recorded in the presence of 50 μM kainate (right). Lines drawn through the data points are least squares fits of a two binding site kinetic model for competitive antagonism. (b) Analysis of equilibrium potency of block of responses to 10 μM NMDA by D-CPP (●) and to 50 μM kainate by CNQX (○); smooth lines were obtained by non-linear regression using the equation for a two-binding site isotherm. (c) Comparison of the association (open column, $\mu M^{-1} s^{-1}$) and dissociation (filled columns, s^{-1}) rate constants for binding of D-CPP and CNQX. k_{on} was calculated from the ratio k_{off}/K_i. Error bars show s.d. for 45–80 observations recorded from 4–5 cells.

(Figure 10a). The rate of recovery from block of responses to kainate by CNQX was analysed by the same two-equivalent site kinetic model described previously for the study of NMDA receptor antagonists. The apparent association and dissociation rate constants for kainate required for this analysis were determined to be $0.42 \mu M^{-1} s^{-1}$ and $31.73 s^{-1}$, respectively (see Benveniste & Mayer, 1991 for methods); the ratio k_{off}/k_{on} was 75.5 μM, consistent with the microscopic dissociation constant of 62 μM, determined from equilibrium dose-response measurements using a two binding site model (Patneau & Mayer, 1990). The dissociation rate constant for CNQX, determined by two-equivalent site analysis for competitive antagonism, was $15.5 \pm 2.2 s^{-1}$, fourteen times faster than that for D-CPP.

An accurate analytical solution for the association rate constant for CNQX could not be obtained from measurement of the time course of onset of action of CNQX in the presence of kainate, because the kinetics of antagonism were too fast to record with our technique. As an alternative, k_{on} was determined from the relationship $k_{on} = k_{off}/K_i$. The value obtained for CNQX was $2.6 \pm 0.4 \times 10^7 M^{-1} s^{-1}$, more than 7 times faster than the experimentally measured association rate constant for D-CPP. As a check of this approach a similar calculation was made for D-CPP; the value obtained, $2.7 \pm 0.2 \times 10^6 M^{-1} s^{-1}$ is in good agreement with that determined directly from kinetic measurements of the response to D-CPP ($3.6 \pm 1.4 \times 10^6 M^{-1} s^{-1}$). These experiments suggest that compared to CNQX, which is itself a very rigid molecule, the association rate constants for conformationally restrained NMDA receptor antagonists which contain a phosphonate moiety are unusually slow. The slow recovery from CNQX-evoked block of AMPA-kainate receptors recorded in experiments on intact preparations (e.g. Long *et al.*, 1990) contrasts with the rapid recovery seen in our concentration jump experiments, and is most likely due to partitioning of CNQX into lipid membranes, making it difficult to remove the drug in the absence of rapid perfusion.

Discussion

Concentration jump analysis, in conjunction with whole cell voltage clamp recording, was used to determine association and dissociation rate constants for a variety of NMDA receptor competitive antagonists acting at the glutamate recognition site. With the resolution of these kinetic parameters, the difference in time course of agonist responses illustrated in Figure 1 and recorded in the presence of the antagonists D-AP7 and LY 257883 can now be explained. Following simultaneous application of NMDA and LY 257883, the initial transient agonist response, to 97% of control, results from an association rate of only $6 s^{-1}$ for 1.5 μM LY 257883, 35 fold slower than the association rate of $210 s^{-1}$ for 100 μM NMDA (Figure 1b, left); for simultaneous application of NMDA and D-AP7, the initial transient agonist response, to only 43% of control results, from an association rate of 240 s^{-1} for 17 μM D-AP7, which is similar to that for 100 μM NMDA (Figure 1a, left). Under conditions where the binding kinetics for agonist are not rate-limiting, and when antagonist binding is pre-equilibrated, the activation of NMDA receptors during a concentration jump application of 100 μM NMDA reaches equilibrium 16 fold faster in the presence of D-AP7 than when LY 257883 is used as an antagonist (Figure 1a and 1b, right). Not surprisingly, this difference is similar to the ratio of 15.6 for the dissociation rate constants measured for D-AP7 and LY 257883 (Table 2).

By examining three parameters (k_{on}, k_{off}, and K_i) for 16 NMDA receptor competitive antagonists, we have resolved some aspects of the molecular mechanisms involved in inhibition of the NMDA receptor. Our results suggest that although conformational restriction can generate antagonists which remain bound to the NMDA receptor antagonist recognition site for several seconds (and thus should be of high potency), the slow forward rate constant for binding of conformationally restrained compounds, which limits the rate at which antagonist molecules bind to the receptor, can significantly reduce potency.

Comparison of voltage clamp K_i measurements to binding data

Radioligand binding assays are now the primary techniques used to determine the relative potency of antagonists *in vitro*. However, differences in assay conditions can generate considerable discrepancy between K_i values determined for individual compounds. For NMDA receptors a discrepancy occurs between K_i values determined by displacement of the agonist [^{3}H]-glutamate versus assays utilizing the antagonists [^{3}H]-CPP or [^{3}H]-CGS 19755. K_i values determined with [^{3}H]-glutamate show approximately 5 fold lower affinity than K_i values determined for the same antagonists in [^{3}H]-CPP or [^{3}H]-CGS 19755 binding experiments (compare x-axis in Figure 11a and b). In both types of experiments, there was reasonable correlation between affinity measured in binding experiments and *in vitro* physiological activity for NMDA receptor antagonists (Figure 11). For antagonist binding measurements the correlation coefficient was 0.753. A number of

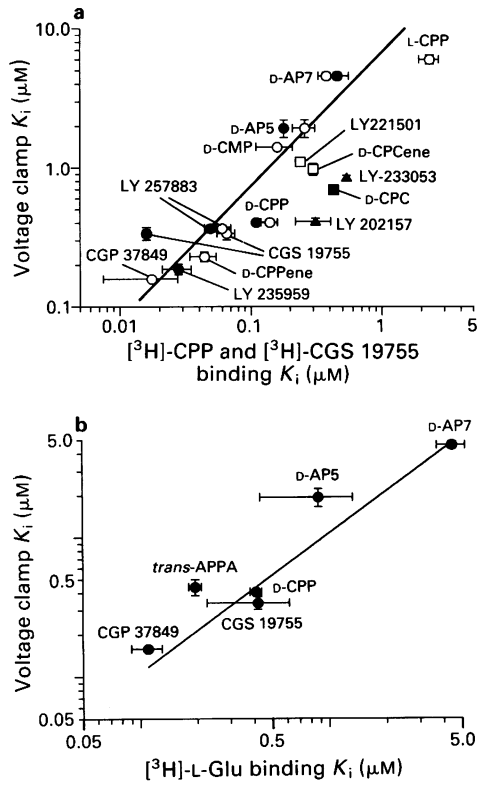

Figure 11 Comparison of NMDA receptor antagonist equilibrium dissociation constants measured in voltage clamp experiments with antagonist dissociation constants measured in binding experiments using displacement of radiolabelled agonist and antagonist: (a) shows a plot of voltage clamp estimates of antagonist K_i vs. K_i values estimated from displacement of [^{3}H]-CPP (open symbols) or [^{3}H]-CGS 19755 (closed symbols) for a series of 16 phosphono- (circles), carboxylic acid- (squares) and tetrazolyl- (triangles) amino acid competitive NMDA receptor antagonists. The line (drawn by eye) illustrates that the phosphono-amino acids show high correlation between ^{3}H antagonist binding and voltage clamp estimates of K_i. (b) Plot of voltage clamp estimates of antagonist K_i vs. K_d values estimated from displacement of [^{3}H]-L-glutamate for a series of 6 phosphono-amino acid NMDA receptor competitive antagonists. The line (drawn by eye) illustrates a high correlation between [^{3}H]-L-glutamate binding and voltage clamp data. Binding data in (a) taken from Aebischer *et al.*, 1989; Fagg *et al.*, 1990; Hays *et al.*, 1990; Hutchison *et al.*, 1989; Ornstein *et al.*, 1991; and personal communications by Drs P. Herrling and P. Ornstein. Binding data in (b) taken from Fagg *et al.* (1990).

points in these plots do not fall within statistically significant confidence intervals of the linear fit; however, K_i values from different laboratories can vary as much as 4 fold for individual compounds, and the overall trend of correlation between binding and voltage clamp measurements is clear. Interestingly, when L-CPP, ω-tetrazoles and dicarboxylic acids were excluded the correlation coefficient increased to 0.963.

The ratio (mean ± s.e.mean) of K_i values from our voltage clamp experiments to K_i values determined from [^{3}H]-CPP and [^{3}H]-CGS 19755 binding, was 6.5 ± 1.0 when data from all 16 antagonists are included, and 7.9 ± 1.2 when L-CPP, ω-tetrazoles, and dicarboxylic acids are excluded (Figure 11a). The correlation coefficient for comparison of [^{3}H]-glutamate binding data and our voltage clamp K_i estimates was 0.97; the ratio of voltage clamp K_i values to [^{3}H]-glutamate K_i estimates is 1.4 ± 0.3 (Figure 11b).

The higher affinity K_i estimates obtained in binding assays using radiolabelled antagonists, vs. estimates obtained using voltage clamp analysis, or glutamate binding, could reflect either distinct agonist and antagonist preferring subtypes of NMDA receptor, or interconverting forms of a single receptor (e.g. Monaghan *et al.*, 1988). Murphy *et al.* (1988) have shown that Scatchard analysis of [^{3}H]-CGS 19755 binding experiments, when done by the centrifugation method, yielded a high affinity binding site for CGS 19755 of K_i 9 nM representing 35% of the total sites, and a low affinity binding site of K_i 0.20 μM, representing 65% of the sites. CPP yielded equilibrium dissociation constants of 19 nM and 0.34 μM, representing 26 and 71% of the binding sites, respectively. The K_i values for the more abundant low affinity site are closer to the glutamate binding K_i values (Fagg *et al.*, 1990) estimated for the racemic mixtures of CPP (0.82 μM) and CGS 19755 (0.84 μM), and our estimates of 0.8 μM and 0.66 μM deduced from voltage clamp data and corrected for the loss of activity in racemic mixtures. We suggest that the low affinity antagonist binding site is the physiologically relevant site for inhibition of NMDA receptor channel activity. The high affinity site appears to be specific for phosphono-amino acids but may not interact strongly with L-glutamate or lower potency antagonists such as the tetrazole and dicarboxylic acid substituted compounds. Our analysis suggests that to obtain good estimates of physiological potency for antagonist action at NMDA receptors, *in vitro* binding assays based on measurements obtained with radiolabelled agonists are preferable to assays conducted with antagonists.

Molecular aspects of ligand binding to NMDA receptors

Geometry, charge and hydrophobicity can all contribute to the interaction between drugs and receptors. Previous work has shown that α-amino, α-carboxylate and ω-acidic moieties are required for high affinity binding of competitive antagonists to NMDA receptors, suggesting that at least three independent sites which recognize positively and negatively charged groups are involved in the interaction of individual antagonist molecules with the receptor (Olverman & Watkins, 1989). Our experiments suggest that the relative mobility of these groups within antagonist molecules, which is influenced by conformational restriction, plays a major role in determining antagonist association and dissociation kinetics at NMDA receptors.

We assume that binding of the α-amino, α-carboxylate and ω-acidic moieties is independent, and that receptor-antagonist complexes with only one or two functional groups bound are unstable. Conformational restriction will influence association kinetics as follows: during collision of antagonist molecules with the receptor, orientation with respect to the antagonist binding site will determine the probability of formation of receptor antagonist complexes with one, two or three functional groups bound. Receptor-antagonist complexes with only one or two functional groups bound will then follow either of two reaction pathways: formation of a more stable complex, with three functional groups bound, or dissociation from the receptor. Conformational flexibility of antagonist molecules would influence the probability that the remaining unbound functional groups could correctly orient to form a more stable receptor-antagonist complex. This hypothesis can explain why the rate of formation of the stable receptor-antagonist complex (i.e. k_{on}) is faster for a flexible molecule like AP5 than for a rigid molecule like CGS 19755. As required by this proposal, it is possible to demonstrate overlay of the functional groups in these antagonists by molecular modelling, suggesting that unconstrained antagonists can assume similar conformations to those of sterically constrained antagonists.

When more than one functional group is involved in ligand binding, the dissociation rate constant should also be influenced by conformational restriction. Statistical arguments suggest that the probability that three independent functional groups will simultaneously dissociate from a receptor binding site is much lower than for dissociation of a single functional group. The binomial distribution was used to estimate the probability for dissociation of one of a total of three functional groups bound to the receptor and compared to the prob-

ability of simultaneous dissociation of all three functional groups. If, for example, the probability of dissociation of each functional group is 0.1, then for a ligand bound to a receptor with three point attachment the probability for dissociation of one of the three equivalent functional groups would be 0.243 while the probability for simultaneous dissociation of all three would be 0.001. As discussed below we propose that rebinding of individual functional groups plays an important role in determining antagonist dissociation kinetics.

For a flexible molecule like AP5 it is possible that following dissociation of the ω-phosphonate group, the methylene chain could flex and allow the ω-phosphonate group to move away from its binding site, leaving the α-amino and α-carboxylate groups still docked. This lower affinity intermediate could then either dissociate completely, or rebind the phosphonate group. It seems likely that for conformationally restricted antagonists like CGS 19755 and CGP 37849 there will be reduced opportunity for movement of the ω-phosphonate, and α-carbon amino and carboxylate groups relative to each other. Thus, following formation of lower affinity intermediates with only one or two functional groups bound, the closer proximity of the free functional groups to their binding sites in conformationally restricted antagonists would increase the probability of rebinding, and lower the probability for complete dissociation of the receptor-antagonist complex; hence k_{off} will be slow for conformationally restricted antagonists.

Differences in the association and dissociation rate constants of piperazine and piperidine analogues are consistent with the above hypothesis that molecular flexibility influences antagonist binding kinetics. The piperazine 4-atom separation analogue, D-CMP, shows significantly faster binding kinetics than CGS 19755, the corresponding piperidine (Table 3). We propose that protonation and deprotonation of the 4-position nitrogen in the piperazine ring allows the aliphatic phosphonate side-chain to flip *cis* and *trans* to the α-carboxylic acid group with very rapid kinetics. This would allow the piperazine antagonist to adopt rapidly the conformation required for binding, but would also be expected to allow faster dissociation; CGS 19755, the piperidine antagonist, which shows slower kinetics, is less flexible due to the fixed geometry of the aliphatic side chain at the 4-position carbon atom. In contrast, Table 4 shows that the 6-atom separation piperazine antagonists CPP and CPC have similar kinetics to their piperidine analogues LY 257883 and LY 221501. Equilibrium binding studies help to resolve this issue and reveal that while the *cis* and *trans* isomers of the 4-atom separation piperidine analogue CGS 19755 differ in potency approximately 14 fold, the *cis* and *trans* isomers of the 6-atom separation piperidine ω-phosphonates (i.e. LY 257883) are equipotent (Hutchison *et al.*, 1989). In addition, the *cis* and *trans* analogues of the piperidine D-CPP-ene are also equipotent (Hutchison *et al.*, 1989). This confirms that stereochemistry at the 4-position is critical for piperazine/piperidine structures with a methyl phosphonate side-chain (4-atom separation analogues), but not for their 6-atom separation counterparts. We interpret this as suggesting that the propyl phosphonate side-chain adds enough flexibility to mimic the effect of the 4-position nitrogen in piperazine structures and compensate for the 4 position stereochemistry.

In addition to conformational restriction, it is possible that antagonist binding kinetics are influenced by increases in entropy associated with binding 6- vs. 4-atom separation antagonists, and by differences in pK_a values for the individual functional groups present in these antagonists. The latter possibility is especially interesting since in AP7 the ω-phosphonate group is known to be only partially ionized at physiological pH (Bigge *et al.*, 1989; Chenard *et al.*, 1990). This raises the possibility that if there is a large difference in the affinity of antagonist molecules with one or two negative charges, calculation of the association rate constant for binding based on the total concentration of antagonist would give an artifically low estimate for k_{on}. This may explain the unusually low association rate constant for binding of phosphonates, compared to analogues containing ω-tetrazole or ω-carboxylate groups, which are fully ionized at physiological pH. In the case of AP5, assuming similar pK_a values measured for AP7, the corrected value for k_{on} would be $7.4 \times 10^7 M^{-1} s^{-1}$, close to the diffusion limit of $10^8 M^{-1} s^{-1}$ expected for low molecular weight ligands (Gutfreund, 1972). A comparable estimate has been obtained for the binding of acetylcholine to the nicotinic receptor at the frog neuromuscular junction, $9 \times 10^7 M^{-1} s^{-1}$ (Colquhoun & Ogden, 1988). The increase in k_{on} observed on introduction of an electron withdrawing double bond in *trans*-APPA and CPP-ene would be consistent with a lowering in pK_a of the ω-phosphonate group if $AP7^{2-}$ was the more active species. Experiments which measure the pH sensitivity of NMDA receptor antagonism should be able to confirm the above hypothesis, and are currently in progress.

An alternative model for NMDA receptor antagonism

The ratio k_{off}/k_{on} vs. K_i determined from equilibrium dose–response measurements was 0.67 ± 0.1 instead of 1, illustrating a systematic error in our method of analysis. To explore one possible source of this error, we developed a model for competitive antagonism in which there were two agonist binding sites, both required for activation of ion channel gating, and both of which could bind a molecule of antagonist, but with the restriction that following binding of one molecule of antagonist, steric occlusion by the antagonist prevents occupation of the second binding site by either agonist or antagonist:

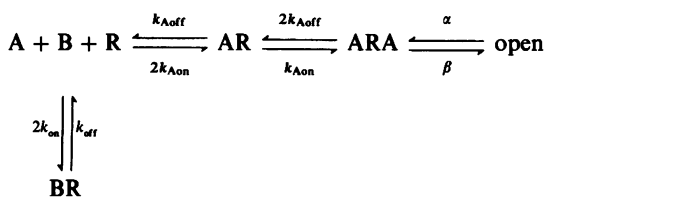

Kinetic and equilibrium experments for D-CPP-ene were reanalysed with this model. The goodness of fit of responses to concentration jump application of D-CPP-ene was similar to that obtained for the 2 agonist-2 antagonist binding site model described earlier, but yielded a 3.5 fold faster association rate constant ($1.7 \times 10^7 M^{-1} s^{-1}$); the dissociation rate constant, $0.62 s^{-1}$ was similar for both models (cf. Table 2). Determination of K_i from the ratio k_{off}/k_{on} yielded a value of 42 ± 16 nM, 3.8 fold higher affinity than the K_i determined with a two site model. Equilibrium dose-inhibition measurements were also well fit, but gave a K_i value of 91 ± 8 nM, 2.5 fold higher affinity than calculated with a two site model (Table 2). However, the ratio k_{off}/k_{on} vs. K_i determined from equilibrium dose-response measurements was 0.46 instead of 1, a larger discrepancy than obtained with the model used for analysis of the bulk of our experiments.

The higher affinity K_i estimates obtained with above model are in slightly better agreement with antagonist binding data, and this again raises the question as to which model is appropriate for analysis of NMDA receptor antagonism. Evidence for two glutamate binding sites on NMDA receptors, both required for activation of ion channel gating, was obtained from analysis of equilibrium dose-response curves (Patneau & Mayer, 1990), and from the kinetics of the response to concentration jump application of glutamate to outside out patches analysed by single channel recording (Clements & Westbrook, 1991). Traditionally it is assumed that competitive antagonists bind to the agonist recognition site; thus one predicts that the NMDA receptor will have at least two recognition sites for glutamate, both of which would be expected to bind competitive antagonists. However, as noted above, steric hinderance might prevent binding of a second antagonist molecule. This possibility is not supported by binding experiments, which

reveal a stoichiometry of 1 : 1 for glutamate and CPP (Thedinga *et al.*, 1989). Further resolution of this issue might occur when the agonist and antagonist binding sites on NMDA receptors are identified by biochemical or molecular biological techniques.

A final consideration of our data shows that although the estimates we obtain for k_{on}, k_{off} and K_i are model-dependent, genuine differences in binding kinetics must underlie the experimentally observed variation in the time course of response to concentration jump application of individual antagonists. As a result, although our estimates for k_{on} and k_{off} may be slightly in error, the analysis of structure-activity relationships described here is empirically correct, and provides insight into the influence of conformational restriction on NMDA receptor antagonist activity that could not have been obtained from equilibrium measurements alone.

The experiments described would not have been possible without the generous gifts of compounds by Drs C. Angst; D. Bennett; S. Borosky G. Fagg; J. Ferkany; P. Herrling; G. Johnson; P. Ornstein; and J.C. Watkins. We thank C. Winters for preparation of cultures. The numerical simulation programme was written by Dr J. Clements. We are especially indebted to Dr P. Ornstein and Professor J.C. Watkins for many helpful discussions. M.B. is an N.R.C. research fellow.

References

AEBISCHER, B., FREY, P., HAERTER, H.P., HERRLING, P., MUELLER, W., OLVERMAN, H.J. & WATKINS, J.C. (1989). Synthesis and NMDA antagonistic properties of the enantiomers of 4-(3-phosphonopropyl)piperazine-2-carboxylic acid (CPP) and of the unsaturated analogue (E)-4-(3-phosphonoprop-2-enyl)piperazine-2-carboxylic acid (CPP-ene). *Helv. Chim. Acta*, **72**, 1043–1051.

ARMSTRONG, D.L. & LESTER, H.A. (1979). The kinetics of tubocurarine action and restricted diffusion within the synaptic cleft, *J. Physiol.*, **294**, 365–386.

BENVENISTE, M. & MAYER, M.L. (1991). A kinetic analysis of antagonist action at NMDA receptors: two binding sites each for glutamate and glycine. *Biophys. J.*, **59**, 560–573.

BENVENISTE, M., MIENVILLE, J.M., SERNAGOR, E. & MAYER, M.L. (1990). Concentration jump experiments with NMDA antagonists in mouse cultured hippocampal neurones. *J. Neurophysiol.*, **63**, 1373–1384.

BIGGE, C.F., DRUMMOND, J.T. & JOHNSON, G. (1989). Synthesis and NMDA receptor binding of 2-amino-7,7-difluoro-7-phosphonoheptanoic acid. *Tetrahedron Lett.*, **30**, 7013–7016.

CHENARD, B.L., LIPINSKI, C.A., DOMINY, B.W., MENA, E.E., RONAU, R.T., BUTTERFIELD, G.C., MARINOVIC, L.C., PAGNOZZI, M., BUTLER, T.W. & TZANG, T. (1990). A unified approach to systematic isosteric substitution for acidic groups and application to NMDA antagonists related to 2-amino-7-phosphonoheptanoate. *J. Med. Chem.*, **33**, 1077–1083.

CHENG, Y.C. & PRUSSOFF, W.H. (1973). Relationship between the inhibition constant (K_i) and the concentration of inhibitor which causes 50 per cent inhibition (I_{50}) of an enzymatic reaction. *Biochem. Pharmacol.*, **22**, 3099–3108.

CHOI, D.W. (1990). Cerebral hypoxia: some new approaches and unanswered questions. *J. Neurosci.*, **10**, 2493–2501.

CLEMENTS, J.D. & WESTBROOK, G.L. (1991). Activation kinetics used to determine number of binding sites on the NMDA channel. *Biophys. J.*, **59**, 353a.

COLQUHOUN, D. & OGDEN, D.C. (1988). Activation of ion channels in the frog end-plate by high concentrations of acetylcholine. *J. Physiol.*, **395**, 131–159.

COLLINGRIDGE, G.L. & LESTER, R.A.J. (1989). Excitatory amino acid receptors in the vertebrate central nervous system. *Pharmacol. Rev.*, **40**, 143–210.

DAVIES, J. & WATKINS, J.C. (1982). Actions of D and L forms of 2-aminophosphonovalerate and 2-amino-4-phosphonobutyrate in the cat spinal cord. *Brain Res.*, **235**, 378–386.

EVANS, R.H., FRANCIS, A.A., JONES, A.W., SMITH, D.A.S. & WATKINS, J.C. (1982). The effects of a series of ω-phosphonic α-carboxylic amino acids on electrically evoked and excitant amino-induced responses in isolated spinal cord preparations. *Br. J. Pharmacol.*, **75**, 65–75.

FAGG, G.E., OLPE, H.-R., POSSA, M.F., BAUD, J., STEINMANN, M., SCHMULTZ, M., PORTET, C., BAUMANN, P., THEDINGA, K., BITTIGER, H., ALLGEIER, H., HECKENDORN, R., ANGST, C., BRUNDISH, D. & DINGWALL, J.G. (1990). CGP 37849 and CGP 39551: novel and potent competitive N-methyl-D-aspartate receptor antagonists with oral activity. *Br. J. Pharmacol.*, **99**, 791–797.

FERKANY, J.W., KYLE, D.J., WILLETS, J., RZESZOTARSKI, W.J., GUZEWSKA, M.E., ELLENBERGER, S.R., JONES, S.M., SACAAN, A.I., SNELL, L.D., BOROSKY, S., JONES, B.E., JOHNSON, K.M., BALSTER, R.L., BURCHETT, K., KAWASAKI, K., HOCH, D.B. & DINGLEDINE, R. (1989). Pharmacological profile of NPC 12626, a novel, competitive N-methyl-D-aspartate receptor antagonist. *J. Pharmacol. Exp. Ther.*, **250**, 100–109.

GUTFREUND, H. (1972). *Enzymes: Physical Principles*. p. 159. London: Wiley Interscience.

HARRISON, N.L. & SIMMONDS, M.A. (1985). Quantitative studies on some antagonists of N-methyl-D-aspartate in slices of rat cerebral cortex. *Br. J. Pharmacol.*, **84**, 381–391.

HAYS, S.J., BIGGE, C.F., NOVAK, P.M., DRUMMOND, J.T., BOBOVSKI, T.P., RICE, M.J., JOHNSON, G., BRAHCE, L.J. & COUGHENOUR, L.L. (1990). New and versatile approaches to the synthesis of CPP-related competitive NMDA antagonists. Preliminary structure-activity relationships and pharmacological evaluation. *J. Med. Chem.*, **33**, 2916–2924.

HENDERSON, G., JOHNSON, J.W. & ASCHER, P. (1990). Competitive antagonists and partial agonists at the glycine modulatory site of the mouse N-methyl-D-aspartate receptor. *J. Physiol.*, **430**, 189–212.

HONORÉ, T., DAVIES, S.N., DREJER, J., FLETCHER, E.J., JACOBSEN, P., LODGE, D. & NIELSEN, F.E. (1988). Quinoxalinediones: potent competitive non-NMDA glutamate receptor antagonists. *Science*, **241**, 701–703.

HEUTTNER, J.E. & BEAN, B.P. (1988). Block of N-methyl-D-aspartate-activated current by the anticonvulsant MK-801; selective binding to open channels. *Proc. Natl. Acad. Sci. U.S.A.*, **85**, 1307–1311.

HUTCHISON, A.J., WILLIAMS, M., ANGST, C., DE JESUS, R., BLANCHARD, L., JACKSON, R.H., WILUSZ, E.J., MURPHY, D.E., BERNARD, P.S., SCHNEIDER, J., CAMPBELL, T., GUIDA, W. & SILLS, M.A. (1989). 4-(phosphonoalkyl)- and 4-(phosphonoalkenyl)-2-piperidinecarboxylic acids: synthesis, activity at N-methyl-D-aspartic acid receptors, and anticonvulsant activity. *J. Med. Chem.*, **32**, 2171–2178.

LONG, S.K., SMITH, D.A.S., SIAREY, R.J. & EVANS, R.H. (1990). Effect of 6-cyano-2,3-dihydroxy-7-nitro-quinoxaline (CNQX) on dorsal root-, NMDA-, kainate- and qusiqualate-mediated depolarization of rat motoneurons *in vitro*. *Br. J. Pharmacol.*, **100**, 850–854.

MACDONALD, J.F., MILJKOVIC, Z. & PENNEFATHER, P. (1987). Use-dependent block of excitatory amino acid currents in cultured neurons by ketamine. *J. Neurophysiol.*, **58**, 251–266.

MAYER, M.L., VYKLICKY JR, L. & CLEMENTS, J. (1989a). Regulation of NMDA receptor desensitization in mouse hippocampal neurons by glycine. *Nature*, **338**, 425–427.

MAYER, M.L., VYKLICKY JR, L. & WESTBROOK, G.L. (1989b). Modulation of excitatory amino acid receptors by group IIB metal cations in cultured mouse hippocampal neurons. *J. Physiol.*, **415**, 329–350.

MELDRUM, B.S., CHAPMAN, A.G., PATEL, S. & SWAN, J. (1989). Competitive NMDA antagonists as drugs. in *The NMDA Receptor*. ed. Watkins, J.C. & Collingridge, G.L. pp. 207–216. Oxford: Oxford University Press.

MONAGHAN, D.T., OLVERMAN, H.L., NGUYEN, L., WATKINS, J.C. & COTMAN, C.W. (1988). Two classes of N-methyl-D-aspartate recognition sites: differential distribution and differential regulation by glycine. *Proc. Natl. Acad. Sci. U.S.A.*, **85**, 9836–9840.

MURPHY, D.E., HUTCHISON, A.J., HURT, S.D. & SILLS, M.A. (1988). Characterisation of the binding of [^{3}H]-CGS 19755: a novel N-methyl-D-aspartate antagonist with nanomolar affinity in rat brain. *Br. J. Pharmacol.*, **95**, 932–938.

OLVERMAN, H.J., JONES, A.W., MEWETT, K.N. & WATKINS, J.C. (1988). Structure/activity relations of N-methyl-D-aspartate receptor ligands as studied by their inhibition of [^{3}H]D-2-amino-5-phosphonopentanoic acid binding in rat brain membranes. *Neuroscience*, **26**, 17–31.

OLVERMAN, H.J. & WATKINS, J.C. (1989). NMDA agonists and com-

petitive antagonists. In *The NMDA Receptor*. ed. Watkins, J.C. & Collingridge, G.L. pp. 19–36. Oxford: Oxford University Press.

ORNSTEIN, P.L., SCHAUS, J.M., CHAMBERS, J.W., HUSER, D.L., LEANDER, J.D., WONG, D.T., PASCHAL, J.W., JONES, N.D. & DETTER, J.B. (1989). Synthesis and pharmacology of a series of 3- and 4-(phosphonoalkyl)pyridine- and piperidine-2-carboxylic acids. Potent N-methyl-D-aspartate receptor antagonists. *J. Med. Chem.*, **32**, 827–833.

ORNSTEIN, P.L., SCHOEPP, D.D., LEANDER, J.D. & LODGE, D. (1991). The development of novel competitive NMDA antagonists as useful therapeutic Agents. Discovery of LY 274614 and LY 233536. In *Excitatory Amino Acids*. ed. Meldrum, B.S., Moroni, F., Simon, R.P. & Woods, J.H. New York: Raven Press, (in press).

PATNEAU, D.K. & MAYER, M.L. (1990). Structure-activity relationships for amino acid transmitter candidates acting at N-methyl-D-aspartate and quisqualate receptors. *J. Neurosci.*, **10**, 2385–2399.

RANG, H.P. (1966). The kinetics of action of acetylcholine antagonists in smooth muscle. *Proc. R. Soc. B*, **164**, 488–510.

SERNAGOR, E., KUHN, D., VYKLICKY, L. & MAYER, M.L. (1989). Open channel block of NMDA receptor responses evoked by tricyclic antidepressants. *Neuron*, **2**, 1221–1227.

SIMON, R.P., SWAN, J.H., GRIFFITHS, T. & MELDRUM, B.S. (1984). Blockade of N-methyl-D-aspartate receptors may protect against ischemic damage in the brain. *Science*, **226**, 850–852.

THEDINGA, K.H., BENEDICT, M.S. & FAGG, G.E. (1989). The N-methyl-D-aspartic acid (NMDA) receptor complex: a stoichiometric analysis of radioligand binding domains. *Neurosci. Lett.*, **104**, 217–222.

ULBRICHT, W. (1981). Kinetics of drug action and equilibrium results at the node of Ranvier. *Physiol. Rev.*, **61**, 785–828.

VERDOORN, T.A. & DINGLEDINE, R. (1988). Excitatory amino acid receptors expressed in *Xenopus* oocytes: agonist pharmacology. *Mol. Pharmacol.*, **34**, 298–307.

VERDOORN, T.A., KLECKNER, N.W. & DINGLEDINE, R. (1989). N-methyl-D-aspartate/glycine and quisqualate/kainate receptors expressed in *Xenopus* oocytes: antagonist pharmacology. *Mol. Pharmacol.*, **35**, 360–368.

VYKLICKY JR. L., BENVENISTE, M. & MAYER, M.L. (1990). Modulation of N-methyl-D-aspartic acid receptor desensitization by glycine in cultured mouse hippocampal neurones. *J. Physiol.*, **428**, 313–331.

(Received February 26, 1991
Revised May 8, 1991
Accepted May 9, 1991)

Br. J. Pharmacol. (1991), **104**, 222–226

Effects of Ca^{2+} antagonists on glutamate release and Ca^{2+} influx in the hippocampus with *in vivo* intracerebral microdialysis

[1]Y. Ming Lu, *J. Tian Zhang, F. Qing Zhao & Y. Fi Qin

Department of Molecular Pharmacology, Naval Neurobiology Research Centre, China Naval Medical College, Nanjing, 210049, China and *Institute of Materia Medica, Chinese Academy of Medical Sciences, Beijing 100050, China

1 The extracellular glutamate content and Ca^{2+} level *in vivo* in rat hippocampus were measured by brain microdialysis following administration of two depolarizing agents (veratridine, KCl) and quinolinic acid (Quin).

2 The two depolarizing agents increased the extracellular glutamate level (to between 280 and 320% basal) and decreased the extracellular Ca^{2+} content (to 48% of basal). However, Quin did not change the glutamate level but decreased the Ca^{2+} content.

3 The effects of Ca^{2+} antagonists on the changes of glutamate and Ca^{2+} level were evaluated in this experimental model. At a dose of 0.5 mg kg^{-1}, i.v., nimodipine (L-type channel blocker) did not produce significant changes in the stimulated-glutamate release. A statistically significant inhibition of Ca^{2+} influx was observed at a dose of 0.05 mg kg^{-1}. In contrast, in those animals receiving the N-type Ca^{2+} antagonist, daurisoline (0.1, 1 or 5 mg kg^{-1}, i.v.), a potent attenuation of both glutamate release and Ca^{2+} influx was found.

4 We propose that the pharmacological properties of Ca^{2+} influx and of neurotransmitter release differ and that nimodipine-sensitive L-type channels may not be very common in nerve terminals but are localized in cell soma. Daurisoline-sensitive N-type channels in nerve terminals have a much greater influence on excitatory amino acid release.

Keywords: Glutamate release; Ca^{2+} influx; multiple Ca^{2+} channels; depolarizing agents; quinolinic acid; nimodipine; daurisoline; intracerebral microdialysis

Introduction

The indispensible role of Ca^{2+} in the release of neurotransmitters is well established. Experimental evidence from various sources has indicated that neurones and other excitable cells may possess several types of voltage-sensitive calcium channels (VSCC) (Carbone & Lux, 1984; Nowycky *et al.*, 1985a). These channels can be distinguished by their biophysical characteristics and also by their sensitivity to drugs, hormones, and toxins (Triggle & Rampe, 1989). One type of VSCC has been characterized in several different tissues by its sensitivity to dihydropyridine drugs (Freedman & Miller, 1984; Miller & Freeman, 1984; Nowycky *et al.*, 1985b). A subject of great current interest is the elucidation of the pharmacological properties of both dihydropyridine-sensitive (L-type channel) and dihydropyridine-insensitive (N-type channels) VSCC. In neurones, a major function of VSCC is to provide Ca^{2+} for triggering the release of neurotransmitters (stimulus-secretion coupling). The evoked release of neurotransmitters from neurones has generally proved to be insensitive to dihydropyridine (Miller & Freedman, 1984). Although transmitter release in general is dihydropyridine-insensitive, high-affinity dihydropyridine binding has been demonstrated on neurones (Miller, 1987). Such observations have produced some confusion and clearly the functions of dihydropyridine-sensitive VSCC in neurones remain to be elucidated. To define further the roles of the various VSCC in neurones, we used brain microdialysis procedure to analyse the effects of an L-type Ca^{2+} channel blocker (nimodipine) and an N-type Ca^{2+} channel antagonist (daurisoline) on transmitter release and Ca^{2+} influx.

[1] Author for correspondence.

Methods

Implantation procedure

Male Sprague-Dawley rats (220–250 g) were used. The animals were placed in a Stoelting stereotoxic apparatus under chloral hydrate (360 mg kg^{-1}, i.p.) anaesthesia. The fibre unit used in the present study was set up as previously described (MacDermott *et al.*, 1986). A single fibre (molecular cut-off 15,000; internal diameter 220 μm; external diameter 310 μm) was straightened with a fine wire inserted through its lumen then bent into a loop. Fast-drying glue was spread over the surface of the fibre except on a 4 mm portion at the tip of the loop, to allow exchange with tissue. Before implantation, each probe was flushed through with distilled water for 15 min (2 μl min^{-1}) and examined microscopically to ensure that there were no leaks. The completed fibre was then unilaterally implanted into the dorsal hippocampus. The coordinates for implantation were 3.5 mm posterior to bregma, 2.6 mm lateral to the midline, and 2.9 mm below dura. The fibre was fixed to the skull with dental acrylic.

In vitro *recovery*

Recovery of glutamate and Ca^{2+} from standard solutions. The tips of the dialysis probes were immersed in 2 ml nominally Ca^{2+}-free Krebs-Ringer Bicarbonate (KRB, composition in mM: NaCl 122, KCl 3, $MgSO_4$ 1.2, KH_2PO_4 0.4 and $NaHCO_3$ 25) and placed in a solution of KRB containing $CaCl_2$ (0.5 mM), glutamate (10 μM) at a flow rate of 2 μl min^{-1}, consecutive six 15 min samples of perfusate were collected. The average recovery of glutamate and Ca^{2+} was determined by use of 3 different fibre units. After 60 min perfusion in KRB + 1 mM $CaCl_2$ and 100 μM glutamate, the fibre was

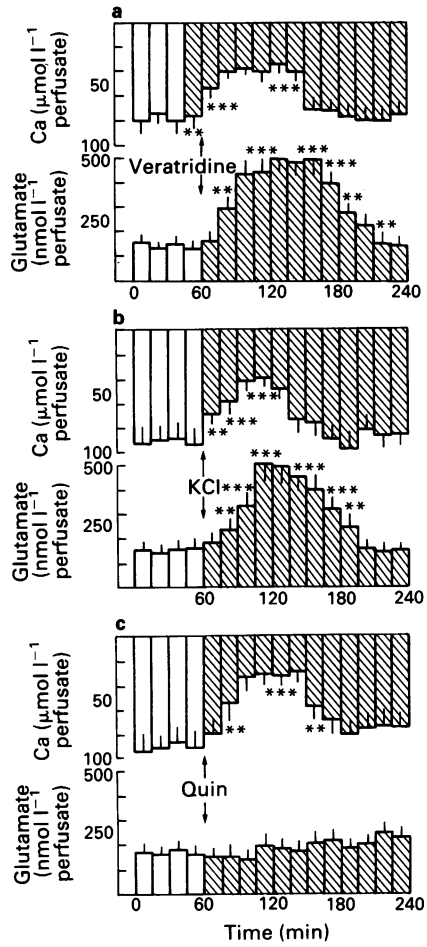

Figure 1 Time-course changes in the perfusate levels of Ca and glutamate from rat hippocampus perfused unilaterally with veratridine (a), KCl (b) and quinolinic acid (Quin, c). Hippocampus dialysis samples were collected at 15-min intervals, before (open colums, basal level) and after (hatched columns) the perfusion of veratridine (0.1 mM), KCl (75 mM) and Quin (80 mM) through the fibre for 60 min (veratridine, 7 rats) and (KCl, 7 rats) and for 30 min (Quin, 7 rats). The data are presented as mean with s.e.mean shown by vertical bars. A typical example of Ca decrease relative to glutamate changes. The arrows indicate time of the perfusion of stimulants. $^{**}P < 0.05$, $^{***}P < 0.01$ vs basal level. Dunnett's two-tailed test.

placed in KRB solution containing 0.5 mM $CaCl_2$ and 10 μM glutamate for 60 min and then again in KRB + 1 mM $CaCl_2$ and 100 μM glutamate for another 60 min. This enabled us to check for fibre unit delay in detecting sudden changes in glutamate and Ca^{2+} concentrations of the extracellular compartment.

In vivo *perfusion*

The conscious rats with the unilaterally implanted fibre, the day after surgery, were simultaneously perfused at a constant rate of 2 μl min^{-1} with KRB, pH 7.4, for measurement of glutamate release, or with KRB nominally Ca^{2+}-free, for determination of Ca^{2+} influx. Fifth min perfusates were collected after 45 min washout. Extracellular Ca^{2+} and glutamate enter the fibre lumen by difference of concentration until equilibrium is reached between two compartments. Changes in the glutamate release and Ca^{2+} influx are then reflected in the Ca^{2+} and glutamate levels of the perfusates. To establish a stable baseline, samples were collected for 60 min before pharmacological treatments; then samples were collected for a minimum of 180 min.

Drug treatment

The drugs were dissolved in vehicles given in parentheses. Collection proceeded for 60 min to determine basal levels of glutamate and Ca^{2+} before the application of drugs in the superfusion stream. After the basal collection period, veratridine (0.1 mM in KRB), quinolinic acid (Quin) (80 mM in KRB) and KCl (75 mM in KRB) were applied through the fibre for 60 min (veratridine, 6–9 rats), 60 min (KCl, 6–8 rats), or 30 min (quinolinic acid, 6–9 rats) to measure the changes of glutamate and Ca^{2+} stimulated by these agents. In the other experiments, specified doses of nimodipine (in propylene glycol) and daurisoline (in propylene glycol) were applied i.v. for 15 min before administration of veratridine, Quin or KCl, to study the direct effects of the drugs on the changes in glutamate and Ca^{2+} induced by these agents.

Glutamate determination

Glutamate was measured by high performance liquid chromatography (h.p.l.c.) after automatic precolumn derivatization with *O*-phthaldialdehyde (OPA) according to the method of Lindroth & Mopper (1979). Thirty μl of the perfusate was mixed with 30 μl of an OPA solution (5.4 mg ml^{-1}) and the reaction product was injected onto a Waters Nucleosil RP-18 h.p.l.c. column 2 min later. The fluorescent reaction products were eluted over a period of 25 min with a mobile phase consisting of 0.1 M citrate: 0.1 M phosphate (4 : 1) buffer, pH 7.0 and methanol (30–70% at a flow rate of 1 ml min^{-1}). The effluent was monitored fluorimetrically (Waters Fluorescence Detector 420 AC) and the data recorded and computed.

Ca^{2+} measurement

Ca^{2+} was measured in an Automatic Atomic Absorption Spectrophotometer (Model GBC 908 AA): 30 μl of the perfusate was added to 1% HCl (70 μl) and the mixed perfusate injected into the meter, the data recorded and computed.

Histological analysis

Animals were killed after perfusion. The correct position of the fibre in the dorsal hippocampus was verified in every animal during histological assessments. Only animals with the probe in the correct position were used for the statistical analysis.

Statistical analysis

The results were calculated as concentration of glutamate (nmol l^{-1} perfusate) and Ca^{2+} (μmol l^{-1} perfusate). The mean values at each time after drug treatment were compared with the basal level, which was the average of 6–9 samples collected immediately preceding drug application. Significant differences were determined by Dunnett's two-tailed test for multiple comparisons and by the non-parametric Mann-Whitney U-test.

Quin and veratridine were obtained from Sigma Chemical Co (St Louis, MO, U.S.A.). Nimodipine was kindly provided by Tanjing Institute of Pharmaceuticals. Daurisoline was obtained from the Department of Medical Chemistry, China Pharmaceutical University. OPA was purchased from Pierce Chemical Co (Rockford IL, U.S.A.).

Results

In vitro *recovery*

By dialysis 12 ± 1.2% of Ca^{2+} and 27.8 ± 1.9% of glutamate were recovered, expressing the mean concentration in the perfusate as a percentage of the concentration of the solution outside the tube. A decrease or increase in Ca^{2+} and glutamate concentration of the external medium was proportion-

Table 1 Effects of nimodipine and daurisoline on the glutamate release caused by veratridine (0.1 mM) infused into rat hippocampus

Drug (mg kg^{-1})	*Basal level* (nM)	*Veratridine* (nM)	*Stim − Basal* (nM)	% *inhibition*
Nimodipine (0.5)	156.4 ± 13.3 (9)	499.2 ± 47.1 (7)	342.8 ± 21.2	
Nimodipine (0.5)	150.0 ± 13.6 (7)	483.4 ± 44.2 (6)	333.4 ± 19.4	
Daurisoline (0.5)	153.3 ± 12.9 (8)	409.6 ± 39.8 (6)**	256.3 ± 13.1	25
(1)	149.5 ± 11.3 (7)	297.6 ± 23.3 (8)***	148.1 ± 9.9	57
(5)	149.2 ± 11.9 (9)	173.4 ± 15.2 (5)***	24.2 ± 2.3	93

Data represent mean and s.e.mean of glutamate (nM) in each 15-min fraction (100–115 min after beginning of perfusion). Veratridine (0.1 mM) was perfused through the fibre for 60 min. Nimodipine and daurisoline were administered i.v. 15 min before the perfusion of veratridine.
**$P < 0.05$, ***$P < 0.1$ vs control alone with Mann-Whitney U-test. The number of animals are given in parentheses.
Stim − Basal was calculated as difference between basal level and veratridine-treated. % inhibition = [1 − (Stim − Basal (Drug))/ Stim − Basal (Control)].

ally reflected in the Ca^{2+} content and glutamate levels of the perfusates in the second 15-min sample collected after changing the solution.

Effects of depolarizing agents and quinolinic acid on control levels of extracellular glutamate in hippocampus dialysates

The basal level of glutamate in hippocampus from the four fractions was 156.8 ± 14.4 nM (mean ± s.e.mean, $n = 7$). The effects of veratridine, KCl and Quin on the extracellular glutamate level are illustrated in Figure 1. When compared with the basal level of glutamate, veratridine and KCl caused a substantial (280–320% of the basal) increase in glutamate level. The glutamate concentration in the perfusate reached a maximum within the 100 min following perfusion of veratridine or KCl and returned to basal over the next 240 min (Figure 1). No significant changes in the glutamate level following perfusion of Quin were detected.

Effects of veratridine, KCl and quinolinic acid on control level of extracellular Ca^{2+} in hippocampus dialysates

A typical example of Ca^{2+} changes relative to glutamate changes is presented in Figure 1. A decrease in Ca^{2+} (40–50% of basal) followed administration of veratridine, KCl and Quin. In particular, glutamate release occurred only following veratridine and KCl but not following Quin. Thus, a clear dissociation between neutrotransmitter release and Ca^{2+} influx was demonstrated.

Effects of nimodipine and daurisoline on evoked changes in extracellular glutamate in hippocampus perfusates

Nimodipine was administered i.v. at increasing doses of 0.05, 0.1 and 0.5 mg kg^{-1} to study the direct effects of the drug on stimulated glutamate release. At all these doses, nimodipine did not produce significant changes in the stimulated glutamate release by depolarizing agents (Tables 1 and 2). In the animal group treated with daurisoline 0.5 mg kg^{-1}, glutamate

Table 2 Effects of nimodipine and daurisoline on the glutamate release caused by KCl (75 mM) infused into rat hippocampus

Drug (mg kg^{-1})	*Basal level* (nM)	KCl (nM)	*Stim − Basal* (nM)	% *inhibition*
Control	156.4 ± 13.3 (9)	443.7 ± 39.8 (7)	287.3 ± 26.5	
Nimodipine (0.5)	150.0 ± 13.6 (7)	456.5 ± 41.0 (6)	306.5 ± 32.1	
Daurisoline (0.5)	153.3 ± 12.9 (8)	386.2 ± 32.4 (6)**	232.9 ± 18.7	19
(1)	149.5 ± 11.3 (7)	277.7 ± 20.1 (8)***	128.2 ± 9.8	55
(5)	149.2 ± 11.9 (9)	169.6 ± 14.9 (5)***	20.4 ± 8.1	93

Data represent mean and s.e.mean of glutamate concentration (nM) in each 15-min fraction (100–115 min after beginning of perfusion). KCl (75 mM) was perfused through the fibre for 60 min. Nimodipine and daurisoline were administered i.v. 15 min before the perfusion of KCl.
**$P < 0.05$, ***$P < 0.01$ vs control alone, Mann-Whitney U-test. The number of animals are given in parentheses.
Stim − Basal was calculated as difference between basal level and KCl-treated. % inhibition = [− (Stim − Basal (Drug))/ Stim-basal (Control)].

Table 3 Effects of nimodipine and daurisoline on decrease in extracellular Ca^{2+} caused by veratridine (0.1 mM) infused into rat hippocampus

Drug (mg kg^{-1})	*Basal level* (μM)	*Veratridine* (μM)	*Stim − Basal* (μM)	% *inhibition*
Control	91.2 ± 8.7 (9)	48.8 ± 3.9 (7)	−42.4 ± 3.2	
Nimodipine (0.05)	92.0 ± 7.9 (7)	57.8 ± 6.2 (6)**	−34.2 ± 2.9	19
(0.1)	90.9 ± 7.9 (8)	68.1 ± 7.1 (6)**	−22.8 ± 1.4	46
(0.5)	89.0 ± 8.1 (7)	76.5 ± 7.1 (8)***	−12.5 ± 0.9	71
Daurisoline (5)	90.9 ± 9.0 (9)	68.4 ± 6.9 (5)***	−22.5 ± 2.1	47

Data represent mean and s.e.mean of Ca^{2+} concentration (μM) in each 15-min fraction (100–115 min after beginning of perfusion). Veratridine (0.1 mM) was perfused through the fibre for 60 min. Nimodipine and daurisoline were administered i.v., 15 min before the perfusion of veratridine.
**$P < 0.05$; ***$P < 0.01$ vs control alone, Mann-Whitney U-test. Number of animals are given in parentheses.
Stim − Basal was calculated as difference between basal level and veratridine-treated. % inhibition = [1 − (Stim − Basal (Drug)/ Stim − Basal (Control)].

release induced by veratridine was significantly reduced (inhibition = 25%, $n = 6$) and KCl-stimulated glutamate release was also blocked (inhibition = 19%, $n = 6$). This effect was even more evident in $5\,mg\,kg^{-1}$ reaching an almost complete suppression of glutamate release induced by veratridine and KCl, respectively (inhibition = 93%, $n = 5$).

Effects of nimodipine and daurisoline on the stimulant-induced decrease in extracellular Ca^{2+}

Tables 3, 4 and 5 show that Ca^{2+} decreases induced by veratridine, KCl and Quin were antagonized by nimodipine ($0.05\,mg\,kg^{-1}$). The percentage inhibition was 19 ($n = 6$), 11 ($n = 6$) and 44 ($n = 6$), respectively. A marked blockade of Ca^{2+} decrease by nimodipine ($0.5\,mg\,kg^{-1}$) was observed (inhibition = 71% ($n = 7$), 71% ($n = 7$), and 92 ($n = 8$), respectively). Veratridine-, KCl- and Quin-stimulated falls in extracellular Ca^{2+} were also prevented by $5\,mg\,kg^{-1}$ of daurisoline (inhibition = 47%, $n = 5$; 39%, $n = 5$ and 64%, $n = 5$, respectively). Neither nimodipine nor daurisoline modified the basal Ca^{2+} level.

Discussion

In the present study, 'brain dialysis' enabled us to measure the extracellular Ca^{2+} changes and transmitter (glutamate) release caused in the hippocampus of a conscious animal by two depolarizing agents (veratridine, KCl) and one excitotoxin (Quin). Our experimental approach does not provide direct evidence of whether Ca^{2+} leaving the extracellular space (reflected in a drop in the ion concentration of the perfusate) enters the intraneuronal compartment. However, most studies have shown that veratridine and KCl-activation raises the cytoplasmic Ca^{2+} concentration in nerve terminals and cell soma (Norris & Bradford, 1985; Mody & Heinemann, 1986) and Ca^{2+} influx stimulated by veratridine and KCl proved to be mediated by VSCC (Nachshen & Blaustein, 1979). Moreover, Ca^{2+} influx by glial cells is not an important site for Ca^{2+} fluxes induced by these depolarizing agents and excitotoxins (Kelly & Krnjevic, 1967; Bowman & Kimelberg, 1984).

A comparative analysis of Ca^{2+} content in brain perfusate and glutamate release at the various times after veratridine or KCl administration showed a close temporal correlation between Ca^{2+} changes and glutamate release. The present data may suggest that an inward Ca^{2+} current is important for triggering glutamate release, although a cause-and-effect relationship cannot be established.

In studies conducted *in vitro*, daurisoline was found to block N-type Ca^{2+} channels selectively (Lu & Liu 1990a, b). In these studies, we had analyzed the depolarization-induced 'fast' phase ^{45}Ca influx into synaptosomes using the same conditions as had been employed in the [^{3}H]-γ-aminobutyric acid release studies. We observed that 'fast' Ca^{2+} influx coupled to neurotransmitter release was potently blocked by daurisoline (IC_{50} 10^{-6} M) but not by nitrendipine. Daurisoline is also less active at L-type channels of smooth muscle cells. More recently, electrophysiological studies (patch clamp) showed that daurisoline inhibited the second inactivating phase of the Ca^{2+} current during strong depolarization in chick dorsal root ganglion (unpublished data). This component of Ca^{2+} current was operated by N-type channels. The ability of daurisoline, which blocked N-type channels, to prevent the fall in Ca^{2+} and glutamate release further suggested that Ca^{2+} influx induced by the agents may be closely involved in the mechanism underlying glutamate release. The inability of Quin, a stimulator of Ca^{2+} influx, to increase glutamate release further suggested that Ca^{2+} influx induced by Qin mainly occurs through VSCC activated by Na^+ entry in nerve cell soma, not in nerve terminals.

The ability of nimodipine to prevent the fall in Ca^{2+} may be the same mechanisms as for Mg^{2+}. Exposure to excess Quin, a potent agonist acting at NMDA receptors, can destroy neurones in the central nervous system and may be responsible for some neurological diseases (i.e. seizures) (Vezzani & Wu, 1988). In this study, we also observed changes

Table 4 Effects of nimodipine and daurisoline on decrease in extracellular Ca^{2+} caused by KCl infused into rat hippocampus

Drug ($mg\,kg^{-1}$)	*Basal level* (μM)	*KCl* (μM)	*Stim − Basal* (μM)	*% inhibition*
Control	91.2 ± 8.7 (9)	56.4 ± 4.3 (7)	−34.8 ± 2.9	
Nimodipine (0.05)	92.0 ± 7.9 (7)	61.0 ± 6.9 (6)**	−31.0 ± 2.3	11
(0.1)	90.9 ± 7.9 (8)	72.3 ± 7.5 (6)**	−18.6 ± 1.1	47
(0.5)	89.0 ± 8.1 (7)	79.0 ± 8.2 (8)***	−10.0 ± 0.9	71
Daurisoline (5)	90.9 ± 9.0 (9)	69.6 ± 7.1 (5)**	−21.3 ± 1.9	39

Data represent mean and s.e.mean of Ca^{2+} concentration (μM) in each 15-min fraction (100–115 min after beginning of perfusion). KCl (75 mM) was perfused through the fibre for 60 min. Nimodipine and daurisoline were administered i.v. 15 min before the perfusion of KCl.
**$P < 0.05$; ***$P < 0.01$ vs control alone, Mann-Whitney U-test. Number of animals are given in parentheses.
Stim − Basal was calculated as difference between basal level and KCl-treated. % inhibition = [1 − (Stim − Basal (Drug))/ Stim − Basal (Control)].

Table 5 Effects of nimodipine and daurisoline on decrease in extracellular Ca^{2+} caused by quinolinic acid (Quin) infused into rat hippocampus

Drug ($mg\,kg^{-1}$)	*Basal level* (μM)	*Quin* (μM)	*Stim − Basal* (μM)	*% inhibition*
Control	91.2 ± 8.7 (9)	42.2 ± 3.0 (7)	−49.0 ± 3.8	
Nimodipine (0.05)	92.0 ± 7.9 (7)	64.8 ± 5.6 (6)**	−27.2 ± 1.9	44
(0.1)	90.9 ± 7.9 (8)	79.7 ± 8.1 (6)***	−11.2 ± 0.8	77
(0.5)	89.0 ± 8.1 (7)	85.0 ± 8.6 (8)***	−4.0 ± 0.2	92
Daurisoline (5)	90.9 ± 9.0 (9)	73.4 ± 7.4 (5)***	−17.5 ± 1.1	64

Data represent mean and s.e.mean of Ca^{2+} concentration (μM) in each 15-min fraction (100–115 min after beginning of perfusion). Quin (80 mM) was perfused through the fibre for 30 min. Nimodipine and daurisoline were administered i.v., 15 min before the perfusion of Quin.
**$P < 0.05$, ***$P < 0.01$ vs control alone, Mann-Whitney U-test. Number of animals are given in parentheses.
Stim − Basal was calculated as difference between basal level and Quin-treated. % inhibition = [1 − (Stim − Basal (Drug))/ Stim − Basal (Control)].

in animal behaviour induced by Quin. The animals presented episodes of tonic rotation of the head, associated with chewing movements. This abnormal animal behaviour was completely blocked by nimodipine ($0.5\,mg\,kg^{-1}$) but not by daurisoline. In fact, we recently reported an antiepileptic effect of nimodipine on excitatory amino acid-induced seizures. The mechanisms involved blocking Ca^{2+} influx into neurones (Lu *et al.*, 1990). This may form the basis of seizures induced by Quin. Therefore, Ca^{2+} channels in cell soma rather than in nerve terminals were responsible for this disorder, because nimodipine can inhibit Quin-induced seizures (Morocutt *et al.*, 1986; Lu *et al.*, 1990). In these studies, no correlations were found between blocking Ca^{2+} influx and seizures induced by Quin, even with large doses of daurisoline. The explanation for this result is that the inhibition of Ca^{2+} influx by daurisoline here, as a consequence of antagonizing Quin-stimulated protein kinase C (CPK) (Lu & Zhao, 1991), did not directly block the VSCC in soma. This did not sufficiently block the excess Ca^{2+} influx evoked and did not prevent convulsions.

In contrast to the effects of daurisoline on glutamate release, the glutamate release evoked by depolarizing agents has been shown to be insensitive to nimodipine, yet Ca^{2+} influx was blocked by nimodipine. How can these observations be explained? It is clear that stimulus-secretion coupling is predominantly mediated by dihydropyridine-insensitive N-type VSCC. Nowycky *et al.* (1985a, b) recently advanced our understanding significantly by demonstrating that chick dorsal root ganglion. (DRG) neurones in culture possessed three distinct types of VSCC. The second type of VSCC (N), of intermediate size, was responsible for the second inactivating phase of the Ca^{2+} current, observed during strong depolarizations. The third VSCC(L), which was also activated by strong depolarizations, was responsible for the non-inactivating component of the current. The pharmacological properties of these types of VSCC proved most interesting. L-type channels were modulated by dihydropyridine agonists and antagonists such as nimodipine, but N-channels were not. Rapid ^{45}Ca flux measurements in synaptosomes have shown that the VSCC that mediate transmitter release in most cases also exhibit voltage inactivation and are nimodipine-insensitive (Lu & Liu, 1990a; Nachshen & Blaustein, 1979). They closely resemble the N-type channels described electrophysiologically. In most cases, such channels may form clusters around transmitter release sites on nerve terminals. It is quite likely that L-type channels may not be very common in nerve terminals and may be preferentially localized in the cell soma, since the concentration of [^{3}H]-nimodipine receptors is much higher in the postsynaptic membrane than on the presynaptic terminal (Pumplin *et al.*, 1991). Our results provide further evidence for this hypothesis.

Our results show that glutamate release and Ca^{2+} influx may be dissociated by different stimulants and differently blocked by calcium antagonists. Daurisoline, by potently inhibiting Ca^{2+} influx and glutamate release, appears to be a useful tool to study VSCC.

References

BOWMAN, C.L. & KIMELBERG, H.K. (1984). Excitatory amino acids directly depolarize rat brain astrocytes in primary culture. *Nature*, **311**, 656–659.

CARBONE, E. & LUX, H.D. (1984). A low voltage activated, fully inactivating Ca channel in vertebrate sensory neurons. *Nature*, **310**, 501–502.

FREEDMAN, S.B. & MILLER, R.J. (1984). Calcium channel activation: A different type of drug action. *Proc. Natl. Acad. Sci. U.S.A.*, 81, 5580–5583.

KELLY, J.S., KRNJEVIC, K. & YIM, G.K. (1967). Unresponsive cells in cerebral cortex. *Brain Res.*, **6**, 767–769.

LINDROTH, P. & MOPPER, K. (1979). High performance liquid chromatographic determination of subpicomole amounts of amino acids by precolumn fluorescence derivatization with *O*-phthaldialdehyde. *Anal. Chem.*, **51**, 1667–1674.

LU, Y.M. & LIU, G.Q. (1990a). Effects of (−)-daurisoline on Ca influx into presynaptic nerve terminals. *Br. J. Pharmacol.*, **101**, 45–48.

LU, Y.M. & LIU, G.Q. (1990b). Effects of (−)-daurisoline on quinolinic acid-induced Ca influx in neurons in freely moving rats. *Acta Pharmacol. Sin.*, **12**, 301–304.

LU, Y.M., ZHANG, J.T. & ZHAO, F.Q. (1990). Effects of nimodipine on L-glutamate induced seizures and Ca influx in the hippocampus in freely moving rats. *Acta Pharmacol. Sin.*, **12**, 297–300.

LU, Y.M. & ZHAO, F.Q. (1991). Effects of (−)-daurisoline on CPK-activities in synaptosomes. *Chin Pharmacol. Bull.*, **7**, 174–179.

MILLER, R.J. (1987). Multiple calcium channels and neuronal function. *Science*, **235**, 46–52.

MILLER, R.J. & FREEDMAN, S.B. (1984). Minireview: are dihydropyridine binding sites voltage-sensitive calcium channels? *Life Sci.*, **34**, 1205–1221.

MACDERMOTT, A.B., MAYER, M.L., WESTBROOK, G.L., SMITH, S.J. & BARKER, J.L. (1986). NMDA-receptor activation increase cytoplasmic calcium concentration in culture spinal cord neurones. *Nature*, **321**, 519–522.

MODY, T. & HEINEMANN, U. (1986). Laminar profiles of the changes in extracellular calcium concentration induced by repetitive stimulation and excitatory amino acids in the rat dentate gyrus. *Neurosci. Lett.*, **69**, 137–142.

MOROCUTT, C., PIERELLI, F. & SANARELLI, L. (1986). Antiepileptic effects of a calcium antagonist (nimodipine) on cefazoline-induced epileptogenic foci in rabbits. *Epilepsia*, **27**, 498–503.

NACHSHEN, D.A. & BLAUSTEIN, M.P. (1979). The effects of some 'organic calcium antagonists' on calcium influx in presynaptic nerve terminals. *Mol. Pharmacol.*, **16**, 579–586.

NORRIS, D.K. & BRADFORD, H.F. (1985). On the specificity of verapamil as a calcium channel-blocker. *Biochem. Pharmacol.*, **34**, 1953–1956.

NOWYCKY, M.C., FOX, A.P. & TSIEN, R.W. (1985a). Three types of neuronal calcium channel with different calcium agonist sensitivity. *Nature*, **316**, 440–443.

NOWYCKY, M.C., FOX, A.P. & TSIEN, R. W. (1985b). Long-opening mode of gating of neuronal calcium channels and its promption by its dihydropyridine calcium agonist Bay K 8644. *Proc. Natl. Acad, Sci. U.S.A.*, **82**, 2178–2182.

PUMPLIN, D.W., REESE, T.S. & LLINAS, R. (1981). Are the presynaptic membrane particles the calcium channels? *Proc. Natl. Acad. Sci., U.S.A.*, **78**, 7210–7216.

TRIGGLE, D.J., & RAMPE, D. (1989). 1,4-dihydropridine activators and antagonists: structural and functional distinctions. *Trends Pharmacol. Sci.*, **10**, 507–511.

VEZZANI, A. & WU, H.Q. (1988). Quinolinic acid-induced seizures, but not nerve cell death, are associated with extracellular Ca^{2+} decrease assessed in the hippocampus by brain dialysis. *Brain Res.*, **454**, 289–297.

(Received July 11, 1990
Revised April 29, 1991
Accepted May 14, 1991)

Br. J. Pharmacol. (1991), **104**, 227–233

Effects of lemakalim on changes in Ca^{2+} concentration and mechanical activity induced by noradrenaline in the rabbit mesenteric artery

Shinichi Ito, Junko Kajikuri, [1]Takeo Itoh & Hirosi Kuriyama

Department of Pharmacology, Faculty of Medicine, Kyushu University, Fukuoka 812 Japan

1 Effects of (−)-cromakalim (lemakalim) on tension and Ca^{2+} mobilization induced by noradrenaline (NA) were investigated by measuring intracellular Ca^{2+} concentration ($[Ca^{2+}]_i$), isometric tension and production of inositol-1,4,5-trisphosphate (IP_3) in smooth muscle strips of the rabbit mesenteric artery.

2 In thin smooth muscle strips, 10 μM NA produced a large phasic, followed by a small tonic increase in $[Ca^{2+}]_i$, which correlated well with the evoked phasic and tonic contractions, respectively. Lemakalim (0.1–10 μM) lowered the resting $[Ca^{2+}]_i$ without a decrease in the resting tension, and also inhibited the increased $[Ca^{2+}]_i$ and tension induced by 10 μM NA, all in a concentration-dependent manner. Glibenclamide (1 μM) inhibited these actions of lemakalim.

3 In Ca^{2+}-free solution containing 2 mM EGTA, NA (10 μM) transiently increased $[Ca^{2+}]_i$, tension and synthesis of IP_3. Lemakalim (over 0.01 μM) inhibited these actions of NA in Ca^{2+}-free solution containing 5.9 mM K^+, but not in Ca^{2+}-free solution containing 128 mM K^+. These actions of lemakalim were prevented by glibenclamide (1 μM). Lemakalim (1 μM) did not modify the increases in $[Ca^{2+}]_i$ and tension induced by 10 mM caffeine.

4 In β-escin-skinned strips, 10 μM NA increased $[Ca^{2+}]_i$ in Ca^{2+}-free solution containing 50 μM EGTA, 3 μM guanosine triphosphate (GTP) and 2 μM Fura 2 after the storage sites were loaded by application of 0.3 μM Ca^{2+} for 2 min, suggesting that Ca^{2+} is released from intracellular storage sites following activation of the α-adrenoceptor. Lemakalim (1 μM) did not inhibit the Ca^{2+} release from storage sites induced by NA.

5 We conclude that lemakalim inhibits NA-induced Ca^{2+} release due to inhibition of NA-induced IP_3 production in a manner dependent on the membrane potential and causes inhibition of the phasic contraction induced by NA.

Keywords: Cromakalim; noradrenaline; inositol-1,4,5-trisphosphate; cellular Ca^{2+} concentration; vascular smooth muscle

Introduction

Cromakalim ((±)-6-cyano-3,4-dihydro-2,2-dimethyl-*trans*-4-(2-oxo-1-pyrrolidyl)-2H-benzo-[b]pyran-3-ol) represents a new class of vasodilator which hyperpolarizes the membrane by opening K^+ channels in vascular smooth muscle cells (for reviews, see Hamilton & Weston, 1989; Quast & Cook, 1989). The effects of cromakalim are stereospecific and confined to the (−)-enantiomer (lemakalim) (Buckingham *et al.*, 1986; Hof *et al.*, 1988). It has been suggested that cromakalim inhibits the activation of the voltage-dependent Ca^{2+} channel as a result of its hyperpolarization of the membrane (Hamilton *et al.*, 1986; Nakao *et al.*, 1988; Standen *et al.*, 1989). In addition, it has also been reported that this agent inhibits refilling of the depleted store sites, as suggested by its reduction of agonist-induced $^{45}Ca^{2+}$ influx (Chiu *et al.*, 1988), possibly through its membrane hyperpolarizing action. These effects may account for the cromakalin-induced inhibition of the tonic phase of contraction that is induced by NA in some vascular smooth muscle tissues and which results from Ca^{2+}-influx (Hamilton & Weston, 1989; Quast & Cook, 1989).

In the rabbit mesenteric artery, noradrenaline (NA) produces a large phasic and a subsequent small tonic contraction, the phasic contraction being mainly due to NA-induced Ca^{2+} release from intracellular storage sites (Itoh *et al.*, 1983). NA causes production of iositol-1,4,5-trisphosphate (IP_3) through hydrolysis of phosphatidylinositol-4,5-bisphosphate (PIP_2), and the IP_3 releases Ca^{2+} from its storage sites in the rabbit mesenteric artery (Hashimoto *et al.*, 1986). Thus, NA may generate its phasic contraction in the smooth muscle of the rabbit mesenteric artery via the action of IP_3. However, the mechanism underlying the cromakalim-induced inhibition of the phasic contraction induced by NA, which may lead to vasodilatation, has not been clearly identified.

In the present study, we have attempted to clarify this mechanism. For this purpose, we used lemakalim ((−)-cromakalim) instead of (±)-cromakalim, and studied its effects on the NA-induced phasic increase in intracellular Ca^{2+} concentration ($[Ca^{2+}]_i$) and tension in Ca^{2+}-containing, or Ca^{2+}-free solution under membrane-polarized and -depolarized conditions. In addition, we have studied the action of this drug on NA-induced Ca^{2+} release in β-escin-skinned smooth muscle strips.

Methods

Male albino rabbits, weighing 1.9–2.5 kg, were anaesthetized with pentobarbitone sodium (40 mg kg^{-1}, i.v.), and then exsanguinated. The third branch of the mesenteric artery was excised immediately and cleaned by removal of connective tissue in Krebs solution at room temperature.

Ca^{2+} and tension measurement

To enable recording of $[Ca^{2+}]_i$ and isometric tension simultaneously, fine circularly-cut strips (0.3–0.5 mm length, 0.04–0.05 mm width, 0.02–0.03 mm thickness) were prepared as previously described (Itoh *et al.*, 1983). Endothelial cells were removed by gentle rubbing of the internal surface of the vessels with small knives. The absence of endothelial cells was confirmed by the inability of acetylcholine (1 μM) to cause relaxation during contractions induced by NA, as described previously (Nishiye *et al.*, 1989). The strip was transferred into a chamber of 0.3 ml volume and mounted horizontally on a

[1] Author for correspondence.

invert-microscope (Diaphoto TMD with special optics for epi-fluorescence, Nikon). The resting tension was adjusted to obtain a maximal contraction in 128 mM K^+.

To enable loading of Fura 2 into smooth muscle cells of the strip, 1 μM acetoxy methyl ester of Fura 2 (Fura 2AM) dissolved in dry dimethyl sulphoxide (1 mM stock solution) was applied for 1 h in Krebs solution at room temperature (20–23°C). The position of the strip was adjusted to the centre of the field with a mask placed in an intermediate image plane to reduce fluorescence from the background (0.04 mm square). The Fura 2 fluorescence emission at 510 nm using an interference filter (centred at 510 nm and full width at half transmission, 20 nm) was passed through the lens (20 times fluor objective lens, Nikon) and collected in a photomultiplier tube (R928, side-on type, Hamamatsu Photonics, Japan) via a dichroic mirror (DM-400, Nikon) which was substituted for the photochanger in a Nikon Diaphoto-TMD microscope. Two alternative excitation wavelengths, 340 nm and 380 nm (each slit 5 nm) were applied by a spectro-fluorimeter (Spex, N.J., U.S.A.) and the data analysed with customized software provided by Spex (DM-3000CM). The ratio of the Fura 2 fluorescence intensities excited by 340 or 380 nm was calculated after subtraction of the background fluorescence. Background fluorescence (including the autofluorescence of the strip) as excited by 340 and 380 nm u.v.-light was measured following application of a solution containing 50 μM ionomycin, 20 mM $MnCl_2$, 110 mM KCl and 10 mM 3-(N-morpholino) propanesulphonic acid (MOPS) (pH 4.8) after the experiment. Under these conditions, the background fluorescence intensity was 10–15% of the Fura 2 signals in smooth muscle strips at either excitation wavelength. Cytosolic Ca^{2+} concentrations were calculated with the formula described by Grynkiewicz *et al.* (1985) and using *in vitro* calibration (Poenie *et al.*, 1986; Becker *et al.*, 1989). The ratio of maximum (F_{max}) to minimum fluorescence (F_{min}) was determined in the calibration solution after subtraction of background excited by either 340 or 380 nm and the 380 signals of Fura 2 were assumed to decrease by 15% in the cell due to the possible intracellular viscosity effects of the dye (Becker et al., 1989). The K_d value for Fura 2 was estimated to be 200 nM (Becker *et al.*, 1989).

We also tried, unsuccessfully, to estimate $[Ca^{2+}]_i$ in some strips by the internal calibration method described by Himpens *et al.* (1989). However, since the value of F_{max} was not consistently bigger than that of 128 mM K^+ in Krebs solution even in very thin strips, we could not use this method in the present experiments.

Experiments on chemically skinned smooth muscle

Chemically skinned smooth muscle strips were made by use of β-escin (Kobayashi *et al.*, 1989). The methods used to make skinned muscles and the compositions of the solution have been described elsewhere (Itoh *et al.*, 1986; Kobayashi *et al.*, 1989). To enable measurement of Ca^{2+} release from the store sites, 0.3 μM Ca^{2+} buffered with 4 mM EGTA was applied for 2 min (to load Ca^{2+} into the store sites) and Ca^{2+} removed from the solution by application of Ca^{2+}-free solution containing 4 mM EGTA for 0.5 min. Then, a solution containing 50 μM EGTA, 3 μM GTP and 2 μM Fura 2 was applied for 2 min. Finally, 10 μM NA with 3 μM GTP was applied for 2 min in a solution containing 50 μM EGTA and 2 μM Fura 2.

Measurement of inositol-1,4,5-trisphospate

Endothelium-denuded strips were equilibrated for over 2 h at 32°C in Krebs solution. After this, the strips were transferred to Ca^{2+}-free Krebs solution containing 2 mM EGTA for 2 min and then 10 μM NA was applied for various times. Lemakalim or glibenclamide was given as pretreatment for 3 min in Krebs solution, for 2 min in Ca^{2+}-free solution and during application of NA. The reaction was stopped by addition of a large amount of ice-cold trichloroacetic acid (final concentration 8%) and the strips were homogenized. The homogenate was centrifuged and the supernatant fraction treated with ether three times and assayed with a radioimmunoassay kit from Amersham International plc. Care was taken to maintain the pH of the homogenate at 9.0–9.5 to optimize the binding properties of the binding protein to IP_3. To minimize the loss of IP_3, teflon tubes were used instead of glassware after homogenization.

Solutions

The ionic composition of the Krebs solution was as follows (mM): Na^+ 137.4, K^+ 5.9, Mg^{2+} 1.2, Ca^{2+} 2.6, HCO_3^- 15.5, $H_2PO_4^-$ 1.2, Cl^- 134 and glucose 11.5. The concentration of K^+ was modified by replacing NaCl with KCl, isosmotically. To prevent both NA outflow from sympathetic nerve terminals and β-adrenoceptor stimulation by exogenously-applied NA, 3 μM guanethidine and 0.3 μM propranolol were added to the Krebs solution throughout the experiment. Ca^{2+}-free Krebs solution was made by substituting an equimolar concentration of $MgCl_2$ for $CaCl_2$ and adding 2 mM EGTA. The solutions were bubbled with O_2 and 5% CO_2, and their pH maintained at 7.3–7.4.

The calibration solution for Ca^{2+} measurement in intact strips contained 11 mM EGTA, 110 mM KCl, 1 mM $MgCl_2$, 2 μM Fura 2 and 20 mM N-2-hydroxyethylpiperazine-N'-2-ethanesulphonic acid (HEPES) (pH 7.1) with or without 11 mM $CaCl_2$.

For experiments on skinned muscle, the composition of the relaxing solution was: 87 mM potassium methanesulphonate (KMS), 20 mM piperazine-N-N'-*bis*-(2-ethanesulphonic acid) (PIPES), 5.1 mM $Mg(MS)_2$, 5.2 mM ATP, 10 mM phosphocreatine and 4 mM ethyleneglycol-*bis*-(β-aminoethyl)-N,N,N'N'-tetraacetic acid (EGTA). To enable measurement of Ca^{2+} release from skinned strips, the concentration of EGTA was reduced to 50 μM and 2 μM Fura 2 added. Various Ca^{2+} concentrations were prepared by adding appropriate amounts of $Ca(MS)_2$ to 4 mM EGTA, based on the calculation reported previously (Itoh *et al.*, 1986). The pH of the solution was adjusted to 7.1 at 25°C with KOH and the ionic strength was standardized at 0.2 M by changing the amount of KMS added.

Drugs

Drugs used were Fura 2, Fura 2AM, EGTA, PIPES, HEPES and MOPS (Dojin, Japan), NA, IP_3, GTP, β-escin and glibenclamide (Sigma), guanethidine (Tokyo Kasei, Japan), ATP (Na salt; Kojin, Japan), propranolol (Nacalai, Japan), A23187 and ionomycin (free acid; Calbiochem), and lemakalim (Beecham).

Statistics

The values recorded were expressed as mean ± s.d., and statistical significance determined by a paired or unpaired Student's *t* test. Probabilities less then 5% ($P < 0.05$) were considered significant.

Results

Effects of lemakalim on changes in $[Ca^{2+}]_i$ *and tension induced by noradrenaline in* Ca^{2+}*-containing solution*

Figure 1 shows traces of the effects of lemakalim on $[Ca^{2+}]_i$ and tension induced by 10 μM NA in a thin smooth muscle strip of the rabbit mesenteric artery. NA was applied for 2 min at 30 min intervals to get reproducible responses and then lemakalim applied for 5 min before, and during subsequent applications of NA. NA (10 μM) produced a transient phasic, followed by a small tonic increase in $[Ca^{2+}]_i$ and in tension. The resting $[Ca^{2+}]_i$ and tension were 151 ± 21 nM and 1.8 ± 0.5 mg, respectively ($n = 8$). Changes in $[Ca^{2+}]_i$ always preceded tension development. Lemakalim (0.01–10 μM) lowered the resting $[Ca^{2+}]_i$ and inhibited the increases in

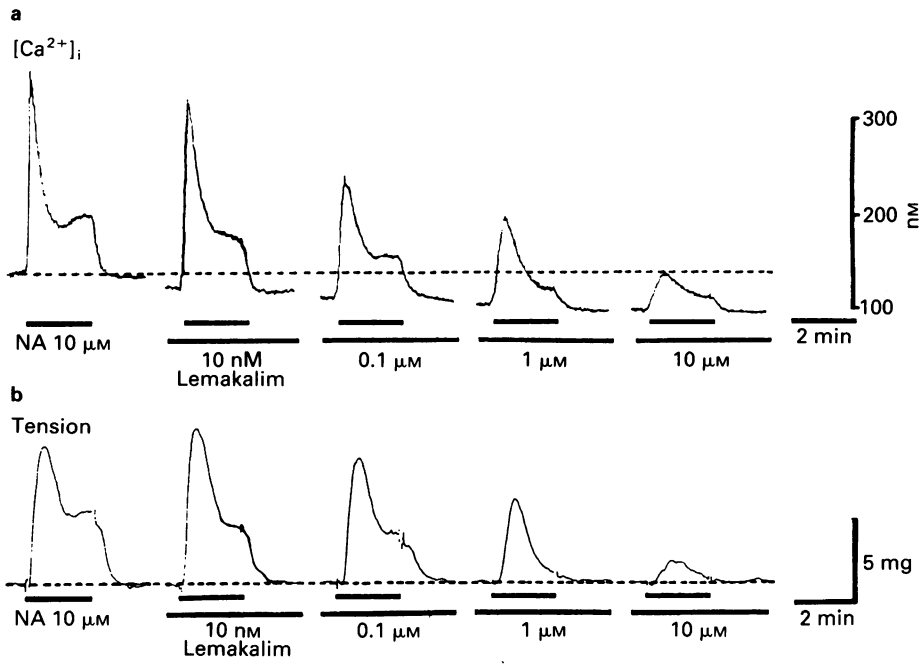

Figure 1 Effects of lemakalim on changes in $[Ca^{2+}]_i$ (a) and tension (b) induced by 10 μM noradrenaline (NA) in a smooth muscle strip of rabbit mesenteric artery. Broken lines indicate resting $[Ca^{2+}]_i$ (a) and tension (b) levels under control conditions. NA (10 μM) was applied for 2 min at 30 min intervals in Krebs solution. Guanethidine (3 μM) and propranolol (0.3 μM) were present throughout the experiment. Lemakalim was given as pretreatment for 5 min and was present during the application of NA. The results illustrated were obtained from a single smooth muscle strip and were reproducible in another 3 strips.

$[Ca^{2+}]_i$ (Figure 1a) and tension (Figure 1b) induced by 10 μM NA, in a concentration-dependent manner. Figure 2 summarizes the effects of lemakalim on the resting $[Ca^{2+}]_i$ and the increase in $[Ca^{2+}]_i$ induced by 10 μM NA ($n = 3$–5). NA (10 μM) increased the $[Ca^{2+}]_i$ to 436 ± 63 nM in the muscle strips ($n = 8$). Lemakalim (0.1–10 μM) lowered the resting $[Ca^{2+}]_i$ and inhibited the evoked increase in $[Ca^{2+}]_i$, both in a concentration-dependent manner (Figure 2). Glibenclamide

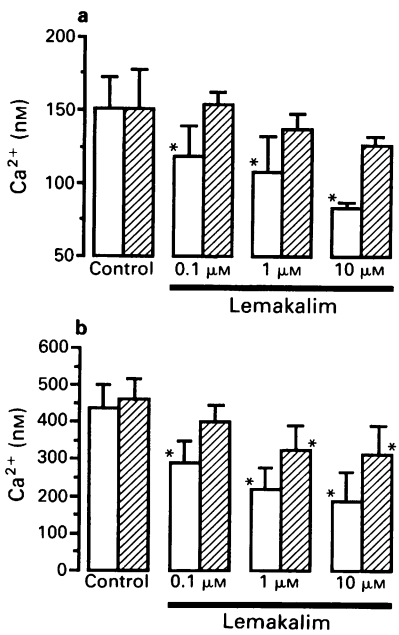

Figure 2 Effects of lemakalim (a) on resting $[Ca^{2+}]_i$ and (b) on active $[Ca^{2+}]_i$ induced by 10 μM noradrenaline (NA) in the presence or absence of 1 μM glibenclamide in smooth muscle strips of rabbit mesenteric artery. The experimental protocol was similar to that described in Figure 1. Glibenclamide (1 μM) was applied for 10 min before, and throughout application of lemakalim. Open columns: control, hatched colums: in the presence of 1 μM glibenclamide. Each column represents mean ($n = 3$–5) with s.d. shown by vertical bars. * Represents statistically significant difference from the control.

(1 μM) itself did not modify resting $[Ca^{2+}]_i$ or the increase induced by 10 μM NA but it did inhibit the effects of 1 μM lemakalim. Figure 3 shows records of the inhibitory effects of 1 μM glibenclamide on the lemakalim-induced inhibition of both the $[Ca^{2+}]_i$ (Figure 3a(i)) and tension (Figure 3b(i)) induced by 10 μM NA in the same smooth muscle strip. The effects of glibenclamide in concentrations over 1 μM were not examined because the vehicle (dimethyl sulphoxide) used to dissolve glibenclamide itself inhibited the NA-contraction (final concentration of vehicle was 0.001%).

Effects of lemakalim on changes in $[Ca^{2+}]_i$ and tension induced by noradrenaline in Ca^{2+}-free solution

In smooth muscle strips of the rabbit mesenteric artery, the phasic contraction induced by NA persists in Ca^{2+}-free solution (Figure 3b(ii)), and this has been supposed to be due to release of Ca^{2+} from storage sites (Itoh *et al.*, 1983). To study the effects of lemakalim on NA-induced Ca^{2+} release, its effects on the increase in $[Ca^{2+}]_i$ and tension induced by 10 μM NA were studied in Ca^{2+}-free solution containing 2 mM EGTA (see Figure 4). At 30 min intervals, NA (10 μM) was applied for 2 min in Ca^{2+}-free solution containing 2 mM EGTA after a 2 min period of Ca^{2+} removal, the strips being kept in Krebs solution (containing 2.6 mM Ca^{2+}) for the 25 min between tests. In Ca^{2+}-free solution containing 2 mM EGTA, the increase in $[Ca^{2+}]_i$ and tension induced by 128 mM K^+ was completely abolished within 15 s. Following application of Ca^{2+}-free solution containing 2 mM EGTA, the resting $[Ca^{2+}]_i$ rapidly decreased from 151 ± 21 to 86 ± 16 nM ($n = 4$) within 1 min and then remained at a new steady level, but the resting tension was not changed significantly (1.6 ± 0.4 to 1.4 ± 0.3 mg, $n = 4$). NA (10 μM) transiently increased $[Ca^{2+}]_i$ (to 234 ± 42 nM, $n = 4$) and tension (to 6.5 ± 1.2 mg, $n = 4$) in Ca^{2+}-free solution. Lemakalim (over 0.1 μM) lowered the resting $[Ca^{2+}]_i$ and inhibited this evoked increase in $[Ca^{2+}]_i$ and tension, in a concentration-dependent manner (Figure 4 and Figure 5). The resting $[Ca^{2+}]_i$ was 81 ± 12 nM in the presence of 0.1 μM lemakalim and 75 ± 11 nM in 1 μM lemakalim ($n = 4$), and these were both significantly different from control ($P < 0.05$ paired t test). However, the resting tension remained unchanged. The

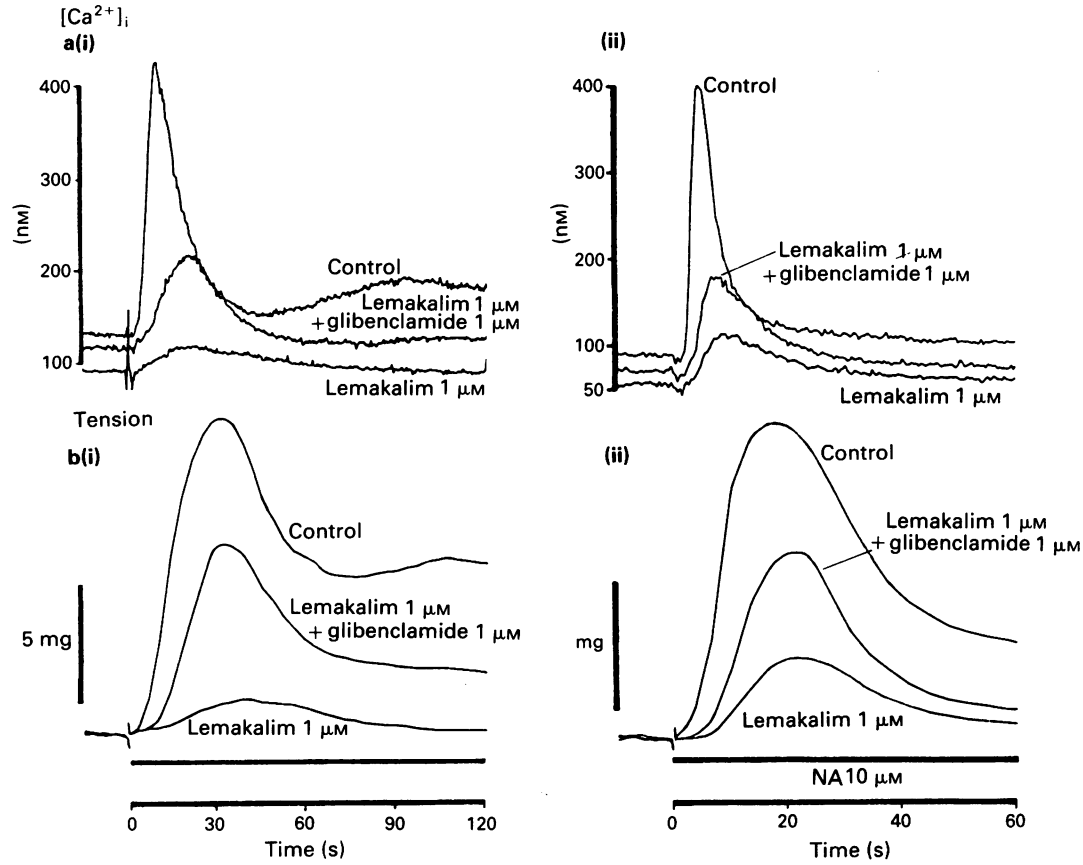

Figure 3 Effects of 1 μM lemakalim, with or without 1 μM glibenclamide, on changes in $[Ca^{2+}]_i$ (a) and tension (b) induced by 10 μM noradrenaline (NA) in Ca^{2+} containing (a(i) and b(i)) and Ca^{2+}-free solution containing 2 mM EGTA (a(ii) and b(ii)) in a smooth muscle strip of rabbit mesenteric artery. NA (10 μM) was applied for 2 min at 30 min intervals in Krebs solution. Guanethidine (3 μM) and propranolol (0.3 μM) were present throughout the experiment. Lemakalin (1 μM) was given as pretreatment for 5 min and was present during application of 10 μM NA. Glibenclamide (1 μM) was applied for 10 min before and throughout application of lemakalim. The results shown were obtained from a single smooth muscle strip and were reproducible in another 3 strips.

maximum $[Ca^{2+}]_i$ induced by 10 μM NA in Ca^{2+}-free solution was 197 $\pm$ 35 nM or 153 $\pm$ 33 nM in the presence of 0.1 μM or 1 μM lemakalim, respectively (Figure 5, $n = 4$; $P < 0.05$, paired t test). The tension induced by 10 μM NA in Ca^{2+}-free solution was inhibited to 81% of control by 0.1 μM lemakalim and to 47% of control by 1 μM lemakalim ($n = 4$). Glibenclamide (1 μM) significantly inhibited the effects of 1 μM lemakalim both on the resting $[Ca^{2+}]_i$, and on the changes in $[Ca^{2+}]_i$ and tension induced by 10 μM NA (Figure 3a(ii) and 3b(ii)). In Ca^{2+}-free solution containing 2 mM EGTA, the

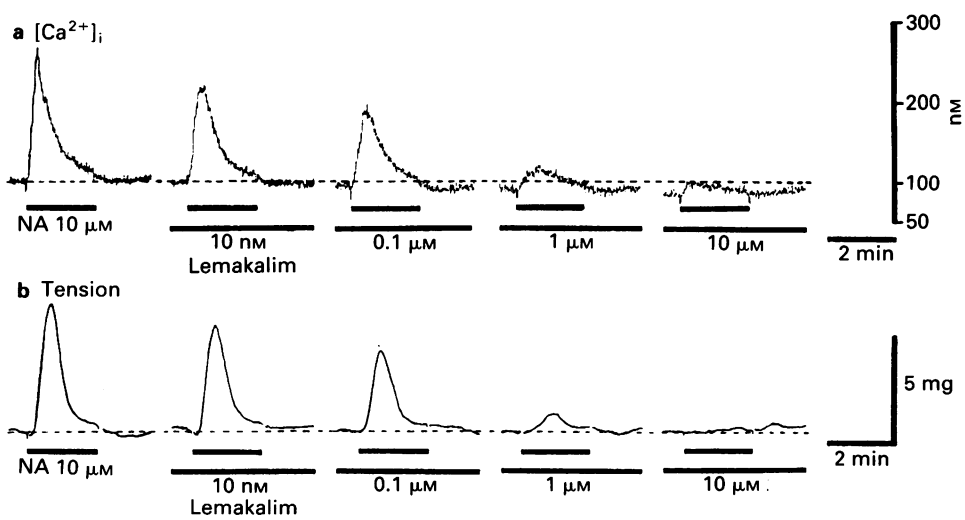

Figure 4 Effects of lemakalim on changes in $[Ca^{2+}]_i$ (a) and tension (b) induced by 10 μM noradrenaline (NA) in Ca^{2+}-free solution containing 2 mM EGTA in a smooth muscle strip of rabbit mesenteric artery. NA (10 μM) was applied for 2 min after a 2 min period of Ca^{2+} removal, then Ca^{2+}-free solution was applied for 1 min to wash out NA. This protocol was repeated at 30 min intervals with the strips being kept in Krebs solution (containing 2.6 mM Ca^{2+}) for the 25 min between tests. Lemakalim was applied for 5 min before and throughout application of NA. Guanethidine (3 μM) and propranolol (0.3 μM) were present throughout the experiment. Broken lines indicate resting $[Ca^{2+}]_i$ (a) and tension (b) level in Ca^{2+}-free solution in the absence of lemakalim. The results illustrated were obtained from a single smooth muscle strip and were reproducible in another 3 strips. N.B. the resting $[Ca^{2+}]_i$ before application of NA was lower in the presence of lemakalim than in control.

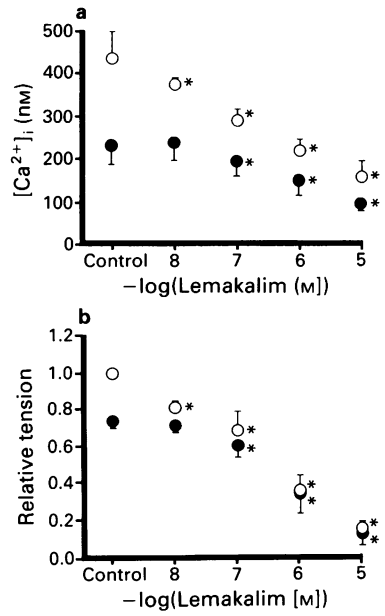

Figure 5 Concentration-dependent effects of lemakalim on increase in $[Ca^{2+}]_i$ (a) and tension (b) induced by 10 μM noradrenaline (NA) in Ca^{2+}-containing (○) or Ca^{2+}-free solution containing 2 mM EGTA (●) in smooth muscle strips of rabbit mesenteric artery. The experimental protocol was similar to that described in Figures 1 and 3. In (b), the maximum amplitude of contraction induced by 10 μM NA in Ca^{2+}-containing solution was normalized as 1.0 for each muscle strip. Each symbol represents mean ($n = 4$) with s.d. shown by vertical bars. * represents statistically significant difference from the value obtained in the absence of lemakalim in either Ca^{2+}-containing or Ca^{2+}-free solution (control).

resting $[Ca^{2+}]_i$ in the presence of 1 μM glibenclamide was 88 ± 12 nM, 88 + 13 nM in 0.1 μM lemakalim with 1 μM glibenclamide and 83 ± 13 nM in 1 μM lemakalim with 1 μM glibenclamide ($n = 3$; $P > 0.05$ when any of these is compared with the resting $[Ca^{2+}]_i$ in the absence of glibenclamide and lemakalim). The maximum $[Ca^{2+}]_i$ induced by 10 μM NA in the presence of 1 μM glibenclamide was 234 ± 26 nM, 201 ± 37 nM in 0.1 μM lemakalim with 1 μM glibenclamide and 169 ± 39 nM in 1 μM lemakalim with 1 μM glibenclamide. These values were not significantly different from the maximum $[Ca^{2+}]_i$ induced by 10 μM NA in the absence of glibenclamide and lemakalim (Figure 5, $n = 3$; $P > 0.05$, paired t test).

Figure 6 shows the effects of 1 μM lemakalim on the increase in $[Ca^{2+}]_i$ and tension induced by 10 μM NA in Ca^{2+}-free solution containing 128 mM K^+. Lemakalim (1 μM) marginally inhibited the maximum increase in $[Ca^{2+}]_i$ and tension induced by 10 μM NA and slightly accelerated decay of both responses. Glibenclamide (1 μM) had no effect on this inhibition.

Lemakalim (0.01–1 μM) had no effect on the increase in $[Ca^{2+}]_i$ and tension induced by 10 mM caffeine in Ca^{2+}-free solution (not shown).

Effects of lemakalim on inositol-1,4,5-trisphosphate production induced by noradrenaline

It has been shown that IP_3 releases Ca^{2+} from intracellular storage sites as a second messenger in smooth muscle cells of the rabbit mesenteric artery (Hashimoto *et al.*, 1986). To investigate further the mechanisms of the inhibitory effects induced by lemakalim during the NA-induced contraction, the effects of lemakalim (0.1 and 1 μM) on the synthesis of IP_3 induced by 10 μM NA were observed in Ca^{2+}-free solution containing 2 mM EGTA. NA transiently increased the amount of IP_3 within 10 s and the effect gradually decayed. The effects of lemakalim (0.1 and 1 μM) on this response were measured 10 s after NA-application and it was found that it inhibited the

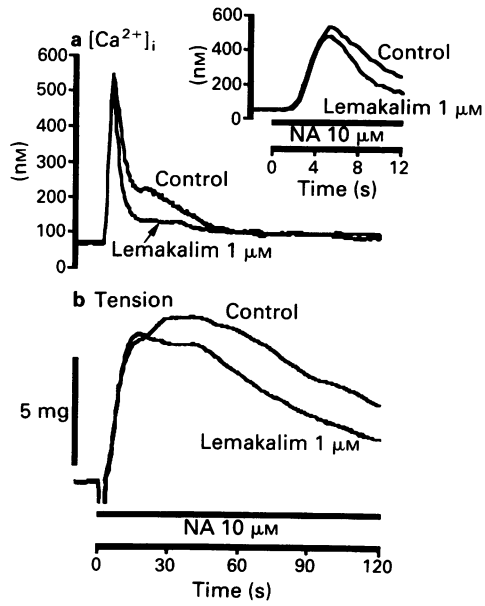

Figure 6 Effects of lemakalim on changes in $[Ca^{2+}]_i$ (a) and tension (b) induced by 10 μM noradrenaline (NA) in Ca^{2+}-free solution containing 2 mM EGTA and 128 mM K^+ in a smooth muscle strip of rabbit mesenteric artery. NA (10 μM) was applied for 2 min after a 2 min period of Ca^{2+} removal by Ca^{2+}-free solution containing 2 mM EGTA with 128 mM K^+, then the Ca^{2+}-free solution was applied for 1 min to wash out NA. This protocol was repeated at 30 min intervals with the strips in Krebs solution (containing 2.6 mM Ca^{2+} with 5.9 mM K^+) for the 25 min between tests. Lamakalim was applied for 5 min before and throughout application of NA. Guanethidine (3 μM) and propranolol (0.3 μM) were present throughout the experiment. In (a) the inset illustrates the initial changes in $[Ca^{2+}]_i$ on an expanded time scale. The results shown were obtained from a single smooth muscle strip and were reproducible in another 3 strips.

synthesis of IP_3 induced by 10 μM NA, in a concentration-dependent manner (Figure 7). Glibenclamide (1 μM) itself did not significantly modify the IP_3 production induced by 10 μM NA but it prevented the inhibitory actions of 0.1 μM lemakalim (Figure 7).

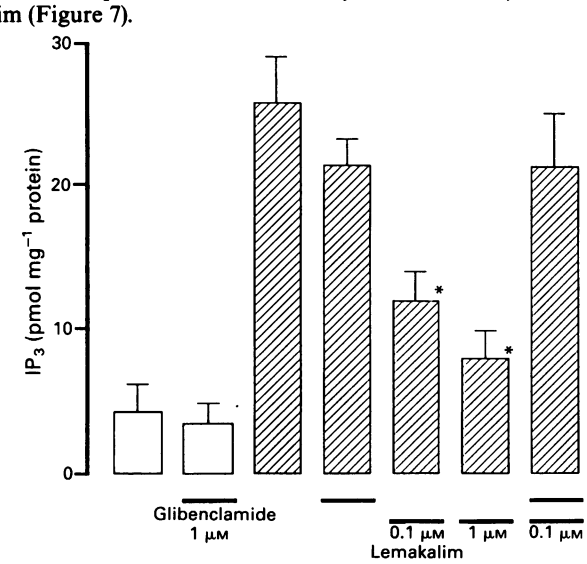

Figure 7 Effects of lemakalim on inositol-1,4,5-trisphosphate (IP_3)-synthesis induced by 10 μM noradrenaline (NA) in Ca^{2+}-free solution in smooth muscle strips of rabbit mesenteric artery. NA (10 μM) was applied for 10 s in Ca^{2+}-free solution containing 2 mM EGTA after a 2 min period of Ca^{2+} removal. Lemakalin (0.1 or 1 μM) was applied for 5 min before, and throughout application of NA. Glibenclamide (1 μM) was applied for 5 min before and throughout application of 10 μM NA or 0.1 μM lemakalim. Results represented are means of 4–8 observations with s.d. shown by vertical bars. * indicates statistically significant difference from response to NA alone ($P < 0.05$). Open columns: strips not stimulated by NA; hatched columns: NA-treated strips.

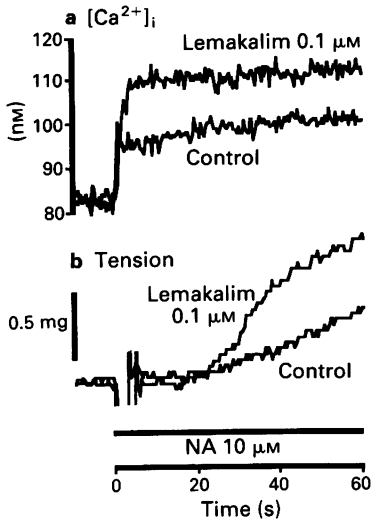

Figure 8 Effects of 0.1 μM lemakalim on increase in Ca^{2+} and tension induced by 10 μM noradrenaline (NA) in β-escin-skinned smooth muscle strips of rabbit mesenteric artery. After strips were skinned by application of 20 μM β-escin for 25 min, 0.3 μM Ca^{2+} buffered with 4 mM EGTA was applied for 2 min, and Ca^{2+}-free solution containing 4 mM EGTA then applied for 0.5 min to remove Ca^{2+} from the solution. Subsequently, 10 μM NA was applied for 2 min in Ca^{2+}-free solution containing 50 μM EGTA, 3 μM GTP and 2 μM Fura 2 following application of Ca^{2+}-free solution containing 50 μM EGTA, 3 μM GTP and 2 μM Fura 2 for 2 min. Lemakalim (0.1 μM) was applied for 2 min before, and throughout application of NA. These results were reproducible in another 2 strips.

Effects of lemakalim on noradrenaline-induced Ca^{2+}-release in chemically skinned smooth muscle strips

To investigate the site of action of lemakalim, the effects of 1 μM lemakalim on NA-induced Ca^{2+} release were observed in smooth muscle strips skinned by a 25 min application of β-escin (20 μM). NA increased $[Ca^{2+}]_i$ and tension in Ca^{2+}-free solution containing 50 μM EGTA. 3 μM GTP and 2 μM Fura 2 application of 0.3 μM Ca^{2+} for 2 min, possibly due to release of Ca^{2+} from its storage sites (Figure 8). Lemakalim (1 μM) did not inhibit, but rather enhanced this evoked increase in Ca^{2+} and tension (Figure 8).

Discussion

(±)-Cromakalim hyperpolarizes the membrane in vascular smooth muscle through activation of the K^+-channel and causes vascular relaxation (Hamilton *et al.*, 1986; Quast, 1987; Nakao *et al.*, 1988; Quast & Baumlin, 1988; Standen *et al.*, 1989). A sulphonylurea, glibenclamide, inhibits the membrane hyperpolarization induced by (±)-cromakalim in smooth muscle cells of the rabbit mesenteric artery (Standen *et al.*, 1989). The effects of cromakalim are stereospecific, the (−)-enantiomer (lemakalim) having a more potent vasodilator action than its racemic form (Buckingham *et al.*, 1986; Hof *et al.*, 1988). In the present experiments, we found that lemakalim lowered the resting $[Ca^{2+}]_i$ in both Ca^{2+}-containing and Ca^{2+}-free solutions and these actions were prevented by glibenclamide. In Ca^{2+}-free solution containing 2 mM EGTA, the extracellular Ca^{2+} has been calculated to be below 10 nM (Itoh *et al.*, 1986) and intracellular Ca^{2+} concentration estimated to be 50–90 nM. Under the above conditions, while influx of Ca^{2+} may be minimized, lemakalim still reduced the $[Ca^{2+}]_i$. Thus, the membrane hyperpolarization may in some way negatively control the resting $[Ca^{2+}]_i$.

In smooth muscle cells of the rabbit mesenteric artery, NA (10 μM) depolarized the membrane and induced oscillatory potential changes (Itoh *et al.*, 1983). NA produced a transient phasic increase in $[Ca^{2+}]_i$ and tension, possibly induced by release of Ca^{2+} from its storage sites, and a subsequent tonic increase which may be due to activation of Ca^{2+}-influx, as suggested by tension measurements in presence or absence of Ca^{2+} (Itoh *et al.*, 1983). Lemakalim (0.01–10 μM) inhibited the increase in $[Ca^{2+}]_i$ and tension induced by 10 μM NA in a concentration-dependent manner. No tonic increases in $[Ca^{2+}]_i$ or tension were induced by NA in Ca^{2+}-free solution containing EGTA. Lemakalim (10 μM) almost abolished the tonic increases in $[Ca^{2+}]_i$ and tension induced by 10 μM NA and glibenclamide prevented these inhibitory actions of lemakalim. These results suggest that lemakalim inhibits the increases in $[Ca^{2+}]_i$ and tension induced by NA through an inhibition of Ca^{2+}-influx.

It has been proposed that NA binds to the α-adrenoceptor and synthesizes IP_3 which releases Ca^{2+} from its store sites in smooth muscle of the rabbit mesenteric artery (Hashimoto *et al.*, 1986). Lemakalim inhibited the Ca^{2+} increase induced by NA, but not by caffeine, in intact smooth muscle strips in Ca^{2+}-free solution containing 5.9 mM K^+. This inhibitory action of lemakalim was prevented by glibenclamide and greatly diminished in Ca^{2+}-free solution containing 128 mM K^+. Lemakalim inhibited the synthesis of IP_3 induced by NA in a concentration-dependent manner and these actions were inhibited by glibenclamide. In Ca^{2+}-free solution containing 2 mM EGTA, nifedipine (a calcium antagonist) inhibited neither the contraction nor the hydrolysis of PIP_2 induced by NA (Kanmura *et al.*, 1983; Itoh *et al.*, 1987). Thus, the present results suggest that lemakalim selectively inhibits the NA-induced Ca^{2+} release, in a manner dependent on the membrane potential, through the inhibition of NA-induced IP_3 synthesis.

It has been reported that smooth muscle skinned with β-escin retains the α receptor-GTP binding protein-phospolipase C coupling mechanism (Kobayashi *et al.*, 1989). In the present experiments, we confirmed this with the finding that NA increased Ca^{2+} and tension in β-escin-treated skinned smooth muscle strips in the presence of GTP and a low concentration of EGTA. Lemakalim (1 μM) did not inhibit, but rather enhanced this response and this absence of an inhibitory action in β-escin skinned smooth muscle (which cannot generate a membrane potential) supports the notion that membrane hyperpolarization may play an essential role in the inhibition of NA-induced synthesis of IP_3 in smooth muscle cells.

In dog brain microsomes, K^+-channel blockers (such as tetraethylammonium, quinine, 4-aminopyridine and barium) inhibit the rate or extent of IP_3-induced Ca^{2+} release (Palade *et al.*, 1989). Thus, it may be that lemakalim increases the amount of stored Ca^{2+} or activates an IP_3-induced Ca^{2+} releasing mechanism through activation of K^+-channels on the storage sites. This remains to be clarified.

In Ca^{2+}-free solution containing 128 mM K^+, lemakalim (1 μM) slightly inhibited the increase in $[Ca^{2+}]_i$ and tension induced by 10 μM NA and slightly accelerated the decay of each response. Glibenclamide (1 μM) did not alter the effects of lemakalim in high K^+ containing solution. Since (±)-cromakalim did not hyperpolarize the membrane of smooth muscle cells of the guinea-pig mesenteric artery in a solution containing 128 mM K^+ (Nakao *et al.*, 1988), the membrane hyperpolarizing action of lemakalim may have been negligible in our experiments under these conditions. These results suggest that some effects of lemakalim other than its membrane hyperpolarizing action may underlie its inhibition of NA-responses in Ca^{2+}-free solution containing 128 mM K^+.

In conclusion, in smooth muscle of the rabbit mesenteric artery, lemakalim lowered the resting $[Ca^{2+}]_i$ and inhibited the active increase in $[Ca^{2+}]_i$ and tension and the synthesis of IP_3 induced by NA. Since glibenclamide consistently inhibited the change in the $[Ca^{2+}]_i$, IP_3 synthesis and tension induced by lemakalim, it is suggested that the membrane hyperpolarization induced by lemakalim may play a role in the inhibition of NA-induced IP_3 synthesis.

We thank Dr R.J. Timms for the language editing. This work was partly supported by Grant-In-Aid from the Ministry of Education of Japan (02807010 and 02404024).

References

BECKER, P.L., SINGER, J.J., WALSH, J.V. & FAY, F.S. (1989). Regulation of calcium concentration in voltage-clamped smooth muscle cells. *Science*, **244**, 211–214.

BUCKINGHAM, R.E., CLAPHAM, J.C., COLDWELL, M.C., HAMILTON, T.C. & HOWLETT, D.R. (1986). Stereospecific mechanism of action of the novel antihypertensive agent BRL 34915. *Br. J. Pharmacol.*, **87**, 78P.

CHIU, P.J.S., TETZLOFF, G., AHN, H. & SYBERTZ, E. (1988). Effects of BRL 34915, a putative K channel opener, on transmembrane ^{45}Ca movements in rabbit aortic smooth muscle. *Eur. J. Pharmacol.*, **155**, 229–237.

GRYNKIEWICZ, G., POENIE, M. & TSIEN, R. Y. (1985). A new generation of Ca^{2+} indicators with greatly improved fluorescence properties. *J. Biol. Chem.*, **260**, 3440–3450.

HAMILTON, T.C. & WESTON, A.H. (1989). Cromakalim, nicorandil and pinacidil: novel drugs which open potassium channels in smooth muscle. *Gen. Pharmacol.*, **20**, 1–9.

HAMILTON, T.C., WEIR, S.W. & WESTON, A.H. (1986). Comparison of the effects of BRL 34915 and verapamil on electrical and mechanical activity in rat portal vein. *Br. J. Pharmacol.*, **88**, 103–111.

HASHIMOTO, T., HIRATA, M., ITOH, T., KANMURA, Y. & KURIYAMA, H. (1986). Inositol 1,4,5-trisphosphate activates pharmacomechanical coupling in smooth muscle of the rabbit mesenteric artery. *J. Physiol.*, **370**, 605–618.

HIMPENS, B., MATTHIJS, G. & SOMLYO, A.P. (1989). Desensitization to cytoplasmic Ca^{2+} and Ca^{2+} sensitivities of guinea-pig ileum and rabbit pulmonary artery smooth muscle. *J. Physiol.*, **413**, 489–503.

HOF, R.P., QUAST, U., COOK, N.S. & BLARER, S. (1988). Mechanism of action, systemic and regional haemodynamics of the potassium channel activator BRL 34915 and its enantiomers. *Circ. Res.*, **62**, 679–686.

ITOH, T., KANMURA, Y. & KURIYAMA, H. (1986). Inorganic phosphate regulates the contraction-relaxation cycle in skinned muscles of the rabbit mesenteric artery. *J. Physiol.*, **376**, 231–252.

ITOH, T., KURIYAMA, H. & SUZUKI, H. (1983). Differences and similarities in noradrenaline- and caffeine-induced mechanical responses in the rabbit mesenteric artery. *J. Physiol.*, **337**, 609–629.

ITOH, T., SATOH, S., ISHIMATSU, T., FUJIWARA, T. & KANMURA, Y. (1987). Mechamisms of flunarizine-induced vasodilation in the rabbit mesenteric artery. *Circ. Res.*, **61**, 446–454.

KANMURA, Y., ITOH, T., SUZUKI, H., ITO, Y. & KURIYAMA, H. (1983). Effects of nifedipine on smooth muscle cells of the rabbit mesenteric artery, *J. Pharmacol. Exp. Ther.*, **226**, 236–248.

KOBAYASHI, S., KITAZAWA, T., SOMLYO, A. V. & SOMLYO, A. P. (1989). Cytosolic heparin inhibits muscarinic and α-adrenergic Ca^{2+} release in smooth muscle. *J. Biol. Chem.*, **264**, 17997–18004.

NAKAO, K., OKABE, K., KITAMURA, K., KURIYAMA, H. & WESTON, A.H. (1988). Characteristics of cromakalim-induced relaxations in the smooth muscle cells of guinea-pig mesenteric artery and vein. *Br. J. Pharmacol.*, **95**, 795–804.

NISHIYE, E., NAKAO, K., ITOH, T. & KURIYAMA, H. (1989). Factors inducing endothelium-dependent relaxation in the guinea-pig basilar artery as estimated from the actions of haemoglobin. *Br. J. Pharmacol.*, **96**, 645–655.

PALADE, P., DETTBARN, C., VOLPE, P., ALDERSON, B. & OTERO, A.S. (1989). Direct inhibition of inositol-1,4,5-trisphosphate-induced Ca^{2+} release from brain microsomes by K^+ channel blockers. *Mol. Pharmacol.*, **36**, 664–672.

POENIE, M., ALDERTON, J., STEINHART, R.A. & TSIEN, R.Y. (1986). Calcium rises abruptly and briefly throughout the cell at the onset of anaphase. *Science*, **233**, 886–889.

QUAST, U. (1987). Effect of the K^+efflux stimulating vasodilator BRL 34915 on $^{86}Rb^+$ efflux and spontaneous activity in guinea-pig portal vein. *Br. J. Pharmacol.*, **91**, 569–578.

QUAST, U. & BAUMLIN, Y. (1988). Comparison of the effluxes of $^{86}Rb^+$ and $^{42}K^+$ elicited by cromakalim (BRL 34915) in tonic and phasic vascular tissue. *Naunyn-Schmiedebergs Arch. Pharmacol.*, **338**, 319–326.

QUAST, U. & COOK, N.S. (1989). Moving together: K^+ channel openers and ATP-sensitive K^+ channels. *Trends Pharmacol.* Sci., **10**, 431–435.

STANDEN, N.B., QUAYLE, J.M., DAVIES, N.W., BRAYDEN, J.E., HUANG, Y. & NELSON, M.T. (1989). Hyperpolarizing vasodilators activate ATP-sensitive K^+ channels in arterial smooth muscle. *Science*, **245**, 177–180.

(Received March 6, 1991
Revised May 2, 1991
Accepted May 13, 1991)

Br. J. Pharmacol. (1991), **104**, 234–238

Muscarinic antagonists attenuate the increase in accumbens and striatum dopamine metabolism produced by clozapine but not by haloperidol

[1]Robert Rivest & *Charles A. Marsden

[1]Department of Pharmacology, Medical School, University of Sherbrooke, Quebec, Canada JIH-5N4 and *Department of Physiology and pharmacology, Medical School, Queen's Medical Centre, University of Nottingham, Nottingham, UK

1 The effect of the muscarinic antagonists, scopolamine and atropine, were examined on the increase in extracellular 3,4-dihydroxyphenylacetic acid (DOPAC) in the nucleus accumbens and the striatum induced by haloperidol and clozapine by use of *in vivo* differential pulse voltammetry with carbon fibre electrodes in anaesthetized rats.

2 Animals received saline (1 ml kg^{-1}, s.c.), scopolamine (1 mg kg^{-1}, o.p.) or atropine (20 μg, i.c.v.) followed 15 min later by saline (10 μl, i.c.v.), haloperidol (1 mg kg^{-1}, s.c.) or clozapine (30 mg kg^{-1}, i.p.) and extracellular DOPAC was simultaneously recorded in the nucleus accumbens and the striatum every 5 min for 60 min after drug administration.

3 Scopolamine or atropine alone had no effect on the DOPAC peak height but attenuated the increase in extracellular DOPAC induced by clozapine in both brain regions. Neither scopolamine nor atropine altered the haloperidol-induced increase in accumbens or striatal extracellular DOPAC.

4 The present results demonstrate that muscarinic antagonists attenuate the increase in accumbens and striatal dopamine metabolism *in vivo* produced by the atypical neuroleptic clozapine but not the haloperidol-induced increase in dopamine metabolism. The results indicate that central muscarinic receptors are involved in the actions on dopaminergic function of clozapine but not haloperidol.

Keywords: Neuroleptics; DOPAC; *in vivo* voltammetry; scopolamine; atropine

Introduction

The attenuation of psychotic symptoms with most neuroleptics is generally associated with the development of extrapyramidal side-effects (Marsden *et al.*, 1975). It is believed that the blockade of dopamine receptors located in the meso-accumbens and meso-cortical dopamine neurones produces the therapeutic effects of the neuroleptics while the extrapyramidal side-effects result from the increase in striatal cholinergic activity that follow the blockade of dopamine receptors in this brain region (Snyder *et al.*, 1974; Meltzer & Stahl, 1976). However, some neuroleptics (e.g. clozapine) are distinguished by having a lower incidence of extrapyramidal side-effects and have been named "atypical" neuroleptics (Herman & Pleasure, 1963; Gerlach & Simmelsgard, 1978).

Clozapine binds with high affinity to histamine and muscarinic receptor sites (Creese *et al.*, 1976; Seeman *et al.*, 1976; Miller & Hiley, 1974; Snyder *et al.*, 1974; Richelson & Nelson, 1984) and with less affinity to dopamine and 5-hydroxytryptamine receptor and α-adrenoceptor sites (Peroutka *et al.*, 1977; Fjalland *et al.*, 1977; Meltzer *et al.*, 1989). It has been suggested that blockade of muscarinic receptors by clozapine helps to prevent the extrapyramidal side-effects common with most neuroleptics (Snyder *et al.*, 1974).

There is evidence that clozapine can effectively prevent cholinergic mediated effects. Thus, clozapine will inhibit oxotremorine induced tremors and physostigmine-induced mortality in mice (Fjalland *et al.*, 1977) and antagonize acetylcholine induced hindgut contractions in the crayfish (Herrling & Misbach-Lesenne, 1982). The anti-cholinoceptor activity of clozapine was shown in a study where clozapine reversed the acetycholine-induced contraction of guinea-pig isolated ileum, reduced tremors induced by oxotremorine in mice and increased pupillary aperture in mice (Sayers & Bürki, 1976). Moreover, Racagni *et al.* (1976) reported that clozapine blocked the increase in acetylcholine content and the decrease in turnover rate induced by arecoline and oxotremorine in the striatum. In contrast, clozapine does not reduce contralateral torsion in guinea-pigs induced by injection of physostigmine into the right carotid artery (De Jonge & Funcke, 1962). It has been reported that clozapine (20 mg kg^{-1}, i.p.) does not increase *in vitro* acetylcholine turnover and release and *in vivo* release in the nucleus accumbens and the striatum (Costa *et al.*, 1978; Compton & Johnson, 1988) although a high dose of clozapine (50 mg kg^{-1}, i.v.) did increase the release of acetylcholine measured by means of push-pull cannulae in the striatum of gallamine-immobilized cat (Costa *et al.*, 1978). Thus while not every study demonstrated clozapine to possess anticholinergic properties, it is generally accepted that one of its actions involves the antagonism of muscarinic receptors.

On the other hand, there is also evidence to support the dopamine antagonist effects of clozapine. For example clozapine attenuates behavioural hyperactivity induced by peripheral or central administration of dopamine agonists in rat (Costall & Naylor, 1976; Chipkin & Latranyi, 1987; Tschanz & Rebec, 1988; Criswell *et al.*, 1989; McMillen *et al.*, 1989; Murray & Waddington, 1990). Moreover, acute administration of clozapine increases the firing rate of dopamine cells in the ventral tegmental area and the substantia nigra (Chiodo & Bunney, 1983) and the release and metabolism of dopamine in the nucleus accumbens and the striatum *in vivo* (Maidment & Marsden, 1987; Stamford *et al.*, 1988; Moghaddam & Bunney, 1990).

Since clozapine has high affinity for muscarinic receptors in the brain and because it is well established that cholinergic and dopaminergic systems interact in the striatum (Sethy & Van Woert, 1974; Le Moine *et al.*, 1990), we have examined whether the blockade of muscarinic receptors with scopolamine or atropine can alter the increase in extracellular 3,4-dihydroxyphenylacetic acid (DOPAC) in the nucleus accumbens and the striatum induced by clozapine and haloperidol.

[1] Author for correspondence at: Department of Psychology, Center for Studies in Behavioral Neurobiology, Concordia University, 1455 de Maisonneuve West, Montreal, Quebec, Canada H3G 1M8.

Extracellular DOPAC was simultaneously recorded in the two brain regions by use of differential pulse voltammetry with carbon fibre electrodes (Rivest *et al.*, 1991).

Methods

Animals

Male Wistar rats (250 and 280 g) were housed, 5 per cage, in a room (21°C) having a 12 h light/dark cycle. Food and water were available *ad libitum*.

Voltametric procedures

Working electrodes, made from one pyrolitic 12 μm carbon fibre, and the reference and auxiliary electrodes were prepared as previously described (Sharp *et al.*, 1984). To obtain sensitivity and adequate separation between ascorbic acid, catechol and indoles, the working electrodes were electrically pretreated by a method based on that of Gonon *et al.* (1980) and modified by Crespi *et al.* (1984). First, working, reference and auxiliary electrodes were immersed in a phosphate buffered saline solution (pH 7.4, 0.1 M) and connected to a polarograph (Princeton Applied Research 174A). A triangular waveform (0 to 3.0 V, 70 Hz) was applied for 10 s, then a continuous potential of +1.5 V, −0.9 V for 5 s each. This was followed by another continuous potential varying from 1.1 V to 1.5 V, depending on the sensitivity of the electrode. Sensitivity and selectivity of the electrodes were examined by performing one voltammetric recording in a phosphate buffered solution containing ascorbic acid (5×10^{-3} M), DOPAC (1×10^{-4} M) and 5-hydroxyindoleacetic acid (5-HIAA, 5×10^{-5} M). Electrodes showing poor separation, low sensitivity or high charging current were discarded. Differential pulse voltammetric parameters for the *in vitro* recording were as follows: potential range: −0.2 to 0.350 V, increase scan rate: 5 mV s^{-1}, pulse amplitude 50 mA, pulse frequency 2 s^{-1}.

Surgery and experimental procedure

Rats were anaesthetized with chloral hydrate (400 mg kg^{-1}, i.p.) which was maintained during the experiment by additional injections (70 mg kg^{-1} h^{-1}). Animals were mounted on a stereotaxic frame with the upper incisor bar set at 3.3 mm below the interaural line. A guide cannula (23 G) was stereotaxically implanted 2 mm above the left lateral ventricle and fixed with dental cement (Espe Durelon). The coordinates used were A/P: −0.2; L: 1.4; V: 4.2, with reference to bregma (Paxinos & Watson, 1982). For the implantation of the voltammetric electrodes, one hole (approximately 2 mm diam) was made in the cranium above the striatum and one above the nucleus accumbens. The dura was carefully ruptured and removed with a hypodermic needle. One working electrode was stereotaxically implanted in the medio-dorsal part of the striatum (A/P: +0.7, L: 3.0, V: 4.0 from the surface of the brain) and another into the nucleus accumbens (A/P: +1.7, L: 1.5, V: 7.0 from the surface of the brain) with reference to bregma (Paxinos & Watson, 1982). Auxiliary and reference electrodes were positioned on the surface of the brain. Electrodes were connected to the polarograph and the DOPAC oxidation peak was recorded every 5 min during a 60 min stabilisation period before the administration of any drugs. To detect DOPAC exclusively, the initial potential applied to the working electrode was set to −50 mV which corresponded with the end of the ascorbic acid peak and the scan was stopped at 200 mV corresponding to the beginning of the 5-HIAA + uric acid peak.

Saline (1 ml kg^{-1}, i.p.) or scopolamine (1 mg kg^{-1}, i.p.), atropine (20 μg, i.c.v.) were administered followed 15 min later by saline (i.c.v.) or haloperidol (1 mg kg^{-1}, s.c.) or clozapine (30 mg kg^{-1}, i.p.). Extracellular DOPAC was recorded every 5 min for the following 60 min.

Histology

The placement of the electrodes was checked histologically. Brains were removed, frozen and sectioned with a microtome, slices mounted on glass slides and stained with cresyl violet for examination. For i.c.v. injection, 2 μl of ink was injected by the same procedure as used for atropine. The brains were removed, sliced transverselly at the injection sites and the dispersion of ink in the ventricle directly checked.

Statistics

The DOPAC peak was recorded every 5 min. Peak heights were measured and converted to a percentage of the basal level calculated from the mean of the last four peaks before drug administration. Differences between groups were assessed by analysis of variance followed by a Scheffe's F Test using Stat-view II Statistical Software, $*P < 0.05$.

Drugs

Scopolamine and atropine (Sigma) were dissolved in saline. Clozapine (Sandoz) was dissolved in saline-HCl 0.3 M and the pH adjusted to 4–5 with saline-NaOH 1 M. Haloperidol (Janssen) was obtained in an injectable ampoule (5 mg ml^{-1}) and was diluted with saline.

Results

Compared with saline (1 ml kg^{-1}, i.p.), scopolamine (1 mg kg^{-1}, i.p.) and atropine (20 μg, i.c.v.) had no effect on extracellular DOPAC in the nucleus accumbers or the striatum (Figure 1 and 2). Haloperidol (1 mg kg^{-1}, s.c.) increased extracellular striatal and accumbens DOPAC (Figure 1 and 2). Pretreatment with scopolamine 15 min before haloperidol produced a small reduction of the increase in dopamine metabolism induced by haloperidol in the nucleus accumbens (Figure 1) but the effect of scopolamine did not reach a significant level ($F = 3.7$, d.f. = 11, 121, $P < 0.08$). Figure 1 shows also that scopolamine did not alter the increase in extracellular DOPAC induced by haloperidol in the striatum ($F = 0.5$, d.f. = 11, 121, $P < 0.51$). The central injection of atropine (20 μg, i.c.v.) 15 min before haloperidol did not reduce the increase in extracellular DOPAC induced by haloperidol either in the nucleus accumbens ($F = 3.5$, d.f. = 9, 99, $P < 0.09$) or the striatum ($F = 0.1$, d.f. = 10, 110, $P < 0.68$). Clozapine (30 mg kg^{-1}, i.p.) also increased the DOPAC peak height in both the nucleus accumbens and the striatum (Figure 3) and pretreatment with scopolamine attenuated this increase in both regions (nucleus accumbens: $F = 17.7$, d.f. = 13, 143, $P < 0.001$; striatum: $F = 24.9$, d.f. = 13, 143, $P < 0.001$). Pretreatment with atropine (20 μg, i.c.v.) also attenuated the effect produced by clozapine in both brain regions (nucleus accumbens: $F = 34.7$, d.f. = 10, 110, $P < 0.001$; striatum: $F = 41.1$, d.f. = 10, 110, $P < 0.001$) (Figure 4).

Discussion

Peripheral or central administration of muscarinic antagonists attenuated the increase in accumbens and striatal extracellular DOPAC induced by the atypical neuroleptic clozapine but not by the typical neuroleptic haloperidol. The present results agree with a previous report suggesting that cholinergic mechanisms may be involved in the effects of clozapine on dopaminergic neurones (Chiodo & Bunney, 1985). In this study, chronic co-administration of haloperidol with a muscarinic antagonist produced a similar response on the firing of dopaminergic neurones in the ventral tegmental area and the substantial nigra to that observed after a chronic treatment with clozapine (Chiodo & Bunney, 1985).

The finding that the muscarinic antagonists attenuated the clozapine-induced increase in striatal and accumbens extra-

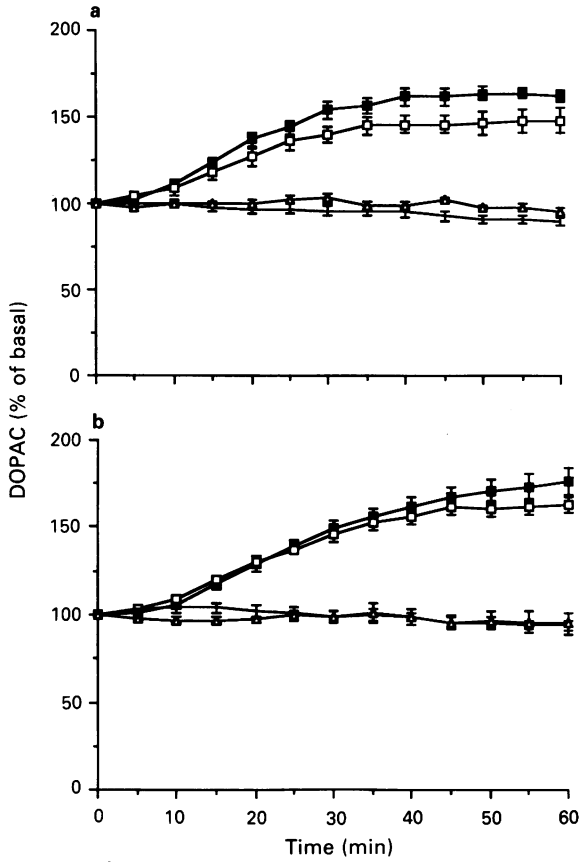

Figure 1 Effect of saline (−), scopolamine (△), haloperidol (■) and scopolamine + haloperidol (□) on extracellular DOPAC in the nucleus accumbens (a) and the striatum (b). Saline (1 ml kg^{-1}, i.p.) or scopolamine (1 mg kg^{-1}, i.p.) were injected followed 15 min later by saline (i.p.) or haloperidol (1 mg kg^{-1}, s.c.). DOPAC peak height was monitored every 5 min for 60 min. The basal extracellular DOPAC level was estimated from the mean of the last four peaks recorded before drug administration and are shown as 100%. Each value is the mean of the recordings made in 6 animals (7 for the group scopolamine + haloperidol); s.e.mean shown by vertical bars. The basal levels of DOPAC in the nucleus accumbens and the striatum were estimated from the DOPAC peak heights *in vitro* and were 41.2 ± 6.4 and 39.4 ± 7.8 (μM ± s.d.) respectively (n = 12).

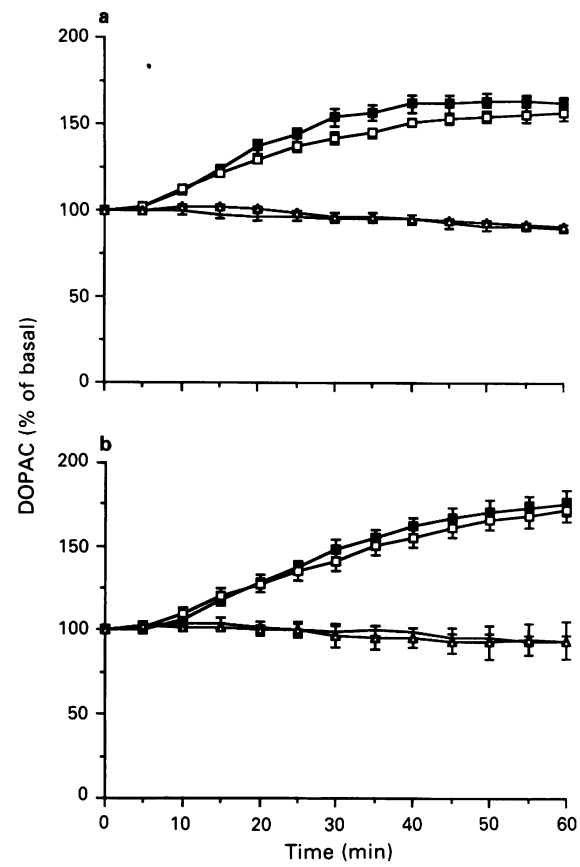

Figure 2 Effect of saline (−), atropine (△), haloperidol (■) and atropine + haloperidol (□) on the extracellular DOPAC in the nucleus accumbens (a) and the striatum (b). Saline (1 ml kg^{-1}, i.p.) or atropine (20 μg, i.c.v.) were injected followed 15 min later by saline (i.p.) or haloperidol (1 mg kg^{-1}, s.c.). DOPAC peak height was monitored every 5 min for 60 min. The basal extracellular DOPAC level was estimated from the mean of the last four peaks recorded before drug administration and are shown as 100%. Each value is the mean of the recordings made in 6 animals (n = 5 for the atropine + saline group); s.e.mean shown by vertical bars.

cellular DOPAC but had no effects on the haloperidol-induced increase may reflect the different profile of the two neuroleptics for affinity at various receptor sites. Clozapine has affinity for a wide range of receptor sites; muscarinic and histamine receptors as well as lower afinity for dopamine, noradrenaline and 5-hydroxytryptamine receptors (Miller & Hiley, 1974; Creese *et al.*, 1976; Seeman *et al.*, 1976; Perry *et al.*, 1983; Richelson & Nelson, 1984; Meltzer *et al.*, 1989). While the increase in dopamine metabolism induced by haloperidol probably involves a specific action at dopamine receptors, it is apparent from the present results that the same effect produced by clozapine is dependent upon the participation of muscarinic receptors. Furthermore, as the effects of clozapine on dopamine metabolism were reduced following intracerebroventricular administration of atropine, the muscarinic receptors involved are situated centrally. It is however possible that a certain quantity of atropine injected into the lateral ventricle leaked to the periphery and produced some effects in which both peripheral and central receptors may have been involved.

It remains to be determined what mechanisms operate in the muscarinic receptor involvement in the clozapine-induced increase in dopamine metabolism. With the doses used in the present study, both muscarinic antagonists markedly attenuated the clozapine-induced increase in extracellular DOPAC in the nucleus accumbens and the striatum. While the present findings suggest that muscarinic receptors play a significant role in the effects of clozapine, it is unlikely that the increase in DOPAC induced by the neuroleptic depends entirely on the blockade of these receptors since neither scopolamine nor atropine increased DOPAC *per se*. Another reason why clozapine is probably not acting as a pure muscarinic antagonist is that while atropine increases acetylcholine but not dopamine release in the striatum (Westerink *et al.*, 1990), clozapine (50 mg kg^{-1}; but not 20 mg kg^{-1}, i.v.) has been reported to increase the release of acetylcholine in the caudate nucleus measured using push-pull cannulae in the gallamine-immobilized cat (Stadler *et al.*, 1974) as well as increasing dopamine release and metabolism in the striatum of the rat (Maidment & Marsden, 1987; Stamford *et al.*, 1988; Moghaddam & Bunney, 1990). However clozapine (20 mg kg^{-1}) has no effect on acetylcholine release *in vitro* in the rat nucleus accumbens and striatum (Compton & Johnson, 1989). To our knowledge, it has not been determined whether clozapine alters acetylcholine release in the rat *in vivo* at the dose used in the present study.

One possibility is that clozapine increases DOPAC by mechanisms that involve the participation of both muscarinic and dopamine receptors. Therefore, clozapine may act on muscarinic receptors located on cholinergic as well as dopaminergic neurones since lesion studies with 6-hydroxydopamine have shown that muscarinic receptors may be located on dopaminergic nerve terminals in the striatum (De Belleroche *et al.*, 1979; Gurwitz *et al.*, 1980). It is feasible that clozapine antagonises muscarinic auto-receptors located on cholinergic terminals resulting in release of acetylcholine that acts on cholinoceptors located on dopaminergic neurones

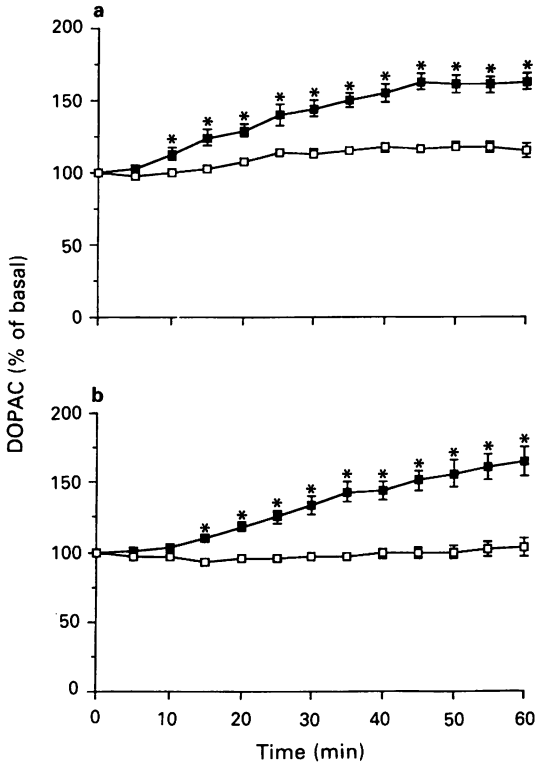

Figure 3 Effect of scopolamine on the increase in extracellular DOPAC induced by clozapine in the nucleus accumbens (a) and the striatum (b). Saline (1 ml kg^{-1}, i.p.) or scopolamine (1 mg kg^{-1}, i.p.) were injected followed 15 min later by clozapine (30 mg kg^{-1}, i.p.). DOPAC peak height was monitored every 5 min for 60 min. Groups are: saline + clozapine (■) and scopolamine + clozapine (□). The basal extracellular DOPAC level was estimated from the mean of the last four peaks recorded before drug administration and are shown as 100%. Each value is the mean of the recordings made in 6 animals (*$P < 0.05$, Scheffe's F Test) for the clozapine group and 9 animals for scopolamine + clozapine group; s.e.mean shown by vertical bars.

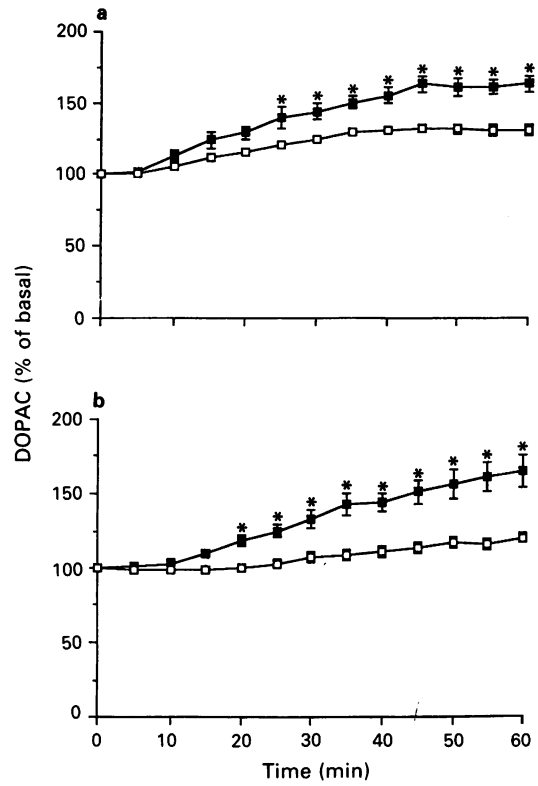

Figure 4 Effect of atropine on the increase in extracellular DOPAC induced by clozapine in the nucleus accumbens (a) and the striatum (b). Saline (1 ml kg^{-1}, i.p.) or atropine (20 μg, i.c.v) were injected followed 15 min later by clozapine (30 mg kg^{-1}, i.p.). DOPAC peak height was monitored every 5 min for 60 min. The basal extracellular DOPAC level was estimated from the mean of the last four peaks recorded before drug administration and are shown as 100%. Groups are: saline + clozapine (■) and atropine + clozapine (□). Each value is the mean of 6 recordings with s.e.mean shown by vertical bars; *$P < 0.05$ (Scheffe's F Test).

to cause an increase in dopamine metabolism. In contrast, by blocking both M_1 and M_2 sites, atropine causes the release of acetylcholine but also blocks the effects of the neurotransmitter on dopamine cells and so has no effect on dopamine metabolism on its own. The effects of clozapine on DOPAC are antagonized by both atropine and scopolamine as under these conditions both M_1 and M_2 sites are antagonized. Further investigations are needed to examine this hypothesis.

An alternative explanation is that the increase in dopamine metabolism by clozapine resulted from the blockade of dopamine receptors but can be regulated by muscarinic function. According to this hypothesis, muscarinic antagonists should attenuate both the clozapine and haloperidol-induced increase in dopamine metabolism. In the present study, scopolamine and atropine caused a small but not significant reduction in the effect produced by haloperidol. In contrast to the present study, earlier reports have suggested that muscarinic antagonists can inhibit haloperidol-induced increases in dopamine metabolism *ex vivo* (Andén & Bédard, 1971; Andén, 1972; Westerink & Korf, 1975). Several factors may account for the difference in the results between these studies and the present one. Thus, while the present study investigated changes in extracellular DOPAC concentrations in the nucleus accumbens and the striatum *in vivo*, the previous work reported changes in tissue dopamine and homovanillic acid concentrations in the nucleus accumbens and the striatum of rats and rabbits. Moreover, the drugs and doses differed as well as the time at which dopamine metabolism was measured following drug treatments.

The present study demonstrates that muscarinic receptors are involved in the increase in dopamine metabolism induced by the atypical neuroleptic clozapine but not by the typical neuroleptic haloperidol after acute administration. The results support the view that the affinity of clozapine for muscarinic receptors is important for the effect of the neuroleptic on dopaminergic systems and may account for the therapeutic profile of the drug.

This work was supported by the Wellcome Trust and by a studentship to R.R. by the FCAR of Quebec.

References

ANDÉN, N.-E. (1972). Dopamine turnover in the corpus striatum and the limbic system after treatment with neuroleptic and anti-acetylcholine drugs. *J. Pharm. Pharmacol.*, **24**, 905–906.

ANDÉN, N.-E. & BÉDARD, P. (1971). Influences of cholinergic mechanisms on the function and turnover of brain dopamine. *J. Pharm. Pharmacol.*, **23**, 460–462.

CHIODO, L.A. & BUNNEY, B.S. (1983). Typical and atypical neuroleptics: differential effects of chronic administration on the activity of A9 and A10 midbrain dopaminergic neurons. *J. Neurosci.*, **3**, 1607–1619.

CHIODO, L.A. & BUNNEY, B.S. (1985). Possible mechanisms by which repeated clozapine administration differentially affects the activity of two subpopulations of midbrain dopamine neurons. *J. Neurosci.*, **5**, 2539–2544.

CHIPKIN, R.E. & LATRANYI, M.B. (1987). Similarity of clozapine and SCH 23390 in reserpinized rats suggests a common mechanism of

action. *Eur. J. Pharmacol.*, **136**, 371–375.

COMPTON, D.R. & JOHNSON, K.M. (1989). Effects of acute and chronic clozapine and haloperidol on in vivo release of acetylcholine and dopamine from striatum and nucleus accumbens. *J Pharmacol. Exp. Ther.*, **248**, 521–530.

COSTA, E., CHENEY, D.L., MAO, C.C. & MORONI, F. (1978). Action of antischizophrenic drugs on the metabolism of γ-aminobutyric acid and acetylcholine in globus pallidus, striatum and n. accumbens. *Fed. Proc.*, **37**, 2408–2414.

COSTALL, B. & NAYLOR, R.J. (1976). A comparison of the abilities of typical neuroleptic agents and of thioridazine, clozapine, sulpiride and metoclopramide to antagonise the hyperactivity induced by dopamine applied intracerebrally to areas of the extrapyramidal and mesolimbic systems. *Eur. J. Pharmacol.*, **40**, 9–19.

CREESE, I., BURT, D.R. & SNYDER, S. (1976). Dopamine receptor binding predicts clinical and pharmacological potencies of antischizophrenic drugs. *Science*, **192**, 481–483.

CRESPI, F., PARET, J., KEANE, P.E. & MORRE, M. (1984). An improved differential pulse voltammetry technique allows the simultaneous analysis of dopaminergic and serotonergic activities in vivo with a single carbon-fibre electrode. *Neurosci. Lett.*, **52**, 159–164.

CRISWELL, H.E., MUELLER, R.A. & BREESE, G.A. (1989). Clozapine antagonism of D-1 and D-2 dopamine receptor-mediated behaviors. *Eur. J. Pharmacol.*, **159**, 141–147.

DE BELLEROCHE, S. & GARDINER, I.M. (1982). Cholinergic action in the nucleus accumbens: modulation of dopamine and acetylcholine release. *J. Pharmacol.*, **75**, 359–365.

DE JONGE, M.C. & FUNCKE, A.B.H. (1962). Sinistrotorsion in guinea pigs as a method of screening central anticholinergic activity. *Arch. Int. Pharmacodyn.*, **137**, 375–382.

FJALLAND, B., CHRISTENSEN, A.V. & HYTTEL, J. (1977). Peripheral and central muscarinic receptor affinity of psychotropic drugs. *Naunyn-Schmiedebergs Arch. Pharmacol.*, **301**, 5–9.

GERLACH, J. & SIMMELSGARD, H. (1978). Tardive dyskinesia during and following treatment with haloperidol, biperiden, thioridazine and clozapine. *Psychopharmacology*, **59**, 105–112.

GONON, F., BUDA, M., CESPUGLIO, R., JOUVET, M. & PUJOL, J.-F. (1980). In vivo electrochemical detection of catechols in the neostriatum of anaesthetized rats: dopamine or DOPAC? *Nature*, **286**, 902–904.

GURWITZ, D., KLOOG, Y., EGOZI, Y. & SOKOLOVSKY, M. (1980). Central muscarinic receptor degeneration following 6-hydroxydopamine lesion in mice. *Life. Sci.*, **26**, 79–84.

HERMAN, E. & PLEASURE, H. (1963). Clinical evaluation of thioridazine and chlorpromazine in chronic schizophrenia. *Disease Nervous System*, **24**, 54–59.

HERRLING, P.L. & MISBACH-LESENNE, B. (1982). Effects of clozapine in a selective muscarinic bioassay and on single cells of the rat hippocampus. *Naunyn-Schmiedebergs Arch. Pharmacol.*, **320**, 20–25.

LE MOINE, C., TISON, F. & BLOCH, B. (1990). D2 dopamine receptors gene expression by cholinergic neurons in the rat striatum. *Neurosci. Lett.*, **117**, 248–252.

MAIDMENT, N.T. & MARSDEN, C.A. (1987). Acute administration of clozapine, thioridazine and metoclopramide increases extracellular DOPAC and decreases estracellular 5-HIAA, measured in the nucleus accumbens and striatum of the rat using *in vivo* voltammetry. *Neuropharmacology*, **26**, 187–193.

MARSDEN, C.D., TARSY, D. & BALDESSARINI, R.J. (1975). Spontaneous and drug-induced movement disorders in psychotic patients. In *Psychiatric Aspects of Neurological Disease*, ed. Benson, D.F. & Blumer, D. p. 219. New York: Grune and Stratton,

MCMILLEN, B.A., DAVANZO, E.A., SONG, A.H., SCOTT, S.M. & RODRIGUEZ, M.E. (1989). Effects of classical and atypical antipsychotic drugs on isolation-induced aggression in male mice. *Eur. J. Pharmacol.*, **160**, 149–153.

MELTZER, H.Y. & STAHL, S.M. (1976). The dopamine hypothesis of schizophrenia: a review. *Schizophr. Bull.*, **2**, 19–76.

MELTZER, H.Y., MATSUBARA, S. & LEE, J.C. (1989). Classification of typical and atypical drugs on the basis of dopamine D-1, D-2 and serotonine$_2$ pKi values. *J. Pharmacol. Exp. Ther.*, **251**, 238–246.

MILLER, R.J. & HILEY, C.R. (1974). Anti-muscarinic properties of neuroleptics and drugs-induced parkinsonism. *Nature*, **248**, 596–597.

MOGHADDAM, B. & BUNNEY, B. (1990). Acute effects of typical and atypical antipsychotic drugs on the release of dopamine from prefrontal cortex, nucleus accumbens, and striatum of the rat: an *in vivo* microdialysis study. *J. Neurochem.*, **54**, 1755–1760.

MURRAY, A.M. & WADDINGTON, J.L. (1990). The interaction of clozapine with dopamine D_1 versus dopamine D_2 receptor-mediated function: behavioural indices. *Eur. J. Pharmacol.*, **186**, 79–86.

PAXINOS, G. & WATSON, C. (1982). The Rat Brain in Stereotaxic Coordinates, New York: Academic press.

PEROUTKA, S.J., U'PRICHARD, D.C., GREENBERG, D.A. & SNYDER, S.H. (1977). Neuroleptic drug interactions with norepinephrine alpha receptor binding sites in rat brain. *Neuropharmacology*, **16**, 549–556.

PERRY, D.B., SIMON, P.R. & U'PRICHARD, D.C. (1983). Interaction of neuroleptic compounds at alpha 2-adrenergic receptor affinity states in bovine caudate nucleus. *Eur. J. Pharmacol.*, **95**, 315–318.

RACAGNI, G., CHENEY, D.L., TRABUCCHI, M. & COSTA, E. (1976). In vivo actions of clozapine and haloperidol on the turnover rate of acetylcholine in rat striatum. *J. Pharmacol. Exp. Ther.*, **196**, 323–332.

RICHELSON, E. & NELSON, A. (1984). Antagonism by neuroleptics of neurotransmitter receptors of normal human brain *in vitro*. *Eur. J. Pharmacol.*, **103**, 197–294.

RIVEST, R., JOLICOEUR, F.B. & MARSDEN, C.A. (1991). Neurotensin causes a greater increase in the metabolism of dopamine in the accumbens than in the striatum *in vivo*. *Neuropharmacology*, **30**, 25–33.

SAYERS, A.C. & BÜRKI, H.R. (1976). Antiacetylcholine activities of psychoactive drugs: a comparison of the [^{3}H] quinuclidinyl benzilate binding assay with conventional methods. *J. Pharm. Pharmacol.*, **28**, 252–253.

SEEMAN, P., LEE, T., CHAU-WONG, M. & WONG, K. (1976). Antipsychotic drug doses and neuroleptic/dopamine receptors. *Nature*, **261**, 717–719.

SETHY, V.M. & VAN WOERT, M.H. (1974). Regulation of striatal acetylcholine concentration by dopamine receptors. *Nature*, **251**, 529–530.

SHARP, T., MAIDMENT, N.T., BRAZELL, M.P., ZETTERSTROM, T., UNGERSTEDT, U., BENNETT, G.W. & MARSDEN, C.A. (1984). Changes in monoamine metabolites measured by simultaneous *in vivo* differential pulse voltammetry and intracerebral dialysis. *Neuroscience*, **12**, 1213–1221.

SNYDER, S.H., GREENBERG, D. & YAMAMURA, H.I. (1974). Antischizophrenic drugs and brain cholinergic receptors. *Arch. Gen. Psychiatry*, **31**, 58–61.

STADLER, H., LLOYD, K.G. & BARTHOLINI, G. (1974). Dopaminergic inhibition of striatal cholinergic neurons: synergistic blocking action of gama-butyrolactone and neuroleptic drugs. *Naunyn-Schmiedebergs Arch. Pharmacol.*, **283**, 129–134.

STAMFORD, J.A., KRUK, Z.L. & MILLAR, J. (1988). Actions of dopamine antagonists on stimulated striatal and limbic dopamine release: an *in vivo* voltammetric study. *Br. J. Pharmacol.*, **94**, 924–832.

TSCHANZ, J.T. & REBEC, G.V. (1988). Atypical antipsychotic drugs block selective components of amphetamine-induced stereotypy. *Pharmacol., Biochem. Behav.*, **31**, 519–522.

WESTERINK, B.H.C., DE BOER, P. & DAMSMA, G. (1990). Dopamine-acetylcholine interaction in the striatum studied by microdialysis in the awake rat: some methodological aspects. *J. Neurosci. Methods*, **34**, 117–223.

WESTERINK, B.H.C. & KORF, J. (1975). Influence of drugs on striatal and limbic homovanillic acid concentration in the rat brain. *Eur. J. Pharmacol.*, **33**, 31–40.

(Received January 24, 1991
Revised May 9, 1991
Accepted May 17, 1991)

Br. J. Pharmacol. (1991), **104**, 239–245

The behavioural properties of CI-988, a selective cholecystokinin$_B$ receptor antagonist

[1]Lakhbir Singh, Mark J. Field, John Hughes, Richard Menzies, Ryszard J. Oles, Caroline A. Vass & Geoffrey N. Woodruff

Parke-Davis Neuroscience Research Centre, Addenbrookes Hospital Site, Hills Road, Cambridge CB2 2QB

1 The behavioural effects of a selective cholecystokinin$_B$ (CCK$_B$) receptor antagonist CI-988 were investigated in rodents.

2 In three rodent tests of anxiety (rat elevated X-maze, rat social interaction test and mouse light/dark box) CI-988 over the dose range 0.001–10.0 mg kg^{-1}, (i.p.) produced an anxiolytic-like action. The magnitude of this effect was similar to that of chlordiazepoxide (CDP). In contrast, the selective CCK$_A$ receptor antagonist, devazepide, was inactive. CI-988 also showed anxiolytic-like action in the rat conflict test but the magnitude of this effect was about 2.5 fold less than that of CDP.

3 Central but not peripheral administration of the selective CCK$_B$ receptor agonist, pentagastrin, like FG 7142, produced an anxiogenic-like action.

4 The pentagastrin-induced anxiety was dose-dependently antagonized by CI-988, whereas devazepide was inactive. However, ten times higher doses of CI-988 were required to block a similar action of FG 7142.

5 In contrast to CDP, CI-988 up to 3000 fold higher doses than those inducing anxiolysis was inactive in tests measuring sedation and ataxia. It also failed to antagonize pentylenetetrazol-induced tonic seizures. Furthermore, CI-988 did not interact with alcohol or barbiturates. Thus, CI-988 appears to be an anxioselective compound.

6 The anxiolytic-like action of CDP in the rat elevated X-maze was dose-dependently antagonized by flumazenil. In contrast, the benzodiazepine receptor antagonist failed to block a similar effect of CI-988.

7 Thus, CI-988 shows anxiolytic-like activity in several animal models of anxiety. The anxiolytic-like effect of CI-988 involves a novel mechanism of action, that is likely to be mediated by selective antagonism of the brain CCK$_B$ receptor. It is suggested that CI-988 should have a better side-effect profile in man than the benzodiazepines.

Keywords: CCK$_A$ receptor; CCK$_B$ receptor; agonist; antagonist; anxiolytic; anxiogenic; sedation

Introduction

The peptide cholecystokinin (CCK) discovered originally in the gastrointestinal tract (Ivy & Oldberg, 1928), is also present in high concentrations in certain regions of the brain (Vanderhaegen *et al.*, 1975), where it exists mainly as the octapeptide in the sulphated and desulphated forms (Dockray, 1976; Rehfeld, 1978). The receptors for CCK have been divided into two types (Innis & Snyder, 1980): the CCK$_A$ receptor that is blocked selectively by devazepide (formerly MK-329, L-364,718; Chang & Lotti, 1986) and is found in discrete brain regions as well as some peripheral tissues (Hill *et al.*, 1987a,b), and the CCK$_B$ receptor that is found throughout the brain (Hill *et al.*, 1987a) and is characterized by the high affinity for the novel antagonists CI-988 (formerly PD 134308) and L-365,260 (Lotti & Chang 1989; Hughes *et al.*, 1990).

It has been reported that CCK may control various physiological events (Zetler, 1985) including hypothermia (Katsuura *et al.*, 1981), analgesia (Zetler, 1980; Kubota *et al.*, 1985), sedation (Zetler, 1981) and satiety (Gibbs *et al.*, 1973). Recent studies have also indicated a role of CCK in anxiety. Thus, animal studies have shown that activation of central CCK$_B$ receptors induces an anxiogenic-like action, whilst antagonism of this receptor leads to anxiolytic-like effects (Hughes *et al.*, 1990; Singh *et al.*, 1991a). Consistent with these data, it has been shown that intravenous administration of CCK-4 in man induces panic-like attacks (De Montigny, 1989; Bradwejn *et al.*, 1990).

The dipeptoid CI-988 is a highly potent and selective CCK$_B$ receptor antagonist (Hughes *et al.*, 1990; Horwell *et al.*, 1991). Recently it has been reported that CI-988 produces anxiolytic-like actions in several experimental models of anxiety (Hughes *et al.*, 1990; Singh *et al.*, 1991a). In the present study, evidence is presented that supports and extends our previous findings that the anxiolytic-like action of CI-988 may involve a specific interaction with the CCK$_B$ receptor. The present data also indicate that unlike benzodiazepines, CI-988 does not possess either anticonvulsant or sedative properties. Furthermore, it does not interact with CNS depressants.

Preliminary accounts of some of these data have already been presented (Field *et al.*, 1991a; Singh *et al.*, 1991b).

[1]Author for correspondence.

Methods

Animals

Male Hooded Lister rats (200–250 g) were obtained from Olac (Bicester, U.K.) and male TO mice (20–25 g) were obtained from Bantin and Kingman (Hull, U.K.). Animals were housed in groups of 6–10 under a 12 h light/dark cycle (lights on at 07 h 00 min) and unless stated otherwise, with food and water *ad libitum*. All behavioural tests were carried out between 10 h 00 min and 17 h 00 min.

Drug administration

Drugs were administered either i.p. or orally (p.o.) before test in a volume of 1 ml kg^{-1} for rats and 10 ml kg^{-1} for mice. Pentagastrin was administered intracerebroventricularly (i.c.v. in 5 μl of the vehicle).

Intracerebroventricular injections

The i.c.v. injections in mice and rats were carried out as described previously (Singh *et al.*, 1990; 1991a). Briefly, rats

were anaesthetized and a 22 gauge stainless steel guide cannula was implanted unilaterally by use of a Kopf stereotaxic frame (anterior posterior = 8.2 mm anterior of interaural line; lateral = +1.4 mm; dorso-ventral = 7.6 mm dorsal to the interaural line according to the atlas of Paxinos & Watson, 1976). Test compounds were administered through an injection cannula extending 1 mm ventral to the guide cannula tip. At the end of the experiment animals were selected randomly and injected with a dye to check the placement of the guide cannula. Mice were briefly anaesthetized with halothane and i.c.v. injections were made at lambda with a 27 gauge needle (3.5 mm long) attached to a 50 μl Hamilton syringe.

Mouse light/dark box

The apparatus was an open-topped box, 45 cm long, 27 cm wide and 27 cm high, divided into a small (2/5) and a large (3/5) area by a partition that extended 20 cm above the walls (Costall *et al.*, 1989a). There was a 7.5 × 7.5 cm opening in the centre of the partition at floor level. The small compartment was painted black and the large compartment white. The white compartment was illuminated by a 60 W tungsten bulb. The laboratory was illuminated by red light. Each mouse was tested by placing it in the centre of the white area and allowing it to explore the novel environment for 5 min. The time spent in the illuminated side was measured (Kilfoil *et al.*, 1989).

Rat social interaction test

The apparatus used was an open-topped box (51 × 51 × 20 cm high) with 17 × 17 cm areas marked on the floor. Two naive rats from separate housing cages were placed into the brightly illuminated box. Their behaviour was scored on a television monitor in an adjacent room, by use of a keyboard linked to an IBM compatible PC over a 5 min period. The arena was cleaned with a solution of Dettol in water (18 ml l^{-1}) between each observation to remove odours. The following behaviours were scored for 5 min as active social interaction (Guy & Gardner, 1985): sniffing, following, grooming, licking, mounting, genital investigation and aggression (which consists of biting, boxing, aggressive grooming, kicking away and full submissive posture).

Rat elevated X-maze

A standard elevated X-maze (Handley & Mithani, 1984; Pellow *et al.*, 1985) was automated as previously described (Field *et al.*, 1991b). The animals were placed on the centre of the X-maze facing one of the open arms. For anxiolytic effects the entries and time spent on the end half sections of the open arms was measured during the 5 min test period (Costall *et al.*, 1989b; Singh *et al.*, 1991a). However, to measure anxiogenic-like actions the total entries and time spent on the open arms was measured (Singh *et al.*, 1991a).

Rat conflict test

Male Hooded Lister rats (food deprived to 75–80% of their free feeding body weight) were trained to press levers for 45 mg food pellets in standard operant chambers (Coulbourn Instruments). The schedule consisted of alternations of four 4 min variable interval (VI) 30 s unpunished periods signalled by chamber lights on and three 3 min fixed ratio (FR) 5 punished periods signalled by chamber lights off. During the punished periods, a 100 ms footshock was given concomitant to food delivery. To study anxiolytic effects, the degree of footshock (100–300 μA) was adjusted for each rat to obtain approximately 80–90% suppression of responding in comparison with unpunished FR5 responding. To measure anxiogenic-like effects the footshock punishment (50–100 μA) was adjusted to obtain approximately 40% suppression.

Upon stable baseline responding, six rats were implanted with a intracerebroventricular (i.c.v.) guide cannula. Test sessions were run once a week and on control days, animals were injected with the appropriate vehicle. Drug effect was expressed as the percentage increase or decrease of the lever-pressing rates during the punished periods and during the unpunished periods on the test day compared with mean performances obtained the two previous days. Rats were only tested if their 2-day control values remained within the following ranges: (1) daily VI30 responses were within 20% of the 2-day mean; (2) daily FR5 responses were within 20% of the 2-day mean; (3) the number of shocks on each control day was at least 2.

Anticonvulsant studies

Pentylenetetrazol (PTZ; 15 mg ml^{-1}, 0.224 ml min^{-1}) was infused i.v. via a tail vein of restrained mice. The latency to tonic seizure was noted. This convulsion represented the end-point of the test and mice were killed immediately after it had occurred. The threshold dose of the convulsant required to elicit this seizure was calculated for each mouse.

Sedation and motor coordination

Mouse rotarod Untrained mice were placed on the accelerating rotarod (accelerating to 15 rev min^{-1} in 120 s) and the time spent on the rotating rotarod was determined.

Rat locomotor activity cages Rats were placed individually in photocell activity cages (45 × 24 × 20 cm). The boxes were fitted with a pair of infrared photocells (in the centre of the long side walls). The locomotor cages were interfaced to an IBM compatible PC. Activity was measured as the number of photocell breaks during a 60 min test period.

Interaction with alcohol and barbiturates

The ability of CI-988 or CDP to potentiate the sedative action of ethanol (0.75 g kg^{-1}, a threshold sedative dose administered p.o. 30 min before test) was examined using the mouse rotarod apparatus. An interaction with sodium pentobarbitone (60.0 mg kg^{-1}, i.p.) was investigated by measuring changes in the sleeping time.

Drugs

The following drugs were used: chlordiazepoxide (CDP, Sigma Chemical Co.), pentagastrin and FG 7142 (N-methyl-β-carboline-3-carboxamide, Research Biochemicals Inc.). Flumazenil (Roche), sodium pentobarbitone (Sagatal, May and Baker). CI-988 (4-{[2-[[3-(1H-indol-3-yl)-2-methyl-1-oxo-2-[[(tricyclo - [3.3.1.1.^{3,7}] - dec - 2 - yloxy) - carbonyl] - amino] - propyl]-amino]-1-phenylethyl]-amino}-4-oxo-[**R**-(**R***,**R***)]-butanoate-*N*-methyl-D-glucamine), L-365,260 [(3**R**)-(+)-N-(2,3-dihydro-1-methyl-2-oxo-5-phenyl-1H-1,4-benzodiazepin-3-yl)-N1-(3-methylphenyl)-urea] and devazepide were synthesized at Parke-Davis Neuroscience Research Centre.

Chlordiazepoxide, flumazenil and FG 7142 were suspended in 1.0% w/v carboxymethylcellulose (CMC) with aid of ultrasonification. CI-988 was dissolved in 0.9% w/v NaCl. Devazepide and L-365,260 were dissolved in 100% ethanol and serially diluted in alcohol and the required concentration was achieved by addition of CMC, so that all solutions contained 10% alcohol. Pentagastrin was dissolved in sodium bicarbonate (50 mM).

Results

Effects of CI-988, L-365,260, CDP and devazepide in the mouse light/dark box

The i.p. administration of CI-988 (0.01–10.0 mg kg^{-1}), L-365,260 (0.01–10.0 mg kg^{-1}) or CDP (2.5–20.0 mg kg^{-1}) 40 min

Table 1 The effect of cholecystokinin (CCK) receptor antagonists in the mouse light/dark box and the rat social interaction test

Compound	*Dose* ($mg\,kg^{-1}$)	*Light/dark box*	*Social interaction*
		TIL (s)	SI (s)
CDP	Veh	79.4 ± 9.7	35.7 ± 1.9
	0.3	—	42.7 ± 3.3
	1.0	—	61.3 ± 6.4*
	3.0	—	68.6 ± 5.6*
	2.5	122.4 ± 15.6	—
	5.0	158.3 ± 15.4*	63.2 ± 4.3*
	10.0	155.4 ± 10.4*	51.3 ± 4.1*
	20.0	157.6 ± 20.5*	—
CI-988	Veh	80.9 ± 7.4	35.7 ± 1.9
	0.001	—	40.4 ± 3.7
	0.01	114.6 ± 14.9	51.9 ± 2.9*
	0.1	132.5 ± 15.1*	57.1 ± 2.3*
	1.0	130.3 ± 10.2*	61.5 ± 1.9*
	3.0	—	60.8 ± 7.7*
	10.0	165.9 ± 21.9*	
L-365,260	Veh	80.0 ± 10.0	45.9 ± 1.4
	0.01	90.2 ± 18.3	—
	0.1	101.3 ± 14.3	—
	0.3	—	46.2 ± 3.1
	1.0	139.3 ± 16.8*	54.1 ± 3.7
	3.0	—	59.1 ± 2.0*
	6.0	—	54.6 ± 2.9
	10.0	134.6 ± 9.7*	45.2 ± 4.3
Devazepide	Veh	87.8 ± 18.3	45.9 ± 1.4
	0.5	94.2 ± 12.0	—
	5.0	77.5 ± 11.1	37.2 ± 2.9
	10.0	59.5 ± 9.1	54.9 ± 7.4
	20.0	103.4 ± 23.8	34.8 ± 1.8
	40.0	—	35.8 ± 3.3

Compounds were administered i.p. 40 min before the 5 min test periods. The time spent by mice in the light side (TIL) of the light/dark box and the social interaction (SI) between pairs of rats is shown in seconds. Results are shown as the means (± s.e.mean) of 8–10 animals per group.
* Significantly different from vehicle-treated controls, $P < 0.05$ (ANOVA followed by Dunnett's t test).

before test, increased dose-dependently the time spent on the illuminated side of the box, with minimum effective doses (MED) of 0.1, 1.0 and 5.0 $mg\,kg^{-1}$ respectively (Table 1). In contrast, devazepide was inactive up to 20 $mg\,kg^{-1}$ (Table 1).

Effects of CI-988, CDP, L-365,260 and devazepide in the rat conflict test

The i.p. administration of CI-988 (0.001–3.0 $mg\,kg^{-1}$), CDP (0.3–5.0 $mg\,kg^{-1}$) or L-365,260 (0.3–3.0 $mg\,kg^{-1}$) 40 min before test dose-dependently increased the active interaction between pairs of rats with MED of 0.01, 1.0 and 3.0 $mg\,kg^{-1}$ respectively (Table 1). As in the light/dark box, the activity of CI-988 was maintained over a wide (1000 fold) dose-range (Table 1). However, at higher doses of L-365,260 and CDP a fall off in the effect was observed (Table 1). As in the light/dark box, devazepide was without effect up to 40 $mg\,kg^{-1}$ (Table 1).

CDP (1.0–30.0 $mg\,kg^{-1}$, i.p.) administered 40 min before test, produced a pronounced increase in punished responding at 3 and 10 $mg\,kg^{-1}$ (Table 2). However, at 30 $mg\,kg^{-1}$, CDP caused a large decrease in punished and unpunished responding (Table 2). CI-988 (0.001–1.0 $mg\,kg^{-1}$, i.p.) induced a small but consistent increase in punished responding at all doses, with a significant effect occurring at 0.01 $mg\,kg^{-1}$ (Table 2). In contrast to CDP, it had no effect on unpunished responding at any of the doses tested (Table 2). The i.c.v. administration of pentagastrin (16 μg/rat) 5 min before test, produced a large decrease in both punished and unpunished responding (Table 2).

Effects of FG 7142 and pentagastrin in the rat elevated X-maze and the mouse light/dark box

The administration of FG 7142 (10.0–30.0 $mg\,kg^{-1}$, i.p.) 30 min before test decreased dose-dependently the entries and time spent by rats on the open arms of the X-maze without affecting the total entries (Figure 1). The MED was 10.0 $mg\,kg^{-1}$ (Figure 1). Similar administration in the mouse also dose-dependently reduced the time spent in the illuminated side of the light/dark box with a MED of 3.0 $mg\,kg^{-1}$ (Figure 1). The i.c.v. administration of pentagastrin (0.08–8.0 μg per animal) 15 min before test produced similar effects to FG 7142 in the two tests (Figure 1), the MED in both tests being 0.8 μg per animal (Figure 1). However, when administered i.p. 30 min before test, pentagastrin (0.1–1.0 $mg\,kg^{-1}$) failed to affect the time spent by mice in the illuminated side of the light/dark box. The mean time (s) spent by control animals in the light side was 117.7 ± 16.2 (± s.e.mean, $n = 10$).

The oral activity of CI-988 in the mouse light/dark box and the rat elevated X-maze

The oral administration of CI-988 (0.001–10.0 $mg\,kg^{-1}$) 40 min before test, increased the percentage time spent and entries made by rats on to the end sections of the X-maze in a dose-related manner (Figure 2). However, it did not alter the total number of entries suggesting a lack of affect on spontaneous locomotor activity. Similarly, CI-988 also increased

Table 2 The effect of CI-988, CDP and pentagastrin in the rat conflict test

Treatments	*Dose* ($mg\,kg^{-1}$)	*Unpunished* % *Increase or decrease*	*Punished*
CDP	1.0	9.4 ± 4.2*	88.6 ± 41.6
	3.0	7.8 ± 5.6	84.8 ± 15.8**
	10.0	−14.5 ± 16.1	137.5 ± 50.7**
	30.0	−62.1 ± 20.9**	3.5 ± 55.0
CI-988	0.001	−1.9 ± 3.9	12.1 ± 11.7
	0.01	−2.6 ± 2.8	25.8 ± 11.8*
	0.1	−0.3 ± 5.6	14.3 ± 9.0
	1.0	−0.3 ± 2.1	7.7 ± 11.8
Pentagastrin	16 μg per rat	−48.3 ± 12.8*	−53.0 ± 13.5**
Pentagastrin + CI-988	16 μg per rat + 0.1 $mg\,kg^{-1}$, i.p.	−10.6 ± 10.3*	−3.6 ± 13.8*

Results are expressed as the mean percentage increase or decrease of lever-pressing rates (± s.e.mean of at least 9 rats per group) on the test day compared with mean performances obtained the two previous days following vehicle administration. Test compounds were administered i.p. 40 min before test. For pentagastrin $n = 6$. Significantly different from previous control days *$P < 0.05$; **$P < 0.01$ (paired Student's t test).

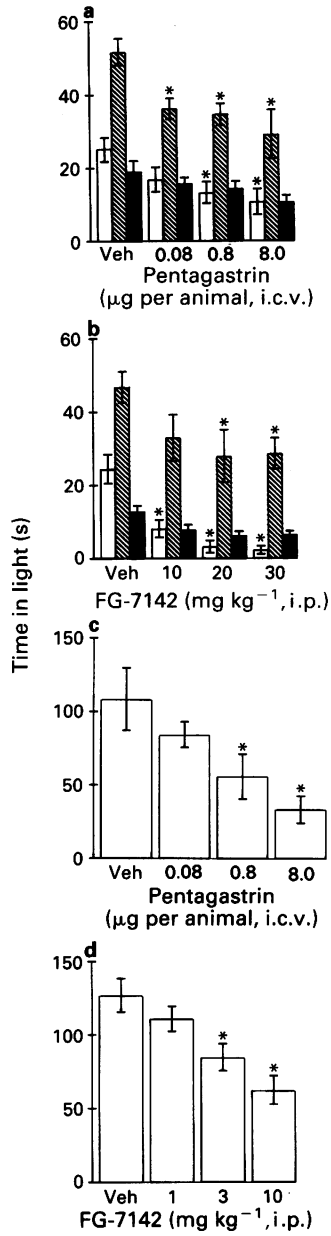

Figure 1 Effect of pentagastrin and FG 7142 in the rat elevated X-maze and the mouse light/dark box. Pentagastrin and FG 7142 were administered i.c.v. and i.p. 15 and 30 min before test, respectively. For the elevated X-maze (a,b), percentage time spent (open columns) and percentage entries (hatched columns) made on to the open arms, and the total number of entries (solid columns) were measured. For the light/dark box (c,d), the time spent in the light side was determined. Results are shown as the mean (vertical bars represent ±s.e.mean) of 10 animals per group. *Significantly different from vehicle-treated controls, $P < 0.05$ (ANOVA followed by Dunnett's t test).

the time spent by mice in the illuminated side of the light/dark box (Figure 2), the MED in the two tests being 0.01 mg kg^{-1} (Figure 2).

Effect of CI-988 on the action of pentagastrin and FG 7142

The effect of a submaximal dose of pentagastrin (0.8 μg per animal, i.c.v.) or FG 7142 (10 mg kg^{-1}, i.p.) in the mouse light/dark box and the rat elevated X-maze was antagonized dose-dependently by oral administration of CI-988 (Figure 3). The doses of CI-988 that completely antagonized the effect of pentagastrin or FG 7142 in both models were 1 and 10 mg kg^{-1},

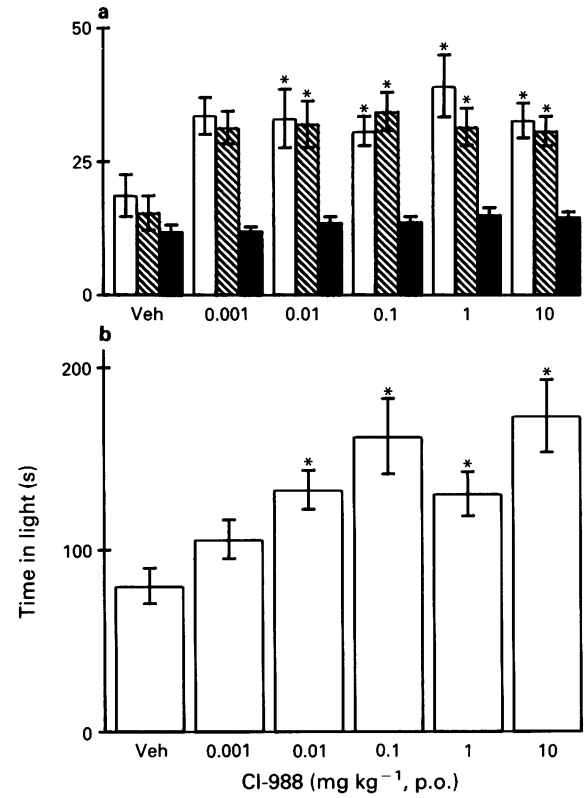

Figure 2 Oral activity of CI-988 in the rat elevated X-maze and the mouse light/dark box. CI-988 was administered orally 40 min before test. For the elevated X-maze (a), percentage time spent (open columns) and entries made (hatched columns) on to the end half sections of the open arms, and the total number of entries (solid columns) were measured. For the light/dark box (b), the time spent in the light side was determined. Results are shown as the mean (vertical bars represent ± s.e.mean) of 10 animals per group. *Significantly different from vehicle-treated controls, $P < 0.05$ (ANOVA followed by Dunnett's t test).

respectively (Figure 3). Moreover, CI-988 (0.1 mg kg^{-1}, i.p.) almost completely antagonized the action of pentagastrin (16 μg per rat, i.c.v.) in the rat conflict test (Table 2). However, unlike CI-988, devazepide (0.1–1.0 mg kg^{-1}, i.p.) was inactive against pentagastrin in the light/dark box (Figure 3). In these antagonism studies none of the treatments affected the total number of entries on the elevated X-maze.

Effect of flumazenil on the action of CI-988 in the rat elevated X-maze

The administration of flumazenil (10.0–100.0 mg kg^{-1}, i.p.) 20 min before a submaximal dose of CDP (3 mg kg^{-1}, i.p.), antagonized dose-dependently the benzodiazepine-induced increase in the entries and time spent on the end half sections of the open arms (Figure 4). At 30.0 mg kg^{-1}, flumazenil almost completely antagonized the action of CDP (Figure 4). In contrast, up to 100 mg kg^{-1} flumazenil failed to antagonize a similar effect of CI-988. In the elevated X-maze, flumazenil (100.0 mg kg^{-1}) had no effect in control animals (Figure 4).

Anticonvulsant activity

The administration of CDP 40 min before test increased dose-dependently (3.0–60.0 mg kg^{-1}, i.p.) the threshold dose of PTZ required to elicit tonic seizures with a MED of 10.0 mg kg^{-1} (Table 3). In contrast, CI-988 up to high doses of 100.0 mg kg^{-1} failed to alter the convulsive dose of PTZ (Table 3).

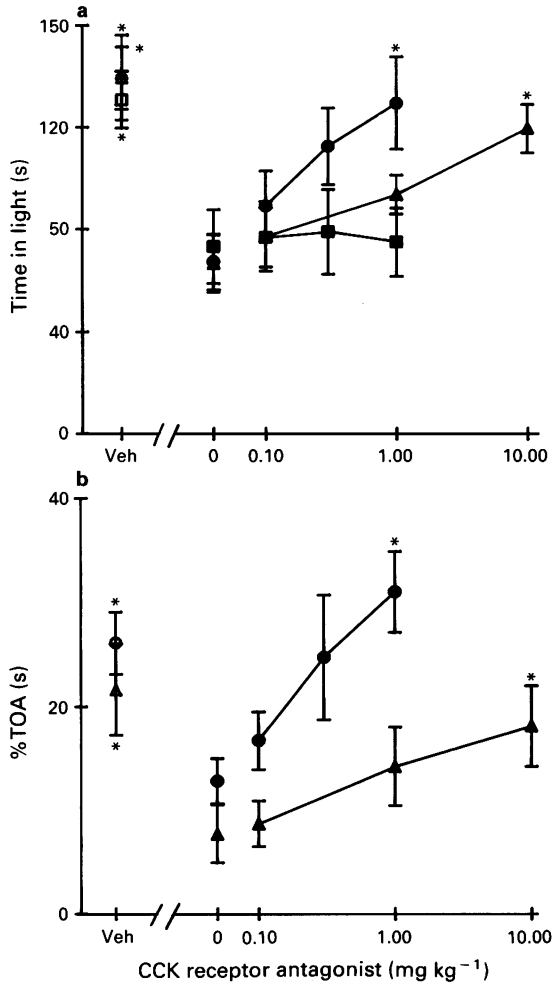

Figure 3 Effect of cholecystokinin (CCK) receptor antagonists on the action of pentagastrin and FG 7142 in the rat elevated X-maze and the mouse light/dark box. Pentagastrin (0.8 μg per animal, i.c.v.) or FG 7142 (10 mg kg^{-1}, s.c.) was administered 15 min before test. The antagonists were administered either orally or i.p. 40 min before test. The time spent in the light side of the light dark box (a) or the percentage time spent on the open arms (%TOA) of the X-maze (b) was measured. Results are shown as the mean (vertical bars represent ± s.e.mean) of 10 animals per group. *Significantly different from respective pentagastrin or FG 7142-treated group, $P < 0.05$ (ANOVA followed by Dunnett's t test). (●) Pentagastrin + CI-988 (p.o.); (■) pentagastrin + devazepide (i.p.); (▲) FG 7142 + CI-988 (p.o.); open symbols show vehicle (Veh)-treated controls as appropriate.

Table 3 The effect of CI-988 and CDP on pentylenetetrazol (PTZ)-induced seizures

Compound	*Dose* (mg kg^{-1}, i.p.)	*MCD of PTZ* (mg kg^{-1}, i.v.)
CDP	Veh	94.5 ± 10.2
	3.0	120.7 ± 13.7
	10.0	168.2 ± 11.9*
	30.0	242.9 ± 20.3*
	60.0	287.5 ± 20.9*
CI-988	Veh	89.0 ± 12.3
	3.0	73.7 ± 8.4
	10.0	76.4 ± 13.9
	30.0	57.1 ± 3.3
	100.0	66.2 ± 7.6

Test compounds were administered i.p. 40 min before infusion of PTZ. The threshold dose of PTZ required to induce tonic seizures was determined. Results are shown as the mean convulsive dose (MCD) of PTZ (±s.e.mean) of 8–10 animals per group.
* Significantly different from vehicle-treated controls, $P < 0.05$ (ANOVA followed by Dunnett's t test).

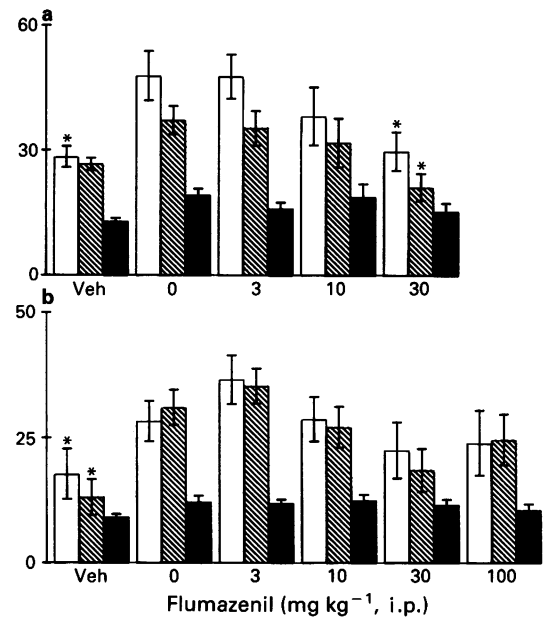

Figure 4 Effect of flumazenil on the action of CI-988 and CDP in the rat elevated X-maze. Flumazenil was administered i.p. 20 min before a submaximal dose of either (a) CDP (3.0 mg kg^{-1}, i.p.) or (b) CI-988 (0.1 mg kg^{-1}, i.p.). Forty minutes later animals were tested on the X-maze and the percentage time spent (open columns) and entries (hatched columns) made on to the end half sections of the open arms, and the total number of entries (solid columns) were measured. Results are shown as the mean (vertical bars represent ± s.e.mean) of 10 animals per group. Vehicle (Veh)-treated animals received appropriate vehicle alone. *Significantly different from the group given CDP or CI-988 alone, $P < 0.05$ (ANOVA followed by Dunnett's t test).

Effects of CDP and CI-988 on locomotor activity in the rat

The administration of CDP 40 min before test, dose-dependently (1.0–30.0 mg kg^{-1}, i.p.) decreased the locomotor activity in the rat with a MED of 10 mg kg^{-1}, the mean activity counts (±s.e.mean) being 49.6 ± 9.2 (cf. control value = 145.9 ± 21.8, $P < 0.05$). In contrast, up to 30 mg kg^{-1} CI-988 was without effect (mean activity counts = 105.8 ± 15.3, $P > 0.05$).

Effects of CDP, CI-988 and pentagastrin on rotarod performance in the mouse

The time spent on the rotating rotarod (TRR) by vehicle-treated animals was (mean ± s.e.mean) 94.4 s ± 12.5 and this was reduced dose-dependently by CDP administered 40 min before the test (1.0–30.0 mg kg^{-1}, i.p.) with a MED of 30.0 mg kg^{-1} (TRR = 10.3 s ± 9.3; significantly different from controls, $P < 0.05$). In contrast, CI-988 was inactive up to high doses of 100.0 mg kg^{-1} (TRR = 46.6 s ± 10.4 cf. control value = 71.5 s ± 10.7, $P > 0.05$).

The TRR by control mice given 5 μl of the vehicle i.c.v. on the revolving rotarod was 115.2 s ± 4.6. This was not affected by i.c.v. administration of pentagastrin (0.08–8.0 μg per mouse) 15 min before test.

Interaction with alcohol and barbiturates

The TRR by control mice was 83.0 s ± 11.6 and was not impaired by oral administration of 0.75 g kg^{-1} ethanol (77.5 s ± 11.9). However, the non-significant decrease in rotarod performance induced by 10 mg kg^{-1} CDP (59.0 s ± 15.4) was significantly potentiated by pretreatment with ethanol (20.7 s ± 8.2, $P < 0.05$). In contrast, no interaction was observed between ethanol and up to 30.0 mg kg^{-1}

CI-988 (TRR by group receiving 30 mg kg^{-1} CI-988 + vehicle = 60.4 s ± 12.5 cf. 62.7 s ± 11.2 for the group given ethanol + 30 mg kg^{-1} CI-988, $P > 0.05$).

The administration of CDP (1.0–30.0 mg kg^{-1}, i.p.) 40 min before sodium pentobarbitone (60.0 mg kg^{-1}, i.p.) dose-dependently increased the sleeping time in mice. The MED of 10 mg kg^{-1} CDP increased the sleeping time from 64.9 min ± 4.5 to 117.8 min ± 20.3 ($P < 0.05$). In contrast, CI-998 at doses up to 30 mg kg^{-1} was without effect (control sleeping time = 57.9 min ± 5.8 cf. 67.7 min ± 11.1 for 30 mg kg^{-1} CI-988, $P > 0.05$).

Discussion

The results presented here indicate that the selective CCK_B receptor antagonist, CI-988, is orally active and produces anxiolytic-like actions in several animal models of anxiety. However, CI-988 does not appear to possess the adverse properties associated with benzodiazepines.

It has been shown that CI-988 is a highly selective antagonist for the CCK_B receptor, the ratio of the K_i values at CCK_A versus the CCK_B receptors being 894 (Hughes *et al.*, 1990; Horwell *et al.*, 1991). Previously it has been reported that CI-988 and L-365,260, another CCK_B receptor antagonist of a different chemical class, produce anxiolytic-like actions in the rat elevated X-maze (Hughes *et al.*, 1990; Singh *et al.*, 1991a). In the present study, both compounds showed anxiolytic-like activity in the rat social interaction test and the mouse light/dark box. In both tests the magnitude of these effects was similar to that of CDP. In contrast, the selective CCK_A receptor antagonist, devazepide, was inactive in both behavioural tests. These results support and extend our previous findings that selective antagonism of the CCK_B receptor leads to anxiolysis (Hughes *et al.*, 1990; Singh *et al.*, 1991a).

The ability of a selective CCK_B receptor agonist, pentagastrin, to produce an anxiogenic-like action further corroborates the role of the CCK_B receptor in anxiety. This is consistent with human studies showing that intravenous administration of selective CCK_B receptor agonists CCK-4 and pentagastrin leads to panic-like attacks (De Montigny, 1989; Abelson & Nesse, 1990; Bradwejn *et al.*, 1990). Previously it has been reported that central administration of pentagastrin or the nonselective CCK receptor agonist, caerulein, produced anxiogenic-like action in the rat (Singh *et al.*, 1991a). In the present study, administration of pentagastrin into the cerebral ventricles produced anxiogenic-like action in the rat elevated X-maze, the mouse light/dark box and the rat conflict test. The lack of effect following systemic administration of pentagastrin indicates a central mechanism of action for this compound. It is known that peripheral administration of CCK receptor agonists can impair motor activity (Crawley *et al.*, 1981) and this could complicate interpretation of the effect on anxiety. However, in the present study the anxiogenic-like effect of pentagastrin occurred at doses that failed to produce sedation in mice or affect spontaneous locomotor activity in the rat elevated X-maze.

The role of brain CCK_A receptors in anxiety at the moment is unclear. In the present study, devazepide was found to be inactive in both the light/dark box and the social interaction test. This is consistent with previous studies showing devazepide to be inactive in the rat elevated X-maze at doses which selectively antagonize the brain CCK_A receptor (Dauge *et al.*, 1989; Singh *et al.*, 1991a). At doses in excess of 20 mg kg^{-1} devazepide was effective in this anxiolytic test (Singh *et al.*, 1991a). However, at these high doses devazepide is known to block brain CCK_B receptors (Boden & Hill, 1988). This makes interpretation of effects obtained with high doses of devazepide difficult. Other behavioural studies have reported devazepide to be active at very low doses in the elevated X-maze and the mouse light/dark box (Hendrie & Dourish, 1990; Ravard *et al.*, 1990). However, in these studies the effect of devazepide was not dose-related and it was only active at one of the doses tested. To confuse the issue further, another selective CCK_A receptor antagonist L-365,031 was found to be inactive (Ravard *et al.*, 1990). Most studies have used devazepide to examine the role of the CCK_A receptor in anxiety. Although devazepide is a highly selective CCK_A receptor antagonist, it has a low water solubility and this leads to different vehicles being used. The possible differences in bioavailability of devazepide in the various vehicles may account for some of the above discrepancies.

The antagonism of pentagastrin response by CI-988 but not by the selective CCK_A receptor antagonist devazepide, is entirely consistent with an involvement of the CCK_B receptor in the anxiolytic-like action of CI-988. It should be noted that the doses of devazepide that failed to antagonize the effect of pentagastrin are 10 times higher than those reported to block the central action of CCK-8S (Dauge *et al.*, 1989). However, a larger dose of CI-988 was required to inhibit pentagastrin-induced anxiety than to produce an anxiolytic-like effect in control animals. This may be a result of pentagastrin producing a more severe form of anxiety than that induced by the exposure of animals to the test conditions. The ability of CI-988 also to antagonize the response to FG 7142 may suggest the usefulness of a CCK_B receptor antagonist in benzodiazepine receptor-mediated anxiety.

The anxiolytic-like action of CI-988 may not involve the benzodiazepine system. This is indicated by the failure of the benzodiazepine receptor antagonist, flumazenil, to antagonize the effect of CI-988 in the rat elevated X-maze. That the action of CI-988 may not involve a benzodiazepine mechanism is also suggested by the contrasting behavioural profiles of CI-988 and benzodiazepines. Thus, in addition to the anxiolytic action, sedation and ataxia are also prominent features of benzodiazepines. CDP showed these effects by impairing rotarod performance in the mouse and by reducing locomotor activity in the rat. As expected, these effects of CDP occurred at doses close to those producing anxiolytic-like effects in the two species. In contrast to CDP, CI-988 at doses up to 3000 fold higher than those producing anxiolysis did not induce sedation or ataxia in either of the species. Furthermore, unlike CDP, CI-988 did not potentiate the sedative actions of alcohol or barbiturates. Also it did not possess an anticonvulsant action. Therefore, the only property that CI-988 shares with benzodiazepines is the anxiolytic-like action. Thus, CI-988 appears to be an anxioselective compound.

It has been reported that agents which produce anxiolytic-like action independently of the benzodiazepine receptor, are either inactive or show weak activity in standard conflict tests (for review see Handley, 1991). However, in the present study CI-988 showed a consistent effect in the rat conflict test but as seen in the primate conflict test (Powell & Barrett, 1991) the activity of CI-988 was confined to a narrow dose-range and was lower in magnitude than CDP. The reason for this difference between the activity of CI-988 in the conflict test and other animal models is unclear. However, as most animal models of anxiety are optimized for benzodiazepines, what is considered to be an 'anxiolytic' activity may be composed of any combination of anxiolytic, sedative, myorelaxant, amnesic or anticonvulsant elements. An anxioselective agent such as CI-988 which does not appear to possess these additional actions may therefore be expected to show a different profile from benzodiazepines.

In conclusion, CI-988 is an orally active compound that induces potent anxiolytic-action in several well established rodent models of anxiety. In most animal models of anxiety, CI-988 is as efficacious and 50–300 fold more potent than CDP but it does not possess sedative, ataxic or anticonvulsant actions even in doses up to 3000 fold higher than those producing anxiolysis. Furthermore, CI-988 does not potentiate the actions of alcohol or barbiturates. Other studies have indicated that at least in mice, CI-988 does not produce dependence syndrome on withdrawal from chronic treatment. Therefore, CI-988 would be predicted to have a much improved side-effect profile in man than benzodiazepines.

References

ABELSON, J.L. & NESSE, R.M. (1990). Cholecystokinin-4 and panic. *Arch. Gen. Psychiatry*, **47**, 395.

BODEN, P. & HILL, R.G. (1988). Effects of cholecystokinin and related peptides on neuronal activity in the ventromedial nucleus of the rat hypothalamus. *Br. J. Pharmacol.*, **84**, 246–252.

BRADWEJN, J., KOSZYCKI, D., SHRIQUI, C. & METERISSIAN, G. (1990). Cholecystokinin tetrapeptide induces panic attacks in patients with panic disorder. *Can. J. Psychiatry*, **35**, 83–85.

CHANG, R.S. & LOTTI, V.J. (1986). Biochemical and pharmacological characterization of an extremely potent and selective nonpeptide cholecystokinin antagonist. *Proc. Natl. Acad. Sci. U.S.A.*, **83**, 4923–4926.

COSTALL, B., JONES, B.J., KELLY, M.E., NAYLOR, R.J. & TOMKINS, D.M. (1989a). Exploration of mice in a black and white box: Validation as a model of anxiety. *Pharmacol. Biochem. Behav.*, **32**, 777–785.

COSTALL, B., KELLY, M.E. & TOMKINS, D.M. (1989b). Use of the elevated plus maze to assess anxiolytic potential in the rat. *Br. J. Pharmacol.*, **96**, 312P.

CRAWLEY, J.N., HAYS, S.E., PAUL, S.M. & GOODWIN, F.K. (1981). Cholecystokinin reduces exploratory behaviour in mice. *Physiol. Behav.*, **27**, 407–411.

DAUGE, V., STEIMES, P., DERRIEN, M., BEAU, N., ROQUES, B.P. & FEGER, J. (1989). CCK-8 effects on motivational and emotional states of rats involve CCK_A receptors of the postereo-median pare of the nucleus accumbens. *J. Pharmacol. Biochem. Behav.*, **34**, 157–163.

DE MONTIGNY, C. (1989). Cholecystokinin tetrapeptide induces panic-like attacks in healthy volunteers. *Arch. Gen. Psychiatry*, **46**, 511–517.

DOCKRAY, G.J. (1976). Immunochemical evidence for cholecystokinin-like peptides in brain. *Nature*, **264**, 564–570.

FIELD, M.J., HUGHES, J., LEWIS, A.S., OLES, R.J., SINGH, L., VASS, C.A. & WOODRUFF, G.N. (1991a). The anxiolytic-like actions of the selective CCK-B receptor antagonist CI-988. *Br. J. Pharmacol.*, **102**, 256P.

FIELD, M.J., LEWIS, A.S., LLOYD, C. & SINGH, L. (1991b). Automation of the rat elevated X-maze test of anxiety. *Br. J. Pharmacol.*, **102**, 304P.

GIBBS, J., YOUNG, R.C. & SMITH, G.P. (1973). Cholecystokinin decreases food intake in rats. *J. Comp. Physiol. Psychol.*, **84**, 488–495.

GUY, A.P. & GARDNER, C.R. (1985). Pharmacological characterisation of a modified social interaction model of anxiety in the rat. *Neuropsychobiol.*, **13**, 194–200.

HANDLEY, S.L. (1991). Serotonin in animal models of anxiety: the importance of stimulus and response. In *Serotonin, Sleep and Mental Disorder*. ed. Idzikowski, C. & Cowen, P. Petersfield: Wrightson Biomedical, (in press).

HANDLEY, S.L. & MITHANI, S. (1984). Effects of alpha-adrenoceptor agonists and antagonists in a maze-exploration model of 'fear'-motivated behaviour. *Naunyn-Schmiedebergs Arch. Pharmacol.*, **327**, 1–5.

HENDRIE, C.A. & DOURISH, C.T. (1990). Anxiolytic profile of the cholecystokinin antagonist devazepide in mice. *Br. J. Pharmacol.*, **99**, 138P.

HILL, D.R., CAMPBELL, N.J., SHAW, T.M. & WOODRUFF, G.N. (1987a). Autoradiographic localization and biochemical characterization of nonpeptide CCK receptors in the rat CNS using highly selective nonpeptide CCK antagonists. *J. Neurochem.*, **7**, 2967–2976.

HILL, D.R., SHAW, T.M. & WOODRUFF, G.N. (1987b). Species differences in the localization of peripheral type cholecystokinin receptors in rodent brain. *Neurosci. Lett.*, **79**, 286–289.

HORWELL, D.C., HUGHES, J., HUNTER, J.C., PRITCHARD, M.C., RICHARDSON, R.S., ROBERTS, E. & WOODRUFF, G.N. (1991). Rationally designed 'dipeptiod' analogues of CCK. alpha-Methyltryptophan derivatives as highly selective and orally active gastrin and CCK-B antagonists with potent anxiolytic properties. *J. Med. Chem.*, **34**, 404–414.

HUGHES, J., BODEN, P., COSTALL, B., DOMENEY, A., KELLY, E., HORWELL, D., HUNTER, J.C., PINNOCK, R.D. & WOODRUFF, G.N. (1990). Development of a class of selective cholecystokinin type B receptor antagonists having potent anxiolytic activity. *Proc. Natl. Acad. Sci., U.S.A.*, **87**, 6728–6732.

INNIS, R.B. & SNYDER, S.H. (1980). Distinct cholecystokinin receptors in brain and pancreas. *Proc. Natl. Acad. Sci. U.S.A.*, **77**, 6917–6921.

IVY, A.C. & OLDBERG, E. (1928). A hormone mechanism for gallbladder contraction and evacuation. *Am. J. Physiol.*, **86**, 599–613.

KATSUURA, G., HIROTA, R. & ITOH, S. (1981). Cholecystokinin—induced hypothermia in the rat. *Experientia*, **30**, 60.

KILFOIL, T., MICHEL, A., MONTGOMERY, D. & WHITING, R.L. (1989). Effects of anxiolytic and anxiogenic drugs on exploratory activity in a simple model of anxiety in mice. *Neuropharmacol.*, **28**, 901–905.

KUBOTA, K., SUGAYA, K., MATSUDA, I., MATSUOKA, Y. & TERAWAKI, Y. (1985). Reversal of antinociceptive effect of cholecystokinin by benzodiazepines and a benzodiazepine antagonist, Ro 15-1788. *Jpn. J. Pharmacol.*, **37**, 101–105.

LOTTI, V.J. & CHANG, R.S.L. (1989). A new potent and selective non-peptide gastrin antagonist and brain cholecystokinin receptor (CCK_B) ligand: L-365,260. *Eur. J. Pharmacol.*, **162**, 273–280.

PAXINOS, G. & WATSON, C. (1976). *The Rat Brain in Stereotaxic Coordinates*. New York: Academic. 2nd Edition.

PELLOW, S., CHOPIN, P., FILE, S.E. & BRILEY, M. (1985). Validation of open:closed arm entries in an elevated Plus-maze as a measure of anxiety in the rat. *J. Neurosci. Meth.*, **14**, 149–167.

POWELL, K.R. & BARRETT, J.E. (1991). Evaluation of the effects of PD 134308 (CI-988), a CCK-B antagonist, on the punished responding of squirrel monkeys. *Neuropeptides* (in press).

RAVARD, S., DOURISH, C.T. & IVERSEN, S.D. (1990). Evidence that the anxiolytic-like effects of the CCK antagonists devazepide and L-365,260 in the elevated plus-maze paradigm in rats are mediated by CCK receptors. *Br. J. Pharmacol.*, **101**, 576P.

REHFELD, J.F. (1978). Immunochemical studies of cholecystokinin. II. Distribution and molecular heterogeneity of cholecystokinin the central nervous system and small intestine of man and dog. *J. Biol. Chem.*, **253**, 4022–4030.

SINGH, L., LEWIS, A.S., FIELD, M.J., HUGHES, J. & WOODRUFF, G.N. (1991a). Evidence for an involvement of the brain cholecystokinin B receptor in anxiety. *Proc. Natl. Acad. Sci., U.S.A.*, **88**, 1130–1133.

SINGH, L., FIELD, M.J., HUGHES, J., VASS, C.A. & WOODRUFF, G.N. (1991b). Central administration of a CCK-B receptor agonist induces anxiety. *Br. J. Pharmacol.*, **102**, 45P.

SINGH, L., OLES, R.J. & TRICKLEBANK, M.D. (1990). Modulation of seizure susceptibility in the mouse by the strychnine-insensitive glycine recognition site of the NMDA receptor/ion channel complex. *Br. J. Pharmacol.*, **99**, 285–288.

VANDERHAEGHEN, J.J., SIGNEAU, J.C. & GEPTS, W. (1975). New peptide acting in the vertebrate CNS with anti-gastrin antibodies. *Nature*, **257**, 604–605.

ZETLER, G. (1980). Analgesia and ptosis caused by caerulein and cholecystokinin octapeptide (CCK-8). *Neuropharmacol.*, **19**, 413–422.

ZETLER, G. (1981). Central depressant effects of caerulein and cholecystokinin octapeptide (CCK-8) different from those of diazepam and haloperidol. *Neuropharmacol.*, **20**, 277–283.

ZETLER, G. (1985). Neuropharmacological profile of cholecystokinin-like peptides. In *Neuronal Cholecystokinin*. ed. Vanderhaeghen, J.J. & Crawley, J.N. pp. 448–469. New York: New York Academic Press.

(Received April 11, 1991
Revised May 14, 1991
Accepted May 16, 1991)

Br. J. Pharmacol. (1991), **104**, 246–250

Evidence against a role for dopamine D_1 receptors in the myocardium of the pig

L.J. Van Woerkens, D.J. Duncker, M.O. Den Boer, E.O. McFalls, L.M.A. Sassen, P.R. Saxena & [1]P.D. Verdouw

Laboratory for Experimental Cardiology, Thoraxcentre and Department of Pharmacology, Erasmus University Rotterdam, P.O. Box 1738, 3000 DR Rotterdam, The Netherlands

1 We investigated the presence of dopamine D_1 receptors in the myocardium of anaesthetized pigs using intravenous infusions of dopamine, alone and after α- and β-adrenoceptor blockade and intracoronary infusions of the selective D_1 receptor agonist, fenoldopam.

2 Intravenous infusion of dopamine (2.5, 5 and 10 $\mu g\,kg^{-1}\,min^{-1}$ for 10 min, $n = 6$) caused dose-dependent changes in heart rate (from 94 ± 6 to 132 ± 10 beats min^{-1}, $P < 0.05$), the maximal rate of rise of left ventricular pressure ($LVdP/dt_{max}$; from 2280 ± 170 to 4800 ± 410 mmHg s^{-1}, $P < 0.05$), mean arterial blood pressure (from 87 ± 5 to 62 ± 3 mmHg) and systemic vascular resistance (from 40 ± 4 to 28 ± 2 mmHg l^{-1} min, $P < 0.05$). The increases in heart rate and $LVdP/dt_{max}$ were abolished when dopamine was infused after α- and β-adrenoceptor blockade. The vasodilator response was, however, only minimally affected.

3 Intravenous infusions of dopamine decreased coronary vascular resistance from 0.90 ± 0.06 to 0.53 ± 0.07 mmHg ml^{-1} min 100 g ($P < 0.05$). This action of dopamine was not observed when dopamine was infused after blockade of the α- and β-adrenoceptors.

4 Pretreatment with α- and β-adrenoceptor blockade had no effect or only slightly attenuated the dopamine-induced decrease in vascular resistance of the brain, kidneys, adrenals and small intestine.

5 In 7 animals, intracoronary doses of 0.04, 0.1, 0.2 and 0.4 $\mu g\,kg^{-1}\,min^{-1}$ of fenoldopam had no effect on coronary venous oxygen content, local myocardial oxygen consumption, coronary blood flow or coronary vascular resistance. However, systemic effects were observed at the highest two doses, as manifested by a drop in mean arterial blood pressure from 82 ± 4 to 72 ± 4 mmHg ($P < 0.05$) due to peripheral vasodilatation (e.g. cerebral vascular bed). Heart rate, $LVdP/dt_{max}$, regional myocardial segment length shortening and left ventricular end-diastolic pressure were not affected at these doses. In 2 animals the infusion rate was increased to 4 $\mu g\,kg^{-1}\,min^{-1}$, but again there was no evidence for coronary vasodilatation.

6 We conclude that the intravenous infusion of dopamine after α- and β-adrenoceptor blockade and the intracoronary infusion of fenoldopam provided no evidence for a major role of D_1 receptors in the coronary circulation of pigs. The absence of any effect of the employed doses of fenoldopam on $LVdP/dt_{max}$ and on regional myocardial segment length shortening also indicates that fenoldopam does not exhibit any inotropic action in this species.

Keywords: Dopamine; fenoldopam; D_1 receptors; systemic haemodynamics; regional blood flows; coronary blood flow; inotropy; pig myocardium

Introduction

Dopamine D_1 receptors have been identified in a number of vascular beds, including the renal, mesenteric and cerebral vasculature (Ueda *et al.*, 1982; Toda, 1983; Hughes & Sever, 1989). However, evidence for their presence in the coronary circulation is limited. Kopia & Valocik (1989) demonstrated a specific D_1 receptor-mediated vasodilatation in the coronary vascular bed of pentobarbitone-anaesthetized dogs following intracoronary infusion of the specific D_1 receptor agonist, fenoldopam. Hieble *et al.* (1987) showed that fenoldopam, in both dogs and rats, increased blood flow to various vascular beds, but not to the heart. Recently, Zhao *et al.* (1990) concluded from their experiments in pentobarbitone-anaesthetized dogs that coronary vasodilatation after intracoronary infusion of fenoldopam was due to a positive inotropic effect of the drug rather than to a direct effect on the coronary vasculature. Furthermore, fenoldopam has failed to relax isolated conduit coronary arteries of humans precontracted by noradrenaline (Hughes & Sever, 1989).

Zhao *et al.* (1990) reported an increased inotropic state during infusion of fenoldopam in dogs, but Hieble *et al.* (1987) found that in the same species the drug reduced the maximal rate of rise of left ventricular pressure ($LVdP/dt_{max}$) and ascribed the latter to a negative inotropic action of the drug. Kopia & Valocik (1989), however, could not confirm either observation, when they infused fenoldopam directly into a coronary artery.

In view of these discrepancies, we used two approaches to investigate the role of D_1 receptors in the myocardium of pigs, a species frequently used in biomedical research. We first determined the responsiveness to intravenous infusions of dopamine alone and after α- and β-adrenoceptor blockade. We then used intracoronary infusions of fenoldopam to evaluate the direct effects of fenoldopam on coronary blood flow and myocardial contractility.

Methods

General

After an overnight fast, 25 cross-bred Landrace × Yorkshire pigs (H.V.C., Hedel, The Netherlands) of either sex and weighing from 22–28 kg were sedated with intramuscular 5 mg kg^{-1} azaperone (Stresnil, Janssen Pharmaceutica, Beerse, Belgium), anaesthetized with intravenous 6 mg kg^{-1} metomidate (Hypnodil, Janssen Pharmaceutica, Beerse, Belgium), intubated and connected to a respirator for intermittent positive pressure ventilation with a mixture of oxygen and nitrous oxide (1 : 2). Respiratory rate and tidal volume were set to

[1]Author for correspondence.

keep arterial blood gases within the normal range: $7.35 < pH < 7.45$; $35\,mmHg < Pco_2 < 45\,mmHg$ and $120\,mmHg < Po_2 < 160\,mmHg$. 7F catheters were placed in the superior caval vein for administration of $150\,mg\,kg^{-1}$ α-chloralose (E. Merck, Darmstadt, Germany) followed by an infusion of a low dose ($5\,mg\,kg^{-1}\,h^{-1}$) of sodium pentobarbitone (Apharma, Arnhem, The Netherlands); for administration of 4 mg of the muscle relaxant pancuronium bromide (Organon Teknika BV, Boxtel, The Netherlands) prior to thoracotomy; and for administration of haemaccel (Behringwerke A.G., Marburg, Germany) to compensate for loss of intravascular volume. Catheters were also positioned in the descending aorta for withdrawal of blood samples and measurement of central aortic blood pressure. A Sensodyn MTC P7 catheter (B. Braun, Medical BV, Uden, The Netherlands) inserted via the left carotid artery was used to measure left ventricular pressure and its first derivative ($LVdP/dt$). After thoracotomy, an electromagnetic flow probe (Skalar, Delft, The Netherlands) was placed around the ascending aorta, and the great cardiac vein was cannulated for subsequent collection of blood for determining haemoglobin concentration and oxygen saturation (OSM2, Radiometer, Copenhagen, Denmark). In 14 of the animals the proximal left anterior descending coronary artery was dissected free and a small cannula inserted for intracoronary infusions of fenoldopam or its solvent.

Regional blood flows

In order to determine regional blood flows, the left atrial appendage was cannulated for injection of a batch of $1–2 \times 10^6$ carbonized plastic microspheres [$15 \pm 1\,\mu m$ (s.d.) in diameter] labelled with ^{46}Sc, ^{95}Nb, ^{103}Ru, ^{113}Sn or ^{141}Ce. Starting 15 s before the injection of microspheres, blood was withdrawn from a femoral artery at a rate of $10\,ml\,min^{-1}$ until 60–65 s after completion of the injection of the microspheres. In the animals which received the intracoronary infusions of fenoldopam, the area perfused by the left anterior descending coronary artery (LADCA) was identified by an intracoronary injection of patent blue violet (Sigma, St. Louis, MO, U.S.A.) at the end of the experiment. Animals were killed with an overdose of sodium pentobarbitone and the heart, the brain (divided into hemispheres, diencephalon, cerebellum and brainstem) adrenals, kidneys and aliquots of the skeletal muscle, skin and small intestine were excised. The heart was fixed in formaldehyde (10% v/v) for 48 h at which point of time the left ventricle was divided into three layers of equal thickness. From the radioactivity in the tissue, blood flows were determined by standard procedures (Saxena *et al.*, 1980).

Myocardial oxygen consumption and contractile function

Myocardial oxygen consumption ($M\dot{V}O_2$) of the LADCA perfused area was calculated as the product of coronary blood flow (microsphere measurements) and the difference in the oxygen contents of the arterial and coronary venous blood.

In the animals in which fenoldopam was infused, regional myocardial segment length shortening was assessed by sonomicrometry (Triton Technology Inc., San Diego, CA, U.S.A.) with a pair of ultrasonic crystals implanted approximately 10 mm apart in the subendocardial layers of the myocardium perfused by the LADCA. From the tracings, systolic segment length shortening (SLS) was calculated as:

$$SLS\ (\%) = 100 \times (EDL - ESL)/EDL,$$

in which EDL and ESL are the segment length at end-diastole and end-systole, respectively.

Experimental protocols

Two series of experiments were performed. In the first series of experiments the effects of dopamine on systemic haemodynamics and regional blood flows were evaluated. To this end 6 pigs received three consecutive 10 min intravenous infusions (2.5, 5 and $10\,\mu g\,kg^{-1}\,min^{-1}$) of dopamine and 5 other animals received four consecutive 10 min intravenous infusions (2.5, 5, 10 and $20\,\mu g\,kg^{-1}\,min^{-1}$) of dopamine after α- and β-adrenoceptor blockade with phentolamine ($1\,mg\,kg^{-1}$) and propranolol ($0.5\,mg\,kg^{-1} + 0.5\,mg\,kg^{-1}\,h^{-1}$), respectively. Systemic haemodynamics, arterial and coronary venous oxygen contents and regional blood flows were determined at baseline and at the end of each infusion rate. In the second series of experiments, the direct effects of fenoldopam on the coronary circulation and the myocardium were evaluated. Hitherto, four incremental doses of fenoldopam (0.04, 0.1, 0.2 and $0.4\,\mu g\,kg^{-1}\,min^{-1}$) were infused directly into the left anterior descending coronary artery for 10 min each in the experimental group ($n = 7$) and the results were compared with those of a control group ($n = 7$), which received equal volumes of the solvent. Systemic haemodynamics, regional myocardial function, arterial and coronary venous oxygen contents and coronary blood flow were determined again at baseline and at the end of each infusion rate.

Drugs

Dopamine hydrochloride (Department of Pharmacy, Academic Hospital Dijkzigt, Rotterdam, The Netherlands), propranolol hydrochloride (gift: ICI-Pharmaceuticals, Rotterdam, The Netherlands) and phentolamine methane-sulphonide (gift: Ciba-Geigy B.V., Arnhem, The Netherlands) were dissolved in physiological saline. Fenoldopam mesylate (gift: Dr F. Lippens, Smith, Kline and Beecham, Rijswijk, The Netherlands) was dissolved in physiological saline containing 1% v/v ethanol and the required doses were obtained by adjusting the infusion rate (from $0.13\,ml\,min^{-1}$ to $2\,ml\,min^{-1}$).

Statistical evaluation

All data are presented as arithmetic mean ± s.e.mean. Statistical analysis was performed by use of a parametric two-way of analysis of variance (random-block design), followed by the Duncan new multiple range test. Statistical significance was accepted for $P < 0.05$.

Results

Intravenous infusions of dopamine without and after α- and β-adrenoceptor blockade

Systemic haemodynamics Intravenous infusion of dopamine caused an increase in heart rate from 94 ± 6 to 132 ± 10 beats min^{-1} ($P < 0.05$) and a decrease in mean arterial blood pressure from 87 ± 5 to 62 ± 3 mmHg ($P < 0.05$); both changes were dose-dependent (Figure 1). Cardiac output did not change, which implies that the hypotensive effect was caused by a reduction of the systemic vascular resistance ($P < 0.05$). $LVdP/dt_{max}$ increased by more than 100%, while left ventricular end-diastolic pressure showed a decrease from 10 ± 1 to 7 ± 1 mmHg ($P < 0.05$).

The animals in which the α- and β-adrenoceptors were blocked had a 20% lower $LVdP/dt_{max}$ at baseline, but other systemic haemodynamic parameters were not significantly different from the animals without adrenoceptor blockade (Figure 1). When dopamine was infused in these animals, the increases in heart rate and in $LVdP/dt_{max}$ were inhibited, but the systemic vasodilator response was only minimally affected (Figure 1).

Myocardial blood flow and oxygen consumption During infusion of the lowest dose of dopamine ($2.5\,\mu g\,kg^{-1}\,min^{-1}$) there was a 10% decrease in left ventricular transmural blood flow, but during the infusion of 5 and $10\,\mu g\,kg^{-1}\,min^{-1}$, transmural blood flow was, respectively, 20% and 50% higher than the baseline flow (Figure 2). The subepicardial layers benefitted

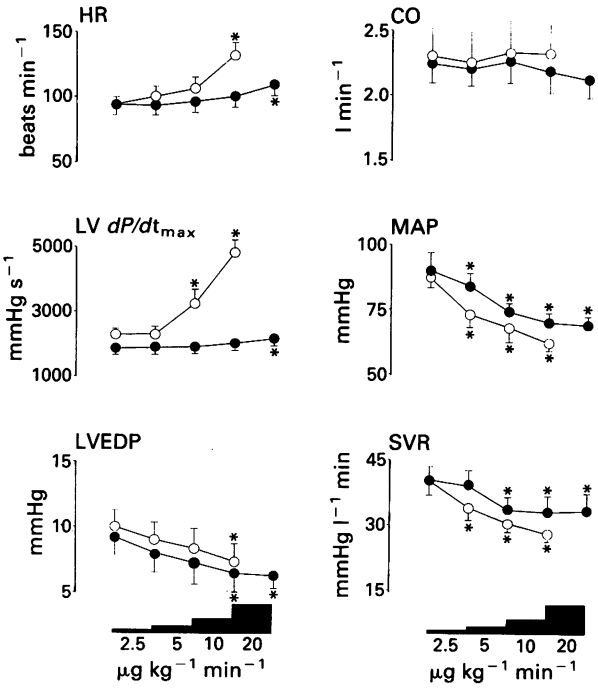

Figure 1 Systemic haemodynamic effects of dopamine alone (○, $n = 6$) and after α- and β-adrenoceptor blockade (●, $n = 5$) in anaesthetized pigs. HR = heart rate (beats min^{-1}); CO = cardiac output ($l\,min^{-1}$); MAP = mean arterial blood pressure (mmHg); $LVdP/dt_{max}$ = maximum rate of rise in left ventricular pressure ($mmHg\,s^{-1}$); LVEDP = left ventricular end-diastolic pressure (mmHg). SVR = systemic vascular resistance ($mmHg\,l^{-1}\,min$). Note that after α- and β-adrenoceptor blockade the dopamine-induced increases in heart rate and $LVdP/dt_{max}$ were almost completely abolished, but that dilatation of the systemic vascular bed was much less affected. *$P < 0.05$ vs baseline.

more from the increase in blood flow than the subendocardial layers as the ratio of the normalized subendocardial and subepicardial blood flows decreased from 1.07 ± 0.04 to 0.97 ± 0.06 ($P < 0.05$). Calculation of the coronary vascular

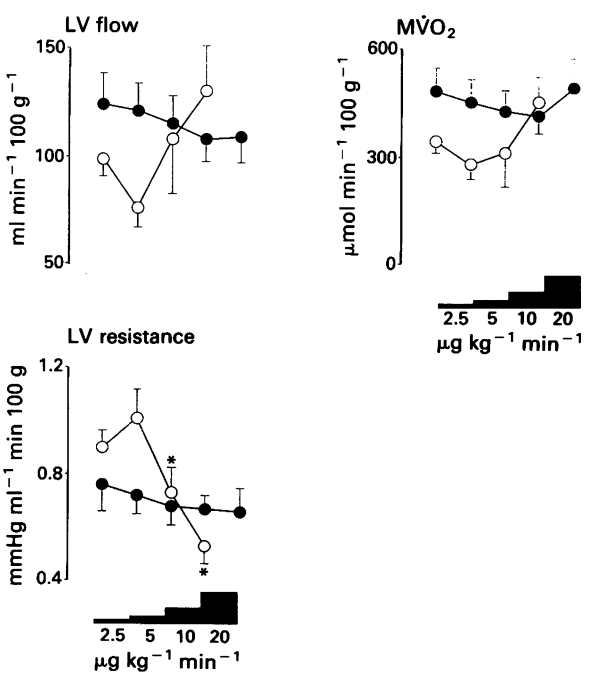

Figure 2 The effect of dopamine on transmural left ventricular blood flow (LV) and left ventricular vascular resistance (LV resistance) and left ventricular oxygen consumption ($M\dot{V}O_2$) in anaesthetized pigs. Data were obtained without (○, $n = 6$) and after α- and β-adrenoceptor blockade (●, $n = 5$). *$P < 0.05$ vs baseline.

resistance revealed no change at $2.5\,\mu g\,kg^{-1}\,min^{-1}$, but decreases of 30% and 50% were observed during the dopamine infusions of 5 and $10\,\mu g\,kg^{-1}\,min^{-1}$, respectively. Myocardial oxygen consumption decreased (by 20%) during infusion of the lowest dose, was not different from baseline during infusion of the middle dose and increased (by 30%) during infusion of the highest dose. The left ventricular systolic pressure-heart rate product, a measure of myocardial oxygen demand, followed a similar pattern.

After blockade of the α- and β-adrenoceptors, the dopamine-induced increases in coronary blood flow were abolished and the decrease in coronary vascular resistance was attenuated. Myocardial oxygen consumption tended to decrease slightly, but levels of statistical significance were not reached. The decrease in myocardial efficiency did not reach levels of statistical significance also.

Regional vascular beds Figure 3 demonstrates the existence of peripheral dopamine receptors in the pig as the decreases in vascular resistances of, in particular the kidneys, adrenals, brain and small intestine, were only minimally affected when dopamine was infused after α- and β-adrenoceptor blockade. The regional differences in the brain were relatively small as after α- and β-adrenoceptor blockade the dopamine-induced decreases in the vascular resistances of the diencephalon, hemispheres, cerebellum and brainstem were maximally $16 \pm 4\%$, $16 \pm 3\%$, $13 \pm 3\%$ and $11 \pm 7\%$, respectively.

Intracoronary infusions of fenoldopam

Systemic haemodynamics As shown in Table 1, intracoronary infusions of fenoldopam up to $0.4\,\mu g\,kg^{-1}\,min^{-1}$ had no effect on cardiac output, heart rate, $LVdP/dt_{max}$ and left ventricular end-diastolic pressure. Mean arterial blood pressure decreased from 82 ± 4 to 72 ± 4 mmHg (12%, $P < 0.05$) with an associated reduction in systemic vascular resistance from 41 ± 3 to $35 \pm 3\,mmHg\,l^{-1}$ min (15%, $P < 0.05$). In 2 of the experiments intracoronary infusions up to $4\,\mu g\,kg^{-1}\,min^{-1}$ were

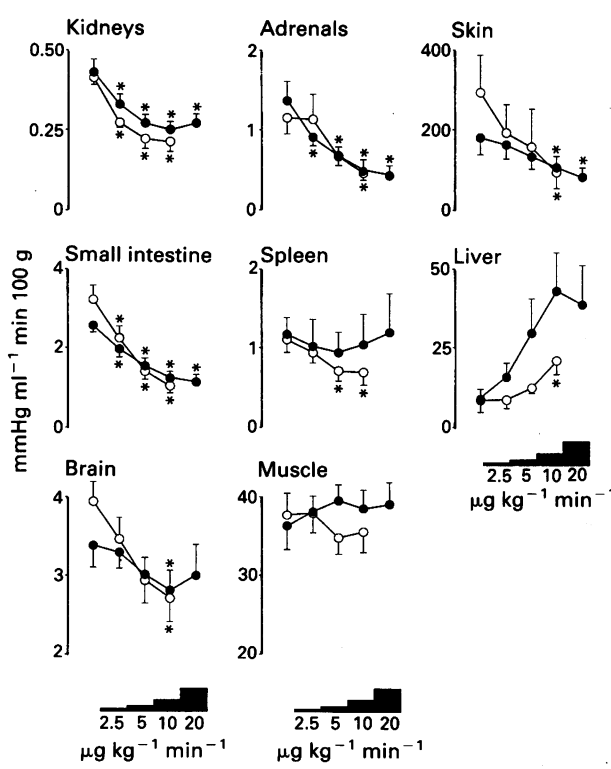

Figure 3 The effect of dopamine on the regional vascular resistance of regional vascular beds. Data were obtained without (○, $n = 6$) and after α- and β-adrenoceptor blockade (●, $n = 5$). *$P < 0.05$ vs baseline.

Table 1 Systemic haemodynamics after continuous intracoronary 10 min infusions of fenoldopam or its solvent in anaesthetized pigs

		Fenoldopam ($\mu g\,kg^{-1}\,min^{-1}$) *or equal volumes of its solvent*				
		0	0.04	0.1	0.2	0.4
HR	Solvent	112 ± 7	110 ± 6	110 ± 5	112 ± 5	113 ± 6
	Fenoldopam	118 ± 8	114 ± 9	114 ± 8	118 ± 9	115 ± 8
MAP	Solvent	89 ± 5	86 ± 9	84 ± 4	85 ± 4	85 ± 6
	Fenoldopam	82 ± 4	80 ± 5	79 ± 4	72 ± 4*	73 ± 6*
CO	Solvent	2.5 ± 0.3	2.5 ± 0.3	2.5 ± 0.3	2.5 ± 0.3	2.4 ± 0.3
	Fenoldopam	2.1 ± 0.2	2.0 ± 0.2	2.1 ± 0.2	2.1 ± 0.2	2.1 ± 0.1
SVR	Solvent	37 ± 3	36 ± 3	36 ± 3	36 ± 3	38 ± 4
	Fenoldopam	41 ± 3	41 ± 3	40 ± 3	35 ± 3*	35 ± 3*
LV$dP/dt_{max}$	Solvent	2360 ± 390	2330 ± 310	2260 ± 330	2430 ± 410	2400 ± 410
	Fenoldopam	2010 ± 320	1850 ± 260	1850 ± 270	1790 ± 280	1880 ± 280
LVEDP	Solvent	7.3 ± 1.1	6.4 ± 1.1	6.5 ± 1.1	6.4 ± 1.1	6.4 ± 1.0
	Fenoldopam	6.9 ± 0.8	7.1 ± 0.8	7.1 ± 0.8	6.8 ± 0.8	7.5 ± 1.0

Data are mean ± s.e.mean; $n = 7$ for the solvent-treated and $n = 7$ for the fenoldopam-treated animals. HR = heart rate (beats min^{-1}); MAP = mean arterial blood pressure (mmHg); CO = cardiac output (1 min^{-1}); SVR = systemic vascular resistance (mmHg l^{-1} min); LV$dP/dt_{max}$ = maximal rate of rise of left ventricular blood pressure (mmHg s^{-1}); LVEDP = left ventricular end-diastolic blood pressure (mmHg).

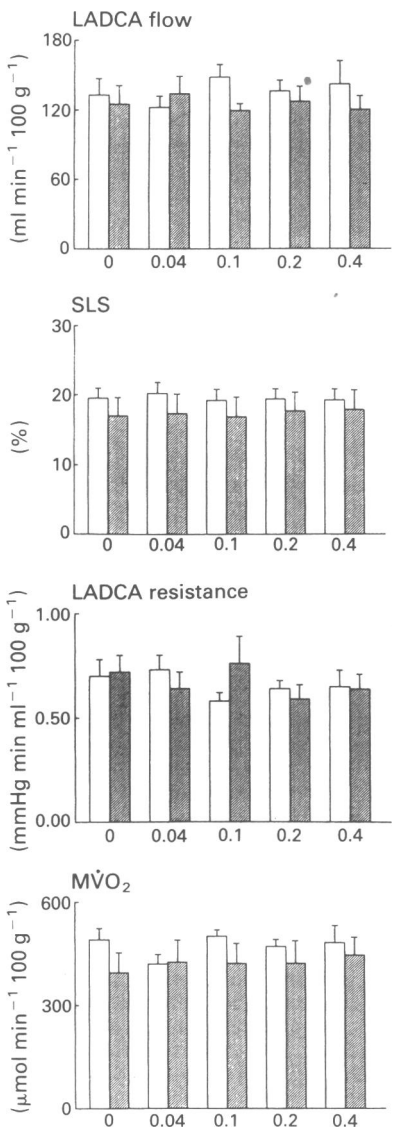

Figure 4 Intracoronary infusions of fenoldopam into the left anterior descending coronary artery (LADCA) had no effect on coronary blood flow, coronary vascular resistance, regional systolic segment length shortening (SLS) or regional myocardial O_2-consumption ($M\dot{V}O_2$); open columns, solvent infusion ($n = 7$); hatched columns, fenoldopam infusion ($n = 7$). Columns represent means and vertical bars represent the standard errors.

used. In these animals there was a further decrease in mean arterial blood pressure by 12 and 18 mmHg, respectively, with a further reduction in systemic vascular resistance. Cardiac output, heart rate and LV$dP/dt_{max}$ were not affected (data not shown in Table 1).

Resistance of the cerebral vascular bed decreased dose dependently from 2.93 ± 0.33 to 2.24 ± 0.23 mm Hg ml^{-1} min 100 g (25%, $P < 0.05$) during the fenoldopam infusions. The resistance of the renal vascular bed was 0.45 ± 0.10 mmHg ml^{-1} min 100 g at baseline and decreased gradually to 0.32 ± 0.04 mmHg ml^{-1} min 100 g at 0.4 $\mu g\,kg^{-1}\,min^{-1}$ fenoldopam. This decrement, however, was not significant compared to the changes in the solvent-treated animals.

Myocardial blood flow, oxygen consumption and contractile function Intracoronary infusions of fenoldopam did not alter transmural blood flow or vascular resistance in the LADCA-perfused region (Figure 4). Since coronary venous oxygen saturation (baseline value: 27 ± 3%) was also not affected, myocardial oxygen consumption was maintained (Figure 4). This observation is not surprising as global and regional parameters of myocardial contractile function, LV$dP/dt_{max}$ (Table 1) and segment length shortening (Figure 4), respectively, did not change.

In the two animals in which fenoldopam was infused at 4 $\mu g\,kg^{-1}\,min^{-1}$, coronary venous oxygen saturation and regional segment length shortening remained constant.

Discussion

The principal findings of this study are that intracoronary infusions of fenoldopam (up to a dose of 0.4 $\mu g\,kg^{-1}\,min^{-1}$) neither affected myocardial blood flow nor myocardial function and oxygen consumption in anaesthetized pigs. The doses used were high enough to cause changes in the peripheral vasculature as reflected by decreases in mean arterial blood pressure and systemic vascular resistance. Furthermore, in two animals the rate of the intracoronary infusions of fenoldopam was increased to 4 $\mu g\,kg^{-1}\,min^{-1}$ without causing any changes in regional myocardial wall motion and coronary venous oxygen saturation, which is a sensitive parameter to detect coronary vasodilatation provided myocardial oxygen consumption does not increase (Duncker *et al.*, 1986; Verdouw *et al.*, 1987; Sassen *et al.*, 1990a,b). These observations suggest that D_1 receptors are of minor importance in the coronary circulation of the anaesthetized pig.

The presence of D_1 receptors in the renal, mesenteric and cerebral vascular beds has now been well established in a

number of species including man, dogs and pigs (Goldberg, 1972; Ueda et al., 1982; Gootman et al., 1983; Toda, 1983; Hughes & Sever, 1989). In contrast, evidence for D_1 receptors in the coronary circulation is inconclusive. In dogs pretreated with α- and β-adrenoceptor antagonists, dopamine has been reported to elicit a D_1 receptor-mediated vasodilatation in coronary conductance vessels (Toda & Hatano, 1979) as well as in arterioles (Schuelke et al., 1971; Kopia & Valocik, 1989). However, in the present experiments in pigs, dopamine-induced coronary vasodilatation was accompanied by increases in heart rate and myocardial contractility, and these effects were absent in animals with α- and β-adrenoceptor blockade. Similarly, fenoldopam-induced coronary vasodilatation has not been consistently observed. While Kopia & Valocik (1989) found coronary vasodilatation after intracoronary administration of $1\,\mu g\,kg^{-1}\,min^{-1}$ fenoldopam in the dog, no such effect was noticed with this drug after intravenous infusion in the same species (Hieble et al., 1987) or after intracoronary infusion in the pig (present experiments). In human isolated coronary arteries precontracted with noradrenaline, fenoldopam failed to elicit a vasodilator response in 6 out of 9 artery segments (6 out of 7 patients) (Hughes & Sever, 1989), implying that the human conduit coronary vessels are devoid of D_1 receptors.

Another controversial point is the potential effects of fenoldopam on myocardial contractility. Hieble et al. (1987) suggested that fenoldopam exerts a negative inotropic action as shown by a 26% decrease in $LVdP/dt_{max}$ during intravenous infusion of the drug. The authors did not take into account that $LVdP/dt_{max}$ depends not only on myocardial contractility but also on heart rate, left ventricular filling pressure and arterial blood pressure (afterload). Since in their study arterial blood pressure decreased by approximately 25%, the effect on dP/dt_{max} cannot be assumed to be secondary to possible cardiodepressant actions of the drug only. In contrast, Zhao et al. (1990) observed that intracoronary infusion of fenoldopam at concentrations up to 5000 nM (equivalent to intracoronary infusions of $1–2\,\mu g\,kg^{-1}\,min^{-1}$ fenoldopam in our experiments) at constant coronary perfusion pressure increased $LVdP/dt_{max}$ in anaesthetized dogs. Kopia & Valocik (1989), using a similar experimental set-up found no change in myocardial function. We also did not observe change in $LVdP/dt_{max}$ or in regional myocardial segment length shortening indicating the absence of a negative inotropic action. Furthermore, to achieve equivalent intracoronary concentrations via intravenous administration one would require a fifty-fold higher dose of the drug. This may be unacceptable because of severe hypotension.

Finally, two points deserve comment. First, it is theoretically possible that in our model a vasodilator response of fenoldopam could not be observed because the coronary vascular bed was already maximally dilated. This seems very unlikely as we have repeatedly shown that in the same model a number of drugs increased coronary blood flow up to 100% (Duncker et al., 1986; Verdouw et al., 1987; Sassen et al., 1990a,b) while in the present study intravenous infusions of dopamine reduced coronary vascular resistance to 60% of baseline. Secondly, it could be argued that the butyrophenone derivative azaperone (Niemegeers et al., 1974), used by us as anaesthetic premedication, may have antagonized a possible vasodilator effect of fenoldopam. This drug has indeed been shown to exhibit antidopamine activity, but the inhibition is at the D_2 receptor site (Fukuchi et al., 1988). Furthermore, intravenous infusion of dopamine in the presence of α- and β-adrenoceptor blockade revealed the existence of dopamine receptors in several peripheral vascular beds.

In conclusion, the lack of effect of intracoronary infusions of high doses of fenoldopam as well as of intravenous infusions of dopamine (after adrenoceptor blockade) on coronary blood flow and myocardial performance provides evidence that D_1 receptors do not play a major physiological role in the coronary circulation and myocardium of pigs. This observation should be taken into account in the study of the effects of agents acting on dopamine receptors.

References

DUNCKER, D.J., VAN DALEN, F.J., HARTOG, J.M., LAMERS, J.M.J., RENSEN, R.J., SAXENA, P.R. & VERDOUW, P.D. (1986). Usefulness of pimobendan in the treatment of heart failure. *Arzneim. Forsch.*, **36**, 1740–1744.

FUKUCHI, I., DAWASHIMA, K., MATSUOKA, Y. & ISHIDA, R. (1988). Neurochemical study of mafoprazine, a new phenylpiperazine derivative. *Jpn. J. Pharmacol.*, **47**, 51–61.

GOLDBERG, L.I. (1972). Cardiovascular and renal actions of dopamine: potential clinical applications. *Pharmacol. Rev.*, **24**, 1–29.

GOOTMAN, N., BUCKLEY, B.J., GOOTMAN, P.M., GRISWOLD, P.G., MELE, J.D. & NUDEL, D.B. (1983). Maturation-related differences in regional circulatory effects of dopamine infusion in swine. *Dev. Pharmacol. Ther.*, **6**, 9–22.

HIEBLE, J.P., OWEN, D.A.A., HARVEY, C.A., BLUMBERG, A.L., VALOCIK, R.E. & DEMARINIS, R.M. (1987). Hemodynamic effects of selective receptor agonists in the rat and dog. *Clin. Exp. Hypertension*, **9**, 889–912.

HUGHES, A.D. & SEVER, P.S. (1989). Action of fenoldopam. A selective dopamine (DA_1) receptor agonist, on isolated human arteries. *Blood Vessels*, **26**, 119–127.

KOPIA, G.A. & VALOCIK, R.E. (1989). Demonstration of specific dopamine-1 receptor-mediated coronary vasodilation in the anesthetized dog. *J. Pharmacol. Exp. Ther.*, **248**, 215–221.

NIEMEGEERS, C.J.E., VAN NUETEN, J.M. & JANSSEN, P.A.C. (1974). Azaperone, a sedative neuroleptic of the butyrophenone series with pronounced anti-aggressive and anti-shock activity. *Arzneim. Forsch.*, **24**, 1798–1806.

SASSEN, L.M.A., SOEI, L.K., KONING, M.M.G. & VERDOUW, P.D. (1990a). The central and regional cardiovascular responses to intravenous and intracoronary administration of the phenyldihydropyridine elgodipine in anaesthetized pigs. *Br. J. Pharmacol.*, **99**, 355–363.

SASSEN, L.M.A., DUNCKER, D.J.G.M., GHO, B.C.G., DIEKMANN, H.W. & VERDOUW, P.D. (1990b). Haemodynamic profile of the potassium channel activator EMD 52692 in anaesthetized pigs. *Br. J. Pharmacol.*, **101**, 605–614.

SAXENA, P.R., SCHAMHARDT, H.C., FORSYTH, R.P. & LOEVE, J. (1980). Computer programs for the radioactive microsphere technique. Determination of experimental circumstances. *Comp. Prog. Biomed.*, **12**, 63–84.

SCHUELKE, D.M., MARK, A.L., SCHMID, P.G. & ECKSTEIN, J.W. (1971). Coronary vasodilation produced by dopamine after adrenergic blockade. *J. Pharmacol. Exp. Ther.*, **176**, 320–327.

TODA, N. (1983). Dopamine vasodilates human cerebral arteries. *Experientia*, **39**, 1131–1132.

TODA, N. & HATANO, Y. (1979). Antagonism by droperidol of dopamine-induced relaxation in isolated dog arteries. *Eur. J. Pharmacol.*, **57**, 231–238.

UEDA, Y., YANO, S. & SAKANASHI, M. (1982). In vitro evidence for dopaminergic receptors in human renal artery. *J. Cardiovasc. Pharmacol.*, **4**, 76–81.

VERDOUW, P.D., SASSEN, L.M.A., DUNCKER, D.J., SCHMEETS, I.O.L., RENSEN, R.J. & SAXENA, P.R. (1987). Nicorandil-induced changes in the distribution of cardiac output and coronary blood flow in pigs. *Naunyn-Schmiedebergs Arch. Pharmacol.*, **336**, 352–358.

ZHAO, R., FENNELL, W.H. & ABEL, F.L. (1990). Effects of dopamine D_1 and dopamine D_2 receptor agonists on coronary and peripheral hemodynamics. *Eur. J. Pharmacol.*, **190**, 193–202.

(Received April 17, 1991
Revised May 21, 1991)

Br. J. Pharmacol. (1991), **104**, 251–257

Mechanism of action of platelet activating factor in the pulmonary circulation: an investigation using a novel isotopic system in rabbit isolated lung

[1]J.P. Seale, [2]S. Nourshargh, [3]P.G. Hellewell & T.J. Williams

Department of Applied Pharmacology, National Heart and Lung Institute, Dovehouse Street, London SW3 6LY

1 Rabbit isolated lungs were perfused via the pulmonary artery with Tyrode solution containing 4.5% Ficoll and 0.1% bovine serum albumin at a constant rate of 20 ml min^{-1}. Lung perfusate was drawn for alternating 5 min periods from two reservoirs, one containing ^{125}I-albumin and the other unlabelled albumin to wash out the intravascular label. Microvascular ^{125}I-albumin leakage was determined from the count remaining at the end of the washout phase with an external gamma scintillation probe. In addition, perfusion pressure was monitored continuously. Each experiment comprised 6 cycles over a total period of 60 min.

2 Infusion of platelet activating factor (PAF, 3 nmol min^{-1} for 10 min) resulted in microvascular ^{125}I-albumin leakage, whereas lyso-PAF was without effect. During PAF infusions there was also an increase in perfusion pressure. Both the permeability and pressor effects of PAF were inhibited by the PAF antagonist L-652731.

3 Infusion of the thromboxane analogue U-46619 (0.6 nmol min^{-1} for 10 min) caused an increase in perfusion pressure but protein accumulation was not significantly different from that observed with control infusions.

4 Bolus injections of PAF (1 nmol) caused increases in perfusion pressure which were reduced by indomethacin, dazmegrel and BW 755C. Bolus injections of PAF, repeated at 30 min intervals caused reproducible pressor responses; however, repeated injections at 60 min intervals resulted in augmented responses. This augmentation did not occur in the presence of indomethacin.

5 Retrograde perfusion of PAF via the pulmonary vein induced increased perfusion pressure and microvascular ^{125}I-albumin leakage. The observed increase in leakage when compared with forward perfusion suggests that PAF produces predominantly arteriolar constriction i.e. proximal to the site of leakage during forward perfusion.

6 These results indicate that PAF is a vasoconstrictor in the rabbit pulmonary circulation and augmented responses occur with repeated injections at 60 min intervals. Cyclo-oxygenase inhibition abolished this vascular hyperresponsiveness induced by PAF. PAF also caused protein accumulation in the lungs. Both these actions of PAF appear to be receptor-mediated because they were inhibited by PAF antagonists. Another pulmonary vasoconstrictor, U-46619 did not cause protein accumulation suggesting that the extravasation of protein with PAF is not merely secondary to changes in vascular tone.

Keywords: PAF; PAF antagonists; thromboxane; oedema; perfused lung; inflammation

Introduction

Platelet activating factor (PAF) was originally described as a putative mediator of anaphylaxis released by rabbit basophils on exposure to antigen (Benveniste *et al.*, 1972). Subsequent investigations have revealed that PAF can be released from other cell types including platelets (Chignard *et al.*, 1980), neutrophils (Lynch *et al.*, 1979; Betz & Henson, 1980), monocytes and macrophages (Arnoux *et al.*, 1980) and endothelial cells (Camussi *et al.*, 1983b). In addition to its effects on platelets, PAF has been shown to be a potent stimulator of other target cells including neutrophils (Goetzl *et al.*, 1980; O'Flaherty *et al.*, 1981), vascular endothelial cells (Handley *et al.*, 1984; Bussolino *et al.*, 1987; Grigorian & Ryan, 1987), vascular smooth muscle cells and bronchial smooth muscle cells (Findlay *et al.*, 1981; Camussi *et al.*, 1983a; Stimler & O'Flaherty, 1983; Baranes *et al.*, 1986).

In vivo, PAF increases microvascular permeability resulting in oedema formation (Vargaftig & Ferreira, 1981; Wedmore & Williams, 1981; Humphrey *et al.*, 1982). In skin, PAF acts synergistically with vasodilator prostaglandins to induce local oedema formation (Wedmore & Williams, 1981; Morley *et al.*, 1983; Archer *et al.*, 1984; Hellewell & Williams, 1986). This PAF-induced increase in vascular permeability appears to result from a direct effect of PAF on vascular endothelial cells since it is unaffected by depletion of circulating neutrophils or platelets (Wedmore & Williams, 1981; Pirotzky *et al.*, 1984). In addition to the effects of exogenously administered PAF, there is evidence that endogenous production of this phospholipid contributes to oedema formation. Thus, PAF antagonists partially suppress oedema in Arthus reactions initiated by immune complex deposition around vessel walls in rabbits (Hellewell & Williams, 1986; Hellewell, 1990) and rats (Camussi *et al.*, 1987; Warren *et al.*, 1989).

The effects of PAF in the lung mimic some of the major pathophysiological characteristics of lung injury. PAF causes pulmonary endothelial damage (Lewis *et al.*, 1983; McManus & Pinckard, 1985), pulmonary oedema and vasoconstriction (Heffner *et al.*, 1983; Hamasaki *et al.*, 1984; Burhop *et al.*, 1986; Christman *et al.*, 1988), increased airway resistance and decreased lung compliance (Halonen *et al.*, 1980; 1981; Christman *et al.*, 1988). Furthermore, PAF has been demonstrated to cause epithelial cell damage and an influx of inflammatory cells into airways and alveoli (Camussi *et al.*, 1983a; Arnoux *et al.*, 1988; Coyle *et al.*, 1988; Lellouch-Tubiana *et al.*, 1988; Sanjar *et al.*, 1990). In animal models of pulmonary dysfunction (associated with endotoxaemia), PAF antagonists are effective inhibitors of haemodynamic changes and lung injury

[1] Present address: Department of Pharmacology, University of Sydney, N.S.W. 2006, Australia.
[2] Author for correspondence.
[3] Present address: British Bio-technology Ltd, Brook House, Watlington Road, Cowley, Oxford, OX4 5LY.

(Chang et al., 1986). Based on these observations, PAF has been proposed to be an important mediator of acute lung injury.

Although the phenomenon of PAF-induced pulmonary oedema is well documented, the precise mechanism by which this effect is mediated is contentious. For example, it is unclear whether oedema formation is due to a change in endothelial cell permeability or whether it is merely a consequence of increased hydrostatic pressure secondary to vasoconstriction (Heffner et al., 1983; Hamasaki et al., 1984; Burhop et al., 1986; Christman et al., 1988; Imai et al., 1988). To investigate the effects of PAF and other inflammatory mediators in the lung under constant flow conditions, we have developed a novel model using *in vitro* lung perfusion. With this system, we have measured simultaneously changes in pulmonary vascular resistance and accurately measured pulmonary microvascular protein leakage. Our results demonstrate that PAF causes potent pulmonary vasoconstriction and increases the permeability of the pulmonary microvasculature and that these processes are dissociable. Parts of this work have been published in abstract form (Seale et al., 1987).

Methods

Animals

Male New Zealand White specific pathogen-free rabbits (2.5–3.5 kg) were purchased from Froxfield Farm, Hampshire and Hacking and Churchill, Huntingdon, Cambridge.

Preparation of isolated perfused lungs

Rabbits were anaesthetized with i.v. sodium pentobarbitone (30 mg kg^{-1}). A tracheostomy was performed and the animals allowed to breathe room air. Heparin (100 iu kg^{-1}) was administered i.v. and the animal killed with an overdose of sodium pentobarbitone. A thoracotomy was immediately performed and a silicone cannula was inserted into the pulmonary artery. The lungs were fully inflated with room air and 100 ml of perfusate at 37°C was flushed through the pulmonary circulation. Effluent perfusate escaped freely through an incision in the left atrium. Perfusion fluid comprised Tyrode solution (pH 7.4) containing 4.5% (w/v) Ficoll 70 and 0.1% (w/v) BSA gassed with 100% oxygen.

Lungs and heart were removed en bloc and suspended by the tracheal cannula. Lungs were inflated with 50–70 ml air and perfusate pumped through the pulmonary circulation at a constant flow of 20 ml min^{-1} (model 5025, Watson-Marlow, Falmouth, Cornwall). Evans blue dye (10 mg ml^{-1}, final concentration) was added to the perfusate for short periods of time so that the distribution of lung perfusate could be visualized. Perfusion pressure (arterial) was recorded continuously with a pressure transducer (Bell and Howell, model 4/327-1, Glasgow, Scotland) connected to a Lectromed MX2P preamplifier and MX212 pen recorder. The lung and apparatus were maintained at 37°C in a thermostatically-controlled perspex box.

In some experiments the lungs were perfused in a retrograde direction. The rabbits were prepared as described but instead of incising the left atrium, a cannula (of the same dimension as the pulmonary artery cannula) was inserted into it through the mitral valve. The lungs were perfused initially in a forward direction (i.e. via the pulmonary artery) at 20 ml min^{-1} for 5 min. The direction of flow was then reversed such that the perfusate entered the pulmonary circulation via the left atrial cannula.

Measurement of extravascular ^{125}I-albumin accumulation

Lung perfusate was drawn for alternating periods of 5 min from two reservoirs, one containing ^{125}I-human serum albumin (20 μg ml^{-1}, 0.05 μCi ml^{-1}) and one containing normal buffer (see below). The change from one reservoir to another was achieved by a solenoid-controlled valve. A gamma detector probe (Nuclear Enterprises Ltd., model DM1-1, Edinburgh, Scotland) fitted with a 25 mm diameter × 3 mm thick NaI crystal was mounted in a lead collimator with a single cylindrical hole (diameter 20 mm × length 15 mm) and positioned adjacent to a segment of well perfused lung, as determined by the infusion of Evans blue dye. ^{125}I-counts were displayed on a scalar ratemeter (Nuclear Enterprises, model SR7) and printed out every 30 s. Before each experiment a volume of the radioactive perfusate containing 100 μg total albumin was placed in the position of the lung in front of the probe to determine the counts per second corresponding to 1 μg of albumin so that radioactivity within the lung could be expressed in terms of μg protein. As shown in Figure 1, the whole system was linked to an Apple IIe microcomputer (Apple Computer, Cupertino, California,

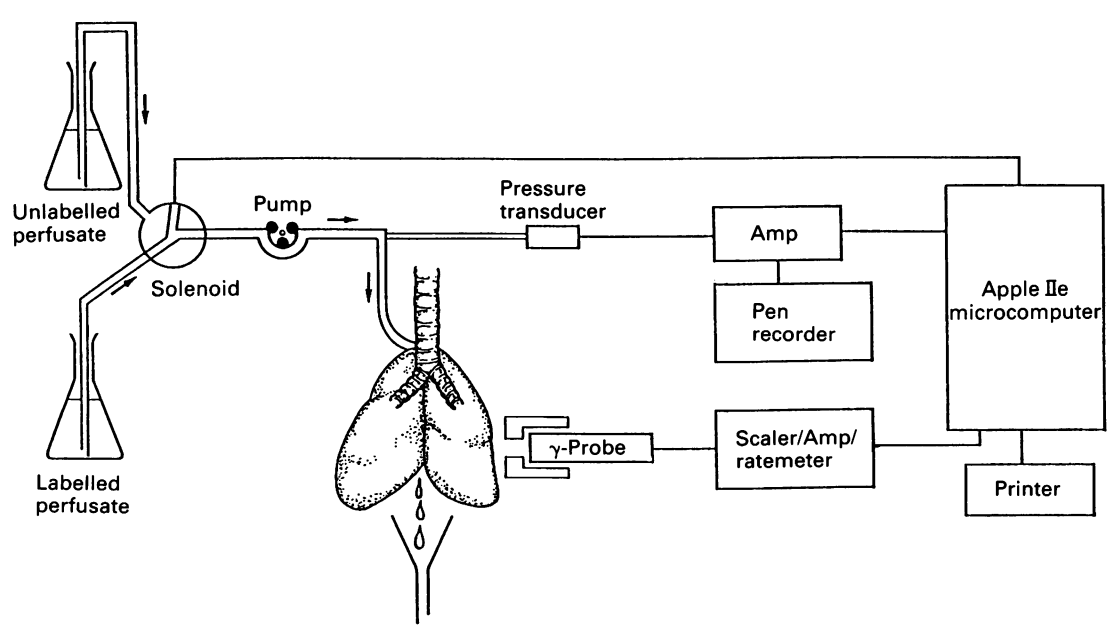

Figure 1 Schematic diagram of experimental apparatus. Lung perfusate was drawn for alternating periods of 5 min from two reservoirs, one of which contained ^{125}I-labelled human serum albumin (labelled perfusate). A gamma-detector probe was positioned adjacent to the pleural surface of the lung. An Apple IIe computer regulated the system and collected data.

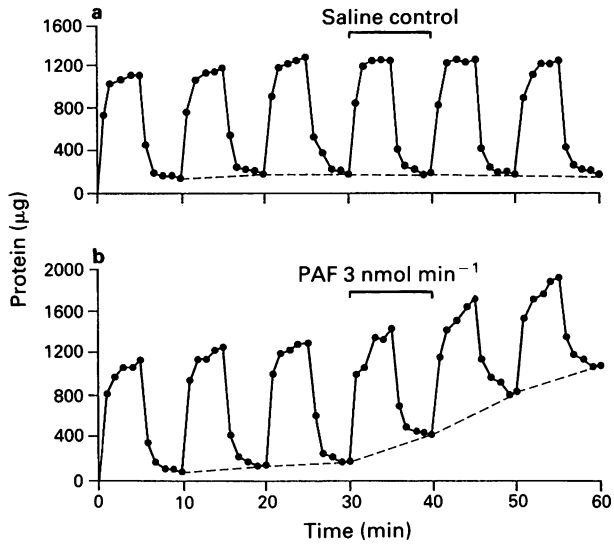

Figure 2 Protein accumulation during six 10 min cycles. Each cycle comprised 5 min 'wash in' of labelled perfusate followed by 5 min 'wash out' with unlabelled buffer. Infusion of PAF during the 4th cycle (b) caused an increase in protein accumulation compared with saline infusion (a).

U.S.A.) which regulated the solenoid and the scalar ratemeter as well as collecting and tabulating the protein-leakage data.

In preliminary experiments with continuous perfusion of labelled albumin it was found that protein leakage could not be accurately measured when superimposed upon a large background signal due to intravascular label. Therefore, a cycling perfusion procedure was devised to wash out the intravascular component periodically as shown in Figure 2. During perfusion with radioactive solution ('wash-in' phase) counts in the lung steadily increased and reached a plateau by 5 min. After starting perfusion with non-radioactive buffer ('washout' phase), there was a rapid fall in counts until a pleateau was reached by 5 min (Figure 2). The residual activity in the collimated region of the lung at the end of each 'wash-out' cycle was used as a measure of extravasated albumin. Three such 10 min cycles (comprising 5 min 'wash-in' and 5 min 'wash-out') were completed. At the start of the 4th cycle, PAF or lyso-PAF (3 nmol min^{-1} in saline containing 0.25% BSA), or saline (containing 0.25% BSA) was infused for 10 minutes (i.e. during the whole of the 4th cycle). In some experiments the stable thromboxane mimetic U-46619 was infused at 0.6 nmol min^{-1}.

Drugs and materials

Bovine serum albumin (BSA, Cohn Fraction V, fatty acid-free), arachidonic acid and indomethacin were purchased from Sigma Chemical Co., Poole, Dorset; Evans blue dye was from BDH Chemicals, Poole, Dorset; platelet activating factor (PAF) was from Bachem, Saffron Walden, Essex; sodium pentobarbitone and mepyramine maleate were from May and Baker, Dagenham, Essex; Ficoll 70 was from Pharmacia Fine Chemicals, Uppsala, Sweden; sterile 0.9% saline (Steriflex) was from the Boots Company, Nottingham, Nottinghamshire; ^{125}I-human serum albumin (50 μCi ml^{-1}, 20 mg albumin ml^{-1}) was from Amersham International plc, Amersham, Buckinghamshire. Sterile Tyrode solution (composition mM: NaCl 148, KCl 2.7, $CaCl_2$ 1.16, $MgCl_2$ 0.5, NaH_2PO_4 0.36, glucose 5.6, $NaHCO_3$ 1.2) was from the Clinical Research Centre media department.

The following were obtained as gifts: 48740 RP (3-(3-pyridyl)-1H,3H-pyrollo [1,2-e]thiazole-7-carboxamide) from Dr P. Sedivy, Rhone-Poulenc Sante, Vitry sur Seine, France; L-652,731 (*trans*-2,5-*bis* (3,4,5-trimethoxy phenyl) tetrahydrofuran) from Dr J.C. Chabala, Merck Sharp & Dohme Research Laboratories, Rahway, New Jersey, U.S.A.; WEB 2086 (3-[4-(2-chlorophenyl)-9-methyl-6H-thieno(3,2-f)(1,2,4-triazolo-(4,3-a)(1-4)-diazepine-2-yl]-1-(4-morpholinyl)-1-propanone) from Dr H. Heuer, Boehringer Ingleheim KG, Ingelheim am Rhein, Germany, BW 755C (3-amino-1-[M-(trifluoromethyl)-phenyl]-2-pyrasoline) was from Wellcome Research Laboratories, Beckenham, Kent; dazmegrel (3-(1H-imidazol-1-yl methyl)-2-methyl-1H-indole-1-propanoic acid) was from Pfizer Central Research, Sandwich, Kent; AH 23848 ([1α(z), 2β,5α]-(±)-7-[5-[[1,1'-biphenyl)-4-yl]methoxy]-2-(4-morpholinyl)-3-oxocyclopentyl]-4 heptenoic acid) was from Dr P.P.A. Humphrey, Glaxo, Ware, Herts; FPL 55712 (7-[3-(4-acetyl-3-hydroxy-2-propylphenoxy)-2-hydroxypropoxy]-4-oxo-8-propyl-4H-1-benzopyran-2-carboxylic acid) was from Fisons Parmaceuticals, Loughborough, Leicestershire; U-46619 (11α,9α-epoxymethano-prostaglandin H_2) was from Dr J. Pike, The Upjohn Company, Kalamazoo, Michigan, U.S.A.

Statistical analysis

Data are presented as the mean ± s.e.mean for n lungs and have been analysed with Student's unpaired t test. A P value of <0.05 was considered statistically significant.

Results

PAF-induced pressor response and protein accumulation in the rabbit lung

As shown in Figure 2, there was little increase in extravascular ^{125}I-albumin over the first three cycles as indicated by the residual activity remaining at the end of the intravascular washout cycles (dashed line). A saline infusion had no detectable effect on label retention (Figure 2a). An infusion of PAF (3 nmol ml^{-1} for 10 min) caused a marked increase in the label remaining at the end of the washout cycles indicating microvascular albumin leakage. Extravascular label continued to rise after stopping the PAF infusion, indicating that leakage persisted. At 60 min, protein accumulation in the collimated area was equivalent to 850 ± 170 μg (n = 10). Infusion of lyso-PAF had no effect on albumin accumulation (Figure 6b), (279 ± 27 μg at 60 min, n = 4 compared with saline controls 250 ± 33 μg, n = 6).

In addition to the enhanced protein leakage, infusion of PAF caused an increase in perfusion pressure. Figure 3 shows the pressor responses plotted against the superimposed ^{125}I wash-out curves from the same experiment. The mechanism of this pressor response was investigated further by use of bolus injections of PAF (1 nmol) in the pulmonary circulation (this resulted in pressor responses of shorter duration than those obtained during PAF infusion and therefore allowed several injections to be given in one lung preparation). In 11 experiments the mean increase in perfusion pressure with PAF injection was 10.5 ± 1.3 mmHg. The effects of a number of inhibitors were tested on the pressor response induced by a bolus (1 nmol) injection of PAF. PAF responses were measured before and after drug administration in the same lung with an interval of 30 min between PAF doses. The PAF-induced vasoconstriction was markedly reduced by indomethacin (at 10 μM, 74% inhibition in 2 experiments), the dual 5-lipoxygenase/cyclo-oxygenase, inhibitor BW 755C (at 50 μM, 57% inhibition in 2 experiments) and by the thromboxane synthesis inhibitor, dazmegrel (at 100 μM, 67% inhibition in 4 experiments). Responses were also inhibited by the thromboxane receptor antagonist, AH23848 (at 1 μM, 50% inhibition in 2 experiments). Injections of arachidonic acid (300 nmol) induced matching pressor responses to PAF at 1 nmol and these arachidonic acid-induced responses were totally inhibited by indomethacin, BW755C and dazmegrel (data not shown). However, the pressor responses to PAF and arachidonic acid were not affected by the sulphidopeptide leukotriene antagonist, FPL 55712 or by the H_1 receptor antagonist, mepyramine. The most effective inhibitors of the constrictor action of PAF were the PAF receptor antagonists 48740 RP,

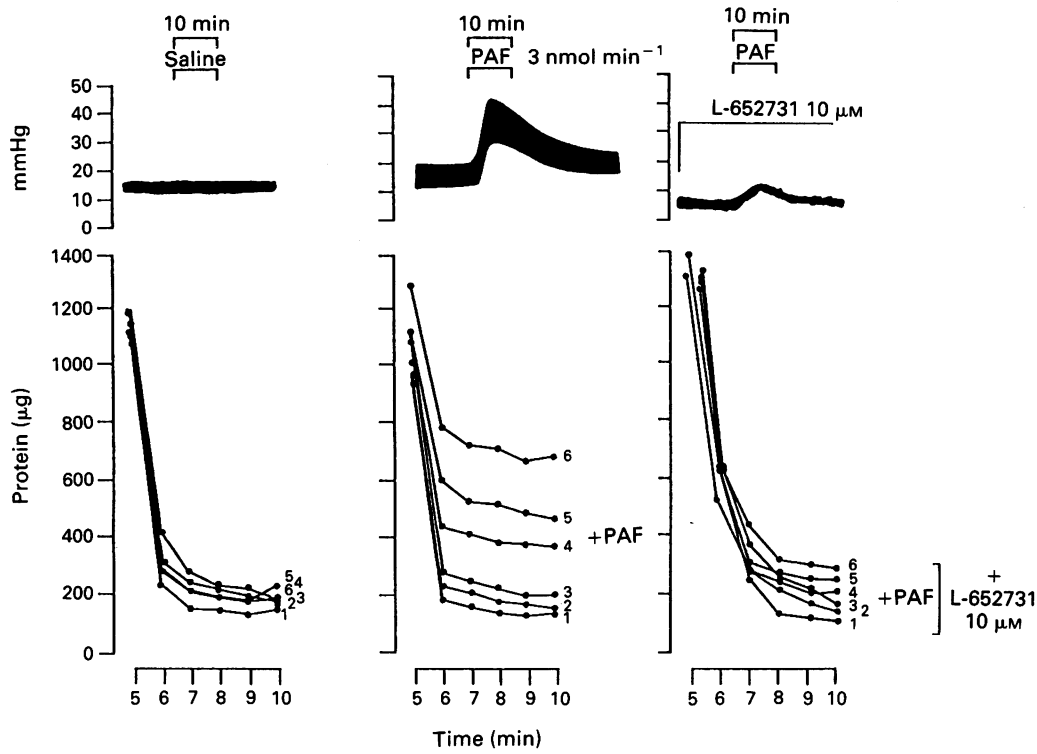

Figure 3 Effects of PAF on perfusion pressure (upper panels) and protein accumulation (lower panels) in sequential 'wash out' cycles (numbered 1–6). During saline infusion there was no increase in pressure and small increments in protein accumulation. Infusion of PAF during 4th cycle caused an increase in perfusion pressure and large increments in protein accumulation (middle panel). These effects of PAF were inhibited by the PAF receptor antagonist, L-652731 (right panel). The traces are representative of four separate experiments.

L-652,731 and WEB 2086, the order of potency being WEB 2086 > L-652,731 > 48740 RP. Complete inhibition of the pressor response was obtained with 1 μM WEB 2086 ($n = 3$ lungs), while greater than 90% inhibition was obtained with 10 μM L-652,731 ($n = 4$ lungs) and 100 μM 48740 RP ($n = 2$ lungs). These results suggest that the constrictor effect of PAF in the pulmonary circulation is mediated partly by a cyclo-oxygenase independent mechanism.

In a series of experiments where protein accumulation was measured, PAF-induced vasoconstriction and protein leakage were almost abolished in the presence of 10 μM L652,731 (Figures 3 and 6).

PAF-induced vascular hyperreactivity

Repeated bolus injections of PAF (1 nmol) at 30 min intervals were found to cause reproducible increases in perfusion pressure in the isolated lung (Figure 4a). However, when injections were made at 1 h intervals then a progressively larger pressor response was observed on each injection (Figure 4b). In three experiments, the mean pressor response on the first injection was 6.0 ± 1.2 mmHg which increased to 14.3 ± 1.9 mmHg on the second and to 19.0 ± 4.0 mmHg on the third, representing an overall increase of 220%. Such increased responsiveness was not observed with injection of histamine (1 μmol) which also induced vasoconstriction in this model (results not shown). To determine whether the PAF-induced vascular hyperreactivity was mediated by cyclo-oxygenase products, the experiment was repeated in the presence of 10 μM indomethacin. As shown in Figure 4c indomethacin blocked the hyperresponsiveness to repeated PAF injections. Similar findings were obtained in two further experiments.

A similar pattern of increased responsiveness as seen with PAF was also evident following injections of the stable thromboxane mimetic drug U-46619 (1 nmol) (Figure 4d); suggesting that the vascular hyperreactivity to PAF is mediated by cyclo-oxygenase products such as endoperoxides and thromboxane A_2.

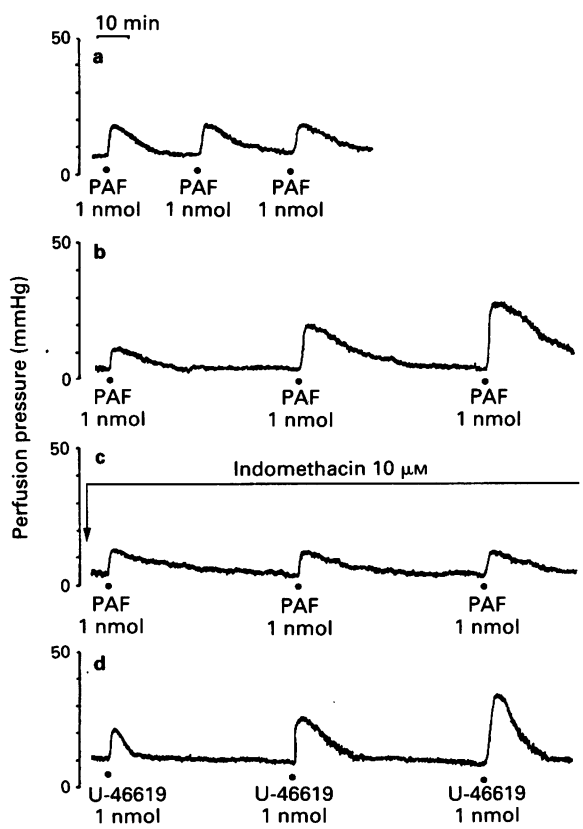

Figure 4 Responses to repeated bolus injections of PAF. Injections at 30 min intervals caused reproducible increases in perfusion pressure (a). Progressively greater pressure responses occurred with each injection of PAF at 60 min intervals (b). This augmentation did not occur in the presence of indomethacin (c). A similar pattern of augmented pressure responses was evident with injections of the thromboxane analogue, U-46619 (d). The results are representative of three separate experiments.

Comparison of responses to PAF and U-46619 in the rabbit lung

Figure 5 compares the pressor responses and protein leakage induced by PAF and U-46619. The pressor responses are plotted against the superimposed individual ^{125}I washout curves from the same experiments. In a series of experiments infusion of U-46619 (0.6 nmol min^{-1}) induced comparable increases in perfusion pressure (31.6 ± 6.0 mmHg, $n = 6$) to those observed with 3 nmol min^{-1} PAF (25 ± 4.0 mmHg, $n = 10$). However only PAF infusions increased protein accumulation (Figure 6a) indicating that in this model protein leakage is not merely a consequence of increased hydrostatic pressure. Furthermore, these results suggest that endogenous thromboxane A_2 is unlikely to be mediating the PAF-induced protein leakage.

PAF-induced protein leakage with retrograde perfusion of lungs

During perfusion of the lungs via a left atrial cannula the PAF-induced increase in perfusion pressure (12.9 ± 2.0 mmHg, $n = 6$) was lower than that observed during forward perfusion (see above). Although background albumin accumulation during retrograde perfusion was marginally higher than during forward perfusion, infusion of PAF resulted in a considerably greater ($P < 0.05$) albumin accumulation than during forward perfusion (Figure 7).

Discussion

PAF is a potent inflammatory mediator with diverse biological actions, including the ability to enhance permeability in microvessels. However, the response of the pulmonary circulation to PAF is poorly understood. It has been suggested that, in rabbit isolated lungs, PAF-induced pulmonary oedema is mediated by thromboxane released from PAF-stimulated platelets (Heffner *et al.*, 1983). In a different species, the guinea-pig, Hamasaki and colleagues (1984) have reported that PAF-induced pulmonary oedema is independent of platelets. More recently, studies in sheep and rabbit lungs, have suggested that the PAF-mediated oedema is a result of vasoconstriction and is not due to any effect on microvascular permeability (Bolin *et al.*, 1986; Burhop *et al.*, 1986).

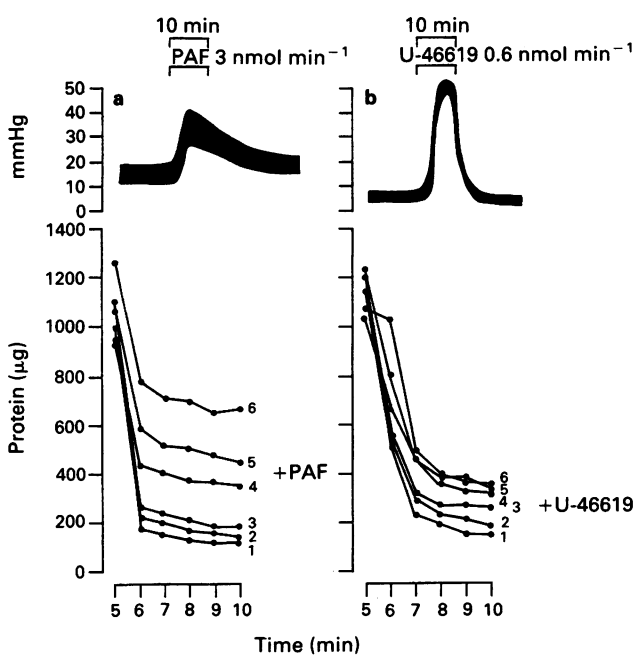

Figure 5 Effects of PAF (a) and U-46619 infusion (b) on perfusion pressure (upper panels) and protein accumulation (lower panels). U-46619 caused an increase in perfusion pressure of similar magnitude to that with PAF, without causing protein accumulation. The results are representative of six separate experiments.

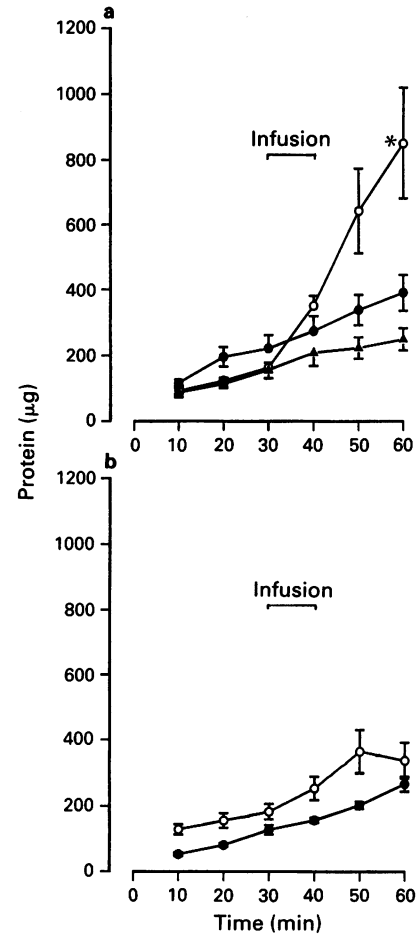

Figure 6 Effects of PAF (a) and U-46619 (b) on protein accumulation. (a) Infusion of PAF (○, 3 nmol min^{-1}, $n = 10$) during the 4th cycle resulted in protein accumulation at 60 min which was significantly greater than control (▲, $n = 6$) ($P < 0.05$). In the presence of the PAF antagonist, L-652731 (●, 10 μM, $n = 4$), the protein accumulation at 60 min was not significantly different from control values. (b) After infusion of U-46619 (○, 0.6 nmol min^{-1}, $n = 6$) during the 4th cycle, protein accumulation at 60 min was not significantly different from protein accumulation after infusion of lyso-PAF (■, 3 nmol min^{-1}, $n = 4$). Each point represents the mean and vertical bars show s.e.mean.

In order to investigate the effects of PAF on the pulmonary microvasculature we developed a novel technique for measuring changes in pulmonary vascular resistance and directly quantifying protein leakage under constant flow conditions in rabbit isolated perfused lungs. We have demonstrated that PAF is a potent vasoconstrictor in rabbit lungs perfused with cell-free Tyrode solution. The PAF-induced pressor response was substantially suppressed by cyclo-oxygenase and thromboxane synthetase inhibitors suggesting that thromboxane and/or endoperoxides contribute to the vasoconstriction. This effect of PAF appears to be receptor-mediated, as three selective antagonists, i.e. 48740 RP (Sedivy *et al.*, 1985), L-652,731 (Hwang *et al.*, 1985) and WEB 2086 (Casals-Stenzel *et al.*, 1987), effectively inhibited the vasoconstriction.

When injections of PAF were repeated at 60 min intervals and pressor responses were recorded, vascular hyperreactivity was detected. With intervals of 30 min between injections no changes in the magnitude of responses were seen, possibly because of a compensating tachyphylactic effect. Indeed, repeated injections of PAF at 15 min intervals resulted in progressively smaller pressor responses (results not shown). The increased vascular responsiveness to PAF seen with 60 min

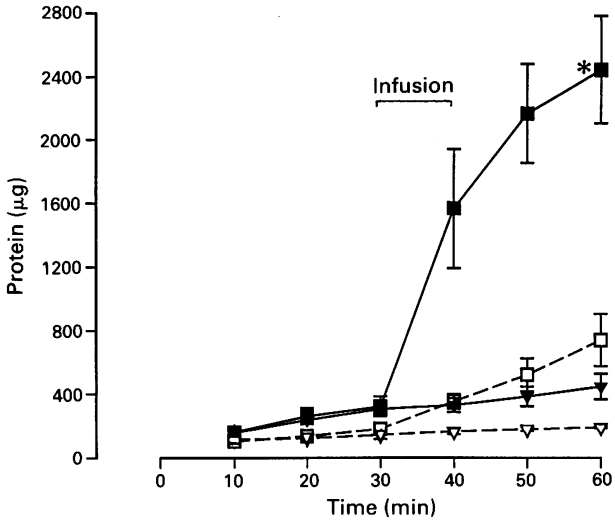

Figure 7 Protein accumulation during retrograde and forward perfusion of PAF 3 nmol min^{-1} and saline/BSA. The closed symbols joined by solid lines represent responses to retrograde perfusion of PAF (■, $n = 6$) and saline (▼, $n = 4$) whilst the open symbols joined by dashed lines represent responses to forward perfusion of PAF (□, $n = 4$) and saline (▽, $n = 3$). The protein accumulation at 60 min during retrograde perfusion of PAF was statistically significantly greater than during forward perfusion (*$P < 0.05$). Each point represents the mean and vertical bars show s.e.mean.

intervals was abolished by indomethacin, suggesting that it is mediated by cyclo-oxygenase products, probably thromboxane since U-46619 also induced the phenomenon. Although PAF-induced airway smooth muscle hyperresponsiveness may be a pathogenic mechanism in clinical asthma, the significance of PAF-induced vascular hyperreactivity is less clear.

As well as being a potent vasoconstrictor, PAF caused increased albumin accumulation in the lungs. To determine whether this effect was secondary to changes in hydrostatic pressure or due to a direct effect on vascular permeability, the stable thromboxane-mimetic, U-46619, was infused into lungs. U-46619 caused comparable increases in perfusion pressure to those occurring with PAF but U-46619 failed to induce protein leakage. These results suggest that the PAF-induced protein leakage was due to an increase in microvascular permeability and not a direct consequence of increased hydrostatic pressure. In addition, these results suggest that although thromboxane endoperoxides contribute to the PAF-induced pulmonary vasoconstriction, they are not involved in the PAF-induced increase in pulmonary microvascular permeability.

During retrograde perfusion, PAF caused both vasoconstriction and protein leakage. However, the extent of the protein leakage was greater than during forward perfusion (despite a smaller increase in perfusion pressure). These findings could be explained if the PAF-induced vasoconstriction occurred predominantly in the pulmonary arterioles, i.e. distal to the site of leakage in the case of retrograde perfusion. Thus, the hydrostatic pressure within the microvessel lumen would be expected to be higher at the site of leakage during retrograde perfusion.

In the present experiments the lungs were perfused with Tyrode solution to eliminate blood elements from the pulmonary circulation. Thus, the vasoconstrictor and permeability effects of PAF probably result from a direct action on vascular smooth muscle and endothelial cells respectively.

In summary, PAF is a potent vasoconstrictor and mediator of increased microvascular permeability in rabbit isolated perfused lungs. The pulmonary vasoconstrictor response is partly mediated by cyclo-oxygenase products probably endoperoxides and/or thromboxane A_2. Our results suggest that thromboxane A_2 or endoperoxides are unlikely to be mediating the protein leakage due to PAF and that protein leakage is due to an effect of PAF on the endothelium i.e. leakage is not secondary to vasoconstriction.

Some of this work was carried out at MRC Clinical Research Centre, Harrow, U.K. S.N. is a Wellcome Trust Postdoctoral Research Fellow and T.J.W. is supported by the National Asthma Campaign. We thank Pfizer Central Research, Sandwich, Kent for financial support. We would also like to acknowledge Mr Mike Smith, from MRC Clinical Research Centre, Harrow, U.K., for developing the computer programme operating the lung system.

References

ARCHER, C.B., PAGE, C.P., PAUL, W., MORLEY, J. & MACDONALD, D.M. (1984). Inflammatory characteristics of platelet activating factor (PAF-acether) in human skin. *Br. J. Dermatol.*, **110**, 45–50.

ARNOUX, B., DUVAL, D. & BENVENISTE, J. (1980). Release of platelet-activating factor (Paf-acether) from alveolar macrophages by the calcium ionophore A23187 and phagocytosis. *Eur. J. Clin. Invest.*, **10**, 437–441.

ARNOUX, B., DENJEAN, A., PAGE, C.P., NOLIBE, D., MORLEY, J. & BENVENISTE, J. (1988). Accumulation of platelets and eosinophils in baboon lung after Paf-acether challenge. *Am. Rev. Respir. Dis.*, **137**, 855–860.

BARANES, J., HELLEGOUARCH, A., LE HAGARAT, M., VIOSSAT, I., AUGUST, M., CHABRIER, P.E., CLOSTRE, F. & BRAQUET, P. (1986). The effects of PAF-acether on the cardiovascular system and their inhibition by a new highly specific PAF-acether receptor antagonist BN 52021. *Pharmacol. Res. Commun.*, **18**, 717–737.

BENVENISTE, J., HENSON, P.M. & COCHRANE, C.G. (1972). Leukocyte-dependent histamine release from rabbit platelets: The role for IgE, basophils and a platelet-activating factor. *J. Exp. Med.*, **136**, 1356–1377.

BETZ, S.J. & HENSON, P.M. (1980). Production and release of platelet-activating factor (PAF); dissociation from degranulation and superoxide production in the human neutrophil. *J. Immunol.*, **125**, 2756–2763.

BOLIN, R.W., ALBERT, R.K. & MARTIN, T.M. (1986). Platelet activating factor (PAF) does not increase vascular permeability in isolated rabbit lungs. *Am. Rev. Respir. Dis.*, **133**, A279.

BURHOP, K.E., GARCIA, J.G.N., SELIG, W.M., LO, S.K., VAN DER LEE, H., KAPLAN, J.E. & MALIK, A.B. (1986). Platelet-activating factor increases lung vascular permeability to protein. *J. Appl. Physiol.*, **61**, 2210–2217.

BUSSOLINO, F., CAMUSSI, G., AGLIETTA, M., BRAQUET, P., BOSIA, A., PESCARMONA, G., SANAVIO, F., D'URSO, N. & MARCHISIO, P.C. (1987). Human endothelial cells are targets for platelet-activating factor. I. Platelet-activating factor induces changes in cytoskeleton structures. *J. Immunol.*, **139**, 2439–2446.

CAMUSSI, G., AGLIETTA, M., MALAVASI, F., TETTA, C., PIACIBELLO, W., SANOVIO, F. & BUSSOLINO, F. (1983a). The release of platelet-activating factor from human endothelial cells in culture. *J. Immunol.*, **131**, 2397–2403.

CAMUSSI, G., PAWLOWSKI, I., SAUNDERS, R., BRENTJENS, J. & ANDRES, G. (1987). Receptor antagonist of platelet activating factor inhibits inflammatory injury induced by in situ formation of immune complexes in renal glomeruli and in the skin. *J. Lab. Clin. Med.*, **110**, 196–206.

CAMUSSI, G., PARLOWSKI, I., TETTA, C., ROFFINELLO, C., ALBERTON, M., BRENTJENS, J. & ANDRES, G. (1983b). Acute lung inflammation induced in the rabbit by local instillation of 1-0-octadecyl-2- acetyl-sn-glyceryl-3-phosphorylcholine or of native platelet activating factor. *Am. J. Pathol.*, **112**, 78–88.

CASALS-STENZEL, J., MUACEVIC, G. & WEBER, K-H. (1987). Pharmacological actions of WEB 2086, a new specific antagonist of platelet activating factor. *J. Pharmacol. Exp. Ther.*, **241**, 974–981.

CHANG, S., HENSON, P.M. & VOELKEL, N.F. (1986). Platelet activating factor mediates endotoxin-induced lung injury in rats. *Am. Rev. Respir. Dis.*, **133**, A278.

CHIGNARD, M., LE CONEDIC, J.P., VARGAFTIG, B.B. & BENVENISTE, J. (1980). Platelet-activating factor (PAF-acether) secretion from platelets: Effect of aggregating agents. *Br. J. Haematol.*, **46**, 455–464.

CHRISTMAN, B.W., LEFFERTS, P.L., KING, G.A. & SNAPPER, J.R. (1988). Role of circulating platelets and granulocytes in PAF-

induced pulmonary dysfunction in awake sheep. *J. Appl. Physiol.*, **64**, 2033–2041.

COYLE, A.J., URWIN, S.C., PAGE, C.P., TOUVAY, C., VILLAIN, B. & BRAQUET, P. (1988). The effect of the selective PAF antagonist BN 52021 on PAF- and antigen-induced bronchial hyper-reactivity and eosinophil accumulation. *Eur. J. Pharmacol.*, **148**, 51–58.

FINDLAY, S.R., LICHTENSTEIN, L.M., HANAHAN, D.J. & PINCKARD, R.N. (1981). The contraction of guinea pig ileal smooth muscle by acetyl glyceryl ether phosphorylcholine. *Am. J. Physiol.*, **241**, C130–C134.

GOETZL, E.J., DERAIN, C.K., TAUBER, A.I. & VALONE, F.H. (1980). Novel effects of 1-0-hexadecyl-2-acyl-SN glycero 3-phosphorycholine mediators on human leukocyte function. Delineation of the specific roles of the aryl substituents. *Biochem. Biophys. Res. Commun.*, **94**, 881–888.

GRIGORIAN, G.Y. & RYAN, U.S. (1987). Platelet-activating factor effects on bovine pulmonary endothelial cells. *Circ. Res.*, **61**, 389–395.

HALONEN, M., PALMER, J.D., LOHMAN, I.C., MCMANUS, L.M. & PINCKARD, R.N. (1980). Respiratory and circulatory alterations induced by acetyl glyceryl ether phosphorylcholine (AFEPC), a mediator of IgE anaphylaxis in the rabbit. *Am. Rev. Respir. Dis.*, **122**, 915–924.

HALONEN, M., PALMER, J.D., LOHMAN, C., MCMANUS, L.M. & PINCKARD, R.N. (1981). Differential effects of platelet depletion on the cardiovascular and pulmonary alterations of IgE anaphylaxis and AGEPC infusion in the rabbit. *Am. Rev. Respir. Dis.*, **124**, 416–421.

HAMASAKI, Y., MOJARAD, M., SAGA, T., TAI, H. & SAID, S.I. (1984). Platelet-activating factor raises airway and vascular pressures and induces oedema in lungs perfused with platelet-free solution. *Am. Rev. Respir. Dis.*, **129**, 742–746.

HANDLEY, D.A., ARBEENY, C.M., LEE, M.L., VAN ALLEN, R.G. & SAUNDERS, R.N. (1984). Effect of platelet activating factor on endothelial permeability to plasma macromolecules. *Immunopharmacology*, **8**, 137–143.

HEFFNER, J.E., SHEEMAKER, S.A., CASHAM, E.M., PATEL, M., MCMURPHY, I.F., MORRIS, H.G. & REPINE, J.E. (1983). Acetyl glyceryl ether phosphorylcholine-stimulated human platelets cause pulmonary hypertension and oedema in isolated rabbit lungs. *J. Clin. Invest.*, **71**, 351–357.

HELLEWELL, P.G. (1990). The contribution of PAF to immune-complex mediated inflammation. In *Platelet Activating Factor in Endotoxin and Immune Diseases*. ed. Handley, D. A., Saunders, R.N., Houlihan, W.J. & Tomesch, J.C. New York: Marcel Dekker, (in press).

HELLEWELL, P.G. & WILLIAMS, T.J. (1986). A specific antagonist of platelet-activating factor suppresses oedema formation in an Arthus reaction but not oedema induced by leukocyte chemoattractants in rabbit skin. *J. Immunol.*, **137**, 302–307.

HUMPHREY, D.M., MCMANUS, L.M., SATOUCHI, K., HANAHAN, D.J. & PINCKARD, R.N. (1982). Vasoactive properties of acetyl glyceryl ether phosphocholine and analogues. *Lab. Invest.*, **46**, 422–427.

HWANG, S.B., LAM, M-H., BIFTU, T., BEATTIE, T.R. & SHEN, T.Y. (1985). Trans-2,5-bis-(3,4,5-trimethoxyphenyl)tetra-hydroguran. An orally active specific and competitive receptor antagonist of platelet activating factor. *J. Biol. Chem.*, **260**, 15639–15645.

IMAI, T., VERCELLOTTI, G.M., MOLDROW, C.F., JACOB, H.S. & WEIR, E.K. (1988). Pulmonary hypertension and edema induced by platelet-activating factor in isolated, perfused rat lungs are blocked by BN52021. *J. Lab. Clin. Med.*, **111**, 211–217.

LELLOUCH-TUBIANA, A., LEFORT, J., SIMON, M-T., PFISTER, A. & VARGAFTIG, B.B. (1988). Eosinophil recruitment into guinea pig lungs after PAF-acether and allergen administration. Modulation by prostacyclin, platelet depletion, and selective antagonists. *Am. Rev. Respir. Dis.*, **137**, 948–954.

LEWIS, J.C., O'FLAHERTY, J.T., MCCALL, C.E., WYKLE, R.L. & BOND, M.G. (1983). Platelet activating factor effects on pulmonary ultrastructure in rabbits. *Exp. Mol. Pathol.*, **38**, 100–108.

LYNCH, J.M., LOTNER, G.Z., BETZ, S.J. & HENSON, P.M. (1979). The release of a platelet-activating factor by stimulated rabbit neutrophils. *J. Immunol.*, **123**,1219–1226.

MCMANUS, J.M. & PINCKARD, R.N. (1985). Kinetics of acetyl glyceryl ether phosphorylcholine (AGEPC)-induced acute lung alterations in the rabbit. *Am. J. Pathol.*, **121**, 55–68.

MORLEY, J., PAGE, C.P. & PAUL, W. (1983). Inflammatory actions of platelet activating factor (Paf-acether) in guinea-pig skin. *Br. J. Pharmacol.*, **80**, 503–509.

O'FLAHERTY, J.T., WYKLE, R.L., MILLER, C.H., LEWIS, J.C., WAITE, M., BASS, D.A., MCCALL, C.E. & DECHATELET, L.R. (1981). 1-0-alkyl-sn-glyceryl-3-phosphorylcholines: A novel class of neutrophil stimulants. *Am. J. Pathol.*, **103**, 70–78.

PIROTZKY, E., PAGE, C.P., ROUBLIN, R., PFISTER, A., PAUL, W., BONNET, J. & BENVENISTE, J. (1984). PAF-acether-induced plasma exudation in rat skin is independent of platelets and neutrophils. *Micro. Endo. Lymph.*, **1**, 107–122.

SANJAR, S., BOUBEKEUR, A.K., CHAPMAN, I.D., SMITH, D., KINGS, M.A. & MORLEY, J. (1990). Eosinophil accumulation in pulmonary airways of guinea-pigs induced by exposure to an aerosol of platelet-activating factor: effect of anti-asthma drugs. *Br. J. Pharmacol.*, **99**, 267–272.

SEALE, J.P., NOURSHARGH, S., HELLEWELL, P.G. & WILLIAMS, T.J. (1987). Responses of the rabbit pulmonary microvasculature to platelet activating factor. *Br. J. Pharmacol.*, **92**, 634P.

SEDIVY, P., CAILLARD, C.G., CARREUTTE, A., DEREGNAUCOURT, J. & MONDOT, S. (1985). 48740 RP: selective anti-PAF agent. In *Advances in Inflammation Research*. ed. Russo-Marie, F., Mencia-Huerta, J.M. & Chignard, M. 10th edition, pp. 171–173. New York: Raven Press.

STIMLER, N.P. & O'FLAHERTY, J.T. (1983). Spasmogenic properties of platelet-activating factor: Evidence for a direct mechanism in the contractile response of pulmonary tissues. *Am. J. Pathol.*, **113**, 75–84.

VARGAFTIG, B.B. & FERREIRA, S.H. (1981). Blockade on the inflammatory effects of PAF by cyclo-oxygenase inhibitors. *Br. J. Med. Res.*, **14**, 187–189.

WARREN, J.S., MANDEL, D.M., JOHNSON, K.J. & WARD, P.A. (1989). Evidence for the role of platelet-activating factor in immune complex vasculitis in the rat. *J. Clin. Invest.*, **83**, 669–678.

WEDMORE, C.V. & WILLIAMS, T.J. (1981). Platelet-activating factor (PAF), a secretory product of polymorphonuclear leukocytes, increases vascular permeability in rabbit skin. *Br. J. Pharmacol.*, **74**, 916-917P.

(Received March 8, 1991
Accepted May 23, 1991)

Br. J. Pharmacol. (1991), **104**, 258–262

The effects of idazoxan and other α_2-adrenoceptor antagonists on food and water intake in the rat

[1]Helen C. Jackson, I.J. Griffin & D.J. Nutt

Reckitt & Colman Psychopharmacology Unit, Department of Pharmacology, School of Medical Sciences, University Walk, Bristol BS8 1TD

1 Idazoxan (1, 3, 10 mg kg^{-1}, i.p.) produced a significant increase in food and water intake in freely feeding rats during the daylight phase.

2 The more selective and specific α_2-adrenoceptor antagonists, RX811059 (0.3, 1, 3 mg kg^{-1}, i.p.) and RX821002 (0.3, 1, 3 mg kg^{-1}, i.p.), did not produce hyperphagia in rats, however, the highest dose produced a significant increase in water intake.

3 The peripherally acting α_2-adrenoceptor antagonist, L-659,066 (1, 3, 10 mg kg^{-1}, i.p.), did not affect food intake in the 4 h following injection, but the highest dose (10 mg kg^{-1}), produced a large increase in water intake.

4 These results indicate that α_2-adrenoceptor antagonists may increase water intake by a peripherally mediated mechanism.

5 The lack of effect of RX811059 and RX821002 on food intake contrasts with the large dose-related increases induced by idazoxan and suggests that the hyperphagic effects of idazoxan are not due to α_2-adrenoceptor blockade but may instead reflect its affinity for a non-adrenoceptor site, a property not shared by the other α_2-antagonists.

Keywords: Idazoxan; α_2-adrenoceptor antagonists; α_2-adrenoceptors; non-adrenoceptor idazoxan binding sites; food intake; water intake

Introduction

As part of a recent experiment investigating the possible involvement of α_2-adrenoceptors in the hyperphagic response to 5-hydroxytryptamine (5-HT) agonists, Sleight *et al.* (1988) found that the α_2-adrenoceptor antagonist idazoxan increased food intake in freely-feeding rats when given alone. This preliminary finding was unexpected, since, despite their widespread use, there have been no other reports of α_2-antagonists stimulating food intake in rats, and paradoxically, α_2-adrenoceptor agonists such as clonidine also elicit feeding (Sanger, 1983; McCabe *et al.*, 1984; Goldman *et al.*, 1985).

In addition to α_2-adrenoceptors, idazoxan has high affinity for non-adrenoceptor idazoxan binding sites (NAIBS; reviewed by Michel & Insel, 1989) which may play a role in control of appetite since they are concentrated in brain areas such as the hypothalamus and area postrema (Hudson *et al.*, 1991). In the current study, we have explored this possibility by comparing the effects of idazoxan on food and water intake in freely-feeding rats with those of the more selective and specific α_2-antagonists RX811059 (Doxey *et al.*, 1985) and RX821002 (Langin *et al.*, 1989). These compounds are structurally similar to idazoxan but have only low affinity for NAIBS (Langin *et al.*, 1990; Mallard *et al.*, 1991). Finally, the α_2-antagonist L-659,066, which does not readily cross the blood-brain barrier (Clineschmidt *et al.*, 1988), has also been used in an attempt to determine whether the site of the effects on appetite of α_2-antagonists is central or peripheral.

Methods

Animals and environment

Male Wistar rats (250–350 g, Bantin & Kingman) were individually housed (in polypropylene cages with metal grid floors) at 23 ± 2°C on a 14:10 h light-dark cycle (lights on at 05 h 00 min) with free access to a powdered standard rat diet (Biosure, Manea, Cambridgeshire) and tap water at all times. The powdered diet was contained in glass feeding jars (10 cm diameter; 8 cm deep) with metal lids. Each lid had a hole (3 cm diameter) cut in it to allow access to the food. Animals were accustomed to these conditions for at least one week before experimentation began.

Experimental procedures

On the day of test, animals were randomly allocated to four treatment groups, each containing six animals. All procedures began at 09 h 00 min so that measurements were carried out during the light period when the food and water intake of control animals was minimal. Feeding jars and water bottles were weighed (to the nearest 0.1 g) at the time of drug administration and after 1, 2, 4 and 24 h to enable the calculation of cumulative food and water intakes. Body weights were recorded at the time of injection (and after 24 h) as a matter of course and any variations in body weight were accounted for by expressing the results as g kg^{-1} rat weight (treatment group means ± s.e.mean). Control rats in the weight range used in this study would normally consume up to 2 g of food and 5 ml of water in the first 4 h of the experiment and 20–25 g of food and 25–30 ml of water over 24 h.

Drugs and injections

The following drugs were used: idazoxan (2-[2-(1,4-benzodioxanyl)]-2-imidazoline; 1, 3, 10 mg kg^{-1}), RX811059 (the 2-ethoxy derivative of idazoxan; 0.3, 1, 3 mg kg^{-1}), RX821002 (2-methoxy idazoxan; 0.3, 1, 3 mg kg^{-1}) and L-659,066 ((2R, 12bS) - N - [2 - (1,3,4,6,7,12b - hexahydro - 2' - oxospiro[2H - benzofuro[2,3 - a]quinolizine - 2,4' - imidazolidin] - 3' - yl)ethyl] methane sulphonamide; 1, 3, 10 mg kg^{-1}). Idazoxan, RX811059 and RX821002 were synthesized at Reckitt & Colman, Hull and L-659,066 was a gift from Merck, Sharp & Dohme, West Point, Pennsylvania, U.S.A. Drug doses are expressed as the hydrochloride salt and all drugs were dissolved in 0.9% saline and administered intraperitoneally in a dose volume of 1 ml kg^{-1}. Doses of drugs were based on those shown by other studies (Clineschmidt *et al.*, 1988; Jackson *et*

[1] Author for correspondence.

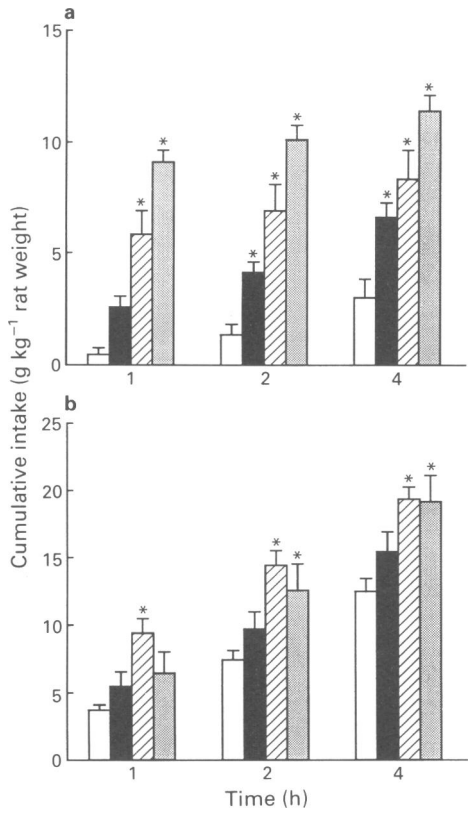

Figure 1 Effect of idazoxan on (a) cumulative food intake and (b) cumulative water intake. Groups of six rats were injected i.p. with either saline (open columns) or doses of idazoxan: 1 mg kg^{-1} (solid columns), 3 mg kg^{-1} (hatched columns) or 10 mg kg^{-1} (stippled columns). Results are expressed as treatment group means; vertical lines represent s.e.mean. Significant differences from control values are indicated by $^*P < 0.05$.

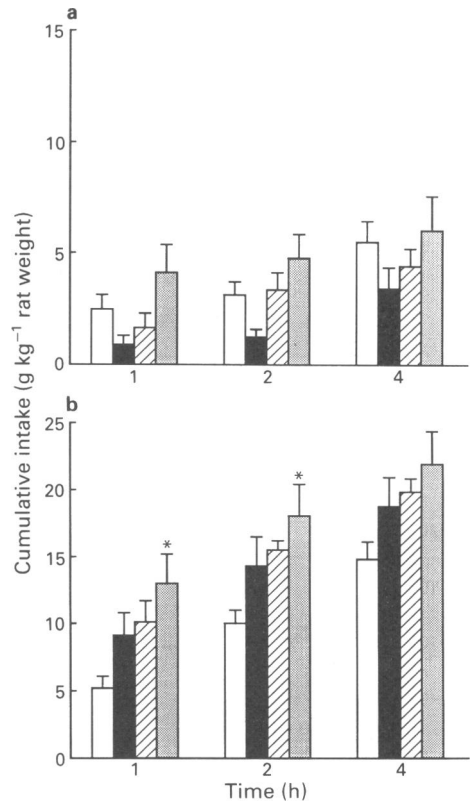

Figure 2 Effect of RX811059 on (a) cumulative food intake and (b) cumulative water intake. Groups of six rats were injected i.p. with either saline (open columns) or doses of RX811059: 0.3 mg kg^{-1} (solid columns), 1 mg kg^{-1} (hatched columns) or 3 mg kg^{-1} (stippled columns). Results are expressed as treatment group means; vertical lines represent s.e.mean. Significant differences from control values are indicated by $^*P < 0.05$.

al., 1990; unpublished observations) to cover the full pharmacological dose-range.

Statistical analysis

Statistical comparisons between mean group intakes were made using analysis of variance and Dunnett's test (two-tailed).

Results

Effects of idazoxan on food and water intake

Idazoxan (1, 3, 10 mg kg^{-1}, i.p.) produced a significant, dose-dependent increase in food intake which became evident within the first hour after drug administration (Figure 1a). Cumulative intakes were still significantly greater than those of the corresponding control group at the 4 h reading. Water consumption was also significantly increased by the two highest doses of idazoxan over the 4 h of the test as shown in Figure 1b. These responses were not clearly dose-related and a lower dose of 1 mg kg^{-1}, i.p. had no effect on drinking behaviour.

Effects of RX811059 and RX821002 on food and water consumption

The α_2-adrenoceptor antagonists RX811059 (0.3, 1, 3 mg kg^{-1}, i.p.) and RX821002 (0.3, 1, 3 mg kg^{-1}, i.p.) did not significantly modify feeding behaviour over the 4 h of the test as shown in Figure 2a and Figure 3a respectively. Water intake, on the other hand, was significantly elevated by RX811059 (3 mg kg^{-1} i.p.; Figure 2b) and RX821002 (3 mg kg^{-1} i.p; Figure 3b) during the first 2 h following injection although cumulative water intakes were comparable with those of the saline-treated controls at the 4 h reading.

Effects of the peripheral α_2-antagonist L-659,066 on feeding and drinking behaviour

The peripheral α_2-antagonist L-659,066 (1, 3, 10 mg kg^{-1}, i.p.) had no effect on food consumption in the rat (Figure 4a). However, the 10 mg kg^{-1} dose produced a large increase in water intake which became apparent in the first hour after injection (Figure 4b). Cumulative water intakes were still significantly greater than control values at the end of the 4 h observation period.

Cumulative 24 h food and water intakes

Idazoxan (1, 3, 10 mg kg^{-1}, i.p.), RX811059 (0.3, 1, 3 mg kg^{-1}, i.p.), RX821002 (0.3, 1, 3 mg kg^{-1}, i.p.) and L-659,066 (1, 3, 10 mg kg^{-1}, i.p.) had no effect on 24 h food and water intake as shown in Table 1. However, water intake of animals treated with high doses of the α_2-adrenoceptor antagonists tended to be lower than controls in the 20 h period between the 4 and 24 h readings (data not shown), and, food intake was significantly ($P < 0.05$) decreased in this interval by the highest (10 mg kg^{-1}) dose of idazoxan (mean food intake $\pm$ s.e. mean in the idazoxan-treated group was 65.1 $\pm$ 2.1 g kg^{-1} rat weight compared with control values of 78.3 $\pm$ 1.8). Body weights were not significantly altered by any of these compounds over a 24 h period apart from the highest dose of

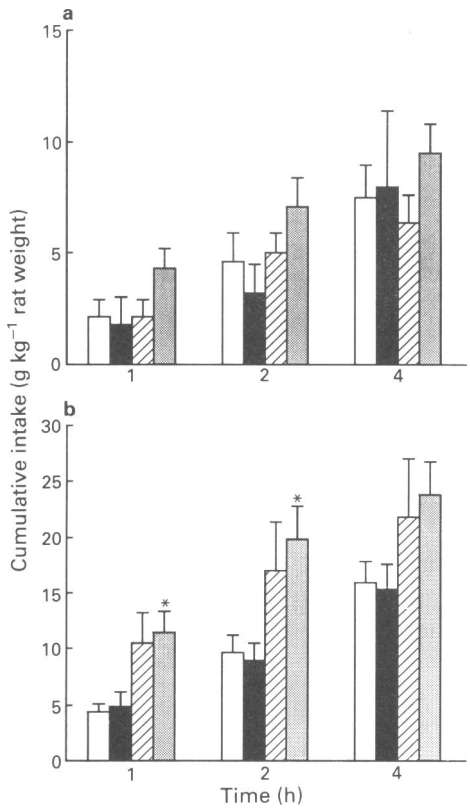

Figure 3 Effect of RX821002 on (a) cumulative food intake and (b) cumulative water intake. Groups of six rats were injected i.p. with either saline (open columns) or doses of RX821002: 0.3 mg kg^{-1} (solid columns), 1 mg kg^{-1} (hatched columns) or 3 mg kg^{-1} (stippled columns). Results are expressed as treatment group means; vertical lines represent s.e.mean. Significant differences from control values are indicated by $^*P < 0.05$.

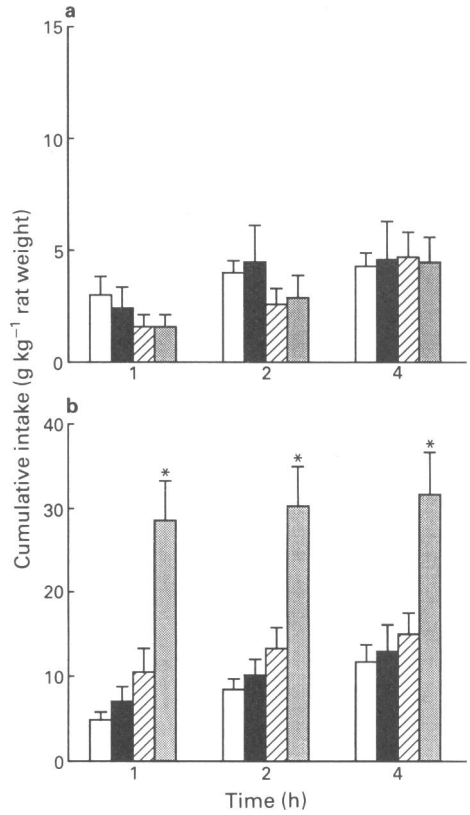

Figure 4 Effect of L659,066 on (a) cumulative food intake and (b) cumulative water intake. Groups of six rats were injected i.p. with either saline (open columns) or doses of L659,066: 1 mg kg^{-1} (solid columns), 3 mg kg^{-1} (hatched columns) or 10 mg kg^{-1} (stippled columns). Results are expressed as treatment group means; vertical lines represent s.e.mean. Significant differences from control values are indicated by $^*P < 0.05$.

L-659,066 (10 mg kg^{-1}, i.p.) which produced a small (1–2%), but significant drop in body weight compared with the saline-treated controls (data not shown).

Discussion

The major findings of this study are that idazoxan increases food and water intake in freely-feeding rats whereas other more selective α_2-adrenoceptor antagonists increase only drinking behaviour.

Table 1 Effect of α_2-adrenoceptor antagonists on food and water intake in the 24 h following drug administration

Treatment (mg kg^{-1}, i.p.)	*Daily intake* (g kg^{-1} rat weight) *Food*	*Water*
Vehicle	81.3 ± 1.8	96.2 ± 1.8
Idazoxan (1)	79.2 ± 2.2	100.7 ± 7.2
Idazoxan (3)	85.2 ± 2.2	106.5 ± 3.2
Idazoxan (10)	77.8 ± 3.0	95.0 ± 5.1
Vehicle	74.6 ± 2.2	91.6 ± 3.6
RX811059 (0.3)	71.6 ± 1.2	93.5 ± 3.5
RX811059 (1)	72.9 ± 2.8	92.4 ± 2.7
RX811059 (3)	68.8 ± 1.3	90.1 ± 5.1
Vehicle	79.4 ± 4.2	99.2 ± 5.2
RX821002 (0.3)	81.8 ± 2.5	91.7 ± 4.9
RX821002 (1)	85.9 ± 3.4	119.3 ± 14.2
RX821002 (3)	77.5 ± 2.0	100.1 ± 7.9
Vehicle	72.0 ± 2.4	82.2 ± 7.8
L-659,066 (1)	72.9 ± 4.9	83.8 ± 6.2
L-659,066 (3)	73.5 ± 2.3	83.9 ± 4.5
L-659,066 (10)	67.4 ± 2.3	98.4 ± 8.0

Values are mean ± s.e.mean.
Treatment groups contained 6 animals.

The mechanisms underlying the stimulatory effects of idazoxan on food intake presumably do not involve noradrenaline released following blockage of presynaptic α_2-adrenoceptors (Walter *et al.*, 1984; Dennis *et al.*, 1987), since RX811059 and RX821002, which would also increase synaptic availability of noradrenaline, did not alter food intake. In accordance with these findings, the α_2-adrenoceptor antagonist, yohimbine, does not increase food consumption in freely-feeding rats (Sanger, 1983). Moreover, although noradrenaline increases feeding in rats, this appears to be due to stimulation of postsynaptic α_2-adrenoceptors located in the paraventricular nucleus of the hypothalamus (Goldman *et al.*, 1985) which would also be blocked in our studies.

Idazoxan-induced feeding may therefore be attributed to a property of this compound other than α_2-adrenoceptor blockade. Stimulation of α_2-adrenoceptors by noradrenaline or clonidine (Leibowitz, 1980; Sanger, 1983; Goldman *et al.*, 1985) increases food intake in rats. Some workers have suggested that idazoxan acts as a partial α_2-agonist in peripheral tissues (Limberger & Starke, 1983), however, there is no evidence for this in the CNS (Galzin *et al.*, 1982; Freedman & Aghajanian, 1984) and it is unlikely that idazoxan-induced feeding is due to activation of α_2-adrenoceptors. In this context, idazoxan produces quite different behavioural effects from α_2-adrenoceptor agonists in rats; clonidine produces sedation (Drew *et al.*, 1979) whereas idazoxan produces behavioural activation (Dickinson *et al.*, 1990) which could result in increased feeding. However, since RX811059 increases locomotor activity in rats (Dickinson *et al.*, 1990), without altering food intake, idazoxan may increase food intake by a more specific effect on appetite.

Another possibility is that idazoxan-induced feeding may be mediated by 5-HT. At high doses idazoxan produces components of the classical 5-HT syndrome such as reciprocal

forepaw treading (Dickinson *et al.*, 1991), a response which has been attributed to activation of 5-HT_{1A}-receptors (Tricklebank *et al.*, 1984). Stimulation of 5-HT_{1A} receptors has also been shown to increase food intake in rats (Dourish *et al.*, 1985). In addition, idazoxan potentiates some of the behavioural effects of 5-HT agonists (Heal *et al.*, 1986; Dickinson *et al.*, 1991) although others, using different test systems, have shown antagonism (Fozard & McDermott, 1985; Marsden & Martin, 1986). It is unlikely that idazoxan interacts directly with 5-HT receptors since *in vitro* studies have shown that the concentration of idazoxan required to displace [^{3}H]-5-HT from its binding sites in rat cerebral cortex is greater than 5 μM (A.C. Lane; personal communication). However, complex interactions between noradrenaline and 5-HT with respect to food intake cannot be discounted.

Finally, idazoxan, but not RX811059, RX821002 or yohimbine, binds with high affinity to NAIBS (Brown *et al.*, 1990; Langin *et al.*, 1990; Mallard *et al.*, 1991). Therefore, it is an exciting possibility that idazoxan-induced feeding may involve activity at these sites. A function for NAIBS has not been described as yet; however, autoradiographial studies have shown that these sites are concentrated in the hypothalamus and area postrema (Hudson *et al.*, 1991), brain areas that have been associated with control of food and water intake. The development of NAIBS-selective ligands should help to clarify this issue.

In addition to effects on food intake, idazoxan also significantly increased drinking in rats. This was not simply a secondary response to increased intake of dry powdered diet since it was also observed for the α_2-adrenoceptor antagonists, RX811059 and RX821002, which do not alter feeding behaviour. Moreover, a similar selective facilitation of water intake has been observed for yohimbine (Sanger, 1983).

Drinking behaviour was also increased in the present study by L-659,066. This α_2-adrenoceptor antagonist acts selectively at α_2-adrenoceptors lying outside the blood-brain barrier following systemic administration (Clineschmidt *et al.*, 1988). This finding suggests that α_2-adrenoceptor antagonist-induced drinking may be peripherally-mediated. However, the possibility that L-659,066 acts at α_2-adrenoceptors located in circumventricular organs cannot be precluded. These structures, which have been implicated in the control of fluid homeostasis, lie within the CNS but are without a blood-brain barrier and are therefore accessible from the peripheral circulation (see Gross, 1987).

The exact mechanisms underlying α_2-adrenoceptor antagonist-induced water intake are unknown. The β-adrenoceptor agonist, isoprenaline, produces copious drinking in rats (Lehr *et al.*, 1967). This is thought to be largely due to its hypotensive effects and its ability to increase renin release in the kidney (Leenen & McDonald, 1974; Ramsay, 1978; Fuller, 1984) although central sites may also be involved (Goldstein *et al.*, 1985). At the level of the kidney, renin generates angiotensin II which is a powerful dipsogen (see Fuller, 1984). In our study, noradrenaline released following presynaptic α_2-adrenoceptor blockade could increase water intake by activation of postsynaptic β-adrenoceptors located in the kidney. Moreover, since α_2-adrenoceptor agonists inhibit renin release in rats (Pettinger *et al.*, 1976), and also inhibit both isoprenaline- and angiotensin-induced drinking (Fregly & Kelleher, 1980; Fregly *et al.*, 1981), α_2-antagonists may increase water intake by removing a tonic inhibitory influence of noradrenaline/α_2-adrenoceptors on water balance. Accordingly, α_2-antagonists potentiate the water intake produced by both isoprenaline and angiotensin II in rats (Fregly *et al.*, 1983).

It is also possible that the effects of α_2-adrenoceptor antagonists on water intake may reflect their cardiovascular actions. Both idazoxan and RX811059 decrease blood pressure in conscious rats (T.L. Berridge, unpublished observations) and this can activate the renin-angiotensin system and therefore increase drinking behaviour (see Fuller, 1984). Furthermore, the drinking induced by α_2-antagonists may be secondary to their effects on urine flow. Such effects have not been extensively investigated in normally-hydrated rats, however, idazoxan has a bimodal effect on urine output in water-loaded animals: low doses inhibit, whereas high doses increase, urination (T.L. Berridge; unpublished observations). In addition, both idazoxan and also the α_2-antagonist efaroxan (Chapleo *et al.*, 1984), produce diuresis in man (unpublished clinical observations). Again the mechanism for this response is unknown but it is unlikely to involve indirect activation of β-adrenoceptors since the β-agonist isoprenaline reduces urine flow in rats (Lehr *et al.*, 1967). Paradoxically, α_2-adrenoceptor agonists also produce diuresis in rats by inhibition of vasopressin secretion in the CNS and its antidiuretic effects in the kidney (Gellai, 1990) which is followed by a secondary increase in drinking (Atkinson *et al.*, 1978; Sanger, 1983).

All of the feeding and drinking responses observed in the current study were relatively short-lasting since 24-hourly intakes were similar to those of the control animals. This could be due to metabolism of the compounds *in vivo* (for example, idazoxan has a half-life in plasma of about 1 h; Lewis *et al.*, 1988) and/or reflect compensatory satiation following the initial feeding and drinking bouts (water intakes of animals treated with high doses of the α_2-antagonists tended to be lower than controls in the 20 h period between the 4 and 24 h readings, and, food intake was significantly decreased in this interval by the highest dose of idazoxan). Interestingly, L-659,066, at a high dose, significantly decreased body weight over 24 h. The reasons for this decrease, which were not observed for the other compounds, are unclear.

In summary, idazoxan increased food intake in rats by a mechanism that does not appear to involve α_2-adrenoceptor blockade since it was not observed following treatment with the selective α_2-antagonists RX811059 or RX821002 or with the peripherally-active compound L-659,066. All four α_2-adrenoceptor antagonists increased drinking in rats and the results with L-659,066 suggest that this may largely be peripherally-mediated. Finally, the unique effects of the α_2-antagonist idazoxan on food intake are interesting since they may be related to its high affinity at NAIBS and suggest that this compound may have some therapeutic value in the treatment of eating disorders.

We would like to thank Merck, Sharp & Dohme for their gift of L-659,066 and Drs S. L. Dickinson (Reckitt & Colman Psychopharmacology Unit) and G. Clarke (Department of Anatomy, University of Bristol) for their helpful discussions.

References

ATKINSON, J., KIRCHERTZ, E.J. & PETERS-HAEFELI, L. (1978). Effect of peripheral clonidine on ingestive behaviour. *Physiol. Behav.*, **21**, 73–77.

BROWN, C.M., MACKINNON, A.C., MCGRATH, J.C., SPEDDING, M. & KILPATRICK, A.T. (1990). α_2-Adrenoceptor subtypes and imidazoline-like binding sites in the rat brain. *Br. J. Pharmacol.*, **99**, 803–809.

CHAPLEO, C.B., MYERS, P.L., BUTLER, R.C.M., DAVIS, J.A., DOXEY, J.C., HIGGINS, S.D., MYERS, M., ROACH, A.G., SMITH, C.F.C., STILLINGS, M.R. & WELBOURN, A.P. (1984). α-Adrenoreceptor reagents. 2. Effects of modification of the 1,4-benzodiazoxan ring system on α-adrenoreceptor activity. *J. Med. Chem.*, **27**, 570–576.

CLINESCHMIDT, B.V., PETTIBONE, D.J., LOTTI, V.J., HUCKER, H.B., SWEENEY, B.M., REISS, D.R., LIS, E.V., HUFF, J.R. & VACCA, J. (1988). A peripherally acting alpha-2 adrenoceptor antagonist: L-659,066. *J. Pharmacol. Exp. Ther.*, **245**, 32–40.

DENNIS, T., L'HEUREUX, R., CARTER, C. & SCATTON, B. (1987). Presynaptic alpha-2 adrenoceptors play a major role in the effects of idazoxan on cortical noradrenaline release (as measured by in vivo dialysis) in the rat. *J. Pharmacol. Exp. Ther.*, **241**, 642–649.

DICKINSON, S.L., GADIE, B. & TULLOCH, I.F. (1990). Specific α_2-adrenoceptor antagonists induce behavioural activation in the rat. *J. Psychopharmacol.*, **4**, 90–99.

DICKINSON, S.L., GADIE, B. & TULLOCH, I.F. (1991). Effects of idazoxan on 5-hydroxytryptamine mediated behaviour in the mouse and rat. *J. Psychopharmacol.* (in press).

DOURISH, C.T., HUTSON, P.H. & CURZON, G. (1985). Low doses of the putative serotonin agonist 8-hydroxy-2-(di-n-propylamino) tetralin (8-OH-DPAT) elicit feeding in the rat. *Psychopharmacol.*, **86**, 197–204.

DOXEY, J.C., LANE, A.C., ROACH, A.G., SMITH, C.F.C. & WALTER, D.S. (1985). Selective α_2-adrenoceptor agonists and antagonists. In *Pharmacology of Adrenoceptors*. ed. Szabadi, E., Bradshaw, C.M. & Nahorski, S.R. pp. 13–22. New York: Macmillan Press.

DREW, G.M., GOWER, A.J. & MARRIOTT, A.S. (1979). α_2-Adrenoreceptors mediate clonidine-induced sedation in the rat. *Br. J. Pharmacol.*, **67**, 133–141.

FOZARD, J.R. & MCDERMOTT, I. (1985). The cardiovascular response to 8-hydroxy-2-(di-n-propylamino)-tetralin (8-OH-DPAT) in the rat. *Br. J. Pharmacol.*, **84**, 69P.

FREEDMAN, J.E. & AGHAJANIAN, G.K. (1984). Idazoxan (RX 781094) selectively antagonises α_2-adrenoreceptors on rat central neurons. *Eur. J. Pharmacol.*, **105**, 265–272.

FREGLY, M.J. & KELLEHER, D.L. (1980). Antidipsogenic effect of clonidine on isoproterenol-induced water intake. *Appetite*, **1**, 279–289.

FREGLY, M.J., KELLEHER, D.L. & GREENLEAF, J.E. (1981). Antidipsogenic effect of clonidine on angiotensin II-, hypertonic saline-pilocarpine- and dehydration-induced water intakes. *Brain Res. Bull.*, **7**, 661–664.

FREGLY, M.J., ROWLAND, N.E. & GREENLEAF, J.E. (1983). Effects of yohimbine and tolazoline on isoproterenol and angiotensin II-induced water intake in rats. *Brain Res. Bull.*, **10**, 121–126.

FULLER, L.M. (1984). The pharmacology of drinking behavior. *Pharmacol. Ther.*, **24**, 179–206.

GALZIN, A.M., LANGER, S.Z. & MORET, C. (1982). RX 781094 antagonises the inhibition by α_2-agonists of [^{3}H]-NA and [^{3}H]-5HT release while enhancing only the release of [^{3}H]-NA. *Br. J. Pharmacol.*, **77**, 447P.

GELLAI, M. (1990). Modulation of vasopressin antidiuretic action by renal α_2-adrenoceptors. *Am. J. Physiol.*, **259**, F1–F8.

GOLDMAN, C.K., MARINO, L. & LEIBOWITZ, S.F. (1985). Postsynaptic α_2-noradrenergic receptors mediate feeding induced by paraventricular nucleus injection of norepinephrine and clonidine. *Eur. J. Pharmacol.*, **115**, 11–19.

GOLDSTEIN, J.M., KNOBLOCH-LITWIN, L.C. & MALICK, J.B. (1985). Behavioral evidence for β-adrenoceptor subsensitivity after subacute antidepressant/α_2-adrenoceptor antagonist treatment. *Naunyn-Schmiedebergs Arch. Pharmacol.*, **329**, 355–358.

GROSS, P.M. (ed.). (1987). *Circumventricular Organs and Body Fluids*. Boca Raton, Florida: CRC Press Inc.

HEAL, D.J., PHILPOT, J., O'SHAUGHNESSY, K.M. & DAVIES, C.L. (1986). The influence of central noradrenergic function on 5-HT$_2$-mediated head-twitch responses in mice: Possible implications for the actions of antidepressant drugs. *Psychopharmacol.*, **89**, 414–420.

HUDSON, AL., MALLARD, N.J. & NUTT, D.J. (1991). Autoradiographic localization of non-adrenoceptor idazoxan binding sites (NAIBS) in rat brain. *Br. J. Pharmacol.*, **102**, 4P.

JACKSON, H.C., DICKINSON, S.L. & NUTT, D.J. (1990). Non-α_2-adrenoceptor idazoxan binding sites are not involved in the proconvulsant action of idazoxan. *Br. J. Pharmacol.*, **100**, 392P.

LANGIN, D., LAFONTAN, M., STILLINGS, M.R. & PARIS, H. (1989). [^{3}H]RX821002: a new tool for the identification of α_{2A}-adrenoceptors. *Eur. J. Pharmacol.*, **167**, 95–104.

LANGIN, D., PARIS, H. & LAFONTAN, M. (1990). Binding of [^{3}H]idazoxan and of its methoxy derivative [^{3}H]RX821002 in human fat cells: [^{3}H]idazoxan but not [^{3}H]RX821002 labels additional non-α_2-adrenergic binding sites. *Molec. Pharmacol.*, **37**, 876–885.

LEENEN, F.H.H. & MCDONALD, R.H. (1974). Effect of isoproterenol on blood pressure, plasma renin activity and water intake in rats. *Eur. J. Pharmacol.*, **26**, 129–135.

LEHR, D., MALLOW, J. & KRUKOWSKI, M. (1967). Copious drinking and simultaneous inhibition of urine flow elicited by beta-adrenergic stimulation and contrary effect of alpha-adrenergic stimulation. *J. Pharmacol. Exp. Ther.*, **158**, 150–163.

LEIBOWITZ, S.F. (1980). Neurochemical systems of the hypothalamus: Control of feeding and drinking behavior and water-electrolyte excretion. In *Handbook of the Hypothalamus, Vol. 1, Part A, Behavioral Studies of the Hypothalamus*. ed. Morgane, P.J. & Panksepp, J. pp. 299–437. New York: Marcel Dekker.

LEWIS, C.J., HAVLER, M.E., HUMPHREY, M.J., LLOYD-JONES, J.G., MCCLEAVY, M.A., MUIR, N.C. & WALTHAM, K. (1988). The pharmacokinetics and metabolism of idazoxan in the rat. *Xenobiotica*, **18**, 519–532.

LIMBERGER, N. & STARKE, K. (1983). Partial agonist effect of 2-[2-(1, 4-benzodioxanyl)]-2-imidazoline (RX 781094) at presynaptic α_2-adrenoreceptors in rabbit ear artery. *Naunyn-Schmiedebergs Arch. Pharmacol.*, **324**, 75–78.

MALLARD, N.J., TYACKE, R., HUDSON, A.L. & NUTT, D.J. (1991). Comparative binding studies of [^{3}H]-idazoxan and [^{3}H]-RX821002 in the rat brain. *Br. J. Pharmacol.*, **102**, 221P.

MARSDEN, C.A. & MARTIN, K.F. (1986). Involvement of 5-HT$_{1A}$- and α_2-receptors in the decreased 5-hydroxytryptamine release and metabolism in rat suprachiasmatic nucleus after intravenous 8-hydroxy-2-(n-dipropylamino) tetralin. *Br. J. Pharmacol.*, **89**, 277–286.

McCABE, J.T., DE BELLIS, M. & LEIBOWITZ, S.F. (1984). Clonidine-induced feeding: Analysis of central sites of action and fiber projections mediating this response. *Brain Res.*, **309**, 85–104.

MICHEL, M.C. & INSEL, P.A. (1989). Are there multiple imidazoline binding sites? *Trends Pharmacol. Sci.*, **10**, 342–344.

PETTINGER, W.A., KEETON, T.K., CAMPBELL, W.B. & HARPER, D.C. (1976). Evidence for a renal α-adrenergic receptor inhibiting renin release. *Circ. Res.*, **38**, 338–346.

RAMSAY, D.J. (1978). Beta-adrenergic thirst and its relation to the renin-angiotensin system. *Fed. Proc.*, **37**, 2689–2693.

SANGER, D.J. (1983). An analysis of the effects of systemically administered clonidine on the food and water intake of rats. *Br. J. Pharmacol.*, **78**, 159–164.

SLEIGHT, A.J., SMITH, R.J., MARSDEN, C.A. & PALFREYMAN, M.G. (1988). Is the hyperphagic response to 8-OH-DPAT a model for 5HT$_{1A}$ receptor responsiveness? *Br. J. Pharmacol.*, **95**, 875P.

TRICKLEBANK, M.D., FORLER, C. & FOZARD, J.R. (1984). The involvement of subtypes of the 5-HT$_1$ receptor and of catecholaminergic systems in the behavioural response to 8-hydroxy-2-(di-n-propylamino)tetralin in the rat. *Eur. J. Pharmacol.*, **106**, 271–282.

WALTER, D.S., FLOCKHART, I.R., HAYNES, M.J., HOWLETT, D.R., LANE, A.C., BURTON, R., JOHNSON, J. & DETTMAR, P.W. (1984). Effects of idazoxan on catecholamine systems in rat brain. *Biochem. Pharmacol.*, **33**, 2553–2557.

(Received February 18, 1991
Revised May 17, 1991
Accepted May 22, 1991)

Br. J. Pharmacol. (1991), **104**, 263–269

Effects of cromakalim on neurally-mediated responses of guinea-pig tracheal smooth muscle

[1]J.F. Burka, J.L. Berry, R.W. Foster, [2]R.C. Small & A.J.Watt

Smooth Muscle Research Group, Department of Physiological Sciences, University of Manchester, Manchester M13 9PT

1 The ability of cromakalim to modulate several different types of neuroeffector transmission has been assessed in guinea-pig isolated trachea.

2 In trachea treated with propranolol (10^{-6} M) and indomethacin (2.8×10^{-6} M), stimulation of the extrinsic vagal nerves evoked contractions which were blocked by hexamethonium (5×10^{-4} M) or by tetrodotoxin (TTX; 10^{-6} M). Cromakalim (10^{-5} M) caused a two fold rightward shift of the frequency-response curve.

3 In carinal trachea treated with propranolol and indomethacin, transmural stimulation evoked an initial, rapid contraction followed by a more sustained secondary contraction. The initial, rapid contractile response was virtually ablated by atropine (10^{-6} M) or by TTX but was resistant to hexamethonium. Cromakalim (10^{-8}–10^{-5} M) caused a concentration-dependent rightward shift of the frequency-response curve for the initial contraction.

4 In carinal trachea treated with atropine, propranolol and indomethacin, transmural stimulation evoked only the secondary (non-adrenergic, non-cholinergic (NANC)) contractile responses. These were markedly reduced by TTX but were resistant to hexamethonium. Cromakalim (10^{-8}–10^{-5} M) suppressed the NANC contractile responses in a concentration-dependent manner. This action could be offset by glibenclamide (10^{-6} M).

5 In trachea treated with atropine, histamine (10^{-4} M), propranolol and indomethacin, transmural stimulation evoked NANC relaxant responses. Cromakalim (up to 10^{-5} M) was without effect on the frequency-response curve for the stimulation of NANC inhibitory nerves.

6 Tested on trachea bathed by drug-free Krebs solution, cromakalim (10^{-7}–10^{-5} M) caused concentration-dependent suppression of tracheal tone. In trachea treated with propranolol and indomethacin, cromakalim (10^{-7}–10^{-5} M) caused concentration-dependent antagonism of acetylcholine (ACh). In trachea treated with atropine, propranolol and indomethacin, cromakalim (up to 10^{-5} M) failed to antagonize effects of either histamine or substance P.

7 It is concluded that cromakalim can inhibit cholinergic (excitatory) neuroeffector transmission in the trachea but only at a concentration having demonstrable inhibitory activity against the action of exogenous ACh and the spontaneous tone of the airways smooth muscle. In contrast, cromakalim may depress NANC excitatory (putative peptidergic) neuroeffector transmission at a concentration below that exerting inhibitory activity on airways smooth muscle. Cromakalim does not concurrently depress NANC inhibitory neuroeffector transmission. Depression of NANC excitatory neuroeffector transmission could explain the ability of cromakalim to suppress airway hyperreactivity or bronchial asthma at doses lacking direct relaxant effect on airways smooth muscle.

Keywords: Cromakalim; trachealis; extrinsic vagal nerves; NANC excitatory nerves; NANC inhibitory nerves; acetylcholine; histamine; substance P

Introduction

The effects of potassium channel openers in suppressing the tone of airway smooth muscle *in vitro* are well established (Allen *et al.*, 1986; Bray *et al.*, 1987; Arch *et al.*, 1988; Nielsen-Kudsk *et al.*, 1988; Paciorek *et al.*, 1990; Berry *et al.*, 1991; Raeburn & Brown, 1991). The effects of potassium channel openers on neurally-mediated responses in the airways have also attracted interest. For example, Hall & Maclagan (1988) observed that cromakalim reduced responses to preganglionic vagal stimulation of guinea-pig isolated trachea in a preparation where intraluminal pressure changes were monitored. Since cromakalim had a relatively greater effect on responses to vagal stimulation than on responses to exogenous acetylcholine, these authors concluded that cromakalim was inhibiting neurotransmitter release.

Subsequent work has suggested that cromakalim may act on the vagal pathway at a site proximal to the postganglionic nerve terminals. McCaig & De Jonckheere (1989), also using the technique of measuring intraluminal pressure of the guinea-pig isolated trachea, demonstrated that cromakalim reduced pressor responses to preganglionic vagal stimulation without reducing those to acetylcholine (ACh) or postganglionic (field) vagal stimulation. An inhibitory effect of cromakalim on cholinergic neuroeffector transmission has also been demonstrated *in vivo* (Ichinose & Barnes, 1990) but these authors, like Hall & Maclagan (1988), concluded that the drug had both pre- and postjunctional inhibitory activity.

Evidence is emerging that potassium channel openers can also depress the activity of excitatory peptidergic nerves supplying the lung. Potassium channel openers have been reported to inhibit contractions to NANC excitatory nerve stimulation of guinea-pig airways *in vivo* (Ichinose & Barnes, 1990) and bronchial smooth muscle *in vitro* (Good & Hamilton, 1991).

The present study was carried out to compare the effects of cromakalim on contractile and relaxant responses of both NANC and cholinergic neural origin in guinea-pig tracheal smooth muscle *in vitro*. In each case we have attempted to determine whether the effect of cromakalim is mediated at a prejunctional (neural) or postjunctional (airway smooth

[1] Present address: Department of Anatomy & Physiology, Atlantic Veterinary College, University of Prince Edward Island, Charlottetown, P.E.I., Canada C1A 4P3.

[2] Author for correspondence.

muscle) site. We have also sought to determine whether the effects of cromakalim on neuronal function are observed at concentrations similar to, or lower than, those causing direct relaxation of airway smooth muscle.

Methods

Tissue preparation

Guinea-pigs (300–500 g) of either sex were killed by stunning and bleeding. Tracheae were excised, cleaned of adhering fat and connective tissue and opened by cutting longitudinally through the cartilage rings diametrically opposite the trachealis. The opened trachea was cut into small segments each containing 4–5 cartilage rings. In experiments involving stimulation of the extrinsic vagus nerve, both the right and left vagus nerves next to the trachea were carefully ligated, cut, and removed with the respective recurrent laryngeal nerves attached to the trachea as described by Clark *et al.* (1981).

The tracheal segments were set up for the isometric recording of tension changes (Coburn & Tomita, 1973) in Krebs solution maintained at 37°C and gassed with 95% O_2: 5% CO_2. In most experiments the Krebs solution contained propranolol (10^{-6} M) and indomethacin (2.8×10^{-6} M). The tissues were subjected to an initial imposed tension of 1.5 g. Thereafter, a period of 60 min was allowed for the dissipation of spontaneous tone, a process facilitated by repeated changes of the bath fluid.

Experiments involving transmural stimulation

Transmural stimulation of tracheal segments was carried out by mounting the tissues between stainless steel electrodes (interelectrode distance 1 cm) connected to a stimulator (S-88, Grass Instruments, Quincy, MA, U.S.A.). A cumulative concentration-response curve was first constructed for ACh (10^{-7} M–10^{-2} M) with a contact time of 3 min for each applied concentration. All subsequent responses to drugs or electrical stimulation were related to the initial E_{max} for ACh identified in this curve. Following repeated washing of the tissue and its return to baseline tone, a frequency-response curve was constructed by use of single pulses (0.5 ms duration) of supramaximal strength (45 V) delivered in trains of 10 s duration every 3 min. Pulse frequency was increased in successive trains in two fold steps from 0.5 Hz to 64 Hz. These procedures were repeated in the absence (i.e. time-matched control) or presence of cromakalim (10^{-7}, 10^{-6} and 10^{-5} M) which was administered 8 min before the reapplication of ACh and transmural stimulation. In similarly-designed experiments, hexamethonium (5×10^{-4} M) or TTX (10^{-6} M) were administered 30 min before the reapplication of ACh or transmural stimulation.

In experiments where responses to NANC nerve stimulation were studied in isolation from cholinergic responses, the Krebs solution contained atropine (10^{-6} M), indomethacin (2.8×10^{-6} M), and propranolol (10^{-6} M). A cumulative concentration-response curve was first constructed for histamine (10^{-6}–10^{-3} M). Transmural stimulation was then performed with a pulse duration of 1 ms in order to achieve optimal activation of NANC neurones (Ellis & Undem, 1990). Frequency-response curves for the stimulation of NANC excitatory and NANC inhibitory nerves were constructed, the former against a background of baseline tone and the latter against a background of submaximal tone induced by histamine (10^{-4} M). Pulse frequency was increased in successive trains (10 s duration) in two fold steps from 0.5 Hz to 32 Hz for NANC excitatory responses and from 0.5 Hz to 64 Hz for NANC inhibitory responses. The time between successive pulse trains was determined by the time required for tissue tone to regain the pre-stimulation value. After initial control responses were established, tissues were washed to restore baseline tone. Cromakalim (0, 10^{-7}, 10^{-6}, or 10^{-5} M) was added for 8 min before reconstructing the concentration-effect curve for histamine and repeating the transmural stimulation.

The initial experiments with NANC excitatory nerve stimulation outlined above revealed that the frequency-response curve for NANC excitatory nerves was markedly depressed when attempts were made to reconstruct it in the same tissue. Accordingly, drug effects against NANC excitatory nerve stimulation were mainly studied by use of pulse trains of 10 s duration repeated at 20 min intervals. Pulse frequency was fixed at 4 Hz. This technique yielded NANC contractile responses that remained constant in amplitude for more than 1 h. Following the administration of several control pulse trains, hexamethonium (5×10^{-4} M), TTX (10^{-6} M) or cromakalim (10^{-8}–10^{-6} M) was added to the bath fluid. Cromakalim was added cumulatively, concentration increments occurring 8 min before each pulse train. Time-matched control tissues were treated identically but were not exposed to hexamethonium, TTX or cromakalim. Following stimulation in the presence of the highest concentration of cromakalim (10^{-6} M), glibenclamide (10^{-6} M) was added to the tissue bath for 30 min and the electrical stimulation was repeated.

In a separate series of experiments involving Krebs solution containing atropine (10^{-6} M), propranolol (10^{-6} M) and indomethacin (2.8×10^{-6} M), cumulative concentration-response curves for substance P (10^{-8}–3×10^{-6} M) and histamine (10^{-6}–10^{-3} M) were constructed before and after the application of cromakalim (0, 10^{-7}, 10^{-6} and 10^{-5} M).

Experiments involving stimulation of the extrinsic vagus nerve

A segment of trachea from the carinal or laryngeal end of the trachea was used with the left or right vagi and recurrent laryngeal nerves attached respectively. The vagus nerve was placed across a bipolar electrode for stimulation with single pulses (0.5 ms) at supramaximal strength (30 V) delivered in trains of 10 s duration every 3 min. The tissue was first exposed to ACh (10^{-3} M) to induce a reference contraction. All subsequent response sizes were measured as a percentage of this standard. Following repeated washing of the tissue and its return to baseline tone, a frequency-response curve was constructed by increasing pulse frequency in successive trains in two fold steps from 0.5 Hz to 64 Hz. Test tissues were then exposed to cromakalim (10^{-5} M) 8 min before reconstruction of the frequency-response curve. Control tissues were treated similarly but were not exposed to cromakalim. Tissues were discarded if the maximal contraction obtained with the initial nerve stimulation was smaller than 20% of that obtained with ACh.

Cromakalim and suppression of the spontaneous tone of the trachea

In these experiments small segments of trachea were set up in drug-free Krebs solution; 20 min later aminophylline (1 mM) was added to the bath fluid in order to determine the recorder pen position at zero tone. The tissue was then washed (bath fluid changes at time 0, 10 min and 20 min) and tone was allowed to recover (40 min). A cumulative concentration-effect curve for cromakalim (10^{-7}–10^{-5} M) was then constructed for which half $\log_{10}$ unit concentration increments were used with a tissue contact time of 8 min for each concentration tested.

Drugs and solutions

Drug concentrations are expressed in terms of the molar concentration of the active species. The following substances were obtained from Sigma: acetylcholine chloride, aminophylline, atropine sulphate, glibenclamide, hexamethonium bromide, histamine dihydrochloride, indomethacin, substance P and tetrodotoxin. Propranolol was obtained from ICI and cromakalim was a gift from SmithKline Beecham Research Laboratories. Stock solutions of most drugs were prepared in

twice-distilled water. Stock solutions of cromakalim and glibenclamide were prepared in 70% w/v ethanol and that of indomethacin in absolute ethanol. A stock solution of substance P was made up immediately before use in 0.1% acetic acid. The Krebs solution had the following composition (mM): Na^+ 143.5, K^+ 5.9, Ca^{2+} 2.6, Mg^{2+} 1.2, Cl^- 127.6, HCO_3^- 25, SO_4^{2-} 1.2, $H_2PO_4^-$ 1.2 and glucose 11.1.

Statistical analysis of results

All log concentration-effect and log stimulation frequency-response results were analysed with MEANCURV (Carpenter, 1986). Of the values obtained, the log EC_{20}, log EC_{50}, log EF_{20} and log EF_{50} values and E_{max} relative to initial control values were used for statistical comparison. Analysis of data from protocols employing response curves obtained in succession was carried out with repeated measures of analysis of variance comparing time and dose on a SPSS computer programme (MANOVA; Norusis, 1988). A paired Student's *t* test was used when data from paired tissues were compared. The null hypothesis was rejected when $P < 0.05$.

Results

Transmural stimulation of trachea

In Krebs solution containing propranolol (10^{-6} M) and indomethacin (2.8×10^{-6} M) the response of tracheal segments to transmural stimulation consisted of an initial, rapid, transient contraction that was often followed by a slower, longer-lasting contraction. As reported by Ellis & Undem (1990), the slow secondary contraction was always observed in tissue segments taken from the carinal end of the organ. In contrast, the secondary slow contraction was observed only in 75% (12/16) of tissue segments taken from the laryngeal end of the trachea.

Both phases of the tracheal response to transmural stimulation were frequency-dependent. When tracheal segments were subjected to repeated stimulation in order to assess the reproducibility of the frequency-response relationship, the frequency-response curve for the initial rapid contraction proved relatively constant in shape and position. However, the frequency-response curve for the secondary slow contraction was markedly depressed on stimulating the tracheal segments for a second time.

The log frequency-response curve for the initial rapid response to transmural stimulation was of relatively shallow slope for frequencies up to 8 Hz. Thereafter the slope of the curve became steeper (Figure 1). The log frequency-response curve for the initial rapid response to transmural stimulation was virtually ablated by atropine (10^{-6} M) or by tetrodotoxin (10^{-6} M). In contrast, it was unaffected by hexamethonium (5×10^{-4} M) (Figure 2). Cromakalim (10^{-8}–10^{-5} M) appeared to induce a concentration-dependent rightward shift of the frequency-response curve. However, only at a concentration of 10^{-5} M did cromakalim significantly increase the log EF_{20} and log EF_{50} values. Cromakalim did not affect the maximum contraction evoked by transmural stimulation (Figure 1).

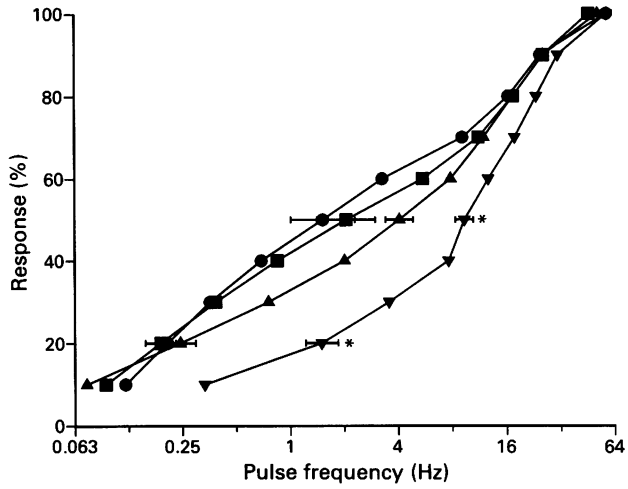

Figure 1 Effects of cromakalim on the initial, rapid contraction evoked by transmural stimulation of guinea-pig isolated trachea. Abscissa scale: pulse frequency (Hz) on a log scale. Ordinate scale: tension developed as a percentage of the response to acetylcholine (10^{-2} M). Pulses (45 V, 0.5 ms duration) were delivered in trains of 10 s duration every 3 min. Propranolol (10^{-6} M) and indomethacin (2.8×10^{-6} M) were present throughout. (●) = log frequency-response curve for time-matched control tissues; (■), (▲), (▼) = log frequency-response curves obtained in tissues treated with 10^{-7}, 10^{-6} and 10^{-5} M cromakalim, respectively. * Indicates a significant ($P < 0.05$) increase in log EF_{20} or log EF_{50} values. Data are means of values from at least 6 tissues; horizontal bars show s.e.mean.

Studies of the slow, secondary (NANC) contractile response of the trachea to transmural stimulation were carried out in Krebs solution containing atropine (10^{-6} M), propranolol

Table 1 Comparison of responses of laryngeal and carinal segments of guinea-pig trachea to transmural stimulation of NANC neurones or to stimulation of the extrinsic vagal (cholinergic) nerves

	NANC inhibitory neurones	*NANC excitatory neurones*	*Vagal cholinergic neurones*
log EF_{20}			
Laryngeal	0.35 ± 0.12 (5)	0.02 ± 0.10 (12)	0.49 ± 0.42 (7)
Carinal	0.34 ± 0.45 (5)	0.15 ± 0.10 (12)	−0.26 ± 0.52* (7)
log EF_{50}			
Laryngeal	0.75 ± 0.16 (5)	0.50 ± 0.10 (12)	0.97 ± 0.40 (7)
Carinal	0.96 ± 0.26 (5)	0.54 ± 0.10 (12)	0.66 ± 0.17* (7)
Maximum response			
	% suppression of response to histamine (10^{-4} M)	*% response to histamine* (10^{-3} M)	*% response to ACh* (10^{-2} M)
Laryngeal	50.0 ± 5.4 (5)	10.6 ± 2.0 (12)	50.6 ± 18.9 (7)
Carinal	24.2 ± 12.0* (5)	17.4 ± 2.9* (12)	48.0 ± 9.3 (7)

Data are means (±s.e.mean) of values from the tabulated (*n*) number of tissues. * Indicates a value significantly ($P < 0.05$) different from the corresponding value from laryngeal segments. Responses to vagal stimulation were recorded in the presence of propranolol (10^{-6} M) and indomethacin (2.8×10^{-6} M). NANC responses to transmural stimulation were recorded in the additional presence of atropine (10^{-6} M). Histamine (10^{-4} M) was also present in the case of NANC relaxant responses.

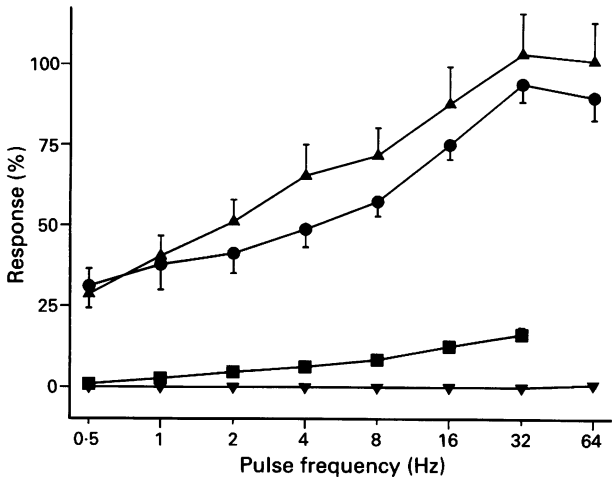

Figure 2 Effects of atropine, tetrodotoxin, and hexamethonium on the initial rapid contraction evoked by transmural stimulation of guinea-pig isolated trachea. Abscissa scale: pulse frequency (Hz) on a log scale. Ordinate scale: tension developed as a percentage of the response to acetylcholine (10^{-2} M). Pulses (45 V, 0.5 ms duration) were delivered in trains of 10 s duration every 3 min. Propranolol (10^{-6} M) and indomethacin (2.8×10^{-6} M) were present throughout. (●) = log frequency-response curve for time matched control tissues; (■), (▲), (▼) = log frequency-response curves obtained in tissues treated with atropine (10^{-6} M), hexamethonium (5×10^{-4} M), or tetrodotoxin (10^{-6} M), respectively. Data are means of values from at least 6 tissues; vertical bars show s.e.mean.

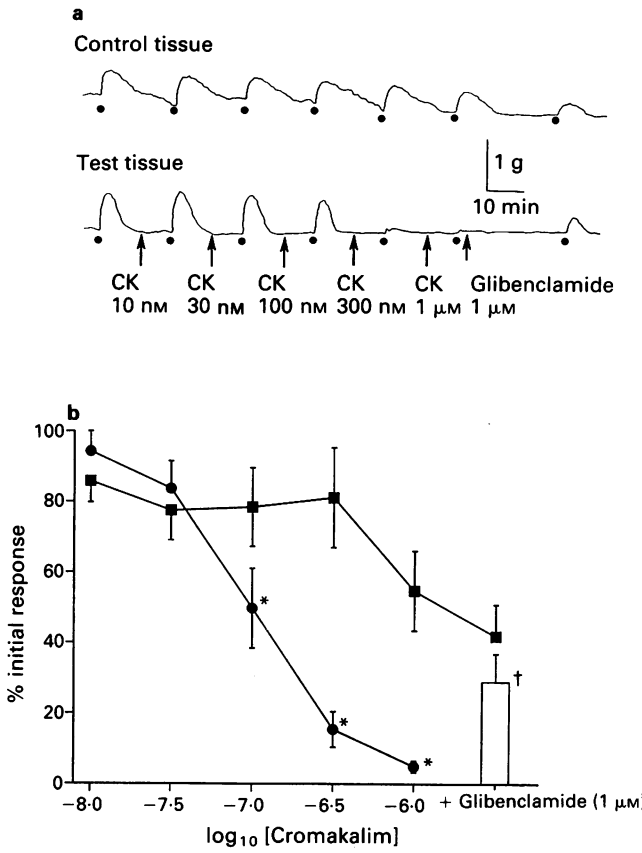

Figure 3 The effects of cromakalim (CK) on the NANC contractile response of carinal segments of guinea-pig isolated trachea to transmural stimulation. (a) Experimental tracings showing the inhibitory effect of cromakalim (10^{-8} M–10^{-6} M, cumulatively applied) on the NANC contractile response to transmural stimulation (●) (45 V pulses of 1 ms duration and 4 Hz frequency delivered in trains of 10 s duration every 20 min). The upper trace represents a time-matched control tissue, the lower the test tissue. Atropine (10^{-6} M), propranolol (10^{-6} M) and indomethacin (2.8×10^{-6} M) were present throughout. Note how glibenclamide (10^{-6} M) applied to the test tissue, was able to offset the inhibitory effect of cromakalim. (b) Log concentration-effect curve for the inhibitory effect of cromakalim against NANC contractile responses evoked by transmural stimulation of carinal segments of guinea-pig trachea (45 V pulses of 1 ms duration and 4 Hz frequency delivered in trains of 10 s duration every 20 min). Atropine (10^{-6} M), propranolol (10^{-6} M), and indomethacin (2.8×10^{-6} M) were present throughout. (■) = response of time-matched control tissues; (●) = response of test tissues. * Indicates a significant ($P < 0.05$) difference between values for the test and time-matched control tissues; † indicates a significant ($P < 0.05$) difference between values of the test tissues in the presence of cromakalim (10^{-6} M) in the presence and absence of glibenclamide (10^{-6} M). Data are means of values from at least 6 tissues; vertical bars show s.e.mean.

(10^{-6} M) and indomethacin (2.8×10^{-6} M). Initially NANC contractile responses of carinal and laryngeal segments of trachea were compared by constructing frequency-response curves. The log EF_{50} values for NANC contractile responses were similar in carinal and laryngeal trachea. However, the maximal NANC contractile response to transmural stimulation was greater in carinal than in laryngeal segments (Table 1).

All further studies of NANC contractile responses were carried out on carinal segments of trachea only. When this tissue was stimulated repetitively at a pulse frequency of 4 Hz, the NANC contractile responses remained relatively constant in amplitude for up to 80 min. Thereafter the responses progressively declined in amplitude (Figure 3a,b). The NANC contractile responses to transmural stimulation were unaffected by hexamethonium (5×10^{-4} M) but were virtually abolished by tetrodotoxin (10^{-6} M) (Figure 4). Cromakalim (10^{-8}–10^{-6} M) applied cumulatively caused concentration-dependent depression of the NANC contractile response to transmural stimulation (log $IC_{50} - 7.06 \pm 0.11$; mean ± s.e.mean, $n = 10$) (Figure 3a,b). Cromakalim (10^{-6} M) inhibited the NANC contractile response by more than 90%. Once the summit of the concentration-effect curve for cromakalim had been reached, the administration of glibenclamide (10^{-6} M; 30 min preincubation) caused the inhibitory action of cromakalim to be offset (Figure 3b).

Studies of NANC relaxant responses to transmural stimulation were carried out in Krebs solution containing atropine (10^{-6} M), histamine (10^{-4} M), propranolol (10^{-6} M) and indomethacin (2.8×10^{-6} M). Comparison of tissue from the laryngeal and carinal ends of the trachea showed that while log EF_{50} values were similar, the maximal relaxant response obtained in carinal tissue was smaller than that obtained in laryngeal tissue (Table 1). NANC relaxant responses to transmural stimulation were unaffected by cromakalim (up to 10^{-5} M) (data not shown).

Effects of cromakalim on vagal stimulation

For anatomical reasons, stimulation of the left vagus nerve required use of a carinal segment of trachea and stimulation of the right vagus nerve required a laryngeal tracheal segment. The log EF_{20} and log EF_{50} values for stimulation of carinal tissue via the left vagus nerve were significantly smaller than the equivalent values for the right vagus nerve and laryngeal segment of trachea. However, the maximum contraction obtainable by nerve stimulation did not differ with location (Table 1). The effects of stimulating the left or right extrinsic vagal nerves were blocked both by hexamethonium (5×10^{-4} M) and by TTX (10^{-6} M). Cromakalim (10^{-5} M) induced a rightward shift of the frequency-response curve for stimulation of the extrinsic vagal nerves, causing a two fold increase in the EF_{50} (Figure 5). When the maximal response to vagal stimulation was measured as a percentage of the contraction evoked by ACh (10^{-3} M), it became evident that cromakalim had additional inhibitory effect. Cromakalim (10^{-5} M) reduced the maximal response from 52.7 ± 5.8% to 37.4 ± 4.7% of the ACh standard (mean ± s.e.mean, $n = 6$ and 9 respectively; $P < 0.05$).

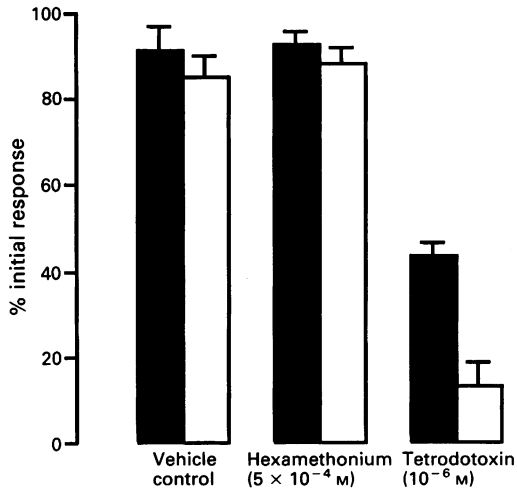

Figure 4 Effects of tetrodotoxin and hexamethonium on the NANC contractile response to transmural stimulation (1 ms pulses of 4 Hz frequency and 45 V strength delivered in trains of 10 s duration every 20 min) of carinal segments of guinea-pig isolated trachea. Atropine (10^{-6} M), propranolol (10^{-6} M) and indomethacin (2.8×10^{-6} M) were present throughout. In each case the solid and open columns represent response height (as a percentage of the initial control) 20 min (solid columns) and 40 min (open columns) after the administration of vehicle, hexamethonium (5×10^{-4} M) or tetrodotoxin (10^{-6} M).

Effects of cromakalim on the spontaneous tone of the trachea and on the actions of exogenous spasmogens

In trachea bathed by normal Krebs solution, cromakalim (10^{-7}–10^{-5} M) produced concentration-dependent suppression of the spontaneous tone of the tissue. The mean (±s.e.mean; $n = 18$) log EC_{50} for the tone suppressant action of cromakalim was -6.35 ± 0.05, a figure significantly ($P < 0.05$; two-tailed unpaired t test) smaller than the corresponding mean log IC_{50} for suppression of contractile responses to transmural stimulation of NANC neurones (see above). The maximal relaxant effect of cromakalim was 73.2 ± 2.5% of that of aminophylline.

Tested in tracheal segments treated with propranolol (10^{-6} M) and indomethacin (2.8×10^{-6} M), cromakalim induced a rightward shift of the ACh concentration-response curve. The EC_{20} and EC_{50} values for ACh were significantly increased (1.8 and 2.5 fold respectively) by cromakalim (10^{-5} M). The maximal contraction induced by ACh was unaffected (Figure 6a).

Tested in trachea treated with atropine (10^{-6} M), propranolol (10^{-6} M) and indomethacin (2.8×10^{-6} M), cromakalim (up to 10^{-5} M) had no effect on contractions induced by histamine

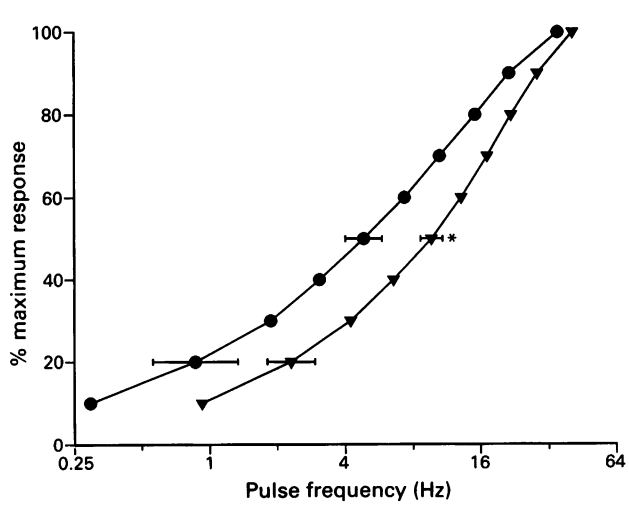

Figure 5 The effects of cromakalim on the contractile response of guinea-pig isolated trachealis to stimulation of its extrinsic vagal nerve supply. Abscissa scale: pulse frequency on a log scale. Ordinate scale: tension developed as a percentage of maximum. (●) = log frequency-response curve obtained in time-matched control tissues; (▼) = log frequency-response curve obtained in test tissues treated with cromakalim (10^{-5} M); 30 V pulses of 0.5 ms duration were delivered in trains of 10 s duration every 3 min. Propranolol (10^{-6} M) and indomethacin (2.8×10^{-6} M) were present throughout. Data are means of values from 9 tissues (carinal trachea with left vagus nerve attached and laryngeal trachea with right vagus nerve attached); horizontal bars show s.e.mean. * Indicates a significant difference between the log EF_{50} values of test and control tissues.

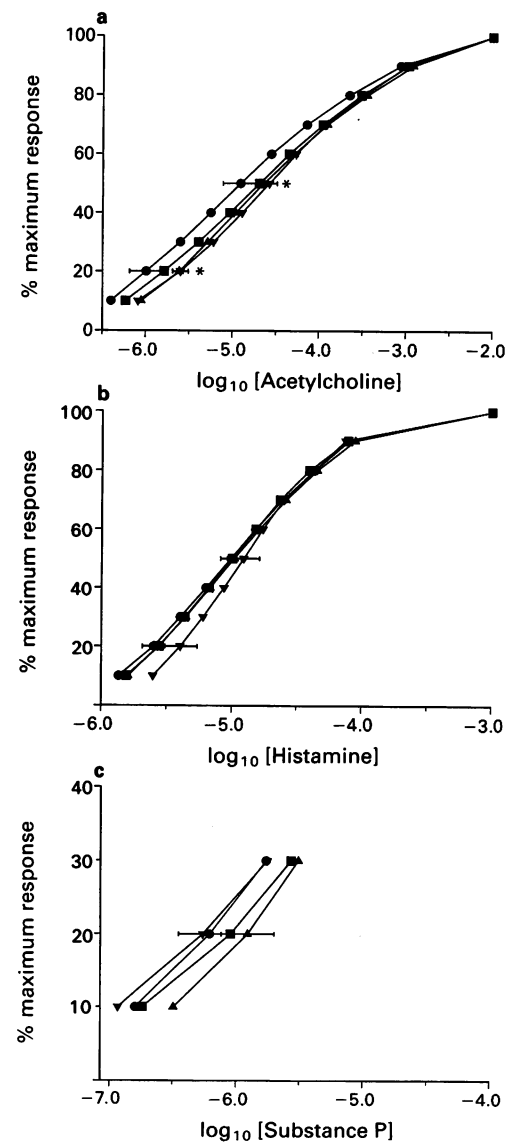

Figure 6 Effects of cromakalim on the contraction of guinea-pig isolated trachealis muscle to (a) acetylcholine, (b) histamine, and (c) substance P. In each panel the abscissa scale indicates the concentration of spasmogen on a log scale. The ordinates represent the tension developed as a % of the E_{max} obtained with acetylcholine (10^{-2} M; a) or histamine (10^{-3} M; b and c). (●) = log concentration-effect curve for the spasmogen as observed in time-matched control tissues; (■), (▲), (▼) = log concentration-effect curves for the spasmogen observed in test tissues treated with 10^{-7} M, 10^{-6} M, and 10^{-5} M cromakalim, respectively. Propranolol (10^{-6} M) and indomethacin (2.8×10^{-6} M) were present throughout the experiments. Atropine (10^{-6} M) was present in the experiments involving histamine and substance P (b and c). Data represent means of values from at least 6 tissues.

or substance P (Figure 6b and c). None of the exogenous spasmogens was affected by hexamethonium (5×10^{-4} M) or TTX (10^{-6} M).

Discussion

Cromakalim and cholinergic neuroeffector transmission in guinea-pig trachea

Stimulation of the extrinsic vagal nerves supplying guinea-pig isolated trachea evokes contractile responses that are suppressed by atropine (Clark *et al.*, 1981), hexamethonium (Clark *et al.*, 1981; present study) or by tetrodotoxin (present study). Such responses are therefore mediated by the preganglionic stimulation of vagal cholinergic neural pathways innervating the trachealis. When carinal segments of guinea-pig trachea are subjected to transmural stimulation in the presence of propranolol and indomethacin, the contractile response is diphasic (Ellis & Undem, 1990; present study). The initial, rapid contractile response is suppressed by atropine and tetrodotoxin (Ellis & Undem, 1990; present study) but is resistant to hexamethonium (present study). The initial contractile response of carinal trachea to transmural stimulation is therefore mediated by the postganglionic activation of vagal cholinergic pathways supplying the trachealis muscle.

That cromakalim inhibits excitatory, cholinergic neuroeffector transmission in guinea-pig trachea is suggested by its ability (at a concentration of 10^{-5} M) to cause rightward shifts in the frequency-response curves to both pre- and postganglionic vagal nerve stimulation (Figure 1). Our finding that cromakalim can inhibit responses to stimulation of preganglionic cholinergic nerves confirms earlier studies (Hall & Maclagan, 1988; McCaig & De Jonckheere, 1989). However, our finding that cromakalim inhibits responses to the postganglionic stimulation of cholinergic pathways contrasts with the observations of McCaig & De Jonckheere (1989). Since inhibitory effects of cromakalim on postganglionic nerve stimulation were observed at a concentration (10^{-5} M) causing marked suppression of the spontaneous tone of the trachea and some antagonism of exogenous acetylcholine (Figure 6a) we must assume that the ability of cromakalim to depress cholinergic neuroeffector transmission includes a postjunctional (on trachealis cells) site of action. In this respect our findings lend support to the *in vivo* observations of Ichinose & Barnes (1990). Assay of neurotransmitter release is clearly required to determine whether a prejunctional action of cromakalim is of any importance in depressing cholinergic neuroeffector transmission in the airways.

Cromakalim and NANC inhibitory neuroeffector transmission in guinea-pig trachea

When guinea-pig trachea is treated with antagonists at muscarinic cholinoceptors and sympatholytic drugs, transmural stimulation elicits relaxant responses attributable to the activation of intramural NANC inhibitory neurones (Coburn & Tomita, 1973; Boyle *et al.*, 1987). The transmitter used by such neurones remains the subject of debate but there is evidence to suggest that it may be vasoactive intestinal polypeptide and/or nitric oxide (Ellis & Farmer, 1989a,b; Li & Rand, 1991). In human airways, NANC inhibitory neurones comprise the principal neural bronchodilator pathway (Richardson & Beland, 1976). The present finding that cromakalim does not attenuate NANC inhibitory neuroeffector transmission in the airways is therefore a good feature of its pharmacological profile bearing in mind its potential use in the chemotherapy of bronchial asthma.

Cromakalim and NANC excitatory neuroeffector transmission in guinea-pig trachea

When guinea-pig trachea is subjected to transmural stimulation in the presence of sympatholytic drugs and an antagonist at muscarinic cholinoceptors, contractile responses are obtained which are attributable to the activation of intramural nerves the transmitter for which may be substance P (Szolcsanyi & Bartho, 1982; Andersson & Grundstrom, 1983; Grundemar *et al.*, 1990; Ellis & Undem, 1990). In the present study such responses were tetrodotoxin-sensitive but hexamethonium-resistant (Figure 4) indicating that the responses were of neural origin but that transmission across cholinergic ganglionic synapses was not involved.

Our demonstration that cromakalim can depress NANC excitatory neuroeffector transmission in guinea-pig trachea is consistent with findings in guinea-pig isolated bronchus (Good & Hamilton, 1991). The IC_{50} for cromakalim-induced suppression of NANC excitatory neuroeffector transmission was significantly smaller than that for cromakalim-induced suppression of spontaneous tone. Furthermore, cromakalim failed to antagonize the contractile effects of exogenous substance P (Figure 6c). These observations suggest that the action of cromakalim in suppressing NANC excitatory neuroeffector transmission may involve inhibition of neurotransmitter release. A similar conclusion has been drawn from the results of *in vivo* studies (Ichinose & Barnes, 1990).

Intramural peptidergic nerves may have pro-inflammatory roles in the airways (Barnes, 1991). Accordingly it may be that cromakalim has important actions on pulmonary peptidergic neurones which may reduce the phenomenon of airway hyperreactivity and relieve the symptoms of bronchial asthma. This idea receives support from the observations that doses of cromakalim too low to cause direct relaxation of airways smooth muscle can suppress airway hyperreactivity in laboratory animals (Chapman *et al.*, 1991) and improve the early morning dip in lung function in patients with nocturnal asthma (Williams *et al.*, 1990).

J.F.B.'s period of study leave in Manchester was supported by the Medical Research Council of Canada and the Wellcome Trust. R.W.F. and R.C.S. were supported by the National Asthma Campaign and Sandoz Pharma Ltd.

References

ALLEN, S.L., BOYLE, J.P., CORTIJO, J., FOSTER, R.W., MORGAN, G.P. & SMALL, R.C. (1986). Electrical and mechanical effects of BRL 34915 in guinea-pig isolated trachealis. *Br. J. Pharmacol.*, **89**, 395–405.

ANDERSSON, R.G.G. & GRUNDSTROM, N. (1983). The excitatory non-cholinergic non-adrenergic nervous system of the guinea-pig airways. *Eur. J. Resp. Dis.*, **64** (Suppl. 131), 141–155.

ARCH, J.R.S., BUCKLE, D.R., BUMSTEAD, J., CLARKE, G.D., TAYLOR, J.F. & TAYLOR, S.G. (1988). Evaluation of the potassium channel activator cromakalim (BRL 34915) as a bronchodilator in the guinea-pig: comparison with nifedipine. *Br. J. Pharmacol.*, **95**, 763–770.

BARNES, P.J. (1991). Neural mechanisms in asthma. In *Handbook of Experimental Pharmacology: Pharmacology of Asthma.* ed. Barnes, P.J. & Page, C.P. pp. 143–166. Berlin: Springer-Verlag.

BERRY, J.L., ELLIOTT, K.R.F., FOSTER, R.W., GREEN, K.A., MURRAY, M.A. & SMALL, R.C. (1991). Mechanical, biochemical and electrophysiological studies of RP 49356 and cromakalim in guinea-pig and bovine trachealis muscle. *Pulm. Pharmacol.*, **4**, 91–98.

BOYLE, J.P., DAVIES, J.M., FOSTER, R.W., MORGAN, G.P., & SMALL, R.C. (1987). Inhibitory responses to nicotine and transmural stimulation in hyoscine-treated guinea-pig isolated trachealis: an electrical and mechanical study. *Br. J. Pharmacol.*, **90**, 733–744.

BRAY, K.M., NEWGREEN, D.T., SMALL, R.C., SOUTHERTON, J.S., TAYLOR, S.G., WEIR, S.W. & WESTON, A.H. (1987). Evidence that the mechanism of action of pinacidil in rat and guinea-pig smooth muscle differs from that of glyceryl trinitrate. *Br. J. Pharmacol.*, **91**, 421–429.

CARPENTER, J.R. (1986). A method for presenting and comparing dose-response curves. *J. Pharmacol. Meth.*, **15**, 283–286.

CHAPMAN, I.D., KRISTERSSON, L., MAZZONI, L., AMSLER, B. & MORLEY, J. (1991). Reversal of induced airway hyper-reactivity by potassium channel openers: PCO 400 and cromakalim. *Br. J. Pharmacol.*, **102,** 335P.

CLARK, L.A., SMALL, R.C. & TURNBULL, M.J. (1981). Do the recurrent laryngeal nerves provide an extrinsic input to non-adrenergic inhibitory neurones in guinea-pig trachealis muscle? *Br. J. Pharmacol.*, **72,** 554–555P.

COBURN, R.F. & TOMITA, T. (1973). Evidence for non-adrenergic inhibitory nerves in the guinea pig trachealis muscle. *Am. J. Physiol.*, **224,** 1072–1080.

ELLIS, J.L. & FARMER, S.G. (1989a). The effects of vasoactive intestinal polypeptide (VIP) antagonists and VIP and peptide histidine isoleucine antisera on non-adrenergic, non-cholinergic relaxations of tracheal smooth muscle. *Br. J. Pharmacol.*, **96,** 513–520.

ELLIS, J.L. & FARMER, S.G. (1989b). Effects of peptidases on non-adrenergic, non-cholinergic inhibitory responses of tracheal smooth muscle: a comparison with effects of VIP- and PHI-induced relaxation. *Br. J. Pharmacol.*, **96,** 521–526.

ELLIS, J.L. & UNDEM, B.J. (1990). Non-adrenergic, non-cholinergic contractions in the electrically field stimulated guinea-pig trachea. *Br. J. Pharmacol.*, **101,** 875–880.

GOOD, D.M. & HAMILTON, T.C. (1991). Effects of BRL 38227 on neurally-mediated responses in guinea-pig isolated bronchus. *Br. J. Pharmacol.*, **102,** 336P.

GRUNDEMAR, L., GRUNDSTROM, N., JOHANSSON, I.G.M., ANDERSSON, R.G.G. & HAKANSON, R. (1990). Suppression by neuropeptide Y of capsaicin-sensitive sensory nerve mediated contraction in guinea-pig airways. *Br. J. Pharmacol.*, **99,** 473–476.

HALL, A.K. & MACLAGAN, J. (1988). Effect of cromakalim on cholinergic neurotransmission in the guinea-pig trachea. *Br. J. Pharmacol.*, **95,** 792P.

ICHINOSE, M. & BARNES, P.J. (1990). A potassium channel activator modulates both excitatory non-cholinergic and cholinergic neurotransmission in guinea pig airways. *J. Pharmacol. Exp. Ther.*, **252,** 1207–1212.

LI, C.G. & RAND, M.J. (1991). Evidence that part of the NANC relaxant response of guinea-pig trachea to electrical field stimulation is mediated by nitric oxide. *Br. J. Pharmacol.*, **102,** 91–94.

McCAIG, D.J. & DE JONCKHEERE, B. (1989). Effect of cromakalim on bronchoconstriction evoked by cholinergic nerve stimulation in guinea-pig isolated trachea. *Br. J. Pharmacol.*, **98,** 662–668.

NIELSEN-KUDSK, J.E., MELLEMKJAER, S., SIGGAARD, C. & NIELSEN, C.B. (1988). Effects of pinacidil on guinea-pig airway smooth muscle contracted by asthma mediators. *Eur. J. Pharmacol.*, **157,** 221–226.

NORUSIS, M.D. (1988). *SPSS/PC + Advanced Statistics V2.0.* Chicago: SPSS Inc.

PACIOREK, P. M., COWLRICK, I.S., PERKINS, R.S., TAYLOR, J.C., WILKINSON, G.F. & WATERFALL, J.F. (1990). Evaluation of the bronchodilator properties of Ro 31-6930, a novel potassium channel opener, in the guinea-pig. *Br. J. Pharmacol.*, **100,** 289–294.

RAEBURN, D.M. & BROWN, T.J. (1991). RP 49356 and cromakalim relax airway smooth muscle in vitro by opening a sulphonylurea-sensitive K^+-channel: a comparison with nifedipine. *J. Pharmacol. Exp. Ther.*, **256,** 480–485.

RICHARDSON, J. & BELAND, J. (1976). Non-adrenergic inhibitory nervous system in human airways. *J. Appl. Physiol.*, **41,** 764–771.

SZOLCSANYI, J. & BARTHO, L. (1982). Capsaicin-sensitive, non-cholinergic, non-adrenergic nervous system of the guinea-pig tracheobronchial smooth muscle. *Neurosc Lett.*, **34,** 247–251.

WILLIAMS, A.J., LEE, T.H., COCHRANE, G.M., HOPKIRK, A., VYSE, T., CHIEW, F., LAVENDER, E., RICHARDS, D.H., OWEN, S., STONE, P., CHURCH, S. & WOODCOCK, A.A. (1990). Attenuation of nocturnal asthma by cromakalim. *Lancet*, **ii,** 334–336.

(Received April 18, 1991
Accepted May 23, 1991)

Br. J. Pharmacol. (1991), **104**, 270–276

Sedation and histamine H_1-receptor antagonism: studies in man with the enantiomers of chlorpheniramine and dimethindene

[1]A.N. Nicholson, Peta A. Pascoe, Claire Turner, *C.R. Ganellin, **P.M. Greengrass, †A.F. Casy & †[2]Amanda D. Mercer

Royal Air Force Institute of Aviation Medicine, Farnborough, Hampshire GU14 6SZ; *Department of Chemistry, University College London, 20 Gordon Street, London WC1H 0AJ; **Pfizer Central Research, Sandwich, Kent CT13 9NJ and †School of Pharmacy and Pharmacology, University of Bath, Claverton Down, Bath BA2 7AY

1 The effects of 10 mg (+)- and (−)-chlorpheniramine and 5 mg (+)- and (−)-dimethindene on daytime sleep latencies, digit symbol substitution and subjective assessments of mood and well-being were studied in 6 healthy young adult humans. Each subject also took 5 mg triprolidine hydrochloride as an active control and two placebos.

2 Daytime sleep latencies were reduced with triprolidine, (+)-chlorpheniramine and (−)-dimethindene, and subjects also reported that they felt more sleepy after (+)-chlorpheniramine and (−)-dimethindene. Performance on digit symbol substitution was impaired with (+)-chlorpheniramine.

3 Changes in measures with (−)-chlorpheniramine and (+)-dimethindene were not different from changes with placebo.

4 In the present study, changes in measures of drowsiness and performance were limited to the enantiomers with high affinity for the histamine H_1-receptor. These findings strongly suggest that sedation can arise from H_1-receptor antagonism alone, and provide further support for the belief that the histaminergic system is concerned with the regulation of alertness in man.

Keywords: Antihistamines; H_1-receptor antagonists; chlorpheniramine; dimethindene; stereoselective effects; sedation in man

Introduction

It is well recognized that many antihistamines lead to drowsiness and impaired performance (Nicholson, 1983; 1987) and, although not demonstrated conclusively, it is believed that such effects are due to antagonism of central histamine H_1-receptors (Quach *et al.*, 1979; Schwartz *et al.*, 1982; Nicholson *et al.*, 1985). Studies in healthy man have shown, however, that the peripheral antihistaminic and central sedative effects of such drugs may be poorly correlated and the question arises whether central depressant effects are related to other pharmacological activity (Peck *et al.*, 1975; Levander *et al.*, 1985). Many antihistamines are not specific H_1-receptor antagonists, and modulation of the activity of neurotransmitters other than histamine could be involved in the sedative effects of a particular drug.

It is in this context that we have carried out the present study in man on the central effects of the enantiomers of two well-established antihistamines, chlorpheniramine and dimethindene, as drowsiness and sedation are reported commonly with each of these drugs. However, the affinities of the isomers for the H_1-receptor indicate a high degree of stereoselectivity (Chang *et al.*, 1979; Borchard *et al.*, 1985), and so studies with the enantiomers may help to resolve whether sedation is related specifically to the steric configuration and is due to H_1-receptor antagonism alone.

Methods

Six healthy volunteers (four females and two males) who were not taking any other medication gave informed consent to participate in the study. The protocol was approved by the RAF Institute of Aviation Medicine Ethics Committee. The subjects were aged between 19 and 28 (mean 23.7) years, and weighed between 50.0 and 95.5 (mean 70.2) kg. They abstained from alcohol and beverages containing caffeine from 18 h 00 min on the evening preceding and on the day of an experiment, and retired at their usual bedtime on the night before an experiment. Subjects ate a light breakfast before arriving at the laboratory. Test sessions commenced at 08 h 30 min, 10 h 00 min, 11 h 00 min and 12 h 30 min, with drug ingestion between the first and second sessions at 09 h 30 min. Each subject took, on separate occasions, 10 mg (+)- and (−)-chlorpheniramine maleate, 5 mg (+)- and (−)-dimethindene maleate, 5 mg triprolidine hydrochloride as an active control, and two placebos. All medication was identical in appearance and the study was double blind. Treatments were arranged in a pseudo-random order balanced for linear sequence, with a placebo among the first and last three drug ingestions, and at least four days separated each assessment.

Each test session was identical. Performance was measured by digit symbol substitution (Nicholson & Stone, 1986), and subjects were trained in this task to achieve a consistent level of performance before the study began. Mood, well-being and alertness were assessed subjectively by use of a series of 12 visual analogue scales (Nicholson & Stone, 1986) and the Stanford Sleepiness Scale (SSS) (Hoddes *et al.*, 1973). After these assessments, sleep latency was measured. Two channels of electroencephalographic (EEG) activity (C_4-A_1 and O_1-A_2) and bilateral electro-oculographic (EOG) activity were recorded with silver-silver chloride electrodes on a Nihon Kohden 4300 Series EEG machine. The paper speed was 10 mm s^{-1} and 70% amplitude frequency response was 0.16 to 35 Hz for the EEG and 1.6 to 15 Hz for the EOG. Subjects lay in bed in individual rooms which were light-proofed, sound-attenuated and temperature-controlled (18 ± 3°C). They were instructed to lie in bed quietly and to try to fall asleep. Each test was ended after the onset of stage 1 (drowsy) sleep or after 20 min if the sleep onset criterion was not met. The latency to stage 1 sleep was determined independently by two analysts, and differences were resolved.

Materials

Racemic chlorpheniramine maleate (Smith, Kline & French) and racemic dimethindene maleate (Zyma) were converted into the free base forms. Samples of (+)- and (−)-chlorpheniramine maleate ($[\alpha]^{24}_D$ + 23.2° and −23.9°, *circa* 1% in

[1] Author for correspondence.
[2] Present address: SmithKline Beecham Pharmaceuticals, Welwyn Garden City, Hertfordshire AL7 1EY.

water, respectively) and (+)- and (−)-dimethindene maleate ($[\alpha]^{24}_D$ + 197.8° and −206.6°, *circa* 1% in methanol, respectively) were obtained by resolution of racemic chlorpheniramine base with D- and L-ditoluoyltartaric acids, and racemic dimethindene base with D- and L-tartaric acids. In each case fractional crystallization was continued until specific rotations of diastereoisomeric salts showed relatively little change on further crystallization.

The products were checked for purity. C, H and N analyses were within 0.4% of the required values, and high performance liquid chromatography (h.p.l.c.) examination (on a Cyclobond I column) gave purities >99%. M.p.'s were 113–115°C and 112–114°C respectively for (+)- and (−)-chlorpheniramine maleate, and 127–129°C for each enantiomer of dimethindene maleate. Additional evidence of optical purity was obtained by chiral h.p.l.c. or ^{1}H n.m.r. methods (Mercer, 1989). The pure enantiomeric drug was triturated with lactose, and capsules were filled with 150 mg of the triturate (or pure lactose for the placebo) to provide doses of 10 mg chlorpheniramine maleate and 5 mg dimethindene maleate. Capsules, each containing two 2.5 mg tablets of triprolidine hydrochloride (Wellcome), were used as the active control.

Measurement of pharmacological activity in vitro

H_1-receptor antagonism was assayed *in vitro* against histamine-induced contraction of guinea-pig ileum. Guinea-pigs of either sex weighing between 400–700 g were used. Immediately after an animal was killed, the terminal ileum was removed, washed and mounted in a 15 ml bath containing magnesium-free Tyrode solution gassed with 95% O_2/5% CO_2 and maintained at 30°C. The tissue was loaded with 0.5 g and contractions in response to histamine were detected by a force transducer and displayed on a potentiometric recorder. Cumulative histamine dose-response curves were obtained prior to and following 8 min incubations with three different concentrations of the antagonist (7–10 observations), and pA_2 values were determined by Schild analysis. The slopes of the Schild plots are indicated in Table 3, and were not significantly different from unity within 95% limits.

The affinities of the enantiomers of chlorpheniramine maleate and dimethindene maleate and of triprolidine hydrochloride for types of central receptor were also determined. Binding assays for radiolabelled prazosin (α_1-adrenoceptors), UK-14304 (5-bromo-6-[2-imidazolin-2-ylamino]-quinoxaline bitartrate) (α_2-adrenoceptors), dihydroalprenolol (β-adrenoceptors), 5-hydroxytryptamine (5-HT) (5-HT_1-receptors), ketanserin (5-HT_2-receptors), 3-quinuclidinyl benzilate (QNB) (muscarinic receptors) and flunitrazepam (benzodiazepine receptors) were conducted on bovine frontal cortex, and for radiolabelled spiperone (dopamine D_2-receptors) on bovine striatum. Assays were also carried out with standard agents. Details of the methods are given in Table 1. Apparent K_i values were calculated from IC_{50} values by the Cheng-Prusoff equation (Cheng & Prusoff, 1973).

Measurement of pharmacological activity in vivo

H_1-receptor antagonism of the enantiomers of dimethindene was assessed *in vivo* against histamine-induced bronchoconstriction in the anaesthetized guinea-pig (Brown *et al.*, 1986). Increasing doses of antagonist were given intravenously and dose-ratios for the displacement of histamine dose-response curves were obtained. The dose of antagonist giving a (dose-ratio − 1) = 10 was determined from a Schild plot.

Statistical analysis of performance, subjective assessment and sleep latency data

Visual analogue scales of mood and well-being were assigned ranks for each subject separately and the principal components of the correlation matrix of the ranks for 12 measures were calculated. Two components were derived and, after varimax rotation, these were identified as measures of sleepiness and feelings associated with mood. Digit symbol substitution scores, SSS ratings and the components derived from the visual analogue scales were investigated by analysis of variance. Sleep latencies were censored at 20 min and so an iterative extension to a standard analysis of variance procedure was used to investigate this measure. Digit symbol substitution scores were screened for possible effects of sequence by analysis of covariance on dummy variables (John & Quenouille, 1977) and if an order effect was found it was used to correct the data.

The assumptions of analysis of variance, homogeneity of variance, normality and additivity, were studied by considering transformations of the raw measures using the maximum likelihood method of Box & Cox (1964). The residuals from an analysis of variance, applied to the data by use of the selected transformation, were then examined after the method of Anscombe (1961) and, if appropriate, this transformation was applied. All of the transformations were logarithmic and so random variation and treatment effects were proportional rather than additive. Back-transformed means are presented for the subjective assessment and sleep latency data.

After analysis of variance, the effects of the drugs on differences between measures before ingestion (08 h 30 min) and those after ingestion (10 h 00 min, 11 h 00 min and 12 h 30 min) were investigated. Two planned comparisons, using the mean differences for six subjects, were made between the two placebos and between the active control (triprolidine 5 mg) and the mean of the two placebos. Each of the remaining drugs was compared with the mean of the two placebos and each enantiomer was compared with its respective isomer by the multiple comparison method of Dunnett (1964). The test of

Table 1 Details of ligand binding assays

Receptor *Bovine frontal cortex:*	*Radioligand*	(nM)	*Non-specific binding defined by* (μM)		*Buffer*	*Incubation time* (min)	*Temp* (°C)
α_1	[^{3}H]-prazosin	0.2	Phentolamine	10.0	50 mM Tris (pH 7.6)	30	25
α_2	[^{3}H]-UK-14304	0.5	Phentolamine	10.0	50 mM Tris (pH 7.6)	30	25
β	[^{3}H]-dihydroalprenolol	2.0	Propranolol	1.0	50 mM Tris (pH 7.6) + 10 mM Mg^{2+}	30	25
5-HT_1	[^{3}H]-5-HT	2.0	5-HT	10.0	50 mM Tris (pH 7.4) + 4 mM Ca^{2+}	30	25
5-HT_2	[^{3}H]-ketanserin	1.0	Spiperone	1.0	50 mM Tris (pH 7.6)	30	25
Muscarinic	[^{3}H]-QNB	0.1	Atropine	1.0	Krebs-50 mM Tris (pH 7.6)	60	25
Benzodiazepine	[^{3}H]-flunitrazepam	0.5	Diazepam	10.0	50 mM Tris (pH 7.6)	60	5
Bovine striatum:							
D_2	[^{3}H]-spiperone	0.2	Butaclamol	1.0	50 mM Tris (pH 7.6)	30	25

References to methods: α_1-adrenoceptor, Greengrass & Bremner (1979); α_2-adrenoceptor, Loftus *et al.* (1984); β-adrenoceptor, Williams *et al.* (1976); 5-HT_1 receptor, Peroutka & Snyder (1979); 5-HT_2 receptor, Leyson *et al.* (1982); muscarinic receptor, Yamamura & Snyder (1974); benzodiazepine receptor, Chiu *et al.* (1982); D_2-dopamine receptor, Leyson *et al.* (1978).

each of these hypotheses was made with a specified size *a posteriori*, and so no account was taken of the composite F test for differences between treatments. The different components of the error term, which applied to each group of comparisons, were tested for homogeneity by Bartlett's test.

Results

The results of the performance measures, sleep latency tests and subjective assessments are shown in Table 2 and Figure 1. With 5 mg triprolidine there was a greater reduction compared with placebo in the latency to stage 1 (drowsy) sleep at 11 h 00 min ($P < 0.01$). Changes in subjective assessments and digit symbol substitution scores were not different from changes with placebo.

Changes in measures with (−)-chlorpheniramine were not different from changes with placebo. With (+)-chlorpheniramine the reduction in sleep latency at 11 h 00 min was more marked than with the (−)-isomer ($P < 0.01$) and with placebo ($P < 0.05$). Increased subjective sleepiness was greater at 11 h 00 min and 12 h 30 min with (+)-chlorpheniramine than with the (−)-isomer (visual analogue scales $P < 0.05$; SSS $P < 0.01$) and with placebo (12 h 30 min, visual analogue scales $P < 0.05$; 11 h 00 min and 12 h 30 min, SSS $P < 0.05$). Impairment of digit symbol substitution was greater at 11 h 00 min and 12 h 30 min with (+)-chlorpheniramine than with the (−)-isomer ($P < 0.05$).

Changes in measures with (+)-dimethindene were not different from those with placebo. With (−)-dimethindene there was a more marked reduction in sleep latency at 11 h 00 min than with the (+)-isomer and with placebo ($P < 0.05$). Subjects reported a greater increase in sleepiness at 12 h 30 min with (−)-dimethindene than with the (+)-isomer ($P < 0.05$). Changes in performance with (−)-dimethindene did not differ from changes with the (+)-isomer or with placebo.

Pharmacological activity in vitro

H_1-receptor antagonist activities of the enantiomers of chlorpheniramine and dimethindene against histamine-induced contraction of the guinea-pig ileum are shown in Table 3. Stereoselectivity ratios were greater than 50 for each pair of enantiomers, with (+)-chlorpheniramine and (−)-dimethindene showing greater potency than their respective isomers. There was some depression of the maximum response with the higher concentrations of (+)-chlorpheniramine (64% at a dose-ratio of 4.5), (−)-chlorpheniramine (30% at a dose-ratio of 3.2) and (−)-dimethindene (31% at a dose-ratio of 5.2), but not with (+)-dimethindene (6% at a dose-ratio of 8.1).

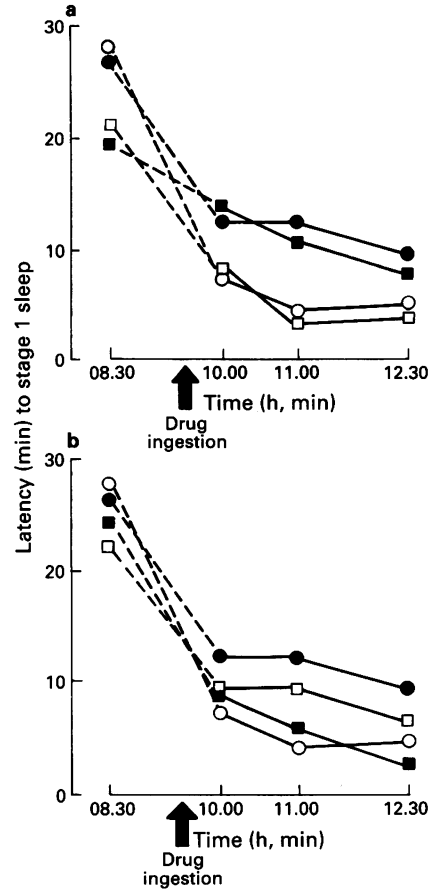

Figure 1 Effect of drugs on sleep latencies (means for 6 subjects). (a) There was a greater reduction in sleep latency from 08 h 30 min to 11 h 00 min with triprolidine (○, $P < 0.01$) and with (+)-chlorpheniramine (□, $P < 0.05$) compared with placebo (●), and with (+)-chlorpheniramine (□) compared with the (−) isomer (■, $P < 0.01$). (b) There was a greater reduction in sleep latency from 08 h 30 min to 11 h 00 min with triprolidine (○, $P < 0.01$) and with (−)-dimethindene (■, $P < 0.05$) compared with placebo (●), and with (−)-dimethindene (■) compared with the (+)-isomer (□, $P < 0.05$).

The results of the radioligand binding assays are shown in Table 4. Standard agents showed nanomolar affinity for their

Table 2 Sleep latencies, subjective sleepiness and performance 1.0 h (08 h 30 min) before and 0.5, 1.5, and 3.0 h (10 h 00 min, 11 h 00 min and 12 h 30 min) after drug ingestion

Measure	*Time* (h)	*Placebo*	*Triprolidine* (mg) 5	*Chlorpheniramine* (mg) (+)10	(−)10	*Dimethindene* (mg) (+)5	(−)5
Sleep latency (min)	0830	26.5	27.5	20.6	19.5	21.9	23 8
	1000	12.6	7.6	7.7	13.1	8.3	8.1
	1100	12.2	3.5[b]	3.3[a, d]	10.5	8.8	3.8[a, c]
	1230	9.0	4.4	3.5	7.2	5.6	2.8
Digit symbol substitution	0830	248.1	224.5	245.7	245.0	249.8	248.8
(number of substitutions)	1000	244.2	239.2	246.0	244.7	250.8	242.8
	1100	242.3	236.2	228.8[c]	245.5	246.3	236.8
	1230	243.6	236.0	232.0[c]	248.3	246.0	241.8
Subjective sleepiness:							
Visual analogue scales	0830	−0.38	−0.16	−0.31	−0.37	−0.42	−0.20
(arbitrary units)	1000	−0.37	−0.06	−0.09	−0.15	−0.34	−0.23
from −1.32 (wide awake)	1100	0.03	0.67	0.98[c]	−0.07	0.19	0.59
to 3.60 (extremely sleepy)	1230	−0.36	0.17	1.12[a, c]	−0.21	0.25	0.74
Standford sleepiness scale	0830	2.51	2.35	2.35	2.69	2.69	2.16
(arbitrary units)	1000	2.44	2.52	2.52	2.52	2.66	2.50
from 1.00 (wide awake)	1100	2.68	3.34	3.79[a, d]	2.69	2.84	2.89
to 7.00 (extremely sleepy)	1230	2.58	2.99	3.97[a, d]	2.52	2.63	3.28[c]

Values are back transformed means for 6 subjects.
Comparisons of differences from before ingestion with placebo: [a]$P < 0.05$; [b]$P < 0.01$.
Comparisons of differences from before ingestion between enantiomers: [c]$P < 0.05$; [d]$P < 0.01$.

Table 3 H_1-histamine receptor antagonist affinities of the enantiomers of chlorpheniramine and dimethindene against histamine-induced contraction of the guinea-pig ileum

Drug	n	pA_2 (95% confidence interval)	*Slope*	*Published* pA_2 values
(+)-Chlorpheniramine	7	9.02 (8.89–9.15)	1.42 ± 0.47	9.30[a]
(−)-Chlorpheniramine	9	7.11 (6.95–7.26)	0.97 ± 0.44	7.84[a]
(+)-Dimethindene	8	7.86 (7.71–8.07)	0.74 ± 0.19	7.80[b]
(−)-Dimethindene	10	9.54 (9.31–9.83)	0.73 ± 0.33	9.10[b]

pA_2 and slope values determined by Schild analysis. Dose-ratios were: 1.17–5.17 for (+)-chlorpheniramine, 1.61–3.80 for (−)-chlorpheniramine, 1.66–9.67 for (+)-dimethindene, and 1.33–5.83 for (−)-dimethindene.

[a] Van den Brink & Lien (1977).

[b] Borchard *et al.* (1985).

respective receptors. (+)-Chlorpheniramine showed similar affinity to (−)-chlorpheniramine for α_1-, β-, 5-HT_1-, muscarinic, D_2- and benzodiazepine receptors, and was less active with respect to α_2- and 5-HT_2-receptors. (−)-Dimethindene was more potent than (+)-dimethindene at 5-HT_2-, muscarinic and D_2-receptors. Triprolidine showed higher affinity for α_1- and 5-HT_2-receptors than for the other receptors. However, with respect to all drugs and all receptors examined, inhibitory concentrations were in the micromolar range.

Pharmacological activity in vivo

(−)-Dimethindene at doses of 0.001, 0.003 and 0.01 μmol kg^{-1} produced dose-related inhibition of histamine-induced increases in airway pressure. Dose-ratios (mean ± s.e.mean, $n = 5$) were 2.9 ± 0.8, 12.0 ± 6.2 and 46.7 ± 26.6, respectively. The dose giving a (dose-ratio − 1) = 10 was 0.003 μmol kg^{-1}. (+)-Dimethindene at doses of 0.01, 0.1, 1.0 and 10.0 μmol kg^{-1} gave dose-ratios of 1.6 ± 0.2, 2·3 ± 0.5, 5·0 ± 1.1 and 21.7 ± 3.9, respectively ($n = 4$ or 5). The dose required to give a (dose-ratio − 1) = 10 was 4.5 μmol kg^{-1}.

Discussion

There is much evidence to suggest that histamine is involved in the control of arousal. Histaminergic pathways originating from the reticular formation project diffusely to the cerebral cortex in a similar way to monoaminergic pathways concerned with alertness (Garbarg *et al.*, 1980; Pollard & Schwartz, 1987). Further, administration of histamine or drugs which enhance histaminergic transmission leads to desynchronization of the EEG and wakefulness (Wolf & Monnier, 1973; Monti *et al.*, 1986; Lin *et al.*, 1988), and histamine may also modulate the activity of medullary neurones (Jones *et al.*, 1983; Bradley *et al.*, 1984). Circadian rhythms in the level of histamine have been found in various regions of the brain (Friedman & Walker, 1968; Orr & Quay, 1975), and the rate of formation of histamine is elevated in rodents during the period of darkness when spontaneous activity is maximal (Schwartz *et al.*, 1976).

Nevertheless, it is possible that pharmacological activity other than H_1 antagonism may give rise to sedation with antihistamines, and the drugs used in the present study, in particular chlorpheniramine, are not specific H_1-receptor antagonists. Chlorpheniramine also modulates the activity of monoamine transmitters, with evidence both *in vitro* and *in vivo* of moderate to marked inhibition of 5-HT, noradrenaline and dopamine uptake compared with drugs, such as tricyclic antidepressants, which have recognised effects on reuptake mechanisms (Carlsson & Lindqvist, 1969; Farnebo *et al.*, 1970; Fuxe *et al.*, 1970; Horn *et al.*, 1971; Lidbrink *et al.*, 1971; Symchowicz *et al.*, 1971; Korduba *et al.*, 1973; Young *et al.*, 1988).

With respect to the other receptors examined, the binding data indicate that interactions of chlorpheniramine and dimethindene occur only at relatively high concentrations. Previous studies have also shown that chlorpheniramine has much lower affinity for peripheral α-adrenoceptors and muscarinic sites than for H_1-receptors (O'Neill & Patil, 1975; Van den Brink & Lien, 1977), and that (+)-chlorpheniramine is similarly less potent at central muscarinic sites (Kubo *et al.*, 1987). Published studies on dimethindene are limited, though the racemic compound has less potent anticholinoceptor than antihistamine receptor activity, both centrally and peripherally, and does not antagonize cardiovascular effects of noradrenaline, adrenaline and acetylcholine in the dog. However, doses of dimethindene which inhibit histamine-induced gastro-intestinal motility also reduce the response to 5-HT (Barrett *et al.*, 1961; Kubo *et al.*, 1987).

In the present study, changes in measures of drowsiness and performance with (−)-chlorpheniramine and (+)-dimethindene, the enantiomers with low affinity for the H_1-receptor, were not different from those with placebo. This would indicate, too, that any other pharmacological activity of these antihistamines is unlikely to be a significant factor in their sedative action, unless such activity is also related to steric configuration. The binding data suggest that this is unlikely. (+)-Chlorpheniramine showed either similar affinity to the

Table 4 Inhibition of radioligand binding at central receptors by the enantiomers of chlorpheniramine and dimethindene, and by triprolidine

Receptor	*Standard agent*	K_i(nM)	Triprolidine	K_i(μM) Chlorpheniramine (+)	Chlorpheniramine (−)	Dimethindene (+)	Dimethindene (−)
α_1	Prazosin	0.15	1.6	2.6	2.7	0.33	0.55
α_2	Phentolamine	3.1	>10.0	>10.0	>10.0	>10.0	>10.0
β	Propranolol	4.1	>10.0	>10.0	>10.0	>10.0	>10.0
5-HT_1	5-HT	1.1	>10.0	>10.0	>10.0	2.8	>10.0
5-HT_2	Ketanserin	1.8	3.3	>10.0	1.9	>10.0	2.2
Muscarinic	Atropine	0.87	>10.0	>10.0	>10.0	>10.0	0.93
Benzodiazepine	Flunitrazepam	2.2	>10.0	>10.0	>10.0	>10.0	>10.0
D_2	Butaclamol	3.3	>10.0	>10.0	>10.0	2.7	0.3

Each value represents the mean of two experiments performed in duplicate, using 5–6 concentrations for each compound.

(−)-isomer, or was less active, at various central receptors, and although (−)-dimethindene was more potent than (+)-dimethindene at 5-HT_2-, muscarinic and dopamine D_2-receptors, inhibitory concentrations were in the micromolar range. It has also been reported previously that the enantiomers of chlorpheniramine have similar affinities for cholinoceptors and adrenoceptors (O'Neill & Patil, 1975; Van den Brink & Lien, 1977). Further, though comparative studies of modulation of 5-HT and noradrenaline activity have not been carried out, it is known that inhibition of dopamine uptake with chlorpheniramine is not stereoselective (Symchowicz *et al.*, 1971).

Although enantiomers share the same physico-chemical properties and should, therefore, be absorbed and penetrate the central nervous system with equal ease, stereoselectivity may lead to pharmacokinetic differences due to differences in protein binding or metabolism (Williams & Lee, 1985; Drayer, 1986; Lam, 1988). Studies have shown that (+)-chlorpheniramine is metabolised more rapidly than the (−)-isomer in rat and rabbit liver microsomes, but not in those of the mouse. Further, when the enantiomers were given as the pseudoracemate, differences in metabolism were potentiated in rabbit, but not rat, microsomes (Thompson & Shioshita, 1981).

Clearly, there are species differences in chlorpheniramine metabolism, and enantiomeric interaction may occur when the isomers are administered together. Studies in man have demonstrated higher serum levels and slower elimination of (+)-chlorpheniramine following both simultaneous and separate administration of the isomers (Miyazaki & Abuki, 1976; Fujiwara *et al.*, 1989). However, it is unlikely that such differences would explain entirely the differential effects of the isomers of chlorpheniramine observed in the present study in which higher doses were used. Further, there is no evidence that the metabolism of dimethindene is influenced by steric configuration.

Previous studies in the cat have indicated that electroencephalographic effects of (−)- and (±)-chlorpheniramine are not related to their ability to antagonize histamine (Faingold & Berry, 1972). However, this does not appear to be the case in man. Sedation with both chlorpheniramine and dimethindene was limited to the enantiomers with high affinity for the histamine H_1-receptor. While (−)-chlorpheniramine and (+)-dimethindene were without effect on the measures tested, (+)-chlorpheniramine and (−)-dimethindene increased the tendency to fall asleep, and subjects reported that they felt more sleepy. (+)-Chlorpheniramine also impaired performance, with lower scores on the digit symbol substitution test.

(+)-Chlorpheniramine is 30–200 times more potent than the (−)-isomer in antagonizing histamine-induced contraction of the guinea-pig ileum (Roth & Govier, 1958; Van den Brink & Lien, 1977), and is approximately 100 times more potent *in vivo* against histamine-induced lethality in guinea-pigs (Roth & Govier, 1958). Marked differences between the activity of the enantiomers have also been observed in rabbit aorta (O'Neill & Patil, 1975). Similarly, there is also evidence for stereoselective antagonism of H_1-receptors in the central nervous system. (+)-Chlorpheniramine inhibits [^{3}H]-mepyramine binding to brain membranes to a greater (up to 240 times) extent than the (−)-isomer in a number of species, including man (Hill *et al.*, 1978; Tran *et al.*, 1978; Chang *et al.*, 1979; Quach *et al.*, 1980). It is of interest that there are no marked species differences in stereoselectivity ratios, even though the ability of chlorpheniramine to displace the labelled ligand varies (Chang *et al.*, 1979).

Dimethindene is a potent H_1 antihistamine, with activity similar to or greater than that of (+)-chlorpheniramine in a number of tests of histamine receptor function (Barrett *et al.*, 1961) and in receptor binding studies (Tran *et al.*, 1978; Kubo *et al.*, 1987). Its stereoselectivity with respect to H_1 sites is less well documented, but (−)-dimethindene is between 20 and 100 times more potent than the (+)-isomer in blocking the response to histamine receptor activation in various guinea-pig tissue preparations (Borchard *et al.*, 1985). In the present study, the stereoselectivity ratio on guinea-pig ileum was greater than 50, and (−)-dimethindene was a more potent inhibitor of histamine-induced bronchoconstriction than the (−)-isomer.

These studies in man with enantiomers of chlorpheniramine and dimethindene strongly suggest that sedation can arise from H_1 antagonism alone. Drugs such as terfenadine, astemizole, loratadine and mequitazine which are either non-sedating or non-sedating at certain therapeutic doses (Clarke & Nicholson, 1978; Nicholson, 1982; Nicholson & Stone, 1982; 1983; Bradley & Nicholson, 1987) usually exhibit poor penetration of the central nervous system, and in some cases possibly lower affinity for central H_1-receptors than for peripheral sites (Quach *et al.*, 1980; Barnett *et al.*, 1984; Ahn & Barnett, 1986; McQuade *et al.*, 1990). The stereoselective activity of two potent antihistamines shown in the present study in man provides further support to the belief that the histaminergic system is concerned with the regulation of alertness.

The authors are indebted to Dr A. Belyavin and Mrs A. Berry (R.A.F. Institute of Aviation Medicine) for statistical advice, to Mr R. C. Blakemore and Dr M. E. Parsons (Smith, Kline and French Research) for ileal assays, and to Mrs M. Pipkin (Smith, Kline and French Research) for the bronchoconstriction measurements.

The authors thank Zyma and Smith, Kline and French Research for gifts of dimethindene and chlorpheniramine, respectively.

A.D.M. gratefully acknowledges support by grants from the S.E.R.C. and Smith, Kline and French Research under the C.A.S.E. scheme.

References

AHN, H.-S. & BARNETT, A. (1986). Selective displacement of [^{3}H]mepyramine binding from peripheral vs. central nervous system receptors by loratadine, a non-sedating antihistamine. *Eur. J. Pharmacol.*, **127**, 153–155.

ANSCOMBE, F.J. (1961). Examination of residuals. *Proc. 4th Berkeley Symp. Math. Statist. Prob.*, **1**, 1–36.

BARNETT, A., IORIO, L.C., KREUTNER, W., TOZZI, S., AHN, H.S. & GULBENKIAN, A. (1984). Evaluation of the CNS properties of SCH29851, a potential non-sedating antihistamine. *Agents Actions*, **14**, 590–597.

BARRETT, W.E., HUEBNER, C.F., RUTLEDGE, R.A., DEITRICH, A. & PLUMMER, A.J. (1961). A pharmacological evaluation of dimethpyridene maleate (Forhistal). *Toxicol. Appl. Pharmacol.*, **3**, 534–544.

BORCHARD, U., HAFNER, D. & HEISE, R. (1985). H_1-antagonistic actions of (+)- and (−)-dimethindene. *Naunyn-Schmiedebergs Arch. Pharmacol.*, **330**, Abstract 42.

BOX, G.E.P. & COX, D.R. (1964). An analysis of transformations. *J.R. Statist. Soc.*, **26B**, 211–232.

BRADLEY, P.B., JONES, H. & ROBERTS, F. (1984). Histamine potentiates the effects of excitatory amino acids on quiescent neurones in the rat medulla. *Br. J. Pharmacol.*, **82**, 195P.

BRADLEY, C.M. & NICHOLSON, A.N. (1987). Studies on the central effects of the H_1-antagonist, loratadine. *Eur. J. Clin. Pharmacol.*, **32**, 419–421.

BROWN, E.A., GRIFFITHS, R., HARVEY, C.A. & OWEN, D.A.A. (1986). Pharmacologial studies with SK&F 93944 (temelastine), a novel histamine H_1-receptor antagonist with negligible ability to penetrate the central nervous system. *Br. J. Pharmacol.*, **87**, 569–578.

CARLSSON, A. & LINDQVIST, M. (1969). Central and peripheral monoaminergic membrane-pump blockade by some addictive analgesics and antihistamines. *J. Pharm. Pharmacol.*, **21**, 460–464.

CHANG, R.S.L., TRAN, V.T. & SNYDER, S.H. (1979). Heterogeneity of histamine H_1-receptors: Species variations in (^{3}H)mepyramine binding of brain membranes. *J. Neurochem.*, **32**, 1653–1663.

CHENG, Y.C. & PRUSOFF, W.H. (1973). Relationship between inhibition constant (K_i) and the concentration of inhibitor which causes 50 percent inhibition (IC_{50}) of an enzymatic reaction. *Biochem.*

Pharmacol., **22**, 3099–3108.

CHIU, T.H., DRYDEN, D.M. & ROSENBERG, H. (1982). Kinetics of (^{3}H)-flunitrazepam binding to membrane bound benzodiazepine receptors. *Mol. Pharmacol.*, **21**, 57–66.

CLARKE, C.H. & NICHOLSON, A.N. (1978). Performance studies with antihistamines. *Br. J. Clin. Pharmacol.*, **6**, 31–35.

DRAYER, D.E. (1986). Pharmacodynamic and pharmacokinetic differences between drug enantiomers in humans: An overview. *Clin. Pharmacol. Ther.*, **40**, 125–133.

DUNNETT, C.W. (1964). New tables for multiple comparisons with a control. *Biometrics*, **20**, 482–491.

FAINGOLD, C.L. & BERRY, C.A. (1972). A comparison of the EEG effects of the potent antihistaminic (DL-chlorpheniramine) with a less potent isomer (L-chlorpheniramine). *Arch. Int. Pharmacodyn.*, **199**, 213–218.

FARNEBO, L.-O., FUXE, K., HAMBERGER, B. & LJUNGDAHL, A. (1970). Effect of some antiparkinsonian drugs on catecholamine neurons. *J. Pharm. Pharmacol.*, **22**, 733–737.

FRIEDMAN, A.H. & WALKER, C.A. (1968). Circadian rhythms in rat mid-brain and caudate nucleus biogenic amine levels. *J. Physiol.*, **297**, 77–85.

FUJIWARA, K., IWAMOTO, K., KAWAI, S. & SAKAMOTO, T. (1989). Behavior of chlorpheniramine *in vivo* after administration of d- and l-chlorpheniramine maleate. *Yakugaku Zasshi*, **109**, 59–64.

FUXE, K., GOLDSTEIN, M. & LJUNGDAHL, A. (1970). Antiparkinsonian drugs and central dopamine neurons. *Life Sci.*, **9**, 811–824.

GARBARG, M., BARBIN, G., LLORENS, C., PALACIOS, J.M., POLLARD, H. & SCHWARTZ, J.C. (1980). Recent developments in brain histamine research: Pathways and receptors. In *Neurotransmitters, Receptors and Drug Action.* ed. Essmann, W.B. pp. 179–202, New York: Spectrum.

GREENGRASS, P.M. & BREMNER, R. (1979). Binding characteristics of ^{3}H-prazosin to rat brain α-adrenergic receptors. *Eur. J. Pharmacol.*, **55**, 323–326.

HILL, S.J., EMSON, P.C. & YOUNG, J.M. (1978). The binding of [^{3}H]mepyramine to histamine H_1-receptors in guinea-pig brain. *J. Neurochem.*, **31**, 997–1004.

HODDES, E., ZARCONE, V., SMYTHE, H., PHILLIPS, R. & DEMENT, W.C. (1973). Quantification of sleepiness: A new approach. *Psychophysiology*, **10**, 431–436.

HORN, A.S., COYLE, J.T. & SNYDER, S.H. (1971). Catecholamine uptake by synaptosomes from rat brain. Structure-activity relationships of drugs with differential effects on dopamine and norepinephrine neurons. *Mol. Pharmacol.*, **7**, 66–80.

JOHN, J.A. & QUENOUILLE, M.H. (1977). *Experiments: Design and Analysis*, pp. 198–199. London: Griffin.

JONES, H., BRADLEY, P.B. & ROBERTS, F. (1983). Excitatory effects of microiontophoretically applied histamine in the rat medulla may be mediated via histamine H_2-receptors. *Br. J. Pharmacol.*, **79**, 282P.

KORDUBA, C.A., VEALS, J. & SYMCHOWICZ, S. (1973). The effect of pheniramine and its structural analogues on 5-hydroxytryptamine in rat and mouse brain. *Life Sci.*, **13**, 1557–1564.

KUBO, N., SHIRAKAWA, O., KUNO, T. & TANAKA, C. (1987). Antimuscarinic effects of antihistamines: Quantitative evaluation by receptor-binding assay. *Jpn. J. Pharmacol.*, **43**, 277–282.

LAM, Y.W.F. (1988). Stereoselectivity: An issue of significant importance in clinical pharmacology. *Pharmacotherapy*, **8**, 147–157.

LEVANDER, S., HAGERMARK, O. & STAHLE, M. (1985). Peripheral antihistamine and central sedative effects of three H_1-receptor antagonists. *Eur. J. Clin. Pharmacol.*, **28**, 523–529.

LEYSON, J.E., GOMMEREN, W. & LADURON, P.M. (1978). Spiperone: A ligand of choice for neuroleptic receptors. 1. Kinetics and characteristics of in vitro binding. *Biochem. Pharmacol.*, **27**, 307–316.

LEYSON, J.E., NIEMERGEERS, C.J.E., VAN NEUTEN, J.M. & LADURON, P.M. (1982). ^{3}H-ketanserin, 9R41468, a selective ^{3}H-ligand for serotonin-2 receptor binding sites. *Mol. Pharmacol.*, **21**, 301–314.

LIDBRINK, P., JONSSON, G. & FUXE, K. (1971). The effect of imipramine-like drugs and antihistamine drugs on uptake mechanisms in the central noradrenaline and 5-hydroxytryptamine neurons. *Neuropharmacology*, **10**, 521–536.

LIN, J.-S., SAKAI, K. & JOUVET, M. (1988). Evidence for histaminergic arousal mechanisms in the hypothalamus of cat. *Neuropharmacology*, **27**, 111–122.

LOFTUS, D.J., STOLK, J.M. & U'PRICHARD, D.C. (1984). Binding of the imidazoline, UK-14,304, a putative full α_2-adrenoceptor agonist, to rat cerebral cortex membranes. *Life Sci.*, **35**, 61–69.

McQUADE, R.D., RICHLAN, K., DUFFY, R.A., CHIPKIN, R.E. & BARNETT, A. (1990). In vivo binding properties of non-sedating antihistamines to CNS histamine receptors. *Drug Dev. Res.*, **20**, 301–306.

MERCER, A.D. (1989). Stereochemical studies of H_1-receptor histamine antagonists. *Ph.D. Thesis, School of Pharmacy and Pharmacology, University of Bath.*

MIYAZAKI, K. & ABUKI, H. (1976). Mass fragmentation determination of d- and l-chlorpheniramine with aid of the stable isotope technique. *Chem. Pharm. Bull.*, **24**, 2572–2574.

MONTI, J.M., PELLEJERO, T. & JANTOS, H. (1986). Effects of H_1- and H_2-receptor agonists and antagonists on sleep and wakefulness in the rat. *J. Neural Trans.*, **66**, 1–11.

NICHOLSON, A.N. (1982). Antihistaminic activity and central effects of terfenadine: A review of European studies. *Arzneim.-Forsch.*, **32**, 1191–1193.

NICHOLSON, A.N. (1983). Antihistamines and sedation. *Lancet*, **ii**, 211–212.

NICHOLSON, A.N. (1987). New antihistamines free of sedative side-effects. *Trends Pharmacol. Sci.*, **8**, 247–249.

NICHOLSON, A.N., PASCOE, P.A. & STONE, B.M. (1985). Histaminergic systems and sleep: Studies in man with H_1 and H_2 antagonists. *Neuropharmacology*, **24**, 245–250.

NICHOLSON, A.N. & STONE, B.M. (1982). Performance studies with the H_1-histamine receptor antagonists, astemizole and terfenadine. *Br. J. Clin. Pharmacol.*, **13**, 199–202.

NICHOLSON, A.N. & STONE, B.M. (1983). The H_1-antagonist mequitazine: Studies on performance and visual function. *Eur. J. Clin. Pharmacol.*, **25**, 563–566.

NICHOLSON, A.N. & STONE, B.M. (1986). Antihistamines: Impaired performance and the tendency to sleep. *Eur. J. Clin. Pharmacol.*, **30**, 27–32.

O'NEILL, P.J. & PATIL, P.N. (1975). Stereoisomers of an antihistamine and the pharmacologic receptors of rabbit aorta. *Pharmacol. Res. Commun.*, **7**, 273–279.

ORR, E. & QUAY, W.B. (1975). Hypothalamic twenty four hour rhythms in histamine, histidine decarboxylase and histamine-N-methyltransferase. *Endocrinology*, **96**, 941–945.

PECK, A.W., FOWLE, A.S.E. & BYE, C. (1975). A comparison of triprolidine and clemastine on histamine antagonism and performance tests in man: implications for the mechanism of drug induced dowsiness. *Eur. J. Clin. Pharmacol.*, **8**, 455–463.

PEROUTKA, S.J. & SNYDER, S.H. (1979). Multiple serotonin receptors: Differential binding of ^{3}H-serotonin, ^{3}H-lysergic acid diethylamide and ^{3}H-spiroperidol. *Mol. Pharmacol.*, **16**, 687–699.

POLLARD, H. & SCHWARTZ, J.-C. (1987). Histamine neuronal pathways and their function. *Trends Neurosci.*, **10**, 86–89.

QUACH, T.T., DUCHEMIN, A.M., ROSE, C. & SCHWARTZ, J.-C. (1979). *In vivo* occupation of cerebral histamine H_1-receptors evaluated with (^{3}H)-mepyramine may predict sedative properties of psychoactive drugs. *Eur. J. Pharmacol.*, **60**, 391–392.

QUACH, T.T., DUCHEMIN, A.M., ROSE, C. & SCHWARTZ, J.-C. (1980). Labelling of histamine H_1-receptors in the brain of the living mouse. *Neurosci. Lett.*, **17**, 49–54.

ROTH, F.E. & GOVIER, W.M. (1958). Comparative pharmacology of chlorpheniramine (Chlor-Trimeton) and its optical isomers. *J. Pharmacol. Exp. Ther.*, **124**, 347–349.

SCHWARTZ, J.-C., BARBIN, G., DUCHEMIN, A.-M., GARBARG, M., LLORENS, C., POLLARD, H., QUACH, T.T. & ROSE, C. (1982). Histamine receptors in the brain and their possible functions. In *Pharmacology of Histamine Receptors.* ed. Ganellin, C. R. & Parsons, M. E. pp. 351–391. Bristol: John Wright & Sons Ltd.

SCHWARTZ, J.-C., BARBIN, G., GARBARG, M., POLLARD, H., ROSE, C. & VERDIERE, M. (1976). Neurochemical evidence for histamine acting as a transmitter in mammalian brain. *Adv. Biochem. Psychopharmacol.*, **15**, 111–126.

SYMCHOWICZ, S., KORDUBA, C.A. & VEALS, J. (1971). Inhibition of dopamine uptake into synaptosomes of rat corpus striatum by chlorpheniramine and its structural analogs. *Life Sci.*, **10**, 35–42.

THOMPSON, J.A. & SHIOSHITA, G.W. (1981). Influence of substrate configuration on chlorpheniramine N-demethylation by hepatic microsomes from rats, rabbits and mice. *Drug Metab. Dispos.*, **9**, 5–9.

TRAN, V.T., CHANG, R.S.L. & SNYDER, S.H. (1978). Histamine H_1-receptors identified in mammalian brain membranes with [^{3}H]mepyramine. *Proc. Natl. Acad. Sci. U.S.A.*, **75**, 6290–6294.

VAN DEN BRINK, F.G. & LIEN, E.J. (1977). pD_2-, pA_2- and pD_2'-values of a series of compounds in a histaminic and a cholinergic system. *Eur. J. Pharmacol.*, **44**, 251–270.

WILLIAMS, L.T., JARETT, L. & LEFKOWITZ, R.J. (1976). Adipocyte β-adrenergic receptors; identification and subcellular localization by (−)-[^{3}H] dihydroalprenolol binding. *J. Biol. Chem.*, **251**, 3096–3104.

WILLIAMS, K. & LEE, E. (1985). Importance of drug enantiomers in clinical pharmacology. *Drugs*, **30**, 333–354.

WOLF, P. & MONNIER, M. (1973). Electroencephalographic behavioural and visceral effects of intraventricular infusion of histamine in the rabbit. *Agents Actions*, **3**, 196.

YAMAMURA, H.I. & SNYDER, S.H. (1974). Muscarinic cholinergic binding in rat brain. *Proc. Natl. Acad. Sci. U.S.A.*, **71**, 1725–1729.

YOUNG, C.S., MASON, R. & HILL, S.J. (1988). Inhibition by H_1-antihistamines of the uptake of noradrenaline and 5-HT into rat brain synaptosomes. *Biochem. Pharmacol.*, **37**, 976–978.

(Received August 27, 1990
Revised May 10, 1991
Accepted May 24, 1991)

Br. J. Pharmacol. (1991), **104**, 277–283

Different mechanisms of action of agents acting on β-adrenoceptors in barium-stimulated and electrically-stimulated rat vas deferens

[1]Alejandro Diaz-Toledo & [2]Aron Jurkiewicz

Department of Pharmacology, Escola Paulista de Medicina, Caixa Postal 20372, 04034 São Paulo, Brazil

1 The relaxation induced by β-adrenoceptor agonists in rat vas deferens was examined under two different experimental conditions: on electrically-induced twitch responses (35 V, 3 ms, 0.07 Hz), and on contractions induced by single doses of barium chloride (300 μM). The experiments were performed in vasa of reserpine-treated rats, after blockade of α-adrenoceptors and extraneuronal uptake with dibenamine (10 μM, 30 min), and neuronal uptake with cocaine (10 μM).

2 When twitch responses were used, the values of pD_2, interpolated from cumulative concentration-response curves for isoprenaline (Iso), adrenaline (Ad), and noradrenaline (NA) showed a rank order of potency consistent with the presence of β_2-adrenoceptors (Iso > Ad ≫ NA).

3 When twitch responses were used, the non-selective β-antagonist, propranolol, caused a concentration-dependent parallel shift to the right of Iso concentration-response curves. Similar shifts were obtained by use of the β_2-antagonist, isopropylmethoxamine (IMA), and higher doses of the β_1-antagonist, practolol, according to the expectations from receptor occupation theory. Practolol presented the lowest value of pK_B, 5.03, corroborating the presence of β_2-adrenoceptors.

4 When twitch responses were used, and Ad or NA employed instead of Iso, the antagonists produced shifts of concentration-response curves which were smaller than expected from theory, precluding the determination of pK_B values. This indicates that other mechanisms are involved besides an interaction with a single population of postsynaptic β_2-adrenoceptors.

5 When barium chloride was used instead of twitch responses, although the potencies of Iso and Ad were increased respectively by about 30 fold and 5 fold, the rank order of potency was still consistent with an interaction with β_2-adrenoceptors. In addition, the antagonists produced parallel and concentration-dependent shifts of the curves of all the agonists, as expected from receptor theory. The values of pK_B for a given antagonist were not modified by interchanging the agonists used, indicating a typical interaction with a single population of β_2-adrenoceptors. When compared to the field-stimulated vas, the values of pK_B for propranolol and IMA against isoprenaline were respectively 1.3 and 0.6 log units larger. These results suggest the β-adrenoceptor agents act by different mechanisms of action in barium-stimulated and electrically-stimulated vas.

6 It is suggested that when barium is used, the effects of agents acting on β-adrenoceptors are mediated only by postsynaptic β_2-receptors, while other complicating factors, probably nerve-dependent presynaptic mechanisms, may be involved with electrical stimulation.

Keywords: β-adrenoceptors; vas deferens; functional antagonism; barium chloride; isoprenaline; noradrenaline; adrenaline; propranolol; practolol; isopropylmethoxamine

Introduction

Previous studies have shown the presence of β_2-adrenoceptors in rat vas deferens, mediating a relaxation of smooth muscle. Almost all the results are based on functional antagonism against electrically-induced twitches (Ganguly & Bhattacharya, 1969; Vohra, 1979; Lotti *et al.*, 1980; Diaz-Toledo & Jurkiewicz, 1980; 1990).

When the reported publications are analysed on the grounds of the two standard pharmacological procedures for receptor classification, namely the determination of the relative potencies of a series of agonists, and the determination of the potencies of competitive antagonists (Furchgott, 1972), at least two groups of incongruities are apparent: (a) there are very few quantitative informations about adrenaline (Ad) and noradrenaline (NA). As a consequence, our knowledge about the rank order of potency for Ad, NA and isoprenaline (Iso), which is one of the main tools for adrenoceptor classification, is still fragmentary. Although Vohra (1979) studied both agonists in the presence and absence of selective and non-selective β-blockers, concentration-response curves and determinations of drug-receptor parameters were not performed, precluding a quantitative analysis and receptor characterization. (b) Data obtained by the use of the competitive antagonist propranolol vs. isoprenaline suggested that the β-agents could be interacting with two receptors (Lotti *et al.*, 1982). In addition, propranolol was also studied by Krstew *et al.* (1982), who were unable to antagonize the effects of NA with this drug. Similar results were reported by May *et al.* (1985) for propranolol against Ad and NA.

The objective of the present study was to obtain quantitative information about the effects and relative potencies of Ad, NA, and Iso, and about the potencies of β-adrenoceptor antagonists. Propranolol and practolol were used respectively as non-selective and β_1-antagonists (Daly & Levy, 1979), and isopropylmethoxamine (IMA) as a β_2-antagonist (Furchgott, 1972). Because of some atypical effects of these agents against electrically-induced twitches, we decided to repeat the experiments by using barium chloride as another functional antagonist.

Methods

Adult male Wistar rats (300–350 g, 6-months old), from our own colony, BAW-2 (Festing, 1980), were pretreated with reserpine (10 mg kg^{-1}, 24 h before death), and killed by a

[1] Visiting Associate Professor at the Escola Paulista de Medicina; present address: Departamento de Farmacologia, Universidad de Concepcion, Chile.

[2] Author for correspondence.

blow on the head. The vasa deferentia were removed, cleared of surrounding tissues, and mounted, under 1 g tension, in 10 ml organ baths containing heated (30°C) and aerated physiological solution of the following composition (mM): NaCl 138, KCl 5.7, $CaCl_2$ 1.8, $NaH_2PO_4 \cdot H_2O$ 0.36, $NaHCO_3$ 15.0 and dextrose 5.5. The isotonic responses to agonists were recorded with tangential writing levers, with a 6 fold amplification.

Concentration-response curves

Pretreatment of the isolated vas deferens In general, when β-agonists were added to the resting vas deferens, no relaxation was observed, except when a tonus was present, caused by an agonist, as for instance barium chloride, or by sequential electrically-induced twitches. In the latter case, Iso, Ad, and NA elicited a dose-dependent decrease of the amplitude of twitches, without affecting the baseline (Diaz-Toledo & Jurkiewicz, 1980; 1990). However, if the concentrations of these agonists were further increased, an undesirable rise in the baseline occurred, due to a well-known concentration-dependent interaction with postsynaptic α-adrenoceptors (Jurkiewicz & Jurkiewicz, 1976); the minimum concentrations of these agonists to start such an increase in the baseline were about 3×10^{-7} M for Ad and NA, and 3×10^{-5} M for Iso (Diaz-Toledo, 1983). To overcome this problem, α-adrenoceptors had to be inactivated in an essentially irreversible manner by a β-haloalkylamine. A single exposure to these agents is able to cause a persistent blockade of the contractile effects of noradrenaline, and also of dopamine, in rat vas deferens (Langeloh & Jurkiewicz, 1982; Busatto & Jurkiewicz, 1985). In the present work we used dibenamine as the alkylating agent (Furchgott & Bursztyn, 1967). This type of pretreatment of the isolated vas, which also included an inhibition of neuronal and extraneuronal uptake, since uptake is supposed to reduce the drug concentration in the vicinity of receptors (Furchgott, 1972; Furchgott *et al.*, 1974) was performed to avoid major sources of error in the estimation of drug-receptor parameters.

After a 30 min equilibrium period, the organs were incubated with dibenamine (10 μM) for 30 min and then washed for 40 min. After this procedure, it was observed, in a group of control experiments, that Ad and NA were unable to cause any contraction of the vas, up to concentrations as high as 10^{-3} M, indicating the inactivation of postsynaptic α-adrenoceptors by dibenamine (Diaz-Toledo, 1983). As an additional control, it was observed that the presynaptic α-adrenoceptor agonist, clonidine, was unable to induce inhibitory effects upon electrically-induced twitches, when added up to a concentration of 3×10^{-5} M, while in preparations which were not treated with dibenamine, a complete inhibition of twitches was observed with a dose of clonidine about 300 times lower (Diaz-Toledo, 1983). To block neuronal uptake, cocaine (10 μM) was added to the bath (Jurkiewicz & Jurkiewicz, 1976), 30 min before the beginning of concentration-response curves, and maintained thereafter. In relation to extraneuronal uptake, other drugs were not used, since dibenamine is known to be an irreversible blocker of this type of removal mechanism (Furchgott, 1972; Furchgott *et al.*, 1974).

The inhibitory effects of β-adrenoceptor agonists were studied in two series of experiments, on contractions elicited by electrical field simulation, or by barium chloride, respectively.

Field stimulation The tissues were mounted between parallel platinum electrodes and continuously field stimulated with submaximal pulses of 35 V, 3 ms and 0.07 Hz. When twitches of constant amplitude were attained, cumulative concentration-response curves were obtained as described by Van Rossum (1963), by increasing agonist concentrations by steps of about 3 (i.e., 1; 3; 10; 30; etc). The inhibitory effects on the electrically evoked contractions were expressed as a percentage of the initial amplitude of twitches.

Barium chloride Barium chloride (300 μM) was used to induce a contraction of rat vas. This contraction, corresponding to less than 50% of barium maximal effect, usually reached a sustained plateau after about 2 min. When the response was steady, a single dose of agonist was added to the bath, and washed out after 2 min. This procedure was repeated at 20 min intervals, by adding the next doses of agonist, that were increased non-cumulatively by a factor of 10 (i.e., 1; 10; 100; etc). Mean concentration-response curves were obtained by measuring the inhibitory effects of the β-adrenoceptor agonist on barium-induced contractions. The effects were expressed as percentages of the barium-induced contraction.

Pharmacological parameters

pK_B *determination* In both experimental procedures, after determination of control concentration-response curves, rat vasa deferentia were incubated with competitive antagonists for 30 min. Then, concentration-response curves were obtained in the presence of an antagonist. Only two concentrations of each antagonist were used in each organ, to avoid tissue desensitization. The latter could also be detected by appropriate controls, in which the curves for agonist were repeated in the absence of antagonist. The pK_B value is assumed to have a theoretical significance, as an estimate of the drug-receptor dissociation constant ($-\log K_B$), and was determined directly from the equation based on the mass law (Arunlakshana & Schild, 1959; Furchgott *et al.*, 1974):

$$-\log K_B = \log(DR - 1) - \log[B]$$

using the values for each concentration of competitive antagonist, [B], and the corresponding dose-ratio for agonist, DR, according to the analytical method described by Mackay (1978). In the case of a typical competitive antagonism, the value of pK_B is expected to be constant in a given experiment, even by increasing the dose of antagonist, since according to the equation above, an increase of the dose of antagonist is expected to cause a proportional increase of $\log(DR - 1)$. If this criterion was not fulfilled, thus indicating a lack of theoretical significance, then the corresponding value of pK_B was not quoted.

pD_2 *value* The values of pD_2 were determined as $-\log ED_{50}$ by linear regression analysis, using all points between 20% and 80% of the maximal response.

Relative potency This parameter was determined as a ratio between ED_{50} values of agonists and that for NA. Thus, the value of 1.0 was arbitrarily assigned to the relative potency of NA.

Drugs

The following drugs were used: (±)-isoprenaline hydrochloride, (−)-noradrenaline ((−)-arterenol) hydrochloride, (−)-adrenaline ((−)-epinephrine) bitartrate, (±)-propranolol hydrochloride (all from Sigma Chemical Co. U.S.A.). Dibenamine hydrochloride (K & K lab. Inc., U.S.A.), cocaine (Merck, West Germany) and reserpine (Ciba-Geygi, Brazil) were also used. Practolol was kindly supplied by Dr B.B. Vargaftig (I. Pasteur, Paris), and isopropylmethoxamine by Prof. R.F. Furchgott (SUNY, U.S.A.).

Statistics

Results are expressed as mean values ± s.e.means. Student's *t* test, analysis of variance and Newman-Keuls' test were used for statistical comparisons. The significance level was considered as $P < 0.05$.

Results

Drug action in electrically stimulated vas

Figure 1 shows concentration-response curves of inhibitory effects of Iso, Ad, and NA on field-stimulated rat vas deferens. The three catecholamines produced concentration-dependent inhibition of the twitch responses and the maximal inhibition was nearly 100% of the twitch. From these data the pD_2 values and relative potencies were determined (Table 1). The concentration-response curves for Iso, Ad and NA, in the absence and presence of propranolol, are shown in Figure 2. The competitive antagonist induced a dose-dependent (10^{-8} M, 10^{-7} M) shift to the right of the concentration-response curve of isoprenaline, as expected from receptor theory. However, propranolol induced an unexpectedly small shift of concentration-response curves of Ad, even with larger doses than in the previous figure (10^{-7} M to 10^{-6} M). Similarly, propranolol (10^{-6} M, 10^{-5} M) was unable to shift the concentration-response curves of NA. When the antagonists were IMA (Figure 3), or practolol (Figure 4), a similar pattern against Iso, Ad, and NA was observed to that obtained by the use of propranolol. Table 1 shows the pK_B values of the different antagonists against the three agonists.

Drug action in rat vas stimulated by barium chloride

Figure 5 illustrates a typical experiment in the barium-stimulated vas deferens, in which the inhibitory effects of isoprenaline were tested in the absence and presence of propranolol. Figures 6, 7, and 8, show concentration-response curves for Iso, Ad and NA, in the absence and presence of two doses of respectively propranolol, IMA, and practolol, obtained from experiments similar to that shown in the previous figure. In contrast with Figures 2, 3, and 4, the shifts of concentration-response curves did not depart from the expectations from Arunlakshana & Schild's equation (1959), whichever agonist or antagonist was used, indicating a typical competitive antagonism. The pD_2 values for the relaxant effects of agonists, and the respective potency ratios (Table 2) were increased in relation to Table 1, but the rank order of potency was maintained. The pK_B values of propranolol, IMA and practolol, determined against Iso, Ad and NA, from the above experiments, are shown in Table 2. It is noteworthy

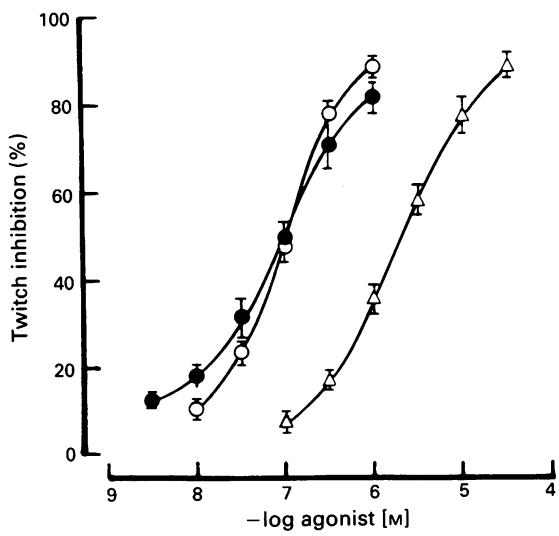

Figure 1 Concentration-response curves obtained in field-stimulated rat vas deferens, for isoprenaline (●), adrenaline (○), and noradrenaline (△). The inhibitory effects are plotted as percentages of the amplitude of electrically-induced twitches immediately before adding the agonist. Vertical lines represent s.e.mean. Each curve is a mean of at least 8 experiments.

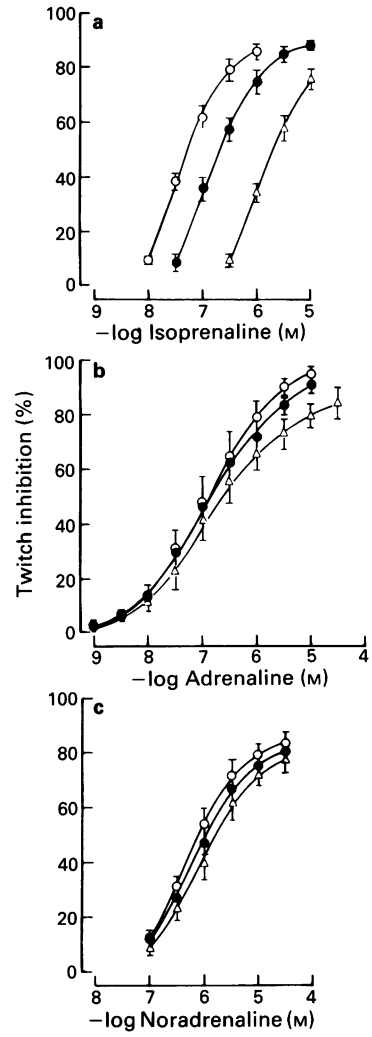

Figure 2 Concentration-response curves obtained in field-stimulated rat vas deferens: (a) for isoprenaline in the absence (○) and presence of propranolol 10^{-8} M (●) and 10^{-7} M (△); (b) for adrenaline in the absence (○) and presence of propranolol 10^{-7} M (●) and 10^{-6} M (△); and (c) for noradrenaline in the absence (○) and presence of propranolol 10^{-6} M (●) and 10^{-5} M (△). Vertical lines represent s.e.mean. Each curve is a mean of at least 8 experiments.

Table 1 Values of pD_2 and relative potencies (Rel Pot) for agonists and pK_B for antagonists, for relaxation mediated by β-adrenoceptors in electrically-stimulated rat vas deferens

			pK_B *for antagonist*		
Agonist	*pD_2*	*Rel Pot*	*Propranolol*	*IMA*	*Practolol*
(±)-Iso	7.25 ± 0.08	29	8.70 ± 0.07	6.70 ± 0.07	5.01 ± 0.04
(−)-Ad	7.10 ± 0.06	21	ND	6.10 ± 0.09	4.60 ± 0.13
(−)-NA	5.79 ± 0.08	1	ND	ND	ND

(±)-Iso, (±)-isoprenaline; (−)-Ad, (−)-adrenaline; (−)-NA, (−)-noradrenaline; IMA, isopropylmethoxamine.
n = at least 8 for each pD_2 and pK_B value. ND = not determined.

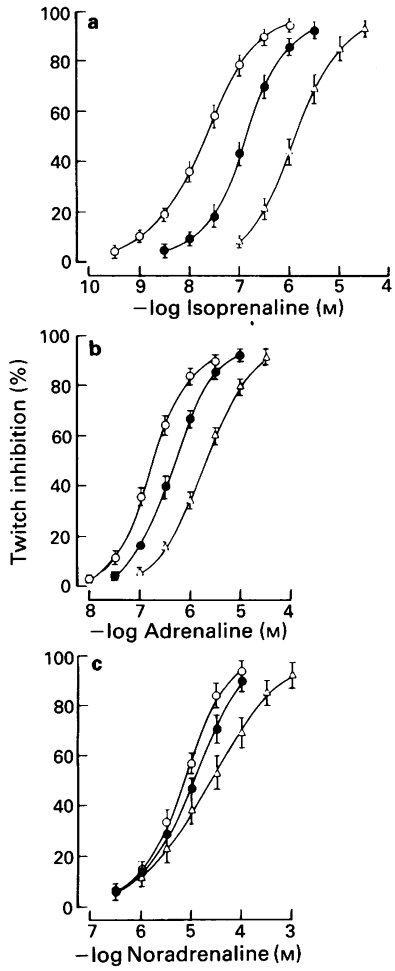

Figure 3 Concentration-response curves obtained in field-stimulated rat vas deferens: (a) for isoprenaline, (b) for adrenaline and (c) for noradrenaline in the absence (○) and presence of isopropylmethoxamine 10^{-6} M (●) and 10^{-5} M (△). Vertical lines represent s.e. mean. Each curve is a mean of at least 8 experiments.

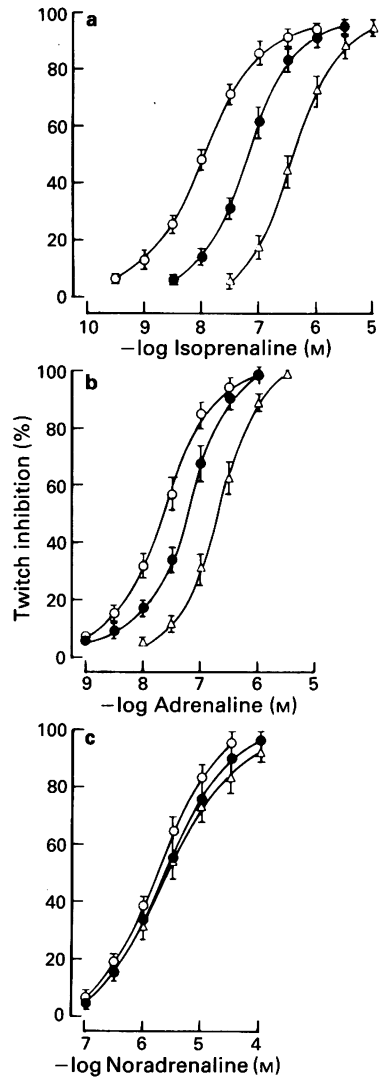

Figure 4 Concentration-response curves obtained in field-stimulated rat vas deferens: (a) for isoprenaline, (b) for adrenaline and (c) for noradrenaline in the absence (○) and presence of practolol 5×10^{-5} M (●) and 5×10^{-4} M (△). Vertical lines represent s.e.mean. Each curve is a mean of at least 8 experiments.

that the pK_B values were not significantly modified by interchanging the agonists, indicating an interaction with a homogeneous receptor population.

Discussion

The results obtained either in field-stimulated vas deferens or in organs contracted by barium chloride, support previous findings that the relaxation induced by β-adrenoceptor agonists are mediated by β_2-adrenoceptors (Ganguly & Bhattacharya, 1969; Vohra, 1979; Lotti *et al.*, 1980; Diaz-Toledo & Jurkiewicz, 1980; 1990). This was indicated, according to Lands *et al.* (1967), by the rank order of potencies for the agonists (Iso > Ad ⩾ NA), when the organ was electrically stimulated (Table 1). The individual values of pD_2 were changed in barium-stimulated vas, leading to a relative increase for isoprenaline and adrenaline potencies but the overall hierarchy was not substantially modified. In addition, the pK_B value for practolol was not very different from 5.0 in all circumstances, corroborating the presence of β_2-adrenoceptors, since values higher than 6.5 would be expected for interactions with β_1-adrenoceptors, as observed in several preparations (Daly & Levy, 1979).

In spite of the similarity of both rank orders of potency, the individual differences on relative potencies and pK_B values (Tables 1 and 2) are an outstanding complication, indicating that the effects induced by β-agonists are mediated by different mechanisms, depending on whether the functional antagonist is barium or electrical stimulation. Furchgott (1972)

Table 2 Values of pD_2 and relative potencies (Rel Pot) for agonists and pK_B for antagonists, for relaxation mediated by β-adrenoceptors in barium-stimulated rat vas deferens

			pK_B *for antagonist*		
Agonist	pD_2	*Rel Pot*	*Propranolol*	*IMA*	*Practolol*
(±)-Iso	8.25 ± 0.13	812	9.96 ± 0.13	7.28 ± 0.08	5.12 ± 0.12
(−)-Ad	7.38 ± 0.15	109	10.10 ± 0.06	7.30 ± 0.09	5.07 ± 0.08
(−)-NA	5.34 ± 0.15	1	9.82 ± 0.11	7.39 ± 0.08	4.90 ± 0.12

Abbreviations as in Table 1.
n = at least 8 for each pD_2 and pK_B value.

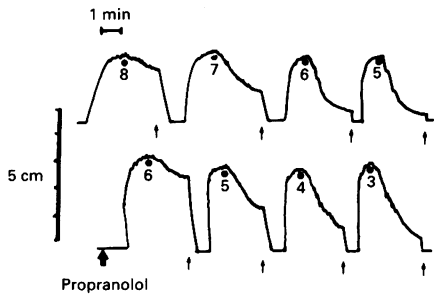

Figure 5 Typical kymograph recording of the relaxation induced by isoprenaline in contractions evoked by barium chloride (300 μM) in rat isolated vas deferens. Isoprenaline was added at dots, and washed out after about 2 min (thin arrows). Intervals between doses were 20 min. Records were obtained in the absence (upper traces) or presence (lower traces) of propranolol (10^{-8} M), added 30 min before barium. In general, 3 to 5 doses of agonist/curve, and 2 doses of antagonist were used in each experiment, except when high doses of noradrenaline (above 10^{-3} M) were needed (see Figures 6, 7 and 8). Isoprenaline concentrations are indicated as −log molar concentrations.

suggested that a greater than three fold difference, in the case of the relative potencies for the same agonist, or a difference of greater than 0.5 in the case of the pA_2 values for the same antagonist, should be considered preliminary evidence for different types of receptors and that a combination of two or more of such differences should be considered strong evidence. In our experiments, a difference larger than three fold was found for the relative potencies of isoprenaline (29:812) and adrenaline (21:109). In addition, the value of pK_B for propranolol against isoprenaline was about 1.3 log units greater, and for IMA almost 0.6 log units greater, when barium was used

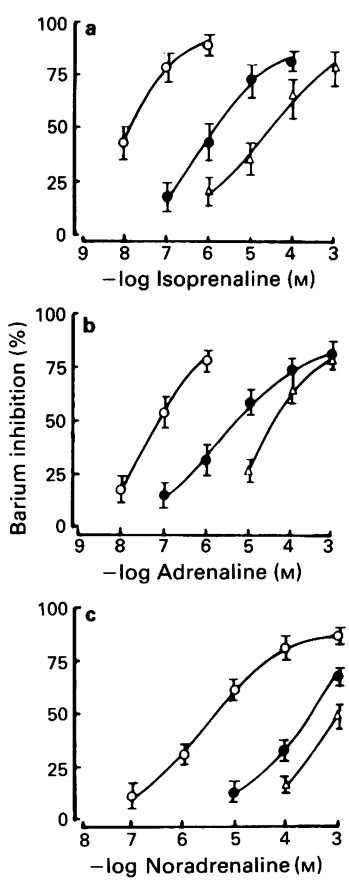

Figure 6 Concentration-response curves obtained in rat deferens contracted by barium chloride 300 μM: (a) for isoprenaline, (b), for adrenaline, and (c) for noradrenaline in the absence (○) and presence of propranolol 10^{-8} M (●) and 10^{-7} M (△). Vertical lines represent s.e.mean. Each curve is a mean of at least 8 experiments.

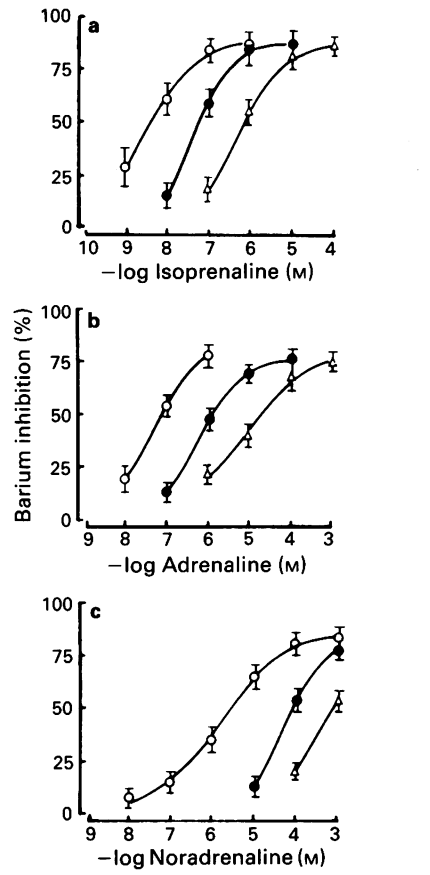

Figure 7 Concentration-response curves obtained in rat vas deferens contracted by barium chloride 300 μM: (a) for isoprenaline, (b) for adrenaline and (c) for noradrenaline, in the absence (○) and presence of isopropylmethoxamine 10^{-6} M (●) and 10^{-5} M (△). Vertical lines represent s.e.mean. Each curve is a mean of at least 8 experiments.

as the functional antagonist. Therefore, these results strongly indicate that relaxations induced in both cases are mediated by different receptor populations.

The experiments with barium, unlike those with electrically-induced twitches, clearly indicated the presence of a homogeneous receptor population. The strongest indication stems from the pK_B values, obtained for each β-blocker, which were independent of the agonist used (Table 2). This is a *sine-qua-non* condition for receptor homogeneity, based on expectations from receptor theory (Arunlakshana & Schild, 1959), as well as on results obtained in a series of pharmacological preparations (Furchgott, 1972; Daly & Levy, 1979).

The atypical results observed when electrically-induced twitches were used instead of barium, indicate the presence of distorting factors. This is probably due to the complexity of the events leading from transmural stimulation to contraction. The involvement of nerve terminals can be demonstrated by the use of tetrodotoxin, which inhibits the electrically-induced twitch in vas (Krstew *et al.*, 1982; May *et al.*, 1985). Electrically-induced twitches depend on the release of reserpine-resistant neurotransmitters, followed by an interaction of these transmitters with muscle receptors. The reduction of the amplitude of twitches, mediated by β-receptors, is supposed to be due to a blockade of this chain of events. On the basis of this assumption it can be hypothesized that two populations of receptors, one of them presynaptic, located in nerve cells, and the second postsynaptic, in muscle cells, would be responsible for the relaxation caused by β-agonists. An interaction with presynaptic receptors would provoke a perturbation of nerve activity, and as a consequence, of transmitter release and contractions. In addition, postsynaptic β-receptors would antagonize the contraction induced by the transmitter-receptor interaction in smooth

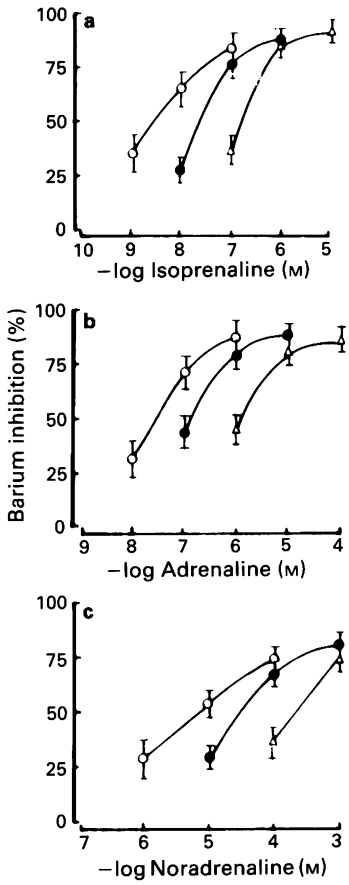

Figure 8 Concentration-response curves obtained in rat vas deferens contracted by barium chloride 300 μM: (a) for isoprenaline, (b) for adrenaline and (c) for noradrenaline, in the absence (○) and presence of practolol 5×10^{-5} M (●) and 5×10^{-4} M (△). Vertical lines represent s.e.mean. Each curve is a mean of at least 8 experiments.

muscle. In barium-stimulated vasa, the interaction of β-agonists with nerve receptors is useless, because the effect of barium is independent of transmitter release. In other words, the presynaptic receptors would also be reached by β-agonists, but this would result in an ineffective, or 'silent' interaction (Jurkiewicz *et al.*, 1971). Therefore, only the interaction of β-agonists with the postsynaptic β_2-adrenoceptors would be effective in barium-stimulated organs.

At least three other publications have advanced the possibility of multi-receptor interaction by β-agonists in the vas: Lotti (1983) suggested the presence of a postsynaptic β_2-adrenoceptor and of a presynaptic β-adrenoceptor, based on anomalous lines obtained in Schild plots, while Krstew *et al.* (1982) and May *et al.* (1985) proposed an interaction with α-adrenoceptors. In relation to our experiments, it is unlikely that α-adrenoceptors are involved, because of at least two pieces of experimental evidence: (a) the inactivation of these receptors by dibenamine was endorsed by the fact that clonidine, a typical presynaptic agonist, was unable to cause a relaxation of the electrically-stimulated vas, as described in Methods, and (b) the difference in pD_2 values, when comparing electrically-stimulated with barium-stimulated vasa, was found to be largest for Iso (compare Tables 1 and 2); if α-adrenoceptors were responsible for this difference, one would expect the pD_2 values for NA and Ad to be most affected, because of their higher affinities for α-adrenoceptors.

Although many precautions have been taken to ensure satisfactory experimental conditions and to exclude the influence of α-adrenoceptors, neuronal and extraneuronal uptake, and release of endogenous noradrenaline, we cannot be sure that this receptor population in nerve tissue, if present, is of β-receptors. In fact, Furchgott (1972) has shown that receptors which cannot be characterized as either α- or β-adrenoceptors can also interact with the so-called β-agonists. From the standpoint of adrenergic transmission, there are a number of publications describing, besides the well-known presence of catecholamines and ATP, the existence, or release, of [Met]enkephalin, neuropeptide Y, and calcitonin gene-related peptide, in vas deferens of different animal species (DePotter *et al.*, 1987; Maggi *et al.*, 1987; Kasarov *et al.*, 1988). Therefore, this two-adrenoceptor hypothesis can only be considered a suggestion rather than conclusive. We believe that a clear answer to this question will only be obtained after a better understanding of at least three inter-related pertinent issues: (a) the role, releasing mechanisms, and interactions of the endogenous substances present in nerve terminals of the vas deferens; (b) a model for functional antagonism (Mackay, 1981) accounting for the hypothesis that we have a double site of action for the β-agents; and (c) a model for competitive antagonism explaining the changes observed for pD_2 and pK_B values (Tables 1 and 2) and the anomalous shifts of dose-response curves due to competitive antagonists (Figures 2, 3, and 4). Although some models have been published in the past (see, for instance, Furchgott *et al.*, 1974) they do not account for the experimental conditions involved here. On the other hand, the presence of two different sites interacting with β-agonists and antagonists has been clearly shown by means of non-functional methods, such as radioligand binding assays (May *et al.*, 1985).

The high pK_B value for propranolol, obtained in organs contracted by barium chloride (Table 2), is in agreement with the pA_2 value obtained by Daly & Levy (1979) in rat aorta (9.45), using the same contracting agent. In relation to the high values for the relative potency of isoprenaline (Table 2), corresponding to a difference larger than 2.5 log units between pD_2 values for Iso and NA, it is noteworthy that when Iso and NA were used against barium in rat aorta and in guinea-pig uterus, similar values were obtained (Daly & Levy, 1979). Further facts on the use of barium chloride as a functional antagonist against other β-agents in vas deferens, have not been reported, to our knowledge. In relation to the pK_B values for propranolol, IMA and practolol against isoprenaline in field-stimulated vas, our data agree with results previously presented for other preparations (Furchgott, 1972; Daly & Levy, 1979).

In summary, it is concluded that the inhibitory effects of β-adrenoceptor agonists on rat vas deferens contracted by barium chloride are mediated by β_2-adrenoceptors. In addition, it is suggested that the inhibitory effects in electrically stimulated vas are mediated by the same receptors, in addition to a second receptor population, the main characteristics of which are still unknown.

References

ARUNLAKSHANA, O. & SCHILD, H.O. (1959). Some quantitative uses of drug antagonists. *Br. J. Pharmacol. Chemother.*, **14**, 48–58.

BUSATTO, P.A. & JURKIEWICZ, A. (1985). Simultaneous measurement of contractile effects in the circular and longitudinal smooth muscle of the rat vas deferens by drugs perfused externally or via the lumen. *Br. J. Pharmacol.*, **85**, 737–746.

DALY, M.J. & LEVY, G.P. (1979). The subclassification of adrenoceptors: evidence in support of the dual-adrenoceptor hypothesis. In *Trends in Autonomic Pharmacology*. Vol. I, ed. Kalsner, S. pp. 347–385, Baltimore: Urban & Schwarzenberg.

DE POTTER, W.P., COEN, E.P., & DE POTTER, R.W. (1987). Evidence for the coexistence and co-release of [met]enkephalin and noradrenaline from sympathetic nerves of the bovine vas deferens. *Neuroscience*, **20**, 855–866.

DIAZ-TOLEDO, A. & JURKIEWICZ, A. (1980). Receptores do sub-tipo beta$_2$ em ducto deferente de rato. *Ciência e Cultura* (São Paulo), **32,** 771 Abs.

DIAZ-TOLEDO, A. & JURKIEWICZ, A. (1990). Dissociation constants and relative efficacies estimated from the functional antagonism of β-adrenoceptor agonists on transmural stimulation in rat vas deferens. *Eur. J. Pharmacol.*, **191,** 157–165.

DIAZ-TOLEDO, A. (1983). Ação de agentes beta-adrenérgicos em ducto deferente de rato. *Doctoral thesis. São Paulo: Escola Paulista de Medicina.*

FESTING, M.F.W. (1980). *International Index of Laboratory Animals,* 4th ed., London: MRC.

FURCHGOTT, R.F. (1972). The classification of adrenoceptors (adrenergic receptors). An evaluation from standpoint of receptor theory. In *Handbook of Experimental Pharmacology,* Vol. 33 (*Catecholamines*), ed. Blaschko, H. & Muscholl, E. pp. 283–335, New York: Springer-Verlag.

FURCHGOTT, R.F. & BURSZTYN, P. (1967). Comparison of dissociation constants and of relative efficacies of selected agonists acting on parasympathetic receptors. *Ann. N.Y. Acad. Sci.*, **144,** 882–899.

FURCHGOTT, R.F., JURKIEWICZ, A. & JURKIEWICZ, N.H. (1974). Antagonism of propranolol to isoproterenol in guinea-pig trachea: Some cautionary findings. *Biochem. Pharmacol.*, **23,** suppl. 1, 220–224.

GANGULY, D.K. & BHATTACHARYA, D.D. (1969). Adrenergic receptors in rat vas deferens. *Arch. Int. Pharmacodyn.*, **185,** 406–412.

JURKIEWICZ, A. & JURKIEWICZ, N.H. (1976). Dual effect of α-adrenoceptor antagonists in rat isolated vas deferens. *Br. J. Pharmacol.*, **56,** 169–178.

JURKIEWICZ, N.H., JURKIEWICZ, A. & VALLE, J.R. (1971). Contractile reserve after maximum doses of full agonists on the rat vas deferens. *Pharmacology,* **5,** 129–144.

KASAROV, L., ELLIS, J., KIRKPATRICK, K., MILNER, P. & BURNSTOCK, G. (1988). Direct evidence for concomitant release of noradrenaline, adenosine 5′-triphosphate and neuropeptide Y from sympathetic nerve supplying the guinea-pig vas deferens. *J. Auton. Nervous System,* **22,** 75–82.

KRSTEW, E., MALTA, E. & RAPER, C. (1982). Comparison of guinea pig uterine and rat vas deferens preparations for assessment of beta$_2$-adrenoceptor-mediated activity. *J. Pharmacol. Methods,* **8,** 279–289.

LANDS, A.M., ARNOLD, A., MACAULIFF, J.P., LUDUENA, F.P. & BROWN, T.G. (1967). Differentiation of receptor systems activated by sympathomimetic amines. *Nature,* **214,** 597–598.

LANGELOH, A. & JURKIEWICZ, A. (1982). Analysis of the effects of dopamine and noradrenaline in relation to the proposed postsynaptic dopamine receptor in rat vas deferens. *Naunyn-Schmiedebergs Arch. Pharmacol.*, **318,** 202–209.

LOTTI, V.J. (1983). Evidence that presynaptic beta-receptors account for the low affinity site in Schild plots for beta-adrenergic antagonists in field stimulated rat vas deferens. *Neurosci. Lett.*, **41,** 195–197.

LOTTI, V.J. CHANG, R.S.L. & KLING, P. (1980). Beta$_2$ selective adrenergic responses in the field-stimulated rat vas deferens. *Eur. J. Pharmacol.*, **68,** 385–386.

LOTTI, V.J., KLING, P. & CERINO, D. (1982). High and low (Gpp(NH)p-sensitive) affinity sites for β_2-adrenergic blockers as antagonists of isoproterenol in the field stimulated rat vas deferens. *Eur. J. Pharmacol.*, **84,** 161–167.

MACKAY, D. (1978). How should values of pD$_2$ and affinity constants for pharmacological competitive antagonists be estimated? *J. Pharm. Pharmacol.*, **30,** 312–313.

MACKAY, D. (1981). An analysis of functional antagonism and synergism. *Br. J. Pharmacol.*, **73,** 127–134.

MAGGI, C.A., SANDICIOLI, P., THEODORSSON-NORHEIM, E. & MELI, A. (1987). Immunoblockade of response to capsaicin in the rat vas deferens: evidence for the involvement of endogenous calcitonin gene-related peptide. *Neurosci. Lett.*, **78,** 63–68.

MAY, J.M., ABEL, P.M. & MINNEMAN, K.P. (1985). Binding of agonists to beta-adrenoceptors in rat vas deferens: relationship to functional response. *Naunyn-Schmiedebergs Arch. Pharmacol.*, **331,** 324–333.

VAN ROSSUM, J.M. (1963). Cumulative dose-response curves II. Technique for the making of dose-response curves in isolated organs and the evaluation of drug parameters. *Arch. Int. Pharmacodyn.*, **143,** 299–330.

VOHRA, M.M. (1979). Evidence for the presence of beta$_2$-inhibitory adrenoceptors in the rat vas deferens. *Gen. Pharmacol.*, **10,** 221–225.

(Received May 7, 1991
Accepted May 29, 1991)

Erratum

Br. J. Pharmacol. (1991), **103**, 1191–1195

M. Shinkai, I. Takayanagi and T. Kato. Facilitatory effects of tachykinins and guanethidine on the acetylcholine output stimulated by nicotine from guinea-pig bladder

The corrected new title for this paper is shown below:

'Contrasting effects of tachykinins and guanethidine on the acetylcholine output stimulated by nicotine from guinea-pig bladder'

British Journal of Pharmacology

VOLUME 104 (1) SEPTEMBER 1991

SPECIAL REPORTS

The purpose of *Special Reports*, which are superseding 'Short Communications', is to provide rapid publication for **new** and **important** results which the Editorial Board considers are likely to be of special pharmacological significance. (Please note that Short Communications are no longer acceptable for publication.) *Special Reports* will have publication priority over all other material and so authors are asked to consider carefully the status of their work before submission.

In order to speed publication there is normally no revision allowed beyond very minor typographical or grammatical corrections. If significant revision is required, the Board may either invite rapid re-submission or, more probably, propose that it be re-written as a Full Paper and be re-submitted for consideration. In order to reduce delays, proofs of *Special Reports* will be sent to authors but **essential corrections must reach the Production Office within 48 hours of receipt.** Authors should ensure that their submitted material conforms exactly to the following requirements.

Special Reports should normally occupy no more than two printed pages of the Journal; two illustrations (Figures or Tables, with legends) are permitted. As a guideline, with type face of 12 pitch and double-line spacing, a page of A4 paper could contain about 400 words. The absolute maximum length of the *Special Report* is 1700 words. For each Figure or Table, please deduct 200 words. The manuscript should comprise a Title page with key words (maximum of 10), a Summary consisting of a single short paragraph, followed by Introduction, Methods, Results, Discussion and References (maximum of 10). In all other respects, the requirements are the same as for Full Papers (see current 'Instructions to Authors').

Papers will be considered for publication on all aspects of pharmacology, including chemotherapy.

Manuscripts (two copies) should be sent to Editorial Office, British Journal of Pharmacology, St. George's Hospital Medical School, Cranmer Terrace, London SW17 0RE. Authors should consult the Instructions to Authors in Vol. 102, 553–559 (1991) and the Nomenclature Guidelines for Authors in Vol. 102, 560–561 (1991). These Instructions and Guidelines also appear with the journal Index for volumes 99–101, 1990.

The *British Journal of Pharmacology* is published monthly by the Scientific & Medical Division, Macmillan Press Ltd.

The journal is covered by *Current Contents*, *Excerpta Medica* and *Index Medicus*.

All business correspondence and reprint requests should be addressed to the Scientific & Medical Division, Macmillan Press Ltd., Houndmills, Basingstoke, Hampshire RG21 2XS, UK. Telephone: (0256) 29242; Fax: (0256) 810526.

Annual subscription prices for 1991 EEC £375, elsewhere £415/US$750 (sterling rate is definitive). Orders must be accompanied by remittance. Cheques should be made payable to Macmillan Press, and sent to: Macmillan Press Ltd., Subscription Department, Brunel Road, Houndmills, Basingstoke, Hampshire RG21 2XS, UK.

Overseas subscribers may make payments into UK Post Office Giro Account No. 5192455. Full details must accompany the payment.

Second Class postage paid at Rahway NJ. US Mailing Agent: Mercury Airfreight International Ltd, Inc., 2323 Randolph Avenue, Avenel, New Jersey, NJ 07001, USA.

Enquiries concerning advertising space or rates should be addressed to: Michael Rowley, Advertisement Manager, Macmillan Press Ltd., 4 Little Essex Street, London WC2R 3LF. Telephone: 071 836 6633; Fax: 071 379 4204.

ISSN 0007–1188

0007–1188/91 $3.50 + $0.00

SPECIAL REPORTS

The purpose of *Special Reports*, which are superseding 'Short Communications', is to provide rapid publication for **new** and **important** results which the Editorial Board considers are likely to be of special pharmacological significance. (Please note that Short Communications are no longer acceptable for publication.) *Special Reports* will have publication priority over all other material and so authors are asked to consider carefully the status of their work before submission.

In order to speed publication there is normally no revision allowed beyond very minor typographical or grammatical corrections. If significant revision is required, the Board may either invite rapid re-submission or, more probably, propose that it be re-written as a Full Paper and be re-submitted for consideration. In order to reduce delays, proofs of *Special Reports* will be sent to authors but **essential corrections must reach the Production Office within 48 hours of receipt.** Authors should ensure that their submitted material conforms exactly to the following requirements.

Special Reports should normally occupy no more than two printed pages of the Journal; two illustrations (Figures or Tables, with legends) are permitted. As a guideline, with type face of 12 pitch and double-line spacing, a page of A4 paper could contain about 400 words. The absolute maximum length of the *Special Report* is 1700 words. For each Figure or Table, please deduct 200 words. The manuscript should comprise a Title page with key words (maximum of 10), a Summary consisting of a single short paragraph, followed by Introduction, Methods, Results, Discussion and References (maximum of 10). In all other respects, the requirements are the same as for Full Papers (see current 'Instructions to Authors').

Still

Number One in Pharmacological Research *

*The latest Journal Citation Reports, from the ISI's Science Citation Index, show that for the second year in succession **British Journal of Pharmacology** is the most intensively cited primary research pharmacology journal in the world.

The last few years have been extraordinarily prolific for British Journal of Pharmacology. Three successive years as the world's second most intensively cited primary research journal in pharmacology have been followed by two successive years in the coveted number one position.

At the same time, the number of excellent quality papers submitted to our editorial office has increased dramatically. As a result, the number of papers published each year has also risen. Indeed in the last nine years the number of papers published each year has doubled.

Naturally, this huge increase in the amount of good material coming in has posed challenges to us. Should we raise our already high editorial standards and reject papers that we would prefer to publish? Or should we delay publication of submitted papers in order to contain the size of the journal?

Of course, we have done neither of these things!

To maintain our position as the world's leading pharmacological research journal we have, since 1990, increased our page size to a smart new A4 format. This has allowed us to print nearly 40% more information on every page. It has also made it easier to print illustrations on the same page as the relevant text.

In addition, we regularly review the editorial process and the composition of the editorial board, to ensure that we maintain British Journal of Pharmacology's reputation for complete coverage of all aspects of basic pharmacology.

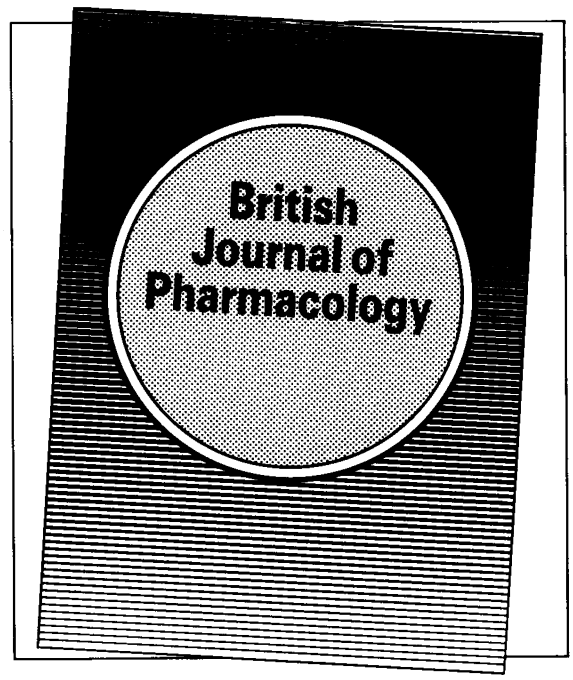

FREE SAMPLE COPY!

If you are not already one of our large family of readers, why not send for your own FREE sample copy of the British Journal of Pharmacology.

To Richard Gedye, Macmillan Press Ltd, Houndmills, Basingstoke, RG21 2XS, UK
Please send me my FREE sample copy of British Journal of Pharmacology

Name _____

Position _____

Address _____

_____

_____

_____

Postal/Zip Code _____

Country _____

BJP M

PREPARATION OF MANUSCRIPTS

Authors are strongly recommended to read the full *Instructions to Authors* and *Nomenclature Guidelines for Authors* (*Br. J. Pharmacol.* 1991, **102,** 553–561) before submitting a manuscript for publication in the *British Journal of Pharmacology.* The manuscript and cover letter should be checked against the following list before mailing.

The original and one copy of the manuscript must be supplied. Manuscripts must be typed in double-line spacing on one side of A4 paper, in type not smaller than 12 characters per inch or 10 point. Both copies to include Tables and a set of labelled Figures. One set of Figures without numbers or letters is also to be included. The text to be arranged in the following subsections:

1. **Title**—To have no more than 150 characters on a separate page, which should also include a Short Title (50 characters maximum) and the name and address of the author for correspondence.
2. **Summary**—To be arranged in numbered paragraphs (Full Papers) or a single paragraph (Special Reports).
   —to include aims, principal results and conclusions.
   —to include Key words (10 maximum) at end of summary.
3. **Introduction**—To contain concise statements of the problem and the aims of the investigation.
4. **Methods**—To have brief but adequate account of the procedures; *full names of drugs (including those referred to by manufacturer's code)*, sources of drugs and statistical tests to be stated.
5. **Results**—To have no repetition of data in Figures, Tables and text.
6. **Discussion**—Findings and conclusions to be placed in context of other relevant work.
   NB Simple repetition of results and unwarranted speculation are not acceptable.
7. **Acknowledgments**—Sources of support. Sources of drugs not widely available commercially.
8. **References**—All references in the text to be included in the Reference List and *vice versa.* References in alphabetical order with complete citations; Journals publishing 'in press' papers identified.
   References to manuscripts submitted to other journals but not yet accepted are not allowed.
9. **Tables**—Each on a separate page and prepared in accordance with current requirements of the Journal.
10. **Figures**—Both labelled and non-labelled Figures to be prepared in accordance with current requirements of the Journal (see *Instructions to Authors,* 1991, vol. **102,** 553–559) and provided with Figure Number and Authors' names on back (*in pencil*)
    —each legend to be typed on a separate page and carrying keys to symbols
11. **Manuscripts**—To be accompanied by a declaration signed by each author that
    (a) results are original
    (b) approval of all persons concerned has been given to submit manuscripts for consideration (see also 12b)
    (c) the same material is neither 'in press' (i.e. is in proof or has definitely been accepted for publication) nor under consideration elsewhere. Furthermore it will not be submitted or published elsewhere before a decision has been reached by the Editorial Board of the *British Journal of Pharmacology* and will not be submitted elsewhere if accepted by the *British Journal of Pharmacology.*
    (d) Copyright assignment is included
12. **Cover letter**—To state clearly
    (a) Corresponding author's full postal address, telephone, telex or Fax number
    (b) where appropriate, that *either* ethical approval has been given for investigation *or* Company or Institutional permission to publish work has been received.
13. **Reminder**—Packaging to be sufficiently robust to protect Figures and to withstand mailing.

Failure to comply with *Instructions to Authors* may lead to substantial delays in processing, review and publication and may even jeopardize acceptance of the manuscript.

BRITISH JOURNAL OF PHARMACOLOGY VOLUME 104 (1) 1991

Filmsetting by Santype International Limited, Salisbury, Wiltshire
and printed in Great Britain by Unwin Brothers Ltd., The Gresham Press, Old Woking, Surrey